Studies on Natural Products: Resistance Modifying Agents, Antibacterials and Structure Elucidation

Simon Gibbons

Acknowledgements
I thank my parents Brian and Gillian for their never-ending love and encouragement of me and my interest in all things phytochemical. I dedicate this thesis to them, to my sister Sarah, my daughters Hannah and Jenny and to my lady Sally. Science can be incredibly seductive and distracting and I apologise to them for when I have been distant and not focusing on their needs. This thesis has a been a psychological journey for me, an anabasis, where I have returned to realising that the only things of value are loving family and God. The rest is a distraction.

Summary

This thesis describes research starting in 1999 on three areas of natural product science, namely bacterial resistance modifying agents, antibacterials and structure elucidation of natural products.

Plants produce an array of structurally-complex and diverse chemical scaffolds and whilst there is an expanding volume of published literature on structure elucidation, there remains a need to understand why these compounds are produced and how they function in terms of biological activity. That can only be properly realised by a full and determined attempt at structure elucidation. This is an important concept as molecular structure describes and precedes function. The chirality and functional group chemistry of natural products *defines* the way in which a compound specifically binds to a receptor, protein or drug target.

My independent research career started with studies on the ability of plant extracts and phytochemicals to modulate the activity of antibiotics that are substrates for bacterial multidrug efflux. These investigations are described in the first section, "Natural Product Resistance Modifying Agents". Studies were, in the first instance, simple assays to look at potentiation and synergy of extracts and pure phytochemicals to potentiate the activity of antibiotics against resistant bacteria. This research evolved to study efflux inhibition, where we learnt much from the collaborations with Professors Piddock (Birmingham), Kaatz (Wayne State) and Bhakta (Birkbeck). Latterly, we were inspired by the highly imaginative and creative work of Dr Paul Stapleton (UCL), to study the plasmid transfer inhibitory effects of natural products; the rationale being that plasmids carry antibiotic-resistance genes and virulence factors. Inhibition of transfer could result in a reduction in the spread of antibiotic resistance and a reduction in pathogenicity.

The second section of this thesis describes antibacterial natural products that were evaluated against clinically-relevant species of bacteria, in the main Gram-positive organisms such as *Staphylococcus aureus* and its methicillin- (MRSA) and multidrug-resistant variants and *Mycobacterium tuberculosis*, the causative agent of tuberculosis, which still continues to affect millions of people globally and for which antibiotic resistance is considerable.

The papers described in this section detail the extraction of the plant and the bioassay-guided isolation of the active compounds, which were then subjected to structure elucidation, using in the majority of cases, Nuclear Magnetic Resonance (NMR) spectroscopy, High-Resolution Mass Spectrometry, and Infrared and Ultraviolet-Visible Spectroscopy. Natural products from the acylphloroglucinol, terpenoid, polyacetylene, alkaloid and sulphide classes are well represented in these publications with some of these antibacterial natural products displaying minimum inhibitory concentrations (MIC) values of less than 1 mg/L against MRSA and *Mycobacterium tuberculosis* strains. These activity levels approach those of existing clinically used antibiotics and this highlights the value of plant natural products as a resource for antibacterial templates.

Mechanistic studies have also been conducted on selected compounds, for example the natural products from *Hypericum acmosepalum* were found to inhibit ATP-

dependent MurE ligase, a key enzyme involved in bacterial cell wall biosynthesis. Other examples included the main component of cinnamon (*Cinnamomum zeylanicum*), an ancient medicinal material cited in the Bible in Exodus, which has been used in antiquity as an anti-infective substance. The main compound from this medicinal material is *trans*-cinnamaldehyde, a simple phenylpropanoid which has been shown to inhibit Acetyl-CoA Carboxylase, a pivotal enzyme that catalyses the first committed step in fatty acid biosynthesis in all animals, plants and bacteria. In collaboration with the marine natural product chemist Professor Vassilios Roussis, we have also been able to characterise the antibacterial activities of marine plants, particularly compounds of the diterpene class that display promising levels of antibacterial activity against MRSA and *S. aureus* strains. Work on the antibacterial properties of *Cannabis sativa* showed that some of the main cannabinoids display excellent potency towards drug-resistant variants of *S. aureus* and support the ancient medicinal usage of *Cannabis* as an anti-infective and wound healing preparation. The acylphloroglucinol class of plant natural products are also noteworthy, particularly from *Hypericum* and Mediterranean medicinal plant species such as Myrtle (*Myrtus communis*), again with MIC values reaching 1 mg/L against pathogenic bacteria. We synthesised some of these acylphloroglucinols and made analogues and not surprisingly, were unable to improve the activity as nature really is the best chemist of all.

The final section describes early and continuing research into the isolation and structure elucidation of natural products from plants and microbes. The rationale for this research is manifold: training for isolation to understand the medicinal use of a plant or microbe, chemotaxonomic investigations, the ecological relevance of phytochemicals in plants that are halophytic and xerophytic and in some cases just plain academic curiosity. These studies use classical phytochemical techniques to isolate and determine the structures of the species of investigation and where possible, absolute stereochemistry is undertaken. It should be noted however that isolation can be *exceptionally challenging and frustrating*. This can be due to the paucity of biomass, low concentrations of compounds, complexity of the resulting natural product mixtures and finally a lack of chemical stability of the products. All of these issues need to be faced before structure determination can even be attempted. A word of caution is therefore needed to the young natural product chemist embarking on their first isolation project. However, words of encouragement are also needed: the isolation of new, chemically complex and exquisitely biologically active molecules is a beautiful endeavour and exceptionally rewarding on many levels.

Table of Contents

Natural Product Resistance Modifying Agents

Escobedo-Martínez, C., Cruz-Morales, S., Fragoso-Serrano, M., Rahman, M.M., Gibbons, S. and Pereda-Miranda, R. (2010). Characterization of a Xylose Containing Oligosaccharide, an Inhibitor of Multidrug Resistance in *Staphylococcus aureus*, from *Ipomoea pes-caprae. Phytochemistry* **71**, 1796-1801.

Piddock, L.J.V., Garvey, M.I., Rahman M.M. and Gibbons, S. (2010). Trimethoprim and epinephrine behave as inhibitors of efflux in Gram negative bacteria. *Journal of Antimicrobial Chemotherapy* **65**, 1215-1223.

Drakulic, B., Stavri, M., Gibbons, S. Cicak, Z., Verbic, T., Juranic, I. and Zloh, M. (2009). Aryldiketo Acids Have Unexpected Antibacterial and Modulation Activity Against MDR *S. aureus* Strains. Structural Insights Based on Similarity and Molecular Interaction Fields. *ChemMedChem* **4**, 1971-1975.

Chérigo, L., Pereda-Miranda, R. and Gibbons. S. (2009). Bacterial resistance modifying tetrasaccharide agents from *Ipomoea murucoides. Phytochemistry* **70**, 222-227.

Chérigo, L., Pereda-Miranda, R., Fragoso-Serrano, M., Jacobo-Herrera, N., Kaatz, G.W. and Gibbons, S. (2008). Multidrug Resistant Bacterial Efflux Pump Inhibitors from the Resin Glycosides of *Ipomoea murucoides. Journal of Natural Products* **71**, 1037-1045.

Lechner, D., Gibbons S. and Bucar, F. (2008). Plant Phenolic Compounds as Ethidium Bromide Efflux Inhibitors in *Mycobacterium smegmatis*. *Journal of Antimicrobial Chemotherapy* **62**, 345-348.

Lechner, D., Gibbons S. and Bucar, F. (2008). Modulation of isoniazid susceptibility by flavonoids in *Mycobacterium*. *Phytochemistry Letters* **1**, 71-75.

Smith, E.C.J., Kaatz, G.W., Seo, S.M., Wareham, N., Williamson E.M. and Gibbons S. (2007). The Phenolic Diterpene Totarol Inhibits Multidrug Efflux Pump Activity in *Staphylococcus aureus*. *Antimicrobial Agents and Chemotherapy* **51**, 4480-4483.

Stavri, M., Piddock L.J.V. and Gibbons, S. (2007). Bacterial efflux pump inhibitors from natural sources. *Journal of Antimicrobial Chemotherapy* **59**, 1247-1260.

Michalet, S., Cartier, G., Stavri, M., David, B., Mariotte, A-M., Dijoux-Franca, M-G., Kaatz, G.W. and Gibbons, S. (2007). *N*-Caffeoylphenalkylamide Derivatives as Bacterial Efflux Pump Inhibitors. *Bioorganic Medicinal Chemistry Letters* **17**, 1755-1758.

Zloh, M. and Gibbons, S. (2007). The role of small molecule – small molecule interactions in overcoming biological barriers for antibacterial

drug action. *Theoretical Chemistry Accounts* **117**, 231-238.

Dickson, R.A., Houghton, P.J., Hylands, P.J. and Gibbons S. (2006). Antimicrobial, Resistance modifying effects, Antioxidant and Free radical scavenging activities of *Mezoneuron benthamianum* Baill., *Securinega virosa* Roxb. & Wlld. and *Microglossa pyrifolia* Lam. *Phytotherapy Research* **20**, 41-45.

Pereda-Miranda, R., Kaatz, G.W. and Gibbons S. (2006). Polyacylated Oligosaccharides from Medicinal Mexican Morning Glory Species as Antibacterials and Inhibitors of Multidrug Resistance in *Staphylococcus aureus*. *Journal of Natural Products* **69**, 406-409.

Cégiéla-Carlioz, P, Bessière J-M, David B, Mariotte A-M, Gibbons, S., Dijoux-Franca, M-G. (2005). Osha Essential Oil Modulates Multidrug-Resistance (MDR) in *Staphylococcus aureus. Flavour and Fragrance Journal* **20**, 671-675.

Gibbons, S., Moser, E. and Kaatz, G.W. (2004). Catechin Gallates inhibit Multidrug resistance (MDR) in *Staphylococcus aureus. Planta Medica* **70**, 1240-1242.

Zloh, M., Kaatz, G.W. and Gibbons, S. (2004). Inhibitors of Multidrug resistance (MDR) have affinity for MDR substrates. *Bioorganic Medicinal Chemistry Letters* **14**, 881-885.

Gibbons, S., Oluwatuyi, M., Veitch, N.C. and Gray, A.I. (2003). Bacterial Resistance Modifying Agents from *Lycopus europaeus*. *Phytochemistry* **62**, 83-87.

Zloh, M. and Gibbons S. (2004). Molecular similarity of MDR inhibitors. *International Journal of Molecular Sciences* **5**, 37-47.

Oluwatuyi, M. Kaatz, G. and Gibbons, S. (2004). Antibacterial and Resistance Modifying Activity of *Rosmarinus officinalis. Phytochemistry* **65**, 3249-3254.

Gibbons, S., Oluwatuyi, M. and Kaatz, G.W. (2003). A Novel Inhibitor of Multidrug Efflux Pumps in *Staphylococcus aureus. Journal of Antimicrobial Chemotherapy* **51**, 13-17.

Gibbons, S. and Udo, E.E. (2000). The effect of reserpine, a modulator of multidrug efflux pumps, on the *in-vitro* activity of tetracycline against clinical isolates of methicillin resistant *Staphylococcus aureus* (MRSA) possessing the *tet*(K) determinant. *Phytotherapy Research* **14**, 139-140.

Natural Product Antibacterials

Brucoli, F., Borrello, M.T., Stapleton, P., Parkinson, G.N. and Gibbons, S. (2012). Structural characterization and antimicrobial evaluation of atractyloside, atractyligenin, and 15-didehydroatractyligenin methyl ester. *Journal of Natural Products* **75**, 1070-1075.

Osman, K., Evangelopoulos, D., Basavannacharya, C., Gupta, A., McHugh, T.D., Bhakta, S. and Gibbons, S. (2012). An Antibacterial from *Hypericum acmosepalum* inhibits ATP dependent MurE ligase from *Mycobacterium tuberculosis*. *International Journal of Antimicrobial Agents* **39**, 124-129.

Shiu, W.K.P., Rahman, M.M., Curry, J., Stapleton, P., Malkinson, J.P. Gibbons, S. (2012). Antibacterial acylphloroglucinols from *Hypericum olympicum*. *Journal of Natural Products* **75**, 336-343.

Guzman J.D., Bucar, F., Gupta, A., Gibbons, S. and Bhakta, S. (2012). Anti-mycobacterials from natural sources: ancient times, antibiotic era and novel scaffolds. *Frontiers in Bioscience* **17**, 1861-1881.

Guzman, J.D., Wube, A., Evangelopoulos, D., Gupta, A., Hüfner, A., Basavannacharya, C., Rahman, M. M., Tomaschitz, C., Bauer, R., McHugh, T., Nobeli, I., Prieto, J., Gibbons, S., Bucar, F. and Bhakta, S. (2011). N-methyl-2-alkenyl-4-quinolones are inhibitors of ATP-dependent MurE ligase of *Mycobacterium tuberculosis*: antibacterial activity, molecular docking and inhibition kinetics. *Journal of Antimicrobial Chemotherapy* **66**, 1766-1772.

Ioannou, E., Quesada, A., Rahman, M.M. Gibbons, S. Vagias, C. and Roussis, V. (2011). Dolabellanes with antibacterial activity from the brown alga *Dilophus spiralis. Journal of Natural Products* **74**, 213-222.

Guzman, J.D., Gupta, A., Evangelopoulos, D., Basavannacharya, C., Pabon, L., Plazas, E.A., Muñoz, D.R., Delgado, W.A., Cuca, L.E., Ribon, W., Gibbons, S. and Bhakta, S. (2010). Anti-tubercular screening of natural products from Colombian plants: 3-methoxy-nordomesticine, an inhibitor of ATP-dependent MurE ligase of *Mycobacterium tuberculosis*. *Journal of Antimicrobial Chemotherapy* **65**, 2101-2107.

Smyrniotopoulos, V. Vagias, C., Rahman, M.M., Gibbons, S. and Roussis, V. (2010). Structure and antibacterial activity of brominated diterpenes from the red alga *Sphaerococcus coronopifolius*. *Chemistry and Biodiversity* **7**, 186-195.

Meades, Jr., G., Henken, R.L., Waldrop, G.L., Rahman, M.M., Gilman, S.D., Kamatou, G.P.P., Viljoen, A.M. and Gibbons S. (2010). Constituents of Cinnamon Inhibit Bacterial Acetyl CoA Carboxylase. *Planta Medica* **76**, 1570-1575.

Smyrniotopoulos, V. Vagias, C., Rahman, M.M., Gibbons, S. and Roussis V. (2010). Ioniols I and II, tetracyclic diterpenes with antibacterial activity

from *Sphaerococcus coronopifolius. Chemistry and Biodiversity* **7**, 666-676.

Stavri, M., Paton, A., Skelton, B.W. and Gibbons, S. (2009). Antibacterial Diterpenes from *Plectranthus ernstii* Codd. *Journal of Natural Products* **72**, 1191-1194.

O'Donnell, G., Poeschl, R., Zimhony, O., Gunaratnam, M., Moreira J.B.C., Neidle, S., Bhakta S., Malkinson, J.P. Boshoff, H., Lenaerts, A. and Gibbons, S. (2009). Bioactive pyridine-*N*-oxide sulphides from *Allium stipitatum. Journal of Natural Products* **79**, 360-365.

Appendino, G., Gibbons, S., Giana, A., Pagani, A., Grassi, G.P., Stavri, M., Smith E. and Rahman, M.M. (2008). Antibacterial phytocannabinoids: a structure-activity study. *Journal of Natural Products* **71**, 1427-1430.

Modaressi, M., Delazar, A., Nazemiyeh, H., Fathi-Azad, F., Smith, E.C.J., Rahman, M.M., Gibbons, S., Nahar, L. and Sarker, S.D. (2008). Antibacterial iridoid glucosides from *Eremostachys laciniata. Phytotherapy Research* **23**, 99-103.

Smyrniotopoulos, V., Vagias, C., Rahman, M.M., Gibbons, S. and Roussis. V. (2008). Brominated antibacterial diterpenes from the red alga *Sphaerococcus coronopifolius*. *Journal of Natural Products* **71**, 1386-1392.

Schinkovitz, A., Stavri, M., Bucar, F. and Gibbons, S. (2008). Antimycobacterial polyacetylenes from *Levisticum officinale. Phytotherapy Research* **22**, 681-684.

Kontiza, I., Stavri, M., Zloh, M., Vagias, C., Gibbons, S. and Roussis, V. (2008). Chemical constituents of marine angiosperm *Cymodocea nodosa* and their antibacterial activity*. Tetrahedron* **64**, 1696-1702.

Sharma, R.J., Negi, D.S. Gibbons, S. and Otsuka H., (2008). Chemical and Antibacterial Constituents of *Skimmia anquetelia. Planta Medica* **74**, 175-177.

Rahman, M.M., Garvey, M., Piddock, L.J.V. and Gibbons, S. (2008). Antibacterial terpenes from the oleo-resin of *Commiphora molmol* (Engl.). *Phytotherapy Research* **22**, 1356-1360.

Smith, E.C.J., Wareham, N., Zloh, M. and Gibbons S. (2008). 2β-acetoxyferruginol – a new antibacterial abietane diterpene from the bark of *Prumnopitys andina. Phytochemistry Letters* **1**, 49-53.

Kokubun, T., Shiu, W.K.P. and Gibbons S. (2007). Inhibitory activities of lichen-derived compounds against methicillin and multidrug-resistant *Staphylococcus aureus. Planta Medica* **73**, 176-179.

Smith, E.C.J., Williamson, E.M., Kaatz, G.W. and Gibbons, S. (2007).

Antibacterials and modulators from immature cones of *Chamaecyparis lawsoniana*. *Phytochemistry* **68**, 210-217.

O'Donnell, G. and Gibbons, S. (2007). Antibacterial Activity of two Canthin-6-one Alkaloids from *Allium neapolitanum*. *Phytotherapy Research* **21**, 653-657.

Zloh, M., Bucar, F. and Gibbons, S. (2007). Quantum Chemical Studies on Structure Activity Relationship of Natural Product Polyacetylenes. *Theoretical Chemistry Accounts* **117**, 247-252.

Xiao, Z.Y., Shiu, W.K.P., Zeng, Y.H., Mu, Q. and Gibbons, S. (2008). A Natural Occurring Inhibitory Agent with Activity against Multidrug Resistant *Staphylococcus aureus* from *Hypericum sampsonii. Pharmaceutical Biology* **46**, 250-253.

Shiu, W.K.P. and Gibbons, S., (2006). Anti-staphylococcal acylphloroglucinols from *Hypericum beanii. Phytochemistry* **67**, 2568-2572.

Stavri, M., Mathew, K.T. and Gibbons, S. (2006). Antimicrobial Constituents of *Scrophularia deserti. Phytochemistry* **67**, 1530-1533.

O'Donnell, G., Bucar, F., Gibbons S. (2006). Phytochemistry and Antimycobacterial activity of *Chlorophytum inornatum. Phytochemistry* **67**, 178-182.

Appendino, G., Maxia, L., Bettoni, P., Locatelli, M., Ballero, M., Stavri, M., Gibbons, S. and Sterner, O. (2006). Antibacterial Galloylated Phloroglucinol Glucosides from Myrtle (*Myrtus communis*). *Journal of Natural Products* **69**, 251-254.

Stavri, M. and Gibbons, S. (2005). The Antimycobacterial Constituents of Dill (*Anethum graveolens*). *Phytotherapy Research* **19**, 938-941.

Smith, E., Williamson, E.M., Zloh, M. and Gibbons, S. (2005). Isopimaric acid from *Pinus nigra* shows activity against multi-drug-resistant and EMRSA strains of *Staphylococcus aureus. Phytotherapy Research* **19**, 538-542.

Gibbons, S., Moser, E., Hausmann, S., Stavri, M., Smith, E. and Clennett, C. (2005). An anti-staphylococcal acylphloroglucinol from *Hypericum foliosum. Phytochemistry* **66**, 1472-1475.

Abebe Wube, A., Bucar, F., Gibbons S. and Asres, K. (2005). Sesquiterpenes of *Warburgia ugandensis* and their Antimycobacterial Activity. *Phytochemistry* **66**, 2309-2315.

Fragoso-Serrano, M., Gibbons, S. and Pereda-Miranda, R. (2005). Anti-staphylococcal and Cytotoxic Compounds from *Hyptis pectinata. Planta Medica* **71**, 278-280.

Stavri, M., Ford, C.H.J., Bucar, F., Streit, B., Hall, M.L., Williamson, R.T., Mathew K.T. and Gibbons, S. (2005). Bioactive constituents of *Artemisia monosperma. Phytochemistry* **66**, 233-239.

Appendino, G., Arnoldi, L. Mercalli, E., Stavri, M., Gibbons, S., Ballero, M. and Maxia, A. (2004). Anti-mycobacterial Coumarins from Sardinian Giant Fennel (*Ferula communis*). *Journal of Natural Products* **67**, 2108-2110.

Gibbons, S. (2004). Anti-Staphylococcal Plant Natural Products. *Natural Product Reports* **21**, 263-277.

Stavri, M., Schneider, R., O'Donnell, G., Lechner, D., Bucar F. and Gibbons, S. (2004). The antimycobacterial components of Hops (*Humulus lupulus*) and their dereplication. *Phytotherapy Research* **18**, 774-776.

Lechner, D., Stavri, M., Oluwatuyi M., Pereda-Miranda, R. and Gibbons, S. (2004). The anti-staphylococcal activity of *Angelica dahurica* (Bai Zhi). *Phytochemistry* **64**, 331-335.

Stavri, M., Mathew, K.T., Bucar, F. and Gibbons S. (2003). Pangelin, an Antimycobacterial Coumarin from *Ducrosia anethifolia. Planta Medica* **69**, 956-959.

Gibbons, S., Fallah, F. and Wright, C.W. (2003). Cryptolepine hydrochloride: a potent anti-mycobacterial alkaloid derived from *Cryptolepis sanguinolenta. Phytotherapy Research* **17**, 434-436.

Gibbons, S., Leimkugel, J., Oluwatuyi, M. and Heinrich, M. (2003). Activity of *Zanthoxylum clava-herculis* extracts against multidrug resistant methicillin-resistant *Staphylococcus aureus* (mdr-MRSA). *Phytotherapy Research* **17**, 274-275.

Schinkovitz, A., Gibbons, S., Stavri, M., Cocksedge, M.J. and Bucar, F. (2003). Ostruthin: An antimycobacterial coumarin from the roots of *Peucedanum ostruthium* Koch. *Planta Medica* **69**, 369-371.

Gibbons, S., Ohlendorf, B. and Johnsen, I. (2002). The genus *Hypericum* - a valuable resource of anti-Staphylococcal leads. *Fitoterapia* **73**, 300-304.

Appendino, G., Bianchi, F., Minassi, A., Sterner, O., Ballero, M. and Gibbons, S. (2002). Oligomeric Acylphloroglucinols from Myrtle (*Myrtus communis*). *Journal of Natural Products* **65**, 334-338.

Structure Elucidation

Page

Stavri, M. Mathew, K.T., Gibson, T., Williamson R.T. and Gibbons, S. (2004). New components of *Artemisia monosperma. Journal of Natural Products* **67**, 892-894.

Gibbons, S., Denny, B.J., Ali-Amine, S., Mathew, K.T., Skelton, B.W., White, A.H. and Gray A.I. (2000). NMR Spectroscopy, X-ray Crystallographic and Molecular Modelling Studies on a new pyranone from *Haloxylon salicornicum* (Moq.) Bunge ex Boiss. *Journal of Natural Products* **63**, 839-840.

Gibbons, S., Mathew, K.T. and Gray, A.I. (1999). A caffeic acid ester from *Halocnemum strobilaceum*. *Phytochemistry* **51**, 465-467.

JOURNAL OF NATURAL PRODUCTS

pubs.acs.org/jnp

Note

Constituents of Two *Dioscorea* Species That Potentiate Antibiotic Activity against MRSA

Gugu F. Sibandze, Paul Stapleton, and Simon Gibbons*

Cite This: *J. Nat. Prod.* 2020, 83, 1696–1700

Read Online

ACCESS | Metrics & More | Article Recommendations | Supporting Information

Dioscorea cotinifolia

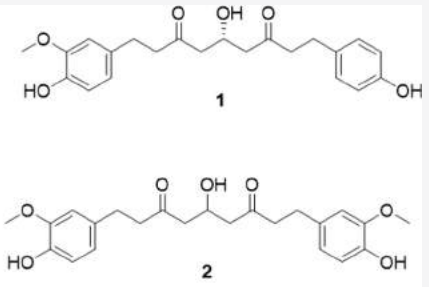

ABSTRACT: The isolation of two diarylnonanoids from *Dioscorea cotinifolia* possessing antibiotic-potentiating activity against resistant strains of *S. aureus* are reported. The diarylnonanoids are a class of natural products similar in structure to the diarylheptanoids, which have a wide spectrum of reported biological activities. One of the diarylnonanoids (**1**) isolated possesses a chiral center, and to deduce its configuration, the modified Mosher ester method was used. Using both 1D and 2D NMR data, as many protons as possible were assigned to both the *R*- and *S*-MTPA esters, and the configuration of the chiral center in **1** was determined to be *R*. Both the chiral and achiral diarylnonanoid (**2**) exhibited potent antibiotic-potentiating activity with the chiral natural product showing a greater tetracycline-potentiating activity than **2**. Interestingly, **2** gave a higher norfloxacin-potentiating activity with a resultant higher efflux pump inhibitory activity. Manipulation of the structure of the diarylnonanoids through synthesis could lead to improved biological activity.

The genus *Dioscorea*, commonly known as the "yam" taxon, is very well-known for its phytochemical diversity. The rhizomes of some species are used as both food and medicine in many parts of the world. Medicinally, the genus is used in the treatment of wounds, sores,[1] rheumatism, and skin problems.[2] Studies on the pharmacological properties of this genus have shown anti-inflammatory, analgesic,[3] antifungal,[1] antitumor,[4] and anthelmintic properties.[5] One of the most useful phytochemicals isolated from the family Dioscoreaceae is diosgenin, which has an important role in the pharmaceutical industry as the precursor for pharmacologically important steroids. Other phytochemicals that have been reported in the family include glycosides, flavonoids, alkaloids, phenols, tannins, triterpenoids,[6] and the diarylheptanoids.[7] In this study, reported are two new diarylnonanoids, an ω-hydroxy fatty acid ester from *Dioscorea cotinifolia* Kunth as well as a bibenzyl from *D. sylvatica* Eckl. var. *sylvatica* with antibiotic-potentiating activity against methicillin-resistant *Staphylococcus aureus* (MRSA). The potential of these compounds to inhibit staphylococcal efflux pumps, which are known be involved in antibiotic resistance, were further investigated.

The diarylnonanoids were isolated from the chloroform extract of the rhizomes of *D. cotinifolia*. Compound **1** was isolated as a yellow solid, while compound **2** was isolated as a yellow amorphous powder. The IR absorption spectra of both compounds showed a C═O bond stretch at 1650 cm^{-1} and an O−H bond stretch at 3300 cm^{-1}. Using their ^{1}H NMR and HRESIMS data, both compounds were identified as 5-hydroxy-1,9-nonane-3,7-diones with different substituents at positions 1 and 9.

The HRESIMS data of compound **1** showed a sodium adduct ion peak $[M + Na]^+$ at m/z 409.1623, corresponding to the pseudomolecular formula, $C_{22}H_{26}O_6Na^+$ (calcd 409.1627; 10 degrees of unsaturation). The ^{1}H NMR data (500 MHz, C_6D_6) revealed the presence of two aromatic ring systems (Table 1). A 1,3,4-trisubstituted aromatic ring system with three aromatic resonances, δ_H 6.46 (1H, d, J = 2.0 Hz), δ_H 6.99 (1H, d, J = 8.0 Hz), and δ_H 6.54 (1H, dd, J = 2.0, 8.0 Hz) accounting for the 4-hydroxy-3-methoxyphenyl moiety of the structure (ring A). For the second ring (B), a 1,4-disustituted

Received: October 13, 2019
Published: May 4, 2020

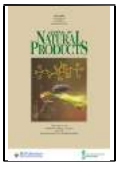

https://dx.doi.org/10.1021/acs.jnatprod.9b01006
J. Nat. Prod. 2020, 83, 1696–1700

Table 1. ^{1}H and ^{13}C NMR Spectroscopic Data and HMBC Correlations of 1 and 2[a]

	1		2		
no.	δ_C, type	δ_H (J in Hz)	δ_C, type	δ_H (J in Hz)	HMBC
1	29.4, CH_2	2.73, t (7.5)	29.9, CH_2	2.73, t (7.5)	3, 2, 2′, 6′, 1′
2	45.8, CH_2	2.29 t (7.5)	45.8, CH_2	2.29, t (7.5)	1′, 1, 3
3	209.2, C		209.3, C		1, 5, 2, 4
4	49.0, CH_2	2.15, dd (7.8, 4.4)	49.1, CH_2	2.16, dd (7.8, 4.3)	6, 3, 5
		2.08, dd (7.8, 4.4)		2.08, dd (7.8, 4.3)	
5	64.9, CH	4.39, m	64.9, CH	4.42, m	3, 7, 4, 6
6	49.1, CH_2	2.12, dd (7.8, 4.4)	49.1, CH_2	2.16, dd (7.8, 4.3)	4, 5, 7
		2.04, dd (7.8, 4.4)		2.08, dd (7.8, 4.3)	
7	209.3, C		209.3, C		5, 9, 6, 8
8	45.6, CH_2	2.22, t (7.5)	45.8, CH_2	2.29, t (7.5)	1″, 7, 9
9	29.3, CH_2	2.68, td (7.5, 2.5)	29.9, CH_2	2.73, t (7.5)	7, 2″, 6″, 1″, 8
1′	133.4, C		133.3, C		5′, 2, 1, 2′
2′	111.7, CH	6.46, d (2.0)	111.8, CH	6.46, d (1.5)	1′, 3′, 4′, 6′, OCH_3 − 3′
3′	147.2, C		147.2, C		
4′	145.2, C		145.2, C		
5′	115.2, CH	6.99, d (8.0)	115.2, CH	6.99, d (8.0)	3′, 1′, 4′
6′	121.6, CH	6.54, dd (8.0, 2.0)	121.6, CH	6.54, dd (8.0, 1.5)	4′, 2′
1″	133.4, C		133.3, C		
2″	130.1, CH	6.85, d (8.5)	111.8, CH	6.46, d (1.5)	
3″	115.9, CH	6.49, d (8.5)	147.2, C		
4″	155.1, C		145.2, C		
5″	115.9, CH	6.49, d (8.5)	115.2, CH	6.99, d (8.0)	
6″	130.1, CH	6.85, d (8.5)	121.6, CH	6.5, dd (8.0, 1.5)	
OCH_3 − 3′	55.7, CH_3	3.20, s	55.7, CH_3	3.21, s	3′
OCH_3 − 3″			55.7, CH_3	3.21, s	3″
OH − 5		3.34, brd			
OH − 4′		5.36, s			
OH − 4″		3.90, brd			

[a]500 MHz for ^{1}H and 125 MHz for ^{13}C, recorded in C_6D_6.

aromatic ring (AA′BB′) system showed two aromatic resonances, each integrating for two protons at δ_H 6.85 (2H, d, J = 8.5 Hz) and δ_H 6.49 (2H, d, J = 8.5 Hz), and therefore suggesting a 4-hydroxyphenyl moiety. A number of key features in the spectroscopic data led to the unambiguous assignment of the structure of **1**.

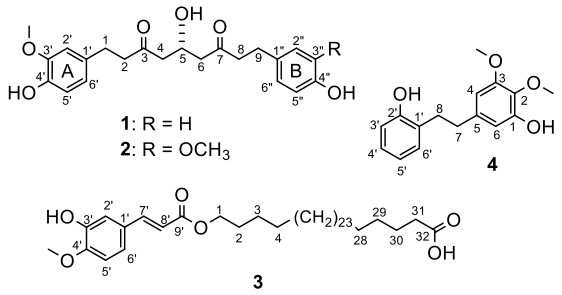

4

3

Two sets of benzylic protons, δ_H 2.73 (2H, t, J = 7.5 Hz) and δ_H 2.68 (2H, dt, J = 7.5 Hz), were apparent along with a pair of deshielded methylene groups (H_2-2 and H_2-8) at δ_H 2.29 (2H, t, J = 7.5 Hz) and δ_H 2.22 (2H, t, J = 7.5 Hz), which showed J correlations with C-1 and C-9, respectively, in the HMBC spectrum. Additionally, H_2-2 and H_2-8 also showed J correlations with the carbonyl resonances at C-3 and C-7. Furthermore, two deshielded methylene groups with resonances at δ_H 2.15, 2.08 (2H, dd, J = 7.8, 4.4 Hz, H_2-4) and δ_H 2.12, 2.04 (2H, dd, J = 7.8, 4.4 Hz, H_2-6) exhibited J correlations with an oxymethine carbon at C-5. A methoxy group resonance on the aromatic ring A at δ_H 3.20 (3H, s), further supported the inference of a 5-hydroxy-1,9-nonane-3,7-dione moiety of **1**. Further resonances at δ_H 3.34 (1H, brd), 5.36 (1H, s), and 3.90 (1H, brd), could be attributed to the three hydroxy groups at C-5, C-4′, and C-4″, respectively.

The ^{13}C NMR spectrum of **1** revealed 22 carbon resonances with seven quaternary carbons missing in the DEPT-135 spectrum, which supported the proposed structure. There were two carbonyl resonances (δ_C 209.2 and 209.3), an oxymethine (δ_C 64.9), and methylenes with different chemical shifts, depending on their proximity to the deshielding oxymethine and carbonyl groups (Table 1). In the HMBC spectrum, the proton at position H-3″ showed J correlations with C-4″ and C-5″. The methylene protons at H-9 showed correlations with C-8 and C-1″, while the methylene protons at H-1 showed correlations with C-2 and C-1′, which enabled the structure of the compound to be confirmed as 5-hydroxy-1-(4-hydroxy-3-methoxyphenyl)-9-(4-hydroxyphenyl)nonane-3,7-dione.

The HRESIMS of **2** showed a sodium adduct ion peak $[M + Na]^+$ peak at m/z 439.1729, corresponding to a pseudomolecular formula, $C_{23}H_{28}O_7Na^+$ (calcd 439.1733; 10 degrees of unsaturation). This was 30 atomic mass units greater than the sodium adduct ion peak observed for **1**, accounting for the addition of an oxymethylene (OCH_2) moiety. The ^{1}H NMR spectrum (500 MHz, C_6D_6) of **2** was highly similar to that of **1** and revealed the absence of a disubstituted aromatic ring (Table 1). The integrals of the resonances in the 1,3,4-trisubstituted aromatic ring were doubled, showing two identical aromatic rings, for which the protons were equivalent.

https://dx.doi.org/10.1021/acs.jnatprod.9b01006
J. Nat. Prod. 2020, 83, 1696−1700

This observation, and the fact that the integrals of the methylenes in the 5-hydroxy-1,9-nonane-3,7-dione moiety were also doubled, led to the conclusion that the structure of **2** possesses symmetry and this could be readily explained by the proposal of **2** as 5-hydroxy-1,9-bis(4-hydroxy-3-methoxyphenyl)nonane-3,7-dione. However, due the exchangeable nature of the hydroxy group protons, they could not be detected in the ^{1}H NMR spectrum of **2** in C_6D_6.

The ^{13}C NMR spectrum of **2** revealed only 13 carbon signals, which again was consistent with the observation of a plane of symmetry at position C-5. The HMBC and COSY data were also highly similar to those of **1**. To verify if compound **1** was not obtained as an artifact, it was isolated from its fraction using preparative TLC with chloroform−acetone−acetic acid (6:4:0.1). Both compounds were isolated with different retention factors, R_f 0.34 for **1** and R_f 0.39 for **2**. It was further hypothesized that if **1** was indeed an artifact, its fragment would be clearly visible in the ESIMS spectra of **2**, run in positive mode, but this was not the case. It was concluded that both compounds are natural products that exist in the plant.

This is the first report of the isolation of diarylnonanoids from the *Dioscorea* genus. Although the diarylheptanoids are similar in structure, and have been previously isolated from the Dioscoreaceae family,[7−10] diarylnonanoids have a 9-carbon chain linking the two aromatic systems. Structurally similar compounds have been isolated from the *Myristica* genus in the plant family Myristicaceae.[11−14] Mosher ester analysis was used to deduce the absolute configuration of the chiral center (C-5) in compound **1**. The Mosher esters, obtained by reacting **1** with both (3*R*)- and (3*S*)-MTPA chloride to yield the (4*S*)- and (4*R*)-MTPA ester, respectively, were analyzed using both 1D and 2D NMR spectroscopy. The data were used to assign as many protons as possible on both the (*R*)- and (*S*)-esters. Since the methylene protons at positions 2 and 8, as well as those in 4 and 6 were overlapped and difficult to distinguish, the benzylic protons at positions 1 and 9, as well as the aromatic protons were used for the analysis. HMQC, HMBC, and COSY spectra were key in the assignments. According to the Kakiswa group,[15] the absolute values of $\Delta\delta$ must be proportional quantitatively to the distance from the MTPA moiety. This condition was met, bringing confidence to the assignment of the hydrogens of the MTPA esters. Using their method, which was later reiterated by Hoye and co-workers,[16] the difference in the chemical shift ($\Delta\delta^{SR}$) was calculated from each of the analogous pairs of protons for both the (*S*)- and (*R*)-MTPA esters.

To determine the absolute configuration, all positive $\Delta\delta^{SR}$ values were assigned to the right side of the model (R_1) in Figure 1 and all the negative $\Delta\delta^{SR}$ values were placed on the left (R_2) (as per the advanced or modified Mosher ester analysis.[15] By applying the Cahn Ingold Prelog system, the priority of the groups on the original carbinol were assigned as 1 (OH), 2 (R_1), 3 (R_2), and 4 (H) and the absolute configuration of the carbinol at C-5 of **1** was determined as (*R*). The name was then assigned as (5*R*)-hydroxy-1-(4-hydroxy-3-methoxyphenyl)-9-(4-hydroxyphenyl)nonane-3,7-dione. The specific optical rotation was determined to be $[\alpha]_D^{20}$ +130.9 (*c* 0.08, $CHCl_3$).

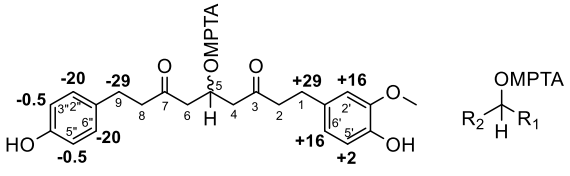

Figure 1. $\Delta\delta^{SR}$ values (bold) for the MTPA ester of **1** (left) and the model used to determine the absolute configuration (right).

The known compounds (*E*)-32-((3-(3-hydroxy-4-methoxyphenyl)isoferuloyl)oxy)dotriacontanoic acid (**3**)[17] and 5-(2-hydroxyphenethyl)-2,3-dimethoxyphenol (**4**)[17,18] were isolated from the chloroform extracts of *D. cotinifolia* and *D. sylvatica* var. *sylvatica*, respectively.

The antibiotic-potentiating activities of compounds **1**−**4** were determined using two MDR *S. aureus* strains possessing characterized efflux proteins, namely, SA-1199B, which is resistant to fluoroquinolones due to overexpression of the NorA MDR pump,[19] and XU212, which is tetracycline-resistant due to the TetK efflux protein.[20] *S. aureus* XU212 is also resistant to most β-lactams due to PBP2a production conferred by the mecA gene.[20] None of the compounds showed inhibitory activity against the *S. aureus* strains, giving minimum inhibitory concentration (MIC) values at >128 mg/L. At subinhibitory concentrations (1/4 or less of the MIC), the compounds caused a 2- or higher-fold reduction in the MIC of the antibiotics when tested against the corresponding resistant strain. Compound **1** was the most active, resulting in a 512-fold reduction in the MIC of tetracycline against the tetracycline-resistant XU212 strain (Table 2). The ω-hydroxy fatty acid ester (**3**) was also very active and resulted in an 8- and 16-fold reduction in the MIC of norfloxacin and tetracycline, respectively.

Table 2. Antibiotic-Potentiating Activity of Compounds 1−4

	MIC (mg/L) of test sample in combination with specified antibiotic (fold reduction) against:	
	S. aureus 1199B (NorA)	*S. aureus* XU212 (TetK)
compound (subinhibitory concentration in mg/L)	norfloxacin @ 32 mg/L	tetracycline @ 128 mg/L
1 (100)	16 (2)	<0.25 (>512)
2 (30)	8 (4)	128
3 (100)	4 (8)	8 (16)
4 (64)	2 (16)	64 (2)
reserpine[a] (20)	16 (2)	64 (2)

[a]Positive control substance.

The possible effect of the isolated compounds to inhibit the active efflux of an antibiotic from cells was investigated using an ethidium bromide accumulation assay. Figure S1 (Supporting Information) and Table S1 (Supporting Information) show the effects of the compounds on the intracellular accumulation of ethidium bromide over time within *S. aureus* 1199B. Reserpine, a known efflux pump inhibitor, showed an increase in intracellular accumulation of ethidium bromide with a resultant increase in fluorescence over a 30 min period of observation. This activity was dose-dependent and at the highest concentration (1/4 MIC), the difference in accumulation (the slope of 2.88) compared to that of the control in the absence of the inhibitor (referred to as the "blank") was the highest obtained (Table 2). Compounds **2** and **4** showed significant efflux pump inhibitory (EPI) activity, with slope

https://dx.doi.org/10.1021/acs.jnatprod.9b01006
J. Nat. Prod. 2020, 83, 1696−1700

differences of 2.45 and 2.68, respectively. Furthermore, their relative final fluorescence (RFF) was similar to that of reserpine. These results led to the conclusion that the antibiotic-potentiating activity of these isolated compounds is due to their EPI activity. **1** gave a lower norfloxacin-potentiating activity, which corresponded to its weaker efflux pump activity compared to **2**. This was interesting because structurally these two compounds are very similar, with only differences in the substitution in the second aromatic ring.

From an observation of the structures of the NorA pump inhibitors isolated in this study, it seems plausible to suggest that the presence of more than one methoxy group as well as at least two phenyl rings is essential for greater EPI activity. This corroborates with the structures of reserpine and verapamil, well-known EPIs, which also possess these structural characteristics. Kaatz and colleagues[21] noted that due to the heterogeneity of reported EPIs, it becomes difficult to characterize the critical structure of an "ideal" NorA inhibitor. However, their recent work on ligand-based pharmacophore modeling suggests that the presence of four pharmacophores facilitate NorA inhibition: (1) a hydrogen-bond acceptor, (2) a positive charge, (3) two aromatic rings, and (4) a hydrophobic region.[22] Although the isolated compounds lacked a positive charge, they possess all the other pharmacophores required and therefore displayed NorA inhibitory properties. The bibenzyl **4** also showed good antibiotic potentiating activity (16-fold reduction in the MIC of norfloxacin).

EXPERIMENTAL SECTION

General Experimental Procedures. The optical rotation of the chiral compound was measured on a PolAAR 21 instrument (Optical Activity Ltd.) using an A2 series polarimeter sample tube with a 100 mm path length. UV−vis absorption spectra were measured on a UV−vis (Spectronic Helios Gamma UV−visible spectrophotometer) and IR spectra were measured on a PerkinElmer 100 FT-IR spectrometer. 1D ^{1}H, ^{13}C, and DEPT-135, and 2D HMQC, HMBC, COSY, and NOESY NMR spectroscopic data were acquired on a Bruker Avance 500 MHz NMR spectrometer. Deuterated solvents and NMR tubes were purchased from Cambridge Isotope Laboratories and Sigma-Aldrich, respectively. Bruker Topspin, version 3.2 software was used to process NMR data. Low-resolution mass spectra were acquired on a LCQ Duo Ion-Trap mass spectrometer (Thermo Fisher Scientific), and a Waters Q-TOF Premier Tandem mass spectrometer was used for high-resolution mass spectrometry. Column chromatography was performed on silica gel 60 (0.04−0.063 mm; Merck) and TLC on Silica gel 60 F254 (Merck) plates. Vanillin-sulfuric acid and *p*-anisaldehyde reagents were used to visualize the TLC plates. All chemicals used were HPLC grade. Chemicals were supplied by either Sigma-Aldrich or Fisher Scientific.

Plant Material. *Dioscorea cotinifolia* (voucher number GM218) and *Dioscorea sylvatica* var. *sylvatica* (voucher number GM217) were collected in March 2014 from Malutha in the southeastern part of Eswatini, Southern Africa. Their exact location was recorded with a Global Position System. Botanical identification was done by Mr. M.N. Dludlu (Botanist; Eswatini Institute for Research in Traditional Medicine, Medicinal and Indigenous Food Plants, University of Eswatini) and voucher specimens were deposited with the Eswatini National Herbarium, Malkerns Research Station, Eswatini.

Extraction and Isolation. The dried and ground rhizomes of *D. cotinifolia* (544 g) were extracted exhaustively in a Soxhlet extractor using hexane, chloroform and methanol to yield 0.08%, 0.3% and 0.9%, respectively, of the crude extracts. The chloroform extract was biologically active in the preliminary tests and therefore subjected to normal-phase SPE with hexane (100%) and subsequently 10% increments of ethyl acetate to yield 11 fractions. After TLC and ^{1}H NMR analysis, fractions 7, 8, 10, and 11 were targeted for the isolation of compounds. Compound **1** (2.5 mg) was isolated from fraction 8 after preparative TLC on silica gel with chloroform−acetone−acetic acid (8:2:0.1). Compound **2** (6.5 mg) was isolated from a combination of fractions 10 and 11 by preparative TLC on silica gel using chloroform−acetone−acetic acid (9:1:0.1), and compound **3** (14.8 mg) was isolated from fraction 7 which was further purified by column chromatography on silica gel using ethyl acetate−hexane (8:2).

The rhizomes of *D. sylvatica* var. *sylvatica* also were successively extracted on an ultrasonic bath with hexane, chloroform and methanol. Fractionation of the chloroform extract by VLC on silica gel led to fraction 6 (227 mg), eluted with hexane-ethyl acetate (50:50). Fraction 6 was purified by column chromatography on silica gel, using petroleum ether (40−60 °C)−ethyl acetate−formic acid (50:50:1) as mobile phases to yield 75 fractions. On the basis of their TLC profile, fractions 10−19 were pooled and further purified by preparative TLC to yield compound **4** (20 mg).

*(5R)-Hydroxy-1-(4-hydroxy-3-methoxyphenyl)-9-(4-hydroxyphenyl)nonane-3,7-dione (**1**).* Yellow solid; $[\alpha]_D^{20}$ +130.9 (*c* 0.08, $CHCl_3$); UV (CH_3CN) λ_{max} (log ε) 223 (4.38), 279 (3.91) nm; IR (film) ν_{max} 3296, 2949, 2837, 2141, 1646, 1450 cm^{-1}; ^{1}H (500 MHz) and ^{13}C NMR (125 MHz, C_6D_6), see Table 1; HRQTOFESIMS *m*/*z* 409.1623 [M + Na]$^+$ (calcd for $C_{22}H_{26}O_6Na^+$, 409.16727).

*5-Hydroxy-1,9-bis(4-hydroxy-3-methoxyphenyl)nonane-3,7-dione (**2**).* Yellow amorphous solid; UV (CH_3CN) λ_{max} (log ε) 201 (4.80), 225 (4.20), 280 (3.85); IR (film) ν_{max} 3335, 2950, 2837, 1652, 1450 cm^{-1}; ^{1}H (500 MHz) and ^{13}C NMR (125 MHz, C_6D_6), see Table 1; HRQTOFESIMS *m*/*z* 439.1729 [M + Na]$^+$ (calcd for $C_{23}H_{28}O_7Na^+$, 439.1733).

Preparation of Mosher's Esters for Spectroscopic Determination of Stereochemistry. Mosher's esters were prepared and analyzed as previously described.[15,16,23,24] Briefly, compound **1** (500 μg) was dissolved in $CDCl_3$ (600 μL) and dry pyridine-d_5 (6 μL). Thereafter, either (*S*)- (+) or (*R*)-(−)-MTPA-Cl (6 μL; Sigma-Aldrich) was added to the reaction mixture and allowed to stand for 24 h in a desiccator. When the reaction was complete the mixture was transferred into an NMR tube and run on a Bruker Avance 500 MHz spectrometer to acquire both 1D and 2D NMR data.

Broth Dilution Assay for Determining the Bacterial Minimum Inhibitory Concentration (MIC). Minimum inhibitory concentrations were determined by the broth dilution assay previously described.[25−27]

Antibiotic-Potentiating Activity. Potentiation of antibiotic activity by the test compounds used a modulation assay adapted from Dickson and co-workers.[28] *S. aureus* strains possessing genes that code for antibiotic resistance against particular antibiotics were used for the experiment; a tetracycline-resistant XU212 strain and the norfloxacin-resistant SA-1199B strain. A subinhibitory concentration (X = 1/4 MIC or less) of the compound was used for the experiment.

Real-Time Ethidium Bromide Accumulation Assay. The efflux pump inhibition activity of the compounds was assessed using real-time analysis of ethidium bromide (EtBr) accumulation in the effluxing *S. aureus* 1199B strain. EtBr is a substrate for various MDR efflux pumps and reversibly binds DNA.[21,29] It enters the cell by diffusion and is pumped out of effluxing cells via an efflux mechanism. Real-time analysis allows for the monitoring of the influx and efflux activity of EtBr within the cell.[30] The assay was performed as described by Ramalhete and co-workers[31] with minor modifications. Fluorescence was measured on a BioTek Synergy HT multidetection plate reader, at excitation and emission wavelengths of 535/590 for 30 min, with readings taken every minute. A positive control (reserpine) and a blank (without EPI) were included in the experiment. The data was processed using Gen5 v1.09 software.

ASSOCIATED CONTENT

Supporting Information

The Supporting Information is available free of charge at https://pubs.acs.org/doi/10.1021/acs.jnatprod.9b01006.

https://dx.doi.org/10.1021/acs.jnatprod.9b01006
J. Nat. Prod. 2020, 83, 1696−1700

HRESIMS and NMR spectra of **1**–**4**; ^{1}H NMR spectra of (R)-MTPA and (S)-MTPA esters of **1**; Ethidium bromide accumulation assay results (PDF)

AUTHOR INFORMATION

Corresponding Author

Simon Gibbons − *Research Department of Pharmaceutical and Biological Chemistry, UCL School of Pharmacy, University College London, London WC1N 1AX, United Kingdom*; Phone: +44 1603 593983; Email: s.gibbons@uea.ac.uk

Authors

Gugu F. Sibandze − *Research Department of Pharmaceutical and Biological Chemistry, UCL School of Pharmacy, University College London, London WC1N 1AX, United Kingdom; Eswatini Institute for Research in Traditional Medicine, Medicinal and Indigenous Food Plants, University of Eswatini, Kwaluseni M201, Eswatini;* orcid.org/0000-0002-5907-2960

Paul Stapleton − *Research Department of Pharmaceutical and Biological Chemistry, UCL School of Pharmacy, University College London, London WC1N 1AX, United Kingdom*

Complete contact information is available at: https://pubs.acs.org/10.1021/acs.jnatprod.9b01006

Notes

The authors declare no competing financial interest.

ACKNOWLEDGMENTS

The authors wish to thank Mr. George Khumalo, a traditional healer who supplied information on the plants studied as well as G. Mavuso, V. Vilane, and S. Dlamini for their assistance in field collections. The Commonwealth Scholarship Commission, award number SZCA-2013-116, University of Eswatini, and UCL School of Pharmacy are greatly appreciated for research funding. We thank Ms. W. Kwok for setting up the ethidium bromide accumulation assay.

REFERENCES

(1) Kelmanson, J. E.; Jäger, A. K.; van Staden, J. *J. Ethnopharmacol.* **2000**, *69*, 241−246.
(2) Cogne, A. L.; Marston, A.; Mavi, S.; Hostettmann, K. *J. Ethnopharmacol.* **2001**, *75*, 51−53.
(3) Mbiantcha, M.; Kamanyi, A.; Teponno, R. B.; Tapondjou, A. L.; Watcho, P.; Nguelefack, T. B. *Evidence-Based Complementary Altern. Med.* **2011**, *2011*, No. 912935.
(4) Sautour, M.; Mitaine-Offer, A. C.; Lacaille-Dubois, M. A. *J. Nat. Med.* **2007**, *61*, 91−101.
(5) Adeniran, A. A.; Sonibare, M. A. *J. Pharmacogn. Phytother.* **2013**, *5*, 196−203.
(6) Subhash, C.; Sarla, S.; Abhay, M. P.; Anoop, B. *Int. Res. J. Pharm.* **2012**, *3*, 289−294.
(7) Dong, S. H.; Nikolić, D.; Simmler, C.; Qiu, F.; van Breemen, R. B.; Soejarto, D. D.; Pauli, G. F.; Chen, S. N. *J. Nat. Prod.* **2012**, *75*, 2168−2177.
(8) Yin, J.; Kouda, K.; Tezuka, Y.; Le Tran, Q.; Miyahara, T.; Chen, Y.; Kadota, S. *Planta Med.* **2004**, *70*, 54−58.
(9) Woo, K. W.; Moon, E.; Kwon, O. W.; Lee, S. O.; Kim, S. Y.; Choi, S. Z.; Son, M. W.; Lee, K. R. *Bioorg. Med. Chem. Lett.* **2013**, *23*, 3806−3809.
(10) Zhang, Y.; Ruan, J.; Li, J.; Chao, L.; Shi, W.; Yu, H.; Gao, X.; Wang, T. *Fitoterapia* **2017**, *117*, 28−33.
(11) Herath, H. M. T. B.; Priyadarshani, A. M. A.; Jamie, J. *Nat. Prod. Lett.* **1998**, *12*, 91−95.
(12) Sen, R.; Bauri, A. K.; Chattopadhyay, S.; Chatterjee, M. *Phytother. Res.* **2007**, *21*, 592−595.
(13) Bauri, A. K.; Foro, S.; Do, N. Q. N. *Acta Crystallogr. Sect. E Crystallogr. Commun.* **2016**, *72*, 1408−1411.
(14) Fajriah, S.; Darmawan, A.; Megawati; Hudiyono, S.; Kosela, S.; Hanafi, M. *Phytochem. Lett.* **2017**, *20*, 36−39.
(15) Ohtani, I.; Kusumi, T.; Ishitsuka, M. O.; Kakisawa, H. *Tetrahedron Lett.* **1989**, *30*, 3147−3150.
(16) Hoye, T. R.; Jeffrey, C. S.; Shao, F. *Nat. Protoc.* **2007**, *2*, 2451−2458.
(17) Liu, H.; Tsim, K. W.; Chou, G. X.; Wang, J. M.; Ji, L. L.; Wang, Z. T. *Chem. Biodiversity* **2011**, *8*, 2110−2116.
(18) Du, D.; Jin, T.; Zhang, R.; Hu, L.; Xing, Z.; Shi, N.; Shen, Y.; Gong, M. *Bioorg. Med. Chem. Lett.* **2017**, *27*, 1467−1470.
(19) Kaatz, G. W.; Seo, S. M.; Ruble, C. A. *Antimicrob. Agents Chemother.* **1993**, *37*, 1086−1094.
(20) Gibbons, S.; Udo, E. E. *Phytother. Res.* **2000**, *14*, 139−140.
(21) Schindler, B. D.; Jacinto, P.; Kaatz, G. W. *Future Microbiol.* **2013**, *8*, 491−507.
(22) Astolfi, A.; Felicetti, T.; Iraci, N.; Manfroni, G.; Massari, S.; Pietrella, D.; Tabarrini, O.; Kaatz, G. W.; Barreca, M. L.; Sabatini, S.; Cecchetti, V. *J. Med. Chem.* **2017**, *60*, 1598−1604.
(23) Breton, R. C.; Reynolds, W. F. *Nat. Prod. Rep.* **2013**, *30*, 501−524.
(24) Dale, J. A.; Mosher, H. S. *J. Am. Chem. Soc.* **1973**, *95*, 512−519.
(25) Andrews, J. M. *J. Antimicrob. Chemother.* **2001**, *48*, 5−16.
(26) Lechner, D.; Stavri, M.; Oluwatuyi, M.; Pereda-Miranda, R.; Gibbons, S. *Phytochemistry* **2004**, *65*, 331−335.
(27) Eloff, J. N. *Planta Med.* **1998**, *64*, 711−713.
(28) Dickson, A. R.; Houghton, P. J.; Hylands, P. J.; Gibbons, S. *Phytother. Res.* **2006**, *20*, 41−45.
(29) Stavri, M.; Piddock, L. J. V; Gibbons, S. *J. Antimicrob. Chemother.* **2007**, *59*, 1247−1260.
(30) Paixão, L.; Rodrigues, L.; Couto, I.; Martins, M.; Fernandes, P.; de Carvalho, C. C. C. R.; Monteiro, G. A.; Sansonetty, F.; Amaral, L.; Viveiros, M. *J. Biol. Eng.* **2009**, *3*, 18.
(31) Ramalhete, C.; Spengler, G.; Martins, A.; Martins, M.; Viveiros, M.; Mulhovo, S.; Ferreira, M. J. U.; Amaral, L. *Int. J. Antimicrob. Agents* **2011**, *37*, 70−74.

International Journal of Antimicrobial Agents 53 (2019) 629–636

Contents lists available at ScienceDirect

International Journal of Antimicrobial Agents

journal homepage: www.elsevier.com/locate/ijantimicag

Inhibiting plasmid mobility: The effect of isothiocyanates on bacterial conjugation

Awo Afi Kwapong[a,b], Paul Stapleton[a], Simon Gibbons[a,*]

[a] Research Department of Pharmaceutical and Biological Chemistry, UCL School of Pharmacy, University College London, 29–39 Brunswick Square, London WC1N 1AX, UK

[b] Department of Pharmaceutics and Microbiology, School of Pharmacy, University of Ghana, Accra, Ghana

ARTICLE INFO

Article history:
Received 9 July 2018
Accepted 20 January 2019

Editor: Dr. S. Dancer

Keywords:
Isothiocyanate
Bacterial conjugation
Conjugative plasmid
Effector protein
Horizontal gene transfer
Plasmid incompatibility group

ABSTRACT

Bacterial conjugation is the main mechanism for the transfer of multiple antimicrobial resistance genes among pathogenic micro-organisms. This process may be controlled by compounds that inhibit bacterial conjugation. In this study, the effects of allyl isothiocyanate, L-sulforaphane, benzyl isothiocyanate, phenylethyl isothiocyanate and 4-methoxyphenyl isothiocyanate on the conjugation of broad-host-range plasmids harbouring various antimicrobial resistance genes in *Escherichia coli* were investigated, namely plasmids pKM101 (IncN), TP114 ($IncI_2$), pUB307 (IncP) and the low-copy-number plasmid R7K (IncW). Benzyl isothiocyanate (32 mg/L) significantly reduced conjugal transfer of pKM101, TP114 and pUB307 to 0.3 ± 0.6%, 10.7 ± 3.3% and 6.5 ± 1.0%, respectively. L-sulforaphane (16 mg/L; transfer frequency 21.5 ± 5.1%) and 4-methoxyphenyl isothiocyanate (100 mg/L; transfer frequency 5.2 ± 2.8%) were the only compounds showing anti-conjugal specificity by actively reducing the transfer of R7K and pUB307, respectively.

1. Introduction

Bacterial conjugation is an adaptive mechanism that allows bacteria to transfer genetic material, effector proteins and/or toxins from one cell to another through a conjugative bridge [1,2]. The genetic material that is transferred via conjugation usually confers a selective advantage to the recipient organism, such as survival, resistance, pathogenicity, infection activities and/or the ability to respond to environmental changes. Conjugation greatly increases bacterial genome plasticity and has immense clinical relevance as a major route for the spread of multiple antimicrobial resistance genes among the microbial community and virulence genes from pathogen to host bacterium [2]. It is therefore imperative to find ways to combat conjugation as a means to decrease the ongoing rise of antimicrobial-resistant infections.

Inhibition of bacterial conjugation has received little research attention because the focus has been on the identification of new classes of antimicrobial agents that target processes essential for bacterial growth such as cell wall biosynthesis, the cell membrane, protein synthesis, nucleic acid synthesis and metabolic activity. This traditional approach has produced many therapeutically useful agents so far, but the challenge is that an antibiotic also introduces selective pressure promoting resistant bacteria and this has led to the current antibiotic resistance crisis. An additional approach for reducing the increasing rate of bacterial antimicrobial resistance dissemination and re-sensitising bacteria to existing antibiotics would be to target non-essential processes such as conjugation, which are less likely to evoke bacterial resistance. This approach could also have a prophylactic use in cosmeceuticals to reduce plasmid transfer. In addition to bacterial conjugation, other non-essential processes such as plasmid replication [3–5] and plasmid-encoded toxin–antitoxin systems [6,7] have been exploited with promising potential in antibacterial therapy.

The few efforts directed towards identifying anti-conjugants include small-molecule inhibitors of *Helicobacter pylori cag* VirB11-type ATPase Cagα [8]. The *cag* genes encode assembly of the conjugative bridge and injection of the CagA toxin into host cells [8,9]. In addition, there have been other reports of promising anti-conjugants, such as dehydrocrepenynic acid [1], linoleic acid [1], 2-hexadecyanoic acid [10], 2-octadecynoic acid [10] and tanzawaic acids A and B [11]. However, these compounds have stability, toxicity or scarcity issues that need to be addressed. Therefore, there is a pressing need to identify safer anti-conjugants to help in the fight against plasmid-mediated transfer and the spread of antimicrobial resistance and virulence.

In this study, four naturally occurring isothiocyanates [allyl isothiocyanate (**1**), L-sulforaphane (**2**), benzyl isothiocyanate (**3**)

* Corresponding author. Tel.: +44 207 753 5913.
E-mail address: simon.gibbons@ucl.ac.uk (S. Gibbons).

https://doi.org/10.1016/j.ijantimicag.2019.01.011
0924-8579/

and phenylethyl isothiocyanate (**4**)] as well as a synthetic isothiocyanate [4-methoxyphenyl isothiocyanate (**5**)] were investigated for their anti-conjugant activity against *Escherichia coli* strains bearing conjugative plasmids with specific antimicrobial resistance genes. Isothiocyanates are usually naturally occurring hydrolytic products of glucosinolates that are commonly found in *Brassica* vegetables. They are produced when damaged plant tissue releases the glycoprotein enzyme myrosinase, which hydrolyses the β-glucosyl moiety of a glucosinolate. This leaves the unstable aglycone thiohydroxamate-*O*-sulfonate, which rearranges to form an isothiocyanate or other breakdown products [12,13]. Other isothiocyanates, such as 4-methoxyphenyl isothiocyanate and methyl isothiocyanate, are synthetically produced and are not naturally occurring.

In addition to anti-conjugant testing, plasmid-curing activity and bacterial growth inhibition were also evaluated to help discriminate between true anti-conjugants and substances that reduce conjugation owing to elimination of plasmids or function by perturbation of bacterial growth or physiology. Isothiocyanates possessing the highest anti-conjugant activities were further investigated for cytotoxicity against human dermal fibroblasts, adult cells (HDFa; C-013-5C).

2. Materials and methods

2.1. Bacterial strains and plasmids

Escherichia coli NCTC 10418 (a susceptible Gram-negative strain), *Staphylococcus aureus* ATCC 25923 (a susceptible Gram-positive strain), *S. aureus* SA-1199B (a fluoroquinolone-resistant strain that overexpresses the multidrug resistance NorA pump) and *S. aureus* XU212 (a tetracycline-resistant strain that overexpresses the multidrug resistance TetK pump) were used for the broth dilution assay. Plasmid-containing *E. coli* strains WP2, K12 J53-2 and K12 JD173 were used as donor strains in the plate conjugation and plasmid elimination assays. *Escherichia coli* ER1793 (streptomycin-resistant) and *E. coli* JM109 (nalidixic-resistant) were used as recipient strains. The conjugative plasmids used were pKM101 [WP2; incompatibility group N (IncN); ampicillin-resistant], TP114 (K12 J53-2; $IncI_2$; kanamycin-resistant) and R7K (K12 J53-2; IncW; ampicillin-, streptomycin- and spectinomycin-resistant), purchased from Deutsche Sammlung von Mikroorganismen und Zellkulturen (DSMZ, Braunschweig, Germany), and conjugative plasmid pUB307 (K12 JD173; IncP; ampicillin-, kanamycin- and tetracycline-resistant), provided by Prof. Keith Derbyshire (Wadsworth Center, New York Department of Health, New York, NY).

2.2. Broth microdilution assay

Antibacterial activity was determined by the broth microdilution assay as described previously [14], which is a modified version of the procedure described in the British Society for Antimicrobial Chemotherapy (BSAC) guide to susceptibly testing [15]. Bacteria were cultured on nutrient agar slants and were incubated at 37 °C for 18 h. A bacterial suspension equivalent to a 0.5 McFarland standard was made from the overnight culture. This was added to Muller–Hinton broth and the test isothiocyanate, which had been serially diluted across a 96-well microtitre plate to achieve a final inoculum of 0.5×10^5 CFU/mL. Minimum inhibitory concentrations (MICs) were determined following 18 h of incubation at 37 °C. This was done by visual inspection after the addition of a 1 mg/mL methanolic solution of 3-[4,5-dimethylthiazol-2-yl]-2,5-diphenyl tetrazolium bromide (MTT) and incubation at 37 °C for 20 min. This experiment was performed in duplicate in two independent experiments.

2.3. Liquid conjugation assay

Donor cells with plasmids pKM101, TP114 and pUB307 were paired with the recipient ER1793. Plasmid R7K donor cells were paired with the recipient JM109. Research has shown that plasmid carriage by host bacteria is associated with some fitness cost (burden) [16,17]. This fitness effect of plasmids plays a vital role in their ability to associate with a new bacterial host. As a consequence of this, different *E. coli* hosts that are known to successfully conjugate [18,19] and to maintain the study plasmids were selected. The liquid conjugation assay was performed as previously described [20] with slight modifications. Equal volumes (20 µL) of donor and recipient cells, for which the CFU/mL had been predetermined (Supplementary Table S1), were introduced into 160 µL of Luria–Bertani broth and the test sample or control. This was incubated at 37 °C for 18 h, after which the number of transconjugants and donor cells was determined using antibiotic-containing MacConkey agar plates. A positive control (linoleic acid [1]) and a negative control (donor, recipient and medium, without drug or test sample) were included in the experiment. The isothiocyanates were evaluated for anti-conjugant activity at a subinhibitory concentration (0.25× MIC). Antibiotics were added at the following concentrations for positive identification of donors, recipients and transconjugants: amoxicillin (30 mg/L); streptomycin sulphate (20 mg/L); nalidixic acid (30 mg/L); and kanamycin sulphate (30 mg/L). Conjugation frequencies were calculated as the ratio of total number of transconjugants (CFU/mL) to the total number of donor cells (CFU/mL) and were expressed as a percentage relative to the negative control. This experiment was performed in duplicate in three independent experiments and the anti-conjugation activity was reported as the mean ± standard deviation (S.D.).

2.4. Plasmid elimination assay

The plasmid elimination assay was performed as described previously [21] with minor modifications. *Escherichia coli* donor strains were subcultured on appropriate antibiotic-containing MacConkey agar plates to ensure plasmid presence. Following incubation of the plates at 37 °C for 18 h, two to three single colonies were selected and were inoculated into Luria–Bertani broth. This was incubated for 18 h at 37 °C and the CFU were determined prior to the assay. Then, 20 µL of the overnight culture was added to a mixture of 180 µL of LB and test sample in a 96-well microtitre plate. This was incubated overnight (18 h) at 37 °C and was subsequently serially diluted, then 20 µL was plated on antibiotic-containing MacConkey agar and was incubated for 18 h at 37 °C. The isothiocyanates were evaluated for plasmid elimination activity at concentrations used in the liquid conjugation assay. Both a positive control (promethazine) [22–24] and negative control (mixture without isothiocyanate or control drug) were included in this experiment. Plasmid elimination was calculated using the equation:

$$\text{Plasmid elimination} = \frac{\text{CFU/mL of control} - \text{CFU/mL of test sample}}{\text{CFU/mL of control}} \times 100$$

Antibiotics and concentrations used in MacConkey agar for positive identification of *E. coli* cells harbouring plasmids were amoxicillin (30 mg/L), kanamycin sulphate (20 mg/L and 30 mg/L) and nalidixic acid (30 mg/L). This experiment was performed in duplicate with three independent experiments.

2.5. Cytotoxicity assay

The isothiocyanates showing anti-conjugant activity were further assessed for their effect on eukaryotic cell growth. The sulforhodamine B (SRB) colorimetric assay was used as described

previously [25] with modifications. Human dermal fibroblasts, adult cells (HDFa; C-013-5C) were grown in a 75-cm^2 culture flask at 37 °C in a humidified atmosphere of 5% carbon dioxide using Dulbecco's modified Eagle's medium supplemented with 10% fetal bovine serum, 1% non-essential amino acids, 0.1% gentamicin and amphotericin B. The grown cells were seeded in a 96-well microtitre plate and the test samples and medium were added. The plates were then incubated at 37 °C in 5% CO_2 for 72 h. Then, 50 µL of cold 40% w/v trichloroacetic acid solution was added, the plate was placed in the fridge for 1 h at 4 °C and was washed four times with distilled water. Cells were then stained with 0.4% w/v SRB solution and were left at room temperature for 1 h. The plate was then rinsed four times with 1% acetic acid and was left overnight (24 h) to dry. Thereafter, 100 µL of 10 mM Tris buffer solution was dispensed into the wells and was agitated in an orbital shaker for 5 min to allow solubilisation of SRB–protein complexes. The optical density (OD) at 510 nm was then measured using a microtitre plate reader (Tecan Infinite® M200; Tecan Life Sciences, Grödig, Austria). The percentage of viable cells was calculated using the equation:

$$\text{Percentage of viable cell} = \frac{\text{OD of test sample} - \text{OD of blank}}{\text{OD of negative control} - \text{OD of blank}} \times 100$$

The experiment was performed as triplicate in three independent experiments, and cytotoxicity was reported as the mean ± S.D.

2.6. Statistical analyses

Statistical analyses were carried out using Excel Data Analysis (Microsoft Corp., Redmond, WA) and GraphPad Prism 7 (GraphPad Software Inc., La Jolla, CA). Welch's *t*-test was used to evaluate differences between the control conjugal transfer frequency and the test compounds. Results with *P*-value of <0.05 were considered statistically significant.

3. Results

3.1. Effect of isothiocyanates on bacterial growth

To test whether the selected isothiocyanates had growth-inhibitory activity against bacterial species and to determine a suitable concentration for their evaluation in the anti-conjugation assay, the isothiocyanates were tested against susceptible Gram-negative (*E. coli* NCTC 10418) and Gram-positive (*S. aureus* ATCC 25923) standard isolates as well as antibiotic-effluxing *S. aureus* strains (SA-1199B and XU212). Table 1 shows the MICs for the tested isothiocyanates. Their inhibitory activity varied from 16 mg/L to >512 mg/L against the evaluated bacteria. The general observation was that, unsurprisingly, the isothiocyanates were marginally more active against the Gram-positive compared with the Gram-negative strains.

3.2. Effect of isothiocyanates on conjugal transfer of plasmids

To investigate whether the selected isothiocyanates had anti-conjugant activity, a range of plasmids belonging to different incompatibility groups (IncN plasmid pKM101, IncI$_2$ plasmid TP114, IncP plasmid pUB307 and IncW plasmid R7K) were employed to test the specificity of conjugation inhibition in *E. coli*. With information about their MIC against *E. coli* NCTC 10418 (a susceptible standard strain) (Table 1), the isothiocyanates were tested at a subinhibitory concentration (0.25× MIC). Fig. 1 shows the effect of the isothiocyanates on conjugal transfer of the test plasmids. The test isothiocyanates exhibited inhibitory activities ranging from a complete reduction in conjugation frequency (0%, considered active) and inhibition of conjugation frequency to <10% (also considered active), to 10–50% (considered moderately active) and >50% (considered inactive) (Supplementary Table S2).

3.3. Elimination of plasmids from Escherichia coli

To determine that the observed anti-conjugant activity was not due to elimination of conjugative plasmids, donor cells were grown in the presence of the test isothiocyanates and the plasmid elimination assay was performed. Fig. 2 shows the effect of the isothiocyanates on conjugative plasmids. The isothiocyanates exhibited varied plasmid-curing activities. Plasmids TP114 (IncI$_2$) and R7K (IncW) were the most eliminated in the donor cells, with elimination percentages ranging from 3.0 ± 0.1% to 77.8 ± 8.0%. Most of the tested isothiocyanates did not have any plasmid-curing effects on pKM101 (IncN), with the exception of allyl isothiocyanate (**1**), which showed a curing effect of 19.4 ± 6.6%. For pUB307 (IncP), a plasmid-curing effect was observed for L-sulforaphane (**2**) (56.7 ± 3.2%) and phenylethyl isothiocyanate (**4**) (64.8 ± 15.4%) (Supplementary Table S3).

3.4. Effect of increasing concentrations of benzyl isothiocyanate (3) on conjugal transfer of plasmids pKM101 (IncN), TP114 (IncI$_2$) and pUB307 (IncP)

With benzyl isothiocyanate (**3**) having shown broad-range anti-conjugant (conjugal reduction to 0.3 ± 0.6–10.7 ± 3.3%; Fig. 1) and the least donor plasmid elimination activity (0–26.5 ± 5.9%; Fig. 2) of all tested compounds, it was further assessed to observe its effect on conjugal transfer at increasing concentrations. Generally, there was a gradual increase in anti-conjugal activity against pKM101 and TP114 with an increase in concentration from 0.125 mg/L to 64 mg/L (Fig. 3), whereas for plasmid pUB307 there was no significant change in the anti-conjugal activity for benzyl isothiocyanate (**3**) and it surprisingly remained active at the low concentrations tested. The observed conjugal transfer of pUB307 in the presence of **3** ranged from 11.3 ± 2.6% to 1.9 ± 2.2% for concentrations of 0.125 mg/L and 64 mg/L, respectively (Supplementary Table S4).

3.5. Effect of increasing concentrations of 4-methoxyphenyl isothiocyanate (5) on conjugal transfer of pUB307

Among the test isothiocyanates, 4-methoxyphenyl isothiocyanate (**5**) was the most active against plasmid pUB307 (IncP) with no plasmid-curing activity. It was therefore evaluated for the effect of increasing concentrations (1–128 mg/L) on the conjugal transfer of plasmid pUB307. The observed activities are shown in Fig. 4. 4-Methoxyphenyl isothiocyanate (**5**) showed a moderate anti-conjugant activity (22.7 ± 1.6%) at the lowest concentration (1 mg/L) and this was steadily maintained up to 32 mg/L, after which there was a sharp increase in conjugal inhibition. Almost complete conjugal inhibition was observed at 128 mg/L (Supplementary Table S5).

3.6. Effect of allyl (1) and benzyl (3) isothiocyanates on normal growth of human dermal fibroblasts, adult cells (HDFa; C-013-5C)

Allyl (**1**) and benzyl (**3**) isothiocyanates that exhibited active to moderate anti-conjugant activity against all test plasmids were further assessed for cytotoxicity against normal cell growth. This was to determine whether the broad-range anti-conjugant activities exhibited by isothiocyanates **1** and **3** were not at cytotoxic concentrations and thus worth pursuing as potential anti-conjugants for further development. The observed cytotoxic activities are shown

Table 1
Minimum inhibitory concentrations (MICs) of isothiocyanates and comparators against *Escherichia coli* and *Staphylococcus aureus* strains.

Isothiocyanate	Chemical structure	MIC (mg/L)			
		E. coli NCTC 10418[a]	*S. aureus* ATCC 25923[a]	*S. aureus* SA-1199B[b]	*S. aureus* XU212[c]
Allyl isothiocyanate (**1**)	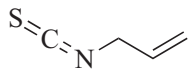	> 512	512	512	> 512
L-sulforaphane (**2**)	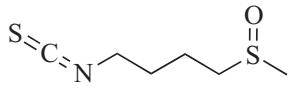	64	64	32	32
Benzyl isothiocyanate (**3**)	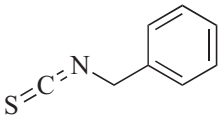	128	256	256	512
Phenylethyl isothiocyanate (**4**)	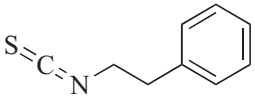	256	16	32	32
4-Methoxyphenyl isothiocyanate (**5**)	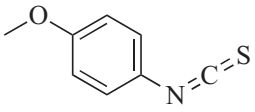	512	256	128	128
Ciprofloxacin	–	<0.0625	<0.0625	–	–
Norfloxacin	–	–	–	32	–
Tetracycline	–	–	–	–	128

[a] Susceptible standard strains.
[b] Fluoroquinolone-resistant strain overexpressing the NorA efflux pump.
[c] Tetracycline-resistant strain overexpressing the TetK efflux pump.

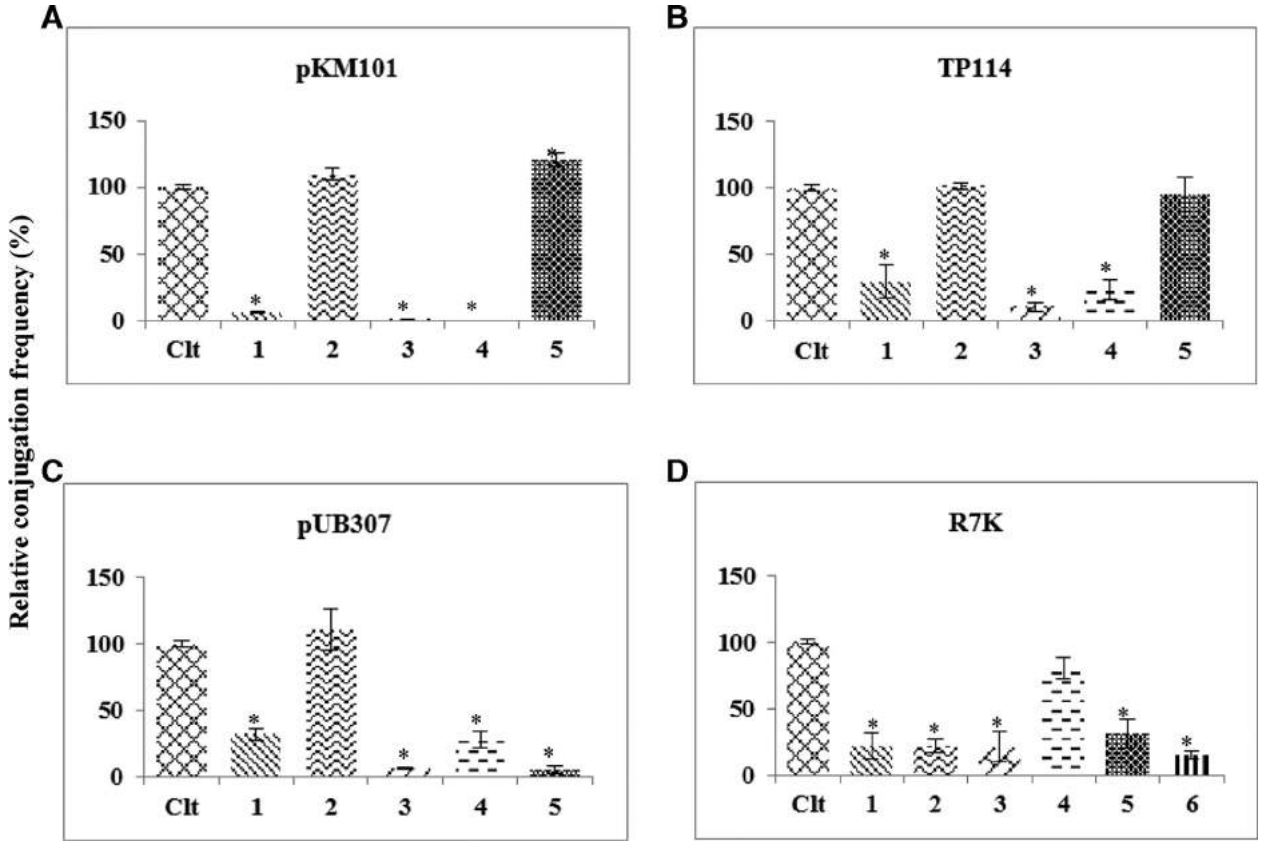

Fig. 1. Effect of selected isothiocyanates on conjugal transfer of (A) IncN plasmid pKM101, (B) $IncI_2$ plasmid TP114, (C) IncP plasmid pUB307 and (D) IncW plasmid R7K, expressed as a percentage relative to the control without test compound (Clt). The isothiocyanates were tested at the following subinhibitory concentrations: allyl isothiocyanate (**1**) (100 mg/L); L-sulforaphane (**2**) (16 mg/L); benzyl isothiocyanate (**3**) (32 mg/L); phenylethyl isothiocyanate (**4**) (64 mg/L); and 4-methoxyphenyl isothiocyanate (**5**) (100 mg/L). Linoleic acid (**6**), a known anti-conjugant for IncW plasmids, was tested at 200 mg/L. Values represent the mean ± standard deviation of at least three independent experiments measured by the plate conjugation assay. * $P < 0.05$ (compared with the control).

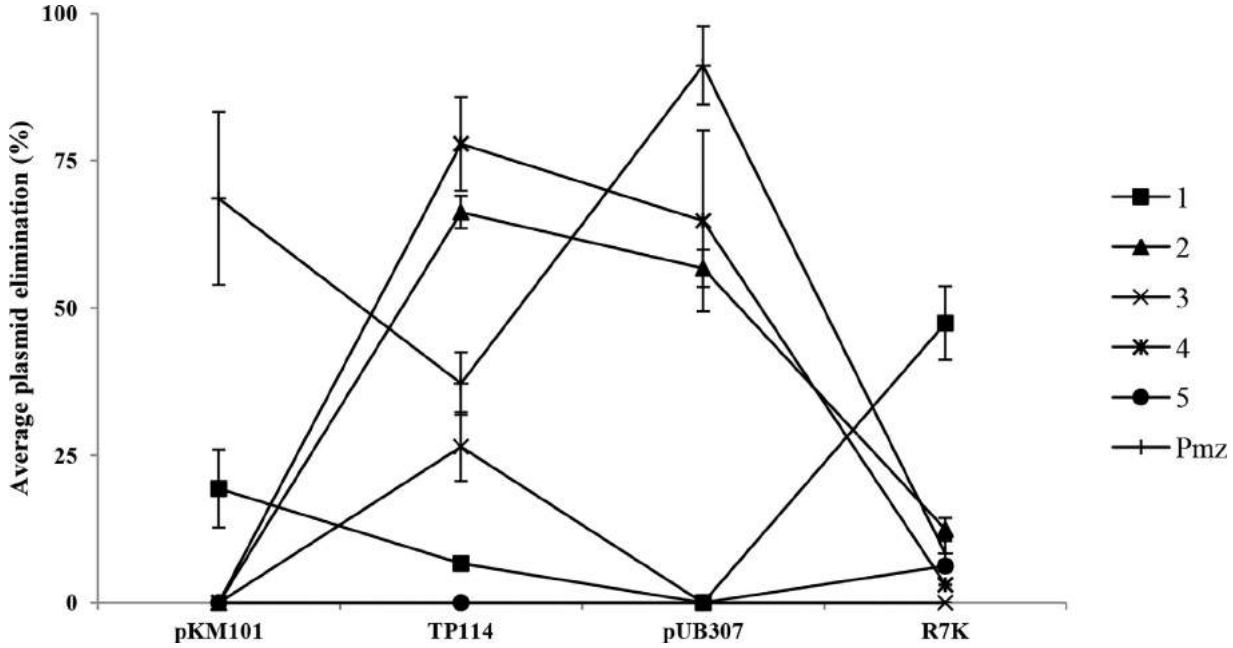

Fig. 2. Plasmid elimination activity of the isothiocyanates. The isothiocyanates were tested at the following concentrations: allyl isothiocyanate (**1**) (100 mg/L); L-sulforaphane (**2**) (16 mg/L); benzyl isothiocyanate (**3**) (32 mg/L); phenylethyl isothiocyanate (**4**) (64 mg/L); 4-methoxyphenyl isothiocyanate (**5**) (100 mg/L); and promethazine (Pmz) (16 mg/L).

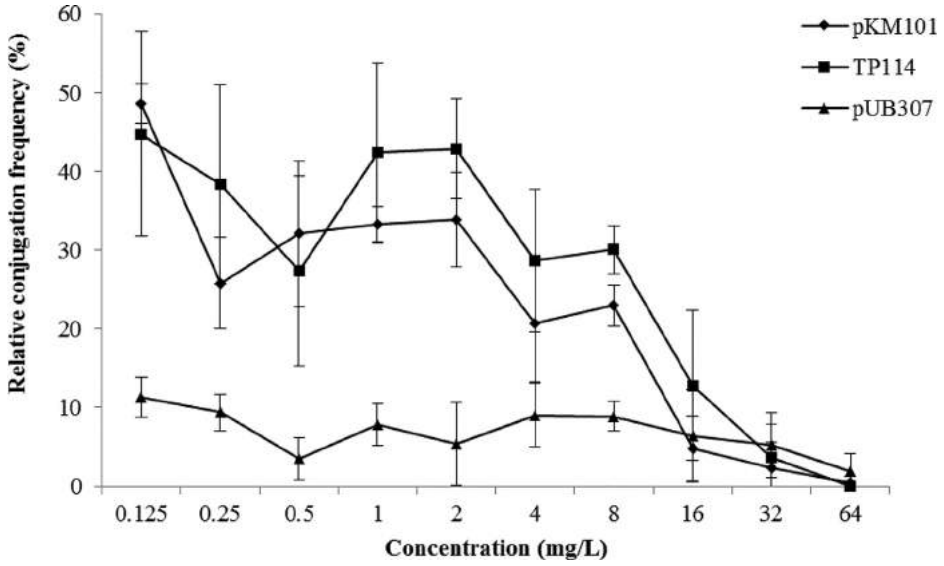

Fig. 3. Effect of increasing concentrations of benzyl isothiocyanate (**3**) on conjugal transfer of plasmids pKM101 (IncN), TP114 ($IncI_2$) and pUB307 (IncP) relative to the control without test sample (100% conjugation frequency). Values represent the mean ± standard deviation of a least three independent experiments measured by the plate conjugation assay.

in Fig. 5. The 50% cytotoxic concentration (CC_{50}) values for allyl (**1**) and benzyl (**3**) isothiocyanates against HDFa cells were 63.9 mg/L (645 μM) and 30.3 mg/L (203 μM), respectively (Supplementary Table S6).

4. Discussion

The discovery of a potent compound that will inhibit the spread of resistance genes and/or resistance mechanisms has clinical relevance, especially in this era of plasmids in species such as *Klebsiella pneumoniae* that are carbapenem-resistant. This is highly timely given the lack of treatment options for infections caused by this pathogen. In line with this, selected isothiocyanates, which are hydrolysis products of glucosinolates commonly found in *Brassica* vegetables, were investigated for the possibility of inhibiting the spread of resistance genes by blocking bacterial conjugation in *E. coli*.

The initial findings from this study showed that allyl isothiocyanate (**1**), L-sulforaphane (**2**), benzyl isothiocyanate (**3**), phenylethyl isothiocyanate (**4**) and 4-methoxyphenyl isothiocyanate (**5**) have some level of antibacterial activity ranging from 16 mg/L to >512 mg/L against susceptible *E. coli* NCTC 10418 and *S. aureus* ATCC 23925 as well as effluxing multidrug-resistant *S. aureus* strains (SA-1199B and XU212) (Table 1). This corroborates the reported antibacterial activity of the isothiocyanates but, owing to the variability in testing methods, bacterial inoculum densities and diversity in susceptibility, it is difficult to compare results [26–32]. The isothiocyanates were found to be less potent compared with

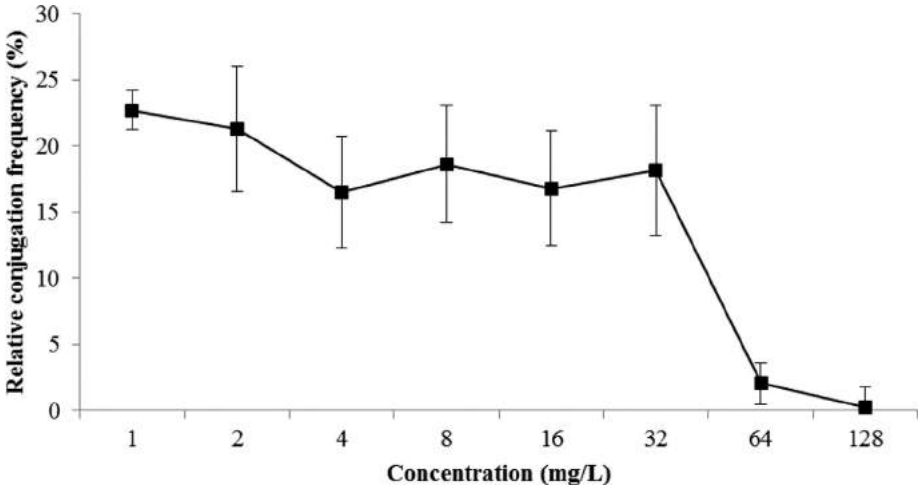

Fig. 4. Effect of increasing concentrations of 4-methoxyphenyl isothiocyanate (**5**) on conjugal transfer of IncP plasmid pUB307 relative to the control without test sample (100% conjugation frequency). Values represent the mean ± standard deviation of a least three independent experiments measured by the plate conjugation assay.

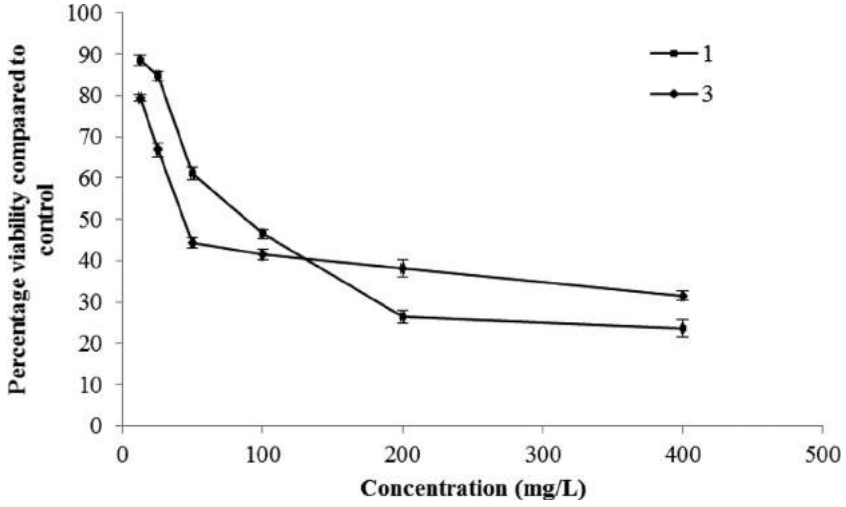

Fig. 5. Effect of allyl (**1**) and benzyl (**3**) isothiocyanates on growth of human dermal fibroblasts, adult cells (HDFa; C-013-5C). Values represent the mean ± standard deviation of a least three independent experiments measured by cytotoxicity assay.

conventional antibiotics, and similar results have been reported by others [26,28,32]. Among the tested isothiocyanates, phenylethyl isothiocyanate (**4**) was the most potent against Gram-positive microbes with MICs ranging from 16 mg/L to 32 mg/L, followed by L-sulforaphane (**2**) (MIC range 32–64 mg/L), which was also the most potent against Gram-negative *E. coli* NCTC 10418. The antibacterial activities of these isothiocyanates have been explained to be due to their ability to cause physical membrane damage [33,34], to interfere with the bacterial redox system that affects the cell membrane potential [34], or disruption of major metabolic processes [35,36].

Regarding the anti-conjugal activity study, broad-range anti-conjugant activity was observed for allyl (**1**) and benzyl (**3**) isothiocyanates at subinhibitory concentrations, with **3** being the most potent among the tested isothiocyanates (Fig. 1). It inhibited the conjugation of plasmids pKM101 (IncN), TP114 ($IncI_2$) and pUB307 (IncP), and selectively cured plasmid TP114 only. Against plasmids pKM101 and TP114, **3** also reduced conjugal transfer by 97.7 ± 3.3% and 96.4 ± 4.2%, respectively, at 32 mg/L (214.46 μM) and its activity gradually declined with decreasing concentrations (Fig. 3). This was not the same for pUB307, where **3** continued to show pronounced activity with a 90.8 ± 2.3% reduction in conjugation even at a low concentration of 0.25 mg/L (1.68 μM). This was interesting as **3** did not show any plasmid-curing activity against this particular plasmid pUB307 or against pKM101, ruling out the fact that the observed anti-conjugation may be due to plasmid elimination. Another area of interest was that **3** exhibited broad-range activity; this could mean that **3** either acts on a common target site on the conjugation machinery or that it causes general cell toxicity. However, considering the MIC (128 mg/L; Table 1) of **3** against the susceptible *E. coli* strain NCTC 10418, the concentrations (≤32 mg/L) used for the conjugation assays were at sub-lethal doses and are less likely to have caused general cell toxicity. With allyl isothiocyanate (**1**), moderate plasmid elimination activity was observed against most of the test plasmids and this may be an indication that its broad-range anti-conjugant activity is due to plasmid curing. The broad-range activities of **1** and **3** prompted their testing against normal growth of human dermal fibroblasts, adult cells (HDFa; C-013-5C). A comparison of the CC_{50} of **3** against HDFa cells (30.30 mg/L; 203.07 μM) with its anti-conjugant concentration against the test plasmids showed that its CC_{50} level was above the concentrations needed to cause a 50% reduction in conjugal transfer of plasmids; pKM101 (CC_{50} = 2.19 mg/L; 14.68 μM); TP114 (CC_{50} = 1.24 mg/L; 8.31 μM); and pUB307 (CC_{50} = 0.34 mg/L; 2.28 μM) (Fig. 5). This suggests that **3** showed anti-conjugant activity at non-toxic concentrations. However, the same cannot be said for allyl isothiocyanate (**1**) because its CC_{50} against HDFa cells

(63.9 mg/L; 644.48 μM) was below the 100 mg/L needed to cause moderate anti-conjugant activity (50–90% reduction) against most of the test plasmids. It is therefore suggested that the concentrations needed to cause a 50% reduction in conjugation is most likely to be closer to the CC_{50} value.

From this study, specificity of anti-conjugal and plasmid-curing activity was observed for 4-methoxyphenyl isothiocyanate (**5**), a synthetic compound. L-sulforaphane (**2**) also exhibited some level of anti-conjugant specificity against the IncW plasmid R7K at 16 mg/L (90.25 μM), but at this same concentration plasmid curing was observed and hence **2** is not a true anti-conjugant (Fig. 2). Anti-conjugant activity of **5** at 100 mg/L (605.29 μM) was pronounced for the IncP plasmid pUB307, with a 94.8 ± 2.8% reduction in conjugation, but it showed minimal inhibition or even promoted conjugation for the other test plasmids (Fig. 1). Its anti-conjugant activity was, however, concentration-dependent (Fig. 4). Regarding the plasmid-curing effect, **5** showed elimination of only the IncW plasmid R7K but it did not have any effect on conjugation of this plasmid. This may give an indication that **5** could have some conjugation promotion factors, and this was observed for pKM101. Conjugation of pKM101 in the presence of **5** exceeded 100% (Fig. 1). The anti-conjugation, plasmid-curing and pro-conjugation activities exhibited by **5** supports its specificity. This suggests that compound **5** acts on a specific target site that may not be common to all plasmids. Consequently, it is less likely for resistance to develop against **5**, unlike other compounds that target general and essential targets of bacteria, which is the case in many instances of antibiotic resistance [37]. A general observation with the test isothiocyanates is that the presence of oxygen, attached to sulphur or an aromatic carbon, conferred some level of anti-conjugal specificity. We therefore hypothesise that the methoxyl substituent on the aromatic ring and the lack of a hydrocarbon chain of **5**, which makes it structurally different from the other test aromatic isothiocyanates, may have contributed to its specificity of activity.

In conclusion, isothiocyanates **3** and **5** were the most promising anti-conjugants identified in this study. Further explorative studies involving structural modification and mechanistic studies of these isothiocyanates could possibly lead to the identification of a potent anti-conjugant. This will help decrease the spread of multidrug resistance genes and multidrug-resistant bacteria, reduce virulence and help reinstate existing antibiotics.

Funding

This work was funded by the Commonwealth Scholarship Commission (CSC), UK [grant no. GHCA-2012-19].

Competing interests

None declared.

Ethical approval

Not required.

Supplementary materials

Supplementary material associated with this article can be found, in the online version, at doi:10.1016/j.ijantimicag.2019.01.011.

References

[1] Fernandez-Lopez R, Machon C, Longshaw CM, Martin S, Molin S, Zechner EL, et al. Unsaturated fatty acids are inhibitors of bacterial conjugation. Microbiology 2005;151:3517–26.
[2] Zechner EL, Lang S, Schildbach JF. Assembly and mechanisms of bacterial type IV secretion machines. Philos Trans R Soc Lond B Biol Sci 2012;367:1073–87.
[3] DeNap JCB, Thomas JR, Musk DJ, Hergenrother PJ. Combating drug-resistant bacteria: small molecule mimics of plasmid incompatibility as antiplasmid compounds. J Am Chem Soc 2004;126:15402–4.
[4] Thomas JR, DeNap JCB, Wong ML, Hergenrother PJ. The relationship between aminoglycosides' RNA binding proclivity and their antiplasmid effect on an IncB plasmid. Biochemistry 2005;44:6800–8.
[5] DeNap JCB, Hergenrother PJ. Bacterial death comes full circle: targeting plasmid replication in drug-resistant bacteria. Org Biomol Chem 2005;3:959–66.
[6] Moritz EM, Hergenrother PJ. Toxin–antitoxin systems are ubiquitous and plasmid-encoded in vancomycin-resistant enterococci. Proc Natl Acad Sci U S A 2007;104:311–16.
[7] Wang NR, Hergenrother PJ. A continuous fluorometric assay for the assessment of MazF ribonuclease activity. Anal Biochem 2007;371:173–83.
[8] Hilleringmann M, Pansegrau W, Doyle M, Kaufman S, MacKichan ML, Gianfaldoni C, et al. Inhibitors of *Helicobacter pylori* ATPase Cagα block CagA transport and *cag* virulence. Microbiology 2006;152:2919–30.
[9] Backert S, Meyer TF. Type IV secretion systems and their effectors in bacterial pathogenesis. Curr Opin Microbiol 2006;9:207–17.
[10] Getino M, Sanabria-Rios DJ, Fernandez-Lopez R, Campos-Gomez J, Sanchez-Lopez JM, Fernandez A, et al. Synthetic fatty acids prevent plasmid-mediated horizontal gene transfer. MBio 2015;6 e01032-15.
[11] Getino M, Fernandez-Lopez R, Palencia-Gandara C, Campos-Gomez J, Sanchez-Lopez JM, Martinez M, et al. Tanzawaic acids, a chemically novel set of bacterial conjugation inhibitors. PLoS One 2016;11:e0148098.
[12] Mithen RF, Dekker M, Verkerk R, Rabot S, Johnson IT. The nutritional significance, biosynthesis and bioavailability of glucosinolates in human foods. J Sci Food Agric 2000;80(Special issue):967–84.
[13] Fahey JW, Zalcmann AT, Talalay P. The chemical diversity and distribution of glucosinolates and isothiocyanates among plants. Phytochemistry 2001;56:5–51.
[14] Andrews JM. Determination of minimum inhibitory concentrations. J Antimicrob Chemother 2001;48:5–16.
[15] A guide to sensitivity testing. Report of Working Party on Antibiotic Sensitivity Testing of the British Society of Antimicrobial Chemotherapy. J Antimicrob Chemother 1991;27(Suppl D):1–50.
[16] San Millan A, MacLean RC. Fitness costs of plasmids: a limit to plasmid transmission. Microbiol Spectr 2017;5. doi:10.1128/microbiolspec.MTBP-0016-2017.
[17] Kottara A, Hall JPJ, Harrison E, Brockhurst MA. Variable plasmid fitness effects and mobile genetic element dynamics across *Pseudomonas* species. FEMS Microbiol Ecol 2018;94. doi:10.1093/femsec/fix172.
[18] Oyedemi BOM, Shinde V, Shinde K, Kakalou D, Stapleton PD, Gibbons S. Novel R-plasmid conjugal transfer inhibitory and antibacterial activities of phenolic compounds from *Mallotus philippensis* (Lam.) Mull. Arg. J Glob Antimicrob Resist 2016;5:15–21.
[19] Kwapong AA, Stapleton P, Gibbons S. A new dimeric imidazole alkaloid plasmid conjugation inhibitor from *Lepidium sativum*. Tetrahedron Lett 2018;59:1952–4.
[20] Rice LB, Bonomo RA. Genetic and biochemical mechanisms of bacterial resistance to antimicrobial agents. In: Lorian V, editor. Antibiotics in laboratory medicine. 5th ed. Philadelphia, PA: Lippincott Williams & Wilkins; 2005. p. 483–4.
[21] Hooper DC, Wolfson JS, McHugh GL, Swartz MD, Tung C, Swartz MN. Elimination of plasmid pMG110 from *Escherichia coli* by novobiocin and other inhibitors of DNA gyrase. Antimicrob Agents Chemother 1984;25:586–90.
[22] Molnar A. Antiplasmid effect of promethazine in mixed bacterial cultures. Int J Antimicrob Agents 2003;22:217–22.
[23] Splenger G, Molnár A, Schelz Z, Amaral L, Sharples D, Molnár J. The mechanism of plasmid curing in bacteria. Curr Drug Targets 2006;7:823–41.
[24] Molnár J, Mándi Y, Splenger G, Amaral L, Haszon I, Turi S, et al. Synergism between antiplasmid promethazine and antibiotics in vitro and in vivo. Mol Biol 2014;34:119. doi:10.4172/2168-9547.1000119.
[25] Skehan P, Storeng R, Scudiero D, Monks A, McMahon J, Vistica D, et al. New colorimetric cytotoxicity assay for anticancer-drug screening. J Natl Cancer Inst 1990;82:1107–12.
[26] Romeo L, Iori R, Rollin P, Bramanti P, Mazzon E. Isothiocyanates: an overview of their antimicrobial activity against human infections. Molecules 2018;23:1–18.
[27] Dufour V, Stahl M, Baysse C. The antibacterial properties of isothiocyanates. Microbiology 2015;161:229–43.
[28] Fahey JW, Haristoy X, Dolan PM, Kensler TW, Scholtus I, Stephenson KK, et al. Sulforaphane inhibits extracellular, intracellular, and antibiotic-resistant strains of *Helicobacter pylori* and prevents benzo[a]pyrene-induced stomach tumors. Proc Natl Acad Sci U S A 2002;99:7610–15.
[29] Kim MG, Lee HS. Growth-inhibiting activities of phenethyl isothiocyanate and its derivatives against intestinal bacteria. J Food Sci 2009;74:M467–71.
[30] Borges A, Abreu AC, Ferreira C, Saavedra MJ, Simoes LC, Simoes M. Antibacterial activity and mode of action of selected glucosinolate hydrolysis products against bacterial pathogens. J Food Sci Technol 2015;52:4737–48.
[31] Nowicki D, Rodzik O, Herman-Antosiewicz A, Szalewska-Pałasz A. Isothiocyanates as effective agents against enterohemorrhagic *Escherichia coli*: insight to the mode of action. Sci Rep 2016;6:22263.
[32] Lu Z, Dockery CR, Crosby M, Chavarria K, Patterson B, Giedd M. Antibacterial activities of wasabi against *Escherichia coli* O157:H7 and *Staphylococcus aureus*. Front Microbiol 2016;7:1403.

[33] Lin CM, Preston JF III, Wei CI. Antibacterial mechanism of allyl isothiocyanate. J Food Prot 2000;63:727–34.
[34] Sofrata A, Santangelo EM, Azeem M, Borg-Karlson AK, Gustafsson A, Pütsep K. Benzyl isothiocyanate, a major component from the roots of *Salvadora persica* is highly active against Gram-negative bacteria. PLoS One 2011;6:e23045.
[35] Abreu AC, Borges A, Simoes LC, Saavedra MJ, Simoes M. Antibacterial activity of phenyl isothiocyanate on *Escherichia coli* and *Staphylococcus aureus*. Med Chem 2013;9:756–61.
[36] Dufour V, Stahl M, Rosenfeld E, Stintzi A, Baysse C. Insights into the mode of action of benzyl isothiocyanate on *Campylobacter jejuni*. Appl Environ Microbiol 2013;79:6958–68.
[37] Smith PA, Romesberg FE. Combating bacteria and drug resistance by inhibiting mechanisms of persistence and adaptation. Nat Chem Biol 2007;3:549–56.

Tetrahedron Letters 59 (2018) 1952–1954

Contents lists available at ScienceDirect

Tetrahedron Letters

journal homepage: www.elsevier.com/locate/tetlet

A new dimeric imidazole alkaloid plasmid conjugation inhibitor from *Lepidium sativum*

Awo Afi Kwapong [a,b], Paul Stapleton [a], Simon Gibbons [a,*]

[a] Research Department of Pharmaceutical and Biological Chemistry, UCL School of Pharmacy, 29-39 Brunswick Square, London WC1N 1AX, United Kingdom
[b] Department of Pharmaceutics and Microbiology, School of Pharmacy, University of Ghana, Ghana

ARTICLE INFO

Article history:
Received 11 December 2017
Revised 6 April 2018
Accepted 10 April 2018
Available online 11 April 2018

Keywords:
Dimeric
Imidazole
Lepidine
Plasmids
Conjugation

ABSTRACT

Phytochemical investigation of the methanolic extract of *Lepidium sativum* seeds led to the isolation of a new compound, named 2-(3-(3-((1*H*-imidazol-2-yl)methyl)-5-methoxyphenoxy)benzyl)-1*H*-imidazole and given the trivial name Lepidine AK (**1**), along with three known compounds; Lepidine E (**2**), Lepidine B (**3**) and 2-(3-(2-((1*H*-imidazol-2-yl)methyl)-6-methoxyphenoxy)benzyl)-1*H*-imidazole (**4**). The structures were elucidated based on NMR spectroscopy, UV, IR and high-resolution electrospray ionization mass spectrometry. The isolated compounds were tested for bacterial conjugation inhibition. Lepidine AK (**1**, 100 μg/mL) reduced the conjugal transfer of the $IncI_2$ plasmid TP114 to 44.7 ± 3.5% but interestingly promoted the conjugation of the IncN plasmid pKM101 to greater than 120%.

Introduction

Lepidium sativum (garden cress) is an annual herb of the family Brassicaceae. It is a native of Egypt and West Asia but is widely farmed in temperate countries globally for its culinary and medicinal uses.[1,2] In China, garden cress seeds are used for the treatment of abdominal colic, asthma, pleurisy and dropsy.[3] In Africa, Ethiopians use the seeds primarily for treatment of throat diseases, asthma, bronchitis, headache and for baking and as a condiment.[4,5] The Mauritians use the seeds for the treatment of hiccough and stomachache.[5] Both seeds and leaves of *L. sativum* are used for the treatment of inflammation, bronchitis, rheumatism and muscular pain in the Unani system of medicine.[3,6] It is also reported to be useful in the treatment of diabetes, hypertension, cough and bleeding piles.[7–9] Phytochemical studies on *L. sativum* have shown the presence of essential oil, glucosinolates, alkaloids, sterols, cyanogenic glycosides (traces), flavonoids, tannins, saponins and triterpenes.[3,6] Bahroun and Damak first reported dimeric imidazole alkaloids for *L. sativum* seeds after which Meinhart Zenk's group isolated five additional analogues.[10]

In this paper, we report the isolation and structural characterization by spectroscopic methods of a new dimeric imidazole alkaloid, 2-(3-(3-((1*H*-imidazol-2-yl)methyl)-5-methoxyphenoxy) benzyl)-1*H*-imidazole (**1**) (Fig. 1) along with three known compounds. The antibacterial activity and inhibition of bacterial conjugal transfer of plasmids of the isolated compounds are reported herein for the first time.

Results and discussion

L. sativum seeds (245 g) were obtained from Seed Parade, UK, and defatted with petroleum ether and subsequently extracted with methanol. The MeOH extract was mixed with water, acidified with concentrated HCl and it was then liquid-liquid extracted with EtOAc. The EtOAc fraction was chromatographed over silica gel 60 (gravity column, 70–230 mesh, column size: 50 × 4 cm). Compound **1** (3.6 mg, *Rf* value: 0.39) was obtained by purification of the column fractions using preparative TLC (silica gel, $CHCl_3$-MeOH-NH_3, 90:9:1, $^{V}/_{V}$).

Compound **1** was isolated as a pale yellow solid and HRTOFE-SIMS gave an *m/z* at 361.1659 $[M+H]^+$, which indicated that its molecular formula was $C_{21}H_{20}N_4O_2$. The ^{1}H and COSY NMR spectra revealed two aromatic rings; di-substituted (A) and tri-substituted (B) aromatic rings. The ^{1}H data was similar to the known compound **4** (2-(3-(2-((1*H*-imidazol-2-yl)methyl)-6-methoxyphenoxy)benzyl)-1*H*-imidazole, only varying in the positioning of the methoxyl and imidazolyl methyl group on the B-ring. The di-substituted aromatic ring was identified by proton resonances at δ_H 6.70 (dd, *J* = 2.0, 1.5 Hz, H-2), 6.86 (dd, *J* = 8.0, 0.5 Hz, H-4), 7.15 (t, *J* = 8.0 Hz, H-5), 6.64 (dd, *J* = 8.0, 2.0 Hz, H-6). The couplings between the aromatic hydrogens, and the meta-coupling of H-2

* Corresponding author.
E-mail address: simon.gibbons@ucl.ac.uk (S. Gibbons).

https://doi.org/10.1016/j.tetlet.2018.04.028
0040-4039/

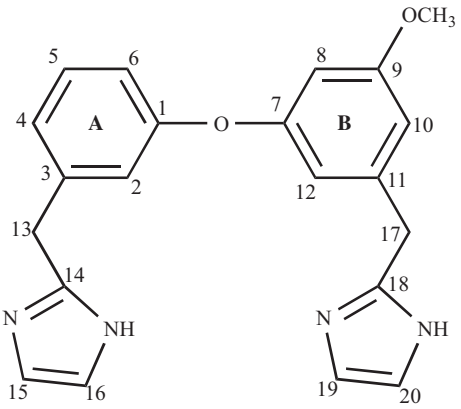

Fig. 1. Structure and numbering of compound **1**.

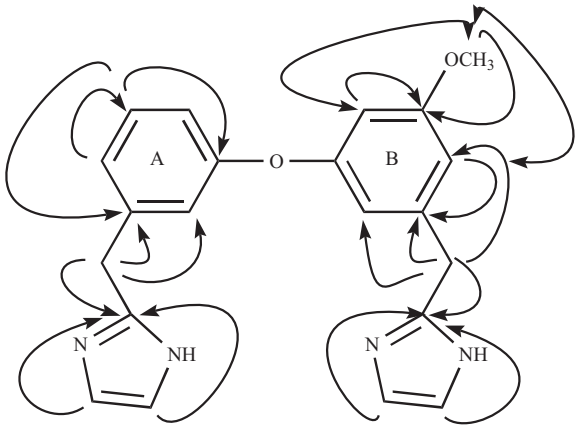

Fig. 2. Key HMBC (single-headed arrows) and NOESY (double-headed arrows) correlations of compound **1**.

by H-6 ($^4J_{HH}$ = 2.0 Hz) confirmed their arrangement on the di-substituted ring. On the B-ring a meta-coupling of a hydrogen signal at δ_H 7.01 (d, J = 1.5 Hz, H-10) to δ_H 6.85 (s, J = 1.5 Hz, H-12) in the COSY spectrum also indicated the presence of an aromatic spin system, which was 1,3,5-tri-substituted (ring B). Both spin systems were confirmed by the HMQC and HMBC correlations (Table 1, Fig. 2). The aromatic rings were linked by oxygen, which was confirmed by a strong IR absorption band at 1053 cm^{-1} (the ether functional group). A $^3J_{H\text{-}C}$ correlation of the methoxyl hydrogens (3H, s, δ_H 3.70) to the aromatic quaternary carbon (δ_C 151.9, C-9) revealed the position of the methoxyl group on the aromatic ring B. It was meta-positioned to the imidazolylmethyl moiety and this was supported by the splitting pattern of the aromatic hydrogens on the ring B. The NOESY spectrum revealed a cross peak between the methoxyl hydrogens (3H, s, δ_H 3.70) and the aromatic hydrogens H-8 and H-10 (δ_H 7.01), which confirmed this structural arrangement. The hydrogen signal at δ_H 6.91 (4H, s, H-15, H-16, H-19 and H-20) and the carbon signals at δ_C 123.3 (2C, C-15 and C-16), 123.0 (2C, C-19 and C-20), 148.1 (C-14) and 148.4 (C-18) accounted for the two-imidazole rings. The signals at δ_H 3.97 (2H, s, H_2-13), δ_c 34.3 (C-13) and δ_H 3.95 (2H, s, H_2-17), δ_c 35.1 (C-17) were identified as the two methylene groups connecting the imidazole rings to the aromatic rings. The IR spectrum confirmed this with the presence of secondary amine functional group absorbance at 2920 cm^{-1}. The combined NMR, IR and HRTOFESIMS spectra data led to an unambiguous assignment of the full structure of compound **1**, as 2-(3-(3-((1*H*-imidazol-2-yl)methyl)-5-methoxyphenoxy)benzyl)-1*H*-imidazole. The known compounds were identified by comparison of their spectroscopic data with reported data as Lepidine E (**2**), Lepidine B (**3**) and 2-(3-(2-((1*H*-imidazol-2-yl)methyl)-6-methoxyphenoxy)benzyl)-1*H*-imidazole (**4**).[10]

Table 1
^{1}H (500 MHz) and ^{13}C NMR (125 MHz) NMR data and HMBC correlations of **1** recorded in methanol d_4.

Position	δ_C, type	δ_H, (J in Hz)	HMBC
1	159.9, C		
2	117.6, CH	6.70, dd (2.0, 1.5)	
3	141.0, C		
4	123.3, CH	6.86, dd (8.0, 0.5)	C-5
5	130.6, CH	7.15, t	C-1, C-3
6	115.6, CH	6.64, dd (8.0, 2.0)	
7	145.6, C		
8	114.5, CH	7.01, s	C-9
9	151.9, C		
10	126.4, CH	7.01, d (1.5)	C-11
11	132.5, C		
12	123.0, CH	6.85, d (1.5)	
13	34.3, CH_2	3.97, s	C-2, C-3, C-4, C-14
14	148.1, C		
15	123.3, CH	6.91, s	C-14
16	123.3, CH	6.91, s	C-14
17	35.1, CH_2	3.95, s	C-10, C-11, C-12, C-18
18	148.4, C		
19	123.0, CH	6.91, s	C-18
20	123.0, CH	6.91, s	C-18
O-Me	56.5, CH_3	3.70, s	C-9

The compounds were tested for their ability to inhibit bacterial plasmid conjugation[11] (Table 2). The essence of this assay is to identify compounds that can inhibit the spread of antibiotic-resistance genes via the bacterial type-IV secretion systems (conjugation machinery). The inhibition of this process is important because of the clinical significance of conjugation machinery in the transfer of toxins and effector proteins directly into eukaryotic target cells, and its involvement in biofilm formation as well as the aforementioned transfer of antibiotic-resistance genes among microorganisms.[12,13]

It was interesting to note that some of the dimeric imidazoles (compounds **2** and **4**) at sub-inhibitory concentration (100 μg/mL) exhibited anti-conjugal activity in *Escherichia coli* while compound **3** at the same concentration enhanced conjugation activity (conjugal transfer frequency, greater than 120%). With compound **1**, the activity varied.

Compound **2** reduced the conjugal transfer frequency of the IncN plasmid pKM101 and $IncI_2$ plasmid TP114 to 31.0 ± 7.0% and 26.0 ± 4.0%, respectively. In comparison to compound **2**, **4** had a slightly better reduction in conjugal transfer frequency, a 28.0 ± 5.0% for IncN plasmid pKM101 and 23.5 ± 4.9% for $IncI_2$ plasmid TP114. Although the difference in anti-conjugal activity for compounds **2** and **4** is marginal, we suspect that the structural differences of substituent groups on the aromatic ring B of the compounds may have contributed to this. At position 8 of the aromatic ring B, compound **2** has a hydroxyl group attached while compound **4** has a methoxyl group. The imidazolylmethyl moiety is attached to position 11 for compound **2**, while for compound **4** it is at the position 12. A general observation made was that, the isolated compounds were similar to each other but only varied in the positioning of the substituent groups on the aromatic ring B (either an hydroxyl or a methoxyl group and an imidazolylmethyl moiety), and this may have influenced the varied outcome of activity against the conjugal transfer of plasmids in *E. coli*.

The only compound, which showed specificity in activity against the tested plasmids strains, was the new imidazole (**1**). It exhibited moderate anti-conjugal activity against the $IncI_2$ plasmid TP114 (transfer frequency 44.0 ± 3.5%) and enhanced the

Table 2
The effect of the isolated dimeric imidazoles on conjugal transfer of plasmids pKM101 and TP114.

Conjugation pair	Compounds (100 μg/mL)					Controls	
Donor	Recipient	1	2	3	4	Novobiocin (10 μg/mL)	No drug
pKM101[a]	ER1793[c]	120 ± 0.0	31.0 ± 7.0	120 ± 0.0	28.0 ± 5.0	–	100.0 ± 0.0
TP114[b]		44.0 ± 3.5	26.0 ± 4.0	120 ± 0.0	23.5 ± 4.0	17.0 ± 4.2	100.0 ± 0.0

The values represent the mean transfer frequency (%) ± standard deviation of at least three independent experiments.
[a] *E. coli strain* WP2 bearing plasmid pKM101 (IncN; ampicillin-resistant).
[b] *E. coli strain* K12 J53-2 bearing plasmid TP114 ($IncI_2$; kanamycin-resistant).
[c] *E. coli strain* ER1793, streptomycin resistant.

conjugation activity of the IncN plasmid pKM101 to greater than 120%. We found this interesting, as specificity would limit its potential use but promotion may have utility in promoting plasmid transfer, which would be useful in many areas of molecular biology. In conclusion, this finding could serve as a good start point for structural modification for improved anti-conjugal activity with specificity. The development of an anti-conjugal molecule has potential druggability in reducing transfer and spread of resistance and reducing virulence.

Structure elucidation

2-(3-(3-((1*H*-imidazol-2-yl)methyl)-5-methoxyphenoxy)benzyl)-1*H*-imidazole (compound **1**).

Pale yellow solid; λ_{max} (log ε) 218 (3.97), 228 (4.18) nm; IR (film) V_{max}: 2919.76, 1045.02, 971.15, 799.93, 610.64 cm^{-1}; ^1H NMR (500 MHz, methanol-d_4) and ^{13}C NMR (125 MHz, methanol d_4): see Table 1; positive HRTOFESIMS *m/z* 361.1659 $[M+H]^+$ (calcd for $C_{21}H_{20}N_4O_2$, 361.1664).

Acknowledgments

We thank Mr. Emmanuel Samuel (UCL School of Pharmacy) for his help with the mass spectrometry. We also thank Commonwealth Scholarship for the financial support to Awo Afi Kwapong.

A. Supplementary data

Supplementary data associated with this article can be found, in the online version, at https://doi.org/10.1016/j.tetlet.2018.04.028.

References

1. Gokavi SS, Malleshi NG, Guo M. *Plant Foods Hum Nutr*. 2004;59:105–111.
2. Nehdi IA, Sbihi H, Tan CP, Al-Resayes SI. *Bioresour Technol*. 2012;126:193–197.
3. Sharma S, Agarwal N, Indian J. *Nat Prod Resour*. 2011;2:292–297.
4. Kloos HJ. *Ethiopian Pharm Assoc*. 1976;2:18–28.
5. Jansen PCM. In: Grubben GJH, Denton OA, eds. *Plant Resources of Tropical African 2. Vegetables*. Wageningen, Netherlands: PROTA Foundation/Backhuys Publishers; 2004:365–367.
6. Ghante MH, Badole SL, Bodhankar SL. In: Preedy VR, Watson RR, Patel VB, eds. *Nuts and seeds in health and disease prevention*. United States of America: Academic Press; 2011:521–526.
7. Eddouks M, Maghrani M, Zeggwagh NA, Michel JB. *J Ethnopharmacol*. 2005;97:391–395.
8. Maghrani M, Zeggwagh NA, Michel JB, Eddouks M. *J Ethnopharmacol*. 2005;100:193–197.
9. Mali RG, Mahajan SG, Mehta AA. *Orient Pharm Exp Med*. 2007;7:331–335.
10. Maier UH, Gundlach H, Zenk MH. *Phytochemistry*. 1998;49:1791–1795.
11. Rice LB, Bonomo RA. In: Lorian V, ed. *Antibiotics in laboratory medicine*. USA: Lippincott Williams & Wilkins; 2005:483–484.
12. Alvarez-Martinez CE, Christie PJ. *Microbiol Mol Biol Rev*. 2009;73:775–808.
13. Zechner EL, Lang S, Schildbach JF. *Philos Trans R Soc Lond B Biol Sci*. 2012;367:1073–1087.

SCIENTIFIC REPORTS

OPEN

Analogues of Disulfides from *Allium stipitatum* Demonstrate Potent Anti-tubercular Activities through Drug Efflux Pump and Biofilm Inhibition

Received: 29 August 2017
Accepted: 19 December 2017
Published online: 18 January 2018

Cynthia A. Danquah[1,2], Eleftheria Kakagianni[1], Proma Khondkar[1,3], Arundhati Maitra[2], Mukhlesur Rahman[4], Dimitrios Evangelopoulos[5], Timothy D. McHugh[5], Paul Stapleton[1], John Malkinson[1], Sanjib Bhakta[2] & Simon Gibbons[1]

Disulfides from *Allium stipitatum*, commonly known as Persian shallot, were previously reported to possess antibacterial properties. Analogues of these compounds, produced by *S*-methylthiolation of appropriate thiols using *S*-methyl methanethiosulfonate, exhibited antimicrobial activity, with one compound inhibiting the growth of *Mycobacterium tuberculosis* at 17 µM (4 mg L^{-1}) and other compounds inhibiting *Escherichia coli* and multi-drug-resistant (MDR) *Staphylococcus aureus* at concentrations ranging between 32–138 µM (8–32 mg L^{-1}). These compounds also displayed moderate inhibitory effects on *Klebsiella* and *Proteus* species. Whole-cell phenotypic bioassays such as the spot-culture growth inhibition assay (SPOTi), drug efflux inhibition, biofilm inhibition and cytotoxicity assays were used to evaluate these compounds. Of particular note was their ability to inhibit mycobacterial drug efflux and biofilm formation, while maintaining a high selectivity towards *M. tuberculosis* H37Rv. These results suggest that methyl disulfides are novel scaffolds which could lead to the development of new drugs against tuberculosis (TB).

We investigated extracts of bulbs from the plant family Alliaceae for their ability to produce antibacterial compounds, and from *Allium neapolitanum*, antibacterial canthinone alkaloids and hydroxy acids were characterised[1]. Of more chemical and pharmacological interest, a study on the Central Asian species *Allium stipitatum*, led to the isolation of three novel pyridine-*N*-oxide alkaloids (**1**–**3**), displaying outstanding potency towards *Mycobacterium tuberculosis* (Fig. 1)[2]. The minimum inhibitory concentrations (MIC) exhibited by these compounds were clinically-relevant and found to range between 2.5–40 µM (0.5–8 mg L^{-1}). Subsequently, a series of structurally-related methyl disulfides were synthesized in an effort to optimize the exceptional antibacterial activity. Structure-activity relationships revealed that the presence of the disulfide moiety was not the only factor responsible for activity, and it is possible that the disulfide is strongly "activated" by the presence of electron-withdrawing functional groups such as pyridine, pyridine-*N*-oxide, pyrimidine and quinoline, whereas phenyl and thiophene were poorly electron withdrawing and therefore had little effect on the "reactivity" of the disulfide bond (Fig. 1)[2]. From compounds **4**–**6**, it was clear that the *N*-oxide was not a prerequisite for antibacterial activity. Based on this rationale, we synthesised a small set of disulphides with proximal electron-withdrawing groups and characterised their antibacterial properties.

[1]Research Department of Pharmaceutical and Biological Chemistry, UCL School of Pharmacy, 29-39 Brunswick Square, London, WC1N 1AX, UK. [2]Department of Biological Sciences, Institute of Structural and Molecular Biology, Birkbeck, University of London, Malet Street, London, WC1E 7HX, UK. [3]Department of Pharmaceutical, Chemical and Environmental Sciences, University of Greenwich, Central Avenue, Chatham Maritime, ME4 4TB, UK. [4]Medicine Research Group, School of Health, Sport and Bioscience, University of East London, Water Lane, London, E15 4LZ, UK. [5]Centre for Clinical Microbiology, UCL Royal Free Hospital, Rowland Hill, London, NW3 2PF, UK. Sanjib Bhakta and Simon Gibbons contributed equally to this work. Correspondence and requests for materials should be addressed to S.B. (email: s.bhakta@bbk.ac.uk) or S.G. (email: simon.gibbons@ucl.ac.uk)

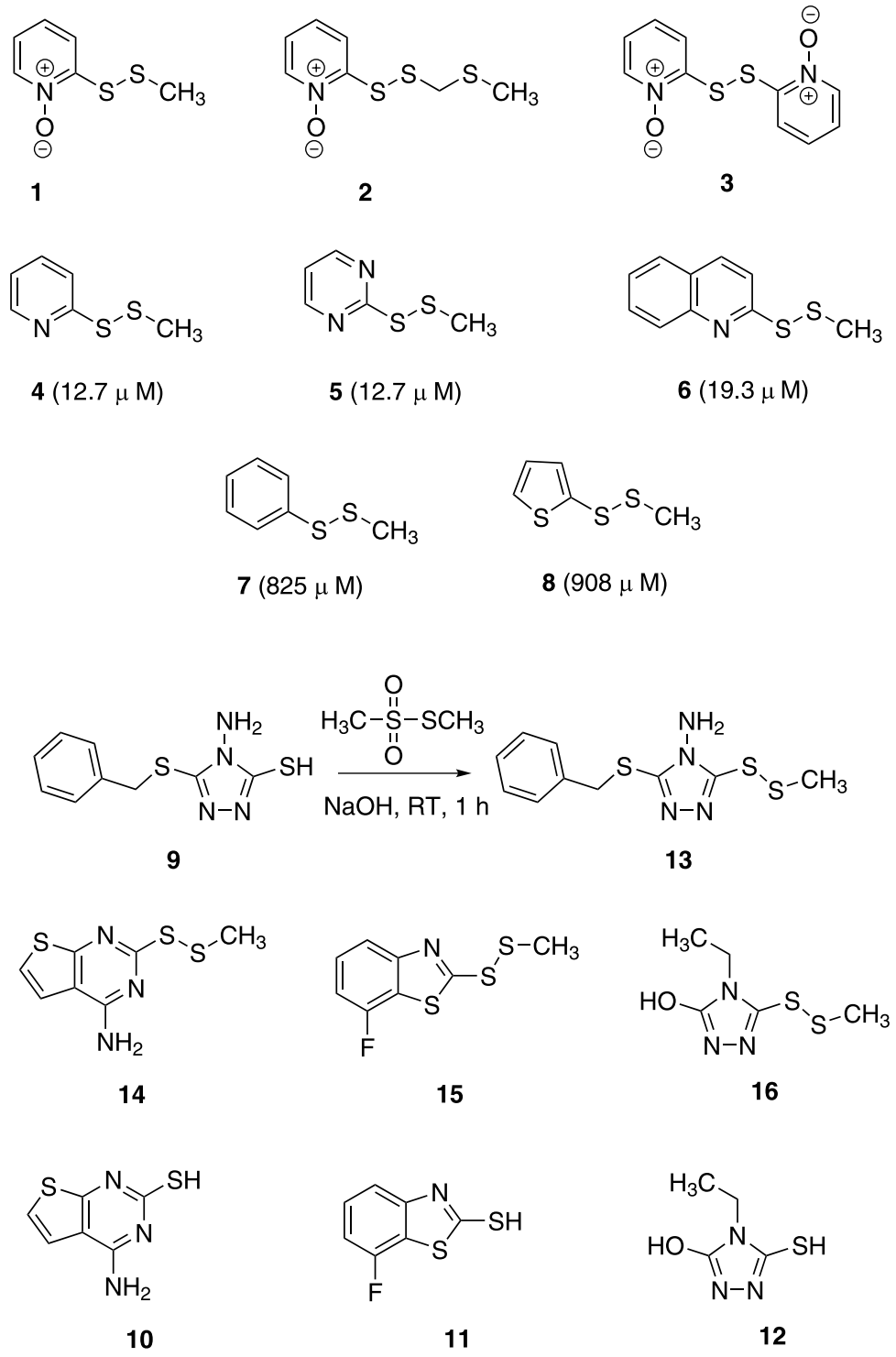

Figure 1. Compounds isolated from *Allium stipitatum* with antibacterial activity (**1**–**3**). Synthesized compounds (**4**–**8**) based on the natural products. MIC values against *S. aureus* are in parentheses. Reaction scheme for the synthesis of compounds (**13**–**16**) and the resulting synthesized methyl disulfides.

Given the continuing issues of multidrug-resistant (MDR) and extensively-drug-resistant (XDR) cases that are increasingly associated with clinically-relevant Gram-positive, Gram-negative and acid-fast human pathogens (such as *Staphylococcus aureus*, *Escherichia coli* and *Mycobacterium tuberculosis* respectively), there is a pressing need to develop new classes of antibacterials[3–5]. Common strategies for effective antimicrobial development are to target novel endogenous effector machinery within a pathogen or to reverse resistance and thereby make the bacteria more susceptible to existing chemotherapy. Increased levels of tolerance towards drugs are observed in bacteria that contain systems to prevent these compounds from reaching their site(s) of action[6]. Within this

Compound	*M. smegmatis*	*M. aurum*	*M. bovis BCG*	*M. tuberculosis H37Rv*	*M. tuberculosis MDR1*	*M. tuberculosis MDR2*	*E. coli (NCTC 10418)*	*Proteus mirabilis -10830*	*K. pneumoniae*	*S. aureus SA-1199B*	*S. aureus XU212*	EMRSA-15	*Ent. faecalis*
13	113 (32)	113 (32)	113 (32)	225 (64)	450 (128)	898 (256)	450 (128)	450 (128)	450 (128)	113 (32)	56 (16)	225 (64)	113 (32)
14	70 (16)	70 (16)	70 (16)	17 (4)	70 (16)	140 (32)	558 (128)	2232 (512)	2232 (512)	70 (16)	70 (16)	70 (16)	140 (32)
15	277 (64)	277 (64)	277 (64)	138 (32)	>2213 (>512)	>2213 (>512)	553 (128)	2213 (512)	>2213 (>512)	138 (32)	69 (16)	69 (16)	69 (16)
16	84 (16)	84 (16)	84 (16)	167 (32)	167 (32)	669 (128)	84 (16)	335 (64)	335 (64)	84 (16)	84 (16)	42 (8)	84 (16)
Norfloxacin	—	—	—	—	—	—	0.4 (0.125)	>200 (>64)	>200 (>64)	200 (64)	25 (8)	2 (0.5)	6 (2)
Isoniazid	29 (4)	4 (0.5)	0.7 (0.1)	0.7 (0.1)	0.7 (0.1)	0.7 (0.1)	—	—	—	—	—	—	—
Rifampicin	10 (8)	0.1 (0.1)	0.6 (0.5)	0.1 (0.1)	—	—	—	—	—	—	—	—	—

Table 1. Minimum Inhibitory Concentrations (MIC) in μM (mg L^{-1}) of the synthesized compounds (**13**–**16**) against non-pathogenic mycobacteria and pathogenic multidrug-resistant clinical isolates of *Mycobacterium tuberculosis*, as well as Gram-positive and Gram-negative bacteria.

paradigm, efflux pump-related multidrug-resistance significantly contributes to a reduction in drug accumulation and often renders antibiotics redundant[7]. This could be circumvented by molecules that interfere with or inhibit antibiotic efflux[8,9]. Additionally, multidrug efflux pumps are often transmembrane proteins that secrete metabolites involved in quorum-sensing[10]. This *cross-talk* between bacteria is believed to be essential for the formation and dispersion of bacterial biofilms[11]. Therefore, inhibition of multidrug efflux pumps is also a strategy to inhibit biofilm formation, which is a major contributor to antimicrobial resistance[11].

The aim of this study was to synthesise the novel disulphide compounds mentioned earlier and comprehensively evaluate their biological activity to optimise the chemical scaffold as a prospective therapeutic lead.

Results

Synthesis of the antibacterial methyl disulfides. To probe the antibacterial potency, efflux and biofilm inhibitory properties, we chose an initial series of aromatic and heterocyclic thiols on the basis of their commercial availability, namely 4-amino-5-(benzylthio)-4*H*-1,2,4-triazole-3-thiol (**9**), 4-aminothieno[2,3-*d*]pyrimidine-2-thiol (**10**), 7-fluorobenzo[*d*]thiazole-2-thiol (**11**) and 4-ethyl-5-mercapto-4*H*-1,2,4-triazol-3-ol (**12**). Each aromatic thiol was treated with *S*-methyl methanethiosulfonate under alkaline conditions to generate the methyl disulfides, compounds **13**–**16** (Fig. 1 and Supplementary Information).

Antibacterial Bioassay of the methyl disulfides. The spot culture growth inhibition (SPOTi) assay is a whole-cell phenotypic screen that is routinely used to identify novel antimicrobial molecules with clinical relevance[12,13]. This rapid but gold-standard assay was applied to evaluate the antimicrobial activity of the synthesized compounds against Gram-positive, Gram-negative and acid-fast bacteria. All of the synthesized methyl disulfides demonstrated antibacterial activity to varying extents (Table 1). Based on the encouraging results when tested against the non-pathogenic model of *M. tuberculosis* organisms, *M. aurum* (ATCC23366) and *M. bovis* BCG (ATCC35734), the compounds were subsequently tested against *M. tuberculosis* H37Rv and its multidrug-resistant clinical isolates (Mtb-MDR1 and Mtb-MDR2). All four compounds showed anti-mycobacterial activities when tested, with compound **14** having the lowest MIC of 17 μM (4 mg L^{-1}), against the virulent *M. tuberculosis* $H37R_V$. Additionally, compounds **13**–**16** exhibited antibacterial activity against the Gram-positive *Staphylococcus aureus* strains (including effluxing multidrug-resistant strains) and *Enterococcus faecalis*. In particular, compounds **14** and **16** were active against *S. aureus* with MIC values ranging between 70–84 μM (16 mg L^{-1}).

Efflux Pump Inhibitory Activity. Multi-drug efflux pumps are a key mechanism through which many pathogens, *M. tuberculosis* in particular, develop intrinsic resistance or tolerance towards xenobiotic compounds[14,15]. Ethidium bromide (EtBr) is a known substrate for these pumps and its accumulation inside the bacterial cell, when the extrusion mechanism is impaired, can be followed by detecting its fluorescence[16]. EtBr is usually quenched in an aqueous environment and fluoresces when interacting with the hydrophobic regions within the bacilli[17]. Verapamil, a calcium channel blocker, is widely used as an inhibitor of efflux in mycobacterial cells and was used as a control in our experiments[15]. All of the compounds showed inhibition of efflux in the whole-cell model (Fig. 2), with compound **14** and **16** being the most active inhibitors, without affecting the cell viability (a concentration of 25% of the MIC was used for the assay).

Methyl disulfides as bacterial biofilm inhibitors. As alluded to earlier, efflux mechanisms are involved in quorum-sensing that in turn plays a pivotal role in biofilm formation[11]. The transcriptional activator LuxR is heavily implicated in quorum sensing and induction of biofilm formation in a variety of bacteria, and is also found in *M. tuberculosis* and *M. leprae*[18,19]. Tubercle bacilli have a natural tendency to form biofilms and other multi-cellular structures, known as cords in liquid culture[20]. Multi-cellular aggregates resembling biofilms have been detected in the acellular rims of granulomas and necrotic lesions[21]. Other species belonging to the *M. tuberculosis* complex (MTBC) such as *M. avium* are known to form stable biofilms in water reservoirs and can invade lung tissues[22]. The ability to form cords and biofilms has been correlated with the pathogen's virulence[22].

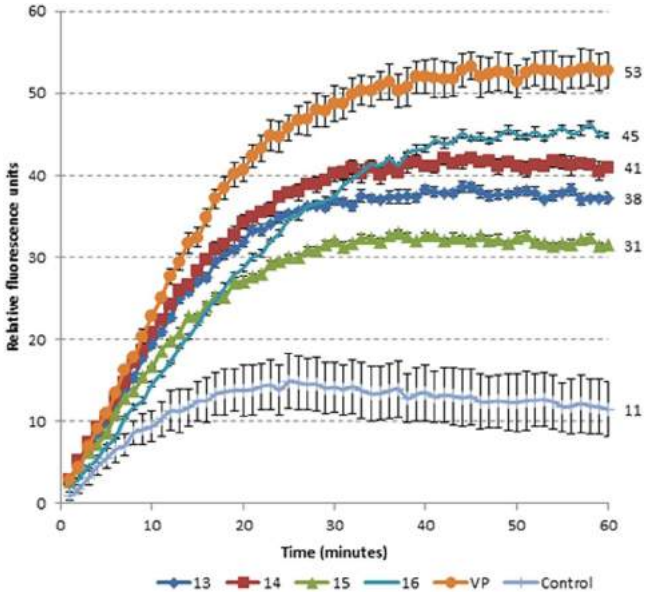

Figure 2. Efflux pump inhibition (EPI) of *M. aurum* under the pressure of methyl disulfides **13**–**16**. Ethidium bromide (EtBr), an efflux pump substrate was used at a final concentration of 1.3 μM (0.5 mg L^{-1}). Its accumulation within the bacterial cells is an indicator of disruption of the efflux mechanism and was detected using fluorescence emissions. Verapamil (VP), a known efflux pump inhibitor, and a drug-free culture were used as positive and negative controls respectively. Low (11–20 rfu) to very high (>50 rfu) inhibition of efflux are represented by the numbers at the side of the graph. The experiments were performed in triplicate ($n = 3$) and the graph was plotted using the averages. (rfu = relative fluorescence units).

Biofilm-deficient mutants of the pathogen show reduced ability to invade epithelial cells as well as to cause infection in mouse models[19].

M. smegmatis, a non-pathogenic model for *M. tuberculosis*, forms stable biofilms at the liquid-air interface within 5 days and was used to test whether the impairment of drug efflux could also inhibit the formation of biofilms in mycobacteria[15]. As compound **14** was found to be the most potent anti-mycobacterial (see Table 1), it was selected for the biofilm inhibition studies. Compound **14** was observed to inhibit the growth of *M. smegmatis* biofilms in a concentration-dependent manner even at sub-MIC levels (Fig. 3a and b) when compared to controls. This finding was further validated through a quantitative crystal violet staining method[23]. Scanning electron microscopic[24] images (Fig. 3c) of *M. smegmatis* biofilms revealed a dense lattice-like network of bacterial cells with rough outer coats that are likely to be composed of extracellular polymeric substances (EPS) such as lipids, proteins and extra-cellular DNA. On treatment with compound **14**, the outer layer of the bacilli became smoother and they appeared to lose the mesh-like inter-cellular connections within the community.

Selectivity. The synthesized compounds showed a range of eukaryotic toxicity profiles against murine macrophage RAW264.7 cells (Table 2). Compound **14** demonstrated a promising SI of 16.

Discussion

The multidrug-resistant *S. aureus* SA-1199B (a strain that overexpresses NorA, a multidrug efflux transporter), proved to be as susceptible to the methyl disulfides as other non-NorA *S. aureus* isolates (Table 1). This indicated that the methyl disulfides may have a mechanism of action that evades NorA-mediated multi-drug efflux.

Interestingly, compound **16** inhibited the Gram-negative bacteria *Klebsiella pneumoniae* and *Proteus mirabilis* at an MIC of 335 μM (64 mg L^{-1}) and whilst this is a moderate activity, it is rare to find compounds demonstrating antibacterial activity toward these organisms. Even the standard antibiotic control used for the assay, norfloxacin, could only inhibit the growth of these organisms at a minimum inhibitory concentration higher than 200 μM (64 mg L^{-1}). The synthesized methyl disulfides exhibited appreciable antibacterial activity against *E. coli*; particularly compound **16** had good antibacterial activity with an MIC value of 84 μM (16 mg L^{-1}).

Overall, the methyl disulfides exhibited inhibitory effects against Gram-positive bacterial strains and acid-fast *Mycobacterium* species. However, their moderate activity against the selected Gram-negative bacteria provided further incentive to investigate the endogenous mechanism(s) of action of these compounds.

Compounds **14** and **16** exhibited whole-cell drug efflux pump inhibitory activities higher than **13** and **15**. Cells treated with the known efflux pump inhibitor verapamil and inhibitor-free cells were used as positive and negative controls in this assay respectively (see Fig. 2).

In terms of the effects of the compounds on *Mycobacterium smegmatis* biofilm formation, the ability of compound **14** to concentration-dependently inhibit biofilm formation, even at sub-MIC levels is particularly noteworthy.

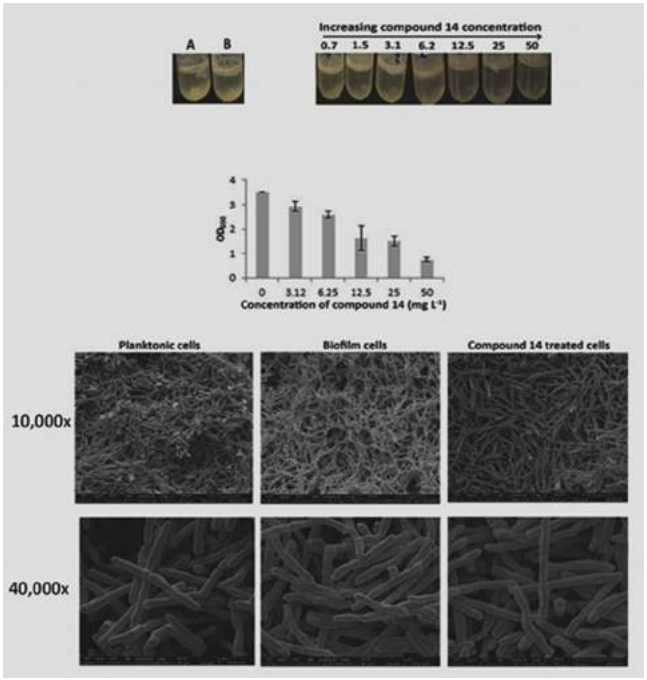

Figure 3. Inhibition of *M. smegmatis* biofilm formation in the presence of varying concentrations of compound **14**. (**a**) Dose-dependent inhibition of *M. smegmatis* biofilm formation, as observed by their thinning in the presence of compound **14**. Tubes A and B are 'no drug' and solvent (0.1% DMSO) controls respectively. Note that the biofilm formation initiated at the air-liquid interface in *M. smegmatis*. A newly-formed biofilm becomes stacked on top of the old layer and generates a downwards push. Once a critical biomass was exceeded, the lower part of the mature biofilm was observed to dissociate and settle at the bottom of the stand-culture-tube (see controls in which no inhibitor was added). (**b**) Crystal violet staining of the biofilms showing a decrease in the intensity of the stain with increasing concentrations of compound **14**. (**c**) SEM images of *M. smegmatis* planktonic, untreated biofilms and biofilms treated with 50 mg L^{-1} of compound **14**.

Compound	MIC[a] *M. tb* H37Rv µM (mg L^{-1})	GIC [b] µM (mg L^{-1})	SI[c]
13	225 (64)	439 (125)	1.95
14	17 (4)	272 (62.5)	16
15	138 (32)	135 (31.3)	0.98
16	167 (32)	40 (7.8)	0.24
INH	0.7 (0.1)	No inhibition	*

Table 2. Cytotoxicity profile of compounds **13**–**16** and selectivity against the murine macrophage cell line RAW 264.7 using the resazurin assay. INH was used as a control drug and shows no effect on the viability of the cells. A drop in the fluorescence levels indicate loss of viability of cells as determined by the reduction in the oxidation of resazurin to resorufin which in turn fluoresces. The experiments were performed in triplicate. [a]MIC - minimum inhibitory concentration. [b]GIC - growth inhibitory concentration. [c]SI - selectivity index, where SI = GIC/MIC (SI calculated using the µM values in Table 2). [d]INH- Isoniazid (control, front-line anti-tubercular drug)*. As no significant inhibition is observed the SI in these cases cannot be calculated.

The efflux pump and biofilm inhibitory effects indicate the possible mechanisms of action of these compounds. This route of antibacterial activity against *Pseudomonas aeruginosa* was also noted by Jakobsen *et al.* (2012) for similar compounds[25]. In addition, allicin, one of the major volatile compounds present in garlic and also a disulfide has been reported to act through permeabilization of cell membranes and inactivation of metabolic enzymes resulting in depletion of intracellular glutathione pools[26,27]. Our ongoing genomic and transcriptomic analyses of bacterial cells under pressure of inhibitor compounds, as well as spontaneous resistant mutants followed by molecular and biochemical investigations of the relevant genes and their recombinant products should provide a deeper insight into the molecular mechanism(s) of action of these compounds.

For compounds **13**, **15** and **16**, the bacterial growth inhibition and macrophage cytotoxicity were similar, indicating poor selectivity for their antibacterial action (Table 2). However for compound **14**, the SI was 16. The SI provides information on the therapeutic potential of compounds as a function of the concentration range at which they are active against pathogenic mycobacteria while remaining non-toxic to mammalian cells. This

provides information on the therapeutic potential of these compound, as a function of the concentration range at which it is active against the growth of pathogenic mycobacteria while remaining non-toxic to mammalian cells (murine macrophages in this case). In conclusion, these synthesized methyl disulfides are new chemical scaffolds that have potential as templates for the discovery of new anti-tubercular leads.

Methods

Materials and synthesis of methyl disulfides. Aromatic thiols 4-amino-5-(benzylthio)-4*H*-1,2,4-triazole-3-thiol (**9**), 4-aminothieno[2,3-*d*]pyrimidine-2-thiol (**10**), 7-fluorobenzo[*d*]thiazole-2-thiol (**11**), 4-ethyl-5-mercapto-4*H*-1,2,4-triazol-3-ol (**12**) were purchased from Sigma-Aldrich, Gillingham, U.K. The method of Kitson and Loomes (1985), for the synthesis of methyl 2- and 4-pyridyl disulfide from 2- and 4-thiopyridone and methyl methanethiosulfonate was adapted and modified as follows. The appropriate thiol (2.5 mmol) was dissolved in water (5 mL) containing NaOH (0.10 g, 2.5 mmol, 1 equiv.) and *S*-methyl methanethiosulfonate (0.315 g, 2.5 mmol, 1 equiv.) added. The solution was stirred for 1 h at room temperature. The cloudy suspension formed was extracted with CH_2Cl_2 (20 mL). The organic phase was then dried with anhydrous sodium sulfate, filtered, and concentrated under reduced pressure to afford the pure disulfide which was subsequently characterized by spectroscopic techniques – NMR, MS, HRMS, UV and IR (Supplementary Information).

Antibacterial assays (whole-cell phenotypic assays). Minimum inhibitory concentrations (MIC) of the compounds against *Mycobacterium* strains were determined using the spot-culture growth inhibition assay (SPOTi)[12,13,28,29]. The lowest concentration at which mycobacterial growth was completely inhibited by the compound was observed directly. Isoniazid and rifampicin were used as antibiotic controls and the experiments repeated in triplicate.

The antibacterial activity of the compounds was tested against Gram-negative bacteria: *Klebsiella pneumoniae*, *Proteus mirabilis* (10830), *Escherichia coli* (NCTC 10418) and Gram-positive bacteria: *Enterococcus faecalis* (12697), methicillin-resistant *Staphylococcus aureus* strains (XU-212 and EMRSA-15) and multidrug-resistant *Staphylococcus aureus* strain SA-1199B using the microtitre broth dilution assay. Norfloxacin served as a positive control. The assay was performed in 96-well plates and each methyl disulfide was tested in quadruplicate to confirm the reliability and reproducibility of the data. The MIC was determined after the addition of 3-(4,5-dim ethylthiazol-2-yl)-2,5-diphenyltetrazolium bromide (MTT) to the 96-well plates. Bacterial growth was indicated by a colour change from yellow to dark blue, which was visually observed. The MIC was recorded as the lowest concentration at which no growth was observed[13,30].

Cytotoxicity assay. Eukaryotic cell toxicity assay was carried out using RAW 264.7 macrophage cells, grown in complete RPMI-1640 medium supplemented with 2 mM l-glutamine and 10% heat-inactivated fetal bovine serum and 1% l-glutamine in a 25 cm^2 vented, screw-cap cell-culture flask (Flowgen Bioscience Ltd., Hessle, UK) and incubated at 37 °C with a supply of 5% CO_2 until confluent growth was observed. Cytotoxicity of the compounds towards the murine macrophages was determined using the resazurin assay[29]. For quantitative analysis, the fluorescence intensity was measured at $\lambda_{ex}560/\lambda_{em}590$ nm using a FLUOstar OPTIMA micro plate reader. The growth inhibitory concentration (GIC) was reported as the lowest concentration of compound at which no viable eukaryotic cells were detected.

Efflux pump inhibition assay. Efflux pump inhibition assays were performed following previously published protocols and modified using *M. aurum* cells[9,15,31]. The effect of the synthesized compounds and verapamil (positive control) on the accumulation of ethidium bromide (EtBr) was determined by measuring fluorescence using a fluorimeter (FLUOstar OPTIMA, BMG Labtech) and fluorescence data was acquired every 60 s for a total period of 60 min. The compounds were used at one quarter of their MICs and EtBr (a known efflux pump substrate) at a concentration of 1.3 µM (0.5 mg L^{-1}).

Biofilm assay (inhibition of biofilm formation). A late log-phase ($OD_{600} = 3.0$) culture of *Mycobacterium smegmatis* was inoculated into Sauton's media as 1:100 dilutions. This preparation (2 mL) was transferred into polypropylene tubes and a range of concentrations of compound **14** 3–218 µM (0.7–50 mg L^{-1}) was then added to each tube. The cap was tightly closed to avoid evaporation of media and the cultures were incubated at 37 °C in a stationary incubator for 5 days. Tubes containing the diluted cultures without any compounds served as inhibitor-free controls and those with only DMSO served as solvent controls. After 5 days, the biofilm samples were observed using the scanning electron microscope[24]. The experiments were performed in triplicate.

Once the biofilms were formed, the medium containing planktonic cells was removed carefully using a hypodermic needle. 1% crystal violet was added to the tubes so as to cover the biofilm and was left for 10 min. The crystal violet solution was discarded and the tubes were washed at least three times until no further stain was present in the washings. Ethanol (95% *v/v* in water) was then added to the tubes and left for 10 min. The solutions were then diluted 1:3 with ethanol and the absorbance of each was measured at 600 nm.

The SEM images were analysed with ImageJ (NIH) software[32]. Each image was calibrated individually and measurements were recorded for at least 200 cells for each condition from a minimum of five fields with varying magnifications.

References

1. O'Donnell, G. & Gibbons, S. Antibacterial activity of two canthin-6-one alkaloids from *Allium neapolitanum*. *Phytother. Res.* **21**, 653–657 (2007).
2. O'Donnell, G. *et al*. Bioactive pyridine-N-oxide disulfides from *Allium stipitatum*. *J. Nat. Prod.* **72**, 360–365 (2009).
3. Gibbons, S. Phytochemicals for bacterial resistance–strengths, weaknesses and opportunities. *Planta Med.* **74**, 594–602 (2008).
4. Davies, J. & Davies, D. Origins and evolution of antibiotic resistance. *Microbiol. Mol. Biol. R.* **74**, 417–433 (2010).
5. Fair, R. J. & Tor, Y. Antibiotics and bacterial resistance in the 21st century. *Perspect. Medicin. Chem.* **6**, 25–64 (2014).

6. Fernandez, L. & Hancock, R. E. Adaptive and mutational resistance: role of porins and efflux pumps in drug resistance. *Clin. Microbiol. Rev.* **25**, 661–681 (2012).
7. Piddock, L. J. Understanding the basis of antibiotic resistance: a platform for drug discovery. *Microbiology* **160**, 2366–2373 (2014).
8. Viveiros, M. *et al*. Inhibitors of mycobacterial efflux pumps as potential boosters for anti-tubercular drugs. *Expert Rev. Anti-Infe.* **10**, 983–998 (2012).
9. Lechner, D., Gibbons, S. & Bucar, F. Plant phenolic compounds as ethidium bromide efflux inhibitors in *Mycobacterium smegmatis*. *J. Antimicrob. Chemother.* **62**, 345–348 (2008).
10. Polkade, A. V., Mantri, S. S., Patwekar, U. J. & Jangid, K. Quorum Sensing: An Under-Explored Phenomenon in the Phylum Actinobacteria. *Front. Microbiol.* **7**, 131 (2016).
11. Baugh, S., Phillips, C. R., Ekanayaka, A. S., Piddock, L. J. & Webber, M. A. Inhibition of multidrug efflux as a strategy to prevent biofilm formation. *J. Antimicrob. Chemother.* **69**, 673–681 (2014).
12. Evangelopoulos, D. & Bhakta, S. Rapid methods for testing inhibitors of mycobacterial growth. *Methods Mol. Biol.* **642**, 193–201 (2010).
13. Guzman, J. D. *et al*. Antitubercular specific activity of ibuprofen and the other 2-arylpropanoic acids using the HT-SPOTi whole-cell phenotypic assay. *BMJ Open* **3**, https://doi.org/10.1136/bmjopen-2013-002672 (2013).
14. Blair, J. M., Webber, M. A., Baylay, A. J., Ogbolu, D. O. & Piddock, L. J. Molecular mechanisms of antibiotic resistance. *Nat. Rev. Microbiol.* **13**, 42–51 (2015).
15. Rodrigues, L. *et al*. Thioridazine and chlorpromazine inhibition of ethidium bromide efflux in *Mycobacterium avium* and *Mycobacterium smegmatis*. *J. Antimicrob. Chemother.* **61**, 1076–1082 (2008).
16. Paixao, L. *et al*. Fluorometric determination of ethidium bromide efflux kinetics in *Escherichia coli*. *J. Biol. Eng.* **3**, 18 (2009).
17. Machado, D. *et al*. Ion Channel Blockers as Antimicrobial Agents, Efflux Inhibitors, and Enhancers of Macrophage Killing Activity against Drug Resistant *Mycobacterium tuberculosis*. *PloS One* **11**, e0149326, https://doi.org/10.1371/journal.pone.0149326 (2016).
18. Santos, C. L., Correia-Neves, M., Moradas-Ferreira, P. & Mendes, M. V. A walk into the LuxR regulators of Actinobacteria: phylogenomic distribution and functional diversity. *PloS One* **7**, e46758, https://doi.org/10.1371/journal.pone.0046758 (2012).
19. Yamazaki, Y. *et al*. The ability to form biofilm influences *Mycobacterium avium* invasion and translocation of bronchial epithelial cells. *Cell. Microbiol.* **8**, 806–814 (2006).
20. Middlebrook, G., Dubos, R. J. & Pierce, C. Virulence and Morphological Characteristics of Mammalian Tubercle Bacilli. *J. Exp. Med.* **86**, 175–184 (1947).
21. Orme, I. M. A new unifying theory of the pathogenesis of tuberculosis. *Tuberculosis* **94**, 8–14 (2014).
22. Vaerewijck, M. J., Huys, G., Palomino, J. C., Swings, J. & Portaels, F. Mycobacteria in drinking water distribution systems: ecology and significance for human health. *FEMS Microbiol. Rev.* **29**, 911–934 (2005).
23. O'Toole, G. A. Microtiter dish biofilm formation assay. *J. Vis. Exp*. https://doi.org/10.3791/2437 (2011).
24. Kulka, K., Hatfull, G. & Ojha, A. K. Growth of *Mycobacterium tuberculosis* biofilms. *J. Vis. Exp*. https://doi.org/10.3791/3820 (2012).
25. Jakobsen, T. H. *et al*. Ajoene, a sulfur-rich molecule from garlic, inhibits genes controlled by quorum sensing. *Antimicrob. Agents Chemother.* **56**, 2314–2325 (2012).
26. Gruhlke, M. C. *et al*. The defense substance allicin from garlic permeabilizes membranes of *Beta vulgaris*, *Rhoeo discolor*, *Chara corallina* and artificial lipid bilayers. *Biochim. Biophys. Acta* **1850**, 602–611 (2015).
27. Müller, A. *et al*. Allicin induces thiol stress in bacteria through S-Allylmercapto modification of protein cysteines. *J. Biol. Chem.* **291**, 11477–11490 (2016).
28. Danquah, C. A., Maitra, A., Gibbons, S., Faull, J. & Bhakta, S. HT-SPOTi: A Rapid Drug Susceptibility Test (DST) to Evaluate Antibiotic Resistance Profiles and Novel Chemicals for Anti-Infective Drug Discovery. *Curr. Protoc. Microbiol.* **40**, 17.8.1–17.8.12, https://doi.org/10.1002/9780471729259.mc1708s40 (2016).
29. Guzman, J. D. *et al*. Anti-tubercular screening of natural products from Colombian plants: 3-methoxynordomesticine, an inhibitor of MurE ligase of *Mycobacterium tuberculosis*. *J. Antimicrob. Chemother.* **65**, 2101–2107 (2010).
30. Gibbons, S. & Udo, E. E. The effect of reserpine, a modulator of multidrug efflux pumps, on the *in vitro* activity of tetracycline against clinical isolates of methicillin resistant *Staphylococcus aureus* (MRSA) possessing the tet(K) determinant. *Phytother. Res.* **14**, 139–140 (2000).
31. Groblacher, B., Maier, V., Kunert, O. & Bucar, F. Putative mycobacterial efflux inhibitors from the seeds of *Aframomum melegueta*. *J. Nat. Prod.* **75**, 1393–1399 (2012).
32. Schneider, C. A., Rasband, W. S. & Eliceiri, K. W. NIH Image to ImageJ: 25 years of image analysis. *Nat. Methods* **9**, 671–675 (2012).

Acknowledgements

C.A.D. and A.M. thank the Ghanaian Education Trust and Wellcome Trust/Birkbeck for supporting their doctoral research studies respectively.

Author Contributions

S.G., S.B., J.M., P.S. and T.D.M. designed the study. C.A.D., E.K., P.K., A.M., M.R. and D.E. collected and analyzed the data. All authors wrote the manuscript text and S.G., J.M., S.B. and A.M. prepared the figures. All authors reviewed and critically revised the manuscript.

Additional Information

Supplementary information accompanies this paper at https://doi.org/10.1038/s41598-017-18948-w.

Competing Interests: The authors declare that they have no competing interests.

Publisher's note: Springer Nature remains neutral with regard to jurisdictional claims in published maps and institutional affiliations.

Journal of Global Antimicrobial Resistance 5 (2016) 15–21

Contents lists available at ScienceDirect

Journal of Global Antimicrobial Resistance

journal homepage: www.elsevier.com/locate/jgar

Novel R-plasmid conjugal transfer inhibitory and antibacterial activities of phenolic compounds from *Mallotus philippensis* (Lam.) Mull. Arg.

Blessing O.M. Oyedemi [a], Vaibhav Shinde [b], Kamlesh Shinde [b], Dionysia Kakalou [a], Paul D. Stapleton [a], Simon Gibbons [a,*]

[a] *Research Department of Pharmaceutical and Biological Chemistry, UCL School of Pharmacy, 29–39 Brunswick Square, London WC1N 1AX, UK*
[b] *Department of Pharmacognosy, Poona College of Pharmacy, Pune 38, India*

ARTICLE INFO

Article history:
Received 13 August 2015
Received in revised form 17 December 2015
Accepted 22 January 2016
Available online 4 March 2016

Keywords:
Multidrug resistance
Bacterial plasmids
Conjugation
Natural products
Antibacterial agent
Anti-plasmid

ABSTRACT

Antimicrobial resistance severely limits the therapeutic options for many clinically important bacteria. In Gram-negative bacteria, multidrug resistance is commonly facilitated by plasmids that have the ability to accumulate and transfer refractory genes amongst bacterial populations. The aim of this study was to isolate and identify bioactive compounds from the medicinal plant *Mallotus philippensis* (Lam.) Mull. Arg. with both direct antibacterial properties and the capacity to inhibit plasmid conjugal transfer. A chloroform-soluble extract of *M. philippensis* was subjected to bioassay-guided fractionation using chromatographic and spectrometric techniques that led to the isolation of the known compounds rottlerin [5,7-dihydroxy-2,2-dimethyl-6-(2,4,6-trihydroxy-3-methyl-5-acetylbenzyl)-8-cinnamoyl-1,2-chromene] and the red compound (8-cinnamoyl-5,7-dihydroxy-2,2,6-trimethylchromene). Both compounds were characterised and elucidated using one-dimensional and two-dimensional nuclear magnetic resonance (NMR). Rottlerin and the red compound showed potent activities against a panel of clinically relevant Gram-positive bacteria, including meticillin-resistant *Staphylococcus aureus* (MRSA). No significant direct activities were observed against Gram-negative bacteria. However, both rottlerin and the red compound strongly inhibited conjugal transfer of the plasmids pKM101, TP114, pUB307 and R6K amongst *Escherichia coli* at a subinhibitory concentration of 100 mg/L. Interestingly, despite the planar nature of the compounds, binding to plasmid DNA could not be demonstrated by a DNA electrophoretic mobility shift assay. These results show that rottlerin and the red compound are potential candidates for antibacterial drug lead development. Further studies are needed to elucidate the mode of inhibition of the conjugal transfer of plasmids.

1. Introduction

The problem of antimicrobial resistance continues to threaten the future of global health and healthcare systems [1]. Microbial infections caused by multidrug-resistant (MDR) Gram-positive bacteria such as *Staphylococcus aureus* as well as Gram-negative bacteria, including among others *Escherichia coli*, *Klebsiella pneumoniae* and *Pseudomonas aeruginosa*, represent an increasingly growing problem. Bacterial plasmids have become broadly recognised as a major contributor to the emergence and burden of antibiotic resistance, especially in Gram-negative bacteria, owing to their ease of mobility across and within bacterial species using highly efficient type IV secretion systems (T4SSs) during conjugation [2]. The T4SSs translocate DNA and protein substrates across the bacterial cell envelope and are widespread within Gram-negative bacteria [3]. Exemplary plasmids comprising different incompatibility (Inc) groups that are of clinical relevance include pUB307 [4], pKM101 [5], TP114 [6], R7K [7] and R6K [8]. Over the years, heterocyclic compounds, intercalators such as ethidium bromide and sodium dodecyl sulphate [9], acridine dyes, surface-active alkyl sulphates [10] and quinolones [11] have been reported as plasmid 'curing' agents. However, most of these compounds are

* Corresponding author. Tel.: +44 020 7753 5913; fax: +44 020 7753 5964.
E-mail address: simon.gibbons@ucl.ac.uk (S. Gibbons).

http://dx.doi.org/10.1016/j.jgar.2016.01.011
2213-7165/

associated with toxicity and mutation [12], thereby rendering them unsuitable as potential drug templates for anti-plasmid activity. Recent studies have shown that plant-derived drugs can interact with plasmids causing plasmid loss from the host cell or inhibiting T4SSs [13]. Furthermore, natural plant products are a rich source of bioactive chemical scaffolds that have yielded antimicrobial drug leads and have been exploited for various diseases. Natural compounds such as phenolics [14] and acylphloroglucinols [15] are capable of modifying the bacterial resistance phenotypes of meticillin-resistant *S. aureus* (MRSA). A novel and promising approach to deal with multidrug resistance and plasmid-encoded antibiotic resistance is to discover new antimicrobial hits that can complement the clinical efficacy of existing antibiotics.

Mallotus philippensis (Lam.) Mull. Arg. (Euphorbiaceae family), commonly known as 'kamala' (Fig. 1A), is a well-known medicinal plant from Asia and Australia producing a wide range of natural products including phenols, diterpenoids, steroids, flavonoids, cardenolides, triterpenoids, coumarins and isocoumarins [16]. The various compounds isolated from different parts of the plant, especially the 'red compound' and rottlerin, have shown antitumour, cytotoxic, antiviral, antileukaemic, antioxidant, anti-inflammatory and immunoregulatory activities [17], antibacterial activity against resistant *Helicobacter pylori* strains [18] and antitubercular activities. In this study, the antibacterial properties of the plant were further investigated, specifically to find agents that had potent activities against Gram-positive bacteria and had the capacity to act as anti-plasmid agents, preventing plasmid transfer between Gram-negative bacteria.

2. Materials and methods

2.1. Chromatographic and spectrometric methods

^{1}H and ^{13}C nuclear magnetic resonance (NMR) spectra were obtained on a Bruker AVANCE CP QNP 500 MHz instrument (Bruker UK Ltd., Coventry, UK). Chromatographic separations using thin layer chromatography (TLC), column chromatography and vacuum liquid chromatography (VLC) were carried out on silica gel GF_{254} (0.25 mm; Merck, Feltham, UK). The mass spectrum was recorded with a matrix-assisted laser desorption/ionisation time-of-flight (MALDI-TOF) mass spectrometer (Voyager-DE Pro; Applied Biosystems, Warrington, UK) at the UCL School of Pharmacy (London, UK).

2.2. Plant material, extraction and isolation

Dried and powdered fruit was collected by two of the authors (VS and KS) from the premises of Poona College of Pharmacy (Pune, India) and a voucher specimen (No. Mat-001) was deposited at the herbarium in the UCL School of Pharmacy.

Red powder (500 g) was exhaustively extracted by cold agitation with solvents of increasing order of polarity (2 L of hexane, chloroform and methanol). The solutions were placed in an ultrasonic bath for 48 h. The resulting extracts were dried under vacuum on a rotary evaporator and were stored in a refrigerator for further analysis. Then, 3 g of the chloroform extract was fractionated using VLC with an increasingly polar gradient of 100% hexane to 100% ethyl acetate and finally 100% methanol, which yielded 21 fractions. These fractions were monitored by TLC using the solvent system containing hexane–ethyl acetate–formic acid (4:6:1). Spots on TLC were visualised by long (365 nm) and short (254 nm) wavelengths as well as being sprayed with 1% (w/v) vanillin–sulphuric acid and heated until a colouration was observed.

Using TLC profiling, similar fractions were pooled together into 10 fractions (F, G, H, I, I2, J, K, M, O and P) and were subjected to antibacterial activity determination against two bacteria (*S. aureus* SA1199B and *S. aureus* XU212) and were evaluated for anti-plasmid activity against *E. coli* harbouring the pKM101 or TP114 plasmids. Fraction K was active in the antibacterial assay with a minimum inhibitory concentration (MIC) of 8 mg/L against SA1199B and 2 mg/L against XU212, whilst fractions J and K were active in the anti-plasmid assay (data not shown). Fractions J and K were pooled to gain sufficient material (10.9 mg) and were subjected to column chromatography using a gradient from 100% toluene to 100% acetone. All fractions obtained were monitored by TLC, yielding a compound with an R_f value of 0.35 with a mixture of hexane–ethyl acetate–formic acid (4:6:1). The fractions that showed single spots were submitted for NMR analysis, which yielded pure compound **1**. The hexane-soluble extract showed antibacterial activity, which led to the bioassay-guided isolation of compound **2**. Both compounds **1** and **2** were then assessed for antibacterial and anti-plasmid activities.

2.3. Bacterial strains and plasmids

All bacterial strains and plasmids were cultured on nutrient agar slopes and were incubated for 24 h at 37 °C prior to MIC

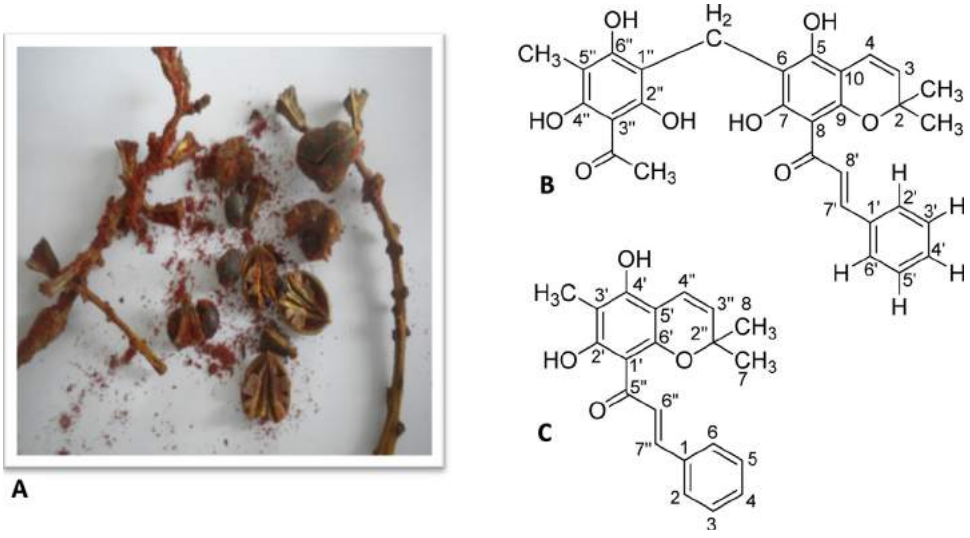

Fig. 1. (a) Photograph of *Mallotus philippensis* (Lam.) Mull. Arg. and (b, c) chemical structure of rottlerin (b) and the red compound (c).

determination. An inoculum turbidity equivalent to a 0.5 McFarland standard (1×10^8 CFU/mL) was prepared in normal saline for each test organism and was then diluted 1:100 in Mueller-Hinton broth just before inoculation of the plates. Strains used in the study included *S. aureus* SA1199B (norfloxacin-resistant, mediated by drug efflux), *S. aureus* SA13373 (meticillin-resistant), MRSA 12981 (meticillin-resistant), MRSA 274829 (meticillin-resistant), MRSA 774812 (meticillin-resistant), MRSA 346724 (meticillin-resistant), ATCC 25923 (standard susceptible *S. aureus* strain), EMRSA-15 and EMRSA-16 (epidemic MRSA strains), XU212 (MRSA and TetK-producer), *S. aureus* RN4220 (macrolide-resistant), *Enterococcus faecalis* 13379 (vancomycin-resistant), *E. faecalis* 12697 (vancomycin-resistant), *E. coli* NCTC 10418, *P. aeruginosa* 10662, *K. pneumoniae* 342, *Bacillus subtilis* BsSOP01 and *Proteus* sp. P10830.

2.4. Minimum inhibitory concentration determination

A volume of 100 μL of sterile Mueller-Hinton broth (Oxoid, Basingstoke, UK) containing 20 mg/L of Ca^{2+} and 10 mg/L of Mg^{2+} was dispensed into the wells of a 96-well microtitre plate (Nunc; 0.3 mL total volume per well). All antibacterial agents were dissolved in dimethyl sulphoxide (DMSO) and were diluted in Mueller-Hinton broth to give a stock solution. Then, 100 μL of the antibacterial agent stock solution (2000 mg/L) was serially diluted into each well and 100 μL of the bacterial inoculum was added to each well to give a final concentration range of 1–512 mg/L. All procedures were performed in duplicate and the plates were incubated for 18 h at 37 °C. Then, 20 μL of a 5 mg/L methanolic solution of 3-[4,5-dimethylthiazol-2-yl]-2,5-diphenyltetrazolium bromide (MTT) (Sigma–Aldrich Ltd, Gillingham, UK) was added to each well and was incubated for 30 min. Blue colouration indicated bacterial growth. The MIC was recorded as the lowest concentration at which no colour change was observed.

2.5. Plasmid conjugation inhibition assay

Plasmid conjugal transfer inhibition was performed by the broth mating method described by Rice and Bonomo [19] with some modifications. A subinhibitory concentration of 100 mg/L was used throughout the assay (0.25 × MIC of rottlerin and the red compound against *E. coli* NCTC 10481; data not shown). Plumbagin at a concentration of 8 mg/L was used as a positive control.

Mating between the plasmid-containing donor strain *E. coli* K12 J53 and the recipient *E. coli* ER1793 was performed in Luria-Bertani broth. Transconjugants were identified by plating bacterial mixtures onto selective media containing the appropriate antibiotics: streptomycin (to select for the recipient) plus either ampicillin (to detect the transfer of pKM101 and pUB307) or kanamycin (to detect the transfer of TP114). Ampicillin and nalidixic acid were used to detect the transfer of R7K or R6K to the recipient *E. coli* JM109. The concentration of the various antibiotics used was 30 mg/L. The transfer frequency was expressed as the number of transconjugant colonies (CFU/mL) per recipient (CFU/mL) and was represented as a percentage of transfer exhibited by plasmid in the absence of the test compound (normalised to 100%). Results were based on at least three independent experiments. Data are expressed as the mean ± S.D. Differences between two mean values were calculated by Student's *t*-test. *P*-values of <0.05 were considered statistically significant and $P < 0.01$ as very significant.

2.6. DNA electrophoretic mobility shift assay (EMSA)

To establish whether the basis of the anti-plasmid activity shown by rottlerin and the red compound was due to direct binding to plasmid DNA, an EMSA [20] was carried out with slight modification. Briefly, 0.5 μg of digested pKM101 DNA was exposed to rottlerin and the red compound (final concentration of 100 mg/L) for 30 min at 37 °C. Samples were electrophoresed on a 0.8% agarose gel at a constant voltage of 40 V for 2–4 h. The gel was subsequently stained with ethidium bromide to visualise the location of the DNA.

3. Results

3.1. Identification of plant compounds

A bioassay-guided isolation approach of extracts of *M. philippensis* was used to detect compounds capable of either directly inhibiting microbial growth or of inhibiting the transfer of plasmids pKM101 and TP114 in *E. coli*. This led to the isolation of compound **1** (2.3 mg) (Fig. 1B). The hexane extract had direct antimicrobial activity towards *S. aureus* SA1199B and gave rise to compound **2** (1.1 mg) (Fig. 1C). The structures of these compounds were identified using detailed one-dimensional and two-dimensional NMR experiments, mass spectrometry and with reference to the literature. The compounds were identified as rottlerin (**1**; Fig. 1B) and the red compound (**2**; Fig. 1C). The red compound gives the kamala plant dust its characteristic red colour. Rottlerin, also known as mallotoxin or kamalin, is 5,7-dihydroxy-2,2-dimethyl-6-(2,4,6-trihydroxy-3-methyl-5-acetylbenzyl)-8-cinnamoyl-1,2-chromene, and the red compound is 8-cinnamoyl-5,7-dihydroxy-2,2,6-trimethylchromene [17]. NMR assignments of the compounds are shown in the Supplementary material for rottlerin and red compound.

3.2. Antimicrobial and anti-plasmid activity of the compounds

The antimicrobial activities of rottlerin and the red compound against MDR *S. aureus* and Gram-negative bacteria are given in Table 1. Noteworthy, rottlerin was active against *E. faecalis* 12697 with an MIC of 1 mg/L, followed by *E. faecalis* 13379, meticillin-resistant *S. aureus* strains MRSA 274829, MRSA 12981 and NorA-overexpressing SA1199B with a consistent MIC of 2 mg/L, which compared favourably with standard antibiotics. Rottlerin demonstrated further MIC values of 4 mg/L against *S. aureus* ATCC 25923 and *B. subtilis* BsSOP01, 8 mg/L against *S. aureus* RN4220 (MsrA), MRSA 346724 and MRSA 774812, 16 mg/L against *S. aureus* XU212 and EMRSA-15, and 32 mg/L against EMRSA-16. The antibacterial activity of the red compound had a common MIC of 32 mg/L against *S. aureus* strains XU212, EMRSA-15 and -16, SA1199B, ATCC 25923 and erythromycin-resistant *S. aureus* RN4220. Both rottlerin and the red compound showed poor activities against the Gram-negative organisms *E. coli*, *P. aeruginosa*, *K. pneumoniae* and *Proteus* sp., with MICs in the range of 256–512 mg/L.

Despite the poor direct antimicrobial potential against Gram-negative organisms, the compounds were evaluated to establish whether they had any capacity to inhibit the conjugative transfer of antibiotic resistance-conferring plasmids amongst *E. coli*. The characteristics of the plasmids investigated are shown in Table 2. The inhibitory effects of rottlerin, the red compound and plumbagin (a compound previously reported to inhibit conjugation) on the plasmid transfer of pKM101, TP114, pUB307, R7K and R6K were evaluated (Figs. 2 and 3). Plumbagin (8 mg/L) had relatively potent capacity to modulate the transfer of several plasmids: transfer frequencies were reduced to 11.0%, 5.7%, 31.8%, 29.8% and 11.2% for pUB307, pKM101, TP114, R6 K and R7K, respectively. Rottlerin (100 mg/L) showed significant transfer inhibitory effects ($P < 0.05$) towards pUB307 (12.67%) and TP114 (3.77%), whilst the inhibitory effects of rottlerin on R7K

Table 1
Minimum inhibitory concentrations (MICs) of the agents against various Gram-positive and Gram-negative bacteria.

Strain	MIC (mg/L)						
	Rottlerin	Red compound	NOR	TET	ERY	OXA	CIP
Staphylococcus aureus SA1199B	2	32	32				
S. aureus ATCC 25923	4	32	32				
Bacillus subtilis BsSOP01	4	NT	0.25				
S. aureus XU212	16	32	0.25				
EMRSA-15	16	32		16			
EMRSA-16	32	32		0.25			
S. aureus RN4220	8	32		0.25			
MRSA 346724	8	NT			32		
MRSA 774812	8	NT				<0.25	
MRSA 274829	2	NT				<0.25	
MRSA 12981	2	NT				128	
Enterococcus faecalis 13379	2	NT				8	
E. faecalis 12697	1	NT					<0.06
Escherichia coli NCTC 10418	512	256					<0.06
Pseudomonas aeruginosa 10662	512	256					≤0.06
Klebsiella pneumoniae 342	512	256					≤0.03
Proteus sp. P10830	512	NT					≤0.03

NOR, norfloxacin; TET, tetracycline; ERY, erythromycin; OXA, oxacillin; CIP, ciprofloxacin; NT, not tested; EMRSA, epidemic meticillin-resistant *S. aureus*.

Table 2
Plasmids used, host and resistance markers.

Plasmid	Plasmid size (kb)	Incompatibility group	Host	Resistance marker
TP114	62.1	IncI2	*Escherichia coli* K12 J53	Km^r
pKM101	35.4	IncN	*E. coli* WP2 uvrA	Ap^r
pUB307:RP1	56.4	IncP	*E. coli* K12 J53	Ap^r, Km^r, Tet^r
R6K	39.4	IncX	*E. coli* K12 J53	Ap^r, Sm^r
R7K	30.3	IncW	*E. coli* K12 J53	Ap^r, Sm^r, Sp^r
R1-drd-19	93.9	IncF11	*E. coli* K12 J53	Ap^r, Cm^r, Km^r, Sm^r, Sp^r, Su^r
Recipient strain				
E. coli ER1793				Sm^r
E. coli JM109				Nal^r

Km, kanamycin; Ap, ampicillin; Tet, tetracycline; Sm, streptomycin; Sp, spectinomycin; Cm, chloramphenicol; Su, sulphonamide; Nal, nalidixic acid.

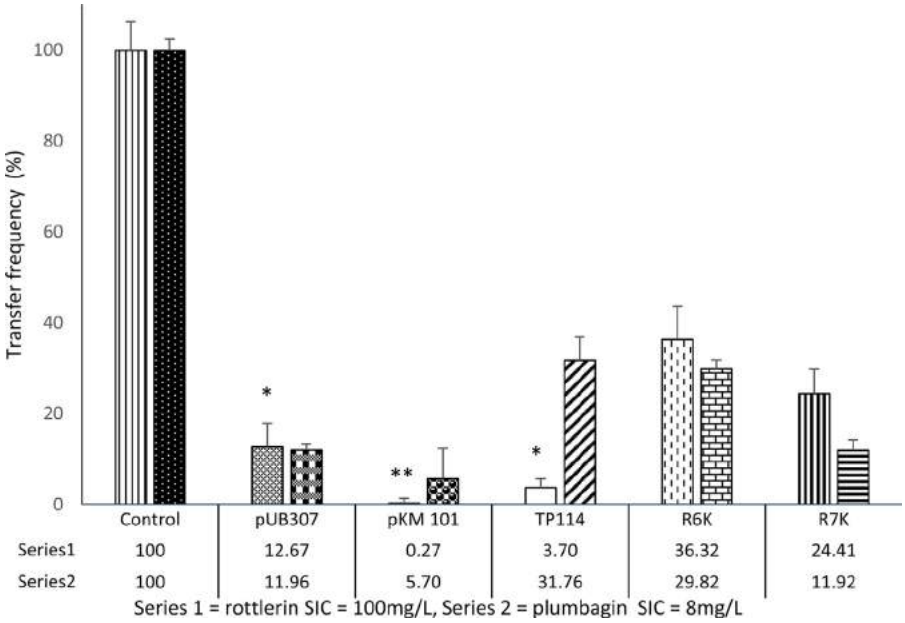

Fig. 2. Plasmid transfer inhibition in the presence of rottlerin (100 mg/L) and plumbagin (8 mg/L). Plasmid transfer in the absence of the drugs is normalised to 100%. Results are expressed as the mean ± S.D. ($n = 3$). $^*P < 0.05$ and $^{**}P < 0.01$ versus positive control at the same point. SIC, subinhibitory concentration.

(24.41%) and R6K (36.32%) were only moderate (Fig. 2). Almost complete inhibition against pKM101 (0.27%; $P < 0.01$) was observed. Likewise, the red compound (100 mg/L) also caused significant transfer inhibition ($P < 0.05$) against pUB307 (29.16%), TP114 (17.33%) and pKM101 (6.23%; $P < 0.01$), indicative of the broad host effect of red compound on the three plasmids tested.

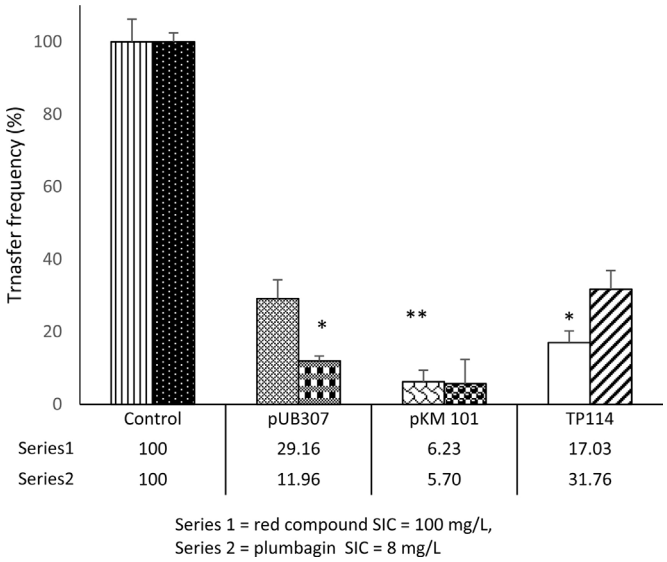

Fig. 3. Plasmid transfer inhibition in the presence of the red compound (100 mg/L) and plumbagin (8 mg/L). Plasmid transfer in the absence of the drugs is normalised to 100%. Results are expressed as the mean ± S.D. ($n = 3$). $^{*}P < 0.05$ and $^{**}P < 0.01$ versus positive control at the same point. SIC, subinhibitory concentration.

3.3. DNA-binding capacities of the compounds

Selective binding of rottlerin and the red compound to plasmid DNA may possibly explain the specificity of activity towards different plasmids. To investigate this, binding of rottlerin, the red compound and actinomycin D (a well-documented DNA-binding agent) to purified pKM101 DNA (the plasmid for which the greatest inhibition of transfer was observed) was conducted and assessed by an EMSA. In contrast to actinomycin D, which exhibited a significant reduction in DNA mobility due to DNA binding by the drug, no shift (or reduction in ethidium bromide fluorescence) in pKM101 mobility was observed (Fig. 4). Consequently, based on this assay, rottlerin and the red compound are less likely to exert their inhibitory effects on plasmid conjugation by directly binding to plasmid DNA.

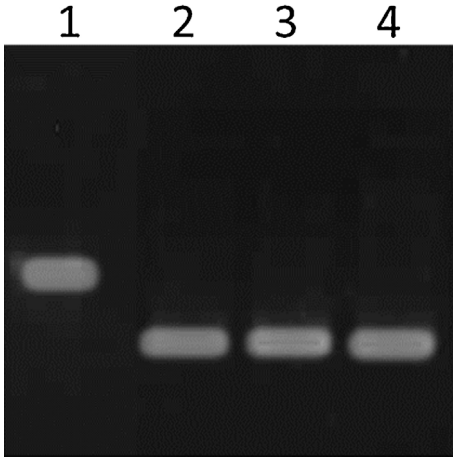

Fig. 4. Electrophoretic mobility shift assay (EMSA) to assess binding of rottlerin and the red compound to plasmid pKM101 DNA. Lane 1, pKM101 plus actinomycin D (a known DNA-binding agent); lane 2, pKM101; lane 3, pKM101 plus the red compound; and lane 4, pKM101 plus rottlerin.

4. Discussion

Mallotus is a fairly large genus rich in valuable phytochemicals such as coumarins and isocoumarins, terpenes, steroids, flavonoids, lignans, chalcones and dimeric chalcone derivatives [16]. These constituent compounds therefore partially justify the ethnomedicinal uses of individual species for the treatment of various ailments.

The red compound primarily serves as a precursor to various chalcone and phloroglucinol derivatives in *Mallotus* spp. Rottlerin is structurally similar to the red compound, except for the presence of the acetophenone moiety. The acetophenone unit is composed of a phloroglucinol backbone and is connected to an aromatic ring via a deshielded CH_2 group, a cinnamoyl group (Ph-CH=CH–CO) and a geminal methyl pair, together with olefinic hydrogens forming a dimethyl-pyran unit. These moieties are very similar to the structural features seen in the red compound, although this has an aromatic-bearing methyl group instead of a benzylic methylene in the case of rottlerin.

Both rottlerin and the red compound displayed notable antibacterial activities against the panel of MRSA strains and MDR Gram-negative bacteria tested, which is reported for the first time. The results identified an additional antibacterial potential of the compounds to their already known antimycobacterial activities [17] and antibacterial properties against *H. pylori* [16]. Rottlerin showed good potency of 1 mg/L against *E. faecalis* 112697 and 2 mg/L against several resistant *S. aureus* strains such as MRSA 274829, MRSA 12981, NorA-overexpressing strain *S. aureus* SA1199B, and *E. faecalis* 13379. In addition, MICs in the range of 4–32 mg/L towards *S. aureus* ATCC 25923, *B. subtilis* BsSOP01, *S. aureus* XU212, EMRSA-15, EMRSA-16 and MRSA 346724 were observed, indicating that rottlerin has a very broad and strong antibacterial activity towards Gram-positive species, which could be harnessed for future antibacterial drug discovery towards MRSA. MRSA continues to pose a health concern, particularly in hospital-acquired infections, and possess an 'exceptional' wide diversity of resistance to many classes of drugs, including tetracyclines, macrolides, aminoglycosides, fluoroquinolones and, in some cases, glycopeptides [21].

Resistance in strains such as *S. aureus* SA1199B, XU212 and RN4220 is promoted by the expression of the efflux pumps NorA, TetK and MsrA, respectively, and these mechanisms have become increasingly important in the current threat of multidrug resistance. *S. aureus* XU212 is an MRSA and overexpresses the TetK (tetracycline) efflux pump, which increases the transport and recognition of tetracycline. MDR *S. aureus* strain SA1199B overexpresses the NorA efflux transporter, in addition to a gyrase mutation, thereby conferring a high level of resistance to certain fluoroquinolones. *S. aureus* RN4220 possesses the MsrA macrolide efflux pump, which binds to macrolides, expelling them from their drug-binding sites [22], whilst epidemic strains of EMRSA are notable for cases of bacteraemia in UK hospitals [23].

The antibacterial effect of the red compound affords a moderate to low range of activity compared with rottlerin. Enhancement of the antibacterial activity of rottlerin against MRSA may be attributable to the acetophenone moiety possessed by this compound. Poor activities of rottlerin and the red compound towards Gram-negative bacteria (*E. coli*, *K. pneumoniae*, *P. aeruginosa* and *Proteus* sp. P10830) almost certainly could be due to poor penetration of the compounds through the bacterial outer membrane [24] or the presence of resistance-nodulation-cell division (RND) efflux pumps in these bacteria, as these compounds are large polyphenolic structures and are possibly RND substrates.

Toxicity studies by other workers have shown that rottlerin has a cytotoxic effect at concentrations higher than IC_{50} values of 9 μM and 8 μM when screened against HL-60 and MIAPCa-2 cells,

respectively [25]. There was also marked cytotoxicity following exposure of SK-Mel-28 cells at 20 μM for a period of 24 h [26]. However, whilst these observations suggest that rottlerin is toxic at high concentrations, this is not the case at the MIC found to be effective towards Gram-positive and Gram-negative bacteria. Further modification of the chemical structure as well as favourable toxicity profiles of the compound suggests a possible therapeutic lead agent.

Plasmids offer numerous unique targets for combating drug-resistant bacteria. Therefore, the use of a single compound that could cause efficient plasmid curing and/or minimise antibiotic resistance transmission is of interest. The decrease in the transfer frequency mediated by the compounds at subinhibitory concentrations is noteworthy because this may lead to reduced maintenance of conjugative plasmids within the bacterial population [27]. The influence of rottlerin was pronounced, with significant reductions in the transfer of plasmids TP114 (96.3%) and pUB307 (87.3%), and most significantly pKM101 (99.7%). Similarly, the red compound displayed significant inhibitory effects on the transfer of pKM101 (93.8%), followed by TP114 (82.7%) and pUB307 (70.8%); the inhibitory effects of rottlerin on R6K and R7K were only moderate. Although the inhibitory activities of the tested compounds differ from those of plumbagin when compared to the given subinhibitory concentration, they are potential active antimicrobial and anti-plasmid agents. Plumbagin (5-hydroxy-2-methyl-1,4-naphthoquinone) reportedly is the first natural compound with established anti-plasmid activity attributable to disruption of DNA gyrase [28,29]. Further studies reported that plasmids, typified by TP181, had increased susceptibility to plumbagin, which can block the rifampicin-induced host-killing system of plasmids to aid survival of plasmid-free strains [30].

Probably, the planar nature of rottlerin and the red compound could facilitate intercalation into plasmid DNA and thus interfere with the conjugation process. Most anti-plasmid compounds, both natural and synthetic, have been shown to possess aromatic moieties that bind into the plasmid and interact with DNA gyrase [31] or disrupt the architecture and partitioning system of the plasmid, an example being phenothiazine [32]. Plant-derived natural products with anti-plasmid activity that have previously been reported include the norditerpene compound 8-epidiosbulbin-*E*-acetate from the bulbs of *Dioscorea bulbifera* [33], and bharangin, a phenolic compound from *Pygmacopremna herbacea* (Roxb.) [34]. Overall, the fact that rottlerin and the red compound could inhibit plasmid transfer in treated cells at subinhibitory concentrations that do not inhibit bacterial growth suggests that the target for these antimicrobial agents could affect plasmid DNA and the replication system in some way that is yet to be determined.

The actinomycin D–DNA bound complex showed a pronounced shift in its DNA migration (Fig. 4) concurring with its well-known capacity to intercalate into DNA [35]. A similar shift in migration was expected for rottlerin and the red compound if direct binding to plasmid DNA was the probable mechanism of action. Whilst no binding was detected, the compounds may have bound to the DNA in sufficiently low quantities or affected the DNA properties in some other way as not to cause any visible shift in DNA migration detectable by the EMSA. A study by Palchaudhuri and Hergenrother [35] noted the importance of molecules that can bind to DNA such as anthracyclines used as anticancer drugs with both antineoplastic and antibacterial properties. Further studies are required to fully eliminate DNA binding as a possible mode of action of the compounds.

5. Conclusion

Undoubtedly it will require significant effort to explore the druggability of anti-plasmid agents but certainly these results represent a step in illustrating that natural plant-derived products have the potential to selectively inhibit plasmid transfer in *E. coli* as well as having direct antibacterial activities against Gram-positive organisms. Since many clinically useful antimicrobial agents are no longer effective owing to the prevalence of strains carrying plasmid-encoded resistance mechanisms, an anti-plasmid approach could rejuvenate antibiotic use, enabling them to be effective once again. Finally, bacteria whose virulence is plasmid-determined could also be targeted with the help of anti-plasmid agents. Research efforts are ongoing to understand the specificity and mode of action of these compounds but, to the best of our knowledge, this is the first report on the inhibitory effects of natural compounds from *M. philippensis* on the conjugal transfer of R-plasmids.

Funding

This work is part of a doctoral research supported by the Commonwealth Scholarship Commission, UK [NGCA-2010-59].

Competing interests

None declared.

Ethical approval

Not required.

Appendix A. Supplementary data

Supplementary data associated with this article can be found, in the online version, at doi:10.1016/j.jgar.2016.01.011.

References

[1] World Health Organization Antimicrobial resistance: global report on surveillance 2014. Geneva, Switzerland: WHO; 2014.
[2] Bennett PM. Plasmid encoded antibiotic resistance: acquisition and transfer of antibiotic resistance genes in bacteria. Br J Pharmacol 2008;153(Suppl. 1):S347–57.
[3] Christie PJ, Whitaker N, González-Rivera C. Mechanism and structure of the bacterial type IV secretion systems. Biochim Biophys Acta 2014;1843:1578–91.
[4] Popowska M, Krawczyk-Balska A. Broad-host-range IncP-1 plasmids and their resistance potential. Front Microbiol 2013;4:44.
[5] Belogurov AA, Delver EP, Rodzevich OV. IncN plasmid pKM101 and IncI1 plasmid Collb-P9 encode homologous antirestriction proteins in their leading regions. J Bacteriol 1992;174:5079–85.
[6] Carattoli A. Resistance plasmid families in Enterobacteriaceae. Antimicrob Agents Chemother 2009;53:2227–38.
[7] Revilla C, Garcillán-Barcia MP, Fernández-López R, Thomson NR, Sanders M, Cheung M, et al. Different pathways to acquiring resistance genes illustrated by the recent evolution of IncW plasmids. Antimicrob Agents Chemother 2008;52:1472–80.
[8] Espinosa M, Cohen S, Couturier M, del Solar G, Diaz-Orejas R, Giraldo R, et al. Plasmid replication and copy number control. In: Thomas CM, editor. The horizontal gene pool: bacterial plasmids and gene spread. Amsterdam, The Netherlands: Taylor & Francis; 2000. p. 281.
[9] Hahn FE, Ciak J. Elimination of resistance determinants from R-Factor R1 by intercalative compounds. Antimicrob Agents Chemother 1976;9:77–80.
[10] Molnár J, Földeák S, Nakamura MJ, Rausch H, Domonkos K, Szabó M. Anti-plasmid activity: loss of bacterial resistance to antibiotics. APMIS Suppl 1992;30:24–31.
[11] Michel-Briand Y, Uccelli V, Laporte J-M, Plesiat P. Elimination of plasmids from Enterobacteriaceae by 4-quinolone derivatives. J Antimicrob Chemother 1986;18:667–74.
[12] Amábile-Cuevas CF, Heinemann JA. Shooting the messenger of antibiotic resistance: plasmid elimination as a potential counter-evolutionary tactic. Drug Discov Today 2004;9:465–7.
[13] Fernandez-Lopez R, Machón C, Longshaw CM, Martin S, Molin S, Zechner EL, et al. Unsaturated fatty acids are inhibitors of bacterial conjugation. Microbiology 2005;151:3517–26.

[14] Maree JE, Khondkar P, Kwapong AA, Oyedemi BM, Aljarba TM, Stapleton P, et al. Bioactive acetophenones from *Plectranthus venteri*. Phytochem Lett 2014;10. cxli–cxliv.
[15] Shiu WKP, Malkinson JP, Rahman MM, Curry J, Stapleton P, Gunaratnam M, et al. A new plant-derived antibacterial is an inhibitor of efflux pumps in *Staphylococcus aureus*. Int J Antimicrob Agents 2013;42:513–8.
[16] Rivière C, Nguyen Thi Hong V, Tran Hong Q, Chataigné G, Nguyen Hoai N, Dejaegher B, et al. *Mallotus* species from Vietnamese mountainous areas: phytochemistry and pharmacological activities. Phytochem Rev 2010;9: 217–53.
[17] Hong Q, Minter DE, Franzblau SG, Arfan M, Amin H, Reinecke MG. Anti-tuberculosis compounds from *Mallotus philippinensis*. Nat Prod Commun 2010;5:211–7.
[18] Zaidi SF, Yoshida I, Butt F, Yusuf MA, Usmanghani K, Kadowaki M, et al. Potent bactericidal constituents from *Mallotus philippinensis* against clarithromycin and metronidazole resistant strains of Japanese and Pakistani *Helicobacter pylori*. Biol Pharm Bull 2009;32:631–6.
[19] Rice LB, Bonomo RA. Genetic and biochemical mechanisms of bacterial resistance to antimicrobial agents. In: Lorian V, editor. Antibiotics in laboratory medicine. 4th ed., Baltimore, MD: Williams & Wilkins; 1996. p. 445–67.
[20] Holden NS, Tacon CE. Principles and problems of the electrophoretic mobility shift assay. J Pharmacol Toxicol Methods 2011;63:7–14.
[21] Gibbons S. Phytochemicals for bacterial resistance—strengths, weaknesses and opportunities. Planta Med 2008;74:594–602.
[22] Poole K. Efflux-mediated antimicrobial resistance. J Antimicrob Chemother 2005;56:20–51.
[23] Gould IM, David MZ, Esposito S, Garau J, Lina G, Mazzei T, et al. New insights into meticillin-resistant *Staphylococcus aureus* (MRSA) pathogenesis, treatment and resistance. Int J Antimicrob Agents 2012;39:96–104.
[24] Cox G, Wright GD. Intrinsic antibiotic resistance: mechanisms, origins, challenges and solutions. Int J Med Microbiol 2013;303:287–92.
[25] Jain SK, Pathania AS, Meena S, Sharma R, Sharma A, Gupta BD, et al. Semi-synthesis of mallotus B from rottlerin: evaluation of cytotoxicity and apoptosis-inducing activity. J Nat Prod 2013;76:1724–30.
[26] Shaikh D, Shaikh A, Rehman B, Shafi S. Antimicrobial and toxicological studies on *Mallotus philippensis* (Kamala powder). Int J Pharm 2012;2:612–8.
[27] Haft RJ, Mittler JE, Traxler B. Competition favours reduced cost of plasmids to host bacteria. ISME J 2009;3:761–9.
[28] Lakshmi VV, Sridhar P, Polasa H. Elimination of multidrug-resistant plasmid in bacteria by plumbagin, a compound derived from a plant. Curr Microbiol 1986;16:159–61.
[29] Bharathi A, Polasa H. Elimination of broad-host-range plasmid vectors in *Escherichia coli* by curing agents. FEMS Microbiol Lett 1991;84:37–40.
[30] Lakshmi VV, Sridhar P, Polasa H. Loss of plasmid linked antibiotic resistance in *Escherichia coli* on treatment with some phenolic compounds. FEMS Microbiol Lett 1996;57:275–8.
[31] Takács D, Cerca P, Martins A, Riedl Z, Hajós G, Molnár J, et al. Evaluation of forty new phenothiazine derivatives for activity against intrinsic efflux pump systems of reference *Escherichia coli*, *Salmonella* Enteritidis, *Enterococcus faecalis* and *Staphylococcus aureus* strains. In Vivo 2011;25:719–24.
[32] Monlár A, Amaral L, Monlár J. Antiplasmid effects of promethazine in mixed bacterial cultures. Int J Antimicrob Agents 2003;22:217–22.
[33] Shriram V, Jahagirdar S, Latha C, Kumar V, Puranik V, Rojatkar S, et al. A potential plasmid-curing agent, 8-epidiosbulbin E acetate, from *Dioscorea bulbifera* L. against multidrug-resistant bacteria. Int J Antimicrob Agents 2008;32:405–10.
[34] Marie-Magdeleine C, Udino L, Philibert L, Bocage B, Archimede H. In vitro effects of cassava (*Manihot esculenta*) leaf extracts on four development stages of *Haemonchus contortus*. Vet Parasitol 2010;173:85–92.
[35] Palchaudhuri R, Hergenrother PJ. DNA as a target for anticancer compounds: methods to determine the mode of binding and the mechanism of action. Curr Opin Biotechnol 2007;18:497–550.

Phytochemistry 95 (2013) 277–283

Contents lists available at ScienceDirect

Phytochemistry

journal homepage: www.elsevier.com/locate/phytochem

Modulators of antibiotic activity from *Ipomoea murucoides*

Berenice Corona-Castañeda [a], Lilia Chérigo [a], Mabel Fragoso-Serrano [a], Simon Gibbons [b], Rogelio Pereda-Miranda [a,*]

[a] Departamento de Farmacia, Facultad de Química, Universidad Nacional Autónoma de México, Ciudad Universitaria, Mexico City 04510DF, Mexico
[b] Department of Pharmaceutical and Biological Chemistry, UCL School of Pharmacy, 29-39 Brunswick Square, London WC1N 1AX, UK

ARTICLE INFO

Article history:
Received 7 May 2013
Received in revised form 7 July 2013
Available online 3 August 2013

Keywords:
Ipomoea murucoides
Convolvulaceae
Structural spectroscopy
Glycolipids
Multidrug-resistance
Gram-positive bacteria
Gram-negative bacteria

ABSTRACT

Reinvestigation of the $CHCl_3$-soluble extract from the flowers of *Ipomoea murucoides*, through preparative-scale recycling HPLC, yielded three pentasaccharides of 11-hydroxyhexadecanoic acid, murucoidins XVII–XIX, in addition to the known murucoidin III and V, all of which were characterized by NMR spectroscopy and mass spectrometry. These compounds were found to be macrolactones of the known pentasaccharides simonic acid B and operculinic acid A. The acylating groups corresponded to acetic, (2*S*)-methyl-butyric, (*E*)-cinnamic and octanoic acids. The esterification sites were established at the C-2 of the second rhamnose and C-3 and C-4 of the third rhamnose. The aglycone lactonization was placed at C-2 or C-3 of the first rhamnose. Bioassays for modulation of antibiotic activity were performed against multidrug-resistant strains of *Staphylococcus aureus*, *Escherichia coli* Rosetta-gami, and two nosocomial pathogens: *Salmonella enterica* sv. Typhi and *Shigella flexneri*. The tested glycolipids did not act as cytotoxic (IC_{50} > 4 μg/mL) nor as antimicrobial (MIC > 128 μg/mL) agents. However, they exerted a potentiation effect on clinically useful antibiotics against the tested bacteria by increasing their antibiotic susceptibility up to four-fold at concentrations of 25 μg/mL.

1. Introduction

The genus *Ipomoea* of the morning glory family (Convolvulaceae) is distinguished by its worldwide distribution in tropical regions as well as for its curative attributes that include laxative properties, which are derived from the presence of high yields of resin glycosides in the whole plant (Eich, 2008; Pereda-Miranda et al., 2010). From a chemical point of view, resin glycosides are mixtures of glycolipids of high molecular mass that are amphipathic in nature due the presence of a hydrophilic portion (the oligosaccharide core) and a hydrophobic aglycone (monohydroxylated fatty acids of fourteen and sixteen carbon atoms) forming the macrolactone (Pereda-Miranda et al., 2010). Important and diverse biological activities of therapeutic interest have been attributed to morning glory resin glycosides (Pereda-Miranda et al., 2010). One of which is their antibacterial activity against resistant nosocomial strains of *Staphylococcus aureus* (Pereda-Miranda et al., 2006).

The main mechanism in the development of bacterial resistance is due to the presence of trans-membrane proteins that confer the phenotype of multidrug-resistance (MDR) to antibiotics, for example the Nor-A and Tet-K pumps. These proteins function as transport systems that are activated to expel antibiotics, preventing the drug from reaching the concentration required to exert their activity within the cell (Savjani et al., 2009; Stavri et al., 2007). Previous studies have described the enhancement of antibiotic susceptibility using microbiologically inactive resin glycosides as inhibitors of efflux pumps in *S. aureus* (Chérigo et al., 2008, 2009; Escobedo-Martínez et al., 2010; Pereda-Miranda et al., 2006). These compounds caused a decrease (at the concentration of 25 μg/mL) of the minimum inhibitory concentration value (MIC; four times, 32–8 μg/mL) of therapeutic antibiotics. Experiments to test the inhibition of extracellular transport of ethidium bromide, a fluorescent agent, have shown that these glycolipids are substrates for MDR efflux pumps (Chérigo et al., 2008; Pereda-Miranda et al., 2006) as well as, in some instances, more potent and effective inhibitors of efflux pumps than reserpine, an alkaloid used as a positive efflux pump inhibitor control (Gibbons, 2008; Li and Nikaido, 2009). These metabolites were also tested for resistance-modulatory activity against *Escherichia coli* Rosetta-gami and two nosocomial pathogens, *Salmonella enterica* sv. Typhi and *Shigella flexneri*. These compounds exerted a potentiation effect of clinically useful antibiotics against the tested Gram-negative bacteria by increasing antibiotic susceptibility up to 64-fold at concentrations of 25 μg/mL (Corona-Castañeda and Pereda-Miranda, 2012).

These findings constitute the starting point for the conceptual approach that guided the present investigation, which is aimed at evaluating new oligosaccharides from *I. murucoides* as potential modulators of the multidrug-resistant (MDR) phenotype in both Gram-positive and -negative bacteria, where active efflux has

* Corresponding author. Tel.: +52 (55) 5622 5288; fax: +52 (55) 5622 5329.
E-mail address: pereda@unam.mx (R. Pereda-Miranda).

0031-9422/$ - see front matter © 2013 Elsevier Ltd. All rights reserved.
http://dx.doi.org/10.1016/j.phytochem.2013.07.007

proven to be one of the most successful detoxification mechanisms. Expanding the knowledge of resin glycoside structural diversity opens the potential for possible therapeutic applications against nosocomial pathogens.

2. Results and discussion

A chemical reinvestigation of *I. murucoides* flowers allowed the isolation of three novel pentasaccharides (**1**–**3**) from their $CHCl_3$-soluble extracts as well as the previously known murucoidins III and V (Chérigo and Pereda-Miranda, 2006). The structures for the new murucoidins XVII–XIX (**1**–**3**) were established by one-dimensional (^1H and ^{13}C NMR) (Tables 1 and 2) and two-dimensional (NMR: COSY, TOCSY, HSQC and HMBC) spectroscopic and spectrometric (FAB-MS negative mode) techniques (Pereda-Miranda et al., 2010). The novel compounds were found to be macrolactones of the known pentasaccharides simonic acid B and operculinic acid A. Evidences for the configuration of constitutive

Table 1
^1H (500 MHz) NMR spectroscopic data of compounds **1**–**3** (pyridine-d_5).[a]

Hydrogen[b]		1	2	3
Fuc	1	4.82 d (7.5)	4.80 d (8.0)	4.73 d (7.5)
	2	4.50 dd (7.5, 9.5)	4.51 dd (8.0, 9.5)	4.16 dd (7.5, 9.5)
	3	4.20 dd (9.5, 2.5)	4.16 dd (9.5, 3.0)	4.07 dd (9.5, 4.0)
	4	3.90*	3.91 sa	3.99 d (3.5, 1.0)
	5	3.81 dq (1.0, 6.5)	3.81 dq (1.0, 6.5)	3.78 dq (1.0, 6.5)
	6	1.52 d (6.5)	1.52 d (6.5)	1.51 d (6.0)
Rha	1	6.32 d (1.0)	6.32 d (1.5)	5.48 d (1.5)
	2	5.20 dd (1.0, 2.5)	5.29 dd (1.5, 3.0)	5.95 dd (2.0, 3.5)
	3	5.66 dd (3.0, 10.0)	5.59 dd (3.0, 9.5)	5.02 dd (3.0, 9.5)
	4	4.67 t (9.5)	4.62 t (9.5)	4.23 sa
	5	4.99 dq (9.5, 6.0)	4.99 dd (9.5, 6.0)	4.43 dq (9.5, 6.0)
	6	1.59 d (6.0)	1.57 d (6.0)	1.62 d (6.0)
Rha′	1	5.57 d (1.5)	5.64 d (1.5)	6.12 d (2.0)
	2	6.03 dd (1.5, 3.5)	5.81 dd (1.5, 3.0)	5.97 dd (2.0, 3.0)
	3	4.63 dd (3.5, 9.0)	4.49 dd (3.0, 9.5)	4.61 dd (3.0, 9.5)
	4	4.26 t (9.5)	4.21 dd (9.5, 9.5)	4.26 dd (9.5, 9.5)
	5	4.39 dq (9.5, 6.0)	4.31 dq (9.5, 6.5)	4.35 dq (9.5, 6.0)
	6	1.62 d (6.0)	1.59 d (6.5)	1.65 d (6.5)
Rha″	1	6.20 d (1.5)	5.89 sa	5.89 d (1.5)
	2	5.14 dd (1.5, 3.0)	4.64 dd (1.5, 3.5)	4.72 dd (1.5, 3.0)
	3	5.88 dd (3.0, 9.5)	4.41 sa	4.49 dd (3.0, 9.5)
	4	6.02 t (9.5)	5.76 t (9.5)	5.81 t (9.5)
	5	4.45 dq (9.5, 6.5)	4.33 dq (9.5, 6.0)	4.33 dq (9.5, 6.5)
	6	1.43 d (6.5)	1.39 d (6.0)	1.38 d (6.5)
Rha‴	1		5.55 d (1.5)	5.64 d (1.5)
	2		4.76 sa	4.85 dd (1.5, 2.5)
	3		4.38 dd (3.5, 9.5)	4.40 dd (2.5, 9.0)
	4		4.25 dd (9.5, 9.5)	4.27 dd (8.0, 9.0)
	5		4.28 dq (9.5, 6.5)	4.25 dq (9.5, 4.5)
	6		1.69 d (6.5)	1.56 d (5.5)
Glc	1	5.09 d (7.5)		
	2	3.87 dd (7.5, 8.8)		
	3	4.12 dd (8.5, 9.0)		
	4	4.14 dd (8.5, 9.0)		
	5	3.84 ddd (2.5, 5.5, 8.0)		
	6a	4.35 dd (11.0, 5.0)		
	6b	4.46 dd (12.5, 3.0)		
Jal	2a	2.26 ddd (2.8, 7.0, 15.0)	2.24 ddd (2.5, 6.5, 15.0)	2.23 ddd (3.5, 9.0, 12.5)
	2b	2.58 dd (2.8, 15.0)	2.92 ddd (2.5, 6.5, 15.0)	2.40 ddd (3.5, 9.0, 12.5)
	11	3.90*	3.87 m	3.86 m
	16	0.96 t (7.0)	0.84 t (7.0)	0.88 t (7.0)
Mba	2	2.45 tq (7.0, 7.0)	2.50 tq (7.0)	2.37 tq (6.5, 7.0)
	2-Me	1.13 d (7.0)	1.20 d (7.0)	1.07 d (7.0)
	3-Me	0.84 t (7.5)	0.94 t (7.5)	0.84 t (7.5)
Mba′	2	2.45 tq (7.0, 7.0)		
	2-Me	1.11 d (7.0)		
	3-Me	0.81 t (7.5)		
Cna	2	6.56 d (16.0)		
	3	7.84 d (16.0)		
	2’	7.32 m		
	3’	7.44 m		
	4’	7.32 m		
Ac	2			2.05 s
Octa	2		2.34 t (7.0)	
	8		0.95 t (7.0)	

[a] Chemical shifts (δ) are in ppm relative to TMS. The spin coupling (J) is given in parentheses (Hz). Chemical shifts marked with an asterisk (*) indicate overlapped signals. Spin-coupled patterns are designated as follows: s = singlet, d = doublet, t = triplet, q = quartet, m = multiplet, brs = broad singlet.
[b] *Abbreviations:* Fuc, fucose; Rha, rhamnose; Glc, glucose, Jal, 11-hydroxyhexadecanoyl; Mba, methylbutanoyl, Cna, cinamoyl, Ac, acetyl, Octa, octanoyl.

Table 2
^{13}C (125 MHz) NMR spectroscopic data of compounds **1**–**3** (pyridine-d_5).[a]

Carbon[b]		1	2	3
Fuc	1	101.5	101.6	104.3
	2	73.6	73.4	80.3
	3	76.5	76.6	73.3
	4	73.6	73.5	73.1
	5	71.2	71.2	70.8
	6	17.2	17.2	17.4
Rha	1	100.0	100.2	98.8
	2	70.0	69.7	73.9
	3	78.0	77.8	69.9
	4	76.0	77.9	79.9
	5	68.0	67.9	68.6
	6	19.2	19.2	19.5
Rha′	1	99.2	99.2	99.2
	2	72.3	73.0	73.0
	3	80.1	80.2	79.6
	4	79.1	79.2	80.0
	5	68.1	68.3	68.1
	6	18.8	18.7	18.8
Rha″	1	103.4	103.6	103.7
	2	69.9	72.6	72.9
	3	72.8	70.2	70.2
	4	71.7	74.8	75.3
	5	68.2	68.1	68.5
	6	17.9	17.9	17.8
Rha‴	1		104.3	104.9
	2		72.5	72.5
	3		72.6	72.6
	4		73.7	73.5
	5		70.8	70.5
	6		18.8	18.6
Glc	1	105.1		
	2	75.2		
	3	78.2		
	4	70.8		
	5	77.7		
	6	62.5		
Jal	1	174.4	174.9	173.1
	2a	34.5	33.7	34.3
	11	79.5	79.3	82.3
	16	14.5	14.4	14.3
Mba	1	175.9	176.3	
	2	41.3	41.6	
	2-Me	16.9	17.0	
	3-Me	11.8	11.8	
Mba′	1	176.1		
	2	41.5		
	2-Me	16.7		
	3-Me	11.6		
Cna	1	166.1		
	2	118.6		
	3	145.2		
	1’	134.7		
	2’	129.2		
	3’	128.5		
	4’	130.7		
Ac	1			170.6
	2			
Octa	1		172.9	
	2		34.4	
	8		14.2	

[a] Chemical shifts (δ) are in ppm relative to TMS.
[b] *Abbreviations:* Fuc, fucose; Rha, rhamnose; Glc, glucose, Jal, 11-hydroxyhexadecanoyl; Mba, methylbutanoyl, Cna, cinamoyl, Ac, acetyl, Octa, octanoyl.

monosaccharides, the anomeric linkages, the sequence of glycosidation, as well as the absolute configuration for the aglycones were published when these oligosaccharides were first elucidated. Also, they are representative cores commonly found in the morning glory resin glycosides, e.g., the Mexican medicinal arborescent members of the genus *Ipomoea*, *I. murucoides* (Chérigo and Pereda-Miranda, 2006) and *I. intrapilosa* (Bah et al., 2007), among others (Pereda-Miranda et al., 2010).

Negative-ion FAB mass spectrometry was particularly useful in determining the exact mass and molecular formulas for **1**–**3**. The mass spectra showed a quasimolecular ion $[M-H]^-$ at *m*/*z* 1297 ($C_{65}H_{101}O_{26}$) for compound **1**, at *m*/*z* 1193 ($[M-H]^-$, $C_{59}H_{101}O_{24}$) for compound **2**, and at *m*/*z* 1109 ($[M-H]^-$, $C_{53}H_{89}O_{24}$) for **3**. In all cases, the characteristic fragment ions common to all branched pentasaccharide resin glycosides were observed for the glycosidic cleavage of each sugar moiety (Chérigo et al., 2008; Escalante-Sánchez et al., 2008; Pereda-Miranda et al., 2005). For example, diagnostic fragments were observed for the aglycone (jalapinoic acid residue: *m*/*z* 271), the aglycone and a methyl pentose residue (*m*/*z* 417), the aglycone and two methyl pentoses (*m*/*z* 545), and the aglycone and three methyl pentoses (*m*/*z* 691) (Bah and Pereda-Miranda, 1996; Pereda-Miranda et al., 2010; Castañeda-Gómez et al., 2013). For compound **1**, the observed ester eliminations at *m*/*z* 1213 ($[M-H]^-$–C_5H_8O [Mba, 84 amu]), 1167 ($[M-H]^-$–C_9H_6O [Cna, 130 amu]), and 1083 ($[M-H]^-$–C_5H_8O–C_9H_6O) allowed for the identification of a triacylated simmonic acid B macrocyclic derivative, while a diacylated derivative of this glycosidic acid was identified for **3** through fragment anions at *m*/*z* 1067 ($[M-H]^-$–C_2H_2O [Ac, 42 amu]) and 837 ($[M-H]^-$–C_2H_2O–C_5H_8O–$C_6H_{10}O_4$). Finally, the fragments at *m*/*z* 1067 ($[M-H]^-$–$C_8H_{14}O$), 963 ($[M-H]^-$–C_5H_8O–$C_6H_{10}O_4$), and 837 ($[M-H]^-$–C_5H_8O–$C_8H_{14}O$–$C_6H_{10}O_4$) also identified a diacylated operculinic acid A derivative for **2** (Castañeda-Gómez et al., 2013).

Murucoidin XVII (**1**) was identified as the intramolecular 1,3″ ester of (11*S*)-hydroxyhexadecanoic acid of *O*-*β*-D-glucopyranosyl-(1→3)-*O*-[4-*O*-(2*S*)-2-methylbutanoyl,3-*O*-cinnamoyl]-α-L-rhamnopyranosyl-(1→4)]-*O*-α-L-rhamnopyranosyl-(1→4)-*O*-α-L-rhamnopyranosyl-(1→2)-*O*-*β*-D-fucopyranoside. In the ^1H NMR spectrum, five anomeric protons were identified through their chemical shifts and coupling constant as doublets (Table 1): 4.82 (7.5 Hz, Fuc), 6.32 (1.0 Hz, Rha), 5.57 (1.5 Hz, Rha′), 6.20 (1.5 Hz, Rha″), and 5.09 ppm (7.5 Hz, Glc). Characteristic signals for the acylating substituents were registered: (a) (2*S*)-methylbutanoic, triplet-like signal at 2.45 ppm (Mba, H-2); (b) cinnamic acid, two doublets at 6.56 (Cna, H-2) and 7.84 (H-3) ppm and two multiplets at 7.32 (H-2′) and 7.44 (H-3′) ppm. The ^{13}C NMR spectrum provided the following information (Table 2): five anomeric carbons between 99.2 and 105.1 ppm, a signal at 62.5 ppm for the hydroxymethylene group of glucose, and four signals corresponding to the carbonyl groups for the three acylating substituents (Mba 174.4 ppm; Mba′ 176.1 ppm; Cna 166.1 ppm) and the macrocyclic lactone (174.4 ppm).

Murucoidin XVIII (**2**) was identified as the intramolecular 1,2″ ester of (11*S*)-hydroxyhexadecanoic acid of *O*-α-L-rhamnopyranosyl-(1→3)-*O*-[[4-*O*-(2*S*)-2-methylbutanoyl]-α-L-rhamnopyranosyl-(1→4)]-*O*-[2-*O*-octanoyl]-α-L-rhamnopyranosyl-(1→4)-*O*-α-L-rhamnopyranosyl-(1→2)-*O*-*β*-D-fucopyranoside. For **2** in the ^1H NMR spectrum (Table 1), the anomeric signals were observed at 4.80 (8.0 Hz, Fuc), 6.32 (1.5 Hz, Rha), 5.64 (1.5 Hz, Rha′), 5.89(1.0 Hz, Rha″), and 5.55 ppm (1.5 Hz, Rha‴). The characteristic signals for the ester substituents were: Mba ($\delta_{H\text{-}2}$ 2.50) and octanoic acid (two triplets, $\delta_{H\text{-}2}$ 2.34 and $\delta_{H\text{-}8}$ 0.95). The ^{13}C NMR spectrum showed: five anomeric carbons (δ_C 99.2–104.3); and three signals for the carbonyl groups: two for the acylating acids (Octa δ_C 172.9 and Mba δ_C 176.3); and the macrolactone (δ_C 174.9) Fig. 1.

The murucoidin XIX (**3**) was identified as the intramolecular 1,2″ ester of (11*S*)-hydroxyhexadecanoic acid of *O*-α-L-rhamnopyranosyl-(1→3)-*O*-[[4-*O*-acetyl]-α-L-rhamnopyranosyl-(1→4)]-*O*-[2-*O*-(2*S*)-2-methylbutanoyl]-α-L-rhamnopyranosyl-(1→4)-*O*-α-L-rhamnopyranosyl-(1→2)-*O*-*β*-D-fucopyranoside. The ^1H NMR spectra of this compound showed five anomeric protons: δ_H 4.73

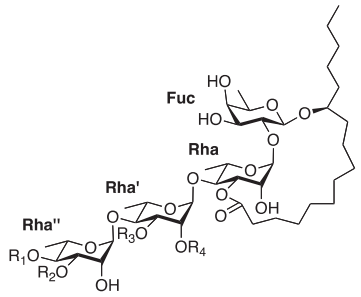

Compound	R_1	R_2	R_3	R_4
1	(2*S*)-methylbutanoyl = Mba	cinamoyl= Cna	β-D-glucopyranosyl= Glc	Mba
2	Mba	H	α-L-rhamnopyranosyl = Rha	*n*-octanoyl

Fig. 1. Chemical structure of murucoidins XVII and XVIII (**1** and **2**).

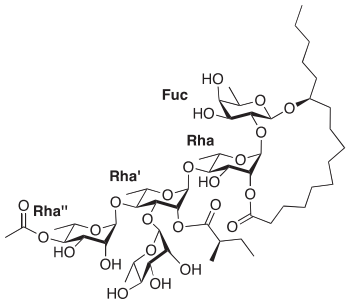

Fig. 2. Chemical structure of murucoidin XIX (**3**).

(7.6 Hz; Fuc), 5.48 (1.5 Hz, Rha), 6.12 (2.0 Hz; Rha′), 5.89 (1.5 Hz, Rha″), and 5.64 (1.5 Hz, Rha‴); 2-methylbutanoic acid (tq, $\delta_{H\text{-}2}$ 2.37) and acetic acid (singlet, δ_H 2.05). The ^{13}C NMR spectrum displayed five signals for the anomeric carbons (δ_C 98.8–104.9) and three carbonyl signals at δ_C 170.6 (Ac), 172.9 (Octa) and 175.5 (macrolactone) Fig. 2.

The acylation sites and glycosidation sequence were assigned by the $^{2,3}J_{CH}$ correlations observed in the HMBC spectrum for all of the compounds (Duus et al., 2000; Pereda-Miranda et al., 2010).The position for macrolactonization was placed at C-2 for compound **3** and at C-3 for compounds **1** and **2** of the second saccharide (Rha), as confirmed by the observed correlation for protons H-2 ($\delta_{H\text{-}2}$ 5.95 for compound **3**) or H-3 ($\delta_{H\text{-}3}$ 5.66 for compound **1** and $\delta_{H\text{-}3}$ 5.59 for **2**). Similarly, the esterification sites were located at C-2 of the second unit of rhamnose (Rha′) at $\delta_{H\text{-}2}$ 6.03, 5.81, and 5.97 for compounds **1**–**3**, respectively, and H-4 of the third unit of rhamnose (Rha″) at $\delta_{H\text{-}4}$ 6.02, 5.76, and 5.81 for all compounds. Additionally, compound **1** displayed another position of acylation at C-3 of Rha″ at $\delta_{H\text{-}3}$ 5.88.

The tested glycolipids were neither cytotoxic (KB: $IC_{50} > 4$ μg/mL) nor antibacterial (Gram-positive: MIC ⩾ 128 μg/mL; Gram-negative: MIC ⩾ 512 μg/mL) (Table 3). However, all of them exhibited a strong antibiotic modulatory activity at a concentration of 25 μg/mL (Table 4). This effect potentiated norfloxacin susceptibility against SA-1199B by four-fold (32–8 μg/mL) for compounds **1** and **2**, and two-fold (32–16 μg/mL) for compound **3** (Table 3). The modulation of antibiotic activity on MDR Gram-negative

Table 3
Susceptibility of *Staphylococcus aureus* to murucoidins XVII–XIX (**1–3**) and their cytotoxicity.[a]

Compound	IC_{50} (μg/mL)			MIC (μg/mL)[c]				
	KB	Hep-2	HeLa	ATCC 25923	XU-212	EMRSA-15	SA-1199B[b]	
							Nor (−)	Nor (+)
1	15.7	6.1	>20	>128	>128	>128	128	8
2	>20	>20	>20	>128	>128	>128	128	8
3	10.8	>20	19.0	>128	>128	>128	128	16
Vinblastine	0.005	0.006	0.001					
Colchicine	0.002	0.003	0.001					
Norfloxacin								32
Reserpine								4

[a] *Abbreviations:* KB, nasopharyngeal carcinoma; Hep-2, laryngeal carcinoma; HeLa, cervix carcinoma; ATCC 25923, standard *S. aureus* strain; EMRSA-15, epidemic methicillin-resistant *S. aureus* strain containing the *mecA* gene; XU-212, a methicillin-resistant *S. aureus* strain possessing the TetK tetracycline efflux protein; SA-1199B, multidrug-resistant *S. aureus* strain over-expressing the NorA efflux pump.

[b] Nor (−) = minimum inhibitory concentration (MIC) value determined in the susceptibility testing; Nor (+) = MIC value determined for norfloxacin in the modulation assay at the concentration of 25 μg/mL of the tested oligosaccharide.

[c] MIC value for norfloxacin in the modulation assay at the concentration of 20 μg/mL of reserpine which was used as positive control for an efflux pump inhibitor.

Table 4
Susceptibility of *Escherichia coli*, *Salmonellaenterica*, and *Shigella flexneri* to murucoidins XVII–XIX (**1–3**).

Compound	MIC (μg/mL)											
	Escherichia coli Rosetta gami				*Salmonella enterica* sv. Typhi				*Shigella flexneri*			
	(−)	Tet (+)	Kan (+)	Cam (+)	(−)	Tet (+)	Kan (+)	Cam (+)	(−)	Tet (+)	Kan (+)	Cam (+)
Antibiotics		128	32	256		1024	1024	512		512	512	256
1	>512	64	8	128	>512	512	512	256	512	256	128	256
2	>512	64	8	128	>512	512	512	256	512	256	128	256
3	>512	64	8	128	>512	512	512	256	512	128	128	256
Reserpine	>512	64	8	128	>512	512	512	256	>512	256	64	128

Abbreviations: (−), minimum inhibitory concentration (MIC) value determined in the susceptibility testing; Tet (+), MIC value determined for tetracycline; Kan(+), MIC value determined for kanamycin; Cam (+), MIC value determined for chloramphenicol in the modulation assay at the concentration of 25 μg/mL of the tested oligosaccharide.

strains was similar to that observed for reserpine, a positive control, in combination with tetracycline, kanamycin, and chloramphenicol. In most of the cases observed, a reduction in MIC was two-fold (Table 4). The highest reduction was observed for compound **3** in combination with tetracycline and kanamycin against *S. flexneri* (512–128 μg/mL). The complexity of the machinery and mechanisms of multidrug efflux in Gram-negative pathogens causes the major difference observed in potency for modulatory activity of the tested glycolipids against both Gram-positive and -negative bacteria, the latter of which are enveloped within a protective double-layer of lipid membranes. Noxious compounds are expelled across these membranes by active transport, providing the pathogens with a permeability barrier to hydrophilic compounds like antibiotics (Stavri et al., 2007). The more complex structure of multidrug efflux pumps in Gram-negative strains includes an inner membrane transporter, a periplasmic fusion protein, as well as an outer membrane channel (Zgurskaya, 2009). This tripartite efflux pump system therefore confers MDR bacteria with the capacity to occupy lethal ecological niches by avoiding the cytotoxic effects of antibiotics and drastically limits the clinical use of these drugs (Corona-Castañeda and Pereda-Miranda, 2012).

3. Concluding remarks

The contemporary recognition of the emergence and proliferation of methicillin-resistant strains of *S. aureus* is an epidemiological challenge as few antibiotics are effective agents in the treatment of nosocomial infections caused by these pathogens. Multidrug-resistant strains of *S. aureus* are often unresponsive to many types of clinically useful antibiotics which can include vancomycin, oxazolidinone, β-lactam and the streptogram in antibiotic categories (Freixas et al., 2012; Shibata et al., 2005). The literature describes a few effective plant-derived efflux pump inhibitors (EPIs) against Gram-positive bacteria (Stavri et al., 2007; Savoia, 2012), but information about EPIs against Gram-negative nosocomial pathogens is much more scarce. From the results obtained by researching into the potential of resin glycosides as EPIs in microbial pathogens (Chérigo et al., 2008, 2009; Escobedo-Martínez et al., 2010; Pereda-Miranda et al., 2006) and mammalian cells (Castañeda-Gómez et al., 2013; Cruz-Morales et al., 2012; Figueroa-González et al., 2012), there is a clear indication of the possibility that these metabolites could be used as synergistic agents in combinatorial therapies, increasing the strength and usefulness of antibiotics that are not effective in the treatment of refractive infections caused by MDR strains.

4. Experimental

4.1. General experimental procedures

Melting points were determined on a Fisher–Johns apparatus and are uncorrected. Optical rotations were measured with a Perkin–Elmer 241 polarimeter. ^{1}H (500 MHz) and ^{13}C (125 MHz) NMR experiments were conducted on a Bruker DMX-500 instrument. The NMR techniques were performed according to a previously described methodology (Bah and Pereda-Miranda, 1996). Negative-ion low and high-resolution FABMS were recorded using a matrix of triethanolamine on a JEOL SX-102A spectrometer. The instrumentation used for HPLC analysis consisted of a Waters 600 E multisolvent delivery system equipped with a Waters 410 differential refractometer detector (Waters Corporation, Milford, MA). Control of the equipment, data acquisition, processing, and management of the chromatographic information were performed by the Empower 2 software program (Waters).

4.2. Plant material

Flowers of *Ipomoea murucoides* were collected at Tepostlán, Morelos, Mexico, on April 10, 2010. The plant material was identified by Dr. Robert Bye and one of the authors (R.P.-M.) through comparison with an authentic plant sample (RP-05) archived at the Departamento de Farmacia, Facultad de Química, UNAM (Chérigo and Pereda-Miranda, 2006). A voucher specimen (Robert Bye 35906) was deposited in the Ethnobotanical Collection of the National Herbarium (MEXUE), Instituto de Biología, UNAM.

4.3. Extraction and isolation of compounds *1–3*

The whole plant material (500 g) was powdered and extracted exhaustively by maceration at room temperature with $CHCl_3$ to afford, after removal of the solvent, a dark brown syrup (35.8 g). The crude mixture of resin glycosides was obtained after fractionation of this extract by open column chromatography over silica gel eluted with a gradient of MeOH in $CHCl_3$. A total of 220 fractions (250 mL each) were collected and combined to give a pool containing a mixture of resin glycosides, which was subjected to fractionation by open column chromatography over reversed-phase C_{18} (330 g) eluted with MeOH to eliminate waxes and pigmented residues. This process provided 30 secondary fractions (30 mL each). Subfractions 18–25 were combined to yield a mixture of lipophilic pentasaccharides (20 g), which were analyzed by reversed-phase C_{18} HPLC using an isocratic elution with CH_3CN–H_2O (95:5). For their resolution, a Symmetry C_{18} column (Waters; 7 μm, 19 × 300 mm), a flow rate of 9 mL/min, and a differential refractometer detector were used. This analysis allowed the comparison with reference solutions of the previously reported resin glycosides (Chérigo et al., 2008), confirming the detection of the following compounds: murucoidin V (t_R 6.9 min), and murucoidin III (t_R 24.6 min). Peaks with t_R values of 9.2 min (peak II), and 16.5 min (peak IV) were collected by the technique of heart cutting and independently reinjected in the apparatus operating in the recycle mode (Pereda-Miranda and Hernández-Carlos, 2002) to achieve total homogeneity after 15 consecutive cycles. These technique yielded pure compounds: compound **1** (25 mg) from peak II, left

region; compound **2** (20 mg) from peak II, right region; and compound **3** (15 mg) from peak IV. Saponification of all compounds yielded (*S*)-(+)-α-methylbutyric acid: $[\alpha]_D$ +10 (*c* 1.0, $CHCl_3$), while compounds **1**–**3** also afforded cinnamic, octanoic and acetic acids, respectively, all of which were purified by HPLC according to previously described methologies (Pereda-Miranda and Hernández-Carlos, 2002; Pereda-Miranda et al., 2005).

4.4. Compound characterization

4.4.1. Murucoidin XVII (*1*)

White powder; mp 133–135 °C; $[\alpha]_D$ −98 (*c* 0.2, MeOH); ^1H and ^{13}C NMR, see Tables 1 and 2; negative-ion FABMS *m*/*z* 1297 $[M-H]^-$ ($C_{65}H_{101}O_{26}$), 1167 [1297−130 (C_9H_6O, cna)]$^-$, 1083 [1167−84 (C_5H_8O, mba)]$^-$, 937 [1083−146 ($C_6H_{10}O_4$, methylpentose)]$^-$, 545 [937−162 ($C_6H_{10}O_5$, deoxyhexose)−146($C_6H_{10}O_4$, methylpentose)−84 (C_5H_8O, mba]$^-$, 417 [545+18 (lactone hydrolysis)−146 ($C_6H_{10}O_4$, methylpentose)]$^-$, 271 [417−146 ($C_6H_{10}O_4$, methylpentose); jalapinolic acid−H]$^-$; HRFABMS *m*/*z* 1297.6576 $[M-H]^-$ (calcd for $C_{65}H_{101}O_{26}$ 1297.6581).

4.4.2. Murucoidin XVIII (*2*)

White powder; mp 123–126 °C; $[\alpha]_D$ −88 (*c* 0.2, MeOH); ^1H and ^{13}C NMR, see Tables 1 and 2; negative-ion FABMS *m*/*z* 1193 $[M-H]^-$ ($C_{59}H_{101}O_{24}$), 1067 [1193−126 ($C_8H_{14}O$, octa)]$^-$, 963 [1193−84 (C_5H_8O, mba)−146($C_6H_{10}O_4$, methylpentose)]$^-$, 837 [963−126 ($C_8H_{14}O$, octa)]$^-$, 545 [837−146($C_6H_{10}O_4$, methylpentose)−146($C_6H_{10}O_4$, methylpentose)]$^-$, 417 [545+18 (lactone hydrolysis)−146 ($C_6H_{10}O_4$, methylpentose)]$^-$, 271 [417−146 ($C_6H_{10}O_4$, methylpentose); jalapinolic acid−H]$^-$; HRFABMS *m*/*z* 1193.6678 $[M-H]^-$ (calcd for $C_{59}H_{101}O_{24}$ 1193.6683).

4.4.3. Murucoidin XIX (*3*)

White powder; mp 150–153 °C; $[\alpha]_D$ −50 (*c* 0.12, MeOH); ^1H and ^{13}C NMR, see Tables 1 and 2; negative FABMS *m*/*z* 1109 $[M-H]^-$ ($C_{53}H_{89}O_{24}$), 1067 [1109−43 (C_2H_3O, ac)]$^-$, 921 [1067−146 ($C_6H_{10}O_4$, methylpentose)]$^-$, 837 [921−84 (C_5H_8O, mba)]$^-$, 545 [837−146 ($C_6H_{10}O_4$, methylpentose)−146 ($C_6H_{10}O_4$, methylpentose)]$^-$, 417 [545+18 (lactone hydrolysis)−146 ($C_6H_{10}O_4$, methylpentose)]$^-$, 271 [417−146 ($C_6H_{10}O_4$, methylpentose); jalapinolic acid−H]$^-$; HRFABMS *m*/*z* 1109.5738 $[M-H]^-$ (calcd for $C_{53}H_{89}O_{24}$ 1109.5744).

4.5. Biological assays

4.5.1. Bacterial strains and media

S. aureus EMRSA-15 containing the mecA gene was provided by Dr. Paul Stapleton, from the UCL School of Pharmacy. Strain XU-212, a methicillin-resistant strain possessing the TetK tetracycline efflux protein, was provided by Dr. E. Udo (Gibbons and Udo, 2000). SA-1199B, which over-expresses the NorA MDR efflux protein (Chérigo et al., 2009) was the generous gift of Professor Glenn Kaatz of Wayne State University. Standard strain *S. aureus* ATCC 25923 was obtained from the ATCC. All strains were cultured on nutrient agar (Oxoid, Basingstoke, UK) before determination of MIC values. Cation-adjusted Mueller–Hinton broth (MHB; Oxoid) containing 20 and 10 mg/L of Ca^{2+} and Mg^{2+}, respectively was used for susceptibility tests. *E. coli* Rosetta-gami was provided by Dr. Federico del Río Portilla, Departamento de Bioquímica, Instituto de Química, UNAM, and was cultured on Luria–Bertani nutrient agar (Sigma) before determination of MIC values. Luria–Bertani broth (LB) was used for susceptibility tests. Nosocomial strains of *S. flexneri* and *S. enterica* sv. Typhi were provided by Dr. Fernando Calzada Bermejo, Unidad de Investigación Médica en Farmacología y Productos Naturales, Centro Médico Nacional Siglo XXI, Instituto Mexicano del Seguro Social, and were cultured on nutrient agar (Mueller–Hinton; Sigma) before determination of MIC values. Mueller–Hinton (MHB) broth was used for susceptibility tests.

4.5.2. Compounds

Tetracycline (purity > 98%), kanamycin (purity > 99%), chloramphenicol (purity > 98%), and reserpine (purity > 98%) were obtained from Sigma. Glycolipids **1**–**3** were purified as previously described by preparative recycling HPLC using a Waters 600 E multi-solvent delivery system equipped with a Waters 410 refractive index detector (Waters) as described above, and their purity was assessed by HPLC, NMR, and FAB-MS as >99%.

4.5.3. Susceptibility testing

MIC values were determined at least in duplicate by standard microdilution procedures. An inoculum density of 1.5×10^8 CFU of each of the test strains was prepared in 0.9% saline by comparison with a McFarland standard. MHB or LB (125 μL) was dispensed into 10 wells of a 96-well microtiter plate (Nunc, 0.3 mL volume per well). All test compounds were dissolved in DMSO before dilution into MHB or LB for use in MIC determinations. The highest concentration of DMSO remaining after dilution (3.125% v/v) caused no inhibition of bacterial growth. Then, compounds **1**–**3** or appropriate antibiotic (125 μL) were individually dispensed into well 1 and serially diluted across the plate (512–1 μg/mL), leaving well 11 empty for the growth control. The final volume was dispensed into well 12, which being free of inoculum served as the sterile control. The inoculum (125 μL) was added into wells 1–11 and the plate was incubated at 37 °C for 24 h. The MIC was defined as the lowest concentration, which yielded no visible growth. Tetracycline, kanamycin, and chloramphenicol were also tested as positive drug controls. A methanolic solution (5 mg/mL) of 3-[4,5-dimethylthiazol-2-yl]-2,5-diphenyltetrazolium bromide (MTT; Sigma) was used to detect bacterial growth by a color change from yellow to dark blue. For the modulation assay, all glycolipids were tested at a final concentration of 25 μg/mL. Two-fold serial dilutions of antibiotics ranging from 512 to 1 μg/mL were added, and the microtiter plates were then interpreted, after inoculum addition and incubation, in the same manner as for MIC determinations. The activity of reserpine at a concentration of 20 μg/mL was also tested as an efflux pump inhibitor (positive control). All samples were tested in duplicate (Corona-Castañeda and Pereda-Miranda, 2012).

4.5.4. Cytotoxicity assay

Nasopharyngeal (KB), cervix (HeLa), and laryngeal carcinoma (Hep-2) cell lines were maintained in RMPI 1640 (10×) medium supplemented with 10% fetal bovine serum. Cell lines were cultured at 37 °C in an atmosphere of 5% CO_2 in air (100% humidity). The cells at log phase of their growth cycle were treated in triplicate with various concentrations of the test samples (0.16–20 μg/mL) and incubated for 72 h at 37 °C in a humidified atmosphere of 5% CO_2. The cell concentration was determined by the NCI sulforhodamine method. Results were expressed as the dose that inhibits 50% control growth after the incubation period (IC_{50}). The values were estimated from a semi log plot of the drug concentration (μg/mL) against the percentage of viable cells. Vinblastine and colchicine were included as positive drug controls (Vichai and Kirtikara, 2006; Figueroa-González et al., 2012).

Acknowledgments

This research was supported by Dirección General de Asuntos del Personal Académico, UNAM (IN212813) and Consejo Nacional de Ciencia y Tecnología (101380-Q). B.C.-C. and L.C. received graduate scholarships from CONACyT. Thanks are due to Georgina Duarte, and Margarita Guzmán ("Unidad de Servicios de Apoyo a

la Investigación", Facultad de Química, UNAM) for the recording of mass spectra.

Appendix A. Supplementary data

Supplementary data associated with this article can be found, in the online version, at http://dx.doi.org/10.1016/j.phytochem.2013.07.007.

References

Bah, M., Pereda-Miranda, R., 1996. Detailed FAB-mass spectrometry and high resolution NMR investigations of tricolorins A–E, individual oligosaccharides from the resins of *Ipomoea tricolor* (Convolvulaceae). Tetrahedron 52, 13063–13080.

Bah, M., Chérigo, L., Taketa, A.T.C., Fragoso-Serrano, M., Hammond, G.B., Pereda-Miranda, R.J., 2007. Intrapilosin I-VII, pentasaccharides from the seeds of *Ipomoea intrapilosa*. J. Nat. Prod. 70, 1153–1157.

Castañeda-Gómez, J., Figueroa-González, G., Jacobo, N., Pereda-Miranda, 2013. Purgin II, a resin glycoside ester-type dimer and inhibitor of multidrug efflux pumps from *Ipomoea purga*. J. Nat. Prod. 76, 64–71.

Chérigo, L., Pereda-Miranda, R., 2006. Resin glycosides from the flowers of *Ipomoea murucoides*. J. Nat. Prod. 69, 595–599.

Chérigo, L., Pereda-Miranda, R., Fragoso-Serrano, M., Jacobo-Herrera, N., Kaatz, G., Gibbons, S., 2008. Inhibitors of bacterial multidrug efflux pumps from the resin glycosides of *Ipomoea murucoides*. J. Nat. Prod. 71, 1037–1045.

Chérigo, L., Pereda-Miranda, R., Gibbons, S., 2009. Bacterial resistance modifying tetrasaccharide agents from *Ipomoea murucoides*. Phytochemistry 70, 222–227.

Corona-Castañeda, B., Pereda-Miranda, R., 2012. Morning glory resin glycosides as modulators of antibiotic activity in multidrug-resistant Gram-negative bacteria. Planta Med. 78, 128–131.

Cruz-Morales, S., Castañeda-Gómez, J., Figueroa-González, G., Mendoza-García, A., Lorence, A., Pereda-Miranda, R., 2012. Mammalian multidrug resistance lipopentasaccharide inhibitors from *Ipomoea alba* seeds. J. Nat. Prod. 75, 1603–1611.

Duus, J.O., Gotfredsen, C.H., Bock, K., 2000. Carbohydrate structural determination by NMR spectroscopy: modern methods and limitations. Chem. Rev. 100, 4589–4614.

Eich, E., 2008. Solanaceae and Convolvulaceae: Secondary Metabolites. Biosynthesis, Chemotaxonomy, Biological and Economic Significance. Springer Verlag, Berlin, pp. 532–572.

Escalante-Sánchez, E., Rosas-Ramírez, D., Linares, E., Bye, R., Pereda-Miranda, R., 2008. Batatinosides II-VI, acylated lipooligosaccharides from the resin glycosides of sweet potato. J. Agric. Food Chem. 56, 9423–9428.

Escobedo-Martínez, C., Cruz-Morales, S., Fragoso-Serrano, M., Mukhlesur, M., Gibbons, S., Pereda-Miranda, R., 2010. Characterization of a xylose containing oligosaccharide, an inhibitor of multidrug resistance in *Staphylococcus aureus*, from *Ipomoea pes-caprae*. Phytochemistry 71, 1796–1801.

Figueroa-González, G., Jacobo-Herrera, N., Zentella-Dehesa, A., Pereda-Miranda, R., 2012. Reversal of multidrug resistance by morning glory resin glycosides in human breast cancer cells. J. Nat. Prod. 75, 93–97.

Freixas, N., Sopena, N., Limón, E., Bella, F., Matas, L., Almirante, B., Pujol, M., 2012. Surveillance of methicillin-resistant *Staphylococcus aureus* (MRSA) in acute care hospitals. Results of the VINCat Program (2008–2010). Enferm. Infecc. Microbiol. Clin. Suppl. 3, 39–42.

Gibbons, S., 2008. Phytochemicals for bacterial resistance-strengths, weaknesses and opportunities. Planta Med. 74, 594–602.

Gibbons, S., Udo, E.E., 2000. The effect of reserpine, a modulator of multidrug efflux pumps, on the in-vitro activity of tetracycline against clinical isolates of methicillin-resistant *Staphylococcus aureus* (MRSA) possessing the tet(K) determinant. Phytother. Res. 14, 139–140.

Li, X.Z., Nikaido, H., 2009. Efflux-mediated drug resistance in bacteria: an update. Drugs 69, 1555–1623.

Pereda-Miranda, R., Escalante-Sánchez, E., Escobedo-Martínez, C., 2005. Characterization of lipophilic pentasaccharides from beach morning glory (*Ipomoeapes-caprae*). J. Nat. Prod. 68, 226–230.

Pereda-Miranda, R., Hernández-Carlos, B., 2002. HPLC Isolation and structural elucidation of diastereomeric niloyl ester tetrasaccharides from Mexican scammony root. Tetrahedron 58, 3145–3154.

Pereda-Miranda, R., Kaatz, G., Gibbons, S., 2006. Polyacylated oligosaccharides from medicinal Mexican morning glory species as antibacterials and inhibitors of multidrug resistance in *Staphylococcus aureus*. J. Nat. Prod. 69, 406–409.

Pereda-Miranda, R., Rosas-Ramírez, D., Castañeda-Gómez, J., 2010. Resin glycosides from the morning glory family. In: Kinghorn, A., Falk, H., Kobayashi, J. (Eds.), Progress in the Chemistry of Organic Natural Products, vol. 92. Springer Verlag, New York, pp. 77–153.

Savjani, J., Gajjar, A., Savjani, K., 2009. Mechanisms of resistance: useful tool to design antibacterial agents for drug-resistant bacteria. Mini Rev. Med. Chem. 9, 194–205.

Savoia, D., 2012. Plant-derived antimicrobial compounds: alternatives to antibiotics. Future Microbiol. 7, 979–990.

Shibata, H., Kondo, K., Katsuyama, R., Kawazoe, K., Sato, Y., Murakami, K., Takaishi, Y., Arakaki, N., Higuti, T., 2005. Alkyl gallates, intensifiers of beta-lactam susceptibility in methicillin-resistant *Staphylococcus aureus*. Antimicrob. Agents Chemother. 49, 549–555.

Stavri, M., Piddock, L., Gibbons, S., 2007. Bacterial efflux pump inhibitors from natural sources. J. Antimicrob. Chemother. 59, 1247–1260.

Vichai, V., Kirtikara, K., 2006. Sulforhodamine B colorimetric assay for cytotoxicity screening. Nat. Protoc. 1, 1112–1116.

Zgurskaya, H., 2009. Multicomponent drug efflux complexes: architecture and mechanism of assembly. Future Microbiol. 4, 912–932.

International Journal of Antimicrobial Agents 42 (2013) 513–518

Contents lists available at ScienceDirect

International Journal of Antimicrobial Agents

journal homepage: http://www.elsevier.com/locate/ijantimicag

A new plant-derived antibacterial is an inhibitor of efflux pumps in *Staphylococcus aureus*

Winnie K.P. Shiu[a], John P. Malkinson[a], M. Mukhlesur Rahman[a,b], Jonathan Curry[a], Paul Stapleton[a], Mekala Gunaratnam[a], Stephen Neidle[a], Shazad Mushtaq[c], Marina Warner[c], David M. Livermore[d], Dimitrios Evangelopoulos[e], Chandrakala Basavannacharya[e], Sanjib Bhakta[e], Bryan D. Schindler[f], Susan M. Seo[f], David Coleman[f], Glenn W. Kaatz[f,g,*], Simon Gibbons[a,**]

[a] *Department of Pharmaceutical and Biological Chemistry, UCL School of Pharmacy, 29–39 Brunswick Square, London WC1N 1AX, UK*
[b] *School of Health, Sport and Bioscience, University of East London, Water Lane, London E15 4LZ, UK*
[c] *Antibiotic Resistance Monitoring & Reference Laboratory, HPA Microbiology Service – Colindale, 61 Colindale Avenue, London NW9 5EQ, UK*
[d] *Norwich Medical School, University of East Anglia, Norwich NR4 7TJ, UK*
[e] *Mycobacteria Research Laboratory, Institute for Structural and Molecular Biology, Department of Biological Sciences, Birkbeck, University of London, London WC1E 7HX, UK*
[f] *The John D. Dingell Department of Veterans Affairs Medical Centre, Detroit, MI 48201, USA*
[g] *Department of Internal Medicine, Division of Infectious Diseases, School of Medicine, Wayne State University, Detroit, MI 48201, USA*

ARTICLE INFO

Article history:
Received 12 July 2013
Accepted 13 August 2013

Keywords:
Hypericum olympicum
Olympicin A
Staphylococcus aureus
MurE ligase

ABSTRACT

An in-depth evaluation was undertaken of a new antibacterial natural product (**1**) recently isolated and characterised from the plant *Hypericum olympicum* L. cf. *uniflorum*. Minimum inhibitory concentrations (MICs) were determined for a panel of bacteria, including: meticillin-resistant and -susceptible strains of *Staphylococcus aureus*, *Staphylococcus epidermidis* and *Staphylococcus haemolyticus*; vancomycin-resistant and -susceptible *Enterococcus faecalis* and *Enterococcus faecium*; penicillin-resistant and -susceptible *Streptococcus pneumoniae*; group A streptococci (*Streptococcus pyogenes*); and *Clostridium difficile*. MICs were 2–8 mg/L for most staphylococci and all enterococci, but were ≥16 mg/L for *S. haemolyticus* and were >32 mg/L for all species in the presence of blood. Compound **1** was also tested against Gram-negative bacteria, including *Escherichia coli*, *Pseudomonas aeruginosa* and *Salmonella enterica* serovar Typhimurium but was inactive. The MIC for *Mycobacterium bovis* BCG was 60 mg/L, and compound **1** inhibited the ATP-dependent *Mycobacterium tuberculosis* MurE ligase [50% inhibitory concentration (IC_{50}) = 75 μM]. In a radiometric accumulation assay with a strain of *S. aureus* overexpressing the NorA multidrug efflux pump, the presence of compound **1** increased accumulation of ^{14}C-enoxacin in a concentration-dependent manner, implying inhibition of efflux. Only moderate cytotoxicity was observed, with IC_{50} values of 12.5, 10.5 and 8.9 μM against human breast, lung and fibroblast cell lines, respectively, highlighting the potential value of this chemotype as a new antibacterial agent and efflux pump inhibitor.

1. Introduction

Plants produce an array of biologically active molecules that have been used as anticancer agents [1], including Taxol®, the camptothecins, the vinca alkaloids and podophyllotoxin derivatives such as etoposide [2]. Less research has been done to evaluate plants as sources of antibacterial agents [3] and among the reports that do exist many lack cytotoxicity data and tested only a few bacterial species. Even fewer studies have attempted to unravel the mechanisms of action for plant products, notable exceptions being studies on (i) the diterpene totarol from many coniferous plants as an inhibitor of FtsZ [4] and of efflux [5] and (ii) epicatechin gallate from green tea, which potentiates β-lactam activity against meticillin-resistant *Staphylococcus aureus* (MRSA) [6].

Nevertheless, plants may be a valuable source of new antibacterials. They must protect themselves against environmental microbes, and plant extracts are widely used as systemic and topical antimicrobials in Western herbal and traditional Chinese

* Corresponding author at: The John D. Dingell Department of Veterans Affairs Medical Centre, Detroit, MI 48201, USA. Tel.: +1 313 576 4491.
** Corresponding author. Tel.: +44 207 753 5913; fax: +44 207 753 5964.
E-mail addresses: gkaatz@juno.com (G.W. Kaatz), simon.gibbons@ucl.ac.uk (S. Gibbons).

0924-8579/$ – see front matter © 2013 Elsevier B.V. and the International Society of Chemotherapy. All rights reserved.
http://dx.doi.org/10.1016/j.ijantimicag.2013.08.007

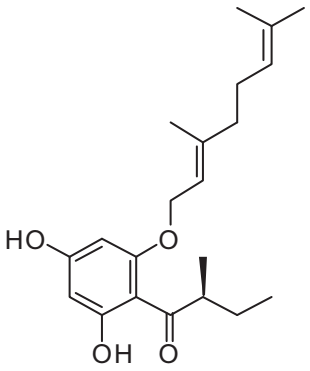

1

Fig. 1. Chemical structure of compound **1**.

medicine as well as in Ayurvedic medicine [7]. Plant extracts are also marketed as 'food materials' with antibacterial properties, such as the various cranberry and bearberry preparations used in the management of urinary tract infections, with bearberry products having better understood chemistry and pharmacology [8]. Also of note are light-activated antibacterial terthiophenes, with minimum inhibitory concentrations (MICs) of 0.022 mg/L for *S. aureus* [9].

We have previously examined plant-derived antibacterials from the acetylene [10], diterpene [11], alkaloid [12] and flavonoid [13] groups. We have focused on acylphloroglucinol products [14], largely due to the considerable antibacterial activities of hyperforin from St John's wort [15], which displayed a MIC of 0.1–1 mg/L for penicillin- and meticillin-resistant *S. aureus* [16]. Acylphloroglucinols are complex natural products with an acylated aromatic-derived core and many prenyl groups, which may be cyclised or oxidised to give a class of chiral products rich in functional groups [17]. Early work on these molecules led to their isolation and characterisation from other *Hypericum* spp. such as *Hypericum drummondii*, which yielded the drummondins, some of which have potent activity towards *S. aureus* (MIC = 0.39 mg/L [18]). Other new acylphloroglucinol products with moderate antibacterial activity [14] were found in *Hypericum foliosum* and *Hypericum beanii*, whilst lipophilic extracts of the aerial parts of *Hypericum olympicum* L. cf. *uniflorum* were found to contain a new acylphloroglucinol antibacterial (**1**), given the trivial name olympicin A (Fig. 1); this was spectroscopically characterised and patented [19,20].

Here we describe the antibacterial spectrum of activity of compound **1** in the presence and absence of blood against multiple bacteria, including *Mycobacterium bovis* BCG, and provide a cytotoxicity evaluation for mammalian cell lines. We additionally examined the ability of compound **1** to inhibit ATP-dependent MurE ligase of *Mycobacterium tuberculosis* as well as to increase the accumulation of the quinolone antibiotic enoxacin by a strain of *S. aureus* overexpressing the NorA major facilitator superfamily (MFS) efflux pump. This work shows the value of simple plant natural product chemotypes as antibacterials and as modifiers of bacterial resistance.

2. Materials and methods

2.1. Isolation of compound *1*

Aerial parts of *H. olympicum* L. cf. *uniflorum* (Kew accession no. **1969-31184**) were collected from the Royal Botanic Garden Kew at Wakehurst Place (Ardingly, UK): 937 g of dried, powdered material was sequentially extracted with 3.5 L of *n*-hexane, dichloromethane (DCM) and methanol using a Soxhlet apparatus (Fisher Scientific, Loughborough, UK). The *n*-hexane and DCM extracts were active against the NorA-overexpressing *S. aureus* strain 1199B (SA-1199B) [21] at 32 mg/L and 16 mg/L, respectively, but had similar profiles by thin-layer chromatography (TLC) (Merck, Darmstadt, Germany). The hexane extract (15.2 g) was fractionated by vacuum-liquid chromatography (VLC) (silica gel $PF_{254+366}$; Merck) using a step-gradient solvent system from 100% hexane to 100% ethyl acetate with a 10% increment and a final methanol wash. VLC fractions 6–8 were active against *S. aureus* SA-1199B at 64 mg/L, had similar TLC profiles and were pooled (total of 842.0 mg). This combined fraction was separated by Sephadex LH-20 (Amersham Biosciences, Little Chalfont, UK) chromatography, giving five fractions eluted with chloroform:methanol (1:1) and one fraction eluted with methanol. The fraction eluted with methanol (80.9 mg) was active at a MIC of 1 mg/L against SA-1199B, and compound **1** (29.1 mg) was isolated from this fraction by preparative TLC [silica; toluene:ethyl acetate:acetic acid (80:18:2), retention factor (R_f) = 0.62]. The compound gave an orange colour reaction with vanillin–sulphuric acid spray on the TLC plate.

2.2. Antibiotics and media

Unless otherwise stated, all chemicals were obtained from Sigma–Aldrich (Poole, UK).

2.3. Bacteria

The bacteria were recent clinical isolates or were reference controls (Table 1). The clinical isolates represented important resistance phenotypes currently prevalent in the UK and worldwide. They comprised: (i) MRSA, including the epidemic MRSA (EMRSA)-15 and -16 strains dominant in the UK [22]; (ii) meticillin-resistant coagulase-negative staphylococci (i.e. *Staphylococcus epidermidis* and *Staphylococcus haemolyticus*); (iii) vancomycin-resistant and -susceptible *Enterococcus faecalis* and *Enterococcus faecium*; (iv) penicillin-resistant and -susceptible *Streptococcus pneumoniae*; (v) group A streptococci (*Streptococcus pyogenes*), which remain universally susceptible to penicillin; and (vi) *Clostridium difficile*. Among the Gram-negative organisms tested were *Escherichia coli* NCTC 10418, *E. coli* STHG69 (multiresistant CMY-4 β-lactamase-producing isolate) and *Pseudomonas aeruginosa* strains NCTC 10662 and NCIB 8626. *M. bovis* BCG ATCC 35734 (Pasteur) was also used. SA-1199B was used in ^{14}C-enoxacin accumulation assays.

2.4. Susceptibility testing

MICs were determined on Iso-Sensitest agar (ISA) by the method of the British Society for Antimicrobial Chemotherapy (BSAC) (http://www.bsac.org.uk) or by microdilution in Iso-Sensitest broth (ISB). Both media were from Oxoid–Thermo Fisher (Basingstoke, UK); ISA was supplemented or not with 5% whole equine blood and ISB with 5% lysed equine blood. Plates were variously incubated at 35–37 °C in (i) air, (ii) air enriched with 5% CO_2 or (iii) under anaerobic conditions. The antimycobacterial activity of compound **1** was determined against slow-growing *M. bovis* BCG using an agar-based spot culture growth inhibition assay as described previously [23]. The front-line antitubercular drug isoniazid was used as a positive control.

2.5. Functional assay for M. tuberculosis MurE activity

The activity of MurE from *M. tuberculosis* was monitored by measuring the release of inorganic phosphate following ATP

Table 1
Minimum inhibitory concentrations (MICs) of compound **1** in Iso-Sensitest broth (ISB) and on Iso-Sensitest agar (ISA) under different atmospheric conditions.

Specimen ID	Species	Phenotype	MIC (mg/L)							
			Air, no blood added		Air, 5% blood added		5% CO_2, blood added		Anaerobic, blood added	
			ISA	ISB	ISA	ISB	ISA	ISB	ISA	ISB
H00057	*Staphylococcus aureus*	EMRSA-16	4	2	>32	>32	>32	>32	32	32
H00520	*S. aureus*	EMRSA-16	2	2	>32	>32	>32	>32	32	32
H00440	*S. aureus*	EMRSA-15	4	4	>32	>32	>32	>32	32	>32
H00156	*S. aureus*	EMRSA-15	4	4	>32	>32	>32	>32	>32	>32
ST797	*S. aureus*	MSSA	8	4	>32	>32	>32	>32	>32	>32
ST841	*S. aureus*	MSSA	8	4	>32	>32	>32	>32	>32	>32
ST862	*S. aureus*	MSSA	8	4	>32	>32	>32	>32	>32	>32
ST870	*S. aureus*	MSSA	2	2	>32	>32	>32	>32	32	>32
CN521	*Staphylococcus epidermidis*	MR-CoNS	8	4	>32	>32	>32	>32	>32	>32
CN515	*Staphylococcus haemolyticus*	MR-CoNS	>32	>32	>32	>32	>32	>32	>32	>32
CN590	*S. haemolyticus*	MS-CoNS	16	16	>32	>32	>32	>32	>32	>32
CN535	*S. epidermidis*	MS-CoNS	4	2	>32	>32	>32	>32	32	>32
H00461	*Enterococcus faecium*	Van^R	4	2	>32	>32	>32	>32	>32	>32
H00473	*E. faecium*	Van^R	4	2	>32	32	>32	32	>32	>32
H00452	*E. faecium*	Van^S	4	2	>32	>32	>32	>32	>32	>32
H00277	*E. faecium*	Van^S	8	2	>32	>32	32	32	32	>32
H00260	*Enterococcus faecalis*	Van^S	4	4	>32	>32	>32	>32	>32	>32
H00666	*E. faecalis*	Van^S	4	4	>32	>32	>32	>32	>32	>32
H00587	*E. faecalis*	Van^R	4	4	>32	>32	>32	>32	>32	>32
H00066	*E. faecalis*	Van^R	4	4	>32	>32	>32	>32	>32	>32
PN2177	*Streptococcus pneumoniae*	Pen^R	(2)[a]	(2)[a]	>32	32	32	32	32	32
PN1847	*S. pneumoniae*	Pen^R	(4)[a]	(2)[a]	>32	32	>32	32	>32	32
H00053	*S. pneumoniae*	Pen^S	(2)[a]	(2)[a]	>32	32	>32	32	>32	>32
H00070	*S. pneumoniae*	Pen^S	(4)[a]	(2)[a]	>32	32	>32	32	>32	32
BS1514	GAS		(4)[a]	(4)[a]	>32	>32	>32	>32	>32	>32
BS1526	GAS		(4)[a]	(4)[a]	>32	>32	>32	>32	>32	>32
BS1531	GAS		(4)[a]	(4)[a]	>32	>32	>32	>32	>32	>32
BS1552	GAS		(4)[a]	(4)[a]	>32	>32	>32	>32	>32	>32
H00518	*Clostridium difficile*	Anaerobe	ng	ng	ng	ng	ng	ng	>32	>32
519	*C. difficile*	Anaerobe	ng	ng	ng	ng	ng	ng	>32	>32
520	*C. difficile*	Anaerobe	ng	ng	ng	ng	ng	ng	>32	>32
522	*C. difficile*	Anaerobe	ng	ng	ng	ng	ng	ng	>32	>32
Standard controls										
NCTC9343	*Bacteroides fragilis*	Anaerobe	ng	ng	ng	ng	ng	ng	>32	>32
ATCC29212	*S. pneumoniae*		(4)[a]	(2)[a]	>32	32	>32	32	>32	32
ATCC29212	*E. faecalis*		4	4	>32	>32	>32	>32	>32	>32
NCTC6571	*S. aureus*		4	4	>32	>32	>32	>32	32	>32
ATCC 35734	*Mycobacterium bovis* BCG	Pasteur	60							

EMRSA, epidemic meticillin-resistant *Staphylococcus aureus*; MSSA, meticillin-susceptible *S. aureus*; MR-CoNS, meticillin-resistant coagulase-negative staphylococci; MS-CoNS, meticillin-susceptible coagulase-negative staphylococci; Van^R, vancomycin-resistant; Van^S, vancomycin-susceptible; Pen^R, penicillin-resistant; Pen^S, penicillin-susceptible; GAS, group A streptococci (*Streptococcus pyogenes*); ng, no growth (all examples were for anaerobes under aerobic growth conditions).

[a] MIC less than or equal to the indicated value, arising when there was no growth at the lowest concentration tested.

hydrolysis [24], with assays performed in final volumes of 50 μL in half-area Costar® microtitre plates (Appleton Woods Ltd., Birmingham, UK). The reaction mixtures comprised 50 ng of recombinant MurE enzyme purified as described previously [25] with 25 mM Bis–Tris–propane/HCl (pH 8.5), 5 mM $MgCl_2$, 50 μM ATP, 50 μM UDP-Mur*N*Ac-L-Ala-D-Glu and 4% (v/v) dimethyl sulphoxide (DMSO) (enzyme reaction) at 37 °C. Then, 2 μL of compound **1** (concentrations of 0.3–100 μM) dissolved in 100% DMSO was added and the reaction was initiated by the addition of 75 μM *meso*-diaminopimelic acid for 30 min at 37 °C. Following this incubation period, release of inorganic phosphate was determined using a Gold Lock Reagent Kit (Innova Biosciences, Cambridge, UK) according to the manufacturer's instructions. Results were corrected for background absorbance of the reaction mixtures and for any non-enzymatic hydrolysis of ATP (control reaction without enzyme). Percent inhibition was calculated for each concentration of compound **1** and was fitted to a non-linear regression model, plotting the sigmoidal dose–response on a semi-log scale to derive the IC_{50} (the inhibitor concentration giving 50% inactivation). All assays were performed in triplicate.

2.6. Cytotoxicity evaluation

The antiproliferative activity of compound **1** was determined for MCF7 (human breast carcinoma), A549 (human lung carcinoma) and WI38 (human fibroblast) cells using the sulforhodamine B assay [26].

2.7. Accumulation of ^{14}C-enoxacin

Accumulation studies using SA-1199B [MIC for compound **1** of 2.9 μM (1 mg/L)] were performed essentially as described previously, modified by the use of a 10-min time course [27]. Control experiments, representing unimpeded NorA activity, included cells incubated only with ^{14}C-enoxacin. Additional experiments were performed using reserpine (33 μM) or a concentration range of compound **1** (10–50 μM; 3.46–17.3 mg/L) in addition to ^{14}C-enoxacin. Three replicates were performed for the control, reserpine, and the 10 μM and 50 μM concentrations of compound **1**, and two replicates were performed for the remainder of the tested concentrations of compound **1**. Comparisons between control, reserpine, and the 10 μM and 50 μM concentrations of

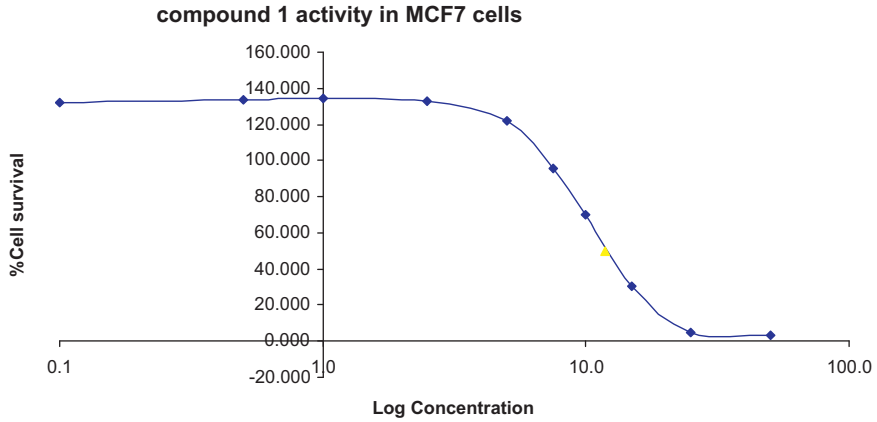

Fig. 2. Activity of compound **1** in human breast cancer cells (MCF7) exposed for 96 h. Cell survival is shown as a percentage of untreated cells.

compound **1** were performed using the statistical functions available within SigmaPlot 12.0 (*t*-test) (SYSTAT Software Inc., Chicago, IL).

Time–kill analyses were performed using SA-1199B and the highest concentration of compound **1** employed in accumulation assays (50 μM). The conditions of the accumulation assay were replicated exactly, resulting in an initial inoculum of SA-1199B of ca. 10^{11} CFU/mL. Following the addition of compound **1**, aliquots were removed at 0, 2, 5 and 10 min and surviving bacteria were enumerated using dilution and plating techniques. Dilutions were sufficient to eliminate any antibiotic carry-over effect.

3. Results

3.1. Susceptibility tests

Enterococci and staphylococci grew under all conditions, whereas the streptococci grew poorly in the absence of blood and *C. difficile* grew only under anaerobic conditions.

Without blood, the MICs of compound **1** for staphylococci, enterococci and streptococci mostly were 2–8 mg/L on ISA and 2–4 mg/L in ISB (Table 1). Exceptions were both of the *S. haemolyticus* isolates, for which MICs were ≥16 mg/L both in ISB and on ISA. The reason(s) for this differential are unknown, but the greater resistance in the species is notable.

Addition of blood raised the MICs of compound **1** to >32 mg/L both on ISA and in ISB for all strains tested, and the values remained at >32 mg/L when the blood-containing media were incubated under 5% CO_2 or under anaerobic conditions. No activity was noted for compound **1** against the Gram-negative organisms *E. coli* or *P. aeruginosa* (MICs > 512 mg/L) (data not shown).

The antimycobacterial activity of compound **1** was determined against the slow-growing vaccine strain *M. bovis* BCG, a close relative to pathogenic *M. tuberculosis*, using an agar-based assay, and the MIC was found to be 60 mg/L.

3.2. Inhibition of MurE ligase

The effect of compound **1** was tested against the recombinant MurE ligase from *M. tuberculosis*, a key enzyme that participates in the early stages of peptidoglycan biosynthesis. This enzyme is conserved in all bacterial species but selects its natural substrates in a species-specific manner [24]. Compound **1** exhibited moderate inhibition of the activity of *M. tuberculosis* MurE ligase, with an IC_{50} of 75 μM (data not shown).

3.3. Cytotoxicity evaluation

The IC_{50} values of compound **1** were determined for MCF7 (human breast carcinoma; Fig. 2), A549 (human lung carcinoma) and WI38 (human fibroblast) cells using the sulforhodamine B assay and were 12.5, 10.5 and 8.9 μM, respectively.

3.4. ^{14}C-enoxacin accumulation

Compound **1** demonstrated a concentration-dependent effect on the accumulation of ^{14}C-enoxacin by *S. aureus* SA-1199B, with increasing concentrations resulting in gradually increasing accumulation (Fig. 3). Both reserpine and compound **1** at 50 μM increased enoxacin accumulation significantly compared with the control ($P = 0.03$ and $P = 0.002$, respectively) and there was a trend towards compound **1** at 50 μM being more effective than reserpine ($P = 0.08$).

Enoxacin accumulation data were validated by time–kill assays, which revealed no effect of 50 μM of compound **1** on the viability of *S. aureus* SA-1199B over a 10-min exposure period (data not shown). This period of time was the same as that employed in the accumulation assays.

4. Discussion

Compound **1** had antibacterial activity against Gram-positive bacteria, with MICs of 2–8 mg/L for staphylococci and enterococci, although with much higher values for *S. haemolyticus*. MICs were generally slightly higher on ISA than in ISB and

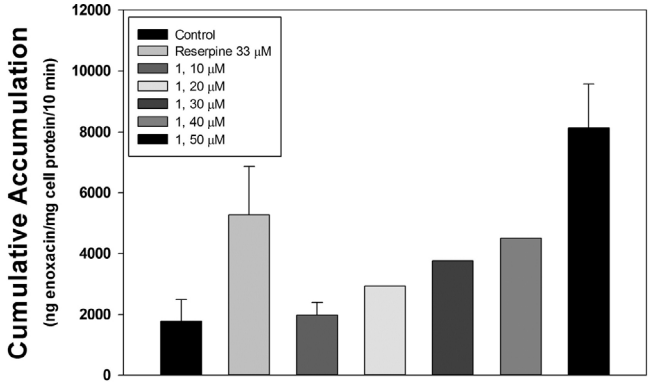

Fig. 3. Accumulation of ^{14}C-enoxacin by *Staphylococcus aureus* 1199B. Concentrations of reserpine and compound **1** used are indicated.

this may reflect binding to agar. The compound probably has similar activity against streptococci as against staphylococci and enterococci, although growth of streptococci is poor without blood and interpretation must be made cautiously.

Blood obviated the activity of compound **1**, raising its MICs to >32 mg/L, irrespective of species and atmospheric conditions. It is likely that compound **1** was bound by albumin or some other blood component. The inactivation is likely to preclude development as a systemic antibiotic but there may be potential for topical use. One example might be the eradication of nasal carriage of MRSA, a role where mupirocin, another antibiotic unsuitable for systemic use, has found a niche. Compound **1** might also remain suitable for minor skin infections such as impetigo caused by *S. aureus*. The natural products mupirocin and retapamulin, both of which are unsuitable for systemic use, likewise are employed in this role. Use in staphylococcal conjunctivitis might also be practicable. Animal experiments could be used to test these possibilities.

Reasons for the lack of activity of compound **1** against any of the Gram-negative bacteria, even at 512 mg/L, are uncertain but efflux was considered a possible contributory factor. In support of this, we have recently shown that strains of *Salmonella* lacking components of efflux pumps such as the pivotal resistance–nodulation–division (RND) pump AcrAB–TolC are susceptible to plant-derived antibacterials such as falcarindiol, which is inactive against their parent strains [28]. However, the activity of compound **1** against Gram-negative isolates was not improved with the addition of the outer membrane permeabilisers ethylene diamine tetra-acetic acid (1 mM) or polyethyleneimine (50 mg/L) (data not shown), and its molecular weight (346 Da) is far below the general exclusion limit for the outer membrane. These data suggest that outer membrane impermeability is not responsible for the lack of activity. Inactivation by chemical modification is another possible mechanism for the lack of activity of compound **1** against Gram-negative bacteria, and further work will be required to investigate this possibility.

Compound **1** inhibited the ATP-depended MurE ligase from *M. tuberculosis*, a cytoplasmic enzyme that participates in the biosynthesis of cell wall peptidoglycan [24]. The key enzymes of the cell wall peptidoglycan biosynthesis pathway are essential for the survival of many bacterial pathogens [29] and there is renewed interest in the search for novel therapeutic targets for tackling existing drug resistance [30,31].

Compound **1** also had some ability to impede efflux. The low accumulation of ^{14}C-enoxacin by SA-1199B in the absence of inhibitors was expected and is the result of overexpression of NorA in this strain (Fig. 3). Compound **1** at 50 μM significantly increased enoxacin accumulation and this concentration was as effective, or perhaps even more effective, than 33 μM reserpine. Increased accumulation of enoxacin is consistent with interference with NorA. As such, it is clear that compound **1** is a NorA inhibitor. Use of concentrations that surpassed the MIC of compound **1** for SA-1199B was not problematic based on time–kill assays, which revealed no effect of compound **1** at 50 μM on the viability of SA-1199B over 60 min.

The pharmacophore of compound **1** may provide a starting point towards the development of a more effective inhibitor, and its weak cytotoxic activity towards cancer and mammalian cell lines suggests that this class of compound may have potential in a topical formulation or, if antibacterial activity in the presence of blood can be enhanced through iterative chemistry, as a lead in the development of a new class of systemic antibiotics. Compounds that are antibacterial and can inhibit efflux processes of bacteria could have potential to treat infections due to multidrug-resistant strains.

Funding: The Heptagon Fund and Union Life Sciences funded this work.

Competing interests: None declared.

Ethical approval: Not required.

References

[1] Cragg GM, Grothaus PG, Newman DJ. Impact of natural products on developing new anti-cancer agents. Chem Rev 2009;109:3012–43.
[2] Felix W, Senn HJ. Clinical study of the new podophyllotoxin derivative, 4′-demethylepipodophyllotoxin 9-(4,6-*o*-ethylidene-β-D-glucopyranoside) (NSC-141540; VP-16-213), in solid tumors. Cancer Chemother Rep 1975;59:737–42.
[3] Gibbons S. Phytochemicals for bacterial resistance—strengths, weaknesses and opportunities. Planta Med 2008;74:594–602.
[4] Jaiswal R, Beuria TK, Mohan R, Mahajan SK, Panda D. Totarol inhibits bacterial cytokinesis by perturbing the assembly dynamics of FtsZ. Biochemistry 2007;46:4211–20.
[5] Smith ECJ, Kaatz GW, Seo SM, Wareham N, Williamson EM, Gibbons S. The phenolic diterpene totarol inhibits multidrug efflux pump activity in *Staphylococcus aureus*. Antimicrob Agents Chemother 2007;51:4480–3.
[6] Stapleton PD, Shah S, Ehlert K, Hara Y, Taylor PW. The β-lactam-resistance modifier (−)-epicatechin gallate alters the architecture of the cell wall of *Staphylococcus aureus*. Microbiology 2007;153:2093–103.
[7] Gautam R, Saklani A, Jachak SM. Indian medicinal plants as a source of antimycobacterial agents. J Ethnopharmacol 2007;110:200–34.
[8] Jahodár L, Jílek P, Páktová M, Dvoráková V. Antimicrobial effect of arbutin and an extract of the leaves of *Arctostaphylos uva-ursi* in vitro. Cesk Farm 1985;34:174–8 [in Czech].
[9] Ciofalo M, Petruso S, Schillaci D. Quantitative assay of photoinduced antibiotic activities of naturally-occurring 2,2′:5′,2-terthiophenes. Planta Med 1996;62:374–5.
[10] Lechner D, Stavri M, Oluwatuyi M, Pereda-Miranda R, Gibbons S. The anti-staphylococcal activity of *Angelica dahurica* (Bai Zhi). Phytochemistry 2004;64:331–5.
[11] Stavri M, Paton A, Skelton BW, Gibbons S. Antibacterial diterpenes from *Plectranthus ernstii*. J Nat Prod 2009;72:1191–4.
[12] O'Donnell G, Gibbons S. Antibacterial activity of two canthin-6-one alkaloids from *Allium neapolitanum*. Phytother Res 2007;21:653–7.
[13] Rahman MM, Gibbons S, Gray AI. Isoflavanones from *Uraria picta* and their antimicrobial activity. Phytochemistry 2007;68:1692–7.
[14] Gibbons S, Moser E, Hausmann S, Stavri M, Smith E, Clennett C. An anti-staphylococcal acylphloroglucinol from *Hypericum foliosum*. Phytochemistry 2005;66:1472–5.
[15] Bystrov NS, Chernov BK, Dobrynin VN, Kolosov MN. The structure of hyperforin. Tetrahedron Lett 1975;32:2791–4.
[16] Schempp CM, Pelz K, Wittmer A, Schöpf E, Simon JC. Antibacterial activity of hyperforin from St John's wort against multiresistant *Staphylococcus aureus* and Gram-positive bacteria. Lancet 1999;353:2129.
[17] Xiao ZY, Mu Q, Shiu WK, Zeng YH, Gibbons S. Polyisoprenylated benzoylphloroglucinol derivatives from *Hypericum sampsonii*. J Nat Prod 2007;70:1779–82.
[18] Jayasuriya H, Clark AM, McChesney JD. New antimicrobial filicinic acid derivatives from *Hypericum drummondii*. J Nat Prod 1991;54:1314–20.
[19] Shiu WK, Rahman MM, Curry J, Stapleton PD, Zloh M, Malkinson JP, et al. Antibacterial acylphloroglucinols from *Hypericum olympicum*. J Nat Prod 2012;75:336–43.
[20] Shiu WKP, Malkinson JP, Gibbons S. UK patent number GB0718023.5. New antibacterial substances from Hypericum. 2007.
[21] Kaatz GW, Seo SM, Ruble CA. Efflux-mediated fluoroquinolone resistance in *Staphylococcus aureus*. Antimicrob Agents Chemother 1993;37:1086–94.
[22] Richardson JF, Reith S. Characterization of a strain of methicillin-resistant *Staphylococcus aureus* (EMRSA-15) by conventional and molecular methods. J Hosp Infect 1993;25:45–52.
[23] Evangelopoulos D, Bhakta S. Rapid methods for testing inhibitors of mycobacterial growth. Methods Mol Biol 2010;642:193–201.
[24] Basavannacharya C, Robertson G, Munshi T, Keep NH, Bhakta S. ATP-dependent MurE ligase in *Mycobacterium tuberculosis*: biochemical and structural characterisation. Tuberculosis (Edinb) 2010;90:16–24.
[25] Guzman JD, Gupta A, Evangelopoulos D, Basavannacharya C, Pabon LC, Plazas EA, et al. Anti-tubercular screening of natural products from Colombian plants: 3-methoxynordomesticine, an inhibitor of MurE ligase of *Mycobacterium tuberculosis*. J Antimicrob Chemother 2010;65:2101–7.
[26] O'Donnell G, Poeschl R, Zimhony O, Gunaratnam M, Moreira JBC, Neidle S, et al. Bioactive pyridine-*N*-oxide sulphides from *Allium stipitatum*. J Nat Prod 2009;72:360–5.
[27] Kaatz GW, Seo SM. Inducible NorA-mediated multidrug resistance in *Staphylococcus aureus*. Antimicrob Agents Chemother 1995;39:2650–5.

[28] Garvey MI, Rahman MM, Gibbons S, Piddock LJ. Medicinal plant extracts with efflux inhibitory activity against Gram-negative bacteria. Int J Antimicrob Agents 2011;37:145–51.
[29] Trepod CM, Mott JE. Elucidation of essential and nonessential genes in the *Haemophilus influenzae* Rd cell wall biosynthetic pathway by targeted gene disruption. Antimicrob Agents Chemother 2005;49:824–6.
[30] Bugg TD, Braddick D, Dowson CG, Roper DI. Bacterial cell wall assembly: still an attractive antibacterial target. Trends Biotechnol 2011;29:167–73.
[31] Munshi T, Gupta A, Evangelopoulos D, Guzman JD, Gibbons S, Keep NH, et al. Characterisation of ATP-dependent Mur ligases involved in the biogenesis of cell wall peptidoglycan in *Mycobacterium tuberculosis*. PLOS ONE 2013;8:e60143.

International Journal of Antimicrobial Agents 37 (2011) 145–151

Contents lists available at ScienceDirect

International Journal of Antimicrobial Agents

journal homepage: http://www.elsevier.com/locate/ijantimicag

Medicinal plant extracts with efflux inhibitory activity against Gram-negative bacteria

Mark I. Garvey[a], M. Mukhlesur Rahman[b], Simon Gibbons[b,**], Laura J.V. Piddock[a,*]

[a] Antimicrobial Agents Research Group, School of Immunity and Infection, College of Medical and Dental Sciences, University of Birmingham, Birmingham B15 2TT, UK
[b] Department of Pharmaceutical and Biological Chemistry, The School of Pharmacy, University of London, 29–39 Brunswick Square, London WC1N 1AX, UK

ARTICLE INFO

Article history:
Received 31 August 2010
Accepted 22 October 2010

Keywords:
Efflux pump inhibitor
Antibiotic resistance
Synergistic interactions

ABSTRACT

It was hypothesised that extracts from plants that are used as herbal medicinal products contain inhibitors of efflux in Gram-negative bacteria. Extracts from 21 plants were screened by bioassay for synergy with ciprofloxacin against *Salmonella enterica* serotype Typhimurium, including mutants in which *acrB* and *tolC* had been inactivated. The most active extracts, fractions and purified compounds were further examined by minimum inhibitory concentration testing with five antibiotics for activity against Enterobacteriaceae and *Pseudomonas aeruginosa*. Efflux activity was determined using the fluorescent dye Hoechst 33342. Eighty-four extracts from 21 plants, 12 fractions thereof and 2 purified molecules were analysed. Of these, 12 plant extracts showed synergy with ciprofloxacin, 2 of which had activity suggesting efflux inhibition. The most active extract, from *Levisticum officinale*, was fractionated and the two fractions displaying the greatest synergy with the five antibiotics were further analysed. From these two fractions, falcarindiol and the fatty acids oleic acid and linoleic acid were isolated. The fractions and compounds possessed antibacterial activity especially for mutants lacking a component of AcrAB–TolC. However, no synergism was seen with the fractions or purified molecules, suggesting that a combination of compounds is required for efflux inhibition. These data indicate that medicinal plant extracts may provide suitable lead compounds for future development and possible clinical utility as inhibitors of efflux for various Gram-negative bacteria.

1. Introduction

Over the last decade there has been a dramatic reduction in the number of pharmaceutical companies developing new antimicrobial agents [1]. In parallel, the number of antibiotic-resistant Gram-negative bacteria has increased [2]. With the reduction in the number of new agents and in antibiotic development, there has been a resurgence of interest in the search for compounds that will restore the activity of licensed antimicrobial agents that until recently had excellent activity against Gram-negative bacteria. In 1998 it was shown that plant-derived compounds have activity against Gram-positive bacteria, in particular *Staphylococcus aureus* [3]. Several compounds, such as reserpine, behave as if they inhibit efflux pumps and hence have become known as efflux pump inhibitors (EPIs) [4]. Since that time, numerous phytochemicals have been shown to have activity against *S. aureus* or other Gram-positive bacteria, or to act as potential EPIs with antimicrobials for Gram-positive bacteria [5–11]. Unfortunately, most of the plant-derived compounds have little or no activity with antibiotics against Gram-negative bacteria and it was suggested that, as many plant pathogens are Gram-negative bacteria, plants may not produce molecules effective against these organisms [5]. None the less, there are many medicinal plants that have traditional usage in various parts of the world in the treatment of infections caused by Gram-negative bacteria [12,13].

Gram-negative bacteria have innate multidrug resistance to many antimicrobial compounds owing to the presence of efflux pumps. In the Enterobacteriaceae, the efflux pump most commonly associated with this innate multidrug resistance is the AcrAB–TolC efflux system.

Homologues of this pump are found in other Gram-negative bacteria, including *Pseudomonas aeruginosa*, *Acinetobacter* spp. and *Campylobacter jejuni* [14]. The presence of these pumps and their broad substrate profile is the cause of the innate resistance to many of the agents that have good antimicrobial activity against Gram-positive bacteria. Overproduction of these efflux pumps confers clinically relevant resistance to many antimicrobial agents, including ciprofloxacin and tigecycline, in Enterobacteriaceae [14].

* Corresponding author. Tel.: +44 121 414 6966; fax: +44 121 414 6819.
** Corresponding author. Tel.: +44 207 753 5913; fax: +44 207 753 5964.
E-mail addresses: simon.gibbons@pharmacy.ac.uk (S. Gibbons), l.j.v.piddock@bham.ac.uk (L.J.V. Piddock).

0924-8579/$ – see front matter © 2010 Elsevier B.V. and the International Society of Chemotherapy. All rights reserved.
doi:10.1016/j.ijantimicag.2010.10.027

We hypothesised that extracts from plants that are used as natural herbal medicines contain molecules that act as EPIs against the efflux pumps of Gram-negative bacteria. Therefore, 84 extracts from 21 medicinal plants were investigated for synergistic activity with ciprofloxacin against *Salmonella enterica* serotype Typhimurium. These plants were chosen as they all have a use in various systems of medicine and some are used as topical antimicrobials, for example *Melissa officinalis*. Extracts were screened for differential activity against strains that either expressed or overproduced the AcrAB–TolC pump but had no activity for mutants in which a component of this pump had been inactivated. In this way, it was hoped to identify extracts that contained an EPI specific for this pump. For those extracts where data suggested active components, the effect upon growth of *Salmonella* spp. as well as inhibition of efflux activity was determined. Two extracts showing the greatest synergy with ciprofloxacin were fractionated and the active molecules were identified.

2. Materials and methods

2.1. Bacterial strains, storage and growth

All bacteria used in this study are listed in Table 1. Construction of mutants derived from *S.* Typhimurium has been described previously [16,19,21,22]. *Salmonella* Typhimurium L3 is a pre-therapy human clinical isolate and L10 is a post-therapy human clinical isolate that overexpresses *acrAB*, both of which have been previously described [20,23]. All bacteria were stored on Protect™ beads (Technical Service Consultants Ltd., Heywood, UK) at −80 °C. Identification of each species was confirmed by Gram-stain and analytical profile index (API 20E; bioMérieux, Marcy-l'Étoile, France).

Table 1
Bacterial strains used in this study.

Strain	Species	Description	Reference/source
L354	*S.* Typhimurium	SL1344	[15]
L109	*S.* Typhimurium	SL1344 *tolC::aph*	[16]
L110	*S.* Typhimurium	SL1344 *acrB::aph*	[16]
L884	*S.* Typhimurium	SL1344 *acrA::aph*	[17]
L785	*S.* Typhimurium	ATCC 15277 (LT2)	[18]
L828	*S.* Typhimurium	ATCC 14028s	[18]
L829	*S.* Typhimurium	ATCC 14028s Δ*tolC*	[19]
L830	*S.* Typhimurium	ATCC 14028s Δ*acrB*	[19]
L831	*S.* Typhimurium	ATCC 14028s Δ*acrAB*	[19]
L3	*S.* Typhimurium	Human pre-therapy clinical isolate, antibiotic-susceptible	[20]
L10	*S.* Typhimurium	Human post-therapy clinical isolate; MDR and overproducing *acrAB*	[20]
A1	*Enterobacter cloacae*	NCTC 10005	NCTC
B14	*Serratia marcescens*	NCTC 2847	NCTC
G1	*Pseudomonas aeruginosa*	NCTC 10662	NCTC
H42	*Klebsiella pneumoniae*	NCTC 10896	NCTC
H43	*K. pneumoniae*	NCTC 9633	NCTC
I114	*Escherichia coli*	NCTC 10538	NCTC
J29	*Morganella morganii*	NCTC 235	NCTC

S. Typhimurium, *Salmonella enterica* serotype Typhimurium; ATCC, American Type Culture Collection; MDR, multidrug-resistant; NCTC, National Culture Type Collection (Health Protection Agency, Colindale, London, UK).

Table 2
List of medicinal plants used in this study.

Plant name	Common name	Family
Anemone nemorosa	Wood anemone	Ranunculaceae
Angelica sinensis	Female ginseng	Apiaceae
Apium graveolens	Dill	Apiaceae
Artemisia abrotanum	Southernwood	Asteraceae
Asclepias tuberosa	Butterfly weed	Apocynaceae
Boswellia serrata	Salai	Burseraceae
Catha edulis	Khat	Celastraceae
Centella asiatica	Gotu kola	Apiaceae
Cinnamomum aromaticum	Cassia cinnamon	Lauraceae
Citrus aurantium	Bitter orange	Rutaceae
Commiphora molmol	Myrrh	Burseraceae
Daucus carota	Wild carrot	Apiaceae
Ephedra funereal	Death Valley ephedra	Ephedraceae
Glycyrrhiza glabra	Liquorice	Leguminosae
Levisticum officinale	Lovage	Apiaceae
Melissa officinalis	Lemon balm	Lamiaceae
Papaver somniferum	Opium poppy	Papaveraceae
Pimpinella anisum	Anise	Apiaceae
Pulmonaria officinalis	Lungwort	Boraginaceae
Thymus vulgaris	Thyme	Lamiaceae
Tussilago farfara	Coltsfoot	Asteraceae

2.2. Media and chemicals

Bacteria were grown on Luria–Bertani (LB) agar plates (Oxoid Ltd., Basingstoke, UK) and in LB broth (Oxoid Ltd.). All antibiotics and other compounds were obtained from Sigma (Poole, UK).

2.3. Extraction of plants

In total, 21 plants were used in this study (Table 2). All plants except *Catha edulis* (purchased locally in London, UK) were purchased from Proline Botanicals (Essendine, UK). Each plant (200–400 g) was extracted at 21 °C sequentially with 300–600 mL of chloroform, methanol and water.

2.4. Fractionation of extracts

Following assessment of bioactivity, the chloroform extract of *Levisticum officinale* (10 g) was fractionated by vacuum liquid chromatography (VLC) on silica gel 60G (Merck Ltd., Lutterworth, UK) using solvent systems of increasing polarity. Fractions were eluted with hexane containing increasing 10% or 20% increments of ethyl acetate (EA) to give fractions A–H (A, 10% EA; B, 20% EA; C, 30% EA; D, 40% EA; E, 50% EA; F, 60% EA; G, 80% EA; and H, 100% EA). Fraction I was eluted with 5% methanol in EA, fraction J with 10% methanol in EA, fraction K with 20% methanol in EA and finally fraction L with 50% methanol in EA.

2.5. Purification of active compounds

Bioassay-directed isolation indicated that the VLC fraction eluted with 30% EA was active. This was purified by preparative thin-layer chromatography (Si Gel; Merck) (mobile phase 20% EA in toluene; double development) yielding falcarindiol (**1**; 450 mg) and levistolide A (**2**; 69 mg) (Fig. 1), which were identified by comparison with literature data [24,25].

2.6. Bioassay screening

Screening with ciprofloxacin in the absence or presence of plant extracts (Table 2), fractions of *L. officinale* and *M. officinalis*, and purified compounds from fractions of the chloroform extract of *L. officinale* for synergistic activity was carried out by bioassay essentially as described previously [26,27]. Six rows of 6 wells (total 36

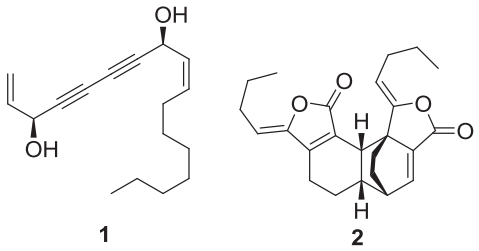

Fig. 1. Structures of falcarindiol (**1**) and levistolide A (**2**).

wells) each of 8-mm diameter were cut out of each agar plate using an agar cutter (Fisher Scientific, Loughborough, UK). Then, 200 μL of sterile Iso-Sensitest™ broth (Oxoid Ltd.) containing ciprofloxacin (0.5, 1 and 2 mg/L) was added to three sets of wells. This volume and concentration gave a zone of inhibition ≥15 mm in diameter. To determine test compound synergism with ciprofloxacin, 200 μL of a solution containing ciprofloxacin (0.5, 1 and 2 mg/L) and the plant extract (100 mg/L) in broth was added to three separate wells. The plates were incubated overnight at 37 °C and the diameters of the inhibition zones were measured. Each experiment contained three technical repeats and was repeated on three separate days. A zone of inhibition of the antibiotic plus test plant extract larger than that of the antibiotic alone was taken to suggest synergy. Positive controls were ciprofloxacin plus L-phenylalanyl-L-arginyl-β-naphthylamide (PAβN) (100 mg/L) or carbonyl cyanide *m*-chlorophenylhydrazone (CCCP) (100 μM), and negative controls were Iso-Sensitest broth alone and plant extract alone to determine whether the plant extract had inherent antimicrobial activity.

2.7. Determination of the minimum inhibitory concentration (MIC) of antibiotics ± synergising extracts, fractions and compounds

The MICs of ciprofloxacin, tetracycline, chloramphenicol, erythromycin and ethidium bromide (EtBr) in the absence or presence of plant extracts and fractions (at 100 mg/L) were determined by the agar doubling dilution method and by the microbroth dilution method [28,29]. MIC determinations were repeated at least three times in independent experiments. Antibiotics, compounds and EPIs were made up and used according to the manufacturer's instructions.

2.8. Determination of the fractional inhibitory concentration index (FICI)

Activity of antibiotics plus the plant extract/fraction/purified compound was determined using the checkerboard technique [30]. The first antibiotic (ciprofloxacin) of a combination was serially diluted along the ordinate of a 96-well microtitre tray; the second agent (e.g. plant extract) was diluted along the abscissa. An inoculum equal to a 0.5 McFarland turbidity standard was prepared from each strain in LB broth. Each well in the microtitre tray was inoculated with 100 mL of the bacterial suspension (at 5×10^5 colony-forming units/mL) and the plates were incubated at 37 °C for 24 h under aerobic conditions. The resulting checkerboard contained each combination of ciprofloxacin and test agent with wells that contained the highest concentration of each agent at opposite corners. The MIC was defined as the lowest concentration of antibiotic that completely inhibited growth of the organism as detected with the naked eye [28]. Synergy was defined as a FICI of ≤0.5, no interaction was defined as a FICI of >0.5–4 and antagonism was defined as a FICI >4 [31].

2.9. Accumulation of Hoechst 33342 ± plant extracts by Salmonella Typhimurium

Efflux activity of five *S.* Typhimurium strains [L3, L10, SL1344, ATCC 15277 (LT2) and ATCC 14028s] was determined by measuring accumulation of the fluorescent dye Hoechst 33342 (bisbenzimide; 2.5 μM) in the absence or presence of known efflux inhibitors (CCCP 100 μM and PAβN 100 mg/L) and in the absence or presence of those plant extracts (at 100 mg/L) revealed to have activity in the bioassay and MIC tests. Measurements were taken at excitation and emission wavelengths of 350 nm and 460 nm, respectively, over 30 min using a FLUOstar OPTIMA (BMG Labtech, Aylesbury, UK) as previously described [32]. Differences in accumulation in the absence of the plant extracts were analysed for statistical significance using the two-tailed Student's *t*-test. *P*-values ≤0.05 were considered significant.

2.10. Growth kinetics ± plant extracts

The growth kinetics of L3, L10, SL1344, ATCC 15277 (LT2) and ATCC 14028s in the absence or presence of plant extracts was determined by monitoring the optical density at 600 nm every 10 min at 37 °C for 24 h using a FLUOstar OPTIMA (BMG Labtech). *Levisticum officinale* chloroform extract and *M. officinalis* methanol extract (at 100 mg/L) were added to the bacterial cultures at mid-logarithmic growth phase (2 h). Samples were also removed and visualised microscopically to detect any gross changes to cell morphology, i.e. filamentation. A two-tailed Student's *t*-test was used to compare the generation times. *P*-values ≤0.05 were considered significant.

3. Results

3.1. Medicinal plant extracts synergise with ciprofloxacin

Plants were extracted with chloroform, methanol and water and were screened to identify those that showed synergy with ciprofloxacin and could be putative EPIs.

Ciprofloxacin was chosen as increased MICs of this agent are often associated with overproduction of the AcrAB–TolC pump. The positive control was PAβN at 100 mg/L, which was the lowest concentration to elicit an effect in this assay. Initial experiments

Table 3
Plant extracts with greatest synergy with ciprofloxacin.

Strain[a]	PAβN	Lo MeOH	Lo $CHCl_3$	Lo Water	M MeOH	M $CHCl_3$	C $CHCl_3$	Pi $CHCl_3$	Pu $CHCl_3$	Pu MeOH
S. Typhimurium SL1344	S	NE	NE	NE	NE	NE	NE	NE	NE	NE
S. Typhimurium ATCC 15277 (LT2)	S	S	S	S	S	NE	S	S	S	S
S. Typhimurium ATCC 14028s	S	S	S	S	S	S	S	S	S	S
Human pre-therapy isolate L3	S	S	S	S	S	S	S	S	S	S
Human post-therapy isolate L10	S	S	S	S	S	S	NE	S	S	S

PAβN, L-phenylalanyl-L-arginyl-β-naphthylamide; Lo, *Levisticum officinale*; M, *Melissa officinalis*; C, *Cinnamomum aromaticum*; Pi, *Pimpinella anisum*; Pu, *Pulmonaria officinalis*; MeOH, methanol extraction; $CHCl_3$, chloroform extraction; water, water extraction; S, synergy (zone of inhibition reproducibly larger than that of antibiotic alone); NE, no effect.

[a] Details of strains are given in Table 1.

were performed with *Salmonella* Typhimurium as a model Gram-negative bacterium and because a defined isogenic set of mutants that lack or overproduce the AcrAB–TolC pump was available. Eighty-four extracts from 21 plants were screened for synergistic activity with ciprofloxacin against *S.* Typhimurium SL1344, ATCC 15277 (LT2), ATCC 14028s, L3 and L10. Of these, 12 extracts showed synergy with ciprofloxacin for these strains, whereas 72 showed little or no activity.

The most active antibiotic-potentiating extracts were those from *L. officinale* (extracted with chloroform, methanol and water), *M. officinalis* (chloroform and methanol), *Cinnamomum aromaticum* (chloroform), *Pimpinella anisum* (chloroform) and *Pulmonaria officinalis* (chloroform and methanol) (Table 3) as well as the chloroform extracts of *Angelica sinensis*, *Tussilago farfara* (methanol) and *Commiphora molmol* (chloroform) (data not shown). Of the extracts investigated, those from *M. officinalis* and *L. officinale* were the most active against strains that either had wild-type levels of AcrAB–TolC or that overproduced AcrAB (Table 4). Chloroform and methanol extracts of *L. officinale* and *M. officinalis* (both 100 mg/L) had no effect on the growth kinetics of the five *Salmonella* strains tested (data not shown), and by MIC determination the extract of *L. officinale* had synergistic activity with ciprofloxacin against most of the strains (Table 4).

3.2. Plant extracts synergise with several antibiotics

Owing to their promising activity, the MICs of the chloroform extract of *L. officinale* and the methanol extract of *M. officinalis* (i.e. those extracts that gave the largest zones of inhibition in the bioassay) were determined in combination with tetracycline, chloramphenicol, erythromycin and EtBr. All extracts showed better activity in liquid media than in agar, with MIC values one to two dilutions lower from the microbroth dilution procedure than with agar (data not shown). No antimicrobial activity was detected at 100 mg/L of either extract; likewise, chloroform and methanol had no activity at the concentration used. Synergy between the extracts from *M. officinalis* and *L. officinale* with tetracycline, chloramphenicol, erythromycin or EtBr was seen for fewer strains than when the plant extracts were combined with ciprofloxacin. None the less, EPI-like activity was detected for both extracts combined with tetracycline, erythromycin and EtBr against wild-type *Salmonella* and the strain in which AcrAB was overproduced. The MIC experiments with the chloroform extract of *L. officinale* indicated that it had synergistic activity with ciprofloxacin and tetracycline for the salmonellae and two *Klebsiella pneumoniae* strains (Table 4). Of interest, the chloroform extract of *L. officinale* also had synergistic activity with ciprofloxacin and EtBr for *Salmonella* Typhimurium in which TolC was not produced and with EtBr for *S.* Typhimurium in which AcrAB was not produced (Table 4). The *M. officinalis* extract had synergistic activity with most antibiotics for the salmonellae and *K. pneumoniae* strains (Table 4).

The extracts of the other plants showing synergistic activity with ciprofloxacin in the bioassay did not reduce the MIC of ciprofloxacin as much as the extracts from *L. officinale* or *M. officinalis*, and when synergy was observed it was seen for fewer bacterial strains. For these reasons, no further experiments were performed with these extracts.

3.3. Activity of fractions derived from the chloroform extract of Levisticum officinale

As the chloroform extract of *L. officinale* showed synergistic activity with more agents and bacteria than that from *M. officinalis*, it was fractionated as the first step to the identification of the active component(s). The chloroform extract of *L. officinale* was subjected to chromatography and 12 fractions (A–L) were obtained.

Table 4
Minimum inhibitory concentrations (MICs) of ciprofloxacin (CIP), tetracycline (TET), chloramphenicol (CHL), erythromycin (ERY) and ethidium bromide (EtBr) in the absence and presence of *Levisticum officinale* and *Melissa officinalis* extracts against Gram-negative bacteria.

Strain[a]	MIC (mg/L)[b]												
	CIP	CIP+Lo	CIP+M	TET	TET+Lo	TET+M	CHL	CHL+Lo	CHL+M	ERY	ERY+Lo	ERY+M	EtBr	EtBr+Lo	EtBr+M
S. Typhimurium L354	0.03	**0.008**	**0.015**	2	**1**	**1**	8	8	8	512	512	512	2048	2048	2048
S. Typhimurium L828	0.03	**0.008**	**0.008**	16	**0.5**	**0.5**	8	8	8	512	**256**	512	2048	1024	2048
S. Typhimurium L829	0.008	**0.004**	0.008	4	**0.5**	**0.5**	1	1	1	8	8	8	16	**8**	16
S. Typhimurium L831	0.008	0.008	0.008	4	**0.5**	**0.5**	2	8	8	64	64	64	64	**32**	64
S. Typhimurium L3	0.008	**0.002**	0.008	4	**0.5**	**0.25**	8	4	8	512	512	512	512	512	512
S. Typhimurium L10	0.06	**0.03**	0.06	8	**4**	**4**	32	**16**	32	512	**256**	512	2048	**1024**	2048
Enterobacter cloacae A1	0.12	**0.06**	0.12	8	**4**	8	4	**2**	4	512	**256**	512	2048	2048	2048
Serratia marcescens B14	0.06	0.06	0.06	64	64	64	4	4	4	256	256	256	2048	2048	2048
Pseudomonas aeruginosa G1	1	1	1	64	64	64	64	64	64	512	512	512	2048	2048	2048
Klebsiella pneumoniae H42	0.06	**0.03**	**0.03**	16	**2**	**4**	128	**64**	128	512	**256**	512	2048	**1024**	**1024**
K. pneumoniae H43	0.12	**0.06**	**0.06**	8	**1**	**2**	4	4	4	512	512	512	2048	**1024**	2048
Escherichia coli I114	0.06	**0.03**	0.06	4	**2**	4	4	4	4	512	512	512	256	256	256
Morganella morganii J29	0.015	**0.008**	0.015	8	8	8	16	16	16	512	512	512	2048	2048	2048

S. Typhimurium, *Salmonella enterica* serotype Typhimurium; Lo, chloroform extract of *L. officinale* extract; M, methanol extract of *M. officinalis*.

[a] Details of strains are given in Table 1.

[b] Bold text indicates synergistic combinations (i.e. MICs for the combination lower than for the antibiotic alone).

Table 5
Minimum inhibitory concentrations (MICs) of ciprofloxacin (CIP) in the absence and presence of the six most active fractions derived from the plant extract from *Levisticum officinale* against a variety of *Salmonella* and Gram-negative bacteria.

Strain[a]	MIC (mg/L)[b]									
	CIP	CIP + Lo	CIP + A	CIP + C	C alone	CIP + F	F alone	CIP + G	CIP + J	CIP + K
S. Typhimurium L354	0.03	**0.008**	0.03	0.03	250	0.03	250	0.03	0.03	0.03
S. Typhimurium L884	0.008	0.008	**0.002**	**0.002**	**64**	**0.008**	250	**0.004**	**0.008**	**0.004**
S. Typhimurium L110	0.008	0.008	**0.002**	**0.004**	**128**	**0.008**	250	**0.004**	**0.008**	**0.004**
S. Typhimurium L109	0.015	0.008	**0.002**	**0.002**	**8**	**0.008**	**128**	**0.004**	0.0015	**0.004**
S. Typhimurium L828	0.03	**0.008**	**0.015**	0.03	250	0.03	250	0.03	0.03	0.03
S. Typhimurium L829	0.008	**0.004**	**<0.001**	**<0.001**	**8**	**0.004**	**128**	**0.004**	0.015	**0.004**
S. Typhimurium L830	0.008	0.008	**<0.001**	**<0.001**	**128**	**0.004**	250	**0.004**	**0.008**	**0.004**
S. Typhimurium L831	0.008	0.008	**<0.001**	**<0.001**	**64**	**0.004**	250	**0.004**	0.008	**0.004**
S. Typhimurium L3	0.008	**0.002**	**<0.001**	**<0.001**	250	0.008	250	0.008	0.008	0.008
S. Typhimurium L10	0.06	**0.03**	**0.03**	0.12	250	0.12	250	**0.03**	0.12	**0.03**
Enterobacter cloacae A1	0.12	**0.06**	0.12	0.12	250	0.12	250	0.12	0.12	0.12
Serratia marcescens B14	0.06	0.06	0.06	0.06	250	0.06	250	0.06	0.06	0.06
Pseudomonas aeruginosa G1	1	1	1	1	250	1	250	1	1	1
Klebsiella pneumoniae H42	0.06	**0.03**	0.06	**0.015**	250	**0.015**	250	**0.015**	**0.015**	**0.015**
K. pneumoniae H43	0.12	**0.06**	0.12	**0.03**	250	**0.03**	250	**0.06**	**0.03**	**0.03**
Escherichia coli I114	0.06	**0.03**	0.06	0.06	250	0.06	250	0.06	0.06	0.06
Morganella morganii J29	0.015	**0.008**	0.015	0.015	250	0.015	250	0.015	0.015	0.015

S. Typhimurium, *Salmonella enterica* serotype Typhimurium; Lo, chloroform extract of *L. officinale*; CIP + letter, indicates the fraction of the chloroform extract of *L. officinale*.
[a] Details of strains are given in Table 1.
[b] Bold text indicates synergistic combinations (i.e. MICs for the combination lower than for the antibiotic alone).

MICs of ciprofloxacin and tetracycline in the absence or presence of each fraction (100 mg/L) were determined. Compared with the chloroform extract of *L. officinale*, few of the fractions had the same synergistic activity with ciprofloxacin. Of interest, fractions A, C, F, G and K synergised with ciprofloxacin for the *Salmonella* mutants in which AcrAB and TolC were not produced, and A, C, G and K also synergised with ciprofloxacin for the two *K. pneumoniae* strains. Fractions A, G and K also had synergistic activity with ciprofloxacin for wild-type *Salmonella* and the clinical isolate that overproduced AcrAB (Table 5). Two fractions (C and F) also had antimicrobial activity alone for the mutant *Salmonella* in which a component of AcrAB–TolC was not produced (Table 5); this was most marked for fraction C.

3.4. Activity of compounds purified from fraction C of Levisticum officinale

As fraction C showed synergistic activity in combination with ciprofloxacin and also antimicrobial activity alone especially against the strains in which *acrB* and *tolC* had been inactivated, this fraction was analysed to identify the active compounds. Nuclear magnetic resonance (NMR) revealed that it contained predominantly the antibacterial fatty acids oleic acid and linoleic acid plus falcarindiol and levistolide A (Fig. 1). These compounds were further purified and the spectral data were in close agreement to those published [24,25]. The absolute stereochemistry of falcarindiol was determined using a modified Mosher's ester method as the 3(*S*), 8(*S*) diastereomer (Fig. 1).

MICs of linoleic acid and falcarindiol were >500 mg/L for the wild-type *Salmonella* SL1344 and ATCC 14028s. For the TolC mutants of these strains the MIC of linoleic acid was 500 mg/L, and the MIC of falcarindiol was 75 mg/L and 125 mg/L, respectively. When linoleic acid was combined with ciprofloxacin MICs of 0.008 mg/L and 0.004 mg/L were obtained for the TolC mutants, and for falcarindiol in combination with ciprofloxacin MIC values <0.001 mg/L were obtained.

Synergistic activity between ciprofloxacin and the compounds for the mutants was confirmed in checkerboard assays, with FICI values of 0.14–0.27 for the combination and the TolC mutants (Table 6). The FICI for ciprofloxacin in combination with the methanol-soluble extract from *M. officinalis* against L3 (pre-therapy isolate) was lower than that for L10 (that overexpresses *acrB*). This suggests that a higher concentration of the putative EPI is required to inhibit growth of L10 owing to the greater production of AcrB by L10. No synergy was seen with this combination for the parental strains, despite it being clearly demonstrated with the extract itself. These data suggest that an EPI-like molecule(s) was lost during the separation process or was inactivated during purification.

3.5. Efflux activity of plant extracts

Accumulation of Hoechst 33342 has been used as a marker for efflux as it is fluorescent and is a substrate of several efflux pumps

Table 6
Fractional inhibitory concentration index (FICI) values of ciprofloxacin (CIP) with plant extracts, fractions and purified molecules for *Salmonella enterica* serotype Typhimurium.

Strain [a]	FICI [b]					
	CIP + Lo	CIP + M	CIP + FC	CIP + FF	CIP + Lin	CIP + Fal
SL1344	0.94	0.97	0.99	0.97	1.34	0.97
SL1344 *tolC::aph*			**0.27**	**0.38**	**0.17**	**0.26**
ATCC 15277 (LT2)	**0.46**	0.59				
ATCC 14028s	**0.48**	**0.41**	1.01	0.98	1.09	1.05
ATCC 14028s Δ*tolC*			**0.32**	**0.33**	**0.14**	**0.14**
Human pre-therapy isolate L3	**0.32**	**0.13**				
Human post-therapy isolate L10	**0.31**	**0.22**				

Lo, *Levisticum officinale* chloroform extract; M, *Melissa officinalis* methanol extract; FC, fraction C from *L. officinale*; FF, fraction F from *L. officinale*; Lin, linoleic acid; Fal, falcarindiol.
[a] Details of strains are given in Table 1.
[b] Bold text indicates synergy [31].

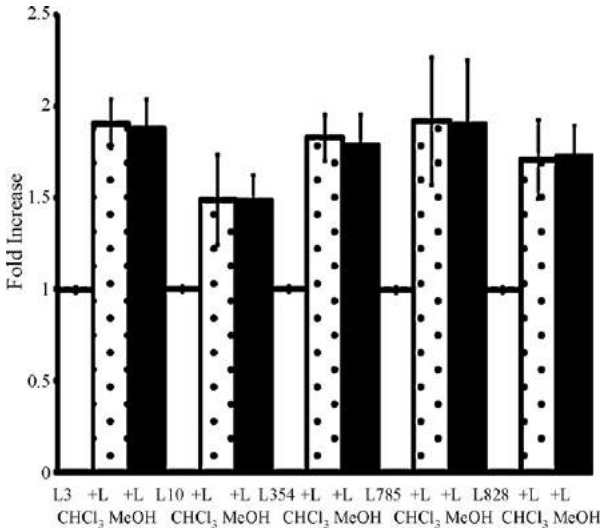

Fig. 2. Accumulation of Hoechst 33342 in the absence or presence of extracts of *Levisticum officinale*. White bars, Hoechst 33342 alone; dotted bars, Hoechst 33342 with chloroform ($CHCl_3$) extract of *L. officinale*; dark grey bars, Hoechst 33342 with methanol (MeOH) extract of *L. officinale*. A value of 1 represents accumulation of Hoechst 33342 in the absence of plant extract; a value >1 indicates increased accumulation of Hoechst 33342 (i.e. reduced efflux). Error bars indicate standard deviations.

including AcrAB–TolC [17,32]. An increase in the amount of Hoechst 33342 accumulated in the presence of an EPI such as PAβN indicates inhibition of efflux [17]. To determine whether synergistic activity displayed by the extracts of *L. officinale* with various antibiotics was due to inhibition of efflux, accumulation of Hoechst 33342 in the presence and absence of 100 mg/L of the chloroform and methanol extracts of *L. officinale* was carried out for five strains of *S.* Typhimurium [SL1344, ATCC 15277 (LT2), ATCC 14028s, L3 and L10]. For the four antibiotic-susceptible wild-type strains of *S.* Typhimurium, both extracts of *L. officinale* increased the amount of Hoechst 33342 accumulated (i.e. reduced efflux) by 1.5–2-fold (Fig. 2). The efflux activity of the strain that overexpressed AcrB (L10) was also reduced by 1.5-fold.

4. Discussion

Many conventional drugs have arisen from natural products, including plants. However, few antimicrobial agents have come from this source, with the vast majority in clinical use derived from products naturally produced by microorganisms [33]. None the less, the use of medicinal and herbal plant remedies to treat infectious diseases is common in many countries [34]. Owing to the continued clinical pressure for novel approaches to combat antibiotic-resistant bacterial infections, there is a need to identify new agents to treat such infections. One approach is to screen for natural products from plants. Plants have already successfully yielded compounds with activities suggesting that they inhibit efflux pumps of Gram-positive bacteria [3,5]. Therefore, in this study we sought to identify medicinal plants that could provide compounds for further antimicrobial drug development. In addition, as there are many clinically licensed antibacterial agents for the treatment of infections by Gram-negative bacteria, but which are effluxed by the various pumps possessed by these bacteria, we sought to screen for activity that suggested efflux inhibition. One desirable property of a putative EPI is that it should synergise with antibiotics for bacteria with wild-type or overproduction of AcrAB–TolC but have no effect on a strain in which AcrAB or TolC are produced. As ciprofloxacin is a substrate of many bacterial efflux pumps [14], the initial experiments used a simple bioassay to identify plant extracts that synergised with this agent [27]. This allowed many plant extracts made under different conditions to be screened with speed. In a prior study, we sought to identify compounds with EPI-like activity and to use this as an aid to predict the common structural features of EPIs and so guide the type of plant from which to make extracts for this study [27]. Of the 84 extracts from the 21 plants, 2 extracts, an ethanol extract from *M. officinalis* (lemon balm) and a chloroform extract of *L. officinale* (lovage root), had the greatest activity in terms of antibiotic potentiation with either the antibiotics ciprofloxacin or tetracycline or the dye EtBr and these data suggest that these extracts contain an inhibitor of efflux. The extract from *L. officinale* had the greatest EPI-like activity and so this was taken forward and fractionated as an initial step to identify the compounds with EPI-like activity. It was surprising to find that none of the 12 fractions of the chloroform extract of *L. officinale* had EPI-like activity, as those fractions that displayed synergy with ciprofloxacin did so in all strains irrespective of the presence or absence of a functional AcrAB–TolC system. These data suggest an interaction with other pumps or another mechanism of synergy. Most interesting was that two fractions (C and F) had some antimicrobial activity alone against all strains including those that lacked TolC. This is highly unusual as the majority of plant extracts display activity only towards Gram-positive bacteria. Fraction C, which had the greatest antimicrobial activity, was further fractionated to identify the compounds conferring the observed antimicrobial activity. Of these, falcarindiol (**1**) had the greatest antimicrobial activity and a strong additive effect to the activity of ciprofloxacin. Falcarindiol has previously been shown to possess antibacterial activity, but for mycobacteria and Gram-positive bacteria and not Gram-negative bacteria [24,35–37]. It is possible that the activity in the fraction was potentiated by the co-isolated fatty acids, and these could have membrane permeabilising activity. As these are ubiquitous in all organisms, this does not entirely explain the data or why so few plant extracts are active against Gram-negative bacteria. Rather, the data suggest that falcarindiol is a substrate of TolC and this may be why it has not been previously identified as having antimicrobial activity for Gram-negative bacteria.

Despite not successfully obtaining the compound(s) that conferred the EPI-like activity in the original plant extract, we postulate that the putative inhibitor of efflux was either lost or was inactivated during fractionation or that it acts in combination with another compound in the plant extract from which it was separated during the fractionation process. Further work to examine reconstituting fractions is required to understand whether a synergistic phenomenon is associated with selected fractions. This will also allow us to conclude whether a putative EPI is being lost in the separation process or is unstable.

Gram-negative plant pathogens such as *Pseudomonas syringae* can cause enormous damage to crop plants [38], and *P. syringae* has been shown to possess a homologue of the tripartite resistance–nodulation–cell division (RND) efflux system MexAB–OprM [39]. This would suggest that plants may not produce chemicals that are active against efflux pumps of Gram-negative plant pathogens. However, the current data suggest that plants do produce molecules with activity against Gram-negative bacteria. Furthermore, we postulate that these molecules are substrates of TolC (and homologues thereof) and associated efflux pumps. Therefore, for plants to withstand infection by these pathogens they need to produce EPIs for the natural antimicrobial agents to be active. It is tempting to speculate that falcarindiol is produced alongside a compound(s) that inhibits efflux.

Lorenzi et al. [40] have recently shown that extracts from plants can also provide compounds with EPI-like activity or antibacterial activity per se. They also found that an extract of an essential oil from a Corsican plant, *Helichrysum italicum*, was able to reduce

the MIC of chloramphenicol for *Enterobacter aerogenes*, *Acinetobacter baumannii* and *P. aeruginosa*. Two fractions of this essential oil and one compound within this oil, geraniol, synergised with chloramphenicol both for the wild-type strain of *E. aerogenes* and its AcrAB mutant. Another recent study by Adonizio et al. [41] showed that medicinal plant extracts can attenuate the virulence of *P. aeruginosa* when explored in the *Caenorhabditis elegans* model system. Although the extracts were from medicinal plants previously used in herbal medicine, the active compounds were not identified. The current data taken together with that of Adonizio et al. [41] and Lorenzi et al. [40] indicate that plants as a source of new and/or novel antimicrobial compounds with activity for Gram-negative bacteria are an underexplored resource. Plant extracts such as those described by ourselves and others provide lead compounds for further exploration and development as antimicrobial agents, as agents to inhibit efflux or for combination with licensed antimicrobials.

Acknowledgments

The authors thank Dr Peter Puplampu for technical support, and Prof. Kim Lewis for helpful discussions whilst writing this manuscript.

Funding: This work was supported by The Leverhulme Trust (project F/00/094/AR).

Competing interests: None declared.

Ethical approval: Not required.

References

[1] Boucher HW, Talbot GH, Bradley JS, Edwards JE, Gilbert D, Rice LB, et al. Bad bugs, no drugs: no ESKAPE! An update from the Infectious Diseases Society of America. Clin Infect Dis 2009;48:1–12.
[2] Livermore D. Has the era of untreatable infections arrived? J Antimicrob Chemother 2009;64(Suppl. 1):i29–36.
[3] Hseih PC, Siegel SA, Rogers B, Davis D, Lewis K. Bacteria lacking a multidrug efflux pump: a sensitive tool for drug discovery. Proc Natl Acad Sci U S A 1998;95:6602–6.
[4] Neyfakh AA, Bidnenko VE, Chen LB. Efflux-mediated multidrug resistance in *Bacillus subtilis*: similarities and dissimilarities with the mammalian system. Proc Natl Acad Sci U S A 1991;88:4781–5.
[5] Tegos G, Stermitz FR, Lemovskaya O, Lewis K. Multidrug pump inhibitors uncover remarkable activity of plant antimicrobials. Antimicrob Agents Chemother 2002;10:3133–41.
[6] Stermitz FR, Cashman KK, Halligan KM, Morel C, Tegos GP, Lewis K. Polyacylated neohesperidosides from *Geranium caespitosum*: bacterial multidrug resistance pump inhibitors. Bioorg Med Chem Lett 2003;13:1915–18.
[7] Belofsky G, Percivill D, Lewis K, Tegos GP, Ekart J. Phenolic metabolites of *Dalea versicolor* that enhance antibiotic activity against model pathogenic bacteria. J Nat Prod 2004;67:481–4.
[8] Belofsky G, Carreno R, Lewis K, Ball A, Casadei G, Tegos GP. Metabolites of the 'smoke tree', *Dalea spinosa*, potentiate antibiotic activity against multidrug-resistant *Staphylococcus aureus*. J Nat Prod 2006;69:261–4.
[9] Cherigo L, Pereda-Miranda R, Fragoso-Serrano M, Jacobo-Herrera N, Kaatz GW, Gibbons S. Inhibitors of bacterial multidrug efflux pumps from the resin glycosides of *Ipomoea murucoides*. J Nat Prod 2008;71:1037–45.
[10] Kumar A, Khan IA, Koul S, Koul JL, Taneja SC, Ali I, et al. Novel structural analogues of piperine as inhibitors of the NorA efflux pump of *Staphylococcus aureus*. J Antimicrob Chemother 2008;61:1270–6.
[11] Timmer A, Günther J, Rücker G, Motschall E, Antes G, Kern WV. *Pelargonium sidoides* extract for acute respiratory tract infections. Cochrane Database Syst Rev 2008;3:CD006323.
[12] Rüegg T, Calderón AI, Queiroz EF, Solís PN, Marston A, Rivas F, et al. 3-Farnesyl-2-hydroxybenzoic acid is a new anti-*Helicobacter pylori* compound from *Piper multiplinervium*. J Ethnopharmacol 2006;103:461–7.
[13] Sawer IK, Berry MI, Brown MW, Ford JL. The effect of cryptolepine on the morphology and survival of *Escherichia coli*, *Candida albicans* and *Saccharomyces cerevisiae*. J Appl Bacteriol 1995;79:314–21.
[14] Piddock LJV. Clinically relevant chromosomally encoded multidrug resistance efflux pumps in bacteria. Clin Microbiol Rev 2006;19:382–402.
[15] Wray C, Sojka WJ. Experimental *Salmonella typhimurium* infection in calves. Res Vet Sci 1978;25:139–43.
[16] Buckley A, Webber MA, Cooles S, Randall LP, La Ragione RM, Woodward MJ, et al. The AcrAB–TolC efflux system of *Salmonella enterica* serovar Typhimurium plays a role in pathogenesis. Cell Microbiol 2006;8:847–56.
[17] Blair JM, La Ragione RM, Woodward MJ, Piddock LJ. The membrane fusion protein AcrA has a distinct role in antibiotic resistance and virulence of *Salmonella enterica* serovar Typhimurium. J Antimicrob Chemother 2009;64:965–72.
[18] Tindall BJ, Grimont PA, Garrity GM, Euzéby JP. Nomenclature and taxonomy of the genus *Salmonella*. Int J Syst Evol Microbiol 2005;55:521–4.
[19] Nishino K, Latifi T, Groisman EA. Virulence and drug resistance roles of multidrug efflux systems of *Salmonella enterica* serovar Typhimurium. Mol Microbiol 2006;59:126–41.
[20] Piddock LJV, White DG, Gensberg K, Pumbwe L, Griggs DJ. Evidence for an efflux pump mediating multiple antibiotic resistance in *Salmonella typhimurium*. Antimicrob Agents Chemother 2000;44:3118–21.
[21] Eaves DJV, Ricci V, Piddock LJV. Expression of *acrB*, *acrF*, *acrB*, *marA* and *soxS* in *Salmonella enterica* serovar Typhimurium: role in multiple antibiotic resistance. Antimicrob Agents Chemother 2004;48:1145–50.
[22] Webber MA, Bailey AM, Blair JMA, Morgan E, Stevens MP, Hinton JC, et al. The global consequence of disruption of the AcrAB–TolC efflux pump in *Salmonella enterica* includes reduced expression of SPI-1 and other attributes required to infect the host. J Bacteriol 2009;191:4276–85.
[23] Piddock LJV, Griggs DJ, Hall MC, Jin YF. Ciprofloxacin resistance in clinical isolates of *Salmonella typhimurium* obtained from two patients. Antimicrob Agents Chemother 1993;37:662–6.
[24] Lechner D, Stavri M, Oluwatuyi M, Pereda-Miranda R, Gibbons S. The anti-staphylococcal activity of *Angelica dahurica* (Bai Zhi). Phytochemistry 2004;65:331–5.
[25] Kaouadji M, De Pachtere F, Pouget C, Chulia AJ, Lavaitte S. Three additional phthalide derivatives, an epoxymonomer and two dimers from *Ligusticum wallichii* rhizomes. J Nat Prod 1986;49:872–7.
[26] Lund ME, Blazevic DJ, Matsen JM. Rapid gentamicin bioassay using a multiple-antibiotic-resistant strain of *Klebsiella pneumoniae*. Antimicrob Agents Chemother 1973;4:569–73.
[27] Piddock LJV, Garvey MI, Rahman MM, Gibbons S. Natural and synthetic compounds such as trimethoprim behave as inhibitors of efflux in Gram-negative bacteria. J Antimicrob Chemother 2010;65:1215–23.
[28] Andrews JM. Determination of minimum inhibitory concentrations. J Antimicrob Chemother 2001;48(Suppl. 1):5–16 [J Antimicrob Chemother 2002;49:1049].
[29] Andrews JM. Determination of minimum inhibitory concentrations. http://www.bsac.org.uk/susceptibility_testing/guide_to_antimicrobial_susceptibility_testing.cfm. BSAC; 2006 [accessed 23 November 2010].
[30] Eliopoulos GM, Moellering R. Antimicrobial combinations. In: Lorian V, editor. Antibiotics in laboratory medicine. 4th ed. Baltimore, MD: Lippincott Williams and Wilkins; 1996. p. 330.
[31] Odds FC, Synergy. antagonism, and what the chequerboard puts between them. J Antimicrob Chemother 2003;52:1–3.
[32] Coldham NG, Webber MA, Woodward MJ, Piddock LJ. A 96-well plate fluorescence assay for assessment of cellular permeability and active efflux in *Salmonella enterica* serovar Typhimurium and *Escherichia coli*. J Antimicrob Chemother 2010;65:1655–63.
[33] Newman D, Cragg G. Natural products as a source of new drugs over the last 25 years. J Nat Prod 2007;70:461–77.
[34] Ankli A, Heinrich M, Bork P, Wolfram L, Bauerfeind P, Brun R, et al. Yucatec Mayan medicinal plants: evaluation based on indigenous uses. J Ethnopharmacol 2002;79:43–52.
[35] Stavri M, Gibbons S. The antimycobacterial constituents of dill (*Anethum graveolens*). Phytother Res 2005;19:938–41.
[36] Schinkovitz A, Stavri M, Gibbons S, Bucar F. Antimycobacterial polyacteylenes from *Levisticum officinale*. Phytother Res 2008;22:681–4.
[37] Chou SC, Everngam MC, Sturtz G, Beck JJ. Antibacterial activity of components from *Lomatium californicum*. Phytother Res 2006;20:153–6.
[38] Arnold DL, Jackson RW, Waterfield NR, Mansfield JW. Evolution of microbial virulence: the benefits of stress. Trends Genet 2007;23:293–300.
[39] Stoitsova SO, Braun Y, Ullrich MS, Weingart H. Characterization of the RND-type multidrug efflux pump MexAB–OprM of the plant pathogen *Pseudomonas syringae*. Appl Environ Microbiol 2008;74:3387–93.
[40] Lorenzi V, Muselli A, Bernardini FA, Berti L, Pagès JM, Amaral L, et al. Geraniol restores antibiotic activities against multidrug-resistant isolates from Gram-negative species. Antimicrob Agents Chemother 2009;53:2209–11.
[41] Adonizio A, Leal SM, Ausubel FM, Mathee K. Attenuation of *Pseudomonas aeruginosa* virulence by medicinal plants in a *Caenorhabditis elegans* model system. Antimicrob Agents Chemother 2008;57:809–13.

J Mol Model (2011) 17:2863–2872
DOI 10.1007/s00894-011-0978-7

ORIGINAL PAPER

In silico screening for antibiotic escort molecules to overcome efflux

Sheikh S. Rahman · Ivana Simovic · Simon Gibbons · Mire Zloh

Received: 15 September 2010 / Accepted: 17 January 2011 / Published online: 8 February 2011

Abstract Resistance to antibiotics is a growing problem worldwide and occurs in part due to the overexpression of efflux pumps responsible for the removal of antibiotics from bacterial cells. The current study examines complex formation between efflux pump substrates and escort molecules as a criterion for an in silico screening method for molecules that are able to potentiate antibiotic activities. Initially, the SUPERDRUG database was queried to select molecules that were similar to known multidrug resistance (MDR) modulators. Molecular interaction fields generated by GRID and the docking module GLUE were used to calculate the interaction energies between the selected molecules and the antibiotic norfloxacin. Ten compounds forming the most stable complexes with favourable changes to the norfloxacin molecular properties were tested for their potentiation ability by efflux pump modulation assays. Encouragingly, two molecules were proven to act as efflux pump modulators, and hence provide evidence that complex formation between a substrate and a drug can be used for in silico screening for novel escort molecules.

Keywords Multidrug resistance · MDR · Efflux pumps · Molecular interaction fields · Escort molecules · In silico screening

Electronic supplementary material The online version of this article (doi:10.1007/s00894-011-0978-7) contains supplementary material, which is available to authorized users.

S. S. Rahman · I. Simovic · S. Gibbons · M. Zloh (✉)
The School of Pharmacy, University of London,
29–39 Brunswick Square,
London WC1N 1AX, UK
e-mail: mire.zloh@pharmacy.ac.uk

Introduction

Multidrug resistance (MDR) to antibiotics is an ever-increasing problem worldwide and occurs due to a number of mechanisms: (i) receptor alteration, where the target site may become altered, resulting in a less efficient interaction between the binding site and drug; (ii) antibiotic modification, where the bacteria may produce novel enzymes that inactivate or alter the drug; or (iii) the removal of the drug from the bacterial cell by efflux pumps (the major mechanism of resistance) [1]. These pumps are membrane-bound proteins that are found in both eukaryotes and prokaryotes, and can be either specific or nonspecific. Efflux pumps that are specific assist the removal of only one compound or a class of compounds, whereas nonspecific efflux pumps assist the removal of a broad range of compounds that are structurally unrelated. It is these nonspecific efflux pumps that lead to MDR.

Bacterial efflux pumps are divided into two major classes based on their energy source. The first are primary transporters that obtain their energy for efflux by hydrolysis of ATP and belong to the ATP-binding cassette (ABC) superfamily. The second are secondary transporters that obtain their energy for efflux in a coupled exchange with H^+ (or Na^+) ions [1]. These secondary transporters are then subdivided into various families based on the size and similarity of their structures: the major facilitator superfamily (MFS), the small multidrug resistance (SMR) family, the resistance nodule cell division (RND) family, and the multidrug and toxic compound extrusion (MATE) family.

There are various ways of combating MDR to restore the antibiotic activity by preventing efflux using a range of structurally unrelated molecules. These efflux pump modulators can come from different sources (natural

products, drugs and synthetic analogues) [2], and their structural diversity indicates that various mechanisms are involved in restoring the action of antibiotics. These mechanisms can be based on affecting the pump function either by removing the energy source using inhibitors such as carbonyl cyanide *m*-chlorophenylhydrazone (CCCP), by abolishing the membrane potential using inhibitors such as valinomycin, or by preventing efflux pump assembly or efflux pump expression. Alternatively, drug efflux can be prevented by intermolecular interactions that efflux pump modulators can form, either through the binding of a molecule to the hydrophobic regions of the binding site [3], or through the formation of a complex between a drug and a modulator. The latter involves two molecules forming a noncovalent complex which is not recognized by the efflux pump [4, 5]. A modulator of MDR complexed with a drug could act as an "escort molecule" to deliver the drug into the bacteria [6].

Small molecule–small molecule interactions may play an important role in biological processes and few experimental studies have confirmed interactions between drugs in solution [7–9]. These interactions can be studied and predicted computationally using different levels of theory; however, these methods do not have the capacity for high-throughput in silico screening where the target is a small molecule. Previously, we demonstrated the use of GRID software and its module GLUE to predict the interaction energies between two small molecules, and reported the link between interaction energies and efflux pump modulation [4, 6]. Furthermore, we have shown the high similarity between MDR inhibitors in terms of shape, lipophilicity and orientation of aromatic moieties [10].

Here, we report the in silico screening process to detect potential escort molecules that could restore the activity of an antibiotic, in this case norfloxacin. The similarity, complex formation, interaction energies and physicochemical properties of complexes between norfloxacin and a small molecule were considered as criteria in this in silico screening process to find suitable escort molecules, where escort molecules may be selected from approved drugs, natural products or nutrients.

Materials and methods

Examination of drug–drug interactions

The GRID22 package [11] consists of six programs including a graphical interface called GREATER and a GRID-based docking program, GLUE. To validate the use of GLUE as a method for detecting complex formation where the target was a small molecule, we used three previously published studies, where the small molecule–small molecule interactions between drug pairs were confirmed using experimental methods [7–9]. The experimental evidence and key interactions were given for complexes of atorvastatin with three antibiotics (ciprofloxacin, gatifloxacin, and ofloxacin), indomethacin with lidocaine, and cocaine with a salt of morphine.

Ionization states of studied molecules were predicted using LigPrep [11] or Avogadro [12]. The molecular mechanics software Macromodel [13, 14] was used to perform a 1000-step energy minimization, followed by a conformational search using the Monte Carlo multiple minima (MCMM) method and the MMFF94s force field [15] for each of the molecules in order to obtain the five most stable representative conformers. These were used as input files for GLUE [16]. GREATER was used to compute the molecular interaction fields (MIF) and to obtain the GRID .kout file required for docking using GLUE. Each of the conformers was used as the target and its corresponding drug pair was defined as the ligand. The eight default GRID probes (H, OH_2, DRY, N1, N+, O, O::, O1) were used, and the box defining the binding site was set to contain whole molecules as a target. To allow flexibility of the ligand, the number of rotatable bonds was set to 5 as the maximum number allowed within GLUE, and the binding energies were calculated without and with considering electrostatic interaction contributions. The docking experiments were repeated by reversing the roles of the ligand and target; i.e. the molecules that were targets in the first docking experiment were set as the ligand in the second docking experiment, and the molecules that were used as the ligands in the first docking experiment were used as the target in the second docking experiment in order to allow for ligand flexibility of both drugs. Vega ZZ [17–20] was used to visualise and analyse the interactions between the two drugs when complexed.

In silico screening strategy and docking experiments

To demonstrate the use of the GRID software for in silico screening, we used the online database of 2,396 already FDA approved and readily available drug molecules, SUPERDRUG [21]. Initially and to minimize the computational time required for computing interaction energies, we screened the database for drug molecules that contain the moieties of known efflux pump inhibitors (reserpine, verapamil, epicatechin gallate, epigallocatechin gallate, biricodar, timcodar, pheophorbide A, 5′-methoxyhydnocarpin, NNC 20-7052, INF55, INF240, INF271, INF277 and INF392). The "build your own structure" feature of the SUPERDRUG database was utilized by evaluating similarity and Tanimoto coefficients [21]. A set of drug molecules with the highest similarity were selected as potential escort molecules for norfloxacin (NOR). The

Table 1 The binding energies of the drug–drug interactions predicted by GLUE

Drug 1	Drug 2	Binding energy (kcal/mol)[a]	Binding energy (kcal/mol)[b]
Ciprofloxacin	Atorvastatin	−20.309	−38.357
Gatifloxacin	Atorvastatin	−14.42	−32.531
Ofloxacin	Atorvastatin	−17.336	−39.459
Indomethacin	Lidocaine	−12.805	−12.742
Morphine	Cocaine	−8.363	−14.343

[a] The binding energies as calculated using GLUE without electrostatic contributions; [b] the binding energies as calculated using GLUE taking into account electrostatic contributions

ionizable groups of 3D structures of these compounds downloaded from the SUPERDRUG database were adjusted to the correct ionized state at pH 7.4 using Avogadro [13]. Final conformations were obtained by VegaZZ using the AM1BCC force field, Gasteiger charges, and a 3000-step energy minimization using the AMMP module.

GRID and GREATER were used as described above to carry out the docking between norfloxacin and selected drug molecules from the SUPERDRUG database. The structures of the drugs identified in SUPERDRUG were used as ligands and subjected to docking protocols using norfloxacin as the target to compute their binding energies.

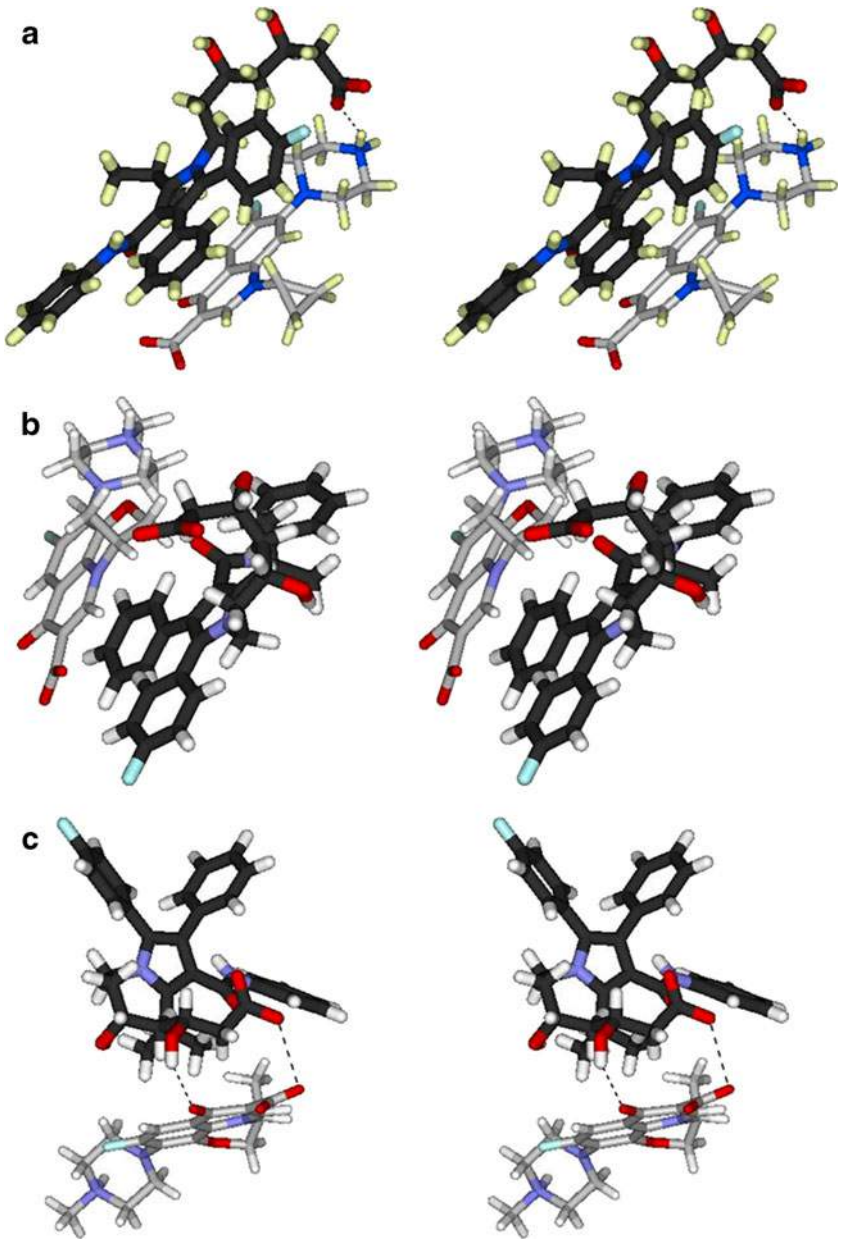

Fig. 1a–c The stereoview representations of noncovalent complexes predicted by GLUE: **a** atorvastatin–ciprofloxacin (conformer with the best binding energy); **b** atorvastatin–gatifloxacin (conformer with the best binding energy); **c** atorvastatin–ofloxacin (conformer with a less favourable binding energy). Atorvastatin is depicted in the *darker shade of grey* and with *thicker sticks*

The results of docking were saved as ligands in noncovalent complexes with norfloxacin, using VegaZZ [17–20], and employed for the prediction of various physicochemical properties of the single molecules as well as their docked complexes, including their surface area (SA), polar surface area (PSA), log*P*, lipole and virtual log*P* properties [22, 23]. The lipophilic surface of each single molecule as well as its docked complex was also calculated using the "surface management" option, where the surface chosen was MLP (molecular lipophilicity potential), the color of the gradient was set to 6, and the probe radius was the default value [24]. Ten drugs with a range of interaction energies, favourable physicochemical properties, and availability for purchase were selected to biologically evaluate their ability to restore the action of norfloxacin against a norfloxacin-effluxing strain of *Staphylococcus aureus*.

Biological evaluation

Alprenolol hydrochloride, apomorphine hydrochloride hemihydrate, bergapten, betaxolol hydrochloride, chlorpromazine hydrochloride, demecolcine, hydroxyzine dihydrochloride, naproxen, paroxetine hydrochloride, pridinol methanesulfonate, and norfloxacin were purchased from Sigma and used without further purification. The assays to test the intrinsic antibacterial activities and potentiating abilities of these molecules are described elsewhere [4]. The assays to test the potentiating activity of these molecules were then repeated as described previously [4], but the mixtures of norfloxacin and the test compounds were left to incubate for 24 h at 37 °C to allow more time for complexation between the two molecules before the addition of 125 μL of the bacterial inoculum (5×10^5 cfu/mL) to wells 1–11.

Results and discussion

A major mechanism of resistance to antibiotics occurs due to the removal of the drug from the bacterial cell by efflux pumps. Here, an in silico screening process to find potential escort molecules was examined by evaluating the complex formation between norfloxacin and chosen small molecules, their interaction energies and their physicochemical properties.

GLUE identifies favourable binding modes between a target and ligands using all of the options and capabilities of the GRID force field and proposes several lower energy poses. The binding energy is expressed by a energy-scoring function which takes into account the steric-repulsion contributions, electrostatic contributions, the hydrophobic contributions and the hydrogen-bonding contributions. Although GLUE suffers from some limitations in the prediction of binding energies, we have previously shown empirically that the ability to restore the activity of antibiotics and anticancer cytotoxics can be qualitatively correlated to binding energies between drugs and known MDR modulators that are lower than −9 kcal mol^{-1}, as predicted by GLUE [5, 6]. In order to examine the use of GLUE for the docking experiments for in silico screening, we have compared the resulting docking complexes to the experimentally predicted complexes for selected pairs of drugs (Table 1). Additionally, we have included two molecules in our study: a known MDR modulator (GG918) [25] and a non-MDR potentiator (aspartame).

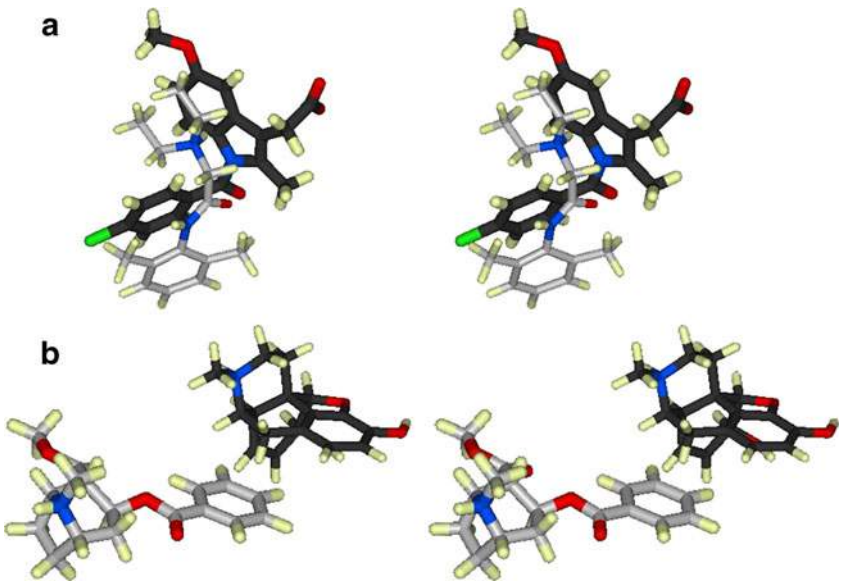

Fig. 2a–b The stereoview representations of predicted noncovalent complexes of **a** lidocaine and indomethacin (indomethacin is shown in a *lighter shade of grey* and with *thicker sticks*) and **b** morphine and cocaine (morphine is depicted in a *darker shade of grey* and with *thicker sticks*)

Can a small molecule be used as a docking target?

The dominant interactions reported in the atorvastatin–ciprofloxacin, atorvastatin–gatifloxacin and atorvastatin–ofloxacin complexes were H-bonding between the carboxylic acid group of atorvastatin and the carboxylic acid group of the fluoroquinolone drugs or the piperazine ring of the fluoroquinolone drugs [7]. The docking experiments performed using GLUE predicted complexation with favourable binding energies, with those that included electrostatic interaction generally being higher (Table 1). However, upon closer inspection of the formed complexes, it was found that results obtained by docking without considering the electrostatic contribution correlated better with the experimental observations.

The most stable ciprofloxacin–atorvastatin complex, obtained without taking into account the electrostatic contributions, exhibited H-bonding interactions between the carboxylic acid group of atorvastatin and the N–H group of the piperazine ring of ciprofloxacin, which is in good agreement with that determined experimentally. For the ofloxacin–atorvastatin and gatifloxacin–atorvastatin complexes, the conformers with the highest binding energies (without taking into account electrostatic contributions) did not exhibit the experimentally determined interactions. However, examining all of the predicted complexes by GLUE, it is found that the experimentally determined interactions are observed but in complexes with less favourable binding energies (Fig. 1).

Umeda et al. suggested that the dominant intermolecular interaction in the case of the lidocaine–indomethacin complex occurs between the carboxylic acid group of indomethacin and the diethyl amino group of lidocaine [9]. The GLUE docking experiments found that the complex formed would be stable, as it exhibits a favourable binding energy, with the most dominant interaction between

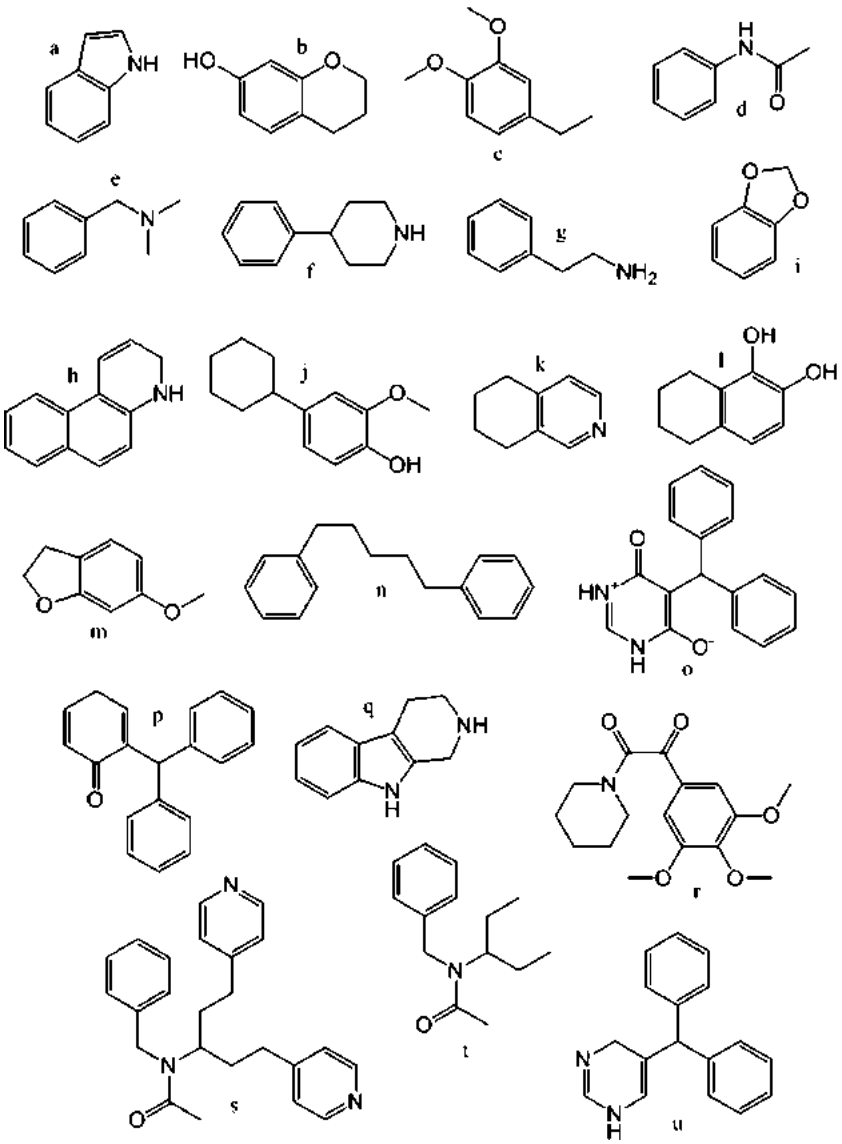

Fig. 3 The moieties extracted from known efflux pump inhibitors (reserpine, verapamil, epicatechin gallate, epigallocatechin gallate, biricodar, timcodar, pheophorbide A, 5′-methoxyhydnocarpin, NNC 20-7052, INF55, INF240, INF271, INF277 and INF392) that were used to screen for potential efflux pump modulator–escort molecules

lidocaine and indomethacin being π–π stacking. Although the carboxylic group and amino group are in proximity, the hydrogen bond is not observed in the complex, which may be a result of the limitations of GLUE in relation to carrying out flexible target docking (Fig. 2a).

With respect to the complex formed between cocaine and morphine, an interaction predicted by DFT calculations occurred between the morphine cavity defined by the two rings containing hydroxyl groups and the cocaine $COOCH_3$ [8]. The results from GLUE for docking indicated a weaker binding energy between cocaine and morphine when excluding electrostatic contributions, and the strongest interactions between the two compounds were aromatic π–π interactions. It can therefore be concluded that weak interactions are not reproduced when computing small molecule–small molecule interactions using GLUE (Fig. 2b). Overall, these computations have shown that interactions seen experimentally can be predicted using GLUE, and that the stronger interactions are more accurately predicted. Despite the observed limitations, it was deemed viable to use GLUE to carry out in silico screening where the target was a small molecule, and in this case an antibiotic.

In silico screening and docking experiments

The SUPERDRUG database [21] is an online source that contains 2,396 3D structures of drug molecules with 108,198 different conformers. This database was used to search for drugs that are similar in structure to known efflux pump inhibitors in order to find drugs that might potentially complex with norfloxacin and therefore act as modulators in vitro (Fig. 3). Eighty-nine drugs with the highest percentage similarities (Tanimoto coefficients) with known efflux pump inhibitors and the moieties of known efflux pump inhibitors were chosen for further studies (see the "Electronic supplementary material", ESM). This set of 89 selected drugs and two control molecules were subjected to docking studies using GLUE with norfloxacin as a target, and it was found that the majority of the drug molecules exhibited favourable interactions with norfloxacin, presenting binding energies of ≤ -10.0 kcal mol^{-1} (see the ESM). As seen earlier, the complex with the lowest most favourable binding energy is not necessarily the complex detected experimentally, so the average binding energy as well as the standard deviation of the GLUE data was also calculated (see the ESM). Two molecules included as a positive control (GG918) and a negative control (aspartame) had the highest and lowest average binding energies, respectively.

To get a better understanding of these docked complexes, VegaZZ was used to assess various physicochemical properties of the single molecules as well as their docked complexes. The interaction energy is an important criterion for the selection of escort molecules [5], but the availability for purchase in pure form and the toxicities of the drugs were considered during the selection process, as these would obviously affect the future use of these drugs as escort molecules. After applying all of the abovementioned criteria, we chose ten molecules for further analysis and biological testing (Table 2).

Table 2 Properties of the ten drugs

Complex (compound and NOR)	Tanimoto coefficient	Most favourable binding energy (kcal/mol)[a]	Average binding energy (kcal/mol)[b]	Change of virtual log*P* (%)	Change of PSA coverage (%)	MIC (μg/ml)	Potentiation[c]
Alprenolol	68.52	−10.237	−8.820	−12.0	−22.8	>512	32 (NC)
Apomorphine	63.27	−15.671	−10.581	−19.5	−3.8	>512	16 (2)
Aspartame*	–	−6.893	−6.277	−64.6	12.2	>512	32 (NC)
Bergapten	39.60	−13.421	−10.136	0.6	−3.8	>512	32 (NC)
Betaxolol	48.15	−10.734	−8.531	14.9	−35.4	>256	32 (NC)
Chlorpromazine	47.69	−14.819	−12.279	49.4	−31.1	64	8 (4)[d]
Demecolcine	53.29	−14.184	−10.446	−27.0	−11.0	>256	32 (NC)
GG918* [29]	–	−15.815	−12.252	64.8	−32.2	>512	4 (8)
Hydroxyzine	50.47	−14.188	−9.601	−25.5	−23.0	>512	32 (NC)
Naproxen	55.77	−12.987	−10.628	64.5	−22.3	>512	32 (NC)
Paroxetine	53.06	−13.881	−11.617	12.2	−18.3	64	32 (NC)
Pridinol	77.08	−12.675	−8.820	71.9	−41.5	>512	32 (NC)

[a] Binding energies without electrostatic forces

[b] The average binding energy without taking into account electrostatic contributions

[c] Decrease in the MIC of norfloxacin (-fold), *NC* no change

[d] Potentiation increased twofold upon incubating chlorpromazine with norfloxacin overnight

The example of the MDR modulator

Three-dimensional structures of the ten chosen drugs complexed with norfloxacin were visualized using VegaZZ. It was apparent that aromatic face-to-face interactions were dominant in most complexes (Fig. 4). In some complexes, these interactions were further stabilized by intermolecular hydrogen bonds. Complexes with hydrogen bonding have a less polar surface exposed to the solvent, as the polar groups tend to interact inside the complex and are thus hidden from the surface.

It was previously reported that the physicochemical properties of an antibiotic change upon complexation, which in turn might enhance the permeability of a drug-escort molecule [6]. The change of virtual log*P*, i.e. ($\mathrm{Vlog}P_{(\mathrm{complex})} - \mathrm{Vlog}P_{(\mathrm{NOR})}$) / $\mathrm{Vlog}P_{(\mathrm{NOR})}$, was used as a measure of the change in lipophilicity of the complex in comparison to norfloxacin on its own. The Vlog*P* of norfloxacin was -3.073, which suggested that it is a hydrophilic antibiotic drug that has a higher affinity for the aqueous phase. The biggest change was observed for a known MDR modulator, GG918, which exhibits the most favourable binding energies and the greatest increase in Vlog*P* (64.8%), while aspartame made the complex even more hydrophilic, with Vlog*P* decreasing (−64.4%).

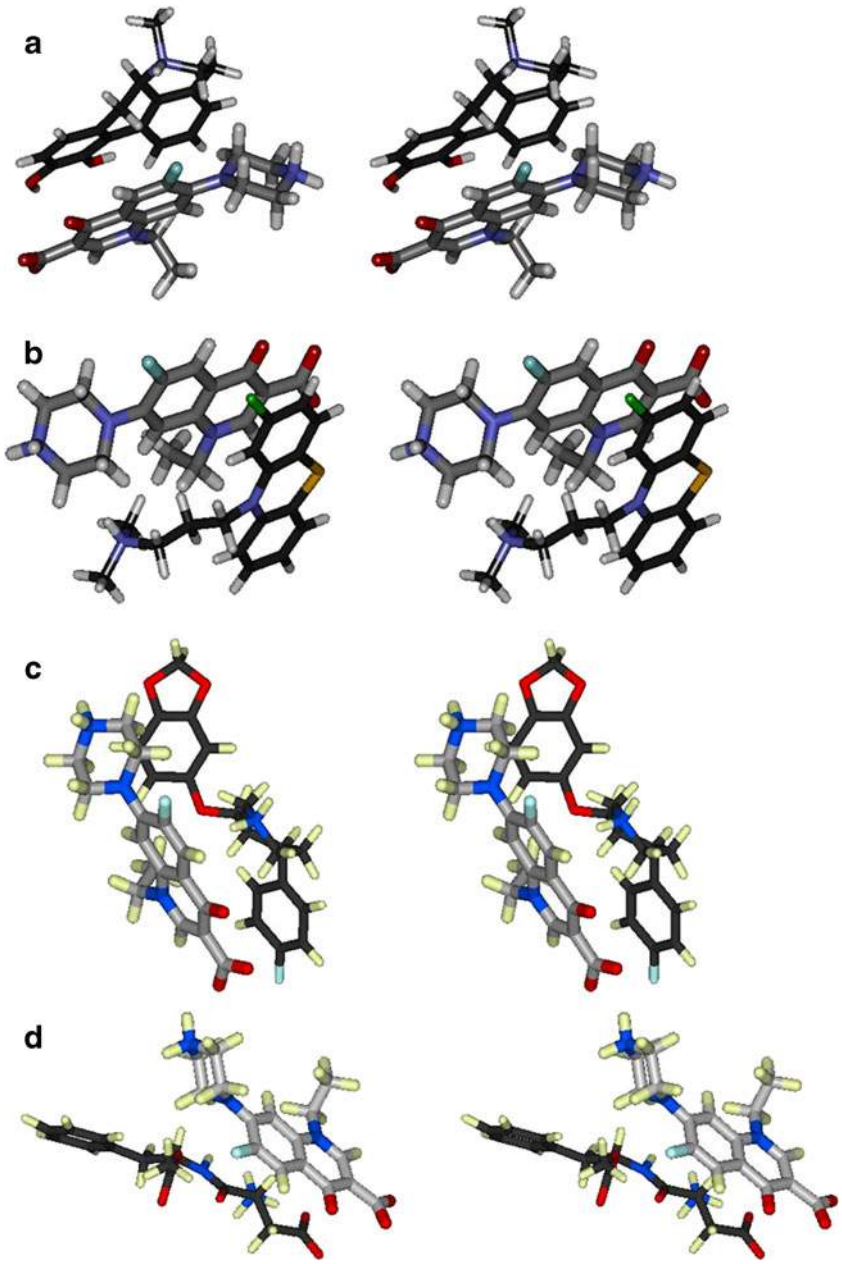

Fig. 4a–d The stereoview representations of noncovalent complexes of **a** apomorphine–norfloxacin, **b** chlorpromazine–norfloxacin, and **c** paroxetine–norfloxacin, which exhibit face-to-face aromatic interactions, and **d** the aspartame–norfloxacin complex (norfloxacin is depicted in a *lighter shade of grey* and with *thicker sticks*)

It was found that after complexation the change in Vlog*P* was positive for the majority of the studied molecules, suggesting that the complexes were less hydrophilic. Hence, complexes have surfaces that are more lipophilic (the average increase in lipophilicity was 19%). Specifically, for chlorpromazine and paroxetine, which exhibited the most favourable average binding energies of the ten studied complexes, we observed increases of 61.4% and 49.4%, respectively. Interestingly, apomorphine exhibited the third most favourable average binding energy, and showed a decrease in lipophilicity of 19.5%.

Furthermore, the polarity of the surface decreased upon complexation, as it was apparent that the percentage of PSA coverage (PSA/SA×100) decreased by 21.8% on average after complexation when compared to the %PSA coverage of norfloxacin (Fig. 5). This indicated a possibility that complexation between the two molecules would enable the antibiotic (norfloxacin) to pass through the membrane with greater ease, as it is well documented in various studies that there is a promising inverse relationship between the polar surface area of a drug molecule and its permeability through the membrane [26, 27].

Evaluation of biological activity

Following in silico screening and analysis of the physicochemical properties, the antibacterial activities and potentiation abilities of the ten chosen molecules were experimentally determined to test whether these molecules potentiated the activity of norfloxacin (Table 2). MIC assays were performed and it was found that chlorpromazine and paroxetine exhibited intrinsic antibacterial activity (MIC=64 μg/ml). The modulation activity assays performed established that chlorpromazine and apomorphine both possessed weak potentiating activity, as they caused the MIC of norfloxacin to decrease two- and fourfold, respectively. This was promising, as apomorphine and chlorpromazine exhibited the most favourable maximum and average binding energies among of the ten tested molecules when docked with norfloxacin (Table 2). Interestingly, chlorpromazine potentiated the activity of norfloxacin twofold when the modulation assay was carried out immediately after mixing the two compounds, but when the two compounds were left in solution overnight before the assay was carried out, the potentiation was fourfold. This has further confirmed our hypothesis that two molecules can form a complex and improve the activity of norfloxacin. However, care needs to be taken when interpreting these results with regards to complex formation between norfloxacin and chlorpromazine, as chlorpromazine is known to change the expression of efflux pumps [28]; nevertheless, an increase of potentiation from twofold to fourfold after incubation suggests that complex formation may also play a role in overcoming resistance.

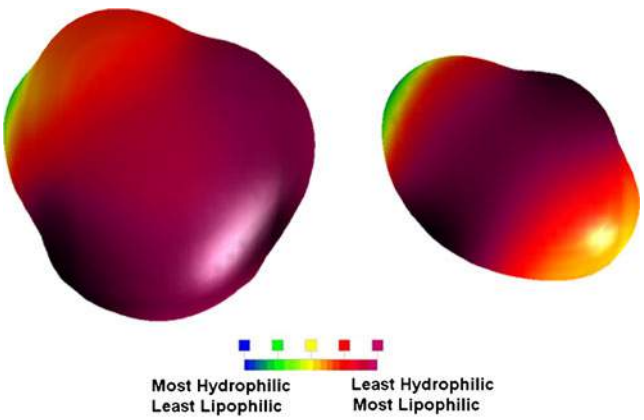

Fig. 5 The molecular lipophilicity (MLP) surface of the norfloxacin–chlorpromazine complex (*left*) and norfloxacin (*right*). The size and position of norfloxacin is the same in both cases. It can be seen that when complexed, the Vlog*P* changes by 49.4%, indicating an increase in lipophilicity

This result agrees well with that computed by GLUE, as chlorpromazine exhibited the best average binding energy and favourable changes in physicochemical properties, and hence would be expected to potentiate the activity of norfloxacin, although not to the same extent as GG918. Apomorphine also exhibited a favourable average binding energy, but the small change in the physicochemical properties suggests that the complex would not increase the permeability of norfloxacin, so this may explain the weaker potentiating activity of the compound compared to GG918 and chlorpromazine.

Paroxetine, bergapten, naproxen and demecolcine were found to have favourable average binding energies, but they did not exhibit any potentiating activity. There are a number of speculations that can be made to explain this. Paroxetine has exhibited intrinsic antibacterial activity, and the modulation assay had to be carried out at a much lower concentration compared to the apomorphine and chlorpromazine concentrations. Demecolcine induces a decrease in Vlog*P* (−27%), as well as a lower change in percentage PSA coverage when complexed with norfloxacin (11% decrease) compared to the change induced by chlorpromazine (31.1% decrease), thus suggesting that the complex formed between demecolcine and norfloxacin would not be able to pass through the membrane as easily, as less polar surface areas yield higher permeability [19, 20]. Bergapten and naproxen lack a nitrogen at the centres of their structures, which is essential for efflux modulation [29].

It was not possible to establish a quantitative correlation between these calculated binding energy values for the studied molecules and their levels of potentiation. It has to be noted that no other interactions were considered in this work, such as interactions between potential escort molecules and membranes. Furthermore, we should bear in mind that the interaction energy and the conformation of a complex depend

on the medium in which the complex is formed. These complexes between a drug and an escort molecule may be formed in water, in a membrane or within a binding site of the efflux pump, and these different environments may affect the binding energies. This will be the subject of further study.

This method of performing a similarity search followed by docking using GLUE was able to identify two new escort molecules (apomorphine and chlorpromazine), as well as a number of molecules that are already known to act in synergy with antibacterial drugs (methdilazine, oxyfedrine and trimeprazine) [30, 31]. It appears that it is possible to discriminate molecules that will not have potentiation ability, such as aspartame. However, this method requires further development and refinement of the criteria to qualitatively predict their ability to restore the activity of an antibiotic.

Conclusions

This study demonstrates that GRID and GLUE can be used in a qualitative way to predict complex formation between two small molecules, and as such it has the potential to be used for in silico screening of modulators of efflux pumps. A combination of similarity search and assessment of interaction energies and physicochemical properties of complexes formed between norfloxacin and potential escort molecules was utilized to search for escort molecules that are able to potentiate the activity of norfloxacin against multidrug-resistant *S. aureus*. Using our approach, among the 2396 molecules available in the SUPERDRUG database, we distinguished three molecules that have aleady demonstrated the ability to act in synergy with antibiotics, and discovered two molecules that modulate the efflux pumps. This study suggests that complexes exhibiting good binding energies and favourable changes to the molecular properties of norfloxacin should restore the activity of this antibiotic. Although our predictions are successful to some extent, the method requires further refinement of the selection criteria. This study could be expanded by querying other databases of molecules, and it has the potential to be utilized for the discovery of escort molecules for other drugs that are effluxed by multidrug-resistant cells.

Acknowledgments The authors would like to thank the Engineering and Physical Sciences Research Council (EPSRC) and the School of Pharmacy for providing financial support and studentship funding.

References

1. Marquez B (2005) Bacterial efflux systems and efflux pumps inhibitors. Biochimie 87:1137–1147. doi:10.1016/j.biochi.2005.04.012
2. Nelson ML (2002) Modulation of antibiotic efflux in bacteria. Curr Med Chem Anti-Infect Agents 1:35–54. doi:10.2174/1568012023355054
3. Ahmed M, Borsch CM, Neyfakh AA, Schuldiner S (1993) Mutants of the *Bacillus subtilis* multidrug transporter Bmr with altered sensitivity to the antihypertensive alkaloid reserpine. J Biol Chem 268:11086–11089
4. Smith E, Williamson E, Zloh M, Gibbons S (2005) Isopimaric acid from *Pinus nigra* shows activity against multidrug-resistant and EMRSA strains of *Staphylococcus aureus*. Phytother Res 19:538–542. doi:10.1002/ptr.1711
5. Zloh M, Kaatz GW, Gibbons S (2004) Inhibitors of multidrug resistance (MDR) have affinity for MDR substrates. Bioorg Med Chem Lett 14:881–885. doi:10.1016/j.bmcl.2003.12.015
6. Zloh M, Gibbons S (2007) The role of small molecule–small molecule interactions in overcoming biological barriers for antibacterial drug action. Theor Chem Acc 117:231–238. doi:10.1007/s00214-006-0149-6
7. Arayne MS, Sultana N, Rizvi SBS, Haroon U (2009) In vitro drug interaction studies of atorvastatin with ciprofloxacin, gatifloxacin, and ofloxacin. Med Chem Res. doi:10.1007/s00044-009-9225-5
8. Garrido JMPJ, Marques MPM, Silva AMS, Macedo TRA, Oliviera-Brett AM, Borges F (2007) Spectroscopic and electrochemical studies of cocaine–opioid interactions. Anal Bioanal Chem 388:1799–1808
9. Umeda Y, Fukami T, Furuishi T, Suzuki T, Makimura M, Tomono K (2007) Molecular complex consisting of two typical external medinicines: intermolecular interaction between indomethacin and lidocaine. Chem Pharm Bull 55:832–836
10. Zloh M, Gibbons S (2004) Molecular similarity of MDR inhibitors. Int J Mol Sci 5:37–47
11. Schrodinger, LLC (2007) LigPrep. Schrodinger, LLC, New York
12. Ali S et al (2011) Avogadro: an open-source molecular builder and visualization tool. http://avogadro.openmolecules.net/
13. Mohamadi F, Richards NGJ, Guida WC, Liskamp R, Lipton M, Caufield C, Chang G, Hendrickson T, Still WC (1990) Macromodel: an integrated software system for modeling organic and bioorganic molecules using molecular mechanics. J Comput Chem 11:440–467
14. Guimarães C, Cardozo M (2008) MM-GB/SA rescoring of docking poses in structure-based lead optimization. J Chem Inf Model 48:958–970. doi:10.1021/ci800004w
15. Halgren TA (1999) MMFF VI. MMFF94s option for energy minimization studies. J Comput Chem 20:720–729
16. Molecular Discovery Ltd (2004) GRID, 22b edn. Molecular Discovery Ltd, Perugia (see http://www.moldiscovery.com/soft_grid.php)
17. Pedretti A, Villa L, Vistoli G (2002) VEGA: a versatile program to convert, handle and viusualize molecular structure on windows-based PCs. J Mol Graph Model 21:47–49. doi:10.1016/S1093-3263(02)00123-7
18. Pedretti A, Villa L, Vistoli G (2003) Atom-Type Description Language: a universal language to recognize atom types implemented in the VEGA program. Theor Chem Acc 109:229–232. doi:10.1007/s00214-002-0402-6
19. Pedretti A, Villa L, Vistoli G (2004) VEGA: an open platform to develop chemo-bio-informatics applications, using plug-in architecture and script programming. J Comput Aided Mol Des 18:167–173. doi:10.1023/B:JCAM.0000035186.90683.f2
20. Drug Design Laboratory (2004–2010) Vega ZZ. Drug Design Laboratory, Milano
21. Goede A, Dunkel M, Mester N, Frommel C, Preissner R (2005) SuperDrug: a conformational drug database. Bioinformatics 21:1751–1753. doi:10.1093/bioinformatics/bti295
22. Broto P, Moreau G, Vandycke C (1984) Molecular structures perception, auto-correlation descriptor and SAR studies: use of the auto-correlation descriptor in the QSAR study of two non-narcotic analgesic series. Eur J Med Chem 19:79–84

23. Ghose AK, Pritchett A, Crippen GM (1988) Atomic physicochemical parameters for three dimensional structure directed quantitative structure–activity relationships. III: Modelling hydrophobic interactions. J Comput Chem 9:80–90
24. Gaillard P, Carrupt PA, Testa B, Boudon A (1994) Molecular lipophilicity potential, a tool in 3D QSAR: method and applications. J Comput Aided Mol Des 8:83–96. doi:10.1007/BF00119860
25. Gibbons S, Oluwatuyi M, Kaatz GW (2003) A novel inhibitor of multidrug efflux pumps in *Staphylococcus aureus*. J Antimicrob Chemother 51:13–17
26. Palm K, Luthman K, Ungell A, Strandlund G, Beigi F, Lundahl P, Artursson P (1998) Evaluation of dynamic polar molecular surface area as predictor of drug absorption: comparison with other computational and experimental predictors. J Med Chem 41:5382–5392. doi:10.1021/jm980313t
27. Remko M, Swart M, Bickelhaupth FM (2006) Theoretical study of structure, pK_a, lipophilicity, solubility, absorption, and polar surface area of some centrally acting antihypertnesives. Bioorg Med Chem 14:1751–1728. doi:10.1016/j.bmc.2005.10.020
28. Bailey AM, Paulsen IT, Piddock LJV (2008) RamA confers multidrug resistance in *Salmonella enterica* via increased expression of acrB, which is inhibited by chlorpromazine. Antimicrob Agents Chemother 52:3604–3611
29. Guz NR, Stermitz FR, Johnson JB, Beeson TD, Willen S, Hsiang JF, Lewis K (2001) Flavonolignan and flavone inhibitors of a *Staphylococcus aureus* multidrug resistance pump: structure–activity relationships. J Med Chem 44:261–268
30. Mazumdar K, Dutta NK, Kumar KA, Dastidar SG (2005) In vitro and in vivo synergism between tetracycline and the cardiovascular agent oxyfedrine HCl against common bacterial strains. Biol Pharm Bull 28:713–717
31. Dutta NK, Mazumdar K, DasGupta A, Dastidar SG (2009) Activity of the phenothiazine methdilazine alone or in combination with isoniazid or streptomycin against *Mycobacterium tuberculosis* in mice. J Med Microbiol 58:1667–1668

Phytochemistry 71 (2010) 1796–1801

Contents lists available at ScienceDirect

Phytochemistry

journal homepage: www.elsevier.com/locate/phytochem

Characterization of a xylose containing oligosaccharide, an inhibitor of multidrug resistance in *Staphylococcus aureus*, from *Ipomoea pes-caprae*

Carolina Escobedo-Martínez [a], Sara Cruz-Morales [a], Mabel Fragoso-Serrano [a], M. Mukhlesur Rahman [b], Simon Gibbons [b], Rogelio Pereda-Miranda [a,*]

[a] Departamento de Farmacia, Facultad de Química, Universidad Nacional Autónoma de México, Ciudad Universitaria, Mexico City 04510, DF, Mexico
[b] Centre for Anti-infective Research, The School of Pharmacy, University of London, 29-39 Brunswick Square, London WC1N 1AX, UK

ARTICLE INFO

Article history:
Received 26 September 2009
Received in revised form 19 March 2010
Available online 30 July 2010

Keywords:
Ipomoea pes-caprae
Convolvulaceae
Staphylococcus aureus
Structural spectroscopy
Multidrug resistance
Resin glycoside
Pentasaccharide

ABSTRACT

Pescaprein XVIII (**1**), a type of bacterial efflux pump inhibitor, was obtained from the $CHCl_3$-soluble resin glycosides of beach morning glory (*Ipomoea pes-caprae*). The glycosidation sequence for pescaproside C, the glycosidic acid core of the lipophilic macrolactone **1** containing D-xylose and L-rhamnose, was characterized by means of several NMR techniques and FAB mass spectrometry. Recycling HPLC also yielded eight non-cytotoxic bacterial resistance modifiers, the two pescapreins XIX (**2**) and XX (**3**) as well as the known murucoidin VI (**4**), pecapreins II (**6**) and III (**7**), and stoloniferins III (**5**), IX (**8**) and X (**9**), all of which contain simonic acid B as their oligosaccharide core. Compounds **1**–**9** were tested for *in vitro* antibacterial and resistance-modifying activity against strains of *Staphylococcus aureus* possessing multidrug resistance efflux mechanisms. All of the pescapreins potentiated the action of norfloxacin against the NorA over-expressing strain by 4-fold (8 μg/mL from 32 μg/mL) at a concentration of 25 μg/mL.

1. Introduction

The genus *Ipomoea* (Convolvulaceae) is a widely known source of complex resin glycosides possessing interesting biological effects (Pereda-Miranda and Bah, 2003; Pereda-Miranda et al., 2010). In Mexico, the herbal drug *Ipomoea pes-caprae* is called "riñonina" and comes from the Spanish word "riñón", which means kidney and reflects the belief of traditional healers that it moderates the "heat" of an infected kidney (Pereda-Miranda et al., 2005). Worldwide, *I. pes-caprae*, commonly known as railroad vine or beach morning glory, is used as an infusion for urinary or kidney complaints, hypertension, skin infections caused by *Mycobacterium tuberculosis*, and in decoctions to treat functional digestive disorders, internal pain, colic, lumbago, dysentery, arthritis, rheumatism, and other inflammatory conditions (De Souza et al., 2000; Pongprayoon et al., 1992).

Previous to this investigation, seven pentasaccharides (pescapreins I–IV and VII–IX) and two tetrasaccharides (pescapreins V and VI) of jalapinolic acid were first reported as a result of the chemical analysis of an herbal store sample of this crude drug (Pereda-Miranda et al., 2005; Escobedo-Martínez and Pereda-Miranda, 2007). A Chinese investigation using wild root samples collected in the Hainan province yielded eight new pentasaccharides, pescaprein X–XVII (Tao et al., 2008). Locally, it is used as an oral decoction to cure rubella as well as to alleviate jellyfish-sting pruritus and applied externally to treat pain and bedsores. The above mentioned investigations have proved that the presence of congeners among the pescaprein series is a result of variations in the type of acylating groups at C-2 of the third saccharide unit (Rha′), and C-2, C-3 and C-4 of the fifth saccharide (Rha‴) in the oligosaccharide core (simonic acid B). It was also reported that this diastereoisomerism at positions C-2 or C-3 could be a consequence of a transesterification via an *ortho*-acid ester intermediate in slightly acidic and neutral aqueous solution (Tao et al., 2008).

Convolvulaceous oligosaccharides have been shown to exert a potentiation effect of norfloxacin against the NorA over-expressing *Staphylococcus aureus* strain SA-1199B (Chérigo et al., 2008, 2009; Pereda-Miranda et al., 2006b). They have demonstrated good activity at low concentrations (10 mM or less) being more active than reserpine, a known efflux pump inhibitor used as a reference control. Therefore, they could be further developed to provide more potent inhibitors of the NorA multidrug efflux pump (Stavri et al., 2007). Departing from this point, the present work was undertaken to emphasize the chemical diversity among the pescaprein series, which indicates their potential to further explore resistance-modifying activity against *S. aureus*. A wild plant collection was used for this investigation because it showed differences in its resin glycoside composition from that of a commercial sample

* Corresponding author. Tel.: +52 55 5622 5288; fax: +52 55 5622 5329.
E-mail address: pereda@unam.mx (R. Pereda-Miranda).

0031-9422/$ - see front matter © 2010 Elsevier Ltd. All rights reserved.
doi:10.1016/j.phytochem.2010.06.018

previously analyzed (Escobedo-Martínez and Pereda-Miranda, 2007; Pereda-Miranda et al., 2005). HPLC isolation of nine pentasaccharides (**1**–**9**) from the $CHCl_3$-soluble resin glycoside mixture is described herein. Several NMR techniques and FABMS were used to characterize the glycosidation sequence of compound **1**, a novel glycosidic acid from the Convolvulaceae family and trivially named pescaproside C.

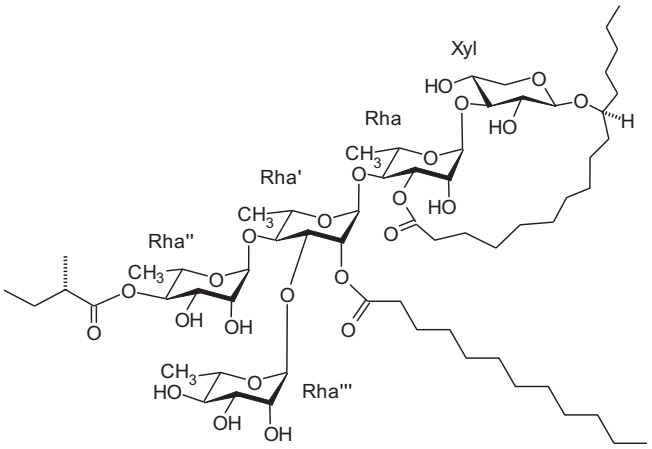

1

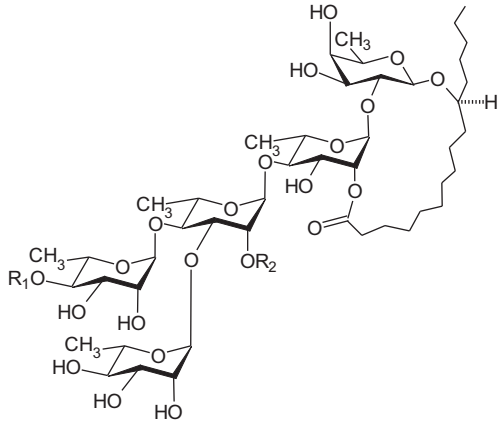

	R_1	R_2
2	methylpropanoyl = iba	*n*-dodecanoyl = dodeca
3	*n*-hexanoyl = hexa	dodeca
8	(2*S*)-methylbutanoyl = mba	*n*-decanoyl = deca
9	mba	dodeca

2. Results and discussion

$CHCl_3$-soluble extracts of the crude drug "riñonina" were fractionated by column chromatography on silica gel. The major fractions, rich in low-polarity resin glycosides, were purified by recycling preparative-scale HPLC (Pereda-Miranda and Hernández-Carlos, 2002), resulting in the isolation of nine glycolipids (**1**–**9**). These compounds showed similar ^1H and ^{13}C NMR spectra and displayed diagnostic signals common for the pescaprein series (Escobedo-Martínez and Pereda-Miranda, 2007; Pereda-Miranda et al., 2005). All compounds displayed the same negative-ion FABMS fragmentation pattern previously described for related resin glycosides, and the resulting diagnostic peaks were useful to confirm the nature of each of their individual pentasaccharide cores (Escobedo-Martínez and Pereda-Miranda, 2007; Pereda-Miranda et al., 2005). For example, compound **1** afforded a pseudomolecular ion $[M-H]^-$ at *m/z* 1235 ($C_{62}H_{107}O_{24}$) in contrast to the ion at *m/z* 1249 for its homologue **7** (pescaprein III), indicating a difference of one methylene group between these compounds which resulted from the presence of the aldopentose xylose instead of a methylpentose, e.g., fucose (Zhou et al., 2007). This 14 mass unit difference was also observed for all common fragment peaks produced by glycosidic cleavage of each sugar moiety at *m/z* 1005, 823, 531, and 403 in compound **1**. This compound exhibited the initial loss of two esterifying groups at *m/z* 1151 $[M-H-C_5H_8O]^-$ and 1053 $[M-H-C_{12}H_{22}O]^-$ which represented the elimination of one unit of α-methylbutyric acid and one of dodecanoic acid, respectively (Chérigo et al., 2008; Escobedo-Martínez and Pereda-Miranda, 2007; Pereda-Miranda et al., 2005).

In the new pescapreins XVIII–XX (**1**–**3**), COSY, TOCSY, and HSQC techniques were used to assign the important ^1H and ^{13}C chemical shifts of each sugar unit (Tables 1 and 2). ROESY and HMBC correlations completed the linkage within the pentasaccharide cores (Duus et al., 2000; Pereda-Miranda et al., 2010). For example, the carbon signals at δ_C 102.1, 75.3, 79.3, 71.5 and 67.2 in compound **1** were assigned to C-1, C-2, C-3, C-4, and C-5 of the xylose, respectively (Zhou et al., 2007). The observed interaction between C-5 (CH_2, δ_C 67.2) and its two attached hydrogens (δ_H 3.65 and 4.30) was the critical HMQC correlation for the assignment of this aldopentose. The ^1H NMR coupling constant for the anomeric proton H-1 ($^3J_{1,2}$ = 7 Hz) was consistent with the β-configuration for D-xylose in the $^4C_1$ conformation (Pereda-Miranda and Bah, 2003). The long-range correlation between H-1 (δ_H 4.89) of this saccharide and C-11 (δ_C 79.5) of the lipidic aglycone in the HMBC spectrum indicated that this unit was the first in the oligosaccharide core. Additional long-range heteronuclear coupling correlations ($^3J_{CH}$) were observed between the following proton and carbon signals: H-1 (δ_H 6.47) of the second saccharide (Rha) and C-3 (δ_C 79.3) of xylose; H-1 (δ_H 5.68) of the second rhamnose (Rha′) and C-4 (δ_C 78.2) of the first rhamnose (Rha); H-1 (δ_H 6.47) of the fourth saccharide (Rha‴) and C-3 (δ_C 80.3) of second rhamnose (Rha′); and H-1 (δ_H 6.47) of the fifth saccharide (Rha″) and C-4 (δ_C 79.8) of second rhamnose (Rha′). The anomeric α configuration in all the L-rhamnose units was deduced from a 2D $^1J_{CH}$ NMR experiment (Duus et al., 2000). These coupling constant values ($^1J_{CH}$ = 170–172 Hz) were 10 Hz higher than that registered for D-xylose ($^1J_{CH}$ = 160 Hz). In conclusion, this new oligosaccharide core for **1**, named pescaproside C, consisted of D-xylose as the first monosaccharide instead of a D-fucose as found in simonic acid B for compounds **2–9** (Escobedo-Martínez and Pereda-Miranda, 2007; Pereda-Miranda et al., 2005). Its structure was determined to be (11*S*)-jalapinolic acid 11-*O*-α-L-rhamnopyranosyl-(1 → 3)-*O*-[α-L-rhamnopyranosyl-(1 → 4)]-*O*-α-L-rhamnopyranosyl-(1 → 4)-*O*-α-L-rhamnopyran- osyl-(1 → 3)-*O*-β-D-xylopyranoside.

Three acylation sites were identified at H-3 of Rha, H-2 of Rha′ and H-4 of Rha″ in the ^1H NMR spectrum of **1**. HMBC studies using long-range heteronuclear coupling correlation located the acylating substituents through the observed connectivities between a specific carbonyl ester group with their vicinal proton resonance ($^2J_{CH}$), in addition to the pyranose ring proton at the site of the esterification ($^3J_{CH}$). Lactonization by the aglycone ($\delta_{C\text{-}1}$ 174.9) was placed at C-3 of the second saccharide (Rha) (δ_H 5.61). The methylbutyroyl group ($\delta_{C\text{-}1}$ 176.3) was located at C-4 of Rha″ (δ_H 5.78); and the additional acyl substituent (*n*-dodecanoic acid; $\delta_{C\text{-}1}$ 173.2) exhibited a $^3J_{CH}$ coupling with the H-2 signal of Rha′ (δ_H 5.84).

The molecular formula calculated from the mass spectra for pescaprein XIX (**2**; $C_{62}H_{107}O_{24}$) and that of pescaprein XX (**3**; $C_{64}H_{111}O_{24}$) indicated that both were diastereosiomers of the known pescaprein II (**6**) and pescaprein IV (**10**), respectively, where by means of 2D NMR analysis the lactonization position was found to be at C-2 of the second saccharide unit instead of at C-3

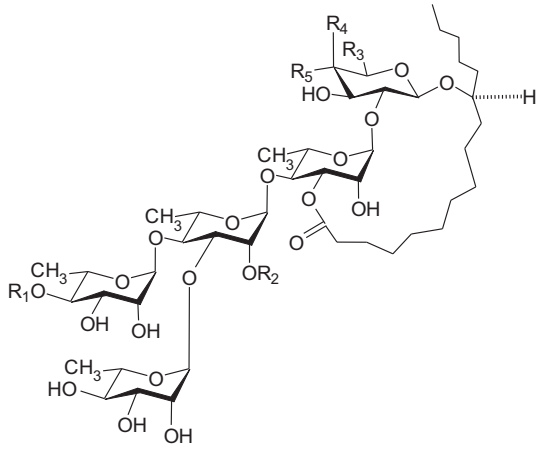

	R_1	R_2	R_3	R_4	R_5
4	mba	dodeca	CH_2OH	H	OH
5	mba	deca	CH_3	OH	H
6	iba	dodeca	CH_3	OH	H
7	mba	dodeca	CH_3	OH	H
10	hexa	dodeca	CH_3	OH	H

(Escobedo-Martínez and Pereda-Miranda, 2007; Pereda-Miranda et al., 2005).

In vitro antibacterial and resistance-modifying activity against strains of *Staphylococcus aureus* possessing multidrug resistance efflux mechanisms indicated that the non-cytotoxic pescapreins **1**–**9** potentiated the action of norfloxacin against the NorA overexpressing strain. They exerted an effect which increased the activity of norfloxacin 4-fold (8 μg/mL from 32 μg/mL) at a concentration of 25 μg/mL (Table 3).

3. Concluding remarks

The novel glycosidation sequence of compound **1** is similar to that of simonic acid B, a commonly found glycosidic acid among the members of the morning glory family (Convolvulaceae), with the only difference being the presence of D-xylopyranose as the first monosaccharide in the oligosaccharide core instead of D-fucose (Pereda-Miranda et al., 2010). In this family, xylose has been reported three times: as part of the tetrasaccharides cuscutic acid B and operculinic acid F from *Cuscuta chinensis* (Du et al., 1998) and *I. operculata* (Noda et al., 1990), respectively, as well as in the pentasaccharide operculinic acid D from *I. operculata* (Ono et al., 1989).

In addition to the results previously reported for other lipophilic oligosaccharides, e.g., the murucoidins (Chérigo et al., 2008, 2009) and orizabins (Pereda-Miranda et al., 2006b), the susceptibility of *Staphylococcus aureus* to the non-cytotoxic pescapreins (**1**–**9**) seems to correlate to the acylation degree of the oligosaccharide core. The lipophilic properties would seem to be an important structural requirement to facilitate cellular uptake to its MDR pump target. Therefore, this type of amphipathic oligosaccharides could be further developed to provide more potent inhibitors of this multidrug efflux pump and facilitate the reintroduction of ineffective antibiotics into clinical use for the treatment of refractive infections.

4. Experimental

4.1. General experimental procedures

All melting points were determined on a Fisher–Johns apparatus and are uncorrected. Optical rotations were measured with a Perkin–Elmer model 241 polarimeter. ^1H (500 MHz) and ^{13}C (125.7 MHz) NMR experiments were conducted on a Bruker DMX-500 instrument. Negative-ion LRFABMS and HRFABMS were recorded using a matrix of triethanolamine on a JEOL SX-102A spectrometer. The instrumentation used for HPLC analysis consisted of a Waters (Millipore Corp., Waters Chromatography Division, Milford, MA) 600E multisolvent delivery system equipped with a refractive index detector (Waters 410). GC–MS was performed on a Hewlett–Packard 5890-II instrument coupled to a JEOL

Table 1
^1H (500 MHz) NMR spectroscopic data of compounds **1**–**3** (pyridine-d_5).[a]

Proton[b]	**1**	2	3
fuc-1		4.73 d (7.5)	4.76 d (7.5)
2		4.16 dd (9.5, 7.5)	4.18 dd (9.4, 7.5)
3		4.07 dd (9.5, 2.5)	4.11 dd (9.4, 3.0)
4		3.99 d (2.5)	4.02 d (3.0)
5		3.77 q (6.5)	3.70 q (6.5)
6		1.51 d (6.5)	1.52 d (6.5)
xyl-1	4.89 d (8.0)		
2	4.25 dd (9.0, 8.0)		
3	4.30 dd (9.0, 8.5)		
4	4.12 ddd (10.5, 8.5, 5.5)		
5	3.65 t (10.8) 4.30 dd (11.0, 5.5)		
rha-1	6.47 d (1.5)	6.16 bs	6.20 d (1.5)
2	5.32 (2.5, 1.5)	6.00 dd (3.0, 1.5)	6.04 dd (3.0, 1.5)
3	5.61 dd (9.5, 2.5)	4.59 dd (9.0, 3.0)	4.61 dd (9.0, 3.0)
4	4.68 dd (9.5, 9.5)	4.31 dd (9.0, 9.0)	4.32 dd (8.5, 8.5)
5	5.07 dq (9.5, 6.0)	4.33–4.36*	4.35–4.41*
6	1.71 d (6.0)	1.65 d (6.0)	1.66 d (6.0)
rha′-1	5.68 d (1.5)	5.48 d (1.5)	5.50 (1.5)
2	5.84 dd (2.5, 1.5)	5.95 dd (3.0, 1.5)	5.99 dd (3.0, 1.5)
3	4.52 dd (9.5, 2.5)	5.01 dd (9.0, 3.0)	5.08 dd (9.0, 3.0)
4	4.23 dd (9.5, 9.5)	4.42–4.45*	4.45–4.50*
5	4.30 dq (9.5, 6.0)	4.21–4.24*	4.31–4.39
6	1.62 d (6.0)	1.61 d (6.0)	1.63 d (6.2)
rha″-1	5.93 bs	5.92 bs	5.97 bs
2	4.63 brs	4.68 brs	4.72 brs
3	4.42 dd (9.5, 3.5)	4.48 dd (9.5, 3.0)	4.53 dd (9.1, 3.5)
4	5.78 dd (9.5, 9.5)	5.78 dd (9.5, 9.5)	5.83 dd (9.6, 9.6)
5	4.36 dq (9.5, 6.0)	4.33–4.36*	4.35–4.41*
6	1.40 d (6.0)	1.38 d (6.0)	1.40 d (6.2)
rha‴-1	5.58 d (1.5)	5.60 d (2.0)	5.63 d (1.5)
2	4.80 brs	4.81 brs	4.86 brs
3	4.53 dd (9.0, 3.0)	4.42–4.45*	4.45–4.50*
4	4.25 dd (9.0, 9.0)	4.21–4.24*	4.31–4.39
5	4.28 dq (9.0, 6.5)	4.29 t (9.5)	4.32 t (9.0)
6	1.72 d (6.0)	1.60 d (6.0)	1.62 d (6.0)
jal-2a	2.26 ddd (15.0, 7.0, 3.0)	2.24 ddd (14.5, 8.0, 4.0)	2.25 ddd (14.0, 7.8, 4.0)
2b	2.95 t (12.0)	2.40 ddd (14.7, 8.5, 3.7)	2.41 ddd (14.5, 8.2, 4.2)
11	3.86 m	3.85 m	3.87 m
16	0.87 t (7.0)	0.87 t (7.5)	0.87 (7.0)
Iba-2		2.63 sept (7.0)	
3		1.16 d (7.0)	
3́		1.19 d (7.0)	
mba-2	2.50 tq (7.0, 6.5)		
2-Me	1.20 d (7.0)		
3-Me	0.94 t (7.5)		
hexa-2			2.32 t (7.5)
6			0.78 t (7.0)
dodeca-2	2.38 t (7.5)	2.30 t (7.5)	2.30 t (7.5)
12	0.93 t (7.0)	0.93 t (7.5)	0.93 t (7.3)

[a] Chemical shifts (δ) are in ppm relative to TMS. The spin coupling (J) is given in parentheses (Hz). Chemical shifts marked with an asterisk (*) indicate overlapped signals. Spin-coupled patterns are designated as follows: s = singlet, bs = broad singlet; brs = broad signal, d = doublet, t = triplet, m = multiplet, q = quartet, sept = septet.

[b] Abbreviations: fuc = fucose; xyl = xylose; rha = rhamnose; jal = 11-hydroxyhexadecanoyl; iba = 2-methylpropanoyl; mba = 2-methylbutanoyl; hexa = hexanoyl; deca = decanoyl; dodeca = dodecanoyl.

Table 2
^{13}C (125 MHz) NMR spectroscopic data of compounds **1**–**3** (pyridine-d_5).[a]

Carbon[b]	1	2	3
fuc-1		104.4	104.3
2		80.2	80.2
3		73.3	73.3
4		73.0	73.0
5		70.8	70.8
6		17.4	17.4
xyl-1	102.1		
2	75.3		
3	79.3		
4	71.5		
5	67.2		
rha-1	100.4	99.1	99.2
2	69.7	73.2	73.2
3	77.8	79.9	79.9
4	78.2	68.4	68.5
5	68.1	70.8	70.5
6	18.2	18.8	18.8
rha′-1	99.2	98.8	98.8
2	73.0	73.9	73.9
3	80.3	79.9	80.0
4	79.8	79.8	79.6
5	67.2	68.6	68.6
6	18.8	18.6	18.6
rha″-1	103.7	103.6	103.6
2	72.7	72.7	72.7
3	70.2	72.6	72.6
4	74.8	74.9	74.8
5	68.3	68.2	68.2
6	17.0	17.9	17.9
rha‴-1	104.4	104.7	104.6
2	72.7	72.6	72.6
3	72.5	70.2	70.2
4	73.7	73.6	73.6
5	70.8	70.7	70.4
6	19.3	19.0	18.4
jal-1	174.9	173.0	173.1
2	33.7	34.2	34.3
11	79.5	82.4	82.3
16	14.3	14.3	14.3
iba-1		176.3	
2		41.5	
3		11.8	
3′		17.0	
mba-1	176.3		
2	41.6		
2-Me	11.8		
3-Me	17.0		
hexa-1			173.1
2			34.2
6			14.3
dodeca-1	173.0	172.9	173.0
2	34.4	34.5	34.2
12	14.4	14.3	14.3

[a] Chemical shifts (δ) are in ppm relative to TMS.
[b] Abbreviations: fuc = fucose; xyl = xylose ; rha = rhamnose; jal = 11-hydroxyhexadecanoyl; iba = 2-methylpropanoyl; mba = 2-methylbutanoyl; hexa = hexanoyl; deca = decanoyl; dodeca = dodecanoyl.

SX-102A spectrometer. GC conditions: HP-5MS (5%-phenyl)-methylpolysiloxane column (30 m × 0.25 mm, film thickness 0.25 μm); He, linear velocity 30 cm/s; 50 °C isothermal for 3 min, linear gradient to 300 °C at 20 °C/min; final temperature hold, 10 min. MS conditions: ionization energy, 70 eV; ion source temperature, 280 °C; interface temperature, 300 °C; scan speed, 2 scans s^{-1}; mass range, 33–880 amu.

4.2. Plant material

The herbal drug "riñonina" was collected in dunes along an upper beach in Las Salinas, Chamela Bay, Jalisco, Mexico in October 2005. A small sample (50 g) was archived at the Departamento de Farmacia, Facultad de Química, UNAM. Macroscopic anatomical features enable the drug to be identified by one of the authors (R.P.-M.) as *Ipomoea pes-caprae* through comparison with a voucher specimen collected at the same location by Dr. Robert Bye (voucher specimen R. Bye 17707) in November 1989 and deposited in the Ethnobotanical Collection of the National Herbarium (MEXU), Instituto de Biología, UNAM.

4.3. Extraction and isolation of compounds *1*–*9*

The whole plant (1 kg) was powdered and extracted exhaustively by maceration at room temperature with $CHCl_3$ to give, after removal of the solvent, a dark-green syrup (15.8 g). The total extract was absorbed on silica gel (25 g) and subjected to column chromatography (CC) over the same normal phase (630 g) with $CHCl_3$ in hexane (1:1 and 1:0), Me_2CO in $CHCl_3$ (1:9, 3:7, and 1:1), Me_2CO in MeOH (1:0 and 1:1) and MeOH. The composition of the 200 fractions obtained (250 mL each) was monitored by TLC (silica gel 60 F254 aluminum sheets, $CHCl_3$–MeOH, 4:1), and identical fractions were combined in eight pools of resin glycosides mixtures (fractions 102–185). These were compared by C_{18} reversed-phase HPLC (Waters column 5 μm, 4.6 × 250 mm) with reference solutions of the previously isolated resin glycosides from this species by an isocratic elution of CH_3CN-MeOH (9:1) at a 0.7 mL/min flow rate, and a sample injection of 10 μL (1 mg/mL). The analysis confirmed a higher complexity in the composition of the less lipophilic fractions 152–165 (pool VII) and 168–185 (pool VIII) eluted with MeOH and differing from that observed for the reference solutions (Escobedo-Martínez and Pereda-Miranda, 2007). The preparative HPLC separations were carried out using a Symmetry C_{18} column (Waters; 7 μm, 19 × 300 mm), using a flow rate of 9 mL/min. The elution was isocratic with CH_3CN–H_2O (4:1) and a sample injection of 500 μL (fraction concentration: 50 mg/mL). The crude fraction VII (150 mg) yielded four major peaks with t_R values of 19.11 (peak I, 16.4 mg), 21.89 (peak II, 14.0 mg), 33.85 (peak III, 30.4 mg), and 43.58 min (peak IV, 24.3 mg) which were collected by the technique of "heart cutting" and independently re-injected to be recycled in order to achieve total homogeneity after twenty consecutive cycles employing an isocratic elution of CH_3CN–MeOH (9:1) with a flow rate of 9 mL/min for all the peaks. Peak I afforded pure major compound **4** (9.7 mg). Peak II afforded compound **5** (7.2 mg). Peak III was split into two peaks during the recycling process to afford pure compounds **1** (14.3 mg) and **6** (12.3 mg). Peak IV yielded compound **7** (22.3 mg). Fraction VIII (200 mg) was subjected to preparative HPLC on the same C_{18} column using an elution with CH_3CN–MeOH (3:7). Eluates across the peaks with t_R values of 23.7 (**8**, 50 mg), 27.5 (**2**, 10 mg), 32.8 (**9**, 40 mg), and 36.8 min (**3**, 4 mg) were collected, independently re-injected, and recycled by 15 consecutive cycles to achieved total purification. All known compounds (**4**–**9**) were identified by comparison of NMR spectroscopic data with published values (Chérigo et al., 2008; Noda et al., 1994, 1998; Pereda-Miranda et al., 2005).

4.4. Compound characterization

4.4.1. Pescaprein XVIII (*1*)

White powder; mp 77–79 °C; $[\alpha]_D$ −42 (*c* 0.1 MeOH); for ^{1}H and ^{13}C NMR spectroscopic data, see Tables 1 and 2; negative FABS *m/z* 1235 [M−H]−, 1151 [M−H−C_5H_8O]$^-$, 1053 [M−H−$C_{12}H_{22}O$]$^-$, 1005 [1151−$C_6H_{10}O_4$]$^-$, 823 [1053−$C_6H_{10}O_4$−C_5H_8O]$^-$, 531[823−2 × 146 ($C_6H_{10}O_4$)]$^-$, 403 [531−128 ($C_6H_{10}O_4$−H_2O]$^-$, 271 [Jal−H]$^-$; HRFAB-MS *m/z*: 1235.7155 [M−H]$^-$ (calcd for $C_{62}H_{107}O_{24}$ requires 1235.7152).

4.4.2. Pescaprein XIX (*2*)

White powder; mp 121–123 °C; $[\alpha]_D$ −32 (*c* 0.5 MeOH); for ^{1}H and ^{13}C NMR spectroscopic data, see Tables 1 and 2; negative FABS

Table 3
Susceptibility of *Staphylococcus aureus* to pescapreins XVIII–XX (**1**–**3**) and known compounds (**4**–**9**) and their cytotoxicity.[a]

Compound	ED_{50} (μg/mL)			MIC (μg/mL)				
	HCT-15	MCF-7	HeLa	ATCC 25923	XU-212	EMRSA-15	SA-1199B[b]	
							Nor (−)	Nor (+)
1	>20	>20	>20	>512	>512	>512	512	8
2	>20	>20	>20	>256	>256	>256	512	8
3	>20	>20	>20	>256	>256	>256	512	8
4	>20	>20	>20	>512	>512	>512	512	8
5	>20	>20	>20	>512	>512	>512	512	8
6	13.4	19.0	12.3	>512	>512	>512	512	8
7	10.0	>20	19.6	>512	>512	>512	512	8
8	>20	>20	>20	>256	>256	>256	512	8
9	>20	>20	>20	>256	>256	>256	512	8
Tetracycline	–	–	–	0.125	64	0.125	0.25	–
Norfloxacin	–	–	–	0.5	8	0.25	–	32
Reserpine	–	–	–	–	–	–	–	8[c]
Vinblastine	0.003	0.007	0.008	–	–	–	–	–

[a] Abbreviations: HCT-15 = colon carcinoma; MCF-7 = breast carcinoma; HeLa = cervix carcinoma; ATCC 25923 = standard *S. aureus* strain; EMRSA-15 = epidemic methicillin-resistant *S. aureus* strain containing the *mecA* gene; XU-212 = a methicillin-resistant *S. aureus* strain possessing the TetK tetracycline efflux protein; SA-1199B = multidrug-resistant *S. aureus* strain over-expressing the NorA efflux pump.
[b] Nor (−) = minimum inhibitory concentration (MIC) value determined in the susceptibility testing; Nor (+) = MIC value determined for norfloxacin in the modulation assay at the concentration of 25 μg/mL of the tested oligosaccharide.
[c] MIC value for norfloxacin in the modulation assay at the concentration of 20 μg/mL of reserpine which was used as positive control for an efflux pump inhibitor.

m/z 1235 $[M-H]^-$, 1165 $[M-H-C_4H_6O]^-$, 837 $[1165-C_{12}H_{22}O-C_6H_{10}O_4]^-$, 673, 545, 417, 271; HRFAB-MS *m/z*: 1235.7153 $[M-H]^-$ (calcd for $C_{62}H_{107}O_{24}$ requires 1235.7152).

4.4.3. Pescaprein XX (**3**)

White powder; mp 120–122 °C; $[\alpha]_D$ −60 (*c* 0.8 MeOH); for ^1H and ^{13}C NMR spectroscopic data, see Tables 1 and 2; negative FABS *m/z* 1263 $[M-H]^-$, 1165 $[M-H-C_6H_{10}O]^-$, 1081 $[M-H-C_{12}H_{22}O]^-$, 837 $[1165-C_{12}H_{22}O-C_6H_{10}O_4]^-$, 673, 545, 417, 271; HRFAB-MS *m/z*: 1263.7452 $[M-H]^-$ (calcd for $C_{64}H_{111}O_{24}$ requires 1263.7465).

4.5. Sugar analysis

Compound **1** (8.5 mg) in 4 N HCl (5 mL) was heated at 90 °C for 2 h. The reaction mixture was diluted with H_2O (2.5 mL) and extracted with Et_2O (15 mL). The aqueous phase was neutralized with 1 N KOH, extracted with *n*-BuOH (20 mL), and concentrated to give a colorless solid. The residue was dissolved in CH_3CN–H_2O and directly analyzed by HPLC: Waters standard column for carbohydrate analysis (3.9 × 300 mm, 10 μm), using an isocratic elution of CH_3CN–H_2O (17:3), a flow rate of 1 mL/min, and a sample injection of 20 μL (sample concentration: 2 mg/mL). Co-elution experiments with standard carbohydrate samples allowed the identification of rhamnose (t_R = 6.9 min) and xylose (t_R = 8.3 min). Each of these eluates was individually collected, concentrated, and dissolved in H_2O. Optical activity was recorded after stirring the solutions for 3 h at room temperature and values were identical for those registered for commercially available samples: L-rhamnose $[\alpha]_D$ +8 (*c* 0.1, H_2O), control $[\alpha]_D$ +7.7 (*c* 0.1, H_2O); D-xylose $[\alpha]_D$ +19 (*c* 0.1, H_2O), control $[\alpha]_D$ +18.8 (*c* 0.1, H_2O). The organic phase was analyzed by GC–MS to allow the detection of two liberated esterifying residues which were identified as: 2-methylbutyric acid (t_R 5.1 min): *m/z* $[M]^+$ 102 (3), 87 (33), 74 (100), 57 (50), 41 (28), 39 (8); and *n*-dodecanoic acid (t_R 11.0 min): *m/z* $[M]^+$ 200 (15), 183 (2), 171 (18), 157 (40), 143 (10), 129 (48), 115 (20), 101 (15), 85 (33), 73 (100), 60 (80), 57 (30), 55 (47), 43 (44), 41 (30) by comparison of their retention times and spectra with those of authentic samples (Chérigo et al., 2008). Previously described methodology was used for the preparation and identification of 4-bromophenacyl (2*S*)-2-methylbutyrate: mp 40–42 °C; $[\alpha]_D$ +18 (*c* 1.0, MeOH) from the resin glycoside mixture pools VII and VIII (20 mg). This transesterification procedure has been used to confirm the absolute configuration for 2-methylbutyric acid (Bah et al., 2007).

4.6. Aglycon identification

A solution of the crude resin glycoside pools VII and VIII (10 mg each) in 5% KOH–H_2O (2.5 mL) was heated until reflux began (95 °C), this being maintained for 3 h. Each reaction mixture was acidified to pH 4.0 and extracted with $CHCl_3$ (20 mL). The aqueous phase was extracted with *n*-BuOH (20 mL), concentrated to dryness and submitted to the same acid-catalyzed hydrolysis described above for the sugar analysis. The organic phase-soluble product was methylated with CH_2N_2 to further perform its separations by HPLC from each of the two resin glycoside fraction as previously described to yield methyl (11*S*)-hydroxyhexadecanoate (jalapinolic acid methyl ester): t_R 16.4 min; mp 42–44 °C; $[\alpha]_D$ +7.3 (*c* 2, $CHCl_3$); ^{13}C NMR: 174.4, 72.0, 51.4, 37.5, 37.4, 34.1, 31.9, 29.6, 29.5, 29.4, 29.2, 29.1, 25.6, 25.3, 24.9, 22.6, 14.1. This aglycon (1 mg) was derivatized by treatment with Sigma Sil-A and analyzed by GC–MS analysis, (t_R 12.8 min): *m/z* $[M]^+$ 358 (0.3), 343 (0.5), 311 (10.5), 287 (59.7), 173 (100), 73 (46.3) (Pereda-Miranda et al., 2006a).

4.7. Biological assays

4.7.1. Bacterial strains and media

Staphylococcus aureus EMRSA-15 containing the *mecA* gene was provided by Dr. Paul Stapleton, The School of Pharmacy, University of London. Strain XU-212, a methicillin-resistant strain possessing the TetK tetracycline efflux protein, was provided by Gibbons and Udo, 2000. SA-1199B, which over-expresses the NorA MDR efflux protein (Kaatz et al., 1993), was provided by Professor Glenn W. Kaatz and standard strain *S. aureus* ATCC 25923 was also used. All strains were cultured on nutrient agar (Oxoid, Basingstoke, UK) before determination of MIC values. Cation-adjusted Mueller–Hinton broth (MHB; Oxoid), containing Ca^{2+} (20 mg/L) and Mg^{2+} (10 mg/L), was used for susceptibility tests.

4.7.2. Susceptibility testing

Minimum inhibitory concentration values (MIC) were determined at least in duplicate by standard microdilution procedures, as recommended by the National Committee for Clinical

Laboratory Standards guidelines (1999). An inoculum density of 5×10^5 cfu of each of the test strains was prepared in 0.9% saline by comparison with a McFarland standard. MHB (125 μL) was dispensed into 10 wells of a 96-well microtiter plate (Nunc, 0.3 mL volume per well). Glycolipids **1–9** were tested at final concentrations ranging from 1 to 512 μg/mL prepared by serial twofold dilutions. All test compounds were dissolved in DMSO before dilution into MHB for use in MIC determinations. The inoculum (125 μL) was added into each well and the plate was incubated at 37 °C for 18 h. For the modulation assay, the pescapreins were tested at final concentrations of 25 μg/mL. Serial doubling dilutions of norfloxacin ranging from 1 to 512 μg/mL were added and the microtitre plates were then interpreted, after inoculum addition and incubation, in the same manner as MIC determinations as previously described (Pereda-Miranda et al., 2006b).

4.7.3. Cytotoxicity assay

Colon (HCT-15), cervix (HeLa), and breast carcinoma (MCF-7) cell lines were maintained in RMPI 1640 (10×) medium supplemented with 10% fetal bovine serum. Cell lines were cultured at 37 °C in an atmosphere of 5% CO_2 in air (100% humidity). The cells at log phase of their growth cycle were treated in triplicate with various concentrations of the test samples (0.16–20 μg/mL) and incubated for 72 h at 37 °C in a humidified atmosphere of 5% CO_2. The cell concentration was determined by the NCI sulforhodamine method (Skehan et al., 1990). Results were expressed as the dose that inhibits 50% control growth after the incubation period (EC_{50}). The values were estimated from a semilog plot of the drug concentration (μg/mL) against the percentage of viable cells.

Acknowledgements

This research was partially supported by Dirección General de Asuntos del Personal Académico, UNAM (IN208307 and IN2173 10) and CONACyT (101380-Q). C.E.-M. and S.C.-M. are grateful to CONACyT for graduate student scholarships. Thanks are due to G. Duarte and M. Guzmán (USAI, Facultad de Química, UNAM) for the recording of mass spectra.

References

Bah, M., Chérigo, L., Taketa, A.T.C., Fragoso-Serrano, M., Hammond, G.B., Pereda-Miranda, R., 2007. Intrapilosins I–VII, pentasaccharides from the seeds of Ipomoea intrapilosa. J. Nat. Prod. 70, 1153–1157.

Chérigo, L., Pereda-Miranda, R., Fragoso-Serrano, M., Jacobo-Herrera, N., Kaatz, G.W., Gibbons, S., 2008. Inhibitors of bacterial multidrug efflux pumps from the resin glycosides of Ipomoea murucoides. J. Nat. Prod. 71, 1037–1045.

Chérigo, L., Pereda-Miranda, R., Gibbons, S., 2009. Bacterial resistance modifying tetrasaccharide agents from Ipomoea murucoides. Phytochemistry 70, 222–227.

De Souza, M.M., Madeira, A., Berti, C., Krogh, R., Yunes, R.A., Cechinel-Filho, V., 2000. Antinociceptive properties of the methanolic extract obtained from Ipomoea pes-caprae (L.). R. Br. J. Ethnopharmacol 69, 85–90.

Du, X.M., Kohinata, K., Kawasaki, T., Guo, Y.T., Miyahara, K., 1998. Components of the ether-insoluble resin glycoside-like fraction from *Cuscuta chinensis*. Phytochemistry 48, 843–850.

Duus, J.Ø., Gotfredsen, C.H., Bock, K., 2000. Carbohydrate structural determination by NMR spectroscopy: modern methods and limitations. Chem. Rev. 100, 4589–5614.

Escobedo-Martínez, C., Pereda-Miranda, R., 2007. Resin glycosides from *Ipomoea pes-caprae*. J. Nat. Prod. 70, 974–978.

Gibbons, S., Udo, E.E., 2000. The effect of reserpine, a modulator of multidrug efflux pumps, on the in-vitro activity of tetracycline against clinical isolates of methicillin resistant *Staphylococcus aureus* (MRSA) possessing the tet(K) determinant. Phytother. Res. 14, 139–140.

Kaatz, G.W., Seo, S.M., Ruble, C.A., 1993. Efflux-mediated fluoroquinolone resistance in *Staphylococcus aureus*. Antimicrob. Agents Chemother. 37, 1086–1094.

National Committee for Clinical Laboratory Standards, 1999. Methods for Dilution Antimicrobial Susceptibility Tests for Bacteria that Growth Aerobically, fifth ed. Villanova, PA, NCCLS, 999, Approved standard M7-A5.

Noda, N., Takahashi, O.M., Fukunaga, T., Kawasaki, T., Miyahara, K., 1990. Four new glycosidic acids, operculinic acids D, E, F, and G, of the ether-soluble crude resin glycosides ("Jalapin") from Rhizoma Jalapae Braziliensis (Roots of *Ipomoea operculata*). Chem. Pharm. Bull. 38, 2650–2655.

Noda, N., Takahashi, N., Kawasaki, T., Miyahara, K., Yang, C.-R., 1994. Stoloniferins I–VII, resin glycosides from *Ipomoea stolonifera*. Phytochemistry 36, 365–371.

Noda, N., Takahashi, N., Miyahara, K., Yang, C.-R., 1998. Stolonifereins VIII–XII, resin glycosides from *Ipomoea stolonifera*. Phytochemistry 48, 837–841.

Ono, M., Kawasaki, T., Miyahara, K., 1989. Resin glycosides V. Identification and characterization of the component organic and glycosidic acids of the ether-soluble crude resin glycosides ("jalapin") from Rhizoma Jalapae Braziliensis (roots of *Ipomoea operculata*). Chem. Pharm. Bull 37, 3209–3213.

Pereda-Miranda, R., Bah, M., 2003. Biodynamic constituents in the Mexican morning glories: purgative remedies transcending boundaries. Curr. Top. Med. Chem. 3, 111–131.

Pereda-Miranda, R., Hernández-Carlos, B., 2002. HPLC isolation and structural elucidation of diastereomeric niloyl ester tetrasaccharides from Mexican scammony root. Tetrahedron 58, 3145–3154.

Pereda-Miranda, R., Escalante-Sánchez, E., Escobedo-Martínez, C., 2005. Characterization of lipophilic pentasaccharides from beach morning glory (*Ipomoea pes-caprae*). J. Nat. Prod. 68, 226–230.

Pereda-Miranda, R., Fragoso-Serrano, M., Escalante-Sánchez, E., Hernández-Carlos, B., Linares, E., Robert, B., 2006a. Profiling of the resin glycoside content of Mexican jalap roots with purgative activity. J. Nat. Prod. 69, 1460–1466.

Pereda-Miranda, R., Kaatz, G.W., Gibbons, S., 2006b. Polyacylated oligosaccharides from medicinal Mexican morning glory species as antibacterial and inhibitors of multidrug resistance in *Staphylococcus aureus*. J. Nat. Prod. 69, 406–409.

Pereda-Miranda, R., Rosas-Ramírez, D., Castañeda-Gómez, J., 2010. Resin glycosides from the morning glory family. In: Kinghorn, A.D., Falk, H., Kobayashi, J. (Eds.), Progress in the Chemistry of Natural Products, vol. 92. Springer, New York, pp. 77–153.

Pongprayoon, U., Baeckström, P., Jacobsson, U., Lindström, M., Bohlin, L., 1992. Antispasmodic activity of β-damascenone and E-phytol isolated from *Ipomoea pes-caprae*. Planta Med. 58, 19–21.

Skehan, P., Storeng, R., Scudiero, D., Monks, A., McMahon, J., Vistica, D., Warren, J.T., Bokesch, H., Kenney, S., Boyd, M.R., 1990. New colorimetric cytotoxicity assay for anticancer-drug screening. J. Natl. Cancer Inst. 82, 1107–1112.

Stavri, M., Piddock, L.J.V., Gibbons, S., 2007. Bacterial efflux pump inhibitors from natural sources. J. Antimicrob. Chemother. 59, 1247–1260.

Tao, H., Hao, X., Liu, J., Ding, J., Fang, Y., Gu, Q., Zhu, W., 2008. Resin glycoside constituents of *Ipomoea pes-caprae* (beach morning glory). J. Nat. Prod. 71, 1998–2003.

Zhou, L.-B., Chen, T.-H., Bastow, K.F., Shibano, M., Lee, K.-H., Chen, D.-F., 2007. Filiasparosides A–D, cytotoxic steroidal saponins from the roots of *Asparagus filicinus*. J. Nat. Prod. 70, 1263–1267.

J Antimicrob Chemother 2010; **65**: 1215–1223
doi:10.1093/jac/dkq079 Advance publication 19 March 2010

Journal of Antimicrobial Chemotherapy

Natural and synthetic compounds such as trimethoprim behave as inhibitors of efflux in Gram-negative bacteria

Laura J. V. Piddock[1]*, Mark I. Garvey[1], M. Mukhlesur Rahman[2] and Simon Gibbons[2]

[1]*Antimicrobial Agents Research Group, School of Immunity and Infection, College of Medical and Dental Sciences, University of Birmingham, Birmingham B15 2TT, UK;* [2]*Department of Pharmaceutical and Biological Chemistry, The School of Pharmacy, University of London, 29–39 Brunswick Square, London WC1N 1AX, UK*

*Corresponding author. Tel: +44-121-414-6966; Fax: +44-121-414-6819; E-mail: l.j.v.piddock@bham.ac.uk

Received 9 December 2009; returned 10 January 2010; revised 17 February 2010; accepted 18 February 2010

Objectives: We hypothesized that small heterocyclic or nitrogen-containing compounds could act as RND efflux pump inhibitors (EPIs). To ascertain possible EPIs, we sought to identify compounds that synergized with substrates of RND efflux pumps for wild-type bacteria and those that overexpress an efflux pump, but had no synergistic activity against strains in which a gene encoding a component of the AcrAB-TolC efflux pump had been inactivated.

Methods: Twenty-six compounds plus L-phenylalanyl-L-arginyl-β-naphthylamide (PAβN) and carbonyl cyanide *m*-chlorophenylhydrazone (CCCP) were screened by bioassay to identify compounds that synergized with ciprofloxacin for a range of Enterobacteriaceae and *Pseudomonas aeruginosa*. The MICs of ciprofloxacin, tetracycline, chloramphenicol, erythromycin and ethidium bromide ± synergizing compounds were determined, and the ability to inhibit the efflux of Hoechst 33342 was measured.

Results: Two compounds, trimethoprim and epinephrine, consistently showed synergy with antibiotics for most strains. The combinations did not show synergy for *Salmonella enterica* serovar Typhimurium in which the AcrAB-TolC efflux pump was inactive. Both compounds inhibited the efflux of Hoechst 33342.

Conclusions: Two compounds, trimethoprim and epinephrine, which are already licensed for use in man, may warrant further analysis as EPIs. The combination of trimethoprim with another antibiotic is a well-used combination in anti-infective chemotherapy, and so combination with another agent, such as a quinolone, may be a viable option and further studies are now required.

Keywords: AcrAB-TolC, antibiotic resistance, EPIs

Introduction

The numbers of antibiotic-resistant bacteria have increased in recent years and such resistance can compromise the efficacy of antimicrobial therapy.[1] Antibiotic-resistant bacteria can be associated with infections with higher mortality than those caused by antibiotic-susceptible strains and fluoroquinolone resistance has been shown to be a particular risk factor for mortality associated with infections by some bacterial species.[2] Fluoroquinolones are also the agents most commonly associated with the selection of constitutive chromosomally mediated multidrug resistance (MDR), frequently presumed to be conferred by the overproduction of chromosomally encoded MDR efflux pumps.[3] The RND efflux pump AcrAB-TolC in Enterobacteriaceae and homologues thereof in other Gram-negative bacteria is the system most commonly associated with innate and acquired chromosomally mediated MDR.[3] Clinical isolates that overexpress efflux pumps usually overproduce this pump and there is an association of MDR mediated by efflux with prior use of fluoroquinolones.[4] In the laboratory, *in vitro* mutants selected after fluoroquinolone exposure comprise various phenotypes, of which ~30% are MDR due to enhanced efflux.[5]

Due to the lack of new antibacterial agents, there is considerable interest in restoring the activity of older antimicrobials. One way to do this is to inhibit the action of MDR efflux pumps that confer innate resistance to these older agents; this is an area of active drug development by pharmaceutical companies.[6] Efflux pump proteins make attractive targets for drug discovery programmes as: (i) inhibition confers multidrug susceptibility; and (ii) a functional RND efflux pump is necessary for mutants resistant to substrates of the pump to be selected,[7–10] and for pathogens to colonize, persist and cause infection in their

hosts.[3,7–9,11] Agents that inhibit efflux (whether innate or enhanced) are termed efflux pump inhibitors (EPIs). However, this is a broad definition that includes agents that: (i) interact with the efflux pump protein(s); (ii) dissipate the proton-motive force required for pump activity, e.g. carbonyl cyanide *m*-chlorophenylhydrazone (CCCP), as in the case of RND family efflux pumps; or (iii) inhibit expression of the efflux pump gene, as has been shown for chlorpromazine and *acrB*.[12] The majority of studies searching for efflux pump inhibitors do so by *in vitro* determination of antimicrobial activity in the presence of the test compound, and by measuring efflux activity in the presence and absence of the test compound. Rarely do studies examine the precise mechanism of action of the presumed EPI. To date, there is only one agent that has been developed as an EPI for Gram-negative bacteria: L-phenylalanyl-L-arginyl-β-naphthylamide (PAβN).[10] This agent is routinely used in the laboratory as a screen to indicate efflux-mediated antibiotic resistance in Gram-negative bacteria. However, PAβN is not used in the clinical setting due to toxicity and bioavailability issues.[7]

Several teams worldwide are searching for molecules whose actions are suggestive of EPIs. Publications predominantly focus on the identification of molecules with activity against Gram-positive bacteria, in particular *Staphylococcus aureus*.[13] More recently, as there is a desperate need for new agents to treat infections by Gram-negative bacteria, the search for inhibitors of efflux has been widened. However, for Gram-negative bacteria such as *Salmonella enterica* serovar Typhimurium, there are no clinically useful EPIs. Building upon the studies by Lomovskaya *et al.*,[10] where PAβN was identified as a *Pseudomonas aeruginosa* MexB inhibitor, other molecules have subsequently been identified to have *in vitro* activity, although as yet none have been licensed for use. Many of the molecules, such as D-ornithinyl-D-homophenylalanyl-3-aminoquinoline, were modified to decrease their *in vivo* toxicity.[14] Data for other molecules suggest that they are also EPIs, including 1-(1-naphthylmethyl)-piperazine, which has been shown to be active against *Acinetobacter baumannii* and Enterobacteriaceae.[15–17] Others have shown that drugs that are currently licensed for uses other than as anti-infective agents, have EPI-like properties; these include selective serotonin reuptake inhibitors[18] and phenothiazines.[12]

We hypothesized that simple heterocyclic nitrogen-containing compounds could also act as inhibitors of efflux in Gram-negative bacteria. Therefore, in a proof-of-principle study, we screened 26 compounds for EPI-like activity by identifying molecules that had synergistic activity with ciprofloxacin for wild-type *Salmonella* Typhimurium and strains that overexpressed the AcrAB-TolC efflux pump, but had no activity against mutants in which AcrA, AcrB or TolC had been inactivated. For those compounds that synergized with ciprofloxacin, the MICs of a range of agents ± the test compound were determined for several different Gram-negative bacterial species. Growth kinetics and, as a measure of efflux activity, accumulation of Hoechst 33342 were determined for the most active compounds.

Materials and methods

Bacterial strains, storage and growth

All bacteria used in this study are listed in Table 1. Construction of mutants derived from *S. enterica* serovar Typhimurium (hereafter referred to as *Salmonella* Typhimurium) strains SL1344 and 14028s with the *acrA*, *acrB* and *tolC* genes disrupted has been described previously.[19–21] *Salmonella* Typhimurium L3 is a human pre-therapy isolate and L10 is a human post-therapy clinical isolate that overexpresses *acrAB*, both of which have been previously described.[4,22] All bacteria were stored on Protect™ beads at −80°C until required. The identification of each species was confirmed by Gram stain and analytical profile index (API 20E; bioMérieux, Marcy l'Étoile, France).

Table 1. Bacterial strains

Strain	Species	Description	Reference/source
L354	*Salmonella* Typhimurium	SL1344	30
L109	*Salmonella* Typhimurium	SL1344Δ*tolC*	21
L785	*Salmonella* Typhimurium	ATCC 15277 (LT2)	31
L828	*Salmonella* Typhimurium	ATCC 14028s	ATCC[a]
L829	*Salmonella* Typhimurium	ATCC 14028s Δ*tolC*	32
L830	*Salmonella* Typhimurium	ATCC 14028s Δ*acrB*	32
L831	*Salmonella* Typhimurium	ATCC 14028s Δ*acrAB*	32
L3	*Salmonella* Typhimurium	human pre-therapy clinical isolate	21
L10	*Salmonella* Typhimurium	human post-therapy MDR clinical isolate, *acrAB*$^{+++}$	21
A1	*Enterobacter cloacae*	NCTC 10005	NCTC[b]
B14	*Serratia marcescens*	NCTC 2847	NCTC[b]
G1	*Pseudomonas aeruginosa*	NCTC 10662	NCTC[b]
H42	*Klebsiella pneumoniae*	NCTC 10896	NCTC[b]
H43	*Klebsiella pneumoniae*	NCTC 9633	NCTC[b]
I114	*Escherichia coli*	NCTC 10538	NCTC[b]
J29	*Morganella morganii*	NCTC 235	NCTC[b]

[a]ATCC, American Type Culture Collection.
[b]NCTC, National Collection of Type Cultures (HPA, Colindale, London, UK).

Media and chemicals

Bacteria were routinely grown on LB agar plates (Oxoid, Basingstoke, UK) and in LB broth (Oxoid). All antibiotics and compounds were obtained from Sigma (Poole, UK).

Bioassay screening

Screening with ciprofloxacin ± 26 test compounds (trimethoprim, cathinone, theobromine, norepinephrine, epinephrine, theophylline, caffeine, quinine, arecoline, atropine, ephedrine, norephedrine, morphine, ergometrine, ergotamine, harmine, harmaline, strychnine, amphetamine, nicotine, papaverine, emetine, quinidine, pilocarpine, salbutamol and ajmaline) for synergistic activity was carried out by bioassay, essentially as described by Lund *et al.*[23] In brief, this consisted of large sterile square dishes (24×24 cm; Fisher Scientific, Loughborough, Leicestershire, UK) containing 250 mL of Iso-Sensitest agar (Oxoid) solidified for 2 h at 4°C. The plates were then air-dried at 50°C for 15 min. An overnight 25 mL culture of *Salmonella* Typhimurium was diluted 1:10000 to obtain 1.72×10^5 cfu/mL (determined by 10 successive replicate plate counts) and then 10 mL of the diluted culture was poured onto the surface of the agar plate. The excess liquid was removed and the plates left to dry at room temperature for 15 min. Six rows of 6 wells (total 36 wells), each of 8 mm diameter, were cut out of each agar plate using an agar cutter (Fisher Scientific) and 200 μL of sterile Iso-Sensitest broth containing ciprofloxacin (0.5, 1 and 2 mg/L) was added to three sets of wells respectively. This volume and concentrations gave a zone of inhibition of ≥15 cm diameter. To determine whether the test compound synergized with ciprofloxacin, 200 μL of a solution containing both ciprofloxacin (0.5, 1 and 2 mg/L respectively) and the test compound (100 mg/L) or epinephrine and trimethoprim (10 mg/L) in broth was added to three separate wells. The plates were incubated overnight at 37°C and the diameters of the zones of growth inhibition were measured. Each experiment contained three technical repeats and was repeated on three separate days. This allowed the inherent variability of the method to be established and statistical analyses of data. A zone of inhibition of the antibiotic plus test compound larger than that of the antibiotic alone was taken to suggest synergy. The positive control was ciprofloxacin plus PAβN (40 mg/L) or CCCP (100 mg/L) and the negative control was Iso-Sensitest broth alone. Compound alone was measured to determine whether the test agent had inherent antimicrobial activity.

Determination of MICs of antibiotics ± synergizing compounds

The MICs of ciprofloxacin, tetracycline, chloramphenicol, erythromycin and ethidium bromide ± test compounds (10 mg/L) or trimethoprim and epinephrine (10 mg/L) were determined by the standardized agar doubling dilution method and by the microbroth dilution method following the BSAC recommended protocol.[24,25] All MIC determinations were repeated at least three times in independent experiments. All antibiotics, compounds and efflux pump inhibitors were made up and used according to the manufacturer's instructions.

Accumulation of Hoechst 33342 ± candidate EPI-like compounds by Salmonella Typhimurium

The efflux activity of five strains [L3, L10, SL1344, ATCC 15277 (LT2) and ATCC 14028s] was determined by measuring the accumulation of the fluorescent dye Hoechst 33342 (bis-benzimide; 2.5 μM) ± known EPIs (100 mg/L CCCP and 40 mg/L PAβN) and ± the putative EPIs (epinephrine and trimethoprim, both at 10 mg/L, and theobromine and norepinephrine, both at 100 mg/L). Measurements were taken at excitation and emission wavelengths of 350 and 460 nm, respectively, over 30 min using a FLUOstar OPTIMA (BMG Labtech, Aylesbury, UK), as previously described.[8] Differences in the accumulation seen ± putative EPI were analysed for statistical significance using the two-tailed Student's *t*-test. *P* values ≤0.05 were taken as significant.

Growth kinetics ± putative EPIs

The growth kinetics of L3, L10, SL1344, ATCC 15277 (LT2) and ATCC 14028s ± putative EPIs were determined by monitoring the optical density at 600 nm every 10 min at 37°C for 24 h using a FLUOstar OPTIMA (BMG Labtech). The putative EPIs (epinephrine and trimethoprim, both at 10 mg/L, and theobromine and norepinephrine, both at 100 mg/L) were added to the bacterial cultures at mid-logarithmic growth phase (2 h). Samples were also removed and visualized microscopically in order to detect any gross changes to cell morphology, i.e. filamentation. A two-tailed Student's *t*-test was used to compare the generation times. *P* values ≤0.05 were taken as significant.

Results

Choice of compounds to investigate for EPI properties

Many EPIs are either nitrogen-containing heterocyclic compounds[15,26] or possess amino acid residues, such as in the case of PAβN.[10] Therefore, we selected a range of natural and synthetic compounds possessing either heterocyclic functional groups or straight chain amino groups. Some of these compounds, e.g. epinephrine, norepinephrine and cathinone, possessed a phenylethylamine moiety, which appears to be a common structural motif in some EPIs.

Identification of compounds that synergized with ciprofloxacin

Twenty-six compounds (listed in the Materials and methods section) plus PAβN and CCCP were screened by bioassay to identify compounds that synergized with ciprofloxacin. In addition to PAβN and CCCP, 13 compounds showed synergy with ciprofloxacin. Of these, trimethoprim, cathinone, theobromine, norepinephrine and epinephrine had the greatest synergy (Figure 1 and Table 2).

The MICs of trimethoprim for all strains were 16–32 mg/L and of epinephrine were 32–64 mg/L. The MICs of theobromine and norepinephrine were >256 mg/L for all strains. *Salmonella* Typhimurium ATCC 14028s and SL1344 in which *acrA*, *acrB*, *acrAB* or *tolC* were inactivated were hypersusceptible to ciprofloxacin, tetracycline, erythromycin, ethidium bromide and chloramphenicol (Table 3 and data not shown). However, the MICs of epinephrine, norepinephrine, trimethoprim and theobromine were the same for the parental strain and the mutants in which the efflux pump gene had been inactivated (data not shown).

When the MICs of ciprofloxacin were determined in combination with the test compounds (at one-quarter to one-half MIC or lower), the synergy observed in the bioassays was not always replicated for all strains (Table 3). Nonetheless, all compounds identified in the bioassay synergized with all antibiotics and ethidium bromide for at least six strains, including NCTC type strains of different species (Tables 3–5). The combination that showed synergy most often was that of trimethoprim with ciprofloxacin.

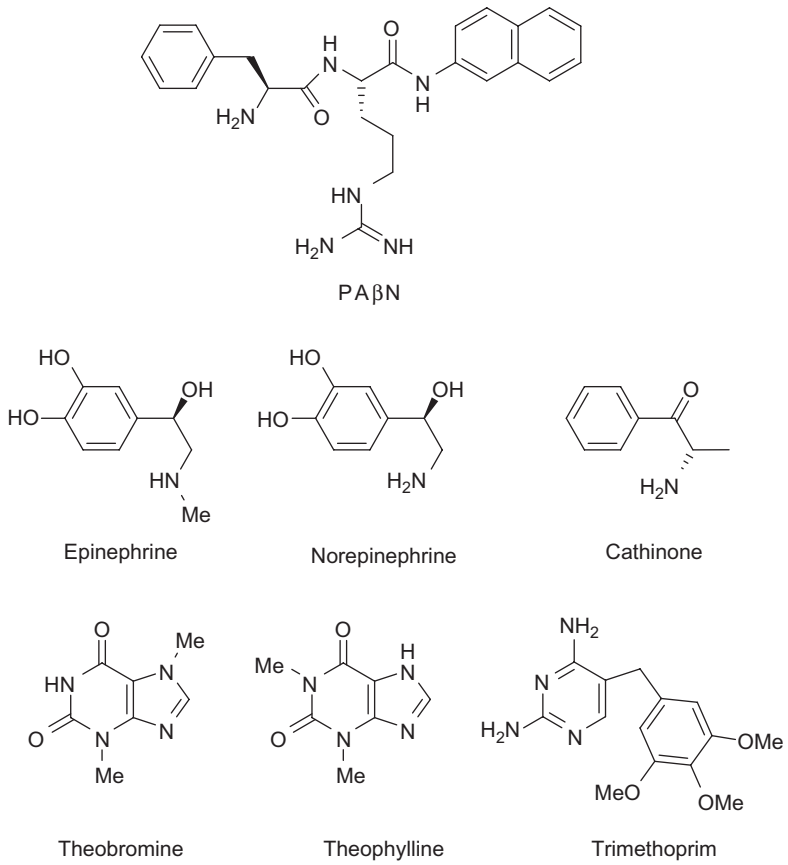

Figure 1. Structures of five test compounds and theophylline compared with that of PAβN.

Table 2. Compounds from the bioassay screen having the greatest synergy with ciprofloxacin

Strain	Description	Ciprofloxacin plus							
		PAβN	TMP	Cat	The	Nre	Ene	Thp	Caf
L354	SL1344	S	S	S	S	S	S	S	S
L785	ATCC 15277 (LT2 wild)	S	S	S	S	S	S	S	NE
L828	ATCC 14028s	S	S	S	S	S	S	NE	S
L3	human pre-therapy clinical isolate	S	S	S	S	S	NE	S	NE
L10	human post-therapy MDR clinical isolate, *acrAB*$^{+++}$	S	S	S	S	S	S	NE	NE

S, synergy; NE, no effect; TMP, trimethoprim; Cat, cathinone; The, theobromine; Nre, norepinephrine; Ene, epinephrine; Thp, theophylline; Caf, caffeine.

The MIC values of ciprofloxacin were reduced by 2–4-fold in the presence of trimethoprim for the wild-type strains of *Salmonella* Typhimurium and NCTC type strains of *Enterobacter cloacae*, *Serratia marcescens*, *P. aeruginosa*, *Klebsiella pneumoniae* and *Escherichia coli* (Table 3). However, no synergy was seen for trimethoprim with ciprofloxacin for the strains of *Salmonella* Typhimurium in which *acrA*, *acrB*, *acrAB* or *tolC* were inactivated. Theobromine with ciprofloxacin also showed synergy for eight other bacterial strains, including wild-type strains of *Salmonella* Typhimurium and NCTC type strains of *E. cloacae*, *P. aeruginosa*, *K. pneumoniae* and *E. coli*. Except for the mutant in which *tolC* had been inactivated, no synergy was seen with this combination, or with mutants in which *acrA*, *acrB* or *acrAB* were inactivated. Ciprofloxacin and epinephrine was also a synergistic combination for some strains/species, but increased activity of the combination versus ciprofloxacin alone was also seen for mutants in which a gene encoding a component of the AcrAB-TolC pump was inactivated. However, the combination had no activity against the parental strains (e.g. L828, Table 3). The combination of ciprofloxacin and norepinephrine was only synergistic for two

strains (one *Salmonella* Typhimurium and the NCTC type strain of *K. pneumoniae*).

Table 3. MIC (mg/L) of ciprofloxacin ± the four most active compounds against Gram-negative bacteria

		CIP plus				
Strain	CIP	PAβN[a]	Ene[b]	Nre[c]	TMP[b]	The[c]
L354	0.06	**0.015**	**0.015**	0.06	**0.015**	0.06
L785	0.03	**0.015**	0.03	0.03	0.03	**0.015**
L828	0.03	**0.015**	0.03	**0.008**	**0.015**	**0.015**
L829	0.008	0.008	**0.002**	0.008	0.008	0.008
L831	0.008	0.008	**0.002**	0.008	0.008	**0.004**
L3	0.008	0.008	0.008	0.008	**0.015**	**0.004**
L10	0.06	**0.015**	0.06	0.06	**0.03**	0.06
A1	0.12	**0.03**	**0.06**	0.12	**0.03**	**0.03**
B14	0.06	0.06	**0.03**	0.06	**0.03**	0.06
G1	1	**0.12**	**0.5**	1	**0.5**	**0.5**
H42	0.06	**0.03**	0.06	0.06	0.06	0.06
H43	0.12	**0.03**	0.12	**0.06**	**0.06**	**0.03**
I114	0.06	**0.03**	0.06	0.06	**0.03**	**0.03**
J29	0.015	**0.008**	0.015	0.015	0.015	0.015

CIP, ciprofloxacin; Ene, epinephrine; Nre, norepinephrine; TMP, trimethoprim; The, theobromine.
Bold text indicates synergistic combinations.
[a]PAβN at 40 mg/L.
[b]TMP and Ene at 10 mg/L.
[c]Nre and The at 100 mg/L.

Epinephrine, norepinephrine, trimethoprim and theobromine synergize with other antibiotics

PAβN showed synergy with ciprofloxacin for 10 strains (Table 3). PAβN also synergized with tetracycline, chloramphenicol and ethidium bromide for seven to nine strains/species (Tables 4 and 5). However, only for *S. marcescens* was synergy seen between PAβN and erythromycin. When the MICs of the four test compounds in combination with other antibiotics were determined, it was revealed that the synergy observed with ciprofloxacin was not always reproduced with the other agents. For instance, norepinephrine and chloramphenicol, norepinephrine and ethidium bromide, and theobromine with erythromycin were not synergistic combinations. However, as seen with ciprofloxacin, trimethoprim in combination with any of the other four agents was synergistic for six to eight strains/species (Tables 4 and 5). Epinephrine in combination with tetracycline, chloramphenicol and ethidium bromide was also synergistic for five to seven strains/species. Theobromine formed a synergistic combination with tetracycline, chloramphenicol and ethidium bromide for three to five strains. Norepinephrine combined with tetracycline or erythromycin showed synergy for three to four strains. Where synergism was observed, the activity for a particular antibiotic was similar, irrespective of the synergizing compound.

Efflux activity of test compounds

Due to the synergistic activity seen for the compounds with some antibiotics and strains in which AcrAB-TolC was produced, and the lack of synergy seen for mutants in which components of this pump were not produced, it was hypothesized that

Table 4. MIC (mg/L) of tetracycline and erythromycin ± the four most active compounds against Gram-negative bacteria

		TET plus						ERY plus				
Strain	TET	PAβN[a]	Ene[b]	Nre[c]	TMP[b]	The[c]	ERY	PAβN[a]	Ene[b]	Nre[c]	TMP[b]	The[c]
L354	8	**4**	**4**	8	**4**	4	512	512	512	512	512	512
L785	16	16	**8**	**8**	**8**	16	512	512	512	512	**256**	512
L828	16	8	16	**8**	**8**	16	512	512	**256**	512	**256**	512
L829	4	4	4	**2**	4	4	8	8	8	8	8	8
L831	4	4	4	**2**	4	4	64	64	64	64	64	64
L3	4	**2**	**2**	4	**2**	4	512	512	512	512	**256**	512
L10	8	**2**	**4**	8	**4**	**4**	512	512	**256**	512	**256**	512
A1	8	**4**	8	8	8	**4**	512	128	512	512	512	512
B14	64	64	64	64	64	**32**	256	**64**	256	256	256	256
G1	64	**8**	64	**32**	64	**32**	512	512	512	**256**	512	512
H42	16	**8**	**8**	16	**8**	16	512	512	512	512	**256**	512
H43	8	8	**4**	8	**4**	8	512	512	512	**256**	**256**	512
I114	4	**2**	4	4	4	4	512	512	512	**256**	512	512
J29	8	**4**	**4**	**4**	**4**	**4**	512	512	512	512	512	512

TET, tetracycline; Ene, epinephrine; Nre, norepinephrine; TMP, trimethoprim; The, theobromine; ERY, erythromycin.
Bold text indicates synergistic combinations.
[a]PAβN at 40 mg/L.
[b]TMP and Ene at 10 mg/L.
[c]Nre and The at 100 mg/L.

Table 5. MIC (mg/L) of chloramphenicol and and ethidium bromide ± the four most active compounds against Gram-negative bacteria

		CHL plus						EtBr plus				
Strain	CHL	PAβN[a]	Ene[b]	Nre[c]	TMP[b]	The[c]	EtBr	PAβN[a]	Ene[b]	Nre[c]	TMP[b]	The[c]
L354	8	**2**	8	8	8	8	2048	**1024**	2048	2048	**512**	2048
L785	8	**2**	8	8	8	8	2048	2048	**1024**	2048	2048	2048
L828	8	**2**	8	8	8	8	2048	2048	**1024**	2048	**1024**	2048
L829	1	1	1	1	1	1	16	16	16	16	16	16
L831	2	2	2	2	2	2	64	**16**	64	64	64	64
L3	8	8	8	8	**4**	**4**	512	512	**256**	512	512	512
L10	32	**8**	**16**	32	**16**	**16**	2048	**512**	2048	2048	**1024**	2048
A1	4	**1**	**2**	4	**2**	4	2048	2048	2048	2048	2048	**1024**
B14	4	4	**2**	4	**2**	4	2048	2048	2048	2048	2048	**1024**
G1	64	**16**	64	64	64	64	2048	**256**	2048	2048	2048	2048
H42	128	**32**	**64**	128	**64**	**64**	2048	**1024**	**1024**	2048	**1024**	2048
H43	4	**1**	**2**	4	**2**	**2**	2048	**1024**	**1024**	2048	**1024**	2048
I114	4	**1**	4	4	4	4	256	**128**	256	256	256	256
J29	16	16	16	16	16	16	2048	2048	**1024**	2048	**1024**	**1024**

CHL, chloramphenicol; Ene, epinephrine; Nre, norepinephrine; TMP, trimethoprim; The, theobromine; EtBr, ethidium bromide.
Bold text indicates synergistic combinations.
[a]PAβN at 40 mg/L.
[b]TMP and Ene at 10 mg/L.
[c]Nre and The at 100 mg/L.

some compounds could be EPIs that target AcrAB-TolC. Therefore, the effect of trimethoprim, epinephrine and theobromine upon the accumulation of Hoechst 33342 was measured for five strains of *Salmonella* Typhimurium (SL1344, LT2, ATCC 14028s, L3 and L10). The growth kinetics of the bacteria were unaffected at the concentrations of compound tested (10 mg/L trimethoprim and epinephrine; 100 mg/L theobromine) (data not shown). A compound with EPI-like properties, such as PAβN, inhibits efflux and so the bacterium is unable to export Hoechst 33342; therefore, the concentration of Hoechst 33342 accumulated by the bacterium increases. Trimethoprim and epinephrine both significantly increased the concentration of Hoechst 33342 accumulated (1.5- and 2–2.5-fold, respectively) (Figures 2 and 3). However, accumulation of Hoechst 33342 by *Salmonella* Typhimurium appeared unaffected by theobromine (data not shown).

Discussion

This proof-of-principle study revealed that combinations of several agents (including trimethoprim) had synergistic antibacterial activity. The compounds were chosen on the basis of being heterocyclic nitrogen-containing 'drug-like' molecules, e.g. the phenylethylamines epinephrine, norepinephrine and cathinone. As ciprofloxacin is a substrate of many efflux pumps in different bacterial species,[3] initial experiments focused upon identifying compounds that displayed synergistic activity with ciprofloxacin in a simple bioassay. Furthermore, to identify possible EPIs, we sought to identify compounds that synergized with substrates of RND efflux pumps for wild-type bacteria and those that overexpress an efflux pump, but had no synergistic activity against strains in which a gene encoding a component of the AcrAB-TolC efflux pump had been inactivated.

Three of the agents identified in the bioassay that synergized with ciprofloxacin, namely epinephrine, norepinephrine and cathinone, are members of the phenylethylamine class of natural product, and all possess this structural motif, as does PAβN. Many of the EPIs identified to date appear to possess either monocyclic or bicyclic (e.g. naphthyl) aromatic rings with side chains possessing nitrogen atoms, for example D-ornithinyl-D-homophenylalanyl-3-aminoquinoline[14] and 1-(1-naphthylmethyl)-piperazine.[15,16]

Where synergy was confirmed in the MIC tests and was seen with a combination of compound plus an antibiotic or ethidium bromide, it was typically seen for NCTC strains of different species. This suggests broad synergistic activity rather than species-specific activity. However, these data require confirmation in studies with a larger number of strains of each species. Two compounds, trimethoprim and epinephrine, consistently showed synergy with antibiotics for most strains. The combinations did not show synergy for strains in which the AcrAB-TolC efflux pump was inactive. These data suggest that trimethoprim and epinephrine either inhibit expression of the genes encoding AcrAB-TolC, as found for *acrB* and chlorpromazine,[12] or interact with a component of the pump directly, as for PAβN and MexB. These hypotheses are supported by data showing that both compounds inhibited the efflux of Hoechst 33342. Whilst trimethoprim and epinephrine appear to be structurally unrelated, they both possess an aromatic ring linked through a chain to a basic nitrogen-containing moiety: a pyrimidine ring in the case of trimethoprim and a primary amine in the case of epinephrine (Figure 1). These appear to be common features of many EPIs, including PAβN, D-ornithinyl-D-homophenylalanyl-3-aminoquinoline and 1-(1-naphthylmethyl)-piperazine. The pyrimidine ring of trimethoprim also bears striking structural and electronic similarity to the A-rings of theobromine and

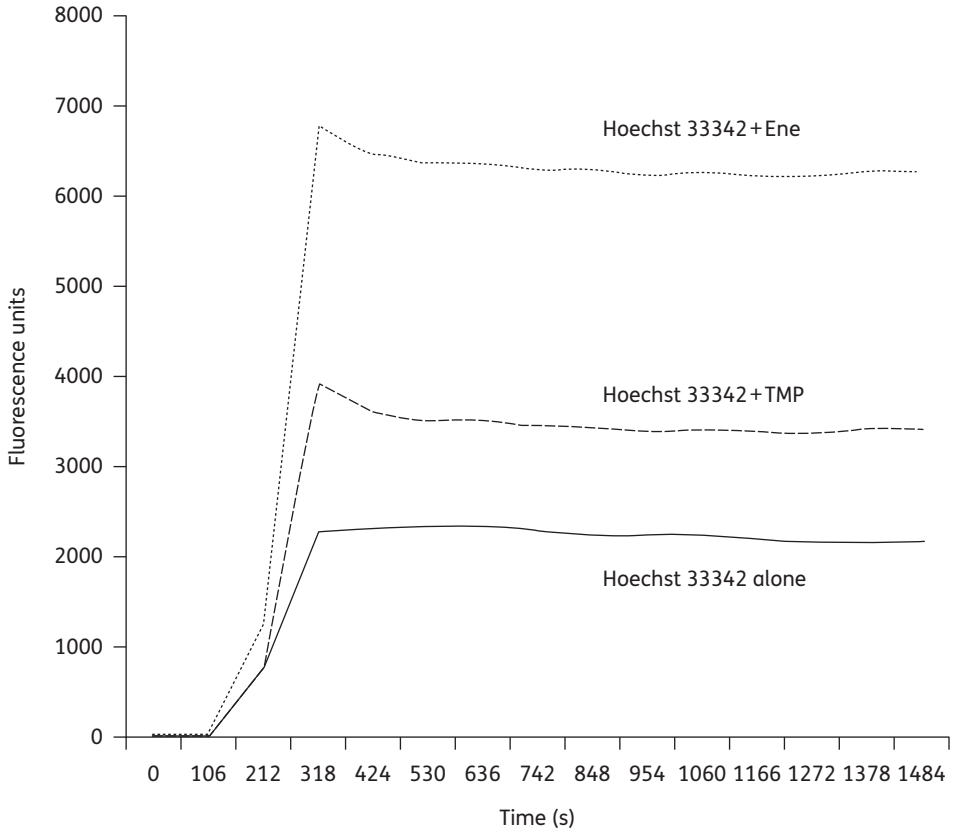

Figure 2. Accumulation of Hoechst 33342 (bis-benzimide) ± epinephrine (Ene; 10 mg/L) or trimethoprim (TMP; 10 mg/L) over 25 min in *Salmonella* Typhimurium SL1344. All compounds were added at time zero.

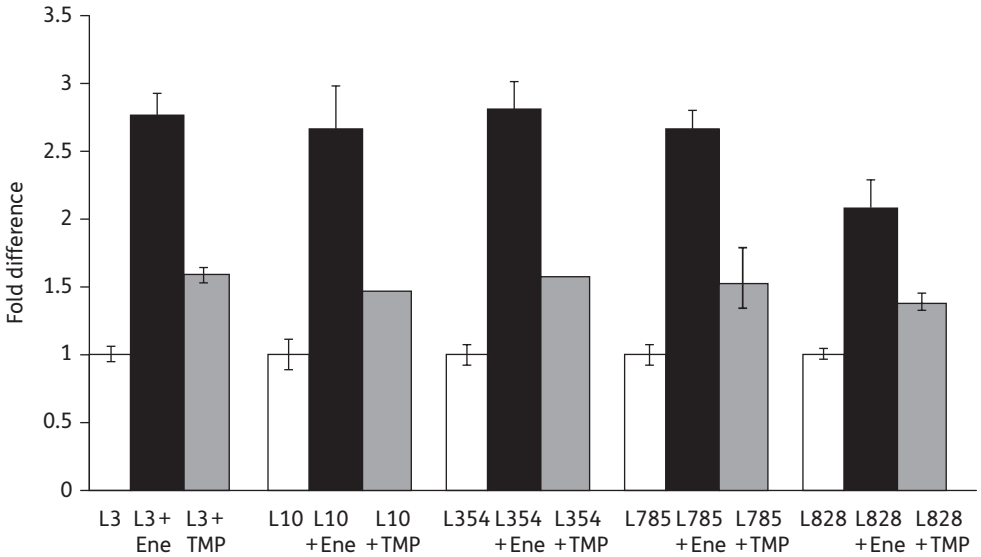

Figure 3. Fold change in accumulation of Hoechst 33342 (bis-benzimide) ± epinephrine (Ene) or trimethoprim (TMP) after 10 min of exposure of *Salmonella* Typhimurium strains L3, L10, SL1344, LT2 and ATCC 14028s (Table 1). All compounds were added at time zero. Hoechst 33342 (bis-benzimide) was added after 2 min.

theophylline. A recent study by Bohnert *et al.*[27] has shown that the AcrB multidrug efflux pump protein contains a hydrophobic phenylalanine-rich binding site. It is possible that aromatic nitrogen-containing EPIs interact and bind at this site via π–π interactions between their aromatic rings and those of the phenylalanine residues.

Two compounds, epinephrine and norepinephrine, had little or no effect upon the activity of ciprofloxacin for *Salmonella* Typhimurium ATCC 14028s. However, this combination was synergistic against mutants lacking *acrAB* or *tolC*. These data suggest that these compounds are substrates of the AcrAB-TolC efflux pump. In the absence of a functional pump, these agents accumulate within the bacterial cell and have an additive antibacterial effect with ciprofloxacin. Furthermore, this suggests that these two compounds have intrinsic antibacterial activity and interact with an intracellular target.

Epinephrine is licensed for the treatment of anaphylactic shock (type 1 hypersensitivity allergic reactions) and is a component of the 'Epi-pen' (British National Formulary; BNF). It is a catecholamine, which is a sympathomimetic monoamine derived from the amino acids phenylalanine and tyrosine. The concentration administered intramuscularly is 1 mg/L, but in a medical emergency 100 mg/L is administered by slow intravenous injection (BNF). Therefore, it is unlikely that a combination of epinephrine plus an antibiotic would be licensed for use as an anti-infective.

Trimethoprim is an inhibitor of dihydrofolate reductase. It is usually administered as a combination antibiotic with another inhibitor of folic acid biosynthesis, sulfamethoxazole (BNF). Therefore, the synergistic and EPI-like behaviour of trimethoprim with other antibiotics is interesting. Synergy of a quinolone with trimethoprim has been reported previously for Gram-negative and Gram-positive bacteria, although the mechanism has not been explored.[28,29] The combination of trimethoprim with another antibiotic, e.g. sulfamethoxazole to give co-trimoxazole, is a well-used combination in anti-infective chemotherapy and so combination with another agent, such as a quinolone, may be a viable option. Although the use of trimethoprim alone has been associated with the selection of trimethoprim-resistant bacteria, this was reduced when in combination with sulfamethoxazole.

In conclusion, we have shown that much simpler aromatic nitrogen-containing compounds than PAβN and D-ornithinyl-D-homophenylalanyl-3-aminoquinoline, which are already licensed for use in man, may warrant further analysis as EPIs. The simplicity of the phenylethylamine and pyrimidine moieties will make these compounds an attractive synthetic target as EPIs.

Funding

This work was supported by The Leverhulme Trust (project F/00 /094/AR).

Transparency declarations

None to declare.

References

1 Taubes G. The bacteria fight back. *Science* 2008; **321**: 356–61.

2 Helms M, Ethelberg S, Mølbak K *et al*. International *Salmonella* Typhimurium DT104 infections, 1992–2001. *Emerg Infect Dis* 2005; **11**: 859–67.

3 Piddock LJ. Clinically relevant chromosomally encoded multidrug resistance efflux pumps in bacteria. *Clin Microbiol Rev* 2006; **19**: 382–402.

4 Piddock LJV, Griggs DJ, Hall MC *et al*. Ciprofloxacin-resistance in clinical isolates of *Salmonella typhimurium* obtained from two patients. *Antimicrob Agents Chemother* 1993; **37**: 662–6.

5 Ricci V, Piddock LJV. Ciprofloxacin selects for multi-drug resistance in *Salmonella enterica* serovar Typhimurium mediated by at least two different pathways. *J Antimicrob Chemother* 2009; **63**: 909–16.

6 Lomovskaya O, Bostian KA. Practical applications and feasibility of efflux pump inhibitors in the clinic—a vision for applied use. *Biochem Pharmacol* 2006; **71**: 910–8.

7 Ricci V, Tzakas P, Buckley A *et al*. Ciprofloxacin-resistant *Salmonella enterica* serovar Typhimurium strains are difficult to select in the absence of AcrB and TolC. *Antimicrob Agents Chemother* 2006; **50**: 38–42.

8 Webber MA, Randall LP, Cooles S *et al*. Triclosan resistance in *Salmonella enterica* serovar Typhimurium. *J Antimicrob Chemother* 2008; **62**: 83–91.

9 Ricci V, Piddock LJV. Only for substrate antibiotics is a functional AcrAB-TolC efflux pump and RamA required to select multidrug resistant *Salmonella* Typhimurium. *J Antimicrob Chemother* 2009 **64**: 654–7.

10 Lomovskaya O, Warren MS, Lee A *et al*. Identification and characterization of inhibitors of multidrug resistance efflux pumps in *Pseudomonas aeruginosa*: novel agents for combination therapy. *Antimicrob Agents Chemother* 2001; **45**: 105–16.

11 Piddock LJ. Multidrug-resistance efflux pumps – not just for resistance. *Nat Rev Microbiol* 2006; **4**: 629–36.

12 Bailey AM, Paulsen IT, Piddock LJV. RamA confers multidrug resistance in *Salmonella enterica* via increased expression of *acrB*, which is inhibited by chlorpromazine. *Antimicrob Agents Chemother* 2008; **52**: 3604–11.

13 Nargotra A, Koul S, Sharma S *et al*. Quantitative structure–activity relationship (QSAR) of aryl alkenyl amides/imines for bacterial efflux pump inhibitors. *Eur J Med Chem* 2009; **44**: 229–38.

14 Renau TE, Léger R, Filonova L *et al*. Conformationally-restricted analogues of efflux pump inhibitors that potentiate the activity of levofloxacin in *Pseudomonas aeruginosa*. *Bioorg Med Chem Lett* 2003; **13**: 2755–8.

15 Pannek S, Higgins PG, Steinke P *et al*. Multidrug efflux inhibition in *Acinetobacter baumannii*: comparison between 1-(1-naphthyl methyl)-piperazine and phenyl-arginine-β-naphthylamide. *J Antimicrob Chemother* 2006; **57**: 970–4.

16 Schumacher A, Steinke P, Bohnert JA *et al*. Effect of 1-(1-naphthyl methyl)-piperazine, a novel putative efflux pump inhibitor, on antimicrobial drug susceptibility in clinical isolates of Enterobacteriaceae other than *Escherichia coli*. *J Antimicrob Chemother* 2006; **57**: 344–8.

17 Kern WV, Steinke P, Schumacher A *et al*. Effect of 1-(1-naphthylmethyl)-piperazine, a novel putative efflux pump inhibitor, on antimicrobial drug susceptibility in clinical isolates of *Escherichia coli*. *J Antimicrob Chemother* 2006; **57**: 339–43.

18 Bohnert JA, Szymaniak-Vits MS, Schuster S *et al*. Antimicrobial action and efflux pump inhibition by selective serotonin reuptake inhibitors (SSRIs) in *Escherichia* (E) *coli* strains over-expressing four different RND efflux pumps. In: *Abstracts of the Forty-ninth Interscience Conference on Antimicrobial Agents and Chemotherapy, San Francisco, CA, 2009*. Abstract E-1457. American Society for Microbiology, Washington, DC, USA.

19 Eaves DJV, Ricci V, Piddock LJV. Expression of *acrB*, *acrF*, *acrB*, *marA* and *soxS* in *Salmonella enterica* serovar Typhimurium: role in multiple antibiotic resistance. *Antimicrob Agents Chemother* 2004; **48**: 1145–50.

20 Buckley A, Webber MA, Cooles S *et al*. The AcrAB-TolC efflux system of *Salmonella enterica* serovar Typhimurium plays a role in pathogenesis. *Cell Microbiol* 2006; **8**: 847–56.

21 Webber MA, Bailey AM, Blair JMA *et al*. The global consequence of disruption of the AcrAB-TolC efflux pump in *Salmonella enterica* includes reduced expression of SPI-1 and other attributes required to infect the host. *J Bacteriol* 2009; **191**: 4276–85.

22 Piddock LJV, White DG, Gensberg K *et al*. Evidence for an efflux pump mediating multiple antibiotic resistance in *Salmonella enterica* serovar Typhimurium. *Antimicrob Agents Chemother* 2000; **44**: 3118–21.

23 Lund ME, Blazevic DJ, Matsen JM. Rapid gentamicin bioassay using a multiple-antibiotic resistant strain of *Klebsiella pneumoniae*. *Antimicrob Agents Chemother* 1973; **4**: 569–73.

24 Andrews JM. Determination of minimum inhibitory concentrations. *J Antimicrob Chemother* 2001; **48** Suppl 1: 5–16.

25 Andrews JM. *Chapter Two. Determination of Minimum Inhibitory Concentrations*. 2006. http://www.bsac.org.uk/susceptibility_testing/guide_to_antimicrobial_susceptibility_testing.cfm (19 January 2010, date last accessed).

26 Gibbons S, Oluwatuyi M, Kaatz GW. A novel inhibitor of multidrug efflux pumps in *Staphylococcus aureus*. *J Antimicrob Chemother* 2003; **51**: 13–7.

27 Bohnert JA, Schuster S, Seeger MA *et al*. Site-directed mutagenesis reveals putative substrate binding residues in the *Escherichia coli* RND efflux pump AcrB. *J Bacteriol* 2008; **190**: 8225–9.

28 Leonard SN, Kaatz GW, Rucker LR *et al*. Synergy between gemifloxacin and trimethoprim/sulfamethoxazole against community-associated methicillin-resistant *Staphylococcus aureus*. *J Antimicrob Chemother* 2008; **62**: 1305–10.

29 Mandal S, Mandal MD, Pal NK. Synergism of ciprofloxacin and trimethoprim against *Salmonella enterica* serovar Typhi isolates showing reduced susceptibility to ciprofloxacin. *Chemotherapy* 2004; **50**: 152–4.

30 Wray C, Sojka WJ. Experimental *Salmonella typhimurium* infection in calves. *Res Vet Sci* 1978; **25**: 139–143.

31 Tindall BJ, Grimont PA, Garrity GM *et al*. Nomenclature and taxonomy of the genus *Salmonella*. *Int J Syst Evol Microbiol* 2005; **55**: 521–4.

32 Nishino K, Latifi T, Groisman EA. Virulence and drug resistance roles of multidrug efflux systems of *Salmonella enterica* serovar Typhimurium. *Mol Microbiol* 2006; **59**: 126–41.

DOI: 10.1002/cmdc.200900273

Aryldiketo Acids Have Antibacterial Activity Against MDR *Staphylococcus aureus* Strains: Structural Insights Based on Similarity and Molecular Interaction Fields

Branko J. Drakulić,*[a] Michael Stavri,[b] Simon Gibbons,[b] Željko S. Žižak,[c] Tatjana Ž. Verbić,[d] Ivan O. Juranić,[d] and Mire Zloh*[b]

Staphylococcus aureus is a major community- and hospital-acquired pathogen.[1] Reports of resistance to antibiotics, including the fluoroquinolone class,[2] have placed a greater emphasis on the development of new drugs for the treatment of both methicillin- (MRSA) and multidrug-resistant (MDR) *S. aureus* strains. Recently, mixed quinolonediketo acid derivatives, which are based on the scaffold of fluoroquinolone antibiotics, were shown to exert significant anti-HIV-1 potency.[3] The γ-diketo moiety is also found in tetracycline, and is therefore potentially important for antibacterial activity. GS-9137 (elvitegravir, CAS 697761-98-1), a 4-quinolone-3-carboxylic acid-based HIV-1 integrase inhibitor is presently in phase III clinical trials.[4] The similarity between these two scaffolds (Figure 1),

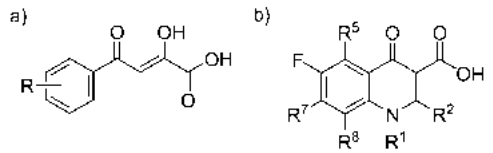

Figure 1. Scaffolds of a) prevailing keto-enol form of ADKs[6,7] and b) fluoroquinolone antibiotics, including substituent numeration.

both of which are integrase inhibitors, inspired our study of aryldiketo acids (ADK) as potential antibacterial agents. To the best of our knowledge, the antibacterial activity of ADK, the scaffold of an important class of HIV-1 integrase inhibitors,[5] has not been reported in the literature so far.

[a] *B. J. Drakulić*
Institute of Chemistry, Technology and Metallurgy, University of Belgrade
Njegoševa 12, 11000 Belgrade (Serbia)
Fax: (+381) 112636061
E-mail: bdrakuli@chem.bg.ac.yu

[b] *M. Stavri, S. Gibbons, M. Zloh*
The School of Pharmacy, University of London
29–39 Brunswick Square, London WC1N 1AX (UK)
Fax: (+44) 2077535964
E-mail: mire.zloh@pharmacy.ac.uk

[c] *Ž. S. Žižak*
Institute for Oncology and Radiology of Serbia
Pasterova 14, 11000 Belgrade (Serbia)

[d] *T. Ž. Verbić, I. O. Juranić*
Faculty of Chemistry, University of Belgrade
Studentski Trg 12-16, 11000 Belgrade (Serbia)

Supporting information for this article is available on the WWW under http://dx.doi.org/10.1002/cmdc.200900273.

4-Phenyl-2,4-dioxobutanoic acids (**1**–**19**) were tested for antibacterial activity against clinical isolates of MDR bacterial strains (Table 1). The synthesis and characterisation of **1**–**7**, **13**–**19** was previously reported.[6,7] Characterisation data for **8**–**12** and **20** are given in the Supporting Information. All compounds (**1**–**10, 12**–**20**) were initially tested for their antibacterial activity against SA-1199B, a strain of *S. aureus* possessing the NorA MDR efflux protein that confers resistance to hydrophilic fluoroquinolones, including norfloxacin.[8] Minimum inhibitory concentration (MIC) values were also compared with those of norfloxacin (**21**),[8] tetracycline, erythromycin and reference fluoroquinolone antibiotics, ciprofloxacin (**22**), levofloxacin (**23**) and moxifloxacin (**24**)[9] (scheme 1S in the Supporting Information).

Table 1. Structures and antibacterial activities of ADKs **1**–**20** against selected MDR *S. aureus* strains.

Compd	R	MIC [μM]						
		SA-1199B[a]	IS-58	XU-212	RN-4220	CD-1281	ATCC-25923	EMRSA-15
1	H	>2660	–	–	–	–	–	–
2	4-Me	>2480	–	–	–	–	–	–
3	4-Et	>2320	–	–	–	–	–	–
4	4-*i*Pr	>2320	–	–	–	–	–	–
5	4-*t*Bu	1030	–	–	–	–	–	–
6	2,5-di-Me	>2320	–	–	–	–	–	–
7	3,4-di-Me	>2320	–	–	–	–	–	–
8	2,4-di-*i*Pr	232	116	464	232	232	232	232
9	2,5-di-*i*Pr	232	232	464	464	464	464	464
10	2,4,6-tri-Et	116	232	232	232	232	232	232
11[b]	2,4,6-tri-*i*Pr	–	–	–	–	–	–	–
12	4-Ph	477	–	–	–	–	–	–
13	β-naphthyl	>2110	–	–	–	–	–	–
14	3-OH	>2460	–	–	–	–	–	–
15	4-OH	>2460	–	–	–	–	–	–
16	4-MeO	>2300	–	–	–	–	–	–
17	4-NO_2	>2160	–	–	–	–	–	–
18	4-F	>2440	–	–	–	–	–	–
19	4-Cl	>2260	–	–	–	–	–	–
20	4-(1*H*-indol-3-yl)	>2220	–	–	–	–	–	–
Norfloxacin[c]		106	–	–	–	–	6.6	3.3
Tetracycline[c]		–	72	288	–	72	–	–
Erythromycin[c]		–	–	–	175	–	–	–

[a] Compounds that exerted an MIC against SA-1199B in concentrations higher than 400 μM were not screened against other strains. [b] Compound was unstable. [c] The MIC determination for these compounds was measured only against relevant resistant strains. – Not measured.

The most promising potency against bacterial strains overexpressing efflux pumps was observed for compounds **8**–**10**, with MIC values comparable to clinically used antibiotics susceptible to MDR. Compounds **5** and **12** exhibited only moderate potency against SA-1199B and were not subjected to studies against other strains. The MIC value of the most potent aryldiketo acids (**8**–**10, 12**) did not change significantly against strains overexpressing efflux pumps or for the standard laboratory strain (ATCC 25923); this indicates that the compounds are possibly not substrates for these efflux pumps. Compounds **8** and **10** were twice as potent as erythromycin and/or tetracycline against bacteria resistant to those antibiotics.

The whole set (**1**–**20**) was also tested for the ability to modulate the activity of norfloxacin against the norfloxacin-resistant NorA-overexpressing strain SA-1199B. The results are given in Table 2; only compounds that had any potentiating effect are given. The presence of several compounds at 25% of their MIC (max 100 $\mu g\,mL^{-1}$) improved the potency of norfloxacin (**21**) by decreasing its MIC value to 53 μM. A further decrease in the concentrations of **15** and **17** did not affect their modulation ability, while compounds **7**, **12** and **20** lost their ability to modulate norfloxacin activity at a lower concentration.

Table 2. Antibacterial activity of norfloxacin against norfloxacin-resistant NorA-overexpressing *S. aureus* strain SA-1199B in the presence of ADKs at two different concentrations.

Compd[a]	R	ADK [μM]	MIC [μM]
Norfloxacin		–	106
7	3,4-di-Me	454	53
		50	106
12	4-Ph	119	53
		50	106
15	4-OH	240	53
		50	53
17	4-NO_2	211	53
		50	53
20	4-(1*H*-indol-3-yl)	430	53
		50	106

[a] No improvement in antibacterial activity of norfloxacin was observed for compounds **1**–**6**, **8**–**11**, **13**–**14**, **16**, **18**–**19**.

Six compounds were selected from for evaluation in a cytotoxicity assay: compounds **8, 10**, **12** with antibacterial activity (MIC) values lower than 400 μM; compounds **15**, **17** able to potentiate the antibacterial action of **21**; indolyl derivative **20**. All tested compounds inhibited 90% of healthy human cell growth at concentrations higher than their MIC value (Supporting Information). A moderate selectivity was observed that could potentially be improved by appropriate structural modifications on the aryl ring.

A common feature for the activity of the two classes of drug is the requirement for metal complexation. Inhibition of HIV-1 integrase by aryldiketo acids is mediated by Mg^{2+} ion complexation to the diketo moiety.[10] We reported the influence of the phenyl substitution pattern in aryldiketo acids on Mg^{2+} complexation.[7] In a similar manner, Mg^{2+} bound to the fluoroquinolone carboxylic acid group at position 3 is necessary for the interaction with prokaryotic gyrase A (GyrA).[11] Notably, ionisation constants for moieties responsible for Mg^{2+} binding in fluoroquinolone antibiotics and aryldiketo acids are similar. Ionisation constants of **5**, **8**–**10**, **12**, **15**, **17**, **19**, **21**–**24** are given in Table 3. pK_a values of **5**, **8**–**10**, **15**, **17**, **19**, were experimentally obtained, pK_a of **12** was calculated by MoKa, while values of **21**–**24** were taken from the literature.

Table 3. Ionisation constants of **5**, **8**–**10**, **12**, **15**, **17**, **19**, **21**–**24**.

Compd	pK_{a1}	pK_{a2}	pK_{a3}	HA^- (%)[c]	A^{2-} (%)[c]	Ref.
5	2.21 ± 0.03	7.77 ± 0.06	–	72.45	27.55	[6]
8	2.04 ± 0.04	7.29 ± 0.03	–	46.51	53.49	–
9	2.33 ± 0.03	7.13 ± 0.04	–	37.59	62.41	–
10	1.99 ± 0.03	6.72 ± 0.03	–	18.98	81.02	–
12	2.35 ± 0.33[a]	6.94 ± 0.59[a]	–	28.01	71.99	–
15	2.29 ± 0.05	7.73 ± 0.01	–	70.42	29.58	[6]
17	1.87 ± 0.06	6.63 ± 0.02	–	83.92	16.03	[6]
19	2.09 ± 0.04	7.30 ± 0.03	–	47.17	52.83	[6]
21	–	6.32 ± 0.005	8.56 ± 0.005	Zwitterion		[18]
22	–	6.23 ± 0.004	8.58 ± 0.004	Zwitterion		[18]
23	–	6.24 ± 0.02	8.26 ± 0.05	Zwitterion		[18]
24	–	6.25 ± 0.02	9.29 ± 0.04	Zwitterion		[19]

[a] Estimated by MoKa v1.0.9;[20] [b] For compounds **21**–**24** pK_{a2} and pK_{a3} refers to ionisations of carboxyl group at C3 and distal nitrogen of heteroalicyclic ring at C7, respectively;[21] [c] % of HA^- refers to the estimated percentage of monoanionic form, % A^{2-} refers to the estimated percentage of dianionic form at physiological pH (7.35).

Furthermore, structural similarity between **1**–**20** and norfloxacin **21** was observed by overlaying the representative conformations of the monoanions of **1**–**20** generated by OMEGA,[12] with the representative conformations of **21** in its zwitterionic form, using ROCS.[13] Visual analysis of the overlays was carried out,[14] and a qualitative correlation between the overlap of important pharmacophoric features of **21**[15,16] with **1**–**20**, and their antibacterial potency was observed (overlaid 3D structures in msv file format are available as Supporting Information). Substituents in positions 1, 3, 4 and 7 of the quinolone core (Figure 1) are a prerequisite for antibacterial activity. The $C(O)CH{=}C(OH)COO^-$ moiety of **1**–**20** overlaps well with the 3-carboxylate and 4-carbonyl positions of the norfloxacin core, which are responsible for binding to cleaved or perturbed DNA and are critical for antimicrobial activity.

Compounds only exhibited notable antibacterial activity if there was additional overlap with the other two pharmacophoric points of **21**, the R^1 ethyl moiety responsible for hydrophobic interaction with the major grove of DNA, and R^7 piperazinyl moiety that directly interacts with GyrA or topoisomerase IV. The *ortho*-phenyl substituents of compounds **8**–**10** overlap with the important R^1 of **21**; those compounds possess MIC values between 116 and 232 μM. As the overlap decreases, and the R^1 position is no longer mimicked, the potency decreases as can be seen for **12** and **5**, with MIC values of 477 and 1030 μM, respectively. Activity diminishes for the remaining compounds lacking phenyl substituents able to overlay the

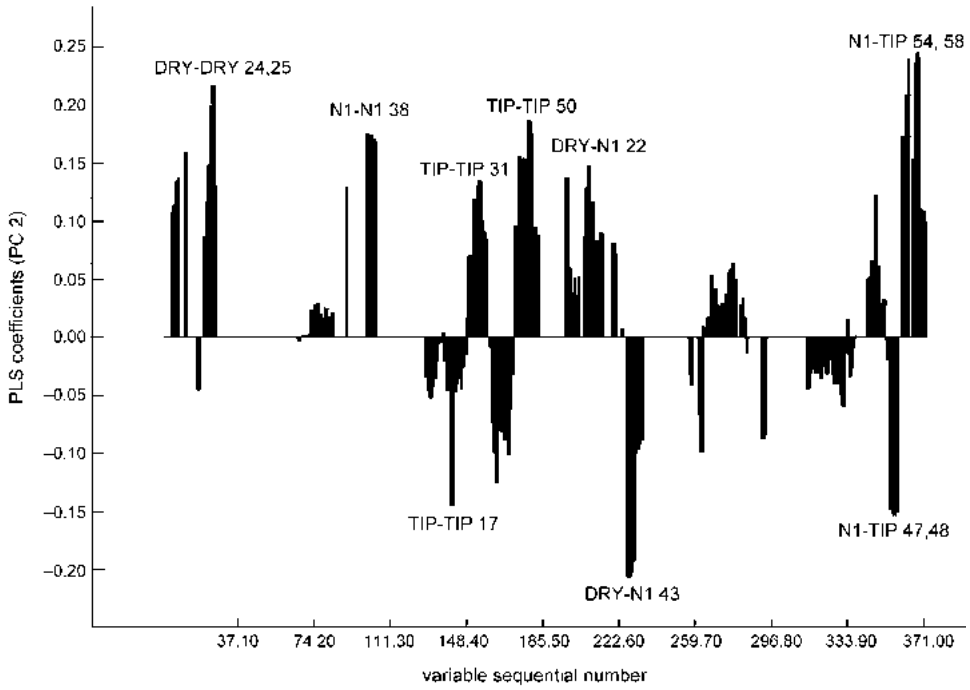

Figure 2. PLS coefficient plot (2 PC) of the ALMOND model show which GRIND variables are correlated to the potency of **5**, **8**–**10**, **12**, **15**, **17**, **19** and **21**–**24**, in their ionised forms against SA-1199B. MIF regions around molecules associated with variables are given in Figures 3 and 4, as well as in panels I and II in the Supporting Information.

R^1 and R^7 positions of **21** (msv files showing overlaid structures of **21**/**15** and **21**/**17** can be found in the Supporting Information).

Further SAR analysis was carried out by including factors other than shape similarity. The protonation states under physiological pH (Table 3) of **5**, **8**–**10**, **12**, **15**, **17**, **19, 21**–**24** were considered as more accurate representation of pH effects on conformation. The molecular interaction fields (MIF) of the active ADKs were compared to those of the fluoroquinolones. The alignment-free 3D QSAR models developed on the basis of GRid INdependent Descriptors (GRIND)[17] were built to provide quantitative representation of pharmacophoric points that are common for these two classes of compounds. The best model was obtained with active molecules (**5**, **8**–**10**, **12**, **15**, **17**, **19**) and reference commercial antibiotics (**21**–**24**) in ionised form at physiological pH (7.35). A necessary approximation was introduced during in silico structure preparation; if a particular molecule (**5**, **8**–**10**, **12**, **15**, **17**, **19**) under physiological pH existed in more than 50% in the A^{2-} form, this molecule was considered to be a dianion. The remaining molecules in the set were treated as monoanions (HA^-). The most favourable interaction regions extracted from molecular interaction fields obtained with N1, DRY and TIP probes (hydrogen bond donor (HBD), hydrophobic and shape, respectively) were correlated with potency of compounds by partial least square (PLS) analysis, and a corresponding PLS coefficient plot is shown in Figure 2. Information about statistics of the model, observed versus calculated log (1/MIC), and detailed descriptions of moieties associated with variables with a high impact on the model and association of variables to particular compounds are given in the Supporting Information. For comparison, a similar model that included the same molecules in their neutral form is also discussed in the Supporting Information.

A structural similarity between moieties of the studied aryldiketo acids (**5**, **8**–**10**, **12**, **15**, **17**, **19**) and fluoroquinolone antibiotics (**21**–**24**) was observed and all of those similar regions were positively correlated with potency. Similarity between the 4-phenyl-4-oxo-2-butenoic moiety of the aryldiketo acids and the quinolone core of compounds **21**–**24** is shown by variables DRY–DRY 24 and 25 (Figure 3a and b). One node of the variable is positioned in proximity to the phenyl rings of both the ADK and quinolone core (interaction energy (IE) $= -1.76$ kcal mol^{-1}), while the other node is positioned in proximity to the 4-oxo-2-butenoic moiety or pyridone C=C double bonds (IE $= -2.08$ kcal mol^{-1}).

The spatial arrangement between the carboxyl group and the *ortho*-alkyl substituent of aryldiketo acids **8**–**10** is similar to the arrangement of the quinolone core 3-carboxyl group and the alkyl substituent in its position 1 (Figure 3c and d), as depicted by the variable TIP–TIP 31.

The similarity between the aroyl moiety (Ar–C(O)–) of the ADKs and the quinolone moiety of compounds **21**–**24** is described by the variable DRY–N1 22 (Figure 4). For aryldiketo acids, the N1 node is associated with the aroylketo group, while the DRY node (IE $= -3.03$ kcal mol^{-1}) is associated with the phenyl ring of ADKs. For the fluoroquinolone molecules, the N1 node (IE $= -6.60$ kcal mol^{-1}) is associated with the keto group in position 3, while the DRY node is situated in close proximity to both the aromatic quinolone core and the alkyl substituent in position 1.

The distinction between fluoroquinolones **21**–**24** and the aryldiketo acids is given by the variable N1–TIP 58. The non-zero value of this variable is found only for the fluoroquinolones (table 7S in the Supporting Information). ADKs, in both neutral and ionised forms, with longer or branched *ortho*-alkyl substituents on the phenyl ring (**8**–**10**), adopted conformations that matched well with the quinolone core and the 1-, 3-, and 4-substituents of compounds **21**–**24**. Along with the quinolone 7-substituent, these are the most important moieties of of the fluoroquinolones, responsible for antibacterial activity.

Although the inclusion of the MG+2 probe (Mg^{2+} ion) did not improve the ALMOND models, it was found that the most favourable interaction regions of this probe with both aryldiketo acids and fluoroquinolones are located in proximity to the

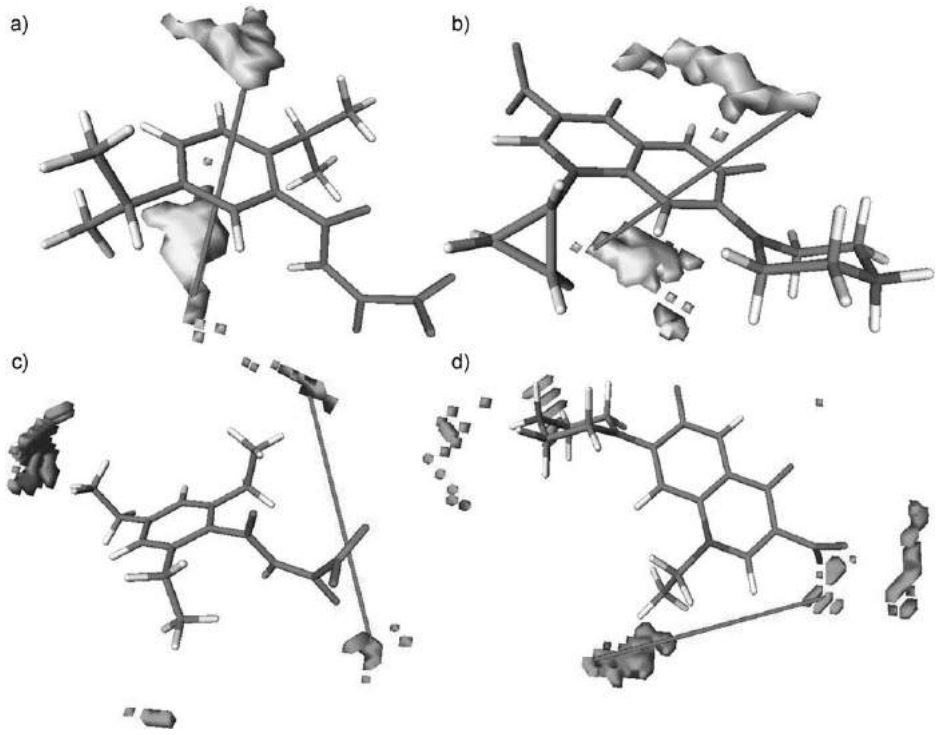

Figure 3. Favourable interaction fields with hydrophobic (up) and shape probes (down). Variable DRY–DRY 25 for a) **9** and b) **22** in their ionised forms at physiological pH. Variable TIP–TIP 31 for c) **10** and d) **21** in their ionised forms at physiological pH.

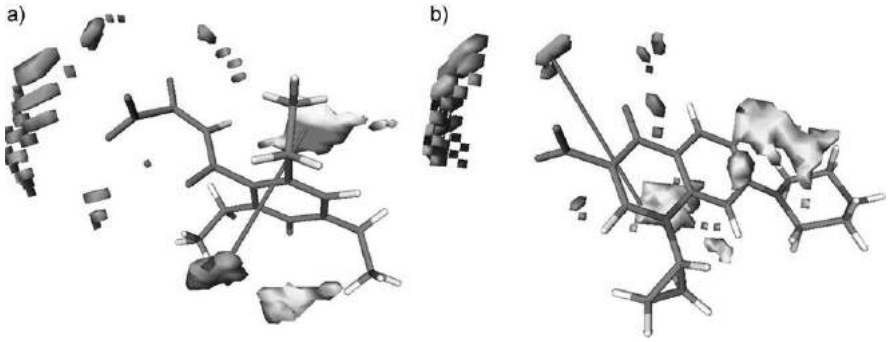

Figure 4. Variable DRY-N1 22 for a) **10** and b) **22** in their ionised forms at physiological pH.

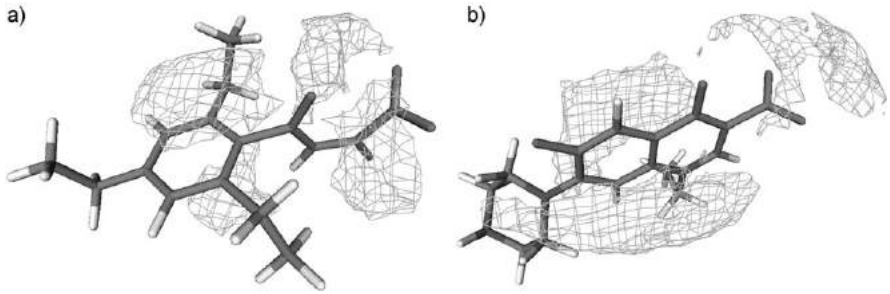

Figure 5. MG+2 GRID probe isocontour levels on −22.2, −4.2 kcal mol^{-1} for **10** and **21**, respectively, in their ionisation states at physiological pH (7.35).

aromatic rings of **1**–**24**. The carboxylate moieties of both aryldiketo acids and fluoroquinolones, which bind the Mg^{2+} ion in the active sites of their respective target enzymes, have to some extent less favourable interaction energies. Similarities of the GRID MG+2 probe isocontour levels on slightly less favourable (less negative) interaction energies are given in Figure 5. So far, only one complex of an aryldiketo acid with the Mg^{2+} ion has been reported.[22] In this complex, the spatial arrangement of the diketo acid C(O)CH=CH(OH)COOH moiety and the Mg^{2+} ion is almost identical to the region around the aryldiketo acids reported here, as predicted by the GRID Mg+2 probe (see 3D msv and mol2 files in the Supporting Information for examples). The observed regions of MG+2 probe favourable interactions will be the subject of a further study.

The potentiation ability of compounds **7**, **12**, **15**, **17** and **20**, can not be explained by the possible complex formation between **21** and ADKs (Supporting Information).[23] The loss of potentiation with decreased compound concentrations indicates that competitive binding of aryldiketo acids might be responsible for overcoming the efflux pumps. The examined aryldiketo acids probably bind to the efflux pumps in a similar position to norfloxacin (**21**) prior to removal from the cell, emphasising the importance of similarities between norfloxacin (**21**) and compounds **15** and **17**.

The antibiotic activity of aryldiketo acids has been reported here for the first time. Some compounds have antibiotic activity against MDR *S. aureus* strains comparable to norfloxacin; furthermore, other compounds have the ability, albeit weak, to potentiate the activity of norfloxacin against effluxing strains. Similarity studies have revealed the importance of the nature of substituents and their position on the aryldiketo acid phenyl moiety on the type of activity (antibacterial/MDR modulation) and their potency. This class of compounds could be a good platform for designing

novel therapeutics that are able to act alone or in synergy with other antibiotics, namely fluoroquinolones. The design, synthesis and evaluation of novel congeners is currently underway.

Acknowledgements

BJD gratefully acknowledge Dr. Francesca Milletti and Prof. Gabriele Cruciani for pK_a *estimations. This work was partially supported by the Ministry of Science of Serbia, grant 142010 (for BJD, TŽV and IOJ).*

Keywords: antibiotics · aryldiketo acids · biological activity · molecular interaction fields · molecular similarity · MRSA

[1] T. M. Perl, *Am. J. Med.* **1999**, *106*, 26S – 37S.
[2] H. M. Blumberg, D. Rimland, D. J. Carroll, P. Terry, I. K. Wachsmuth, *J. Infect. Dis.* **1991**, *163*, 1279 – 1285.
[3] R. Di Santo, R. Costi, A. Roux, M. Gaetano, G. C. Crucitti, A. Iacovo, F. Rosi, A. Lavecchia, L. Marinelli, C. Di Giovanni, E. Novellino, L. Palmisano, M. Andreotti, R. Amici, C. M. Galluzzo, L. Nencioni, A. T. Palamara, Y. Pommier, C. Marchand, *J. Med. Chem.* **2008**, *51*, 4744 – 4750.
[4] L. A. Sorbera, N. Serradell, *Drugs Future* **2006**, *31*, 310 – 313.
[5] J. Deng, R. Dayam, L. Q. Al-Mawsawi, N. Neamati, *Curr. Pharm. Des.* **2007**, *13*, 129 – 141.
[6] T. Ž. Verbic, B. J. Drakulić, M. F. Zloh, J. R. Pecelj, G. V. Popović, I. O. Juranić, *J. Serb. Chem. Soc.* **2007**, *72*, 1201 – 1216.
[7] T. Ž. Verbic, B. J. Drakulić, M. Zloh, I. O. Juranić, *Lett. Org. Chem.* **2008**, *5*, 692 – 699.
[8] G. W. Kaatz, S. M. Seo, C. A. Ruble, *Antimicrob. Agents Chemother.* **1993**, *37*, 1086 – 1094.
[9] S. Gibbons, M. Oluwatuyi, G. W. Kaatz, *Aureus. J. Antimicrob. Chemoth.* **2003**, *51*, 13 – 17.
[10] C. Marchand, A. A. Johnson, R. G. Karki, G. C. Pais, X. Zhang, K. Cowansage, T. A. Patel, M. C. Nicklaus, T. R. Burke Jr. , Y. Pommier, *Mol. Pharmacol.* **2003**, *64*, 600 – 609.
[11] C. Sissi, E. Perdona, E. Domenici, A. Feriani, A. J. Howells, Maxwell, A. M. Palumbo, *J. Mol. Biol.* **2001**, *311*, 195 – 203.
[12] J. Boström, J. R. Greenwood, J. Gottfries, *J. Mol. Graph. Mod.* **2003**, *21*, 449 – 462; www.eyesopen.com/products/applications/omega.html (Last accessed: October 14, 2009).
[13] J. E. J. Mills, P. M. Dean, *J. Cold Reg. Eng. J. Comput-Aided Mol. Des.* **1996**, *10*, 607 – 622; www.eyesopen.com/products/applications/rocs.html (Last accessed: October 14, 2009).
[14] M. Zloh, S. Gibbons, *Int. J. Mol. Sci.* **2004**, *5*, 37 – 47.
[15] L. R. Peterson, *Clin. Infect. Dis.* **2001**, *33*, S180 – S186.
[16] S. Emami, A. Shafiee, A. Foroumadi, *Mini-Rev. Med. Chem.* **2006**, *6*, 375 – 386.
[17] a) M. Pastor, G. Cruciani, I. McLay, S. Pickett, S. Clementi, *J. Med. Chem.* **2000**, *43*, 3233 – 3243; b) F. Fontaine, M. Pastor, F. Sanz, *J. Med. Chem.* **2004**, *47*, 2805 – 2815; c) ALMOND version 3.3.0, Molecular Discovery Ltd., Perugia (Italy); www.moldiscovery.com (Last accessed: October 14, 2009).
[18] A. Llinàs, R. C. Glen, J. M. Goodman, *J. Chem. Inf. Model.* **2008**, *48*, 1289 – 1303.
[19] M-H. Langloisa, M. Montaguta, J-P. Dubosta, J. Grellet, M-C. Saux, *J. Pharm. Biomed. Anal.* **2005**, *37*, 389 – 393.
[20] F. Milletti, L. Storchi, G. Sforna, G. Cruciani, *J. Chem. Inf. Mod.* **2007**, *47*, 2172 – 2181; MoKa version 1.0.9, Molecular Discovery Ltd., Perugia (Italy); www.moldiscovery.com (Last accessed: October 14, 2009).
[21] M. S. Burkhead, H. Wang, M. Fallet, E. M. Gross, *Anal. Chim. Acta* **2008**, *613*, 152 – 162.
[22] A. Bacchi, M. Biemmi, M. Carcelli, F. Carta, C. Compari, E. Fisicaro, D. Rogolino, M. Sechi, M. Sippel, C. A. Sotriffer, T. W. Sanchez, N. Neamati, *J. Med. Chem.* **2008**, *51*, 7253 – 7264.
[23] M. Zloh, G. W. Kaatz, S. Gibbons, *Bioorg. Med. Chem. Lett.* **2004**, *14*, 881 – 885.

Received: July 6, 2009
Revised: October 10, 2009
Published online on October 23, 2009

Phytochemistry 70 (2009) 222–227

Contents lists available at ScienceDirect

Phytochemistry

journal homepage: www.elsevier.com/locate/phytochem

Bacterial resistance modifying tetrasaccharide agents from *Ipomoea murucoides*

Lilia Chérigo [a], Rogelio Pereda-Miranda [a,*], Simon Gibbons [b]

[a] Departamento de Farmacia, Facultad de Química, Universidad Nacional Autónoma de México, Ciudad Universitaria, Mexico City 04510DF, Mexico
[b] Centre for Pharmacognosy and Phytotherapy, The School of Pharmacy, University of London, 29-39 Brunswick Square, London WC1N 1AX, UK

ARTICLE INFO

Article history:
Received 15 September 2008
Received in revised form 9 November 2008
Available online 10 January 2009

Keywords:
Ipomoea murucoides
Convolvulaceae
Staphylococcus aureus
Structural spectroscopy
Multidrug resistance
Resin glycoside
Tetrasaccharide
NMR

ABSTRACT

As part of an ongoing project to identify oligosaccharides which modulate bacterial multidrug resistance, the $CHCl_3$-soluble extract from flowers of a Mexican arborescent morning glory, *Ipomoea murucoides*, through preparative-scale recycling HPLC, yielded five lipophilic tetrasaccharide inhibitors of *Staphylococcus aureus* multidrug efflux pumps, murucoidins XII–XVI (**1**–**5**). The macrocyclic lactone-type structures for these linear hetero-tetraglycoside derivatives of jalapinolic acid were established by spectroscopic methods. These compounds were tested for in vitro antibacterial and resistance modifying activity against strains of *Staphylococcus aureus* possessing multidrug resistance efflux mechanisms. Only murucoidin XIV (**3**) displayed antimicrobial activity against SA-1199B (MIC 32 μg/ml), a norfloxacin-resistant strain that over-expresses the NorA MDR efflux pump. The four microbiologically inactive (MIC > 512 μg/ml) tetrasaccharides increased norfloxacin susceptibility of this strain by 4-fold (8 μg/ml from 32 μg/ml) at concentrations of 25 μg/ml, while murucoidin XIV (**3**) exerted the same potentiation effect at a concentration of 5 μg/ml.

1. Introduction

All Mexican medicinal arborescent members of the genus *Ipomoea* (Convolvulaceae) share two therapeutic properties: the raw flowers, used antiseptically, are rubbed directly on skin infections, itching and rashes, and as decoctions, plasters and poultices, and in some instances the leaves, stem and bark are used for rheumatism, inflammation, and muscular pain (Chérigo and Pereda-Miranda, 2006). "Cazahuate", Nahuatl (Aztec language) for "tree to cure mange", is the vernacular name in contemporary Mexican Spanish for this group of arborescent species belonging to the genus *Ipomoea* series Arborescentes, e.g., *Ipomoea murucoides* Roem. et Schult. In the 16th century account of Mexican pre-Hispanic herbolaria "De la Cruz-Badiano Codex" (Emmart, 1940), the antiseptic properties for this medicinal plant complex are confirmed in a description of how Aztec healers used this herbal drug to prevent hair loss.

Murucoidins, a series of related lipophilic pentasaccharides of jalapinolic acid, were first reported in the chemical analysis of resin glycosides from this crude drug (Chérigo and Pereda-Miranda, 2006). A second investigation followed for the identification of new resin glycoside inhibitors of bacterial growth and in some instances inhibitors of multidrug efflux to treat infections resulting from multidrug-resistant *S. aureus* strains. All tested murucoidins exerted a potentiation effect of norfloxacin against the NorA over-expressing strain SA-1199B by increasing the activity 4-fold (8 μg/ml from 32 μg/ml) at concentrations of 5–25 μg/ml (Chérigo et al., 2008). This work was undertaken to increase the recognition of chemical diversity of the target oligosaccharides which modulate bacterial multidrug resistance, basically by isolating compounds from a new plant collection of *I. murucoides* that displayed variations in its resin glycoside composition.

2. Results and discussions

$CHCl_3$-soluble extracts of a new collection of the crude drug "Cazahuate" were compared by C_{18} reversed-phase HPLC with reference solutions of the previously reported resin glycosides from this species (Chérigo et al., 2008). This analysis confirmed a higher complexity in their composition and allowed the detection of the known pentasaccharides stoloniferin I, pescaprein III, intrapilosin I, and murucoidins I–V, as well as five new constituents, murucoidins XII–XVI (**1**–**5**) which were separated and purified by using a recycling HPLC technique (Pereda-Miranda and Hernández-Carlos, 2002). Several NMR techniques and FABMS were used to characterize their structures which were found to be macrolactones of the known operculinic acids C and E, linear hetero-tetraglycosides of jalapinolic acid, with *n*-dodecanoic or (2*S*)-methylbutyric acids esterifying the C-2 or C-3 positions on the second rhamnose unit of the oligosaccharide core and (2*S*)-methylbutyric acid at C-4 on the third rhamnose moiety.

A small portion of the glycosidic mixture was saponified to liberate an H_2O-soluble mixture of five oligosaccharides of jalapinolic acid: the major products were identified as operculinic acid A and

* Corresponding author. Tel.: +52 55 5622 5288; fax: +52 55 5622 5329.
E-mail addresses: pereda@unam.mx, pereda@prodigy.net.mx (R. Pereda-Miranda).

0031-9422/$ - see front matter © 2008 Elsevier Ltd. All rights reserved.
doi:10.1016/j.phytochem.2008.12.005

simonic acids A and B by HPLC retention time comparison with those of authentic samples (Chérigo et al., 2008). Two additional glycosidic acids represented minor constituents and were characterized as operculinic acid C: (11*S*)-hydroxyhexadecanoate 11-*O*-α-L-rhamnopyranosyl-(1 → 4)-*O*-α-L-rhamnopyranosyl-(1 → 4)-*O*-α-L-rhamnopyranosyl-(1 → 2)-β-D-fucopyranoside, and operculinic acid E: (11*S*)-hydroxyhexadecanoate 11-*O*-α-L-rhamnopyranosyl-(1 → 4)-*O*-α-L-rhamnopyranosyl-(1 → 4)-*O*-α-L-rhamnopyranosyl-(1 → 2)-β-D-glucopyranoside, both previously isolated from *I. operculata* (Ono et al., 1989). Evidence for the absolute stereochemistry of the sugars, the configuration of the anomeric linkages as well as the sequence of glycosidation was published when their oligosaccharide cores were first elucidated (Ono et al., 1989, 1990). Sugar analysis confirmed that all monosaccharides were in ther naturally occurring form as previously described (Chérigo et al., 2008).

Negative-ion FAB mass spectra generated by murucoidins XII and XIII (**1–2**) were found to be very similar, with a pseudomolecular $[M–H]^-$ ion at *m/z* 1119, and therefore these constituents represented diastereoisomeric tetrasaccharides of molecular formula $C_{57}H_{100}O_{21}$. Compounds **3** afforded a FAB mass spectrum with the $[M–H]^-$ ion at *m/z* 1103 ($C_{57}H_{99}O_{20}$). Careful analysis of the negative FABMS generated by these tetrasaccharides **1–3** confirmed the nature of the oligosaccharide core for each glycolipid. The observed difference of 16 mass units in all diagnostic fragments for **3** in relation with **1** and **2** indicated the presence of a 6-deoxy-hexose (fucose) instead of the hexose unit (glucose). The initial loss of the dodecanoyl group afforded a peak at *m/z* 937 in **1** and **2** representing $[M–H–C_{12}H_{22}O]^-$, while the same elimination in **3** afforded the peak at *m/z* 921. The subsequent elimination of the methylbutyroyl unit (84 mass units) in **1** and **2** afforded a peak at *m/z* 853 $[937–C_5H_8O]^-$, and the peak *m/z* 837 in **3**. The ions produced by the rupture of each of the glycosidic linkages afforded the series of peaks at *m/z* 707, 561, 433 and 271 in **1** and **2** and at *m/z* 691 $[1067–2 \times 146\ (C_6H_{10}O_4)–C_5H_8O]^-$, 545 $[691–146\ (C_6H_{10}O_4)]^-$, which indicated that the lactonization was located at the first rhamnose unit (Rha), 417 $[545 + H_2O – 146\ (C_6H_{10}O_4)]^-$, and 271

Table 1
^{1}H (500 MHz) NMR spectroscopic data of compounds **1–5** (pyridine-d_5).[a]

Proton[b]	1	2	3	4	5
glc-1	4.99 *d* (8.0)	5.00 *d* (8.0)			
2	4.30* *dd* (8.0, 8.0)	4.30* *dd* (8.0, 8.0)			
3	4.30* *dd* (8.0, 8.0)	4.30* *dd* (8.0, 8.0)			
4	4.17 *dd* (9.0, 9.0)	4.16 *dd* (9.0, 9.0)			
5	3.90*	3.90 *ddd* (2.0, 5.5, 9.0)			
6a	4.38 *dd* (5.6, 12.0)	4.40* *m*			
6b	4.52 *dd* (2.8, 12,0)	4.52 *dd* (3.0, 11.7)			
fuc-1			4.79 *d* (7.5)	4.69 *d* (7.5)	4.73 *d* (7.5)
2			4.54*dd* (7.5, 9.5)	4.14 *dd* (7.5, 9.5)	4.14 *dd* (7.5, 9.5)
3			4.19 *dd* (3.0, 9.5)	4.00 *dd* (3.0, 9.5)	4.07 *dd* (3.0, 9.5)
4			3.92*	3.97 *m*	3.97 *brs*
5			3.82 *dq* (1.0, 6.5)	3.72 *dq* (1.0, 6.5)	3.77 *dq* (1.0, 6.5)
6			1.52 *d* (6.5)	1.50 *d* (6.5)	1.50 *d* (6.5)
rha-1	6.49 *d* (1.0)	6.51 *d* (1.5)	6.39 *d* (2.0)	5.49 *d* (2.0)	5.47 *d* (2.0)
2	5.28 *dd* (1.0, 3.0)	5.25 *dd* (1.5, 3.0)	5.25 *dd* (2.0, 3.0)	5.92 *dd* (2.0, 3.5)	5.90 *dd* (2.0, 3.5)
3	5.59 *dd* (3.0, 9.5)	5.69 *dd* (3.0, 9.5)	5.66 *dd* (2.5, 9.5)	4.99 *dd* (3.5, 9.5)	5.00 *dd* (3.5, 9.5)
4	4.63 *t* (9.5)	4.76 *t* (9.5, 9.5)	4.71 *t* (9.5)	4.20 *t* (9.5)	4.22 *t* (9.5)
5	5.08 *dq* (6.5, 9.5)	5.16 *dq* (6.5, 9.5)	5.08 *dq* (6.0,9.5)	4.45 *dq* (6.5, 9.5)	4.45 *dq* (9.5, 6.5)
6	1.75 *d* (6.5)	1.75 *d* (6.5)	1.59 *d* (6.0)	1.64 *d* (6.5)	1.63 *d* (6.5)
rha′-1	5.57 *d* (1.5)	5.91 *d* (1.5)	5.89 *d* (1.5)	6.01 *d* (2.0)	6.16 *d* (2.0)
2	5.78 *dd* (1.5, 3.5)	4.71 *dd* (1.5, 3.0)	4.70 *dd* (1.5, 3.0)	5.95 *dd* (2.0, 3.5)	4.87 *dd* (2.0, 3.0)
3	4.59 *dd* (3.5, 9.5)	5.72 *dd* (3.0, 9.5)	5.71 *dd* (3.0, 9.5)	4.66 *dd* (3.5, 9.5)	5.74 *dd* (3.0, 9.5)
4	4.26 *t* (9.5, 9.5)	4.57 *t* (9.5, 9.5)	4.56 *t* (9.5, 9.5)	4.24 *t* (9.5, 9.5)	4.58 *t* (9.5, 9.5)
5	4.37 *dq* (6.0, 9.5)	4.43 *dq* (6.5, 9.5)	4.40 *dq* (6.0, 9.5)	4.38 *dq* (6.5, 9.5)	4.42 *dq* (6.5, 9.5)
6	1.69 *d* (6.0)	1.61 *d* (6.5)	1.58 *d* (6.0)	1.71 *d* (6.5)	1.65 *d* (6.5)
rha″-1	6.16 *d* (1.5)	5.68 *d* (1.5)	5.68 *d* (1.5)	6.13 *d* (1.5)	5.75 *d* (1.5)
2	4.77 *dd* (1.5, 3.0)	4.47 *dd* (1.5, 3.0)	4.46 *dd* (1.5, 3.5)	4.81 *brs*	4.53 *brs*
3	4.48 *dd* (3.0, 9.5)	4.40* *m*	4.38 *dd* (3.5, 9.5)	4.55 *dd* (3.0, 9.5)	4.47 *dd* (3.0, 9.5)
4	5.80 *t* (9.5)	5.76 *t* (9.5)	5.75 *t* (9.5, 9.5)	5.83 *t* (9.5, 9.5)	5.79 *t* (9.5, 9.5)
5	4.41 *dq* (6.0, 9.5)	4.32 *dq* (6.5, 9.5)	4.30 *dq* (6.0, 9.5)	4.43 dq (6.5, 9.5)	4.34 *dq* (6.5, 9.5)
6	1.44 *d* (6.0)	1.36 *d* (6.5)	1.35 *d* (6.0)	1.44 *d* (6.5)	1.35 *d* (6.5)
jla-2a	2.24 *ddd* (3.0, 8.0, 11.7)	2.13 *ddd* (3.7, 7.8, 11.5)	2.14 *ddd* (3.5, 7.0, 12.0)	2.22 *ddd* (3.5, 7.0, 12.0)	2.21 *ddd* (3.7, 8.0, 11.5)
2b	2.72 *ddd* (3.0, 8.0, 11.7)	2.25 *ddd* (3.7, 7.8, 11.5)	2.23 *ddd* (3.5, 7.0, 12.0)	2.44 *ddd* (3.5, 7.0, 12.0)	2.35 *ddd* (3.7, 8.0, 11.5)
11	3.90*	3.96 *m*	3.92*	3.84 *m*	3.85 *m*
16	1.00 *t* (7.0)	0.99 *t* (7.0)	0.99 *t* (7.0)	0.88 *t* (7.0)	0.88 *t* (7.5)
mba-2	2.52 *tq* (7.0, 7.0)	2.48 *tq* (7.0, 7.0)	2.47 *tq* (7.0,7.0)	2.40 *tq* (7.0, 7.0)	2.45* tq (7.0, 7.0)
2-Me	1.22 *d* (7.0)	1.20 *d* (7.0)	1.20 *d* (7.0)	1.21 *d* (7.0)	1.19 *d* (7.0)
3-Me	0.95 *t* (7.5)	0.92 *t* (7.5)	0.92 *t* (7.5)	0.94 *t* (7.5)	0.91 *t* (7.5)
mba′-2				2.51 *tq* (7.0, 7.0)	2.45* *tq* (7.0,7.0)
2-Me				1.08 *d* (7.0)	1.13 *d* (7.0)
3-Me				0.85 *t* (7.5)	0.86 *t* (7.5)
dodeca-2a	2.27 *ddd* (7.5, 7.5, 15.0)	2.30 *ddd* (7.5, 7.5, 15.0)	2.27 *ddd* (7.0, 7.0, 15.0)		
2b	2.35 *ddd* (7.5, 7.5, 15.0)	2.39 *ddd* (7.5, 7.5, 15.0)	2.38 *ddd* (7.0, 7.0, 15.0)		
12	0.87 *t* (7.5)	0.87 *t* (7.0)	0.88 *t* (7.5)		

[a] Chemical shifts (δ) are in ppm relative to TMS. The spin coupling (*J*) is given in parentheses (Hz). Chemical shifts marked with an asterisk (*) indicate overlapped signals. Spin-coupled patterns are designated as follows: *s* = singlet, *d* = doublet, *t* = triplet, *q* = quartet, *m* = multiplet, *brs* = broad singlet.
[b] Abbreviations: fuc = fucose; rha = rhamnose; glc = glucose, jal = 11-hydroxyhexadecanoyl; mba = methylbutanoyl, dodeca = dodecanoyl.

[417–146 ($C_6H_{10}O_4$)]$^-$ in **3**, as previously reported for related tetrasaccharides of the tricolorin series (Bah and Pereda-Miranda, 1996). Therefore, operculinic acid E represented the oligosaccharide core for compounds **1** and **2** and operculinic acid C for **3**. A similar diastereoisomerism was observed for murucoidins XV (**4**) and XVI (**5**). Both compounds were also macrolactone derivatives of operculinic acid C and displayed in the negative-ion FAB mass spectrum a pseudomolecular [M–H]$^-$ ion at *m/z* 1005, which allowed for the calculation of a molecular formula of $C_{50}H_{86}O_{20}$. The initial elimination of two methylbutyroyl units produced the peaks at *m/z* 921 [M–H–C_5H_8O]$^-$ and 837 [921–C_5H_8O]$^-$. The lactonization was also located at the first rhamnose unit (Rha) by the observed peak at *m/z* 545, as previously reported (Pereda-Miranda et al., 2005) for related pentasaccharides of the murucoidin (Chérigo and Pereda-Miranda, 2006) and pescaprein series (Pereda-Miranda et al., 2005).

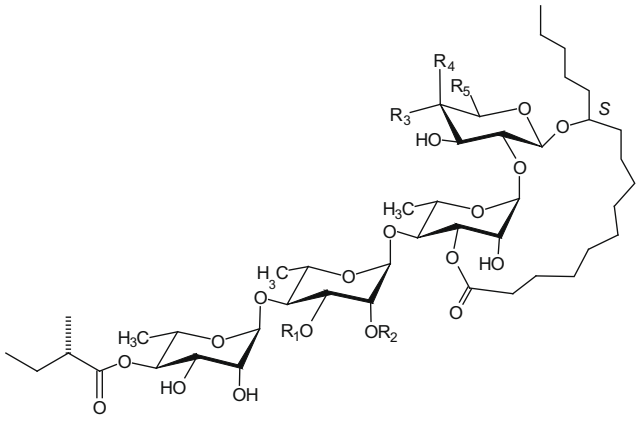

	R_1	R_2	R_3	R_4	R_5
1	H	*n*-dodecanoyl	OH	H	CH_2OH
2	*n*-dodecanoyl	H	OH	H	CH_2OH
3	*n*-dodecanoyl	H	H	OH	CH_3

Table 2
^{13}C (125 MHz) NMR spectroscopic data of compounds **1–5** (pyridine-d_5).[a]

Carbon[b]	1	2	3	4	5
glc-1	101.4	101.5			
2	75.1	75.0			
3	79.8	79.8			
4	72.0	72.0			
5	78.2	78.3			
6	62.8	62.8			
fuc-1			101.7	104.4	104.2
2			73.1	79.9	80.1
3			76.9	73.5	73.4
4			73.6	72.9	72.9
5			71.2	70.9	70.8
6			17.2	17.4	17.3
rha-1	100.2	100.3	100.3	98.6	98.5
2	69.5	69.6	69.7	73.7	73.9
3	77.9	78.9	78.9	69.9	70.2
4	79.3	76.2	76.1	80.8	80.9
5	67.9	67.6	67.4	68.7	68.7
6	19.2	19.5	19.3	19.3	19.3
rha′-1	100.7	102.6	102.5	100.2	103.3
2	74.3	70.4	70.4	73.9	69.8
3	70.8	75.6	75.5	70.7	75.8
4	80.8	78.4	78.3	80.8	78.1
5	68.5	69.1	69.0	68.6	68.7
6	18.7	18.5	18.5	18.9	18.8
rha″-1	103.7	103.7	103.7	103.8	103.2
2	72.3	72.7	72.6	72.4	72.7
3	70.2	70.1	70.0	70.3	70.1
4	75.1	74.8	74.7	75.2	74.7
5	68.0	68.2	68.1	68.1	68.1
6	17.9	17.9	17.8	18.0	17.8
jal-1	174.9	174.4	174.4	173.1	173.0
2	34.2	34.6	34.6	34.3	34.2
11	79.3	79.8	79.8	82.4	82.4
16	14.6	14.6	14.6	14.3	14.3
mba-1	176.3	176.3	176.3	175.9	176.0
2	41.6	41.5	41.5	41.6	41.5
2-Me	17.0	17.0	17.0	16.7	16.9
3-Me	11.8	11.8	11.7	11.6	11.7
mba'-1				176.4	176.3
2				41.3	41.5
2-Me				17.1	16.8
3-Me				11.8	11.6
dodeca-1	173.2	172.6	172.6		
2	34.4	34.5	34.4		
12	14.3	14.3	14.3		

[a] Chemical shifts (δ) are in ppm relative to TMS.
[b] Abbreviations: fuc = fucose; rha = rhamnose; glc = glucose, jal = 11-hydroxyhexadecanoyl; mba = methylbutanoyl; dodeca = dodecanoyl.

The ^1H NMR spectrum of these compounds showed signals of four anomeric protons, and when compared with the values previously reported for operculinic acids C and E (Ono et al., 1989), exhibited the acylation shifts for H-3 of Rha, H-2 or H-3 of Rha′, and H-4 of Rha″. HMBC studies using long-range heteronuclear coupling correlation ($^{2,3}J_{CH}$) provided evidence for the location of each ester substituent at the oligosaccharide core (Duus et al., 2000; Pereda-Miranda and Bah, 2003). Thus, the site of lactonization by the aglycone for compounds **1–3** ($\delta_{C\text{-}1}$ 174) could be placed at C-3 (δ_H 5.59–5.69) of the second saccharide (Rha), while for compounds **4** and **5**, the lactonization by the aglycone ($\delta_{C\text{-}1}$ 173) was placed at C-2 (δ_H 5.90) of the same sugar unit; a methylbutyroyl group ($\delta_{C\text{-}1}$ 176) was located at C-4 of Rha″ (δ_H 5.75–5.83) in all murucoidins; and the additional acyl substituent, dodecanoic acid ($\delta_{C\text{-}1}$ 173) in compounds **1–3**, or methylbutyric acid ($\delta_{C\text{-}1}$ 176) in compounds **4** and **5**, exhibited a $^3J_{CH}$ coupling with either H-2 (δ_H 5.72 in compound **1** and δ_H 5.95 in compound **4**) or H-3 (δ_H 5.71–5.74 in compounds **2**, **3**, and **5**) signal of Rha′.

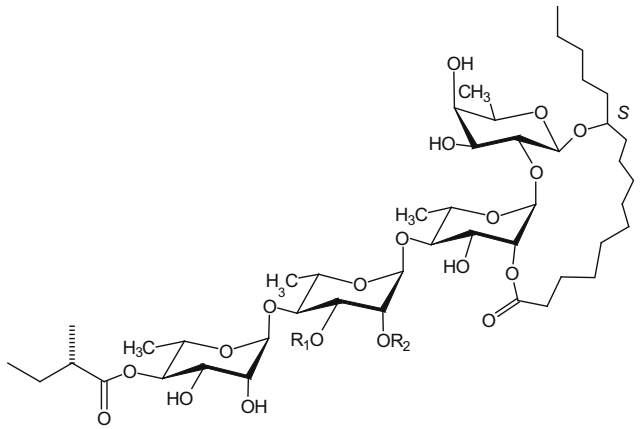

	R_1	R_2
4	H	(2*S*)-methylbutanoyl
5	(2*S*)-methylbutanoyl	H

Table 3
Susceptibility of *Staphylococcus aureus* to murucoidins XII–XVI (**1**–**5**) and their cytotoxicity.[a]

Compound	ED_{50} (μg/ml)			MIC (μg/ml)				
	KB	Hep-2	HeLa	ATCC 25923	XU−212	EMRSA−15	SA−1199B[b]	
							Nor (−)	Nor (+)
1	17.1	>20	>20	>512	>512	>512	512	8
2	>20	>20	>20	>512	>512	>512	512	8
3	13.6	3.6	16.0	>512	>512	>512	32	8[c]
4	19.0	16.4	15.5	>512	>512	>512	512	8
5	14.1	>20	15.9	>512	>512	>512	512	8
Tetracycline	–	–	–	0.125	64	0.125	0.0.25	–
Norfloxacin	–	–	–	0.5	8	0.25	–	32
Reserpine	–	–	–	–	–	–	–	8[d]
Vinblastine	0.003	0.007	0.008	–	–	–	–	–

[a] Abbreviations: KB = nasopharyngeal carcinoma; Hep-2 = laryngeal carcinoma; HeLa = cervix carcinoma; ATCC 25923 = standard *S. aureus* strain; EMRSA-15 = epidemic methicillin-resistant *S. aureus* strain containing the *mecA* gene; XU-212 = a methicillin-resistant *S. aureus* strain possessing the TetK tetracycline efflux protein; SA-1199B = multidrug-resistant *S. aureus* strain over-expressing the NorA efflux pump.
[b] Nor (−) = minimum inhibitory concentration (MIC) value determined in the susceptibility testing; Nor (+) = MIC value determined for norfloxacin in the modulation assay at the concentration of 25 μg/ml of the tested oligosaccharide.
[c] MIC value for norfloxacin in the modulation assay at the concentration of 5 μg/ml of the tested oligosaccharide.
[d] MIC value for norfloxacin in the modulation assay at the concentration of 20 μg/ml of reserpine which was used as positive control for an efflux pump inhibitor.

Only murucoidins XIV (**3**) displayed antimicrobial activity at the concentration tested against SA-1199B (MIC 8 μg/ml), a *Staphylococcus aureus* strain that over-expresses the NorA MDR efflux pump. All of the murucoidins strongly potentiated the action of norfloxacin against this NorA over-expressing strain (Gibbons et al., 2003; Oluwatuyi et al., 2004) in experiments using a sub-inhibitory concentration of these oligosaccharides (Table 3). Compounds **1–5** exerted a potentiation effect which increased the activity of norfloxacin by 4-fold (8 μg/ml; from 32 μg/ml) at concentrations of 5–25 μg/ml. These increments in norfloxacin susceptibility were similar to those observed for the orizabins, tetrasaccharides from the resin glycoside mixture of Mexican scammony (*Ipomoea orizabensis*), and the lipophilic pentasaccharides previously isolated from *I. murucoides* (Chérigo et al., 2008; Pereda-Miranda et al., 2006). These compounds are amphiphilic with very similar logP values and they could cause non-specific membrane disruption, however if this was the case, all of these molecules would be active and the norfloxacin modulating activity could not be observed.

3. Concluding remarks

This is the first report of the presence of tetraglycosidic lactones of jalapinolic acid in a tree-like morning glory species since the section Arborescentes is characterized by the presence of pentasaccharides (Chérigo and Pereda-Miranda, 2006; Bah et al., 2007). The observed variation in the resin glycoside composition of *I. murucoides* flowers seems to depend on the geographical distribution of this species and deserves further studies.

The potential use as therapeutic agents of this class of bacterial resistance modifiers for new efflux pump inhibitors is under investigation in view of the fact that by combining these plant non-cytotoxic products with commercial antibiotics could facilitate the reintroduction of ineffective antibiotics into clinical use for the treatment of refractive infections caused by multidrug-resistant *S. aureus* strains.

4. Experimental

4.1. General experimental procedures

All melting points were determined on a Fisher–Johns apparatus and are uncorrected. Optical rotations were measured with a Perkin–Elmer model 241 polarimeter. ^1H (500 MHz) and ^{13}C (125.7 MHz) NMR experiments were conducted on a Bruker DMX-500 instrument. The NMR techniques were performed in accordance with previously described methodology (Bah and Pereda-Miranda, 1996). Negative-ion low and high-resolution FAB–MS were recorded using a matrix of triethanolamine on a JEOL SX-102A spectrometer. The instrumentation used for HPLC analysis consisted of a Waters (Millipore Corp., Waters Chromatography Division, Milford, MA) 600 E multisolvent delivery system equipped with a refractive index detector (Waters 410).

4.2. Plant material

Flowers of *I. murucoides* were collected at Tepostlán, Morelos, Mexico, on April 15, 2001. The plant material was identified by Dr. Robert Bye and one of the authors (R.P.-M.) through comparison with an authentic plant sample (RP-05) archived at the Departamento de Farmacia, Facultad de Química, UNAM (Chérigo y Pereda-Miranda, 2006). A voucher specimen (Robert Bye 35906) was deposited in the Ethnobotanical Collection of the National Herbarium (MEXUE), Instituto de Biología, UNAM.

4.3. Extraction and isolation of compounds *1–5*

The whole plant material (500 g) was powdered and extracted exhaustively by maceration at room temperature with $CHCl_3$ to afford, after removal of the solvent, a dark brown syrup (35.8 g). The crude extract was subjected to column chromatography over silica gel (500 g) using gradients of CH_2Cl_2 in hexane (1:1 and 1:0), Me_2CO in CH_2Cl_2 (1:9 and 3:7), and MeOH in Me_2CO–CH_2Cl_2 (0.5:2.5:7, 1:2:7, 2:1:7). A total of 250 fractions (200 ml each) were collected, examined by TLC and combined in eight fractions. Fraction IV (eluates 122–126; MeOH–Me_2CO–CH_2Cl_2, 1:2:7) and fraction V (eluates 127–132; MeOH–Me_2CO–CH_2Cl_2, 2:1:7) were combined to give a pool containing a mixture of resin glycosides (18 g) which was subjected to fractionation by open column chromatography over reversed-phase C_{18} (150 g) eluted with MeOH. This process provided 40 secondary fractions (25 ml each). The subfraction 14–18 yielded a mixture of lipophilic resin glycosides (9.6 g) which were analyzed by reversed-phase HPLC using an isocratic elution with CH_3CN–MeOH (9:1). For their resolution, a Waters Symmetry C_{18} column (300 × 19 mm), a flow rate of 9 ml/min, and a refractive index detector were used. Peaks with t_R values of 7.0 (28 mg, peak I), 7.8 (18.6 mg, peak II), 12.6 min (26 mg, peak III), 13.4 (16.5 mg, peak IV), 14.0 min (25.8 mg, peak V), 16.5 (18 mg, peak VI), 19.5 min (20 mg, peak VII), 22.0

(21.3 mg, peak VIII), 23.0 min (29 mg, peak IX), 24.9 (35.6 mg, peak X), and 30.5 (60 mg, peak XI) were collected by the technique of heart cutting and independently re-injected in the apparatus operating in the recycle mode to achieve total homogeneity after 15 consecutive cycles. An isocratic elution with CH_3CN–MeOH (7:3) was used for those peak with t_R values higher to 15 min. These techniques afforded pure murucoidin XIII (**2**, 15 mg) from peak III, murucoidin XII (**1**, 14 mg) from peak V, murucoidin XIV (**3**, 6 mg) from peak VII, and murucoidin XVI (**5**, 12 mg) from peak IX. Peak XI afforded murucoidin IV (28 mg) and murucoidin XV (**4**, 16 mg). Co-elution experiments with reference solutions of previously reported resin glycosides allowed the detection of the following compounds: murucoidin V from peak I (13.5 mg), stoloniferin I (10.2 mg) from peak II, murucoidin I (8.4 mg) from peak IV, pescaprein III (7.3 mg) from peak VI, murucoidin II (9.1 mg) from peak VIII, and murucoidin III (15 mg) from peak X. All known compounds were identified by comparison of NMR data with published values (Bah et al., 2007; Chérigo y Pereda-Miranda, 2006; Pereda-Miranda et al., 2005).

4.4. Compound characterization

4.4.1. Murucoidin XII (1)

White powder; mp 100–104 °C; $[\alpha]_D$–78° (*c* 0.2, MeOH); ^1H and ^{13}C NMR, see Tables 1 and 2; negative FABMS *m/z* 1119 $[M–H]^-$, 937 $[M–H–C_{12}H_{22}O]^-$, 853 $[937–C_5H_8O]^-$, 707 $[853–C_6H_{10}O_4]^-$, 561, 433, 271; HRFABMS *m/z* 1119.6676 $[M–H]^-$ (calcd for $C_{57}H_{99}O_{21}$ requires 1119.6679).

4.4.2. Murucoidin XIII (2)

White powder; mp 96–98 °C; $[\alpha]_D$–67° (*c* 0.1, MeOH); ^1H and ^{13}C NMR, see Tables 1 and 2; negative FABMS *m/z* 1119 $[M–H]^-$, 937 $[M–H–C_{12}H_{22}O]^-$, 853 $[937–C_5H_8O]^-$, 707 $[853–C_6H_{10}O_4]^-$, 561 $[707–C_6H_{10}O_4]^-$, 433 $[561–128]^-$, 271; HRFABMS *m/z* 1119.6674 $[M–H]^-$ (calcd for $C_{57}H_{99}O_{21}$ requires 1119.6679).

4.4.3. Murucoidin XIV (3)

White powder; mp 125–127 °C; $[\alpha]_D$–60° (*c* 0.47, MeOH); ^1H and ^{13}C NMR, see Tables 1 and 2; negative FABMS *m/z* 1103 $[M–H]^-$, 921 $[M–H–C_{12}H_{22}O]^-$, 837 $[921–C_5H_8O]^-$, 691 $[837–C_6H_{10}O_4]^-$, 545 $[691–C_6H_{10}O_4]^-$, 417, 271; HRFABMS *m/z* 1103.6724 $[M–H]^-$ (calcd for $C_{57}H_{99}O_{20}$ requires 1103.6729).

4.4.4. Murucoidin XV (4)

White powder; mp 108–111 °C; $[\alpha]_D$–66° (*c* 0.60, MeOH); ^1H and ^{13}C NMR, see Tables 1 and 2; negative FABMS *m/z* 1005 $[M–H]^-$, 921 $[M–H–C_5H_8O]^-$, 837 $[921–C_5H_8O]^-$, 775 [921–146 $C_6H_{10}O_4]^-$, 691 $[775–C_5H_8O]^-$, 545 $[691–C_6H_{10}O_4–C_5H_8O]^-$, 417, 271; HRFABMS *m/z* 1005.5630 $[M–H]^-$ (calcd for $C_{50}H_{85}O_{20}$ requires 1005.5634).

4.4.5. Murucoidin XVI (5)

White powder; mp 125–127 °C; $[\alpha]_D$–29° (*c* 0.35, MeOH); ^1H and ^{13}C NMR, see Tables 1 and 2; negative FABMS *m/z* 1005 $[M–H]^-$, 921 $[M–H–C_5H_8O]^-$, 691 $[921–C_5H_8O–C_6H_{10}O_4]^-$, 545 $[691–C_6H_{10}O_4]^-$, 417, 271; HRFABMS *m/z* 1005.5629 $[M–H]^-$ (calcd for $C_{50}H_{85}O_{20}$ requires 1005.5634).

4.5. Alkaline hydrolysis of resin glycoside mixture

A solution of the crude resin glycoside mixture (100 mg) in 5% KOH–H_2O (5 ml) was heated at 95 °C for 4 h. The reaction mixture was acidified to pH 4.0 and extracted with $CHCl_3$ (30 ml). The organic layer was washed with H_2O, dried over anhydrous Na_2SO_4, and evaporated under reduced pressure. The aqueous phase was extracted with *n*-BuOH (20 ml) and concentrated to dryness. The residue extracted (42 mg) from the aqueous phase was methylated with CH_2N_2 to further perform the separation by HPLC of the methyl ester derivatives, using a Waters μBondapak NH_2 column (7.8 × 300 mm), an isocratic elution with CH_3CN–H_2O (5:1), a flow rate of 3 ml/min, and a sample injection of 500 μl (20 mg/ml). This procedure yielded operculinic acid C methyl ester (6.4 mg, t_R = 5.8 min), operculinic acid E methyl ester (8.6 mg, t_R = 10.9 min), simonic acid A methyl ester (4.3 mg, t_R = 14.0 min), operculinic acid A methyl ester (8.6 mg, t_R = 20.9 min), and simonic acid B methyl ester (14.7 mg, t_R = 28.2 min), which were identified by comparison of their physical constants and NMR data with published value (Ono et al., 1989, 1990).

The residue from the organic phase was analyzed by GC–MS to allow the detection of the major liberated esterifying residues which were identified as 2-methyl propanoic, 2-methyl butanoic, and *n*-dodecanoic acids by comparison of their retention times and spectra with those of authentic samples as previously described (Bah et al., 2007; Chérigo et al., 2008). Previously described procedures were used for the preparation and identification of 4-bromophenacyl (2*S*)-2-methylbutyrate from the resin glycoside mixture: mp 40–42 °C; $[\alpha]_D$ + 18 (*c* 1.0, MeOH) (Pereda-Miranda and Hernández-Carlos, 2002).

4.6. Biological assays

4.6.1. Bacterial strains and media

Staphylococcus aureus EMRSA-15 containing the *mecA* gene was provided by Dr. Paul Stapleton, The School of Pharmacy, University of London. Strain XU-212, a methicillin-resistant strain possessing the TetK tetracycline efflux protein, was provided by Dr. E. Udo (Gibbons and Udo, 2000). SA-1199B, which over-expresses the NorA MDR efflux protein (Kaatz et al., 1993), and *S. aureus* ATCC 25923 were also used. All strains were cultured on nutrient agar (Oxoid, Basingstoke, UK) before determination of MIC values. Cation-adjusted Mueller–Hinton broth (MHB; Oxoid) containing 20 and 10 mg/l of Ca^{2+} and Mg^{2+}, respectively was used for susceptibility tests.

4.6.2. Susceptibility testing

Minimum inhibitory concentration values (MIC) were determined at least in duplicate by standard microdilution procedures. An inoculum density of 5×10^5 cfu of each of the test strains was prepared in 0.9% saline by comparison with a McFarland standard. MHB (125 μl) was dispensed into 10 wells of a 96-well microtiter plate (Nunc, 0.3 ml volume per well). All test compounds were dissolved in DMSO before dilution into MHB for use in MIC determinations. The highest concentration of DMSO remaining after dilution (3.125% v/v) caused no inhibition of bacterial growth. Then, glycolipids **1–5** or appropriate antibiotic (125 μl) were dispensed into well 1 and serially diluted across the plate (512–1 μg/ml), leaving well 11 empty for the growth control. The final volume was dispensed into well 12, which being free of inoculum served as the sterile control. The inoculum (125 μl) was added into wells 1–11 and the plate was incubated at 36 °C for 18 h. The MIC was defined as the lowest concentration which yielded no visible growth. Tetracycline and norfloxacin from Sigma (Poole, UK) were also tested as positive drug controls. A methanolic solution (5 mg/ml) of 3-[4,5-dimethylthiazol-2-yl]-2,5-diphenyltetrazoliium bromide (MTT; Lancaster) was used to detect bacterial growth by a color change from yellow to dark blue. For the modulation assay, the murucoidins were tested at final concentrations of 25 or 5 μg/ml. Serial doubling dilutions of norfloxacin ranging from 1 to 512 μg/ml were added and the microtitre plates were then interpreted, after inoculum addition and incubation, in the same manner as MIC determinations. The activity of reserpine at a con-

centration of 20 μg/ml was also tested as an efflux pump inhibitor for comparison purposes. All samples were tested in duplicate.

4.6.3. Cytotoxicity assay

Nasopharyngeal (KB), cervix (HeLa), and laryngeal carcinoma (Hep-2) cell lines were maintained in RMPI 1640 (10×) medium supplemented with 10% fetal bovine serum. Cell lines were cultured at 37 °C in an atmosphere of 5% CO_2 in air (100% humidity). The cells at log phase of their growth cycle were treated in triplicate with various concentrations of the test samples (0.16–20 μg/ml) and incubated for 72 h at 37 °C in a humidified atmosphere of 5% CO_2. The cell concentration was determined by the NCI sulforhodamine method (Skehan et al., 1990) Results were expressed as the dose that inhibits 50% control growth after the incubation period (EC_{50}). The values were estimated from a semilog plot of the drug concentration (μg/ml) against the percentage of viable cells. Vinblastine was included as a positive drug control.

Acknowledgements

This research was partially supported by Consejo Nacional de Ciencia y Tecnología (45861-Q) and Dirección General de Asuntos del Personal Académico, UNAM (IN208307). R.P.-M. was on sabbatical leave at the Centre for Pharmacognosy and Phytotherapy (The School of Pharmacy, UL) with the final support of DGAPA (UNAM). L.C. is grateful to DGAPA for a graduate scholarship. Thanks are due to G. Duarte and M. Guzmán (USAI, Facultad de Química, UNAM) for the recording of mass spectra and to Dr. Mabel Fragoso-Serrano (Facultad de Química, UNAM) for HPLC technical assistance.

References

Bah, M., Chérigo, L., Taketa, A.T.C., Fragoso-Serrano, M., Hammond, G.B., Pereda-Miranda, R., 2007. Intrapilosins I–VII, pentasaccharides from the seeds of *Ipomoea intrapilosa*. J. Nat. Prod. 70, 1153–1157.

Bah, M., Pereda-Miranda, R., 1996. Detailed FAB-Mass spectrometry and high resolution NMR investigations of tricolorins A–E, individual oligosaccharides from the resins of *Ipomoea tricolor* (Convolvulaceae). Tetrahedron 52, 13063–13080.

Chérigo, L., Pereda-Miranda, R., 2006. Resin glycosides from the flowers of *Ipomoea murucoides*. J. Nat. Prod. 69, 595–599.

Chérigo, L., Pereda-Miranda, R., Fragoso-Serrano, M., Jacobo-Herrera, N., Kaatz, G.W., Gibbons, S., 2008. Inhibitors of bacterial multidrug efflux pumps from the resin glycosides of *Ipomoea* murucoides. J. Nat. Prod. 71, 1037–1045.

Duus, J.Ø., Gotfredsen, C.H., Bock, K., 2000. Carbohydrate structural determination by NMR spectroscopy: modern methods and limitations. Chem. Rev. 100, 4589–5614.

Emmart, E.W., 1940. The Badianus Manuscript (Codex Barberini, Latin 241). An Aztec Herbal of 1552. The Johns Hopkins Press, Baltimore.

Gibbons, S., Oluwatuyi, M., Veitch, N.C., Gray, A.I., 2003. Bacterial resistance modifying agents from *Lycopus europaeus*. Phytochemistry 62, 83–87.

Gibbons, S., Udo, E.E., 2000. The effect of reserpine, a modulator of multidrug efflux pumps, on the in-vitro activity of tetracycline against clinical isolates of methicillin resistant *Staphylococcus aureus* (MRSA) possessing the tet(K) determinant. Phytother. Res. 14, 139–140.

Kaatz, G.W., Seo, S.M., Ruble, C.A., 1993. Efflux-mediated fluoroquinolone resistance in *Staphylococcus aureus*. Antimicrob. Agents Chemother. 37, 1086–1094.

Oluwatuyi, M., Kaatz, G.W., Gibbons, S., 2004. Antibacterial and resistance modifying activity of *Rosmarinus officinalis*. Phytochemistry 65, 3249–3254.

Ono, M., Kawasaki, T., Miyahara, K., 1989. Resin glycosides V. Identification and characterization of the component organic and glycosidic acids of the ether-soluble crude resin glycosides (“jalapin”) from Rhizoma Jalapae Braziliensis (roots of *Ipomoea operculata*). Chem. Pharm. Bull. 37, 3209–3213.

Ono, M., Fukunaga, T., Kawasaki, T., Miyahara, K., 1990. Resin glycosides VIII. Four glycosidic acids, operculinic acids D, E, F, and G of the ether-soluble crude resin glycosides (“jalapin”) from rhizoma jalapae braziliensis (roots of *Ipomoea operculata*). Chem. Pharm. Bull. 38, 2650–2655.

Pereda-Miranda, R., Bah, M., 2003. Biodynamic constituents in the Mexican morning glories: purgative remedies transcending boundaries. Curr. Top. Med. Chem. 3, 111–131.

Pereda-Miranda, R., Escalante-Sánchez, E., Escobedo-Martínez, C., 2005. Characterization of lipophilic pentasaccharides from beach morning glory (*Ipomoea pes-caprae*). J. Nat. Prod. 68, 226–230.

Pereda-Miranda, R., Hernández-Carlos, B., 2002. HPLC isolation and structural elucidation of diastereomeric niloyl ester tetrasaccharides from Mexican scammony root. Tetrahedron 58, 3145–3154.

Pereda-Miranda, R., Kaatz, G.W., Gibbons, S., 2006. Polyacylated oligosaccharides from medicinal Mexican morning glory species as antibacterial and inhibitors of multidrug resistance in *Staphylococcus aureus*. J. Nat. Prod. 69, 406–409.

Skehan, P., Storeng, R., Scudiero, D., Monks, A., McMahon, J., Vistica, D., Warren, J.T., Bokesch, H., Kenney, S., Boyd, M.R., 1990. New colorimetric cytotoxicity assay for anticancer-drug screening. J. Natl. Cancer Inst. 82, 1107–1112.

Inhibitors of Bacterial Multidrug Efflux Pumps from the Resin Glycosides of *Ipomoea murucoides*[⊥]

Lilia Chérigo,[†] Rogelio Pereda-Miranda,*[,†] Mabel Fragoso-Serrano,[†] Nadia Jacobo-Herrera,[†] Glenn W. Kaatz,[‡] and Simon Gibbons[§]

Departamento de Farmacia, Facultad de Química, Universidad Nacional Autónoma de México, Ciudad Universitaria, Mexico City 04510 DF, Mexico, Department of Internal Medicine, Division of Infectious Diseases, John D. Dingell Veterans Affairs Medical Center and Wayne State University School of Medicine, Detroit, Michigan 48201, and Centre for Pharmacognosy and Phytotherapy, The School of Pharmacy, University of London, 29-39 Brunswick Square, London WC1N 1AX, U.K.

Received March 10, 2008

A reinvestigation of the $CHCl_3$-soluble extract from flowers of the Mexican medicinal arborescent morning glory, *Ipomoea murucoides*, through preparative-scale recycling HPLC, yielded six new pentasaccharides, murucoidins VI−XI (**1**−**6**), as well as the known pescaprein III (**7**), stoloniferin I (**8**), and murucoidins I−V (**9**−**13**). Their structures were characterized through the interpretation of their NMR spectroscopic and FABMS data. Compounds **1**−**6** were found to be macrolactones of three known glycosidic acids identified as simonic acids A and B, and operculinic acid A, with different fatty acids esterifying the same positions, C-2 on the second rhamnose unit and C-4 on the third rhamnose moiety. The lactonization site of the aglycone was placed at C-2 or C-3 of the second saccharide unit. The esterifying residues were composed of two short-chain fatty acids, 2-methylpropanoic and (2*S*)-methylbutyric acids, and two long-chain fatty acids, *n*-dodecanoic (lauric) acid and the new (8*R*)-(−)-8-hydroxydodecanoic acid. For the latter residue, its absolute configuration was determined by analysis of its Mosher ester derivatives. All members of the murucoidin series exerted a potentiation effect of norfloxacin against the NorA overexpressing *Staphylococcus aureus* strain SA-1199B by increasing the activity 4-fold (8 μg/mL from 32 μg/mL) at concentrations of 5−25 μg/mL. Stoloniferin I (**8**) enhanced norfloxacin activity 8-fold when incorporated at a concentration of 5 μg/mL. Therefore, this type of amphipathic oligosaccharide could be developed further to provide more potent inhibitors of this multidrug efflux pump.

In the New World flora there are 13 tree-like morning glory species in the genus *Ipomoea* series *Arborescentes*, most of them are confined to Mexico and nearby Central America.[1] These species have long been of medicinal and economical interest to the native people, who coexist with them in the same ecosystem. In central Mexico, six species collectively called "cazahuate"[2] are a conspicuous floristic element of the seasonal dry tropical forest. They have been used since Prehispanic times[3] and share several morphological features, e.g., trees with large white flowers and funnel-shaped corollas, and the same therapeutic application to treat itching, rashes, and other infections by rubbing the raw flowers directly on the skin. Traditional healers continue to use decoctions of this medicinal plant complex[4−6] considered to be of "cold-nature"[7] to reduce excessive body heat[8] and relieve uncomfortable "water and cold" symptoms believed to be produced by abrupt climatic changes resulting in diseases considered to be "hot", e.g., rheumatism, inflammation, and ear pain.

This paper presents the results of a second investigation based on the chemical analysis of the resin glycoside mixture obtained from the flowers of *Ipomoea murucoides* Roem. et Schult. Six new acylated pentasaccharides of jalapinolic acid, murucoidins VI−XI (**1**−**6**), as well as the known pescaprein III (**7**), stoloniferin I (**8**), and murucoidins I−V (**9**−**13**) were separated and purified by a recycling HPLC technique, and their structures were characterized through the interpretation of NMR spectroscopic and FABMS data. The antimicrobial potential of these complex macrocyclic lactones was evaluated against a panel of *Staphylococcus aureus* strains overexpressing specific efflux pumps as a starting point for the development of new bacterial inhibitors to treat infections resulting from multidrug-resistant *S. aureus* strains.[9,10]

Results and Discussion

A small portion of the resin glycoside fractions, obtained from the $CHCl_3$-soluble extract, was submitted to saponification and yielded a water-soluble solid product that was resolved by HPLC into three glycosidic derivatives of jalapinolic acid and an organic solvent-soluble oily acidic fraction. The glycosidic acids were identified as simonic acid A, (11*S*)-jalapinolic acid 11-*O*-α-L-rhamnopyranosyl-(1→3)-*O*-[α-L-rhamnopyranosyl-(1→4)]-*O*-α-L-rhamnopyranosyl-(1→4)-*O*-α-L-rhamnopyranosyl-(1→2)-β-D-glucopyranoside,[11] simonic acid B, (11*S*)-jalapinolic acid 11-*O*-α-L-rhamnopyranosyl-(1→3)-*O*-[α-L-rhamnopyranosyl-(1→4)]-*O*-α-L-rhamnopyranosyl-(1→4)-*O*-α-L-rhamnopyranosyl-(1→2)-β-D-fucopyranoside,[5,11] and operculinic acid A, (11*S*)-jalapinolic acid 11-*O*-β-D-glucopyranosyl-(1→3)-*O*-[α-L-rhamnopyranosyl-(1→4)]-*O*-α-L-rhamnopyranosyl-(1→4)-*O*-α-L-rhamnopyranosyl-(1→2)-β-D-fucopyranoside,[5,12] previously obtained from *Ipomoea batatas*,[11] *I. stolonifera*,[13] *I. operculata*,[14] *I. leptophylla*,[15] *I. murucoides*,[5] and *I. intrapilosa*.[16]

The major liberated fatty acids were identified as 2-methylpropanoic (iba), 2-methylbutanoic (mba), and *n*-dodecanoic acids by GC-MS comparison of their spectra and retention times with those of authentic samples.[5,17] The new (8*R*)-(−)-8-hydroxydodecanoic acid (**14**) was also liberated as one of the hydrolyzed products recovered from the organic-soluble fraction obtained from the saponification of murucoidin X (**5**).

Individual constituents of the remaining portion of these resin glycoside fractions were separated and purified by a recycling HPLC technique,[18] using a semipreparative reversed-phase column. These procedures led to the isolation and structural characterization of six new compounds, for which the names murucoidins VI−XI (**1**−**6**) have been proposed. All compounds displayed the same fragmentation pattern produced by glycosidic cleavage in their negative-ion FABMS, as previously described for the pescaprein[19] and murucoidin[5] series. Common fragment peaks reported for the

* To whom correspondence should be addressed. Tel: +52-55-5622-5288. Fax: +52-55-5622-5329. E-mail: pereda@servidor.unam.mx.
[†] Universidad Nacional Autónoma de México.
[‡] John D. Dingell Veterans Affairs Medical Center and Wayne State University.
[§] University of London.
[⊥] This work was taken in part from the Ph.D. thesis of L. Chérigo.

10.1021/np800148w CCC: $40.75
Published on Web 05/24/2008

resin glycosides[20,21] were observed in all mass spectra, confirming the branched pentasaccharide core, and the resulting diagnostic peaks also indicated the nature of the esterifying moieties. For example, murucoidin X (**5**) gave a pseudomolecular $[M - H]^-$ ion at *m/z* 1265, indicating a molecular formula of $C_{63}H_{110}O_{25}$. The ions at *m/z* 1181 $[M - H - C_5H_8O]^-$ and 1067 $[M - H - C_{12}H_{22}O_2]^-$ suggested the presence of a methylbutyric acid and a monohydroxydodecanoic acid as esterifying residues. The subsequent losses produced by glycosidic cleavage of each sugar moiety afforded peaks at *m/z* 691 $[1067 - 2 \times 146\ (C_6H_{10}O_4) - C_5H_8O]^-$, 545 $[691 - 146\ (C_6H_{10}O_4)]^-$, which indicated that the lactonization was located at the first rhamnose unit (Rha), 417 $[545 + H_2O - 146\ (C_6H_{10}O_4)]^-$, and 271 $- [417 - 146\ (C_6H_{10}O_4)]^-$.

Common features in both ^{1}H and ^{13}C NMR spectra of all six new compounds (**1**−**6**) were noted (Tables 1 and 2). All ^{1}H NMR spectra showed significantly downfield shifted signals for the proton on C-2 or C-3 of the first rhamnose unit (rha) and on H-2 and H-3 of the second and third rhamnose units (rha′ and rha″), suggesting esterification at these positions. The multiplets with splitting patterns as ddd centered at δ 2.80 and 2.25 showed cross-peaks in their COSY and TOCSY spectra, revealing the macrocyclic lactone-type structure for all the murucoidins because these signals correspond to the nonequivalent diastereotopic protons of the CH_2-2 of the aglycone (11*S*-hydroxyhexadecanoic acid, jal) when forming a ring.[20,21] The following spectroscopic features were observed: (a) the carbonyl resonance of the lactone functionality (δ 173−174) was assigned by the ^2J coupling with each of the methylene protons on the adjacent C-2 position of jalapinolic acid in all compounds **1**−**6**; (b) the lactonization site at C-3 (δ_C 77) of the second saccharide (rha) was established by the observed ^3J coupling between this carbonyl carbon and its downfield shifted geminal proton (δ 5.6) in murucoidins VI (**1**) and IX−XI (**4**−**6**); for compounds **2** and **3**, the lactonization at C-2 (δ_C 70) was identified by the $^3J_{C-H}$ coupling and corroborated by the significant downfield shift for its geminal proton (δ 5.0) in comparison with the same resonance in the rest of the compounds with the Rha C-3 macrocyclic ring closure; (c) all murucoidins showed signals for one short-chain fatty acid residue esterifying position C-4 at Rha″ (δ_C 73); H-2 of these moieties was used as a diagnostic resonance centered at δ 2.4−2.5 (1H, tq) for the methylbutanoyl group (mba) in murucoidins VI (**1**), VIII (**3**), X (**5**), and XI (**6**) and at δ 2.5−2.6 (1H, septet) for the methylpropanoyl group (iba) in murucoidins VII (**2**) and IX (**4**); (d) the C-2 methylene equivalent protons were observed as a triplet signal at δ 2.4 for the long-chain fatty acid esterifying residues in **1**, **5**, and **6**. In all cases it was possible by HMBC analysis[21,22] to establish the links between a specific carbonyl ester group with their corresponding vicinal proton resonance ($^2J_{CH}$) and the pyranose ring proton at the site of esterification ($^3J_{CH}$). For example, the 8-hydroxydodecanoyl residue in murucoidin X (**5**) was identified through the observed $^2J_{CH}$ coupling between the carbonyl resonance at δ 172.9 with the triplet-like signal for the vicinal methylene protons (δ 2.3, 2H) and its location at C-2 of Rha′ by the $^3J_{CH}$ coupling with the signal at δ 5.8. Therefore, the remaining esterified position (C-4 Rha″ δ_H 4.2; δ_C 73) represented the location of the additional ester linkage for the methylbutanoyl group.

From the TOCSY experiment,[22] edited ^{1}H NMR subspectra for each individual monosaccharide moiety were obtained for all oligosaccharides and permitted the assignment of their resonances (Table 1). Homonuclear spin decoupling experiments were carried out to verify coupling constants. The anomeric configuration in each sugar unit was deduced from 2D $^1J_{CH}$ NMR experiments. For D-sugars in the $^4C_1$ conformation, the α-anomeric configuration (β-equatorial C−H bond) has a $^1J_{CH}$ value of 170 Hz, which is 10 Hz higher than that for the β-anomer (α-axial C−H bond; ca. 160 Hz).[22] From the anomeric signals in the ^{13}C NMR spectra of the glycosidic acids (i.e., simonic acids A and B and operculinic acid C), $^1J_{CH}$ values for fucose (159 Hz) and glucose (164 Hz) supported the β-anomeric configuration. The α-configuration was deduced for the rhamnose units ($^1J_{CH}$ = 170−172 Hz).[20] All monosaccharides were in their naturally occurring form (D-glucose, D-fucose, and L-rhamnose), as confirmed by optical rotation measurements of the acid-liberated individual monosaccharides.

The structure of the new acylating acid residue obtained from the saponification of murucoidin X (**5**) was further supported by its chemical transformations to its silylated methyl ester derivative (**16**).[17] Its mass spectrum indicated that the hydroxyl group was attached at the C-8 position in a fatty acid chain of 12 carbons since the α-cleavage[23] on either side of the trimethylsiloxyl group gave the diagnostic ions at *m/z* 245 $[C_9H_{16}O_3TMS]^+$ and 159 $[C_5H_{10}OTMS]^+$. In compound **5**, the presence of the C-8 hydroxyl group in the aglycone was also recognized by the downfield shift (α-effect ca. +41 ppm)[24] on C-8 (δ_C 75) and the β-effects on C-7 and C-9 (δ_C 38), which resulted in shifts to higher frequency ($\Delta\delta$ = +8 ppm)[24] in comparison with the same resonances in the *n*-dodecanoic acid (δ_C 29−30).[25] To determine the stereochemistry at the C-8 position, compound **15** was converted to the Mosher esters **17** and **18** with (*S*)- and (*R*)-α-methoxy-α-trifluoromethylphenylacetyl (MTPA) chloride, and their ^{1}H NMR spectra were recorded.[26] The chemical shift difference ($\Delta\delta = \delta_S - \delta_R$) between corresponding Me-12 protons was positive ($\Delta\delta$ = +0.059 ppm), allowing the confirmation of a C-8 *R* absolute configuration through the application of the configurational model proposed by Kakisawa and associates (Scheme 1).[27] This result is consistent with the previously reported chemical shift differences ($\Delta\delta$ = +0.057 ppm) at the terminal methyl signals that are separated by as much as four methylene groups from the asymmetric carbon.[28] It is also in accordance with the observation that synthetic monohydroxylated fatty acids with a dextrorotatory optical activity have an *S* absolute configuration and their levoisomers have the opposite, *R* configuration.[29] The acylating 8-(*R*)-hydroxydodecanoic acid of murucoidin X (**5**) represents the first levorotatory monohydroxylated aglycone in the Convolvulaceae family.

Only murucoidins I (**9**), VI (**1**), and VII (**2**) displayed antimicrobial activity at the concentration tested against SA-1199B (MIC 32 μg/mL), a *Staphylococcus aureus* strain that overexpresses the NorA MDR efflux pump. This may be explained by a loss in "fitness" of this strain due to overexpression of this MDR pump when compared to the other strains. All of the murucoidins strongly potentiated the action of norfloxacin against this NorA overexpressing strain[30] in experiments using a subinhibitory concentration of these oligosaccharides (Table 3). They exerted a potentiation effect, which increased the activity of norfloxacin by 4-fold (8 μg/mL from 32 μg/mL) at concentrations of 5−25 μg/mL; stoloniferin I (**8**) enhanced norfloxacin activity 8-fold when incorporated at a concentration of 5 μg/mL. These strong potentiation effects were similar to those previously observed for the amphipathic orizabins,[9] which are tetrasaccharides from the Mexican scammony (*Ipomoea orizabensis*). An ethidium efflux inhibition assay utilizing SA-1199B[31] demonstrated that compound **8** had modest inhibitory activity (Figure 1) in comparison with the strong activity previously reported for orizabin IX, which was more efficacious than reserpine.[9] This decrease in activity could be due to solubility issues, since the murucoidins are extremely nonpolar and at higher concentrations the broth solution became cloudy as a result of test compound precipitation. Compound **11** had no efflux inhibitory activity; the basis for its profound effect on the norfloxacin MIC in the modulation assay currently is unknown and deserves further attention.

The amphipathic properties of these compounds resulting from the acylation of some of the free hydroxyl groups of the oligosaccharide core and the lipophilic alkyl chains of their aglycones would seem to be important in facilitating cellular uptake to its MDR pump target. To verify this hypothesis, the modulatory activity of two

Table 1. ^{1}H NMR Data of Compounds **1**−**6** (500 MHz)[a]

proton[b]	1	2	3	4	5	6
glc-1	5.03 d (7.5)	4.90 d (7.5)	4.91 d (7.5)			
2	4.28 dd (7.5, 8.0)	3.90 dd (7.5, 8.5)	3.90 dd (7.5, 8.5)			
3	4.30 dd (8.0, 9.0)	4.12* dd (8.5, 9.0)	4.16* dd (8.5, 9.0)			
4	4.15 t (9.0, 9.0)	4.12* dd (9.0, 9.5)	4.16* dd (9.0, 9.0)			
5	3.90 ddd (2.4, 5.0, 9.0)	3.88 m	3.88 ddd (2.5, 6.0, 9.0)			
6a	4.33–4.35	4.33 dd (6.0, 12.5)	4.32 dd (6.0, 12.0)			
6b	4.54* dd (3.0, 10.0)	4.47 dd (3.0, 12.5)	4.48 dd (2.5, 12.0)			
fuc-1				4.82 d (8.0)	4.82 d (7.5)	4.82 d (8.0)
2				4.53 dd (8.0, 9.5)	4.55 dd (7.5, 9.5)	4.52 dd (8.0, 9.5)
3				4.20 dd (4.0, 9.5)	4.20 dd (3.5, 9.5)	4.19* dd (3.0, 9.5)
4				3.92 m	3.92 d (3.5)	3.90 m
5				3.82 dq (0.5, 6.5)	3.82 dq (0.7, 6.5)	3.83 q (6.5)
6				1.52 d (6.5)	1.53 d (6.5)	1.52 d (6.5)
rha-1	6.46 d (1.6)	5.57 d (2.0)	5.59 d (1.5)	6.35 d (1.5)	6.35 d (1.5)	6.35 d (1.5)
2	5.32 brs	6.06 dd (2.0, 3.5)	6.07 dd (1.5, 3.5)	5.32 dd (1.5, 2.5)	5.32 dd (1.5, 3.0)	5.25 brs
3	5.62 dd (3.0, 9.8)	5.04 dd (3.5, 9.0)	5.09 dd (3.5, 9.0)	5.60 dd (2.5, 9.8)	5.61 dd (3.0, 9.5)	5.66 dd (3.0, 10.0)
4	4.69 t (9.8)	4.21 dd (9.0, 9.0)	4.24* dd (9.0, 9.5)	4.65 dd (9.8, 9.8)	4.64 dd (9.5, 9.5)	4.68 t (10.0, 10.0)
5	5.10 dq (6.4, 9.8)	4.38* dq (6.0, 9.0)	4.38* dq (6.0, 9.5)	5.00 dq (6.0, 9.8)	5.03 dq (6.0, 9.5)	4.95 brs
6	1.72 d (6.4)	1.58 d (6.0)	1.58 d (6.0)	1.57 d (6.0)	1.58 d (6.0)	1.59 d (6.0)
rha′-1	5.68 d (1.6)	6.13 d (2.0)	6.16 d (1.5)	5.60 d (2.0)	5.66 d (1.5)	5.63 d (1.5)
2	5.84 dd (1.6, 3.0)	5.96 dd (2.0, 3.0)	5.97 dd (1.5, 3.5)	5.78 dd (2.0, 3.0)	5.82 dd (1.5, 3.5)	6.00 dd (1.5, 3.5)
3	4.54* dd (3.0, 3.0)	4.59 dd (3.0, 9.0)	4.61 dd (3.5, 9.0)	4.50 (3.0, 9.0)	4.52* dd (3.5, 9.5)	4.63 dd (3.5, 9.0)
4	4.33 dd (9.0, 9.0)	4.25 dd (9.0, 9.5)	4.27 dd (9.0, 9.5)	4.23 dd (9.0, 9.5)	4.25* dd (9.5, 9.5)	4.35 dd (9.5, 9.5)
5	4.37 dq (6.0, 9.0)	4.32 dq (6.0, 9.5)	4.38* dq (6.0, 9.5)	4.33–4.35* dq (6.0, 9.5)	4.34 dq (6.0, 9.5)	4.31 dq (6.0, 9.5)
6	1.62 d (6.0)	1.64 d (6.0)	1.65 d (6.0)	1.59 d (6.0)	1.60 d (6.0)	1.62 d (6.0)
rha″-1	5.93 brs	5.88 brs	5.91 d (1.0)	5.88 d (1.5)	5.92 brs	6.21 d (2.0)
2	4.63 dd (1.3, 3.3)	4.70 brs	4.71 dd (1.0, 3.0)	4.63 brs	4.63 dd (1.5, 3.5)	4.89 dd (2.0, 3.0)
3	4.42 dd (3.3, 9.7)	4.47 dd (3.0, 9.0)	4.47 dd (3.0, 9.5)	4.42 dd (3.0, 9.5)	4.41 dd (3.5, 9.5)	4.45 dd (3.0, 9.0)
4	5.78 t (9.7)	5.79 t (9.0)	5.82 t (9.5)	5.80 t (9.5)	5.78 t (9.5)	5.73 t (9.0, 9.0)
5	4.33–4.35*	4.38* dq (6.0, 9.0)	4.36 dq (6.5, 9.5)	4.33–4.35* dq (6.0, 9.5)	4.36 dq (6.0, 9.5)	4.37 dq (6.0, 9.0)
6	1.40 d (6.3)	1.38 d (6.0)	1.40 d (6.5)	1.39 d (6.0)	1.39 d (6.0)	1.40 d (6.0)
rha‴-1	5.57 d (1.3)	5.62 d (1.5)	5.65 d (1.0)	5.57 d (1.5)	5.57 d (1.0)	
2	4.79 dd (1.3, 3.1)	4.83 brs	4.84 dd (1.0, 3.5)	4.80 brs	4.79 dd (1.0, 3.5)	
3	4.50 dd (3.1, 9.4)	4.40 dd (3.0, 9.0)	4.41 dd (3.5, 9.0)	4.46 dd (3.0, 9.5)	4.52 dd (3.5, 9.5)	
4	4.23 t (9.4)	4.23 dd (9.0, 9.0)	4.25* dd (9.5, 9.0)	4.26* m	4.25* dd (9.5, 9.5)	
5	4.27 dq (6.0, 9.4)	4.32* dq (6.0, 9.0)	4.38* dq (6.0, 9.5)	4.26* m	4.30 dq (6.0, 9.5)	
6	1.71 d (6.0)	1.55 d (6.0)	1.57 d (6.0)	1.70 d (6.0)	1.71 d (6.0)	
glc-1						5.09 d (7.5)
2						3.96 t (7.5, 9.0)
3						4.14 *dd (9.0,9.0)
4						4.14 * dd (9.0, 9.0)
5						3.88 ddd (3.0, 6.0, 9.0)
6a						4.39 dd (6.0, 12.0)
6b						4.48 dd (3.0, 12.0)
jal-2a	2.25 ddd (3.8, 7.2, 13.6)	2.25 ddd (3.5, 8.0, 12.0)	2.25 ddd (3.5, 8.0, 12.0)	2.24 ddd (3.5, 7.9, 12.5)	2.27 ddd (2.8, 8.0, 11.5)	2.28 ddd (3.0, 7.8, 13.0)
2b	2.91 ddd (3.8, 7.2, 13.6)	2.40 ddd (3.5, 7.0, 12.0)	2.40 ddd (3.5, 8.0, 12.0)	2.83 ddd (3.5, 7.9, 12.5)	2.92 ddd (2.8, 8.0, 11.5)	2.70 dd (2.5, 13.0)
11	3.90 m	3.87 m	3.87 m	3.88 m	3.87 m	3.87 m
16	0.93 t (7.0)	0.83 t (7.0)	0.83 t (7.0)	0.93 t (7.0)	0.95 t (7.0)	0.94 t (7.0)
mba-2	2.50 tq (7.0, 7.0)	2.36 tq (7.0, 7.0)	2.37 tq (7.0, 7.0)	2.48 tq (7.0, 7.0)	2.50 tq (7.0, 7.0)	2.50 tq (7.0, 7.0)
2-Me	1.20 d (7.0)	1.07 d (7.0)	1.08 d (7.0)	1.21 d (7.0)	1.21 d (7.0)	1.20 d (7.0)
3-Me	0.94 t (7.5)	0.85 t (7.5)	0.85 t (7.0)	0.94 t (7.5)	0.94 t (7.5)	0.93 t (7.0)
mba′−2			2.50 tq (7.5, 7.5)			

Table 1. Continued

proton[b]	1	2	3	4	5	6
2-Me			1.20 d (7.0)			
3-Me			0.93 t (7.5)			
iba-2		2.63 sept (7.0, 7.0)		2.54 sept (7.0, 7.0)		
3		1.19 d (7.0)		1.12 d (7.0)		
3′		1.16 d (7.0)		1.17 d (7.0)		
dodeca-2	2.38 t (7.4)					2.42 t (7.5)
12	0.87 t (7.0)					0.87 t (7.5)
8-hydroxydodeca-2					2.42 t (7.5)	
12					0.87 t (7.0)	

[a] Data in C_5D_5. Chemical shifts (δ) are in ppm relative to TMS. The spin coupling (J) is given in parentheses (Hz). Chemical shifts marked with an asterisk (*) indicate overlapped signals. Spin-coupled patterns are designated as follows: s = singlet, d = doublet, t = triplet, q = quartet, m = multiplet, brs = broad signal, sept = septet. [b] Abbreviations: fuc = fucose; rha = rhamnose; glc = glucose; jal = 11-hydroxyhexadecanoyl; mba = 2-methylbutanoyl; iba = 2-methylpropanoyl; dodeca = dodecanoyl; 8-hydroxydodeca = 8-hydroxydodecanoyl.

Table 2. ^{13}C NMR Data of Compounds **1**−**6** (125 MHz)[a]

carbon[b]	1	2	3	4	5	6
glc-1	101.4	104.5	104.6			
2	75.3	82.0	82.0			
3	79.8	76.5	76.5			
4	72.1	71.9	71.9			
5	79.8	77.9	78.0			
6	62.8	62.8	62.8			
fuc-1				101.6	101.6	101.5
2				73.4	73.4	73.5
3				76.7	76.7	76.5
4				73.6	73.6	73.5
5				71.3	71.3	71.2
6				17.2	17.2	17.2
rha-1	100.3	98.8	98.8	100.3	100.3	100.1
2	69.7	73.7	73.7	69.8	69.8	69.9
3	77.8	69.9	70.0	77.9	77.8	77.9
4	78.1	79.8	79.8	77.4	78.0	76.5
5	68.0	68.7	68.5	67.9	67.9	68.0
6	19.4	19.3	19.4	19.2	19.2	19.2
rha′-1	99.2	99.3	99.1	99.1	99.2	99.3
2	72.9	73.0	73.1	72.8	73.0	72.3
3	80.0	79.8	79.8	79.8	80.2	80.2
4	79.8	80.1	80.1	79.4	79.2	78.6
5	68.3	68.2	68.2	68.4	68.3	67.9
6	18.7	18.8	18.8	18.8	18.8	18.7
rha″-1	103.7	103.8	103.8	103.9	103.7	103.4
2	72.6	72.7	72.8	72.6	72.6	72.3
3	70.2	70.2	70.2	70.2	70.2	70.2
4	74.8	74.9	74.8	74.8	74.8	75.2
5	68.1	68.5	68.7	68.2	68.2	68.1
6	17.9	17.8	17.9	17.9	17.9	18.0
rha‴-1	104.3	104.9	104.9	104.4	104.3	
2	72.6	72.5	72.5	72.6	72.7	
3	72.5	72.5	72.5	72.6	72.5	
4	73.7	73.5	73.5	73.6	73.7	
5	70.8	68.7	68.7	70.7	70.8	
6	18.7	18.6	18.6	18.8	18.8	
glc-1						104.8
2						75.2
3						78.5
4						70.7
5						79.5
6						62.5
jal-1	174.9	173.4	173.3	174.8	174.9	174.6
2	33.7	34.3	34.3	33.8	33.7	34.1
11	79.4	82.8	82.8	79.4	79.3	79.5
16	14.4	14.5	14.3	14.4	14.4	14.4
mba-1	176.3	175.5	175.5	176.3	176.3	176.3
2	41.6	41.5	41.5	41.6	41.6	41.5
2-Me	17.0	16.1	16.8	17.0	17.0	16.9
3-Me	11.8	11.8	11.7	11.8	11.8	11.7
mba′-1			176.3			
2			41.5			
2-Me			17.0			
3-Me			11.7			
iba-1		176.9		176.0		
2		34.5		34.2		
3		19.3		19.1		
3′		19.1		19.1		
dodeca-1	172.9					173.5
2	34.4					34.5
12	14.3					14.3
8-hydroxydodeca-1					172.9	
2					34.4	
7					38.4	
8					75.2	
9					38.3	
12					14.3	

[a] Data in C_5D_5. Chemical shifts (δ) are in ppm relative to TMS. [b] Abbreviations: fuc = fucose; rha = rhamnose; glc = glucose; jal = 11-hydroxyhexadecanoyl; mba = methylbutanoyl; iba = methylpropanoyl; dodeca = dodecanoyl; 8-hydroxydodeca = 8-hydroxydodecanoyl.

tetrasaccharides, tricolorins A and E (SA-1199B, MIC 8 μg/mL), and their peracetylated derivatives (SA-1199B, MIC >256 μg/mL)

Scheme 1[a]

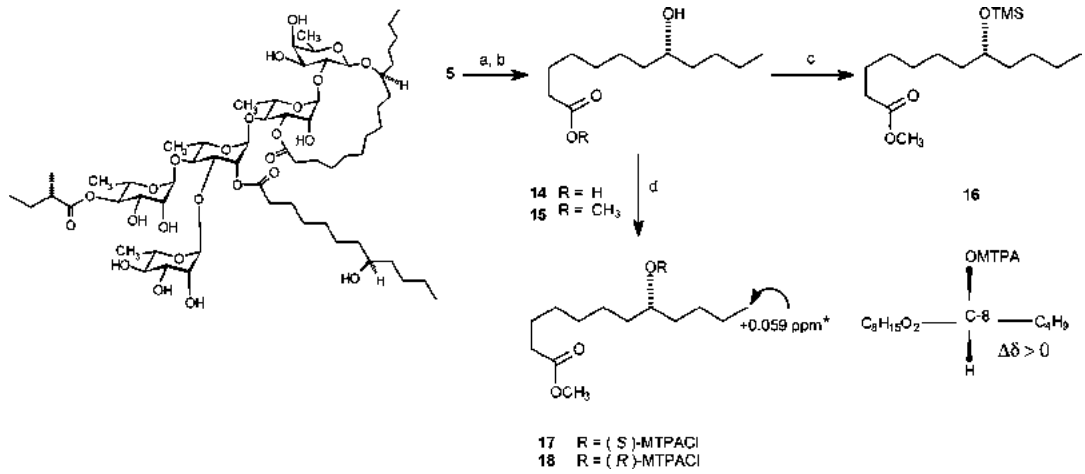

[a] Key: (a) KOH, (b) CH_2N_2, (c) TMSiCl, pyridine, 70 °C, 15 min, (d) (*R*)-MTPACl or (*S*)-MTPACl, DMAP, pyridine, 70 °C, 5 h. *$\Delta\delta = \delta$(**17**) − δ(**18**).

Table 3. Susceptibility of *Staphylococcus aureus* to Selected Convolvulaceous Oligosaccharides and their Cytotoxicity[a]

	ED_{50} (μg/mL)			MIC (μg/mL)				
							SA-1199B[b]	
compound	KB	Hep-2	HeLa	ATCC 25923	XU-212	EMRSA-15	Nor (−)	Nor (+)
1	>20	>20	>20	>512	512	256	32	8[c]
2	>20	>20	>20	>512	512	256	32	8[c]
3	17.9	14.2	16.4	>512	>512	>512	>512	8
4	>20	10.2	12.4	>512	>512	>512	>512	8
5	15.8	>20	>20	>512	>512	>512	>512	8
6	12.1	>20	>20	>512	>512	>512	>512	32
7	15.7	4.7	>20	>512	>512	>512	>512	32
8	>20	>20	>20	>512	256	512	64	8[c]
9	>20	>20	>20	>512	512	256	32	8[c]
10	>20	>20	16.0	>512	>512	>512	>512	8
11	15.4	10.7	>20	>512	>512	>512	>512	8
12	15.0	4.0	>20	>512	>512	>512	>512	8
13	>20	>20	13.2	>512	256	128	64	8[c]
orizabin IX	>20	>20	5.2	>512	>512	256	512	<2[d]
tricolorin A	1.0	1.6	4.7	16	8	4	8	32[e]
tricolorin E	10.6	>20	1.0	16	8	8	8	32[e]
tetracycline				0.125	64	0.125	0.25	
norfloxacin				0.5	8	0.25		32
reserpine								8[f]
vinblastine	0.003	0.007	0.008					

[a] Abbreviations: KB = nasopharyngeal carcinoma; Hep-2 = laryngeal carcinoma; HeLa = cervix carcinoma; ATCC 25923 = standard *S. aureus* strain; XU-212 = a methicillin-resistant *S. aureus* strain possessing the TetK tetracycline efflux protein; EMRSA-15 = epidemic methicillin-resistant *S. aureus* strain containing the *mecA* gene; SA-1199B = multidrug-resistant *S. aureus* strain overexpressing the NorA efflux pump. [b] Nor (−) = minimum inhibitory concentration (MIC) value determined in the susceptibility testing; Nor (+) = MIC value determined for norfloxacin in the modulation assay at the concentration of 25 μg/mL of the tested oligosaccharide. [c] MIC value for norfloxacin in the modulation assay at the concentration of 5 μg/mL of the tested oligosaccharide. [d] MIC value for norfloxacin in the modulation assay at the concentration of 1 μg/mL of the tested oligosaccharide. [e] MIC value for norfloxacin in the modulation assay at the subinhibitory concentration of 2 μg/mL of the tested oligosaccharide. [f] MIC value for norfloxacin in the modulation assay at the concentration of 20 μg/mL of reserpine, which was used as positive control for an efflux pump inhibitor.

was tested in order to compare their effects with those obtained for the orizabin[9] and murucoidin series. The antimicrobial tricolorins and their peracetylated derivatives exhibited no modulatory activity at the subinhibitory concentration of 2 μg/mL for the natural products and 25 μg/mL for the derivatives. The loss of activity for the highly acylated compounds is a comparable situation to the inactivity recorded for the polar analogue[9] since the cellular uptake is not facilitated, probably in this case, by the formation of complex aggregates or micelles that could induced membrane perturbation, provoking an imbalance in the maintenance of cellular homeostasis.[32] Surprisingly, the antimicrobial tricolorins A and B did not display a potentiation effect in combination with norfloxacin. It seems possible that compounds that are nonpolar will not interact with the membrane efflux pumps and those that are too polar are poorly membrane soluble. Therefore, convolvulaceous plants may elaborate an array of amphipathic mixtures of glycolipids to confer selective advantages against microbial infections through a combination of several mechanisms of action; for example, the tricolorin series are cytotoxic, while the murucoidin series exert their action through inhibition of multidrug resistance pumps (Table 3), as previously reported for the structurally related acylated disaccharides found in the leaf exudates of *Geranium* species (Geraniaceae).[33] The most important result from the standpoint of the murucoidins' potential use as therapeutic agents is that by combining these plant noncytotoxic products with commercial antibiotics, which are substrates for these MDR pumps, the treatment of refractive infections caused by effluxing staphylococci could be alleviated. The use of bacterial resistance modifiers such as this type of complex oligosaccharides as prototypes for new efflux pump inhibitors could facilitate the reintroduction of therapeutically ineffective antibiotics into clinical use (e.g., ciprofloxacin) and might even contribute to the suppression of the emergence of new multidrug-resistant bacterial strains, which are a major cause of clinical infections.[10,34] Extracts that have been standardized on these mixtures of glycosides (e.g., orizabins) would also find utility in the development of antiseptic creams to replace or be used in

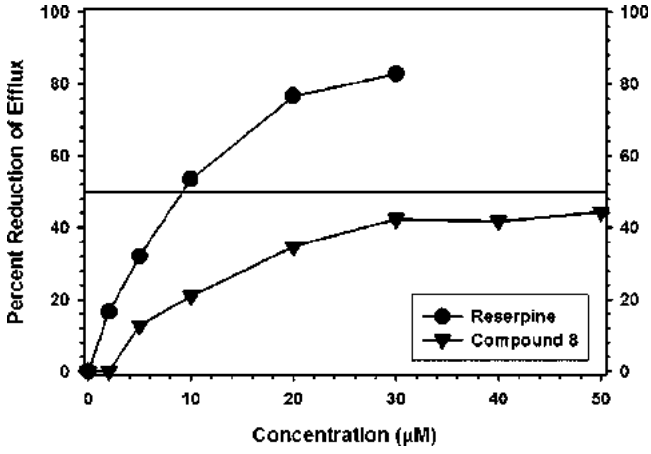

Figure 1. Ethidium efflux inhibition assay against SA-1199B strain cells. The horizontal line indicates 50% efflux inhibition.

combination with mupirocin and fusidic acid, which have wide usage in containment of *S. aureus* and its methicillin-resistant variants in the clinical setting.

Experimental Section

General Experimental Procedures. Melting points were determined on a Fisher-Johns apparatus and are uncorrected. Optical rotations were measured with a Perkin-Elmer 241 polarimeter. ^{1}H (500 MHz) and ^{13}C (125 MHz) NMR experiments were conducted on a Bruker DMX-500 instrument. The NMR techniques were performed according to a previously described methodology.[18,21] Negative-ion LRFABMS and HRFABMS were recorded using a matrix of triethanolamine on a JEOL SX-102A spectrometer. The instrumentation used for HPLC analysis consisted of a Waters 600 E multisolvent delivery system equipped with a Waters 410 differential refractometer detector (Waters Corporation, Milford, MA). Control of the equipment, data acquisition, processing, and management of the chromatographic information were performed by the Empower 2 software program (Waters). GC-MS was performed on a Hewlett-Packard 5890-II instrument coupled to a JEOL SX-102A spectrometer. GC conditions: HP-5MS (5%-phenyl)-methylpolysiloxane column (30 m × 0.25 mm, film thickness 0.25 μm); He, linear velocity 30 cm/s; 50 °C isothermal for 3 min, linear temperature gradient to 300 at 20 °C/min; final temperature hold, 10 min. MS conditions: ionization energy, 70 eV; ion source temperature, 280 °C; interface temperature, 300 °C; scan speed, 2 scans s^{-1}; mass range, 33−880 amu.

Plant Material. Flowers of *Ipomoea murucoides* were collected at the campus of the Universidad Autónoma del Estado de Morelos, Cuernavaca, Morelos, Mexico, on December 12, 2004. The voucher specimens were archived at the Departamento de Farmacia, Facultad de Química, UNAM. Macroscopic anatomical features enabled the collected material to be identified by one of the authors (R.P.-M.) through comparison with a voucher specimen deposited at the HUMO herbarium collection (voucher no. 1520).

Extraction and Isolation. The whole plant material (425 g) was powdered and extracted exhaustively by maceration at room temperature with $CHCl_3$ to afford, after removal of the solvent, a dark brown syrup (39 g). The crude mixture of resin glycosides was obtained after fractionation of this extract by open column chromatography over silica gel eluted with a gradient of MeOH in $CHCl_3$. A total of 220 fractions (250 mL each) were collected and combined to give a pool containing a mixture of resin glycosides, which was subjected to fractionation by open column chromatography over reversed-phase C_{18} (330 g) eluted with MeOH to eliminate waxes and pigmented residues. This process provided 30 secondary fractions (30 mL each). Subfractions 19−25 were combined to yield a mixture of lipophilic pentasaccharides (20 g), which were analyzed by reversed-phase C_{18} HPLC using an isocratic elution with CH_3CN−MeOH (9:1). For their resolution, a Symmetry C_{18} column (Waters; 7 μm, 19 × 300 mm), a flow rate of 9 mL/min, and a differential refractometer detector were used. This analysis allowed the comparison with reference solutions of the previously reported resin glycosides,[5,19] confirming the detection of the following compounds: murucoidin V (**13**, t_R 6.9 min), stoloniferin I (**8**, t_R 7.3 min), murucoidin I (**9**, t_R 13.0 min), pescaprein III (**7**, t_R 16.3 min), murucoidin II (**10**, t_R 21.9 min), murucoidin III (**11**, t_R 24.6 min), and murucoidin IV (**12**, t_R 30.3 min). The eluates across the peaks with t_R values of 7.9 min (peak I), 9.6 min (peak II), 14.3 min (peak III), 17.9 min (peak IV), 18.4 min (peak V), and 22.4 min (peak VI) were collected by the technique of heart cutting and independently reinjected in the apparatus operating in the recycle mode[18,35] to achieve total homogeneity after 15 consecutive cycles. These techniques afforded pure compounds **5** (29 mg) from peak II, **1** (3 mg) from peak III, **2** (3.1 mg) from peak IV, **6** (4.2 mg) from peak V, and **3** (3.0 mg) from peak VI. An isocratic elution with CH_3CN−H_2O (7:3) was used for the resolution of peak I from a complex mixture of related minor oligosaccharide to afford pure major compound **4** (t_R = 24.4 min, 3.2 mg).

Murucoidin VI (1): white powder; mp 143−145 °C; $[\alpha]_D$ −38 (*c* 0.1, MeOH); ^{1}H and ^{13}C NMR, see Tables 1 and 2; negative FABMS *m/z* 1265 $[M - H]^-$, 1181 $[M - H - C_5H_8O]^-$, 1083 $[M - H - C_{12}H_{22}O]^-$, 853 $[1083 - C_6H_{10}O_4$ (methylpentose) $- C_5H_8O]^-$, 561 $[853 - 2 \times 146\ (C_6H_{10}O_4)]^-$, 433 $[561 - 128]^-$, 271 $[Jal - H]^-$; HRFABMS *m/z* 1265.7256 $[M - H]^-$ (calcd for $C_{63}H_{109}O_{25}$ requires 1265.7258).

Murucoidin VII (2): white powder; mp 141−143 °C; $[\alpha]_D$ −39 (*c* 0.11, MeOH); ^{1}H and ^{13}C NMR, see Tables 1 and 2; negative FABMS *m/z* 1153 $[M - H]^-$, 1083 $[M - H - C_4H_6O]^-$, 937 $[1083 - C_6H_{10}O_4]^-$, 791 $[937 - C_6H_{10}O_4]^-$, 561, 433, 271; HRFABMS *m/z* 1153.6000 $[M - H]^-$ (calcd for $C_{55}H_{93}O_{25}$ requires 1153.6006).

Murucoidin VIII (3): white powder; mp 150−152 °C; $[\alpha]_D$ −20 (*c* 0.09, MeOH); ^{1}H and ^{13}C NMR, see Tables 1 and 2; negative FABMS *m/z* 1167 $[M - H]^-$, 1083 $[M - H - C_5H_8O]^-$, 937 $[1083 - C_6H_{10}O_4]^-$, 853 $[937 - C_5H_8O]^-$, 561, 433, 271; HRFABMS *m/z* 1167.6159 $[M - H]^-$ (calcd for $C_{56}H_{95}O_{25}$ requires 1167.6162).

Murucoidin IX (4): white powder; mp 156−158 °C; $[\alpha]_D$ −74 (*c* 0.07, MeOH); ^{1}H and ^{13}C NMR, see Tables 1 and 2; negative FABMS *m/z* 1137 $[M - H]^-$, 1053 $[M - H - C_5H_8O]^-$, 991 $[M - H - C_6H_{10}O_4]^-$, 921 $[991 - C_4H_6O]^-$, 837 $[921 - C_5H_8O]^-$, 545 $[837 - 2 \times 146\ (C_6H_{10}O_4)]^-$, 417 $[545 - 128]^-$, 271 $[Jal - H]^-$; HRFABMS *m/z* 1137.6051 $[M - H]^-$ (calcd for $C_{55}H_{93}O_{24}$ requires 1137.6057).

Murucoidin X (5): white powder; mp 128−130 °C; $[\alpha]_D$ −53 (*c* 0.15, MeOH); ^{1}H and ^{13}C NMR, see Tables 1 and 2; negative FABMS *m/z* 1265 $[M - H]^-$, 1181 $[M - H - C_5H_8O]^-$, 1067 $[M - H - C_{12}H_{22}O_2]^-$, 691 $[1067 - 2 \times 146\ (C_6H_{10}O_4) - C_5H_8O]^-$, 545 $[691 - 146\ (C_6H_{10}O_4)]^-$, 417, 271; HRFABMS *m/z* 1265.7254 $[M - H]^-$ (calcd for $C_{63}H_{109}O_{25}$ requires 1265.7258).

Murucoidin XI (6): white powder; mp 156−158 °C; $[\alpha]_D$ −50 (*c* 0.32, MeOH); ^{1}H and ^{13}C NMR, see Tables 1 and 2; negative FABMS *m/z* 1265 $[M - H]^-$, 1181 $[M - H - C_5H_8O]^-$, 1083 $[M - H - C_{12}H_{22}O]^-$, 921 $[1083 - 162\ (C_6H_{10}O_5) - C_5H_8O]^-$, 545 $[921 - 2 \times 146\ (C_6H_{10}O_4) - C_5H_8O]^-$, 417, 271; HRFABMS *m/z* 1265.7253 $[M - H]^-$ (calcd for $C_{63}H_{109}O_{25}$ requires 1265.7258).

Alkaline Hydrolysis of Resin Glycoside Mixture. A solution of the crude resin glycoside mixture (100 mg) in 5% KOH−H_2O (5 mL) was refluxed at 95 °C for 3 h. The reaction mixture was acidified to pH 4.0 and extracted with $CHCl_3$ (30 mL). The organic layer was washed with H_2O, dried over anhydrous Na_2SO_4, and evaporated under reduced pressure. The aqueous phase was extracted with *n*-BuOH (20 mL) and concentrated to dryness. The residue from the organic phase was directly analyzed by GC-MS to allow the detection of three peaks. MS for the minor constituents with <5% of total chromatogram integration were not recorded. The major constituents were identified as 2-methylpropanoic acid (t_R 4.12 min), *m/z* $[M]^+$ 88 (10), 73 (27), 60 (3), 55 (5), 45 (7), 43 (100), 41 (40), 39 (10), 29 (6), 27 (24); 2-methylbutanoic acid (t_R 7.2 min), *m/z* $[M]^+$ 102 (3), 87 (33), 74 (100), 57 (50), 41 (28), 39 (8); and *n*-dodecanoic acid (t_R 17.8 min), *m/z* $[M]^+$ 200 (15), 183 (2), 171 (18), 157 (40), 143 (10), 129 (48), 115 (20), 101 (15), 85 (33), 73 (100), 60 (80), 57 (30), 55 (47), 43 (44), 41 (30). Previously reported procedures[18] were used for the preparation and identification of 4-bromophenacyl (2*S*)-2-methylbutyrate from the resin glycoside fraction: mp 41−42 °C; $[\alpha]_D$ +18.2 (*c* 1.0, MeOH).

The residue extracted (35 mg) from the aqueous phase was subjected to preparative HPLC on a Waters μBondapak NH_2 column (7.8 × 300 mm; 10 μm). The elution was isocratic with CH_3CN−H_2O (4:1), using a flow rate of 4 mL/min and a sample injection of 500 μL (35 mg/mL). This procedure yielded simonic acid A (6.3 mg, t_R = 4.8 min), operculinic acid C (8.2 mg, t_R = 10.9 min), and simonic acid B (17.0

Chart 1

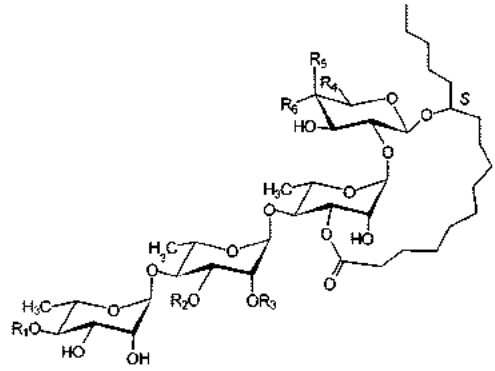

	R_1	R_2	R_3	R_4	R_5	R_6
1	(2*S*)-methylbutanoyl = mba	α-L-rhamnopyranosyl = rha	*n*-dodecanoyl = dodeca	CH_2OH	H	OH
4	methylpropanoyl = iba	rha	mba	CH_3	OH	H
5	mba	rha	(8*R*)-hydroxydodecanoyl	CH_3	OH	H
6	mba	β-D-glucopyranosyl = glc	dodeca	CH_3	OH	H
7	mba	rha	dodeca	CH_3	OH	H
8	mba	rha	mba	CH_3	OH	H
13	mba	glc	mba	CH_3	OH	H

Chart 2

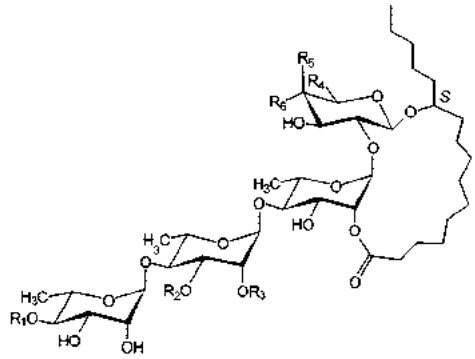

	R_1	R_2	R_3	R_4	R_5	R_6
2	iba	rha	mba	CH_2OH	H	OH
3	mba	rha	mba	CH_2OH	H	OH
9	H	rha	mba	CH_3	OH	H
10	iba	rha	mba	CH_3	OH	H
11	mba	rha	mba	CH_3	OH	H
12	mba	glc	mba	CH_3	OH	H

mg, t_R = 17.0 min), which were identified by comparison of their physical constants and NMR data with published values.

Sugar Analysis. A solution of fractions IV and V (15 mg) in 4 N HCl (10 mL) was heated at 90 °C for 2 h. The reaction mixture was diluted with H_2O (5 mL) and extracted with Et_2O (30 mL). The aqueous phase was neutralized with 1 N KOH, extracted with *n*-BuOH (30 mL), and concentrated to give a colorless solid (5.7 mg). The residue was dissolved in CH_3CN-H_2O and directly analyzed by HPLC: Waters standard column for carbohydrate analysis (μBondapak NH_2; 3.9 × 300 mm, 10 μm), using an isocratic elution of CH_3CN-H_2O (17:3), a flow rate of 1 mL/min, and a sample injection of 20 μL (sample concentration: 5 mg/mL). Co-elution experiments with standard carbohydrate samples allowed the identification of rhamnose (t_R = 5.9 min), fucose (t_R = 7.7 min), and glucose (t_R = 10.1 min). Each of these eluates was individually collected, concentrated, and dissolved in H_2O. Optical activity was recorded after stirring the solutions for 2 h at room temperature: L-rhamnose $[\alpha]_{598}$ +8, $[\alpha]_{578}$ +8, $[\alpha]_{546}$ +9, $[\alpha]_{436}$ +15, $[\alpha]_{365}$ +21 (*c* 0.1, H_2O); D-fucose $[\alpha]_{598}$ +81, $[\alpha]_{578}$ +83, $[\alpha]_{546}$ +94, $[\alpha]_{436}$ +155, $[\alpha]_{365}$ +236 (*c* 0.1, H_2O); D-glucose $[\alpha]_{598}$ +50, $[\alpha]_{578}$ +51, $[\alpha]_{546}$ +57, $[\alpha]_{436}$ +97, $[\alpha]_{365}$ +150 (*c* 0.1, H_2O).

Alkaline Hydrolisis of Murucoidin X (5). Approximately 22 mg of **5** was dissolved in 1 mL of MeOH and 5% $KOH-H_2O$ (4 mL). The solution was refluxed at 95 °C for 2 h. The reaction mixture was acidified to pH 4.0 and extracted three times with 5 mL of Et_2O. The organic layer was washed with H_2O, dried over anhydrous Na_2SO_4, and evaporated under reduced pressure. A small aliquot was directly analyzed by GC-MS with two peaks detected. These were 2-methylbutyric acid (t_R 8.0 min) and 8-hydroxydodecanoic acid (**14**, t_R 25.0 min): *m/z* $[M - OH - H_2O]^+$ 181 (8), 115 (13), 97 (17), 87 (19), 83 (8), 73 (84), 69 (15), 60 (100), 57 (40), 55 (35), 45 (15), 43 (27), 41 (30). The remaining ether extract was reacted with excess diazomethane, concentrated, and analyzed by normal-phase HPLC; for the resolution of this reaction mixture, a normal-phase column (19 × 150 mm, 10 μm), an isocratic elution with hexane−EtOAc (4:1), a flow rate of 2 mL/min, and a differential refractometer were used. The eluates across the peaks with t_R value of 6 min (2-methylbutyric acid methyl ester, $[\alpha]_D$ +10 (*c* 0.1, $CHCl_3$)) and 12.5 min (8-hydroxydodecanoic acid methyl ester (**15**)) were collected and concentrated to dryness. Compound **15** was dissolved in 0.25 mL of pyridine-d_5 and divided into two portions. An aliquot was derivatized with Sigma Sil-A for 15 min at 70 °C. GC-MS analysis gave one peak (**16**, t_R 5.1 min): 274 $[M - 28]^+$ (1.2), 271 $[M - 31]^+$ (2.3), 255 (7), 245 (29), 216 (10), 159 (65), 141 (26), 103 (18), 95 (37), 75 (40), 73 (100). Half of the second aliquot was treated with 4-(dimethylamino)pyridine (3 mg, previously heated at 70 °C for 3 h) and dry pyridine-d_5 (0.75 mL) in NMR tubes.[25] (*R*)-(+)-α-Methoxy-α-trifluoromethylphenylacetyl (MTPA) chloride was added (20 μL). The reaction was allowed to stand at 70−75 °C for 5 h under an atmosphere of N_2. NMR spectra were then recorded at 500 MHz by acquiring the reaction mixture. Further purification was performed as follows. The mixture was transferred from the NMR tubes into a vial. Saturated aqueous $NaHCO_3$ and Et_2O were added to the mixture and stirred vigorously for 5 min. Water (5 mL) was added and the mixture was extracted with $CHCl_3$. The organic phases were washed with 0.5 N HCl, dried with anhydrous Na_2SO_4, and concentrated. The crude residue was purified by normal-phase HPLC using an isocratic elution with hexane−EtOAc (7:3) and a flow rate of 3 mL/min to give the (*S*)-MTPA ester (**17**, t_R 7.5 min). NMR spectra in $CDCl_3$ were recorded after purification. Treatment of the remaining compound **15** with (*S*)-(−)-MTPA chloride as described above yielded the (*R*)-MTPA ester (**18**, t_R 6.9 min).

The aqueous phase from the saponification of compound **5** was extracted with *n*-BuOH (5 mL) and concentrated to give a colorless solid (5 mg). The residue was methylated with CH_2N_2, and the physical and spectroscopic constants (^1H and ^{13}C NMR) registered for the product were identical in all aspects to those previously reported[11] for simonic

acid B methyl ester: white powder; mp 113−115 °C; $[\alpha]_D$ −82.5 (*c* 1.0, MeOH); HRFABMS *m/z* 1015.5322 $[M - H]^-$ (calcd for $C_{47}H_{83}O_{23}$ requires 1015.5325).

(8*R*)-(−)-8-Hydroxydodecanoic Acid Methyl Ester (15): oil; $[\alpha]_{598}$ −15.6, $[\alpha]_{578}$ −16.3, $[\alpha]_{546}$ −16.8, $[\alpha]_{436}$ −18.8, $[\alpha]_{365}$ −20 (*c* 0.1, $CHCl_3$); ^{1}H NMR (400 MHz, $CDCl_3$) δ_H 3.67 (3H, s, OMe), 3.59 (1H, m, H-8), 2.34 (2H, t, J = 7.5 Hz, H-2), 1.64 (2H, m, H-3), 1.46−1.07 (14H, m, H_2-4-H_2-7, and H_2-9-H_2-11), 0.90 (3H, t, J = 7.2, H-12); HRESIMS *m/z* 229.1805 (calcd for $C_{13}H_{25}O_3$, 229.1803).

Bacterial Strains and Media. *Staphylococcus aureus* EMRSA-15 containing the *mecA* gene was provided by Dr. Paul Stapleton, The School of Pharmacy, University of London. Strain XU-212, a methicillin-resistant strain possessing the TetK tetracycline efflux protein, was provided by Dr. E. Udo.[36] SA-1199B, which overexpresses the NorA MDR efflux protein,[37] and *S. aureus* ATCC 25923 were also used. All strains were cultured on nutrient agar (Oxoid, Basingstoke, UK) before determination of MIC values. Cation-adjusted Mueller-Hinton broth (MHB; Oxoid) containing 20 and 10 mg/L of Ca^{2+} and Mg^{2+}, respectively, was used for susceptibility tests.

Susceptibility Testing. Minimum inhibitory concentration values (MIC) were determined at least in duplicate by standard microdilution procedures, as recommended by the National Committee for Clinical Laboratory Standards guidelines.[38] An inoculum density of 5×10^5 cfu of each of the test strains was prepared in 0.9% saline by comparison with a McFarland standard. MHB (125 μL) was dispensed into 10 wells of a 96-well microtiter plate (Nunc, 0.3 mL volume per well). Glycolipids **1**−**13** were tested at final concentrations ranging from 1 to 512 μg/mL prepared by serial 2-fold dilutions. All test compounds were dissolved in DMSO before dilution into MHB for use in MIC determinations. The highest concentration of DMSO remaining after dilution (3.125% v/v) caused no inhibition of bacterial growth. The MIC was defined as the lowest concentration that yielded no visible growth. Tetracycline and norfloxacin from Sigma (Poole, UK) were also tested as positive drug controls. For the modulation assay, the murucoidins were tested at final concentrations of 25 or 5 μg/mL, and the glycolipids orizabin IX and tricolorins A and E at 2 μg/mL. Serial doubling dilutions of norfloxacin in the range 1−512 μg/mL were added, and the microtiter plates were then interpreted in the same manner as MIC determinations. The activity of reserpine at a concentration of 20 μg/mL was also tested as an efflux pump inhibitor for comparison purposes. All samples were tested in duplicate.

Ethidium Efflux Assay. SA-1199B, which overexpresses NorA, was loaded with EtBr as previously described, and the effect of varying concentrations of compounds **8** and **11** on EtBr efflux efficiency was determined to generate a dose−response profile for each oligosaccharide.[37,39] The effect of reserpine was also determined as a positive control. Assays were performed in duplicate, and mean results were expressed as the percentage reduction of total efflux observed for SA-1199B in the absence of inhibitors. This was calculated as follows: [(efflux in the absence of inhibitor − efflux in the presence of inhibitor)/efflux in the absence of inhibitor] × 100.

Cytotoxicity Assay. Nasopharyngeal (KB), cervix (HeLa), and laryngeal carcinoma (Hep-2) cell lines were maintained in RMPI 1640 (10×) medium supplemented with 10% fetal bovine serum. Cell lines were cultured at 37 °C in an atmosphere of 5% CO_2 in air (100% humidity). The cells at log phase of their growth cycle were treated in triplicate with various concentrations of the test samples (0.16−20 μg/mL) and incubated for 72 h at 37 °C in a humidified atmosphere of 5% CO_2. The cell concentration was determined by the NCI sulforhodamine method.[40] Results were expressed as the dose that inhibits 50% control growth after the incubation period (ED_{50}). The values were estimated from a semilog plot of the drug concentration (μg/mL) against the percentage of viable cells. Vinblastine was included as a positive drug control.

Acknowledgment. This research was partially supported by Consejo Nacional de Ciencia y Tecnología (45861-Q) and Dirección General de Asuntos del Personal Académico, UNAM (IN208307). R.P.-M. was on sabbatical leave at the Centre for Pharmacognosy and Phytotherapy (The School of Pharmacy, UL) with the financial support of DGAPA (UNAM). L.C. is grateful to DGAPA for a graduate scholarship. N.J.-H. received posdoctoral scholarships from CONACyT and DGAPA. Thanks are due to G. Duarte and M. Guzmán (USAI, Facultad de Química, UNAM) for the recording of mass spectra.

References and Notes

(1) Felger, R.; Austin, D. F. *Sida* **2005**, *21*, 1293–1303.
(2) The Mexican term "cazahuate" is derived from the Nahuatl ("cuauhzahuatl") words for tree ("quauitl") and mange ("zahuatl"). This medicinal plant complex of arborescent morning glories is composed of six related tree-like *Ipomoea* species: *I. arborescens* (Kunth) G. Don, *I. bracteata* Cav., *I. intrapilosa* Rose, *I. murucoides* Roem. & Schult, *I. pauciflora* Martens & Galeotti, and *I. wolcottiana* Rose.
(3) Emmart, E. W. *The Badianus Manuscript (Codex Barberini, Latin 241). An Aztec Herbal of 1552*; The Johns Hopkins Press: Baltimore, 1940; p 215.
(4) A medicinal plant complex consists of an assemblage of herbal drugs that are taxonomically different at the specific, generic, and/or familial level but that share a common name, one or more key morphological features, certain organoleptic characteristics, and one therapeutic application. For examples, see: (a) Linares, E.; Bye, R. *J. Ethnopharmacol.* **1987**, *19*, 153–183. (b) Pereda-Miranda, R.; Fragoso-Serrano, M.; Escalante-Sánchez, E.; Hernández-Carlos, B.; Linares, E.; Bye, R. *J. Nat. Prod.* **2006**, *69*, 1460–1466.
(5) Chérigo, L.; Pereda-Miranda, R. *J. Nat. Prod.* **2006**, *69*, 595–599.
(6) Baytelman, B. *Acerca de Plantas y Curanderos. Etnobotánica y Antropología Médica en el Estado de Morelos*; Instituto Nacional de Antropología e Historia: Mexico, 1993; pp 91−92.
(7) Argueta Villamar, A.; Cano Asseleih, L. M.; Rodarte, M. E. *Atlas de las Plantas de la Medicina Tradicional Mexicana*; Instituto Nacional Indigenista: Mexico City, 1994; Vol. 1, p 351.
(8) Indian and mestizo populations in Latin America traditionally classified foods, illnesses, medicine, and people as "hot" or "cold". A hot−cold imbalance must be redressed by the ingestion of contrary elements. For the hot−cold dichotomy, see: (a) López Austin, A. *The Human Body and Ideology. Concepts of the Ancient Nahuas*; University of Utah Press: Salt Lake City, UT, 1988; pp 270−282. (b) Ortiz de Montellano, B. R. *Aztec Medicine, Health, and Nutrition*; Rutgers University Press: New Brunswick, NJ, 1990; pp 213−235. (c) Foster, G. M. *Hippocrates' Latin American Legacy. Humoral Medicine in the New World*; Gordon and Breach: Langhorne, 1994; pp 165−195.
(9) Pereda-Miranda, R.; Kaatz, G. W.; Gibbons, S. *J. Nat. Prod.* **2006**, *69*, 406–409.
(10) Stavri, M.; Piddock, L. J. V.; Gibbons, S. *J. Antimicrob. Chemother.* **2007**, *59*, 1247–1260.
(11) Noda, N.; Yoda, S.; Kawasaki, T.; Miyahara, K. *Chem. Pharm. Bull.* **1992**, *40*, 3163–3168.
(12) (a) Ono, M.; Kubo, K.; Miyahara, K.; Kawasaki, T. *Chem. Pharm. Bull.* **1989**, *37*, 241–244. (b) Ono, M.; Kubo, K.; Miyahara, K.; Kawasaki, T. *Chem. Pharm. Bull.* **1989**, *37*, 3209–3213.
(13) Noda, N.; Takahashi, N.; Kawasaki, T.; Miyahara, K.; Yang, C.-R. *Phytochemistry* **1994**, *36*, 365–371.
(14) Ono, M.; Kawasaki, T.; Miyahara, K. *Chem. Pharm. Bull.* **1989**, *37*, 3209–3213.
(15) Barnes, C. C.; Smalley, M. K.; Manfredi, K. P.; Kindscher, K.; Loring, H.; Sheeley, D. M. *J. Nat. Prod.* **2003**, *66*, 1457–1462.
(16) Bah, M.; ChéRigo, L.; Taketa, A. T. C.; Fragoso-Serrano, M.; Hammond, G. B.; Pereda-Miranda, R. *J. Nat. Prod.* **2007**, *70*, 1153–1157.
(17) Pereda-Miranda, R.; Fragoso-Serrano, M.; Escalante-Sánchez, E.; Hernández-Carlos, B.; Linares, E.; Bye, R. *J. Nat. Prod.* **2006**, *69*, 1460–1466.
(18) Pereda-Miranda, R.; Hernández-Carlos, B. *Tetrahedron* **2002**, *58*, 3145–3154.
(19) Pereda-Miranda, R.; Escalante-Sánchez, E.; Escobedo-Martínez, C. *J. Nat. Prod.* **2005**, *68*, 226–230.
(20) Pereda-Miranda, R.; Bah, M. *Curr. Top. Med. Chem.* **2003**, *3*, 111–131.
(21) (a) Bah, M.; Pereda-Miranda, R. *Tetrahedron* **1996**, *52*, 13063–13080. (b) Bah, M.; Pereda-Miranda, R. *Tetrahedron* **1997**, *53*, 9007–9022. (c) Escalante-Sánchez, E.; Pereda-Miranda, R. *J. Nat. Prod.* **2007**, *70*, 1029–1034.
(22) Duus, J. Ø.; Gotfredsen, C. H.; Bock, K. *Chem. Rev.* **2000**, *100*, 4589–5614.
(23) Ahmad, I.; Sherwani, M. R. M.; Hasan, S. Q.; Ahmad, M. S., Jr.; Osman, S. M. *Phytochemistry* **1983**, *22*, 493–494.
(24) Wehrli, F. W.; Wirthlin, T. W. *Interpretation of Carbon-13 NMR Spectra*; John Wiley & Sons: London, 1983; pp 36−37.
(25) http://riodb01.ibase.aist.go.jp/sdbs/cgi-bin/direct_frame_top.cgi
(26) (a) Rieser, M. J.; Hui, Y.-H.; Rupprecht, J. K.; Kozlowski, J. F.; Wood, K. V.; McLaughlin, J. L.; Hanson, P. R.; Zhuang, Z.; Hoye, T. R. *J. Am. Chem. Soc.* **1992**, *114*, 10203–10213. (b) Fragoso-Serrano, M.; González-Chimeo, E.; Pereda-Miranda, R. *J. Nat. Prod.* **1999**, *62*, 45–50. (c) Su, B.-N.; Park, E. J.; Mbwambo, Z. H.; Santarsiero, B. D.; Mesecar, A. D.; Fong, H. H. S.; Pezzuto, J. M.; Kinghorn, A. D. *J. Nat. Prod.* **2002**, *65*, 1278–1282.
(27) Ohtani, I.; Kusumi, T.; Kashman, Y.; Kakisawa, H. *J. Am. Chem. Soc.* **1991**, *113*, 4092–4096.

(28) Ono, M.; Yamada, F.; Noda, N.; Kawasaki, T.; Miyahara, K. *Chem. Pharm. Bull.* **1993**, *41*, 1023–1026.
(29) (a) Masaoka, Y.; Sakakibara, M.; Mori, K. *Agric. Biol. Chem.* **1982**, *46*, 2319–2324. (b) Sugai, T.; Mori, K. *Agric. Biol. Chem.* **1984**, *48*, 2155–2156. (c) Kitagawa, I.; Baek, N. I.; Kawashima, K.; Yokokawa, Y.; Yoshikawa, M.; Ohashi, K.; Shibuya, H. *Chem. Pharm. Bull.* **1996**, *44*, 1680–1692.
(30) (a) Gibbons, S.; Oluwatuyi, M.; Veitch, N.; Gray, A. I. *Phytochemistry* **2003**, *6*, 83–87. (b) Oluwatuyi, M.; Kaatz, G. W.; Gibbons, S. *Phytochemistry* **2004**, *65*, 3249–3254.
(31) Gibbons, S.; Oluwatuyi, M.; Kaatz, G. W. *J. Antimicrob. Chemother.* **2003**, *51*, 13–17.
(32) Rencurosi, A.; Mitchell, E. P.; Cioci, G.; Pérez, S.; Pereda-Miranda, R.; Imberty, A. *Angew. Chem., Int. Ed.* **2004**, *43*, 5918–5922.
(33) Stermitz, F. R.; Cashman, K. K.; Halligan, K. M.; Morel, C.; Tegos, G. P.; Lewis, K. *Bioorg. Med. Chem. Lett.* **2003**, *13*, 1915–1918.
(34) Hershberger, E.; Donabedian, S.; Konstantinou, K.; Zervos, M. *J. Clin. Infect. Dis.* **2004**, *38*, 92–98.
(35) Kubo, I.; Nakatsu, T. *LC-GC* **1990**, *8*, 933–939.
(36) Gibbons, S.; Udo, E. E. *Phytother. Res.* **2000**, *14*, 139–140.
(37) Kaatz, G. W.; Seo, S. M.; Ruble, C. A. *Antimicrob. Agents Chemother.* **1993**, *37*, 1086–1094.
(38) National Committee for Clinical Laboratory Standards. *Methods for Dilution Antimicrobial Susceptibility Tests for Bacteria that Growth Aerobically,* fifth ed.; NCCLS: Villanova, PA, 1999; Approved standard M7-A5.
(39) Kaatz, G. W.; Seo, S. M.; O'Brien, L.; Wahiduzzaman, M.; Foster, T. J. *Antimicrob. Agents Chemother.* **2000**, *44*, 1404–1406.
(40) (a) Skehan, P.; Storeng, R.; Scudiero, D.; Monks, A.; McMahon, J.; Vistica, D.; Warren, J. T.; Bokesch, H.; Kenney, S.; Boyd, M. R. *J. Natl. Cancer Inst.* **1990**, *82*, 1107–1112. (b) Angerhofer, C. K.; Guinaudeau, H.; Wongpanich, V.; Pezzuto, J. M.; Cordell, G. A. *J. Nat. Prod.* **1999**, *62*, 59–66.

NP800148W

Journal of Antimicrobial Chemotherapy (2008) **62**, 345–348
doi:10.1093/jac/dkn178
Advance Access publication 21 April 2008

JAC

Plant phenolic compounds as ethidium bromide efflux inhibitors in *Mycobacterium smegmatis*

Doris Lechner[1], Simon Gibbons[2] and Franz Bucar[1]*

[1]Institute of Pharmaceutical Sciences, Department of Pharmacognosy, Karl-Franzens-University of Graz, Universitaetsplatz 4/I, A-8010 Graz, Austria; [2]Centre for Pharmacognosy and Phytotherapy, The School of Pharmacy, University of London, 29-39 Brunswick Square, London WC1N 1AX, UK

Received 27 November 2007; returned 30 January 2008; revised 28 February 2008; accepted 1 April 2008

***Background*: One-third of the world's population is infected with the dormant tuberculosis bacillus, and there have been no new antimycobacterial compounds with new modes of action for over 30 years. Extensively drug-resistant tuberculosis is resistant to first- and second-line drugs, which can have severe side effects, and requires the breakthrough of new antituberculotics and resistance-modifying agents. Efflux pumps can cause multidrug resistance and have recently evoked much interest as promising new targets in antimicrobial therapy.**

***Objectives*: The study was performed to set up an ethidium bromide (EtBr) efflux assay in *Mycobacterium smegmatis* mc^{2}155 for testing plant natural compounds as mycobacterial efflux pump inhibitors (EPIs).**

***Methods*: After determining the MICs of the putative EPIs, they were tested for synergistic effects with EtBr prior to the efflux assay.**

***Results*: We established an EtBr efflux assay in *M. smegmatis* mc^{2}155. The isoflavone biochanin A exhibited efflux pump inhibiting activity comparable to that of verapamil. The flavone luteolin and the stilbene resveratrol were less active.**

***Conclusions*: A new assay was established to observe the EtBr efflux in *M. smegmatis* and was applied to evaluate plant phenolic compounds. Our results highlighted that the isoflavonoid biochanin A exhibited better EPI activities than other flavonoids in mycobacteria.**

Keywords: isoflavonoids, biochanin A, efflux pumps, mycobacteria

Introduction

Mycobacterial infections including *Mycobacterium tuberculosis* as well as fast-growing strains are increasing globally. The additional prevalence of multidrug-resistant (MDR) strains and extensively drug-resistant tuberculosis[1] stimulates an urgent need for the development of new drugs for the treatment of mycobacterial infections. The mycobacterial cell wall barrier and active multidrug efflux pumps are involved in intrinsic and acquired resistance of these pathogens to many commonly used antibiotics.[2] Efflux pumps can be specific for a class of antibiotics or responsible for MDR.[3] They are attractive antibacterial targets, and the co-administration of an efflux pump inhibitor (EPI) with an antibiotic has progressed to human clinical trials.[4] Effective bacterial EPIs should decrease the intrinsic resistance of bacteria to antibiotics, reverse acquired resistance and reduce the frequency of emergence of resistant mutant strains.[5] According to Stavri *et al*.,[6] there have been no natural EPIs for mycobacteria identified so far.

Every class of the five existing families of efflux pumps is present in *M. tuberculosis*.[2] Reserpine is an inhibitor of ATP-dependent pumps, verapamil inhibits P-glycoprotein and bacterial efflux pumps in general,[2] and chlorpromazine affects potassium flux across the membrane in *Staphylococcus aureus* and the yeast *Saccharomyces cerevisiae*.[7] A feature of all of these compounds is their ability to inhibit potassium transport processes.[8] These inhibitors were used as reference substances to evaluate the extent of possible efflux inhibition in *Mycobacterium smegmatis* mc^{2}155, which expresses many putative efflux pumps.[9] In this paper, we present for the first time

*Corresponding author. Tel: +43-316-3805531; Fax: +43-316-3809860; E-mail: franz.bucar@uni-graz.at

plant natural products with inhibiting effects on ethidium bromide (EtBr) efflux of *M. smegmatis* mc^{2}155.

Materials and methods

Chemicals

EtBr (Sigma-Aldrich, Steinheim, Germany) was dissolved in water. Isoniazid (Sigma-Aldrich) and carbonyl cyanide *m*-chlorophenylhydrazone (CCCP; Fluka/Sigma-Aldrich) were dissolved in DMSO (Merck Darmstadt, Germany). The following test compounds were dissolved in DMSO: Biochanin A, daidzein and formononetin (Fluka, Sigma-Aldrich). Baicalin 95%, baicalein 98%, resveratrol, chlorpromazine hydrochloride, verapamil hydrochloride 98% and reserpine were purchased from Sigma-Aldrich. Luteolin was acquired from Carl RothKG, Karlsruhe, Germany.

Bacterial strains and growth conditions

M. smegmatis mc^{2}155 ATCC 700084 (LGC Promochem, Teddington, Middlesex, UK) was used throughout the study. Bacterial cells were grown on Columbia Blood Agar (CBA; Oxoid, Basingstoke, England, UK) supplemented with 7% defibrinated horse blood (Oxoid) at 37°C under aerobic conditions for 2–3 days prior to assays. MIC and modulation assays were performed in cation-adjusted Mueller–Hinton Broth (MHB; Oxoid).

Difco™ Middlebrook 7H9 Broth (Becton, Dickinson and Company, Le Pont de Claix, France) supplemented with 10% BBL™ Middlebrook OADC Enrichment (Becton, Dickinson and Company, Shannon, Ireland) and 0.05% Tween 80 (for molecular biology, Sigma-Aldrich) or 0.4% Difco™ Glycerol (Becton, Dickinson and Company, Sparks, MI, USA) was used for efflux experiments.

MIC assay and modulation assay

MICs were determined as described previously.[10] Briefly, a standard MIC determination of serially diluted test compounds in Ca^{2+}- and Mg^{2+}-adjusted MHB using bacterial inocula with a density of 5×10^5 cfu/mL was conducted. Plates were incubated at 37°C for 72 h. Isoniazid was used as a positive control.

Test compounds were further screened for their synergistic effects with EtBr prior to efflux assays. Compounds were dissolved in DMSO and diluted in MHB at subinhibitory concentrations. The concentration of the modulators remained the same throughout the experiment, whereas the antibiotics were serially diluted for MIC determination with and without modulator, respectively. A 'modulation factor' (MF) was used to express the modulating effects of compounds on MIC (EtBr).

$$\mathrm{MF} = \mathrm{MIC\ (antibiotic)}/\mathrm{MIC\ (antibiotic} + \textit{modulator})$$

The fractional inhibitory concentration index (FICI)[11] expressed the effect of the combination of antibacterial agents:

$$\mathrm{FICI} = \mathrm{FIC\ (A)} + \mathrm{FIC\ (B)}$$

$$\mathrm{FIC\ (A)} = \mathrm{MIC\ (A\ in\ the\ presence\ of\ B)}/\mathrm{MIC\ (A\ alone)}$$

$$\mathrm{FIC\ (B)} = \mathrm{MIC\ (B\ in\ the\ presence\ of\ A)}/\mathrm{MIC\ (B\ alone)}$$

Synergism, FICI ≤ 0.5; antagonism, FICI ≥ 4.0; and no interaction, FICI > 0.5–4.0.

EtBr efflux assay

This assay was adapted for *M. smegmatis* mc^{2}155 following a method by Kaatz *et al.*[12] for inhibitors of the proton motive force driven multidrug pump NorA in *S. aureus*.

M. smegmatis mc^{2}155 was cultivated on CBA under aerobic conditions at 37°C for 2–3 days, which was then used for inoculating an overnight culture[13] in Tween 80-containing Middlebrook 7H9 broth. This culture was incubated overnight at 37°C, 160 rpm in sterile 50 mL centrifugal tubes and diluted 1:100 in the same medium. Large-scale cultures were grown to mid-exponential phase ($OD_{600} \sim 0.8$–1.0) at 37°C, 80 rpm for 16–24 h.

Cells were loaded with 100 μM of the proton conductor CCCP and 5 μM EtBr and further incubated for 1 h at 37°C. The inoculum was adjusted to $OD_{600} = 0.40$ (0.39–0.41) with EtBr- and CCCP-containing Middlebrook 7H9 (with OADC and Tween 80), 4 mL aliquots were spun down with 5000 **g** for 10 min at 20°C and the pellets were put on ice immediately. Cell pellets were resuspended in 2 mL of glycerol-containing Middlebrook 7H9. EtBr efflux from the cells was monitored at room temperature with a spectrofluorimeter (Perkin Elmer LS50B Luminescence Spectrometer) under constant stirring. The excitation and emission wavelengths used were 530 nm (slit width = 5.0 nm) and 600 nm (slit width = 10.0 nm), respectively, and readings were taken every minute for 10 min. The loss of fluorescence indicated efflux activity. The low background fluorescence of the medium was subtracted from sample and control measurements. Controls without the test compounds were carried out at the beginning and end of the assay, showing that the bacteria did not loose EtBr while stored on ice. Each concentration of the test compounds and the controls was measured at least in duplicate (active compounds at least in triplicate). Mean results were expressed as the percentage reduction of total efflux, which was observed for test strains in the absence of inhibitors for 10 min. Fluorescence levels of all controls and samples had to be within a coefficient of variation of maximal 20%.

Table 1. MICs and modulation factors of compounds for *M. smegmatis* mc^{2}155

Compound	MIC (mg/L)	Concentration as modulator (mg/L)	Modulation factor (EtBr)
Baicalein	64	32	2
Baicalin	256	32	1
Biochanin A	256	10	4–8
		32	16–32
Daidzein	>256	64	1
Formononetin	256	64	1
Genistein	256	32	2
Luteolin	32	8	2
		16	2
Myricetin	32	16	1
Resveratrol	64	16	2
Chlorpromazine	64	8	1
		16	2
Reserpine	>128	20	2
		40	4
Verapamil	>256	20	1–2
		40	2

MIC of isoniazid = 2 mg/L and MIC of EtBr = 16 mg/L.
Modulation factor = MIC (EtBr)/MIC (EtBr + modulator); $n = 4$–8.

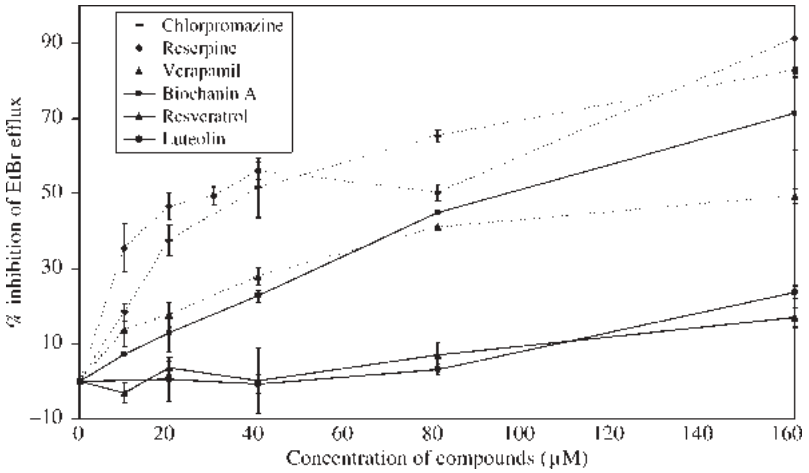

Figure 1. Ethidium efflux inhibition assay from *M. smegmatis* mc^{2}155 cells. Standard EPIs (broken lines): chlorpromazine, bars; reserpine, filled diamonds; verapamil, filled triangles. Test compounds (continuous lines): biochanin A, filled squares; resveratrol, filled triangles; luteolin, filled circles. Values represent means ± SD, $n = 2–6$.

Results

Minimum inhibitory concentrations

The majority of the compounds exhibited weak antimycobacterial activities (Table 1).

Modulating activities

All compounds were further tested for modulating activities of EtBr at subinhibitory concentrations. Biochanin A was shown to be the best modulator and could decrease the MIC of EtBr 4- to 8-fold at 10 mg/L and 16- to 32-fold at 32 mg/L. The FICI between biochanin A and EtBr showed synergism (FICI = 0.25).[11]

With the exception of baicalin, formononetin, daidzein and myricetin, all tested compounds could modulate the MIC of EtBr at least to a small extent.

EtBr efflux inhibition experiments

We validated the EtBr efflux assay using reserpine, which demonstrated efflux inhibition of 91.31 ± 9.36% at 160 μM. Each known EPI tested showed efflux inhibition in *M. smegmatis* mc^{2}155 cells. From all compounds tested, only biochanin A achieved inhibition levels comparable to the standard EPI controls. Luteolin and resveratrol were much less active and myricetin was inactive (Figure 1).

Discussion

The modulation assay with EtBr as an antibiotic seems to be an appropriate pre-screening for flavonoids as EPIs. Therefore, compounds that are able to decrease the MIC of EtBr (MIC = 16 mg/L) in *M. smegmatis* mc^{2}155 should be further tested in the efflux assay. This can be illustrated by comparison of biochanin A, luteolin and myricetin, which show decreasing modulation factors as well as decreasing efflux-inhibiting activities.

The modulation assay also appears to be suitable for bioassay-guided isolation for mycobacterial EPIs, for example from crude plant extracts. As we did not utilize an overexpressing strain, this might explain the quite high concentrations of EPIs to achieve efflux inhibition.

Luteolin exhibited the same antimycobacterial activity as myricetin, but stronger synergism with EtBr. This showed that the hydroxy group at C-3 as well as the number of hydroxyl groups in ring B of flavones influenced EtBr-modulating but not antimycobacterial activity.

The free hydroxyl group in ring B of daidzein slightly increased the modulating activity when compared with formononetin with a *para*-methoxy group in ring B. In contrast, the *para*-methoxy group of biochanin A strongly enhanced the modulating activity when compared with its parent compound genistein. Comparison of biochanin A and formononetin illustrated the relevance of a hydroxy group at C-5 for EtBr-modulating and efflux-inhibiting activities of isoflavones. Comparing baicalin and its aglycone baicalein showed that glycosylation of the hydroxy group at C-7 of flavones reduced antimycobacterial as well as modulating activities, respectively.

Biochanin A showed comparable efflux inhibitory effects to the reference EPIs. The isoflavone biochanin A and its metabolite genistein are potentiators of the antibacterial activities of norfloxacin and berberine in wild-type *S. aureus*,[14] and the authors assumed an inhibiting effect on MDR pumps. Biochanin A might also reverse MDR by inhibiting the P-glycoprotein function in human breast cancer cells and was shown to increase [^{3}H]daunomycin accumulation much more than the positive control verapamil.[15] Combining our results with those of previous literature, biochanin A can override efflux mediated resistance in mammalian as well as bacterial cells.

The experiments of this study were performed on a fast-growing mycobacterial strain, and we emphasize that conclusions on the effects on *M. tuberculosis* should be drawn with care. However, the results obtained with the isoflavonoid biochanin A should stimulate investigations of this class of compounds as inhibitors of mycobacterial efflux pumps.

Acknowledgements

We would like to thank Dr José A. Aínsa (Grupo de Genetica de Micobacterias, Departamento de Microbiologia, Facultad de Medicina, Universidad de Zaragoza, Spain) for helpful discussions. Many thanks to Professor Klaus Groschner and members

of the Institute of Pharmaceutical Sciences, Department of Pharmacology, University of Graz for discussion and technical assistance. The Austrian Academy of Sciences is thanked for the award of a studentship for D. Lechner.

Funding

The Austrian Academy of Sciences awarded a studentship for D. L. (Doc-Fforte 22076). Financial support was provided by the Karl-Franzens-University of Graz.

Transparency declarations

None to declare.

References

1. WHO. XDR-TB Extensively drug-resistant tuberculosis. http://www.who.int/tb/challenges/xdr/en/index.html (9 April 2008, date last accessed).

2. De Rossi E, Ainsa JA, Riccardi G. Role of mycobacterial efflux transporters in drug resistance: an unresolved question. *FEMS Microbiol Rev* 2006; **30**: 36–52.

3. Cattoir V. Efflux-mediated antibiotics resistance in bacteria. *Pathol Biol (Paris)* 2004; **52**: 607–16.

4. Lynch AS. Efflux systems in bacterial pathogens: an opportunity for therapeutic intervention? An industry view. *Biochem Pharmacol* 2006; **71**: 949–56.

5. Marquez B. Bacterial efflux systems and efflux pumps inhibitors. *Biochimie* 2005; **87**: 1137–47.

6. Stavri M, Piddock LJV, Gibbons S. Bacterial efflux pump inhibitors from natural sources. *J Antimicrob Chemother* 2007; **59**: 1247–60.

7. Kaatz GW, Moudgal VV, Seo SM *et al*. Phenothiazines and thioxanthenes inhibit multidrug efflux pump activity in *Staphylococcus aureus*. *Antimicrob Agents Chemother* 2003; **47**: 719–26.

8. Amaral L, Martins M, Viveiros M. Enhanced killing of intracellular multidrug-resistant *Mycobacterium tuberculosis* by compounds that affect the activity of efflux pumps. *J Antimicrob Chemother* 2007; **59**: 1237–46.

9. Li X-Z, Zhang L, Nikaido H. Efflux pump-mediated intrinsic drug resistance in *Mycobacterium smegmatis*. *Antimicrob Agents Chemother* 2004; **48**: 2415–23.

10. Stavri M, Schneider R, O'Donnell G *et al*. The antimycobacterial components of hops (*Humulus lupulus*) and their dereplication. *Phytother Res* 2004; **18**: 774–6.

11. European Committee for Antimicrobial Susceptibility Testing (EUCAST) of the European Society of Clinical Microbiology and Infectious Diseases (ESCMID). Terminology relating to methods for the determination of susceptibility of bacteria to antimicrobial agents. *Clin Microbiol Infect* 2000; **6**: 503–8.

12. Kaatz GW, Seo SM, O'Brien L *et al*. Evidence for the existence of a multidrug efflux transporter distinct from NorA in *Staphylococcus aureus*. *Antimicrob Agents Chemother* 2000; **44**: 1404–6.

13. Parish T, Stoker NG. Electroporation of mycobacteria. *Methods Mol Biol* 1995; **47**: 237–52.

14. Morel C, Stermitz FR, Tegos G *et al*. Isoflavones as potentiators of antibacterial activity. *J Agric Food Chem* 2003; **51**: 5677–9.

15. Chung SY, Sung MK, Kim NH *et al*. Inhibition of P-glycoprotein by natural products in human breast cancer cells. *Arch Pharmacal Res* 2005; **28**: 823–8.

Available online at www.sciencedirect.com
ScienceDirect
Phytochemistry Letters 1 (2008) 71–75
PHYTOCHEMISTRY LETTERS
www.elsevier.com/locate/phytol

Modulation of isoniazid susceptibility by flavonoids in *Mycobacterium*

Doris Lechner [a], Simon Gibbons [b], Franz Bucar [a,*]

[a] *Institute of Pharmaceutical Sciences, Department of Pharmacognosy, Karl-Franzens-University, Universitätsplatz 4/I, 8010 Graz, Austria*
[b] *Centre for Pharmacognosy and Phytotherapy, The School of Pharmacy, University of London, 29-39 Brunswick Square, London WC1N 1AX, UK*

Received 24 October 2007; received in revised form 10 January 2008; accepted 11 January 2008
Available online 20 March 2008

Abstract

In the course of a project to identify plant natural products which modulate the susceptibility of different strains of fast-growing mycobacteria to the first-line antituberculotic isoniazid (INH), several flavonoids without significant antimycobacterial activities at the tested concentrations were screened for their ability to decrease the minimum inhibitory concentrations (MICs) of INH. Flavonoids with different substitution patterns, namely epicatechin, isorhamnetin, kaempferol, luteolin, myricetin, quercetin, rutin and taxifolin were tested to examine structure–activity relationships (SARs) of these compounds. Different mycobacterial strains, i.e. *Mycobacterium smegmatis* (ATCC 14468), *M. smegmatis* mc^2155 (ATCC 700084), *M. smegmatis* $mc^2$2700, *M. phlei* (ATCC 11758) and *M. fortuitum* (ATCC 6841) were used. The strongest synergistic effects were observed in *M. smegmatis* mc^2155 followed by *M. phlei*, whereas the tendency of INH potentiation by certain flavonoids remained the same within each strain. Myricetin was the most efficient intensifier of INH susceptibility in all tested strains causing a decrease of the MIC of INH up to 64-fold at 16 μg/ml, followed by quercetin. Structure–activity relationships of flavonoids as intensifiers of INH susceptibility in mycobacteria indicate that they overlap with SARs for their radical-scavenging properties, however the potentiation of INH activity cannot only be explained by their radical-scavenging activity alone.

Keywords: Mycobacteria; Isoniazid susceptibility; Resistance modulation; Flavonoids; Myricetin

1. Introduction

Infections associated with mycobacteria including *Mycobacterium tuberculosis* are increasing worldwide and the additional prevalence of multidrug-resistant (MDR) strains requires the development of new drugs for the therapy of mycobacterial infections. One third of the world's population is infected with the dormant tuberculosis (TB) bacillus (Cantrell et al., 2001; Eddleston and Pierini, 1999; Smith et al., 2004). TB can usually be treated with a regime of the four first-line anti-TB drugs isoniazid (INH), rifampicin (RIF), pyrazinamide (PZA) and ethambutol (EMB) (Blumberg et al., 2003). In case of misuse, MDR strains are likely to develop. Most drug-resistant clinical isolates of the tubercle bacillus are resistant to isoniazid (Marrakchi et al., 2000). The treatment of MDR-TB takes more time with second-line drugs (cycloserine, ethionamide/prothionamide, streptomycin, amikacin/kanamycin, capreomycin, *p*-aminosalicylic acid, and fluoroquinolones), which are more expensive and also have more side-effects (WHO, 2007). Extensively drug-resistant tuberculosis (XDR-TB) is resistant to first- and second-line drugs and is usually a result of misuse, mismanagement or non-patient compliance due to side-effects (WHO, 2007). The INH resistance mechanisms of mycobacteria are very complex (Viveiros et al., 2002). Fifty to 60% of the strains have individual mutations of genes encoding a catalase-peroxidase (*katG*), an enzyme of the mycolic acid pathway (*inhA*), and a β-ketoacyl-acyl carrier protein synthetase (*kasA*). INH resistance has furthermore been related to INH neutralization by the over-production of arylamine *N*-acetyltransferase, by limitation of NAD^+-binding proteins, and by the overexpression of anti-oxidant enzymes that compensate for the loss of function of the KatG protein (Hillas et al., 2000; Viveiros et al., 2002; Zhao et al., 2006). In 20% of all INH-resistant strains there still remain mechanisms that are different to those mentioned above (Viveiros et al., 2002). Recent research has given evidence that resistance to INH can also be mediated by energy-dependent efflux pumps (Choudhuri et al., 1999; De Rossi et al., 2006; Pasca et al., 2005) and that the induction of high level resistance to INH may be due to the activation or induction of an efflux

* Corresponding author. Tel.: +43 316 3805531; fax: +43 316 3809860.
E-mail address: franz.bucar@uni-graz.at (F. Bucar).

1874-3900/$ – see front matter
doi:10.1016/j.phytol.2008.01.002

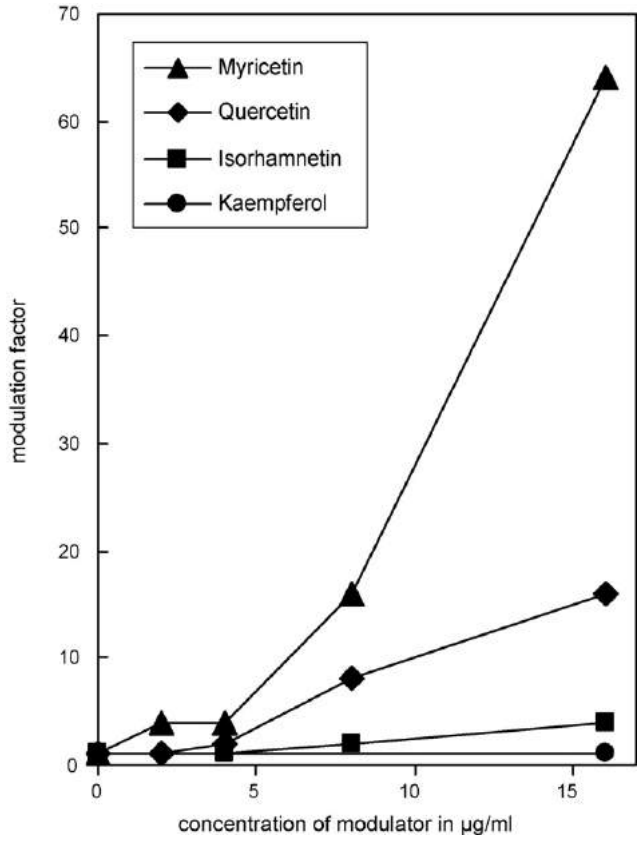

Fig. 1. Modulation of INH susceptibility by various concentrations of flavonols with different B-ring substitution patterns in *M. smegmatis* mc^{2}155.

pump mechanism (Colangeli et al., 2005; Gumbo et al., 2007; Viveiros et al., 2002).

In an ongoing project to identify new antimycobacterial compounds from plants, we screened flavonoids, which in combination with INH, decreased the minimum inhibitory concentrations (MICs) of INH against different mycobacterial strains. At present, a lot of research concerning compounds that reduce the risk of development of resistance to chemotherapeutic agents in anti-cancer and antimicrobial therapy is going on. Roufogalis et al. (2007) describe the flavonoid methylvitexin as an inhibitor of resistance mediated by a cell transporter protein and in particular P-glycoprotein and/or the breast cancer resistance protein. In earlier investigations, catechin has been described to potentiate the action of streptomycin against the tubercle bacillus in mice and decreases the incidence of pulmonary tuberculosis fourfold (Martin et al., 1949), indicating the potential of flavonoids as resistance modifying compounds. In a recent study by Brown et al. (2007) the antimycobacterial activity of the flavonoids butein and isoliquiritigenin could be related to their inhibitory effect on fatty acid and mycolic acid biosynthesis.

In this paper we present the INH modulating activities of (−)-epicatechin, isorhamnetin, kaempferol, luteolin, myricetin, quercetin, rutin and taxifolin in *M. smegmatis*, *M. smegmatis* mc^{2}155, *M. smegmatis* mc^{2}2700, *M. fortuitum* and *M. phlei* which could be co-administered with anti-TB chemotherapy to prevent or overcome resistance to INH (Fig. 1).

2. Results and discussion

All investigated flavonoids were screened for antimycobacterial activities prior to modulation assays (Fig. 2). Each tested compound caused at least a twofold decrease of the MICs of INH at subinhibitory concentrations. MICs and modulation factors are summarized in Tables 1 and 2.

Only three of the tested flavonoids, i.e. myricetin, quercetin and luteolin showed moderate antimycobacterial activities with MIC values ranging from 32 to 64 µg/ml. (−)-Epicatechin as well as rutin exhibited weak activities from 128 to 256 µg/ml against *M. fortuitum*.

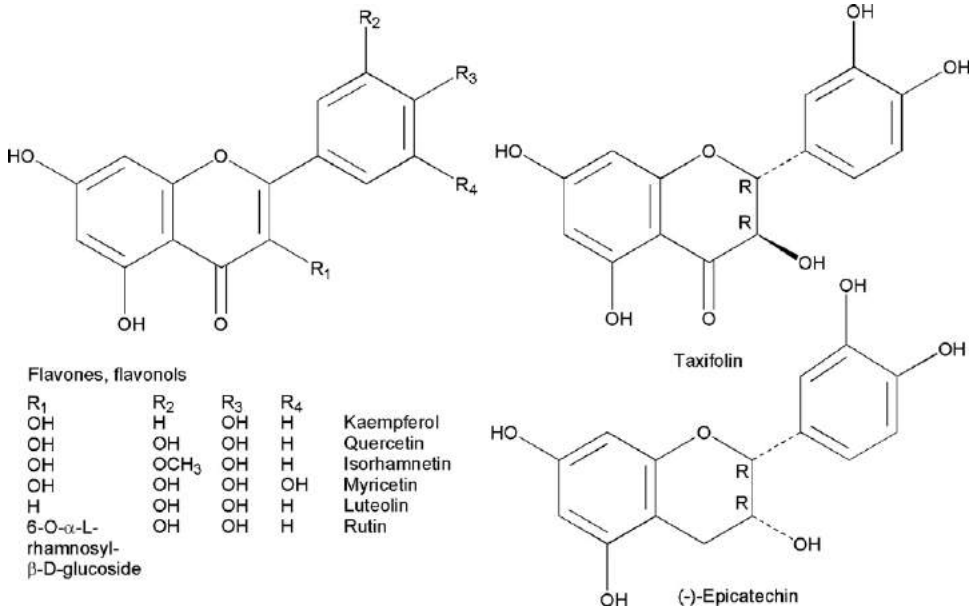

Fig. 2. Structures of the investigated compounds.

Table 1
Minimum inhibitory concentrations (MIC values, μg/ml) of flavonoids

Compound	Strains				
	M. smegmatis mc^{2}155	*M. smegmatis* (ATCC 14468)	*M. smegmatis* mc^{2}2700	*M. fortuitum*	*M. phlei*
(−)-Epicatechin	>128	>128	>128	>128	>128
Isorhamnetin	>256	>128	>128	>128	>256
Kaempferol	>256	>128	>128	>128	256
Luteolin	128–256	>128	16–32	32	64–128
Myricetin	32	64	64	>128	64
Quercetin	>256	128	64	>256	>256
Rutin	>128	>128	>128	128	>128
Taxifolin	>128	>128	>128	>128	>128
INH	2	(1–)2	2(–4)	1(–2)	4
EMB	2	0.5	1	4	0.5
RIF	32	64	32	8	0.5

The SARs for these flavonoids as modulators of isoniazid activity indicate that they overlap SARs for their radical-scavenging properties. Their radical-scavenging activity is enhanced by the number of hydroxy groups, a 2,3-double bond in conjugation with a 4-oxo group and an orthodiphenolic structure, especially as a pyrogallol group in ring B as seen in myricetin (Pietta, 2000). Glycosylation (blocking the 3-OH in C-ring) and the lack of OH or presence of a methoxy in B-ring decrease the radical-scavenging effect (Sroka, 2005). The catechol group in ring B is the major structure for radical-scavenging capacity of flavonoids. It has better electron-donating properties and is a radical target, whereas the 2,3-double bond conjugated with the 4-oxo group is responsible for electron delocalization (Pietta, 2000). Nevertheless their modulating activities cannot only be explained by these moieties. According to these criteria decreasing activities should be found in the following order: myricetin > quercetin > rutin/luteolin/taxifolin > (−)-epicatechin > isorhamnetin/kaempferol. This order fits only for the most active flavonoids myricetin and quercetin as well as for the weakest compound kaempferol.

For comparison we conducted our modulation screening of INH activity against different mycobacterial strains. Most modulators showed the strongest INH potentiation against *M. smegmatis* mc^{2}155, a strain which expresses different efflux pumps. Comparison of modulation results between this strain and *M. smegmatis* (ATCC 14468) could indicate efflux inhibition. *M. smegmatis* mc^{2}2700 overexpresses the fatty acid synthase gene (fas 1) from *M. tuberculosis* (Zimhony et al., 2004). Antimycobacterial screening against this strain and *M. smegmatis* (ATCC 14468) could reveal if a compound inhibits FAS-I, a target of the activated antituberculotic pyrazinamide (Zimhony et al., 2000; Zimhony et al., 2004). Remarkably, *M. tuberculosis* has both types of fatty acid synthase systems found in nature: FAS-I is usually found in eukaryotes other than plants, and FAS-II is found in bacteria and plants (Duncan, 2004).

Luteolin showed an approximately eightfold reduced MIC against *M. smegmatis* mc^{2}2700 compared to other *M. smegmatis* strains. This indicates that luteolin could be a potential inhibitor of FAS-I. As luteolin-7-glucoside turned out to be the first plasmodial FAS-II inhibiting natural product targeting the malarial FabI enzyme (Kirmizibekmez et al., 2004), we further tested luteolin-7-glucoside and luteolin-5-glucoside, respectively. Both compounds were inactive, which clearly demonstrates that the 5-hydroxy as well as the 7-hydroxy group are essential for the antimycobacterial activity of luteolin. However, they moderately decreased the MIC of INH twofold in *M. smegmatis* mc^{2}2700.

Myricetin with a 2,3-double bond and three hydroxyl groups in ring B was by far the most active compound concerning modulating activity, however it also exhibited moderate

Table 2
Modulation factors and reference concentrations of flavonoids against different strains of mycobacteria (nt, not tested)

Compound	[C] (μg/ml)	Strains				
		M. smegmatis mc^{2}155	*M. smegmatis* (ATCC 14468)	*M. smegmatis* mc^{2}2700	*M. fortuitum*	*M. phlei*
(−)-Epicatechin	32	16	4	4	4	8
Isorhamnetin	32	8	1–2	2	2	4
Kaempferol	32	2	2	1	2	2
Luteolin	32	4	2	nt	nt	32
	8	nt	nt	2	2	4–8
Myricetin	16	64	8	8	8	16
Quercetin	16	16–32	2	8	4	8–16
Rutin	32	2	4	2	2	4
Taxifolin	32	4	4	2	2	1

antimycobacterial activity (MIC = 32 μg/ml). In combination it exhibited a synergistic and not additive antibiotic effect with INH with a fractional inhibitory concentration index (FICI) of 0.2. Myricetin was the most active INH modulator and could decrease the MIC of INH 16-fold at a concentration of 8 μg/ml and 64-fold at a concentration of 16 μg/ml, respectively in *M. smegmatis* mc^2155. Myricetin did not decrease the MIC values of other antibiotics such as ethambutol, rifampicin, streptomycin, ciprofloxacin or tetracycline. This further supports the synergistic activity and specificity for INH potentiation. Quercetin turned out to be the second active compound lacking one hydroxy group in ring B compared to myricetin. A comparison between quercetin and luteolin indicated that the 3-hydroxy group enhances both antimycobacterial and potentiation activities, respectively. Kaempferol was the least active compound and highlighted the importance of the presence of adjacent hydroxy groups in ring B for potentiation activity of flavonoids when compared to quercetin or luteolin. This SAR was also supported by the stronger activity of quercetin compared to isorhamnetin. Correlations between the structures of kaempferol and taxifolin showed that the number of hydroxyl groups in ring B (catechol groups) and the 3-hydroxyl seemed to be more important for potentiation activity than the 2,3-double bond.

Flavonoids are known inhibitors of multidrug resistance proteins (MRP) with efflux activity (Bobrowska-Hagerstrand et al., 2003). Myricetin can override *in vitro* cellular MRP1- and MRP2-mediated vincristine resistance (van Zanden et al., 2005). We therefore assume that our tested flavonoids could also inhibit mycobacterial efflux pumps and that the mode of action of INH potentiation is not only mediated by their antioxidant activity. INH is a prodrug and susceptible to oxidative reactions catalyzed by KatG resulting in an IN-NAD (INH-nicotinamide adenine dinucleotide) adduct molecule (Zhao et al., 2006). The IN-NAD adduct molecule is a strong inhibitor of InhA, a key enzyme involved in the biosynthesis of mycolic acids for the mycobacterial cell wall. Low concentrations of H_2O_2 are necessary so that KatG can efficiently catalyze the INH activation. It is possible that the flavonoids additionally keep the H_2O_2 level low (Zhao et al., 2006). Another hypothesis is that the antioxidants remove a natural substrate of KatG and therefore provide more peroxidase activity with INH (Magliozzo, 2007, pers. commun.). Nevertheless flavonoids seem to be potential adjuvants in anti-TB therapy. Further *in vivo* studies are necessary to assess if they can facilitate the lowering of INH dosages in chemotherapy, therefore reduce toxic side-effects, lead to better patient compliance and also prevent or overcome acquired resistance to INH.

3. Experimental section

3.1. General experimental procedures

Flavonoids were purchased from Carl Roth KG Karlsruhe, Germany. Purities were checked by TLC or HPLC. Isoniazid, ethambutol, rifampicin, streptomycin sulfate and tetracyclin were supplied by Sigma–Aldrich Chemie Gmbh, Steinheim, Germany. Ciprofloxacin was obtained from Bayer HealthCare, Leverkusen, Germany.

3.2. Bacterial strains

Bacteria were obtained from the American Type Culture Collection: *M. smegmatis* (ATCC 14468), *M. smegmatis* mc^2155 (ATCC 700084), *M. fortuitum* (ATCC 6841) and *M. phlei* (ATCC 11758). The *M. smegmatis* $mc^2 2700$ strain overexpresses the fatty acid synthase gene (fas 1) from *M. tuberculosis* (Zimhony et al., 2004) and was a generous gift from Dr. Oren Zimhony, Infectious Diseases Unit, Kaplan Medical Center, Hebrew University and Hadassah Medical School, Jerusalem. All strains were cultured on Columbia Blood Agar (Oxoid Ltd., Basingstoke, Hampshire, England) supplemented with 7% defibrinated horse blood (Oxoid) under aerobic conditions and incubated for 72 h at 37 °C prior to MIC determinations or modulation assays, respectively.

3.3. Minimum inhibitory concentration

An *in vitro* assay was used to exclude antimycobacterial activity of the flavonoids or to choose subinhibitory concentrations for the modulation assay. Compounds and standard antibiotics were dissolved in DMSO and serially diluted (twofold) with cation adjusted Mueller Hinton Broth (MHB, Oxoid) to particular concentrations in a 96-well microtiter plate (Iwaki, Microplate 96-well/flat bottom, 0.35 ml well capacity). Bacterial inoculum (density of 5×10^5 cfu/ml after dilution of an inoculum adjusted to Mac Farland turbidity standard 0.5) was added to the wells and the plate was incubated at 37 °C for 72 h. The MIC was recorded as the lowest concentration at which no growth was observed after the addition of 20 μl of a 5 mg/ml methanolic solution of 3-[4,5-dimethylthiazol-2-yl]-2,5-diphenyltetrazolium bromide (MTT; Sigma) and incubation for 30 min. A blue colouration indicated bacterial growth, whereas wells without bacterial growth stayed yellow. DMSO and INH controls were included in all assays. The highest final DMSO concentrations were 62.5 μl DMSO/ml in MIC determinations and 72.9 μl/ml in modulation assays, respectively. For modulation assays, flavonoids were dissolved in DMSO and diluted into MHB at different subinhibitory concentrations. These media were then used for the minimum inhibitory concentration assay to screen for synergistic effects with INH. Results were obtained from experiments carried out in at least duplicate.

The extent of MIC modulation was expressed by the modulation factor (MF):

$$\mathrm{MF} = \frac{\mathrm{MIC\,(antibiotic)}}{\mathrm{MIC\,(antibiotic + modulator)}}$$

A modulation factor of 16 indicated a 16-fold reduction of MIC in the presence of a modulator in a certain concentration.

The fractional inhibitory concentration index expressed the effect of the combination of antibacterial agents:

$$\mathrm{FICI} = \mathrm{FIC(A)} + \mathrm{FIC(B)},$$

$$\mathrm{FIC(A)} = \frac{\mathrm{MIC(A\ in\ the\ presence\ of\ B)}}{\mathrm{MIC(A\ alone)}},$$

$$\mathrm{FIC(B)} = \frac{\mathrm{MIC(B\ in\ the\ presence\ of\ A)}}{\mathrm{MIC(B\ alone)}}$$

Synergism: FICI $\leq$ 0.5, antagonism: FICI $\geq$ 2, additive effects: FICI = 0.5–1.0, indifferent effects: FIC >1 to <2 (European Committee for Antimicrobial Susceptibility Testing (EUCAST) of the European Society of Clinical Microbiology and Infectious Diseases (ESCMID), 2000).

Acknowledgement

The Austrian Academy of Sciences is thanked for the award of a studentship to D. Lechner (Doc-Fforte 22076).

References

Blumberg, H.M., Burman, W.J., Chaisson, R.E., Daley, C.L., Etkind, S.C., Friedman, L.N., Fujiwara, P., Grzemska, M., Hopewell, P.C., Iseman, M.D., Jasmer, R.M., Koppaka, V., Menzies, R.I., O'Brien, R.J., Reves, R.R., Reichman, L.B., Simone, P.M., Starke, J.R., Vernon, A.A., 2003. American Thoracic Society/Centers for Disease Control and Prevention/Infectious Diseases Society of America: Treatment of tuberculosis. Am. J. Respir. Crit. Care Med. 167, 603–662.

Bobrowska-Hagerstrand, M., Wrobel, A., Mrowczynska, L., Soderstrom, T., Shirataki, Y., Motohashi, N., Molnar, J., Michalak, K., Hagerstrand, H., 2003. Flavonoids as inhibitors of MRP1-like efflux activity in human erythrocytes. A structure–activity relationship study. Oncol. Res. 13, 463–469.

Brown, A.K., Papaemmanouil, A., Bhowruth, V., Bhatt, A., Dover, L.G., Besra, G.S., 2007. Flavonoid inhibitors as novel antimycobacterial agents targeting Rv0636, a putative dehydratase enzyme involved in *Mycobacterium tuberculosis* fatty acid synthase II. Microbiology 153, 3314–3322.

Cantrell, C.L., Franzblau, S.G., Fischer, N.H., 2001. Antimycobacterial plant terpenoids. Planta Med. 67, 685–694.

Choudhuri, B.S., Sen, S., Chakrabarti, P., 1999. Isoniazid accumulation in *Mycobacterium smegmatis* is modulated by proton motive force-driven and ATP-dependent extrusion systems. Biochem. Biophys. Res. Commun. 256, 682–684.

Colangeli, R., Helb, D., Sridharan, S., Sun, J., Varma-Basil, M., Hazbon, M.H., Harbacheuski, R., Megjugorac, N.J., Jacobs Jr., W.R., Holzenburg, A., Sacchettini, J.C., Alland, D., 2005. The *Mycobacterium tuberculosis* iniA gene is essential for activity of an efflux pump that confers drug tolerance to both isoniazid and ethambutol. Mol. Microbiol. 55, 1829–1840.

De Rossi, E., Ainsa, J.A., Riccardi, G., 2006. Role of mycobacterial efflux transporters in drug resistance: An unresolved question. FEMS Microbiol. Rev. 30, 36–52.

Duncan, K., 2004. Identification and validation of novel drug targets in tuberculosis. Curr. Pharm. Des. 10, 3185–3194.

Eddleston, M., Pierini, S., 1999. Oxford Handbook of Tropical Medicine. Oxford University Press.

European Committee for Antimicrobial Susceptibility Testing (EUCAST) of the European Society of Clinical Microbiology and Infectious Diseases (ESCMID), 2000. Terminology relating to methods for the determination of susceptibility of bacteria to antimicrobial agents. Clin. Microbiol. Infect. 6, 503–508.

Gumbo, T., Louie, A., Liu, W., Ambrose Paul, G., Bhavnani Sujata, M., Brown, D., Drusano, G.L., 2007. Isoniazid's bactericidal activity ceases because of the emergence of resistance, not depletion of *Mycobacterium tuberculosis* in the log phase of growth. J. Infect. Dis. 195, 194–201.

Hillas, P.J., Del Alba, F.S., Oyarzabal, J., Wilks, A., De Montellano, P.R.O., 2000. The AhpC and AhpD antioxidant defense system of *Mycobacterium tuberculosis*. J. Biol. Chem. 275, 18801–18809.

Kirmizibekmez, H., Calis, I., Perozzo, R., Brun, R., Doenmez, A.A., Linden, A., Rueedi, P., Tasdemir, D., 2004. Inhibiting activities of the secondary metabolites of *Phlomis brunneogaleata* against parasitic Protozoa and plasmodial enoyl-ACP reductase, a crucial enzyme in fatty acid biosynthesis. Planta Med. 70, 711–717.

Marrakchi, H., Laneelle, G., Quemard, A., 2000. InhA, a target of the antituberculous drug isoniazid, is involved in a mycobacterial fatty acid elongation system, FAS-II. Microbiology 146, 289–296.

Martin, G.J., Carley Jr., J., Moss, J.N., 1949. Agylcone flavonoids in experimental chemotherapy. Exp. Med. Surg. 7, 391–393.

Pasca, M.R., Guglierame, P., De Rossi, E., Zara, F., Riccardi, G., 2005. mmpL7 gene of *Mycobacterium tuberculosis* is responsible for isoniazid efflux in *Mycobacterium smegmatis*. Antimicrob. Agents Chemother. 49, 4775–4777.

Pietta, P.-G., 2000. Flavonoids as antioxidants. J. Nat. Prod. 63, 1035–1042.

Roufogalis, B., Marks, D., Duke, R., 2007. A method of treatment with flavonoids for overcoming acquired or inherent resistance to chemotherapeutic compounds. PCT Int. Appl. 57.

Smith, C.V., Sharma, V., Sacchettini, J.C., 2004. TB drug discovery: Addressing issues of persistence and resistance. Tuberculosis 84, 45–55.

Sroka, Z., 2005. Antioxidative and antiradical properties of plant phenolics. Z. Naturforsch. C: J. Biosci. 60, 833–843.

van Zanden, J.J., de Mul, A., Wortelboer, H.M., Usta, M., van Bladeren, P.J., Rietjens, I.M.C.M., Cnubben, N.H.P., 2005. Reversal of in vitro cellular MRP1 and MRP2 mediated vincristine resistance by the flavonoid myricetin. Biochem. Pharmacol. 69, 1657–1665.

Viveiros, M., Portugal, I., Bettencourt, R., Victor, T.C., Jordaan, A.M., Leandro, C., Ordway, W., Amaral, L., 2002. Isoniazid-induced transient high-level resistance in *Mycobacterium tuberculosis*. Antimicrob. Agents Chemother. 46, 2804–2810.

WHO. (2007). XDR-TB Extensively drug-resistant tuberculosis. URL in August 2007, http://www.who.int/tb/xdr/en/index.html.

Zhao, X., Yu, H., Yu, S., Wang, F., Sacchettini, J.C., Magliozzo, R.S., 2006. Hydrogen peroxide-mediated isoniazid activation catalyzed by *Mycobacterium tuberculosis* catalase-peroxidase (KatG) and its S315T mutant. Biochemistry 45, 4131–4140.

Zimhony, O., Cox, J.S., Welch, J.T., Vilcheze, C., Jacobs Jr., W.R., 2000. Pyrazinamide inhibits the eukaryotic-like fatty acid synthetase I (FASI) of *Mycobacterium tuberculosis*. Nat. Med. 6, 1043–1047.

Zimhony, O., Vilcheze, C., Jacobs Jr., W.R., 2004. Characterization of *Mycobacterium smegmatis* expressing the *Mycobacterium tuberculosis* fatty acid synthase I (fas1) gene. J. Bacteriol. 186, 4051–4055.

ANTIMICROBIAL AGENTS AND CHEMOTHERAPY, Dec. 2007, p. 4480–4483 Vol. 51, No. 12
0066-4804/07/$08.00+0 doi:10.1128/AAC.00216-07

The Phenolic Diterpene Totarol Inhibits Multidrug Efflux Pump Activity in *Staphylococcus aureus*▽

Eileen C. J. Smith,[1] Glenn W. Kaatz,[2,3] Susan M. Seo,[3] Neale Wareham,[4] Elizabeth M. Williamson,[5] and Simon Gibbons[1]*

Centre for Pharmacognosy and Phytotherapy, The School of Pharmacy, University of London, 29-39 Brunswick Square, London WC1N 1AX, United Kingdom[1]; The John D. Dingell Department of Veteran's Affairs Medical Centre[2] and Department of Internal Medicine, Division of Infectious Diseases, School of Medicine, Wayne State University,[3] Detroit, Michigan 48201; Stiefel International R&D, Whitebrook Park, 68 Lower Cookham Road, Maidenhead, Berkshire SL6 8XY, United Kingdom[4]; and Department of Pharmacy, University of Reading, Whiteknights, Reading, Berks RG6 6AJ, United Kingdom[5]

Received 13 February 2007/Returned for modification 23 March 2007/Accepted 24 July 2007

The phenolic diterpene totarol had good antimicrobial activity against effluxing strains of *Staphylococcus aureus*. Subinhibitory concentrations reduced the MICs of selected antibiotics, suggesting that it may also be an efflux pump inhibitor (EPI). A totarol-resistant mutant that overexpressed *norA* was created to separate antimicrobial from efflux inhibitory activity. Totarol reduced ethidium efflux from this strain by 50% at 15 μM (1/4× MIC), and combination studies revealed marked reductions in ethidium MICs. These data suggest that totarol is a NorA EPI as well as an antistaphylococcal antimicrobial agent.

Efflux is a common resistance mechanism employed by bacteria. Multidrug resistance (MDR) pumps can confer resistance to bile, hormones, and other substances produced by the host and may play a role in host colonization (24). The NorA MDR pump of *Staphylococcus aureus* effluxes a broad spectrum of compounds, including fluoroquinolones, quaternary ammonium compounds, ethidium bromide, rhodamine, and acridines (17). In addition to MDR pumps, there are those that are specific for a particular class of antibiotics; an example is TetK, which is also found in *S. aureus* and effluxes only tetracyclines.

There is significant interest in plant compounds which may inhibit bacterial efflux pumps. An example is the plant alkaloid reserpine, which inhibits both TetK and NorA (7, 21) but unfortunately is toxic at the concentrations required for this activity (17). An effective efflux pump inhibitor (EPI) could have significant benefits, including restoration of antibiotic sensitivity in a resistant strain (13) and a reduction in the dose of antibiotic required, possibly reducing adverse drug effects. It has also been demonstrated that use of an EPI with an antibiotic delays the emergence of resistance to that antibiotic (16). A new EPI lead compound (MP-601,205), which is in phase I clinical trials, has recently been described (15). A hybrid molecule of the synthetic MDR pump inhibitor INF_{55} (17) and the natural product berberine was effective in vivo in curing an enterococcal infection in a *Caenorhabditis elegans* nematode infection model (2). Therefore, the prospects for producing EPIs which could be used clinically are encouraging.

Conifer oleoresin, secreted as a defense mechanism against predators, has long been valued for its antiseptic properties. In this study, the phenolic diterpene totarol (Fig. 1) was isolated from the immature cones of *Chamaecyparis nootkatensis*. Here we demonstrate that totarol has both antibacterial and EPI activity against *S. aureus*, providing further evidence that effective EPI lead compounds can be isolated from plants.

Unless stated otherwise, all reagents were obtained from Sigma-Aldrich Company Ltd., Dorset, United Kingdom. Cation-adjusted Mueller-Hinton broth was obtained from Oxoid and was adjusted to contain 20 mg/liter Ca^{2+} and 10 mg/liter Mg^{2+}.

The strains of *S. aureus* used are listed in Table 1. Strains overexpressing various efflux-related resistance mechanisms were employed and will be referred to as "effluxing strains," including strains XU212 (*tetK*), RN4220 (*msrA*), and SA-1199B (*norA*). SA-K1758 is a derivative of *S. aureus* NCTC 8325-4 having the *norA* gene deleted and replaced with an *erm* cassette (25). To help separate antimicrobial from efflux inhibitory activity, a totarol-resistant mutant of SA-K1758 (SA-K3090) was produced by employing gradient plates. The *norA* gene and promoter were amplified from SA-1199B and cloned into pCU1, producing pK364 (1). This plasmid was transduced into SA-K3090 using phage 85, resulting in SA-K3092 (6).

Totarol was isolated from the immature cones of *Chamaecyparis nootkatensis* (Bedgebury Pinetum, Goudhurst, Kent), and a voucher specimen was placed in the herbarium at the School of Pharmacy (voucher specimen no. ECJS/008). Soxhlet extraction on 500 g of cones was carried out using 3.5 liters of solvents of increasing polarity: hexane, chloroform, acetone, and methanol. Vacuum-liquid chromatography was performed on 2 g of the chloroform extract using Merck Silica Gel 60 (VWR, Leicestershire United Kingdom), commencing elution with 100% chloroform with a gradient of 10% increments to 100% ethyl acetate. The solvent was then changed to ethyl acetate-acetone (50:50), followed by 100% acetone and finishing with acetone-methanol (50:50). Fraction 3 (852 mg) was

* Corresponding author. Mailing address: Centre for Pharmacognosy and Phytotherapy, The School of Pharmacy, University of London, 29-39 Brunswick Square, London WC1N 1AX, United Kingdom. Phone: 44 207 7535913. Fax: 44 207 7535909. E-mail: simon.gibbons@pharmacy.ac.uk.

▽ Published ahead of print on 30 July 2007.

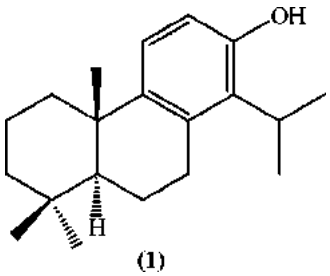

(1)

FIG. 1. Structure of totarol.

subjected to preparative reverse-phase high-pressure liquid chromatography using an XTerra MS C_{18} column (300 mm by 19 mm by 10 μm) (Waters, Hertfordshire, United Kingdom). Samples (65 mg) were eluted with acetonitrile-H_2O (70:30) for 30 min, and the acetonitrile concentration was then increased in a gradient up to 100% over 5 min and held for 2 min. Four high-pressure liquid chromatography runs yielded 39.0 mg totarol.

Gas chromatography-mass spectrometry (GC-MS) analysis was carried out using an Agilent 6890 GC coupled to an Agilent 5973 mass selective detector. An HP-5ms capillary column of 30 m in length with a diameter of 250 μm was used with a nonpolar stationary phase of 5% phenylmethylsiloxane and a film thickness of 0.25 μm. Samples were introduced into the system using split injection with a split ratio of between 5:1 and 10:1 and an injector temperature of 250°C. Helium was used as the carrier gas at an average linear velocity of 50 cm/s. The initial oven temperature was 50°C, and the temperature was increased after 5 min at a rate of 5°C to a maximum of 300°C. The MS was run in EI mode. One-dimensional (1D) and 2D nuclear magnetic resonance (NMR) spectra were recorded on a Bruker Avance 500-MHz spectrometer and processed using XWin NMR 3.5 software. Samples were dissolved in deuterated chloroform, which was also used as the internal solvent standard. Extensive 1D and 2D NMR experiments and GC-MS facilitated the structure elucidation of the isolated diterpene (Fig. 1), and the spectral data were in close agreement with the literature values for totarol (23).

MIC and modulation assays were performed using a broth dilution technique as described previously (29). Totarol was assayed at half the MIC in modulation assays, and reserpine was used as a control. Checkerboard combination studies using ethidium bromide (EtBr) and totarol were performed as described previously (4). Totarol concentrations included in combination experiments were ≤1/4 of its respective MIC. Increasing concentrations of totarol and reserpine were assayed for their ability to inhibit EtBr efflux from SA-K3092 using methods exactly as previously described (12).

TABLE 2. Results of modulation assays for totarol and reserpine

Test compound (concn, μg/ml)	MIC (μg/ml) of indicated drug for indicated strain with/without test compound (fold inhibition)		
	Tetracycline, XU212 (TetK)	Norfloxacin, SA1199B (NorA)	Erythromycin, RN4220 (MsrA)
Totarol (1)	128/32 (4)	32/8 (4)	128/16 (8)
Reserpine (20)	128/32 (4)	32/4 (8)	128/128 (0)

Totarol exhibited good antibacterial activity, having an MIC of 2 μg/ml against *S. aureus* ATCC 25923 and effluxing strains. EtBr MICs for NCTC 8325-4, SA-K1758 (*norA* null), SA-K3090, and SA-K3092 (plasmid-based *norA* overexpresser) were 6.25, 0.63, 0.63, and 100 μg/ml, respectively, demonstrating the marked increase in EtBr MIC associated with *norA* overexpression. The totarol MICs for these strains were 2.5, 1.25, 16, and 16 μg/ml, respectively, indicating that totarol is not a substrate for NorA.

At half the MIC, the modulatory activity of totarol against effluxing strains was comparable to that seen for reserpine (Table 2). Of particular note was the observation of a totarol-mediated eightfold reduction in the MIC of erythromycin against strain RN4220, which expresses the macrolide-specific MsrA pump, whereas reserpine had no activity as a modulator against this strain. No inhibitors of the MsrA pump have so far been reported; however, some caution must be exercised in defining totarol as an inhibitor of MsrA, as it has been suggested that the MsrA protein may not be an efflux pump (26).

Isobolograms illustrating the effect of totarol on EtBr MICs of test strains are presented in Fig. 2. The effect of totarol on strains overexpressing NorA (SA-1199B and K3092) is evident and is consistent with an inhibitory effect on NorA function.

The activity of totarol against effluxing strains of *S. aureus* suggested that it may be an EPI. To test this possibility, a dose-response efflux inhibition assay was performed using SA-K3092 (Fig. 3). The concentration at which totarol inhibited EtBr efflux by 50% (IC_{50}) (15 μM or 4.29 μg/ml) was approximately one-fourth of the MIC for this strain. Reserpine is a more efficient inhibitor of EtBr efflux in this test system, having an IC_{50} of 8 μM.

This is the first report of antibacterial and modulatory ac-

TABLE 1. Study strains

Strain	Relevant characteristic(s)	Reference(s)
ATCC 25923	Control strain	7
XU212	Clinical isolate, has TetK efflux pump, erythromycin resistant	7
RN4220 (*msrA*)	Transformed with pSK265 into which the gene for the MsrA efflux protein has been cloned	26
SA-1199	Clinical isolate, methicillin susceptible	10
SA-1199B	NorA-overproducing derivative of SA-1199, also has A116E GrlA substitution	10, 11
NCTC 8325-4	Commonly used laboratory strain	
SA-K1758	*norA* deletion mutant of NCTC 8325-4	25
SA-K3090	SA-K1758, resistant to totarol	This study
SA-K3092	SA-K3090(pK364)	This study
EMRSA-15	Clinical isolate, methicillin and erythromycin resistant	27

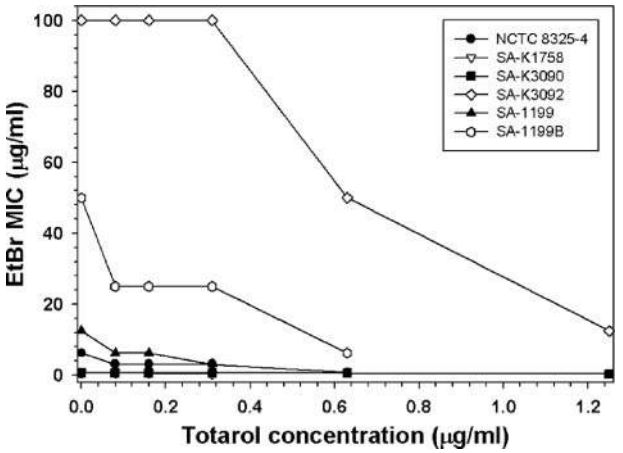

FIG. 2. Isobolograms demonstrating the effect of totarol on EtBr MICs.

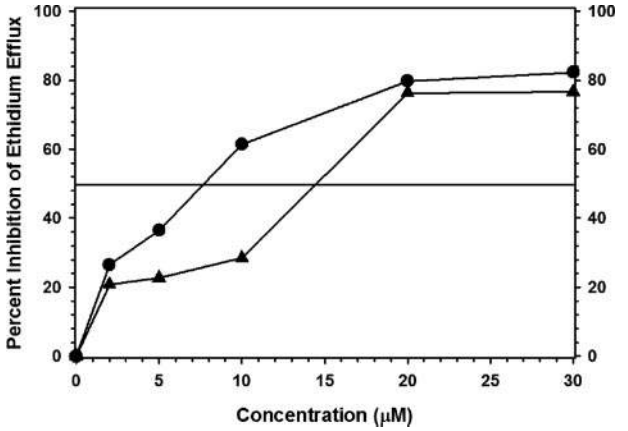

FIG. 3. Inhibition of EtBr efflux in SA-K3092 by reserpine (●) and totarol (▲). The horizontal line indicates the IC_{50}.

tivities for totarol against effluxing strains of *S. aureus*. Efflux inhibition results using a mutant with an elevated totarol MIC indicated successful separation of antibacterial and modulatory activities. An IC_{50} for EtBr efflux at one-quarter of the MIC indicated that the antibacterial activity of totarol is not likely to be contributing to its activity as a modulator and that it does function as a weak EPI. Totarol's activity as a modulator has also been reported against mycobacteria. Mossa et al. (19) found the compound was active against several species (MIC, 2.5 μg/ml) and that at half of the MIC it caused an eightfold potentiation of isoniazid activity.

The antibacterial activity of totarol and its activity as a potentiator of methicillin activity against methicillin-resistant *S. aureus* (MRSA) have previously been reported (14, 20, 22). Various reductions in the MIC of methicillin against MRSA strains have been reported when used with totarol at half of the MIC. At least an 8-fold reduction in MIC, from >32 to 4 μg/ml, was noted by one group (22), but others observed a 16-fold reduction in MIC against one MRSA strain but only a 2-fold reduction against a different strain (20). For comparison, in this study we assayed totarol against the clinical isolate EMRSA-15 and found a 50-fold potentiation of oxacillin activity (data not shown). Nicolson et al. (22) studied the expression levels of PBP2′, and concluded that potentiation of methicillin activity by totarol is by interference with the synthesis of this MRSA-specific PBP. Obviously this would not be the mode of action in non-MRSA effluxing strains. The presence of other efflux pumps for which totarol may be a substrate is one possible reason for the difference in activity.

The mode of antibacterial action of totarol is not known. Several possibilities have been suggested, including inhibition of bacterial respiratory transport (8), but others have found that totarol inhibits growth of anaerobic bacteria (28). Another possibility is disruption of membrane phospholipids, leading to loss of membrane integrity (18). Increased leakage of protons through the mitochondrial membrane was observed by one group, although at a higher totarol concentration than required for antibacterial activity (5). Most recently, inhibition of bacterial cytokinesis by targeting the FtsZ protein, which forms the Z ring, was reported (9). In some instances it has been found that the presence of a modulator can have a negative effect on antibiotic activity (29, 30). It is possible that the modulator may interact with the antibiotic substrate, perhaps leading to reduced bioavailability of the drug (31).

Totarol reduces NorA-mediated EtBr efflux, but the mechanism(s) of this effect is not known. Whether totarol acts directly, i.e., by binding to the pump, or indirectly, perhaps by binding the pump substrate or affecting the assembly, conformation, or even the translation of the pump, remains to be determined.

There is a potentially useful separation between the antibacterial activity of totarol and its cytotoxicity. Clarkson et al. (3) reported antiplasmodial activity for totarol against a chloroquine-resistant strain of *Plasmodium falciparum* at an IC_{50} of 4.29 μM, which was 40-fold less than its cytotoxic activity against CHO cells. A recent report suggested differential inhibitory effects on mammalian and bacterial cell proliferation, with only weak inhibition of HeLa cell proliferation in the presence of totarol (9). The activity of totarol as an antibacterial, modulator and EPI seen in this study, together with results from others, suggests that totarol would be a good lead candidate for further development in the search for effective drugs against resistant *S. aureus*.

We thank Stiefel International R&D Ltd. for the award of a studentship and postdoctoral funding to E. C. J. Smith and The Engineering and Physical Sciences Research Council for a multiproject equipment grant (no. GR/R47646/01).

We thank Bedgebury Pinetum, Goudhurst, Kent, United Kingdom, for the supply of conifer material.

REFERENCES

1. **Augustin, J., R. Rosenstein, B. Weiland, U. Schneider, N. Schell, G. Engelke, K. Entian, and F. Götz.** 1992. Genetic analysis of epidermin biosynthetic genes and epidermin-negative mutants of *Staphylococcus epidermidis*. Eur. J. Biochem. **204:**1149–1154.
2. **Ball, A. R., G. Casadei, S. Samosom, J. B. Bremner, F. M. Ausubel, T. I. Moy, and K. Lewis.** 2006. Conjugating berberine to a multidrug efflux pump inhibitor creates an effective antimicrobial. ACS Chem. Biol. **1:**594–600.
3. **Clarkson, C., C. C. Musonda, K. Chibale, W. E. Campbell, and P. Smith.** 2003. Synthesis of totarol amino alcohol derivatives and their antiplasmodial activity and cytotoxicity. Bioorg. Med. Chem. **11:**4417–4422.
4. **Eliopoulos, G. M., and R. C. Moellering, Jr.** 1991. Antimicrobial combinations, p. 432–492. *In* V. Lorian (ed.), Antibiotics in laboratory medicine. Williams and Wilkins, Baltimore, MD.
5. **Evans, G. B., R. H. Furneaux, G. J. Gainsford, and M. P. Murphy.** 2000. The

synthesis and antibacterial activity of totarol derivatives. 3. Modification of ring-B. Bioorg. Med. Chem. **8:**1663–1675.
6. **Foster, T. J.** 1998. Molecular genetic analysis of staphylococcal virulence. Methods Microbiol. **27:**433–454.
7. **Gibbons, S., and E. E. Udo.** 2000. The effect of reserpine, a modulator of multidrug efflux pumps, on the *in vitro* activity of tetracycline against clinical isolates of methicillin resistant *Staphylococcus aureus* (MRSA) possessing the *tet*(K) determinant. Phytother. Res. **14:**139–140.
8. **Haraguchi, H., H. Ishikawa, and I. Kubo.** 1996. Mode of antibacterial action of totarol, a diterpene from *Podocarpus nagi*. Planta Med. **62:**122–125.
9. **Jaiswal, R., T. K. Beuria, R. Mohan, S. K. Mahajan, and D. Panda.** 2007. Totarol inhibits bacterial cytokinesis by perturbing the assembly dynamics of FtsZ. Biochemistry **46:**4211–4220.
10. **Kaatz, G. W., S. I. Barriere, D. R. Schaberg, and R. Fekety.** 1987. The emergence of resistance to ciprofloxacin during therapy of experimental methicillin-susceptible *Staphylococcus aureus* endocarditis. J. Antimicrob. Chemother. **20:**753–758.
11. **Kaatz, G. W., S. M. Seo, and C. A. Ruble.** 1993. Efflux-mediated fluoroquinolone resistance in *Staphylococcus aureus*. Antimicrob. Agents Chemother. **37:**1086–1094.
12. **Kaatz, G. W., S. M. Seo, L. O'Brien, M. Wahiduzzaman, and T. J. Foster.** 2000. Evidence for the existence of a multidrug efflux transporter distinct from NorA in *Staphylococcus aureus*. Antimicrob. Agents Chemother. **44:**1404–1406.
13. **Kaatz, G. W.** 2005. Bacterial efflux pump inhibition: a potential means to recover clinically relevant activity of substrate antimicrobial agents. Curr. Opin. Investig. Drugs **6:**191–198.
14. **Kubo, I., H. Muroi, and M. Himejima.** 1992. Antibacterial activity of totarol and its potentiation. J. Nat. Prod. **55:**1436–1440.
15. **Lomovskaya, O., and K. A. Bostian.** 2006. Practical applications and feasibility of efflux pump inhibitors in the clinic—a vision for applied use. Biochem. Pharmacol. **71:**910–918.
16. **Markham, P. N., and A. A. Neyfakh.** 1996. Inhibition of the multidrug transporter NorA prevents emergence of norfloxacin resistance in *Staphylococcus aureus*. Antimicrob. Agents Chemother. **40:**2673–2674.
17. **Markham, P. N., E. Westhaus, K. Klyachko, M. E. Johnson, and A. A. Neyfakh.** 1999. Multiple novel inhibitors of the NorA multidrug transporter of *Staphylococcus aureus*. Antimicrob. Agents Chemother. **43:**2404–2408.
18. **Micol, V., C. R. Mateo, S. Shapiro, F. J. Aranda, and J. Villalain.** 2001. Effects of (+)-totarol, a diterpenoid antibacterial agent, on phospholipid model membranes. Biochim. Biophys. Acta **1511:**281–290.
19. **Mossa, J. S., F. S. El-Feraly, and I. Muhammad.** 2004. Antimycobacterial constitutents from *Juniperus procera*, *Ferula communis* and *Plumbago zeylanica* and their *in vitro* synergistic activity with isonicotinic acid hydrazide. Phytother. Res. **18:**934–937.
20. **Muroi, H., and I. Kubo.** 1996. Antibacterial activity of anacardic acid and totoral, alone and in combination with methicillin against methicillin-resistant *Staphylococcus aureus*. J. Appl. Bacteriol. **80:**387–394.
21. **Neyfakh, A. A., C. M. Borsch, and G. W. Kaatz.** 1993. Fluoroquinolone resistance protein NorA of *Staphylococcus aureus* is a multidrug efflux transporter. Antimicrob. Agents Chemother. **37:**128–129.
22. **Nicolson, K., G. Evans, and P. W. O'Toole.** 1999. Potentiation of methicillin activity against methicillin-resistant *Staphylococcus aureus* by diterpenes. FEMS Microbiol. Lett. **179:**233–239.
23. **Nishida, T., I. Wahlberg, and C. R. Enzell.** 1977. Carbon-13 nuclear magnetic resonance spectra of some aromatic diterpenoids. Org. Mag. Reson. **9:**203.209.
24. **Piddock, L. J. V.** 2006. Multidrug-resistance efflux pumps—not just for resistance. Nat. Rev. Microbiol. **4:**629–636.
25. **Price, C. T. D., G. W. Kaatz, and J. E. Gustafson.** 2002. The multidrug efflux pump NorA is not required for salicylate-induced reduction in drug accumulation by *Staphylococcus aureus*. Int. J. Antimicrob. Agents **20:**206–213.
26. **Reynolds, E., J. I. Ross, and J. H. Cove.** 2003. *Msr*(A) and related macrolide/streptogramin resistance determinants: incomplete transporters? Int. J. Antimicrob. Agents **22:**228–236.
27. **Richardson, J. F., and S. Reith.** 1993. Characterisation of a strain of methicillin-resistant *Staphylococcus aureus* (EMRSA-15) by conventional and molecular methods. J. Hosp. Infect. **25:**45–52.
28. **Shapiro, S., and B. Guggenheim.** 1998. Inhibition of oral bacteria by phenolic compounds. 1. QSAR analysis using molecular connectivity. Quant. Struct. Activity Relationships **17:**327–337.
29. **Smith, E., E. Williamson, M. Zloh, and S. Gibbons.** 2005. Isopimaric acid from *Pinus nigra* shows activity against multidrug-resistant and EMRSA strains of *Staphylococcus aureus*. Phytother. Res. **19:**538–542.
30. **Tegos, G., F. R. Stermitz, O. Lomovskaya, and K. Lewis.** 2002. Multidrug pump inhibitors uncover remarkable activity of plant antimicrobials. Antimicrob. Agents Chemother. **46:**3133–3141.
31. **Zloh, M., G. W. Kaatz, and S. Gibbons.** 2004. Inhibitors of multidrug resistance (MDR) have affinity for MDR substrates. Bioorg. Med. Chem. Lett. **14:**881–885.

Journal of Antimicrobial Chemotherapy (2007) **59**, 1247–1260
doi:10.1093/jac/dkl460
Advance Access publication 4 December 2006

JAC

Bacterial efflux pump inhibitors from natural sources

Michael Stavri[1], Laura J. V. Piddock[2] and Simon Gibbons[1]*

[1]Centre for Pharmacognosy and Phytotherapy, The School of Pharmacy, University of London, 29-39 Brunswick Square, London WC1N 1AX, UK; [2]Antimicrobial Agents Research Group, Division of Immunity and Infection, The Medical School, University of Birmingham, Birmingham B15 2TT, UK

The rapid spread of bacteria expressing multidrug resistance (MDR) has necessitated the discovery of new antibacterials and resistance-modifying agents. Since the initial discovery of bacterial efflux pumps in the 1980s, many have been characterized in community- and hospital-acquired Gram-positive and Gram-negative pathogens, such as *Staphylococcus aureus*, *Pseudomonas aeruginosa*, *Escherichia coli* and, more recently, in mycobacteria. Efflux pumps are able to extrude structurally diverse compounds, including antibiotics used in a clinical setting; the latter are rendered therapeutically ineffective. Antibiotic resistance can develop rapidly through changes in the expression of efflux pumps, including changes to some antibiotics considered to be drugs of last resort. It is therefore imperative that new antibiotics, resistance-modifying agents and, more specifically, efflux pump inhibitors (EPIs) are characterized. The use of bacterial resistance modifiers such as EPIs could facilitate the re-introduction of therapeutically ineffective antibiotics back into clinical use such as ciprofloxacin and might even suppress the emergence of MDR strains. Here we review the literature on bacterial EPIs derived from natural sources, primarily those from plants. The resistance-modifying activities of many new chemical classes of EPIs warrant further studies to assess their potential as leads for clinical development.

Keywords: MDR, MRSA, *Staphylococcus aureus*, NorA, efflux, *Mycobacterium*, *Pseudomonas*, *Escherichia*, modulators

Introduction

Staphylococcus aureus is an important community- and major hospital-acquired pathogen.[1,2] This organism is cause for considerable concern due to its ability to acquire resistance towards the newest antibacterial drugs currently on the market. In the UK, the number of death certificates citing methicillin-resistant *S. aureus* (MRSA) trebled from 398 in 1998 to 1168 in 2004.[3] These figures are believed to be a conservative estimate of the actual number of deaths as a result of MRSA. Similar data are available for many developed countries. Fluoroquinolones were thought to be useful anti-staphylococcal agents, but resistance quickly emerged.[4–6] Resistance to vancomycin, once thought of as the drug of last resort for the treatment of MRSA, has now been described in a strain in the USA.[7,8] MRSA resistant to linezolid, an anti-staphylococcal oxazolidinone have already been reported.[9] This leaves the streptogramin mixture quinupristin/dalfopristin and the cyclic lipopeptide daptomycin as the drugs for the treatment of methicillin-susceptible *S. aureus* (MSSA) and MRSA, although resistance has been reported to these drugs as well. Should widespread resistance to these agents emerge, substances that can increase susceptibility to currently licensed agents would be a very attractive option.

Gram-negative bacteria and mycobacteria both possess thick outer membranes that are highly hydrophobic, providing these organisms with a permeability barrier[10] especially towards hydrophilic compounds such as macrolide antibiotics like erythromycin.[11] This in part explains the greater resistance observed by Gram-negative bacteria as opposed to Gram-positive organisms. Various mechanisms provide bacteria with resistance to antibiotics; these include target-site modification and antibiotic inactivation. Resistance to macrolides,[12] vancomycin,[13] β-lactams,[14,15] fluoroquinolones[16] and aminoglycosides[17] has been achieved by target-site alteration, while antibiotic inactivation mechanisms have accounted for resistance towards β-lactams,[18] aminoglycosides[19] and chloramphenicol.[20] These mechanisms are important to bacteria to provide resistance, but do so to only a single class of compound. To become multidrug resistant a bacterium must acquire multiple mechanisms, and whilst many species have done so the spectra of resistances vary. Many efflux pumps are encoded chromosomally and their presence enhances resistance mediated by these individual mechanisms. Problems also now exist with the prevalence of human pathogenic bacteria overexpressing pumps and conferring multidrug resistance (MDR). A single pump can provide bacteria with resistance to a wide array of chemically and structurally diverse

*Corresponding author. Tel: +44-207-7535913; Fax: +44-207-7535909; E-mail: simon.gibbons@pharmacy.ac.uk

compounds. The problems of resistant Gram-positive and Gram-negative bacteria highlight the urgent need for new drugs with new modes of action and/or combination therapy to treat infections caused by resistant human pathogens such as *S. aureus*, *Pseudomonas aeruginosa* and *Mycobacterium tuberculosis*.

Here we review the literature concerning bacterial resistance modulators from natural sources and will highlight plants with the potential of discovering new bacterial efflux pump inhibitors (EPIs). The majority of EPIs discussed are putative inhibitors of efflux pumps of the highly problematic human pathogen *S. aureus*. This review also explores the problems posed by Gram-negative bacteria and mycobacteria possessing efflux mechanisms as a mechanism of resistance towards clinically relevant drugs and how EPIs may be one way of tackling this mechanism of resistance.

Bacterial efflux families

The phenomenon of microbial multidrug efflux was first reported by Ball *et al*.[21] and McMurry *et al*.[22] for the efflux of tetracycline in *Escherichia coli*. This resistance was transferable between strains and was encoded by *tet* (tetracycline) determinants, which were encoded either on plasmids or transposons.[23,24] Since this initial discovery, further efflux systems have been identified in Gram-positive and Gram-negative bacteria and, more recently, in mycobacteria. Bacterial efflux transporters can be divided into five main families primarily based on amino acid sequence homology.[25] These are the major facilitator (MF) superfamily, the resistance-nodulation-division (RND) family, the small MDR (SMR) family, the ATP binding cassette (ABC) family and the multiple antibiotic and toxin extrusion (MATE) family. The first three families achieve the energy required to extrude a drug out of the cell via the proton motive force in a proton-drug antiport system, whilst the MATE family is driven by the exchange of either proton or sodium ions. In contrast, the ABC family couples drug extrusion with the hydrolysis of ATP.[25] Efflux of drugs from Gram-positive bacteria is mediated by a single cytoplasmic membrane-located transporter of the MF, SMR or ABC families.[25] The efflux pumps in Gram-negative bacteria are more complex due to the presence of an outer membrane; they form a tripartite protein channel, which requires a protein that traverses the periplasm known as the membrane fusion protein (MFP) and an outer membrane efflux protein (OEP) along with the cytoplasmic membrane-located transporter. It is not uncommon for an organism to code for more than one efflux pump, which may either be expressed constitutively or induced in direct response to the presence of a substrate. *P. aeruginosa* constitutively expresses the MexAB-OprM multidrug efflux pump, which is the main member of the RND family in this organism.[26] However, *P. aeruginosa* also have the MexXY-OprM pump, which is inducible in the presence of any of its substrates, such as aminoglycosides.[27] Multidrug efflux pumps therefore contribute to the intrinsic resistance of *P. aeruginosa*.[26]

Bacterial efflux pumps offer potential targets to combat problematic infectious diseases such as those caused by MRSA, *E. coli* and *P. aeruginosa*. In Gram-positive organisms, the pumps studied in greatest detail include the NorA, Tet(K) and Msr(A) transporters.[28] In Gram-negative bacteria, studies have focused on the tripartite AcrAB-TolC and MexAB-OprM efflux pumps of *E. coli* and *P. aeruginosa*, respectively,[28] and also the FloR efflux pump of *Salmonella enterica* serovar Typhimurium.[29] The Tap and DrrAB efflux proteins of mycobacteria, including *M. tuberculosis*, can extrude a range of chemically diverse compounds.[25,28]

A genetic approach to determine the consequences of inhibiting the efflux pumps of *P. aeruginosa* was undertaken by Lomovskaya *et al*.;[30] inhibition significantly decreased MICs for both antibiotic-susceptible and -resistant bacteria, reversed acquired resistance, and resulted in a decreased frequency of emergence of *P. aeruginosa* mutants highly resistant to fluoroquinolones. It is therefore imperative to identify agents that can block efflux and, in so doing, extend the life of existing antibacterial drugs. Currently there are no EPIs on the market that can be used in combination with a drug that is a pump substrate to recover its clinical utility. However, the concept of using a compound that inhibits resistance together with a conventional antibiotic is well proven and co-amoxiclav is an important example.[31]

Screening for EPIs

It has been known for many years that some antibiotics exert synergy when used together and the chequerboard assay[32] has been used to identify such agents. Variations of this method have been applied to identify potential inhibitors of efflux pumps.

The modulation assay is a quick and easy method to identify potential EPIs in Gram-positive and Gram-negative bacteria. An initial study of the antibacterial activity of an extract or crude fractions is necessary to guard against false-positive results. A concentration, normally 4-fold lower than the MIC, is chosen when performing a potentiation assay. The modulation assay[33,34] requires a sub-inhibitory concentration of a crude fraction or pure compound to be dissolved in dimethylsulphoxide (DMSO) and diluted in Mueller–Hinton broth. Serial doubling dilutions of a drug known to be a substrate for an efflux transporter, such as norfloxacin for the NorA protein, is added and microtitre plates are then interpreted in the same manner as MIC determinations. All samples are tested in duplicate.

The chequerboard assay identifies synergic combinations of antimicrobial agents and has been used to screen for potential EPIs. Serial 2-fold dilutions of a pump substrate, such as norfloxacin or berberine for the NorA pump, as well as 2-fold dilutions of a fraction or test compound will result in microtitre wells with a different combination of pump substrate and fraction or test compound concentration.[35,36]

The berberine uptake assay[37] has also been used in bioassay-guided isolation of MDR inhibitors. Crude extracts and fractions are tested in the presence and absence of a sub-inhibitory concentration of this antibacterial alkaloid. Bacterial growth in the absence of berberine and no growth in its presence can be taken as an indicator of the presence of an MDR inhibitor in the extract.[38] This is an important screening tool enabling many fractions to be tested quickly and easily.

The ethidium bromide efflux inhibition assay[39,40] is a more detailed study of the potentiation activity of a test compound. Ethidium bromide is a substrate for a number of MDR efflux pumps. The activity of putative inhibitors can be measured fluorometrically due to the retention of fluorescence over time if efflux is reduced. Similar efflux assays can be performed with acriflavine or pyronin Y.[40]

Accumulation studies have been used to identify potential EPIs. Various substrates that have been used in accumulation studies include ethidium bromide,[26,39] norfloxacin,[41,42] berberine[37,43] and novobiocin.[44] Assays can be performed in a number of ways to determine the effect of a potential efflux inhibitor on a bacterial strain possessing an efflux pump. One method is the incorporation of an efflux inhibitor midway through a time-course assay in order to detect a difference in fluorescence. Another method is to run two separate time-course assays, one in the absence and one in the presence of an inhibitor to determine any effect a test compound may have as a potential inhibitor. An increase in drug accumulation only in the presence of an inhibitor indicates that the inhibitor is a blocker of an efflux mechanism.[45]

EPIs from plant sources

Work on staphylococcal efflux pumps has really only advanced in the past 2 years, with the identification of MDR transporters in addition to NorA. All data prior to this time on staphylococci and EPIs are either genetic or microbiological with little or no biochemistry. *S. aureus* has multiple transporters encoded by its genome, some of which are now known to transport antimicrobials, and there is poor evidence that the EPIs described to date interact solely with the NorA protein; reversal of resistance in NorA overexpressing strains is indicative but not conclusive; so, too, is the absence of activity versus strains lacking NorA. Overexpression, disruption or deletion of one pump can affect the expression of other MDR transporters.[46] A microbiological assay and even an efflux assay only gives the total phenotype, which is the sum of all transporter activity present in the bacterial cell at that time. Only crystal structure data of the purified protein and the inhibitor co-crystallized can really provide detailed information about binding. Experiments with pure protein are those that provide conclusive evidence.

The antihypertensive plant alkaloid reserpine (**1**) (Figure 1) was first isolated from the roots of *Rauwolfia vomitoria* Afz.[47] Its EPI activity was originally demonstrated against the Bmr efflux pump, which mediates tetracycline efflux in *Bacillus subtilis*.[48] Klyachko *et al*.[49] demonstrated that reserpine interacts directly with the Bmr protein at amino acids phenylalanine-143, valine-286 and phenylalanine-306, which form a reserpine-binding site. Reserpine also potentiated the activity of tetracycline (a 4-fold reduction in MIC) in two clinical isolates of MRSA, IS-58 and XU212, which possessed the Tet(K) efflux protein.[50] Reserpine also reversed NorA-conferred MDR,[51] and Kaatz and Seo[52] showed that it enhanced the activity of norfloxacin against *S. aureus*. NorA is one of the major MDR transporters in *S. aureus* and causes a significant decrease in susceptibility towards fluoroquinolones. In a study carried out by Schmitz *et al*.,[53] the MICs of the fluoroquinolones ciprofloxacin, moxifloxacin and sparfloxacin in the presence of reserpine were lowered by as much as 4-fold in 48, 21 and 11 of 102 *S. aureus* isolates tested, respectively. Fluoroquinolone resistance in *Streptococcus*

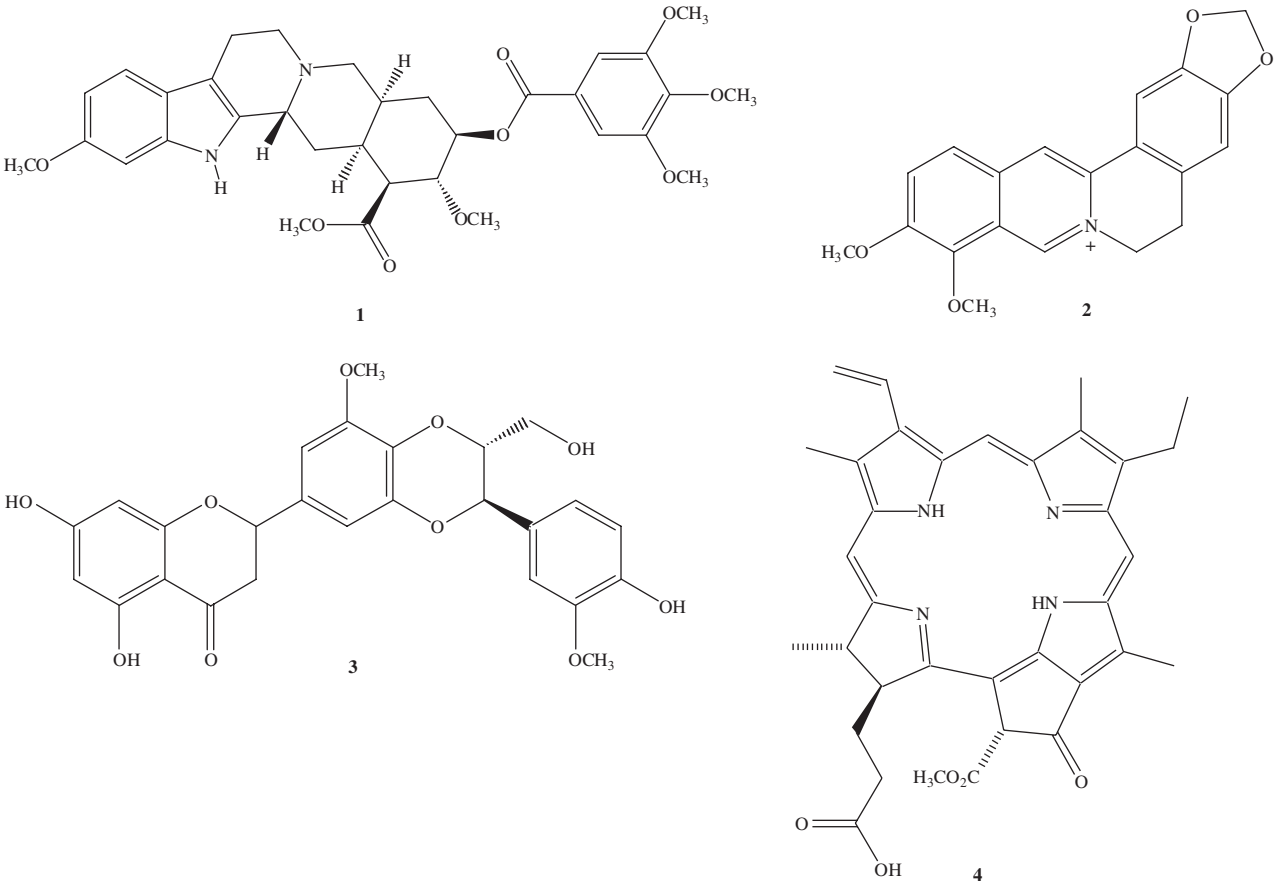

Figure 1. Chemical structures of compounds **1–4**.

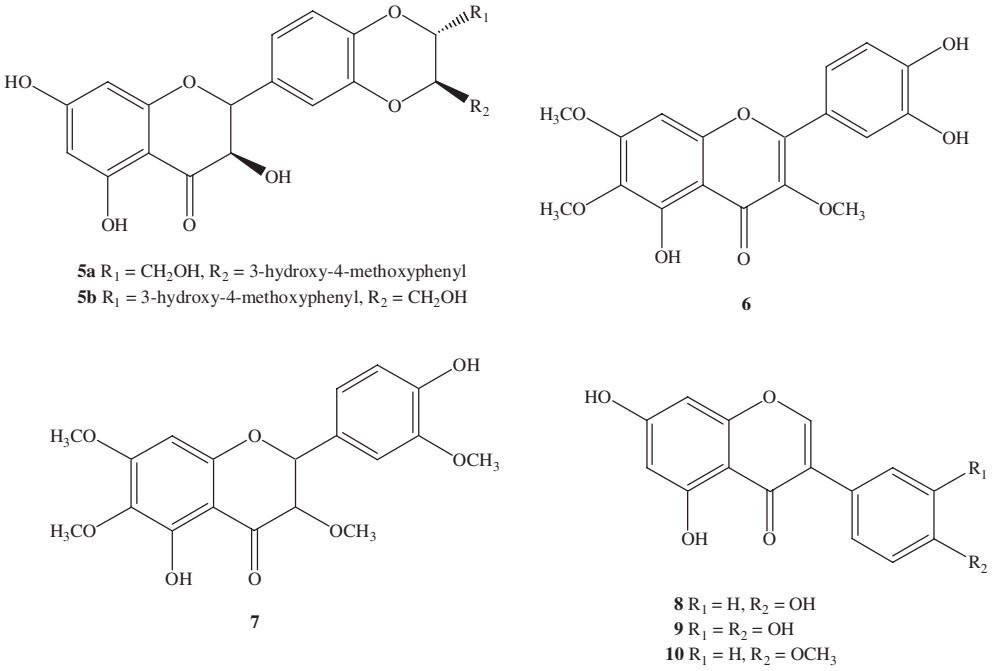

Figure 2. Chemical structures of compounds **5–10**.

pneumoniae has also been negated in the presence of reserpine.[54,55] In 1999 Gill *et al*.[56] identified PmrA, which has 43% amino acid similarity with NorA. Subsequent reduction of norfloxacin MIC against a norfloxacin-resistant construct (R6N) in the presence of reserpine led the authors to interpret that reserpine inhibited the PmrA protein. However, this interaction has not been conclusively proven. Fluoroquinolone accumulation studies using strain R6N as compared with R6 (wild-type) resulted in a decrease in the accumulation of these drugs.[57] However, the addition of reserpine at a concentration used in potentiation assays failed to increase fluoroquinolone accumulation suggesting that this compound interacts with another protein other than PmrA.[57] An ABC transporter associated with ciprofloxacin resistance has recently been identified by Marrer *et al*.[58] and subsequent deletion of this transporter resulted in these *S. pneumoniae* strains being conferred multidrug susceptible.[59]

A number of MDR pump inhibitors against the human pathogen *S. aureus* have been described by the Lewis group. Berberine (**2**), isolated from *Berberis fremontii*, is an alkaloid with only weak antibacterial activity (MIC = 256 mg/L) against a wild-type strain of *S. aureus*.[60] However, the isolation of the flavonolignan 5′-methoxyhydnocarpin-D (5′-MHC-D) (**3**) and a synergistic study between these two compounds led to a 16-fold increase in the antibacterial activity of berberine (MIC = 16 mg/L).[60] 5′-MHC-D also had a synergistic effect with several other NorA substrates, including norfloxacin.

The isolation of the porphyrin pheophorbide *a* (**4**) from *Berberis* species and a further flavonolignan, silybin (**5**) (Figure 2) a diastereomeric mixture of **5a** and **5b**, from Milk thistle (*Silybum marianum*)[38,61] also demonstrated synergistic activity against *S. aureus*.

There have also been a number of methoxylated flavones[62] and isoflavones[63] described as putative inhibitors of the MDR pump NorA in the presence of subinhibitory concentrations of berberine and the fluoroquinolone norfloxacin. The flavones chrysosplenol-D (**6**) (MIC = 25 mg/L with 30 mg/L berberine) and chrysoplenetin (**7**) (MIC = 6.25 mg/L with 30 mg/L berberine), isolated from *Artemisia annua* (Asteraceae), were shown previously to potentiate the activity of the antimalarial artemisinin against *Plasmodium falciparum*.[64] Both **6** and **7** are weakly antibacterial against *S. aureus* and this is not an uncommon feature for a potentiator to also exert a direct antibacterial effect. Care must be taken when interpreting results to ensure that activity is solely due to potentiation and not by direct inhibition. It is likely that these compounds act against a MDR efflux pump, to which artemisinin is a substrate, in *P. falciparum*, in a similar manner as in *S. aureus*. The active isoflavones from *Lupinus argenteus*, genistein (**8**), orobol (**9**) and biochanin A (**10**) also reduced the MIC of berberine (16-fold) and norfloxacin (4-fold).

A study of popular horticultural taxa such as *Geranium* has led to the isolation of putative inhibitors of *S. aureus* NorA, these included the polyacylated neohesperidosides (**11** and **12**) (Figure 3) from *G. caespitosum*.[65] The pentaester, **12**, increased the activity of berberine, ciprofloxacin, norfloxacin and rhein, an antibacterial component of rhubarb.

An investigation of *Dalea versicolor* (Fabaceae) ‘mountain delight’ resulted in the isolation of phenolic metabolites that enhanced the activity of berberine, erythromycin and tetracycline against *S. aureus*.[66] The chalcone (**13**) enhanced the activity such that the MICs were comparable to those for a mutant lacking NorA, suggesting that this agent is an inhibitor of NorA. This compound, along with the stilbene (**14**), also increased the activity of these antibiotics against *Bacillus cereus* with activity being the greatest in combination with berberine. This alkaloid is a substrate for the NorA efflux pump and a genomic comparison has revealed the presence of a Bmr homologue in this species, which is a homologue of NorA. Together with the activity data recorded against *S. aureus*, it is suggested that agent **13** is a putative EPI of the NorA efflux pump.

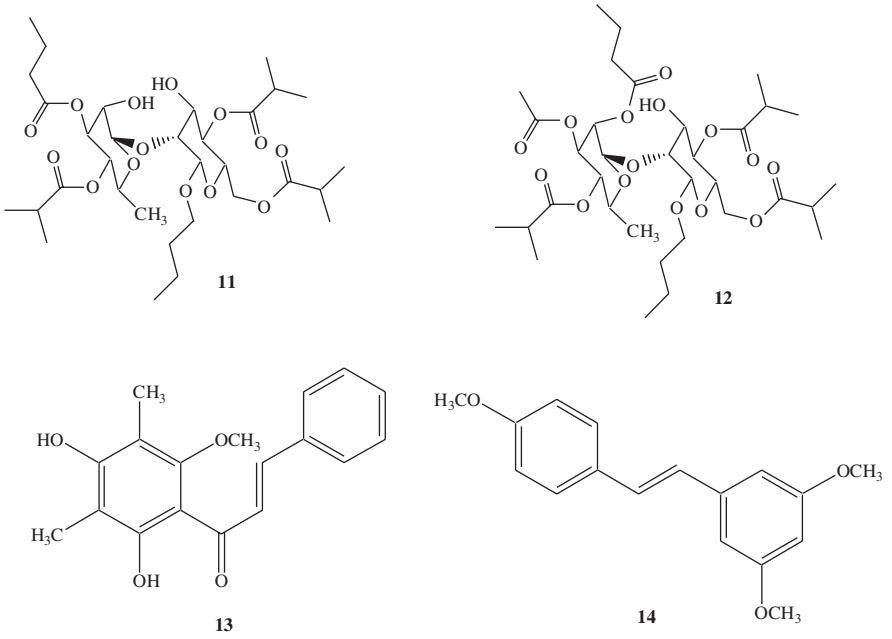

Figure 3. Chemical structures of compounds **11–14**.

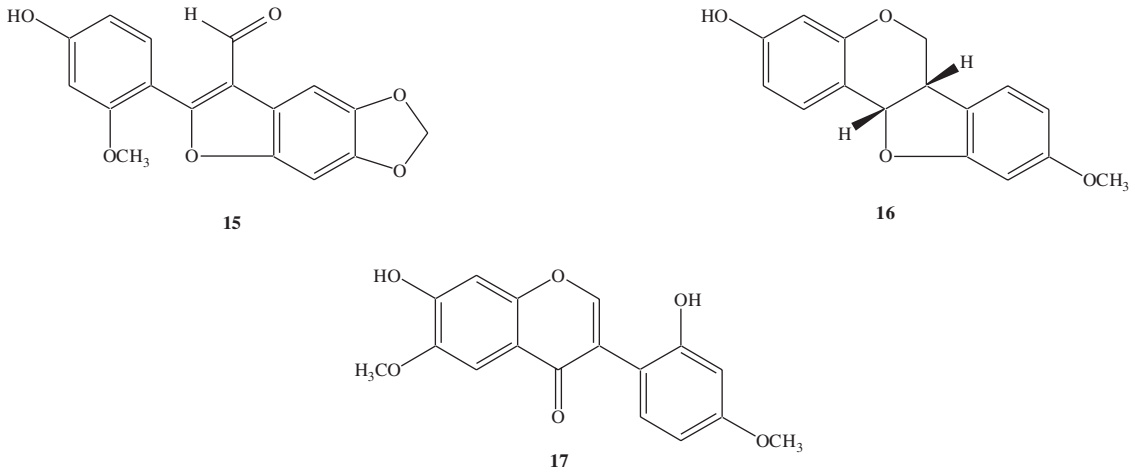

Figure 4. Chemical structures of compounds **15–17**.

A new arylbenzofuran aldehyde (spinosan A) (**15**), a known pterocarpan (**16**) and isoflavone (**17**) (Figure 4) were isolated from another *Dalea* species, the 'smoke tree', *Dalea spinosa*, which exerted a potentiation activity in the presence of berberine.[35] All three compounds enhanced berberine activity against the wild-type strain of *S. aureus*, lowering the MIC 4- to 8-fold. These compounds also caused an increased activity of berberine against an isogenic NorA mutant lowering the MIC 2- to 15-fold, but none was active against the NorA over-expressing mutant. It is likely that agents **15–17** cause inhibition of an efflux pump other than NorA.

A phytochemical investigation of Mexican Morning Glory species[67] led to the isolation of three oligosaccharides exerting a potentiation effect of norfloxacin against the NorA overexpressing *S. aureus* strain SA-1199B. The amphipathic orizabin XIX (**18**) (Figure 5) increased the activity of norfloxacin 4-fold (8 mg/L from 32 mg/L) at a concentration of 25 mg/L. Whilst orizabin IX (**19**) enhanced norfloxacin activity 16-fold when incorporated at a concentration of 1 mg/L. The ethidium efflux inhibition assay utilizing SA-1199B demonstrated that orizabin IX and another orizabin, orizabin XV (**20**), were nearly equipotent. The authors have not taken the possibility of quenching into account. It has recently been demonstrated that high intracellular concentrations of ethidium bromide result in a decrease in fluorescence due to self-quenching.[68] These oligosaccharides showed good activity at low concentrations (10 μM or less) being more active than reserpine and they could be further developed to provide more potent inhibitors of this multidrug efflux pump. The acylation of some of the free hydroxyl groups of the oligosaccharide and the lipophilic alkyl chain would seem to be important in facilitating cellular uptake to its MDR pump target.

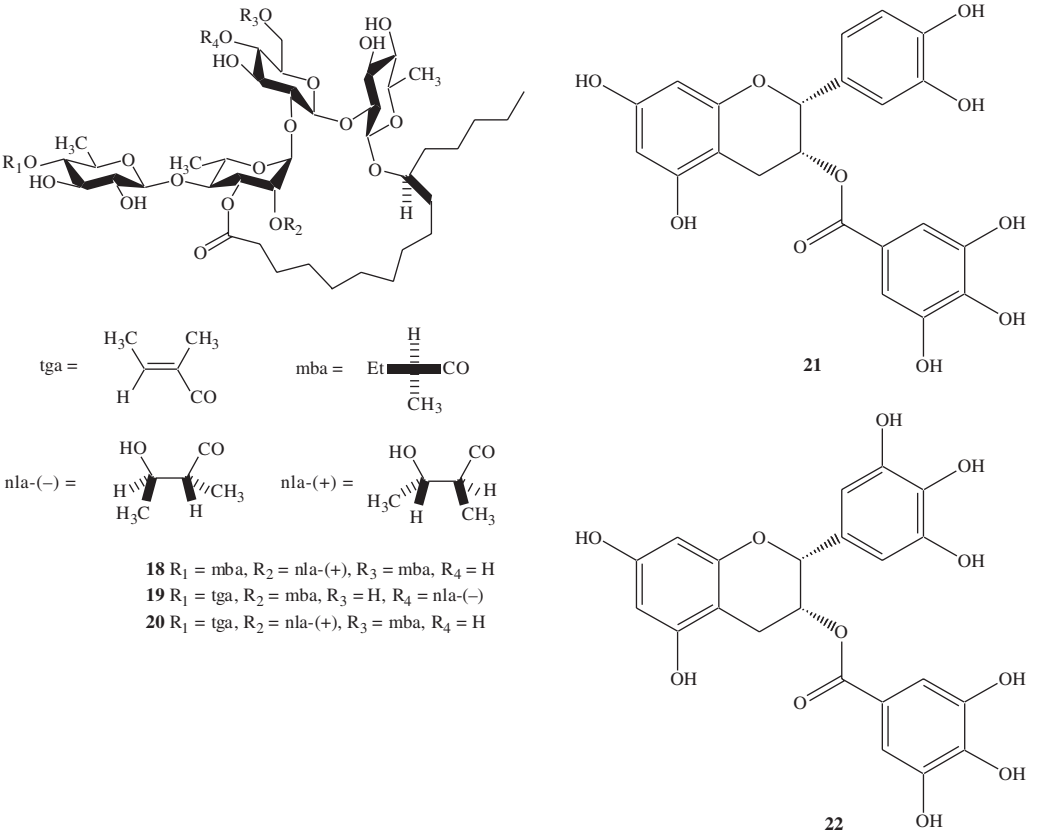

Figure 5. Chemical structures of compounds **18–22**.

The catechin gallates are another group of phenolic metabolites that have provided interest, initially by Hamilton-Miller's group, due to their ability to reverse methicillin resistance in MRSA.[69–71] Modulation assays of epicatechin gallate (**21**) and epigallocatechin gallate (**22**) in 96-well microtitre plates showed these compounds reduced the MIC of norfloxacin 4-fold against SA-1199B at a concentration of 20 mg/L.[72] As both compounds possess moderate antibacterial activity against this strain, the ethidium efflux inhibition assay was performed to verify this activity. The authors have not taken the possibility of quenching into account. Both compounds were found to weakly inhibit the NorA efflux pump, with epicatechin gallate **21** being slightly more potent. Interestingly, both compounds were reported to enhance efflux at low concentrations (Figure 6) resulting in the authors hypothesizing the presence of two binding sites on the NorA transporter, one with a high affinity for catechins and another with a low affinity.[72] Low concentrations of catechins would result in the high-affinity binding sites being occupied preferentially and therefore enhancing efflux. However, an increased concentration of catechins would result in the low-affinity sites being bound as well resulting in the reversal of efflux enhancement to one of a mild efflux inhibitor. Further work to study the low concentration of catechins could help to understand how these pumps are controlled. Another hypothesis for these data could be that catechins interact with another pump. Epigallocatechin gallate has also been shown to enhance tetracycline activity in Tet(K) resistant staphylococci.[73] At a concentration of 30 mg/L epigallocatechin gallate caused a 4- and 8-fold increase in the activity of tetracycline in *Staphylococcus epidermidis* and

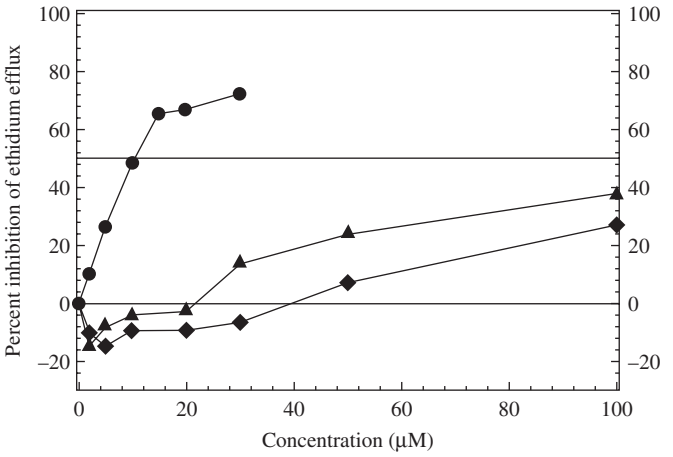

Figure 6. Inhibition of ethidium efflux by catechin gallates. Reserpine was included for comparative purposes. Filled circles, reserpine; filled triangles, epicatechin gallate (**21**); filled diamonds, epigallocatechin gallate (**22**).

S. aureus, respectively. A tetracycline uptake and release study was performed on resistant and susceptible *S. epidermidis* with and without pre-treatment with **22** (50 mg/L) over a 15 min time-course. The tetracycline release curve was steeper in the resistant strain, without **22**, than that of the susceptible strain, indicating greater efflux of the resistant strain.[73] The curves were shallower when strains were pre-treated with **22** indicating a greater retention of tetracycline within the cells.[73] Roccaro *et al.*[73] then

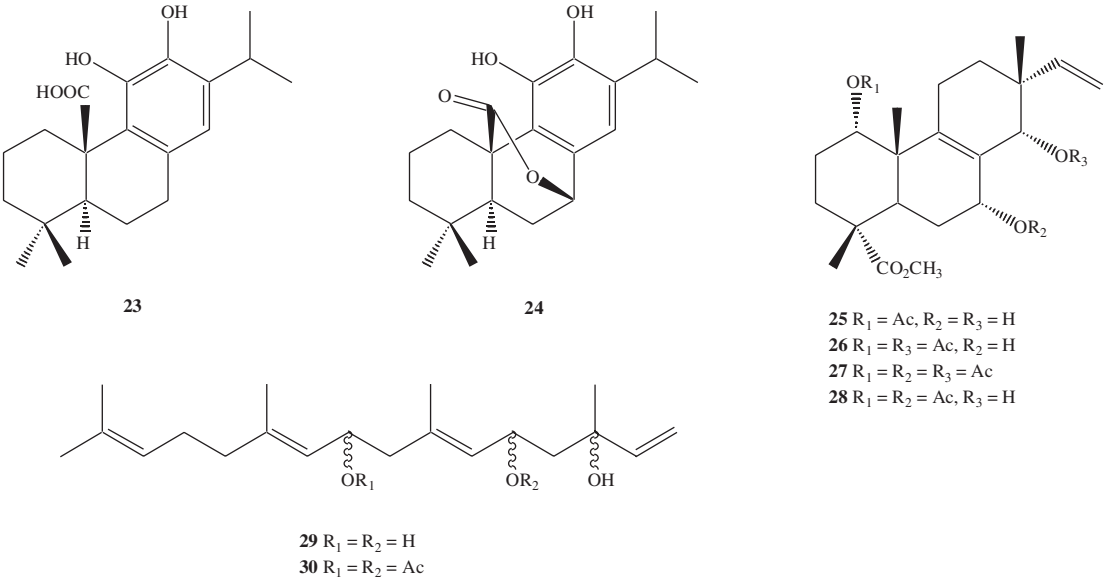

Figure 7. Chemical structures of compounds **23–30**.

performed the same experiments with protoplasts of *S. epidermidis* cells to confirm that **22** acts against Tet(K) rather than binding to peptidoglycan. The results obtained with protoplasts were not affected under these circumstances, indicating that peptidoglycan did not affect the uptake and release of tetracycline. The tetracycline-susceptible isolates of these species showed an 8-fold reduction in the MIC of tetracycline, so whilst epigallocatechin gallate appears to be an inhibitor of the Tet(K) pump, it may also cause inhibition of an as yet undefined efflux mechanism.

The abietane diterpenes carnosic acid (**23**) and carnosol (**24**) (Figure 7), isolated from the popular herb Rosemary (*Rosmarinus officinalis*), were identified as potentiators of tetracycline and erythromycin against *S. aureus* strains possessing the Tet(K) and Msr(A) efflux pumps, respectively.[34] Both **23** and **24** enhanced tetracycline activity against *S. aureus* XU212, possessing the Tet(K) efflux protein, at a concentration of 10 mg/L. Carnosic acid also enhanced the activity of erythromycin, causing an 8-fold reduction in MIC (32 mg/L from 256 mg/L) against the erythromycin-resistant strain RN4220 which expresses the Msr(A) efflux protein. An ethidium efflux inhibition assay incorporating carnosic acid against strain SA-1199B identified this compound as a moderately active potentiator of norfloxacin against the NorA pump with an IC_{50} of 50 μM (16.6 mg/L), equivalent to approximately one quarter of the MIC for the strain. The authors did not take the possibility of quenching into account.

As part of a project to identify natural plant products with modulation activity, an extract of *Lycopus europaeus* (Lamiaceae) was investigated. *L. europaeus* is also commonly known as Gipsywort in Britain and the lipophilic extract caused a potentiation of tetracycline and erythromycin against strains IS-58 and RN4220 of *S. aureus* possessing multidrug efflux pumps Tet(K) and Msr(A), respectively.[33] Bioassay-guided isolation of the hexane extract led to the isolation of six metabolites that included four isopimarane diterpenes (**25**–**28**) (Figure 7) and two oxidized geranylgeranyl diterpenes (**29** and **30**). Various chromatographic techniques were used to isolate these compounds and the activity of each fraction was tracked by modulation assay until the active components were purified. None of these compounds was active at 512 mg/L. However, when incorporated into the Mueller–Hinton broth at a concentration of 10 mg/L each of these compounds reduced the MIC of tetracycline and erythromycin 2-fold against *S. aureus* IS-58 [Tet(K)] and *S. aureus* RN4220 [Msr(A)]. Interestingly, there were no differences in activities of these diterpenes, despite the structural differences between the isopimarane and geranylgeranyl groups. None of the compounds was able to enhance norfloxacin activity against *S. aureus* 1199B that overexpresses NorA. A common feature of these six compounds is that they are highly lipophilic, suggesting that this is a key factor for an inhibitor of MDR efflux pumps of Gram-positive bacteria.

Baicalein (**31**) (Figure 8), a trihydroxy flavone isolated from the leaves of the commonly used herb thyme (*Thymus vulgaris*), was identified as possessing a strong synergic activity when used in conjunction with tetracycline or the β-lactam antibiotics oxacillin, cefmetazole and ampicillin against MRSA.[74] Baicalein is weakly antibacterial (MIC = 100 mg/L) but at 25 mg/L, it reduced the MIC of tetracycline from 4 to 0.12 mg/L against the MRSA clinical isolate OM481. This compound reduced the MIC of tetracycline against another MRSA isolate, OM584, this time by a factor of four. Expression of an *S. aureus*-derived *tet*(K) gene into an *E. coli* host led to a 16-fold increase in MIC, but in the presence of baicalein this was again reduced 4-fold. There was also a decrease in MIC detected in the *E. coli* strain not expressing the Tet(K) efflux protein. MRSA OM481 did not possess the Tet(K) protein indicating that baicalein (**31**) may inhibit another MDR pump in these MRSA isolates or have more than one mechanism of action, such as interfering with the integrity of the cell wall.

A biological evaluation of grapefruit oil, which can be isolated from the species *Citrus paradisi*, has highlighted some of the components as potential modulators of efflux pumps in MRSA strains. Fractionation of the grapefruit oil led to the characterization of a coumarin derivative (**32**), a bergamottin epoxide

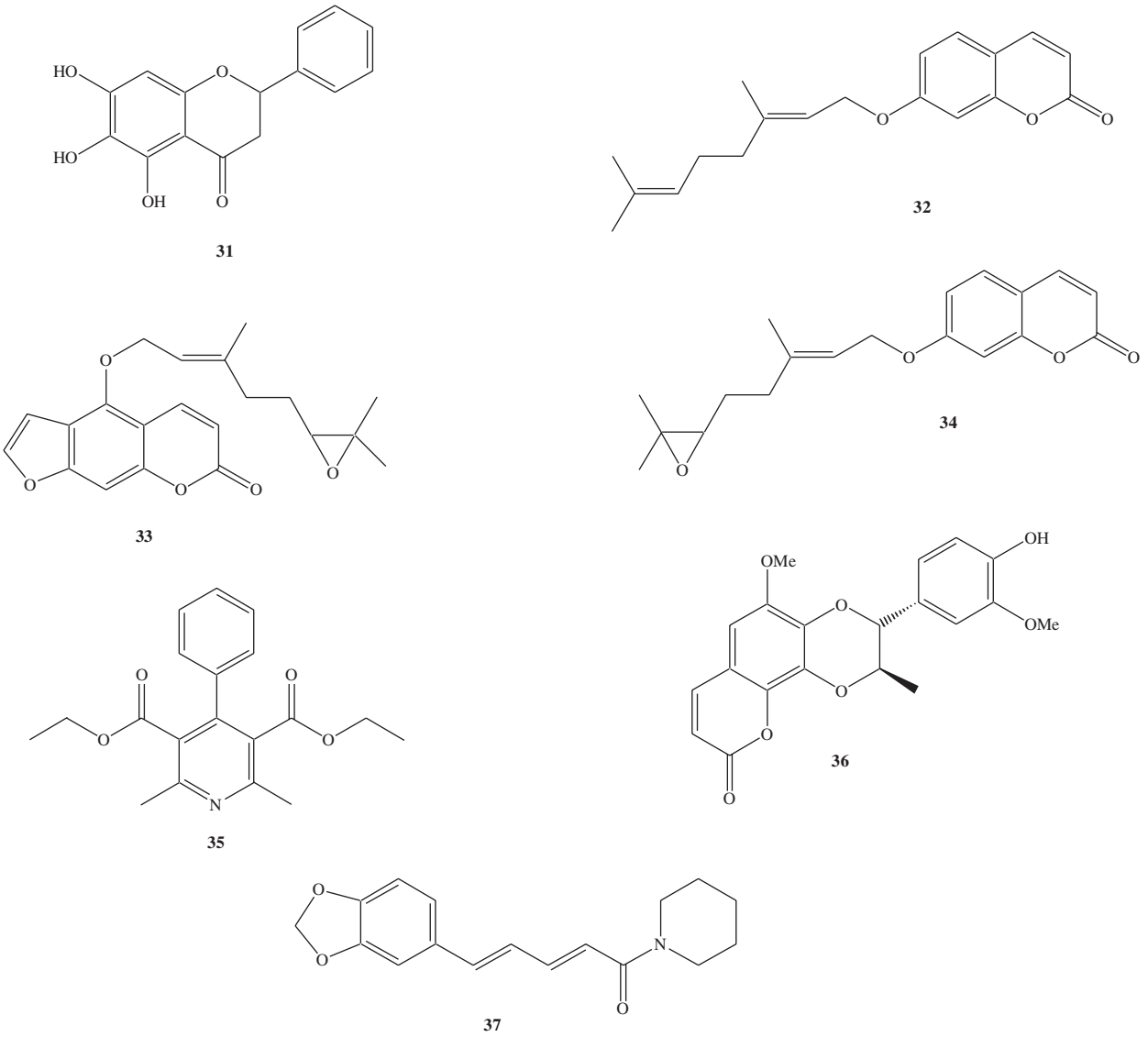

Figure 8. Chemical structures of compounds **31–37**.

derivative (**33**) and a coumarin epoxide derivative (**34**) (Figure 8) able to enhance the activity of ethidium bromide and norfloxacin.[75] Both **32** and **34** caused a 2-fold reduction in MIC of ethidium bromide whilst **33** caused a 6-fold reduction. **33** and **34** also caused a 20-fold reduction in the MIC of norfloxacin against MRSA strains but not against MSSA strains. Kristiansen *et al*.[76] have suggested that MRSA strains may be more susceptible than MSSA to chlorpromazine, which inhibits multidrug efflux pump activity. Whilst MICs of oxacillin were lowered in the presence of chlorpromazine complete resistance reversal was not achieved. However, these data indicate that efflux may play a role in providing MRSA strains with resistance to antibiotics such as the penicillins. This view is supported by recent work performed on 12 MRSA strains that showed an up-regulation of efflux genes including *norA*, *erm*(A) and *erm*(B).[77]

Bioassay-guided fractionation of an extract of *Jatropha elliptica* (Euphorbiaceae) led to the isolation of the penta-substituted pyridine, 2,6-dimethyl-4-phenyl-pyridine-3,5-dicarboxylic acid diethyl ester (**35**),[78] which is not antibacterial but does augment ciprofloxacin and norfloxacin activity against *S. aureus* SA-1199B. The coumarin lignan propacine (**36**) also showed moderate activity as a modulator in combination with ciprofloxacin against this strain. The activity of this compound is proposed by Marquez *et al*.[78] to be due to the lignan portion of the molecule based on the flavonolignan work published by Guz *et al*.[79] Work on plants belonging to the family Euphorbiaceae has resulted in the isolation of inhibitors of the mammalian MDR transporter *P*-glycoprotein, including a jatrophane diterpene that caused a 2-fold greater inhibition of daunomycin efflux, with respect to cyclosporin A, at a concentration of 5 μM.[80–82] So it is unsurprising that activity towards bacterial efflux mechanisms is also being reported.

Piperine (**37**) (Figure 8), a major plant alkaloid within the family Piperaceae including black pepper (*Piper nigrum*) and long pepper (*Piper longum*), has recently been reported to enhance the accumulation of ciprofloxacin by *S. aureus* with similar results being obtained when reserpine is substituted.[83] At concentrations of 12.5 and 25 mg/L, **37** caused a 2-fold reduction of the MIC

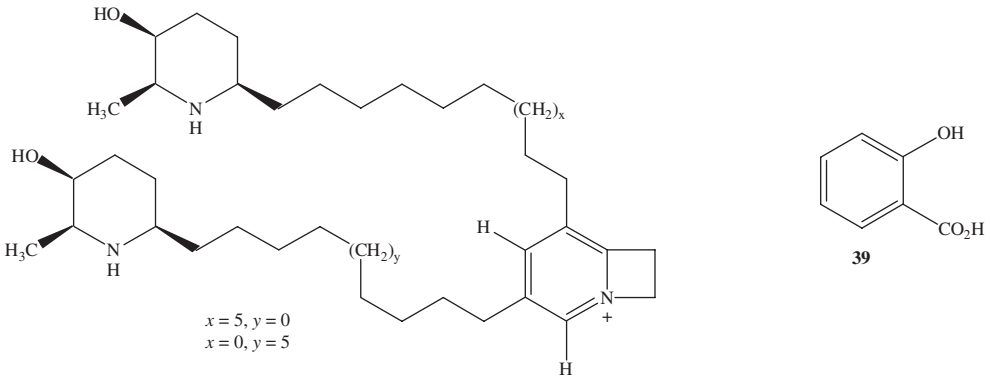

38

39

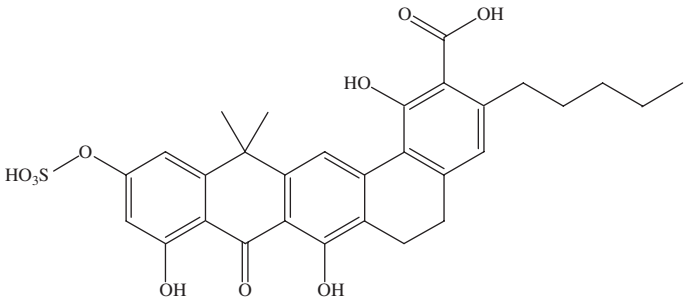

40

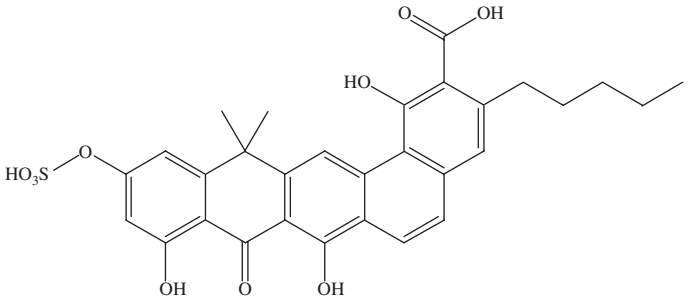

41

Figure 9. Chemical structures of compounds **38–41**.

of ciprofloxacin. This plant alkaloid was also able to reduce the MIC of ciprofloxacin against MRSA strain 15187 from >16 to 8 mg/L. A ciprofloxacin-resistant mutant strain of *S. aureus* also exhibiting an increased MIC against ethidium bromide was rendered susceptible by the addition of piperine. Reserpine exerted a similar effect at an equal concentration. Both of these compounds are substrates for NorA and therefore it is plausible that piperine acts as an inhibitor of this transporter.

In an evaluation of Kuwaiti plants for bacterial resistance-modifying activity, the extracts of *Prosopis juliflora* (Mimosaceae) were studied. This species is known to produce piperidine alkaloids such as julifloridine, juliflorine and juliprosine with some possessing a direct antibacterial activity.[84] The methanol extract was identified to possess resistance-modifying activity by causing a reduction in MIC of norfloxacin against *S. aureus* 1199B. Extensive bioassay-guided fractionation led to the isolation of the active constituent, **38** (Figure 9), and accurate mass determination indicated a molecular formula of $C_{40}H_{72}N_3O_2$. This compound possesses both lipophilic and hydrophilic properties.[85] The large size and lipophilicity of this piperidine alkaloid is a common feature of many known active potentiators against Gram-positive bacteria. From the HMBC spectra, **38** has a pyridine ring attached to a four-membered ring system that should be highly strained and unstable.[85] Mass spectrometry also indicated the presence of two piperidine rings, one with 13 methylenes attached to it and the other with 8 methylenes attached. The two alkylated piperidine ring systems and the 6:4 heterocyclic ring system provided the correct molecular formula. However, there is ambiguity as to the placement of the alkyl chains and only single crystal X-ray structural analysis will provide a definitive answer. The presence of four-membered rings possessing a quaternary nitrogen is very rare both in nature and as synthetic compounds and those described from the literature are brominated on the four-membered ring system.[86] **38** exhibited good potentiation activity against *S. aureus* SA-1199B (NorA), by inhibiting ethidium efflux with an IC_{50} of 7 μM. This is slightly better than reserpine (IC_{50} = 10 μM) but not as active as the synthetic compound

GG918.[87] The authors did not take the possibility of quenching into account. **38** also exerted an antibacterial activity against a panel of MDR MRSA strains with MIC values of 4 mg/L.

Salicylic acid (**39**), a simple phenolic present in many plant species, has recently been shown to induce a reduction of both the antibiotic ciprofloxacin and MDR substrate ethidium bromide for *S. aureus*.[88] This is the reverse of what would be expected for a putative EPI. This has been demonstrated by accumulation studies of ciprofloxacin and ethidium bromide in the presence and absence of this agent. An ethidium efflux assay in the presence of salicylic acid also resulted in an increase in efflux of the MDR substrate ethidium as compared with the assay performed in its absence. Inactivation of NorA did not alter the ability of salicylate to induce increased ciprofloxacin and ethidium resistance. This indicates that NorA is not essential for salicylate-induced MDR for *S. aureus*.[88]

Microbial-derived EPIs

EPIs derived from microbial sources have been relatively scarce to date. The ability of microorganisms to produce antimicrobial compounds as part of their 'chemical arsenal' needs to be combated by susceptible microbes through the evolution of drug resistance. MDR pumps are an example, with an ability to extrude a number of chemically diverse antibiotics with the expression of just a single efflux mechanism. It would therefore seem logical that, as is the case with plants,[60] microorganisms would evolve to produce a second compound that could nullify the effect of MDR pumps in a competing microorganism resulting in the accumulation of the antimicrobial compound to a level that would be static or cidal.

Screening of microbial fermentations has resulted in the characterization of two new natural product EPIs.[89] The MDR inhibitors were isolated from *Streptomyces* MF-EA-371-NS1, which is a new strain closely related to *Streptomyces vellosus*.[89] EA-371α (**40**) and EA-371δ (**41**) (Figure 9) both inhibited the MDR pump MexAB-OprM of *P. aeruginosa* PAM1032, which overexpresses this pump. At a concentration of 0.625 mg/L both compounds caused a 4-fold reduction in the MIC of levofloxacin. An 8-fold reduction of this fluoroquinolone was effected at 1.25 and 2.5 mg/L of EA-371δ and EA-371α, respectively. These compounds were not active against the triple pump deletion strain PAM1626.

Plant extracts exhibiting potentiating activity

The identification of plants able to inhibit efflux pumps is important as they provide a potential for lead optimization and future use with an existing antibacterial rendered ineffective due to MDR pumps in both Gram-positive and Gram-negative bacteria.

Berberis aetnensis, an endemic plant on the volcano Mount Etna,[90] has been shown to exert a synergistic interaction in combination with ciprofloxacin. The modulation activity was located in the chloroform extract, which was fractioned further into yellow and green subfractions, obtained from the leaves of this plant. These lowered the MIC of ciprofloxacin for strains of *S. aureus*, *E. coli* and *P. aeruginosa*. Analytical thin-layer chromatography of the chloroform extract with an authentic sample of pheophorbide *a* indicated the presence of this compound.[90] The results were similar to those obtained when ciprofloxacin was added to commercial pheophorbide *a* at a concentration of 0.5 mg/L. The authors also hypothesized on the presence of 5′-MHC-D, which was isolated previously from *Berberis* species.[38] However, it is plausible that 5′-MHC-D was not present, but rather that an additional metabolite may provide a similar synergistic activity. It is also possible that there were further compounds in this leaf extract that possessed a potentiating activity when combined with a drug such as ciprofloxacin. An interesting finding was that the weaker dilutions (23.3 and 45 mg/L) of the chloroform extracts exhibited a far greater activity than the more concentrated extracts (233 and 450 mg/L). There is the possibility that the putative EPI or EPIs in this leaf extract actually binding to a high-affinity binding site of an efflux pump causing greater inhibition only at low concentration, but at a higher leaf extract concentration would result in low-affinity binding sites being occupied therefore causing a reduction in activity. Strains of *S. aureus*, *E. coli* and *P. aeruginosa* were 33-fold more susceptible to ciprofloxacin at these lower concentrations. It is possible that at high concentration the efflux inhibitors may form complexes with ciprofloxacin reducing the bioavailability of the fluoroquinolone causing a reduction in MIC.[91,92] At lower extract concentrations there would be a greater concentration of ciprofloxacin and efflux inhibitor in the free state to exert their activities. A control to assess the possible interference caused by the solvent used to dissolve the plant extracts in the potentiation assay was not stated.

Extracts of *Mezoneuron benthamianum* (Caesalpinaceae) and *Securinega virosa* (Euphorbiaceae) exerted a potentiation activity against fluoroquinolone-, tetracycline- and erythromycin-resistant strains of *S. aureus*. The ethanol extract of *M. benthamianum* and chloroform extract of *S. virosa* reduced the MIC of norfloxacin against *S. aureus* 1199B by a factor of 4.[93] The petroleum spirit extract of *M. benthamianum* also caused inhibition of the same strain but to a lesser degree and also caused a 2-fold reduction in MIC of tetracycline (64 mg/L from 128 mg/L) against *S. aureus* XU212, containing the Tet(K) transporter.

The methanolic extract of *Punica granatum* (pomegranate) caused an increase in ethidium bromide uptake in *S. aureus* RN-7044, containing the pWBG32 plasmid encoding for an ethidium bromide efflux mechanism.[94] This extract exhibited synergic interactions with chloramphenicol, gentamicin, ampicillin, tetracycline and oxacillin against most of the 30 MRSA and MSSA clinical isolates tested.[94] The effect of methanol alone to assess possible interference in the potentiation assay was not stated by the authors.

Extracts of *Commiphora molmol*, *Centella asiatica*, *Daucus carota*, *Citrus aurantium* and *Glycyrrhiza glabra* showed good activity against three strains of *S. enterica* serovar Typhimurium that overexpress the AcrAB-TolC efflux protein (L. J. V. Piddock and S. Gibbons, unpublished data). This is the main efflux transporter located in the Enterobacteriaceae and is a homologue of the MexAB-OprM transporter, with the capability of extruding many structurally diverse chemicals including tetracyclines, fluoroquinolones and chloramphenicol. Some enhancing activity by the extracts was also detected with the wild-type strains, but not for those that lacked components of the AcrAB-TolC efflux pump when tested with nalidixic acid, chloramphenicol or tetracycline. However, significant reductions were recorded with each plant extract in combination with any of the three drugs tested against strains overexpressing AcrAB-TolC. The reduction

in MIC of these drugs ranged from 4-fold up to 32-fold. No enhancing activity was demonstrated by the extracting solvent alone. These extracts are of interest as they represent an efflux transporter that is difficult to inhibit due to the greater resistance afforded to the Gram-negative cells due to the presence of the outer membrane.

Conclusions

MDR due to the expression of efflux pumps is an increasing clinical problem, rendering many antibiotics redundant. Novel antibiotics with new modes of action are urgently required to suppress the rise of MDR bacteria. An alternative approach would be to identify molecules that can interfere with the process of efflux. Currently there are no EPI/antimicrobial drug combinations on the market, although research into identifying potential EPIs is ongoing both in academic institutions as well as the pharmaceutical industry.[79,95] Success has already been achieved in mammalian cells with resistance modifying agents of *P*-glycoprotein, one of the major MDR mechanisms in cancer cells.[96] Identifying EPIs from natural sources is still in its infancy and the number of research groups seeking inhibitors is small. No natural products have been taken up for further development as much of the data acquired for putative EPIs are only preliminary, resulting from potentiation assays and accumulation and efflux studies. Biochemical studies to provide conclusive evidence of an EPI/protein interaction are required as well as toxicity and small *in vivo* studies to ascertain the pharmacokinetic and toxicity data for potential EPIs. Reserpine is an example of a natural product that has not been further developed; it is neurotoxic at concentrations required to inhibit the efflux pump NorA of *S. aureus*.[97] The cost and time required to identify potential EPIs is another problem.[40] However, the chemical diversity that plants and microorganisms provide, as well as their requirement to biosynthesize such compounds to combat competitors for nutrients, should make the search for EPIs from such sources an attractive option.

This review has highlighted a number of bacterial EPIs derived from natural sources, primarily from plants. The activities of some of these compounds are appreciable and warrant further study as possible candidates for lead optimization. It is our belief that plants should be further exploited for their potential to produce compounds capable of blocking the mechanism of efflux. There is an ecological rationale for the production of natural products that modify bacterial resistance. It has been speculated that plants have evolved compounds which evade MDR mechanisms and that plant antimicrobials might be developed into broad-spectrum antibiotics in combination with inhibitors of MDR.[37]

Some of the compounds described exerted both an antibacterial and potentiating activity. An important issue when identifying a potential EPI is to ensure that the activity being displayed is due to the interference of efflux rather than any other antibacterial activity.

Resistance-modifying compounds active against Gram-positive bacteria tend to be large, lipophilic molecules. To our knowledge, there have been no natural EPIs with enhancing activities for mycobacteria. This can partly be attributed to the fact that the characterization of efflux pumps of this genus has been reported more recently than for Gram-positive or Gram-negative bacteria. There is an urgent need to identify new anti-tuberculosis (TB) compounds due to the high incidence levels of MDR-TB cases. MDR pumps can extrude both first- and second-line drugs such as isoniazid, ethambutol, fluoroquinolones and aminoglycosides.[98] EPIs could increase the lifespan of these drugs, especially as there have been no new antimycobacterial compounds with new modes of action for over 30 years.

The vast majority of EPIs described so far are active against Gram-positive bacteria, particularly *S. aureus*. It is perhaps the Gram-negative species of *Pseudomonas*, *Escherichia* and *Acinetobacter* that will be the most problematic bacteria to treat in the future. These organisms have an intrinsic resistance afforded to them by their thick, lipophilic outer membrane. This view has been strengthened by the dearth of MDR inhibitors described against Gram-negative bacteria in this paper.

Acknowledgements

We would like to thank Dr Mark Webber for data mining the *Bacillus cereus* genome for homologues of Bmr.

Transparency declarations

None to declare.

References

1. Perl TM. The threat of vancomycin resistance. *Am J Med* 1999; **106**: 26–37S.

2. Rotun SS, McMath V, Schoonmaker DJ *et al*. *Staphylococcus aureus* with reduced susceptibility to vancomycin isolated from a patient with fatal bacteremia. *Emerg Infect Dis* 1999; **5**: 147–9.

3. Office for National Statistics. Deaths involving MRSA: England and Wales, 2000–2004. *Health Stat Q* 2006; **29**: 63–8.

4. Blumberg HM, Rimland D, Carroll DJ *et al*. Rapid development of ciprofloxacin resistance in methicillin-susceptible and -resistant *Staphylococcus aureus*. *J Infect Dis* 1991; **163**: 1279–85.

5. Harnett N, Brown S, Krishnan C. Emergence of quinolone resistance among clinical isolates of methicillin-resistant *Staphylococcus aureus* in Ontario, Canada. *Antimicrob Agents Chemother* 1991; **35**: 1911–13.

6. Coronado VG, Edwards JR, Culver DH *et al*. Ciprofloxacin resistance among nosocomial *Pseudomonas aeruginosa* and *Staphylococcus aureus* in the United States. *Infect Control Hosp Epidemiol* 1995; **16**: 71–5.

7. Public Health Dispatch. Vancomycin-resistant *Staphylococcus aureus*. *Morbid Mortal Weekly Rep* 2002; **51**: 902.

8. CDC. *Staphylococcus aureus* resistant to vancomycin. *Morbid Mortal Weekly Rep* 2002; **51**: 565–7.

9. Tsiodras S, Gold HS, Sakoulas G *et al*. Linezolid resistance in a clinical isolate of *Staphylococcus aureus*. *Lancet* 2001; **358**: 207–8.

10. Nikaido H. Prevention of drug access to bacterial targets: permeability barriers and active efflux. *Science* 1994; **264**: 382–8.

11. Poole K. Mechanisms of bacterial biocide and antibiotic resistance. *J Appl Microbiol* 2002; **92**: 55–64S.

12. Leclercq R, Courvalin P. Bacterial resistance to macrolide, lincosamide, and streptogramin antibiotics by target modification. *Antimicrob Agents Chemother* 1991; **35**: 1267–72.

13. Cetinkaya Y, Falk P, Mayhall CG. Vancomycin-resistant enterococci. *Clin Microbiol Rev* 2000; **13**: 686–707.

14. Chambers HF. Methicillin resistance in staphylococci: molecular and biochemical basis and clinical implications. *Clin Microbiol Rev* 1997; **10**: 781–91.

15. Hiramatsu K, Cui L, Kuroda M *et al*. The emergence and evolution of methicillin-resistant *Staphylococcus aureus*. *Trends Microbiol* 2001; **9**: 486–93.

16. Hooper DC. Mechanisms of action and resistance of older and newer fluoroquinolones. *Clin Infect Dis* 2000; **31**: S24–8.

17. Wright GD. Aminoglycoside-modifying enzymes. *Curr Opin Microbiol* 1999; **2**: 499–503.

18. Thompson KS, Smith ME. Version 2000: the new β-lactamases of Gram-negative bacteria at the dawn of the new millenium. *Microbes Infect* 2000; **2**: 1225–35.

19. Wright GD, Berghuis AM, Mobashery S. Aminoglycoside antibiotics. Structures, functions, and resistance. *Adv Exp Med Biol* 1998; **456**: 27–69.

20. Murray IA, Shaw WV. *O*-Acetyltransferases for chloramphenicol and other natural products. *Antimicrob Agents Chemother* 1997; **41**: 1–6.

21. Ball PR, Shales SW, Chopra I. Plasmid-mediated tetracycline resistance in *Escherichia coli* involves increased efflux of the antibiotic. *Biochem Biophys Res Commun* 1980; **93**: 74–81.

22. McMurry LM, Petrucci RE Jr, Levy SB. Active efflux of tetracycline encoded by four genetically different tetracycline resistance determinants in *Escherichia coli*. *Proc Natl Acad Sci USA* 1980; **77**: 3974–7.

23. Chopra I, Roberts MC. Tetracycline antibiotics: mode of action, applications, molecular biology and epidemiology of bacterial resistance. *Microbiol Mol Biol Rev* 2001; **65**: 232–60.

24. Roberts MC. Update on acquired tetracycline resistance genes. *FEMS Microbiol Lett* 2005; **245**: 195–203.

25. Piddock LJV. Clinically relevant bacterial chromosomally encoded multi-drug resistance efflux pumps. *Clinl Microbiol Rev* 2006; **19**: 382–402.

26. Li XZ, Poole K, Nikaido H. Contributions of MexAB-OprM and an EmrE homolog to intrinsic resistance of *Pseudomonas aeruginosa* to aminoglycosides and dyes. *Antimicrob Agents Chemother* 2003; **47**: 27–33.

27. Aires JR, Kohler T, Nikaido H *et al*. Involvement of an active efflux system in the natural resistance of *Pseudomonas aeruginosa* to aminoglycosides. *Antimicrob Agents Chemother* 1999; **43**: 2624–8.

28. Poole K. Efflux mediated antimicrobial resistance. *J Antimicrob Chemother* 2005; **56**: 20–51.

29. Arcangioli MA, Leroy-Setrin S, Martel JL *et al*. A new chloramphenicol and florfenicol resistance gene flanked by two integron structures in *Salmonella typhimurium* DT104. *FEMS Microbiol Lett* 1999; **174**: 327–32.

30. Lomovskaya O, Lee A, Hoshino K *et al*. Use of a genetic approach to evaluate the consequences of inhibition of efflux pumps in *Pseudomonas aeruginosa*. *Antimicrob Agents Chemother* 1999; **43**: 1340–6.

31. Esposito S, Noviello S. *In-vitro* sensitivity of amoxicillin/clavulanic acid (Augmentin) to isolated β-lactamases and *in-vitro* antibacterial activity. *J Chemother* 1990; **2**: 167–70.

32. Lorian V. *Antibiotics in Laboratory Medicine*. Baltimore: Williams and Wilkins, 1996.

33. Gibbons S, Oluwatuyi M, Veitch N *et al*. Bacterial resistance modifying agents from *Lycopus europaeus*. *Phytochemistry* 2003; **62**: 83–7.

34. Oluwatuyi M, Kaatz GW, Gibbons S. Antibacterial and resistance modifying activity of *Rosmarinus officinalis*. *Phytochemistry* 2004; **65**: 3249–54.

35. Belofsky G, Carreno R, Lewis K *et al*. Metabolites of the 'smoke tree', *Dalea spinosa*, potentiate antibiotic activity against multidrug-resistant *Staphylococcus aureus*. *J Nat Prod* 2006; **69**: 261–4.

36. Marchetti O, Moreillon P, Glauser MP *et al*. Potent synergism of the combination of fluconazole and cyclosporine in *Candida albicans*. *Antimicrob Agents Chemother* 2000; **44**: 2373–81.

37. Tegos G, Stermitz FR, Lomovskaya O *et al*. Multidrug pump inhibitors uncover remarkable activity of plant antimicrobials. *Antimicrob Agents Chemother* 2002; **46**: 3133–41.

38. Stermitz FR, Tawara-Matsuda J, Lorenz P *et al*. 5'-Methoxyhydnocarpin-D and pheophorbide A: *Berberis* species components that potentiate berberine growth inhibition of resistant *Staphylococcus aureus*. *J Nat Prod* 2000; **63**: 1146–9.

39. Kaatz GW, Seo SM, O'Brien L *et al*. Evidence for the existence of a multidrug efflux transporter distinct from NorA in *Staphylococcus aureus*. *Antimicrob Agents Chemother* 2000; **44**: 1404–6.

40. Kaatz GW, Moudgal VV, Seo SM *et al*. Phenothiazines and thioxanthenes inhibit multidrug efflux pump activity in *Staphylococcus aureus*. *Antimicrob Agents Chemother* 2003; **47**: 719–26.

41. Kaatz GW, Moudgal VV, Seo SM. Identification and characterization of a novel efflux-related multidrug resistance phenotype in *Staphylococcus aureus*. *J Antimicrob Chemother* 2002; **50**: 833–8.

42. Kaatz GW, Seo SM, Ruble CA. Efflux-mediated fluoroquinolone resistance in *Staphylococcus aureus*. *Antimicrob Agents Chemother* 1993; **37**: 1086–94.

43. Samorsorn S, Bremner JB, Ball A *et al*. Synthesis of functionalised 2-aryl-5-nitro-1*H*-indoles and their activity as bacterial NorA efflux pump inhibitors. *Bioorg Med Chem Lett* 2006; **14**: 857–65.

44. Baranova N, Nikaido H. The baeSR two-component regulatory system activates transcription of the *yegMNOB* (*mdtABCD*) transporter gene cluster in *Escherichia coli* and increases its resistance to novobiocin and deoxycholate. *J Bacteriol* 2002; **184**: 4168–76.

45. Kaatz GW, Moudgal VV, Seo SM *et al*. Phenylpiperidine selective serotonin reuptake inhibitors interfere with multidrug efflux pump activity in *Staphylococcus aureus*. *Int J Antimicrob Agents* 2003; **22**: 254–61.

46. Piddock LJV. Multidrug-resistance efflux pumps—not just for resistance. *Nat Rev Microbiol* 2006; **4**: 629–36.

47. Poisson J, Le Hir A, Goutarel R *et al*. Isolation of reserpine from roots of *Rauwolfia vomitoria* Afz. *C R Hebd Seances Acad Sci* 1954; **238**: 1607–9.

48. Neyfakh AA, Bidnenko VE, Chen LB. Efflux-mediated multi-drug resistance in *Bacillus subtilis*: similarities and dissimilarities with the mammalian system. *Proc Natl Acad Sci USA* 1991; **88**: 4781–5.

49. Klyachko KA, Schuldiner S, Neyfakh AA. Mutations affecting substrate specificity of the *Bacillus subtilis* multidrug transporter Bmr. *J Bacteriol* 1997; **179**: 2189–93.

50. Gibbons S, Udo EE. The effect of reserpine, a modulator of multidrug efflux pumps, on the *in vitro* activity of tetracycline against clinical isolates of methicillin resistant *Staphylococcus aureus* (MRSA) possessing the *tet*(K) determinant. *Phytother Res* 2000; **14**: 139–40.

51. Neyfakh AA, Borsch CM, Kaatz GW. Fluoroquinolone resistance protein NorA of *Staphylococcus aureus* is a multidrug efflux transporter. *Antimicrob Agents Chemother* 1993; **37**: 128–9.

52. Kaatz GW, Seo SM. Inducible NorA-mediated multidrug resistance in *Staphylococcus aureus*. *Antimicrob Agents Chemother* 1995; **39**: 2650–5.

53. Schmitz FJ, Fluit AC, Luckefahr M *et al*. The effect of reserpine, an inhibitor of multidrug efflux pumps, on the *in-vitro* activities of ciprofloxacin, sparfloxacin and moxifloxacin against clinical isolates of *Staphylococcus aureus*. *J Antimicrob Chemother* 1998; **42**: 807–10.

54. Brenwald NP, Gill MJ, Wise R. The effect of reserpine, an inhibitor of multi-drug efflux pumps, on the *in-vitro* susceptibilities of fluoroquinolone-resistant strains of *Streptococcus pneumoniae* to norfloxacin. *J Antimicrob Chemother* 1997; **40**: 458–60.

55. Markham PN. Inhibition of the emergence of ciprofloxacin resistance in *Streptococcus pneumoniae* by the multidrug efflux inhibitor reserpine. *Antimicrob Agents Chemother* 1999; **43**: 988–9.

56. Gill MJ, Brenwald NP, Wise R. Identification of an efflux pump gene, *pmrA*, associated with fluoroquinolone resistance in *Streptococcus pneumoniae*. *Antimicrob Agents Chemother* 1999; **43**: 187–9.

57. Piddock LJV, Johnson MM. Accumulation of ten fluoroquinolones by wild-type and efflux mutant *Streptococcus pneumoniae*. *Antimicrob Agents Chemother* 2002; **46**: 813–20.

58. Marrer E, Satoh T, Johnson MM *et al*. Global transcriptome analysis of the responses of a fluoroquinolone-resistant *Streptococcus pneumoniae* mutant and its parent to ciprofloxacin. *Antimicrob Agents Chemother* 2006; **50**: 269–78.

59. Robertson GT, Doyle TB, Lynch AS. Use of an efflux-deficient *Streptococcus pneumoniae* strain panel to identify ABC-class multidrug transporters involved in intrinsic resistance to antimicrobial agents. *Antimicrob Agents Chemother* 2005; **49**: 4781–3.

60. Stermitz FR, Lorenz P, Tawara JN *et al*. Synergy in a medicinal plant: antimicrobial action of berberine potentiated by 5′-methoxyhydnocarpin, a multidrug pump inhibitor. *Proc Natl Acad Sci USA* 2000; **97**: 1433–7.

61. Stermitz FR, Beeson TD, Mueller PJ *et al*. *Staphylococcus aureus* MDR efflux pump inhibitors from a *Berberis* and a *Mahonia* (sensu strictu) species. *Biochem Syst Ecol* 2001; **29**: 793–8.

62. Stermitz FR, Scriven LN, Tegos G *et al*. Two flavonols from *Artemisia annua* which potentiate the activity of berberine and norfloxacin against a resistant strain of *Staphylococcus aureus*. *Planta Med* 2002; **68**: 1140–1.

63. Morel C, Stermitz FR, Tegos G *et al*. Isoflavones as potentiators of antibacterial activity. *J Agric Food Chem* 2003; **51**: 5677–9.

64. Liu KCS, Yang SL, Roberts MF *et al*. Antimalarial activity of *Artemisia annua* flavonoids from whole plants and cell cultures. *Plant Cell Rep* 1992; **11**: 637–40.

65. Stermitz FR, Cashman KK, Halligan KM *et al*. Polyacylated neohesperidosides from *Geranium caespitosum*: bacterial multidrug resistance pump inhibitors. *Bioorg Med Chem Lett* 2003; **13**: 1915–8.

66. Belofsky G, Percivill D, Lewis K *et al*. Phenolic metabolites of *Dalea versicolor* that enhance antibiotic activity against model pathogenic bacteria. *J Nat Prod* 2004; **67**: 481–4.

67. Pereda-Miranda R, Kaatz GW, Gibbons S. Polyacylated oligosaccharides from medicinal Mexican morning glory species as antibacterials and inhibitors of multidrug resistance in *Staphylococcus aureus*. *J Nat Prod* 2006; **69**: 406–9.

68. Babayan A, Nikaido H. In *Pseudomonas aeruginosa* ethidium bromide does not induce its own degradation or the assembly of pumps involved in its efflux. *Biochem Biophys Res Commun* 2004; **324**: 1065–8.

69. Yam TS, Hamilton-Miller JMT, Shah S. The effect of a component of tea (*Camellia sinensis*) on methicillin resistance, PBP2′ synthesis, and β-lactamase production in *Staphylococcus aureus*. *J Antimicrob Chemother* 1998; **42**: 211–16.

70. Hamilton-Miller JMT, Shah S. Disorganization of cell division of methicillin-resistant *Staphylococcus aureus* by a component of tea (*Camellia sinensis*): a study by electron microscopy. *FEMS Microbiol Lett* 1999; **176**: 463–9.

71. Hamilton-Miller JMT, Shah S. Activity of the tea component epicatechin gallate and analogues against methicillin-resistant *Staphylococcus aureus*. *J Antimicrob Chemother* 2000; **46**: 852–3.

72. Gibbons S, Moser E, Kaatz GW. Catechin gallates inhibit multidrug resistance (MDR) in *Staphylococcus aureus*. *Planta Med* 2004; **70**: 1240–2.

73. Roccaro AS, Blanco AR, Giuliano F *et al*. Epigallocatechin-gallate enhances the activity of tetracycline in staphylococci by inhibiting its efflux from bacterial cells. *Antimicrob Agents Chemother* 2004; **48**: 1968–73.

74. Fujita M, Shiota S, Kuroda T *et al*. Remarkable synergies between baicalein and tetracycline, and baicalein and β-lactams against methicillin-resistant *Staphylococcus aureus*. *Microbiol Immunol* 2005; **49**: 391–6.

75. Abulrob AN, Suller MTE, Gumbleton M *et al*. Identification and biological evaluation of grapefruit oil components as potential novel efflux pump modulators in methicillin-resistant *Staphylococcus aureus* bacterial strains. *Phytochemistry* 2004; **65**: 3021–7.

76. Kristiansen MM, Leandro C, Ordway D *et al*. Phenothiazines alter resistance of methicillin-resistant strains of *Staphylococcus aureus* (MRSA) to oxacillin *in vitro*. *Int J Antimicrob Agents* 2003; **22**: 250–3.

77. Pruneau M, Moisan H, Malouin F. Transcriptomics of antibiotic resistance and virulence genes in methicillin-resistant *Staphylococcus aureus*. In: *Abstracts of the Forty-fifth Interscience Conference on Antimicrobial Agents and Chemotherapy, Washington, DC, 2005*. Poster C1-906. American Society for Microbiology, Washington, DC, USA.

78. Marquez B, Neuville L, Moreau NJ *et al*. Multidrug resistance reversal agent from *Jatropha elliptica*. *Phytochemistry* 2005; **66**: 1804–11.

79. Guz NR, Stermitz FR, Johnson JB *et al*. Flavonolignan and flavone inhibitors of a *Staphylococcus aureus* multidrug resistance pump: structure-activity relationships. *J Med Chem* 2001; **44**: 261–8.

80. Hohmann J, Molnar J, Redei D *et al*. Discovery and biological evaluation of a new family of potent modulators of multidrug resistance: reversal of MDR of mouse lymphoma cells by new natural jatrophane diterpenoids isolated from *Euphorbia* species. *J Med Chem* 2002; **45**: 2425–31.

81. Hohmann J, Redei D, Forgo P *et al*. Jatrophane diterpenoids from *Euphorbia mongolica* as modulators of the multidrug resistance of tumor cells. *J Nat Prod* 2003; **66**: 976–9.

82. Corea G, Fattorusso E, Lanzotti V *et al*. Advances of structure-activity relationships and discovery of the potent lead pepluanin A. *J Med Chem* 2004; **47**: 988–92.

83. Khan IA, Mirza ZH, Kumar A *et al*. Piperine, a phytochemical potentiator of ciprofloxacin against *Staphylococcus aureus*. *Antimicrob Agents Chemother* 2006; **50**: 810–12.

84. Ahmad A, Khan KA, Ahmad VU *et al*. Antibacterial activity of juliflorine isolated from *Prosopis juliflora*. *Planta Med* 1986; **4**: 285–8.

85. Gibbons S. Plants as a source of bacterial resistance modulators and anti-infective agents. *Phytochem Rev* 2005; **4**: 63–78.

86. Anderson S, Glover EE, Vaughan KD. The *N*-amination and subsequent oxidation by bromine of imidazo[1,5-α] pyridines. *J Chem Soc Perk Trans* 1976; **1**: 1722–4.

87. Gibbons S, Oluwatuyi M, Kaatz GW. A novel inhibitor of multidrug efflux pumps in *Staphylococcus aureus*. *J Antimicrob Chemother* 2003; **51**: 13–17.

88. Price CTD, Kaatz GW, Gustafson JE. The multidrug efflux pump NorA is not required for salicylate-induced reduction in drug accumulation by *Staphylococcus aureus*. *Int J Antimicrob Agents* 2002; **20**: 206–13.

89. Lee MD, Galazzo JL, Staley AL *et al*. Microbial fermentation-derived inhibitors of efflux-pump-mediated drug resistance. *Farmaco* 2001; **56**: 81–5.

90. Musumeci R, Speciale A, Costanzo R *et al*. *Berberis aetnensis* C. Presl. extracts: antimicrobial properties and interaction with ciprofloxacin. *Int J Antimicrob Agents* 2003; **22**: 48–53.

91. Smith E, Williamson E, Zloh M *et al*. Isopimaric acid from *Pinus nigra* shows activity against multidrug-resistant and EMRSA strains of *Staphylococcus aureus*. *Phytother Res* 2005; **19**: 538–42.

92. Zloh M, Kaatz GW, Gibbons S. Inhibitors of multidrug resistance (MDR) have affinity for MDR substrates. *Bioorg Med Chem Lett* 2004; **14**: 881–5.

93. Dickson RA, Houghton PJ, Hylands PJ *et al*. Antimicrobial, resistance-modifying effects, antioxidant and free radical scavenging activities of *Mezoneuron benthamianum* Baill., *Securinega virosa* Roxb. &Wlld. and *Microglossa pyrifolia* Lam. *Phytother Res* 2006; **20**: 41–5.

94. Braga LC, Leite AAM, Xavier KGS *et al*. Synergic interaction between pomegranate extract and antibiotics against *Staphylococcus aureus*. *Can J Microbiol* 2005; **51**: 541–7.

95. Lomovskaya O, Warren MS, Lee A *et al*. Identification and characterization of inhibitors of multidrug resistance efflux pumps in

Pseudomonas aeruginosa: novel agents for combination therapy. *Antimicrob Agents Chemother* 2001; **45**: 105–16.

96. Teodori E, Dei S, Martelli C *et al*. The functions and structure of ABC transporters: implications for the design of new inhibitors of Pgp and MRP1 to control multidrug resistance (MDR). *Curr Drug Targets* 2006; **7**: 893–909.

97. Markham PN, Neyfakh AA. Inhibition of the multi-drug transporter *norA* prevents emergence of norfloxacin resistance in *Staphylococcus aureus*. *Antimicrob Agents Chemother* 1996; **40**: 2673–4.

98. De Rossi E, Ainsa JA, Riccardi G. Role of mycobacterial efflux transporters in drug resistance: an unresolved question. *FEMS Microbiol Rev* 2006; **30**: 36–52.

Available online at www.sciencedirect.com
ScienceDirect
Bioorganic & Medicinal Chemistry Letters 17 (2007) 1755–1758
Bioorganic & Medicinal Chemistry Letters

N-Caffeoylphenalkylamide derivatives as bacterial efflux pump inhibitors

Serge Michalet,[a,*] Gilbert Cartier,[a] Bruno David,[b] Anne-Marie Mariotte,[a] Marie-Geneviève Dijoux-franca,[a] Glenn W. Kaatz,[c] Michael Stavri[d] and Simon Gibbons[d]

[a]*DPM UMR 5063 CNRS-UJF, Equipe de Pharmacognosie, UFR de Pharmacie de Grenoble, Domaine de La Merci, 38706 La Tronche cedex, France*
[b]*Centre de Recherche des Substances Naturelles, UMS CNRS/IRPF No. 2597, 3, rue des Satellites, 31432 Toulouse, France*
[c]*Department of Internal Medicine, Division of Infectious Diseases, School of Medicine, Wayne State University and the John D. Dingell Department of Veteran Affairs Medical Center, Detroit, MI 48201, USA*
[d]*Centre for Pharmacognosy and Phytotherapy, School of Pharmacy, University of London, 29/39 Brunswick Square, WC1N 1AX London, UK*

Received 16 October 2006; revised 15 December 2006; accepted 16 December 2006
Available online 22 December 2006

Abstract—As part of an ongoing project to identify plant natural products as efflux pump inhibitors (EPIs), bioassay-guided fractionation of the methanolic extract of *Mirabilis jalapa* Linn. (Nyctaginaceae) led to the isolation of an active polyphenolic amide: *N*-*trans*-feruloyl 4′-*O*-methyldopamine. This compound showed moderate activity as an EPI against multidrug-resistant (MDR) *Staphylococcus aureus* overexpressing the multidrug efflux transporter NorA, causing an 8-fold reduction of norfloxacin MIC at 292 μM (100 μg/mL). This prompted us to synthesize derivatives in order to provide structure–activity relationships and to access more potent inhibitors. Among the synthetic compounds, some were more active than the natural compound and *N*-*trans*-3,4-*O*-dimethylcaffeoyl tryptamine showed potentiation of norfloxacin in MDR *S. aureus* comparable to that of the standard reserpine.

In recent years bacterial resistance to antibiotics has become a serious problem of public health that concerns almost all antibacterial agents. Among the mechanisms involved (target modification, enzymatic inactivation or reduction of accumulation within the cell), active efflux has received particular attention since it has been recognised as one of the most important causes of intrinsic antibiotic resistance in bacteria.[1]

One species is particularly resistant to treatment, notably *Staphylococcus aureus*. This pathogen has evolved from the MRSA phenotype (methicillin-resistant *S. aureus*) to the VRSA phenotype (vancomycin-resistant *S. aureus*), whereas vancomycin was the drug of last-resort for treatment of MRSA.[2] Resistance has also been reported for newer agents such as linezolid and daptomycin.[3,4]

Of particular concern is the presence of multidrug resistance (MDR) efflux pumps that extrude a wide range of structurally unrelated compounds. The NorA protein of *S. aureus* is a drug/proton antiporter belonging to the major facilitator family (MFS) of transporters and is responsible for the efflux of substances such as norfloxacin, ciprofloxacin, ethidium bromide and acriflavin.[5,6] It has been recognised as one of the major efflux pumps protecting *S. aureus* from antibiotics.[7]

One of the strategies employed to overcome bacterial resistance is the use of EPIs that could restore antibiotic activity in resistant strains. This approach is promising as it would be a way to improve the efficacy and/or extend the clinical utility of existing antibiotics.[8] The combination of a resistance inhibitor with an antibiotic has already proven its efficacy with the clavulanic acid/amoxicillin association. Furthermore, this combination can reduce the in vitro frequency of emergence of resistant mutant strains.[9] At present this combination therapy is taken into account by a number of pharmaceutical companies and several strategies are being developed by different groups.[10]

Keywords: EPI; *Staphylococcus aureus*; *N*-Hydroxycinnamic acid derivatives; *Mirabilis jalapa*.
* Corresponding author. Tel.: +33 4 76 51 86 88; fax: +33 4 76 63 71 65; e-mail: sergemichalet@yahoo.fr

0960-894X/$ - see front matter © 2007 Elsevier Ltd. All rights reserved.
doi:10.1016/j.bmcl.2006.12.059

Plants use antimicrobials to protect themselves from environmental stresses, but unlike fungi or bacteria activities are often weak and with a narrow spectrum. This poses the interesting question of how plants react towards increasing antimicrobial resistance. Some authors postulate that plants use an anti-MDR strategy to potentiate their antimicrobials.[11] This is the case for the alkaloid berberine which has a weak antimicrobial activity that is significantly enhanced by 5′-methoxyhydnocarpin (5′-MHC), a flavonolignan produced by the same *Berberis* species.[12] 5′-MHC does not have any antibacterial activity on its own but potentiates the activity of berberine by inhibiting its efflux. A number of inhibitors produced by plants as secondary metabolites and belonging to many chemical classes have been identified but few are potent and have a broad spectrum of action.[13] This includes the alkaloid reserpine which is used as a standard but cannot be used in therapy because of its toxicity. Searching for inhibitors from natural sources is therefore an attractive strategy to access a greater range of active compounds.

In this context, previous screening of ornamental and exotic plants showed activity associated with extracts of *Mirabilis jalapa* Linn. (Nyctaginaceae) in reversing fluoroquinolone resistance in *S. aureus* overexpressing the NorA MDR efflux pump (SA-1199B strain).[14] This plant is used in folk medicine as an anti-infective.[15,16] Bioassay-guided fractionation of the methanolic extract from leaves and stems of *M. jalapa* led to the isolation of an active phenolic compound, namely *N-trans*-feruloyl 4′-*O*-methyldopamine, which has already been reported in the plant kingdom.[17] This compound caused an 8-fold reduction of norfloxacin MIC when tested at 100 μg/mL (292 μM). Synthesis of derivatives was then undertaken as this small molecule was a good starting point for structure–activity relationships (SARs), and could be a good candidate for combination therapy.

We chose couplings between cinnamic acid derivatives and amines that occur in nature, as our project was to identify active compounds from natural sources. Several structure–activity relationship criteria were examined: substitution on the aromatic ring on each part, methoxy or hydroxyl substitution influence, double bond influence, aromatic ring nature on the amine part (we chose here to test tryptamine combinations as indolic compounds are known to be good inhibitors).[18] We chose *N-trans*-3,4-*O*-dimethylcaffeoyl dopamine as lead compound as it showed the same activity as the natural compound, and its asymetrical substitution allowed us to have a better understanding of the influence of each substituant (i.e., hydroxyl or methoxy) on each part of the molecule. Each time, one part of the lead compound was conserved and the other part was varied in order to provide structure–activity relationships that could lead to further optimisation. Compounds were obtained by coupling of a cinnamic acid (or dihydrocinnamic acid in the case of compound **8**) derivative with the corresponding amine in DMF in the presence of triethylamine and BOP (benzotriazol-1-yloxy-tris-(dimethylamino)-phosphonium hexafluorophosphate) as a coupling agent (Scheme 1).[19] Nine compounds were synthesized and their related activities are presented in Table 1.[20] MICs of the modulators were determined when good potentiation was observed; a good resistance reverser should actually not show any antibacterial effect at the tested concentrations.

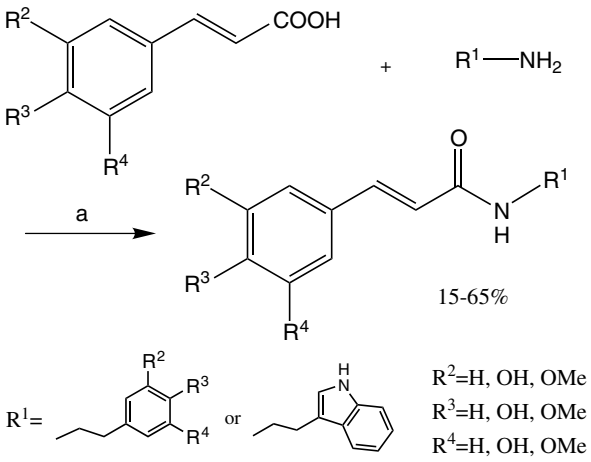

Scheme 1. Reagents and condition: (a) BOP, Et_3N, DMF, 20 h. Compound **8** was prepared with 3,4-dimethoxy-dihydrocinnamic acid.

Interpretation of the results led us to draw several conclusions:

- For the cinnamic part: an hydroxyl substitution on the aromaticring appears to be better than methoxy or unsubstituted (compound **2** versus compounds **1** and **6**); the double bond is essential for activity.
- For the amine part: trisubstitution on the aromatic ring led to a decrease in activity but antibacterial activity was observed (compound **5**); methoxy substitution gave better results than hydroxyl substitution (compound **3** vs compound **1**) which, in turn, were better than no substitution (compound **1** vs compound **7**); tryptamine combinations showed the best results (compound **9**).

Among the 9 compounds tested, compound **9** showed potentiation of norfloxacin comparable to that of the reference alkaloid reserpine. In order to confirm the inhibitory mechanism, we performed an efflux inhibition assay using ethidium bromide (EtBr), a good substrate of NorA, whose efflux can be measured by loss of fluorescence within the cell (Fig. 1).[21,22]

Based on estimation of IC_{50}, compound **9** was approximately 2-fold less active than reserpine at inhibiting EtBr efflux (Fig. 1). However, this difference disappeared at a concentration of 30 μM for each compound.

Structure–activity relationships (SARs) showed that better activities were obtained when the phenyl ring on the cinnamic portion was substituted with 2 hydroxyls. According to this result, we would expect *N-trans*-caffeoyl tryptamine (dihydroxylated equivalent of compound **9**) to be more active than compound **9**. It

Table 1. Potentiation of norfloxacin MIC on SA-1199B strain cells by synthetic compounds

Compound	Formula	[Concentration]/fold reduction of norfloxacin MIC
1 (lead)	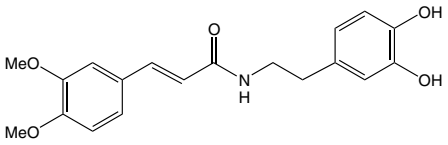	[292 μM]/**8** [146 μM]/**4**
2	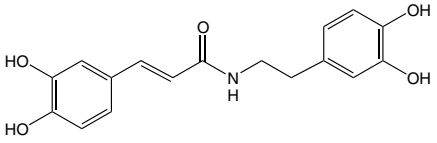	[317 μM]/**8** [63 μM]/**4** MIC ⩾ 406 μM
3	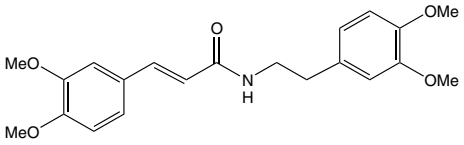	[162 μM]/**8** [54 μM]/**2**
4	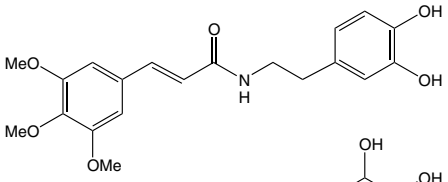	[268 μM]/**4**
5	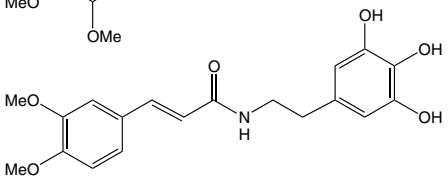	[56 μM]/**0** MIC = 356 μM
6	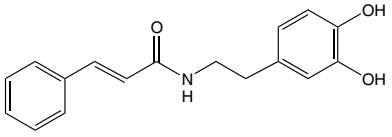	[353 μM]/**16** [70 μM]/**4** MIC > 452 μM
7	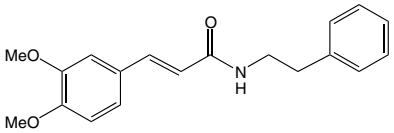	[322 μM]/**4**
8	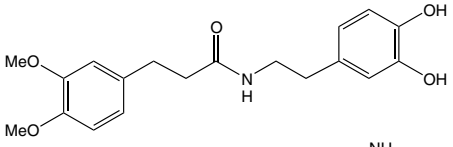	[290 μM]/**0**
9	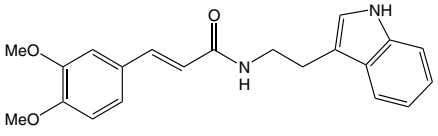	[286 μM]/**16** [57 μM]/**8** [29 μM]/**4** MIC > 366 μM

would also be interesting to evaluate whether this type of compound would be a good EPI in Gram-negative bacteria or in other models.

In summary, we have demonstrated that *N*-cinnamoylphenalkylamides are a class of EPIs that could be used to potentiate the bactericidal effect of antibiotics such as norfloxacin in multidrug-resistant pathogenic bacteria such as *S. aureus*. The ease of synthesis and the small size of these compounds make them potential candidates for SARs as EPIs in multidrug efflux systems.

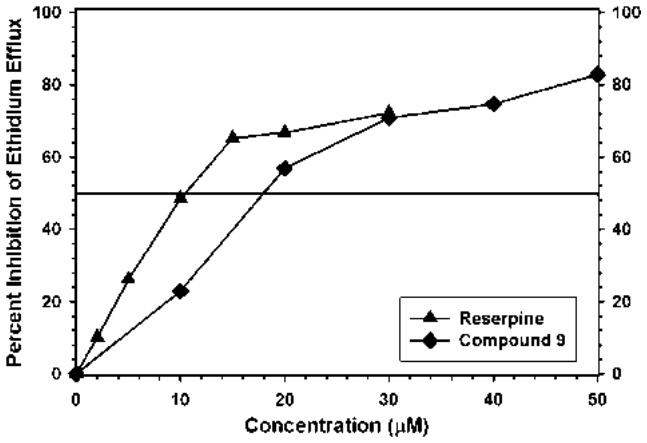

Figure 1. Ethidium efflux inhibition assay from SA-1199B strain cells: (▲) reserpine; (♦) compound **9**.

Acknowledgments

We are thankful to Institut Klorane (Laboratoires Pierre Fabre) for a PhD studentship for S. Michalet. Region Rhône-Alpes is also acknowledged for the Eurodoc scholarship program.

References and notes

1. Ryan, B. M.; Dougherty, T. J.; Beaulieu, D.; Chuang, J.; Dougherty, B. A.; Barrett, J. F. *Expert Opin. Investig. Drugs* **2001**, *10*, 1409.
2. Hiramatsu, K. *Lancet Infect. Dis.* **2001**, *1*, 147.
3. Tsiodras, S.; Gold, H.; Sakoulas, G.; Eliopoulos, G.; Wennersten, C.; Venkataraman, L.; Moellering, R. C.; Ferraro, M. J. *Lancet* **2001**, *358*, 207.
4. Hershberger, E.; Donadebian, S.; Konstantinou, K.; Zervos, M. J. *Clin. Infect. Dis.* **2004**, *38*, 92.
5. Neyfakh, A. A.; Borsh, C. M.; Kaatz, G. W. *Antimicrob. Agents Chemother.* **1993**, *37*, 128.
6. Nakae, T.; Yoshihara, E.; Yoneyama, H. *J. Infect. Chemother.* **1997**, *3*, 173.
7. Hsieh, P. C.; Siegel, S. A.; Rogers, B.; Davis, D.; Lewis, K. *Proc. Natl. Acad. Sci. U.S.A.* **1998**, *95*, 6602.
8. Lynch, A. S. *Biochem. Pharmacol.* **2006**, *71*, 949.
9. Schmitz, F.-J.; Fluit, A. C.; Luckefahr, M.; Engler, B.; Hofmann, B.; Verhoef, J.; Heinz, H.-P.; Hadding, U.; Jones, M. E. *J. Antimicrob. Chemother.* **1998**, *42*, 807.
10. Poole, K.; Lomovskaya, O. *Drug Discovery Today* **2006**, *3*, 145.
11. Stermitz, F. R.; Lorenz, P.; Tawara, J. N.; Zenewicz, L. A.; Lewis, K. *Proc. Natl. Acad. Sci. U.S.A.* **2000**, *97*, 1433.
12. Stermitz, F. R.; Tawara-Matsuda, J. N.; Lorenz, P.; Muller, P.; Zenewicz, L. A. *J. Nat. Prod.* **2000**, *63*, 1146.
13. Gibbons, S. *Nat. Prod. Rep.* **2004**, *21*, 263.
14. Cegiela-Carlioz, P. Ph.D. thesis, University of Grenoble I, April 2004.
15. Siddiqui, S.; Siddiqui, B. S.; Adil, Q.; Begum, S. *Fitoterapia* **1990**, *61*, 471.
16. Kusamba, C.; Byamana, K.; Mbuyi, W. M. *J. Ethnopharmacol.* **1991**, *35*, 197.
17. Cutillo, F.; d'Abrosca, B.; DellaGreca, M.; Di Marco, C.; Golino, A.; Previtera, L.; Zarrelli, A. *Phytochemistry* **2003**, *64*, 1381.
18. Samosorn, S.; Bremner, J. B.; Ball, A.; Lewis, K. *Bioorg. Med. Chem.* **2006**, *14*, 857.
19. Analytical data for new compounds: for Compound **1**: ^{1}H NMR (400 MHz, CD_3OD): δ 7.46 (d, 1H, J = 15.6 Hz), δ 7.16 (d, 1H, J = 2.0 Hz), δ 7.13 (dd, 1H, J_1 = 8.4 Hz; J_2 = 2.0 Hz), δ 6.97 (d, 1H, J = 8.4 Hz), δ 6.70 (d, 1H, J = 8.0 Hz), δ 6.69 (d, 1H, J = 2.0 Hz), δ 6.57 (dd, 1H, J_1 = 8.0 Hz; J_2 = 2.0 Hz), δ 6.46 (d, 1H, J = 15.6 Hz), 3.87 (s, 3H); 3.87 (s, 3H), δ 3.48 (t, 2H, J = 7.6 Hz), δ 2.68 (t, 2H, J = 7.6 Hz), RMN ^{13}C (100 MHz, CD_3OD): δ 167.6; δ 150.8; δ 149.3; δ 144.9; δ 143.4; δ 140.2; δ 130.7; δ 128.0; δ 121.8; δ 119.6; δ 118.3; δ 115.5; δ 115.0; δ 111.3; δ 109.9; δ 55.0; δ 55.0; δ 41.2; δ 34.6. EIMS: m/z = 343 [M^+]. For Compound **4**: RMN ^{1}H (400 MHz, CD_3OD): δ 7.45 (d, 1H, J = 15.6 Hz), δ 6.87 (s, 2H); δ 6.71 (d, 1H, J = 8.0 Hz), δ 6.69 (d, 1H, J = 2.0 Hz), δ 6.57 (dd, 1H, J_1 = 8.0 Hz; J_2 = 2.0 Hz), δ 6.52 (d, 1H, J = 15.6 Hz), δ 3.87 (s, 3H), δ 3.87 (s, 3H), δ 3.80 (s, 3H), δ 3.48 (t, 2H, J = 6.8 Hz), δ 2.62 (t, 2H, J = 6.8 Hz); RMN ^{13}C (100 MHz, CD_3OD): δ 167.2; δ 155.4; δ 144.6; δ 143.5; δ 142.3; δ 140.2; δ 130.9; δ 130.8; δ 120.0; δ 119.6; δ 117.6; δ 115.5; δ 115.0; δ 114.9; δ 114.6; δ 104.9; δ 59.8; δ 55.3; δ 55.3; δ 41.1; δ 34.6. EIMS: m/z = 373 [M^+]. For Compound **5**: RMN ^{1}H (400 MHz, CD_3OD): δ 7.39 (d, 1H, J = 15.6 Hz), δ 7.08 (d, 1H, J = 2.0 Hz), δ 7.05 (dd, 1H, J_1 = 8.0 Hz; J_2 = 2.0 Hz), δ 6.89 (d, 1 H, J = 8.4 Hz), δ 6.39 (d, 1H, J = 15.6 Hz), δ 6.62 (s, 2H), δ 3.80 (s, 3H), 3.79 (s, 3H), δ 3.39 (t, 2H, J = 7.2 Hz), δ 2.57 (t, 2H, J = 7.2 Hz); RMN ^{13}C (100 MHz, CD_3OD): δ 167.6; δ 150.8; δ 149.4; δ 145.7; δ 140.2; δ 131.3; δ 130.1; δ 128.1; δ 121.8; δ 118.4; δ 118.4; δ 111.4; δ 110.1; δ 107.3; δ 107.3; δ 55.1; δ 55.1; δ 41.0; δ 34.9. EIMS: m/z = 359 [M^+]. For Compound **8**: RMN ^{1}H (400 MHz, $CDCl_3$): δ 6.70 (d, 1H, J = 8.4 Hz), δ 6.68 (d, 1H, J = 8.0 Hz), δ 6.60 (d, 1H, J = 1.6 Hz), δ 6.59 (dd, 1H, J_1 = nd; J_2 = 1,6 Hz), δ 6.54 (d, 1H, J = 2.0 Hz), δ 6.38 (dd, 1H, J_1 = 8.0 Hz; J_2 = 2.0 Hz), δ 5.71 (t, 1H, J = 5.6 Hz), δ 3.75 (s, 3H), δ 3.72 (s, 3H), δ 3.31 (m, 2H), δ 2.78 (t, 2H, J = 7.2 Hz), δ 2.49 (t, 2H, J = 7.2 Hz), δ 2.35 (t, 2H, J = 7.6 Hz); RMN ^{13}C (100 MHz, $CDCl_3$): δ 173.5; δ 148.9; δ 147.5; δ 144.3; δ 143.1; δ 133.1; δ 130.6; δ 120.5; δ 120.4; δ 115.6; δ 115.4; δ 111.8; δ 111.5; δ 56.0; δ 55.9; δ 41.01; δ 38.7; δ 34.8; δ 31.3. EIMS: m/z = 345 [M^+]. For Compound **9**: RMN ^{1}H (400 MHz, $CDCl_3$): δ 7.97 (s, 1H), δ 7.60 (d, 1H, J = 8.0 Hz), δ 7.54 (d, 1H, J = 15.6 Hz), δ 7.37 (d, 1H, J = 8.0 Hz), δ 7.17 (td, 1H, J_1 = 8.0 Hz; J_2 = 7.2 Hz; J_3 = 1.2 Hz), δ 7.10 (td, 1H, J_1 = 8.0 Hz; J_2 = 7.2 Hz; J_3 = 1.2 Hz), δ 7.03 (s, 1H), δ 7.01 (dd, 1H, J_1 = 8.8 Hz, J_2 = 2.4 Hz), δ 6.96 (d, 1H, J = 1.6 Hz), δ 6.79 (d, 1H, J = 8.4 Hz), δ 6.24 (d, 1H, J = 15.6 Hz), δ 6.12 (t, 1H, J = 6.0 Hz), δ 3.87 (s, 3H), δ 3.84 (s, 3H), δ 3.72 (m, 2H), δ 3.02 (t, 2H, J = 6.8 Hz); RMN ^{13}C (100 MHz, $CDCl_3$): δ 167.6; δ 150.8; δ 149.4; δ 140.2; δ 136.6; δ 128.0; δ 127.3; δ 122.0; δ 121.8; δ 120.9; δ 118.4; δ 118.2; δ 117.9; δ 111.9; δ 111.3; δ 110.8; δ 110.0; δ 55.0; δ 55.0; δ 40.2; δ 25.0. EIMS: m/z = 350 [M^+].
20. Modulation assays were conducted according to National Committee for Clinical Laboratory Standards, 1999. Methods for dilution antimicrobial susceptibility tests for bacteria that grow aerobically, 5th ed. Norfloxacin MIC on SA-1199B cell is 100 μM (32 μg/mL), and the reference alkaloid reserpine causes an 8-fold reduction of norfloxacin MIC at 33 μM (20 μg/mL).
21. *Ethidium bromide assay*: EtBr is a substrate for many MDR pumps, including NorA. The efficiency of efflux pumps for which EtBr is a substrate can be assessed fluorometrically by the loss of fluorescence over time from cells loaded with EtBr. SA-1199B was loaded with EtBr as described previously and the effects of varying concentrations of compound **9** and reserpine were determined to generate dose–response profiles. The total time course for the efflux assay was 5 min. Assays were performed in duplicate and mean results were expressed as the percentage reduction of total efflux observed for test strains in the absence of inhibitors.
22. Kaatz, G. W.; Seo, S. M.; O'Brien, L.; Wahiduzzaman, M.; Foster, T. J. *Antimicrob. Agents Chemother.* **2000**, *44*, 1404.

Theor Chem Acc (2007) 117: 231–238
DOI 10.1007/s00214-006-0149-6

REGULAR ARTICLE

Mire Zloh · Simon Gibbons

The role of small molecule–small molecule interactions in overcoming biological barriers for antibacterial drug action

Received: 21 June 2005 / Accepted: 5 December 2005 / Published online: 22 June 2006

Abstract The ineffectiveness of antibiotics against bacteria can be caused by multidrug resistance (MDR) or by an outer membrane, which restricts the penetration of amphipathic compounds into Gram-negative bacteria. Remarkable activities of plant antimicrobials in the presence of MDR modulators have been observed against a series of MDR and Gram-negative bacteria (Tegos et al., Antimicrob Agents Chemother 46:3133, 2002). Assuming that modulators of MDR might form complexes with substrates of efflux pumps Zloh et al., Biogr Med Chem Lett 14:881, 2004), we have evaluated interaction energies between antimicrobials and MDR modulators reported in Tegos et al. (Antimicrob Agents Chemother 46:3133, 2002). In this paper, we can confirm that modulation activity against the efflux pump NorA in *Staphylococcus aureus* correlates with the interaction energies between MDR modulator INF271 and antibacterials. Additionally, the change of log *P* of complexes might be responsible for overcoming the membrane impermeability in Gram-negative bacteria and increasing the antibacterial activity in the presence of the modulator MC207110. This suggests that interactions between small molecules may play an important role in overcoming biological barriers in bacteria.

Keywords Multidrug resistance · MDR · Antibiotic activity · MDR modulators · Intermolecular interactions · GRID

1 Introduction

Plants produce compounds that can be effective antimicrobials if they find their way into the cell of the pathogen [3]. Production of multidrug resistance (MDR) inhibitors by the plant would be one way to ensure delivery of the antimicrobial compound.

Gram-negative bacteria have an effective permeability barrier, comprised of the outer membrane, which restricts the penetration of amphipathic compounds. Additionally these bacteria possess multidrug resistance pumps (MDRs), which extrude toxins across this barrier. There is a direct assumption that the apparent ineffectiveness of plant antimicrobials is largely due to the permeability barrier. This hypothesis was tested in a study by Tegos and co-workers by evaluating a combination of MDR mutants and MDR inhibitors [1].

Several important results that have greatly raised our interest were observed in [1]. It was shown that the modulators INF271 and MC207110 significantly potentiated the actions of most antimicrobials in the panel against *Bacillus megaterium* and *Staphylococcus aureus*. The plant antimicrobials resveratrol and coumestrol showed little direct activity, and the MDR inhibitors caused little potentiation of activity by these antimicrobials. Gossypol presented an interesting anomaly: the activity of this plant antimicrobial decreased by approximately tenfold in the presence of INF_{271} in the mutant type, and a fourfold decrease in activity was observed in the MDR *norA* strain. Rhein, plumbagin, resveratrol, gossypol, coumestrol, pyrithione and berberine – all showed similar patterns of activity against Gram-negative species. All were relatively ineffective against most species in the panel, but the activity of each compound was strongly potentiated by MDR inhibitors against several of the species. This suggests that a high level of activity of an antimicrobial against a given species was achieved in the presence of modulators of MDRs responsible for efflux of the tested compound.

It is believed that MDR inhibitors often reverse multidrug resistance by competing for the transport system responsible for MDR, but overall the mechanism of MDR inhibition is not well understood. The relationships between drug structure and MDR, and inhibitor structure and MDR inhibition are still obscure, except for the molecule lipophilicity. MDR inhibitors may bind directly to the efflux protein, however, we have proposed that these inhibitors could also function

M. Zloh (✉)
University of London, Department of Pharmaceutical and Biological Chemistry, The School of Pharmacy, 29/39 Brunswick Square, London, WC1N 1AX, UK
E-mail: mire.zloh@ulsop.ac.uk

S. Gibbons
University of London, Centre for Pharmacognosy and Phytotherapy, The School of Pharmacy, 29/39 Brunswick Square, London, WC1N 1AX, UK

as 'chaperones' by binding therapeutics outside the cell [2], increasing their lipophilicity (a key feature of all known MDR inhibitors) and therefore facilitating their entry into the cell. Furthermore, we have proposed that inhibitors of MDR have affinity for substrates of efflux transporters, and that they may form complexes. The experimental evidence has shown that indole-3-carbinol may have an affinity for substrates of P-glycoprotein (P-gp) and bind them to form a complex that may facilitate entry of the drug [4].The small molecule–small molecules interactions could play a key role in this large inhibitor–antibiotic complex formation and overcome biological barriers. Such a complex would effectively be a 'Trojan horse' that would not be recognised as a substrate by the pump mechanism. This complex may then dissociate to allow the inhibitor to bind to the pump causing inhibition of efflux and release of drug to its target.

We have used molecular modelling methods to rationalise results of the study by Tegos et al. Antimicrobials modelled were asarinin, esculetin, bisnorargemonine, 13-hydroxylupanine, coumestrol, rhein, plumbagin, pyrithione, resveratrol, gossypol, and berberine (Scheme 1). Bisnorargemonine and 13-hydroxylupanine were not discussed in detail, since they do not possess antibacterial activity. The interaction between antimicrobials and well-characterised MDR inhibitors INF271 and MC207110 (Scheme 2) was predicted by the Glue docking module of Grid22 [5]. Molecular properties of complexes with most favourable interaction energies were evaluated using VegaZZ software [6, 7]. The possibility of complex formation, correlation of antibacterial activity with interaction energies and increase of octanol/water partition coefficient, ($\log P$) of antibacterial-MDR inhibitor complex might provide a new insight into the mechanism of MDR modulation.

2 Computational methods

2.1 Model building and conformational analysis of antibacterials and MDR inhibitors

The initial structures of INF271, MC207110 and a series of antibacterials were sketched using ChemDraw Ultra 7.0.1, converted into three-dimensional (3D) models and saved as mol2 files by Chem3D Ultra 7.0.0 [8]. These structures were imported into Macromodel [9], atom and bond types were adjusted and minimised with the MMFFs force field parameters [10]. The generalised Born/surface area continuum (GB/SA) solvent model for H_2O [11] implemented in MacroModel was used to simulate an aqueous environment, with a constant dielectric function ($\varepsilon = 1$). An extended non-bonded cutoff (van der Waals: 8 Å; electrostatics: 20 Å) was used.

Using the optimised structures, a systematic conformational search on each molecule was performed. Monte Carlo conformational analysis (500 steps) was used for all compounds. The energy cutoff was set to $\Delta E = 10$ kJ/mol above the lowest energy conformation. The ensembles of generated structures were clustered using the program Xcluster. All structure sets were analysed using the cluster analysis program Xcluster [12].

2.2 Prediction of interaction energies between antibacterials and MDR inhibitors

Representative structures of inhibitors and drugs were used as input files for GRID 22 software [5]. The whole molecule was considered during calculations and all GRID parameters were kept at their default values. Glue, the GRID-docking programme, was used to find possible interactions for an antibacterial molecule with an inhibitor molecule as a target. All interactions were examined by using GROUP probes implemented in the Glue software representing relevant functional groups of drug molecules. Reported interaction energies by Glue 1.0 software were used as a criteria for evaluating the probability of MDR modulation. Complexes between antibacterials and modulators that exhibited the most favourable interaction energies were saved as mol2 files and imported into MacroModel. The complexes were further optimised using MMFFs force field.

The MINTA calculations of free energy [13] of single molecules and complexes were used to predict relative binding energies of different antibacterials to a given modulator by using a thermodynamic cycle.

2.3 Calculation of molecular properties

Molecular lipophilicity potential (MLP) is a structure–property descriptor that visualises the lipophilic properties of the molecule on its 3D surface and was calculated by projecting the Broto–Moreau lipophilicity atomic constants on the molecular surface [14]. The virtual log P, Broto log P and lipole, of all single molecules and complexes were evaluated by Vega ZZ software [6, 7]. Vega ZZ software was used to produce figures.

The correlations between different calculated values and activities were examined by the Gretl software package [15].

3 Results and discussion

The antibacterial activity of a series of plant antimicrobials was measured in the absence and in the presence of two different MDR inhibitors [1]. The aim of this study was to find a rationale for interesting observations found in [1]. It was shown previously that modulators of efflux pump activity may have an affinity for antibacterial and anticancer drugs [2]. Here, we have hypothesised that small molecules could interact between themselves and produce complexes to overcome biological barriers such cell efflux pumps and the membranes of Gram-negative bacteria.

The possible complex formation between modulators and antibacterials was examined by molecular modelling. The initial structures of antibacterial and modulator molecules were imported and optimised using Macromodel [9] and MMFFs forcefield [10]. At least five different conformations of each molecule were obtained by a Monte Carlo conformational search and Xcluster analysis [12]. The interaction

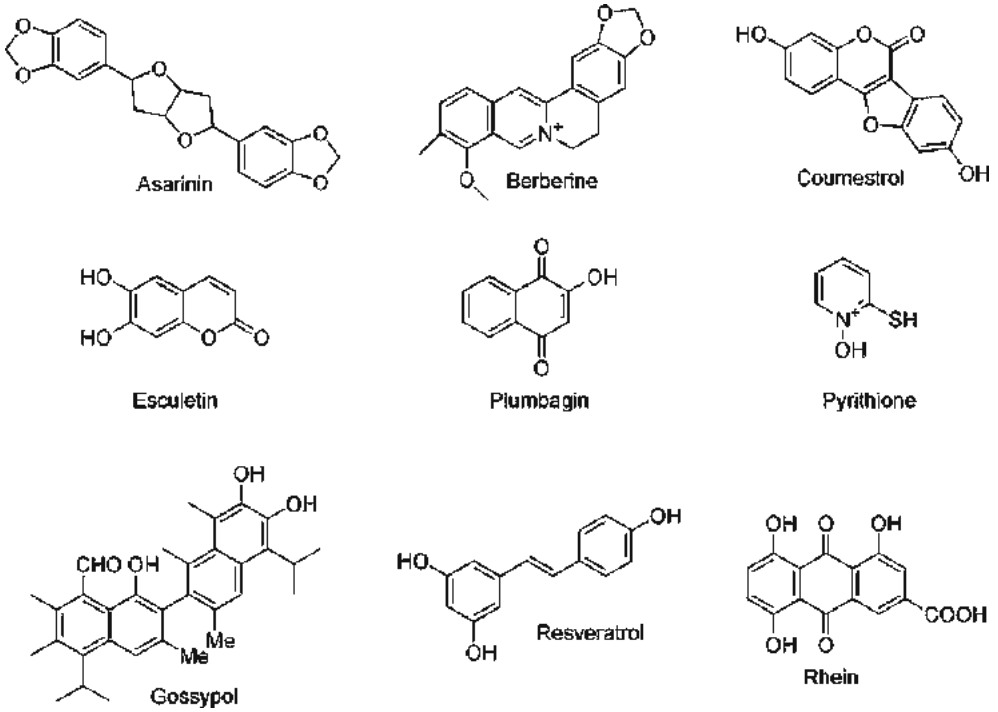

Scheme 1

between molecules was investigated using Grid 22 [5] and its docking module Glue 1.0. Both modulators were set as targets with five different conformations for each and binding affinity was tested for several different conformations of antibacterial molecules with rotational freedom for three bonds in ligands.

The complexes with most favourable interaction energies were selected for further analysis: calculation of change of free energy during complexation by Minta [13] and log *P* calculation by Vega ZZ [6, 7]. Generally, a good agreement was observed between interaction energies calculated by Grid and Minta, so potentiation of the drug activity was correlated with interaction energy determined by Grid.

To compare the effects of MDR modulators on activity, the potentiation was calculated by dividing the minimum inhibitory concentration (MIC) of the antibiotic in the presence of a modulator by the value of the MIC where the antibacterial was acting on its own. The increase of activity in the presence of a modulator would give a value larger than 1, while decrease of activity would result in potentiation being lower than 1. If the value of potentiation is 1, a change in activity was not detected.

3.1 Modulation of MDR efflux pump activity in Gram-positive bacterial strains

In the first instance, the correlation between interaction energies and levels of potentiation were examined for two strains of Gram-positive bacteria *S. aureus*, without and with overexpression of the NorA MDR efflux pump. The interac-

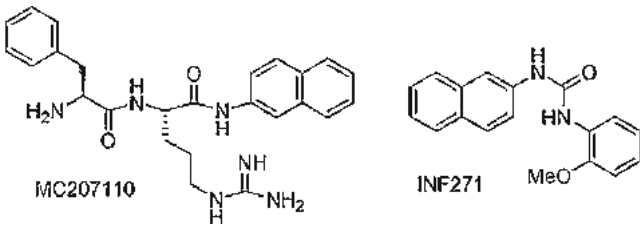

Scheme 2

tion energies calculated by Grid and Minta, levels of potentiation, change of log *P* and the levels of potentiation for each of the molecules in the presence of the INF271 modulator are shown in Table 1. Interaction energies between INF271 and all molecules are negative and indicate favourable interactions and therefore suggest that complexes might be formed in an aqueous solution.

3.1.1 Potentiation of antibacterial activity against S. aureus in the absence of the efflux pump NorA

Most antimicrobials had significantly higher activity (higher level of potentiation) in the presence of INF271 against *S. aureus* [1]. This is unexpected, since the *S. aureus* isolate lacks overexpression of the NorA MDR efflux pump and the MDR inhibitor should not have any effect on antibacterial activity. It was proposed that action of other unidentified MDRs [16] could be inhibited and is therefore highly likely to be responsible for this potentiation. Although, the presence of such MDR pumps cannot be overlooked, we are proposing that the formation of an antibacterial-inhibitor complex

could increase antibacterial drug uptake though increasing the lipophilicity.

Drug lipophilicity can be correlated to its permeation in biological systems [17]. Log *P* is the one of the principal parameters to evaluate lipophilicity of chemical compounds and is used as a standard property in determination of potential drug molecules in Lipinski's "rule of 5" [18]. Log *P* coefficients are correlated to passive permeation in biomembranes only when hydrogen-bonding and electrostatic effects are not rate-limiting [19]. MLP calculations can evaluate relationship between conformation and lipophilicity by projecting the Broto–Moreau lipophilicity atomic constants on the molecular surface [14]. Therefore, the MLP calculations were performed on single molecules as well as on all the structures of complexes predicted by Glue.

As shown in Table 1, the change of log *P* is at least 70% as a result of complex formation. Maps of electrostatic potentials for rhein and the rhein–INF271 complex are shown in Fig. 1, suggesting how the lipophilicity is increased through complex formation. The possible complex formation might change the lipophilicity of a complex and its log *P*, consequently it could change the permeability into the cell, therefore overcoming the biological barriers such as MDR pumps or bacterial membranes.

A similar conclusion can be drawn from the potentiation of the antibacterial activity against *S. aureus* in the presence of the MC207110 inhibitor (Table 2). The potentiation is observed for the molecules whose Δ log *P* was above 70%, with the exception of berberine and asarinin, whose log *P* on their own were high (above 4.3).

3.1.2 Potentiation of antibacterial activity against S. aureus overexpressing NorA

Strains of *S. aureus* that overexpress the NorA efflux pump present an additional biological barrier for antibacterial molecules. We have derived an empirical rule that could be used to predict the potentiation of the antibacterial activity in the presence of an MDR inhibitor, the potentiation will be observed if the interaction energy between a modulator and the drug (antibacterial) predicted by Grid and is greater than 9− kcal/mol and smaller than 18 kcal/mol [2]. Although, the rule was an attempt to present a complex picture in a simplified manner, in the set of nine examined molecules in the presence of INF271 the behaviour of six were correctly predicted. The berberine–INF271 pair exhibited a potentiation of 3.32 and the complex had the greatest stabilisation energy of −14.61 kcal/mol (Fig. 2.)

The potentiation for coumestrol, plumbagin and pyrithione was not correctly predicted. The prediction of potentiation of pyrithione has failed due to the small interaction energy; however, pyrithione is a small molecule and consequently the calculated interaction energies would be proportionally smaller. At the present time, we cannot explain the false prediction of potentiation of activity of plumbagin and coumestrol.

Table 1 Potentiation of antibacterial activities of complexes between antibacterials and INF271 modulator against Gram-positive bacteria in correlation with interaction energies and molecular properties

Molecule	Molecular properties						Interaction energies				*S. aureus* [a]		*S. aureus* NorA [a]	
	Log *P*	Δ Log *P*	Lipole	Δ Lipole (%)	Vitual log *P*	Δ Virtual log *P* (%)	E_{grid} kcal/mol	$\Delta\Delta G_c$ (kcal/mol)	$\Delta\Delta G_j$ kcal/mol	ΔH (kj/mol)	MIC (μg/ml) [1]	Potentiation	MIC (μg/ml) [1]	Potentiation
Resveratrol	6.16	156.94	2.17	59.55	5.32	112.58	−10.81	−6.35	−26.56	−22.59	125	2.00	250	4.00
Gossypol	8.94	72.80	1.61	−50.94	6.61	38.79	−18.17	−8.98	−37.61	−41.92	3.12	0.10	1.95	0.25
Coumestrol	7.49	101.07	2.10	21.52	5.25	59.11	−12.35	−3.50	−16.11	−15.60	250	2.00	250	1.00
Rhein	4.25	773.10	1.89	53.74	3.28	552.80	−12.07	−7.17	−30.01	−30.02	4.0	6.45	4	6.45
Plumbagin	4.79	368.76	2.25	11.37	4.02	266.40	−10.14	−6.03	−25.24	−23.17	0.78	2.52	0.31	1.00
Pyrithione	4.23	816.70	1.98	6.74	4.46	361.05	−7.02	−3.93	−16.45	−17.84	0.62	3.88	0.16	2.00
Berberine	8.14	86.16	0.56	−72.32	6.24	45.19	−14.61	−8.61	−36.00	−36.69	250	128.21	3.25	3.32
Esculetin	5.38	232.55	1.50	47.77	3.99	148.58	−7.21	−6.57	−27.50	−26.24	31.25	2.00	15.62	1.00
Asarinin	8.08	87.27	1.55	−22.80	5.52	44.70	−14.85	−8.76	−36.66	−28.71	62.50	4.00	31.25	2.00

The log *P*, lipole and virtual log *P* were calculated by the Broto method implemented in Vega ZZ [6, 7]. Δ values are given as percent change compared to values of antibacterial on its own. E_{grid} is the interaction energy calculated by Grid [5]. ΔΔ G values were estimated by Minta [13] and Δ H was calculated by Macromodel [9] and MMFFs force filed [10] MIC values are reported activities of antibacterials without MDR inhibitor and potentiation was calculated by dividing the MIC of the antibacterial in the presence of MDR inhibitor by the MIC of antibacterial on its own–results taken from [1] [a] it Staphylococcus aureus without and with overexpression of the NorA MDR efflux pump, respectively

Table 2 Potentiation of antibacterial activities of complexes between antibacterials and MC207110 modulator against Gram-positive bacteria in correlation with interaction energies, molecular properties and change of molecular properties compared to single molecule

Molecule	Log *P*	Δ Log *P*	E_{grid} (kcal/mol)	ΔΔ G_J(kcal/mol)	ΔΔ G_c (kJ/mol)	Δ *H*(kJ/mol)	Potentiation	
							S. aureus[a]	*S. aureus* NorA[a]
Resveratrol	3.16	316	−11.58	−24.54	−5.86	−23.84	1.00	1.00
Gossypol	5.93	14.68	−13.68	−47.97	−11.46	−51.45	1.00	1.00
Coumestrol	4.48	20.38	−12.25	−18.25	−4.36	−23.17	1.00	1.00
Rhein	1.25	155.85	−9.32	−38.02	−9.09	−47.35	2.00	6.45
Plumbagin	1.78	74.34	−8.37	−26.42	−6.32	−27.57	2.52	1.00
Pyrithione	1.22	164.64	−7.54	−12.86	−3.08	−20.16	3.88	2.00
Berberine	5.13	17.37	−16.60	−37.27	−8.91	−44.43	8.00	2.01
Esculetin	2.38	46.88	−6.51	−34.49	−8.24	−34.92	1.00	1.00
Asarinin	5.07	17.59	−11.48	−31.78	−7.60	−25.54	2.00	2.00

The Δ log *P* is defined as a percent change of log *P* of a complex compared to values of antibacterial on its own by the Broto method implemented in Vega ZZ [6, 7]. E_{grid} is the interaction energy calculated by Grid [5], ΔΔ *G* values were estimated by Minta [13] and Δ *H* was calculated by Macromodel [9] and MMFFs force filed [10] The potentiation was calculated by dividing the MIC of the antibacterial in the presence of the MDR inhibitor by the MIC of the antibacterial on its own – results taken from [1]
[a] *S. aureus* without and with overexpression of the NorA MDR efflux pump, respectively

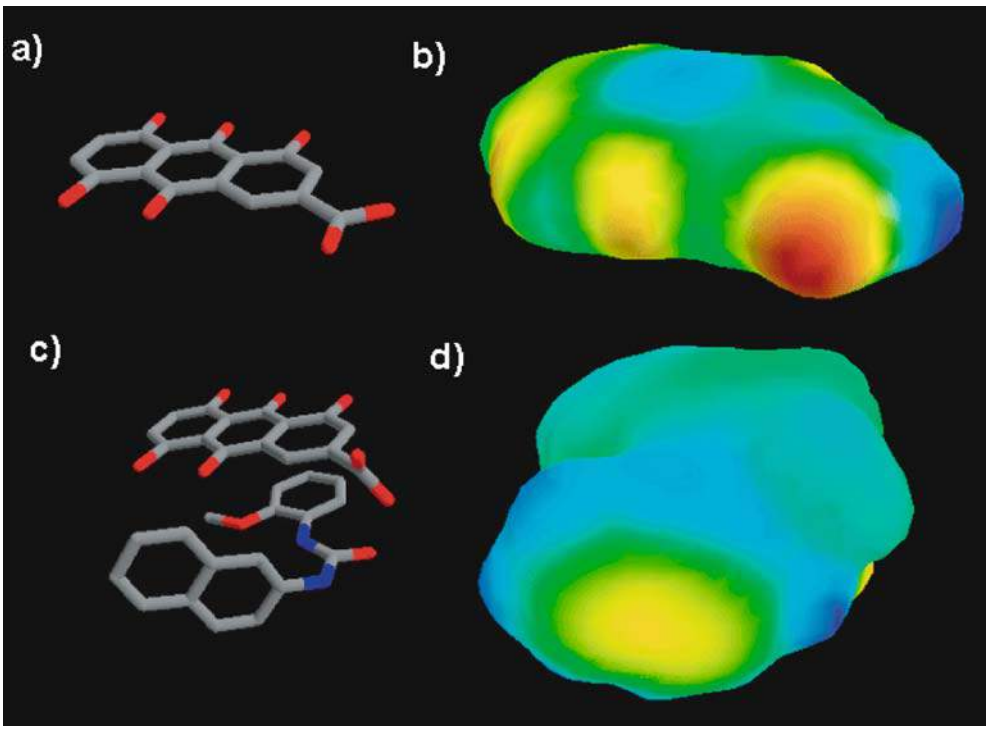

Fig. 1 Structures of rhein (**a**) and rhein–INF271 complex (**b**)and their maps of elestrostatic potentials (**c** and **d**, respectively). Complex was determined using Grid software [5] and structures were optimised using Macromodel [9] and MMFFs force field [10]

A similar combination of interaction energies and log *P* changes could be used to explain the potentiation of antibacterial activity in the presence of the MC207110 modulator (Table 2). For example, berberine and rhein complexes had their interaction energies higher than −9 kcal/mol and their activities were potentiated. However, molecules that had interaction energies higher than −9 kcal/mol and their activities were not potentiated by the presence of MC207110 did not have a significant increase of the log *P* after complex formation to increase uptake. Observed correlations between potentiation and Δ log *P* was 0.6478, while the correlation with interaction energy E_{grid} was only 0.1083.

Figure 2 presents maps of electrostatic potentials for resveratrol and plumabgin, suggesting that the shape of the complex might play a role in MDR modulation. Therefore, we believe that by using a combination of better-defined rules, that include interaction energies, log *P* and shape of a complex, it would be possible to predict the potentiation for an antibacterial drug–MDR modulator pair.

3.1.3 Unusual behaviour of gossypol

The presence of INF271 did not potentiate the activity of gossypol, and it decreased by approximately tenfold in the wild

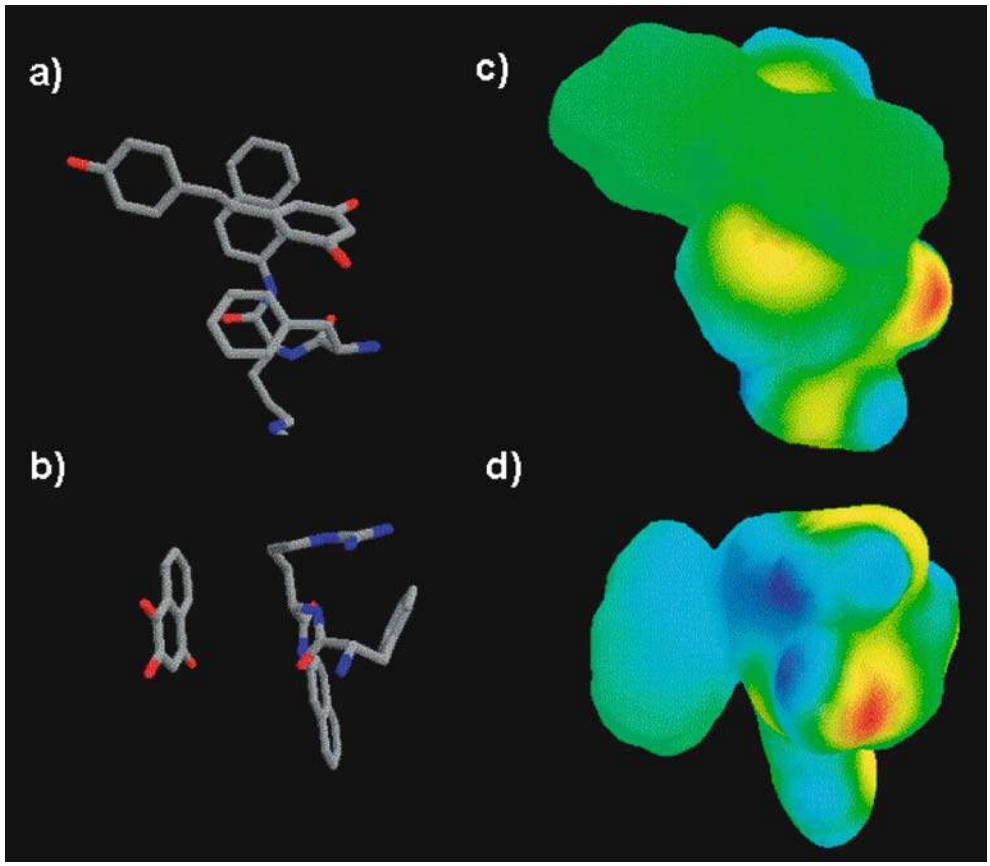

Fig. 2 Structures of resveratrol–MC207110 (**a**) and plumabgin– MC207110 (**b**) complexes andcorresponding maps of elestrostatic potentials (**c** and **d**, respectively). Complexes were determined using Grid software [5] and structures were optimised using Macromodel [9] and MMFFs force field [10]

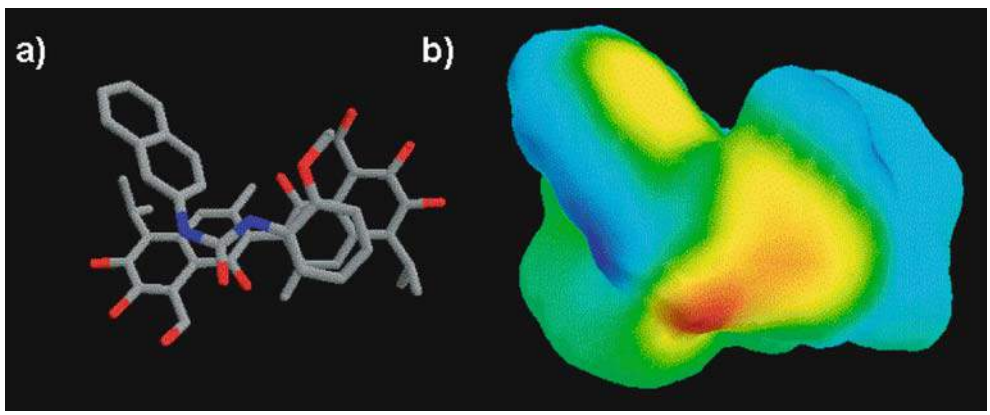

Fig. 3 Structure and map of elestrostatic potentials of gossypol and INF271 complex. Complex was determined using Grid software [5] and structure was optimised using Macromodel [9] and MMFFs force field [10]

type, and fourfold in the NorA strain of *S. aureus* [1]. Similar behaviour was reported with abietic acid and the MDR modulator reserpine [20]. NMR and molecular modelling studies have indicated that a highly interacting complex between reserpine and abietic acid was formed that could decrease activity due to poor availability of abietic acid to act on the drug target. Interestingly, the interaction energy between gossypol and INF271 was −18.17 kcal/mol, indicating that the complex formed between these two molecules (Fig. 3) could be stable and not disassociate at the target site, thus decreasing the activity of the antibiotic in the presence of INF271. In a similar fashion, α-tocopherol has a higher energy of interaction with MDR inhibitors than substrates (−19.06 kcal/mol with GG918) [2] and it has been shown to reverse the effects

Table 3 Potentiation of antibacterial activities of complexes between antibacterials and MC207110 modulator against Gram- negative bacteria in correlation with interaction energies, molecular properties and change of molecular properties compared to the single molecule

MC207110	Δ log *P*	Lipole	E_{grid} (kcal/mol)	Potentiation										
				EC	*EC tolC*	*PA*O1	*PA mexAB*	*SEST*	PS	*XC*	*AT*	*ER*	*ECA*	*SM*
Resveratrol	31.6	4.35	−11.58	4.00	255.10	16.00	16.00	127.88	16.00	32.01	4.00	8.00	128.21	8.00
Gossypol	14.7	2.93	−13.68	4.00	16.01	4.00	2.00	4.00	1.00	16.01	2.00	31.95	2.00	3.99
Coumestrol	20.4	2.72	−12.25	8.00	1.00	2.00	8.00	8.00	2.00	2.00	4.00	1.00	16.01	2.00
Rhein	155.8	1.73	−9.32	80.00	8.00	2.00	4.00	5.00	51.20	80.00	2.00	16.00	16.00	10.24
Plumbagin	74.3	2.98	−8.37	20.00	2.56	16.00	16.00	10.00	5.13	64.10	8.01	10.00	16.03	8.33
Pyrithione	164.6	1.96	−7.54	12.50	25.00	6.40	6.45	3.23	1.56	3.13	12.50	6.25	12.50	12.80
Berberine	17.4	4.05	−16.60	4.00	1.00	2.00	1.00	4.00	4.00	2.00	2.00	2.00	4.00	222.22
Esculetin	46.9	3.61	−6.51	4.00	4.00	2.00	2.00	4.00	4.00	4.00	2.00	4.00	4.00	4.00
Asarinin	17.6	3.81	−11.48	4.00	4.00	2.00	1.00	4.00	4.00	4.00	2.00	4.00	4.00	4.00

The log *P* and lipole were calculated by the Broto method implemented in Vega ZZ [6, 7], Δ values are given as percent change compared to values of antibacterial on its own. E_{grid} is the interaction energy calculated by Grid [5], and Δ *H* was calculated by Macromodel [9] and MMFFs force filed [10] MIC values are reported activities of antibacterials without MDR inhibitor and potentiation was calculated by dividing the MIC of the antibacterial in the presence of MDR inhibitor by the MIC of antibacterial on its own – results taken from [1] *EC Escherichia coli* K-12; *EctolC E. coli tolC mutant PA01 Pseudomonas aeruginosa* PA767; *PAmexAB P.* aeruginosa K119; *SEST Salmonella enterica* serovar Typhimurium; *PS P. syringae* pv. *maculicola* ES4326 *; XC Xanthomonas campestris* XCC528; *; AT Agrobacterium tumefaciens* GV3101 *ER Erwinia rhapontici* Er1 *; ECA Erwinia carotovora* ATCC 358; *SM Sinorhizobium meliloti* Rm1021

Table 4 Potentiation of antibacterial activities of complexes between antibacterials and INF271 modulator against Gram-negative bacteria in correlation with interaction energies, molecular properties and change of molecular properties compared to a single molecule

INF271	Δ log *P*	Lipole	E_{grid}(kcal/mol)	Potentiation										
				EC	*EC tolC*	*PA*O1	*PA mexAB*	*SEST*	PS	*XC*	*AT*	*ER*	*ECA*	*SM*
Resveratrol	156.9	2.17	−10.81	2.00	255.10	4.00	2.00	2.00	2.00	2.00	4.00	4.00	4.00	2.00
Gossypol	72.8	1.61	−18.17	1.00	2.00	2.00	1.00	1.00	1.00	2.00	2.00	4.00	2.00	3.99
Coumestrol	101.1	2.10	−12.35	2.00	0.06	2.00	2.00	2.00	2.00	1.00	2.00	1.00	4.00	4.00
Rhein	773.1	1.89	−12.07	5.00	2.00	2.00	1.00	5.00	25.60	40.00	2.00	2.00	2.00	4.00
Plumbagin	368.8	2.25	−10.14	2.00	1.00	2.00	2.00	2.00	2.56	2.08	2.00	5.12	4.01	2.08
Pyrithione	816.7	1.98	−7.02	2.00	2.00	3.20	2.00	1.00	1.00	1.56	3.13	1.00	2.00	2.00
Berberine	86.2	0.56	−14.61	2.00	2.00	2.00	1.00	2.00	2.00	2.00	2.00	2.00	4.00	2.00
Esculetin	232.5	1.50	−7.21	2.00	2.00	2.00	2.00	2.00	2.00	2.00	2.00	2.00	2.00	2.00
Asarinin	87.3	1.55	−14.85	2.00	2.00	2.00	1.00	2.00	2.00	2.00	2.00	2.00	2.00	2.00

The log *P* and lipole were calculated by the Broto method implemented in Vega ZZ [6, 7], Δ values are given as percent change compared to values of antibacterial on its own. E_{grid} is the interaction energy calculated by Grid [5], and Δ *H* was calculated by Macromodel [9] and MMFFs force filed [10] MIC values are reported activities of antibacterials without MDR inhibitor and potentiation was calculated by dividing the MIC of the antibacterial in the presence of MDR inhibitor by the MIC of antibacterial on its own – results taken from [1]
EC E. coli K-12; EctolC E. coli tolC mutant; PA01 - P. aeruginosa PA767; PAmexAB Pseudomonas aeruginosa K119; SEST Salmonella enterica serovar Typhimurium; PS P. syringae pv. maculicola ES4326 XC X. campestris XCC528; AT A. tumefaciens GV3101 ER Erwinia rhapontici Er1; ECA Erwinia carotovora ATCC 358; SM Sinorhizobium meliloti Rm1021

of MDR inhibitors [20]. This supports the hypothesis of the importance of small molecule–small molecule interactions role in overcoming MDR.

3.2 Modulation of antibacterial activity in Gram-negative bacterial strains in the presence of MDR modulators

The potentiation of activity of antibacterials in the presence of MDR inhibitors MC207110 and INF271 are shown in Tables 3 and 4, respectively. In Gram-negative bacteria, the situation is more complex, due to the presence of an additional outer membrane and efflux pumps in some of the bacterial strains. As shown in the previous sections, there is the possibility of complex formation between drugs and inhibitors that could affect the uptake of a drug. However, the same cutoff point of −9 kcal/mol for the interaction energy determined by Grid cannot applied, since the potentiation was observed even if the interaction energy was as low as −6 kcal/mol.

The increase of the lipophilicity and log *P* could be used to explain the potentiation of antibacterial activity in the presence of MDR modulators from different structural classes. A high correlation was observed between the % increase of log *P* and potentiation, for example the correlation coefficient between these two variables was 0.69 in the case of *Escherichia coli* K-12, while the correlation coefficient between potentiation and interaction energy was only 0.27. However, the opposite correlations were observed for *Sinorhizobium meliloti* Rm1021, the correlation coefficient between interaction energy and potentiation was high (0.66), while the correlation coefficient between potentiation and % increase of log *P* was only −0.23.

Similar correlations were observed for the potentiation of drug action in the presence of the INF271 modulator. The potentiation of drug action against *Xanthomonas campestris* XCC528 (*X. campestris)* in the presence of INF271 was in good correlation with the % increase of log *P* (0.59) and a small correlation with interaction energy (−0.13). In the case

of *P. aeruginosa* K1119 (*P. aeruginosa mexAB*) the correlation coefficient between the energy of interaction and potentiation was 0.766 with no correlation with % increase of log *P*.

Although these observations provide general support to the hypothesis, more precise and specific rules for predicting the potentiation of the drug action in the presence of a modulator could be derived from more extensive studies carried out for each strain of Gram-negative bacteria.

4 Conclusion

Complex formation between antibacterial drugs and MDR modulators was predicted by molecular modelling. It was shown that the potentiation of the antibacterial activity could be correlated to interaction energies between complexes and/or log *P* of formed complexes. The unusual decrease in antibacterial activity of gossypol in the presence of INF271 modulator, could be explained by complex formation with strong interactions, thus preventing drug action.

The Grid and Glue software could be used to predict the antibacterial activity potentiation for a drug–inhibitor pair and could find use as a quick screen for new MDR modulators of efflux activity of *S. aureus* overexpressing NorA.

More comprehensive models that include interaction energies and log *P* predictions could be developed to evaluate different MDR modulators and their ability to potentiate drug activity against Gram-negative bacteria.

It is possible that small molecule–small molecule interactions could play an important role in overcoming biological barriers in drug delivery.

References

1. Tegos G, Stermitz FR, Lomovskaya O, Lewis K (2002) Antimicrob Agents Chemother 46:3133
2. Zloh M, Kaatz GW, Gibbons S (2004) Biogr Med Chem Lett 14:881
3. Stermitz FR, Lorenz P, Tawara JN, Zenewicz L, Lewis K (2000) Proc Natl Acad Sci USA 97:1433
4. Arora A, Seth K, Kalra N, Shukla Y (2005) Toxicol Appl Pharm 202:237
5. Goodford PJ (1985) J Med Chem 28:849
6. Pedretti A, Villa L, Vistoli G (2002) J Mol Graph 21:47
7. Pedretti A, Villa L, Vistoli G (2003) Theor Chem Acc 109:229
8. ChemOffice Ultra 2002: CambridgeSoft (2001)
9. Mohamadi F, Richards N, Guida W, Liskamp R, Lipton M, Caulfield C, Chang G, Hendrickson T, Still W (1990) J Comput Chem 11:440
10. Cramer CJ, Truhlar DG (1995) In: Lipkowitz KB, Boyd DB (eds) Reviews in computational chemistry Vol 6. VCH, New York, pp 1–72
11. Still WC, Tempczyk A, Hawley RC, Hendrickson T (1990) J Am Chem Soc 112:6127
12. Shenkin P, McDonald Q (1994) J Comput Chem 15:899
13. Kolossvary I (1997) J Phys Chem A 101:9900
14. Gaillard P, Carrupt PA, Testa B, Boudon A (1994) J CAMD, 8:83
15. Gretl 1.3.2 http://gretl.sourcegforge.net/
16. Kaatz GW, Seo SM, O'Brien L, Wahiduzzaman M, Foster TJ (2000) Antimicrob Agents Chemother 44:1404
17. Testa B, Carrupt, P-A, Gaillard P, Billois F, Weber P (1996) Pharm Res 13:335
18. Lipinski CA (1997) Adv Drug Del Rev 23:3
19. Mälkiä A, Murtomäki L, Urtti A, Kontturi K (2004) Eur J Pharm Sci 23:13
20. Smith E, Williams E, Zloh M, Gibbons S (2005) Phytother Res 19:538

PHYTOTHERAPY RESEARCH
Phytother. Res. **20**, 41–45 (2006)
Published online in Wiley InterScience (www.interscience.wiley.com). **DOI**: 10.1002/ptr.1799

Antimicrobial, Resistance-Modifying Effects, Antioxidant and Free Radical Scavenging Activities of *Mezoneuron benthamianum* Baill., *Securinega virosa* Roxb. &Wlld. and *Microglossa pyrifolia* Lam.

R. A. Dickson[1], P. J. Houghton[1]*, P. J. Hylands[1] and S. Gibbons[2]

[1]Pharmacognosy Research, Pharmaceutical Sciences Research Division, KCL, 150 Stamford Street, London SE1 9NH, UK
[2]Centre for Pharmacognosy and Phytotherapy, Department of Pharmaceutical and Biological Chemistry, The School of Pharmacy, University of London, UK

Mezoneuron benthamianum*, *Securinega virosa* and *Microglossa pyrifolia* are used in folk medicine in Ghana for the treatment of dermal infections and wounds. Petroleum spirit, chloroform and ethanol extracts of the plants were tested for antimicrobial activity against a battery of organisms using the agar well diffusion technique and a serial dilution microassay. The resistance modifying activities of these extracts on standard antibiotics against *Staphylococcus aureus* possessing efflux mechanisms of resistance have also been assessed. A 4-fold potentiation of the activity of norfloxacin was observed for ethanol and chloroform extracts of *M. benthamianum* and *S. virosa*, respectively, whilst the petroleum spirit extract resulted in a 2-fold potentiation with minimum inhibitory concentration (MIC) values in the range 8–16 μg/mL. Ethanol extracts of all three species, the petroleum spirit extract of *M. benthamianum* and the chloroform extracts of *M. benthamianum* and *S. virosa*, showed interesting antimicrobial activities. Antioxidant and free radical scavenging activities using DPPH spectrophotometric and TBA lipid peroxidation assays were also conducted. Of the five extracts that showed antioxidant activities, the petroleum spirit and chloroform extracts of *M. benthamianum* rated most highly by displaying strong free radical scavenging activity with IC_{50} values of 15.33 and 19.72 μg/mL, respectively. Lipid peroxidation inhibition provided by the same two extracts also produced the lowest IC_{50} values for all the extracts tested, of 23.15 and 30.36 μg/mL. These findings therefore give some support to the ethnopharmacological use of the plants in the treatment of various skin diseases and wounds, as well as demonstrating the potential of some of the plants as sources of compounds possessing the ability to modulate bacterial multidrug resistance. Copyright © 2006 John Wiley & Sons, Ltd.

Keywords: Mezoneuron benthamianum; *Securinega virosa*; *Microglossa pyrifolia*; antimicrobial; MDR; efflux; resistance modifying effects; antioxidant effects.

INTRODUCTION

Mezoneuron benthamianum Baill. (Caesalpinaceae), *Securinega virosa* Roxb. &Wlld. (Euphorbiaceae) and *Microglossa pyrifolia* Lam. (Asteraceae) are plants found mostly in secondary forest in Ghana and find use in the treatment of infections and wounds (Irvine, 1961; Abbiw, 1990; Burkill, 1994). In most cases a paste is made from the plant materials, mixed with vehicles such as shea butter or palm kernel oil and this is then applied topically to the affected areas. Infusions made from palm-wine (an alcoholic beverage), the local gin or decoctions may also be drunk.

Plants have been found to be useful in accelerating wound healing, a complex process involving the interplay of many biochemical and cellular mediators. Microbial infections, especially due to *Staphylococcus*, *Streptococcus* and *Pseudomonas* species, and the presence of oxygen free radicals, are known impediments to wound healing (Hollinworth, 1997). Any agent capable of eliminating or reducing the number of microorganisms present in a wound, as well as reducing the levels of ROS, may facilitate the wound healing process.

The ever increasing resistance of human pathogens to current antimicrobial agents is a serious medical problem resulting in the need for novel antibiotic prototypes (Kinghorn, 1999). Methicillin-resistant *Staphylococcus aureus* (MRSA) is one of the most problematic bacteria to treat in patients and to eradicate from hospitals. In the UK alone, there have been increments in the number of death certificates citing MRSA, with 47 citations in 1993 rising to 398 in 1998 (Crowcroft and Catchpole, 2002). Multidrug resistance (MDR) pumps of MRSA protect the cells from antibiotics such as fluoroquinolones, tetracycline and a number of amphipathic cations. Certain natural products, for example reserpine, have been found to be able to block these efflux pumps (Gibbons, 2004) and thereby reduce the MIC of norfloxacin and other antibiotics.

* Correspondence to: Professor P. J. Houghton, Pharmacognosy Research, Pharmaceutical Sciences Research Division, King's College London, 150 Stamford Street, London SE1 9NH, UK.
E-mail: Peter.houghton@kcl.ac.uk
Contract/grant sponsor: Commonwealth Scholarship Commission, UK.

Received 16 August 2005
Accepted 16 September 2005

Such compounds could restore the efficacy of antibiotics against which resistance has arisen. Reserpine, however, has been found to be toxic in humans at an effective concentration so non-toxic alternatives are needed. The extracts under investigation were therefore tested for their antibiotic modulatory activities.

Although there are no previous antimicrobial reports on the roots of any of the species examined, studies on the leaves of *M. benthamianum* have resulted in the isolation of gallic acid and gallic derivatives that possess antibacterial activity (Cordell and Binutu, 2000). The antibacterial activities of securinine and viroallosecurnine, both of which are alkaloids from the leaves of *S. virosa*, have also been reported (Saito *et al.*, 1964; Mensah *et al.*, 1988). Additionally, some acetylenic glycosides possessing antibacterial activity have been isolated from the leaves of *M. pyrifolia* (Rucker *et al.*, 1992). There are, however, no reports on the antioxidant properties of these plants. This study sought to examine the *in vitro* antimicrobial and antioxidant activities of different crude preparations of the root bark of these species, with the objective of investigating the validity of their traditional uses. The studies also sought to examine whether or not these plants could serve as a source of plant-derived natural products that modulate bacterial multidrug resistance (MDR) in effluxing strains of *S. aureus*.

MATERIALS AND METHODS

Plant materials. The root bark of *M. benthamianum*, *S. virosa* and *M. pyrifolia*, with voucher specimen numbers RADMB11, RADSV22 and RADMP44 respectively, were collected from the Amansie West district and Akwapim Mampong in the Eastern and Ashanti regions of Ghana. The plants were authenticated by Dr Blagogee a taxonomist, at the Centre for Scientific Research into Plant Medicine (CSRPM), Mampong Akwapim, Ghana, where voucher specimens have been deposited. DPPH, bovine brain extract and all other substances used were obtained from Sigma-Aldrich Co. Ltd.

Extraction of plant materials. The root bark of *M. benthamianum*, *S. virosa* and *M. pyrifolia* were washed with water, chopped into smaller pieces, air dried at room temperature for 1 week and then oven dried at 45 °C for 5 h, coarsely powdered and extracted with petroleum spirit, chloroform, ethanol and water (500 mL) respectively for 24 h each in a Soxhlet apparatus. The yields are given in Table 1.

Antimicrobial activity. The antimicrobial activities of the different extracts from the three plants were determined using the agar well diffusion and micro dilution assay procedures as outlined by Vanden Berghe and Vlietinck (1991) and Eloff (1998), respectively.

Agar well diffusion technique. Crude extracts were prepared at concentrations of 5 mg/mL using 2% aqueous DMSO with slight heating on a water bath, sonicated and filter sterilized using a 0.25 μm Millipore filter. Wells of 7 mm diameter were made in 20 mL nutrient agar (Oxoid) seeded with 20 μL of a suspension of test organisms containing 10^5 CFU/mL under aseptic conditions. 100 μL of extracts were fed into wells, allowed to diffuse for 1 h and then incubated at 37 °C for 24 h, after which time they were examined for zones of inhibition. All experiments were carried out in triplicate.

Table 1. Percentage yield of various solvents

Plant species	Solvent	Yield (%)
Mezoneuron benthamianum	Petroleum spirit	1.5
	Chloroform	1.1
	Ethanol	4.3
	Water	5.33
Securinega virosa	Petroleum spirit	1.0
	Chloroform	3.1
	Ethanol	3.6
	Water	4.1
Microglossa pyrifolia	Petroleum spirit	2.1
	Chloroform	3.4
	Ethanol	5.9
	Water	7.0

Determination of minimum inhibitory concentration (MIC). Stock solutions of all extracts were prepared by dissolving 4 mg of the extract in 80 μL DMSO. The mixture of DMSO and the extract was sonicated to ensure thorough mixing. Sterile water was added to make the volume up to 2 mL in a sterile bottle. This was then sonicated to ensure complete mixing. The stock mixture was passed through a pyrogenic filter to sterilize the solution and serially diluted to arrive at concentrations between 1000 μg/mL and 7.8 μg/mL. The inocula of microorganisms were prepared from broth cultures and serial dilutions made to achieve a suspension of approximately 10^5 CFU/mL. For every experiment, a sterility check (2% DMSO and medium), negative control (2% DMSO, medium and inoculum) and positive control (2% DMSO, medium, inoculum and water-soluble antibiotic) were included. In general, the 96-well plates were prepared by dispensing into each well 100 μL each of an appropriate medium, test extracts and 20 μL of the inoculum. A double strength nutrient broth and Sabouraud's dextrose agar media were employed for the bacterial and fungal assays, respectively. The contents of each well were mixed thoroughly with a multi-channel pipette and the microtitre plates incubated at temperatures and for periods of time appropriate to the organism under study. For the bacteria, the growth of the microorganisms was determined by adding 20 μL of a 5% solution of tetrazolium salt (MTT) and incubating for a further 10 minutes. Clear wells indicated inhibition of the growth of organism, whilst dark coloured wells indicated absence of inhibition. 200 μg/mL of miconazole and tetracycline served as positive controls for antifungal and antibacterial activity respectively. Yeasts were incubated at 30 °C and bacteria at 37 °C respectively for 24 h and the dermatophytes were maintained at 26 °C for 2 weeks. After the specified times the plates were examined for growth. The fungi were examined in daylight and MTT used for the bacteria. The MIC of the preparations was the lowest concentration in the medium that completely inhibited the visible growth. All experiments were performed in triplicate.

Modulation assay. The modulation assay was performed using 10 μg/mL doses of the extracts, well below the concentration shown to inhibit growth (minimum inhibitory concentrations in the range 64–128 μg/mL). The assay was directed towards finding the modulating effect of these extracts when combined with the standard antibiotics, norfloxacin, tetracycline and erythromycin, in 96-well plates on multi-drug resistant strains of *Staphylococcus aureus* which were resistant to these antibiotics *via* efflux mechanisms. 125 μL of a 10 μg/mL solution of the crude extracts were prepared using Mueller-Hinton broth and were placed in wells of the first three rows of the 96-well plates. Wells in rows 4 and 5 were filled with 125 μL of broth containing 10 μg/mL of reserpine, a control drug with modulation activity, which served as a positive control. Wells in the remaining rows as well as rows 1–5 were then filled with norfloxacin of different concentrations ranging from 512 μg/mL to 1 μg/mL. 125 μL of an overnight culture of bacteria containing approximately 10^5 CFU/mL were added to each well, except the wells of column 12 (sterile control). The plates were incubated at 37 °C for 24 h after which 20 μL of MTT (thiazole blue tetrazolium salt) solution was added to each well and the plate incubated for a further 30 min. Inhibition of bacterial growth was visible as a clear well, whilst the presence of growth was detected by the presence of a dark blue colouration in the well resulting from the formation of a complex between the dehydrogenase enzyme in the live bacteria and the tetrazolium salt. Modulation assays were compared with MIC assays for antibiotics and modulation was observed where a potentiation of antibiotic activity (a lowering of MIC) occurred. All experiments were performed in triplicate under aseptic conditions.

Microorganisms used. The following bacterial and fungal strains obtained from the UK National Culture Collection and School of Pharmacy, University of London were used in the bioassay: *Micrococcus flavus [M.f]* (NCTC 7743), *Bacillus subtillis [B.s]* (NCTC 10073), *Staphylococcus aureus [S.a]* (NCTC4163), multidrug-resistant *S. aureus* SA-1199B (over-expressing the NorA MDR transporter), tetracycline-resistant *S. aureus* XU 212 (TetK expresser), erythromycin-resistant *S. aureus* RN 4220 (expresser of the MsrA, macrolide pump), *Streptococcus faecalis [S.f]* (NCTC 775), *Salmonella abony [S.ab]* (NCIMB6017), *Pseudomonas aeruginosa [P.a]* (NCIMB 10421), *Escherichia coli [E.c]* (NCTC 9002), *Klebsiella aerogenes [Ka]* (NCTC 5055), *Candida albicans [C.a]* (NCPF 3179), *Saccharomyces cerevisiae [S.c]* (NCTC 080178), *Trichophyton interdigitale [T.i]* (NCPF 654) and *Microsporum gypseum [M.g]* (NCPF261)

Antioxidant activity. 20 μL of 100 μg/mL extracts were monitored initially for antioxidant activity on TLC (solvent system: petroleum spirit, ethyl acetate 4:1) using 0.2% of the stable free radical 2,2-diphenyl-1-picrylhydrazyl (DPPH) in methanol, and antioxidant compounds in the extracts gave clear zones against a purple background (Cuendet *et al.*, 1997).

Scavenging activity on DPPH radical. The free radical scavenging activity of the extracts was measured by the 2,2-diphenyl-1-picrylhydrazyl (DPPH) method described by Brand-Williams *et al.* (1995). Briefly, a 0.1 mM solution of DPPH in ethanol was prepared and 1.0 mL of this solution was added to 0.5 mL of the samples in different concentrations. After 20 min, the absorbance was measured at 525 nm. The DPPH radical scavenging activity was calculated according to the following equation. DPPH solution alone served as control (A_0).

$$\text{DPPH}^{\bullet}\ \text{scavenging activity}\ (\%) = [(A_0 - A_1)/A_0] \times 100$$

where A_0 is the absorbance of the control and A_1 is the absorbance in the presence of the test substance.

Antioxidant activity against the formation of lipid peroxide. The lipid peroxidation assay was performed to determine the inhibition of Fe^{2+}/ascorbate-induced lipid peroxidation (LPO) on bovine brain liposomes by each of the active extracts (Galvez *et al.*, 2005).

RESULTS AND DISCUSSION

The chloroform extract of *S. virosa* was the most active extract showing activity against 13 test organisms including some dermatophytes with MIC values ranging from 15.6 μg/mL to over 1000 μg/mL The highest diameter of zone of inhibition (22 mm) observed for the agar well diffusion method, was given by this extract against *M. flavus* (Tables 2 and 3). The ethanol extract of this plant showed some activity although the inhibition zone was smaller. The petroleum spirit, chloroform and ethanol extracts of *M. benthamianum* produced good MIC values of between 31.2 and 1000 μg/mL for both gram-positive and gram-negative bacteria and some dermatophytes (Table 3). Of the three extracts of *M. pyrifolia*, only the ethanol extract showed antimicrobial effects which were poor to moderate with MIC values no less than 500 μg/mL.

The petroleum spirit, chloroform and ethanol extracts of *M. benthamianum* and *S. virosa* exhibited modulation effects when combined with standard antibiotics against resistant strains of *S. aureus* (Table 4). For example, the ethanol extract of *M. benthamianum* and the chloroform extract of *S. virosa* produced a 4-fold potentiation of norfloxacin activity against the norfloxacin-resistant strain of *S. aureus* possessing the efflux pump NorA. This is the major characterized drug pump in this pathogen and this result compares well with the MDR inhibitor reserpine, particularly given that the extract is chemically complex and the concentration of the extract in the broth was only 10 μg/mL compared with 20 μg/mL for reserpine. It is likely that purification of this extract will lead to a more potent modulator than reserpine and this work is currently underway. The petroleum spirit extract of *M. benthamianum* showed a 2-fold potentiation in this respect. This extract also produced good potentiation effects on the tetracycline MIC by a 2-fold reduction of tetracycline concentration needed to inhibit growth of the strain possessing the TetK efflux mechanism. All the extracts were inactive against erythromycin resistant *S. aureus* which possesses the MsrA macrolide transporter. This mechanism is also unaffected by reserpine although GG-918, an inhibitor of the mammalian MDR protein p-glycoprotein, has recently been reported to modulate

Table 2. Antimicrobial effect (zone of inhibition in mm) of crude extracts

Test organism	Extract					
	MBP	MBC	MBE	SVC	SVE	MPE
Staphylococcus aureus	14	14	15	13	13	12
Bacillus subtilis	16	13	19	17	9	0
Micrococcus flavus	15	12	18	19	19	13
Streptococcus feacali	13	0	10	11	11	13
Escherichia coli	0	0	0	0	0	0
Pseudomonas aeruginosa	12	0	15	12	12	12
Salmonella abony	0	0	0	0	0	0
Klebsiella aerogenes	0	0	0	0	0	0
Candida albicans	0	0	0	0	0	0
Saccharomyces cerevisae	0	0	0	0	0	0

MBP, MBC, MBE, petroleum spirit, chloroform and ethanol extracts of *M. benthamianum.*
SVC, SVE and MPE, chloroform, ethanol extracts of *S. virosa* and *M. pyrifolia.*
Concentration of extracts, 5 mg/mL; – , no inhibition observed; All tests were done in triplicate; Tetracyline and miconazole served as positive controls for antibacterial and antifungal assays respectively.

Table 3. Mean minimum inhibitory concentration (MIC; μg/mL) of different extracts on various microorganisms, $n = 3$

Test organism	Extract							
	MBP	MBC	MBE	SVC	SVE	MPE	Tetracycline	Miconazole
Bacteria								
Staphylococcus aureus	125	250	125	125	500	>1000	2.5	NT
MDR-SA-1199B	64	128	64	64	0	0	NT	NT
Bacillus subtilis	125	250	62.5	250	500	500	5	NT
Micrococcus flavus	250	500	31.2	250	500	>1000	1	NT
Streptococcus feacali	>1000	0	500	500	1000	1000	5	NT
Escherichia coli	0	0	0	500	0	0	10	NT
Pseudomonas aeruginosa	1000	0	500	>1000	>1000	0	20	NT
Salmonella abony	0	0	0	15.6	0	0	2.5	NT
Klebsiella aerogenes	0	0	0	250	0	0	5	NT
Yeast/Fungi								
Candida albicans	0	0	0	1000	0	0	NT	10
Saccharomyces cerevisae	0	0	0	>1000	0	0	NT	10
Trichophyton interdigitale	0	0	125	125	0	0	NT	20
Microsporum floccosum	0	0	125	250	0	0	NT	20

MBP, MBC, MBE, petroleum spirit, chloroform and ethanol extracts of *M. benthamianum.*
SVC, SVE and MPE, chloroform, ethanol extracts of *S. virosa* and *M. pyrifolia.*
MDR-SA-1199B possesses the NorA MDR transporter, – no inhibition observed; NT, not tested; All tests were done in triplicate. Tetracycline and miconazole served as positive controls for antibacterial and antifungal assays, respectively.

erythromycin activity against this strain (Gibbons *et al.*, 2003).

Five of the extracts demonstrated antioxidant and free radical scavenging activities. The petroleum spirit and chloroform extracts of *M. benthamianum* demonstrated the highest antioxidant properties with IC_{50} values of 15.33 μg/mL and 19.72 μg/mL for free radical scavenging activity and 23.15 and 30.36 μg/mL respectively for inhibition of lipid peroxidation of bovine brain extract liposomes (Table 5). On the basis of the antimicrobial, resistance modifying, antioxidant and free radical scavenging effects that have been observed for different extracts, the traditional use of lipophilic preparations of these species is supported. Further isolation of the various compounds responsible for these activities is underway in our laboratories.

Acknowledgement

Funding for this work was provided by the Commonwealth Scholarship Commission, UK. We want to gratefully acknowledge the assistance rendered by Dr Blagogee of the Centre for Scientific Research into Plant Medicine (CSRPM), Mampong Akwapim, Ghana, the local herbalists and the technicians of the Department of Pharmacy, KCL.

REFERENCES

Abbiw D. 1990. *Useful Plants of Ghana.* Intermediate Technical Publications and Royal Botanic Gardens: Kew UK, 199–200.

Brand-Williams W, Cuvelier ME, Berset C. 1995. Use of a free radical method to evaluate antioxidant activity. *Lebensm Wiss Technol* **28**: 25–30.

Table 4. Antimicrobial susceptibility of test strains in the absence and presence of extracts and reserpine a naturally occurring MDR inhibitor

	MIC of test strain expressing the indicated efflux pump (μg/mL)		
Antimicrobial agent	SA-1199B (NorA)	XU212 (TetK)	RN4220 (MsrA)
Norfloxacin	32	NT	NT
+MBE	8		
+MBC	32		
+MBP	16		
+SVC	8		
+Reserpine	8		
+Tetracycline	NT	128	NT
+MBE		–	
+MBC		128	
+MBP		64	
+SVC		–	
+Reserpine		32	
+Erythromycin	NT	NT	256
+MBE			–
+MBC			–
+MBP			–
+SVC			–
+Reserpine			256

Test extracts, 10 μg/mL; reserpine, 20 μg/mL; NT, not tested; –, not active at highest concentration. MBE, MBC, MBP, ethanol, chloroform and petroleum spirit extracts of *M. benthamianum* and SVC, chloroform extract of *S. virosa.*

Table 5. IC_{50} values (μg/mL) for free radical scavenging activity and inhibition of lipid peroxidation of bovine brain extract liposomes by extracts

Extract	IC_{50} DPPH	IC_{50} TBA
MPC	53.81	73.11
SVC	26.17	45.76
MPE	47.31	51.84
MBP	15.33	23.15
MBC	19.72	30.36
Catechin	15.13	NA
Propyl gallate	NA	0.582

Catechin and propyl gallate served as positive controls for DPPH and TBA assays, respectively. NA, not applicable.

Burkill HM. 1994. *The Useful Plants of West Tropical Africa*. The Trustees of the Royal Botanic Gardens: Kew, 755.

Cordell GA, Binutu OA. 2000. Gallic acid derivatives from *Mezoneuron benthamianum* leaves. *Pharm Biol* **38**: 284–286.

Crowcroft NS, Catchpole M. 2002. Mortality from methicillin-resistant *Staphylococcus aureus* in England and Wales: analysis of death certificates. *Br Med J* **325**: 1390–1391.

Cuendet M, Hostettman K, Potterat O. 1997. Iridoid glycosides with free radical scavenging properties from *Fagraeae blumei. Helv Chim Acta* **80**: 1144–1152.

Eloff JN. 1998. Which extract should be used for the screening and isolation of antimicrobial components from plants? *J Ethnopharmacol* **60**: 1–8.

Galvez M, Martin-Cordero C, Houghton PJ, Ayuso MJ. 2005. Antioxidant activity of methanol extracts obtained from *Plantago* species. *J Agric Food Chem* **53**: 1927–1933.

Gibbons S. 2004. Anti-Staphylococcal plant natural products. *Nat Prod Rep* **21**: 263–277.

Gibbons S, Oluwatuyi M, Kaatz GW. 2003. A novel inhibitor of multidrug efflux pumps in *Staphylococcus aureus. J Antimicrob Chemother* **51**: 13–17.

Hollinworth H.1997. The management of infected wounds. *Professional Nurse* **12**: 8–11.

Irvine FR. 1961. *Woody Plants of Ghana*. Oxford University Press: London, 312–313

Kinghorn AD. 1999. *Phytochemical Resources for Medicine and Agricultur*e, Nigg HN, Seigler D (eds). Plenum Press: New York, 75–94.

Mensah LJ, Gleye J, Moulis C, Fouraste I. 1988. Alkaloids from the leaves of *Phyllanthus discoideus. J Nat Prod* **51**: 1113–1115.

Rucker G, Kehrbaums S, Sakulas H, Lawong B, Goeltenboth F. 1992. Medicinal plants from Papua New Guinea. 2. Acetylenic glucosides from *Microglossa pyrifolia. Planta Med* **58**: 266–269.

Saito S, Iwamoto T, Tanaka T *et al.* 1964. Two new alkaloids, viroallosecurinine and securine isolated from *Securinega virosa* Pax. and Hoff. *Chem Ind* **11**: 1263.

Vanden Berghe DA, Vlietinck AJ. 1991. *Screening Methods for Antibacterial and Antiviral Agents from Higher Plants,* K Hostettmann (ed.). Methods in Plant Biochemistry VI. Assays for Bioactivity. Academic Press: London, 47–69.

Polyacylated Oligosaccharides from Medicinal Mexican Morning Glory Species as Antibacterials and Inhibitors of Multidrug Resistance in *Staphylococcus aureus*[⊥]

Rogelio Pereda-Miranda,*[,†] Glenn W. Kaatz,[‡] and Simon Gibbons[§]

Departamento de Farmacia, Facultad de Química, Universidad Nacional Autónoma de México, Ciudad Universitaria, 04510 DF Mexico, Department of Internal Medicine, Wayne State University School of Medicine, Detroit, Michigan 48201, and Centre for Pharmacognosy and Phytotherapy, The School of Pharmacy, University of London, 29−39 Brunswick Square, London WC1N 1AX, U.K.

Received June 23, 2005

Twenty-two convolvulaceous oligosaccharides selected from the tricolorin (**1**−**7**), scammonin (**8**, **9**), and orizabin (**10**−**22**) series were evaluated for activity against a panel of *Staphylococcus aureus* strains possessing or lacking specific efflux pumps. The minimum inhibitory concentrations (MIC values) for most of the amphipatic compounds ranged from 4 to 32 μg/mL against XU-212 (possessing the TetK multidrug efflux pump) and SA-1199B (overexpressing the NorA multidrug efflux pump), compared with 64 and 0.25 μg/mL, respectively, for tetracycline. This activity was shown to be bactericidal. Two microbiologically inactive members of the orizabin series (**10**, **20**) increased norfloxacin susceptibility of strain SA-1199B. At low concentrations, compound **10** was a more potent inhibitor of multidrug pump-mediated EtBr efflux than reserpine. The wide range of antimicrobial activity displayed by these compounds is an example of synergy between related components occurring in the same medicinal crude drug extract, i.e., microbiologically inactive components disabling a resistance mechanism, potentiating the antibiotic properties of the active substances. These results provide an insight into the antimicrobial potential of these complex macrocyclic lactones and open the possibility of using these compounds as starting points for the development of potent inhibitors of *S. aureus* multidrug efflux pumps.

There are few available antibiotics that can be used to treat life-threatening infections caused by methicillin-resistant *Staphylococcus aureus* (MRSA) strains.[1,2] Unfortunately, resistance to the main antibiotic used in its treatment, the glycopeptide vancomycin, has become more frequent[3] and is cause for considerable concern in hospitals and in community life. While the newest oxazolidinone and streptogramin-type antibiotics have been heralded as a solution to therapeutic difficulties associated with MRSA infections, resistance to linezolid (an oxazolidinone) has been reported for vancomycin-resistant *Enterococcus faecium*.[4] Staphylococcal resistance to this antibiotic[5] and to other recently developed agents has also emerged.[6] Clearly, there is an urgent need to identify new compounds that display a broad spectrum of antibiotic activity and develop these leads into new drugs to treat multidrug-resistant (MDR) and methicillin-resistant variants of *S. aureus*. This would alleviate the present situation where few back-up leads are available to complement glycopeptides, oxazolidones, or daptomycin.[7]

Facing this need, we have evaluated the inhibitory activity of a series of oligosaccharides[8,9] from the convolvulaceous resin glycosides on four *S. aureus* strains as well as the effect of the interaction of two inactive natural products when tested combined with norfloxacin on an MDR strain that effluxes this antibiotic. Previously, tricolorins A−E (**1**−**5**) have displayed antimicrobial properties with MIC values in the range 1−40 μg/mL against a standard *S. aureus* strain (ATCC 6538) and toward *Mycobacterium tuberculosis* (MIC 16−32 μg/mL),[10] suggesting the potential of this class of natural bioactive polyacylated oligosaccharides[11] as new antibacterial agents. The current investigation also acknowledges the growing interest in plants historically used in medical treatments as a possible source of antimicrobial agents.[12]

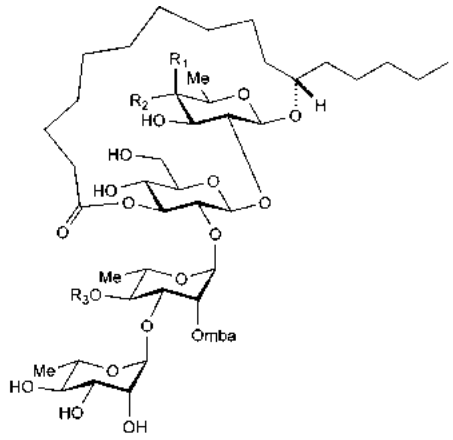

1 : R_1 = OH, R_2 = H, R_3 = mba
2 : R_1 = OH, R_2 = H, R_3 = iba
3 : R_1 = OH, R_2 = H, R_3 = nla-(−)
5 : R_1 = H, R_2 = OH, R_3 = mba

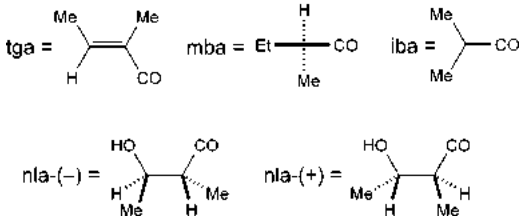

The MIC of all tested compounds was determined against two effluxing strains (SA-1199B and XU-212), an epidemic methicillin-resistant strain (EMRSA-15), and a standard *S. aureus* strain (ATCC 25923), and the data are presented in Table 1. All the amphipathic tetrasaccharides from the tricolorin series (**1**−**5**) exhibited an inhibitory activity against *S. aureus* ATCC 25923, with MIC values

[⊥] Dedicated to Dr. Norman R. Farnsworth of the University of Illinois at Chicago for his pioneering work on bioactive natural products.

* To whom correspondence should be addressed. Tel: +52-55-5622-5288. Fax: +52-55-5622-5329. E-mail: pereda@servidor.unam.mx.
[†] Universidad Nacional Autónoma de México.
[‡] Wayne State University.
[§] University of London.

10.1021/np050227d CCC: $33.50
Published on Web 10/20/2005

Table 1. Susceptibility of *Staphylococcus aureus* to Selected Convolvulaceous Oligosaccharides

code	compound	MIC (μg/mL)			
		ATCC 25923	XU-212	SA-1199B	EMRSA-15
1	tricolorin A	16	8	8	4
2	tricolorin B	32	16	16	16
3	tricolorin C	32	16	32	32
4	tricolorin D	16	32	32	32
5	tricolorin E	16	8	8	8
6	tricolorin F	>512	>512	>512	>512
7	tricolorin J	>256	>256	>256	>256
8	scammonin I	32	128	32	32
9	scammonin II	256	512	512	128
10	orizabin IX	>512	>512	512	256
11	orizabin X	16	32	4	4
12	orizabin XI	16	32	4	4
13	orizabin XII	>512	>512	256	512
14	orizabin XIII	8	32	4	8
15	orizabin XIV	16	64	8	8
16	orizabin XV	128	512	32	16
17	orizabin XVI	8	128	16	8
18	orizabin XVII	8	32	4	8
19	orizabin XVIII	32	64	64	64
20	orizabin XIX	128	512	512	256
21	orizabin XX	64	>512	8	32
22	orizabin XXI	8	64	8	16
tetracycline		0.08	64	0.25	0.15
norfloxacin		2	16	32	0.5

of 16−32 μg/mL, and toward the effluxing strains with MIC values of 4−32 μg/mL. Not surprisingly, the polar compounds tricolorins F (**6**) and J (**7**) exhibited no antibacterial activity at the concentrations employed. This correlation between lipophilicity and antibacterial activity where the more lipophilic compounds are significantly more active than their polar analogues has been found in other natural products.[10,13] Where growth inhibition by tested compounds was noted, an aliquot of the culture was plated out on nutrient agar and incubated for 24 h. No growth was detected for any of the active compounds, indicating a bactericidal mode of action.

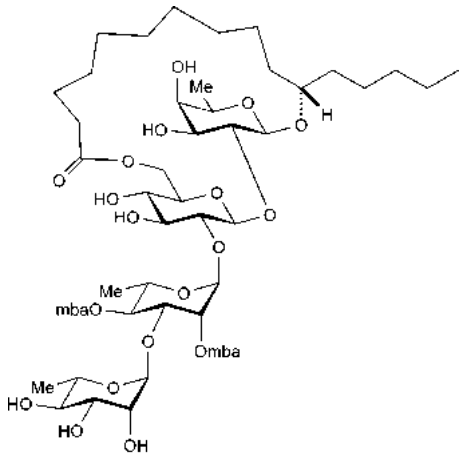

4

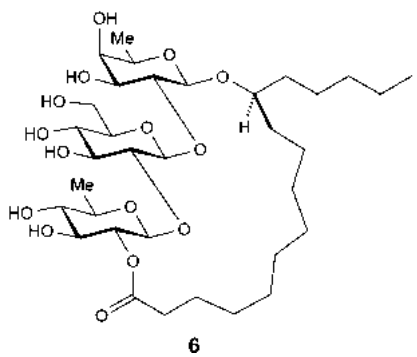

6

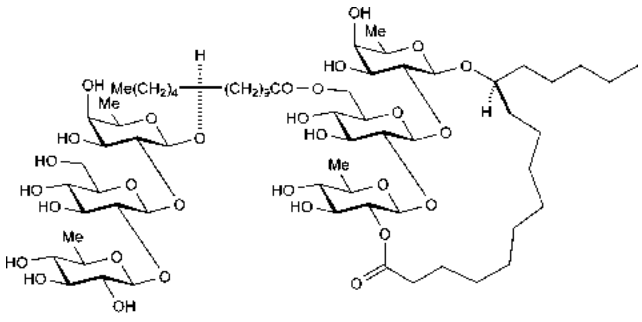

7

The size of the lactone ring was not crucial for antibacterial activity because the potency of the larger macrocyclic structure of the orizabin series was similar to that of the tricolorin series. It would be interesting to evaluate a higher number of related compounds so as to elaborate conclusions related to the influence of the degree, type, and position of acylation on the activity of these oligosaccharides. However, the following observations can be drawn from our results: (a) the more highly acylated compounds had no direct effect against *S. aureus* (MIC > 512 μg/mL), as indicated by the displayed inactivity of peracetylated derivatives of tricolorin A (**1**), scammonin I (**8**), and orizabin XI (**12**); (b) the activity against *S. aureus* produced by the diesters (**2**−**5**, **8**) was similar to that of tricolorin A (**1**); (c) the monoester compound **9** (scammonin II) was inactive and did not show a potentiation of activity in combination with a subinhibitory dose of the antibiotic norfloxacin; (d) the substitution of (2*S*,3*S*)-nilic acid (nla) by its enantiomer (2*R*,3*R*) in the orizabin series (**11**−**22**), as the esterifying moiety at position C-2 of the inner rhamnose unit, causes, in most of the cases, a 4-fold reduction in the inhibition, e.g., orizabin XII (**13**) versus orizabin XIII (**14**); this effect could be a consequence of a slight difference in the conformations adopted by the macrocyclic structure in each of the diasteroisomeric pairs, modifying their interactions with the microorganism target membranes; (e) the interchange of the other esterifying residues, i.e., tiglic (tga), methylbutyric (mba), and isobutyric (iba) acids, at the remaining

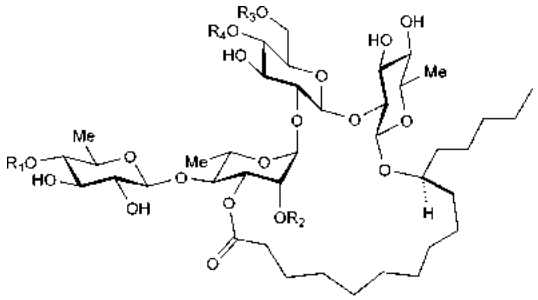

	R_1	R_2	R_3	R_4
8	tga	mba	H	H
9	H	mba	H	H
10	tga	mba	H	nla-(−)
11	tga	nla-(−)	iba	H
12	tga	nla-(+)	iba	H
13	tga	iba	nla-(−)	H
14	tga	iba	nla-(+)	H
15	tga	nla-(−)	mba	H
16	tga	nla-(+)	mba	H
17	tga	mba	nla-(−)	H
18	tga	mba	nla-(+)	H
19	mba	nla-(−)	mba	H
20	mba	nla-(+)	mba	H
21	mba	mba	nla-(−)	H
22	mba	mba	nla-(+)	H

esterifying positions on the oligosaccharide core does not produce any major effect in the inhibitory activity.

The amphipatic orizabins IX (**10**) and XIX (**20**) displayed a strong synergistic effect in combination with norfloxacin. Alone, these compounds had no antimicrobial activity at the concentration tested (MIC > 256 μg/mL), but they strongly potentiated the action of norfloxacin in experiments using a subinhibitory concentration of these oligosaccharides. Orizabin XIX (**20**) at 25 μg/mL reversed norfloxacin resistance 4-fold (8 versus 32 μg/mL) for SA-1199B, while orizabin IX (**10**) at 1 μg/mL completely inhibited SA-1199B growth in the presence of 2 μg/mL of norfloxacin.

Ethidium bromide (EtBr) is a substrate for many multidrug efflux pumps, including NorA of *S. aureus*. The efficiency of any pump for which EtBr is a substrate can be assessed fluorometrically by the loss of fluorescence over time from cells loaded with EtBr.[14] Orizabins IX (**10**) and XV (**16**) were nearly equipotent with respect to the inhibition of EtBr efflux by SA-1199B, with a slight advantage observed for compound **16** (Figure 1). At lower concentrations (less than 10 μM) both test compounds were more efficacious than reserpine. However, at 10 μM or higher their effects reached a plateau and became inferior to that of reserpine. This falloff in activity was due to solubility issues, since above 30 μM the broth solution became cloudy as a result of test compound precipitation. These data suggest that both compounds hold promise as leads in the search for more potent inhibitors of *S. aureus* multidrug efflux pumps.

From the standpoint of their potential use as therapeutic agents, the most important result is that these convolvulaceous oligosaccharides exert their action through inhibition of the multidrug resistance pumps, as previously reported for the structurally related acylated disaccharides found in the leaf exudates of *Geranium* species (Geraniaceae).[15] Therefore, combining these plant products with antibiotics that are substrates for these MDR pumps (e.g., orizabin IX (**10**)/ciprofloxacin) could improve the treatment of refractive infections caused by effluxing staphylococci.

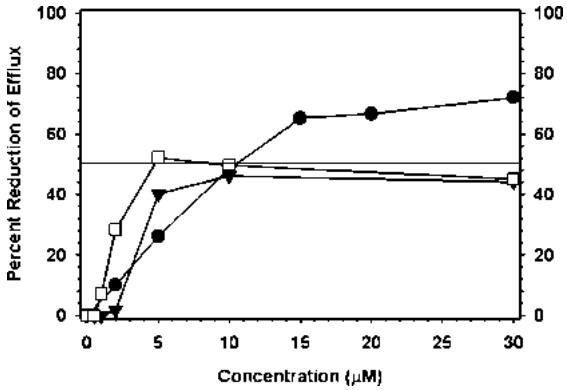

Figure 1. Ethidium efflux inhibition assay from SA-1199B strain cells: (●) reserpine; (▼) compound **10**; (□) compound **16**. The horizontal line indicates 50% efflux inhibition.

The cross activity displayed between members of the tricolorin and orizabin series could represent an example of synergy[16] between related components in medicinal crude drug extracts, with microbiologically inactive compounds disabling a resistance mechanism (e.g., compounds **10**, **16**, and **20**), therefore potentiating the antimicrobial activity of the antibiotic substances.[17] Our results suggest that convolvulaceous plants may elaborate an array of amphipatic oligosaccharides, many of which have evolved to confer selective advantage against microbial attack to plants.[18] This evolutionary process may have potential in the discovery of new antibacterial leads.

Experimental Section

Bacterial Strains and Media. *Staphyloccocus aureus* EMRSA-15 containing the *mecA* gene was provided by Dr. Paul Stapleton, The School of Pharmacy, University of London. Strain XU-212, a methicillin-resistant strain possessing the TetK tetracycline efflux protein, was provided by E. Udo.[19] SA-1199B, which overexpresses the NorA MDR efflux protein,[20] and *S. aureus* ATCC 25923 were also used. All strains were cultured on nutrient agar (Oxoid, Basingstoke, UK) before determination of MIC values. Cation-adjusted Mueller-Hinton broth (MHB; Oxoid) containing 20 and 10 mg/L of Ca^{2+} and Mg^{2+} was used for susceptibility tests.

Antibiotics and Chemicals. Tetracycline and norfloxacin were obtained from Sigma (Poole, UK). Individual glycolipids from the $CHCl_3$ extracts of *Ipomoea tricolor* Cav. and *I. orizabensis* (Pelletan) Ledebour ex Steudel were purified as previously described.[8,9] Glycolipids **1**−**22** were isolated from their respective crude resin mixtures by preparative recycling HPLC using a Waters 600 E multisolvent delivery system equipped with a Waters 410 differential refractometer detector (Waters, Milford, MA). For purification of the tricolorins (**1**−**7**), elution was isocratic (CH_3CN-H_2O, 4:1; flow rate = 3.5 mL/min) on a reversed-phase C_{18} column (20 × 250 mm; 15 μm; ISCO) and a sample injection of 500 μL (100 mg/mL). To perform the separations of compounds **8**−**22**, an HPLC system equipped with an NH_2 column (19 × 150 mm; 10 μm, μBondapak, Waters) was used, and elution was also conducted isocratically (CH_3CN-H_2O, 95:5; flow rate = 4 mL/min).

Susceptibility Testing. Minimum inhibitory concentration values (MIC) were determined at least in duplicate by standard microdilution procedures, as recommended by the National Committee for Clinical Laboratory Standards guidelines.[21] An inoculum density of 5×10^5 cfu of each of the test strains was prepared in 0.9% saline by comparison with a MacFarland standard. MHB (125 μL) was dispensed into 10 wells of a 96-well microtiter plate (Nunc, 0.3 mL volume per well). Glycolipids **1**−**22** were tested at final concentrations ranging from 1 to 512 μg/mL prepared by serial 2-fold dilutions. All test compounds were dissolved in DMSO before dilution into MHB for use in MIC determinations. The highest concentration of DMSO remaining after dilution (3.125% v/v) caused no inhibition of bacterial growth. The MIC was defined as the lowest concentration that yielded no visible growth.

Ethidium Efflux Assay. SA-1199B, which overexpresses NorA, was loaded with EtBr as previously described, and the effect of varying concentrations of compounds **10** and **16** on EtBr efflux efficiency was determined to generate a dose−response profile for each oligosaccharide.[20,22] The effect of reserpine was also determined for comparative purposes. Assays were performed in duplicate, and mean results were expressed as the percentage reduction of total efflux observed for SA-1199B in the absence of inhibitors.

Acknowledgment. We thank Dr. Mabel Fragoso-Serrano (Facultad de Química, UNAM) for assistance during the purification of the test compounds. This research was partially supported by grants from Dirección General de Asuntos del Personal Académico (UNAM: IN214205-2), Consejo Nacional de Ciencia y Tecnología de México (45861-Q), La Academia Mexicana de Ciencias, and The Royal Society, UK.

References and Notes

(1) Chang, F.-Y.; MacDonald, B. B.; Peacock, J. E.; Musher, D. M.; Triplett, P.; Mylotte, J. M.; O'Donnell, A.; Wagener, M. M.; Yu, V. L. *Medicine* **2003**, *82*, 322−332.
(2) Lowy, F. *New Engl. J. Med*. **1998**, *339*, 520−532.
(3) (a) Centers for Disease Control and Prevention. *Am. J. Infect. Control* **2001**, *29*, 404−421. (b) Centers for Disease Control and Prevention. *Morb. Mortal. Wkly. Rep.* **2002**, *51*, 565−567. (c) Centers for Disease Control and Prevention. *Morb. Mortal. Wkly. Rep.* **2002**, *51*, 902. (d) Centers for Disease Control and Prevention. *Morb. Mortal. Wkly. Rep.* **2004**, *53*, 322−323.
(4) Gonzales, R. D.; Schreckenberger, P. C.; Graham, M. B.; Kelkar, S.; DenBesten, K.; Quinn, J. P. *Lancet* **2001**, *357*, 1179.
(5) (a) Tsiodras, S.; Gold, H. S.; Sakoulas, G.; Eliopoulos, G. M.; Wennersten, C.; Venkataraman, L.; Moellering, R. C.; Ferraro, M. J. *Lancet* **2001**, *358*, 207−208. (b) Wilson, P.; Andrews, J. A.; Charlesworth, R.; Walesby, R.; Singer, M.; Farrell, D. J.; Robbins, M. *J. Antimicrob. Chemother*. **2003**, *51*, 186−188.
(6) Hershberger, E.; Donabedian, S.; Konstantinou, K.; Zervos, M. J. *Clin. Infect. Dis.* **2004**, *38*, 92−98.
(7) Livermore, D. M. *Int. J. Antimicrob. Agents* **2000**, *16*, S3−S10.
(8) (a) Bah, M.; Pereda-Miranda, R. *Tetrahedron* **1996**, *52*, 1306−13080. (b) Bah, M.; Pereda-Miranda, R. *Tetrahedron* **1997**, *53*, 9007−9022.
(9) (a) Hernández-Carlos, B.; Bye, R.; Pereda-Miranda, R. *J. Nat. Prod.* **1999**, *62*, 1096−1100. (b) Pereda-Miranda, R.; Hernández-Carlos, B. *Tetrahedron* **2002**, *58*, 10251−10260.
(10) Rivero-Cruz, I.; Acevedo, L.; Guerrero, J. A.; Martínez, S.; Bye, R.; Pereda-Miranda, R.; Franzblau, S.; Timmermann, B. N.; Mata, R. *J. Pharm. Pharmacol*. **2005**, *57*, 1117−1126.
(11) Pereda-Miranda, R.; Bah, M. *Curr. Top. Med. Chem*. **2003**, *3*, 111−131.
(12) Cowan, M. M. *Clin. Microbiol. Rev.* **1999**, *12*, 564−582.
(13) Cantrell, C. L.; Franzblau, S. G.; Fisher, N. H. *Planta Med.* **2001**, *67*, 685−694.
(14) Gibbons, S.; Oluwatuyi, M.; Kaatz, G. W. *J. Antimicrob. Chemother.* **2003**, *51*, 13−17.
(15) Stermitz, F. R.; Cashman, K. K.; Halligan, K. M.; Morel, C.; Tegos, G. P.; Lewis, K. *Bioorg. Med. Chem. Lett.* **2003**, *13*, 1915−1918.
(16) Williamson, E. M. *Phytomedicine* **2001**, *8*, 401−409.
(17) Stermitz, F. R.; Lorenz, P.; Tawara, J. N.; Zenewicz, L. A.; Lewis, K. *Proc. Natl. Acad. Sci.* **2000**, *97*, 1433−1437.
(18) Dixon, R. A. *Nature* **2001**, *411*, 843−847.
(19) Gibbons, S.; Udo, E. E. *Phytother. Res.* **2000**, *14*, 139−140.
(20) Kaatz, G. W.; Seo, S. M.; Ruble, C. A. *Antimicrob. Agents Chemother.* **1993**, *37*, 1086−1094.
(21) National Committee for Clinical Laboratory Standards. *Methods for Dilution Antimicrobial Susceptibility Tests for Bacteria that Grow Aerobically*, 5th ed.; NCCLS: Villanova, PA, 1999; Approved standard M7-A5.
(22) Kaatz, G. W.; Seo, S. M.; O'Brien, L.; Wahiduzzaman, M.; Foster, T. J. *Antimicrob. Agents Chemother.* **2000**, *44*, 1404−1406.

NP050227D

FLAVOUR AND FRAGRANCE JOURNAL
Flavour Fragr. J. 2005; **20**: 671–675
Published online 14 September 2005 in Wiley InterScience (www.interscience.wiley.com). DOI: 10.1002/ffj.1584

Modulation of multi-drug resistance (MDR) in *Staphylococcus aureus* by Osha (*Ligusticum porteri* L., Apiaceae) essential oil compounds

Pascale Cégiéla-Carlioz,[1] Jean-Marie Bessière,[2] Bruno David,[3] Anne-Marie Mariotte,[1] Simon Gibbons[4] and Marie-Geneviève Dijoux-Franca[1]*

[1] Laboratoire de Pharmacognosie, Département de Pharmacochimie Moléculaire (DPM), UMR 5063 CNRS-UJF, Domaine de La Merci, 38706 La Tronche cedex, France
[2] Laboratoire de Phytochimie, Ecole Nationale Supérieure de Chimie de Montpellier, 4 Rue de l'Ecole Normale, 34000 Montpellier, France
[3] Centre de Recherche sur les Substances Naturelles, UMS CNRS/IRPF No. 2597, Institut de Recherche Pierre Fabre, ISTMT, 3 Rue des Satellites, 31400 Toulouse, France
[4] Centre for Pharmacognosy and Phytotherapy, School of Pharmacy, University of London, 29–39 Brunswick Square, London WC1N 1AX, UK

Received 12 December 2003; Revised 02 November 2004; Accepted 09 December 2004

ABSTRACT: In a continuing project to characterize natural compounds with activity as modulators of MDR in *Staphyloccocus aureus*, Osha essential oil and extracts were evaluated. The aim of this work was to identify the active components as MDR modulators in the oil from the roots of *Ligusticum porteri* Coulter & Rose (Apiaceae). This essential oil was obtained by steam distillation or by solvent extraction and analysed by gas chromatography–mass spectrometry. Forty-two components were identified. Sabinyl acetate (1) (56.6%), (*Z*)-ligustilide (2) (12.9%) and sabinol (3) (3.3%) were the major components of water-distilled essential oil, while (*Z*)-ligustilide (2) (39.1%), sabinyl acetate (1) (34.6%) and 4-terpinyl acetate (4) (3.1%) were the major components of the dichloromethane extract. At a concentration of 100 μg/ml, the oil from hydrodistillation caused a two-fold potentiation, and the oil from solvent extraction caused a four-fold potentiation of the activity of the fluoroquinolone antibiotic norfloxacin against a norfloxacin-resistant strain possessing the NorA MDR efflux transporter, the major chromosomal drug pump in this pathogen. Copyright © 2005 John Wiley & Sons, Ltd.

KEY WORDS: *Ligusticum porteri*; Apiaceae; essential oil; chemical composition; *Staphylococcus aureus*; MDR modulation

Introduction

The development and use of antibiotics for the chemotherapy of bacterial infections was one of the most remarkable accomplishments in medicine of the last century. Multidrug-resistant (MDR) organisms such as methicillin-resistant *Staphylococcus aureus* (MRSA) are becoming common causes of infections in the acute and long-term care units in hospitals. Consequently, there is a clear and urgent need to discover and develop new effective and non-toxic drugs that are able to reverse MDR. In a continuing project to characterize natural products with activity as modulators of MDR in *Staphyloccocus aureus*,[1] *Ligusticum porteri* Coulter & Rose (Apiceae) (Osha) essential oil was evaluated.

The genus *Ligusticum* includes 60 species with worldwide distribution in many non-coastal western states in the USA. Osha is a perennial herb which grows throughout much of the Rocky Mountains, from northern Wyoming to Chihuahua, Mexico.[2] Osha is widely employed in traditional medicine in south-western USA and in northern Mexico as a treatment for cough, sore throat and stomach ache. Powdered roots are used in order to prevent infections.[3]

Apiaceae essential oils have been shown to contain monoterpenes, sesquiterpenes and phenylpropanoids, and some genera include ligustilides.[4] Numerous studies have been published on the chemical composition of organic extracts or essential oil in the genus *Ligusticum*, but only a few have reported on their biological activities. The present report is the first account of the chemical composition and biological activity of *L. porteri* (Osha) oil. The composition of volatile fractions obtained with two different procedures were studied, using gas chromatography–mass spectrometry (GC–MS) analysis. The modulation activity of Osha oil and its major components were evaluated using a strain of *Staphylococcus aureus* possessing the Nor(A) MDR efflux pump.

* Correspondence to: M.-G. Dijoux-Franca, Laboratoire de Pharmacognosie, Département de Pharmacochimie Moléculaire (DPM), UMR 5063 CNRS-UJF, Domaine de La Merci, 38706 La Tronche Cedex, France.
E-mail: Marie-Genevieve.Dijoux@ujf-grenoble.fr
Contract/grant sponsor: Institut de Recherche Pierre Fabre, France.
Contract/grant sponsor: Institut Klorane, France.
Contract/grant sponsor: Région Rhône-Alpes, France.

Experimental

Plant Material

Powdered dry roots of *L. porteri* were purchased in April 2002 from Proline Botanicals Ltd. A voucher specimen was deposited at the University of London School of Pharmacy (Batch No. SG-PC 2002-1).

General Experimental Procedures

Analysis by GC–MS was carried out using the same conditions as previously described by Brun *et al*.[6] on a non-polar DB1 column (Macherey–Nagel) (25 m × 0.20 mm i.d., 0.25 μm film thickness). ^{1}H-NMR (400 MHz) and ^{13}C-NMR (100 MHz) spectra were recorded in $CDCl_3$ on a Bruker Avance 400 spectrometer at 22 °C. Chemical shift values (δ) are reported in parts per million (ppm) relative to tetramethylsilane (TMS $\delta = 0$) as internal standard and coupling constants (*J* values) are given in Hz. EI Mass spectra were recorded on a R210C instrument coupled with a computer IPC (P2A) MSCAN WALLIS. TLC was carried out on 60 F_{254} mm (Macherey–Nagel) pre-coated plates and spots were visualized by spraying with sulphuric acid (40% in MeOH) followed by heating.

Preparation and Fractionation of Extracts

Powdered dry roots (50 g) were submitted to steam distillation for 3 h, according to the standard procedures for hydrodistillation described in the *Pharmacopée Française* (10th edn).[5] This extraction yielded 1.5 ml pale yellow essential oil (4.5% dry weight).

A 100 g sample of the dry ground *L. porteri* roots were successively extracted twice with dichloromethane, acetone and MeOH at room temperature for 1 h, in a sonicator. Following filtration, the solvent was removed under reduced pressure and the CH_2Cl_2 extract (85.2 g) [C0], the Me_2CO extract (7.6 g) [A0] and the MeOH extract (19.3 g) [M0], respectively were obtained.

Isolation of sabinyl acetate **(1)**

Initially, an aliquot of the CH_2Cl_2 extract (C0, 2 g) was applied to silica gel column chromatography (Silicagel 60 Macherey–Nagel), which was eluted with a toluene–EtOAc gradient; the eluates were collected as fractions C1-1 to C1-12. Compound **1** (382 mg; C1-1) was obtained with 100% toluene.

Isolation of the (Z)-ligustilide **(2)**

Next, the MeOH extract (M0; 19 g) was partitioned with H_2O:CH_2Cl_2 (50:50). The CH_2Cl_2 extract (M1-1, 1 g) was obtained. Then, M1-1 was applied to a Sephadex LH-20 cc (column chromatography) and eluted with CH_2Cl_2:MeOH (70:30) to yield 13 fractions (M2-1 to M2-13). M2-1 (368 mg) was submitted to a MPLC on a diol (Lichroprep®, Merck) column chromatograph and eluted with a cyclohexane–CH_2Cl_2–MeOH gradient to yield 26 fractions (M3-1 to M3-26). The M3-1 fraction (53 mg) was obtained in 100% cyclohexane. Finally, M3-1 was applied to a silica gel column chromatograph (Silicagel 60 Macherey-Nagel), which was eluted with a cyclohexane–CH_2Cl_2–MeOH gradient and 21 fractions were collected (M4-1 to M4-21). Compound **2** (M4-10, 8 mg) was eluted with cyclohexane:CH_2Cl_2 (80:20).

Sabinyl acetate **(1)**

Pale yellow oil; visible by quenching at 254 nm. EI–MS (relative intensity %) *m/z*: 194 $[M]^+$ (5), 154 (4), 134 (22), 119 (38), 109 (11), 92 (100), 91 (84), 32 (10). ^{1}H-NMR ($CDCl_3$): 0.75 (dd, 4.5Hz, 2.1Hz, 1H, H-4a), 0.77 (dd, 4.5Hz, 2.1Hz, 1H, H-4b), 0.84 (d, 6.9Hz, 3H, H-9), 0.90 (d, 6.8Hz, 3H, H-10), 1.45 (sept, 6.8Hz, 1H, H-8), 1.97 (s, 3H, H-2′), 2.02 (t, 3Hz, 1H, H-3), 2.13 (dd, 7.7Hz, 2.1Hz, 1H, H-6a), 2.17 (dd, 7.7Hz, 2.1Hz, 1H, H-6b), 5.03 (s, 1H, H-7a), 5.06 (s, 1H, H-7b), 5.41 (d, 7.6Hz, 1H, H-1). ^{13}C-NMR ($CDCl_3$): 18.6 (C-4), 19.5 (C-9), 19.6 (C-10), 21.4 (C-2′), 29.3 (C-6), 32.3 (C-3), 35.6 (C-8), 36.9 (C-5), 76.1 (C-1), 100.6 (C-7), 152.2 (C-2), 170.2 (C-1′).

(Z)-ligustilide **(2)**

Yellow oil; white coloration under UV light at 366 nm. EI–MS (70 eV, relative intensity %) *m/z*: 190 $[M]^+$ (20), 161 (55), 148 (71), 134 (17), 105 (77), 91 (28), 77 (62), 55 (100). ^{1}H- and ^{13}C-NMR spectra were assigned by comparison with the literature data.[7]

Bacterial Strains

Multidrug-resistant *Staphylococcus aureus* strain SA-1199B (fluoroquinolone-resistant) was provided by Professor Glenn W. Kaatz (Wayne State University) and was cultured on nutrient agar (Oxoid) and incubated for 24 h at 37 °C prior to determination of MIC.

MIC

Mueller–Hinton Broth (MHB) (Oxoid) was adjusted to contain 20 mg/L and 10 mg/L of Ca^{2+} and Mg^{2+} respectively. This was achieved by dissolving 83.7 mg $MgCl_2.6H_2O$ and 73.4 mg $CaCl_2.2H_2O$ in 1l MHB. An inoculum density of 5×10^5 cfu of the test organism was prepared in normal saline (9 g/l) by comparison with a

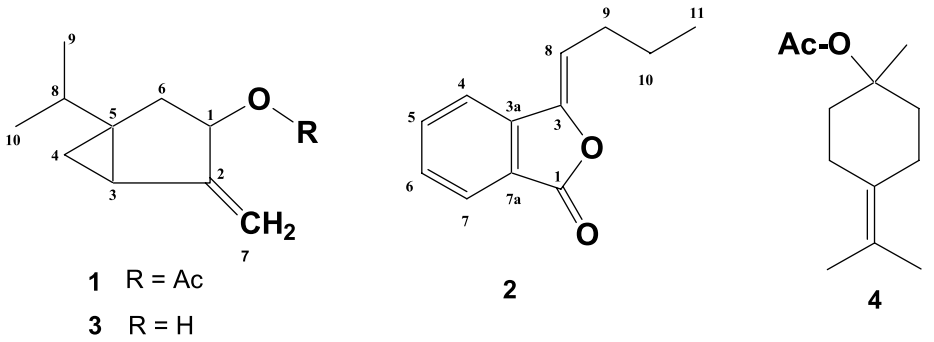

Figure 1. Major compounds of the essential oil from hydrodistillation and from the dichloromethane extract of *Ligusticum porteri*

MacFarland standard. MHB (125 µl) was dispensed into 10 wells of a 96-well microtitre plate (Nunc, 0.3 ml/well). A stock solution of norfloxacin (8.192 mg/ml) was prepared by dissolving the antibiotic in DMSO (Sigma) and diluting in MHB to give a final DMSO concentration of 0.625%. A DMSO control was included in all assays. 125 µl test solution (2048 µg/ml) was serially diluted (two-fold) into each of the wells. 125 µl inoculum was then added to each of the wells, resulting in a test compound range of 512 to 1 µg/ml. The plate was then incubated at 37 °C for 18 h and the MIC was recorded as the lowest concentration at which no growth was observed. Norfloxacin and reserpine were obtained from Sigma Chemical Co. For the modulation of resistance experiment, reserpine was incorporated into the MHB to give a concentration of 20 µg/ml; test samples were incorporated into the MHB to give a concentration of 100 µg/ml or 50 µg/ml for (*Z*)-ligustilide **2**, which also demonstrated antibacterial activity. In the case of the modulation assay, **1**, **2** and reserpine were dissolved in DMSO and diluted into MHB to give final concentrations of 100, 50 and 20 µg/ml, respectively. This medium was then used in the MIC assay.

Results

Volatile compounds obtained by hydrodistillation and solvent extraction of the powdered roots were investigated by GC–MS. Overall, 42 components were identified from their retention indices[8,9] and mass spectral data.[8,10,12,13]

The results are listed in Table 1 with percentage composition. This analysis showed that there were fewer compounds in the solvent extract compared to the essential oil (30 compounds vs. 41, respectively). Furthermore, the content of the major compounds varied. The essential oil and solvent extract were dominated by terpenes (73.4% and 46.5%, respectively) and by phthalides (14.4% and 41.1%, respectively). Sabinol **3** was not present in the solvent extract. Sabinyl acetate **1** (56.6%), (*Z*)-ligustilide **2** (12.9%) and sabinol **3** (3.3%) (Figure 1) were the major components of the essential oil from hydrodistillation, while (*Z*)-ligustilide **2** (39.1%), sabinyl acetate **1** (34.6%) and 4-terpinyl acetate **4** (3.1%) were the major components of the dichloromethane extract.

A ^{13}C-NMR spectrum of the oil was recorded in order to check the identification of the major components. The major peaks could be assigned to sabinyl acetate **1**.

Additionally, Osha essential oil and the solvent extract were evaluated for bacterial resistance modifying activity against a strain of multidrug-resistant (MDR) *Staphylococcus aureus* (Table 2). At a non-bacteriostatic concentration (100 µg/ml), the oil caused a two-fold potentiation and the solvent extract caused a four-fold potentiation of the activity of the fluoroquinolone antibiotic norfloxacin against a norfloxacin-resistant strain of *S. aureus*. This strain was resistant due to the presence of the norfloxacin effluxing MDR transporter NorA, the major characterized chromosomal drug pump in this species.[14] The oil and the solvent extract significantly restored the bacterial sensitivity to the antibiotic. The MIC of norfloxacin decreased from 32 µg/ml (when tested alone) to 16 µg/ml and 8 µg/ml when co-administrated with essential oil and organic extract, respectively. These activities compare favourably with reserpine (at concentration, c = 10 µg/ml), which caused a four-fold reduction in norfloxacin MIC against the same strain (Table 2).

Although the activities of these extracts seem moderate, it should be realized that both essential oil and solvent extract have a complex composition. The pure isolated compounds are likely to be more active than the crude essential oil or extract.

The major pure compounds of the essential oil and the dichloromethane extract were also tested for their potentiation of norfloxacin activity against *S. aureus* SA-1199B (Table 2). With **1**, a two-fold reduction of norfloxacin MIC against this strain (at 100 µg/ml) was observed. Compound **2** showed weak growth inhibition activity at 128 µg/ml and a two-fold reduction in the MIC of norfloxacin against SA-1199B (at 50 µg/ml). Sabinyl acetate **1** and (*Z*)-ligustilide **2** therefore exhibit

Table 1. Chemical composition of essential oil and dichloromethane extract from roots of *Ligusticum porteri*

Compounds	Retention indices	Essential oil (%)	Dichloromethane extract (%)
α-Thujene	926	0.05	
α-Pinene	942	0.1	
Sabinene	973	0.4	0.1
β-Pinene	978	0.3	
Myrcene	997	0.1	
α-Phellandrene	1003	0.3	0.1
α-Terpinene	1017	0.2	
p-Cymene	1018	0.9	0.2
β-Phellandrene	1026	0.4	
Limonene	1027	0.1	1.8
γ-Terpinene	1056	0.3	0.2
cis-Thujone	1103	0.03	
1,3,8-Menthatriene	1112	0.1	
α-Phellandrene-1,2-epoxide	1115	1.9	0.6
Sabinol (**3**)*	1132	3.3	
Pentylbenzene	1161	2.1	1.5
Terpinen-4-ol	1170	0.8	0.1
α-Terpineol	1181	0.1	
Thymyl methylether	1228	0.05	0.4
Carvacryl methylether	1254	0.9	0.4
Isothujyl acetate	1273	0.2	0.1
trans-Pinocarveyl acetate	1273	0.1	
Bornyl acetate	1284	1.8	0.9
Sabinyl acetate (**1**)*	1287	56.6	34.6
4-Vinylguaiacol	1299	0.4	
4-Terpinyl acetate (**4**)	1338	0.1	3.1
α-Terpinyl acetate	1348	1.3	0.8
o-Methyleugenol	1389	1.1	0.5
2,5-Dimethoxy-*p*-cymene	1407	0.3	0.2
α-Barbatene	1413	0.3	0.4
β-Funebrene	1423	0.1	0.1
Widdrene	1441	0.2	0.3
β-Barbatene	1444	1.3	1.5
Myristicin	1498	0.8	0.6
(–)-Kessane	1500	0.6	0.4
Liguloxide	1505	0.5	0.4
α-Chamigrene	1507		0.1
Elemicin	1531	0.5	0.4
(*Z*)-3-Butylidenephthalide	1637	0.8	0.8
α-Eudesmol	1658	0.2	0.1
(*Z*)-Ligustilide (**2**)	1698	12.9	39.1
(*E*)-Ligustilide	1749	0.2	0.8
Identified compounds		88.1	96.2

* Undetermined isomer.

Table 2. Minimum inhibitory concentrations (MICs) and potentiation of norfloxacin activity against *Staphylococcus aureus* SA-1199B (NorA)

Extract or pure compound	Antibacterial activity MIC (μg/ml)	MDR reversal	
		Concentration (μg/ml)	Norfloxacin MIC (μg/ml)
Essential oil	>512	100	16
Dichloromethane extract	512	100	8
(*Z*)-Ligustilide (**2**)	128	50	16
Sabinyl acetate (**3**)	>512	100	16
Norfloxacin	32	32	32
Reserpine	—	20	2

moderate potentiation of the activity of the norfloxacin against a norfloxacin-effluxing strain of *S. aureus* compared to the effect of reserpine.[15]

Discussion

This study showed the presence of numerous compounds that have not been described previously in *L. porteri*. A number of publications have described important factors that influence the composition of the oil throughout the process of extraction (hydrodistillation, hydrodiffusion, solvent extraction or supercritical fluid extraction).[8,16] This report is another example of the influence of the extraction procedure.

Neither the essential oil nor the CH_2Cl_2 extract exhibited a bacteriostatic activity against the MDR *S. aureus* strain, while they both restored the sensitivity of this strain to norfloxacin. As the organic extract was the more efficient modulator ($MIC_{norfloxacin}$ = 8 μg/ml), it was supposed that the main component of this extract would be responsible for the activity. Sabinyl acetate and (*Z*)-ligustilide were therefore tested but revealed moderate activity ($MIC_{norfloxacin}$ = 16 μg/ml). These results suggest that separately the pure components are less active than the complex mixture. This indicated that the activity could be related to either the associated compounds, in a synergistic mode of action, or to the mixture itself.

Even if the resistance-modifying activities of (*Z*)-ligustilide and sabinyl acetate are moderate, these compounds are present in high concentration in Osha and are amenable to semi-synthetic modification, which could give rise to useful structure–activity information. These components add to our knowledge of natural compounds as bacterial MDR modulators.

Finally, (*Z*)-ligustilide has also been shown to have weak antiviral properties[17] and activity against Gram-negative bacteria and yeast microorganisms. This is the first report of its anti-bacterial activity against an MDR strain of *S. aureus* possessing a multidrug efflux-mediated mechanism of resistance.

Acknowledgements—The authors are grateful to the Institut de Recherche Pierre Fabre, the Institut Klorane and the Région Rhône-Alpes (EURODOC program) for their financial support.

References

1. Gibbons S, Oluwatuyi M, Veitch NC, Gray AI. *Phytochemistry* 2003; **62**: 83–87.
2. Bye RA, Linares E. *J. Ethnobiol*. 1986; **6**: 289–306.
3. Linares E, Bye RA. *J. Ethnopharmacol*. 1987; **19**: 153–183.
4. Gillespie SG, Duszynski JN. *Planta Med*. 1998; **64**: 392.
5. *Pharmacopée Française*, 10th edn. Maisonneuve SA: Paris, 1983.
6. Brun G, Bessière JM, Dijoux-Franca MG, David B, Mariotte AM. *Flavour Fragr. J*. 2001; **16**: 116–119.
7. Gijbels MJM, Scheffer JJC, Baerheim Svendsen A. *Planta Med*. 1982; **44**: 207–211.
8. Jennings WG, Shibamato T. *Qualitative Analysis of Flavor and Fragrance Volatiles by Glass Capillary Gas Chromatography*. Academic Press: New York; 1980; 9.
9. Kondjoyan N, Berdague JL. *A Compilation of Relative Retention Indices for Analysis of Aromatic Compounds*. Laboratoire Flaveur: INRA de Theix, St Genès Champanelle, France, 1996.
10. Pacakova V, Feltl L. *Chromatographic Retention Indices*. Ellis Horwood: New York, 1992.
11. Mc Lafferty FW, Staufer DB. *The Wiley/NBS Registry of Mass Spectral Data*. Wiley Interscience: New York, 1989.
12. The NIST Mass Spectral Search Program for the NIST/EPA/NIM Mass Spectral Library, version 1.7, build 11/05/1999.
13. Adams RP. *Identification of Essential Oil Components by Gas Chromatography/Mass Spectroscopy*. Allured: Carol Stream, IL, 1995.
14. Ubukata K, Itoh-Yamashita N, Konno M. *Antimicrob. Agents Chemother*. 1989; **33**: 1535–1539.
15. Gibbons S, Udo EE. *Phytother. Res*. 2000; **14**: 139–140.
16. Jean FI, Deslauriers H, Collin GJ *et al. J. Essent. Oil Res*. 1990; **2**: 37–44.
17. Beck JJ. *Diss. Abstr. Int. (B)* 1997; **57**: 4391.

Catechin Gallates Inhibit Multidrug Resistance (MDR) in *Staphylococcus aureus*

Simon Gibbons[1], Elisabeth Moser[1], Glenn W. Kaatz[2]

Abstract

Epicatechin gallate (**1**) and epigallocatechin gallate (**2**) were evaluated for their antibacterial and efflux inhibitory activity against a wild-type and three multidrug-resistant (MDR) strains of *Staphylococcus aureus.* Compound **2** was more active than **1** based on minimum inhibitory concentrations (MICs; 32 – 64 versus 64 – > 512 μg/mL, respectively). When incorporated into the growth medium at 20 μg/mL, both compounds exhibited a four-fold potentiation of the activity of norfloxacin against a norfloxacin-resistant strain of *S. aureus* overexpressing the NorA multidrug efflux pump. Against this strain **1** was moderately more potent than **2** as an inhibitor of ethidium efflux, but at $\leq$ 20 μM both compounds paradoxically stimulated efflux. This phenomenon has not been encountered previously in the analysis of inhibitors of multidrug efflux.

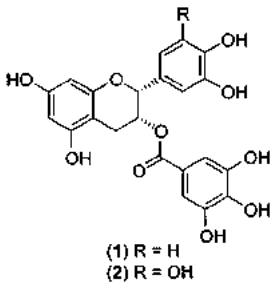

(1) R = H
(2) R = OH

Multidrug-resistance (MDR) is a phenomenon found in many species of bacteria, fungi and tumour cells [1]. In many cases membrane-based proteins are responsible and mediate the efflux of antibiotics and antitumour agents from cells, leading to a low and ineffective intracellular drug concentration [2]. MDR mechanisms recognise many structurally unrelated substrates and it is likely that they are naturally present as part of the detoxifying mechanisms in xenobiotic removal [3].

In clinical strains of *Staphylococcus aureus,* including those that are methicillin-resistant (MRSA), a number of efflux proteins have been described. These include the MsrA [4] and TetK [5] efflux mechanisms, which have a degree of specificity for certain macrolide and tetracycline antibiotics, respectively. The QacA [6] multidrug efflux protein has also been described which transports quaternary ammonium salts (antiseptics). The major characterised MDR efflux mechanism in *S. aureus* is the NorA protein which was originally characterised as effluxing norfloxacin, a member of the fluoroquinolone class of antibiotics [7]. Like QacA, the NorA transporter is a true MDR protein and recognises a wide array of structurally unrelated compounds as substrates. Inhibition of this mechanism would render resistant strains susceptible to substrate antibiotics and *in vivo* data have demonstrated that the use of an inhibitor and antibiotic in combination greatly reduces the rate of emergence of antibiotic resistant variants [8].

Previous work on the characterisation of natural product *Staphylococcal* resistance modifying agents has highlighted a variety of structurally unrelated compounds from several biosynthetic classes including flavones, flavonolignans, porphyrins, indole alkaloids, polyacylated neohesperidosides and diterpenes [9]. How these diverse compounds function as inhibitors is not clear, although it has been postulated that the MDR inhibitor reserpine binds to a hydrophobic region of the Bmr MDR transporter of *Bacillus subtilis* causing inhibition of efflux [10]. We recently conducted molecular modelling studies on the potential of complex formation between MDR inhibitors and drug substrates and have proposed that there is affinity between these two groups [11]. The formation of such complexes may facilitate entry of the drug into the cell and effectively cloak it from efflux by the MDR pump.

Much work has been conducted by the research group of Hamilton-Miller on the ability of epicatechin gallate (**1**) to reverse methicillin-resistance in MRSA [12], [13], [14]. Reversal of this resistance would render MRSA strains susceptible to the beta-lactam class of antibiotics. This natural product appears to act by inhibiting the synthesis of penicillin binding protein 2′ (PBP2′) and is selective in that it affects only *Staphylococci* that synthesise PBP2′. In the presence of a β-lactam antibiotic, **1** renders MRSA strains sensitive and an electron microscopy study has shown that **1** affects cell wall morphology of resistant strains whereas sensitive strains are unaffected. Compound **1** was also reported to be weakly bacteriostatic toward MRSA strains (MIC = 512 μg/mL) [13]. This resistance modifying activity prompted us to study the ability of **1** and the related tea catechin **2** to inhibit the growth of strains possessing MDR efflux mechanisms and as inhibitors of the NorA efflux protein.

MIC values of the test compounds are shown in Table **1**. The antibacterial activity of both **1** and **2** was similar to that of norfloxacin against SA-1199B, which overexpresses the NorA MDR efflux pump. Epigallocatechin gallate (**2**) was more active than epicatechin gallate (**1**) against the remaining tetracycline (XU212) and erythromycin (RN4220) effluxing strains and the standard ATCC strain. The difference in activity is quite marked for the slight difference in the presence of one additional hydroxy group on the B ring of the flavonoid nucleus in compound **2** compared to compound **1**. If the antibacterial target of these compounds is a pro-

Affiliation: [1] Centre for Pharmacognosy and Phytotherapy, The School of Pharmacy, University of London, London, U.K. · [2] Division of Infectious Diseases, Department of Internal Medicine, School of Medicine, Wayne State University and the John D. Dingell Department of Veterans Affairs Medical Center, Detroit, Michigan, U.S.A.

Correspondence: Dr. Simon Gibbons · Centre for Pharmacognosy and Phytotherapy · The School of Pharmacy · University of London · 29–39 Brunswick Square · London WC1N 1AX · U.K. · Phone: +44-207-753-5913 · Fax: +44-207-753-5909 · E-mail: simon.gibbons@ulsop.ac.uk

Received: March 26, 2004 · **Accepted:** July 10, 2004

Bibliography: Planta Med 2004; 70: 1240–1242 · © Georg Thieme Verlag KG Stuttgart · New York · DOI 10.1055/s-2004-835860 · ISSN 0032-0943

Table **1** Minimum inhibitory concentrations (in μg/mL) of catechin gallates and standard antibiotics. Efflux protein possessed by each strain is indicated

S. aureus strain	*Compound 1*	*Compound 2*	*Norfloxacin*	*Tetracycline*	*Erythromycin*
SA-1199B (NorA)	64	32	32	0.25	0.25
XU-212 (TetK)	> 512	64	8	128	> 512
RN4220 (MsrA)	256	64	2	0.25	128
ATCC 25923	> 512	32	2	0.5	0.25

tein then the presence of an additional phenolic OH group may be important for binding, although this could be offset by poor cellular absorption.

The ability of subinhibitory concentrations of **1** or **2** (20 μg/mL) to potentiate the activity of norfloxacin against SA-1199B was evaluated by their incorporation into Mueller-Hinton broth and measurement of the norfloxacin MIC. Both compounds potentiated the activity of norfloxacin by 4-fold. The MDR inhibitor reserpine was used as a positive control and at a concentration of 10 μg/mL resulted in an identical reduction in norfloxacin MIC (Table **2**).

Given that both compounds possess antibacterial activity, it was considered likely that the potentiation effects observed in combination with norfloxacin were the result of an additive antibacterial effect. We therefore assessed the ability of both compounds to inhibit efflux of ethidium bromide from cells with the NorA transporter (see Fig. **1**). We observed that both compounds were weak inhibitors of ethidium efflux with **1** being slightly more potent than **2**. The phenolic hydroxy group in the B ring of the catechin nucleus in **2** may result in reduced cellular uptake and thus a reduced ethidium efflux-inhibitory effect. Intriguingly, at low concentrations both compounds potentiated efflux and this phenomenon has not been reported before for a bacterial efflux system. Such a paradoxical effect on efflux may be the result of interaction of the catechins with high- and low-affinity binding sites on the NorA transporter. The high affinity sites, which would be occupied at low catechin concentrations, may augment the interaction of substrate with the transporter or even improve the kinetics of transport. There is precedence for such an effect in that certain natural products have been observed to activate calcium-activated potassium channels [15]. High catechin concentrations may inhibit efflux by interaction with low-affinity sites on NorA, which in turn reduces transport efficiency. Crystallisation of NorA in the presence of either catechin would be required to test this hypothesis.

Table **2** Susceptibility of SA-1199B to norfloxacin (in μg/mL) in the absence and presence of 20 μg/mL of **1**, **2,** or 10 μg/mL reserpine

No inhibitor	*1*	*2*	*Reserpine*
32	8	8	8

Given the ability of these compounds to inhibit the growth of MDR strains of *S. aureus*, the action of **1** as a methicillin-resistance reversing agent and their mild efflux inhibition properties, it seems to us that this class may have potential as drug leads. Enhancement of the lipophilicity of the catechin gallate skeleton, which is a key characteristic of good MDR inhibitors, would improve their cellular uptake but it is important that the antibacterial and methicillin reversal characteristics are conserved.

Materials and Methods

Epicatechin gallate (**1**) (98%, $[\alpha]_D^{24}$: –100°, *c*, 0.12, MeOH), epigallocatechin gallate (**2**) (95%, $[\alpha]_D^{24}$: –160°, *c*, 0.20, MeOH), tetracycline, norfloxacin, and erythromycin were obtained from Sigma Chemical Co., Poole, UK. ^{1}H-NMR spectra of **1** and **2** were recorded to prove identity and copies of spectra are available from the author on request. *S. aureus* RN4220 containing plasmid pUL5054, which carries the gene encoding the MsrA macrolide efflux protein, was provided by J. Cove [4]. Strain XU-212, which possesses the TetK tetracycline efflux protein, was provided by E. Udo [16]. SA-1199B, which overexpresses the *norA* gene encoding the NorA MDR efflux protein, has been described previously [17]. *S. aureus* ATCC 25923 was obtained from the American Type Culture Collection.

MICs were determined in triplicate by a broth microdilution technique according to NCCLS guidelines, using *S. aureus* ATCC 25923 as a quality control strain [18]. The effects of **1, 2** (20 μg/mL) and reserpine (10 μg/mL) on norfloxacin MIC also were de-

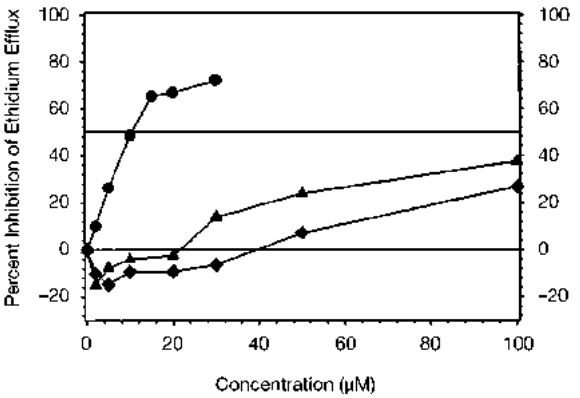

Fig. **1** Inhibition of ethidium efflux by catechin gallates. Reserpine was included for comparative purposes. Filled circles, reserpine; filled triangles, epicatechin gallate (**1**); filled diamonds, epigallocatechin gallate (**2**).

termined. These compounds were dissolved in DMSO before dilution into Mueller-Hinton broth for use in MIC determinations, and the highest concentration of DMSO remaining after dilution (2.5% [v/v]) caused no inhibition of bacterial growth (data not shown).

Ethidium bromide (EtBr) is a substrate for many Gram-positive MDR pumps, including NorA. The efficiency of efflux pumps for which EtBr is a substrate can be assessed fluorometrically by the loss of fluorescence over time from cells loaded with EtBr. SA-1199B was loaded with EtBr as previously described, and the effect of varying concentrations of **1**, **2** and reserpine on EtBr efflux was determined to generate a dose-response profile for each compound [19]. Results were expressed as percent reduction of the total efflux observed for test strains in the absence of inhibitors.

References

[1] Ling V. Multidrug resistance: molecular mechanisms and clinical relevance. Cancer Chemother Pharmacol 1997; 40 (Suppl): S3 – 8
[2] Bradley G, Ling V. P-glycoprotein, multidrug resistance and tumor progression. Cancer Metastasis Rev 1994; 13: 223 – 33
[3] Neyfakh AA. The ostensible paradox of multidrug recognition. J Mol Microbiol Biotechnol 2001; 3: 151 – 4
[4] Ross JI, Eady EA, Cove JH, Cunliffe WJ, Baumberg S, Wootton JC. Inducible erythromycin resistance in staphylococci is encoded by a member of the ATP-binding transport super-gene family. Mol Microbiol 1990; 4: 1207 – 14
[5] Guay GG, Khan SA, Rothstein DM. The *tet*(K) gene of plasmid pT181 of *Staphylococcus aureus* encodes an efflux protein that contains 14 transmembrane helices. Plasmid 1993; 30: 163 – 6
[6] Littlejohn TG, Paulsen IT, Gillespie MT, Tennent JM, Midgley M, Jones IG, Purewal AS, Skurray RA. Substrate specificity and energetics of antiseptic and disinfectant resistance in *Staphylococcus aureus*. FEMS Microbiol Lett 1992; 74: 259 – 65
[7] Ubukata K, Itoh-Yamashita N, Konno M. Cloning and expression of the *norA* gene for fluoroquinolone resistance in *Staphylococcus aureus*. Antimicrob Agents Chemother 1989; 33: 1535 – 9
[8] Markham PN, Westhaus E, Klyachko K, Johnson ME, Neyfakh AA. Multiple novel inhibitors of the NorA multidrug transporter of *Staphylococcus* aureus. Antimicrob Agents Chemother 1999; 43: 2404 – 8
[9] Gibbons S. Anti-staphylococcal plant natural products. Nat Prod Repts 2004; 21: 263 – 77
[10] Ahmed M, Borsch CM, Neyfakh AA, Schuldiner S. Mutants of the *Bacillus subtilis* multidrug transporter Bmr with altered sensitivity to the antihypertensive alkaloid reserpine. J Biol Chem 1993; 268: 11086 – 9
[11] Zloh M, Kaatz GW, Gibbons S. Inhibitors of Multidrug resistance (MDR) have affinity for MDR substrates. Bioorg Med Chem Lett 2004; 14: 881 – 5
[12] Yam TS, Hamilton-Miller JMT, Shah S. The effect of a component of tea (*Camellia sinensis*) on methicillin resistance, PBP2′ synthesis, and beta-lactamase production in *Staphylococcus aureus*. J Antimicrob Chemother 1998; 42: 211 – 6
[13] Hamilton-Miller JM, Shah S. Disorganization of cell division of methicillin-resistant *Staphylococcus aureus* by a component of tea (*Camellia sinensis*): a study by electron microscopy. FEMS Microbiol Lett 1999; 176: 463 – 9
[14] Hamilton-Miller JM, Shah S. Activity of the tea component epicatechin gallate and analogues against methicillin-resistant *Staphylococcus aureus*. J Antimicrob Chemother 2000; 46: 852 – 3
[15] Nardi A, Calederone V, Chericoni S. Natural modulators of large-conductance calcium-activated potassium channels. Planta Medica 2003; 69: 885 – 92
[16] Gibbons S, Udo EE. The effect of reserpine, a modulator of multidrug efflux pumps, on the *in-vitro* activity of tetracycline against clinical isolates of methicillin resistant *Staphylococcus aureus* (MRSA) possessing the *tet*(K) determinant. Phytother Res 2000; 14: 139 – 40
[17] Kaatz GW, Seo SM, Ruble CA. Efflux-mediated fluoroquinolone resistance in *Staphylococcus aureus*. Antimicrob Agents Chemother 1993; 37: 1086 – 94
[18] Jo B. National Committee for Clinical laboratory Standards, Methods for Dilution Antimicrobial Susceptibility Tests for Bacteria that Grow Aerobically. 1999; Fifth Edition Approved Standard M7-A5. NCCLS, Villanova, PA,
[19] Kaatz GW, Seo SM, O'Brien L, Wahiduzzaman M, Foster TJ. Evidence for the existence of a multidrug efflux transporter distinct from NorA in *Staphylococcus aureus*. Antimicrob Agents Chemother 2000; 44: 1404 – 6

Available online at www.sciencedirect.com
SCIENCE DIRECT
Bioorganic & Medicinal Chemistry Letters
Bioorganic & Medicinal Chemistry Letters 14 (2004) 881–885

Inhibitors of multidrug resistance (MDR) have affinity for MDR substrates

Mire Zloh,[a,*] Glenn W. Kaatz[b] and Simon Gibbons[c,*]

[a]*Department of Pharmaceutical and Biological Chemistry, The School of Pharmacy, University of London, 29–39 Brunswick Square, London WC1N 1AX, UK*
[b]*Division of Infectious Diseases, Department of Internal Medicine, School of Medicine, Wayne State University and the John D. Dingell Department of Veterans Affairs Medical Center, Detroit, MI 48201, USA*
[c]*Centre for Pharmacognosy and Phytotherapy, The School of Pharmacy, University of London, 29–39 Brunswick Square, London WC1N 1AX, UK*

Received 16 September 2003; revised 12 November 2003; accepted 3 December 2003

Abstract—Multidrug-resistance (MDR) occurs in many bacterial species and tumour cells. MDR functions by membrane proteins which export drugs from cells, resulting in a low ineffective concentration of the drug. We have shown by molecular modelling that inhibitors of MDR have affinity for substrates of MDR transporters. This affinity may facilitate drug entry into cells and a large inhibitor–drug complex may be a poorer substrate for the MDR mechanism. This complex would effectively 'cloak' the drug rendering it unavailable for efflux.

Multidrug-resistance (MDR) occurs in many bacteria, fungi and tumour cells[1] and this phenomenon is responsible for exporting drugs from cells, resulting in a low ineffective concentration of the drug.[2] A common feature of MDR mechanisms is their ability to recognise many structurally unrelated substrates[3] and remove them from the cell, and inhibitors of these transport processes are thought to act by directly binding to hydrophobic regions of MDR proteins causing inhibition of xenobiotic removal.[4] A number of these transporters have been characterised for mammalian cells including *p*-glycoprotein (*p*-gp)[2] and multidrug resistance related protein (MRP),[5] both of which confer resistance to cytotoxic agents. In Gram-positive and Gram-negative bacteria, MDR pumps such as NorA[6] (*Staphylococcus aureus*) and MexAB-OprM[7] (*Pseudomonas aeruginosa*) export a wide array of antiseptics and antibiotics including fluoroquinolones.

It is not known exactly how inhibitors of MDR transporters function but there are a few proposed mechanisms of action: direct binding of inhibitor to one or more binding sites on the protein therefore blocking transport as either competitive or non-competitive inhibitors,[2] depletion of pump energy by inhibiting binding of ATP and modifying protein conformation by an inhibitor interaction with the cell membrane.[8] There is indirect evidence by Ahmed et al.,[9] that reserpine does bind to a hydrophobic region of the Bmr MDR transporter of *Bacillus subtilis* causing inhibition of efflux.

It seemed possible to us that inhibitors of MDR may have an affinity for substrates and bind them to form a complex which may facilitate entry of the drug into the cell and also importantly from the perspective of MDR inhibition, this complex may not be recognised by the transporter. In the cell this complex could then dissociate to release inhibitor and drug. To investigate our hypothesis, we conducted a series of molecular modelling experiments to study the affinity that inhibitors of MDR phenomena have with MDR substrates.

The modelling work presented here was performed using ChemOffice 2002,[10] GRID 20,[11] Molden,[12] and Viewer Lite 5.0[13] software packages. In order to model the MDR inhibitors, antibiotics and anticancer drugs, molecular mechanical and semi-empirical theory were used. The structures of each molecule were initially drawn by ChemDraw. Each 2D structure was converted

Keywords: MDR; Multidrug-resistance; Molecular modelling; Mechanism; Bacteria; Tumour.
* Corresponding authors. Tel.: +44-20-7753-5879; fax: +44-20-7753-5964; (M.Z.); tel.: +44-20-7753-5913, fax: +44-20-7753-5909 (S.G.); e-mail: mire.zloh@ulsop.ac.uk; simon.gibbons@uslop.ac.uk

0960-894X/$ - see front matter © 2003 Elsevier Ltd. All rights reserved.
doi:10.1016/j.bmcl.2003.12.015

into 3D structure by Chem3D, followed by molecular mechanics minimization using MM2 force field. MM2 parameters used here are from the full MM2 Parameter Set including π-systems, as provided by N. L. Allinger and implemented in Chem3D.[10]

The resulting structures were further subjected to altered simulated annealing protocol consisting of 4 ps molecular dynamics at 300 K to explore conformational space. Five visibly different structures (not necessarily lowest energy conformations) for each molecule were chosen from the trajectory and subjected to 2 ps molecular dynamics at 100 K. The last structure in the trajectory was minimized using MM2 energy minimization and further optimized using MOPAC 2000 and the AM1 method. MM2 and Mopac 2000 were implemented in the Chem3D software. Semi-empirical AM1 geometries of MDR inhibitors and drugs were used as input files for GRID 20 software. The whole molecule was considered during calculations and all GRID parameters were kept at their default values. Inhibitor molecules were chosen to be target molecules during calculations, since those were generally larger than drug molecules. All interactions were examined by using GROUP probes implemented in GRID software representing relevant functional groups of drug molecules. All reported interaction energies were predicted using GRID20 software.

This study was conducted on inhibitors of *p*-glycoprotein mediated MDR and between cytotoxic drugs which are substrates of this mechanism (Table 1). Additionally, inhibitors of bacterial MDR in combination with fluoroquinolone antibiotics, some of which are substrates for the bacterial MDR efflux systems NorA and MexAB–OprM, were also studied (Table 1). We have examined pairs of MDR inhibitor–drug (substrate) which have experimental data showing that the inhibitor restores activity of the drug.[14–24]

For inhibitors which showed reversal of MDR, the energy of interaction of the drug with corresponding inhibitor was calculated by GRID 20 software as negative and greater than −10 kcal/mol, which indicated that it was highly likely that these pairs have the ability to form a complex. Table 1 shows the energy of interaction for a wide range of MDR inhibitor–drug complexes and to highlight these findings, below we discuss selected examples from the anticancer and antibacterial fields of MDR.

Specifically, the anticancer drugs doxorubicin and vinblastine were shown to bind to reserpine (Fig. 1a and b) at the same moiety of the reserpine molecule, notably the A, B and C-rings, although the mode of binding of these two drugs to reserpine is different. In the case of doxorubicin, an interaction was observed between its aromatic rings and those of the inhibitor, whilst in the case of the vinblastine–reserpine complex, the aromatic region of reserpine fitted into the curvature of the vinblastine molecule (Fig. 1b) being perpendicular to the aromatic rings of vinblastine. In both cases the energy of interactions are comparable.

For the inhibitor GG918, four combinations with the cytotoxic drugs doxorubicin, topotecan, mitoxantrone and vinblastine were studied. For all of these complexes, the cytotoxic drug bound to the middle portion of GG918, which links the acridone and isoquinoline moieties, and the interaction appears to be non-specific, with topotecan (Fig. 1c) having the highest energy of interaction (Table 1). Drug–inhibitor complex pairs represented here have the highest energy of interaction and it must be noted that a range of other complex conformations were detected. Although the position of the drug with respect to inhibitor is different, most significantly, the same part of the inhibitor is involved in all complexes, even with different drugs.

This non-specificity of interaction possibly enables the MDR inhibitor to recognise and bind a wide array of structurally unrelated drugs and to restore their efficacy.

α-Tocopherol, which has been shown to reverse the effects of MDR inhibitors,[16] has a higher energy of interaction with MDR inhibitors than substrates (−19.06 kcal/mol with GG918). Furthermore, it binds to the same portion of the inhibitor as the substrates (Fig. 1d) suggesting that it may function by preferentially binding to the inhibitor and therefore preventing the formation of an inhibitor–drug complex.

Four inhibitors of bacterial MDR were chosen with fluoroquinolones as efflux substrates. Two of these, reserpine and GG918 have been shown to be inhibitors of Gram-positive MDR transporters such as the *S. aureus* NorA system.[17] The last two, MC-002,595 and MC-207,110 are inhibitors of the MexAB–OprM and AcrAB–TolC MDR efflux mechanisms found in Gram-negative species.[18]

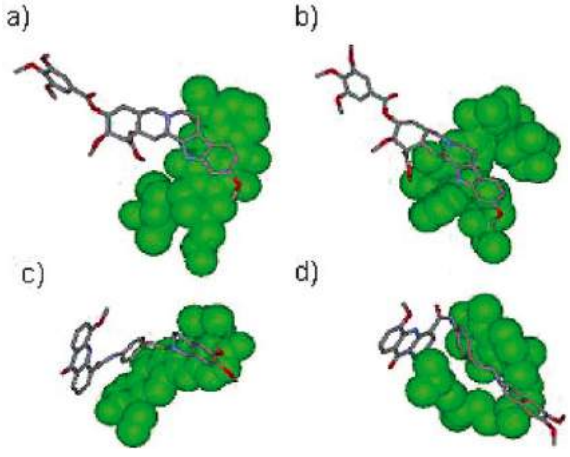

Figure 1. Highest interaction energy complexes between MDR inhibitors and ligand molecules (ligand molecules are represented in green): (a) binding between A, B and C rings of reserpine and doxorubicin, indicating π–π stacking between aromatic moieties of the two molecules; (b) reserpine and vinblastine interaction depicting the aromatic region of reserpine fitting into the curvature of the vinblastine molecule. The A, B and C rings of reserpine are perpendicular to the aromatic rings of vinblastine; (c) GG918 and topotecan complex; (d) GG918 and α-tocopherol complex depicting the position of the ligand molecule binding strongly to the binding site for substrates.

In all cases of the reserpine–fluoroquinolone antimicrobial agent complexes, the binding site is the same for that as the anticancer drugs, being binding to the first three rings of the reserpine structure as demonstrated in Figure 2a for the norfloxacin–reserpine complex. Again all energies of interaction were comparable, although modes of binding were not the same. For GG918, the binding site of the fluoroquinolones to the inhibitor is also the same region as that for the anticancer drugs as represented in Figure 2b

Table 1. Interaction energies between different drugs and MDR inhibitors calculated by GRID 20 software in correlation with the reported MDR inhibition

Drug	MDR Inhibitor	Inhibition	Interaction energy (kcal/mol)
Doxorubicin	Reserpine	2.9[a,14]	−12.01
Vinblastine	Reserpine	8.0[a,14]	−11.63
Mitoxantrone	GG918	1.2–1850[b,15]	−13.02
Topotecan	GG918	1.0–23[b,15]	−16.15
Doxorubicin	GG918	~58% reduction[c,16]	−13.42
Vinblastine	GG918	~95% reduction[c,16]	−15.89
α-Tocopherol	GG918	Reversal of MDR inhibition[16]	−19.06
Norfloxacin	Reserpine	4[d,17]	−13.29
Ciprofloxacin	Reserpine	8[d,17]	−12.94
Levofloxacin	Reserpine	2[d,17]	−13.32
Moxifloxacin	Reserpine	2[d,17]	−12.95
Norfloxacin	GG918	8[d,17]	−13.57
Ciprofloxacin	GG918	8[d,17]	−13.94
Levofloxacin	GG918	2[d,17]	−15.24
Moxifloxacin	GG918	0[d,17]	−14.58
NPN	MC-002,595	2.3[e,18]	−12.97
Levofloxacin	MC-207,110	2–64[f,18]	−13.75
Vincristine	JTV-519	3.7[g,19]	−15.05
Taxol	JTV-519	24.8[g,19]	−13.18
Etoposide (VP-16)	JTV-519	2.6[g,19]	−13.18
Doxorubicin	JTV-519	2.7[g,19]	−15.59
Actinomycin D	JTV-519	3[g,19]	−12.15
STI571	JTV-519	3.1[g,19]	−13.10
Taxol	VX-710	Successful in clinical trial[20]	−10.64
Daunorubicin	XR-9576	IC_{50} = 38.18 nM[21]	−14.98
Vincristine	Sinensetin	72.28[h,22]	−10.1
Doxorubicin	Indomethacin	0.251/NA[i,23]	−18.60
Doxorubicin	Sulindac	0.368/0.449[i,23]	−15.23
Doxorubicin	Tolmetin	0.357/0.467[i,23]	−13.05
Vincristine	Indomethacin	0.301/NA[i,23]	−16.66
Vincristine	Sulindac	0.462/0.241[i,23]	−16.10
Vincristine	Tolmetin	NA/0.593[i,23]	−15.73
Etoposide	Indomethacin	0.916/0.534[i,23]	−15.50
Etoposide	Sulindac	0.681/0.463[i,23]	−15.02
Etoposide	Tolmetin	NA/0.745[i,23]	−12.58
Taxol	Indomethacin	2.234/1.227[i,23]	−12.90
Taxol	Sulindac	1.539/1.233[i,23]	−12.43
Taxol	Tolmetin	1.349/NA[i,23]	−9.18
Doxorubicin	Tetrandrine	5.4–20.4[j,23]	−12.89
Doxorubicin	Verapamil	~33% reduction[c,16]	−12.73
Vinblastine	Verapamil	~88% reduction[c,16]	−12.53
α-Tocopherol	Verapamil	Reversal of inhibition[16]	−15.39
Doxorubicin	Clofazimine	~40% reduction[c,16]	−23.70
Vinblastine	Clofazimine	~94% reduction[c,16]	−20.25
α-Tocopherol	Clofazimine	Reversal of inhibition[16]	−29.55
Doxorubicin	B669	~31% reduction[c,16]	−20.59
Vinblastine	B669	~95% reduction[c,16]	−17.94
α-Tocopherol	B669	Reversal of inhibition[16]	−20.80
Doxorubicin	α-Tocopherol	0% reduction[c,16]	−13.64
Vinblastine	α-Tocopherol	0% reduction[c,16]	−14.24
Norfloxacin	Agent from *Lycopus europeus*	No inhibitory activity[25]	−8.51

[a] Fold increase, IC_{50} for drug alone/IC_{50} for drug in the presence of inhibitor.
[b] DMF, dose modifying factor defines as the IC_{50} for the chemotherapy drug without GG918 divide by IC_{50} with GG918.
[c] Approximate percentage for the level of inhibition of cell growth in the presence of cytotoxic drug in the presence and absence of inhibitor using H69/LX4 cells. This was calculated using the percentage growth value of inhibitor + drug divided by the value for drug.
[d] Fold reduction in minimum inhibitory concentration (MIC) of antibiotic in the presence of inhibitor.
[e] Fold reduction in fluorescence in presence of inhibitor (128 μg/mL) compared to absence of inhibitor.
[f] Ratio between the MIC without efflux pump inhibitor (EPI) and the MIC in the presence of a potentiating concentration of EPI.
[g] Relative resistance determined by dividing the IC_{50} values of drugs with or without the inhibitors by that without the reversing agents.
[h] Chemosensitizing index IC_{50} (vincristine)/IC_{50} (vincristine + inhibitor).
[i] Combination index (CI) values, a quantitative measure of drug interaction in terms of an additive (CI = 1), synergistic (CI < 1) or antagonistic (CI > 1) effect. Values quoted for two different cell lines (A549/DLKP). NA is not available.
[j] Fold-reversal, ratio of the IC_{50} for doxorubicin alone versus the IC_{50} for doxorubicin in the presence of the modulating agent.

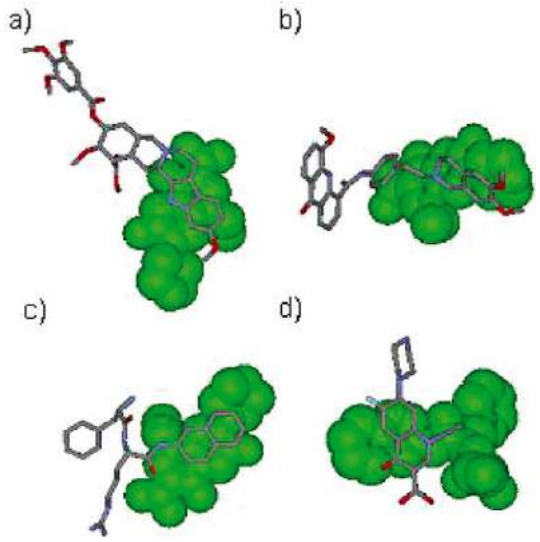

Figure 2. Highest interaction energy complexes between MDR inhibitors and substrates for bacterial MDR (substrate molecules are represented in green): (a) reserpine strongly binds norfloxacin at the same binding site for anticancer drugs, namely rings A, B and C; (b) binding site of GG918 for norfloxacin is the same as for the topotecan complex; (c) the aromatic moiety of the MC-207,110 strongly binds the antibiotic levofloxacin and (d) the interaction between MC-002,595 and NPN involves π–π stacking of the aromatic rings.

for the GG918-norfloxacin complex, and energies of interactions are given in Table 1. Interestingly, a recently isolated plant natural product from *Lycopus europaeus*,[25] which did not modulate the activity of norfloxacin and therefore is not an inhibitor of NorA in *S. aureus,* showed a low energy of interaction with norfloxacin (−8.51 kcal/mol). Whilst this compound possesses similar lipophilic properties to reserpine, it is a non-aromatic highly chiral non-planar compound, which may account for its low predicted interaction with aromatic planar achiral norfloxacin. This would again support the importance of complex formation between MDR inhibitor and drug for reversal of MDR.

The inhibitors of the MexAB–OprM and AcrAB–TolC MDR transporters, MC-207,110 and MC-002,595, have a similar binding site for all fluoroquinolones investigated, being the quinoline portion of the molecule. In Fig 2c and d, complexes between MC-207,110 and levofloxacin, and MC-002,595 and NPN (*N*-phenylnaphthylamine, a fluorescent substrate for the AcrAB–TolC mechanism), are shown. Interaction energies are within the range of 1 kcal/mol for both substrate–inhibitor complexes investigated. Again, as in the previous case, each inhibitor bound the substrate at the same site on the inhibitor but with a different portion of each substrate.

Interestingly, the Gram-positive bacterial MDR inhibitors reserpine and GG918 do not inhibit Gram-negative pumps such as MexAB–OprM and this has been explained as being presumably due to differences in cell wall architecture. Looking at the structures of MC-002,595 and MC-207,110, both inhibitors possess lipophilic regions which are probably important for complex formation and transport into the membrane, and hydrophilic moieties (which are lacking in reserpine and GG918) such as the two primary amine groups. These may be important in facilitating transport of the complex across the hydrophilic domain of the periplasmic space, which is present between the two membranes of Gram-negative bacteria.

At the present time, we cannot correlate the predicted energy of interaction with inhibitory potential due to the fact that the experimental efflux/modulation results come from different in vivo and in vitro studies, and the levels of MDR inhibition were not reported explicitly or were reported using different criteria. We propose three empirical correlations:

1. A low predicted interaction energy (< -9 kcal/mol) results in absence of MDR inhibition.
2. Optimal predicted interaction energy for MDR inhibition is generally greater than −10 kcal/mol. The exception is combinations of taxol and inhibitors (sulindac, tolmetin and indomethacin) where interaction energies were between −9 and −13 kcal/mol, but MDR inhibition was not detected in the experimental studies.[23] However, these interaction energies are lower than interaction energies between other drugs and the same set of MDR inhibitors in that study.[23]
3. A high interaction energy between non-drug molecule and inhibitor molecule results in reversal of MDR inhibition.

Our results lead to the conclusion that it is highly likely that inhibitors of MDR have affinity for substrates of efflux transporters, and that they may form complexes which could have a number of roles in the mechanism of MDR inhibition. These complexes may facilitate entry of drugs into the cell and secondly the drug in such a complex may be hidden from MDR transporters. The structural moieties which are present in many MDR inhibitors have been described[26] and some of these, notably quinoline and benzyl moieties are found in the drug-binding sites of MDR inhibitors in this study for example GG918 and MC-002,595.

This study may change the perception of MDR inhibition and open further research to find compounds which have good drug-binding capabilities and readily form complexes whilst retaining features which enhance membrane permeability and imperviousness to efflux.

References and notes

1. Ling, V. *Cancer Chemotherapy and Pharmacology* **1997**, *40* (Suppl), S3.
2. Bradley, G.; Ling, V. *Cancer Metastasis Rev.* **1994**, *13*, 223.
3. Neyfakh, A. A. J. *Mol. Microbiol. Biotechnol.* **2001**, *3*, 151.
4. Neyfakh, A. A. *Molecular Microbiology* **2002**, *44*, 1123.
5. Cole, S. P. C.; Bhardwaj, G.; Gerlach, J. H.; Mackie, J. E.; Grant, C. E.; Almquist, K. C.; Stewart, A. J.; Kurz, E. U.; Duncan, A. M. V.; Deeley, R. G. *Science* **1992**, *258*, 1650.
6. Ubukata, K.; Itoh-Yamashita, N.; Konno, M. *Antimicrob. Agents Chemother.* **1989**, *33*, 1535.

7. Li, X. Z.; Nikaido, H.; Poole, K. *Antimicrob. Agents Chemother*. **1995**, *39*, 1948.
8. Ambudkar, S. V.; Dey, S.; Hrycyna, C. A.; Ranmachandra, M.; Pastan, I.; Gottesman, M. M. *Annu. Rev. Pharmacol. Toxicol*. **1999**, *39*, 361.
9. Ahmed, M.; Borsch, C. M.; Neyfakh, A. A.; Schuldiner, S. *J. Biol. Chem*. **1993**, *268*, 11086.
10. ChemOffice Ultra 2002: CambridgeSoft, 2001.
11. Goodford, P. J. *J. Med. Chem*. **1985**, *28*, 849.
12. Schaftenaar, G.; Noordik, J. H. *J. Comput.-Aid. Mol. Des*. **2000**, *14*, 123.
13. ViewerLite 5.0, Accelerys Inc, 2002.
14. Bhat, U. G.; Winter, M. A.; Pearce, H. L.; Beck, W. T. *Mol. Pharmacol*. **1995**, *48*, 682.
15. de Bruin, M.; Miyake, K.; Litman, T.; Robey, R.; Bates, S. E. *Cancer Lett*. **1999**, *146*, 117.
16. Van Rensburg, C. E. J.; Joone, G.; Anderson, R. *Cancer Lett*. **1998**, *127*, 107.
17. Gibbons, S.; Oluwatuyi, M.; Kaatz, G. W. *Journal of Antimicrobial Chemotherapy* **2003**, *51*, 13.
18. Lomovskaya, O.; Warren, M. S.; Lee, A.; Galazzo, J.; Fronko, R.; Lee, M.; Blais, J.; Cho, D.; Chamberland, S.; Renau, T.; Leger, R.; Hecker, S.; Watkins, S.; Hoshino, K.; Ishida, H.; Lee, V. J. *Antimicrob. Agents Chemother*. **2001**, *45*, 105.
19. Chea, X. F.; Nakajimaa, Y.; Sumizawaa, T.; Ikedaa, R.; Rena, X. Q.; Zhenga, C. L.; Mukaia, M.; Furukawaa, T.; Haraguchia, M.; Gaoa, H.; Sugimotob, Y.; Akiyamaa, S. *Cancer Lett*. **2002**, *187*, 111.
20. Seiden, M. V.; Swenerton, K. D.; Matulonis, U.; Campos, S.; Rose, P.; Batist, G.; Ette, E.; Garg, V.; Fuller, A.; Harding, M. W.; Charpentier, D. *Gynecologic Oncology* **2002**, *86*, 302.
21. Roe, M.; Folkes, A.; Ashworth, P.; Brumwell, J.; Chima, L.; Hunjan, S.; Pretswell, I.; Dangerfield, W.; Ryder, H.; Charlton, P. *Bioorg. Med. Chem. Lett*. **1999**, *9*, 595.
22. Choi, C. H.; Sun, K. H.; An, C. S.; Yoo, J. C.; Hahm, K. S.; Lee, I. H.; Sohng, J. K.; Kim, Y. C. *Biochemical and Biophysical Research Communications* **2002**, *295*, 832.
23. Duffy, C. P.; Elliott, C. J.; O'Connor, R. A.; Heenan, M. M.; Coyle, S.; Cleary, I. M.; Kavanagh, K.; Verhaegen, S.; O'Loughlin, C. M.; NicAmhlaoibh, R.; Clynes, M. *Eur. J. Cancer* **1998**, *34*, 1250.
24. Fua, L. W.; Zhangb, Y. M.; Lianga, Y. J.; Yanga, X. P.; Pana, Q. C. *Eur. J. Cancer* **2002**, *38*, 418.
25. Gibbons, S.; Oluwatuyi, M.; Veitch, N. C.; Gray, A. I. *Phytochemistry* **2003**, *62*, 83.
26. Klopman, G.; Shi, L. M.; Ramu, A. *Mol. Pharmacol*. **1997**, *52*, 323.

PERGAMON

Phytochemistry 62 (2003) 83–87

PHYTOCHEMISTRY

www.elsevier.com/locate/phytochem

Bacterial resistance modifying agents from *Lycopus europaeus*

Simon Gibbons[a,*], Moyosoluwa Oluwatuyi[a], Nigel C. Veitch[b], Alexander I. Gray[c]

[a]*Centre for Pharmacognosy and Phytotherapy, The School of Pharmacy, University of London, 29–39 Brunswick Square, London WC1N 1AX, UK*

[b]*Jodrell Laboratory, Royal Botanic Gardens, Kew, Richmond, Surrey TW9 3DS, UK*

[c]*Department of Pharmaceutical Sciences, University of Strathclyde, 27 Taylor Street, Glasgow G2 0NR, UK*

Received 31 July 2002; accepted 12 September 2002

Abstract

As part of an ongoing project to identify plant natural products which modulate bacterial multidrug resistance (MDR), bioassay-guided isolation of an extract of *Lycopus europaeus* yielded two new isopimarane diterpenes, namely methyl-1α-acetoxy-7α 14α-dihydroxy-8,15-isopimaradien-18-oate (**1**) and methyl-1α,14α-diacetoxy-7α-hydroxy-8,15-isopimaradien-18-oate (**2**). The structures were established by spectroscopic methods. These compounds and several known diterpenes were tested for in vitro antibacterial and resistance modifying activity against strains of *Staphylococcus aureus* possessing the Tet(K), Msr(A), and Nor(A) multidrug resistance efflux mechanisms. At 512 μg/ml none of the compounds displayed any antibacterial activity but individually in combination with tetracycline and erythromycin, a two-fold potentiation of the activities of these antibiotics was observed against two strains of *S. aureus* that were highly resistant to these agents due to the presence of the multidrug efflux mechanisms Tet(K) (tetracycline resistance) and Msr(A) (macrolide resistance).

Keywords: Lamiaceae; *Lycopus europaeus*; *Staphylococcus aureus*; Multidrug resistance; MDR; Modulation; Isopimarane diterpenes

1. Introduction

Methicillin-resistant *Staphylococcus aureus* (MRSA) is one of the major causes of nosocomial infections and until recently, all strains of MRSA were susceptible to the glycopeptides, such as vancomycin; however, intermediate resistance to this antibiotic has been reported (Sieradzki et al., 1999). Whilst new anti-staphylococcal agents such as linezolid offer some respite, resistance to this agent has been reported in vancomycin-resistant *Enterococcus faecium* (Gonzales et al., 2001) and it is likely that this pattern will emerge in the staphylococci. MRSA strains produce a series of multidrug resistance (MDR) efflux pumps such as Tet(K), Msr(A), Nor(A) and Qac(A) which confer resistance to a wide range of structurally unrelated antibiotics and antiseptics (Marshall and Piddock, 1997). These MDR pumps are part of an array of cytoplasmic membrane transport systems involved primarily in the uptake of essential nutrients, the excretion of toxic compounds and the maintenance of cellular homeostasis (Paulsen et al., 1996).

In a continuing project to identify plant natural products that modify bacterial resistance in MRSA, we screened an extract from *Lycopus europaeus* L. (Lamiaceae), which in combination with either tetracycline or erythromycin reduced the minimum inhibitory concentrations (MICs) of these antibiotics against two strains of *S. aureus* possessing multidrug efflux pumps. *L. europaeus*, commonly known as Gipsywort in Britain, is a native perennial of river and canal banks (Philips, 1977) and is known to have anti-thyreotropic and anti-gonadotropic activities, which are attributed to phenolic compounds (Bucar and Kartnig, 1995). Previous phytochemical studies on the constituents of this species have focused on isopimarane type diterpenoids (Jeremic et al., 1985) and straight chain aliphatic precursors of cyclic diterpenes (Hussein and Rodriguez, 2000).

This paper deals with the isolation and structure elucidation of two new and four known compounds and their bacterial resistance modifying activity.

* Corresponding author. Tel.: +44-207-7535913; fax: +44-207-7535909.

E-mail address: simon.gibbons@ulsop.ac.uk (S. Gibbons).

0031-9422/03/$ - see front matter © 2003 Elsevier Science Ltd. All rights reserved.
PII: S0031-9422(02)00446-6

Table 1
^1H (400MHz) and ^{13}C NMR (100 MHz) spectral data for **1** and **2** in $CDCl_3$

Position	**1**		**2**	
	^1H (*J* in Hz)	^{13}C	^1H (*J* in Hz)	^{13}C
1	4.90 *t* (3.0)	72.9	4.84 *t* (2.8)	72.8
2	1.88 *m*	21.7	1.85 *m*	21.7
3	1.45 *m*	30.0	1.37 *m*	29.9
4		46.5		46.5
5	2.84 *dd* (13.2, 1.8)	35.0	2.80 *dd* (12.8, 1.6)	34.8
6	1.45, 1.83 *m*	29.6	1.37, 1.65 *m*	29.5
7	4.16 *br d* (3.5)	68.2	3.87 *br s*	66.8
8		130.2		128.4
9		142.3		144.6
10		42.0		42.3
11	1.82, 1.95 *m*	20.0	1.82, 1.95 *m*	20.1
12	1.45, 1.72 *m*	30.7	1.46, 1.66 *m*	31.4
13		39.9		39.3
14	3.87 *br s*	78.3	5.31 *s*	79.0
15	6.00 *dd* (18.5, 10.6)	142.2	5.90 *dd* (18.0, 11.2)	141.5
16	5.10 *dd* (10.6, 1.2)	114.6	4.98 *dd* (11.2, 0.8)	
	5.15 *dd* (18.5, 1.2)		4.99 *dd* (18.0, 0.8)	113.8
17	1.02 *s*	23.2	0.89 *s*	23.4
18		178.1		178.1
19	1.24 *s*	16.6	1.17 *s*	16.6
20	1.05 *s*	18.8	0.99 *s*	18.8
OAc	2.08 *s*	21.3, 170.7	2.02, 2.00 *s*	21.3, 21.3, 171.1, 170.7
OMe	3.71 *s*	52.2	3.64 *s*	52.2
OH	3.00 *br s*, 3.16 *br s*		2.11 *br s*	

2. Results and discussion

By VLC and reverse phase preparative HPLC compound (**1**) was isolated as a colourless crystalline solid. Accurate FAB-MS indicated a molecular formula of $C_{23}H_{34}O_6$ and characteristic signals in the ^1H NMR spectrum for one acetyl group (δ_H 2.08, s) and one methoxyl substituent (δ_H 3.71, s) suggested that (**1**) was a diterpene. Further signals in the ^1H and ^{13}C spectra (Table 1) for three tertiary methyl singlets [δ_H 1.02 (3H-17), 1.24 (3H-19) and 1.05 (3H-20)], an olefin (δ_H 6.00, H-15, dd, $J = 18.5$, 10.6 Hz), an exocyclic methylene (δ_H 5.10 and 5.15, 2H) and two additional olefinic carbons (δ_C 130.2, C-8, 142.3, C-9; Table 1) were typical of isopimarane diterpenes which have been previously isolated from this species (Hussein et al., 1999; Hussein and Rodriguez, 2000).

HMBC (Table 2) and COSY spectra were acquired to identify long-range ^1H–^{13}C and ^1H–^1H connectivities respectively. In the HMBC spectrum, methyl H-19 exhibited a ^2J correlation to C-4 and ^3J correlations to C-3, C-5 and to the carbonyl carbon of C-18 (δ_C 178.1). The methoxyl protons at δ_H 3.71 also showed a ^3J correlation to the C-18 carbonyl, indicating the presence of a methyl ester at C-18, which is a common feature of *Lycopus* diterpenes (Hussein et al., 1999). The proton attached to C-5 (δ_H 2.84, 1H, dd, $J = 13.2$, 1.8 Hz) showed a COSY correlation to H_2-6 (δ_H 1.45, 1.83, 2H, m) which further correlated to an oxymethine proton (H-7, 4.16, br d, $J = 3.5$ Hz) which in the HMBC spectrum, showed correlations to two olefinic carbons (C-8 and C-9). This C-9 carbon was correlated with the C-20 methyl, which exhibited additional correlations to C-10 (^2J), C-5 and C-1 (^3J). A proton attached to the carbon at C-1 was deshielded with respect to H-7 (δ_H 4.90, t, $J = 3.0$ Hz) and exhibited a ^3J correlation to a carbonyl carbon of the acetate group indicating that the acetate group should be placed at C-1. Further signals in the HMBC, COSY and DEPT-135 spectra of **1** showed correlations from H-1 to C-3 (CH_2) and H-1 to a methylene of C-2 indicating the presence of methylene groups at C-2 and C-3 and completing the A and B rings of the diterpene nucleus.

Methyl-17 displayed a correlation to a quaternary carbon (C-13, ^2J) and ^3J correlations to a methylene

Table 2
Long-range ^1H-^{13}C connectivities detected in HMBC experiments for **1** and **2**

Position	**1** Correlated C-atom HMBC (H→C)		**2** Correlated C-atom HMBC (H→C)	
	^2J	^3J	^2J	^3J
1	C-10	C-3, C-5, C=O		C-3, C-5
2	C-1	C-4		
3				
5	C-4, C-10	C-3, C-7, C-9, C-18, C-19, C-20	C-4, C-10	C-3, C-7, C-9, C-18, C-19, C-20
6	C-7	C-10	C-7	C-4, C-10
7	C-8	C-5, C-9		
11	C-9, C-12	C-8, C-13		C-8, C-10
12	C-11, C-13	C-15, C-17	C-13	C-9, C-14, C-15, C-17
14	C-8, C-13	C-9/C-15, C-17	C-8, C-13	C-9, C-12, C-15, C-17, C=O
15	C-13	C-12, C-14, C-17	C-13	C-14, C-17
16	C-15	C-13	C-15	C-13
17	C-13	C-12, C-14, C-15	C-13	C-12, C-14, C-15
19	C-4	C-3, C-5, C-18	C-4	C-3, C-5, C-18
20	C-10	C-1, C-5, C-9	C-10	C-1, C-5, C-9
OAc	C=O		C=O	
OMe		C-18		C-18

(C-12), an oxygenated methine carbon of C-14 ($\delta_C = 78.3$) and to an olefinic carbon (C-15, 142.2) whose attached proton coupled to the exocyclic methylene group in the COSY spectrum. Couplings between C-12 methylene and the allylic C-11 methylene in the COSY spectrum and ^2J and ^3J correlations between H_2-11 and C-9 and C-8 in the HMBC spectrum completed the isopimarane skeleton. From the molecular formula and the ^1H and ^{13}C chemical shifts of C-7 and C-14, hydroxyl groups must be placed at these positions. This was supported by the presence of two broad singlets (δ 3.00, 3.16) which are attributed to hydroxyl protons.

The relative stereochemistry of (**1**) was established by inspection of ^1H and NOESY spectra. The magnitude of the observed coupling constants for H-1 ($J = 3.0$ Hz) and H-7 ($J = 3.2$ Hz) indicated an equatorial (β) orientation for these protons and therefore that the acetate and hydroxyl groups at these positions be axial (α). In the NOESY spectrum a through-space interaction between H-7 and H-14 indicated that they were on the same face of the molecule (Fig. 1) and that the hydroxyl group at C-14 should also be axial (α). This was supported by a NOESY correlation between the proton at H-14 and methyl-17 indicating that they are on the same face and are both β. This is in agreement with the stereochemistry of related compounds isolated from this plant (Hussein et al., 1999). Compound (**1**) is therefore assigned as methyl-1α-acetoxy-7α,14α-dihydroxy-8,15-isopimaradien-18-oate.

By accurate FAB-MS, compound (**2**) solved for a molecular formula of $C_{25}H_{36}O_7$ and signals in the ^1H and ^{13}C NMR spectra were almost identical to those of (**1**) (Table 1) but with the presence of an additional acetate group. With respect to compound (**1**), H-14 (δ_H 5.31) was downfield shifted by 1.44 ppm indicating that esterification by the acetate had taken place at this position. This was corroborated by examination of the HMBC spectrum, which showed a correlation between H-14 and the carbonyl group of the acetate. Full HMBC analysis again led to the placement of acetate at C-1, and hydroxyl at C-7 of the isopimarane nucleus. The stereochemistry of (**2**) was identical to that of (**1**) with H-1 displaying a small coupling to H_2-2 (δ_H 4.84, $J = 2.8$ Hz), implying an equatorial (α) orientation for H-1. H-7 was a broad singlet and did not display any discernable coupling to H_2-6. As with compound (**1**), a NOESY experiment again showed correlations between H-7 and H-14 and between H-14 and methyl-17 indicating that compound (**2**) is methyl-1α,14α-diacetoxy-7α-hydroxy-8,15-isopimaradien-18-oate.

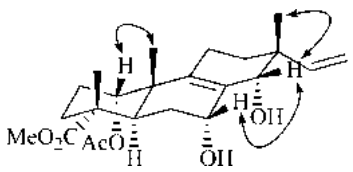

Fig. 1. Selected NOE connectivities for compound **1**.

Four additional compounds (**3**–**6**) were also isolated from the hexane extract and were identical to those isolated previously from *L. europaeus* on comparison of their ^1H and ^{13}C data with that published (Hussein et al., 1999; Hussein and Rodriguez, 2000). Compound **6** has previously been isolated from *Geigeria* species and data is in close agreement with that published (Bohlmann et al., 1982).

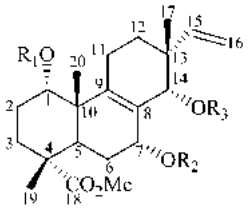

1 $R_1 = Ac$, $R_2 = R_3 = H$
2 $R_1 = R_3 = Ac$, $R_2 = H$
3 $R_1 = R_2 = R_3 = Ac$
4 $R_1 = R_2 = Ac$, $R_3 = H$

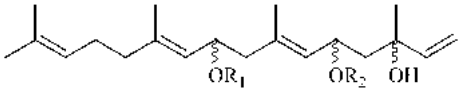

5 $R_1 = R_2 = H$
6 $R_1 = R_2 = Ac$

Compounds **1**–**6** showed no antibacterial activity at 512 μg/ml against any of the MDR strains of *S. aureus*. When each of the diterpenes were incorporated into the growth medium at low concentration (10 μg/ml), a two fold reduction in the MICs of tetracycline and erythromycin was observed against two strains which possessed the tetracycline Tet(K) and macrolide Msr(A) MDR efflux transporters respectively (Table 3). Surprisingly, there were no differences in activities of these diterpenes, despite the obvious structural differences between the groups **1**–**4** and **5** and **6**. These compounds modulated the activities of the antibiotics by halving the concentration of antibiotic needed to inhibit the growth of the drug resistant bacteria. Interestingly, no resistance

Table 3
MICs of test strains in the absence and presence of **1**–**6**[a] and reserpine

Strain (MDR efflux protein)	Tetracycline	Erythromycin	Norfloxacin[b]
IS-58 (TetK)	128, 64, **32**[c]	–	–
RN4220 (MsrA)	–	256, 128, **256**	–
SA-1199B (NorA)	–	–	32, 32, **2**

[a] 10 μg/ml. All MICs were determined in duplicate.
[b] MICs in the absence and presence of **1**–**6** are expressed in μg/ml.
[c] Figures in bold denote MICs in the presence of reserpine at 20 μg/ml.

modifying activity was observed against a strain possessing the Nor(A) efflux system, the major MDR transporter in *S. aureus*. The MDR inhibitor reserpine (Beck et al., 1988) caused a four-fold reduction in the MIC of tetracycline against the tetracycline-resistant strain and an eight-fold reduction in the MIC of norfloxacin against the fluoroquinolone (Nor(A)) resistant strain. Reserpine did not however affect the MIC of erythromycin against the erythromycin-resistant (Msr(A) producing) strain.

Previously discovered modulators of MDR in *S. aureus* have been described for strains possessing the Nor(A) efflux mechanism. These compounds are from many structural classes, including natural products such as flavonolignans, flavones and porphyrins (Stermitz et al., 2000a, b) and synthetic naphthylamides (Markham et al., 1999). A common feature of all of these resistance modifying agents is however, a high degree of lipophilicity which is also apparent in compounds **1**–**6**. This property is presumably important for interaction with the efflux proteins which are membrane bound. Further work is underway to find more potent and broad spectrum alternatives to counter the wide array of multidrug efflux mechanisms produced by *S. aureus*.

3. Experimental section

3.1. General experimental procedures

Melting points were determined on a Gallenkamp apparatus. Optical rotations were measured on a Bellingham and Stanley ADP 200 polarimeter. UV spectra were recorded on a Perkin-Elmer UV/vis spectrophotometer and IR spectra were recorded on a Nicolet 360 FT-IR spectrophotometer. ^{1}H NMR (400 MHz) and ^{13}C NMR (100 MHz) spectra were recorded in $CDCl_3$ on Bruker DRX, AVANCE and AMX 400 spectrometers. Chemical shift values (δ) are reported in parts per million (ppm) relative to tetramethylsilane (TMS $\delta = 0$) as internal standard and coupling constants (*J* values) are given in Hertz. ^{1}H–^{1}H COSY, HMBC and HSQC experiments were recorded with gradient enhancements using sine shaped gradient pulses. FAB Mass spectra were recorded on a VG ZAB-SE instrument. Vacuum liquid chromatography on Merck Si gel 60 $PF_{254+366}$ and preparative HPLC using Waters Delta 600 were used for fractionation and isolation. TLC was carried out on Kieselgel 60 F_{254} (Merck) pre-coated plates and spots were visualized by spraying with Vanillin-Sulphuric acid followed by heating.

3.2. Plant material

Plant material used in this study was collected in September 2000 from Wilstone, Hertfordshire, UK on the verge of the Aylesbury arm of the Grand Union Canal and a voucher specimen SG01/09/2000 has been deposited at the Centre for Pharmacognosy and Phytotherapy at the University of London School of Pharmacy.

3.3. Extraction and isolation

Air-dried and powdered herb (450 g) was exhaustively extracted in a Soxhlet apparatus with a series of solvents (3 l) in order of increasing polarity (hexane, chloroform, ethyl acetate, acetone and methanol). Extracts were dried under vacuum in a rotary evaporator. Vacuum liquid chromatography (VLC) was carried out on the hexane extract (23.6 g) with silica gel using a step gradient system with 10% increments from 100% hexane to 100% EtOAc and finally 10% methanol in EtOAc yielding 12 fractions. Preparative reverse phase HPLC (on two coupled 40 × 100 mm 6 μm Nova-Pak HR C_{18} columns) using a gradient system from 100% water to 100% acetonitrile over 30 min was carried out on VLC fractions 8 (862.1 mg) and 10 (272.4 mg) yielding compounds **1** (57.2 mg) and **2** (11.4 mg) respectively.

3.4. Bacterial strains

S. aureus RN4220 containing plasmid pUL5054, which carries the gene encoding the MsrA macrolide efflux protein, was provided by J. Cove (Ross et al., 1989). Strain IS-58, which possesses the TetK tetracycline efflux protein, was provided by E. Udo (Gibbons and Udo, 2000). SA-1199B, which overexpresses the *norA* gene encoding the NorA MDR efflux protein was provided by G. Kaatz (Kaatz et al., 1993). All strains were cultured on nutrient agar (Oxoid) and incubated for 24 h at 37 °C prior to MIC determination.

3.5. Minimum inhibitory concentration (MIC)

Tetracycline, norfloxacin, and erythromycin were obtained from Sigma Chemical Co. Mueller-Hinton broth (MHB; Oxoid) was adjusted to contain 20 and 10 mg/l of Ca^{2+} and Mg^{2+}, respectively. An inoculum density of 5×10^5 cfu of each of the test organisms was prepared in normal saline (9 g/l) by comparison with a MacFarland standard. MHB (125 μl) was dispensed into 10 wells of a 96-well microtitre plate (Nunc, 0.3 ml volume per well). Tetracycline and erythromycin were dissolved in MHB to give stock solutions. A stock solution of norfloxacin was prepared by dissolving the antibiotic in DMSO (Sigma) and dilution in MHB to give a final concentration of 0.625%. A DMSO control was included in all assays.

Antibiotics were serially diluted into each of the wells followed by the addition of the appropriate bacterial inoculum. The plate was incubated at 37 °C for 18 h

and the MIC recorded as the lowest concentration at which no growth was observed. This was facilitated by the addition of 20 μl of a 5 mg/ml methanolic solution of 3-[4,5-dimethylthiazol-2-yl]-2,5-diphenyltetrazolium bromide (MTT; Sigma) to each of the wells and incubation for 20 min. A blue colouration indicated bacterial growth.

In the case of the modulation assay, diterpenes and reserpine were dissolved in DMSO and diluted into MHB to give final concentrations of 10 and 20 μg/ml, respectively. This medium was then used in the minimum inhibitory concentration assay.

3.6. Methyl-1α-acetoxy-7α,14α-dihydroxy-8,15-isopimaradien-18-oate (*1*)

Colourless crystals; mp 150–153 °C; $[\alpha]_D^{25}$ +0.08 ($CHCl_3$; *c* 0.12); UV λ_{max} (MeOH) nm (log ε): 217 (2.22); IR ν_{max} (thin film) cm^{-1}: 2950,1723, 1645, 1434, 1372, 1241, 1028, 754; ^1H NMR and ^{13}C NMR ($CDCl_3$): see Table 1; HRFAB-MS (*m*/*z*): 429.2268 $[M+Na]^+$ (calcd. for $C_{23}H_{34}O_6Na$, 429.2253).

3.7. Methyl-1α,14α-diacetoxy-7α-hydroxy-8,15-isopimaradien-18-oate (*2*)

Pale yellow oil; $[\alpha]_D^{25}$−0.01 ($CHCl_3$; *c* 0.8); UV λ_{max} (MeOH) nm (log ε): 215 (2.16); IR ν_{max} (thin film) cm^{-1}: 3409, 2931, 1723, 1641, 1433, 1372, 1234; 1145, 1028, 965, 751; ^1H NMR and ^{13}C NMR ($CDCl_3$): see Table 1; HRFAB-MS (*m*/*z*): 581.1538 $[M+Cs]^+$ (calcd. for $C_{25}H_{36}O_7Cs$, 581.1515).

Acknowledgements

The EPSRC is thanked for the award of a studentship to M. Oluwatuyi and the Royal Society is thanked for a project grant (Grant No. 21595) to S. Gibbons.

References

Beck, W.T., Cirtain, M.C., Glover, C.J., Felsted, R.L., Safa, A.R., 1988. Effects of indole alkaloids on multidrug resistance and labeling of P-glycoprotein by a photoaffinity analog of vinblastine. Biochemical and Biophysical Research Communications 153, 959–966.

Bohlmann, F., Zdero, C., Ahmed, M., 1982. New sesquiterpene lactones, geranyllinalol derivatives and other constituents from *Geigeria* species. Phytochemistry 21, 1679–1691.

Bucar, F., Kartnig, T.H., 1995. Flavone glucuronides of *Lycopus virginicus*. Planta Medica 61, 378–380.

Gibbons, S., Udo, E.E., 2000. The effect of reserpine, a modulator of multidrug efflux pumps, on the *in-vitro* activity of tetracycline against clinical isolates of methicillin resistant *Staphylococcus aureus* (MRSA) possessing the *tet*(K) determinant. Phytotherapy Research 14, 139–140.

Gonzales, R.D., Schreckenberger, P.C., Graham, M.B., Kelkar, S., DenBesten, K., Quinn, J.P., 2001. Infections due to vancomycin-resistant *Enterococcus faecium* resistant to linezolid. Lancet 357, 1179.

Hussein, A.A., Rodriguez, B., Martinez-Alcazar, M., Cano, F.H., 1999. Diterpenoids from *Lycopus europaeus* and *Nepeta septemcrenata*: revised structures and new isopimarane derivatives. Tetrahedron 55, 7375–7388.

Hussein, A.A., Rodriguez, B., 2000. Isopimarane diterpenoids from *Lycopus europaeus*. Journal of Natural Products 63, 419–421.

Jeremic, D., Macura, S., Milosavljevic, S., Vajs, V., 1985. A novel pimara-8(9),15-diene from *Lycopus europaeus*. Tetrahedron 41, 357–364.

Kaatz, G.W., Seo, S.M., Ruble, C.A., 1993. Efflux-mediated fluoroquinolone resistance in *Staphylococcus aureus*. Antimicrobial Agents and Chemotherapy 37, 1086–1094.

Markham, P.N., Westhaus, E., Klyachko, K., Johnson, M.E., Neyfakh, A.A., 1999. Multiple novel inhibitors of the NorA multidrug transporter of *Staphylococcus aureus*. Antimicrobial Agents and Chemotherapy 43, 2404–2408.

Marshall, N.J., Piddock, L.J.V., 1997. Antibacterial efflux systems. Microbiologia 13, 285–300.

Paulsen, I.T., Brown, M.H., Skurray, R.A., 1996. Proton-dependent multidrug efflux systems. Microbiology Reviews 60, 575–608.

Philips, R., 1977. Wild Flowers of Britain. Pan books, London.

Ross, J.I., Farrell, A.M., Eady, E.A., Cove, J.H., Cunliffe, W.J., 1989. Characterisation and molecular cloning of the novel macrolide-streptogramin B resistance determinant from *Staphylococcus epidermidis*. Journal of Antimicrobial Chemotherapy 24, 851–862.

Sieradzki, K., Roberts, R.B., Haber, S.W., Tomaz, A., 1999. The development of vancomycin resistance in a patient with methicillin-resistant *Staphylococcus aureus* infection. The New England Journal of Medicine 340, 517–523.

Stermitz, F.R., Lorenz, P., Tawara, J.N., Zenewicz, L.A., Lewis, K., 2000a. Synergy in a medicinal plant: antimicrobial action of berberine potentiated by 5′-methoxyhydnocarpin, a multidrug pump inhibitor. Proceedings of the National Academy of Sciences of the United States of America 97, 1433–1437.

Stermitz, F.R., Tawara-Matsuda, J., Lorenz, P., Mueller, P., Zenewicz, L., Lewis, K., 2000b. 5′-Methoxyhydnocarpin-D and pheophorbide A: *Berberis* species components that potentiate berberine growth inhibition of resistant *Staphylococcus* aureus. Journal of Natural Products 63, 1146–1149.

Int. J. Mol. Sci. **2004**, *5*, 37-47

International Journal of
Molecular Sciences
ISSN 1422-0067

www.mdpi.org/ijms/

Molecular Similarity of MDR Inhibitors

Mire Zloh[1*] and Simon Gibbons[2]

[1] University of London School of Pharmacy, Department of Pharmaceutical and Biological Chemistry, 29-39 Brunswick Square, London WC1N 1AX, UK Tel: + 44 (0) 20 7753 5879, Fax: +44 (0) 20 7753 5964, E-mail: mire.zloh@ulsop.ac.uk, URL: http://www.ulsop.ac.uk/depts/pharmchem/zloh.html

[2] University of London School of Pharmacy, Centre for Pharmacognosy and Phytotherapy, 29-39 Brunswick Square, London WC1N 1AX, UK Tel: + 44 (0) 20 7753 5913, E-mail: simon.gibbons@ulsop.ac.uk, URL: http://www.ulsop.ac.uk/depts/cog-pages/sg.html

* Author to whom correspondence should be addressed.

Received: 10 April 2003 / Accepted: 31 August 2003 / Published: 30 January 2004

Abstract: The molecular similarity of multidrug resistance (MDR) inhibitors was evaluated using the point centred atom charge approach in an attempt to find some common features of structurally unrelated inhibitors. A series of inhibitors of bacterial MDR were studied and there is a high similarity between these in terms of their shape, presence and orientation of aromatic ring moieties. A comparison of the lipophilic properties of these molecules has also been conducted suggesting that this factor is important in MDR inhibition.

Keywords: MDR, multidrug resistance, inhibitor, molecular similarity, SAR, *ab initio*.

Introduction

MDR or multidrug resistance is responsible for many forms of resistance in bacteria, fungi and human tumours [1]. This resistance functions by the presence of membrane bound efflux pumps, which actively export therapeutics from the cell resulting in a low intracellular ineffective concentration of the drug [2]. These pumps recognize a wide variety of structurally unrelated compounds [3] and it is believed that MDR inhibitors bind directly to the hydrophobic region of the efflux pump thus preventing the drug transport [4].

There has been much research conducted to find inhibitors of these proteins, particular in human tumour resistance as reviewed by Stouch and Gudmundsson [5]. Some progress has been reported on

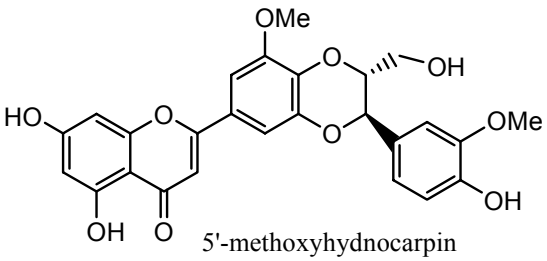

5'-methoxyhydnocarpin

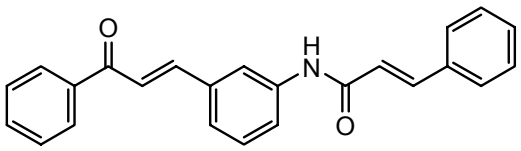

INF 240

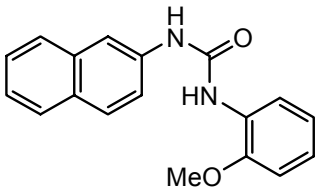

INF 271

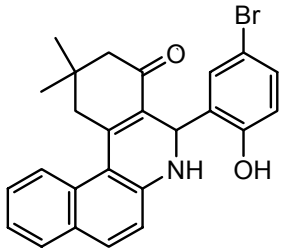

INF 277

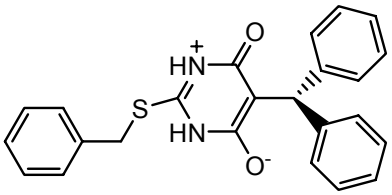

INF 392

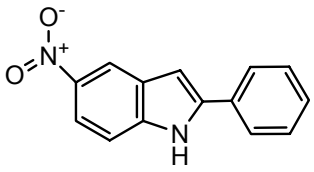

INF 55

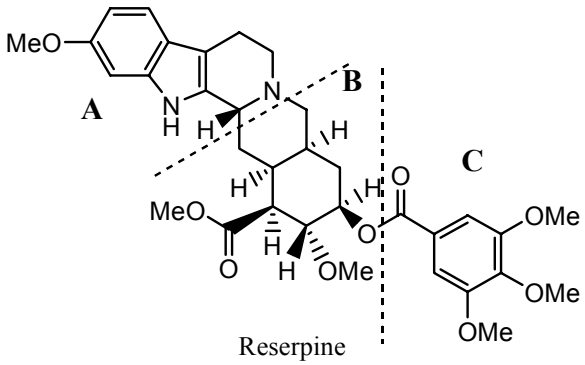

Reserpine

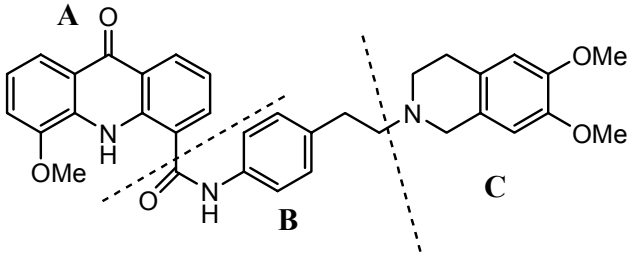

GG918

Scheme 1

the structure-activity relationships (SARs) for inhibitors of bacterial efflux pumps [6], but further work is necessary to fully explain the mechanism of MDR efflux inhibition, since most potent inhibitors of the NorA MDR pump of *Staphylococcus aureus* come from totally different chemical classes. This is unusual since it seems that there is no common pharmacophore that causes inhibition of MDR.

We have modelled and explored biomolecular similarities of a series of representative MDR inhibitors of the NorA pump from different classes (Scheme 1) on the basis of molecular interaction potentials and report here some structural features required for MDR inhibition.

Computational Methods

The inhibitors studied were optimized by Gamess-US *ab initio* software package [7] and HF/6-311G(*) basis set (except for the INF 277 where we have used HF/6-31G(*) basis set). The molecular similarity was evaluated by MIPSIM software [8] using COMP module and a classical atom-centred point-charge distribution (PTC_MEP) approach. The reserpine and GG918 molecules were too big for the MIPSIM calculations, and were spilt into 3 units for comparison with other inhibitors (denoted as A, B and C in Scheme 1). The theoretical values of logP, surface area and volume were calculated by SciLogP 3.0 [9], Vega [10] and Chem3D [11] software packages. Visualization of the results was achieved by ViewerLite [12] and ICM Lite [13] software packages.

Results and Discussion

The efflux pump NorA plays an important role in resistance to fluoroquinolone antibiotics of the major human pathogen *Staphylococcus aureus*, which is highly problematic in the clinical environment [14]. The restoration of antibiotic efficacy could be achieved by using inhibitors, molecules that potentiate the activity of standard antibiotics against MDR cells. Efflux inhibitors are from a wide range of structural classes and representative molecules for different classes were studied here. The experimental results of MDR modulation for chosen inhibitors are shown in Table 1. These results are taken from the literature [15] or from one of the authors [16, 17]. Compounds with no potential for MDR inhibition are shown in Scheme 2. It is believed that inhibitors of these transport processes act by directly binding to hydrophobic regions of MDR proteins causing inhibition of antibiotic removal [4]. Since a wide range of MDR inhibitors have been discovered and with no apparent pharmacophore detected, we have assumed that interactions important for MDR inhibition must be non-specific. The molecular electrostatic potential could be very important for the formation of a potential hydrogen bond network and other interactions between MDR inhibitor and efflux pump, and it could also play a significant role in molecular recognition.

In the absence of an explanation for the MDR inhibition mechanism, we have decided to evaluate the importance of molecular electrostatic potential in these processes. The *ab initio* optimised geometries of selected inhibitors of the NorA efflux pump were compared using atom-centred point-

Table 1. MDR modulation results for NorA inhibitors (5'-MHC depicted 5'-methoxyhydnocarpin).

Inhibitor	Drug	Inhibition	Reference
INF 240	Ciprofloxacin	0.12*	Markham et al., 1999. [15]
INF 271	Ciprofloxacin	0.12*	Markham et al., 1999. [15]
INF 277	Ciprofloxacin	0.15*	Markham et al., 1999. [15]
INF 392	Ciprofloxacin	0.28*	Markham et al., 1999. [15]
INF 55	Ciprofloxacin	0.25*	Markham et al., 1999. [15]
5'-MHC	Norfloxacin	4**	Stermitz et al., 2000. [18]
Reserpine	Norfloxacin	4**	Gibbons et al., 2003. [16]
GG918	Norfloxacin	8**	Gibbons et al., 2003a. [16]
Diterpene from *Lycopus europaeus*	Norfloxacin	ND	Gibbons et al., 2003b. [16]
Epigallocatechin-3-O-gallate	Norfloxacin	ND	Gibbons, unpublished data [2003]

*FIC index - <0.5 is considered to be indicator of synergistic activity.

**Fold reduction in minimum inhibitory concentration (MIC) of antibiotic in the presence of inhibitor.

ND - no drug potentiation.

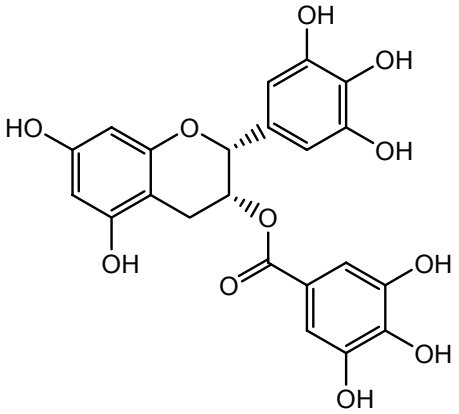

Epigallocathechin-3-O-gallate

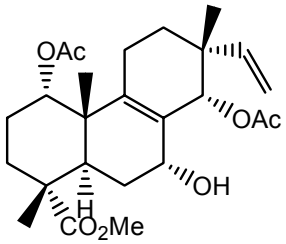

Diterpene from *Lycopus europaeus*

Scheme 2

charge distribution and results are presented in Table 2 in the form of a similarity matrix. Reserpine and GG918 had to be split into three portions, and those are defined in the Scheme 1.

The similarity index for all pairs of inhibitors was between 0.644 and 0.932, depending on the size of the compared molecules. The results for the parts of reserpine and GG918 are to be taken with caution due to the relatively small sizes of examined moieties. Direct correlation between similarity and fold of modulation cannot be fully examined due to differences in the representation of experimental data, however, the following could be emphasised:

a) INF 271 and INF 277 have a similar potency of MDR inhibition and similarity index is also high – 0.817;
b) 5'-methoxyhydnocarpin (5'-MHC) and INF 240 are potent MDR inhibitors and have a high similarity index.

Due to the difference in the size of molecules, a more detailed analysis was carried out by visually comparing inhibitors.

Table 2. Final similarity matrix for MDR inhibitors of the NorA pump calculated by MIPSIM using point charges. Three parts of reserpine were denoted as Reserpine A, Reserpine B and Reserpine C, and three parts of GG918 were denoted as GG918 A, GG918 B, and GG918 C. Similarity between parts that belong to the same molecule were not considered.

	5'-MHC	INF 240	INF 271	INF 277	INF 392	INF 55
5'-MHC	1.000					
INF 240	0.840	1.000				
INF 271	0.735	0.733	1.000			
INF 277	0.704	0.673	0.817	1.000		
INF 392	0.740	0.751	0.781	0.722	1.000	
INF 55	0.729	0.707	0.866	0.803	0.725	1.000
Reserpine A	0.690	0.735	0.870	0.754	0.719	0.932
Reserpine B	0.691	0.616	0.817	0.813	0.739	0.808
Reserpine C	0.699	0.649	0.717	0.695	0.677	0.737
GG918 A	0.669	0.713	0.818	0.755	0.707	0.915
GG918 B	0.644	0.703	0.759	0.699	0.670	0.839
GG918 C	0.716	0.692	0.795	0.722	0.646	0.824
Diterpene from *Lycopus europaeus*	0.681	0.566	0.763	0.807	0.722	0.720
Epigallocatechin-3-O-gallate	0.682	0.670	0.825	0.868	0.733	0.750

From the figures of the best fit between pairs of inhibitors, some observations are apparent:

a) 5'-methoxyhydnocarpin and INF 240 have the same shape and some polar groups in a similar position (Figure 1). Note the absence of nitrogen atom in 5'-MHC;
b) INF 271 and INF 277 have a similar shape and both have a nitrogen atom in the middle of the molecule (Figure 2);
c) INF 55 is planar and different in shape compared to INF 271, however both molecules have a nitrogen atom in the middle of molecule and aromatic rings from both molecules are almost parallel to each other (Figure 3);
d) there is high similarity between INF 271 and parts of Reserpine and GG918 (Figure 4 and Figure 5, respectively), again with a nitrogen atom in the middle of the molecule;
e) all potent MDR inhibitors have aromatic rings in the areas that contain high similarity.

In Figures 6 and 7, similarities between epigallocatechin-3-O-gallate (EGG) and two Influx compounds are depicted. However, EGG is not a potentiator of drugs in bacterial MDR processes, and possibly is therefore not an inhibitor of bacterial MDR efflux. This can possibly be explained by visually examining the best fit between EGG and the two Influx compounds (INF271 and INF277). The similarity index is very high for both of these combinations but it can be observed that there is a poor fit between EGG and the aromatic moieties of both of these compounds. Looking at the fit between INF277 and the diterpene from *Lycopus europaeus,* there is a high calculated similarity but again this diterpene is not a potentiator of MDR drugs and this is probably due to the poor fit that this has with aromatic moieties of other MDR inhibitors e.g. INF277 (Figure 8).

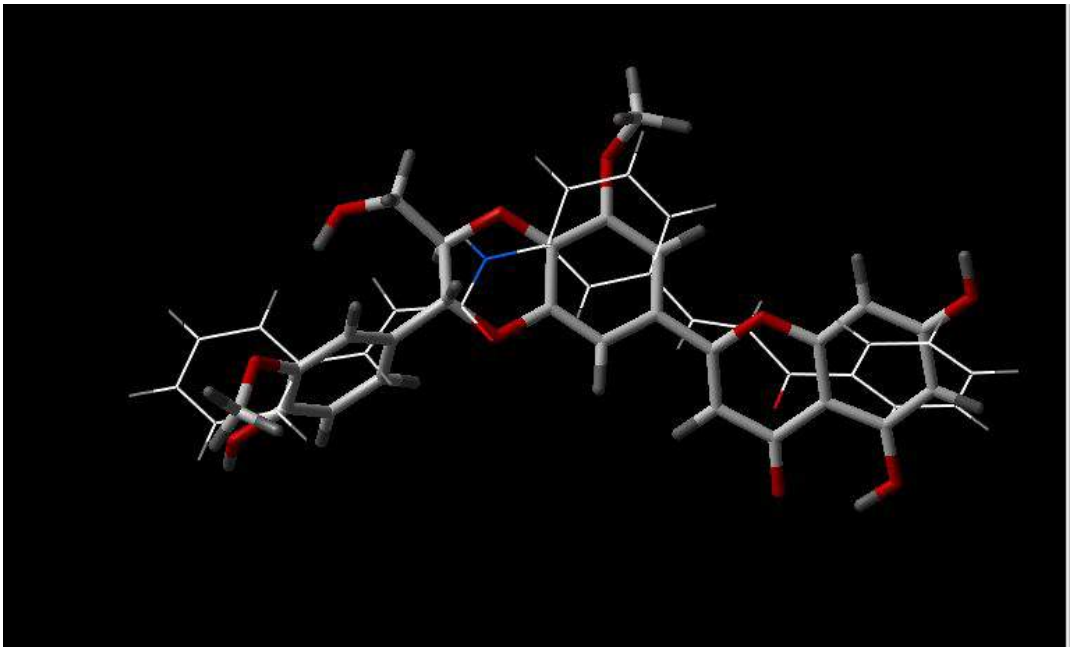

Figure 1. Best fit of optimized 5'-methoxyhydnocarpin (sticks) and INF 240 (wireframe) structures.

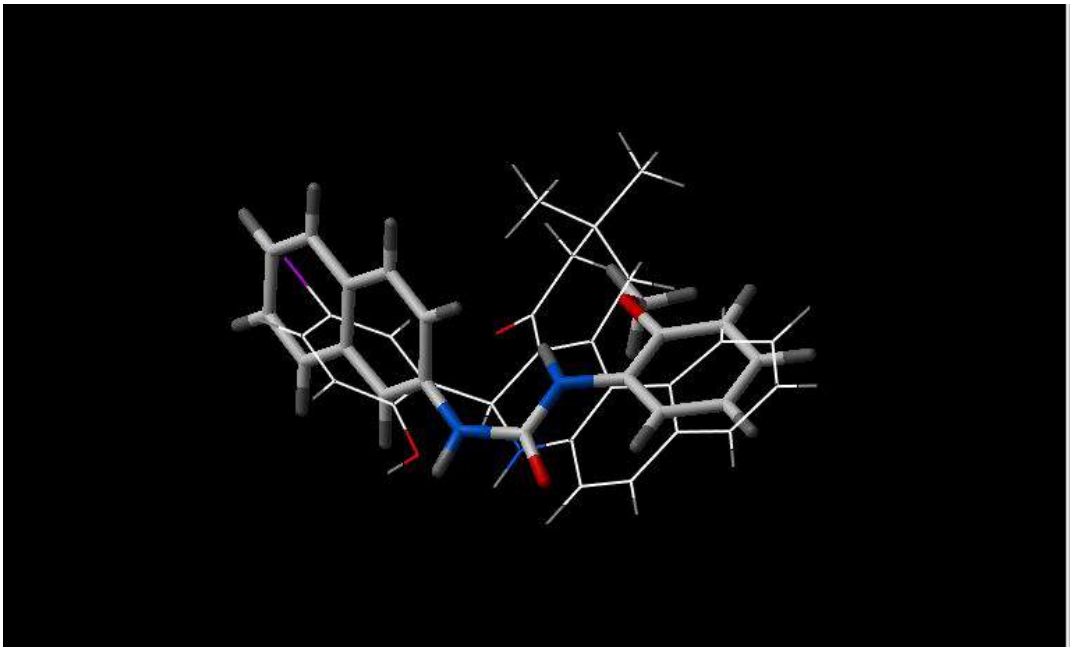

Figure 2. Best fit of optimised INF 271 (sticks) and INF 277 (wireframe) structures.

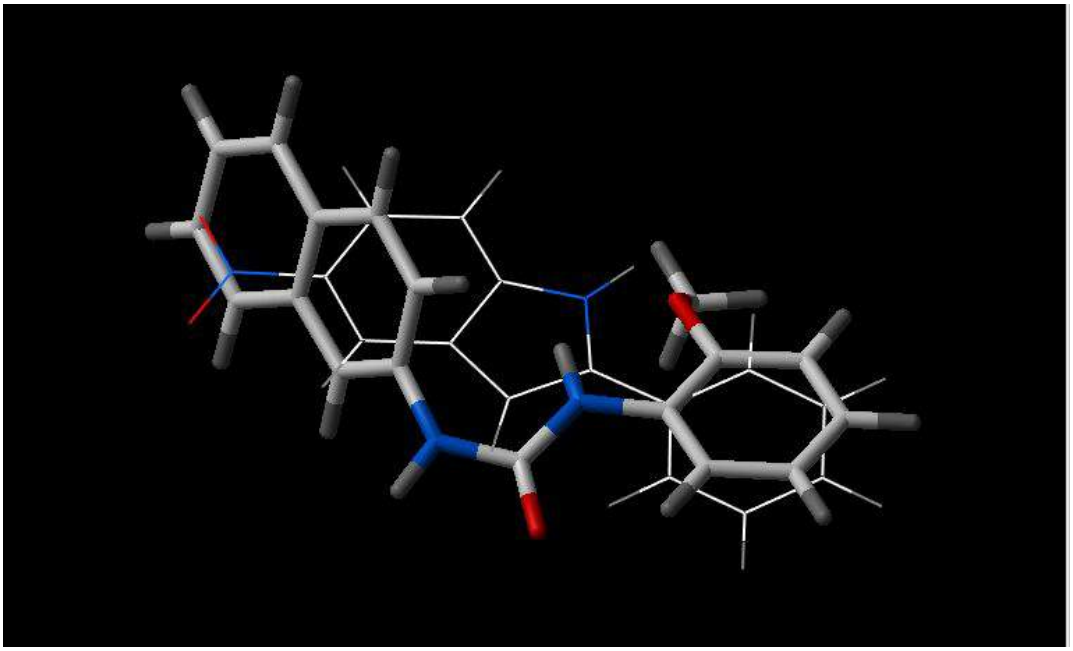

Figure 3. Best fit of optimised INF 271 (sticks) and INF 55 (wireframe) structures.

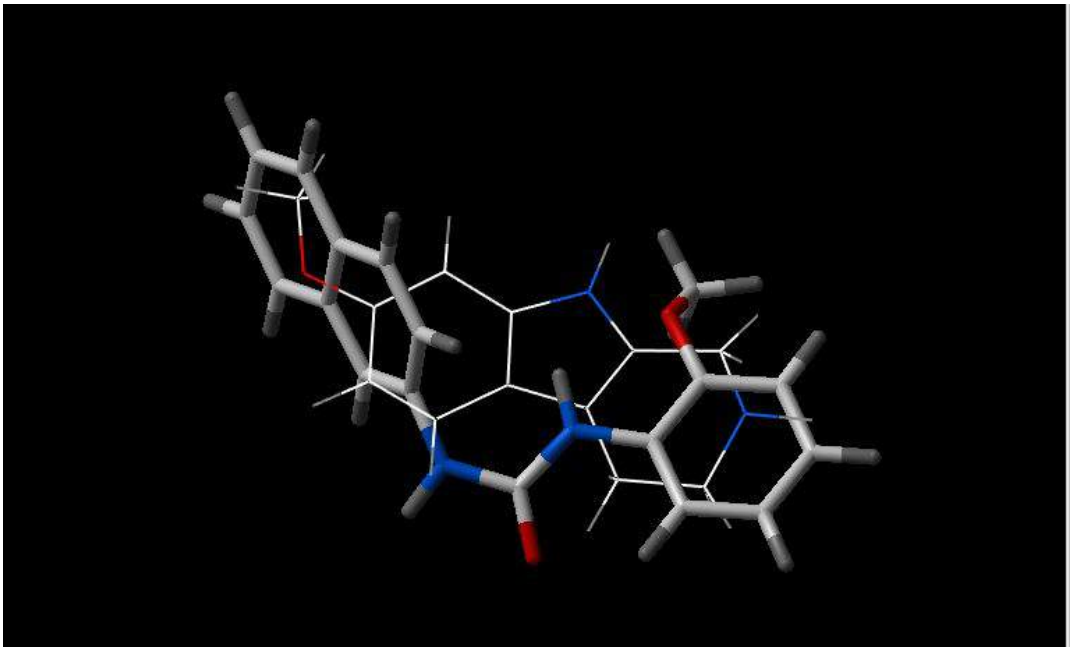

Figure 4. Best fit of optimised INF 271 (sticks) and Reserpine A (wireframe) structures.

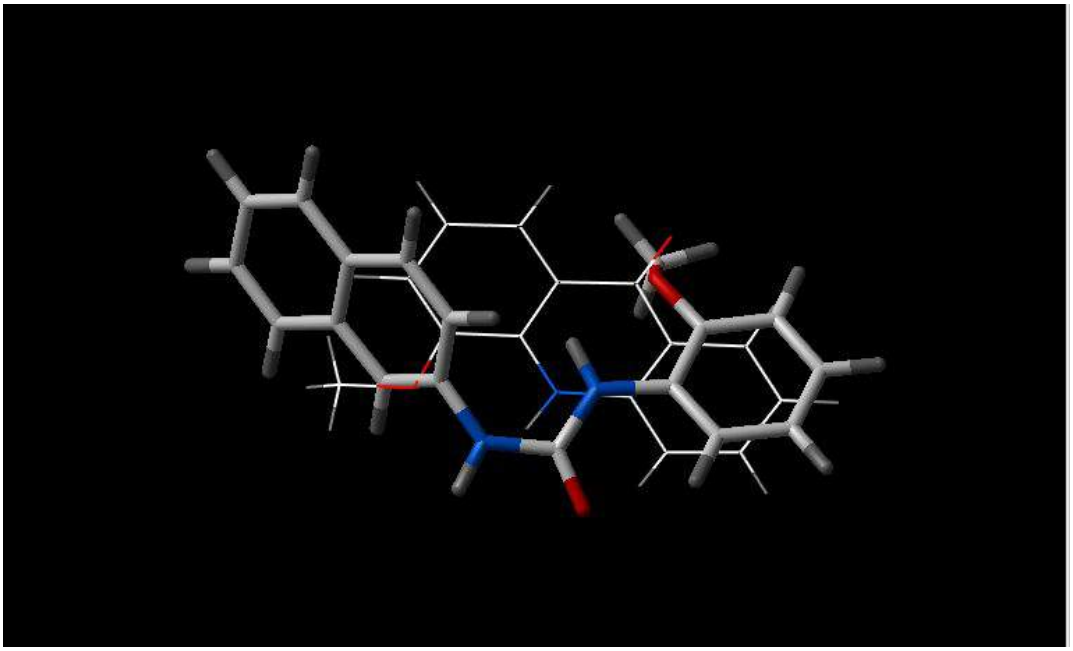

Figure 5. Best fit of optimised INF 271 (sticks) and GG918 A (wireframe) structures.

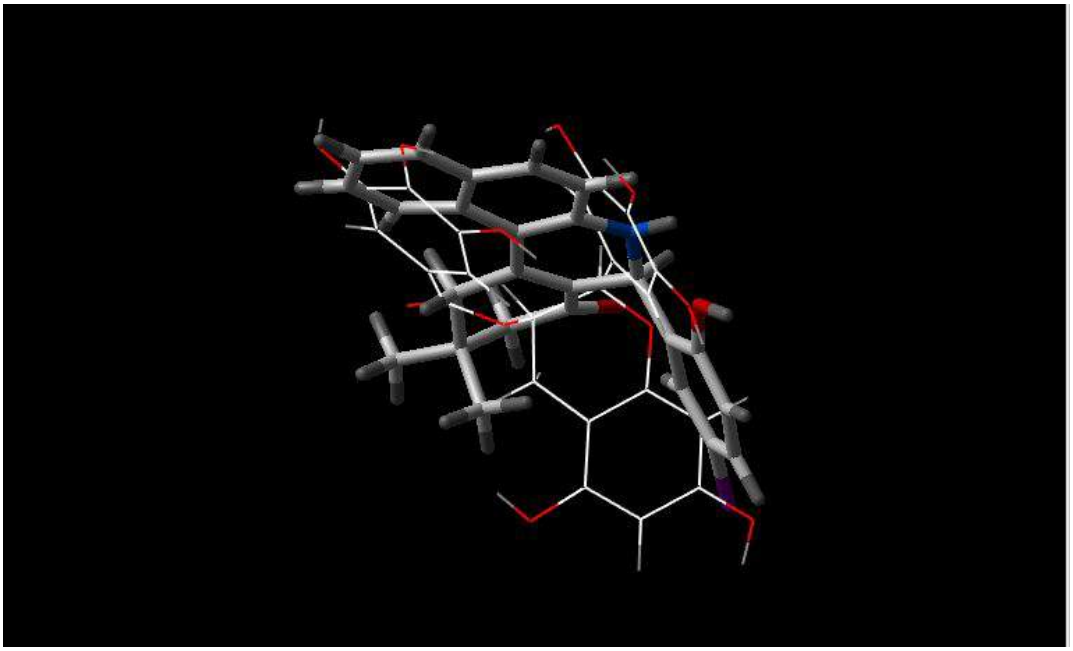

Figure 6. Best fit of optimised INF277 (sticks) and Epigallocatechin-3-O-gallate (wireframe) structures.

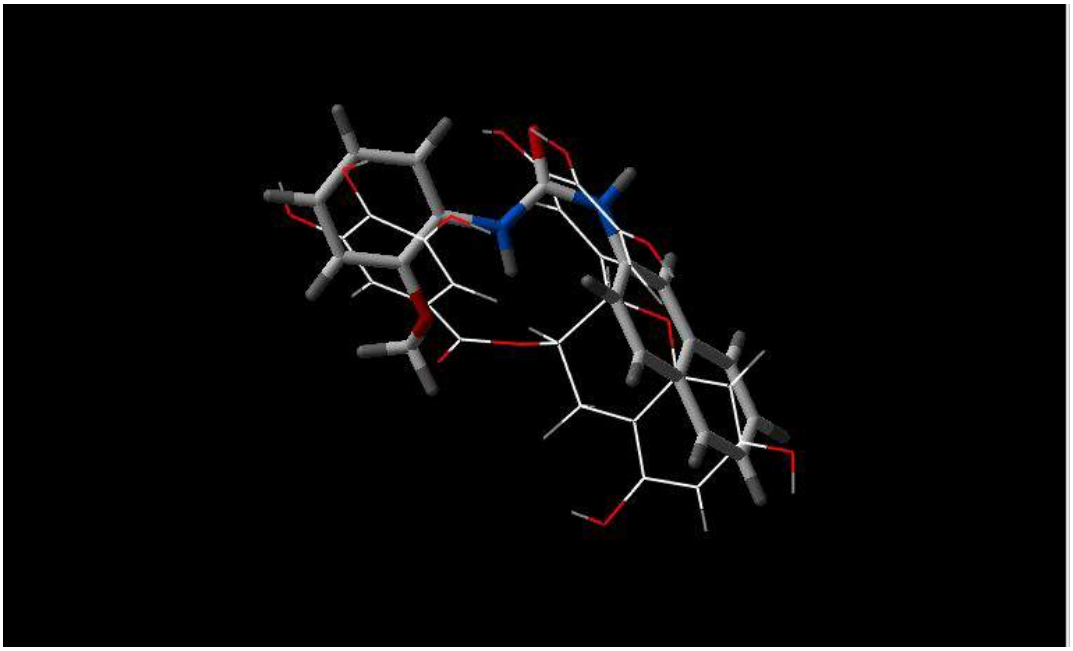

Figure 7. Best fit of optimised INF271 (sticks) and Epigallocatechin-3-O-gallate (wireframe) structures.

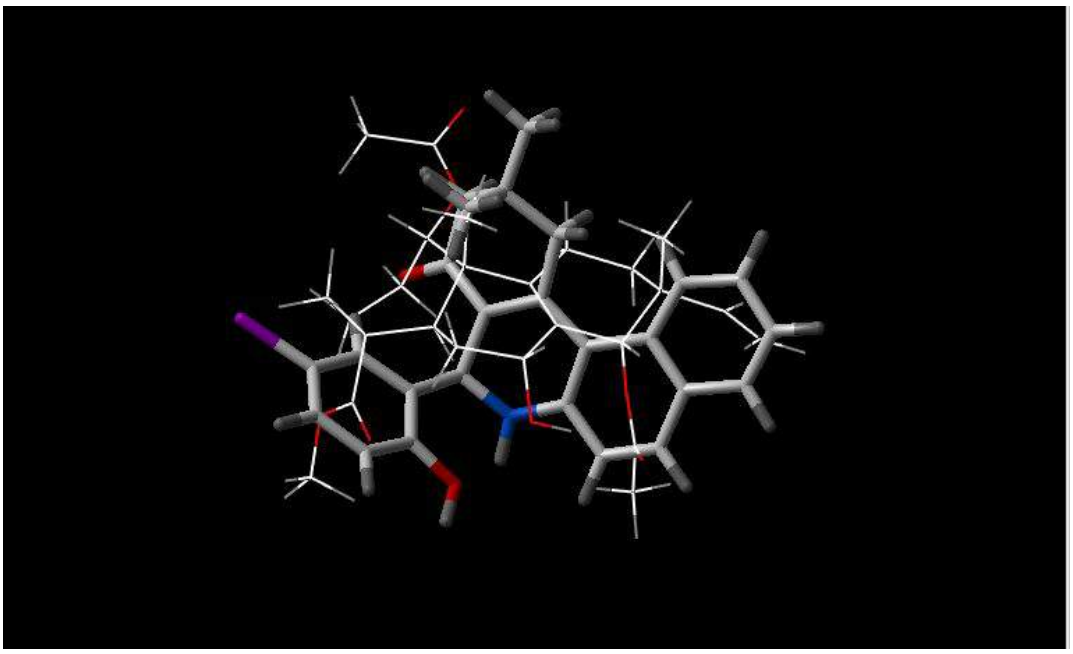

Figure 8. Best fit of optimised INF277 (sticks) and diterpene from *Lycopus europaeus* (wireframe) structures.

We have also studied some theoretical parameters i.e. clogP and logP, (Table 3), however there is no obvious correlation with MDR modulation results. However clogP is generally lower for non-MDR inhibitors, the exception to this is INF55, which is a small molecule and one of the poorest MDR inhibitor of the INF series.

Table 3. Theoretically calculated values of clogP, logP, surface area and volume of all studied MDR inhibitors and non potentiators by different methods.

Inhibitor	clogP (Chem3D)	logP (Chem3D)	logP (SciLogP)	logP (Vega)	lipole (Vega)	Surface area (A^2)	Volume (A^3)
5'-MHC	3.47	2.33	6.23	5.43	2.92	482.9	410.5
INF 240	5.14	4.73	6.04	3.03	1.43	396.5	328.5
INF 271	4.28	3.38	5.67	3.76	2.77	316.9	263.9
INF 277	6.02	5.12	6.02	6.73	2.29	408.0	361.2
INF 392	4.25	5.60	6.15	4.48	1.29	419.8	354.0
INF 55	0.93	3.68	5.09	4.92	5.12	248.7	207.2
Reserpine	3.85	2.69	6.08	4.38	1.10	656.0	546.6
GG918	4.21	5.03	6.12	5.60	0.89	629.9	536.0
Diterpene from *Lycopus europaeus*	2.45	3.65	6.23	3.34	0.73	497.84	425.59
Epigallocatechin-3-O-gallate	1.49	2.07	6.21	6.62	2.61	429.3	363.6

Conclusions

This study has shown that there is a high similarity between inhibitors of the NorA MDR transporter with similarity index higher than 0.6. However, there is no obvious correlation between similarity index and potential as MDR inhibitor, since some non-potentiators have high similarity index with MDR inhibitors. The important feature that differentiates inhibitors and non-inhibitors is the shape of the molecule and relative position of the aromatic moieties present in the molecule.

Although in most inhibitors there is a nitrogen atom in the middle of the molecule, it is not essential, for example 5'-MHC has no such feature. This confirms the assumption that the interactions occurring during MDR inhibition must be non-specific. The shape of the molecule, aromatic rings and presence of some polar atoms will determine the potency of MDR inhibition. This study should be expanded to encompass a further series of inhibitor and non-inhibitor molecules of MDR processes of NorA in order to derive rules for the *in silico* screening for MDR inhibitors.

References

1. Ling, V. *Cancer Chemotherapy and Pharmacology* 1997, *40,* Suppl:S3-8.
2. Bradley, G.; Ling, V. *Cancer Metastasis Rev.* 1994, *13,* 223-233.
3. Neyfakh, A.A. *J. Mol. Microbiol. Biotechnol.* 2001, *3*, 151-154.
4. Neyfakh, A.A. *Molecular Microbiology* 2002, *44,* 1123-1130.
5. Stouch, T.R.; Gudmundsson, O. *Advanced Drug Delivery Reviews* 2002, *54*, 315-328.
6. Guz, N. R.; Stermitz, F.R.; Johnson, J.B.; Beeson, T.D.; Willen, S.; Hsiang, J.F.; Lewis, K. *J. Med. Chem.* 2001, *44,* 261-268.
7. Schmidth, M.W.; Baldridge, K.K.; Boatz, J.A.; Elbert, S.T.; Gordon, M.S.; Jensen, J.H.; Koseki, S.; Matsunaga, N.; Nguyen, K.A.; Su, S.J.; Windus, T.L.; Dupuis, M.; Montgomery, J.A. *Journal of Computational Chemistry* 1993, *14,* 1347-1363.
8. Sanz, F.; Manaut, F.; Rodriguez, J.; Lozoya E.; Lopez-de-Briñas, E. *Journal of Computer-Aided Molecular Design* 1993, *7*, 337-347.
9. SciLogP 3.0, SciVision, Inc. 1999.
10. Pedretti, A.; Villa, L.; Vistoli, G. *J. Mol. Graph.*, 2002, *21*, 47-49.
11. Chem3D Ultra, CambridgeSoft 2001.
12. ViewerLite 5.0, Accelerys Inc 2002.
13. ICM Lite, MolSoft, 2002.
14. Kaatz, G.W.; Seo, S.M.; Ruble, C.A. *Antimicrob. Agents. Chemother.* 1993, *37*, 1086-1094.
15. Markham, P.N.; Westhaus, E.; Klyachko, K.; Johnson, M.E.; Neyfakh, A.A. *Antimicrobial Agents and Chemotherapy* 1999, *43,* 2404-2408.
16. Gibbons, S.; Oluwatuyi, M. Kaatz, G.W. *Journal of Antimicrobial Chemotherapy* 2003, *51*, 13-17.
17. Gibbons, S. ; Oluwatuyi, M.; Veitch, N.C. Gray, A.I. *Phytochemistry* 2003, *62*, 83-87.
18. Stermitz, F.R.; Lorenz, P.; Tawara, J.N.; Zenewicz, L.A. Lewis, K. *PNAS* 2000, *97*, 1433-1437.

Available online at www.sciencedirect.com
SCIENCE DIRECT®
Phytochemistry 65 (2004) 3249–3254
PHYTOCHEMISTRY
www.elsevier.com/locate/phytochem

Antibacterial and resistance modifying activity of *Rosmarinus officinalis*

Moyosoluwa Oluwatuyi [a], Glenn W. Kaatz [b], Simon Gibbons [a,*]

[a] *Centre for Pharmacognosy and Phytotherapy, The School of Pharmacy, University of London, 29-39 Brunswick Square, London WC1N 1AX, UK*
[b] *Division of Infectious Diseases, Department of Internal Medicine, School of Medicine, Wayne State University and the John D. Dingell Department of Veteran Affairs Medical Center, Detroit, MI 48201, USA*

Received 8 October 1994

Abstract

As part of a project to characterise plant-derived natural products that modulate bacterial multidrug resistance (MDR), bioassay-guided fractionation of a chloroform extract of the aerial parts of *Rosmarinus officinalis* led to the characterisation of the known abietane diterpenes carnosic acid (**1**), carnosol (**2**) and 12-methoxy-*trans*-carnosic acid. Additionally, a new diterpene, the *cis* A/B ring junction isomer of 12-methoxy-*trans*-carnosic acid, 12-methoxy-*cis*-carnosic acid (**5**), was isolated.

The major components were assessed for their antibacterial activities against strains of *Staphylococcus aureus* possessing efflux mechanisms of resistance. Minimum inhibitory concentrations ranged from 16 to 64 μg/ml. Incorporation of **1** and **2** into the growth medium at 10 μg/ml caused a 32- and 16-fold potentiation of the activity of erythromycin against an erythromycin effluxing strain, respectively. Compound **1** was evaluated against a strain of *S. aureus* possessing the NorA multidrug efflux pump and was shown to inhibit ethidium bromide efflux with an IC_{50} of 50 μM, but this activity is likely to be related to the inhibition of a pump(s) other than NorA. The antibacterial and efflux inhibitory activities of these natural products make them interesting potential targets for synthesis.

Keywords: Abietane diterpenes; Multidrug-resistance; *Staphylococcus aureus*; MDR; MRSA; Efflux inhibitors; Antibacterial

1. Introduction

Bacteria are exceptionally adept at acquiring resistance to antibiotics and antiseptic agents. Amongst some of the most problematic clinically relevant pathogens at present, methicillin-resistant *Staphylococcus aureus* (MRSA) ranks as one of the most difficult bacteria to treat in patients and eradicate from hospital environments. In the UK there has been a significant increase in the number of death certificates which mention MRSA, with 47 citations in 1993 rising to 398 in 1998 (Crowcroft and Catchpole, 2002).

New antibiotics and strategies are therefore needed to deal with this threat. The difficulty in treating MRSA infections is compounded by the fact that many strains also possess efflux pumps such as the specific TetK and MsrA transporters, which export certain tetracyclines and macrolides, and the multidrug resistance (MDR) proteins NorA and QacA which confer resistance to a wide range of structurally unrelated antibiotics and antiseptics (Marshall and Piddock, 1997). The discovery of therapeutically useful compounds which are inhibitors of these processes and antibacterial in their own right could improve the containment, treatment, and eradication of these strains.

* Corresponding author. Tel.: +44 207 753 5913; fax: +44 207 753 5909.
E-mail address: simon.gibbons@ulsop.ac.uk (S. Gibbons).

0031-9422/$ - see front matter © 2004 Elsevier Ltd. All rights reserved.
doi:10.1016/j.phytochem.2004.10.009

In an ongoing project which aims to identify plant natural products that modulate resistance in MDR strains of *S. aureus* (Gibbons et al., 2003a), an evaluation of the constituents of the chloroform extract of *Rosmarinus officinalis* (Lamiaceae) was undertaken. *Rosmarinus officinalis* L., commonly referred to as rosemary, belongs to the mint family. It is a popular herb in many western countries, with global cultivation and an exceptionally wide usage in the Mediterranean countries from where it originates. Rosemary has a long list of claims pertaining to its medicinal uses including antibacterial (Del Campo et al., 2000) and antioxidant properties (Ozcan, 2003). It is known to be an effective chemopreventive agent (Plouzek et al., 1999), an antimutagenic (Minnunni et al., 1992) and has been shown to be non-toxic in animal models (Lemonica et al., 1996).

Previous investigations into the effect of natural plant-derived chemicals on the activity of the plasma membrane-associated glycoprotein, P-glycoprotein (P-gp), which is the major MDR mechanism in mammalian tumour cells (Bradley and Ling, 1994), showed that an extract of rosemary inhibits P-gp-mediated drug efflux (Plouzek et al., 1999). Furthermore, it has also been shown that GG918, a known P-gp inhibitor, enhances the in vitro activity of certain antibacterial agents against strains of MDR *S. aureus* (Gibbons et al., 2003b). Additionally, we have evaluated other members of this plant family that potentiate the activity of antibiotics towards effluxing MRSA strains (Gibbons et al., 2003a). In view of these findings, we hypothesised that an extract of rosemary may inhibit the in vitro efflux of antibacterial agents in strains of *S. aureus* expressing multidrug efflux pumps. We report here for the first time the antibacterial and resistance modifying activities of this species against MDR strains of *S. aureus*.

2. Results and discussion

The major components of rosemary, carnosic acid (**1**), carnosol (**2**) and 4′,7-dimethoxy-5-hydroxy-flavone (**3**) were isolated by a combination of vacuum liquid chromatography (VLC), sephadex LH-20 column chromatography, thin-layer chromatography and recrystallisation. The structures of these compounds were established by extensive spectroscopic studies using 1 and 2-D NMR spectroscopy and mass spectrometry (ESI). The ^{1}H and ^{13}C data of **1**–**3** were compared with the literature and are in close agreement with that published (Dimayuga et al., 1991; Schwarz and Ternes, 1992; Yang et al., 1995).

Compound **4** was isolated as colourless crystals solving for the molecular formula of $C_{21}H_{30}O_4$ by ESI-MS. Examination of the ^{13}C NMR spectrum showed characteristic signals between 110 and 150 ppm pointing to a diterpene with an aromatic system, a moiety also found in **1** and **2** (Table 1). Signals in the ^{1}H NMR spectrum (Table 1) for four methyl groups (δ_H 0.92, 0.96 and 1.16 ($2 \times CH_3$)) and an aromatic proton (δ_H 6.42, s) further suggested that this compound was an abietane diterpene similar to compounds previously isolated from this plant (Inatani et al., 1982; Schwarz and Ternes, 1992). The presence of a carbon signal at 61.9 ppm was consistent with the presence of a methoxyl group in the molecule (δ_H 3.71, s). Full 2-dimensional analysis including COSY, HMQC and HMBC spectra (Table 2) led to the assignment of this compound as 12-methoxy-*trans*-carnosic acid and the data (Table 1) are in close agreement with those published for this natural product (Al-Hazimi et al., 1987).

Table 1
^{1}H (500 MHz) and ^{13}C NMR (125 MHz) spectral data for **4** and **5** in CD_3OD

Position	Compound **4**		Compound **5**	
	^{1}H (*J* in Hz)	^{13}C	^{1}H (*J* in Hz)	^{13}C
1	3.56 *dd* (13, 3)	36.7	3.59 *dd* (13, 3)	36.9
2	1.51 *m*	22.1	1.49 *m*	22.1
3	1.31, 1.47 *m*	43.6	1.38, 1.44 *m*	43.7
4		35.6		35.2
5	1.41 *m*	56.4	1.44 *m*	56.1
6	1.88 *d* (2)	20.5	1.88 *br m*	20.4
	2.57 *m*		1.41 *m*	
7	2.75	33.9	2.88 *br s*	33.7
8		135.7		135.2
9		129.5		129.0
10		35.6		35.2
11		151.5		154.5
12		145.2		145.3
13		140.9		140.4
14	6.42 *s*	118.9	6.56 *s*	118.5
15	3.15 *sept.*	28.1	3.18 *sept.*	27.7
16	1.16 *dd* (8, 0.5)	24.4	1.24 *d* (6.5)	23.9
17	1.16 *dd* (8, 0.5)	24.7	1.24 *d* (6.5)	24.1
18	0.96 *s*	33.9	1.01 *s*	33.7
19	0.92 *s*	22.3	0.98 *s*	23.2
20		180.7		182.6
OMe	3.65 *s*	61.9	3.83 *s*	61.2

Table 2
Long-range ^{1}H–^{13}C connectivities detected in HMBC experiments for **4** and **5**

Position	Compound **4**, Correlated C-atom, HMBC (H→C)		Compound **5**, Correlated C-atom, HMBC (H→C)	
	^{2}J	^{3}J	^{2}J	^{3}J
1				
2		C-10		
3	C-2	C-4		C-18
5	C-4			
6				
7		C-5		C-8
14	C-13	C-7, C-12, C-15		C-7, C-9, C-12
15		C-12, C-14, C-16, C-17		
OMe	C-12			C-12

Compound **5** was isolated as colourless crystals solving for the molecular formula of $C_{21}H_{30}O_4$ by ESI-MS. The ^{13}C NMR and ^1H data (Table 1) were very closely related to that of **4**. Full HMBC analysis (Table 2) suggested that **5** was a methoxylated aromatic abietane diterpene of very similar structure to **4**. However, the ^1H NMR spectrum was different on the basis of the chemical shifts of the H_2-6 methylene protons. H-6(α) of **5** resonated at 1.88 ppm, which was consistent with that observed in **4**, but H-6β of **5** (δ_H 1.41, m) was different by 1.16 ppm in comparison to H-6β of **4** (δ_H 2.57, m). In compound **4**, due to the *trans* A/B ring junction, there is a 1,3 through-space interaction between the carboxyl group at C-10 (C-20) and the beta axially oriented H-6 (Fig. 1). This accounts for the large differences in the chemical shifts of H-6β and H-6α. This difference was not seen in **5** although all other resonances are comparable. We propose that this discrepancy is based on a different A/B ring junction architecture for **5** compared to **4** and that in compound **5** the carboxyl group (C-20) at C-10 is *cis* with respect to H-5. This would remove any through-space interactions to H-6β. Compound **5** is therefore assigned as 12-methoxy-*cis*-carnosic acid and is described here for the first time.

A paucity of sample prohibited further biological evaluation of **5** whilst the diterpenes (**1**, **2** and **4**) and the methoxyflavone **3** showed minimum inhibitory concentrations (MIC) ranging from 16 to 64 μg/ml against a panel of staphylococci capable of effluxing various drugs (Table 3). Of these strains, RN4220 and XU212 are erythromycin and tetracycline resistant, respectively, due to the presence of the MsrA and TetK efflux proteins which confer a high level of resistance to these agents. Strain SA-1199B overproduces the NorA MDR efflux protein, the major drug pump in *S. aureus* and was resistant to norfloxacin (Table 3). However, some of this resistance is also the result of a GrlA subunit substitution known to correlate with diminished fluoroquinolone susceptibility (Ala116 → Glu; Kaatz and Seo, 1997).

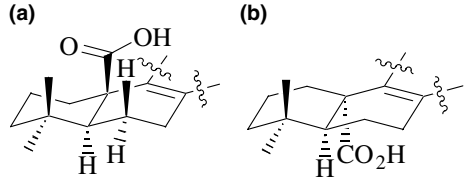

Fig. 1. (a) Partial structure for **4** showing a *trans* A/B ring junction. Carboxyl group at C-10 is in close proximity to H-6β. (b) Partial structure for **5** showing a *cis* A/B ring junction. Carboxyl group at C-10 is unable to deshield H-6β.

The two major components, carnosic acid (**1**) and carnosol (**2**) were incorporated into the bacterial growth medium and tested for their ability to enhance the activity of antibiotics against resistant effluxing strains (Table 4). At 10 μg/ml, carnosic acid (**1**) and carnosol (**2**) showed a 2- and 4-fold potentiation of tetracycline activity against XU212 (TetK possessing strain), respectively, while carnosic acid showed an impressive 8-fold potentiation of erythromycin activity against the macrolide resistant strain possessing MsrA. These results compare favourably with reserpine, our control MDR inhibitor which potentiated tetracycline and norfloxacin activity 4-fold but showed no effect against the erythromycin-resistant strain. At 10 μg/ml neither (**1**) nor (**2**) potentiated norfloxacin activity against SA-1199B. Despite the presence of a substitution in GrlA known to correlate with fluoroquinolone resistance in SA-1199B, inhibition of NorA by reserpine or other inhibitors still has been shown to result in MIC reductions which for reserpine we again demonstrated (Gibbons et al., 2003b; Kaatz et al., 2003a; Kaatz et al., 2003b). This observation indicated that at the tested concentration neither (**1**) nor (**2**) has activity against the NorA multidrug efflux pump.

A study of the effect of carnosic acid (**1**) on ethidium bromide (EtBr) efflux was conducted using SA-1199B (Fig. 2). EtBr is a substrate for many MDR pumps and when bound to DNA fluoresces and therefore the effects of inhibition of efflux can be assessed fluorometrically. Carnosic acid had modest efflux inhibitory activity with an IC_{50} of 50 μM (16.6 μg/ml), which is equivalent to approximately one-fourth its MIC for SA-1199B. A similar level of inhibition was observed with 10 μM reserpine (Fig. 2). On the surface this result may seem surprising in that there was no observable potentiation of norfloxacin activity against SA-1199B by (**1**) at 10 μg/ml (30 μM) or any of the other compounds tested at the given concentrations in the MIC assay. As a 2-fold potentiation of norfloxacin was observed in the total extract during screening, it is possible that the component responsible for this activity is yet to be identified. It also is possible that the effect on ethidium efflux observed for (**1**) against SA-1199B is

Table 3
MICs of **1–4** and standard antibiotics in μg/ml

Strain (MDR efflux protein)	**1**	**2**	**3**	**4**	Tetracycline	Erythromycin	Norfloxacin
XU212 (TetK)	32	16	16	64	128	–	–
RN4220 (MsrA)	32	16	32	16	–	256	–
SA-1199B (NorA)	64	16	32	64	–	–	32

All MICs were determined in duplicate.

Table 4
Antimicrobial susceptibility of test strains in the absence and presence of 10 μg/ml of **1**, **2**, or 20 μg/ml the MDR efflux inhibitor reserpine

Antimicrobial agent	MIC[a] of test strain expressing the indicated efflux protein		
	XU212 (TetK)	RN4220 (MsrA)	SA-1199B (NorA)
Tetracycline	128	ND	ND
+carnosic acid (**1**)	64		
+carnosol (**2**)	32		
+reserpine	32		
Erythromycin	ND	256	ND
+carnosic acid (**1**)		32	
+carnosol (**2**)		256	
+reserpine		256	
Norfloxacin	ND	ND	32
+carnosic acid (**1**)			32
+carnosol (**2**)			32
+reserpine			8
Ethidium bromide	ND	ND	16
+carnosic acid (**1**)			8
+carnosol (**2**)			ND
+reserpine			8

[a] MIC, minimum inhibitory concentration, in μg/ml.

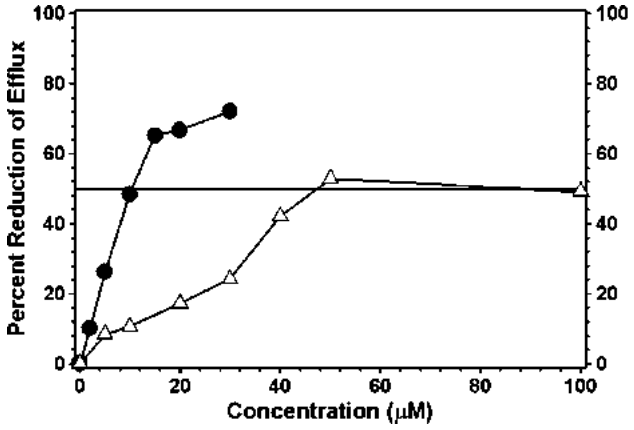

Fig. 2. Ethidium efflux inhibition assay, SA-1199B. Filled circles, reserpine; open triangles, carnosic acid (**1**).

related to an inhibitory effect on a pump(s) other than NorA for which ethidium is a substrate. Such pumps are highly likely to exist based on a detailed analysis of *S. aureus* genome data in the public domain (see http://66.93.129.133/transporter/wb/index2.html). The 2-fold potentiation of the antibacterial activity of ethidium by (**1**) (Table 4) and the modest inhibition of ethidium efflux correlate with and support this hypothesis.

Previously discovered modulators of MDR in *S. aureus* have been described. These compounds are from many structural classes including natural products such as terpenes, flavones, flavonolignans, porphyrins (Stermitz et al., 2000a,b; Gibbons et al., 2003a; Gibbons, 2004) and synthetic naphthylamides (Markham et al., 1999). Since impermeability of the bacterial membrane is deemed as a resistance mechanism, it follows that compromising this barrier by its permeabilisation would be an effective approach to combating antimicrobial resistance (Nikaido, 1998; Hancock, 1997). A common characteristic of all these agents appears to be the high degree of lipophilicity, a feature which is important for the interaction with membrane bound efflux proteins and the ability to overcome membrane impermeability.

Inhibition of bacterial cell growth is a traditional method of screening for natural antimicrobial and resistance modifying agents. We have demonstrated that rosemary constituents have antimicrobial and resistance modifying activity. While the antimicrobial activity might not be of clinical importance, the resistance modifying action is of interest since there is no known resistance modifying agent in use in the clinic presently. GG918, a synthetic mammalian tumour MDR inhibitor, has been shown to have broad spectrum resistance modifying activity against strains of *S. aureus* possessing multidrug efflux resistance mechanisms (Gibbons et al., 2003b) and is currently in clinical trials for the reversal of mammalian tumour resistance. Rosemary is a commonly used herb which is readily available, inexpensive, and has been shown to be relatively non-toxic (Plouzek et al., 1999). Its use as a potentiator of antibacterial agents rendered ineffective against MDR *S. aureus* once established might prove useful. Structure-activity studies may reveal a derivative of (**1**) having a broader spectrum of pump-inhibitory activity, including NorA.

3. Experimental

3.1. General experimental procedures

NMR spectra were recorded on Bruker AVANCE 400 and 500 MHz spectrometers. Chemical shift values (δ) were reported in parts per million (ppm) relative to appropriate internal solvent standard and coupling constants (J values) are given in Hertz. Mass spectra were recorded on VG ZAB-SE instrument (FAB-EIMS) and Finnigan navigator (ESMS). IR spectra were recorded on a Nicolet 360 FT-IR spectrophotometer and UV spectra on a Perkin–Elmer UV/Visible spectrophotometer.

3.2. Plant material

The powdered herb of *Rosmarinus officinalis* was supplied by Herbal Apothecary (Batch number 03213).

3.3. Extraction and isolation

500 g of air-dried and powdered herb was extracted at room temperature using 3×3 l of chloroform. The resulting extract was dried under vacuum to yield 73 g

of extract. Vacuum liquid chromatography (VLC) was carried out on 10 g of extract on silica gel eluting with hexane containing 10% increments of ethyl acetate to yield 12 fractions. Carnosic acid (**1**), carnosol (**2**) and 4′,7-dimethoxy-5-hydroxy-flavone (**3**) were isolated as a crude mixture by vacuum liquid chromatography (VLC) on silica gel eluting with 70% ethyl acetate in hexane (fraction 8). **1** and **2** were further purified using sephadex LH-20 and recrystallised from chloroform/methanol. Compound **3** was purified by a C_{18} TLC plate eluting with MeOH–H_2O (9:1). 12-methoxy-*trans*-carnosic acid (**4**) and 12-methoxy-*cis*-carnosic acid (**5**) were isolated from VLC fractions 5 following separation on a C-18 SPE cartridge and purification by TLC on a silica gel plate eluting with $CHCl_3$–MeOH (97:3) to give (**4**) (5.4 mg) and diethyl ether–petrol (1:1) to give (**5**) (2.3 mg).

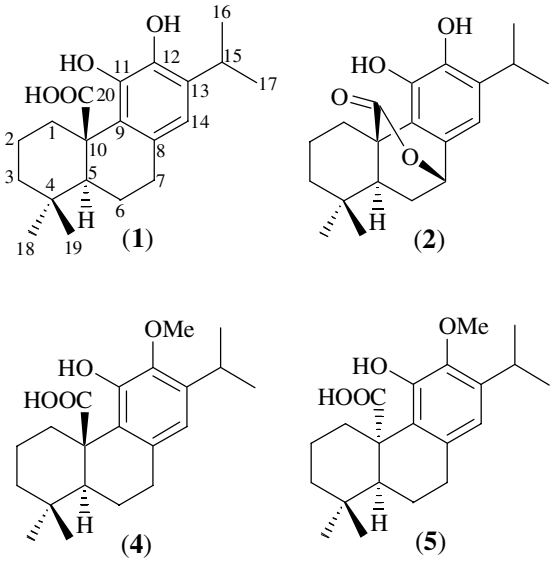

3.4. Bacterial strains and antibacterial assay

S. aureus strains RN4220, XU212, and SA-1199B that overexpress *msrA*, *tetK* and *norA*, respectively, were employed. *msrA* and *tetK* expressing strains were the generous gifts of J. Cove (University of Leeds, UK) and E. Udo (Kuwait University, Kuwait), whereas the origin of SA-1199B is as described in Kaatz et al. (1993). Test strains were cultured on nutrient agar and incubated for 24 h at 37 °C prior to MIC determination. An inoculum turbidity equivalent to No. 0.5 tube of the McFarland scale of each test organism was prepared in normal saline. MICs were determined in duplicate by the microdilution assay as previously described (Gibbons and Udo, 2000). The potentiating effect of these compounds was determined by dissolving in DMSO before diluting into MHB for use in the MIC determinations. A DMSO control also was included.

3.5. Ethidium efflux assay

Ethidium bromide (EtBr) is a substrate for many MDR pumps, including NorA. The efficiency of efflux pumps for which EtBr is a substrate can be assessed fluorometrically by the loss of fluorescence over time from cells loaded with EtBr. SA-1199B was loaded with EtBr exactly as described previously and the effects of varying concentrations of (**1**) and reserpine were determined to generate dose–response profiles (Kaatz et al., 2000). The total time course for the efflux assay was 5 min. Assays were performed in duplicate and mean results were expressed as the percentage reduction of total efflux observed for test strains in the absence of inhibitors.

3.6. 12-Methoxy-trans-carnosic acid (*4*)

Colourless crystals; $[\alpha]_D^{21} + 250(c\ 0.04)$; UV ($CH_3OH$) λ_{max} (log ε): 226 (3.39), 276 (1.71); IR ν_{max} (thin film) cm^{-1}: 2959, 2360, 2342, 1734, 1457, 1364, 1229, 668; ^1H NMR and ^{13}C NMR (CD_3OD): see Table 1; ESI-MS (*m*/*z*): 347.2 $[M + H]^+$ (calc. for $C_{21}H_{31}O_4$, 347.2).

3.7. 12-Methoxy-cis-carnosic acid (*5*)

Colourless crystals; $[\alpha]_D^{21} + 50(c\ 0.06)$; UV ($CH_3OH$) λ_{max} (log ε): 224 (3.30), 277 (0.8); IR ν_{max} (thin film) cm^{-1}: 2959, 2360, 2342, 1734, 1559, 1457, 1367, 1221, 668; ^1H NMR and ^{13}C NMR (CD_3OD): see Table 1; ESI-MS (*m*/*z*): 347.2 $[M + H]^+$ (calc. for $C_{21}H_{31}O_4$, 347.2).

Acknowledgement

We thank the EPSRC for a PhD studentship (GR/N64496/01) for M. Oluwatuyi and for a multi project equipment grant (GR/R47646/01).

References

Al-Hazimi, G.M.H, Miana, A.G., Deep, M.S.H., 1987. Terpenoids from *Salvia lanigera*. Phytochemistry 26, 1091–1093.

Bradley, G., Ling, V., 1994. P-glycoprotein, multidrug resistance and tumour progression. Cancer and Metastasis Review 13, 223–233.

Crowcroft, N.S., Catchpole, M., 2002. Mortality from methicillin-resistant *Staphylococcus aureus* in England and Wales: analysis of death certificates. British Medical Journal 325, 1390–1391.

Del Campo, J., Amiot, M.J., Nguyen-The, C., 2000. Antimicrobial effect of rosemary extracts. Journal of Food Production 63, 1359–1368.

Dimayuga, R.E., Garcia, S.K., Nielsen, P.H., Christophersen, C., 1991. Traditional medicine of baja california sur (Mexico). III. Carnosol. A diterpene antibiotic from *Lepechinia hastate*. Journal of Ethnopharmacology 31, 43–48.

Gibbons, S., 2004. Anti-staphylococcal plant natural products. Natural Product Reports 21, 263–277.

Gibbons, S., Udo, E.E., 2000. The effect of reserpine, a modulator of multidrug efflux pumps, on the in vitro activity of tetracycline against clinical isolates of methicillin resistant *Staphylococcus aureus* (MRSA) possessing the tet(K) determinant. Phytotherapy Research 14, 139–140.

Gibbons, S., Oluwatuyi, M., Veitch, N.C., Gray, A.I., 2003a. Bacterial resistance modifying agents from *Lycopus europaeus*. Phytochemistry 62, 83–87.

Gibbons, S., Oluwatuyi, M., Kaatz, G.W., 2003b. A novel inhibitor of multidrug efflux pumps in *Staphylococcus aureus*. Journal of Antimicrobial Chemotherapy 51, 13–17.

Hancock, R.E.W., 1997. The bacterial outer membrane as a drug barrier. Trends in Microbiology 5, 37–42.

Inatani, R., Nobuji, N., Hidetsugu, F., Haruo, S., 1982. Structure of a new antioxidative phenolic diterpene isolated from rosemary (*Rosmarinus officinalis* L.). Agricultural and Biological Chemistry 46, 1661–1666.

Kaatz, G.W., Seo, S.M., 1997. Mechanisms of fluoroquinolone resistance in genetically related strains of *Staphylococcus aureus*. Antimicrobial Agents and Chemotherapy 41, 2733–2737.

Kaatz, G.W., Seo, S.M., Ruble, C.A., 1993. Efflux-mediated fluoroquinolone resistance in *Staphylococcus aureus*. Antimicrobial Agents and Chemotherapy 37, 1086–1094.

Kaatz, G.W., Seo, S.M., O'Brien, L., Wahiduzzaman, M., Foster, T.J., 2000. Evidence for the existence of a multidrug efflux transporter distinct from NorA in *Staphylococcus aureus*. Antimicrobial Agents and Chemotherapy 44, 1404–1406.

Kaatz, G.W., Moudgal, V.V., Seo, S.M., Kristiansen, J.E., 2003a. Phenothiazines and thioxanthenes inhibit multidrug efflux pump activity in *Staphylococcus aureus*. Antimicrobial Agents and Chemotherapy 47, 719–726.

Kaatz, G.W., Moudgal, V.V., Seo, S.M., Bondo-Hansen, J., Kristiansen, J.E., 2003b. Phenylpiperidine selective serotonin reuptake inhibitors interfere with multidrug efflux pump activity in *Staphylococcus aureus*. International Journal of Antimicrobial Agents 22, 263–264.

Lemonica, I.P., Demasceno, D.C., Di-Stasi, L.C., 1996. Study of the embryonic effects of an extract of rosemary (*Rosmarinus officinalis* L.). Brazilian Journal of Medical and Biological Research 29, 223–227.

Marshall, N.J., Piddock, L.J.V., 1997. Antibacterial efflux systems. Microbiologia 13, 285–300.

Markham, P.N., Westhaus, E., Klyachko, K., Johnson, M.E., Neyfakh, A.A., 1999. Multiple novel inhibitors of the NorA multidrug transporter of *Staphylococcus aureus*. Antimicrobial Agents and Chemotherapy 43, 2404–2408.

Minnunni, M., Wolleb, U., Mueller, O., Pfeifer, A., Aeschbacher, H.U., 1992. Natural antioxidants as inhibitors of oxygen species induced mutagenicity. Mutation Research 269, 193–200.

Nikaido, H., 1998. The role of outer membrane and efflux pumps in the resistance of Gram-negative bacteria. Can we improve drug access?. Drug Research Update 1, 93–98.

Ozcan, M., 2003. Antioxidant activity of rosemary, sage, and sumac extracts and their combinations on stability of natural peanut oil. Journal of Medicinal Food 6, 267–270.

Plouzek, C.A., Ciolino, H.P., Clarke, R., Yeh, G.C., 1999. Inhibition of P-glycoprotein activity and reversal of multidrug resistance in vitro rosemary extract. European Journal of Cancer 35, 1541–1545.

Schwarz, K., Ternes, W., 1992. Antioxidative Constituents of *Rosmarinus officinalis* and *Salvia officinalis*. Zeitschrift Fur Lebensmittel Untersuchung und Forschung 195, 99–103.

Stermitz, F.R., Lorenz, P., Tawara, J.N., Zenewicz, L.A., Lewis, K., 2000a. Synergy in a medicinal plant: antimicrobial action of berberine potentiated by 5′-methoxyhydrocarpin, a multidrug pump inhibitor. Proceedings of the National Academy of Sciences of the United States of America 97, 1433–1437.

Stermitz, F.R., Tawara-Matsuda, J., Lorenz, P., Mueller, P., Zenewicz, L.A., Lewis, K., 2000b. 5′-methoxyhydrocarpin-D and pheophorbide A: *Berberis* species components that potentiate berberine growth inhibition of resistant *Staphylococcus aureus*. Journal of Natural Products 63, 1146–1149.

Yang, O.H., Suh, D., Han, B.H., 1995. Isolation and characterisation of platelet-activating factor receptor binding antagonist from *Biota orientalis*. Planta Medica 61, 37–40.

Journal of Antimicrobial Chemotherapy (2003) **51**, 13–17
DOI: 10.1093/jac/dkg044

JAC

Original articles

A novel inhibitor of multidrug efflux pumps in *Staphylococcus aureus*

Simon Gibbons[1]*, Moyosoluwa Oluwatuyi[1] and Glenn W. Kaatz[2]

[1]Centre for Pharmacognosy and Phytotherapy, The School of Pharmacy, University of London, 29–39 Brunswick Square, London WC1N 1AX, UK; [2]Division of Infectious Diseases, Department of Internal Medicine, School of Medicine, Wayne State University and the John D. Dingell Department of Veterans Affairs Medical Center, Detroit, MI 48201, USA

Received 16 September 2002; returned 8 October 2002; revised 11 October 2002; accepted 15 October 2002

GG918, a synthetic inhibitor of P-glycoprotein-mediated mammalian tumour multidrug resistance, was found to be equipotent to reserpine in enhancing the *in vitro* activity of norfloxacin and ciprofloxacin against strains of *Staphylococcus aureus* expressing distinct efflux-related multidrug resistance pumps. Four- to eight-fold reductions in MICs of these fluoroquinolones were observed for SA-1199B, a strain that overexpresses NorA (the major *S. aureus* multidrug transporter), and SA-K2068, which possesses a multidrug efflux-related pump distinct from NorA. Neither inhibitor potentiated the activity of newer fluoroquinolones such as levofloxacin or moxifloxacin by more than two-fold, and this effect was observed only in SA-1199B and SA-K2068. GG918 and reserpine exposure resulted in two- to four-fold reductions in norfloxacin and ciprofloxacin MICs in a fluoroquinolone-susceptible control strain and in strains expressing the MsrA and TetK proteins, which mediate efflux-related resistance to macrolides and tetracyclines, respectively, suggesting inhibition of as yet uncharacterized pumps for which norfloxacin and ciprofloxacin are substrates. In the MsrA- and TetK-expressing strains no more than a two-fold augmentation of erythromycin or tetracycline activity was observed with either inhibitor, suggesting minimal, if any, inhibitory activity against these efflux proteins. Using GG918 as a lead compound, a structure–activity evaluation may reveal a more potent and broader spectrum inhibitor of *S. aureus* antibiotic efflux pumps.

Keywords: multidrug efflux, GG918, *Staphylococcus aureus*

Introduction

Multidrug (MDR) efflux is an increasingly reported phenomenon and has been described for many organisms, including bacteria, fungi and protozoa, and as a mechanism of resistance in mammalian tumour cells.[1] Bacteria possess a wide array of drug efflux proteins and a number of clinically relevant species, most notably *Staphylococcus aureus*, *Pseudomonas aeruginosa* and *Escherichia coli*, utilize these transporters as part of their resistance strategy.[2] Many of these efflux mechanisms export an extensive range of structurally unrelated antibiotics from the cell, resulting in a reduced intracellular concentration and thus reduced susceptibility.

Examples of efflux-related resistance mechanisms that have been described for *S. aureus* include those conferred by QacA and NorA, which are MDR transporters, and the more specific MsrA and TetK transport proteins.[3–6] These export proteins were originally described to efflux quaternary ammonium salts (antiseptics), fluoroquinolones, macrolides and tetracyclines, respectively, although these efflux proteins, especially QacA and NorA, actively export a broad array of structurally dissimilar drugs from the bacterial cell.

GG918 (Figure 1) is a synthetic compound that was originally discovered as part of a screening programme designed to identify inhibitors of mammalian P-glycoprotein (P-gp). P-gp is an ABC-type transporter that exports numerous anti-

*Corresponding author. Tel: +44-20-7753-5913; Fax: +44-20-7753-5909; E-mail: simon.gibbons@ulsop.ac.uk

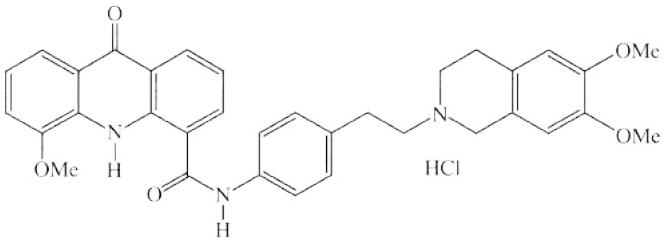

Figure 1. Structure of GG918.

neoplastic agents from cancer cells, making them drug resistant.[1,7] It has been shown that co-administration of GG918 with paclitaxel significantly increases the systemic exposure to this anti-neoplastic agent.[8] Toxicities associated with GG918 were not observed in this study and the mean maximal serum concentration of the compound was 0.43 ± 0.27 mg/L. The mean area under the plasma concentration–time curve of paclitaxel after oral administration of 1 g of GG918 was comparable to that achieved with oral paclitaxel in combination with another P-gp inhibitor, cyclosporin A.[9] Unlike cyclosporin A, GG918 has no known immunosuppressive activity and may be a better candidate for clinical use as a P-gp inhibitor.

Previous work on inhibitors of MDR pumps in *S. aureus* includes the screening of a synthetic library against the NorA MDR transporter.[10] These inhibitors acted in a synergic manner with ciprofloxacin and dramatically suppressed the emergence of ciprofloxacin-resistant *S. aureus* upon *in vitro* exposure to the drug. Other inhibitors of MDR pumps in *S. aureus* include the anti-hypertensive plant alkaloid reserpine, the porphyrin pheophorbide A, 5′-methoxyhydnocarpin D (a flavonolignan) and selected flavones.[11] The antimicrobial activity of berberine, a natural antibiotic found in some plants and also a NorA substrate, was found to be potentiated by low concentrations of 5′-methoxyhydnocarpin D by inhibition of its efflux.[12] Identification of effective inhibitors of NorA and other *S. aureus* efflux pumps could restore the clinical utility of pump substrates, which prompted the current investigation of the activity of GG918 as an inhibitor of such pumps.

Materials and methods

Bacterial strains and media

S. aureus RN4220 containing plasmid pUL5054, which carries the gene encoding the MsrA macrolide efflux protein, and strain CD-1281, which possesses the TetK tetracycline efflux protein, were generously provided as gifts from J. Cove (University of Leeds, UK) and C. Dowson (University of Warwick, UK), respectively. SA-1199B, which overexpresses the NorA MDR efflux protein, SA-K2068, which exhibits an MDR efflux phenotype conferred by a pump distinct from NorA, and *S. aureus* ATCC 25923 were also used.[13,14] All strains were cultured on nutrient agar (Oxoid, Basingstoke, UK) before determination of MICs. Cation-adjusted Mueller–Hinton broth (MHB; Oxoid) was used for susceptibility tests.

Antibiotics and chemicals

Tetracycline, norfloxacin and erythromycin were obtained from Sigma (Poole, UK). Ciprofloxacin, levofloxacin and moxifloxacin were obtained from their respective manufacturers. GG918 was provided by GlaxoSmithKline (Stevenage, UK).

Susceptibility tests

MICs were determined at least in duplicate by microdilution techniques according to the NCCLS guidelines, using *S. aureus* 25923 as a quality control strain.[15] The effects of GG918 and reserpine (final concentrations 10 and 20 mg/L, respectively) on MICs were also determined. Both of these compounds were dissolved in DMSO before dilution into MHB for use in MIC determinations. The highest concentration of DMSO remaining after dilution (25%, v/v) caused no inhibition of bacterial growth (data not shown).

Ethidium efflux

Ethidium bromide (EtBr) is a substrate for many Gram-positive MDR pumps, including NorA. The efficiency of efflux pumps for which EtBr is a substrate can be assessed fluorometrically by the loss of fluorescence over time from cells loaded with EtBr. SA-1199B and SA-K2068 were loaded with EtBr as previously described, and the effect of varying concentrations of reserpine and GG918 on EtBr efflux was determined to generate a dose–response profile for each compound.[16] Results were expressed as percentage reduction of the total efflux observed for test strains in the absence of inhibitors.

Results and discussion

Susceptibility data for test strains in the presence and absence of inhibitors are shown in Table 1. Neither reserpine nor GG918 by themselves had inhibitory activity against any test strain at the concentrations employed (data not shown). The presence of either compound resulted in at least a four-fold reduction in norfloxacin MICs for all strains possessing efflux-related resistance phenotypes, regardless of that phenotype. With respect to ciprofloxacin, a four-fold or greater potentiation of activity was observed only with SA-1199B and SA-K2068; no more than two-fold MIC changes were observed for the other test strains. The inhibitors only minimally augmented the activity of levofloxacin and moxifloxacin, which are more recently developed fluoroquinolones with

Table 1. MICs of test strains (mg/L)

Antimicrobial[a]	RN4220 (MsrA)	CD-1281 (TetK)	SA-1199B (NorA)	SA-K2068 (MDR)	ATCC 25923
Norfloxacin	1	1	32	8	0.5
+Reserpine	0.25 (4)[b]	0.25 (4)	8 (4)	1 (8)	0.125 (4)
+GG918	0.25 (4)	0.25 (4)	4 (8)	2 (4)	0.25 (2)
Ciprofloxacin	0.25	0.25	8	4	0.125
+Reserpine	0.125 (2)	0.125 (2)	1 (8)	0.5 (8)	0.063 (2)
+GG918	0.25 (NC)	0.125 (2)	1 (8)	1 (4)	0.125 (NC)
Levofloxacin	0.25	0.25	2	1	0.125
+Reserpine	0.25 (NC)	0.25 (NC)	1 (2)	0.5 (2)	0.125 (NC)
+GG918	0.25 (NC)	0.25 (NC)	1 (2)	0.5 (2)	0.125 (NC)
Moxifloxacin	0.125	0.125	0.25	0.25	0.031
+Reserpine	0.125 (NC)	0.125 (NC)	0.125 (2)	0.125 (2)	0.031 (NC)
+GG918	0.125 (NC)	0.125 (NC)	0.25 (NC)	0.25 (NC)	0.031 (NC)
Erythromycin	64	0.5	0.25	0.5	0.125
+Reserpine	64 (NC)	0.25 (2)	0.125 (2)	0.5 (NC)	0.125 (NC)
+GG918	32 (2)	0.25 (2)	0.125 (2)	0.5 (NC)	0.125 (NC)
Tetracycline	0.25	32	0.125	1.0	0.25
+Reserpine	0.25 (NC)	16 (2)	0.063 (2)	0.5 (2)	0.25 (NC)
+GG918	0.125 (2)	16 (2)	0.063 (2)	0.5 (2)	0.25 (NC)

[a]Antimicrobials were tested alone, or in combination with reserpine (20 mg/L) or GG918 (10 mg/L).
[b]Fold reductions are given in parentheses.
MDR, non-NorA multidrug efflux phenotype; NC, no change.

improved potency compared with ciprofloxacin against *S. aureus*.

The presence of GG918 or reserpine resulted in no more than a two-fold reduction in erythromycin and tetracycline MICs for all strains. The equivalence in activity regardless of the efflux-related resistance trait present suggests that the modest MIC reductions observed are not related to specific inhibition of MsrA or TetK.

Overall, the effects of GG918 and reserpine on susceptibility data were equivalent for all test strains. In general, the activities of norfloxacin and ciprofloxacin were the most potentiated. This was especially true for SA-1199B, which overexpresses NorA, and SA-K2068, which possesses a novel non-NorA MDR pump. Both norfloxacin and ciprofloxacin are quite hydrophilic molecules with small substituents at the C7 and C8 positions, characteristics that make them more favourable substrates for NorA, and probably for the SA-K2068 efflux pump.[17] The lack of significant activity of either inhibitor on MICs of levofloxacin and moxifloxacin for strains bearing these pumps may relate to molecular hydrophobicity in the case of levofloxacin and structural features in the case of both compounds, characteristics that may reduce recognition and transport.

The sequence of the *S. aureus* genome has recently been published, and examination of the data reveals the presence of up to 17 open reading frames encoding putative drug transporters.[18] The four-fold potentiation of norfloxacin activity by inhibitors in RN4220 (MsrA), CD-1281 (TetK) and ATCC 25923, strains not possessing known quinolone efflux systems, is likely to be related to the inhibition of one or more of these as yet uncharacterized pumps. These data indicate that GG918 and reserpine may have more affinity for MDR-type pumps than for more limited spectrum pumps such as MsrA and TetK, or at least for pumps for which fluoroquinolones are substrates.

The effect of inhibitors on the EtBr efflux capability of SA-1199B and SA-K2068 compared with the effect observed for reserpine is shown in Figure 2. For SA-1199B, concentrations of ≤10 μM GG918 were more potent than the same concentrations of reserpine. Both inhibitors were very potent versus SA-K2068, with GG918 appearing more effective at concentrations of ≤5 μM. These data indicate that at low concentrations GG918 is more potent than reserpine as an inhibitor of MDR pump-mediated EtBr efflux in *S. aureus*.

The development of efflux pump inhibitors, which could be used in conjunction with existing antibiotics, could extend the useful lifetime of some antibiotics by improving therapeutic efficacy and by suppressing the emergence of resistant variants that might otherwise arise during treatment. The former phenomenon has been evaluated in an animal model of a *P. aeruginosa* infection caused by a strain overexpressing the MexAB–OprM MDR efflux system, with treatment consisting of levofloxacin plus inhibitor or levofloxacin alone.[19] Improved therapeutic efficacy was observed in animals treated with the combination versus those treated with only levofloxacin. The latter phenomenon has been demonstrated

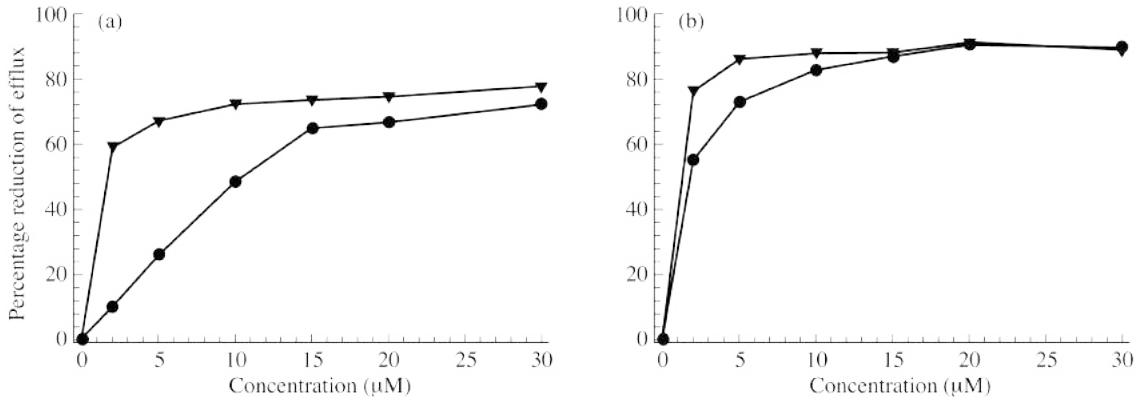

Figure 2. Effect of inhibitors on ethidium bromide efflux; the data presented are means of duplicate experiments. (a) SA-1199B; (b) SA-K2068; inverted filled triangles, GG918; filled circles, reserpine.

for both NorA and PmrA, a recently described *Streptococcus pneumoniae* MDR transporter, where it has been shown that the combination of reserpine and a fluoroquinolone markedly reduced the emergence of resistant variants *in vitro* compared with what was observed with the fluoroquinolone alone.[10,20] However, the concentrations of reserpine required for the observed effect were not clinically relevant as the potential for adverse effects, such as neurotoxicity, eliminates the use of reserpine as an efflux pump inhibitor in the clinical setting.

GG918 is a first step toward developing an inhibitor active against *S. aureus* antibiotic efflux pumps, especially NorA. A further effort to identify an even more potent compound with a good toxicity profile and broader spectrum of activity seems reasonable. The combination of a broad-spectrum MDR pump inhibitor with antibiotics that are known pump substrates could reduce the morbidity and mortality that might result from a delay in the institution of effective therapy for serious *S. aureus* infections.

Acknowledgements

Drs Edet Udo, Jon Cove and Professor Christopher Dowson are thanked for the provision of bacterial strains. Glaxo-SmithKline are thanked for the provision of GG918. We thank the Royal Society (Grant No. 21595) for a research grant to S. Gibbons and the EPSRC for a PhD studentship for M. Oluwatuyi.

References

1. Ling, V. (1997). Multidrug resistance: molecular mechanisms and clinical relevance. *Cancer Chemotherapy and Pharmacology* **40**, *Suppl.*, S3–8.

2. Marshall, N. J. & Piddock, L. J. V. (1997). Antibacterial efflux systems. *Microbiologia* **13**, 285–300.

3. Littlejohn, T. G., Paulsen, I. T., Gillespie, M. T., Tennent, J. M., Midgley, M., Jones, I. G. *et al.* (1992). Substrate specificity and energetics of antiseptic and disinfectant resistance in *Staphylococcus aureus*. *FEMS Microbiology Letters* **74**, 259–65.

4. Ubukata, K., Itoh-Yamashita, N. & Konno, M. (1989). Cloning and expression of the *norA* gene for fluoroquinolone resistance in *Staphylococcus aureus*. *Antimicrobial Agents and Chemotherapy* **33**, 1535–9.

5. Ross, J. I., Eady, E. A., Cove, J. H., Cunliffe, W. J., Baumberg, S. & Wootton, J. C. (1990). Inducible erythromycin resistance in staphylococci is encoded by a member of the ATP-binding transport super-gene family. *Molecular Microbiology* **4**, 1207–14.

6. Guay, G. G., Khan, S. A. & Rothstein, D. M. (1993). The *tet*(K) gene of plasmid pT181 of *Staphylococcus aureus* encodes an efflux protein that contains 14 transmembrane helices. *Plasmid* **30**, 163–6.

7. Hyafil, F., Vergely, C., Du Vignaud, P. & Grand-Perret, T. (1993). *In vitro* and *in vivo* reversal of multidrug resistance by GF120918, an acridonecarboxamide derivative. *Cancer Research* **53**, 4595–602.

8. Malingré, M. M., Beijnen, J. H., Rosing, H., Koopman, F. J., Jewell, R. C., Paul, E. M. *et al.* (2001). Co-administration of GF120918 significantly increases the systemic exposure to oral paclitaxel in cancer patients. *British Journal of Cancer* **84**, 42–7.

9. Malingré, M. M., Terwogt, J. M., Beijnen, J. H., Rosing, H., Koopman, F. J., van Tellingen, O. *et al.* (2000). Phase I and pharmacokinetic study of oral paclitaxel. *Journal of Clinical Oncology* **18**, 2468–75.

10. Markham, P. N., Westhaus, E., Klyachko, K., Johnson, M. E. & Neyfakh, A. A. (1999). Multiple novel inhibitors of the NorA multidrug transporter of *Staphylococcus aureus*. *Antimicrobial Agents and Chemotherapy* **43**, 2404–8.

11. Guz, N. R., Stermitz, F. R., Johnson, J. B., Beeson, T. D., Willen, S., Hsiang, J. *et al.* (2001). Flavonolignan and flavone inhibitors of a *Staphylococcus aureus* multidrug resistance pump: structure–activity relationships. *Journal of Medicinal Chemistry* **44**, 261–8.

12. Stermitz, F. R., Lorenz, P., Tawara, J. N., Zenewicz, L. A. & Lewis, K. (2000). Synergy in a medicinal plant: antimicrobial action of berberine potentiated by 5′-methoxyhydnocarpin, a multidrug pump inhibitor. *Proceedings of the National Academy of Sciences, USA* **97**, 1433–7.

13. Kaatz, G. W., Seo, S. M. & Ruble, C. A. (1993). Efflux-mediated fluoroquinolone resistance in *Staphylococcus aureus*. *Antimicrobial Agents and Chemotherapy* **37**, 1086–94.

14. Kaatz, G. W., Moudgal, V. V. & Seo, S. M. (2002). Identification and characterization of a novel efflux-related multidrug resistance phenotype in *Staphylococcus aureus*. *Journal of Antimicrobial Chemotherapy* **50**, 833–8.

15. National Committee for Clinical Laboratory Standards. (1999). *Methods for Dilution Antimicrobial Susceptibility Tests for Bacteria that Grow Aerobically—Fifth Edition: Approved Standard M7-A5*. NCCLS, Villanova, PA, USA.

16. Kaatz, G. W., Seo, S. M., O'Brien, L., Wahiduzzaman, M. & Foster, T. J. (2000). Evidence for the existence of a multidrug efflux transporter distinct from NorA in *Staphylococcus aureus*. *Antimicrobial Agents and Chemotherapy* **44**, 1404–6.

17. Takenouchi, T., Tabata, F., Iwata, Y., Hanzawa, H., Sugawara, M. & Ohya, S. (1996). Hydrophilicity of quinolones is not an exclusive factor for decreased activity in efflux-mediated resistant mutants of *Staphylococcus aureus*. *Antimicrobial Agents and Chemotherapy* **40**, 1835–42.

18. Kuroda, M., Ohta, T., Uchiyama, I., Baba, T., Yuzawa, H., Kobayashi, I. *et al*. (2001). Whole genome sequencing of methicillin-resistant *Staphylococcus aureus*. *Lancet* **357**, 1225–40.

19. Renau, T. E., Leger, R., Flamme, E. M., Sangalang, J., She, M. W., Yen, R. *et al*. (1999). Inhibitors of efflux pumps in *Pseudomonas aeruginosa* potentiate the activity of the fluoroquinolone levofloxacin. *Journal of Medicinal Chemistry* **42**, 4928–31.

20. Markham, P. N. (1999). Inhibition of the emergence of ciprofloxacin resistance in *Streptococcus pneumoniae* by the multidrug efflux inhibitor reserpine. *Antimicrobial Agents and Chemotherapy* **43**, 988–9.

PHYTOTHERAPY RESEARCH
Phytother. Res. **14**, 139–140 (2000)

SHORT COMMUNICATION

The Effect of Reserpine, a Modulator of Multidrug Efflux Pumps, on the *in vitro* Activity of Tetracycline Against Clinical Isolates of Methicillin Resistant *Staphylococcus aureus* (MRSA) Possessing the *tet*(K) Determinant

Simon Gibbons[1]* and E. E. Udo[2]

[1]Centre for Pharmacognosy and Phytotherapy, The School of Pharmacy, University of London, 29–39 Brunswick Square, London WC1N 1AX, UK
[2]Department of Microbiology, Faculty of Medicine, Kuwait University, P.O. Box 24923, Safat 13110, Kuwait

As part of a screening programme to identify modulators of multidrug efflux in methicillin resistant *Staphyloccocus aureus* (MRSA), we have validated our assays using the antihypertensive plant alkaloid reserpine. Clinical isolates of MRSA were resistant to tetracycline and shown to possess the *tet*(K) determinant which encodes for the Tet(K) efflux protein, which conferred high level resistance to tetracycline (MIC = 128 μg/mL). In the presence of reserpine, a known inhibitor of multidrug resistance (mdr) efflux pumps, this MIC was significantly reduced (MIC = 32 μg/mL).

Keywords: efflux; MRSA; Tet(K); multidrug resistance; mdr.

INTRODUCTION

The occurrence and proliferation of methicillin resistant *Staphylococcus aureus* (MRSA) is cause for great concern in the clinical environment due to the few effective therapeutic agents that can be used against this organism (Horikawa *et al.*, 1999). The last group of antibiotics available for the treatment of MRSA are the glycopeptides, typically vancomycin, but unfortunately resistance to this agent has already been encountered in Japan (Hiramatsu *et al.*, 1997) and the United States (Martin and Wilcox, 1997; Perl, 1999; Rotun *et al.*, 1999), and more recently in the United Kingdom (unpublished report on vancomycin resistance in *Staphylococcus aureus* at Glasgow Royal Infirmary, June 1999).

Efflux is an important mechanism of resistance in many clinically relevant pathogens, notably, *Streptococcus pneumoniae* (Markham, 1999), *Pseudomonas aeruginosa* and *Neisseria gonorrhoeae* (Marshall and Piddock, 1997). In *Staphylococcus aureus*, efflux mechanisms have been demonstrated to confer resistance to macrolides, fluoroquinolones and the tetracyclines *via* the Msr(A) (Ross *et al.*, 1990), Nor(A) (Ng *et al.*, 1994) and Tet(K) (Guay *et al.*, 1993) efflux proteins respectively. The *tet*(K) gene encodes for an hydrophobic, 50.6 KDa membrane bound protein that actively effluxes tetracycline and is assumed to confer resistance to this agent (Guay *et al.*, 1993).

We have been screening elements of the Kuwaiti flora for modulators of Tet(K) mediated resistance in clinical isolates of MRSA and have validated our assays using the multidrug efflux inhibitor reserpine, which has been shown to modulate resistance in bacteria possessing the NorA and Bmr efflux mechanisms (Ng *et al.*, 1994).

* Correspondence to: Dr S. Gibbons, The School of Pharmacy, 29–39 Brunswick Square, London, WC1N 1AX, UK.

MATERIALS AND METHODS

Bacterial strains. MRSA strains IS-58 and XU212 were cultured from clinical isolates from the Ibn Sina and Adan hospitals, respectively. *S. aureus* standard strain ATCC 25923 was obtained from the American Type Culture Collection. All strains were cultured on nutrient agar (Oxoid) prior to determination of minimum inhibitory concentration.

Primer details for the *tet*(K) gene. The *tet*(K) gene in strains IS-58 and XU212 was detected in polymerase chain reaction (PCR) experiments using two 18- mer oligonucleotide primers, synthesis based on the DNA sequence of the *S. aureus* plasmid, pT181, which encodes a tetracycline efflux protein. The sequences were: primer K1, 5′-CAG CAG ATC CTA CTC CTT-3′ corresponding to nucleotides 531 to 549 and primer K2, 5′-TCG ATA GGA ACA GCA GTA-3′, which is complementary to nucleotides 682 to 700 of the *tet*(K) gene and separated by 168 base pairs.

Protocol for PCR. The PCR mixture consisted of 3 μL of template DNA, 10 pmol of K1 and K2 primers and 45 μL of PCR supermix (Gibco BRL). DNA amplification was carried out for 30 cycles in a final volume of 50 μL of reaction mixture as follows: denaturation at 94 °C (1 min),

Received 30 July 1999
Accepted 10 October 1999

Table 1. Minimum inhibitory concentrations (MICs) for test organisms

	MIC (μg/mL) of tetracycline	
Strain		+R
XU212	128	32
IS-58	128	32
ATCC 25923	0.16	0.16

+R, MIC measured in the presence of reserpine at a concentration of 10 μg/mL.

annealing at 55 °C (1 min) and extension at 72 °C for 1 min. After amplification, 15 μL of product was analysed by agarose gel 1.5% (w/v) electrophoresis in Tris buffer and stained with ethidium bromide. The amplified DNA was visualized under UV light and photographed.

Determination of Minimum Inhibitory Concentration (MIC). Mueller-Hinton broth (MHB) (Oxoid) was adjusted to contain 20 mg/L and 10 mg/L of Ca^{2+} and Mg^{2+} respectively. An inoculum density of 10^5 cfu of each of the test organisms was prepared in normal saline (0.9 g/L). MHB (125 μL) was dispensed into 10 wells of a 96-well microtitre plate (Nunc, 0.3 mL volume) and then 125 μL of tetracycline (2048 μg/mL) (Sigma Chemical Co.) was serially diluted (2 fold) into each of the wells. 125 μL of inoculum was then added to each of the wells, which resulted in a tetracycline concentration range of 512–1 μg/mL. The plate was then incubated at 36 °C for 18 h and the MIC was recorded as the lowest concentration at which no growth was observed. In the case of ATCC 25923 *Staphylococcus aureus*, a tetracycline concentration range of 10–0.02 μg/mL was used.

For the modulation of resistance experiment, reserpine (Sigma Chemical Co.) was incorporated into the MHB to give a final concentration of 10 μg/mL.

RESULTS AND DISCUSSION

MRSA strains IS-58 and XU212 were highly resistant to tetracycline (Table 1) and exhibited MICs of 128 μg/mL as a result of the presence of the *tet*(K) determinant which encodes for the Tet(K) efflux protein. When compared with the standard ATCC 25923 strain, IS-58 and XU212 exhibited an 800 fold increase in resistance to tetracycline, which renders the use of this antibiotic against these organisms as therapeutically redundant.

The incorporation of the antihypertensive plant alkaloid reserpine into the medium, clearly affected the MIC of tetracycline in the MRSA strains and lowered the MIC by a factor of 4. In contrast, the incorporation of reserpine into the medium did not effect the MIC for the standard ATCC strain.

This 4-fold decrease in MIC is in good agreement with data for MICs recorded in the presence and absence of reserpine of norfloxacin resistant *S. aureus* possessing the Nor(A) fluoroquinolone efflux protein (Ng *et al*., 1994).

This is, we believe, the first report of a reduction of MIC in clinical isolates of MRSA possessing the Tet(K) efflux protein in the presence of reserpine.

Modulators of drug resistance would clearly have benefit for the treatment of multidrug resistant (mdr) strains of bacteria for which the majority of therapeutic antibiotics are of no further clinical use. Inhibitors of drug efflux mechanisms could, in combination, greatly extend the useful lifetime of older conventional antibiotics, for example with the tetracyclines. This concept of resistance modulation could be extended to other multidrug resistant pathogens such as fluoroquinolone resistant *Streptococcus pneumoniae*, azole resistant *Candida albicans* or macrolide resistant *Escherichia coli*, all of which produce efflux proteins as part of their resistance mechanisms (Markham, 1999; Cannon *et al*., 1998, Marshall and Piddock, 1997).

REFERENCES

Cannon, R. D., Fischer, F. J., Niimi, K., Niimi, M., and Arisawa, M. (1998). Drug pumping mechanisms in *Candida albicans*. *Jpn J. Med. Mycol.* **39**, 73–78.

Guay, G. G., Khan, S. A., and Rothstein, D. M. (1993). The *tet*(K) gene of plasmid pT181 of *Staphylococcus aureus* encodes an efflux protein that contains 14 transmembrane helices. *Plasmid* **30**, 163–166.

Hirimatsu, K., Hanaki, H., Ino, T., Yabuta, K., Oguri, T., and Tenover, F. C. (1997). Methicillin-resistant *Staphylococcus aureus* clinical isolates with reduced vancomycin susceptibility. *J. Antimicrob. Chemother.* **40**, 135–136.

Horikawa, M., Noro, T., and Kamei, Y. (1999). *In vitro* anti-methicillin-resistant *Staphylococcus aureus* activity found in extracts of marine algae indigenous to the coastline of Japan. *J. Antibiot.* **52**, 186–189.

Markham, P. N. (1999). Inhibition of the emergence of ciprofloxacin resistance in *Streptococcus pneumoniae* by the multidrug efflux inhibitor reserpine. *Antimicrob. Agents. Chemother.* **43**, 988–989.

Marshall, N. J., and Piddock, L. J. V. (1997). Antibacterial efflux systems. *Microbiologia* **13**, 285–300.

Martin, R., and Wilcox, K. R. (1997). Update: *Staphylococcus aureus* with reduced susceptibility to vancomycin, United States. *MMWR* **46** (35), 813–815.

Ng, E. Y. W., Trucksis, M., and Hooper, D. C. (1994). Quinolone resistance mediated by *norA:* physiologic characterization and relationship to *flqB,* a quinolone resistance locus on the *Staphylococcus aureus* chromosome. *Antimicrob. Agents. Chemother.* **38**, 1345–1355.

Perl, T. M. (1999). The threat of vancomycin resistance. *Am. J. Med.* **106**, (5A), 26S–37S.

Ross, J. I., Eady, E. A., Cove, J. H., Cunliffe, W. J., Baumberg, S., and Wootton, J. C. (1990). Inducible erythromycin resistance in staphylococci is encoded by a member of the ATP-binding transport super-gene family. *Mol. Microbiol.* **4**, 1207–1214.

Rotun, S. S., Schoomaker, D. J., Maaupin, P. S., Tenover, F. C., Hill, B. C., and Ackman, M. (1999). *Staphylococcus aureus* with reduced susceptibility to vancomycin isolated from a patient with fatal bacteraemia. *Emerg. Infect. Dis.* **5**, 147–149.

European Journal of Medicinal Chemistry 155 (2018) 255–262

Contents lists available at ScienceDirect

European Journal of Medicinal Chemistry

journal homepage: http://www.elsevier.com/locate/ejmech

Short communication

Total synthesis of acylphloroglucinols and their antibacterial activities against clinical isolates of multi-drug resistant (MDR) and methicillin-resistant strains of *Staphylococcus aureus*

M. Mukhlesur Rahman [a, b], Winnie K.P. Shiu [a, 1], Simon Gibbons [a], John P. Malkinson [a, *]

[a] Research Department of Pharmaceutical and Biological Chemistry, UCL School of Pharmacy, 29-39 Brunswick Square, London, WC1N 1AX, UK
[b] Medicine Research Group, School of Health, Sport and Bioscience, University of East London, Stratford Campus, Water Lane, London, E15 4LZ, UK

ARTICLE INFO

Article history:
Received 29 March 2018
Received in revised form
22 May 2018
Accepted 24 May 2018
Available online 25 May 2018

Keywords:
Acylphloroglucinols
Total synthesis
Anti-staphylococcal
MRSA

ABSTRACT

Bioassay-directed drug discovery efforts focusing on various species of the genus *Hypericum* led to the discovery of a number of new acylphloroglucinols including (*S*,*E*)-1-(2-((3,7-dimethylocta-2,6-dien-1-yl) oxy)-4,6-dihydroxyphenyl)-2-methylbutan-1-one (**6**, olympicin A) from *H. olympicum*, with MICs ranging from 0.5 to 1 mg/L against a series of clinical isolates of multi-drug-resistant (MDR) and methicillin-resistant *Staphylococcus aureus* (MRSA) strains. The promising activity and interesting chemistry of olympicin A prompted us to carry out the total synthesis of **6** and a series of analogues in order to assess their structure-activity profile as a new group of antibacterial agents. Following the synthesis of **6** and structurally-related acylphloroglucinols **7**–**15** and **18**–**24**, their antibacterial activities against a panel of *S. aureus* strains were evaluated. The presence of an alkyloxy group consisting of 8–10 carbon atoms *ortho* to a five-carbon acyl substituent on the phloroglucinol core are important structural features for promising anti-staphylococcal activity.

1. Introduction

In the era of antibiotic resistance, natural products notably from plants, microbes and marine organisms continue to be an important source of lead compounds for drug discovery. Since the discovery of penicillin from *Penicillium notatum*, researchers have focused on natural resources, mostly microorganisms, for effective and safe antibiotics. Although plants have been well documented for their production of biologically-active metabolites including anticancer agents such as paclitaxel (Taxol®) [1], antimalarial drugs (artemisinin) [2], narcotic analgesics (morphine) [3] and cardioactive agents such as digoxin [4], this area has been underexploited for antimicrobial drug discovery. However, there are numerous reports of plants being used as systemic and topical antimicrobial agents in Ayurvedic [5] and Traditional Chinese Medicine [6] as well as in western herbal medicine [7] because of their self-protection strategy to counter bacteria and fungi in their own environment [8].

Due to the burgeoning global problem of anti-microbial resistance (AMR), there is an increasing need for new chemistries to supplement the dwindling antibiotic arsenal [9]. St John's Wort (*Hypericum perforatum*), a medicinal plant used widely as an antidepressant in herbal medicine, has been reported to produce hyperforin, an antibacterial metabolite with a minimum inhibitory concentration (MIC) value of 0.1 mg/L against methicillin-resistant *Staphylococcus aureus* (MRSA) and penicillin-resistant variants [10]. Our bioassay-directed drug discovery efforts to identify potent anti-staphylococcal agents from various species of the genus *Hypericum* led to the discovery of a number of acylphloroglucinols including (*S*,*E*)-1-(2-((3,7-dimethylocta-2,6-dien-1-yl)oxy)-4,6-dihydroxyphenyl)-2-methylbutan-1-one (**6**) (trivial name olympicin A) from *H. olympicum* [11] with MIC values of 0.5–1 mg/L against a series of MRSA strains. The potential activity and the complex but interesting chemistry of such acylphloroglucinol compounds prompted us to carry out the total synthesis of olympicin A and its related analogues in order to assess their structure-activity profile as a new group of antibacterial agents. Here we report the total synthesis of olympicin A (**6**) and a series of

* Corresponding author.
E-mail address: j.malkinson@ucl.ac.uk (J.P. Malkinson).
[1] Present Address: 16 Royal Swan Quarter, Leret Way, Leatherhead, Surrey KT22 7JL, UK.

https://doi.org/10.1016/j.ejmech.2018.05.038
0223-5234/

acylphloroglucinols (**7**–**22**) that are structurally related to **6**, as well as their antibacterial activities against a panel of multi-drug-resistant (MDR) and methicillin-resistant *Staphylococcus aureus* strains.

2. Results and discussion

2.1. Synthesis of (S)-(2-methylbutanoyl)phloroglucinols with ortho alkyloxy variants

(*S*,*E*)-1-(2-((3,7-Dimethylocta-2,6-dien-1-yl)oxy)-4,6-dihydroxyphenyl)-2-methylbutan-1-one (**6**) (trivial name olympicin A), a promising antibacterial acylphloroglucinol isolated from *H. olympicum*, and its analogues with variable *ortho* alkyloxy substituents were synthesised in four steps starting from (*S*)-2-methylbutanoic acid (**1**) (Scheme 1) with typical overall yields of 10–12%. This general approach involved Friedel-Crafts acylation of phloroglucinol (**3**) with (*S*)-2-methylbutanoyl chloride (**2**) to give the intermediate ketone (*S*)-2-methyl-1-(2,4,6-trihydroxyphenyl) butan-1-one (**4**), which was regioselectively protected as the bis-silyl derivative **5** prior to alkylation of the remaining free phenolic hydroxyl group (and simultaneous deprotection). The structures of all intermediate compounds were confirmed unambiguously by NMR spectral data.

In the first step, commercially available (*S*)-2-methylbutanoic acid (**1**) was treated with thionyl chloride to form the corresponding acid chloride (*S*)-2-methylbutanoyl chloride (**2**; 93% yield), which was isolated by distillation. The boiling point of **2** was 119–120 °C, which was in good agreement with the literature [12]. The structural identity of **2** was confirmed by mass spectrometry, and ^{1}H and ^{13}C NMR spectroscopy (section 4.2.1).

Friedel-Crafts acylation of phloroglucinol (**3**) with (*S*)-2-methylbutanoyl chloride (**2**) in the presence of $AlCl_3$, CS_2 and nitrobenzene led to the formation of (*S*)-2-methyl-1-(2,4,6-trihydroxyphenyl)butan-1-one (**4**; 54% yield), which was purified by VLC. Unreacted phloroglucinol and nitrobenzene were easily separated from **4** during purification and successful acylation was verified by mass spectrometry and NMR spectral data (section 4.2.2). In addition to the presence of the signals that were typical for a 2-methylbutanoyl substituent, the ^{1}H NMR spectrum showed a singlet at δ_H 5.81, integrating for two equivalent *meta* aromatic hydrogen atoms, consistent with the plane of symmetry in **4**.

Initial efforts to protect two (*para* and one *ortho*) of the three phenolic hydroxyl groups in **4** utilised methoxymethyl (MOM) ether protecting groups. Isolated yields were generally poor (below 20%) and this approach was ultimately abandoned as the acidic conditions required for MOM ether deprotection also resulted in cleavage of the required geranyl ether in the target compound **6**. The use of silyl ethers for the desired bis-protection proved more successful. Compound **4** was treated with TBDMS-Cl (2.1 molar equivalents) under basic reaction conditions, forming (*S*)-1-(2,4-bis((*tert*-butyldimethylsilyl)oxy)-6-hydroxyphenyl)-2-methylbutan-1-one (**5**) in an improved 81% yield, after purification by VLC over silica gel. Small quantities of mono-protected derivatives were also identified in the reaction mixture. The presence of a hydrogen-bonded hydroxyl (δ_H 13.43) and two *meta*-coupled ($J = 2.0$ Hz) hydrogen atoms with two different chemical shifts (δ_H 5.85 and 6.04) confirmed the protection of the hydroxyl groups with TBDMS at one *ortho* and the *para* position. Intramolecular hydrogen bonding between the hydrogen of the one remaining free phenolic hydroxyl and the carbonyl oxygen of the acyl substituent, as well as its lower steric accessibility, are likely to account for the excellent regioselectivity of this bis-silyl ether protection.

The final step in the synthesis of the (*S*)-2-methylbutanoylphloroglucinol series involved the alkylation of the free *ortho* phenolic hydroxyl of **5** using the appropriate alkyl bromide. Treatment of a solution of (*S*)-1-(2,4-bis((*tert*-butyldimethylsilyl)oxy)-6-hydroxyphenyl)-2-methylbutan-1-one (**5**) with geranyl bromide in the presence of K_2CO_3 yielded (*S*,*E*)-1-(2-((3,7-dimethylocta-2,6-dien-1-yl)oxy)-4,6-dihydroxyphenyl)-2-methylbutan-1-one (**6**; typically 9–16% yield), which was purified by VLC over silica gel. The original intention had been to alkylate the free *ortho* phenolic hydroxyl followed by silyl ether deprotection in a subsequent step, but the conditions used in the alkylation unexpectedly led to simultaneous TBDMS group removal. While this suggested the possibility of direct alkylation (geranylation) of unprotected **4**, attempts to achieve this generally resulted in very poor conversion (less than 5% yields) of starting acylphloroglucinols to typically *ca.* 1:1 mixtures of *ortho* and *para* mono-alkylated products, which were difficult to separate from unreacted starting materials.

The NMR data of **6** were identical to those of the new acylphloroglucinol we reported from *H. olympicum* [11]. The alkyl (geranyl) substituent included an oxymethylene group (δ_H 4.56 d, $J = 6.5$ Hz, geranyl C-1), the hydrogen atoms of which showed long-range (^{3}J) ^{1}H-^{13}C correlations with a deshielded aromatic carbon atom (δ 162.6, aromatic C-2) of the acylphloroglucinol nucleus and two carbons associated with an olefinic group (δ 118.2, geranyl C-2; δ 142.4, geranyl C-3). Together with the non-equivalence (asymmetry) of the aromatic C-H signals, this confirmed successful *ortho* *O*-alkylation. In a similar manner, a series of other *ortho* alkyloxy acylphloroglucinols (**7**–**15**, Fig. 1) was synthesised, purified and characterised. The final ether substituents were varied to include both saturated and unsaturated linear and branched alkyl/alkenyl groups such as prenyl (**7**), farnesyl (**8**), 3,7-dimethyloctyl (reduced geranyl; **9**), 3-methylbutyl (reduced prenyl; **10**), benzyl (**11**), octyl (**12**), decyl (**13**), dodecyl (**14**) and octadecyl (**15**) groups. In each analogue, the C-1 oxymethylene hydrogen atoms of the alkyl substituent demonstrated key HMBC interactions with the aromatic C-

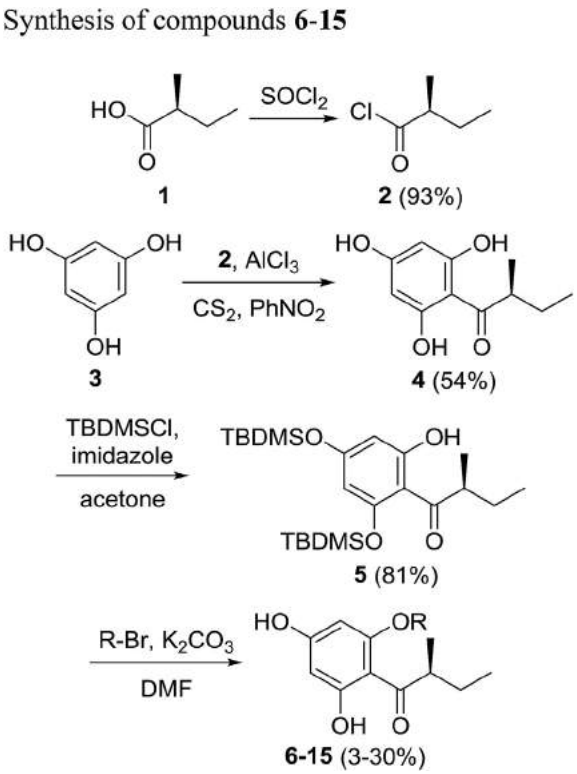

Scheme 1. Synthesis of compounds **6**–**15**.

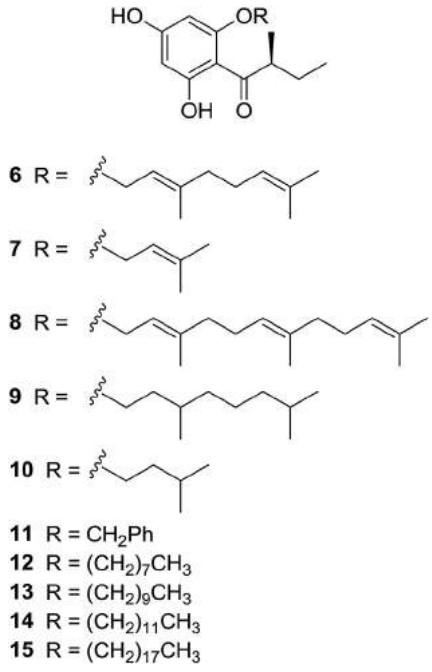

Fig. 1. (*S*)-(2-Methylbutanoyl)phloroglucinols with *ortho* alkyloxy variants.

2 (*ortho*) carbon atom of the acylphloroglucinol core, allowing confirmation of the successful desired *ortho* alkylation in compounds **7**–**15**. The yield of the final alkylation/deprotection step was typically quite low at around 30% (though much lower for **8** and **10**). Isolated by-products often included recovered **4**, along with small quantities of bis-alkylated (*ortho* plus *para*) and occasionally *para* alkylated derivatives.

2.2. Synthesis of ortho geranylated acylphloroglucinols with acyl variants

The acyl chloride used in the initial Friedel-Crafts acylation of phloroglucinol was varied to generate, after elaboration as described above, a series of geranylated acylphloroglucinol analogues (Fig. 2), incorporating simple linear acyl substituents such as propanoyl (**19**), butanoyl (**20**), pentanoyl (**21**), decanoyl (**22**) and octadecanoyl (**23**) as well as aromatic acyl substituents such as benzoyl (**24**). Commercially available acetylphloroglucinol was also used to synthesise *ortho* geranylated acetylphloroglucinol (**18**).

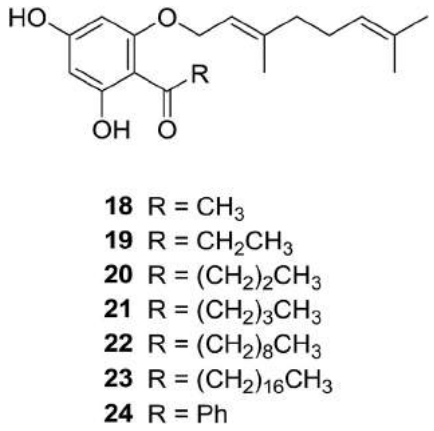

Fig. 2. *Ortho* geranylated acylphloroglucinols with acyl variants.

Regioselective di-protection of two (*para* and one *ortho*) of the three hydroxyl groups of the acylphloroglucinol (**16**) moiety again using TBDMS-Cl, followed by alkylation with geranyl bromide and simultaneous deprotection of the silyl ethers (**17**) yielded the corresponding *ortho* geranylated acylphloroglucinols **18**–**24** (Scheme 2). Final products were purified by SPE over silica gel and confirmed by NMR spectroscopy. Again, a key aspect in the confirmation of the structures of each of the compounds was the use of 2D-HMBC, in which the C-1 oxymethylene hydrogen atoms of the geranyl substituent demonstrated ^{3}J correlations with the C-2 (*ortho*) carbon of the acylphloroglucinol.

2.3. Antibacterial activity of acylphloroglucinols

The antibacterial activities (Table 1) of the acylphloroglucinol series were assessed against a panel of clinical isolates of multidrug-resistant (MDR) and methicillin-resistant *Staphylococcus aureus* (MRSA), notably SA1199B, XU212, RN4220, EMRSA15 and EMSA16. These organisms represent a group of effluxing strains that are resistant to common antibiotics including certain fluoroquinolones (SA1199B), tetracycline (XU212) and macrolides (erythromycin; RN4220). These strains were chosen as antibacterials that are not substrates for these MDR pumps are clinically desirable. It was evident from Table 1 that the (*S*)-2-methylbutanoylphloroglucinol derivatives with geranyl (**6**; the natural product olympicin A) and 3,7-dimethyloctyl (reduced geranyl; **9**) ether substituents at the *ortho* position were found to be highly active with MIC values of 0.5–1 mg/L. The effect on activity of replacing the geranyl substituent with shorter and longer alkyl/alkenyl groups (prenyl, farnesyl, 3-methylbutyl, 3,7-dimethyloctyl) can also be observed. We found that increasing the chain length from geranyl (**6**) to farnesyl (**8**) resulted in a dramatic loss of activity, evidenced by an increase in MIC values from 0.5 to 1 mg/L to in excess of 512 mg/L (no inhibition of the growth of any of the strains of bacteria was seen at the highest concentration of **8** tested), while decreasing the chain length from geranyl to prenyl (**7**) showed at least a two-fold reduction in activity. These results suggested an optimal length for the alkyloxy group in terms of antibacterial activity, which may imply a specific molecular target

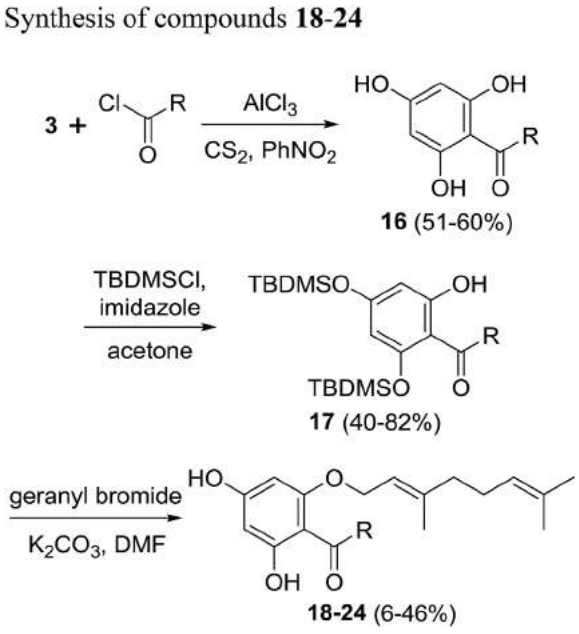

Scheme 2. Synthesis of compounds **18**–**24**.

Table 1
MICs (in mg/L) of compounds (**8**–**24**) against standard, multi-drug resistant (MDR) and methicillin-resistant strains of *Staphylococcus aureus*.

Compound	SA1199B	XU212	ATCC25941	RN4220	EMRSA15	EMRSA16
6	1	0.5	1	1	1	0.5
7	16	4–8	8	8	16	4
8[a]	>512	>512	>512	>512	>512	>512
9	0.5–1	1	1	0.5	0.5–1	0.25
10	2	4	2	2	2–4	2–4
11	8	4	4	4–8	8	4
12	0.25–0.5	0.5	0.25–0.5	0.5	0.5	0.25
13	2	2–4	1–2	1	0.5–1	0.25
14	16	64	128	8	16	16
15[a]	>512	>512	>512	>512	>512	>512
18	8	8	16	8	16	4
19	2	1	2	1	2	1
20	2	2	2	2	2	1
21	1	0.5	0.5	0.5	1	0.5
22	512	64	512	256	512	64
23[a]	>512	>512	>512	>512	>512	>512
24	1	1	1	1	1	0.5
Norfloxacin	32	8	0.5	0.5	0.5	256
Vancomycin	0.25	0.5	0.25	0.5	0.25	0.25

[a] No inhibition of growth was apparent at the highest concentration tested.

or a requirement for a particular lipophilicity for the mechanism of action. In addition, the 3-methylbutyl (**10**) and 3,7-dimethyloctyl (**9**) derivatives were as active as the prenyl or geranyl derivatives respectively, suggesting that the presence of the double bonds in the alkyl side chain (and the consequent reduction in conformational freedom) might not have any significant role in antibacterial activity. The most potent compound in terms of its activity against the six *S. aureus* strains was **12**, an (*S*)-(2-methylbutanoyl)phloroglucinol with a straight chain octyl ether substituent – the same continuous linear chain length as the geranyl and 3,7-dimethyloctyl derivatives – at the *ortho* position phenolic hydroxyl.

Among the *ortho* geranylated acylphloroglucinol series, the pentanoyl derivative (**21**) demonstrated the highest activity with MICs of 0.5–1 mg/L, making it comparable in activity to the parent natural product **6**. The octadecanoyl analogue (**23**) did not show any inhibition of bacterial growth at any of the concentrations tested, indicating that there was clearly an optimal chain length (number of carbon atoms) for the acyl substituent. Geranylated analogues containing three to seven carbon atoms in their acyl substituents (aliphatic or aromatic) seem be most active.

3. Conclusion

The acylphloroglucinol natural product olympicin A was synthesised from commercial phloroglucinol over three straightforward steps (Friedel-Crafts acylation, regioselective silyl protection, and simultaneous deprotection/*O*-alkylation). The same approach provided access to a series of *ortho* alkyloxy and acyl analogues. Evaluation of the activities of the analogues against several strains of MRSA seemed to indicate that the presence of an alkyloxy group consisting of 8–10 carbon atoms *ortho* to a five-carbon-atom acyl substituent is an important structural feature for promising anti-staphylococcal activity within this class of acylphloroglucinol antibiotics. The most potent derivative **12** – the octyl ether analogue of olympicin A – demonstrated improved activity over the natural product against all MRSA strains tested. The most promising acylphloroglucinols identified in this study are being evaluated for their clinical potential as systemic and topical antibacterial agents. A more diverse range of structural analogues, including those incorporating side-chain functionality, is also being synthesised in an effort to better understand the structure-activity relationships of this class of agents. At present we do not fully understand how these compounds function. However, given that the most active compounds all have a hydrophobic portion, comprised of an ether and an acyl functionality, capable of membrane interaction, and a hydrophilic diphenolic moiety, it is probable that their target is cell-wall located.

4. Experimental section

4.1. General methods

All chemicals and reagents used for the syntheses were purchased from Sigma-Aldrich, Gillingham, UK. UV spectra were recorded on a Thermo Electron Corporation Helios spectrophotometer and IR spectra were recorded on a Nicolet 360 FT-IR spectrophotometer. NMR spectra (both 1D and 2D) were recorded on a Bruker AVANCE 500 MHz spectrometer (500 MHz for ^{1}H and 125 MHz for ^{13}C). Chemical shift values (δ) are reported in parts per million (ppm) and are calibrated relative to residual solvent peaks as internal standards, and coupling constants (J values) are expressed in Hz. Detailed assignments of NMR spectra can be found in the Supporting Information. Mass spectra were recorded on a Finnigan MAT 95 high resolution, double focusing, magnetic sector mass spectrometer. Accurate mass measurement was achieved using voltage scanning of the accelerating voltage. This was nominally 5 kV and an internal reference of heptacosa was used. Resolution was set between 5000 and 10000. Both TLC and preparative TLC were performed using silica gel 60 PF_{254} plates (Merck). Vacuum liquid chromatography (VLC) columns were packed with silica gel 60 PF_{254} (Merck), while solid phase extraction (SPE) was performed using 10 g pre-packed SPE columns (SiGel60) using mobile phases of hexane and ethyl acetate of increasing polarity.

4.2. Synthesis of intermediate and final compounds

4.2.1. Synthesis of (S)-2-methylbutanoyl chloride (2) [12]

(*S*)-2-Methylbutanoic acid (**1**; 10 g, 97.91 mmol) and thionyl chloride (10.71 mL, 146.9 mmol, 1.5 equiv) were heated together at 80–90 °C under reflux for 2 h. Distillation of the reaction mixture afforded (*S*)-2-methylbutanoyl chloride as a colourless liquid (10.89 g, 90.72 mmol, 93%). $[\alpha]_D^{22}$ +10.1 (*c* 0.54, $CHCl_3$); b.p. 119–120 °C; ^{1}H NMR (500 MHz, $CDCl_3$): δ_H 0.95 (3H, t, $J = 7.5$ Hz), 1.26 (3H, d, $J = 7.5$ Hz), 1.59 (1H, m), 1.80 (1H, m), 2.80 (1H, q, $J = 7.0$ Hz); ^{13}C NMR (125 MHz, $CDCl_3$): δ_C 11.3, 16.7, 26.7, 53.1, 177.8; HRMS (ESI) *m/z*: $[M\text{-}H]^-$ Calcd for C_5H_8OCl 119.0264; Found 119.0263.

4.2.2. Synthesis of (S)-2-methyl-1-(2,4,6-trihydroxyphenyl)butan-1-one (4) [13]

Phloroglucinol (**3**; 10.81 g, 85.8 mmol) in carbon disulphide (50 mL) was transferred into a two-necked round-bottomed flask and allowed to stir while aluminium trichloride (46.43 g, 351.8 mmol, 4.1 equiv) was added. Nitrobenzene (40 mL) was then added to the solution over 30 min. The solution was then heated under reflux at 55 °C for 30 min. A solution of 2-methylbutanoyl chloride (**2**) (10.89 g, 85.8 mmol) dissolved in 5 mL nitrobenzene was added to the reaction mixture over 30 min, followed by heating for another 30 min. The reaction mixture was allowed to cool with stirring and then poured into an ice-water bath (400 mL). 100 mL of 3 M hydrochloric acid was then added and the mixture extracted with diethyl ether (3 × 500 mL). The organic solvents were removed under reduced pressure. The oily residue containing the acylphloroglucinol was subjected to VLC over SiGel PF254 using hexane and EtOAc of increasing polarity. The VLC fraction eluted with 30–45% EtOAc in hexane gave (*S*)-2-methyl-1-(2,4,6-

trihydroxyphenyl)butan-1-one as a pale yellow oil (9.71 g, 46.19 mmol, 54%). $[\alpha]_D^{22}$ +8.5 (*c* 0.35, $CHCl_3$); UV ($CHCl_3$) λ_{max} (log ε): 240 (4.17), 290 (3.97) nm; IR ν_{max} (thin film) cm^{-1}: 3297, 1628, 1602, 1222; ^1H NMR (500 MHz, CD_3OD): δ_H 0.88 (3H, t, $J = 7.5$ Hz), 1.11 (3H, d, $J = 6.5$ Hz), 1.33 (1H, m), 1.78 (1H, m), 3.84 (1H, m), 5.81 (2H, s); ^{13}C NMR (125 MHz, CD_3OD): δ_C 12.4, 17.2, 28.2, 46.7, 96.0, 96.0, 105.3, 165.8, 165.8, 211.4; HRMS (ESI) *m/z*: $[M-H]^-$ Calcd. for $C_{11}H_{13}O_4$ 209.0814; Found 209.0813.

4.2.3. Synthesis of (S)-1-(2,4-bis((tert-butyldimethylsilyl)oxy)-6-hydroxyphenyl)-2-methylbutan-1-one (**5**) [14]

Acylphloroglucinol **4** (9.71 g, 46.19 mmol) was dissolved in part in dry acetone (150 mL) and transferred into a 250 mL round bottom flask. Imidazole (3.43 g, 138.6 mmol, 3 equiv) was added to the solution and the reaction mixture stirred for 5 min followed by the addition of TBDMS-Cl (14.61 g, 97.0 mmol, 2.1 equiv). The reaction mixture was stirred for 2 h at room temperature. Acetone was removed from the reaction mixture under reduced pressure and the residue taken up in chloroform and washed with 1 M HCl (150 mL). The organic layer was dried using anhydrous magnesium sulphate, filtered and the solvent was removed under reduced pressure. The crude product purified by VLC over silica gel using hexane and EtOAc of increasing polarity. VLC fractions eluted with 2.5–7.5% EtOAc in hexane afforded (*S*)-1-(2,4-bis((*tert*-butyldimethylsilyl)oxy)-6-hydroxyphenyl)-2-methylbutan-1-one as a pale yellow oil (16.4 g, 37.26 mmol, 81%). $[\alpha]_D^{22}$ +4.9 (*c* 0.39, $CHCl_3$); UV ($CHCl_3$) λ_{max} (log ε): 239 (4.26), 290 (4.23) nm; IR ν_{max} (thin film) cm^{-1}: 3276, 2973, 1688, 1572, 1531,1256, 1131, 1072, 850; ^1H NMR (500 MHz, $CDCl_3$): δ_H 0.23 (2 × 3H, s), 0.32 (2 × 3H, s), 0.88 (3H, t, $J = 7.5$ Hz), 0.97 (3 × 3H, s), 0.99 (3 × 3H, s), 1.12 (3H, d, $J = 6.5$ Hz), 1.43 (1H, m), 1.78 (1H, m), 3.82 (1H, m), 5.85 (1H, d, $J = 2.0$ Hz), 6.04 (1H, d, $J = 2.0$ Hz), 13.43 (1H, s); ^{13}C NMR (125 MHz, $CDCl_3$): δ_C -4.2, -3.7, 11.0, 16.9, 18.1, 18.9, 25.5, 26.5, 26.1, 45.0, 102.0, 103.1, 108.4, 158.8, 161.7, 166.5, 210.5; HRM (ESI) *m/z*: $[M-H]^-$ Calcd. for $C_{23}H_{41}O_4Si_2$ 437.2549; Found 437.2554.

4.2.4. Synthesis of (S,E)-1-(2-((3,7-dimethylocta-2,6-dien-1-yl)oxy)-4,6-dihydroxy-phenyl)-2-methylbutan-1-one (olympicin A) (**6**)

TBDMS-protected acylphloroglucinol **5** (6.6 g, 15.0 mmol) was dissolved in dry DMF (100 mL) and anhydrous potassium carbonate (3.1 g, 22.5 mmol, 1.5 equiv) was added. The mixture was stirred for approximately 5 min followed by the addition of geranyl bromide (3.43 mL, 18 mmol, 1.2 equiv). The mixture was heated at 80 °C for 3 h with stirring. The reaction mixture was poured over water and extracted with chloroform. The solvent in the organic layer was removed under reduced pressure. The crude product was purified by chromatography over silica gel by VLC. Compound **6** was eluted with 9:1 hexane-ethyl acetate and removal of the solvents under reduced pressure yielded the title compound as a pale yellow oil (450 mg, 1.3 mmol, 8.7%). All spectral data were identical to those of the natural product [11]. $[\alpha]_D^{22}$ +6.0 (*c* 0.30, $CHCl_3$); UV ($CHCl_3$) λ_{max} (log ε): 239 (4.06), 240 (4.23) nm; IR ν_{max} (thin film) cm^{-1}: 3357, 2965, 2931, 1623, 1589, 1458, 1212, 1165, 1087, 825; ^1H NMR (500 MHz, $CDCl_3$): δ_H 0.88 (3H, t, $J = 7.5$ Hz), 1.12 (3H, d, $J = 6.5$ Hz), 1.36 (1H, m), 1.61 (3H, s), 1.69 (3H, s), 1.74 (3H, s), 1.79 (1H, m), 2.10 (2H, m), 2.13 (2H, m), 3.68 (1H, m), 4.56 (2H, d, $J = 6.5$ Hz), 5.10 (1H, m), 5.44 (1H, br s), 5.50 (1H, m), 5.91 (1H, d, $J = 2.0$ Hz), 5.98 (1H, d, $J = 2.0$ Hz), 14.10 (1H, s); ^{13}C NMR (125 MHz, $CDCl_3$): δ_C 11.9, 16.5, 16.6, 17.7, 25.7, 26.2, 26.9, 39.5, 46.2, 65.6, 91.5, 96.5, 105.9, 118.2, 122.6, 132.0, 142.4, 161.9, 162.6, 167.5, 210.4; HRMS (ESI) *m/z*: $[M-H]^-$ Calcd. for $C_{21}H_{29}O_4$ 345.2071; Found 345.2067.

4.2.5. Synthesis of compounds **7**–**15** from TBDMS-protected acylphloroglucinol **5**

Compounds **7**–**15** were synthesised from TBDMS-protected acylphloroglucinol **5** using the procedure as described for **6** above but replacing the geranyl bromide with the appropriate alkyl bromide.

4.2.5.1. (S)-1-(2,4-Dihydroxy-6-((3-methylbut-2-en-1-yl)oxy)phenyl)-2-methylbutan-1-one (**7**).

Synthesised using 0.259 mmol of **5** and 0.311 mmol of prenyl bromide. Isolated after SPE (SiGel; hexane/EtOAc 9:1) as a pale yellow oil (15 mg, 0.054 mmol, 21%). $[\alpha]_D^{22}$ +5.2 (*c* 0.30, MeOH); UV (MeOH) λ_{max} (log ε): 239 (4.36), 290 (3.97) nm; IR ν_{max} (thin film) cm^{-1}: 3423, 2968, 2914, 1630, 1595, 1560, 1420, 1350, 1200; ^1H NMR (500 MHz, $CDCl_3$): δ_H 0.88 (3H, t, $J = 7.5$ Hz), 1.13 (3H, d, $J = 6.5$ Hz), 1.33 (1H, m), 1.76 (3H, s), 1.78 (1H, m), 1.82 (3H, s), 3.66 (1H, m), 4.55 (2H, d, $J = 6.5$ Hz), 5.51 (1H, t, $J = 6.5$ Hz), 5.70 (1H, br s), 5.93 (1H, d, $J = 2.0$ Hz), 6.00 (1H, d, $J = 2.0$ Hz), 14.07 (1H, br s); ^{13}C NMR (125 MHz, $CDCl_3$): δ_C 12.0, 16.7, 18.4, 25.9, 27.1, 46.3, 65.8, 91.7, 96.7, 106.1, 118.6, 139.3, 162.3, 162.8, 167.7, 210.6; HRMS (ESI) *m/z*: $[M-H]^-$ Calcd. for $C_{16}H_{21}O_4$ 277.1445; Found 277.1453.

4.2.5.2. (S)-1-(2,4-Dihydroxy-6-(((2E,6E)-3,7,11-trimethyldodeca-2,6,10-trien-1-yl)oxy)phenyl)-2-methylbutan-1-one (**8**).

Synthesised using 0.925 mmol of **5** and 1.11 mmol of farnesyl bromide. Isolated after SPE (SiGel; hexane/EtOAc 92:8) as a yellow oil (25 mg, 0.060 mmol, 6.5%). $[\alpha]_D^{22}$ +6.7 (*c* 0.51, MeOH); UV (MeOH) λ_{max} (log ε): 239 (4.09), 285 (4.22) nm; IR ν_{max} (thin film) cm^{-1}: 314, 1529, 1442, 1292, 1166, 1074, 821; ^1H NMR (500 MHz, $CDCl_3$): δ_H 0.90 (3H, t, $J = 7.5$ Hz), 1.13 (3H, d, $J = 6.5$ Hz), 1.37 (1H, m), 1.61 (3H, s), 1.62 (3H, s), 1.69 (3H, s), 1.75 (3H, s), 1.80 (1H, m), 1.99 (2H, s), 2.07 (2H, s), 2.11 (2H, m), 2.13 (2H, m), 3.67 (1H, m), 4.57 (2H, d, $J = 6.5$ Hz), 5.08 (1H, m), 5.12 (1H, m), 5.52 (1H, m), 5.93 (1H, d, $J = 2.5$ Hz), 5.99 (1H, d, $J = 2.5$ Hz), 14.05 (1H, s); ^{13}C NMR (125 MHz, $CDCl_3$): δ_C 12.1, 16.2, 16.8, 16.9, 17.9, 25.9, 26.5, 26.9, 27.0, 39.7, 39.9, 46.3, 65.9, 91.8, 96.7, 106.1, 118.4, 123.7, 124.5, 131.6, 135.9, 142.7, 162.3, 162.8, 167.7, 210.6; HRMS (ESI) *m/z*: $[M-H]^-$ Calcd. for $C_{26}H_{37}O_4$ 413.2698; Found 413.2697.

4.2.5.3. (2S)-1-(2-((3,7-Dimethyloctyl)oxy)-4,6-dihydroxyphenyl)-2-methylbutan-1-one (**9**).

Synthesised using 1.073 mmol of **5** and 1.289 mmol of 1-bromo-3,7-dimethyloctane. Isolated after SPE (SiGel; hexane/EtOAc 9:1) as a colourless oil (110 mg, 0.313 mmol, 29%). $[\alpha]_D^{22}$ +4.4 (*c* 0.40, $CHCl_3$); UV ($CHCl_3$) λ_{max} (log ε): 239 (3.99), 290 (4.21) nm; IR ν_{max} (thin film) cm^{-1}: 3233, 2964, 2921, 1661, 1583, 1432, 1241, 1103, 1057; ^1H NMR ($CDCl_3$): δ_H 0.88 (3H, t, $J = 7.5$ Hz), 0.89 (6H, d, $J = 6.5$ Hz), 0.97 (3H, d, $J = 6.5$ Hz), 1.15 (3H, d, $J = 6.5$ Hz), 1.18 (2H, m), 1.19 (1H, m), 1.35 (3H, m), 1.43 (1H, m), 1.54 (1H, m), 1.66 (3H, m), 1.82 (1H, m), 1.89 (1H, m), 3.72 (1H, m), 4.04 (2H, d, $J = 6.5$ Hz), 5.36 (1H, br s), 5.93 (1H, d, $J = 2.0$ Hz), 5.99 (1H, d, $J = 2.0$ Hz), 14.05 (1H, s); ^{13}C NMR ($CDCl_3$): δ_C 11.7, 16.8, 19.6, 22.6, 24.6, 26.6, 28.0, 29.9, 36.0, 37.5, 39.2, 46.0, 66.7, 91.5, 96.5, 105.8, 162.4, 162.8, 167.4, 210.4; HRMS (ESI) *m/z*: $[M+H]^+$ Calcd. for $C_{21}H_{35}O_4$ 351.2531; Found 351.2529.

4.2.5.4. (S)-1-(2,4-Dihydroxy-6-(isopentyloxy)phenyl)-2-methylbutan-1-one (**10**).

Synthesised using 0.579 mmol of **5** and 0.695 mmol of 1-bromo-3-dimethylbutane. Isolated after SPE (SiGel; hexane/EtOAc 9:1) as a yellow oil (5 mg, 0.018 mmol, 3.1%). $[\alpha]_D^{22}$ + 3.5 (*c* 0.34, MeOH); UV (MeOH) λ_{max} (log ε): 242 (4.39), 288 (4.09) nm; IR ν_{max} (thin film) cm^{-1}: 333, 1631, 1593, 1258, 1110; ^1H NMR (500 MHz, $CDCl_3$): δ_H 0.89 (3H, t, $J = 7.5$ Hz), 0.98 (6H, d, $J = 6.5$ Hz), 1.14 (3H, d, $J = 6.5$ Hz), 1.41 (1H, m), 1.73 (2H, m), 1.80 (1H, m), 1.81 (1H, m), 3.69 (1H, m), 4.02 (2H, d, $J = 6.5$ Hz), 5.40 (1H, br s), 5.92 (1H, d, $J = 2.0$ Hz), 5.99 (1H, d, $J = 2.0$ Hz), 14.17 (1H, s);

^{13}C NMR (125 MHz, $CDCl_3$): δ_C 11.7, 16.8, 22.5 (2C), 25.2, 26.6, 37.7, 46.0, 67.5, 91.5, 96.5, 105.8, 162.4, 162.8, 167.4, 210.4; HRMS (ESI) *m/z*: $[M\text{-}H]^-$ Calcd. for $C_{16}H_{23}O_4$ 279.1602; Found 279.1598.

*4.2.5.5. (S)-1-(2-(Benzyloxy)-4,6-dihydroxyphenyl)-2-methylbutan-1-one (**11**).* Synthesised using 0.934 mmol of **5** and 1.121 mmol of benzyl bromide. Isolated after SPE (SiGel; hexane/EtOAc 8:2) as a pale yellow oil (85 mg, 0.283 mmol, 30%). $[\alpha]_D^{22}$ + 4.2 (*c* 0.32, MeOH); UV (MeOH) λ_{max} (log ε): 241 (4.30), 289 (3.94) nm; IR ν_{max} (thin film) cm^{-1}: 3239, 2958, 1624, 1568, 1500, 1456, 1383, 1255, 1161, 1105, 751; ^{1}H NMR (500 MHz, $CDCl_3$): δ_H 0.68 (3H, t, $J = 6.5$ Hz), 1.00 (3H, d, $J = 6.5$ Hz), 1.29 (1H, m), 1.71 (1H, m), 3.57 (1H, m), 5.08 (2H, s), 6.00 (1H, d, $J = 2.0$ Hz), 6.01 (1H, d, $J = 2.0$ Hz), 7.38–7.42 (5H, m), 14.00 (1H, s); ^{13}C NMR (125 MHz, $CDCl_3$): δ_C 11.7, 16.8, 26.9, 46.2, 71.6, 92.0, 97.1, 106.1, 128.4 (2C), 128.8, 129.0 (2C), 135.6, 162.2, 162.5, 167.8, 210.6; HRMS (ESI) *m/z*: $[M+H]^+$ Calcd. for $C_{18}H_{21}O_4$ 301.1440; Found 301.1430.

*4.2.5.6. (S)-1-(2,4-Dihydroxy-6-(octyloxy)phenyl)-2-methylbutan-1-one (**12**).* Synthesised using 0.893 mmol of **5** and 1.931 mmol of 1-bromooctane. Isolated after SPE (SiGel; hexane/EtOAc 92:8) as a pale yellow oil (82 mg, 0.255 mmol, 29%); $[\alpha]_D^{22}$ + 6.1 (*c* 0.45, MeOH); UV (MeOH) λ_{max} (log ε): 239 (4.39), 288 (3.98) nm; IR ν_{max} (thin film) cm^{-1}: 3328, 2928, 2857, 1621, 1591, 1444, 1377, 1212, 1158, 1102, 826, 754; ^{1}H NMR (500 MHz, $CDCl_3$): δ_H 0.89 (3H, t, $J = 7.5$ Hz), 0.90 (3H, t, $J = 7.5$ Hz), 1.16 (3H, d, $J = 7.0$ Hz), 1.26–1.40 (8H, m), 1.38 (1H, m), 1.46 (2H, m), 1.81 m (1H, m), 1.85 (2H, m), 3.72 (1H, q, $J = 6.5$ Hz), 4.00 (2H, t, $J = 6.5$ Hz), 5.42 (1H, br s), 5.91 (1H, d, $J = 2.0$ Hz), 5.99 (1H, d, $J = 2.0$ Hz), 14.06 (1H, s); ^{13}C NMR (125 MHz, $CDCl_3$): δ_C 12.0, 14.3, 17.1, 22.8, 26.5, 26.9, 29.3, 29.4, 29.5, 32.0, 46.3, 69.4, 91.5, 96.8, 106.2, 162.2, 163.0, 167.8, 210.5; HRMS (ESI) *m/z*: $[M+H]^+$ Calcd. for $C_{19}H_{31}O_4$ 323.2222; Found 323.2211.

*4.2.5.7. (S)-1-(2-(Decyloxy)-4,6-dihydroxyphenyl)-2-methylbutan-1-one (**13**).* Synthesised using 0.936 mmol of **5** and 1.123 mmol of 1-bromodecane. Isolated after SPE (SiGel; hexane/EtOAc 9:1) as a yellow oil (96 mg, 0.264 mmol, 28%). $[\alpha]_D^{22}$ + 4.5 (*c* 0.25, MeOH); UV (MeOH) λ_{max} (log ε): 243 (4.33), 292 (3.99) nm; IR ν_{max} (thin film) cm^{-1}: 3327, 2926, 2855, 1739, 1621, 1592, 1443, 1368, 1216, 1156, 1103, 827, 752; ^{1}H NMR (500 MHz, $CDCl_3$): δ_H 0.88 (3H, t, $J = 7.5$ Hz), 0.89 (3H, t, $J = 7.5$ Hz), 1.17 (3H, d, $J = 6.5$ Hz), 1.28–1.31 (12H, m), 1.34 (1H, m), 1.46 (2H, m), 1.81 (1H, m), 1.84 (2H, m), 3.72 (1H, q, $J = 6.5$ Hz), 4.00 (2H, t, $J = 6.5$ Hz), 5.92 (1H, d, $J = 2.0$ Hz), 6.00 (1H, d, $J = 2.0$ Hz), 14.16 (1H, s); ^{13}C NMR (125 MHz, $CDCl_3$): δ_C 12.0, 14.3, 17.3, 26.5, 26.6, 29.1, 29.4, 29.5, 29.6, 29.8, 29.9, 32.0 (8C), 46.3, 69.3, 91.6, 96.8, 106.2, 162.3, 163.0, 167.7, 210.6; HRMS (ESI) *m/z*: $[M+H]^+$ Calcd for $C_{22}H_{37}O_4$ 365.2692; Found 365.2699.

*4.2.5.8. (S)-1-(2-(Dodecyloxy)-4,6-dihydroxyphenyl)-2-methylbutan-1-one (**14**).* Synthesised using 0.913 mmol of **5** and 1.096 mmol of 1-bromododecane. Isolated after SPE (SiGel; hexane/EtOAc 92:8) as a pale yellow oil (98 mg, 0.259 mmol, 28%). $[\alpha]_D^{22}$ + 4.7 (*c* 0.30, MeOH); UV (MeOH) λ_{max} (log ε): 238 (4.32), 290 (3.99) nm; IR ν_{max} (thin film) cm^{-1}: 3327, 2924, 2854, 1739, 1622, 1593, 1456, 1366, 1216, 1160, 1109, 827; ^{1}H NMR (500 MHz, $CDCl_3$): δ_H 0.88 (3H, t, $J = 7.5$ Hz), 0.89 (3H, t, $J = 7.5$ Hz), 1.16 (3H, d, $J = 6.5$ Hz), 1.28–1.30 (16H, m), 1.35 (1H, m), 1.46 (2H, m), 1.83 m (1H, m), 1.86 (2H, m), 3.73 (1H, q, $J = 6.5$ Hz), 4.00 (2H, t, $J = 6.5$ Hz), 5.92 (1H, d, $J = 2.0$ Hz), 6.00 (1H, d, $J = 2.0$ Hz), 6.02 (1H, br s), 14.19 (1H, s); ^{13}C NMR (125 MHz, $CDCl_3$): δ_C 12.0, 14.3, 17.1, 22.9, 26.9, 26.5, 29.3, 29.5, 29.6, 29.77 (2C), 29.8, 29.9, 32.1, 46.3, 69.4, 91.7, 96.8, 106.1, 162.5, 163.0, 167.7, 210.7; HRMS (ESI) *m/z*: $[M+H]^+$ Calcd. for $C_{23}H_{39}O_4$ 379.2848; Found 379.2864.

*4.2.5.9. (S)-1-(2,4-Dihydroxy-6-(octadecyloxy)phenyl)-2-methylbutan-1-one (**15**).* Synthesised using 0.9 mmol of **5** and 1.079 mmol of 1-bromooctadecane. Isolated after SPE (SiGel; hexane/EtOAc 92:8) as a colourless oil (118 mg, 0.255 mmol, 28%). $[\alpha]_D^{22}$ + 4.2 (*c* 0.35, MeOH); UV (MeOH) λ_{max} (log ε): 244 (4.32), 289 (3.98) nm; IR ν_{max} (thin film) cm^{-1}: 3328, 2923, 2853, 1738, 1623, 1593, 1455, 1373, 1214, 1159, 1104, 774; ^{1}H NMR (500 MHz, $CDCl_3$): δ_H 0.89 (3H, t, $J = 7.5$ Hz), 0.91 (3H, t, $J = 7.5$ Hz), 1.16 (3H, d, $J = 6.5$ Hz), 1.27–1.33 (28H, m), 1.42 (1H, m), 1.46 (2H, m), 1.81 (1H, m), 1.85 (2H, m), 3.73 (1H, q, $J = 6.5$ Hz), 4.00 (2H, t, $J = 6.5$ Hz), 5.92 (1H, d, $J = 2.0$ Hz), 6.00 (1H, d, $J = 2.0$ Hz), 6.07 (1H, br s), 14.12 (1H, s); ^{13}C NMR (125 MHz, $CDCl_3$): δ_C 12.0, 14.3, 17.1, 22.9, 26.5, 26.9, 29.3, 29.6, 29.8–29.9 (11C), 32.2, 46.3, 69.4, 91.6, 96.8, 106.1, 162.3, 163.0, 167.8, 210.6; HRMS (ESI) *m/z*: $[M+H]^+$ Calcd for $C_{29}H_{51}O_4$ 463.3787; Found 463.3796.

*4.2.6. Synthesis of compounds **18**–**24** from phloroglucinol*

The first step in the synthesis of compounds **19**–**24** was the Friedel-Crafts acylation of phloroglucinol using the appropriate acyl (propionyl, butyryl, pentanoyl, decanoyl, octadecanoyl and benzoyl) chloride using the procedure described for **4** above. Compound **18** was synthesised starting from commercially available acetylphloroglucinol. TBDMS protection of each acylphloroglucinol **16** was achieved according to the procedure described for **5** above. Finally, the TBDMS-protected acylphloroglucinols **17** were simultaneously deprotected and geranylated at the *ortho* phenolic hydroxyl as described for compound **6** to produce compounds **18**–**24**. Further details of the experimental procedures used for the synthesis of compounds **18**–**24**, including full compound characterisation data for the corresponding precursor acylphloroglucinols and TBDMS-protected acylphloroglucinols, are included in the Supporting Information.

*4.2.6.1. (E)-1-(2-((3,7-Dimethylocta-2,6-dien-1-yl)oxy)-4,6-dihydroxyphenyl)ethanone (**18**).* Isolated after SPE (SiGel; hexane/EtOAc 8:2) as a pale yellow oil (45 mg, 0.148 mmol, 4.3% over two steps starting from commercial acetylphloroglucinol). UV (MeOH) λ_{max} (log ε): 244 (4.36), 288 (3.97) nm; IR ν_{max} (thin film) cm^{-1}: 3136, 2909, 1737, 1621, 1561, 1464, 1373, 1284, 1259, 1222, 1165, 1104, 1071, 822, 756; ^{1}H NMR (500 MHz, $(CD_3)_2CO$): δ_H 1.59 (3H, s), 1.64 (3H, s), 1.77 (3H, s), 2.11–2.16 (4H, m), 2.55 (3H, s), 4.64 (2H, d, $J = 6.5$ Hz), 5.11 (1H, m), 5.56 (1H, m), 5.93 (1H, d, $J = 2.0$ Hz), 56.03 (1H, d, $J = 2.0$ Hz), 13.91 (1H, s); ^{13}C NMR (125 MHz, $(CD_3)_2CO$): δ_C 16.7, 17.8, 25.9, 27.0, 33.2, 40.1, 66.4, 92.8, 96.6, 106.1, 119.9, 124.7, 132.2, 142.6, 164.0, 166.0, 168.3, 203.5. HRMS (ESI) *m/z*: $[M+H]^+$ Calcd. for $C_{18}H_{25}O_4$ 305.1753; Found 305.1766.

*4.2.6.2. (E)-1-(2-((3,7-Dimethylocta-2,6-dien-1-yl)oxy)-4,6-dihydroxyphenyl)propan-1-one (**19**).* Isolated after SPE (SiGel; hexane/EtOAc 9:1) as a yellow oil (50 mg, 0.157 mmol, 2.6% over three steps starting from **3**). UV (MeOH) λ_{max} (log ε): 243 (4.32), 289 (3.99) nm; IR ν_{max} (thin film) cm^{-1}: 3310, 2973, 2937, 1622, 1594, 1448, 1376, 1220, 1166, 1100, 828, 756; ^{1}H NMR (500 MHz, $CDCl_3$): δ_H 1.15 (3H, t, $J = 7.0$ Hz), 1.61 (3H, s), 1.68 (3H, s), 1.74 (3H, s), 2.10 (2H, m), 2.13 (2H, m), 3.03 (2H, q, $J = 7.0$ Hz), 4.57 (2H, d, $J = 6.5$ Hz), 5.10 (1H, m), 5.51 (1H, m), 5.53 (1H, br s), 5.91 (1H, d, $J = 2.0$ Hz), 5.98 (1H, d, $J = 2.0$ Hz), 14.05 (1H, br s); ^{13}C NMR (125 MHz, $CDCl_3$): δ_C 9.0, 16.9, 18.0, 25.9, 26.5, 37.8, 39.7, 66.0, 91.7, 96.6, 106.3, 118.6, 123.8, 132.3, 142.4, 162.4, 163.2, 167.4, 207.0; HRMS (ESI) *m/z*: $[M+H]^+$ Calcd. for $C_{19}H_{27}O_4$ 319.1909; Found 319.1917.

*4.2.6.3. (E)-1-(2-((3,7-Dimethylocta-2,6-dien-1-yl)oxy)-4,6-dihydroxyphenyl)butan-1-one (**20**).* Isolated after SPE (SiGel; hexane/EtOAc 94:6) as a pale yellow oil (110 mg, 0.331 mmol, 5.7% over three steps starting from **3**). UV (MeOH) λ_{max} (log ε): 243 (4.39), 290

(3.99) nm; IR ν_{max} (thin film) cm^{-1}: 3317, 2970, 1739, 1606, 1435, 1366, 1215, 745; ^1H NMR (500 MHz, $CDCl_3$): δ_H 0.97 (3H, t, $J = 6.5$ Hz), 1.61 (3H, s),1.69 (3H, s), 1.71 (2H, s), 1.74 (3H, s), 2.10 (2H, m), 2.13 (2H, m), 2.97 (2H, t, $J = 7.0$ Hz), 4.54 (2H, d, $J = 6.5$ Hz), 5.10 (1H, m), 5.50 (1H, t, $J = 6.5$ Hz), 5.91 (1H, s, HO4), 5.93 (1H, d, $J = 2.0$ Hz), 5.99 (1H, d, $J = 2.0$ Hz), 14.10 (1H, s); ^{13}C NMR (125 MHz, $CDCl_3$): δ_C 14.2, 16.9, 17.9, 18.9, 25.9, 26.5, 39.7, 46.5, 65.9, 92.1, 96.6, 106.0, 118.4, 123.8, 132.2, 142.7, 162.43, 163.4, 167.3, 206.9. HRMS (ESI) m/z: $[M+H]^+$ Calcd. for $C_{20}H_{29}O_4$,333.2066; Found 333.2057.

*4.2.6.4. (E)-1-(2-((3,7-Dimethylocta-2,6-dien-1-yl)oxy)-4,6-dihydroxyphenyl)pentan-1-one (**21**).* Isolated after SPE (SiGel; hexane/EtOAc 8:2) as a colourless oil (95 mg, 0.274 mmol, 2.2% over three steps starting from **3**). UV (MeOH) λ_{max} (log ε): 239 (4.36), 290 (3.97) nm; IR ν_{max} (thin film) cm^{-1}: 3263, 2957, 2929, 1739, 1621, 1569, 1416, 1346, 1198, 1164, 1102, 827, 791; ^1H NMR (500 MHz, $CDCl_3$): δ_H 0.92 (3H, t, $J = 6.5$ Hz), 1.37 (2H, q, $J = 6.5$ Hz), 1.61 (3H, s), 1.64 (2H, m), 1.69 (3H, s), 1.74 (3H, s), 2.10 (2H, m), 2.13 (2H, m), 3.00 (2H, m), 4.55 (2H, d, $J = 6.5$ Hz), 5.10 (1H, t, $J = 6.5$ Hz), 5.50 (1H, t, $J = 6.5$ Hz), 5.92 (1H, d, $J = 2.0$ Hz), 5.99 (1H, d, $J = 2.0$ Hz), 6.38 (1H, s), 14.04 (1H, s); ^{13}C NMR (125 MHz): δ_C 14.2, 16.9, 17.9, 22.8, 25.9, 26.5, 27.4, 39.6, 44.4, 65.9, 91.9, 96.6, 106.1, 118.4, 123.8, 132.2, 142.6, 162.9, 163.1, 167.4, 206.8; HRMS (ESI) m/z: $[M+H]^+$ Calcd. for $C_{21}H_{31}O_4$ 347.2222; Found 347.2223.

*4.2.6.5. (E)-1-(2-((3,7-Dimethylocta-2,6-dien-1-yl)oxy)-4,6-dihydroxyphenyl)decan-1-one (**22**).* Isolated after SPE (SiGel; hexane/EtOAc 96:4) as a colourless oil (85 mg, 0.204 mmol, 4.2% over three steps starting from **3**). UV (MeOH) λ_{max} (log ε): 244 (4.39), 293 (3.98) nm; IR ν_{max} (thin film) cm^{-1}: 3309, 2924, 2854, 1738, 1620, 1594, 1445, 1376, 1206, 1167, 1097, 829, 754; ^1H NMR (500 MHz, $CDCl_3$): δ_H 0.88 (3H, t, $J = 6.5$ Hz), 1.26 (12H, br s), 1.35 (2H, m), 1.61 (3H, s), 1.68 (3H, s), 1.74 (3H, s), 2.09 (2H, m), 2.13 (2H, m), 2.99 (2H, m), 4.56 (2H, d, $J = 6.5$ Hz), 5.11 (1H, t, $J = 6.5$ Hz), 5.51 (1H, t, $J = 6.5$ Hz), 5.92 (1H, d, $J = 2.0$ Hz), 5.99 (1H, d, $J = 2.0$ Hz), 14.12 (1H, s); ^{13}C NMR (125 MHz, $CDCl_3$): δ_C 14.4, 16.9, 17.9, 22.9, 25., 25.9, 26.6, 29.6, 29.7–29.8 (3C), 32.2, 39.8, 44.7, 65.9, 91.8, 96.6, 106.1, 118.5, 123.8, 132.2, 142.6, 163.0, 163.1, 167.5, 206.5; HRMS (ESI) m/z: $[M+H]^+$ Calcd. for $C_{26}H_{41}O_4$ 417.3005; Found 417.3001.

*4.2.6.6. (E)-1-(2-((3,7-Dimethylocta-2,6-dien-1-yl)oxy)-4,6-dihydroxyphenyl)octadecan-1-one (**23**).* Isolated after SPE (SiGel; hexane/EtOAc 96:4) as a pale yellow oil (650 mg, 1.230 mmol, 19% over three steps starting from **3**). UV (MeOH) λ_{max} (log ε): 237 (4.18), 286 (3.87) nm; IR ν_{max} (thin film) cm^{-1}: 3020, 2924, 2854, 1715, 1662, 1447, 1214, 1097, 829, 750; ^1H NMR (400 MHz, $CDCl_3$): δ_H 0.89 (3H, t, $J = 6.8$ Hz), 1.26–1.35 (34H, br s), 1.62 (3H, s), 1.69 (3H, s), 1.75 (3H, s), 2.10 (2H, m), 2.13 (2H, m), 2.99 (2H, m), 4.55 (2H, d, $J = 6.5$ Hz), 5.10 (1H, t, $J = 6.5$ Hz), 5.50 (1H, t, $J = 6.5$ Hz), 5.91 (1H, d, $J = 2.0$ Hz), 5.98 (1H, d, $J = 2.0$ Hz), 14.12 (1H, s); ^{13}C NMR (100 MHz, $CDCl_3$): δ_C 14.3, 16.9, 17.9, 22.9, 25.3, 25.9, 26.5, 29.6, 29.8–29.9 (15C′), 32.1, 39.7, 44.7, 65.9, 91.7, 96.6, 106.3, 118.5, 123.8, 132.2, 142.5, 162.6, 163.1, 167.5, 206.7; HRMS (ESI) m/z: $[M+H]^+$ Calcd. for $C_{34}H_{57}O_4$ 529.4257; Found 529.3710.

*4.2.6.7. (E)-(2-((3,7-Dimethylocta-2,6-dien-1-yl)oxy)-4,6-dihydroxyphenyl) (phenyl) methanone (**24**).* Isolated after SPE (SiGel; hexane/EtOAc 9:1) as a pale yellow oil (96 mg, 0.262 mmol, 10% over three steps starting from **3**); UV (MeOH) λ_{max} (log ε): 237 (4.45), 288 (3.99) nm; IR ν_{max} (thin film) cm^{-1}: 3308, 2970, 2923, 1738, 1621, 1590, 1446, 1376, 1271, 1154, 1095, 825, 752; ^1H NMR (500 MHz, $CDCl_3$): δ_H 1.52 (3H, s), 1.61 (3H, s), 1.71 (3H, s), 1.85 (2H, m), 1.94 (2H, m), 4.21 (2H, d, $J = 6.5$ Hz), 4.61 (1H, t, $J = 6.5$ Hz), 5.05 (1H, m), 5.89 (1H, d, $J = 2.0$ Hz), 6.07 (1H, d, $J = 2.0$ Hz), 7.36 (2H, dt, $J = 8.0$, 1.5 Hz), 7.42 (1H, d, $J = 8.0$ Hz), 7.49 (2H, dt, $J = 8.0$, 1.5 Hz), 12.27 (1H, s); ^{13}C NMR (125 MHz, $CDCl_3$): δ_C 16.8, 17.9, 25.9, 26.4, 39.4, 65.5, 92.4, 96.5, 106.2, 118.1, 124.0, 127.6 (2C), 127.8, 130.7, 132.0, 140.7, 142.5, 162.4, 163.5, 165.9, 200.1; HRMS (ESI) m/z: $[M+H]^+$ Calcd. for $C_{23}H_{27}O_4$ 367.1909; Found 367.1893.

4.3. Antibacterial assay against Staphylococcus aureus

Unless otherwise stated, all chemicals were obtained from Sigma-Aldrich, Gillingham, UK. Cation-adjusted Mueller-Hinton broth (MHB) was obtained from Oxoid and was adjusted to contain 20 mg/L and 10 mg/L of Ca^{2+} and Mg^{2+}, respectively. The *S. aureus* strains used in this study included ATCC 25923, SA-1199B, RN4220, XU212, EMRSA-15 and EMRSA-16. A standard laboratory strain, ATCC 25923, which is sensitive to antibiotics like tetracycline [15], was also used in this study. SA-1199B over-expresses the NorA MDR efflux pump [16], RN4220 possesses the MsrA macrolide efflux protein [17], XU212 is a Kuwaiti hospital isolate which is an MRSA strain possessing the TetK tetracycline efflux pump [15], whilst the EMRSA-15 strain [18] and EMRSA-16 strain [19] are epidemic in the UK. These strains were the generous gift of Dr Paul Stapleton (UCL).

All *S. aureus* strains were cultured on nutrient agar (Oxoid) and incubated for 24 h at 37 °C prior to MIC determination. A stock solution of norfloxacin was prepared by dissolving the antibiotic (2 mg) in DMSO (244 μL; Sigma) and diluting 16-fold with MHB to obtain the desired starting concentration (512 mg/L) of antibiotic. Similarly, stock solutions of the test compounds were prepared by initial dissolution in DMSO followed by dilution with MHB to produce target concentrations of 512 mg/L. No significant precipitation was noted for any of the test compounds when stock solutions were prepared at this concentration. An inoculum density of 5×10^5 colony forming units (cfu/mL) of each bacterial strain was prepared in normal saline (9 g/L) by comparison with a 0.5 Mac-Farland turbidity standard.

During the experiment, MHB (125 μL) was added to each well of a 96-well plate, save for the final column which was left empty. 125 μL of the stock solution of the compound to be tested (or the control antibiotic norfloxacin) was then added to the MHB in the first well. Using a multi-channel pipette, the contents of the first well were mixed thoroughly, followed by the transfer of 125 μL of the well contents to the second well. This two-fold serial dilution process was continued up until the tenth well, and the final 125 μL solution was added to the final (empty) well. The inoculum (125 μL) of each bacterium at a density of 5×10^5 cfu/mL was added to all wells except those in the final column. The final concentrations of each test compound thus ranged from 128 mg/L to 0.25 mg/L in the initial evaluation (similarly, the final concentrations of DMSO in the assays ranged from 1.56% *v/v* at the highest concentration of test compound to 0.0031% *v/v* at the lowest). The contents of the wells in columns 11 and 12 represented growth control (bacteria but no compound) and sterility control (compound but no bacteria) respectively. Every assay was performed in duplicate. The microtitre plates were then incubated at 37 °C for the appropriate incubation time. For the MIC determination, 20 μL of a 5 mg/mL methanolic solution of 3-(4,5-dimethylthiazol-2-yl)-2,5-diphenyltetrazolium bromide (MTT) was added to each of the wells, followed by incubation for 20 min. Bacterial growth was indicated by a colour change from yellow to dark blue. The MIC was recorded as the lowest concentration at which no growth was observed [11]. If no growth was observed at any of the concentrations tested, the assay was repeated starting with a stock solution of lower concentration. If growth was observed at all of the concentrations tested, the assay was repeated starting with a stock solution of higher concentration.

Acknowledgements

This work was supported by the Heptagon Fund (Heptagon 96/SoP16).

Appendix A. Supplementary data

Supplementary data related to this article can be found at https://doi.org/10.1016/j.ejmech.2018.05.038.

References

[1] G.M. Cragg, P.G. Grothaus, D.J. Newman, Impact of natural products on developing new anti-cancer agents, Chem. Rev. 109 (2009) 3012–3043.
[2] A. Butler, T. Hensman, Drugs for the fever, Educ. Chem. 37 (2000) 151.
[3] G. Patrick, The opioid analgesic, in: An Introduction to Medicinal Chemistry, fifth ed., Oxford University Press, Oxford, 2013, p. 632.
[4] A. Hollman, Digoxin comes from *Digitalis lanata*, Br. Med. J. 312 (1996) 912.
[5] R. Gautam, A. Saklani, S.M. Jachak, Indian medicinal plants as a source of antimycobacterial agents, J. Ethnopharmacol. 110 (2007) 200–234.
[6] Z. Wang, P. Yu, G. Zhang, L. Xu, D. Wang, L. Wang, X. Zeng, Y. Wang, Design, synthesis and antibacterial activity of novel andrographolide derivatives, Bioorg. Med. Chem. 18 (2010) 4269–4274.
[7] M. Oluwatuyi, G.W. Kaatz, S. Gibbons, Antibacterial and resistance modifying activity of *Rosmarinus officinalis*, Phytochemistry 65 (2004) 3249–3254.
[8] G. O'Donnell, R. Poeschl, O. Zimhony, M. Gunaratnam, J.B.C. Moreira, S. Neidle, D. Evangelopoulos, S. Bhakta, J.P. Malkinson, H.I. Boshoff, A. Lenaerts, S. Gibbons, Bioactive pyridine-N-oxide sulphides from *Allium stipitatum*, J. Nat. Prod. 72 (2009) 360–365.
[9] J. O'Neill, Tackling Drug-resistant Infections Globally: Final Report and Recommendations the Review on Antimicrobial Resistance, 2016.
[10] C.M. Schempp, K. Pelz, A. Wittmer, E. Schöpf, J.C. Simon, Antibacterial activity of hyperforin from St John's wort against multi-resistant *Staphylococcus aureus* and Gram-positive bacteria, Lancet 353 (1999) 2129.
[11] W.K.P. Shiu, M.M. Rahman, J. Curry, P.D. Stapleton, M. Zloh, J.P. Malkinson, S. Gibbons, Antibacterial acylphloroglucinols from *Hypericum olympicum* L. cf. uniflorum, J. Nat. Prod. 75 (2012) 336–343.
[12] M.J. Begley, L. Crombie, R.C.F. Jones, C.J. Palmer, Synthesis of the *Mammea* coumarins. Part 4. Stereochemical and regiochemical studies, and synthesis of (-)-mammea B/BB, J. Chem. Soc. Perk. T. 1 (1) (1987) 353–357.
[13] L. Crombie, R.C.F. Jones, C.J. Palmer, Synthesis of the *Mammea* coumarins. Part 1. The coumarins of the mammea A, B, and C series, J. Chem. Soc. Perk. T. 1 (1) (1987) 317–331.
[14] A. Liu, K. Dillon, R.M. Campbell, D.C. Cox, D.M. Huryn, Synthesis of E-selectin inhibitors: use of an aryl-cyclohexyl ether as a disaccharide scaffold, Tetrahedron Lett. 37 (1996) 3785–3788.
[15] S. Gibbons, E.E. Udo, The effect of reserpine, a modulator of multidrug efflux pumps, on the *in vitro* activity of tetracycline against clinical isolates of methicillin resistant *Staphylococcus aureus* (MRSA) possessing the *tet*(K) determinant, Phytother Res. 14 (2000) 139–140.
[16] G.W. Kaatz, S.M. Seo, C.A. Ruble, Efflux-mediated fluoroquinolone resistance in *Staphylococcus aureus*, Antimicrob. Agents Chemother. 37 (1993) 1086–1094.
[17] J.L. Ross, A.M. Farrell, E.A. Eady, J.H. Cove, W.J.J. Cunliffe, Characterisation and molecular cloning of the novel macrolide-streptogramin B resistance determinant from *Staphylococcus epidermidis*, Antimicrob. Agents Chemother. 24 (1989) 851–862.
[18] J.F. Richardson, S. Reith, Characterization of a strain of methicillin-resistant *Staphylococcus aureus* (EMRSA-15) by conventional and molecular methods, J. Hosp. Infect. 25 (1993) 45–52.
[19] R.A. Cox, C. Conquest, C. Mallaghan, R.R.A. Marples, Major outbreak of methicillin-resistant *Staphylococcus aureus* caused by a new phage-type (EMRSA-16), J. Hosp. Infect. 29 (1995) 87–106.

RSC Advances

PAPER

View Article Online
View Journal | View Issue

Cite this: *RSC Adv.*, 2016, **6**, 43518

Benzocyclohexane oxide derivatives and neolignans from *Piper betle* inhibit efflux-related resistance in *Staphylococcus aureus*†

Zhong-Lin Sun,[a] Jian-Ming He,[a] Shuang-Ying Wang,[a] Ru Ma,[a] Proma Khondkar,[b] Glenn W. Kaatz,[c] Simon Gibbons[b] and Qing Mu*[a]

Received 20th April 2016
Accepted 26th April 2016

DOI: 10.1039/c6ra10199b

www.rsc.org/advances

This research seeks to address the problem of methicillin-resistant *Staphylococcus aureus* (MRSA) by discovering synergistic antibacterial natural substances from traditional Chinese herbs using antibacterial bioassays. Six compounds, including three neolignans (−)-acuminatin (**1**), (−)-denudatin B (**2**), puberulin D (**3**), and three benzocyclohexane oxide derivatives ferrudiol (**4**), ellipeiopsol B (**5**) and zeylenol (**6**), were isolated and purified by silica gel and reverse-phase silica gel column chromatography, and the chemical structures were determined through NMR spectroscopy, MS, together with CD and calculated CD spectroscopic methods. Synergistic activity was determined using strain SA1199B, a strain that overexpresses the major *S. aureus* multidrug transporter, NorA. Compounds **1–6** showed synergistic activity combined with norfloxacin against SA1199B, with FICI values of 0.13, 0.25, 0.25, 0.52, 0.08 and 0.27 respectively. The synergistic effects of the benzocyclohexane oxide derivatives with norfloxacin were further demonstrated through strain growth kinetics experiments. In the mechanistic experiment, the compounds showed significant accumulation and/or inhibition effects for EtBr efflux in SA1199B. These active compounds showed no toxicity to HEK293T cells at a concentration of 100 μM in the cytotoxicity evaluation experiments. Combined with efflux pump inhibitors, classic antibiotics that are substrates for efflux pumps may yet play a role in the therapy of drug-resistant bacteria where a lower dose could result in improved safety.

1. Introduction

Over the past few decades, there has been a dramatic decrease in the number of pharmaceutical companies developing new antimicrobial drugs.[1] Methicillin-resistant *Staphylococcus aureus* (MRSA) is still cause for concern due to the small number of compounds that can be used therapeutically for this organism and resistance associated with their use.[2] A supplemental strategy to overcome resistance is to develop agents that can suppress bacterial resistance mechanisms, and such agents are known as resistance-modifying agents (RMAs).[3] These compounds may work by synergism, which is defined as a phenomenon in which two or more different compounds are combined to enhance their individual activity,[4] and this approach is now widely recognized and can be directly applied to the development of new pharmaceuticals.[5]

Whilst there are different kinds of mechanisms of drug-resistance, multidrug-resistance (MDR)-related efflux is a common and important one, and has been reported for many organisms, including bacteria, fungi and protozoa, and also as a mechanism of resistance in human tumor cells.[6] Examples of efflux-related resistance mechanisms that have been reported for *S. aureus* include those conferred by QacA and NorA, which are MDR transporters.[7] Fluoroquinolone resistance, facilitated by the NorA efflux protein,[6] has been shown to be a particular risk factor for mortality associated with infections by *S. aureus*.[8] Therefore, in our research, we have studied the effects of plant natural products on *S. aureus* strain SA1199B, which is fluoroquinolone resistant by means of increased NorA production as well as a critical amino acid substitution within the quinolone resistance-determining region of GrlA.[9] We evaluated the *in vitro* synergism of extracts of *Piper betle* Linn. (Piperaceae) with the fluoroquinolone antimicrobial drug norfloxacin against *S. aureus* strains by the broth microdilution method.[10]

P. betle is widely distributed in Yunnan, Guangxi and the Guangdong province of China,[11] and cultivated in India for its leaves, which are used for chewing.[12] Experimentally, the extracts and herbal material of *P. betle* have been shown to

[a]*School of Pharmacy, Fudan University, Shanghai 201203, China. E-mail: muqing2200@gmail.com*

[b]*Research Department of Pharmaceutical and Biological Chemistry, UCL School of Pharmacy, London WC1N 1AX, UK*

[c]*The John D. Dingell Department of Veteran's Affairs Medical Centre and Department of Internal Medicine, Division of Infectious Diseases, School of Medicine, Wayne State University, Detroit, Michigan 48201, USA*

† Electronic supplementary information (ESI) available. See DOI: 10.1039/c6ra10199b

possess many kinds of curative properties such as laxative, aphrodisiac, antimicrobial,[13] antioxidant[14] and to improve appetite.[15] The plant is rich in phenolics,[16] methyl piperbetol, piperol A and piperol B,[17] and some benzocyclohexane oxide derivatives and neolignans.[18] In this report, we studied the chemical constituents of *P. betle*, guided by an antibacterial synergistic assay, and a series of preliminary mechanistic experiments were carried out.

2. Materials and methods

2.1. General experimental instruments and materials

The silica gel (100–400 mesh) used in column chromatography was purchased from Qingdao Marine Chemical Plant, China. ^{1}H and ^{13}C NMR spectra were obtained on a Varian Mercury Plus 400 MHz spectrometer. EI-MS spectra were measured with an Agilent 5973N MSD mass spectrometer. IR spectra and UV spectra were recorded on an Avatar 360 ESP FTIR spectrophotometer and a HITACHI U-2900 spectropolarimeter, respectively. Fractions obtained from column chromatography were monitored by thin layer chromatography (TLC) (silica gel plate HGF254, Yantai Huangwu Chemical Plant, Yantai, China). Optical density was recorded on a Multiskan FC (Thermo Co. Ltd, USA), and fluorescence was recorded on a Tecan M 1000 plate reader (Tecan Co. Ltd., Switzerland).

2.2. Extraction and bioactivity-guided isolation

P. betle was collected in Mengla County, Yunnan Province of China, in December of 2002, and identified by Professor Xu You-Kai, Professor of Xishuangbanna Botanic Garden in Yunnan province, the Chinese Academic of Science. A voucher specimen (148888) was deposited at the Herbarium and used in identifying the plant by professor You-Kai, and in the same time, we also saved a plant sample in our lab in School of Pharmacy, Fudan University. 100 g air dried leaves of *P. betle* were extracted using 95% ethanol by maceration and 10.8 g resinous extract was obtained. The resulting resin was then extracted using chloroform by solid–liquid extraction and yielded a gum (3 g). The total chloroform extract, was dissolved in acetone and mixed with silica gel and then subjected to silica gel and eluted with a gradient of chloroform–acetone (99 : 1–7 : 3). Fractions A–H were obtained by TLC monitoring with similar eluents. All of the eight fractions were subjected to Middle Chromatogram Isolated (MCI) gel to remove chlorophyll. Under the guidance of the synergistic activity, some fractions were further separated selectively and six compounds were obtained. Compound **1**, named (−)-acuminatin (8 mg) was isolated from fraction B by silica gel column chromatography with elution of petroleum ether–acetone (95 : 5). Compounds **2** and **3**, named (−)-denudatin B (10 mg) and puberulin D (3 mg), were both obtained from fraction C. Compound **2** was isolated by forward silica gel column chromatography with elution of petroleum ether–ethyl acetate (9 : 1) while compound **3** was obtained by high-pressure liquid chromatography (HPLC) preparation with elution of methanol–water (8 : 2). Fraction E was further separated to obtain compound **4**, named ferrudiol (12 mg), by silica gel column chromatography with elution of chloroform–acetone (95 : 5). Compounds **5** and **6**, named ellipeiopsol B (20 mg) and zeylenol (35 mg), were isolated from fraction F by silica gel column chromatography and Sephadex LH-20 gel column chromatography. The structures of all the compounds were deduced from spectroscopic methods (NMR spectroscopy and mass spectrometry) and all the resulting data were in good agreement with the literature.

2.3. HPLC fingerprint

The chloroform extract and six compounds (**1–6**) were dissolved in methanol, respectively. Each solution (2 mg mL^{-1}) was subjected on the HPLC (10 μL, Agilent 1200) using an autosampler at 25 °C. The specifications and models of using column are eclipse XDB-C18, 5 μm, 4.6 × 250 mm (Agilent). The eluent flow rate was set to 1.0 mL min^{-1} propelled by an Agilent 1200 series G1312B SL binary pump, with ultra-pure water and HPLC-grade methanol (solutions A and B) eluting using the gradient method: started with 50% B, changing to 70% B within 30 min, then changing to 90% B within 40 min, the total time was 75 min. UV detector was used and the signal of compounds was monitored at a wavelength of 254 nm.

2.4. Electronic circular dichroism (ECD) spectral calculations

The absolute configurations of the six compounds were predicted by a quantum chemical calculation using Gaussian 09.[19] The geometries of all compounds were optimized at the B3LYP/6-31G level of density functional theory (DFT). The Electronic Circular Dichroism (ECD) spectra were then calculated using the time dependent DFT (TDDFT) method at the B3LYP/6-311++G** level in the solvent methanol.

2.5. Antibacterial minimum inhibitory concentration (MIC) assay

Five *Staphylococcus aureus* strains (SA1199B, XU212, RN4220, EMRSA-15 and EMRSA-16) were used in experiments, all of which had a drug-resistance phenotype. Strain SA1199B, which overexpresses the *nor*A gene encoding the NorA MDR efflux pump, was the generous gift of Professor Glenn W. Kaatz.[20] Strain XU212, which possesses the TetK tetracycline efflux protein, was provided by Dr Edet Udo.[21] Strain RN4220, was provided by Dr Jon Cove.[22] Strains EMRSA-15 and strain EMRSA-16, which are epidemic methicillin-resistant (MRSA) strains, were the kind gift of Dr Paul Stapleton.[23]

Minimum inhibitory concentration (MICs) values were determined following the guidelines of Clinical Laboratory Standards Institute.[24] Mueller-Hinton broth (MHB; Oxoid), was used which was supplemented with 20 and 10 mg L^{-1} of Ca^{2+} and Mg^{2+} respectively. All bacterial suspensions were adjusted to 5×10^{5} cfu mL^{-1} for the bioassay. 2% DMSO in broth served as the negative control and vancomycin (Sigma Chemical Co. Ltd) served as the positive control. All compounds and chloroform extract were dissolved in DMSO respectively and then diluted with MHB, added into 96-well microtiter plate, with a concentration of 512 mg L^{-1} in upmost row and each

following row (B–H) contained half concentration of the previous one. Both controls and treatments were tested in duplicate. After incubation at 37 °C for 24 h, 20 μL of 3-[4,5-dimethylthiazol-2-yl]-2,5-diphenyltetrazolium bromide (MTT; Biosharp) solution (5 mg mL^{-1}) was added into each well to determined MIC. MTT colorimetric assay was performed to determine the MIC values. The minimum concentrations for colour appearing from black to yellow (completely inhibited the visible bacterial growth) were recorded as the MIC values against test strains.

2.6. Synergy tests

The five drug-resistant *S. aureus* strains described above were used in broth microdilution antimicrobial checkerboard assays[10,25] to examine for the presence of a synergistic interaction. The rows of a 96-well microtiter plate contained compounds isolated with a concentration of 128 mg L^{-1} in upmost row (A) and each following row (B–G) contained half concentration of the previous one. Row (H) contained no compounds but MHB. A similar procedure was carried out along columns (1–12) with concentration of specific antibiotics ranging from 256 to 0.5 mg L^{-1}. All of the treatments were tested in duplicate wells. MTT colorimetric assay was performed to determine the MIC values, which were used to evaluate the effects of the combination of compounds and antibiotics by calculating the fractional inhibitory concentration index (FICI) according to the formula:

$$\mathrm{FICI} = \frac{\mathrm{MIC\ (antibiotic\ combined\ with\ compound)}}{\mathrm{MIC\ (antibiotic\ alone)}} + \frac{\mathrm{MIC\ (compound\ combined\ with\ antibiotic)}}{\mathrm{MIC\ (compound\ alone)}}$$

"Synergy" effects were defined when the FICI was less than or equal to 0.5. When the FICI was greater than 0.5 and less than or equal to 4.0 this was regarded as an "indifference" effect; whilst "antagonistic" effects were observed when the FICI was greater than 4.0.[26] An isobologram was constructed to depict the results of the checkerboard assay and the FICI values.

2.7. EtBr efflux assay

Those compounds for which an adequate amount existed were chosen for an efflux assay as previously described.[27] Test organisms were grown overnight in cation-adjusted MHB until the $OD_{620} = 0.4$ and then followed by the addition of carbonyl cyanide *m*-chlorophenylhydrazone (CCCP, Across Organic) and EtBr (Sigma) (final concentrations, 100 μM (20.5 mg L^{-1}) and 25 μM (2.725 mg L^{-1}), respectively). After incubation at room temperature for 20 min, 4 mL of the inocula was pelleted at 13 000*g* for 5 min and then re-suspended in 3 mL of fresh MHB containing CCCP or the tested compounds (final concentrations, all 100 μM) (35.6 mg L^{-1} for compound **2**, 48.8 mg L^{-1} for compound **4** and 38.4 mg L^{-1} for compound **5** and **6**). Fluorescence of the suspension was monitored continuously (excitation and emission wavelengths were 530 and 600 nm, respectively; slit width was 5 nm) every five min for one hour. All tested compounds and the control were measured in triplicate.

2.8. EtBr accumulation assay

Ferrudiol (**4**), ellipeiopsol B (**5**) and zeylenol (**6**) were subjected to the EtBr accumulation assay by the fluorometric method due to their adequate quantity. This assay was conducted according to a modification of reported methods.[28] Organisms were grown overnight in cation-adjusted MHB until the OD_{620} reached 0.4. Then 3 mL of the inoculum was collected by centrifugation at 13 000*g* for 5 min and re-suspended using fresh MHB to adjust the OD_{620} to 0.4. Culture medium (50 μL) and an equal volume of CCCP and test compounds (final concentrations, all 100 μM) (20.5 mg L^{-1} for CCCP, 48.8 mg L^{-1} for compound **4** and 38.4 mg L^{-1} for compound **5** and **6**) were added to a 96-well plate containing 100 μL of EtBr (final concentration, 12.5 μM) (1.36 mg L^{-1}). The 96-well plate was filled with 200 μL of the suspension and monitored continuously by the fluorescence of the suspension (excitation and emission wavelengths were 530 and 600 nm, respectively; slit width was 5 nm) every five min for one hour. All tested compounds and the control were measured in triplicate.

2.9. Growth curves

Growth kinetics was determined according to Garvey[29] with some modifications. The growth kinetics of strain SA1199B in the absence or presence of the benzocyclohexane oxide derivatives were determined by monitoring the optical density at 620 nm every 2 h at 37 °C for 12, 24, 36 and 48 h using a microwell reader (Multiskan FC, Thermo). The final concentration of compounds and norfloxacin both alone and in combination with each other were 128 mg L^{-1} and 4 mg L^{-1}. All tested compounds and the control were measured in triplicate.

2.10. Cytotoxicity evaluation

To determine whether the benzocyclohexane oxide derivatives were toxic, a cytotoxicity assay using a human embryonic kidney cell line (HEK293T) with the method of the 3-(4,5-dimethylthiazol-2-yl)-2,5-diphenyltetrazolium bromide (MTT) assay was carried out and the cell viability was measured according to Lu with some modifications.[30] Cells were plated into 96-well plates at a cell density of 5×10^3 cells per well and allowed to grow in a 5% CO_2 incubator. After 24 h, the medium was removed and replaced by fresh medium containing the tested compounds that were dissolved in DMSO and diluted to various concentrations (final concentrations were 100, 30, 10, 3, 1 μM respectively) with complete medium (RPMI 1640 + 10% FBS) before the experiment, and the final concentration of DMSO was 0.1%. After 24 hours incubation, cultures were incubated in 200 μL of medium with 20 μL of 5 mg mL^{-1} MTT solution for 4 hour at 37 °C. The medium with MTT was removed, and 150 μL of DMSO was added to each well to dissolve the formazan. The absorbance at 490 nm was measured with a microwell reader (Multiskan FC, Thermo). The inhibitory percentage of each compound at various concentrations was

calculated, and the IC_{50} value was determined. All tested compounds and the control were measured in triplicate.

3. Results

3.1. Extraction and isolation

Compounds **1–6** were identified as the known chemical constituents (−)-acuminatin (**1**),[31] (−)-denudatin B (**2**),[31] puberulin D (**3**),[32] ferrudiol (**4**),[33–35] ellipeiopsol B (**5**)[34,35] and zeylenol (**6**)[34,35] (Fig. 1) by comparison of their physical properties and spectral data (ESI Tables S1 and S2†) with the literature. The chemical systematic name of the compound **3** is (7*S*,8*S*,1′*R*,5′*R*,6′*S*)-$\Delta^{2',8'}$-6′-acetoxy-3′-methoxy-3,4-methylenedioxy-4′-oxo-8.1′,7.5′-neolignan,[32] which was given a trivial name as puberulin D in this manuscript. The absolute configuration of compounds **1–6** were determined by comparison of their circular dispersion (CD) spectra with those reported and with the quantum chemical calculated CD spectra (ESI Fig. S1†). The purities of all six compounds were ≥95% as determined by HPLC (Fig. S2†).

3.2. HPLC fingerprint

The HPLC fingerprint with well resolved peak separation for the chloroform extract of *P. betle* was obtained (Fig. 2). Compounds **1–6** were unambiguously recognized in the fingerprint by comparing with their retention time (Fig. 2). The retention time of (−)-acuminatin (**1**) was 41.473, which is the peak with retention time 41.418 in the fingerprint. We can were also able to identify the peaks for (−)-denudatin B (**2**), puberulin D (**3**), ferrudiol (**4**), ellipeiopsol B (**5**) and zeylenol (**6**) in the fingerprint with a retention time 31.431 min, 29.531 min, 39.988 min, 16.740 min and 11.281 min, respectively. The relative percentage contents of compounds **1–6** were 6.3%, 9.4%, 4.1%, 10.5%, 9.5% and 11.3% respectively. Total contents of the six compounds were more than fifty percent.

3.3. Antibacterial minimum inhibitory concentration (MIC) assay

The chloroform extract and compounds **1–6** were assayed for antibacterial activity against all test strains of *S. aureus*, and none had any significant antibacterial effect in that all MICs exceeded 512 mg L^{-1}.

3.4. Synergy tests

The five drug-resistant *S. aureus* strains described above and antibiotics to which the strains were resistant were employed. The results showed that compounds **1–6** showed significant synergistic effects with norfloxacin against strain SA1199B,

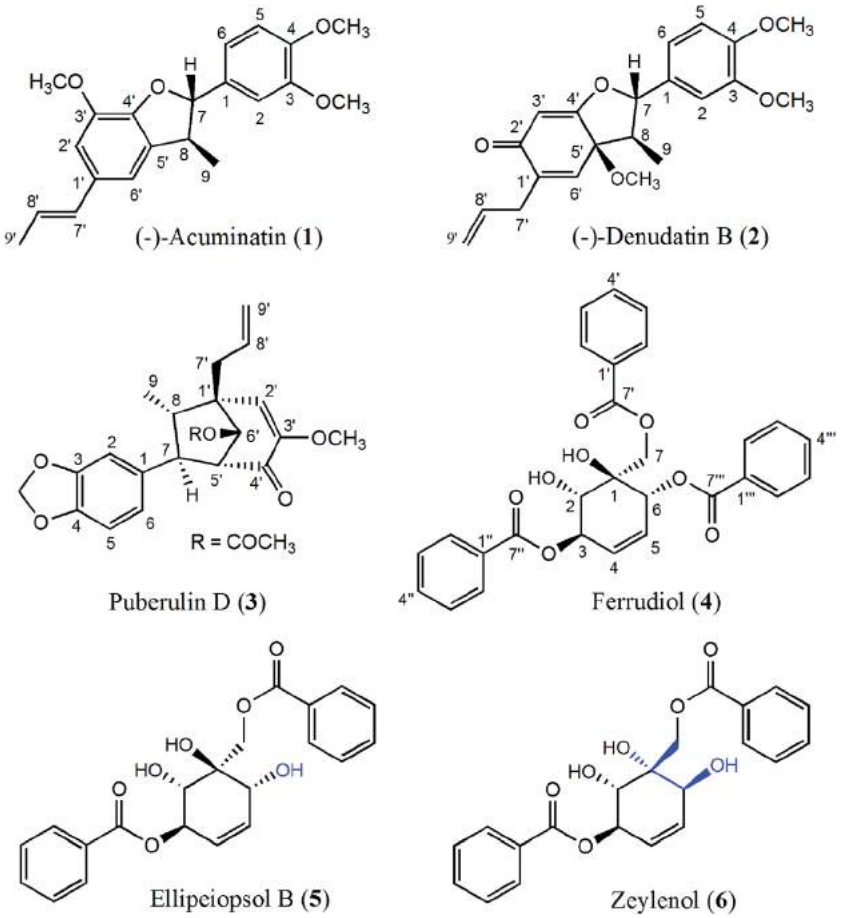

Fig. 1 Chemical structures of compounds **1–6** isolated from *Piper betle*.

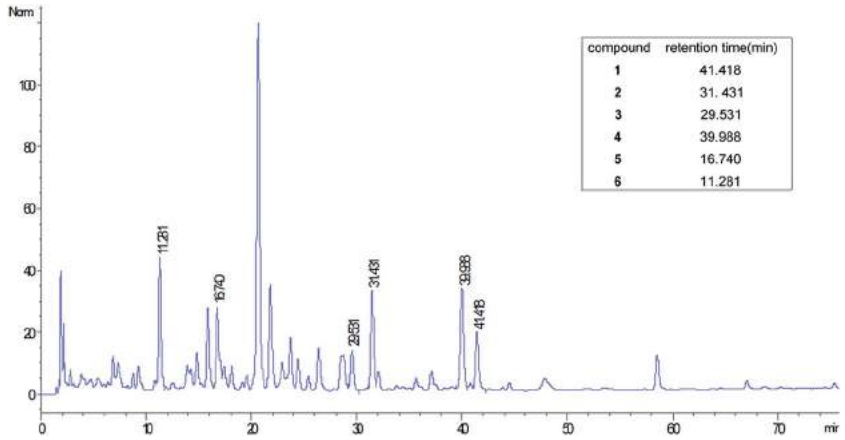

Fig. 2 The HPLC fingerprint of chloroform extract.

which overexpresses the *norA* gene encoding the NorA MDR efflux pump, but no synergetic effects were observed for the other four strains (XU212, RN4220, EMRSA-15 and EMRSA-16). (−)-Acuminatin (**1**), (−)-denudatin B (**2**), puberulin D (**3**), ferrudiol (**4**), ellipeiopsol B (**5**) and zeylenol (**6**) reduced the MIC of norfloxacin against SA1199B by eight-, four-, four-, two-, sixteen- and eight-fold respectively. This resulted in a concentration decrease of the antibiotic from 64 to 8 mg L^{-1}, 128 to 32 mg L^{-1}, 64 to 16 mg L^{-1}, 64 to 32 mg L^{-1}, 64 to 4 mg L^{-1} and 64 to 8 mg L^{-1}, respectively (Table 1). The FICI of the combinations were 0.13, 0.25, 0.25, 0.52, 0.08, 0.27, respectively and we were able to construct an isobologram depicting the synergistic effects for the six compounds (ESI Fig. S3†).

3.5. EtBr efflux assay

All compounds were subjected to an EtBr efflux assay by the fluorometric method without (−)-acuminatin (**1**) and puberulin D (**3**) due to their limited quantity. As shown in Fig. 3, ferrudiol (**4**), ellipeiopsol B (**5**) and zeylenol (**6**) had moderate efflux pump inhibitory effects against SA1199B (Fig. 3a, b and d), whereas (−)-denudatin B (**2**) demonstrated a strong efflux inhibitory effect against this strain (Fig. 3c). Within the first half hour, ferrudiol (**4**) showed a similar efflux pump inhibitory effect compared with the positive control CCCP, while a stronger effect than CCCP over the subsequent half hour was observed (Fig. 3a). Zeylenol (**6**) showed a similar activity compared with CCCP within one hour (Fig. 3b) and (−)-denudatin B (**2**) exhibited a stronger activity than CCCP within one hour (Fig. 3c). Ellipeiopsol B (**5**) showed a stronger activity than CCCP, but with a weaker effect than CCCP over the second half hour (Fig. 3d).

3.6. EtBr accumulation assay

Ferrudiol (**4**), ellipeiopsol B (**5**) and zeylenol (**6**) exhibited EtBr accumulation effects with strain SA1199B (Fig. 4). They all increased the concentrations of EtBr compared with the vehicle

Table 1 Minimum inhibitory concentrations (MIC) and fractional inhibition concentration indices (FICI) of six compounds from *Piper betle* for *S. aureus* SA1199B[a]

		MIC (mg L^{-1})			
Drug-resistant strain	Agent	Alone	Combination	FIC	FICI
SA1199B	(−)-Acuminatin (**1**)	>512	2	<0.004	<0.13
	Norfloxacin	64	8	0.125	
	(−)-Denudatin B (**2**)	>512	2	<0.004	<0.25
	Norfloxacin	128	32	0.25	
	Puberulin D (**3**)	>512	2	<0.004	<0.25
	Norfloxacin	64	16	0.25	
	Ferrudiol (**4**)	>512	8	<0.02	<0.52
	Norfloxacin	64	32	0.5	
	Ellipeiopsol B (**5**)	>512	8	<0.02	<0.08
	Norfloxacin	64	4	0.06	
	Zeylenol (**6**)	>512	8	<0.02	<0.27
	Norfloxacin	64	16	0.25	

[a] (1) FICI ≤ 0.5 is defined as synergy; 0.5 < FICI ≤ 1 as additive; 0.5 < FICI ≤ 4 as indifferent; 4 < FICI as antagonistic. (2) All six compounds have no direct inhibitory effects on five strains and no synergetic effects combined with the other four strains, so data about those was not listed in above table.

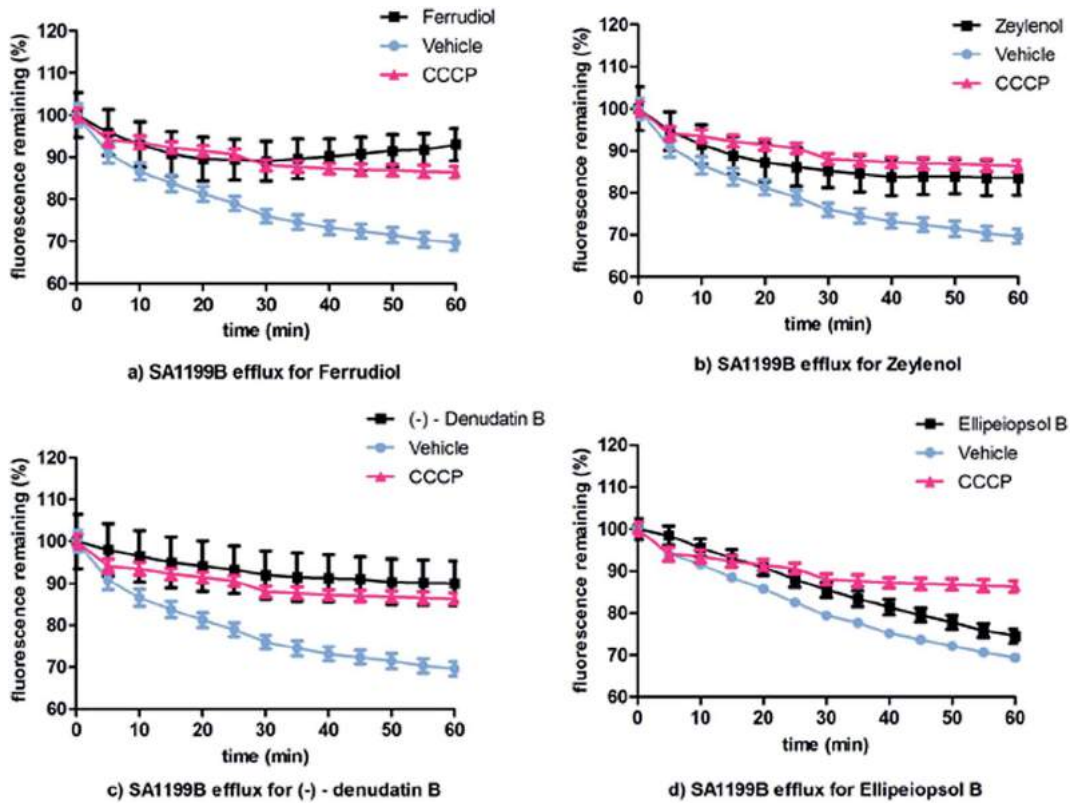

Fig. 3 EtBr efflux inhibitory effects of ferrudiol (**4**), zeylenol (**6**), (−)-denudatin B (**2**) and ellipeiopsol B (**5**) against *S. aureus* SA1199B.

control, especially ellipeiopsol B (**5**), showing stronger activity than the positive control CCCP (Fig. 4c). Zeylenol (**6**) had a similar activity compared with CCCP (Fig. 4b) and ferrudiol (**4**) showed a weaker activity compared to CCCP but with a significantly stronger effect than the control vehicle (Fig. 4a).

3.7. Growth curves

Time-growth experiments of SA1199B in the absence or presence of norfloxacin and compounds alone and in combination with each other are shown in Fig. 5. The ordinate represents the increased several times of OD value. The results suggested that the increase of strain growth in a mixture of norfloxacin and compounds was less than strain growth with norfloxacin or compounds alone. All three of the tested compounds ferrudiol (**4**), ellipeiopsol B (**5**) and zeylenol (**6**) alone showed weak growth inhibitory activity within the first 30 h, while no activity within the last 18 h was observed. Interestingly, SA1199B with norfloxacin and the test compounds exhibited a lower OD value increase than with SA1199B and norfloxacin alone within 48 h (Fig. 5).

3.8. Cytotoxicity evaluation

In terms of the cytotoxic activity of the benzocyclohexane oxide derivatives, ferrudiol (**4**), ellipeiopsol B (**5**) and zeylenol (**6**) showed no toxicity with IC_{50} values within the concentration of 100 μM for HEK293T cells, a human embryonic kidney cell line. As shown in the ESI Fig. S5,† within the 1–100 μM L^{-1} (<48.8 mg L^{-1} for compound **4**, <38.4 mg L^{-1} for compound **5** and **6**) concentration range of all three compounds the viability of HEK293T was approximately 100%. The compounds on their own had no cytotoxicity and did not increase the toxicity of norfloxacin compared with norfloxacin alone within the antibacterial effect concentration (ESI Fig. S6†).

4. Discussion

In the primary experiment, the chloroform extract of *Piper betle* showed no direct bacterial growth inhibition but had a marginal synergistic effect together with the antibiotics. Under the guidance of a synergistic bacterial assay employing a checkerboard methodology in combination with chromatography, three neolignans [(−)-acuminatin (**1**), (−)-denudatin B (**2**) and puberulin D (**3**)] and three benzocyclohexane oxide derivatives [ferrudiol (**4**), ellipeiopsol B (**5**) and zeylenol (**6**)] were isolated from the extract. These compounds were isolated from other *Piper* species such as *P. cubeba*, *P. puberulum* and so on previously. All six compounds showed no direct bacterial inhibition but had significant synergistic activity with norfloxacin against strain SA1199B. The MIC values of the antibiotic combined with the compounds was several times less than that of the antibiotic alone (Table 1). The six compounds were known compounds, but there are no reports on their synergistic activities on drug-resistant strains. Considering the tested strain SA1199B overexpressing the NorA efflux pump, we

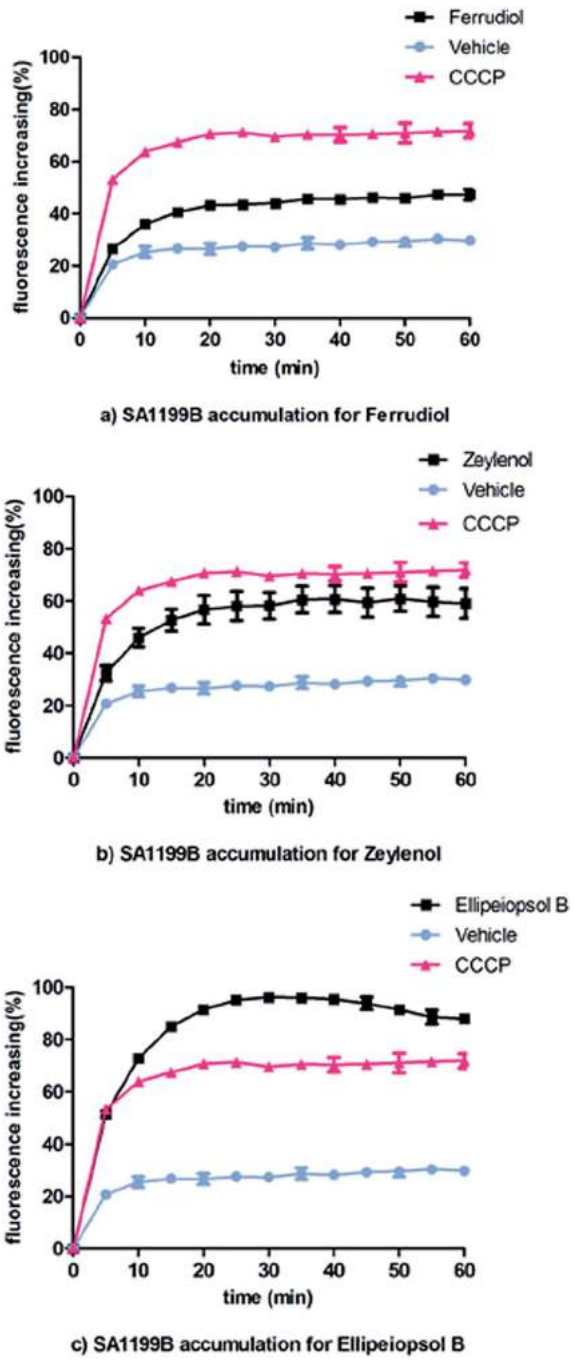

Fig. 4 EtBr accumulation effects of ferrudiol (**4**), zeylenol (**6**) and ellipeiopsol B (**5**) against *S. aureus* SA1199B.

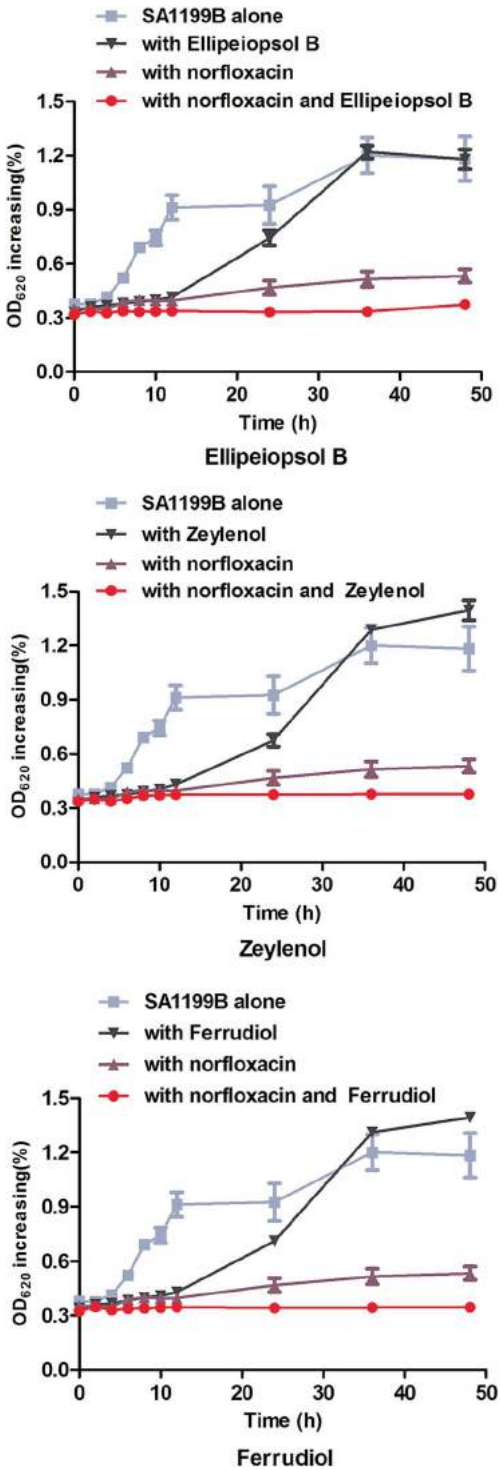

Fig. 5 Time-growth of SA1199B in the absence or presence of norfloxacin and benzocyclohexane oxide derivatives.

postulated that the synergistic effects were as a result of NorA inhibition.

All tested compounds showed a similar inhibitory activity on strain SA1199B compared with the positive control (CCCP) in the EtBr efflux and accumulation assays (Fig. 3 and 4). These results indicated that efflux pump inhibition may contribute to the synergistic effects of these compounds against SA1199B.

In order to further confirm the synergistic effects, growth kinetics in the presence and absence of compounds were determined. The synergistic effects were obvious since the OD value increase of SA1199B with norfloxacin and compounds was lower than that with norfloxacin alone (Fig. 5), while the OD value of SA1199B with compounds alone was almost the same as SA1199B grown in isolation. The exact synergistic effects on the growth kinetics of the strain need further confirmation at the CFU level.

ESI Fig. S5 and S6† suggested that the synergistic activity of the compounds showed no inhibition on bacteria and no toxicity on mammalian cells within synergistic effect concentration, which was encouraging and warrants further investigation of the characteristics of these compounds as promising drug hits to overcome resistance in *Staphylococcus aureus*.

5. Conclusion

The conclusion can be drawn that these compounds may have specific inhibitory effects against the NorA efflux pump of strain SA1199B, which contributes to their synergistic effects with antibiotics against this strain. Synergy may be a promising strategy to resolve problems caused by drug-resistant strains because the compounds with synergistic effects will not cause a reduction of bacterial growth, reducing the likelihood of the formation of new drug-resistant mutants. Some of the classical antibiotics could be re-introduced into a clinical role in the therapy of infections caused by selected drug-resistant bacteria, resulting in the use of lower doses and potentially an improved safety profile. Furthermore, these compounds had no cytotoxic effects on the human embryonic kidney cell line (HEK293T) within the antibacterial effect concentration. This approach may have utility against multi-drug resistant *Staphylococcus aureus*.

Acknowledgements

This work was supported by the NSFC grant (21172041) of China.

References

1 H. W. Boucher and G. H. Talbot, *Clin. Infect. Dis.*, 2009, **48**, 1–12.
2 H. Grundmann, M. Aires-de-Sousa, J. Boyce and E. Tiemersma, *Lancet*, 2006, **368**, 874–885.
3 A. C. Abreu, A. J. McBain and M. Simose, *Nat. Prod. Rep.*, 2012, **29**, 1007–1021.
4 E. M. Williamson, *Phytomedicine*, 2001, **8**, 401–409.
5 H. Wagner and G. Ulrich-Merzenich, *Phytomedicine*, 2009, **16**, 97–110.
6 S. Gibbons, M. Oluwatuyi and G. W. Kaatz, *J. Antimicrob. Chemother.*, 2003, **51**, 13–17.
7 T. G. Littlejohn, I. T. Paulsen, M. T. Gillespie, J. M. Tennent, M. Midgley, I. G. Jones, A. S. Purewal and R. A. Skurrsy, *FEMS Microbiol. Lett.*, 1992, **74**, 259–265.
8 M. Helms, S. Ethelberg, K. Mølbak and the DT104 Study Group, *Emerging Infect. Dis.*, 2005, **11**, 859–867.
9 G. W. Kaatz and S. M. Seo, *Antimicrob. Agents Chemother.*, 1997, **41**, 2733–2737.
10 S. Hemaiswarya, A. Kruthiventi and M. Doble, *Phytomedicine*, 2008, **15**, 639–652.
11 Editorial Committee of Chinese Bencao of the State Administration of Traditional Chinese Medicine of the People's Republic of China., Zhong Hua Ben Cao, Shanghai Science and Technology Press, Shanghai, 1999.
12 K. Ghosh and T. K. Bhattacharya, *Molecules*, 2005, **10**, 798–802.
13 S. N. Tewari and M. Nayak, *Trop. Agric.*, 1991, **68**, 373–375.
14 L. Arambewela, M. Arawwawala and D. Rajapaksa, *Int. J. Food Sci. Technol.*, 2006, **41**, 10–14.
15 S. M. Prabu, M. Muthumani and K. Shagirtha, *Saudi J. Biol. Sci.*, 2012, **19**, 229–239.
16 C. K. Wang and M. J. Wu, *J. Chin. Agric. Chem. Soc.*, 1996, **34**, 638–647.
17 H. W. Zeng, Y. Y. Jiang, D. G. Cai, J. Bian, K. Long and Z. L. Chen, *Planta Med.*, 1997, **63**, 296–298.
18 V. S. Parmar, S. C. Jain, K. S. Bisht, R. Jain, P. Taneja, A. Jha, O. D. Tyagi, A. K. Prasad, J. Wengel, C. E. Olsen and P. M. Boll, *Phytochemistry*, 1996, **46**, 591–673.
19 M. J. Frisch, *Gaussian09, (Revision B.01)*, Wallingford CT, 2009.
20 G. W. Kaatz, S. M. Seo and C. A. Ruble, *Antimicrob. Agents Chemother.*, 1993, **37**, 1086–1094.
21 E. E. Udo and S. Gibbons, *Phytother. Res.*, 2000, **14**, 139–140.
22 J. I. Ross, A. M. Farrell, E. A. Eady, J. H. Cove and W. J. Cunliffe, *J. Antimicrob. Chemother.*, 1989, **24**, 851–862.
23 J. F. Richardson and S. Reith, *J. Hosp. Infect.*, 1993, **25**, 45–52.
24 Clinical and Laboratory Standards Institute, CLSI, M100-S25, Wayne, USA., PA, 2015.
25 F. Iten, R. Saller, G. Abel and J. Reichling, *Planta Med.*, 2009, **75**, 1231–1236.
26 A. J. Hiyas, A. S. C. Arlene, A. E. Keivan, T. B. Johnna, T. M. Kathryn, N. G. Tyler, J. R. Scott, E. C. Robert, H. O. Nicholas and B. C. Nadja, *J. Nat. Prod.*, 2011, **74**, 1621–1629.
27 D. Lechner, S. Gibbons and F. Bucar, *J. Antimicrob. Chemother.*, 2008, **62**, 345–348.
28 L. J. V. Piddock, M. I. Garvey, M. M. Rahman and S. Gibbons, *J. Antimicrob. Chemother.*, 2010, **65**, 1215–1223.
29 M. I. Garvey, M. M. Rahman, S. Gibbons and L. J. V. Piddock, *Int. J. Antimicrob. Agents*, 2011, **37**, 145–151.
30 Y. L. Lu, Y. K. Li, M. X. Li, D. Chen and T. Wu, *Synth. React. Inorg., Met.-Org., Nano-Met. Chem.*, 2014, **44**, 859–863.
31 Y. Ma, G. Q. Han and Y. Y. Wang, *Acta Pharmacol. Sin.*, 1993, **28**, 370–373.
32 J. M. David, M. Yoshida and O. R. Gottlieb, *Phytochemistry*, 1993, **36**, 491–499.
33 L. Wirasathien, T. Pengsuparp, M. Moriyasu, K. Kawanishi and R. Suttisri, *Acta Pharmacol. Sin.*, 2006, **29**, 497–502.
34 G. R. Schulte and B. Ganem, *Tetrahedron Lett.*, 1982, **23**, 4299–4302.
35 A. Kijjoa, J. Bessa, M. M. M. Pinto, C. Anatachoke, A. M. S. Silva, G. Eaton and W. Herz, *Phytochemistry*, 2002, **59**, 543–554.

JOURNAL OF NATURAL PRODUCTS

Article

pubs.acs.org/jnp

Antistaphylococcal Prenylated Acylphoroglucinol and Xanthones from *Kielmeyera variabilis*

Aline Coqueiro,[†,∥,∇] Young H. Choi,[†] Robert Verpoorte,[†] Karthick B. S. S. Gupta,[‡] Maria De Mieri,[§] Matthias Hamburger,[§] Maria C. M. Young,[⊥] Paul Stapleton,[∥] Simon Gibbons,[*,∥] and Vanderlan da S. Bolzani[*,∇]

[†]Natural Products Laboratory, Institute of Biology, Leiden University, Sylviusweg 72, Leiden, 2333 BE, The Netherlands

[‡]NMR Facility, Leiden Institute of Chemistry, Leiden University, Einsteinweg 55, Leiden, 2333 CC, The Netherlands

[§]Division of Pharmaceutical Biology, University of Basel, Klingelbergstrasse 50, Basel, CH-4056, Switzerland

[⊥]Section of Plant Physiology and Biochemistry, Institute of Botany, São Paulo, 01061-970, Brazil

[∥]Research Department of Pharmaceutical and Biological Chemistry, UCL School of Pharmacy, 29-39 Brunswick Square, London, WC1N 1AX, United Kingdom

[∇]Department of Organic Chemistry, Institute of Chemistry, São Paulo State University, Prof. Francisco Degni 55, Araraquara, 14800-900, Brazil

Supporting Information

ABSTRACT: Bioactivity-guided fractionation of the EtOH extract of the branches of *Kielmeyera variabilis* led to the isolation of a new acylphoroglucinol (**1**), which was active against all the MRSA strains tested herein, with pronounced activity against strain EMRSA-16. Compound **1** displayed an MIC of 0.5 mg/L as compared with an MIC of 128 mg/L for the control antibiotic norfloxacin. The structure of the new compound was elucidated by 1D and 2D NMR spectroscopic analysis and mass spectrometry, and experimental and calculated ECD were used to determine the absolute configurations. The compounds *β*-sitosterol (**2**), stigmasterol (**3**), ergost-5-en-3-ol (**4**), and osajaxanthone (**5**) also occurred in the *n*-hexane fraction. The EtOAc fraction contained nine known xanthones: 3,6-dihydroxy-1,4,8-trimethoxyxanthone (**6**), 3,5-dihydroxy-4-methoxyxanthone (**7**), 3,4-dihydroxy-6,8-dimethoxyxanthone (**8**), 3,4-dihydroxy-2-methoxyxanthone (**9**), 5-hydroxy-1,3-dimethoxyxanthone (**10**), 4-hydroxy-2,3-dimethoxyxanthone (**11**), kielcorin (**12**), 3-hydroxy-2-methoxyxanthone (**13**), and 2-hydroxy-1-methoxyxanthone (**14**), which showed moderate to low activity against the tested MRSA strains.

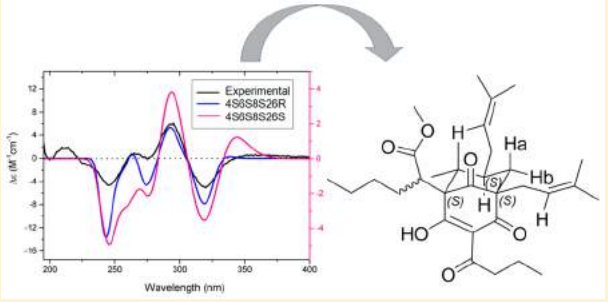

The genus *Kielmeyera* belongs to the family Clusiaceae and occurs exclusively in South America. Among the 47 known species of this genus, 45 are native to Brazilian ecosystems. These plants grow mainly in the Brazilian Cerrado Biome, specifically in the Midwest region.[1]

Kielmeyera variabilis Mart., commonly known in Brazil as "malva-do-campo", is a medicinal tree used in Brazilian folk medicine to treat several tropical diseases, including schistosomiasis, leishmaniasis, malaria, and fungal and bacterial infections.[2] Previous work has shown that species belonging to the family Clusiaceae produce xanthones and phoroglucinol derivatives that possess antibacterial activity against methicillin-resistant *Staphylococcus aureus* (MRSA).[3,4] Previous studies on *K. variabilis* Mart. have shown that this species contains prenylated xanthones with molluscicidal activity[5,6] and flavonoids with antioxidant properties.[7]

Resistance to methicillin, a form of penicillin, among *S. aureus* began to be noted at the beginning of the 1960s. Since then, these organisms have developed mechanisms of resistance to many different classes of antimicrobial agents, making treatment options severely limited. Infection with MRSA is therefore a serious public health concern that has called for the development of new antibacterial drugs to overcome microbial resistance.[8]

Natural products bearing different structural patterns can be active against resistant strains, so the screening of natural product extracts from microorganisms or plants still constitutes a valid strategy to discover new lead compounds with antibiotic properties.

As part of an ongoing SisBiota CNPq/FAPESP Biodiscovery Program, which aims to discover new sources of bioactive compounds in the Brazilian flora, this investigation evaluated

Special Issue: Special Issue in Honor of John Blunt and Murray Munro

Received: September 26, 2015
Published: February 22, 2016

DOI: 10.1021/acs.jnatprod.5b00858
J. Nat. Prod. 2016, 79, 470−476

the potential of *K. variabilis* Mart. against multidrug-resistant strains. Bioassay-guided fractionation helped to define the bioactive compounds and prove that this plant is applicable as an antimicrobial agent in traditional folk medicine.

RESULTS AND DISCUSSION

Successive extraction of the dried and pulverized *K. variabilis* branches and leaves with EtOH afforded an extract for a preliminary activity screening assay against the multidrug-resistant strain SA-1199B, which overexpresses the NorA efflux pump and has a Gyr-A mutation.[11]

Partitioning of the EtOH extracts of *K. variabilis* branches and leaves by liquid−liquid extraction resulted in four fractions (*n*-hexane, EtOAc, *n*-BuOH, and aqueous MeOH) for each plant part. Tests on all fractions against strain SA-1199B permitted the selection of the most promising fraction to start the bioassay-guided fractionation (Table 1).

Table 1. Antimicrobial Activity of the Extracts and Fractions of *K. variabilis* Branches and Leaves against the Strain SA-1199B

plant part	extract and fractions	MIC (mg/L)
branches	EtOH	32
	n-hexane	16
	EtOAc	64
	n-BuOH	256
	aqueous MeOH	>512
leaves	EtOH	128
	n-hexane	64
	EtOAc	128
	n-BuOH	256
	aqueous MeOH	>512
positive control	norfloxacin	32

The crude EtOH extract of the branches was 4 times more active (MIC of 32 mg/L) than the crude EtOH extract of the leaves (MIC of 128 mg/L) and had activity comparable to the activity of the standard norfloxacin (MIC of 32 mg/L) against the fluoroquinolone-resistant organism. The antibacterial activity of the *n*-hexane fraction of the branches (MIC of 16 mg/L) was higher than the corresponding EtOH extract (MIC of 32 mg/L) and even slightly higher than the activity of the control norfloxacin (MIC of 32 mg/L). This showed that the fractionation process potentiated the activity of the branches extract by concentrating the most active compound(s) in the *n*-hexane fraction.

Bioassay-guided fractionation of the most active fraction permitted identification of the bioactive compound. Fractionation of the *n*-hexane fraction of the branches on a Sephadex LH-20 column led to six subfractions (Fr1 to Fr6). Evaluation of the antibacterial activity of these subfractions showed that Fr1 (756.5 mg) was the most active, with an MIC of 2 mg/L, and therefore Fr1 was 8-fold more potent than the *n*-hexane fraction (MIC of 16 mg/L).

A phytochemical study on the most active subfraction identified compound **1** as the bioactive compound underlying the activity of the EtOH extract of *K. variabilis* branches. The activities of Fr1 and compound **1** were assessed at concentrations ranging from 512 to 0.5 mg/L against a panel of multidrug-resistant *S. aureus* strains with clinical relevance and different mechanisms of resistance. Fr1 also contained the steroids *β*-sitosterol (**2**), stigmasterol (**3**),[16] and ergost-5-en-3-ol (**4**). The nonactive subfraction Fr6 contained the xanthone osajaxanthone (**5**),[17] which we did not test due to the low sample size of this compound.

Among the tested strains were SA-1199B, a multidrug-resistant strain that overexpresses the NorA efflux pump[11] and possesses a gyrase-encoding gene mutation that also confers a high level of resistance to some fluoroquinolones;[18] RN4220, a macrolide-resistant strain;[10] XU212, a clinical MRSA strain that is resistant to tetracycline and bears the TetK efflux pump;[9] ATCC 25923, a standard laboratory strain;[9] and the epidemic methicillin-resistant strains EMRSA-15 and EMRSA-16.[13]

Compound **1** accounted for the activity of the *n*-hexane fraction of the branches. Its activity was similar to or higher than the activity of fraction Fr1. Compared with the positive control norfloxacin, its activity was higher against strains SA-1199B and XU212. It also displayed pronounced activity against the epidemic methicillin-resistant strain EMRSA-16; its MIC was 0.5 mg/L as compared with the MIC of the control (128 mg/L). The activities of compound **1** and the control were similar for the strains ATCC 25923, RN4220, and EMRSA-15.

The mixture of **2** and **3** and of individual compounds **2**, **3**, and **4** did not exhibit any activity against the *S. aureus* strains. Knowing that these compounds are nonactive, their identification was conducted by NMR and GC-MS without isolating them from these mixtures.

Minimum bactericidal concentration (MBC) assays conducted with active compound **1** permitted determination whether this compound exerted a bacteriostatic or bactericidal effect. For these assays, a 10 μL sample was removed from the wells of a plate used to determine the MIC values of compound **1** against SA-1199B (where no bacterial growth had occurred). This volume was plated onto drug-free media. After 24 h of incubation, bacteria grew on the drug-free plates. Hence, compound **1** inhibited the organisms by exerting a bacteriostatic effect.

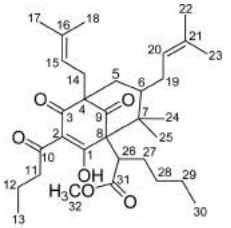

1

The HRESIMS of compound **1** revealed an $[M + H]^+$ ion *m*/*z* at 529.3547 in the positive mode. Combined with ^{13}C NMR data, this information permitted assignment of the molecular formula of compound **1** as $C_{32}H_{48}O_6$. Two vinyl protons, four vinylic methyl groups, and four allylic protons in the ^1H NMR spectrum suggested the presence of two isopent-2-enyl side chains. HMBC correlations of H-11a, H-11b, H-12a, and H-12b with the carbonyl C-10 and COSY correlations of H-11b to H-11a and H-12b and of H-12b to H_3-13 demonstrated the presence of an *n*-butanoyl chain. A ^{13}C NMR resonance at δ 174.1 (C-31) correlated with H_3-32 (δ 3.65) in the HMBC spectrum is typical of a methoxy group and revealed the presence of an ester carbonyl group. The presence of one methine (δ_C 38.7), three methylene (δ_C 39.9, 37.3, and 22.7), and one methyl carbon (δ_C 15.2) correlated by HMBC reveals the presence of a hexanoyl chain. This chain is confirmed by correlations of H-26 (δ 3.29) and H-27 (δ 2.34) with the ester

DOI: 10.1021/acs.jnatprod.5b00858
J. Nat. Prod. 2016, 79, 470−476

carbonyl C-31 and the correlations of H-26, H-29 (δ 1.43 and 1.52), and H-30 (δ 0.94) with C-28 (δ 37.3).

The ^{13}C NMR spectrum displayed the characteristic resonances of a bicyclic [3.3.1] nonane ring system with three quaternary carbons (δ_C 64.7, 49.2, and 69.5), a methine (δ_C 48.6), a methylene (δ_C 39.5), an enolized 1,3-diketo system (δ_C 114.7, 199.7, and 195.5), and a nonconjugated carbonyl (δ 209.4). Together, these data suggested that compound **1** was a polyisoprenylated phloroglucinol derivative.[4,19−22]

HMBC correlations facilitated establishment of the substitution pattern of the nonane ring system. Correlation of H-26 with C-1, C-9, and C-31 indicated that the ester carbonyl group was connected to the nonane system at C-8. HMBC correlation of H-5a with C-14 and C-19 showed connection of the isoprenyl side chains to C-4 and C-6. By elimination, the 1-butanoyl moiety was linked at C-2. The methyl groups Me-24 (δ 1.20) and Me-25 (δ 1.37) correlated with each other and with C-7 and C-8 (Figure 1).

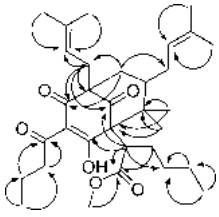

Figure 1. Key correlations observed in the HMBC NMR spectrum of compound **1**.

Proton H-5a had two large coupling constants, i.e., 14.3 Hz, consistent with its geminal coupling to H-5b, and 10.4 Hz, due to an axial−axial coupling with H-6. These data indicated that H-6 was in the axial position, with the C-6 isoprenyl side chain equatorially oriented.[23]

NOESY studies aided the determination of the relative configuration assignments and supported the delineated stereochemistry. Key NOE correlations between H-6 (δ 1.41), the methyl protons at δ 1.20 (H_3-24), and H-5b (δ 2.12) shown in Figure 3a demonstrated that they were all oriented on the same face of the bicyclic [3.3.1] nonane ring,

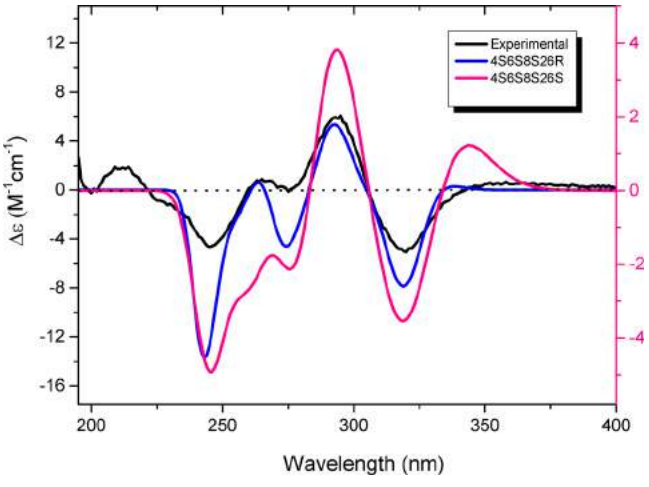

Figure 2. Comparison of experimental and calculated (weighted) ECD spectra of **1** for the two stereoisomers 4*S*,6*S*,8*S*,26*S*, 4*S*,6*S*,8*S*,26*R*. The calculations were performed with TDDFT at the cam-B3LY/6-31G** level in MeOH.

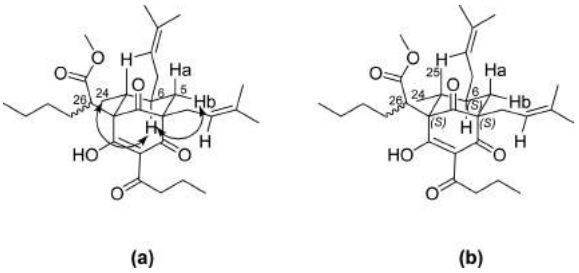

Figure 3. Key correlations observed in the NOESY NMR spectra of compound **1** (a) and absolute configuration of the bicyclic [3.3.1] nonane ring determined by ECD (b).

which placed H-5b and H_3-24 in an 1,3-diequatorial position relative to each other and in a chair conformation in relation to the cyclohexanone ring.

The absolute configuration of **1** was stablished by comparison of its experimental electronic circular dichroism (ECD) curve with those predicted using TDDFT theory. On the basis of geometrical considerations, four possible isomers were conceivable: 4*S*,6*S*,8*S*,26*S*, 4*S*,6*S*,8*S*,26*R*, 4*R*,6*R*,8*R*,26*S*, and 4*R*,6*R*,8*R*,26*R*.

The 4*S*,6*S*,8*S* absolute configuration of the bicyclic [3.3.1] nonane ring, was assigned by the similarity of the experimental and calculated spectra at the cam-B3LY/6-31G** level in MeOH (Figure 2). However, this method was not able to clearly discriminate between the 26*R* and 26*S* configurations, since the calculated spectra for the 4*S*,6*S*,8*S*,26*S* and 4*S*,6*S*,8*S*,26*R* epimers are very similar.

Therefore, the structure of kielmeyeracin (**1**) was established as shown in Figure 3b.

Phytochemical investigation of the EtOAc fraction, i.e., the second most active fraction of *K. variabilis* branches, resulted in the identification of nine xanthones: 3,6-dihydroxy-1,4,8-trimethoxyxanthone (**6**), 3,5-dihydroxy-4-methoxyxanthone (**7**),[24] 3,4-dihydroxy-6,8-dimethoxyxanthone (**8**),[25] 3,4-dihydroxy-2-methoxyxanthone (**9**),[26] 5-hydroxy-1,3-dimethoxyxanthone (**10**),[25,26] 4-hydroxy-2,3-dimethoxyxanthone (**11**),[27,28] kielcorin (**12**),[26] 3-hydroxy-2-methoxyxanthone (**13**),[29] and 2-hydroxy-1-methoxyxanthone (**14**).[30] Although these xanthones were previously isolated from the genus *Kielmeyera*, no studies on the antimicrobial action of these compounds exist. Kielcorin is the only xanthone that has been previously reported for the species *K. variabilis*.[5,6] The amount of xanthones **6**, **7**, and **8** obtained here permitted their testing and identification in a mixture. 1D and 2D NMR techniques, ESIMS, and comparison with literature data enabled the identification of all of the xanthones. The Supporting Information shows the NMR and MS data.

Microbial infections stimulate higher plants to synthesize xanthones related to phytoalexins via a passive defense system. Natural xanthones are potent MRSA inhibitors,[31] and prenylated xanthones show the highest antimicrobial activity.[32,33]

The antimicrobial potential of the isolated oxygenated xanthones was evaluated against the same panel of *S. aureus* strains (Table 4).

The xanthones displayed moderate to weak antibacterial action. Xanthone **9** had the highest activity: MICs varied between 16 and 64 mg/L. The most pronounced activity was observed against the most resistant strain, EMRSA-16. Among the pure tested compounds, xanthone **9** is the only one bearing

DOI: 10.1021/acs.jnatprod.5b00858
J. Nat. Prod. 2016, 79, 470−476

Table 2. In Vitro Antibacterial Activity (MIC in mg/L) of Subfractions and Compounds Isolated from the *n*-Hexane Fraction of *K. variabilis* Branches against Different *S. aureus* Strains

fraction and compounds	SA-1199B	XU212	ATCC 25923	RN4220	EMRSA-15	EMRSA-16
Fr1	2	0.5	1	0.5	1	0.5
1	2	0.25	1	0.25	1	0.5
2 + **3**	>512	>512	>512	>512	>512	>512
2 + **3** + **4**	>512	>512	>512	>512	>512	>512
norfloxacin	32	8	0.5	0.5	0.5	128

Table 3. NMR Spectroscopic Data (600 MHz, Pyridine-d_5) for Compound 1

position	δ_C, type	δ_H (J in Hz)	HMBC
1	199.7, C		
2	114.7, C		
3	195.5, C		
4	64.7, C		
5	39.5, CH_2	a: 2.26 dd (14.3, 10.4)	3, 4, 6, 14, 19
		b: 2.12 overlapped	
6	48.6, CH	1.41 m	
7	49.2, C		
8	69.5, C		
9	209.4, C		
10	203.7, C		
11	41.7, CH_2	a: 3.27 m	10, 13
		b: 3.05 ddd (15.2, 8.9, 6.2)	10, 13
12	19.4, CH_2	a: 1.71 m	10, 11, 13
		b: 1.78 m	10, 11, 13
13	14.5, CH_3	0.95 t (7.5)	11, 12
14	29.4, CH_2	a: 2.80 dd (14.6, 6.8)	3, 4, 5, 9, 15, 16
		b: 2.89 dd (14.6, 8.0)	3, 4, 5, 9, 15, 16
15	121.2, CH	5.64 br t	14, 17, 18
16	134.7, C		
17	26.7, CH_3	1.74 s	15, 16, 18
18	18.3, CH_3	1.67 s	15, 16, 17
19	29.7, CH_2	a: 1.88 br	
		b: 2.10 overlapped	
20	124.3, CH	4.93 br t	19, 22, 23
21	133.5, C		
22	26.5, CH_3	1.69 s	20, 21, 23
23	18.3, CH_3	1.55 s	20, 21, 22
24	25.4, CH_3	1.20 s	7, 8, 25
25	22.6, CH_3	1.37 s	7, 8
26	38.7, CH	3.29 m	1, 8, 9, 27, 28, 31
27	39.9, CH_2	2.34 br	31
28	37.3, CH_2	a: 2.01 br	
		b: 1.81 m	
29	22.7, CH_2	a: 1.52 m	28, 30
		b: 1.43 m	28, 30
30	15.2, CH_3	0.94 t (7.5)	28, 29
31	174.1, C		
32	52.0, OCH_3	3.65 s	31

a catechol group in the structure. In the present work, the activity of oxygenated xanthones was lower than the activities reported for some prenylated xanthones. Indeed, the prenyl groups can serve as modulators of lipid affinity and cellular bioavailability. The presence of a nonpolar group enhances membrane permeability, which accounts for the higher antimicrobial potential of prenylated xanthones[32,33] as compared with the oxygenated xanthones investigated in this study.

The bioassay-guided fractionation applied in this study led to the isolation of the new compound kielmeyeracin (**1**), which displayed strong antibacterial activity against methicillin-resistant *S. aureus* strains. This compound exhibited activity similar to or higher than the activity of the control norfloxacin, mainly against EMRSA-16. *K. variabilis* Mart. proved to have a high antimicrobial potential, which correlated with the use of this plant in folk medicine. Isolation of the bioactive compound makes both this molecule and the plant of interest for further studies on the mechanism of anti-MRSA action and for future in vivo investigations.

EXPERIMENTAL SECTION

General Experimental Procedures. Optical rotation was measured on a PerkinElmer polarimeter (model 341) equipped with a sodium lamp (589 nm) and a 10 cm microcell. UV spectra were obtained on a Shimadzu UV-1800 instrument. The ECD spectra were recorded in MeOH with a Chirascan spectrometer. NMR spectra of compound **1** were recorded on a Bruker 600 Avance II NMR spectrometer (Bruker, Bellerica, MA, USA) in pyridine-d_5 (298 K), at 600 and 150 MHz for ^{1}H and ^{13}C NMR, respectively. 1D and 2D NMR spectra of xanthones and steroids were recorded on a Varian INOVA 500 (11.7 T) spectrometer with TMS as the internal standard. The HRESIMS of compound **1** was performed on a Bruker UPLC system (Dionex 3000) coupled to a Bruker (micrOTOF II) time-of-flight mass spectrometer, equipped with an electrospray interface (ESI). A Bruker Daltonics utrOTOFQ with ESI operating in the positive and negative mode was used to confirm the molecular weight of the xanthones. A Varian ProStar chromatography system with diode array detector was employed to profile the extracts. A Varian ProStar chromatography unit operating at λ = 254 nm was used to accomplish the preparative isolation. The following columns were employed: a Phenomenex Luna Phenyl-Hexyl and a Phenomenex Luna C_{18} column (5 μm, 250 × 4.6 mm, analytical), a Phenomenex Luna Phenyl-Hexyl preparative column (10 μm, 250 × 21.2 mm), and a preparative Phenomenex C_{18} column (10 μm, 250 × 21.2 mm). The mixtures of steroids were analyzed by gas chromatography coupled to a mass detector (GC-MS) with split injector 20:1; the injected volume was 1 μL. The injector temperature was 280 °C, and the temperature of the interface was 300 °C. The initial column temperature was 50 °C, held for 3 min, which was followed by a temperature rise to 295 °C at 2 °C/min. The temperature was kept at 295 °C for an additional 20 min. The total run time was 145.5 min. Helium was employed as the carrier gas at an average linear velocity of 1 mL/min. The ionization mode was electron ionization (EI) in the positive mode with an impact energy of 70 eV. The identities of the isolated compounds were confirmed by comparing ^{1}H and ^{13}C NMR signals with literature values and high-resolution MS data (Supporting Information).

Plant Material. The leaves and branches of *K. variabilis* were collected in Fazenda Campininha in Mogi-Guaçú, state of São Paulo, Brazil, in January 2007. The plant was identified by Dr. Inês Cordeiro (IBt-SMA). A voucher specimen (SP 346310) was deposited in the herbarium "Maria E. P. Kauffman" of the Botanic Institute of São Paulo, state of São Paulo, Brazil.

Extraction. Air-dried and ground leaves and branches were exhaustively extracted by maceration with EtOH at room temperature separately. After filtration, the solvent was evaporated at low

DOI: 10.1021/acs.jnatprod.5b00858
J. Nat. Prod. 2016, 79, 470−476

Table 4. In Vitro Antibacterial Activity (MIC in mg/L) of Xanthones Isolated from *K. variabilis*

compounds	SA-1199B	XU212	ATCC 25923	RN4220	EMRSA-15	EMRSA-16
6 + **7** + **8**	64	64	128	64	128	32
9	32	32−16	64	32	64	16
10	128−64	>512	128	>512	>512	64
11	128−64	128	128	>512	>512	64
12	>512	>512	>512	>512	>512	>512
13	64	64	64	64	64	32
14	64	128	64	64	64	32
norfloxacin	32	8	0.5	0.5	0.5	128

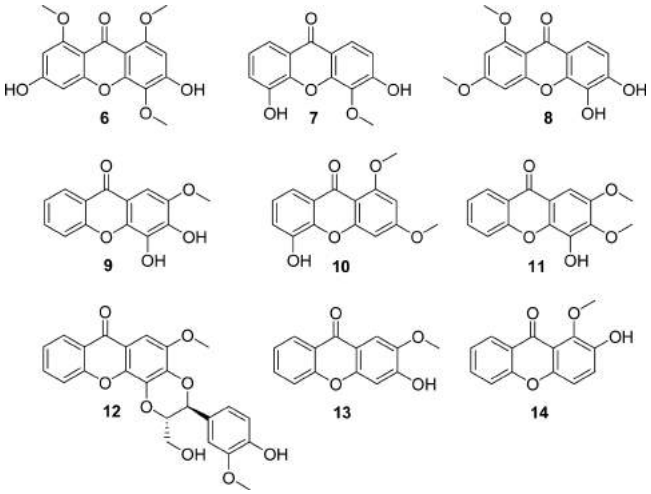

Figure 4. Chemical structure of xanthones **6**−**14**.

temperature (<40 °C) under reduced pressure, to yield a thick syrup. The EtOH extracts were dispersed in MeOH/H_2O (4:1) and successively partitioned with *n*-hexane, EtOAc, and *n*-BuOH. Samples of the EtOH extracts, the *n*-hexane, EtOAc, and *n*-BuOH fractions, and the lyophilized aqueous MeOH fractions were further used in the antimicrobial tests.

Isolation of the Compounds in the *n*-Hexane Fraction of *K. variabilis* Branches. The *n*-hexane fraction (1.0 g) was subjected to a Sephadex LH-20 column, eluted with a gradient of *n*-hexane/$CHCl_3$ from 90:10, v/v, to 0:100, v/v, followed by isocratic elution with $CHCl_3$/MeOH (50:50, v/v). The fractions were analyzed by analytical TLC and grouped into seven subfractions (Fr1−Fr7); part of fraction Fr1 (740 mg) was purified on a silica gel column using a gradient of *n*-hexane/EtOAc (100:0 to 0:100, v/v) and EtOAc/MeOH (100:0 to 0:100, v/v). Fractions were grouped on the basis of the TLC profile, to give 17 subfractions (Fr1.1−Fr1.17). Subfraction Fr1.8 (222.7 mg) was repurified by solid-phase extraction (SPE) on silica gel; a gradient system of *n*-hexane/EtOAc (0:100 to 100:0, v/v) as eluent yielded four subfractions (Fr1.8.1−Fr1.8.4). Part of subfraction Fr1.8.1 (50 mg) was subjected to preparative TLC with *n*-hexane/EtOAc (95:5, v/v) as eluent, which afforded compound **1** (23.5 mg). The other part of subfraction Fr1.8.1 (172.7 mg) was purified by preparative HPLC on a C_{18} column with an isocratic solvent system of MeCN/H_2O (97:3, v/v), which also yielded compound **1** (28.3 mg). Purification of fraction Fr1.10 (48.3 mg) by normal-phase PTLC with *n*-hexane/EtOAc (90:10, v/v) as eluent gave four subfractions (Fr1.10.1−Fr1.10.4). Subfraction Fr1.10.3 (26.6 mg) was subjected to normal-phase PTLC again using $CHCl_3$/MeOH (99:1, v/v) as eluent. This procedure afforded six subfractions (Fr1.10.3.1−Fr1.10.3.6). Fr1.10.3.2 (11.9 mg) consisted of a mixture of compounds **2** and **3**. Subfraction Fr1.11 (17.9 mg) was also subjected to normal-phase PTLC with *n*-hexane/EtOAc (85:15, v/v) as eluent, to give four subfractions (Fr1.11.1−Fr1.11.4). Fr1.11.2 (6.9 mg) comprised a mixture of compounds **2**, **3**, and **4**. Purification of Fr6 by normal-phase PTLC with *n*-hexane/EtOAc (30:70, v/v) as eluent resulted in 10 subfractions (Fr1.6.1−Fr1.6.10). Subfraction Fr1.6.4 (1.0 mg) was identified as compound **5**.

Isolation of the Xanthones in the EtOAc Fraction of *K. variabilis* Branches. The ethyl acetate fraction was subjected to HPLC separation. The compounds were purified on a preparative column (Phenomenex C_{18} column, 10 μm, 250 × 21.2 mm; flow rate of 1 mL/min, 80 min), eluted with MeOH/H_2O (50:50, v/v) + 0.1% HOAc, to yield 12 fractions (Fr1−Fr12). All fractions were analyzed by 1D and 2D NMR and MS. Fraction Fr1 (23.7 mg) consisted of a mixture of three compounds identified as compounds **6**, **7**, and **8**. Fr3 (25.6 mg), Fr5 (50.1 mg), Fr7 (30.2 mg), and Fr11 (30.4 mg) were pure and comprised compounds **9**, **10**, **11**, and **12**, respectively. Fraction Fr9 (26.7 mg) was repurified by semipreparative HPLC (Phenomenex Luna Phenyl-Hexyl column; 10 μm, 250 × 21.2 mm; flow rate of 12 mL/min, 60 min) eluted with MeOH/H_2O (50:50, v/v) + 0.1% HOAc, to afford compounds **13** and **14**.

Kielmeyeracin (**1**): yellow oil; $[\alpha]^{25}_{D}$ −70 (*c* 0.1, MeOH); UV (MeOH) λ_{max} (log ε) 201 (4.20), 284 (4.15); ECD (*c* = 0.5 mM; MeOH) λ_{max} ($\Delta\varepsilon$) 214 (0.78); 225 sh (−0.35); 248 (−1.75); 265 sh (0.35); 293 (2.39); 320 (−2.06); ^{1}H NMR (pyridine-d_5, 600 MHz) and ^{13}C NMR (pyridine-d_5, 150 MHz), see Table 3; ESIMS (positive) *m*/*z* 529.3547 $[M + H]^+$ (calcd for $C_{32}H_{49}O_6$, 529.3537).

Antibacterial Activity Testing. *Bacterial Strains.* The susceptibility test involved the standard *S. aureus* reference strain ATCC 25923 and the clinical MRSA isolate XU212 bearing the TetK efflux pump, obtained from Dr. E. Udo.[9] The MsrA macrolide-resistant strain RN4220 was provided by Dr. J. Cove.[10] Strain SA-1199B, which overexpresses the NorA MDR efflux pump, was a gift from Prof. Glenn Kaatz.[11] The strains EMRSA-15[12] and EMRSA-16[13] were supplied by Dr. Paul Stapleton.

Minimum Inhibitory Concentration (MIC). To determine the MIC, the strains were first cultured on nutrient agar (Oxoid) and incubated for 24 h at 37 °C. An inoculum density of 1 × 10^6 cfu/mL of each *S. aureus* strain was prepared in normal saline (9 g/L) by comparison with a 0.5 MacFarland turbidity standard and appropriate dilution. The positive control antimicrobial agent norfloxacin (Sigma-Aldrich Chemical Co. LLC) and the samples were dissolved in DMSO and diluted in cation-adjusted Mueller-Hinton broth (MHB) to give a starting concentration of 1024 mg/L. With the aid of Nunc 96-well microtiter plates, 125 μL of MHB was dispensed into wells 1−11. Then, 125 μL of the test compound or the appropriate antibiotic was dispensed into well 1 and serially diluted across the plate, leaving well 11 empty as a growth control. The remaining volume from well 10 was dispensed into well 12, which served as the sterility control for the prepared samples. Finally, the bacterial inoculum (125 μL) was added to wells 1−11, and the plate was incubated at 37 °C for 18 h. A DMSO control was also included. For MIC determination, 20 μL of a 5 mg/mL MeOH solution of 3-[4,5-dimethylthiazol-2 yl]-2,5-diphenyltetrazolium bromide (MTT; Sigma) was added to each of the wells and incubated for 20 min. A color change from yellow to dark blue indicated bacterial growth. The lowest concentration at which no growth was observed was determined as the MIC.[11] Mueller-Hinton broth (Oxoid) was adjusted to contain Ca^{2+} at 20 mg/L and Mg^{2+} at 10 mg/L.

Minimum Bactericidal Concentration (MBC). Sample preparation followed the same protocol used for the MIC assays, and the samples were added to the same inoculum density of the SA-1199B strain. The

DOI: 10.1021/acs.jnatprod.5b00858
J. Nat. Prod. 2016, 79, 470−476

96-well plates were incubated at 37 °C for 24 h. After incubation, 10 μL of each solution at different concentrations of the tested compound was transferred to Petri dishes containing drug-free culture medium (Mueller-Hinton agar). The Petri plates were then incubated for a further 24 h. MBC was obtained by observing the growth of colonies in Petri dishes after 24 h of incubation; ≥99.9% reduction in the number of bacterial cells as compared with the starting inoculum was considered as the bactericidal end point. MBC values equivalent to or exhibiting no more that a 2-fold difference from the MIC of the agent indicated a bactericidal drug. An MBC value 8-fold higher than the MIC indicated a bacteriostatic drug.

Computational Methods. Conformational analysis of **1** was performed with Schrödinger MacroModel 9.8 (Schrödinger, LLC, New York) employing the OPLS2005 (optimized potential for liquid simulations) force field in H_2O. Ten conformers within a 2 kcal/mol energy window from the global minimum were selected for geometrical optimization and energy calculation applying DFT with the Becke's nonlocal three-parameter exchange and correlation functional and the Lee−Yang−Parr correlation functional level (B3LYP) using the B3LYP/6-31 G** basis set in the gas phase with the Gaussian 09 program package.[14] Vibrational evaluation was done at the same level to confirm minima. Excitation energy (denoted by wavelength in nm), rotator strength dipole velocity (R_{vel}), and dipole length (R_{len}) were calculated in MeOH by TD-DFT/CAM-B3LYP/6-31G**, using the SCRF method, with the CPCM model. ECD curves were obtained on the basis of rotator strengths with a half-band of 0.3 eV using SpecDis v1.61.[15] ECD spectra were calculated from the spectra of individual conformers according to their contribution calculated by Boltzmann weighting.

■ ASSOCIATED CONTENT

Supporting Information

The Supporting Information is available free of charge on the ACS Publications website at DOI: 10.1021/acs.jnatprod.5b00858.

Bioguided fractionation scheme; ^{1}H NMR, ^{13}C NMR, HSQC, HMBC, ^{1}H−^{1}H COSY, NOESY, and HRESIMS spectra for compound **1**; chromatograms of isolation and the spectroscopic and spectrometric data of xanthones (PDF)

■ AUTHOR INFORMATION

Corresponding Authors

*Tel: +44 207 7535913. Fax: +44 207 7535964. E-mail: simon.gibbons@ucl.ac.uk.

*Tel: +55 (16)3301-9660. Fax: +55 16 3322-2308. E-mail: bolzaniv@iq.unesp.br.

Notes

The authors declare no competing financial interest.

■ ACKNOWLEDGMENTS

This work was funded by grants 06/61187-7 from the São Paulo Research Foundation (FAPESP) as part of the Biodiversity Virtual Institute Program (www.biota.org.br) grant 03/02176-7, and BEX 5285/12-7, from Ciências sem Fronteiras, CAPES Foundation, Ministry of Education of Brazil. The authors also thank Dr. A. Camilo Alécio for GC-MS analysis of the steroids, Dr. M. Pivatto for processing of the LC-MS data of xanthones, and Dr. M. Smiesko for computational facilities and technical assistance in interpreting calculated results.

■ DEDICATION

Dedicated to Professors John Blunt and Murray Munro, of the University of Canterbury, for their pioneering work on bioactive marine natural products.

■ REFERENCES

(1) Barros, M. A. G. *Acta Bot. Bras.* **2002**, *16*, 113−122.

(2) Alves, T. M. A.; Silva, A. F.; Brandão, M.; Grandi, T. S. M.; Smânia, E. F.; Smânia, A., Jr.; Zani, C. L. *Mem. Inst. Oswaldo Cruz* **2000**, *95*, 367−373.

(3) Klaiklay, S.; Sukpondma, Y.; Rukachaisirikul, V.; Phongpaichit, S. *Phytochemistry* **2013**, *85*, 161−166.

(4) Xiao, Z. Y.; Mu, Q.; Shiu, W. K. P.; Zeng, Y. H.; Gibbons, S. *J. Nat. Prod.* **2007**, *70*, 1779−1782.

(5) Pinheiro, L.; Cortez, D. A. G.; Vidotti, G. J.; Young, M. C. M.; Ferreira, A. G. *Quim. Nova* **2003**, *26*, 157−160.

(6) Pinheiro, L.; Nakamura, C. V.; Filho, B. P. D.; Ferreira, A. G.; Young, M. C. M.; Cortez, D. A. G. *Mem. Inst. Oswaldo Cruz* **2003**, *98*, 549−552.

(7) Coqueiro, A.; Regasini, L. O.; Skrzek, S. C. G.; Queiroz, M. M. F.; Silva, D. H. S.; Bolzani, V. S. *Molecules* **2013**, *18*, 2376−2385.

(8) http://www.niaid.nih.gov/topics/antimicrobialresistance/examples/mrsa/Pages/history.aspx.

(9) Gibbons, S.; Udo, E. E. *Phytother. Res.* **2000**, *14*, 139−140.

(10) Ross, J. I.; Farrell, A. M.; Eady, E. A.; Cove, J. H.; Cunliffe, W. J. *J. Antimicrob. Chemother.* **1989**, *24*, 851−862.

(11) Kaatz, G. W.; Seo, S. M.; Ruble, C. A. *Antimicrob. Agents Chemother.* **1993**, *37*, 1086−1094.

(12) Richardson, J. F.; Reith, S. *J. Hosp. Infect.* **1993**, *25*, 45−52.

(13) Cox, R. A.; Conquest, C.; Mallaghan, C.; Maples, R. R. *J. Hosp. Infect.* **1995**, *29*, 87−106.

(14) Frisch, M. J.; Trucks, G. W.; Schlegel, H. B.; Scuseria, G. E.; Robb, M. A.; Cheeseman, J. R.; Scalmani, G.; Barone, V.; Mennucci, B.; Petersson, G. A.; Nakatsuji, H.; Caricato, M.; Li, X.; Hratchian, H. P.; Izmaylov, A. F.; Bloino, J.; Zheng, G.; Sonnenberg, J. L.; Hada, M.; Ehara, M.; Toyota, K.; Fukuda, R.; Hasegawa, J.; Ishida, M.; Nakajima, T.; Honda, Y.; Kitao, O.; Nakai, H.; Vreven, T.; Montgomery Jr., J. A.; Peralta, J. E.; Ogliaro, F.; Bearpark, M. J.; Heyd, J.; Brothers, E. N.; Kudin, K. N.; Staroverov, V. N.; Kobayashi, R.; Normand, J.; Raghavachari, K.; Rendell, A. P.; Burant, J. C.; Iyengar, S. S.; Tomasi, J.; Cossi, M.; Rega, N.; Millam, N. J.; Klene, M.; Knox, J. E.; Cross, J. B.; Bakken, V.; Adamo, C.; Jaramillo, J.; Gomperts, R.; Stratmann, R. E.; Yazyev, O.; Austin, A. J.; Cammi, R.; Pomelli, C.; Ochterski, J. W.; Martin, R. L.; Morokuma, K.; Zakrzewski, V. G.; Voth, G. A.; Salvador, P.; Dannenberg, J. J.; Dapprich, S.; Daniels, A. D.; Farkas, Ö.; Foresman, J. B.; Ortiz, J. V.; Cioslowski, J.; Fox, D. J. *Gaussian 09*; Gaussian, Inc.: Wallingford, CT, USA, 2009.

(15) Bruhn, T.; Hemberger, A. S. Y.; Bringmann, G. *Spec Dis* version 1.61; University of Wuerzburg: Germany, 2014.

(16) Matida, A. K.; Rossi, M. H.; Blumenthal, E. E. A.; Schuquel, I. T. A.; Malheiros, A.; Vidotti, G. J. *Anais Assoc. Bras. Quim.* **1996**, *45*, 147−151.

(17) Mondal, M.; Puranic, V. G.; Argade, N. P. *J. Org. Chem.* **2006**, *71*, 4992−4995.

(18) Appendino, A.; Gibbons, S.; Giana, A.; Pagani, A.; Grassi, G.; Stavri, M.; Smith, E.; Rahman, M. M. *J. Nat. Prod.* **2008**, *71*, 1427−1430.

(19) Bokesh, H. R.; Groweiss, A.; McKee, T. C.; Boyd, M. R. *J. Nat. Prod.* **1999**, *62*, 1197−1199.

(20) Liu, X.; Yang, X.-W.; Chen, C.-Q.; Wu, C.-Y.; Zhang, J.-J.; Ma, J.-Z.; Wang, H.; Y, L.-X.; Xu, G. *J. Nat. Prod.* **2013**, *76*, 1612−1618.

(21) Cuesta-Rubio, O.; Padron, A.; Castro, H. V.; Pizza, C.; Rastrelli, L. *J. Nat. Prod.* **2001**, *64*, 973−975.

(22) Piccinelli, A. L.; Cuesta-Rubio, O.; Chica, M. B.; Mahmood, N.; Pagano, B.; Pavone, M.; Barone, V.; Rastrelli, L. *Tetrahedron* **2005**, *61*, 8206−8211.

(23) Fukuyama, Y.; Minami, H.; Kuwayama, A. *Phytochemistry* **1998**, *49*, 853−857.

(24) Zhang, Z.; ElSohly, H. N.; Jacob, M. R.; Pasco, D. S.; Walker, L. A.; Clark, A. M. *Planta Med.* **2002**, *68*, 49−54.
(25) Walia, S.; Mukerjee, S. K. *Phytochemistry* **1984**, *23*, 1816−1817.
(26) Pinto, M. M. M.; Mesquita, A. A. L.; Gottlieb, O. R. *Phytochemistry* **1987**, *26*, 2045−2048.
(27) Corrêa, D. B.; Silva, L. G.; Gottlieb, O. R.; Gonçalves, S. J. *Phytochemistry* **1970**, *9*, 447−451.
(28) Gottlieb, O. R.; Magalhães, M. T.; Pereira, O. S.; Mesquita, A. A. L.; Corrêa, D. B.; Oliveira, G. G. *Phytochemistry* **1970**, *9*, 2537−2544.
(29) Habib, A. M.; Reddy, K. S.; McCloud, T. G.; Chang, C.-J.; Cassady, J. M. *J. Nat. Prod.* **1987**, *50*, 141−145.
(30) Sobral, I. S.; Souza-Neta, L. C.; Costa, A. N.; Guedes, M. L. S.; Martins, D.; Cruz, F. G. *Rev. Bras. Farmacogn.* **2009**, *19*, 686−689.
(31) Saleem, M.; Nazir, M.; Ali, M. S.; Hussain, H.; Lee, Y. S.; Riaz, N.; Jabbar, A. *Nat. Prod. Rep.* **2010**, *27*, 238−254.
(32) Panthong, K.; Pongcharoen, W.; Phongpaichit, S.; Walter, C. T. *Phytochemistry* **2006**, *67*, 999−1004.
(33) Boonsri, S.; Karalai, C.; Ponglimanont, C.; Kanjana-opas, A.; Chantrapromma, K. *Phytochemistry* **2006**, *67*, 723−727.

DOI: 10.1021/acs.jnatprod.5b00858
J. Nat. Prod. 2016, 79, 470−476

Phytochemistry Letters 10 (2014) cxli–cxliv

Contents lists available at ScienceDirect

Phytochemistry Letters

journal homepage: www.elsevier.com/locate/phytol

Bioactive acetophenones from *Plectranthus venteri*☆

Johanna E. Maree [a], Proma Khondkar [b], Awo A. Kwapong [b], Blessing M. Oyedemi [b], Tariq M. Aljarba [b], Paul Stapleton [b], Alvaro M. Viljoen [a], Simon Gibbons [b,*]

[a] Department of Pharmaceutical Sciences, Tshwane University of Technology, Private Bag X680, Pretoria 0001, South Africa
[b] Department of Pharmaceutical and Biological Chemistry, UCL School of Pharmacy, 29-39 Brunswick Square, London WC1N 1AX, United Kingdom

ARTICLE INFO

Article history:
Received 17 September 2014
Received in revised form 14 October 2014
Accepted 16 October 2014
Available online 31 October 2014

Keywords:
Plectranthus venteri
Lamiaceae
Acetophenones
Bacterial plasmid transfer inhibition

ABSTRACT

In a project to investigate the chemistry of South African *Plectranthus* species, from the dichloromethane extract of the aerial parts of *Plectranthus venteri*, we isolated two known natural product acetophenones, namely 2-hydroxy-3,4,5,6-tetramethoxy-acetophenone (**1**) and 2-hydroxy-4,5,6-trimethoxy-acetophenone (**2**). Structures were assigned using NMR spectroscopy and HRTOFESIMS. Compound **1** was previously synthesised as a precursor to the polymethoxylated flavone nobiletin. The acetophenones exhibited remarkable inhibitory activities against the transfer of the IncW plasmid R7K in a bacterial plasmid transfer inhibition assay.

1. Introduction

Plectranthus is the largest genus of the Lamiaceae and is represented by approximately 350 species, mostly occurring in Africa, India, Japan, Malaysia and Australia. Fifty-three of these species occur abundantly in South Africa (Van Jaarsveld, 2006). Several species are used as traditional medicine in South Africa for the treatment of various conditions ranging from coughs, wounds, gastrointestinal disorders, skin infections and for pain (Hutchings et al., 1996; Lukhoba et al., 2006). *Plectranthus* is considered paraphyletic as all *Plectranthus* species have a common ancestor but the genus does not include all the descendants of the shared ancestor (Potgieter et al., 2009). *Plectranthus* differs from the other members of the Lamiaceae as the two lipped corolla has exerted stamens attached to its throat, the bracts are smaller than the leaves and the 5-toothed calyx enlarges after fertilisation (Van Jaarsveld, 2006). The infrageneric taxonomy of *Plectranthus* remains challenging due to the lack of well-defined morphological characters. As a result of taxonomic ambiguity, numerous species have been incorrectly placed in closely related genera such as *Coleus*, *Solenostemon* and *Englerastrum* (Lukhoba et al., 2006). Furthermore, species previously assigned to *Plectranthus* now form part of the distant genus *Isodon* (Paton et al., 2004). In a project to study the chemistry of this interesting genus, we conducted a phytochemical investigation of *Plectranthus venteri* van Jaarsv. & L. Hankey, a narrow endemic to the Sekukuniland region of South Africa, which was only discovered in 1997. In order to justify the traditional uses against infectious diseases, we also focused on the antibacterial activities of the compounds isolated from this plant. Purified compounds were evaluated in a bacterial plasmid transfer inhibition assay with plasmids harbouring antibiotic-resistance genes. The rationale for this was that a reduction in plasmid transfer could result not only in a reduction of antibiotic resistance in a bacterial population, but also contribute to a reduction of virulence of a selected bacterial species.

2. Results and discussion

Compound **1** was isolated as an orange oil and HRQTOFESIMS gave an *m/z* at 257.1012 $[M+H]^+$, which indicated that its molecular formula was $C_{12}H_{16}O_6$. The ^1H NMR spectrum (Figure 1, supporting information) was very simple, accounted for all 16 hydrogens and was reminiscent of a methoxylated acetophenone (Parsons et al., 1994) (Fig. 1). An acetyl methyl group (δ_H 2.66), four methoxyl groups (δ_H 3.79, 3.84, 3.94 and 4.07) and a highly deshielded hydrogen-bonded hydroxyl group (δ_H 13.23) accounted for all positions of the aromatic acetophenone core. Given that the hydroxyl group had to be *ortho* to the acetyl group for maximal H-bonding with the carbonyl oxygen of the acetyl group, the structure of the compound could readily be assigned as

☆ This paper forms part of a special issue of Phytochemistry Letters dedicated to the memory of Andrew Marston (1953–2013), outstanding Phytochemist who is much missed by his friends.

* Corresponding author. Tel.: +44 207 753 5913; fax: +44 207 753 5964.
E-mail address: simon.gibbons@ucl.ac.uk (S. Gibbons).

http://dx.doi.org/10.1016/j.phytol.2014.10.021
1874-3900/

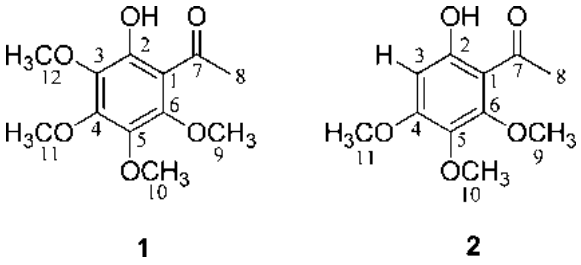

Fig. 1. Structures and numbering for compounds **1** and **2**.

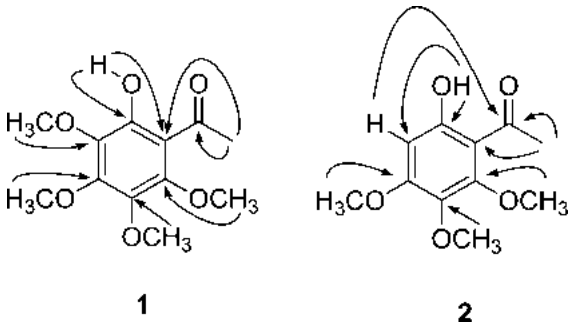

Fig. 2. HMBC correlations for compounds **1** and **2**.

2-hydroxy-3,4,5,6-tetramethoxy-acetophenone. To confirm this nomenclatural assignment, full 2-dimensional NMR spectral analyses, including HMBC spectroscopy, were carried out to unambiguously assign all ^{1}H and ^{13}C resonances (Figure 2, supporting information). The acetyl methyl hydrogens (H_3-8) showed a ^{2}J correlation to a carbonyl carbon (δ_c 204.5) and to an aromatic quaternary carbon, to which this acetyl group was directly attached (C-1, δ_C 110.4) (Fig. 2). The hydrogen-bonded hydroxyl hydrogen correlated to C-2, C-1 and to an oxygen-bearing aromatic quaternary carbon (C-3), which was also coupled to by the hydrogens of a methoxyl group (H_3-12). The three remaining methoxyl groups each coupled to their respective aromatic oxygen-bearing quaternary carbons (C-4, C-5 and C-6). Full assignment of the precise resonances of each methoxyl was achieved by careful inspection of the NOESY spectrum. Methoxyl H_3-12 showed a correlation to H_3-11, which coupled to H_3-10 which in turn coupled to H_3-9. In combination with the HSQC spectrum, we were therefore able to unambiguously assign all of their respective ^{1}H and ^{13}C resonances (Table 1). Compound **1** was therefore assigned as 2-hydroxy-3,4,5,6-tetramethoxy-acetophenone. This compound had previously been isolated as an alkaline hydrolysis degradation product from two separate studies from a polymethoxylated chromone conyzorigun from *Ageratum conyzoides* (Adesogan and Okunade, 1978) and the flavone 5,6,7,8,3′,4′,5′-heptamethoxyflavone from *Eupatorium coelestinum* (Le-Vam and Pham, 1979). Additionally, it was isolated from the Liverwort *Adelanthus decipens* (Rycroft et al., 1998). This is however, the first report of its full ^{13}C NMR data. This compound was previously synthesised using the microwave-assisted technique in a study on the inhibitory effects on melanogenesis by polymethoxylated acetophenones and polymethoxylated flavones (Tsukayama et al., 2007). The ^{1}H NMR data are in very close agreement with the natural and synthetic compound. **1** was also synthesised as a precursor to the synthesis of the *Citrus* polymethoxylated flavone nobiletin in a study of its use as a stimulator of neuronal cell signalling by positron emission tomography (Asakawa et al., 2011).

The ^{1}H and ^{13}C resonances for compound **2** (Table 1) were highly similar to those of **1** with the exception of the absence of one methoxyl group and the presence of an aromatic hydrogen (δ_H 6.21), again indicating a methoxylated acetophenone. HRQTOFE-SIMS gave an *m/z* at 227.0920 $[M+H]^+$, which indicated that its molecular formula was $C_{11}H_{14}O_5$. Signals in the ^{1}H NMR spectrum (Table 1 and Figure 3 (supporting information)) included a highly deshielded hydrogen-bonded hydroxyl hydrogen (δ_H 13.49), an aromatic hydrogen (δ_H 6.21), three methoxyl groups (δ_H 3.76, 3.86 and 3.97) and an acetyl methyl group (δ_H 2.63).

Inspection of the HMBC and ^{13}C spectra (Fig. 2 and Figure 4 (supporting information)) allowed unambiguous assignment of all resonances and again confirmed that compound **2**, like compound **1**, was a methoxylated acetophenone. The difference between the two compounds was identified by an HMBC correlation from the phenolic hydroxyl hydrogen to the carbon bearing an aromatic hydrogen (δ_H 6.21), therefore fixing the position of the aromatic hydrogen *ortho* to the hydroxyl group. Compound **2** was therefore assigned as 2-hydroxy-4,5,6-trimethoxy-acetophenone and has been previously isolated from *Erigeron breviscapus* (Chun et al., 2003).

Both compounds were evaluated for their ability to inhibit conjugal transfer of plasmid-mediated antibiotic resistance in *Escherichia coli*. The compounds exhibited significant inhibitory activities against the transfer of the IncW plasmid R7K with an 85% and 87% reduction in the presence of **1** and **2**, at a concentration of 100 mg/L, respectively. This activity was comparable to that of linoleic acid, a known anti-conjugation agent for IncW plasmids (Fernandez-Lopez et al., 2005). At 100 mg/L, linoleic acid gave a 92% reduction in the transfer of the R7K IncW plasmid. The activity of **1** and **2** were found to be specific as they were poorly active (with a 35% or below reduction) in limiting the transfer of the IncN plasmid pKM101, the $IncI_2$ plasmid TP114 and the IncP plasmid pUB307. At a concentration of 10 mg/L, novobiocin significantly

Table 1
^{1}H (500 MHz) and ^{13}C (125 MHz) NMR spectral data and HMBC correlations of **1** and **2** recorded in $CDCl_3$.

1					**2**				
Position	^{1}H	^{13}C	^{2}J	^{3}J	Position	^{1}H	^{13}C	^{2}J	^{3}J
1	–	110.4			1	–	108.4		
2	–	154.7			2	–	161.9		
3	–	136.7			3	6.21	96.1	C2, C4	C1, C5
4	–	151.6			4	–	160.1		
5	–	138.0			5		134.7		
6	–	153.8			6	–	155.3		
7	–	204.5			7	–	203.6		
8	2.66	32.6	C7	C1	8	2.63	32.2	C7	C1
9	4.07	61.6		C6	9	3.97	61.1		C5
10	3.79	61.5		C5	10	3.76	61.1		C4
11	3.94	61.3		C4	11	3.86	56.2		C3
12	3.84	61.2		C3	OH	13.49		C2	C1
OH	13.23		C2	C1, C3	–	–			

inhibited the transfer of pKM101, TP114, pUB307 and R7K with an 81.7%, 83%, 72.5% and 99.4% reduction respectively. Whilst novobiocin is known to eliminate various plasmids, its activity is concentration dependent (Hooper et al., 1984). These results indicate that the simple methoxylated acetophenone core is worthy of further anti-plasmid investigation, particularly with respect to the methoxyl substitution pattern and the number and type of functional groups around the acetophenone nucleus. *Plectranthus* is known for its medicinal value and there are previous reports of antimicrobial activity of some species of *Plectranthus* (Rijo et al., 2011; Awadh Ali et al., 2012) but according to our knowledge this is the first report of plasmid inhibitory activity from this genus.

The most frequently cited ethnobotanical uses of *Plectranthus* species, which account for more than 85% of all reported uses, relates to their medicinal properties (Lukhoba et al., 2006). *Plectranthus* species have a profound biosynthetic capacity to produce diverse phytochemicals from secondary cell metabolism, which are predominantly diterpenoids and triterpenoids with confirmed biological properties. These phytochemicals continue to be an interesting source of new drugs, drug leads and new chemical entities with *Plectranthus* being no exception. Extracts of *Plectranthus barbatus* are used in slimming formulations due to its reported fat breakdown stimulation (Lukhoba et al., 2006). Forskolin isolated from *P. barbatus*, served as a prototype for the development of more potent water-soluble compounds with selective activation of adenylyl cyclase. The most potent water-soluble forskolin derivative produced is 6-(3-dimethylaminopropionyl)-forskolin hydrochloride. This forskolin derivative was the first clinically available adenylyl cyclase activator used for post-operative management of cardiac surgery patients (Paul et al., 2013). Considering that *Plectranthus* species accumulate interesting bioactive molecules and given their illustrious use in African traditional medicine, a concerted effort is required to systematically explore South African species which hitherto remain neglected.

3. Experimental

3.1. Extraction and isolation

The leaves of *P. venteri* were collected from Kirstenbosch National Botanical Gardens (KBNBG) and Walter Sisulu National Botanical Gardens (WSNBG) in July 2010. The samples were air-dried at room temperature, milled (Retsch® MM 400 ball mill, Haan, Germany) to a fine powder and sieved (500 μm sieve, Endecotts Ltd., London, United Kingdom) to obtain a homogenous particle size. Each sample was placed in conical flask and extracted with dichloromethane (CH_2Cl_2) (Fisher Scientific UK Ltd., Loughborough, United Kingdom). The mixture was sonicated for 10 min at 25 °C (Sonorex Digital 10P, Bandelin Electronic™, Berlin, Germany) and subsequently allowed to settle for 5 min. The supernatant was removed and placed into round bottom flasks. This procedure was repeated three times before drying the combined extract with a rotary evaporator (Multivapor P-12, Büchi Labortechnik AG©, Switzerland) at 40 °C and the extract was stored at 2 °C.

5 g of *P. venteri* dichloromethane extract was subjected to silica gel (Merck) VLC yielding 15 fractions. A stepwise gradient elution procedure from 100% hexane to 100% ethyl acetate followed by methanol 10% increments in ethyl acetate was used as mobile phase. The fraction eluted with 80% hexane: 20% ethyl acetate was concentrated under vacuum to yield 1425 mg of solid. This fraction was then extracted with methanol to give a methanol soluble portion and an insoluble residue. The methanol soluble portion was subjected to p-TLC (toluene:ethyl acetate (9:1, v/v)) to give 28.4 mg of **1** (R_f value: 0.43) and 33.2 mg of **2** (R_f value: 0.52).

3.2. Structure elucidation

1D and 2D NMR spectra were recorded on a Bruker AVANCE 500 MHz spectrometer and processed using XWin NMR 3.5 software. Samples were dissolved in deuterated-chloroform, which was also used as the internal solvent standard and referenced to 7.26 ppm.

3.3. Exact mass measurement

Twenty μL of the sample in methanol was injected using a Waters 1525 μ Binary HPLC pump system connected to a Waters Sample Manager Autosampler. An isocratic mode was utilised 50% methanol–50% water 0.1% formic acid with the flow rate of 0.2 mL/min. The capillary eluent was continuously directed into a Waters LCT Premier XE. Exact mass measurements were carried out automatically using the LCT Premier's integral LockSpray dual-electrospray source. The LockSpray dual-electrospray source was operated in both positive- and negative-ion ESI mode with full MS scans over 2 min time period of the direct infusion isocratic run. The LCT Premier mass spectrometer was calibrated prior the accurate mass measurement with sulfadimethoxine $[M+H]^+$ with m/z value of 311.0814 and leucine enkephalin $[M]^+$, m/z value of 556.2771. The LCT Premier XE mass spectrometer was operated in W-mode with the following parameters: the source capillary was 2300 V, sample cone 60 V, desolvation temperature 400 °C, source temperature 80 °C, cone gas flow 50, and desolvation gas flow 450 °C. The analyser parameters were TOF flight tube 7200 V, reflectron 1800 V, pusher voltage 895, MCP 1800.

3.4. Bacterial plasmid transfer inhibition assay

3.4.1. Materials and reagents

Amoxicillin, kanamycin sulphate, nalidixic acid, streptomycin, novobiocin, linoleic acid and dimethyl sulfoxide were purchased from Sigma–Aldrich (Poole, UK). MacConkey agar, Luria–Bertani (LB) broth and phosphate buffered saline (PBS) were obtained from Fisher Scientific UK Ltd.

3.4.2. Bacterial strains and plasmids

Plasmid-containing *E. coli* strain K12 J53 was used as the donor and *E. coli* ER1793 (streptomycin-resistant) and *E. coli* JM109 (nalidixic-resistant) were recipients in the bacterial conjugation assay. Conjugative transfer of plasmids pKM101 (IncN; ampicillin-resistant), TP114 ($IncI_2$; kanamycin-resistant), pUB307 (IncP; ampicillin-, kanamycin- and tetracycline-resistant) and R7K (IncW; ampicillin-, streptomycin- and spectinomycin-resistant), which were obtained from Dr. Paul Stapleton, were evaluated. Antimicrobial agents were used at the following concentrations to select for the appropriate plasmid: kanamycin sulphate (20 mg/L), amoxicillin (30 mg/L), streptomycin sulphate (20 mg/L) and nalidixic acid (30 mg/L).

3.4.3. Bacterial plasmid conjugation assay

Both recipients *E. coli* ER1793 and JM109 and plasmid-containing donor *E. coli* K12 J53 strains were incubated separately overnight (16 h) at 37 °C in LB broth. Samples of the overnight cultures were retained for colony-forming unit (cfu/mL) determinations. Bacterial conjugation was performed as described by Rice and Bonomo (2005) with slight modification with equal volumes of the donor and recipient. Compounds were evaluated for anti-conjugative activity at a concentration of 100 mg/L. Transconjugants (recipient cells carrying the donated plasmid) and donor cells were identified by inoculating 100 μL of serial dilutions of the overnight conjugation mixture on appropriate antibiotic selective MacConkey agar plates. The

transfer frequency was calculated as the ratio of total number of transconjugants (cfu/mL) to the total number of donor (cfu/mL). Novobiocin and linoleic acid were used as the positive controls. All experiments were performed in triplicate and the mean determined. The difference between the control transfer frequency and the compounds were evaluated by Student's *t*-test. Values of $p < 0.05$ were statistically significant.

3.5. 2-Hydroxy-3,4,5,6-tetramethoxy-acetopheonone (**1**)

Orange oil; λ_{max} (log ε) 219 (3.91), 280 (3.82) nm; IR (film) ν_{max} 2941, 1744, 1624, 1589, 1406, 1363, 1313, 1281, 1260, 1214, 1097, 1017, 988, 899, 849 cm^{-1}; ^{1}H NMR and ^{13}C NMR ($CDCl_3$): see Table 1; HRTOFESIMS *m*/*z* 257.1012 $[M+H]^+$ (Calcd for $C_{12}H_{17}O_6$ 257.1025).

3.6. 2-Hydroxy-4,5,6-trimethoxy-acetopheonone (**2**)

Orange oil; λ_{max} (log ε) 216 (4.01), 280 (4.03) nm; IR (film) ν_{max} 2944, 1615, 1592, 1363, 1277, 1253, 1219, 1105, 1081, 1021, 997, 966, 930, 868, 824 cm^{-1}; HRTOFESIMS *m*/*z* 227.0920 $[M+H]^+$ (Calcd for $C_{11}H_{15}O_5$ 227.0919).

Acknowledgements

We thank Mr. Emmanuel Samuel for his help in facilitating mass spectrometry and Ms. Kersti Karu for running HRTOFESIMS. Dr. Ernst van Jaarsveld (Kistenbosch Botanical Garden) and Mr. Andrew Hankey (Walter Sisulu Botanical Garden) are thanked for assisting in access and collection of plant material. The National Research Foundation (South Africa) and the Commonwealth Split-fellowship Programme (United Kingdom) are thanked for financial support (ZACN-2010-247).

Appendix A. Supplementary data

Supplementary data associated with this article can be found, in the online version, at http://dx.doi.org/10.1016/j.phytol.2014.10.021.

References

Adesogan, E.K., Okunade, A.L., 1978. Structure of conyzorigun, a new chromone from *Ageratum conyzoides*. J. Chem. Soc., Chem. Commun. 152 .

Asakawa, T., Hiza, A., Nakayama, M., Inai, M., Oyama, D., Koide, H., Shimizu, K., Wakimoto, T., Harada, N., Tsukada, H., Oku, N., Kan, T., 2011. PET imaging of nobiletin based on a practical total synthesis. Chem. Commun. 47, 2868–2870.

Chun, L., Honggao, L., Xuanli, Y., Huachun, G., 2003. Advances in studies on *Erigeron breviscapus*. Chin. Wild Plant Resour. 1, 002.

Fernandez-Lopez, R., Machon, C., Longshaw, C.M., Martin, S., Molin, S., Zechner, E.L., Espinosa, M., Lanka, E., De La Cruz, F., 2005. Unsaturated fatty acids are inhibitors of bacterial conjugation. Microbiology 151, 3517–3526.

Hooper, D.C., Wolfson, J.S., Mchugh, G.L., Swartz, M.D., Tung, C., Swartz, M.N., 1984. Elimination of plasmid pMG110 from *Escherichia coli* by novobiocin and other inhibitors of DNA gyrase. Antimicrob. Agents Chemother. 25, 586–590.

Hutchings, A., Scott, A.H., Lewis, G., Zululand, U.O., Cunningham, A.B., Institute, N.B., 1996. Zulu Medicinal Plants: An Inventory. University of Natal Press.

Le-Vam, N., Pham, T.V.C., 1979. Two new flavones from *Eupatorium coelestinum*. Phytochemistry 18, 1859–1861.

Lukhoba, C.W., Simmonds, M.S.J., Paton, A.J., 2006. Plectranthus: a review of ethnobotanical uses. J. Ethnopharmacol. 103, 1–24.

Awadh Ali, N.A., Al-Fatimi, M.A., Crouch, R.A., Denkert, A., Setzer, W.N., Wessjohann, L., 2012. Antimicrobial, Antioxidant, and Cytotoxic Activities of the Essential Oil of *Tarchonanthus camphoratus*. Nat. Prod. Commun. 7, 1099–1102.

Parsons, I.C., Gray, A.I., Hartley, T.G., Waterman, P.G., 1994. Acetophenones and coumarins from stem bark and leaves of *Melicope stipitata*. Phytochemistry 37, 565–570.

Paton, A.J., Springate, D., Suddee, S., Otieno, D., Grayer, R.J., Harley, M.M., Willis, F., Simmonds, M.S.J., Powell, M.P., Savolainen, V., 2004. Phylogeny and evolution of basils and allies (Ocimeae, Labiatae) based on three plastid DNA regions. Mol. Phylogenet. Evol. 31, 277–299.

Rijo, P., Rodríguez, B., Duarte, A., Simões, M.F., 2011. Antimicrobial properties of *Plectranthus ornatus* extracts, 11-acetoxyhalima-5,13-dien-15-oic acid metabolite and its derivatives. Nat. Prod. J. 1, 57–64.

Paul, M., Radha, A., Kumar, D.S., 2013. On the high value medicinal plant, *Coleus forskohlii* briq. Hygeia J.D. Med. 5, 69–78.

Potgieter, C.J., Edwards, T.J., Van Staden, J., 2009. Pollination of *Plectranthus* spp. (Lamiaceae) with sigmoid flowers in southern Africa. S. Afr. J. Bot. 75, 646–659.

Rice, L.B., Bonomo, R.A., 2005. Genetic and biochemical mechanisms of resistance to antimicrobial agents. In: Lorian, V. (Ed.), Antibiotics in Laboratory Medicine. Lippincott Williams & Wilkins, USA, pp. 483–484.

Rycroft, D.S., Cole, W.J., Rong, S., 1998. Highly oxygenated naphthalene and acetophenones from the liverwort *Adelanthus decipiens* from the British Isles and South America. Phytochemistry 48, 1351–1356.

Tsukayama, M., Kusunoki, E., Hossain, M.M., Kawamura, Y., Hayashi, S., 2007. Miscrowave-assisted efficient synthesis of polymethoxyacetophenones and natural polymethoxyflavones, and their inhibitory effects on melanogenesis. Heterocycles 711589–711600.

Van Jaarsveld, E., 2006. The Southern African Plectranthus and the Art of Turning Shade to Glade. Fernwood Press, Simon's Town, pp. 176.

JOURNAL OF NATURAL PRODUCTS

Note

pubs.acs.org/jnp

In Vitro Antibacterial Activity of Prenylated Guanidine Alkaloids from *Pterogyne nitens* and Synthetic Analogues

Aline Coqueiro,[†,‡] Luis Octávio Regasini,[†] Paul Stapleton,[‡] Vanderlan da Silva Bolzani,*[,†] and Simon Gibbons*[,‡]

[†]Department of Organic Chemistry, Institute of Chemistry, São Paulo State University, Rua Prof. Francisco Degni 55, Araraquara14800-900, Brazil

[‡]Department of Pharmaceutical and Biological Chemistry, UCL School of Pharmacy, 29-39 Brunswick Square, London WC1N 1AX, United Kingdom

Supporting Information

ABSTRACT: The present investigation deals with the antibiotic activity of eight natural guanidine alkaloids and two synthetic analogues against a variety of clinically relevant methicillin-resistant *Staphylococcus aureus* strains. Galegine (**1**) and pterogynidine (**2**) were the most potent compounds, with a minimum inhibitory concentration of 4 mg/L, to all tested strains. The preliminary chemical features correlating to anti-MRSA activity showed that the size of the side chain and the substitution pattern in the guanidine core played a key role in the antibacterial activity of the imino group. Guanidine alkaloids **1** and **2** are promising molecular models for further synthetic derivatives and, thus, for medicinal chemistry studies.

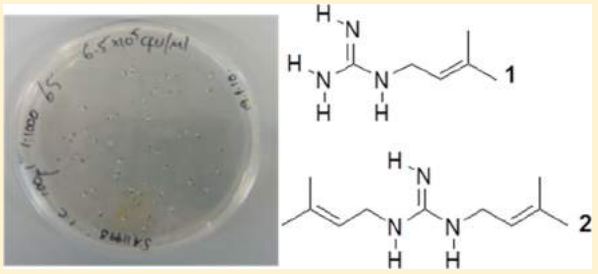

When antimicrobials were made available for therapeutic use over 60 years ago, they were considered miracle drugs. However, their indiscriminate use and popularity have contributed to the appearance of many resistant bacterial strains, which has made antimicrobials progressively less effective over the past decade. Infectious diseases caused by methicillin-resistant *Staphylococcus aureus* (MRSA) currently constitute a major public health concern in hospitals and communities, and these bacteria have developed resistance to the most commonly used antibiotics.[1] Indeed, *S. aureus* has acquired resistance to many classes of antibiotics including the glycopeptide family (such as vancomycin and teicoplanin), oxazolidinones (linezolid), and a combination of streptogramins (quinupristin and dalfopristin).[2] Therefore, developing new classes of antibiotics to overcome the issue of drug resistance is mandatory.[3]

Natural products remain a superb source of chemical diversity and potential drugs. Thousands of natural products have been isolated, some of which exhibit great antimicrobial potential for medicinal use.[4] Despite the potent antibacterial activity of some plant secondary metabolites[2] and the ability of some of these compounds to modify the resistance associated with MDR strains[5] and efflux pumps,[6] plants are still an underexplored and underexploited source of antimicrobial agents.

In our current research on biologically active natural products from Brazilian biodiversity, we have screened extracts obtained from many plant species collected mainly in the Cerrado and the Atlantic Forest, two biomes in the State of São Paulo seriously threatened by extinction.[7] *Pterogyne nitens* Tul. (Fabaceae, Caesalpinioideae) is one of these species and is catalogued in our database ($NuBBE_{DB}$).[8]

Pterogyne nitens is a native tree of South America and is popularly known as "balsam", "cocal", "yvira-ró", and "amendoinzeiro". It bears attractive flowers and fruits and, therefore, has application as an ornamental plant.[9] Although scientists have not frequently reported the medicinal uses of this species, the Paraguayan population has used aqueous preparations from the stem bark of *P. nitens* to treat ascariasis.[10] Our previous phytochemical studies on the leaves, flowers, fruits, bark, and roots of *P. nitens* led to the isolation of guanidine alkaloids, which are unusual in plants, as well as flavones, flavonols, and terpenoids.[11−15] Several articles have reported that these guanidine alkaloids possess different biological activities including cytotoxic, antimutagenic, anti-angiogenic, pro-apoptotic, and antifungal actions.[11,16−20] While guanidine alkaloids belonging to marine sources display a broad spectrum of actions,[21] few studies have dealt with higher plants, where these compounds rarely occur.

As part of the SisBiotaCNPq/FAPESP Biodiscovery and CIBIFar Programs, which aim to search for new antibacterial agents from the Brazilian flora, this investigation evaluated the antibacterial activity of eight guanidine alkaloids from *P. nitens* and two synthetic analogues using different multi-drug-resistant strains.

In the present work, we tested a panel of *Staphylococcus aureus* strains with clinical relevance, possessing different

Received: March 28, 2014
Published: August 4, 2014

mechanisms of resistance. Among these, we tested strain SA-1199B, a multi-drug-resistant strain that overexpresses the NorA efflux pump[22] and also possesses a gyrase-encoding gene mutation that in addition to NorA confers a high level of resistance to some fluoroquinolones;[23] a macrolide-resistant strain (RN4220);[24] a clinical MRSA (XU212), resistant to tetracycline bearing the TetK efflux pump;[25] a standard laboratory strain (ATCC25923);[25] and the methicillin-resistant strains EMRSA-15[26] and EMRSA-16.[27] All of the natural guanidine alkaloids (**1**−**8**) and two synthetic analogues (**9** and **10**) were tested against the six *S. aureus* strains, and the minimum inhibitory concentration (MIC) was determined for the active alkaloids. All the guanidine alkaloids were tested at concentrations ranging from 512 to 0.5 mg/L.

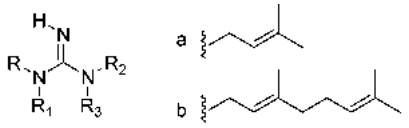

	R	R_1	R_2	R_3
1	H	H	H	a
2	H	a	H	a
3	H	b	H	b
4	H	H	b	b
5	CH_3	b	CH_3	b

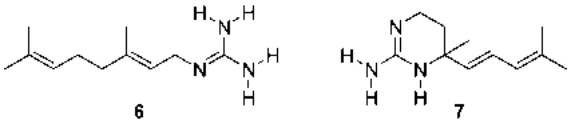

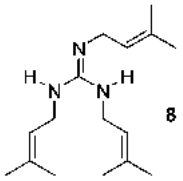

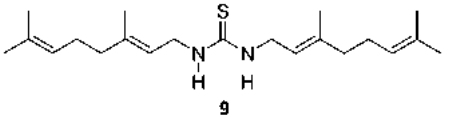

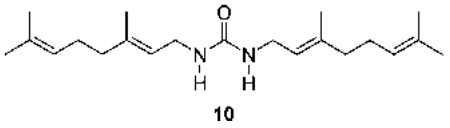

With the exception of alchorneine (**8**), which was inactive (MIC > 512 mg/L), all of the natural alkaloids displayed activity stronger than or similar to norfloxacin against *S. aureus* SA-1199B, XU212, and EMRSA-16 strains. Galegine (**1**) and pterogynidine (**2**) were the most potent compounds among the investigated natural guanidines for all tested strains (Table 1).

Previous work with synthetic guanidines has shown the antimicrobial potential of these compounds against drug-resistant pathogens.[28,29] Fair et al. showed that, by replacement of hydroxyl or amine groups with guanidine groups, the derivatives were superior binders of the bacterial ribosomal A-site compared to their parent compounds, demonstrating a potent effect.[29] The guanidines are strong bases, and the reactivity of this chemical group can be attributed to the electron-donating nitrogen atoms that are present in a planar structure, which can participate in well-defined directional hydrogen bonds.

Due to the similarities of the structures of the tested guanidine alkaloids, it was possible to suggest preliminary chemical features that were correlated to anti-MRSA activity.

The most active compounds **1** and **2** possess one and two prenyl groups, respectively, and showed the same MIC values (4 mg/L) for all tested strains, but when the prenyl groups were substituted by one or two geranyl groups, the activity decreased (**3**, **4**, and **6**: MICs of 8−32 mg/L), being independent of which position the group was introduced. The same phenomenon was observed for compound **7**, a cyclic guanidine, and **5**, which possesses two methyl substituents in the guanidine core. Compounds **3**−**7** had poorer activity when compared to the prenylated guanidines (**1** and **2**). Interestingly, guanidine **8** (*N*-1,*N*-2,*N*-3-tri-isopentenylguanidine), the only compound possessing at least one substituent on each nitrogen, was the sole inactive compound.

This information showed that the size of the side chain and the substitution pattern in the guanidine core appeared to play a key role in the antibacterial activity. This may be attributed to the fact that an increase in the size of the side chain decreased the electron donation ability of the nitrogen. When three of the nitrogen atoms in the guanidine core were substituted (e.g., **8**), the steric effects could affect the reactivity and binding of these molecules. This spatial shielding effect makes potential interactions more difficult and less likely. The steric effect means that it would be more difficult to get close enough to allow attack by the lone pair of the nitrogen or to form hydrogen bonds.

The side chains can also serve as modulators of lipid affinity and, therefore, cellular bioavailability; so when the size or number of side chains is increased, this enhances the membrane permeability but may result in poorer aqueous solubility, leading to a loss of activity.[23]

To confirm the importance of the imino group in the antimicrobial activity of the guanidines, we tested two analogues of nitensidine A that were synthesized by replacing the imino nitrogen atom in nitensidine A by sulfur (nitensidine AT) and oxygen (nitensidine AU). The antimicrobial activity of nitensidine A was reduced by replacing the imino nitrogen by sulfur (S), and the activity was extinguished when the imino group was substituted by oxygen (O). These results confirmed the requirement of the imino nitrogen atom for antibacterial activity. Nitensidine AU (**10**) did not show activity (MIC > 512 mg/L); however the oxygen atom can also participate in hydrogen bonds, and while they can contribute to the activity, they are not crucial. On the other hand, the basicity of the imino nitrogen in the guanidine core seems to play a key role in the antimicrobial activity.

The steric effect was not high for galegine (**1**) and pterogynidine (**2**), demonstrating that one or two prenyl groups did not interfere in the interaction of the imino group and were optimal in this study in terms of lipophilicity and could explain the noteworthy activity of **1** and **2**. These compounds were 8 times more potent than norfloxacin against the multi-drug-resistant strain that overexpresses the NorA efflux transporter (SA-1199B) and 32 times more potent than norfloxacin against the most resistant strain, EMRSA-16.

dx.doi.org/10.1021/np500281c | *J. Nat. Prod.* 2014, 77, 1972−1975

Table 1. In Vitro Antibacterial Activity (MIC in mg/L and μM) of Guanidine Alkaloids 1−8 from *Pterogyne nitens* and the Synthetic Analogues 9 and 10 against *Staphylococcus aureus* Strains

compound	SA-1199B	RN4220	XU212	ATCC25943	EMRSA-15	EMRSA-16
1	4/31.4	4/31.4	4/31.4	4/31.4	4/31.4	4/31.4
2	4/20.5	4/20.5	4/20.5	4/20.5	4/20.5	4/20.5
3	32/96.5	16/48.3	8/24.1	16/48.3	32−16/96.5−48.3	16−8/48.3−24.1
4	32/96.5	16/48.3	8/24.1	16/48.3	32/96.5	8/24.1
5	32/89.0	16/44.5	8/22.2	16/44.5	32/89.0	8/22.2
6	32/163.8	16/81.9	8/40.9	16/81.9	16/81.9	8/40.9
7	32/165.6	16/82.8	8/41.4	32−16/165.6−82.8	32/165.6	16−8/82.8−41.4
8	>512	>512	>512	>512	>512	>512
9	128/367.5	128/367.5	128/367.5	128/367.5	>512	64−32/183.8−91.9
10	>512	>512	>512	>512	>512	>512
norfloxacin	32/100.2	0.5/1.6	8/25.1	0.5/1.6	0.5/1.6	128/400.8

In a previous study by Regasini et al., on the cytotoxicity of guanidine alkaloids, a larger number of prenyl groups elicited more potent activity.[11] The authors found that **7** was the most active alkaloid against a number of cell lines; compounds **1**, **2**, and **6** were inactive against all of the human tested cell lines.[11] On the basis of this information, we concluded that toxicity against bacteria was selective and that compounds **1** and **2**, which did not harm tested human cell lines in a previous study, were the most active against prokaryotic cells.

The minimum bactericidal concentration (MBC) assays were conducted on the most active alkaloids—galegine (**1**) and pterogynidine (**2**)—to verify whether they possessed a bactericidal or bacteriostatic effect. Ten microliters of sample from the wells of a plate used to determine the MIC values of compounds **1**−**7** against SA-1199B was removed where no growth was observed (i.e., the MIC and above) and plated out onto drug-free media. After 24 h incubation, no growth was observed at the MIC or higher, indicating that the compound had killed the organism, rather than just inhibiting its growth, suggesting that these agents had bactericidal activities; the MIC and MBC values were 4 mg/L.

Guanidine alkaloids from *P. nitens* displayed antibacterial activity against multi-drug-resistant strains (MRSA). Galegine and pterogynidine were effective against different strains, mainly SA-1199B and MRSA-16, which were resistant to the standard drug norfloxacin. Therefore, guanidine alkaloids **1** and **2** are promising hits for further medicinal chemistry investigations to synthesize anti-MRSA drug leads. Further studies on these bactericidal compounds are necessary to determine the mechanism of action involved in the activity against MRSA.

EXPERIMENTAL SECTION

Plant Material. Leaves and branches of *Pterogyne nitens* Tul., Fabaceae, were collected from the Botanic Garden of São Paulo (São Paulo, Brazil) by Dr. Maria C. M. Young in May 2003 and January 2005, respectively, and identified by Dr. Inês Cordeiro (IBt-SMA). Two voucher specimens (SP203419 and SP204319b) were deposited at the State Herbarium "Maria Eneida Kaufmann" of the Institute of Botany (São Paulo, Brazil).

Test Compounds. The extraction, isolation, and the physicochemical and spectroscopy data of the guanidine alkaloids **1**−**8** from leaves and stem branches of *P. nitens* Tul. have been previously described by Regasini and co-workers.[11,17] The synthesis, purification, and identification of nitensidines AT (**9**) and AU (**10**) were previously reported by Tajima et al.[30]

Bacterial Strains. A standard *S. aureus* susceptibility testing reference strain (ATCC 25923) and a clinical MRSA isolate (XU212) bearing the TetK efflux pump were obtained from Dr. E. Udo.[25] Strain RN4220, which is resistant to the macrolide erythromycin, was provided by Dr. J. Cove.[24] EMRSA-15[26] and EMRSA-16[27] were provided by Dr. Paul Stapleton. Strain SA-1199B, which overexpresses the NorA MDR efflux pump, was the gift of Prof. Glenn W. Kaatz.[23]

Minimum Inhibitory Concentration. All of the strains were cultured on nutrient agar (Oxoid) and incubated for 24 h at 37 °C prior to MIC determination. An inoculum density of 1×10^6 cfu/mL of each *S. aureus* strain was prepared in normal saline (9 g/L) by comparison with a 0.5 MacFarland turbidity standard and appropriate dilution. Norfloxacin and the samples were dissolved in DMSO and diluted in cation-adjusted Mueller-Hinton broth (MHB) to give a starting concentration of 1024 μg/L. Using Nunc 96-well microtiter plates, 125 μL of MHB was dispensed into wells 1−11. Then, 125 μL of the test compound or the appropriate antibiotic was dispensed into well 1 and serially diluted across the plate, leaving well 11 empty for growth control. The final volume was dispensed into well 12, which was free of MHB or inoculum and served as the sterile control. Finally, the bacterial inoculum (125 μL) was added to wells 1−11, and the plate was incubated at 37 °C for 18 h. A DMSO control was also included. For MIC determination, 20 μL of a 5 mg/mL methanol solution of 3-[4,5-dimethylthiazol-2 yl]-2,5-diphenyltetrazolium bromide (MTT; Sigma) was added to each of the wells and incubated for 20 min. A color change from yellow to dark blue indicated bacterial growth. The MIC was recorded as the lowest concentration at which no growth was observed.[22] Norfloxacin was used as positive control and was purchased from Sigma Chemical Co. Mueller-Hinton broth (Oxoid) was adjusted to contain 20 mg/L Ca^{2+} and 10 mg/L Mg^{2+}.

Minimum Bactericidal Concentration. The samples were prepared using the same protocol that was employed for the MIC assays and were added to the same inoculum density of the SA-1199B strain. The 96-well plates were incubated at 37 °C for 24 h. After incubation 10 μL of each solution at different concentrations of the tested compound were transferred to Petri dishes containing the corresponding drug-free culture medium (Mueller-Hinton agar). The Petri plates were then incubated for a further 24 h. The MBC was obtained by observing the growth of colonies on Petri dishes after 24 h of incubation; an observed 99.9% reduction in bacterial cell numbers from the starting inoculum was considered as the bactericidal end point. MBC values equivalent to or exhibiting no more than a 2-fold difference from the MIC of the agent would indicate a bactericidal drug. An MBC value of 8-fold or higher than the MIC would indicate a bacteriostatic drug.

ASSOCIATED CONTENT

Supporting Information

The authors declare no competing financial interest. This material is available free of charge via the Internet at http://pubs.acs.org.

AUTHOR INFORMATION

Corresponding Authors

*(V. S. Bolzani) Tel: +55-16-3301-9660. Fax: +55-16-3322-2308. E-mail: bolzaniv@iq.unesp.br.

*(S. Gibbons) Tel: +44-207-7535913. Fax: +44-207-7535964. E-mail: simon.gibbons@ucl.ac.uk.

Notes

The authors declare no competing financial interest.

ACKNOWLEDGMENTS

This work was funded by grants 06/61187-7, 03/00886-7, and 2011/51313-3 from São Paulo Research Foundation (FAPESP), awarded to V.S.B., A.C., and L.O.R, as part of the Biota-FAPESP, the Biodiversity Virtual Institute Program (www.biotasp.org.br). We also acknowledge CNPq, CAPES, and FAPESP for researcher and student fellowships.

REFERENCES

(1) Amábile-Cuevas, C. F. *Am. Sci.* **2003**, *91*, 138−149.

(2) Gibbons, S. *Nat. Prod. Rep.* **2004**, *21*, 263−277.

(3) Saleem, M.; Nazir, M.; Ali, M. S.; Hussain, H.; Lee, Y. S.; Riaz, N.; Jabbar, A. *Nat. Prod. Rep.* **2010**, *27*, 238−254.

(4) Behal, V. *Folia Microbiol.* **2001**, *46*, 363−370.

(5) Stavri, M.; Piddock, L. J. V.; Gibbons, S. *J. Antimicrob. Chemother.* **2007**, *59*, 1247−1260.

(6) Smith, E. C.; Kaatz, G. W.; Seo, S. M.; Wareham, N.; Williamson, E. M.; Gibbons, S. *Antimicrob. Agents Chemother.* **2007**, *51*, 4480−4483.

(7) Myers, N.; Mittermeier, R. A.; Mittermeier, C. G.; Fonseca, G. A. B.; Kent, J. *Nature* **2000**, *403*, 853−858.

(8) http://nubbe.iq.unesp.br/portal/nubbedb.html, accessed in July 2014.

(9) Lorenzi, H. *Árvores Brasileiras: Manual de Identificação e Cultivo de Plantas Arbóreas do Brasil*; Plantarum: Nova Odessa, 1998; p 151.

(10) Crivos, M.; Martínez, M. R.; Pochettino, M. L.; Remorini, C.; Sy, A.; Teves, L. *J. Ethnobiol. Ethnomed.* **2007**, *3*, 1−12.

(11) Regasini, L. O.; Castro-Gamboa, I.; Silva, D. H. S.; Furlan, M.; Barreiro, E. J.; Ferreira, P. M. P.; Pessoa, C.; Lotufo, L. V. C.; Moraes, M. O.; Young, M. C. M.; Bolzani, V. S. *J. Nat. Prod.* **2009**, *72*, 473−476.

(12) Fernandes, D. C.; Regasini, L. O.; Vellosa, J. C. R.; Pauletti, P. M.; Castro-Gamboa, I.; Bolzani, V. S.; Oliveira, O. M. M.; Silva, D. H. S. *Chem. Pharm. Bull.* **2008**, *56*, 723−726.

(13) Regasini, L. O.; Fernandes, D. C.; Castro-Gamboa, I.; Silva, D. H. S.; Furlan, M.; Bolzani, V. S. *Quim. Nova* **2008**, *31*, 802−806.

(14) Regasini, L. O.; Vellosa, J. C. R.; Silva, D. H. S.; Furlan, M.; Oliveira, O. M. M.; Khalil, N. M.; Brunetti, I. L.; Young, M. C. M.; Barreiro, E. J.; Bolzani, V. S. *Phytochemistry* **2008**, *69*, 1739−1744.

(15) Regasini, L. O.; Vieira-Júnior, G. M.; Fernandes, D. C.; Bolzani, V. S.; Cavalheiro, A. J.; Silva, D. H. S. *J. Chil. Chem. Soc.* **2009**, *54*, 218−221.

(16) Bolzani, V. S.; Gunatilaka, A. A. L.; Kingston, D. G. I. *J. Nat. Prod.* **1995**, *58*, 1683−1688.

(17) Regasini, L. O.; Pivatto, M.; Scorzoni, L.; Benaducci, T.; Fusco-Almeida, A. M.; Giannini, M. J. S. M.; Barreiro, E. J.; Silva, D. H. S.; Bolzani, V. S. *Braz. J. Pharmacogn.* **2010**, *20*, 706−711.

(18) Regasini, L. O.; Oliveira, C. M.; Vellosa, J. C. R.; Oliveira, O. M. M. F.; Silva, D. H. S.; Bolzani, V. S. *Afr. J. Biotechnol.* **2008**, *7*, 4609−4613.

(19) Lopes, F. C. M.; Rocha, A.; Pirraco, A.; Regasini, L. O.; Silva, D. H. S.; Bolzani, V. S.; Azevedo, I.; Carlos, I. Z.; Soares, R. *BMC Complementary Altern. Med.* **2009**, *9*, 1−11.

(20) Duarte, R. A.; Mello, E. R.; Araki, C.; Bolzani, V. S.; Silva, D. H. S.; Regasini, L. O.; Silva, T. G. A.; Morais, M. C. C.; Ximenes, V. F.; Soares, C. P. *Tumor Biol.* **2010**, *31*, 513−522.

(21) Berlinck, R. G. S. *Nat. Prod. Rep.* **2002**, *19*, 617−649.

(22) Kaatz, G. W.; Seo, S. M.; Ruble, C. A. *Antimicrob. Agents Chemother.* **1993**, *37*, 1086−1094.

(23) Appendino, A.; Gibbons, S.; Giana, A.; Pagani, A.; Grassi, G.; Stavri, M.; Smith, E.; Rahman, M. *J. Nat. Prod.* **2008**, *71*, 1427−1430.

(24) Ross, J. I.; Farrell, A. M.; Eady, E. A.; Cove, J. H.; Cunliffe, W. J. *J. Antimicrob. Chemother.* **1989**, *24*, 851−862.

(25) Gibbons, S.; Udo, E. E. *Phytother. Res.* **2000**, *14*, 139−140.

(26) Richardson, J. F.; Reith, S. *J. Hosp. Infect.* **1993**, *25*, 45−52.

(27) Cox, R. A.; Conquest, C.; Mallaghan, C.; Maples, R. R. *J. Hosp. Infect.* **1995**, *29*, 87−106.

(28) Hensler, M. E.; Bernstein, G.; Nizet, V.; Nefzi, A. *Bioorg. Med. Chem. Lett.* **2006**, *16*, 5073−5079.

(29) Fair, R. J.; Hensler, M. E.; Thienphrapa, W.; Dam, Q. N.; Nizet, V.; Tor, Y. *ChemMedChem* **2012**, *7*, 1237−1244.

(30) Tajima, Y.; Nakagawa, H.; Tamura, A.; Kadioglu, O.; Satake, K.; Mitani, Y.; Murase, H.; Regasini, L. O.; Bolzani, V. S.; Ishikawa, T.; Fricker, G.; Efferth, T. *Phytomedicine* **2014**, *21*, 323−332.

JOURNAL OF NATURAL PRODUCTS

Note

pubs.acs.org/jnp

Biological Evaluation of Hyperforin and Its Hydrogenated Analogue on Bacterial Growth and Biofilm Production

Brigida Immacolata Pia Schiavone,[†] Antonio Rosato,[†] Muraglia Marilena,[†] Simon Gibbons,[‡] Ezio Bombardelli,[§] Luisella Verotta,*[,⊥] Carlo Franchini,[†] and Filomena Corbo[†]

[†]Department of Pharmacy, University of Bari "Aldo Moro", 70124 Bari, Italy

[‡]Department of Pharmaceutical and Biological Chemistry, UCL School of Pharmacy, London WC1N 1AX, U.K.

[§]Indena SpA, 20139 Milan, Italy

[⊥]Department of Chemistry, University of Milan, 20133 Milan, Italy

ABSTRACT: Bacterial biofilms are organized communities of microorganisms, embedded in a self-produced matrix, growing on a biotic surface and resistant to many antimicrobial agents when associated with a medical device. These biofilms require the development of new strategies for the prevention and treatment of infectious disease, including the potential use of natural products. One interesting natural product example is *Hypericum*, a plant genus that contains species known to have antimicrobial properties. The major constituent of *Hypericum perforatum* is an unstable compound named hyperforin (**1**); for this reason it was not believed to play a significant role in the pharmacological effects. In this investigation a hydrogenated hyperforin analogue (**2**) was tested on several ATCC and clinical isolate strains, in their planktonic and biofilm form (*Staphylococcus aureus*, MRSA, and *Enterococcus faecalis*). Compound **2** was effective against planktonic and biofilm cultures, probably due to higher stability, showing the percentage of cells killed in the range from 45% to 52%. These results are noteworthy from the point of view of future development of these polyprenylated phloroglucinols as potential antibiotics.

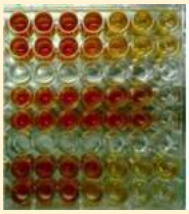

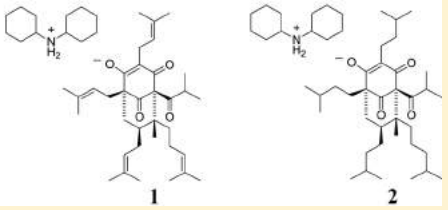

Despite significant progress made in microbiology and the control of microorganisms, sporadic incidents of epidemics due to drug-resistant microorganisms represent an enormous threat to global public health. In recent years, the use of medical implants such as catheters, pacemakers, prosthetic heart valves, and joint replacements has increased dramatically. These devices can become colonized by microorganisms that form a biofilm consisting of a mono- or multilayer of cells embedded within a matrix of extracellular polymeric material.[1−7] Release of microorganisms from the biofilm may initiate an acute disseminated infection. Implant-associated infections are difficult to resolve, because biofilm microorganisms are resistant to both host defense mechanisms and antibiotic therapy.[1,2,6] Bacterial biofilms have received increasing attention over the past decade,[1,7] and a number of model systems have been devised for studying the colonization of various solid surfaces by bacteria. In vitro investigations with pathogenic bacteria have shown that biofilm bacteria have a substantially reduced sensitivity to clinically important antibiotics compared with cells of the same organism in the dispersed form.[2] Although the majority of implant infections are caused by Gram-positive bacteria, notably staphylococci, infections due to Gram-negative bacteria and fungi tend to be more serious.[3] New drugs are needed to combat these pathogens. Antimicrobial compounds of plant origin have enormous therapeutic potential, not only because they mitigate infectious diseases but since they may also lack adverse side effects associated with antimicrobial agents. One interesting example is *Hypericum*, a plant genus that biosynthesizes secondary metabolites known to have antimicrobial properties.[8]

St. John's Wort (*Hypericum perforatum* L.) (Hypericaceae) extracts have been used in European folk medicine for centuries in a variety of indications, including skin injuries and burns. A petroleum ether extract of the aerial parts of *H. perforatum* was reported to be active against Gram-positive bacteria.[9] A major constituent of lipophilic extracts of *H. perforatum* is the prenylated acylphloroglucinol hyperforin, accompanied by 10% of its homologue adhyperforin and a number of oxidized acylphloroglucinols derived from the parent compounds.[10] In fact, hyperforin is unstable, in particular when exposed to light and air since the enolized β-dicarbonyl system and the prenyl groups are involved readily in oxidative reactions.[10,11] For this reason, hyperforin was not believed to play a significant role in the pharmacological effects of the extracts. However, it was recently shown that the extraction of the plant material under controlled conditions results in extracts containing 1−5% hyperforin, which can be maintained, if appropriately stored, for prolonged periods.[12] An *H. perforatum* extract obtained by supercritical extraction of the dried herb with carbon dioxide contains a much higher proportion of hyperforin (more than 20%), which does not deteriorate even after prolonged storage. From such an extract, pure hyperforin can be isolated through

Received: May 16, 2013
Published: August 27, 2013

previous treatment with dicyclohexylamine and crystallization of the dicyclohexylamonium salt (DCHA) salt (**1**). In this salt form, hyperforin demonstrates good stability so that biological assays can be readily performed. Additionally, a slight increase in water solubility is also observed.[13−16a,b]

Hyperforin can be hydrogenated in quantitative yields to give the corresponding octahydro derivative (**2**). This shows an increase in lipophilicity and a considerably higher stability due to the absence of the double bonds.

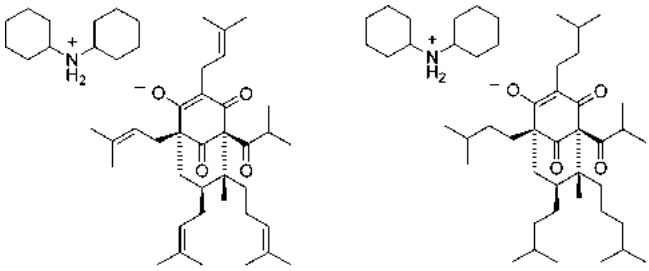

1 **2**

Compounds **1** and **2** were tested for inhibition of bacterial growth and biofilm formation against a panel of clinically relevant pathogens, comprising the American Type Culture Collection (ATCC) strains *Staphylococcus aureus* ATCC 29213, methicillin-resistant *Staphylococcus aureus* ATCC 43300 (MRSA), *Enterococcus faecalis* ATCC 29212, and *Escherichia coli* ATCC 25922, and a clinical isolate of methicillin-resistant *Staphylococcus aureus* (*Staphylococcus aureus* Ig5). Growth inhibitory properties against planktonic strains were tested for the ability to prevent biofilm formation. Minimum biofilm inhibitory concentration (MBIC), which represents the lowest concentration of an antimicrobial agent resulting in no detectable biofilm growth, was determined against biofilms formed on 96-well microtiter plates using the XTT reduction assay. Reduction of the tetrazolium salt (XTT) is a commonly used method for determining microbial cell viability. It measures metabolic activity and requires the addition of an electron coupling reagent. The viability of all strains was decreased by octahydrohyperforin DCHA salt (**2**) in the biofilm assay compared to the untreated control. Interestingly, for hyperforin DCHA salt (**1**) there was no significant difference in the reduction of XTT in biofilm cells.

Compounds **1** and **2** demonstrated antimicrobial activity against the Gram-positive bacteria tested (*S. aureus*, MRSA, *E. faecalis*), but not against the Gram-negative bacterium (*E. coli*), in agreement with previous studies.[17] The minimum inhibitory concentration (MIC) was defined as the lowest concentration of antimicrobial agent that inhibited visible bacterial growth after overnight incubation. The MIC values of **2** were 4-fold higher than those for **1** for all sensitive strains tested, as reported in Table 1. The MIC values obtained for **1** were comparable to the results obtained by other investigators.[17] Five percent (v/v) DMSO and ethanol were used in the dilution of the drugs and did not show any antimicrobial activity against the planktonic bacteria (data not shown). Each experiment was performed in triplicate.

Antimicrobial activity testing for biofilm was evaluated in a 96-well plate assay, as described above, and the results are shown in Table 2 and in Figures 1 and 2. The converted amount of XTT is a measure of the metabolic activity of the microorganisms in the biofilm. In Table 2, the efficacy of compounds **1** and **2** is expressed as a percentage reduction of

Table 1. Minimum Inhibitory Concentration (MIC) Results of Compounds 1 and 2 and Norfloxacin (Nor) against Bacterial Strains Tested in Suspension

	MIC (μg/mL)		
bacterial strain	**1**	**2**	Nor
S. aureus ATCC 29213	1	4	2
S. aureus ATCC 25923	1	4	2
S. aureus ATCC 43300	1	4	4
S. aureus EMRSA-15	2		0.5
S. aureus SA1199B	2	4	32
S. aureus XU212	0.5	1	4
S. aureus RN4220		1	1
S. aureus Ig5	1	4	2
E. faecalis ATCC 29212	1	4	4
E. coli ATCC 25922	R[a]	R[a]	0.12

[a]R = resistant.

Table 2. Minimum Biofilm Inhibitory Concentration (MBIC) Results in μg/mL and Percentage Reduction of Microbial Cell Viability of Octahydrohyperforin DCHA and Hyperforin DCHA against Bacterial Strains Tested in Biofilms

	1		**2**	
	MBIC		MBIC	
bacterial strain	μg/mL	%	μg/mL	%
S. aureus ATCC 29213	25	45	150	52
S. aureus ATCC 43300	25	21	37.5	47
E. faecalis ATCC 29212	25	34	37.5	45
S. aureus Ig5	25	33	37.5	52

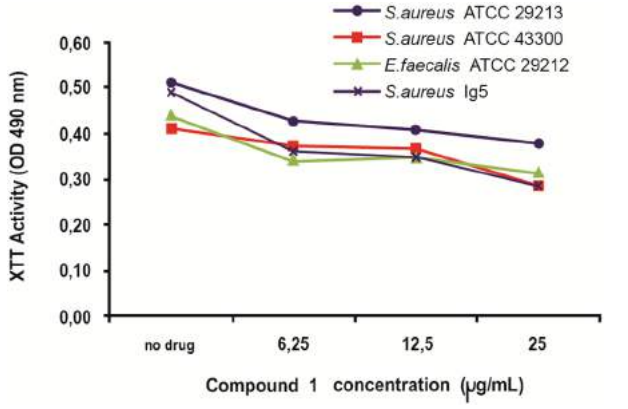

Figure 1. Metabolic activities of biofilms exposed to different concentrations of compound **1**. Metabolic activity is expressed as the optical density of treated biofilms compared to that for untreated biofilms (control).

the microorganisms in the biofilm as compared to an untreated biofilm. In this assay, PEG-200 was used as alternative solvent for **2** to promote its passage through the matrix of the biofilm. The results showed that for strains *S. aureus* ATCC 29213 and *E. faecalis* ATCC 29212 a percentage reduction of 52% at 150 μg/mL and a percentage reduction of 45% at 37.5 μg/mL were observed. *S. aureus* ATCC 43300 showed a reduction of 47% at 37.5 μg/mL, and the isolated strain *S. aureus* Ig5 (MRSA) was reduced to 45% at 150 μg/mL. Despite the fact that *S. aureus* Ig5 (a clinical isolate of MRSA) and *S. aureus* ATCC 43300 (MRSA) showed the same MIC value of 4 μg/mL, their MBIC

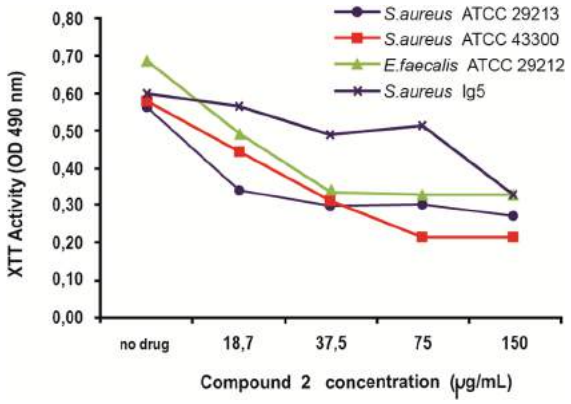

Figure 2. Metabolic activities of biofilms exposed to different concentrations of compound **2**. Metabolic activity is expressed as the optical density of treated biofilms compared to that for untreated biofilms (control).

values were different. To obtain the same percentage reduction for *S. aureus* Ig5, it was necessary to increase the concentration of **2** four times. These results clearly showed that clinical isolates, such as *S. aureus* Ig5, are less sensitive compared to their ATCC counterpart strains.

Compound **1**, at the highest test concentration used of 25 μg/mL, showed moderate activity for *S. aureus* ATCC 29213, with a 45% reduction, and demonstrated low activity for the other strains, with the lowest percentage reduction being 50%. The MIC values of **1** and **2** were similar and in the range 0.5−4 μg/mL (Table 1). Notably, the reduction of the prenyl side chains of hyperforin gave only a moderate increase in MIC and only a slight reduction of biological activity, which is somewhat surprising given the difference in chemical reactivity between the two compounds. Of clinical interest, both compounds displayed good potency against the tetracycline-resistant *S. aureus* strain (XU212), which is also a MRSA strain.

The direct antibacterial activities of compounds **1** and **2** are noteworthy, particularly given that they were found active toward multidrug-effluxing and MRSA strains at low MIC values (Table 1). Once stability issues are resolved, it is entirely plausible that these agents could be formulated into topical products to facilitate in the decolonization of mupirocin- or fusidic acid-resistant MRSA strains, which continues to be a pressing clinical issue.

The activities of **1** and **2** against biofilms also may be advantageous. Biofilms are especially problematic since they exhibit increased resistance to antibiotics. Using a variety of mechanisms, bacteria in biofilms can be 10 to 1000 times more resistant than their planktonic counterparts.[18] Along with the reduced antibiotic penetration in biofilms, these exopolysaccharide structures limit oxygen and nutrient diffusion and allow for the development of persister cells within the matrix, which results in slow- or nongrowing bacteria that reduce the antibacterial effects of many antibiotics.[19] Due to the high failure rate of commonly used antibiotics, it is reasonable to consider alternative treatments, and this study offers evidence that a natural compound can be a feasible candidate.

The aim of this study was to assess the antimicrobial efficacy of **1** and **2** against common microorganisms involved in infectious diseases and to determine the antimicrobial activity against planktonic and biofilm cells. In fact, previous investigations have demonstrated the efficacy of *Hypericum* constituents against *S. aureus* ATCC and MRSA biofilms.[20] In the present study, the XTT assay was performed to evaluate biofilm formation by four strains. The XTT assay indirectly measures microbial activity; it is reduced by dehydrogenase enzymes, present in the electron transport system, to a water-soluble formazan dye. The XTT assay shows an excellent correlation with other biofilm susceptibility methods, such as the AlamarBlue assay and viable counts, and offers the benefits of simplicity, relative cost, compatibility, and, most importantly, high reproducibility and a lack of toxicity.

As shown in Table 3, compound **1** was more effective against planktonic cells compared to **2**, with the MIC value of **1** being

Table 3. Minimum Inhibitory Concentration (MIC) Results in μg/mL against Bacterial Strains in Suspension and Minimum Biofilm Inhibitory Concentration (MBIC) Results in μg/mL and Percentage Reduction of Microbial Cell Viability of Compounds 1 and 2 against Bacterial Strains Tested in Biofilms

	1			2		
	MIC	MBIC		MIC	MBIC	
bacterial strain	μg/mL	μg/mL	%	μg/mL	μg/mL	%
S. aureus ATCC 29213	1	25	45	4	150	52
S. aureus ATCC 43300	1	25	21	4	37.5	47
E. faecalis ATCC 29212	1	25	34	4	37.5	45
S. aureus Ig5	1	25	33	4	37.5	52
E. coli ATCC 25922	R[a]			R		

[a]R = resistant.

4-fold greater than that of **2**. In clinical terms, **1** may have use for the treatment of Gram-positive bacterial infections, but it showed only weak utility to treat biofilm-associated infections. When cells were grown as surface-attached biofilms in order to mimic a device-related infection, **1** lacked the ability to inhibit cells within the biofilms. This may suggest that this agent, although effective against bacteria in suspension, for example in bloodstream infections, may not be the most suitable substance for treating biofilm-mediated device-related infections. These observations are probably related to the facile degradation of hyperforin in oxygenated conditions and correlate with insights made in the traditional uses of *Hypericum* to treat topical infections.

Compound **2** was effective against planktonic and biofilm cultures, probably due to its higher stability than **1**. In biofilms treated with **2**, the percentage of cells killed ranged from 45% to 52%. The obtained results suggested that this compound may be used in the development of an antibiofilm drug. This is noteworthy from the point of view of the potential development of polyprenylated phloroglucinols as antibiotics. Octahydrohyperforin **2** is readily obtainable by hydrogenation of a crude *H. perforatum* lipophilic extract without the need to isolate the parent compound (hyperforin, **1**). The stability of octahydrohyperforin to oxygen, light, and temperature also indicates that this agent could have topical utility.

EXPERIMENTAL SECTION

Test Compounds. Hyperforin DCHA (**1**) was a generous gift from Indena SpA, Milan, Italy. Octahydrohyperforin DCHA (**2**) was obtained from **1** as reported in L. Verotta et al.[21] Compound purity was >95% (Indena Drug Master File).

Bacterial Strains and Culture Conditions. The bacteria used in this study were *Staphylococcus aureus* ATCC 29213, *Staphylococcus*

aureus ATCC 43300, *Enterococcus faecalis* ATCC 29212, and *Staphylococcus aureus* Ig5 (clinical MRSA isolate). A standard *S. aureus* strain (ATCC 25923) and a clinical isolate (XU212), which possesses the TetK efflux pump and is also a MRSA strain, were obtained from Dr. E. Udo.[22] Strain RN4220, which has the MsrA macrolide efflux pump, was provided by Dr. J. H. Cove.[23] EMRSA-15[24] was obtained from Dr. P. Stapleton, UCL School of Pharmacy. Strain SA1199B, which overexpresses the NorA MDR efflux pump, was a gift of Professor G. W. Kaatz.[25] Norfloxacin was obtained from Sigma Chemical Co. Mueller-Hinton broth (MHB; Oxoid) was adjusted to contain 20 mg/L Ca^{2+} and 10 mg/L Mg^{2+}. All the strains were stored at −70 °C in nutrient broth (Muller-Hinton II broth, MHBII, Becton Dickinson, France) containing 15% glycerol, until used. Cultures were grown on MHBII from 100 μL of frozen culture and incubated aerobically for approximately 4 h at 37 °C.

Antibacterial Agents. Compound **1** was freshly prepared in dimethyl sulfoxide (DMSO) and diluted in CaMHB before use, and **2** was dissolved in absolute ethanol for planktonic susceptibility tests and in sterile polyethylene glycol-200 for biofilm susceptibility tests.

Planktonic Susceptibility Testing. The minimum inhibitory concentration was determined for each strain in planktonic culture according to the Clinical and Laboratory Standards Institute (CLSI, M7-A6, 2003) as previously reported.[26] Serial 2-fold dilutions of **1** and **2** were prepared in 96-well microtiter plates with concentrations ranging, respectively, from 16 to 0.25 μg/mL and from 256 to 0.25 μg/mL. CaMHB was used to perform all dilutions. To ensure that the solvents themselves had no antibacterial activity, a control test was carried out by using them at their maximum concentration in the medium. *S. aureus* ATCC 25953 was included as a control strain in each test, and all results were within the published data.[17] All MIC tests were performed in triplicate.

Minimum Inhibitory Concentration Assay Determination. Overnight cultures of each strain were made up in 0.9% saline to an inoculum density of 5×10^5 colony-forming units (cfu) by comparison with a MacFarland standard. Norfloxacin was dissolved in DMSO and then diluted in MHB to give a starting concentration of 512 μg/mL. Using Nunc 96-well microtiter plates, 125 μL of MHB was dispensed into wells 1−11. Then, 125 μL of the test compound or the appropriate antibiotic was dispensed into well 1 and serially diluted across the plate, leaving well 11 empty for the growth control. The final volume was dispensed into well 12, which being free of MHB or inoculum served as the sterile control. Finally, the bacterial inoculum (125 μL) was added to wells 1−11, and the plate was incubated at 37 °C for 18 h. A DMSO control (3.125%) was also included. All MICs were determined in duplicate. The MIC was determined as the lowest concentration at which no growth was observed. A methanol solution (5 mg/mL) of 3-[4,5-dimethylthiazol-2-yl]-2,5-diphenyltetrazoliium bromide (MTT; Lancaster, UK) was used to detect bacterial growth by a color change from yellow to blue.

Culturing of Biofilms. Biofilms were developed according to the method of Stepanović et al.,[27] with some minor modifications. Strains were streaked from frozen cultures and grown overnight at 37 °C on a Tryptic soy agar plate with 2% glucose.[27] A number of colonies were suspended in Tryptic soy broth (TSB, Merck KGaA, Germany) with 2% glucose to a density of approximately 10^5 cfu/mL. Briefly, 200 μL of each bacterial suspension was transferred in a 96-well, flat-bottom, tissue culture-treated microtiter plate (IWAKI, Tokio, Japan), to promote biofilm formation; the plates were incubated aerobically on a horizontal shaker for 4 h at 37 °C. After the suspension was gently drawn off and replaced by sterile medium, the plate was incubated for 24 h at 37 °C to obtain mature biofilms.[28] Each strain was tested in triplicate.

Treatment with Antimicrobial Compound. Following incubation, the plate was rinsed twice with phosphate-buffered saline (PBS) to remove loosely attached planktonic cells, and a serial dilution of the antimicrobial compound was added to each well. TSB with 2% glucose was used to perform all dilutions. Compound **1** was tested at a concentration ranging from 150 to 18.7 μg/mL, while **2** was evaluated from 25 to 6.25 μg/mL. Biofilms were incubated for 18 h at 37 °C on a horizontal shaker, and control antibiotic-free biofilms were included in each experiment.

Quantification of Viable Cells in a Biofilm Using the XTT Assay. The XTT assay was used to quantify the number of viable cells in each of the wells following antimicrobial compound treatment in comparison with biofilms formed in the presence of TSB (control). This method has been used extensively for the quantification of viable bacterial cells in a biofilm.[29] It measures the reduction of a tetrazolium salt (2,3-bis[2-methoxyloxy-4-nitro-5-sulfophenyl]-2*H*-tetrazolium-5-carboxanilide, Sigma-Aldrich, St. Louis, MO, USA) by metabolically active cells to a colored, water-soluble formazan derivative that can be easily quantified colorimetrically. Briefly, an XTT solution (1 mg/mL) was prepared in PBS and sterilized through a 0.22 μm pore size filter. Menadione solution (Fluka, Newport News, VA, USA) (0.4 mM) was prepared in DMSO before each assay. Following antimicrobial compound exposure, the plate was rinsed with PBS to remove loosely attached cells and dried in an inverted position at 37 °C for 20 min, and then 180 μL of PBS and 20 μL of the XTT−menadione solution (12.5 times the volume of the XTT solution was mixed with 1 volume of the menadione solution) were added to each well. The plate was incubated for 2 h at 37 °C on a horizontal shaker in the dark.[30] Reduction of XTT (oxidative activity) was then measured at 492 nm using a Perkin-Elmer Wallac Victor3 microplate reader.

AUTHOR INFORMATION

Corresponding Author

*E-mail: luisella.verotta@unimi.it. Tel: (+39) 0250314114. Fax: (+39) 0250314106.

Notes

The authors declare no competing financial interest.

REFERENCES

(1) Characklis, W. G.; Wilderer, P. A. *Structure and Function of Biofilms*; Wiley: Chichester, UK, 1989.

(2) Costerton, J. W.; Cheng, K. J.; Geesey, G. G.; Ladd, T. I.; Nickel, J. C.; Dasgupta, M.; Marrie, T. J. *Annu. Rev. Microbiol.* **1987**, *41*, 435−464.

(3) Dougherty, S. H. *Rev. Infect. Dis.* **1988**, *10*, 1102−1117.

(4) Elliott, T. S. J. *J. Med. Microbiol.* **1988**, *27*, 161−167.

(5) Goldmann, D. A.; Pier, G. B. *Clin. Microbiol. Rev.* **1993**, *6*, 176−192.

(6) Gristina, A. G. *Science* **1987**, *237*, 1588−1595.

(7) Melo, L. F.; Bott, T. R.; Fletcher, M.; Capdeville, B. *Biofilms - Science and Technology*; Kluwer Academic Publishers: Dordrecht, The Netherlands, 1992.

(8) Saddiqe, Z.; Naeem, I.; Mimoona, A. *J. Ethnopharmacol.* **2010**, *131*, 511−521.

(9) Reichling, L. J.; Weseler, A.; Saller, R. *Pharmacopsychiatry* **2001**, *34* (Suppl. 1), S116−S118.

(10) Verotta, L. *Curr. Top. Med. Chem.* **2003**, *3*, 187−201.

(11) Wolfender, J. L.; Verotta, L.; Belvisi, L.; Fuzzati, N.; Hostettmann, K. *Phytochem. Anal.* **2003**, *14*, 290−297.

(12) Chatterjee, S. S.; Noldner, M.; Koch, E.; Erdelmeier, C. *Pharmacopsychiatry* **1998**, *31* (Suppl. 1), 7−15.

(13) Maisenbacher, P.; Kovar, K. A. *Planta Med.* **1992**, *58*, 351−354.

(14) Orth, H. C. J.; Rentel, C.; Schmidt, P. C. *J. Pharm. Pharmacol.* **1999**, *51*, 193−200.

(15) Orth, H. C. J.; Schmidt, P. C. *Pharm. Ind.* **2000**, *62*, 60−63.

(16) (a) Orth, H. C. J.; Hauer, H.; Erdelmeier, C. A. J.; Schmidt, P. C. *Pharmazie* **1999**, *54*, 76−77. (b) Verotta, L.; Appendino, G.; Belloro, E.; Jakupovic, J.; Bombardelli, E. *J. Nat. Prod.* **1999**, *62*, 770−772.

(17) Gibbons, S. *Nat. Prod. Rep.* **2004**, *21*, 263−277.

(18) Olson, K. M.; Starks, C. M.; Williams, R. B.; O'Neil-Johnson, M.; Huang, Z.; Ellis, M.; Reilly, J. E.; Eldridge, G. R. *Antimicrob. Agents Chemother.* **2011**, *55*, 3691−3695.

(19) Rose, W. E.; Poppens, P. T. *J. Antimicrob. Chemother.* **2009**, *63*, 485−488.

(20) Sarkisian, A. A.; Janssen, M. J.; Matta, H.; Henry, G. E.; LaPlante, K. L.; Rowley, D. C. *Phytother. Res.* **2012**, *26*, 1012−1016.
(21) Verotta, L.; Appendino, G.; Bombardelli, E.; Brun, R. *Bioorg. Med. Chem. Lett.* **2007**, *17*, 1544−1548.
(22) Gibbons, S.; Udo, E. E. *Phytother. Res* **2000**, *14*, 139−140.
(23) Ross, J. I.; Farrell, A. M.; Eady, E. A.; Cove, J. H.; Cunliffe, W. J. *J. Antimicrob. Chemother.* **1989**, *24*, 851−862.
(24) Richardson, J. F.; Reith, S. *J. Hosp. Infect.* **1993**, *25*, 45−52.
(25) Kaatz, G. W.; Seo, S. M.; Ruble, C. A. *Antimicrob. Agents Chemother.* **1993**, *37*, 1086−1094.
(26) (a) Armenise, D.; Muraglia, M.; Florio, M. A.; De Laurentis, N.; Rosato, A.; Carrieri, A.; Corbo, F.; Franchini, C. *Arch. Pharm. Chem. Life Sci.* **2012**, *345*, 407−416. (b) Catalano, A.; Carocci, A.; Defrenza, I.; Muraglia, M.; Carrieri, A.; Van Bambeke, F.; Rosato, A.; Corbo, F.; Franchini, C. *Eur. J. Med. Chem.* **2013**, in press.
(27) Stepanović, S.; Vukovic, D.; Hola, V.; Di Bonaventura, G.; Djukic, S.; Irkovic, I. C.; Ruzicka, F. *APMIS* **2007**, *115*, 891−899.
(28) Hübner, N. O.; Matthes, R.; Koban, I.; Rändler, C.; Müller, G.; Bender, C.; Kindel, E.; Kocher, T.; Kramer, A. *Skin Pharmacol. Physiol.* **2010**, *23* (Suppl. 1), 28−34.
(29) Pettit, R. K.; Weber, C. A.; Kean, M. J.; Hoffmann, H.; Pettit, G. R.; Tan, R.; Franks, K. S.; Horton, M. L. *Antimicrob. Agents Chemother.* **2005**, *49*, 2612−2617.
(30) Chaieb, K.; Zmantar, T.; Souiden, Y.; Mahdouani, K.; Bakhrouf, A. *Microb. Pathogen.* **2011**, *50*, 1−5.

PHYTOTHERAPY RESEARCH
Phytother. Res. **28**: 784–787 (2014)
Published online 22 August 2013 in Wiley Online Library
(wileyonlinelibrary.com) **DOI**: 10.1002/ptr.5053

SHORT COMMUNICATION

Flavonoid glycosides from the stem bark of *Margaritaria discoidea* demonstrate antibacterial and free radical scavenging activities

Edmund Ekuadzi,[1] Rita Dickson,[1] Theophilus Fleischer,[2] Kofi Annan,[2] Dominik Pistorius,[3] Lukas Oberer[4] and Simon Gibbons[5]*

[1]Department of Pharmacognosy, Faculty of Pharmacy and Pharmaceutical Sciences, College of Health Sciences, Kwame Nkrumah University of Science and Technology, Kumasi, Ghana
[2]Department of Herbal Medicine, Faculty of Pharmacy and Pharmaceutical Sciences, College of Health Sciences, Kwame Nkrumah University of Science and Technology, Kumasi, Ghana
[3]Natural Product Unit, Novartis Institutes for Biomedical Research, Basel 4056, Switzerland
[4]Analytical Sciences, Novartis Institutes for BioMedical Research, Basel 4056, Switzerland
[5]Department of Biological and Pharmaceutical Chemistry, UCL School of Pharmacy, 29-39 Brunswick Square, London WC1N 1AX, UK

One new flavonoid glycoside, along with three known flavonoid glycosides were isolated from the stem bark of *Margaritaria discoidea*, which is traditionally used in the management of wounds and skin infections in Ghana. The new flavonoid glycoside was elucidated as hydroxygenkwanin-8-*C*-[α-rhamnopyranosyl-(1 → 6)]-β-glucopyranoside (1) on the basis of spectroscopic analysis. The isolated compounds demonstrated free-radical scavenging as well as some level of antibacterial activities. Microorganisms including *Staphylococcus aureus* are implicated in inhibiting or delaying wound healing. Therefore, any agent capable of reducing or eliminating the microbial load present in a wound as well as decreasing the levels of reactive oxygen species may facilitate the healing process. These findings therefore provide some support to the ethnopharmacological usage of the plant in the management of wounds. Copyright © 2013 John Wiley & Sons, Ltd.

Keywords: Margaritaria discoidea; flavonoid glycosides; margadiscoside; fagovatin; antibacterial activities; antioxidant activities.

INTRODUCTION

Margaritaria discoidea (Baill.) G.L. Webster (Euphorbiaceae), previously referred to as *Phyllanthus discoideus*, is a tree that finds use in ethnomedicine as a treatment against wounds and infectious skin diseases (Abbiw, 1990; Irvine, 1961). Earlier phytochemical investigations have shown the presence of eight *Securinega* alkaloids (Fehler, 2000; Mensah *et al*., 1988; Weenen *et al*., 1990) and betulinic acid (Calixto *et al*., 1998). In an earlier work, we reported the antibacterial, antioxidant and anti-inflammatory activities of the 70% ethanol extract of the *M. discoidea* leaves and stem bark (Dickson *et al*., 2010). Here, we identify and characterize the compounds that may be contributing to the biological activities observed in our earlier study. The isolation, structure elucidation, antioxidant and antibacterial activities of one new flavone glycoside (**1**) along with three known flavonoid glycosides (**2**, **3** and **4**) are reported herein for the first time in this species. The structure of compound **1** was established using NMR spectroscopy, IR, UV and MS data (Fig. 1).

Extracts of *Margaritaria discoidea* are well known as wound healing remedies in Ghana. The presence of these compounds may contribute in part to the wound healing benefits derived from the plant when used traditionally.

* Correspondence to: Professor Simon Gibbons, Department of Biological and Pharmaceutical Chemistry, UCL School of Pharmacy, 29–39 Brunswick Square, London WC1N 1AX, UK.
Email: simon.gibbons@ucl.ac.uk

MATERIALS AND METHODS

General experimental procedures. NMR spectra were recorded on a Bruker AV-III-600 spectrometer equipped with a 1.7 mm TXI cryoprobe. The mass spectra were performed by ESI in positive-ion mode using an LTQ Orbitrap XL mass spectrometer (ThermoScientific). IR spectra were measured as a solid film with a Bruker Hyperion 2000 FTIR microscope connected to a Vertex 70 spectrometer. Flash chromatography was carried out on RediSep R_f normal phase disposable columns. Prep LC/MS was carried out on an Agilent Technologies 1200 series Chromatograph fitted with an Agilent 1100 series LC/MSD quadrupole mass spectrometer.

Plant material. The stem bark of *M. discoidea* was collected from Kente in the Amansie Central District in June 2009. A voucher specimen (KNUST/HM1/2010/S003) has been deposited at the Department of Pharmacognosy Herbarium.

Extraction and isolation of compounds. The dried powdered stem bark (2.5 kg) was successively Soxhlet-extracted using petroleum ether (50.50 g), EtOAc (208.75 g) and 70% EtOH (386.25 g). The resulting extracts were evaporated on a rotary evaporator under reduced pressure at a temperature of less than 40 °C. 20 g of the 70% EtOH extract was

Received 26 March 2013
Revised 06 June 2013
Accepted 08 July 2013

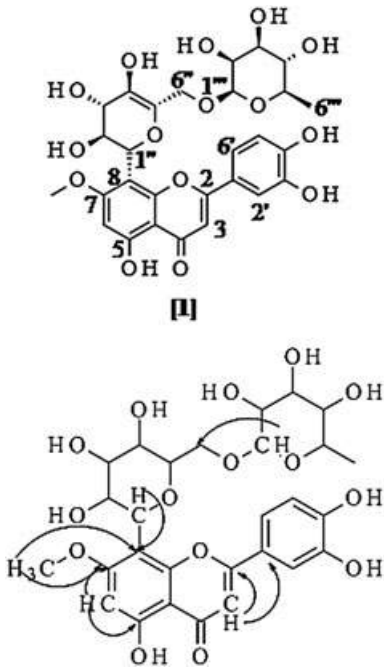

Figure 1. Selected COSY (bold faced bonds) and HMBC (arrows) correlations of compound **1**.

Table 1. Antibacterial activity of isolated compounds

	MIC (μg/mL)			
Microorganisms	**1**	**2**	**3**	**4**
Gram-positive				
Bacillus subtilis NCTC 10073	500	500	>500	>500
Staphylococcus aureus ATCC 25923	500	500	>500	>500
Gram-negative				
Proteus vulgaris NCTC 4635	500	500	500	500
Pseudomonas aeruginosa ATCC 27853	500	500	>500	>500

All experiments were carried out in triplicates. MIC readings for all wells were the same. 200 μg/mL of amoxicillin served as positive control. MIC readings for all wells of the same compound were identical.

Table 2. IC50 values (μg/mL) for free radical scavenging activity of the isolated compounds

Compounds	IC_{50} DPPH (μg/mL)
1	17.45
2	20.34
3	68.94
4	24.88
n-Propyl gallate	7.983

All experiments were carried out in triplicates. *n*-Propylgallate served as positive control.

subjected to silica gel Flash Chromatography (≤4 bar) using a ternary gradient consisting of C_6H_{14}, EtOAc and MeOH starting with nonpolar conditions and gradually of increasing polarities to yield fractions A (0.07 g), B (1.06 g), C (3.72 g), D (2.89 g) and E (3.66 g). Fraction D was subjected to prep-LC/MS using a SunFire C-18 Optimal Bed Density column (150 × 30 mm; 5 μm particle diameter; Waters) with a flow rate of 60 mL/min and a mobile phase of H_2O and MeCN, each containing 0.1% HCOOH, with a linear gradient from 10% to 30% MeCN in 15 min to yield fractions D1 (58.20 mg), D2 (18.05 mg) and D3 (9.30 mg). Fraction D3 afforded pure compound **2** (9.30 mg; 0.0072%w/w). Further fractionation of D1 and D2 on a Luna Phenyl-Hexyl column (150 × 21 mm; 5 μm particle diameter; Phenomenex) with a flow rate of 24 mL/min and a mobile phase of H_2O and MeCN, each containing 0.1% HCOOH, with a linear gradient from 15% to 40% MeCN in 15 min yielded compounds **3** (7.50 mg; 0.0058%w/w), **4** (7.88 mg; 0.0061%w/w) and **1** (1.42 mg; 0.0011% w/w), respectively.

Bioactivity of isolated compounds. *Broth microdilution assay.* Minimal inhibitory concentration values of the compounds were determined based on a broth micro-well dilution method (Eloff, 1998). The iocula of microorganisms were prepared from 12-h broth cultures, and serial dilutions were made to achieve a suspension of approximately 10^5 CFU/mL. Growth of the microorganisms was determined by adding 20 μL of a 5% solution of tetrazolium salt and incubating for a further 30 minutes. Amoxycillin was included as the positive control. All experiments were carried out in triplicate.

Free radical scavenging activity (DPPH method). The isolated compounds were compared to *n*-propyl gallate (in methanol), and the DPPH method (Blois, 1958) was used. A 20 mg/L solution of DPPH in methanol was prepared, and 3 mL of this solution was added to 1 mL each of the test compounds at 1, 0.5, 0.1 and 0.05 mg/mL in methanol. After 3 min, the absorbance was measured at 517 nm using a T90+ UV/VIS Spectrometer (PG Instruments Limited). 1 mL of methanol was added to 3.0 mL DPPH solution which served as a negative control. All experiments were carried out in triplicate. Inhibition of radical scavenging was calculated according to the following equation:

$$\%\ \text{DPPH scavenging activity} = [(A_0 - A_1)/A_0] \times 100$$

with A_0 being the absorbance of the control, and A_1, the absorbance in the presence of the test sample. Data were presented as % DPPH scavenging effect against concentration and the IC_{50} determined.

RESULTS AND DISCUSSION

Compound **1** was obtained as a yellow amorphous solid. Its IR spectrum exhibited absorption bands for an α, β-unsaturated ketonic functional group (1652 and 1607 cm^{-1}) and hydroxyl groups (3381 cm^{-1}). The UV spectrum of **1** in methanol displayed two major absorption peaks at 245.4 (with a shoulder) and 346.2 nm +indicative of a flavone natural product with

Table 3. 1H and 13C NMR chemical shifts of compounds 1 and 2 (in DMSO-d6, 600 MHz)

	1		2	
Carbon no.	Chemical shifts (ppm) ^{1}H NMR	Chemical shifts (ppm) ^{13}C NMR	Chemical shifts (ppm) ^{1}H NMR	Chemical shifts (ppm) ^{13}C NMR
2	-	164.3; 164.1	-	165.5; 164.0
3	6.70	102.5	6.88 (*s*); 6.86 (*s*)	103.4
4	-	182.0; 181.7	-	182.5; 182.0
5	-	160.3; 159.5	-	159.5; 160.5
6	6.78; 6.80	91.0; 90.1	-	110.0
7	-	164.8; 163.6	-	165.3; 164.0
8	-	109.5; 109.4	6.85 (*s*); 6.84 (*s*)	91.0; 92.0
9	-	156.8; 156.6	-	156.8; 157.0
10	-	107.0	-	104.0; 104.5
C-1′	-	104.6; 104.1	-	121.0
C-2′	7.42	112.8	7.98 (*d*, 7.3 Hz)	129.0
C-3′	-	146.1	6.95 (*d*, 8.8 Hz)	116.0
C-4′	-	156.8	-	161.7
C-5′	6.83	115.8	6.95 (*d*, 8.8 Hz)	116.0
C-6′	7.45	119.4	7.98 (*d*, 7.3 Hz)	129.0
8-*C*-Glc			6-*C*-Glc	
C- 1″	4.58 (*d*, 9.9 Hz); 4.60 (*d*, 9.9 Hz)	72.9	4.58 (*d*, 9.9 Hz); 4.60 (*d*, 9.9 Hz)	73.0; 72.5
C- 2″	3.97 (*t*, 8.8, 8. 8 Hz); 4.17 (*t*, 8.8, 8.8 Hz)	70.2	3.97 (*t*, 8.8, 8. 8 Hz); 4.17 (*t*, 8.8, 8.8 Hz)	70. 2
C- 3″	3.20 (*m*); 3.22 (*m*)	70.7	3.20 (*m*); 3.22 (*m*)	79.5
C- 4″	3.10 (*m*); 3.05 (*m*)	70.6	3.10 (*m*); 3.05 (*m*)	71.0
C- 5″	3.17 (*m*); 3.15 (*m*)	78.9; 78.8	3.17 (*m*); 3.15 (*m*)	81.0
C- 6″	3.88 (*m*); 3.30 (*m*)	66.6; 66.6	3.88 (*m*); 3.30 (*m*)	68.0
6″-*O*-Rha			6″-*O*-Rha	
C – 1	4.51(*d*, 4.8 Hz)	100.6; 100.3	4.51(*d*, 4.8 Hz)	101.5
C – 2	3.73 (*m*)	71.9	3.73 (*m*)	70.0
C – 3	3.35 (*m*)	79.9	3.35 (*m*)	79.5
C – 4	3.14 (*m*)	70.5	3.14 (*m*)	70.8
C – 5	3.56 (*d*, 5.5 Hz)	70.2	3.56 (*d*, 5.5 Hz)	69.0
C – 6	1.12 (*d*, 6.2 Hz) 1.09 (*d*, 5.9 Hz)	17.9	1.12 (*d*, 6.2 Hz) 1.09 (*d*, 5.9 Hz)	18.2
7-OCH_3	3.85 (*s*); 3.90 (*s*)	56.5; 56.3	3.88 (*s*); 3.90 (*s*)	57.0
5-OH	13.55	-	13.48	-

a 3′,4′- or a 3′,4′,5′-oxygenation pattern in the B-ring (Mabry *et al*., 1970). The high-resolution MS signal at *m/z* 609.18140 $[M+H]^+$, in combination with the observed isotopic intensities was indicative for a molecular formula of $C_{28}H_{32}O_{15}$.

The ^{1}H and ^{13}C NMR spectra of **11** showed duplication of signals revealing two rotamers which slowly interconverted via rotation about the *C*-glycosidic bond (Lewis *et al*., 2000). The ^{1}H NMR spectrum of **1** showed signals at δ_H 6.83 (*d*), 7.42 (*s*) and 7.45 (*d*) assignable to H-5′, H-2′ and H-6′, respectively, confirming that ring B was a 3′,4′-oxygenated phenyl moiety. A singlet at δ_H 3.85 indicated the presence of one methoxy group which was assignable to position 7. The ^{1}H NMR spectrum also showed a signal at δ_H 6.70 that was characteristic for the H-3 resonance of a flavone. A broad singlet at δ_H 13.55 was due to the 5-OH group which formed a hydrogen bond with the carbonyl group at C-4 of the flavone. The ^{1}H NMR spectrum also showed the presence of sugar moieties in **1** with two anomeric proton signals at δ_H 4.58 (*d*, *J* =9.9 Hz) and δ_H 4.51 (*d*, *J* = 4.8 Hz). The signal at δ_H 4.51 together with a methyl resonance at δ_H 1.15 (3H, *d*, 6.2 Hz) were both typical of a rhamnopyranosyl residue (Yahara *et al*., 2000).

The HMBC spectrum of **1** showed ^{2}J and ^{3}J correlations between the anomeric proton of Glc, H-1#x02BA; (δ_H 4.58) and C-8 (δ_C 104.6/104.0) and C-7 (δ_C164.8/163.6), confirming C-8 as the position of the *C*-glycosidic linkage. Thus, the singlet at δ_H 6.78/6.80 was unambiguously assigned to H-6. The site of substitution of the additional α-rhamnose moiety was confirmed to be the 6″-OH of the Glc moiety which was β-linked to the flavone aglycone. This was further confirmed by HMBC correlations between H-1‴ (δ_H 4.51) and C-6#x02BA; (66.59/66.57). On the basis of the above evidence, the flavonoid glycoside was characterized as hydroxygenkwanin-8-*C*-[*α*-rhamnopyranosyl-(1 → 6)]-*β*-glucopyranoside and trivially called margadiscoside.

The known compounds, genkwanin-6-*C*-[*α*-rhamnopyranosyl-(1 → 6)]-*β*-glucopyranoside (**2**) (Qasim *et al*., 1987), kaempferol-3-*O*-*α*-rhamnopyranosyl-(1 → 2)-*β*-glucopyranoside-7-*O*-*α*-rhamnopyranoside (**3**) (Mulinacci *et al*., 1995) and kaempferol-3-*O*-*α*-rhamnopyranosyl-(1 → 2)-[*α*-rhamnopyranosyl-(1 → 6)]-*β*-glucopyranoside-7-*O*-*α*-rhamnopyranoside (**4**) (Kite *et al*., 2007) are reported for the first time in this species. Also being reported for the first time are the full ^{13}C NMR data of compound **2**.

The antibacterial activity of compounds **1–4** is shown in Table 1. All of the test compounds exhibited weak

antibacterial activities with their minimum MIC values being 500 μg/mL. Even though the antibacterial activity is not high, the results could be said to be interesting as the various compounds isolated may be said to be contributing individually to the antibacterial effects observed. In the free radical scavenging assay using DPPH, the flavonoid glycosides displayed predictably intense effects (Table 2). Flavonoids have been reported to exhibit free radical scavenging properties (Pietta, 2000). The wound healing process may be hampered by microbial infection and oxygen free radicals leading to the formation of chronic non-healing ulcers (Houghton *et al*., 2005). For the isolated compounds to have shown antibacterial and antioxidant activities, they may reduce the possibility of this happening. Thus, the antibacterial and antioxidant properties of the isolated compounds, however mild, may be contributing in part to the wound healing effects of the plant. The presence of betulinic acid and the alkaloids, securinine and phyllantidine, which have been isolated from the ethyl acetate fraction of the plant, was reported in literature to possess antibacterial, antioxidant and anti-inflammatory effects (Nguemfo *et al*., 2009; Fulda *et al*., 1999; Schuhly *et al*., 1999; Wachter *et al*., 1999, Nick *et al*., 1995; Mensah *et al*., 1990 & 1988). These may also be contributing to the wound healing effects of the plant as observed in folk medicine in Ghana.

Hydroxygenkwanin-8-*C*-[*α*-rhamnopyranosyl (1 → 6)]-*β*-glucopyranoside (1)

Yellow amorphous compound, UV: λ_{max} (MeOH) 245.4 (with a shoulder) and 346.2 nm. IR: ν_{max} 1652 and 1607 (*α*, *β*-unsaturated ketonic function) and hydroxyls 3381 (O–H) cm^{-1}. ^{1}H and ^{13}C NMR data: Table 3.

Genkwanin-6-*C*-[*α*-rhamnopyranosyl (1 → 6)]-*β*-glucopyranoside (2)

Brown amorphous compound, UV: λ_{max} (MeOH) 270.7 and 337.3 nm. IR: ν_{max} 1652 and 1608 (*α*, *β*-unsaturated ketonic function) and hydroxyls 3393 (O–H) cm^{-1} ^{1}H and ^{13}C NMR data: Table 3.

Acknowledgement

Novartis is hereby gratefully acknowledged for sponsoring Edmund Ekuadzi to participate in the Novartis Diversity and Inclusion Next Generation Scientist Programme in their Natural Product Unit in Basel, Switzerland.

Conflict of Interest

The authors have declared that there is no conflict of interest.

REFERENCES

Abbiw D. 1990. Useful Plants of Ghana. Intermediate Technical Publications and Royal Botanic Gardens, Kew UK.

Blois MS. 1958. Antioxidant determination by the use of a stable free radical. *Nature* **181**: 1199–1200.

Calixto JB, Santos ARS, Filho VC, Yunes RA. 1998. A review of the plants of the genus *Phyllanthus*: their chemistry, pharmacology and therapeutic potential. *Med Res Rev* **18**(4): 225–258

Dickson RA, Fleischer TC, Ekuadzi E, Mensah AY, Annan K, Woode E. 2010. Antibacterial, Antioxidant and Anti-inflammatory Properties of *Margaritaria discoidea*, a Wound Healing Remedy from Ghana. *Phcog J.* **2**(17): 32–39.

Eloff JN. 1998. A sensitive and quick microplate method to determine the minimal inhibitory concentration of plant extracts for bacteria. *Planta Med* **64**(8): 711–713.

Fehler K. 2000. Isolierung und Identifizierung von Alkaloiden aus der Euphorbiaceae *Margaritaria discoidea*. Fraβhemmer gegen Termite Schedorhinotermes lamianus, Universität Hamburg.

Fulda S, Jeremias I, Steiner HH, Pietsch T. Debatin KM. 1999. Betulinic acid: A new cytotoxic agent against malignant brain-tumor cells. *Int J Cancer* **82**: 435–441.

Houghton PJ, Hylands PJ, Mensah AY, Hensel A, Deters AM. 2005. *In vitro* tests and ethnopharmacological investigations: Wound healing as an example. *J Ethnopharmacol* **100**:100–107.

Irvine FR. 1961. Woody plants of Ghana. Oxford University Press: London.

Kite GC, Stoneham CA, Veitch NC. 2007. Flavonol tetraglycosides and other constituents from leaves of *Styphnolobium japonicum* (Leguminosae) and related taxa. *Phytochemistry* **68**: 1407–1416.

Lewis KC, Maxwell AR, McLean S, Reynolds WF, Enriquez RG. 2000. Room-temperature (^{1}H, ^{13}C) and variable-temperature (^{1}H) NMR studies on spinosin. *Magn Reson Chem* **38**: 771–774.

Mabry TJ, Markham KR, Thomas MB. 1970. The systematic identification of flavonoids. *Springer-Verlag*: **35–164**.

Mensah JL, Gleye J, Moulis C, Fouraste I. 1988. Alkaloids from the leaves of *Phyllanthus discoideus*. *J. Nat.Prod*. **51**: 1113–1115.

Mensah JL, Lagarde I, Ceschin C, Michel G, Gleye J, Fouraste, I. 1990. Antibacterial activity of the leaves of *Phyllanthus discoideus*. *J Ethnopharmacol* **28**: 129–133.

Mulinacci N, Vincieri FF, Baldi A, Bambagiotti-Alberti M, Sendl A, Wagner H. 1995. Flavonol glycosides from *Sedum telephium* subspecies maximum leaves. . *Phytochemistry* **38**: 531–533.

Nguemfo EL, Dimo T, Dongmo AB, Azebaze AGB, Alaoui K, Asongalem EA, Cherrah Y, Kamtchouing P. 2009. Anti-oxidative and anti-inflammatory activities of some isolated constituents from the stem bark of *Allanblackia monticola* Staner L.C. (Guttiferae). *Inflammopharmacology* **17**: 37–41.

Nick A, Wright AD, Rali T, Sticher O. 1995. Antibacterial triterpenoids from *Dillenia papuana* and their structure–activity relationships. *Phytochemistry* **40**: 1691–1695.

Pietta PG. 2000. Flavonoids as antioxidants. *J Nat Prod* **63**: 1035–1042.

Qasim MA, Roy SK, Kamil M, Ilyas M. 1987. A new glycosyl flavone from *Fagraea obovata* Wall. *Phytochemistry* **26**: 2871–2872.

Schuhly W, Heilmann J, Calis I, Sticher O. 1999. New triterpenoids with antibacterial activity from *Zizyphus joazeiro*. *Planta Med* **65**: 740–743.

Wachter GA, Valcic S, Flagg ML, Franzblau SG, Montenegro G, Suarez E. Timmermann BN. 1999. Antitubercular activity of pentacyclic triterpenoids from plants of Argentina and Chile. *Phytomedicine* **6**: 341–345.

Weenen H, Nkunya MHH, Bray DH, Mwasumbi LB, Kinabo LB, Kilimali VAEB, Wijnberg JBPA. 1990. Antimalarial activity of Tanzanian medicinal plants. *Planta Med* **56**(4): 371.

Yahara S, Kohjyoumab M, Kohoda H. 2000. Flavonoid glycosides and saponins from *Astragalus shikokianus*. *Phytochemistry* **53**: 469–471.

PHYTOTHERAPY RESEARCH
Phytother. Res. **27**: 993–998 (2013)
Published online 16 August 2012 in Wiley Online Library
(wileyonlinelibrary.com) **DOI**: 10.1002/ptr.4823

Antimycobacterials from Lovage Root (*Ligusticum officinale* Koch)

Juan David Guzman,[1,2] Dimitrios Evangelopoulos,[1] Antima Gupta,[1] Jose M. Prieto,[2] Simon Gibbons[2]* and Sanjib Bhakta[1]*

[1]Mycobacteria Research Laboratory, Department of Biological Sciences, Institute of Structural and Molecular Biology, Birkbeck, University of London, Malet Street, London WC1E 7HX, UK
[2]Department of Pharmaceutical and Biological Chemistry, UCL School of Pharmacy, 29-39 Brunswick Square, London WC1N 1AX, UK

The *n*-hexane extract of Lovage root was found to significantly inhibit the growth of both *Mycobacterium smegmatis* mc^{2}155 and *Mycobacterium bovis* BCG, and therefore a bioassay-guided isolation strategy was undertaken. (*Z*)-Ligustilide, (*Z*)-3-butylidenephthalide, (*E*)-3-butylidenephthalide, 3-butylphthalide, α-prethapsenol, falcarindiol, levistolide A, psoralen and bergapten were isolated by chromatographic techniques, characterized by NMR spectroscopy and MS, and evaluated for their growth inhibition activity against *Mycobacterium tuberculosis* H_{37}Rv using the whole-cell phenotypic spot culture growth inhibition assay (SPOTi). Cytotoxicity against RAW 264.7 murine macrophage cells was employed for assessing their degree of selectivity. Falcarindiol was the most potent compound with a minimum inhibitory concentration (MIC) value of 20 mg/L against the virulent H_{37}Rv strain; however, it was found to be cytotoxic with a half-growth inhibitory concentration (GIC_{50}) in the same order of magnitude (SI < 1). Interestingly the sesquiterpene alcohol α-prethapsenol was found to inhibit the growth of the pathogenic mycobacteria with an MIC value of 60 mg/L, being more specific towards mycobacteria than mammalian cells (SI ~ 2). Colony forming unit analysis at different concentrations of this phytochemical showed mycobacteriostatic mode of action. Copyright © 2012 John Wiley & Sons, Ltd.

Keywords: Ligusticum officinale Koch; Lovage; tuberculosis; cytotoxicity; α-prethapsenol.

INTRODUCTION

More than 8.5 million new cases of tuberculosis (TB) and 1.1 million deaths were estimated globally in 2010 according to the World Health Organization report (WHO, 2011). TB remains a global health emergency for several reasons, namely the appearance of multi-drug and extensively drug-resistant strains (M/XDR-TB), and immunosuppression-associated HIV/AIDS epidemic. Novel, safer and more effective drugs with no interaction with antiretroviral therapies are required for treating drug-resistant strains. Moreover, there are no specific drugs designed for treating latent TB. The TB Alliance sponsorship is putting a huge effort towards bringing a complete pipeline of anti-TB drugs; however, more research in early stages of drug discovery is necessary to fuel the pipeline. Natural products are an outstanding source of bioactive chemical scaffolds which can potentially lead to novel therapeutics for a wide array of diseases (Newman and Cragg, 2012). Several interesting anti-mycobacterials have been isolated from natural sources such as hirsutellones, manzamines or saringosterol 24-epimers and many other classes (Guzman *et al*., 2012). Large anti-TB bioprospecting screening programmes are currently in progress, and there is a renewed interest in natural sources for finding novel antimycobacterials (Ashforth *et al*., 2010).

The genus *Ligusticum* belongs to the Apiaceae plant family, a large and economically important group of herbaceous plants commonly used in traditional medicine in America, Europe and Asia. The species *Ligusticum porteri*, *Ligusticum officinale* and *Ligusticum chuanxiong* are medicinally important representatives of each respective region (Zschocke *et al*., 1998). Lovage (*Ligusticum officinale* Koch syn *L. levisticum*) is a traditional culinary ingredient in Britain for making soups, for aromatizing meats and as a seasonal winter beverage as a cordial. This species has been widely used for medicinal purposes in Europe from Mediterranean Greece and Italy to Scandinavia (Andrews, 1941). Even today in rural areas, the root is employed as a diuretic, spasmolytic and as a carminative material (Toulemonde *et al*., 1987). The major phytochemical compounds of Apiaceae species are the phthalide lactones and their non-aromatic dihydro- and tetrahydro- derivatives, which can exist principally as monomers or dimers (Beck and Chou, 2007). Ligustilide is a common dihydrophthalide present in *Ligusticum* species displaying interesting biological properties notably acting as a powerful neuroprotective agent (Wu *et al*., 2011). Further important phyto-constituents of *Ligusticum* species are the polyacetylenes such as falcarindiol and falcarinol, which have been previously isolated from Lovage root and found to be mycobacterial growth inhibitors (Schinkovitz *et al*., 2008b). In this work, a bioassay-guided isolation of antimycobacterial constituents of Lovage root was undertaken in an attempt to isolate potentially active novel antitubercular compounds.

* Correspondence to: Professor Simon Gibbons, Department of Pharmaceutical and Biological Chemistry, UCL School of Pharmacy, 29–39 Brunswick Square, London WC1N 1AX, UK; Dr Sanjib Bhakta, Mycobacteria Research Laboratory, Department of Biological Sciences, Institute of Structural and Molecular Biology, Birkbeck, University of London, Malet Street, London WC1E 7HX, UK.
E-mail: simon.gibbons@ucl.ac.uk; s.bhakta@bbk.ac.uk

Received 31 May 2012
Revised 23 July 2012
Accepted 25 July 2012

MATERIALS AND METHODS

Microbial strains, cells and culture media. *Mycobacterium smegmatis* mc^{2}155 (ATCC 700084), *Mycobacterium bovis* BCG Pasteur (ATCC 35734), *Mycobacterium tuberculosis* H_{37}Rv (ATCC 27294) and mouse RAW264.7 macrophage cells (ATCC TIB71) were used in this study. Middlebrook 7H9, Middlebrook 7H10 media, oleic acid, albumin, dextrose and catalase (OADC) and ADC supplements were purchased from BD Diagnostics. All other media and reagents were purchased from Sigma-Aldrich unless otherwise stated.

Plant material, fractionation and purification of natural products. *Ligusticum officinale* Koch (batch number 37129) roots (490 g) obtained from Proline Botanicals Ltd, were ground using an electric mill, and the material was then exhaustively extracted using a Soxhlet apparatus with 2.5 L of *n*-hexane, 2.5 L of chloroform and finally 2.5 L of methanol. After filtration and removal of solvents under reduced pressure using a rotary evaporator, 7.5 g of an oily *n*-hexane extract, 1.1 g of chloroform extract and 13 g of methanol extract were obtained. The *n*-hexane extract (7.2 g) was fractionated using vacuum liquid chromatography eluting with hexane and ethyl acetate mixtures. Eighteen fractions named H1 to H18 were collected. Fraction H5, H6, H7 and H8 were chromatographed on solid-phase extraction (SPE) cartridge packed with normal phase silica (10 g, Strata, Phenomenex) eluting with hexane, ethyl acetate mixtures. Thereafter, the fractions were further fractionated by column chromatography (CC) or preparative thin-layer chromatography (PTLC) in silica gel. A schematic representation of the fractionation and purification is shown in Fig 1B. Compounds **1** and **2** were obtained as colorless amorphous solids from fraction H5S1 by CC eluting with toluene/ethyl acetate 9:1 (*v/v*). Compounds **3** and **4** were also isolated as amorphous colorless solids from fraction H5S2 by PTLC eluting with toluene/ethyl acetate 95:5 (*v/v*). Compound **5** was obtained as colorless crystals by CC from fraction H6S2 eluting with toluene/acetone 96:4 (*v/v*). Compound **6** was isolated as yellow oil directly from fraction H7 by SPE in the hexane/ethyl acetate 8:2 (*v/v*) fraction. Compounds **7**, **8** and **9** were obtained from H8S3 fraction by PTLC eluting with 100 mL of toluene/ethyl acetate 9:1 (*v/v*) containing five drops of formic acid. Mono and bidimensional ^{1}H and ^{13}C NMR spectroscopy (Bruker Avance 400) and mass spectrometry (Thermo Navigator) were employed for chemical characterisation of the isolated chemical products.

Antimycobacterial testing. At each step of the chemical fractionation of the extract, the spot culture growth inhibition assay (SPOTi) was performed as previously described (Evangelopoulos and Bhakta, 2010). Initially, the *n*-hexane, chloroform and methanol extracts were tested against both *M. smegmatis* mc^{2}155 and *M. bovis* BCG at 200, 100, 50, 25, 10 and 0 mg/L concentration. Thereafter, each sub-fraction that was obtained was tested only against *M. bovis* BCG at 100, 50, 25, 10, 5 and 0 mg/L. Briefly, extracts were dissolved in DMSO at 200 g/L concentration, while fractions and compounds were dissolved at 100 g/L. A one thousand-fold dilution was prepared from the stock and dispensed in 6 or 24-well plates (5 or 2 μL, respectively). Then, 5 mL or 2 mL of molten Middlebrook 7H10 (MB7H10) agar supplemented with 0.5% glycerol and 10% OADC, were added to each well, and the plates were allowed to stand for 10 min without a lid. Then, 5 or 2 μL of an appropriately diluted (around 10^6 colony forming unit (CFU)/mL) mid-log phase liquid culture of the mycobacteria grown in Middlebrook 7H9 (MB7H9) broth, was carefully dispensed into the middle of each well. The plates were incubated at 37°C for two days for *M. smegmatis* mc^{2}155 and for two weeks for *M. bovis* BCG. Minimum inhibitory concentrations (MICs) were determined visually after the incubation period. All the pure compounds were

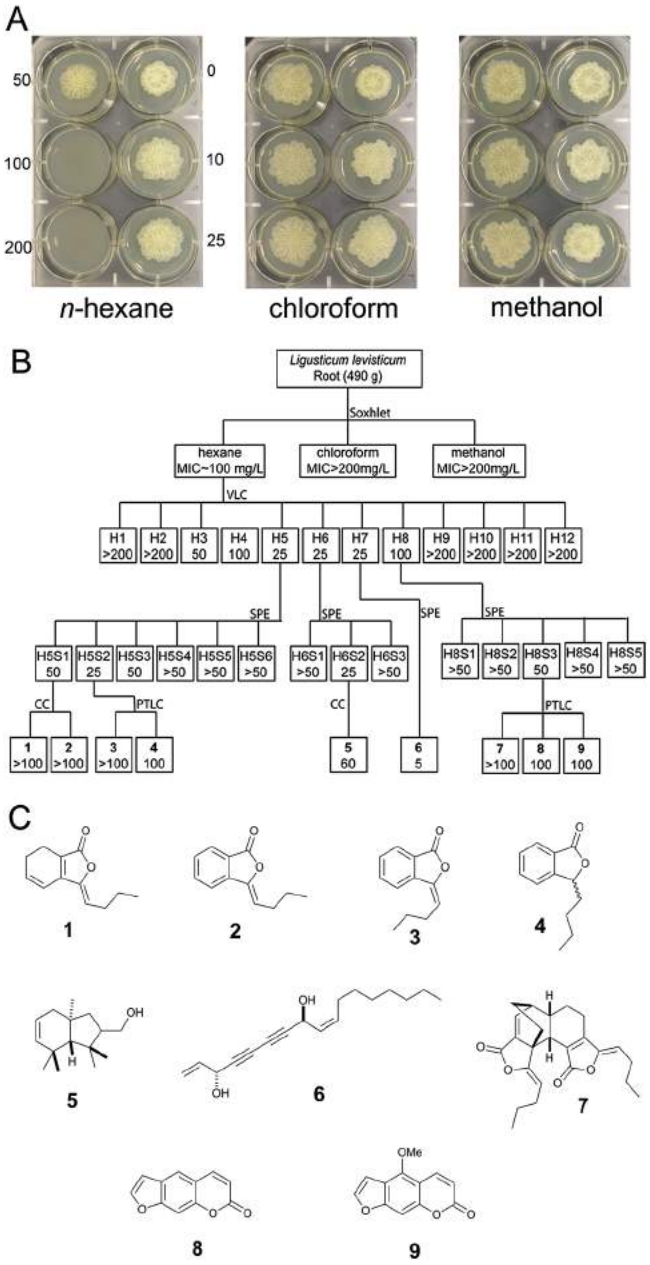

Figure 1. Antimycobacterial activity and chemical fractionation of the roots of *Ligusticum officinale*. (A) SPOTi assay of the three extracts of Lovage root against *M. bovis* BCG. (B) Schematic representation of the bioassay-guided fractionation of the extracts. The number under the fraction code represents its MIC value in mg/L against *M. bovis* BCG. Vacuum liquid chromatography (VLC), solid-phase extraction (SPE), column chromatography (CC) and preparative thin-layer chromatography (PTLC) were employed for fractionation/purification. (C) Chemical structures of compounds **1–9**. This figure is available in colour online at wileyonlinelibrary.com/journal/ptr.

tested against *Mycobacterium tuberculosis* $H_{37}Rv$ using a similar procedure in a biosafety level III (BSL-3) laboratory. Isoniazid was included in all experiments as a positive control at 10, 1, 0.1, 0.05, 0.01 and 0 mg/L concentrations and DMSO was included as a negative control at 0.1% (*v/v*).

Cytotoxicity assay. Mouse macrophage cells (RAW 264.7) were cultured according to a previously described method (Gupta and Bhakta, 2012). The cytotoxicity assay was performed in 96-well cell culture black flat-bottom plates (Costar; Appleton Woods) in triplicate. First, 16 μL of 50 g/L stock solutions of isolated compounds were placed in triplicate in the first row containing 200 μL of RPMI-1640 medium, and then twofold serially diluted. To each well, 100 μL of diluted macrophage cells (5×10^5 cells/mL) was added. After 48 h of incubation, the macrophage cells were washed twice with PBS, and fresh RPMI-1640 medium was added to each well. Plates were then treated with 30 μL of freshly prepared 0.01% resazurin filtered-sterilized solution and incubated for 16 h at 37°C. The change in color and the fluorescence intensity was recorded at $\lambda_{ex} = 560$ nm, $\lambda_{em} = 590$ nm using a fluorometer microplate reader (OPTIMA, BMG LABTECH GmbH). The half growth inhibitory concentrations (GIC_{50}) were determined based on fluorescence intensity, and the selectivity index (SI) was calculated as the ratio between the GIC_{50} against RAW 264.7 macrophages and the MIC against *M. tuberculosis* $H_{37}Rv$ for all of the compounds.

Growth curve and CFU counting. Prethapsenol **5** was further evaluated against *M. bovis* BCG growing in liquid culture media. To four rolling bottles containing 90 mL of MB7H9 and 10 mL of ADC enrichment were added 50, 100 and 150 μL of a 50 g/L stock of compound **5** and completed with 150, 100 and 50 μL of DMSO respectively. A control was included by adding 200 μL of pure DMSO. A 1:100 inoculum dilution (around 10^7 cells) of a mid-log phase liquid culture of *M. bovis* BCG were added to each rolling culture, and then the four bottles were incubated at 37°C in a roller incubator set at 2 rpm. The optical density at 600 nm (OD_{600}) was measured every day for two weeks. After 4 days, when the DMSO control reached 1.8 absorbance units (mid-exponential phase), an aliquot of the culture was diluted to 10^{-5}, 10^{-6}, 10^{-7} and 10^{-8} with MB7H9, and spread into Petri dishes containing solidified MB7H10 agar enriched with 10% OADC. The plates were sealed and incubated for three weeks at 37°C. Thereafter, emerging cell colonies were counted and the mean and standard deviation calculated among the three experimental replicates.

Stability experiment. Eight microliters of α-prethapsenol (**5**) dissolved in DMSO at 50 g/L were added to 1992 μL of MB7H9 medium containing 0.5% glycerol, 0.05% Tween 80 and 10% ADC, to achieve a final concentration of 200 mg/L. A pure sample of α-prethapsenol was prepared by diluting an aliquot of 10 μL of the DMSO stock with 990 μL of methanol to achieve a concentration of 500 mg/L. A sample of supplemented MB7H9 was also included. All three samples were dispensed into 2 mL HPLC vials. The analysis was performed on an Agilent 1100 HPLC instrument using a reverse phase C-18 column (Phenomenex 10 cm, 4.7 mm, 5 μm) and a gradient mobile phase of water and acetonitrile, going from 90% water and 10% acetonitrile to 100% acetonitrile at 30 minutes after injection. The flow rate was 1.0 mL/min, the volume injected was 10 μL and a photodiode array detector was used continuously at 220 nm. Samples were maintained at 37°C and analyzed on day 0, 4, 14 and 28. The amount of α-prethapsenol was determined by calculating the area under the peak of each HPLC chromatogram.

RESULTS

The bioassay-guided isolation of chemical entities from the roots of *L. officinale* was carried out by evaluating the activity against *M. bovis* BCG at each step of chemical fractionation process. Initially, only the lowest polarity solvent extract obtained from the roots showed activity (Fig 1A). More polar chloroform and methanol extracts were inactive at the highest concentration tested (200 mg/L). The *n*-hexane extract completely inhibited both *M. smegmatis* mc^2155 and *M. bovis* BCG growth at 100 mg/L. Upon vacuum liquid chromatography fractionation, the antimycobacterial activity principally concentrated into three fractions (H5-H7) having MIC values of 25 mg/L (Fig 1B). Further fractionation and purification of H5 led to the isolation of four monomers of ligustilides, namely (*Z*)-ligustilide (**1**), (*Z*)-3-butylidenephthalide (**2**), (*E*)-3-butylidenephthalide (**3**)

Table 1. MIC values against two slow-growing mycobacterial species and cytotoxicity and selectivity against the murine macrophage cell line RAW 264.7

Compound	MIC *M. tuberculosis* $H_{37}Rv$ (mg/L)	MIC *M. bovis* BCG (mg/L)	GIC_{50} Macrophages RAW264.7 (mg/L)	Selectivity index (GIC_{50}/MIC_{H37Rv})
1	>100	>100	250	<2.5
2	>100	>100	250	<2.5
3	>100	>100	250	<2.5
4	100	100	200	2
5	60	60	125	2.1
6	20	5	5	0.25
7	>100	>100	200	<2
8	>100	100	100	<1
9	>100	100	100	<1
Isoniazid	0.1	0.1	3000[a]	30000

[a]Value taken from reference (Gupta and Bhakta, 2012)

and 3-butylphthalide (**4**). Their NMR and MS spectra were in agreement with previously reported data (Miyazawa *et al.*, 2004; Schinkovitz *et al.*, 2008a). α-Prethapsenol (**5**), a sesquiterpenoid recently isolated for the first time from the roots of *Ligusticum grayi* (Cool *et al.*, 2010), was obtained from H6. More than 300 mg of pure falcarindiol (**6**) were recovered from H7. Unambiguous identification was achieved by NMR and MS spectra analysis and comparison with reported data (Lechner *et al.*, 2004). A dimer of (*Z*)-ligustilide, levistolide A (**7**) and two furanocoumarins psoralen (**8**) and bergapten (**9**) were obtained from fraction H8 and characterized by NMR and MS spectra (Kaouadji *et al.*, 1986; Masuda *et al.*, 1998). The chemical structures of the isolated compounds are depicted in Fig 1C.

All of the ligustilides (**1–4**) displayed low potency against slow-growing mycobacterial species having MIC values ≥ 100 mg/L (Table 1). The saturated chain of compound **4** slightly improved the activity in comparison with both geometric configurations of the alkenes **2–3**. Half-growth inhibition concentrations (GIC_{50}) against macrophage RAW 264.7 cells were also comparable for the ligustilides with values between 200 and 250 mg/L. Their specificity against mycobacteria in relation to the mammalian cell line was low (SI < 2.5). The sesquiterpene alcohol α-prethapsenol (**5**) displayed an MIC value of 60 mg/L against both *M. bovis* BCG and *M. tuberculosis* $H_{37}Rv$. At higher concentrations of **5**, the growth of the bacteria was completely inhibited resulting in clear wells on the SPOTi assay. The cytotoxicity profile of α-prethapsenol indicated that it had certain selectivity towards killing mycobacteria in comparison with the macrophage cell line with an SI value of 2.1. Falcarindiol (**6**) was obtained in high yields from Lovage roots (0.1% *w/w*) and as found previously by several authors (Deng *et al.*, 2008; Schinkovitz *et al.*, 2008b) it is a potent inhibitor of *M. tuberculosis* growth displaying in this study an MIC value of 5 mg/L against *M. bovis* BCG and 20 mg/L against *M. tuberculosis* $H_{37}Rv$. However, falcarindiol was found to be toxic towards mammalian RAW264.7 cells, being able to kill half the population at a concentration of 5 mg/L. The SI was therefore less than 1, suggesting the possibility of a specific mammalian metabolic interference. Levistolide A (**7**) was inactive against mycobacteria showing an MIC value higher than 100 mg/L. This dimer had a RAW264.7 macrophage GIC_{50} value of 200 mg/L. Furanocoumarins psoralen **8** and bergapten **9** were both inhibitory to *M. bovis* BCG at 100 mg/L, and their cytotoxicity towards murine macrophages was in the same order of magnitude as the MIC suggesting poor selectivity.

The sesquiterpene alcohol α-prethapsenol (**5**) was selected for further study against *M. bovis* BCG in a liquid culture-based assay. The growth curve under different concentrations of **5** was constructed (Fig 2A). An extended lag phase of growth was observed when the concentration was equal or higher than the MIC. At 75 mg/L, four more days of incubation were required for the bacteria to attain the exponential growth observed in the untreated control (Fig 2A). A minor delay of the lag phase was also noted at a concentration of 50 mg/L concentration of **5**. CFU counts however showed only a minor decrease in cell viability when treated with a concentration > MIC, and after removal of the pressure of the compound, high numbers of bacteria were able to grow (Fig 2B). Initially, it was thought that α-prethapsenol might be chemically unstable in MB7H9 media at 37°C, and therefore a stability experiment was undertaken. After one month of incubation in MB7H9 at usual growth conditions, the same amount of the small molecule was measured by reverse phase HPLC (Fig 2C), indicating high stability under these conditions.

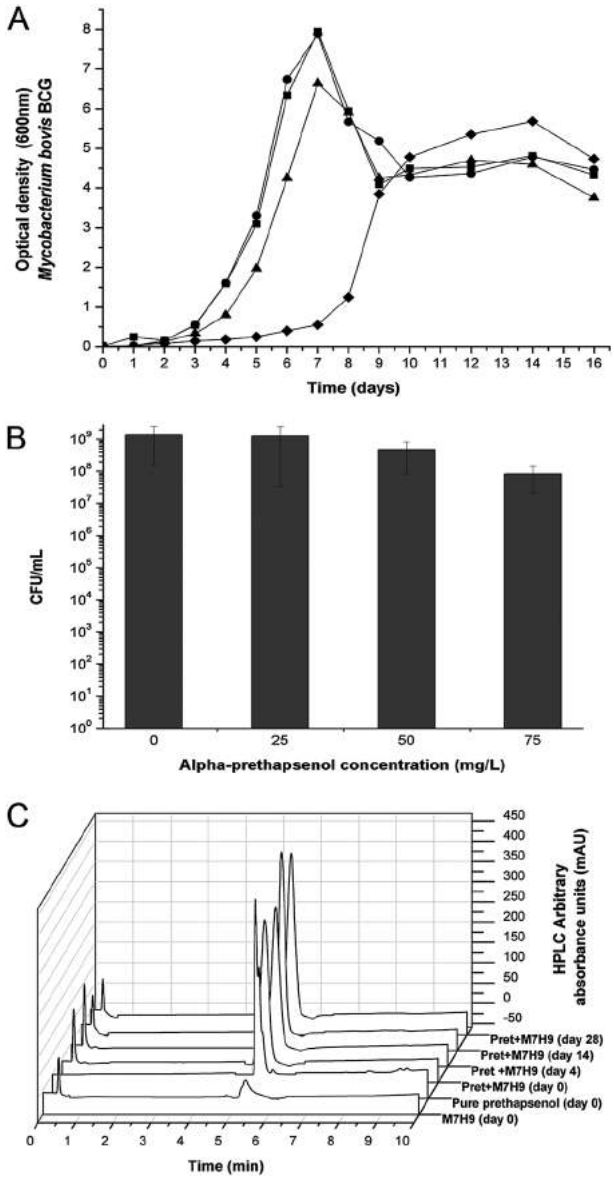

Figure 2. Effect of different concentrations of α-prethapsenol (**5**) on the growth of *M. bovis* BCG and stability experiment of α-prethapsenol. (A) Growth curve of *M. bovis* BCG under three different concentrations of **5**. The concentrations 0, 25, 50 and 75 mg/L are represented as circles, squares, triangles and diamonds, respectively. (B) Number of colony forming units of *M. bovis* BCG treated with different concentrations of **5** at day 4. Each bar represents the mean CFU ± SD (C) HPLC chromatograms of MB7H9, pure α-prethapsenol and incubated in MB7H9 media at 37°C analyzed at different time points.

DISCUSSION

The ligustilide monomers **1–4** and dimer **7** isolated in this study from Lovage root were found to be weak inhibitors of mycobacterial growth and only compound **4** showed inhibition at the highest concentration tested.

(*Z*)-Ligustilide **1** isolated from Osha root (*Ligusticum porteri*) has been found to inhibit the growth of *Staphylococcus aureus* at 128 mg/L, showing potentiation of norfloxacin against an efflux-mediated *S. aureus* drug-resistant strain (Cégiéla-Carlioz *et al*., 2005). Other bacteria and viruses (Beck and Stermitz, 1995) but also cancer cell lines (Kan *et al*., 2008) have been reported to be inhibited at high concentration of **1**, and all these results point out a general mechanism of action affecting different types of cells. However, there is the possibility that other ligustilide-related compounds appearing in the complex fraction H-5/H-6 at lower concentration could be responsible for the high activity of these fractions. In particular, we observed by NMR analysis a small fraction containing a 1:1 mixture of an epoxy-ligustilide and (*Z*)-butylidenephtalide which was more active than **2** alone, but the low quantity of this fraction prevented full chemical and biological characterisation.

Interestingly, the novel sesquiterpene skeleton of α-prethapsenol (**5**) was found to be active against both *M. bovis* BCG and *M. tuberculosis* H_{37}Rv strains. No closely related structures have been shown to possess antimicrobial effects. Other sesquiterpenoids such as the benzoylated dihydroagarofuranoids isolated from *Microtropis* species (Chen *et al*., 2007), the sesquiterpenelactones based on germacrane, eudesmane or guaiane skeletons (Fischer *et al*., 1998; Vongvanich *et al*., 2006) or farnesol (Rajab *et al*., 1998) have shown significant antitubercular activity, but they share little structural similarity to **5**. In other words, this compound might be affecting the bacteria through a particular unknown biochemical mechanism while being less active against eukaryotic cell lines. Related compounds have been found in *L. grayi* (Cool *et al*., 2010), and a systematic anti-tubercular screening of these entities may underpin more potent natural products.

Falcarindiol (**6**) showed high potency but little selectivity. It is considered to be more active towards eukaryotic cells than bacteria, a not very appealing result for TB-drug discovery research; however, this compound may have an essential role to play in future cancer-drug discovery, and efforts in this direction are being made (Zaini *et al*., 2012). Furanocoumarins **8** and **9** showed low antimycobacterial activity and selectivity suggesting a non-specific mechanism of action, although other coumarins such as umbelliferone, scopoletin, xanthyletin and (*S*)-marmesin have been found to be active with MIC values in the range 40–60 mg/L (Chiang *et al*., 2010).

M. bovis BCG cells were able to grow exponentially after one week of incubation with concentrations of the prethapsane alcohol **5** above its MIC. This natural product was found to be stable when dissolved in MB7H9 media and maintained under the conditions of incubation, and therefore it is reasonable to think that the concentration of **5** remains unchanged during the assay, although a bio-modification mechanism cannot be ruled out at this point. It seems sensible to suggest that BCG growth was delayed by **5**, without notable bacterial killing as the CFU counting remained in the same order of magnitude for all treatments, indicating a shift towards the viable but non-replicating physiological state of mycobacteria. The bacteriostatic effect of **5** was consistent with the lag-phase extension seen in the growth curve because onset of exponential growth phase is dependent on sufficient supply of essential biomolecules. It is known that in the lag phase, bacterial cells prepare primordial molecules (nucleosides triphosphates, sugars, metals and cofactors) and enzymes for sustained cell division (Rolfe *et al*., 2012), and therefore we hypothesize that **5** may interfere with one or several steps of this transient adaptation.

Acknowledgements

The authors would like to acknowledge Bloomsbury Colleges, University of London for a Research Studentship to JDG and Medical Research Council, UK for a New Investigators Research Grant award (code G0801956) to SB. The authors are grateful to Professor Simon Croft for his generous support with the TB culture facility at the London School of Hygiene and Tropical Medicine.

Conflict of Interest

The authors have declared that there is no conflict of interest.

REFERENCES

Andrews AC. 1941. Alimentary use of Lovage in the Classical period. *Isis* **33**: 514–518.

Ashforth EJ, Fu C, Liu X, *et al*. 2010. Bioprospecting for antituberculosis leads from microbial metabolites. *Nat Prod Rep* **27**: 1709–1719.

Beck JJ, Chou S-C. 2007. The structural diversity of phthalides from the Apiaceae. *J Nat Prod* **70**: 891–900.

Beck JJ, Stermitz FR. 1995. Addition of methyl thioglycolate and benzylamine to (Z)-ligustilide, a bioactive unsaturated lactone constituent of several herbal medicines. An improved synthesis of (*Z*)-ligustilide. *J Nat Prod* **58**: 1047–1055.

Cégiéla-Carlioz P, Bessière J-M, David B, Mariotte A-M, Gibbons S, Dijoux-Franca M-G. 2005. Modulation of multi-drug resistance (MDR) in *Staphylococcus aureus* by Osha (*Ligusticum porteri* L., Apiaceae) essential oil compounds. *Flavour Frag J* **20**: 671–675.

Chen J-J, Chou T-H, Peng C-F, Chen I-S, Yang S-Z. 2007. Antitubercular dihydroagarofuranoid sesquiterpenes from the roots of *Microtropis fokienensis*. *J Nat Prod* **70**: 202–205.

Chiang C-C, Cheng M-J, Peng C-F, Huang H-Y, Chen I-S. 2010. A novel dimeric coumarin analog and antimycobacterial constituents from *Fatoua pilosa*. *Chem Biodivers* **7**: 1728–1736.

Cool LG, Vermillion KE, Takeoka GR, Wong RY. 2010. Irregular sesquiterpenoids from *Ligusticum grayi* roots. *Phytochemistry* **71**: 1545–1557.

Deng S, Wang Y, Inui T, *et al*. 2008. Anti-TB polyynes from the roots of *Angelica sinensis*. *Phytother Res* **22**: 878–882.

Evangelopoulos D, Bhakta S. 2010. Rapid methods for testing inhibitors of mycobacterial growth. *Antibiotic Resistance Protocols, Methods in Molecular Biology* **642**: 279.

Fischer NH, Lu T, Cantrell CL, Castaneda-Acosta J, Quijano L, Franzblau SG. 1998. Antimycobacterial evaluation of germacranolides in honour of professor G.H. Neil Towers 75th birthday. *Phytochemistry* **49**: 559–564.

Gupta A, Bhakta S. 2012. An integrated surrogate model for screening of drugs against *Mycobacterium tuberculosis*. *J Antimicrob Chemother* **67**: 1380–1391.

Guzman JD, Gupta A, Bucar F, Gibbons S, Bhakta S. 2012. Antimycobacterials from natural sources: ancient times, antibiotic era and novel scaffolds. *Front Biosci* **17**: 1861–1881.

Kan WLT, Cho CH, Rudd JA, Lin G. 2008. Study of the antiproliferative effects and synergy of phthalides from *Angelica sinensis* on colon cancer cells. *J Ethnopharmacol* **120**: 36–43.

Kaouadji M, De Pachtere F, Pouget C, Chulia AJ, Lavaitte S. 1986. Three additional phthalide derivatives, an epoxymonomer and two dimers, from *Ligusticum wallichii* rhizomes. *J Nat Prod* **49**: 872–877.

Lechner D, Stavri M, Oluwatuyi M, Pereda-Miranda R, Gibbons S. 2004. The anti-staphylococcal activity of *Angelica dahurica* (Bai Zhi). *Phytochemistry* **65**: 331–335.

Masuda T, Takasugi M, Anetai M. 1998. Psoralen and other linear furanocoumarins as phytoalexins in *Glehnia littoralis*. *Phytochemistry* **47**: 13–16.

Miyazawa M, Tsukamoto T, Anzai J, Ishikawa Y. 2004. Insecticidal effect of phthalides and furanocoumarins from *Angelica acutiloba* against *Drosophila melanogaster*. *J Agric Food Chem* **52**: 4401–4405.

Newman DJ, Cragg GM. 2012. Natural products as sources of new drugs over the 30 years from 1981 to 2010. *J Nat Prod* **75**: 311–335.

Rajab MS, Cantrell CL, Franzblau SG, Fischer NH. 1998. Antimycobacterial activity of (*E*)-phytol and derivatives: A preliminary structure-activity study. *Planta Med* **64**: 2–4.

Rolfe MD, Rice CJ, Lucchini S, *et al*. 2012. Lag phase is a distinct growth phase that prepares bacteria for exponential growth and involves transient metal accumulation. *J Bacteriol* **194**: 686–701.

Schinkovitz A, Pro SM, Main M, *et al*. 2008a. Dynamic nature of the ligustilide complex. *J Nat Prod* **71**: 1604–1611.

Schinkovitz A, Stavri M, Gibbons S, Bucar F. 2008b. Antimycobacterial polyacetylenes from *Levisticum officinale*. *Phytother Res* **22**: 681–684.

Toulemonde B, Paul F, Noleau I. 1987. Phtalides from Lovage (*L. officinale* Koch). In Flavour Science and Technology, Martens M, Dalett A, Russwurm H (eds). John Wiley and Sons: New York; 89–94.

Vongvanich N, Kittakoop P, Charoenchai P, Intamas S, Sriklung K, Thebtaranonth Y. 2006. Antiplasmodial, antimycobacterial, and cytotoxic principles from *Camchaya calcarea*. *Planta Med* **72**: 1427–1430.

WHO. 2011. Global tuberculosis control *WHO report* 1–8.

Wu X-m, Qian Z-m, Zhu L, *et al*. 2011. Neuroprotective effect of ligustilide against ischaemia-reperfusion injury via up-regulation of erythropoietin and down-regulation of RTP801. *Br J Pharmacol* **164**: 332–343.

Zaini RG, Brandt K, Clench MR, Le Maitre CL. 2012. Effects of bioactive compounds from carrots (*Daucus carota* L.), polyacetylenes, beta-carotene and lutein on human lymphoid leukaemia cells. *Anticancer Agents Med Chem* **12**: 640–652.

Zschocke S, Liu J-H, Stuppner H, Bauer R. 1998. Comparative study of roots of *Angelica sinensis* and related umbelliferous drugs by thin layer chromatography, high-performance liquid chromatography, and liquid chromatography – mass spectrometry. *Phytochem Anal* **9**: 283–290.

JOURNAL OF NATURAL PRODUCTS

Article

pubs.acs.org/jnp

Antimicrobial Phenolics and Unusual Glycerides from *Helichrysum italicum* subsp. *microphyllum*

Orazio Taglialatela-Scafati,*[,†] Federica Pollastro,[‡] Giuseppina Chianese,[†] Alberto Minassi,[‡] Simon Gibbons,[§] Warunya Arunotayanun,[§] Blessing Mabebie,[§] Mauro Ballero,[⊥] and Giovanni Appendino*[,‡]

[†]Dipartimento di Chimica delle Sostanze Naturali, Università di Napoli Federico II, Via Montesano 49, 80131 Napoli, Italy

[‡]Dipartimento di Scienze Farmaceutiche, Università del Piemonte Orientale, Via Bovio 6, 28100, Novara, Italy

[§]Department of Pharmaceutical and Biological Chemistry, UCL School of Pharmacy, 29-39 Brunswick Square, London WC1N 1AX, U.K.

[⊥]Dipartimento di Scienze Botaniche and Consorzio per lo Studio dei Metaboliti Secondari (COSMESE), Università di Cagliari, Viale S. Ignazio 13, 09123 Cagliari, Italy

S *Supporting Information*

ABSTRACT: During a large-scale isolation campaign for the heterodimeric phloroglucinyl pyrone arzanol (**1a**) from *Helichrysum italicum* subsp. *microphyllum*, several new phenolics as well as an unusual class of lipids named santinols (**5a–c**, **6–8**) have been characterized. Santinols are angeloylated glycerides characterized by the presence of branched acyl- or keto-acyl chains and represent a hitherto unreported class of plant lipids. The antibacterial activity of arzanol and of a selection of *Helichrysum* phenolics that includes coumarates, benzofurans, pyrones, and heterodimeric phloroglucinols was evaluated, showing that only the heterodimers showed potent antibacterial action against multidrug-resistant *Staphylococcus aureus* isolates. These observations validate the topical use of *Helichrysum* extracts to prevent wound infections, a practice firmly established in the traditional medicine of the Mediterranean area.

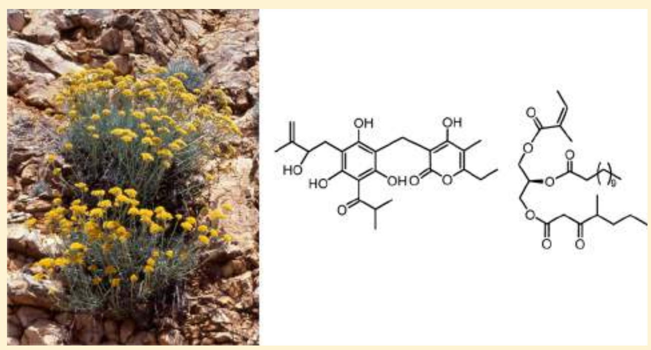

Helichrysum italicum L. (family Asteraceae), a plant endemic to the Mediterranean area, is known to contain a poorly characterized cortisone-like principle named helichrysine.[1] The structure of helichrysine has long been elusive, but the identification of the heterodimeric phloroglucinyl pyrone arzanol (**1a**), a major constituent of *H. italicum*,[2] as a potent dual inhibitor of pro-inflammatory transcription factors (NF-κB)[2] and inflammatory enzymes [(mPGES)-1,5-LO][3] suggests that helichrysine might consist of arzanol and/or related compounds. As a prelude to preclinical in vivo studies, a large-scale isolation of arzanol from a Sardinian variety of *H. italicum* [*H. italicum* subsp. *microphyllum* (Willd.) Nyman] especially rich in this compound[2] was carried out. In the course of this study, we have characterized several minor constituents of the plant, including an unprecedented class of lipids and several phenolics. The availability of these compounds provided the opportunity to study in a systematic way a second important property of helichrysine, namely, its antibacterial activity.[1,4] Therefore, this report presents an account of the structure elucidation of the minor constituents of this plant and a study of the antibacterial action of the major phenolics from *H. italicum* against multidrug-resistant and methicillin-resistant variants of *Staphylococcus aureus* (MRSA), an important agent of nosocomial infections and a growing medical emergency.[5]

■ RESULTS AND DISCUSSION

Apart from arzanol (**1a**, ca. 0.32% on dried plant basis), the aerial parts of *H. italicum* subsp. *microphyllum* contain large amounts (ca. 0.40%) of ursolic acid (**2**) and phenolics belonging to three structural types: pyrones (both homo- and heterodimeric), benzofurans (bitalin esters), and prenylcoumarates. Ursolic acid could be obtained in high purity from crude extracts by the Passerini method, namely, a brief (10 min) reflux in acetone, cooling to obtain a crude triterpenoid mixture, and then recrystallization from methanol.[6] The presence of large amounts of ursolic acid, a poorly soluble compound, complicated the fractionation of the extract, but it was found that, as an alternative to the Passerini method, this compound could also be largely removed by liquid/liquid

Special Issue: Special Issue in Honor of Lester A. Mitscher

Received: October 12, 2012
Published: December 24, 2012

partition of the extract between petroleum ether and aqueous methanol. Ursolic acid has a low solubility in both phases and remained undissolved during the partition of the crude extract between these two solvents. The two "de-triterpenated" phases were then independently fractionated by gravity column chromatography on silica gel to afford six major fractions (A–F).

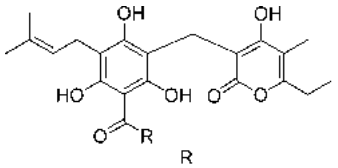

R

1a -CH_3

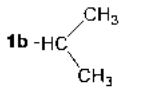

1b -HC(CH_3)(CH_3)

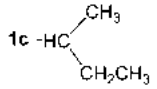

1c -HC(CH_3)(CH_2CH_3)

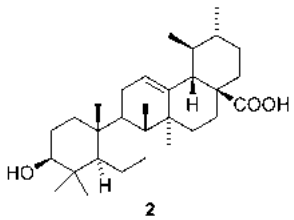

2

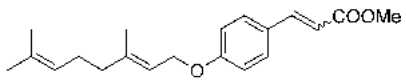

3a; *E*
3b; *Z*

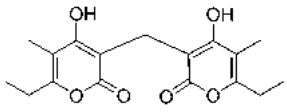

4

The petroleum ether phase (fraction A) contained neryl acetate, the hallmark compound of the *Helichrysum* essential oils from the Tyrrhenian area,[7] and the *O*-geranylated isomeric coumarates **3a**,**b**,[8] which could be separated by preparative HPLC on silica gel and could also be isolated from the aqueous methanol phase. Alkoxycinnamates have attracted considerable attention because of their action against drug-resistant *Mycobacterium*,[9] but the concentration of these compounds in the extract (overall, ca. 35 ppm in the dried plant material) was too low to be associated with a specific activity.

The remaining fractions were obtained by gravity column chromatography purification of the aqueous methanol phase. Fraction B was crystallized from ether to afford the dimeric pyrone helipyrone (**4**).[10] The mother liquors afforded a series of angeloylated lipids (**5a–c**, **6–8**) that have been named santinols in honor of Leonardo Santini, the pioneer in the study of the medicinal use of *Helichrysum*.[1,11] By gravity column chromatography, a major glyceride was obtained apparently pure in terms of its ^{1}H NMR spectrum, but ESIMS revealed a mixture of homologues, eventually resolved by RP-HPLC to afford pure santinols A1–A3 (**5a–c**).

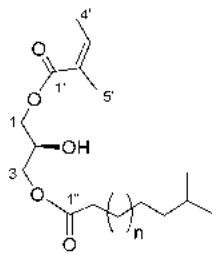

5a n = 5
5b n = 7
5c n = 9

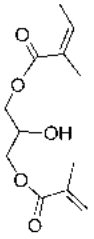

6

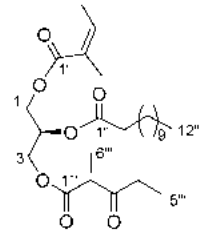

7

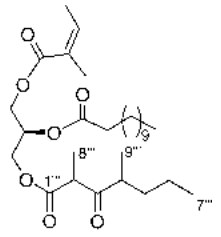

8

Santinol A1 (**5a**) ($C_{20}H_{36}O_5$, HR-ESIMS) was obtained as an optically active 1,3-diacylglycerol. The ^{1}H NMR spectrum of **5a** ($CDCl_3$) showed a partially overlapped cluster of five resonances between δ 4.14 and 4.28, which, with the help of the COSY and HSQC spectra, could be deconvoluted and assigned to a 1,3-diacylated glycerol. The presence of an angelate group was evidenced by the appearance of typical ^{1}H (δ_H 1.90, 3H, brs; 6.12, 3H, q; 1.99, 3H, d) and ^{13}C NMR resonances, and the *Z* configuration of the stereogenic double bond was confirmed by the detection of a NOE correlation between the olefinic signal and the allylic methyl (H_3-5′). Molecular formula considerations and the presence of a terminal branching identified the second acyl moiety as isolauric acid, an unusual C-12 fatty acid. The 1,3-acylation pattern was assessed by chemical shift considerations (the downfield resonance of the diastereotopic oxymethylene protons) and confirmed by the detection of HMBC cross-peaks between the methylene protons and the ester carbonyls (angelate carbonyl at δ 168.3; isolaurate carbonyl at δ 174.4). The presence of two markedly different acyl moieties provided a rationale for applying the modified Mosher's method[12] to assess the absolute configuration of **5a**. To this aim, **5a** was reacted with *R*- or *S*-MTPA chloride [MTPA = methoxy-(trifluoromethyl)phenylacetic acid], obtaining the corresponding *S* (**5d**) and *R* (**5e**) monoesters. Analysis of $\Delta\delta$ ($S - R$) values for protons of the glycerol moiety (Figure 1) indicated,

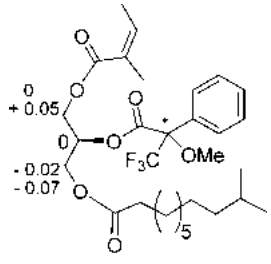

5d *S*
5e *R*

Figure 1. Application of the modified Mosher's method for the absolute configuration at C-2 of santinol A1 (**5a**).

dx.doi.org/10.1021/np3007149 | *J. Nat. Prod.* 2013, 76, 346–353

according to Mosher's model,[12] a 2*S* configuration for the natural product. Santinols A2 (**5b**) and A3 (**5c**) differed from **4a** only for the length of the saturated acyl moiety, an isomyristate and an isopalmitate, respectively. Since **5b** and **5c** share with **5a** a positive optical rotation, it seemed reasonable to assume that they share the same *S* configuration at the stereogenic center.

Santinol B (**6**, $C_{13}H_{20}O_5$) was optically inactive, and its NMR spectra showed a 1,3-diangeloylated glycerol. Thus, the ^{1}H NMR spectrum of **6** showed, apart from the signals of the glycerol protons, only the resonances of the angelate protons, while the ^{13}C NMR spectrum showed only seven signals (two for the glycerol unit and five for the two angeloyl residues).

Santinol C (**7**, $C_{26}H_{44}O_7$) was found to be a triacyl glycerol. Analysis of its ^{1}H and ^{13}C NMR data identified, apart from the resonances of the glycerol backbone and of the angeloyl and lauryl moieties, also those of a 2-methyl-3-oxovaleroyl group. Thus, the COSY spectrum disclosed the presence, within this acyl moiety, of a methyl-bearing methine, in addition to the expected ω-methyl-bearing methylene, located between two carbonyl groups by analysis of the HMBC cross-peaks [correlation between the methyl doublet at δ 1.34 (H-3−6‴) and the ester carbonyl at δ 170.3 and with a ketone carbonyl resonating at δ 206.0]. The correlation of the methyl triplet H_3-5‴ with C-3‴ indicated that an ethyl group bound to the ketone carbonyl completed the structure of this residue. 2-Methyl-3-oxovaleric acid is an important marker for the diagnosis of propionic acidemia, a genetic disease caused by a defect in the biotin-dependent carboxylation of propionyl CoA,[13] but has not been detected before in natural glycerides. The HMBC spectrum also defined the attachment of the acyl units, since the glyceryl methine (H-2, δ 5.35) showed a cross-peak with the ester carbonyl at δ 173.0 of the lauryl group.

Santinol D (**8**) ($C_{29}H_{50}O_7$) was found to be closely related to santinol C, differing only for the homologation of the α-methyl-branched acyl moiety to 2,4-dimethyl-3-oxo-enanthate. In particular, the COSY spectrum of this acyl moiety disclosed two different spin systems (H-2‴−H_3-8‴ and a C_5 residue spanning from H_3-9‴ to H_3-7‴), for which the proton resonances were associated with those of the corresponding carbons by a HSQC experiment. Analysis of the HMBC cross-peak (H_3-8‴ with both the ester carbonyl at δ 170.3 and a ketone carbonyl at δ 209.3 along with the cross-peak of H_3-9‴ with the same ketone carbonyl) made it possible to combine the two spin systems into a final β-dicarbonyl acyl moiety, while the HMBC cross-peaks of H_2-3 with C-1″ secured the attachment of this unit at *O*-3. Given the structural resemblances of santinols C and D with santinol A, especially in relation to the presence and location of the angeloyl moiety, it seems reasonable to assume that they share the same 2*S* configuration, while the configuration of the methyl-bearing acyl chain stereocenters of **6** and **7** could not be assigned. The branched acyl moiety of santinol D is unknown as a natural product and is structurally related to the pyrone moiety of arzanol (**1a**) and helipyrone (**4**), differing, however, by the location of the methyl groups. While a biogenetic polyketide derivation seems obvious for the fatty acyl moieties of santinols, their *raison d'être* is unclear. They could either represent aborted attempts to convert short ketide moieties into pyrones, the major constituents of the plant, or, otherwise, have a more precise and yet elusive role, with a general inclusion in cell membranes being ruled out by their low isolation yields (ca. 0.001%). Unusual lipids have been isolated from the Mediterranean plant *Thapsia garganica* L.,[14] suggesting that the distribution of this compound class deserves systematic studies.

Apart from the santinols, fraction C also contained a mixture of medium- and long-chain tremetone derivatives. The oleyl and the nonanoyl esters of bitalin A (**9a**,**b**),[15] both new compounds, could be obtained pure from this complex mixture. The isolation of an odd-number fatty acid ester was somewhat surprising and was confirmed by comparison with an authentic sample prepared by the esterification of bitalin A with nonanoic acid. Shorter chain esters of this benzofuran derivative were obtained from fractions D and E, along with the monomeric pyrone micropyrone (**10**).[2] While the acetate (**9c**), the isobutyrate (**9e**), and the α-methylbutyrate (**9f**) ester are known,[16] the propionate (**9d**) and the isocaproate (**9g**) are new. The structure elucidation of the new esters of bitalin A was straightforward. Consequently, the benzofuran core showed the signals (data for **9d** as an example) of two ABX systems, one aromatic (δ_H 7.81, 7.80, and 6.82) and the other aliphatic (δ_H 5.39, 3.42, and 3.20), and of an oxymethylene (δ_H 4.70 and 4.63), an sp^2-*exo*methylene (δ_H 5.37 and 5.39), and one acetyl (δ_H 2.53), while the acyl moieties were all common structural elements of phytochemicals. All tremetone esters showed a negative sign of optical rotation, suggesting the same configuration at the single stereogenic center of the dihydrobenzofuran core.

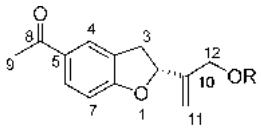

R
9a Oleoyl
9b *n*-Nonanoyl
9c Acetyl
9d Propionyl
9e *i*-Butyryl
9f α-Methylbutyryl
9g *i*-Caproyl

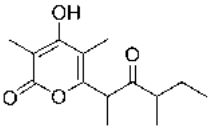

10

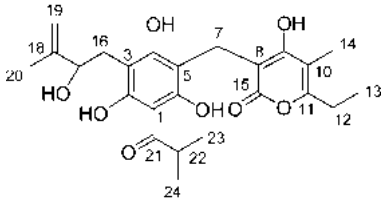

11

Fraction F contained heterodimeric pyrones. Arzanol (**1a**), the major constituent of the plant, could be crystallized from ether, and chromatographic purification of the mother liquors afforded the known less polar homologues **1b** and **1c**[16] and the novel more polar derivative **11**, which we have named heliarzanol. The heterodimer **1c** shows a stereogenic center in its acyl moiety. Given the polyketide derivation of acylphloroglucinols, it seems reasonable to assume that **1c** is assembled from an isoleucine-derived acyl starter. If so, the configuration of the stereogenic carbon on **1c** should be *S*.

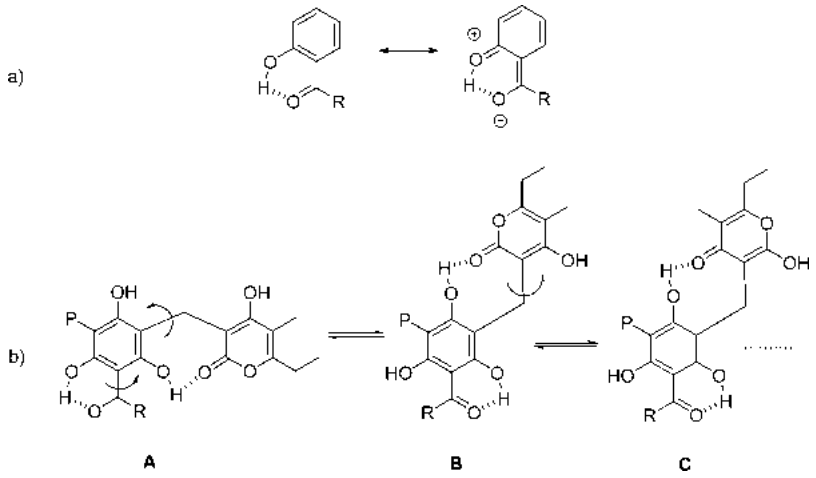

Figure 2. (a) Resonance-enhanced hydrogen bonding in *ortho*-hydroxylated phenones. (b) Possible rotameric and tautomeric processes involved in arzanol-type heterodimers (P = prenyl group; R = alkyl group).

Table 1. MIC (μg/mL) Values of a Selection of Phenolics from *Helichrysum italicum* subsp. *microphyllum* (ns > 128 μg/mL)

compound	SA1199B	Xu212	ATCC25943	RN4220	EMRSA15	EMRSA16
arzanol (**1a**)	1	4	1	2	4	2
micropyrone (**10**)	ns	ns	ns	128	ns	128
helipyrone (**4**)	ns	ns	64	12	ns	128
3a	ns	ns	ns	ns	ns	ns
3b	ns	ns	ns	ns	ns	ns
9a	ns	ns	ns	ns	ns	ns
9b	ns	ns	ns	ns	ns	ns
9c	ns	ns	ns	ns	ns	ns
methylarzanol (**12**)	ns	ns	ns	ns	ns	ns
cycloarzanol A (**13**)	128	128	32	32	128	ns
cycloarzanol B (**14**)	ns	ns	ns	ns	ns	ns
15a	32	128	128	32	32	128
15b	4	8	4	4	8	8
15c	16	4	8	2	6	8
15d	1	16	1	2	2	2
15e	128	ns	64	128	128	128
15f	16	16	8	8	16	8
norfloxacin	32	8	0.5	0.5	0.5	128

Heliarzanol (**11**), $C_{24}H_{30}O_8$ by HRESIMS, was identified as an arzanol-type compound on the basis of its NMR data. The ^{13}C NMR spectrum of **11** showed 24 well-resolved signals and the resonances typical of the *Helichrysum* phloroglucinyl α-pyrones (from C-1 to C-15), with differences, however, on the prenyl moiety. Accordingly, the ^1H NMR spectrum of **11** ($CDCl_3$, 500 MHz) showed signals typical of the arzanol heterodimeric motif, including a deshielded methyl singlet (CH_3-14, δ 1.95), an ethyl group, and a methylene broad singlet (H_2-7, δ 3.70). The resonances of an additional methyl singlet (δ 1.86), a sp^2 methylene group, and six multiplets, sorted as an isopropyl and a CH_2CH-OH moiety by means of a 2D COSY spectrum, were also evident in the ^1H NMR spectrum of heliarzanol (**11**). Association of all the proton resonances with those of the directly bound carbon atoms was obtained by the HSQC spectrum, and this allowed the correct interpretation of the HMBC spectrum. In addition to allowing the unambiguous location of methyl and ethyl groups on the pyrone moiety and confirming the presence of the methylene bridge (cross-peaks of H_2-7 with C-4, C-5, C-6, C-8, C-9, C-15) to connect the two rings, the HMBC spectrum also allowed the identification of substituents at C-1 and C-3. In particular, the deshielded isopropyl methine at δ 3.11 showed HMBC cross-peaks with a ketone carbonyl (δ 204.1) and with C-1 (δ 106.1), while cross-peaks of the oxymethine at δ 4.34 (H-17) with C-3, C-20, and the sp^2 carbons C-18 and C-19 allowed the elucidation of the C-3 side chain and defined the full planar structure of heliarzanol as shown in **11**.

Some nonexchangeable signals in the ^1H and ^{13}C NMR spectra of arzanol and its analogues were rather broad at room temperature and were sharpened by heating to 60 °C, suggesting the presence of slow conformational interconversion between different rotameric and/or tautomeric forms. *ortho*-Hydroxylated phenones show resonance-enhanced hydrogen bonding (Figure 2a) that slows rotation around the bond linking the acyl moiety to the aromatic ring.[17] As the phenolic hydroxy groups adjacent to the methylene bridge can form intramolecular hydrogen bonding with the oxygen function at C-2 and C-4 of the pyrone moiety, the rotameric equilibrium could, in principle, involve the interconversion of extensively hydrogen-bonded conformations around the bonds that link the phloroglucinyl core to its acyl and pyronylmethyl substituents (Figure 2b, rotamers A and B). Since the 4-hydroxypyrone ring can, in turn, exist in two distinct tautomeric

forms, this scenario is further complicated by the involvement of different tautomeric forms of the pyrone moiety and rotation around the other bond of the pivotal methylene linker (cf., **B** and **C** in Figure 2b). These conformational issues are quite general for homo- and heterodimeric acylphloroglucinols,[18] an important class of natural products, but have not yet been investigated systematically.

Extracts of *Helichrysum* are used in folk medicine for the management of bacterial infection of the skin and the oral cavity, a use backed up by clinical observations[1] and by the development in the former Soviet Union of arenarin (a mixture of phloroglucinols from *Helichrysum arenarium* L.) as a skin and eye antibacterial agent.[4,19] It was therefore interesting to evaluate if, and to what extent, the phenolics from *Helichrysum* have significant activity against multidrug-resistant bacterial strains, a current medicinal urgency in both hospital and community settings especially for *Staphylococcus aureus*.[5]

Multidrug- and methicillin-resistant strains of *S. aureus* can efflux antibiotics from the cell by means of a pump in the cytoplasmic membrane. Some of these pumps, such as NorA and QacA, are able to efflux a range of antibiotics, antiseptics, and structurally unrelated compounds.[20] Other pumps are more specific, for example TetK, which effluxes tetracycline. Simple, nonprenylated acylphloroglucinol derivatives show, in general, only modest antibacterial activity, enhanced, however, by *C*-prenylation.[21] The very potent antibacterial action of arzanol demonstrated enhanced activity by the addition of a pyrone substituent. Arzanol had notable activities against *S. aureus* 1199B, which overexpresses the NorA pump (1 μg/L), EMRSA-16 (2 μg/L), and XU 212 (4 μg/L), all of which were lower than the MIC of the standard control antibiotic norfloxacin (Table 1). By analogy with the results of the anti-inflammatory assays,[2] the bitalin esters (**9a**–**g**) were inactive, as were the coumarates and the simple pyrone micropyrone (**10**), while the pyrone homodimer helipyrone (**4**) was only marginally active. The chimeric structure of arzanol, combining two distinct polyketide elements with prenylation and heterodimerization, seems therefore optimized for bioactivity, in terms of both antibacterial and anti-inflammatory action.

Having validated arzanol (**1a**) as a lead structure for antibacterial activity, we also investigated the activity of some derivatives of the natural product and synthetic analogues available from a study on the total synthesis of arzanol.[22] Remarkably, both methylation of the pyrone moiety (**12**) and cyclization of the prenyl moiety (**13**, **14**) led to loss of activity (Table 1), suggesting that hydroxylation of the *ortho*-position of the phloracetophene core and of the pyrone moiety were critical for the antibacterial activity of arzanol, again in perfect analogy with the results of anti-inflammatory evaluation.[3] The development of a total synthesis of the natural product made it possible to also evaluate the effect of the introduction of a substituent on the methylene linker and of the simplification of the pyrone substitution pattern. The introduction of a substituent on the methylene linker [methyl (**15a**), hexyl (**15b**), phenyl (**15c**)] led to a modest decrease in their antibacterial activity and not to an increase of potency, as seen in the MICs value ranges (1–128 μg/L). On the other hand, the replacement of the pyrone moiety of the natural product with dehydroacetic acid led to a substantial retention of activity both in the natural product series (**15d**) and in its substituted analogues **15e** and **15f**. Taken together, these observations show that the antibacterial action of arzanol is critically sensitive to changes involving the hydroxy groups, while the pyrone

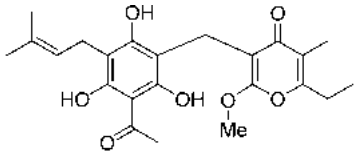

12

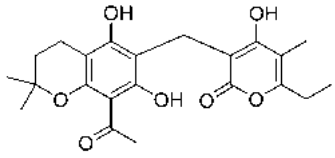

13

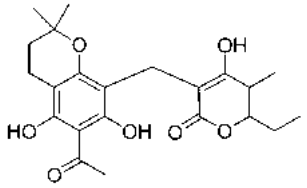

14

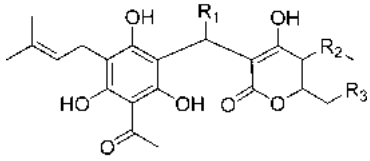

	R_1	R_2	R_3
15a	Me	Me	Et
15b	*n*-Hexanoyl	Me	Et
15c	Phenyl	Me	Et
15d	H	H	H
15e	Me	H	H
15f	*n*-Hexanoyl	H	H

substitution pattern can be simplified and the introduction of a substituent on the methylene linker may provide no advantage. The potent activity of arzanol and its strict structure–activity relationships suggested that a specific target underlies its antibacterial activity. Arzanol is a powerful inhibitor of the transition-metal (iron, copper)-promoted oxidative degradation of lipids (linoleic acid, cholesterol)[23] and inhibits pro-inflammatory targets involving redox reactions [(mPGES)-1,5-LO].[3] It is therefore tempting to speculate that it might interfere with a bacterial target that uses a transition metal redox system.

The anti-inflammatory and antibacterial action of helichrysine was investigated clinically in the 1940s, at the onset of research on corticosteroids and antibiotics.[1] The extraordinary success of these agents made interest in helichrysine fade quickly, despite its excellent clinical performance[1] and the observation that its clinical profile summarized the action of both classes of drugs. Seventy years later, we believe that arzanol (**1a**) has the potential to play a role in addressing the major limitations of antibiotics and corticosteroids, namely, the selection of resistant strains for the former and the development of side-effects for the latter.

EXPERIMENTAL SECTION

General Experimental Procedures. Optical rotations ($CHCl_3$) were measured at 589 nm on a JASCO P2000 polarimeter, and IR spectra on a FT-IR Thermo Nicolet apparatus. ^1H (500 MHz) and ^{13}C

dx.doi.org/10.1021/np3007149 | *J. Nat. Prod.* 2013, 76, 346–353

(125 MHz) NMR spectra were measured on a Varian INOVA spectrometer. Chemical shifts were referenced to the residual solvent signal ($CDCl_3$: δ_H = 7.26, δ_C = 77.0, CD_3OD: δ_H = 3.34, δ_C = 49.0). Homonuclear ^1H connectivities were determined by the COSY experiment. One-bond heteronuclear $^1H-^{13}C$ connectivities were determined with the HSQC experiment. Through-space ^1H connectivities were evidenced using a ROESY experiment with a mixing time of 250 ms. Two- and three-bond $^1H-^{13}C$ connectivities were determined by gradient 2D HMBC experiments optimized for a $^{2,3}J$ = 9 Hz. Low- and high-resolution ESIMS were obtained on a LTQ OrbitrapXL (Thermo Scientific) mass spectrometer. Silica gel 60 (70–230 mesh) and RP-18 used for gravity column chromatography were purchased from Macherey-Nagel. Reactions were monitored by TLC on Merck 60 F254 (0.25 mm) plates, which were visualized by UV inspection and/or staining with 5% H_2SO_4 in ethanol and heating. Organic phases were dried with Na_2SO_4 before evaporation. HPLC separations were achieved on a Knauer apparatus equipped with a refractive index detector. The Knauer HPLC apparatus was used to purify all final products. LUNA (normal-phase, SI60, or reversed-phase RP-18, 250 × 4 mm) (Phenomenex) columns were used, with 0.7 mL/min as flow rate.

Plant Material. Flowered aerial parts of *H. italicum* subsp. *microphyllum* were collected around Arzana (Sardinia) at the beginning of July 2010. The plant material was identified by M.B., and a voucher specimen (number 729/10) is kept at the General Herbarium of the Botany Department of the University of Cagliari.

Extraction and Isolation. Powdered nonwoody aerial parts (flowers and leaves, 5 kg) of *H. italicum* subsp. *microphyllum* were extracted at room temperature with acetone (2 × 15 L). Evaporation of the solvent left a black, gummy residue (202 g, 4.0%), part of which (50 g) was partitioned between petroleum ether (1.5 L) and aqueous methanol (1:9, 1.5 L). A 5 L round-bottom flask was used, connected to a rotatory evaporator stirring motor. After stirring for 1 h in a water bath at 30 °C, the two phases were separated to afford, after evaporation, 10.3 g of petroleum ether phase and 29.4 g of aqueous methanol phase. The semisolid material resisting partition (8.2 g) was purified by refluxing in acetone (200 mL) for 10 min. Cooling at room temperature and then in the refrigerator at 4 °C afforded 5.1 g (0.40%) of crude ursolic acid, which was further purified from impurities of oleanolic acid by recrystallization from methanol. The petroleum ether phase (11.3 g) was dissolved in methanol (300 mL) and then cooled at 4 °C overnight. After filtration of the copious precipitate of waxes and triglycerides, the filtrate (7 g) was purified by filtration over neutral alumina and further fractionated by gravity column chromatography on silica gel (200 g, petroleum ether–EtOAc, 9:1, as eluant) to afford neryl acetate (290 mg), ω-oleoyloxylinalol,[2] and a mixture of the coumarates **3a**,**b** (42 mg, ca. 35 ppm in the dry plant material), which could be separated by preparative HPLC (petroleum ether–EtOAc, 9:1, as eluant). The aqueous methanol phase (24.7 g) was fractionated coarsely by gravity column chromatography on silica gel (400 g, petroleum ether–EtOAc gradient) into five fractions (B–F), and, in turns, these were variously purified. Fraction B (3.4 g) was crystallized from ether to afford helipyrone (**4**, 320 mg, 256 ppm from the dry plant material). The mother liquors were further purified by gravity column chromatography on silica gel (150 g, petroleum ether–EtOAc, 7:3) to afford the bitalin A ester **9a** (21 mg, 17 ppm in the dried plant material) and **9b** (35 mg, 28 ppm in the dried plant material) and a mixture of santinol diesters and triesters. This was further fractionated by HPLC on normal phase (hexane–EtOAc, 8:2) to afford two subfractions, which eventually yielded pure compounds by further chromatographic separation. The mixture of santinols A1–A3 (ca. 200 mg, 160 ppm in the dried plant material) was resolved using MeOH–H_2O, 93:7, as eluant, affording santinol A1 (**5a**, 15.3 mg, 12.2 ppm in the dried plant material), santinol A2 (**5b**, 8.6 mg, 70 ppm in the dried plant material), and santinol A3 (**5c**, 7.1 mg, ca. 60 ppm in dried plant material). The second, less polar santinol subfraction (180 mg) was subjected to chromatography over a silica gel column (230–400 mesh) eluting with a solvent gradient of increasing polarity from *n*-hexane to EtOAc. Fractions eluted with *n*-hexane–EtOAc (9:1) were rechromatographed by HPLC (*n*-hexane–EtOAc, 9:1) to give santinols D (**8**, 3.7 mg, ca. 3 ppm in dried plant material) and C (**7**, 2.5 mg, ca. 2 ppm in the dried plant material). Fractions eluted with *n*-hexane–EtOAc, 8:2, were subjected to repeated HPLC chromatography (*n*-hexane–EtOAc, 85:15), affording santinol B (**6**, 1.5 mg, ca. 1 ppm in the dried plant material). Fractions D (1.6 g) and E (1.1 g) contained, along with micropyrone (**10**, overall yield 130 ppm on dried plant material after trituration with ether of a combination of two subfractions), a complex mixture of esters of bitalin A, from which pure compounds were obtained using a combination of chromatographic purifications on silica gel. Thus, a mixture of **9d** and **9g** (126 mg) obtained from the purification of fractions D and E by gravity column chromatography on silica gel was subjected to HPLC (*n*-hexane–EtOAc, 8:2) to yield **9d** (2.0 mg) and **9g** (1.1 mg). Fraction F was crystallized from ether to afford arzanol (3.1 g) as a yellow powder. The mother liquors (2.9 g) were fractionated by gravity colum chromatography to afford a further 600 mg of arzanol (overall yield 3.0%) and a mixture of analogues (250 mg), which was resolved by preparative HPLC on normal-phase silica gel (hexane–EtOAc, 55:45), affording pure heliarzanol (**11**, 4.5 mg, 3.6 ppm in dried plant material), **1b** (12 mg, 10 ppm in dried plant material), and **1c** (31 mg, 25 mg in dried plant material).

*Santinol A1 (**5a**):* colorless oil; $[\alpha]_D$ +3.5 (*c* 0.2, $CHCl_3$); ^1H NMR ($CDCl_3$, 500 MHz) δ 6.12 (1H, dq, *J* = 7.4, 2.0 Hz, H-3′), 4.28 (1H, overlapped, H-1a), 4.23 (1H, overlapped, H-3a), 4.22 (1H, overlapped, H-1b), 4.16 (1H, overlapped, H-3b), 4.14 (1H, m, H-2), 2.35 (2H, t, *J* = 7.8 Hz, H_2-2″), 1.99 (3H, d, *J* = 7.4 Hz, H_3-4′), 1.90 (3H, brs, H_3-5′), 1.63 (1H, m, H-10″), 1.60 (2H, overlapped, H_2-3″), 1.25 (10H, m, H_2-4″ to H_2-8″), 1.15 (2H, m, H_2-9″), 0.87 (6H, d, *J* = 6.7 Hz, H_3-11″ and H_3-12″); ^{13}C NMR ($CDCl_3$, 125 MHz) δ 174.4 (s, C-1″), 168.3 (s, C-1′), 139.6 (d, C-3′), 127.4 (s, C-2′), 68.6 (d, C-2), 65.4 (t, C-3), 65.2 (t, C-1), 39.4 (t, C-9″), 34.4 (t, C-2″), 29.6 (t, C-4″ to C-8″), 28.0 (d, C-10″), 25.3 (t, C-3″), 22.9 (q, C-11″ and C-12″), 20.9 (q, C-5′), 16.2 (q, C-4′); (+) ESIMS *m*/*z* 379 $[M + Na]^+$; HRESIMS *m*/*z* 379.2456 (calcd for $C_{20}H_{36}O_5Na$, 379.2460).

*Santinol A2 (**5b**):* colorless oil; $[\alpha]_D$ +3.2 (*c* 0.2, $CHCl_3$); ^1H NMR spectrum ($CDCl_3$, 500 MHz) was identical to that of **5a**, except for the integration of the signal at δ_H 1.25 (14H); (+) ESIMS *m*/*z* 407 $[M + Na]^+$; HRESIMS *m*/*z* 407.2777 (calcd for $C_{22}H_{40}O_5Na$, 407.2773).

*Santinol A3 (**5c**):* colorless oil; $[\alpha]_D$ +2.7 (*c* 0.2, $CHCl_3$); ^1H NMR spectrum ($CDCl_3$, 500 MHz) was identical to that of **5a** except for the integration of the signal at δ_H 1.25 (18H); (+) ESIMS *m*/*z* 435 $[M + Na]^+$; HRESIMS *m*/*z* 435.3090 (calcd for $C_{24}H_{44}O_5Na$, 435.3086).

Mosher Ester Analysis of Santinol A1. Santinol A1 (**5a**, 2.0 mg) was treated with *R*-MTPA chloride (30 μL) in 400 μL of dry pyridine with a catalytic amount of DMAP overnight at room temperature. The solvent was then removed, and the product was purified by HPLC (*n*-hexane–EtOAc, 85:15) to obtain the *S*-MTPA ester **5d** (1.8 mg). When santinol A1 (**5a**, 2.0 mg) was treated with *S*-MTPA chloride, following the same procedure, 1.7 mg of the *R*-MTPA ester **5e** was obtained.

*Santinol A1 (S)-MTPA ester **5d**:* ^1H NMR (500 MHz, $CDCl_3$) δ (selected values) 5.58 (1H, m, H-2), 4.44 (1H, dd, *J* = 12.3, 3.5 Hz, H-3a), 4.37 (1H, dd, *J* = 12.3, 4.0 Hz, H-1a), 4.30 (1H, dd, *J* = 12.3, 6.0 Hz, H-1b), 4.14 (1H, dd, *J* = 12.3, 7.2 Hz, H-3b); ESIMS (positive ion) *m*/*z* 595 $[M + Na]^+$.

*Santinol A1 (R)-MTPA ester **5e**:* ^1H NMR (500 MHz, $CDCl_3$) δ (selected values) 5.58 (1H, m, H-2), 4.46 (1H, dd, *J* = 12.3, 3.5 Hz, H-3a), 4.37 (1H, dd, *J* = 12.3, 4.0 Hz, H-1a), 4.25 (1H, dd, *J* = 12.3, 6.0 Hz, H-1b), 4.21 (1H, dd, *J* = 12.3, 7.2 Hz, H-3b); ESIMS (positive ion) *m*/*z* 595 $[M + Na]^+$.

*Santinol B (**6**):* colorless oil; ^1H NMR ($CDCl_3$, 500 MHz) δ 6.15 (2H, dq, *J* = 7.4, 2.0 Hz, H-3′ = H-3″), 4.24–4.22 (4H, m, H_2-1 and H_2-3), 4.20 (1H, m, H-2), 1.99 (6H, d, *J* = 7.4 Hz, H-4′ = H-4″), 1.88 (6H, brs, H_3-5′ and H_3-5″); ^{13}C NMR ($CDCl_3$, 125 MHz) δ 167.4 (s, C-1′ = C-1″), 139.7 (d, C-3′ = C-3″), 127.7 (s, C-2′ = C-2″), 68.5 (d, C-2), 65.0 (t, C-1 = C-3), 20.9 (q, C-5′ = C-5″), 16.1 (q, C-4′ = C-4″); (+) ESIMS *m*/*z* 279 $[M + Na]^+$; HRESIMS *m*/*z* 279.1211 (calcd for $C_{13}H_{20}O_5Na$, 279.1208).

*Santinol C (**7**):* colorless oil; $[\alpha]_D$ −8.5 (*c* 0.1 in $CHCl_3$); ^1H NMR ($CDCl_3$, 500 MHz) δ 6.12 (1H, dq, *J* = 7.0, 2.0 Hz, H-3′), 5.35 (1H,

m, H-2), 4.37 (1H, dd, J = 12.3, 3.5 Hz, H-3a), 4.35 (1H, dd, J = 12.3, 4.0 Hz, H-1a), 4.21 (1H, overlapped, H-3b), 4.20 (1H, overlapped, H-1b), 3.55 (1H, q, J = 7.1 Hz, H-2‴), 2.60 (1H, m, H-4‴a,), 2.54 (1H, m, H-4‴b), 2.30 (2H, t, J = 7.5 Hz, H_2-2″), 1.99 (3H, d, J = 7.0 Hz, H_3-4′), 1.88 (3H, brs, H_3-5′), 1.60 (2H, m, H_2-3″), 1.34 (3H, d, J = 7.1 Hz, H_3-6‴), 1.26 (16H, m, from H_2-4″ to H_2-11″), 1.06 (3H, t, J = 7.2 Hz, H_3-5‴), 0.88 (3H, t, J = 6.9 Hz, H_3-12″); ^{13}C NMR ($CDCl_3$, 125 MHz) δ 206.1 (s, C-3‴), 173.0 (s, C-1″), 170.3 (s, C-1‴), 167.4 (s, C-1′), 139.7 (d, C-3′), 127.7 (s, C-2′), 68.6 (d, C-2), 63.3 (t, C-3), 62.0 (t, C-1), 52.6 (d, C-2‴), 35.1 (t, C-4‴), 34.4 (t, C-2″), 29.9 (t, C-4″ to C-11″), 25.8 (t, C-3″), 20.8 (q, C-5′), 16.1 (q, C-4′), 14.7 (q, C-12″), 13.1 (q, C-6‴), 8.8 (q, C-5‴); (+) ESIMS m/z 491 $[M + Na]^+$; HRESIMS m/z 491.2993 (calcd for $C_{26}H_{44}O_7Na$, 491.2985).

*Santinol D (**8**):* colorless oil; $[\alpha]_D$ +24.9 (c 0.4 in $CHCl_3$); ^{1}H NMR ($CDCl_3$, 500 MHz) δ 6.13 (1H, dq, J = 7.0, 2.0 Hz, H-3′), 5.35 (1H, m, H-2), 4.37 (1H, dd, J = 12.3, 3.5 Hz, H-3a), 4.35 (1H, dd, J = 12.3, 4.0 Hz, H-1a), 4.21 (1H, overlapped, H-3b), 4.20 (1H, overlapped, H-1b), 3.76 (1H, q, J = 7.1 Hz, H-2‴), 2.80 (1H, m, H-4‴), 2.30 (2H, t, J = 7.5 Hz, H_2-2″), 1.99 (3H, d, J = 7.0 Hz, H_3-4′), 1.87 (3H, brs, H_3-5′), 1.60 (2H, m, H_2-3″), 1.55 (2H, m, H-5‴), 1.34 (3H, d, J = 7.1 Hz, H_3-8‴), 1.26 (16H, m, from H_2-4″ to H_2-11″), 1.25 (2H, m, H_2-6‴), 1.13 (3H, d, J = 7.1 Hz, H-9‴), 0.88 (3H, t, J = 6.9 Hz, H_3-12″), 0.87 (3H, t, J = 7.0 Hz, H-7‴); ^{13}C NMR ($CDCl_3$, 125 MHz) δ 209.3 (s, C-3‴), 173.0 (s, C-1″), 170.3 (s, C-1″), 167.5 (s, C-1′), 139.7 (d, C-3′), 127.6 (s, C-2′), 68.6 (d, C-2), 63.3 (t, C-3), 62.0 (t, C-1), 52.9 (d, C-2‴), 43.5 (d, C-4‴), 34.4 (t, C-2″), 33.5 (t, C-5‴), 29.9 (from C-4″ to C-11″), 25.8 (t, C-3″), 20.5 (t, C-6‴), 20.5 (q, C-5′), 16.3 (q, C-4′), 15.5 (q, C-9‴), 14.7 (q, C-12″), 14.1 (q, C-7‴), 13.2 (q, C-8‴); (+) ESIMS m/z 533 $[M + Na]^+$; HRESIMS m/z 533.3457 (calcd for $C_{29}H_{50}O_7Na$, 533.3454).

*Oleoylbitalin A (**9a**):* waxy gum; $[\alpha]_D$ −75 (c 0.2, $CHCl_3$); ^{1}H NMR ($CDCl_3$, 500 MHz) δ 7.82 (1H, s, H-4), 7.79 (1H, d, J = 6.2 Hz, H-6) 6.82 (1H, d, J = 6.2 Hz, H-7), 5.40 (1H, t, J = 8.0 Hz, H-2), 5.38 (2H, brs, H-9′ and H-10′), 5.36 (1H, brs, H-11a), 5.32 (1H, brs, H-11b), 4.71 (1H, d, J = 13.2 Hz, H-12a), 4.66 (1H, d, J = 13.2 Hz, H-12b), 3.44 (1H, dd, J = 15.0, 8.0 Hz, H-3a,), 3.20 (1H, dd, J = 15.0, 8.0 Hz, H-3b), 2.53 (3H, s, H_3-9), 2.28 (2H, t, J = 7.2 Hz, H_2-2′), 2.00 (6H, brs, H_2-3′, H_2-8′ and H_2-11′), 1.28 (22H, brs), 0.86 (3H, t, J = 7.2 Hz, H_3-18′); ^{13}C NMR ($CDCl_3$, 125 MHz) δ 196.6 (s, C-8), 173.1 (s, C-1′), 163.2 (s, C-7a), 142.7 (s, C-10), 131.1 (s, C-5), 130.6 (d, C-9′ and C-10′), 130.5 (d, C-4), 127.2 (s, C-3a), 124.8 (d, C-6), 114.6 (t, C-11), 109.1 (d, C-7), 84.0 (d, C-2), 64.1 (t, C-12), 34.8 (t, C-3), 33.9, 33.8, 33.6 (t, C-2′, C-8′, and C-11′), 31.7 (t, C-16′), 29.8, 29.7, 29.5, 29.4, 29.3 (t, C-4′, C-5′, C-6′, C-7′, C-12′, C-13′, C-14′, and C-15′), 26.7 (q, C-9), 25.3 (t, C-3′), 22.5 (t, C-17′), 14.1 (q, C-18′); (+) ESIMS m/z 505 $[M + Na]^+$; HRESIMS m/z 505.3294 (calcd for $C_{31}H_{46}O_4Na$, 505.3294).

*Nonanoylbitalin A (**9b**):* waxy gum; $[\alpha]_D$ −65 (c 0.2, $CHCl_3$); ^{1}H NMR ($CDCl_3$, 500 MHz) δ 7.82 (1H, s, H-4), 7.79 (1H, d, J = 6.2 Hz, H-6), 6.82 (1H, d, J = 6.2 Hz, H-7), 5.39 (1H, t, J = 8.0 Hz, H-2), 5.36 (1H, brs, H-11a), 5.27 (1H, brs, H-11b), 4.73 (1H, d, J = 13.2 Hz, H-12a), 4.67 (1H, d, J = 13.2 Hz, H-12b), 3.48 (1H, dd, J = 15.0, 8.0 Hz, H-3a,), 3.20 (1H, dd, J = 15.0, 8.0 Hz, H-3b), 2.53 (3H, s, H_3-9), 2.27 (2H, t, J = 7.2 Hz, H_2-2′), 1.58 (4H, m, H_2-3′ and H_2-4′), 1.28 (8H, brs, H_2-5′- H_2-8′), 0.86 (3H, t, J = 7.2 Hz, H_3-3′); ^{13}C NMR ($CDCl_3$, 125 MHz) δ 196.0 (s, C-8), 172.9 (s, C-1′), 162.7 (s, C-7a), 142.3 (s, C-10), 131.4 (s, C-5), 130.2 (d, C-4), 127.2 (s, C-3a), 125.7 (d, C-6), 114.7 (t, C-11), 109.4 (d, C-7), 84.0 (d, C-2), 64.2 (t, C-12), 34.9 (t, C-3), 34.1 (t, C-2′), 31.8 (t. C-7′), 29.4, 29.3 (t, C-6′ and C-5′), 28.7 (t, C-4′), 26.7 (q, C-9), 25.0 (t, C-3′), 22.5 (t, C-8′), 13.8 (q, C-9′); (+) ESIMS m/z 381 $[M + Na]^+$; HRESIMS m/z 381.2056 (calcd for $C_{22}H_{30}O_4Na$, 381.2042).

*Propanoylbitalin A (**9d**):* colorless, amorphous solid; $[\alpha]_D$ −52.8 (c 0.2, $CHCl_3$); ^{1}H NMR ($CDCl_3$, 500 MHz) δ 7.81 (1H, s, H-4), 7.80 (1H, d, J = 6.2 Hz, H-6) 6.82 (1H, d, J = 6.2 Hz, H-7), 5.39 (1H, t, J = 8.0 Hz, H-2), 5.37 (1H, brs, H-11a), 5.29 (1H, brs, H-11b), 4.70 (1H, d, J = 13.2 Hz, H-12a), 4.63 (1H, d, J = 13.2 Hz, H-12b), 3.42 (1H, dd, J = 15.0, 8.0 Hz, H-3a,), 3.20 (1H, dd, J = 15.0, 8.0 Hz, H-3b), 2.53 (3H, s, H_3-9), 2.37 (2H, q, J = 7.2 Hz, H_2-2′), 1.16 (3H, t, J = 7.2 Hz, H_3-3′); ^{13}C NMR ($CDCl_3$, 125 MHz) 196.7 (s, C-8), 171.5 (s, C-1′), 163.7 (s, C-7a), 142.5 (s, C-10), 131.0 (s, C-5), 130.5 (d, C-4), 127.0 (s, C-3a), 125.7 (d, C-6), 114.9 (t, C-11), 109.2 (d, C-7), 84.2 (d, C-2), 64.1 (t, C-12), 34.6 (t, C-3), 28.1 (t, C-2′), 26.4 (q, C-9), 10.1 (q, C-3′); (+) ESIMS m/z 297 $[M + Na]^+$; HRESIMS m/z 297.1105 (calcd for $C_{16}H_{18}O_4Na$, 297.1103).

*Isocaproylbitalin A (**9g**):* colorless, amorphous solid; $[\alpha]_D$ −43.1 (c 0.1, $CHCl_3$); ^{1}H NMR ($CDCl_3$, 500 MHz) δ 7.81 (1H, s, H-4), 7.80 (1H, d, J = 6.2 Hz, H-6) 6.82 (1H, d, J = 6.2 Hz, H-7), 5.39 (1H, t, J = 8.0 Hz, H-2), 5.37 (1H, brs, H-11a), 5.29 (1H, brs, H-11b), 4.70 (1H, d, J = 13.2 Hz, H-12a), 4.63 (1H, d, J = 13.2 Hz, H-12b), 3.42 (1H, dd, J = 15.0, 8.0 Hz, H-3a), 3.20 (1H, dd, J = 15.0, 8.0 Hz, H-3b), 2.53 (3H, s, H_3-9), 2.25 (2H, t, J = 7.0 Hz, H_2-2′), 1.70 (1H, m, H-3′), 1.58 (2H, m, H_2-3′), 0.95 (6H, d, J = 7.0 Hz, H_3-5′ and H_3-6′); ^{13}C NMR ($CDCl_3$, 125 MHz) δ 196.7 (s, C-8), 171.3 (s, C-1′), 163.7 (s, C-7a), 142.5 (s, C-10), 131.0 (s, C-5), 130.5 (d, C-4), 127.0 (s, C-3a), 125.7 (d, C-6), 114.9 (t, C-11), 109.2 (d, C-7), 84.2 (d, C-2), 64.1 (t, C-12), 35.5 (t, C-3′), 34.6 (t, C-3), 31.8 (t, C-2′), 28.2 (d, C-4′), 26.4 (q, C-9), 23.0 (q, C-5′ and C-6′); (+) ESIMS m/z 339 $[M + Na]^+$; HRESIMS m/z 339.1582 (calcd for $C_{19}H_{24}O_4Na$, 339.1572).

*Heliarzanol (**11**):* pale yellow, amorphous solid; $[\alpha]_D$ +17.4 (c 0.15, CH_3OH); IR (KBr) ν_{max} 3331, 3000, 1675, 1625, 1570, 1321, 1175 cm^{-1}; ^{1}H NMR ($CDCl_3$, 500 MHz) δ 4.89 (2H, brs, H_2-19), 4.34 (1H, bt, J = 7.3 Hz, H-17), 3.70 (2H, brs, H_2-7), 3.22 (1H, dd, J = 11.5, 7.3 Hz, H-16a), 3.11 (1H, hept, J = 6.9 Hz, H-22), 2.85 (1H, dd, J = 11.5, 7.3 Hz, H-16b), 2.55 (2H, q, J = 6.9 Hz, H_2-12), 1.95 (3H, s, H_3-14), 1.86 (3H, brs, H_3-20), 1.20 (6H, d, J = 6.9 Hz, H_3-23 and H_3-24), 1.19 (3H, q, J = 6.9 Hz, H_3-13); ^{13}C NMR ($CDCl_3$, 125 MHz) δ 204.1 (s, C-21), 169.4 (s, C-15), 168.7 (s, C-9), 161.9 (s, C-4), 161.4 (s, C-11), 161.1 (s, C-6), 159.5 (s, C-2), 144.2 (s, C-18), 111.6 (t, C-19), 109.0 (s, C-10), 107.9 (s, C-3), 107.0 (s, C-5), 106.1 (s, C-1), 103.5 (s, C-8), 79.6 (d, C-17), 32.2 (t, C-16), 30.1 (d, C-22), 24.9 (t, C-12), 20.0 (q, C-23 and C-24), 19.2 (t, C-7), 18.1 (q, C-20), 11.9 (q, C-13), 10.0 (q, C-14); (−) ESIMS m/z 445 $[M - H]^-$; HRESIMS m/z 445.1866 (calcd for $C_{24}H_{29}O_8$, 445.1862).

*Synthesis of Nonanoylbitalin A (**9b**).* A solution of bitalin A (obtained by hydrolysis with methanolic KOH of a mixture of its esters, 104 mg, 0.45 mmol) in CH_2Cl_2 (3 mL) was treated sequentially with nonanoic acid (66 mg, 4.95 mmol, 1.1 molar equiv), DCC (108 mg, 4.95 mmol, 1.1 molar equiv), and DMAP (47 mg, 0.8 molar equiv). After stirring 12 h at room temperature, the reaction was diluted with ether (ca. 6 mL) and filtered over neutral alumina and then silica gel to obtain 119 mg (60%) of **9b** as a colorless, waxy solid, identical (^{1}H and ^{13}C NMR and MS) with the compound obtained by isolation.

Biological Assays. *Bacterial Strains.* Strain XU212, which possesses the TetK tetracycline efflux pump and is also resistant to methicillin and erythromycin, was a hospital isolate. XU212 and standard strain ATCC 25923 were obtained from Dr. Edet Udo.[24] Strain SA-1199B overexpresses the NorA MDR efflux pump and was provided by Prof. Glenn Kaatz.[25] RN4220, which has the MsrA macrolide efflux protein, was provided by J. Cove.[26] The epidemic methicillin-resistant strains EMRSA-15 and EMRSA-16 are hospital isolates[27,28] and were obtained from Dr. Paul Stapleton. All strains were cultured on nutrient agar (Oxoid) and incubated overnight at 37 °C prior to assay.

Minimum Inhibitory Concentration (MIC) Determination. Sterile Mueller-Hinton broth (MHB; Oxoid) (100 μL) containing 20 and 10 mg/L of Ca^{2+} and Mg^{2+}, respectively, was dispensed into 11 of the wells of a 96-well microliter plate (Nunc, 0.3 mL volume per well). All antibacterial agents apart from norfloxacin were dissolved in dimethylsulfoxide and diluted in MHB to give a stock solution. Then, 100 μL of the antibacterial agent stock solution (concentration 512 mg/L) was serially diluted into each well, and 100 μL of the bacterial innoculum was added to each well to give a final concentration range of 128−0.25 μg/L in the wells. All procedures were performed in duplicate, and the plates incubated for 18 h at 37 °C. A 20 μL aliquot of a 5 mg/L methanolic solution of 3-[4,5-dimethylthiazol-2-yl]-2,5-diphenyltetrazolium bromide (MTT; Sigma) was added to each well and incubated for 30 min. A blue coloration

indicated bacterial growth. The MIC was recorded as the lowest concentration at which no visible growth was observed.

■ ASSOCIATED CONTENT

Supporting Information

This material is available free of charge via the Internet at http://pubs.acs.org.

■ AUTHOR INFORMATION

Corresponding Author

*Tel: + 39 081 678509 (O.T.-S.); +39 0321 373744 (G.A.). Fax: + 39 081 678552 (O.T.-S.); +39 0321 0.375621 (G.A.). E-mail: scatagli@unina.it (O.T.-S.); appendino@pharm.unipmn.it (G.A.).

Notes

The authors declare no competing financial interest.

■ ACKNOWLEDGMENTS

We are grateful to MURST (Italy) for financial support (Project 2009RMW3Z5: Metodologie sintetiche per la generazione di diversità molecolare di rilevanza biologica). Mass and NMR spectra were recorded at "Centro di Servizio Interdipartimentale di Analisi Strumentale", Università di Napoli "Federico II".

■ DEDICATION

Dedicated to Dr. Lester A. Mitscher, of the University of Kansas, for his pioneering work on the discovery of bioactive natural products and their derivatives

■ REFERENCES

(1) Santini, L. *Minerva Med.* **1952**, *43*, 714−719.

(2) Appendino, G.; Ottino, M.; Marquez, N.; Bianchi, F.; Giana, A.; Ballero, M.; Sterner, O.; Fiebich, B. L.; Muñoz, E. *J. Nat. Prod.* **2007**, *70*, 608−612.

(3) Bauer, J.; Koeberle, A.; Dehm, F.; Pollastro, F.; Appendino, G.; Northoff, H.; Rossi, A.; Sautebin, L.; Werz, O. *Biochem. Pharmacol.* **2011**, *81*, 259−268.

(4) Negrash, A. K.; Pertsev, I. M.; Khristenko, L. A.; Salo, D. P. *Khim.-Farm. Zh.* **1977**, *11*, 107−110.

(5) Gibbons, S. *Nat. Prod. Rep.* **2004**, *21*, 263−277.

(6) Passerini, M.; Ridi, M.; Papini, P. *Ann. Chim.* **1954**, *74*, 783−786.

(7) Angioni, A.; Barra, A.; Arlorio, M.; Coisson, J. D.; Russo, M. T.; Pirisi, F. M.; Satta, M.; Cabras, P. *J. Agric. Food Chem.* **2003**, *51*, 1030−1034.

(8) Weyerstahl, P.; Marschall, H.; Bork, W.-R.; Reiner, S.; Wahlburg, H.-C. *Flav. Fragr. J.* **1995**, *10*, 297−311.

(9) (a) Zapesochnaya, G. G.; Dzyadevich, T. V.; Karasartov, B. S. *Khim Prir. Soedin* **1990**, 409−410. (b) Lakshmanan, D.; Werngren, J.; Jose, L.; Suja, K. P.; Nair, M. S.; Varma, R. L.; Mandayoor, S.; Hoffner, S.; Kumar, R. A. *Fitoterapia* **2011**, *82*, 757−761.

(10) Haensel, R.; Cybulski, E. M.; Cubukcu, B.; Mericli, A. H.; Bohlmann, F.; Zdero, C. *Phytochemistry* **1980**, *19*, 639−644.

(11) Leonardo Santini (1904−1983), an Italian physician, carried out the first systematic studies on the clinical anti-inflammatory properties of *H. italicum* (Santini, L. *Atti Soc. Lomb. Sci. Med. Biol.* **1949**, *5*, 18). Santini summarized the results of almost two decades of clinical observation on *H. italicum* in a review article that appeared in 1952.[1] On the basis of these studies, extracts of various *Helichrysum* species were introduced to the Italian pharmaceutical market for the treatment of cough. The quality and origin of these extracts were questioned by L. Santini (personal communication of his son, Maurizio Santini, to G.A.), and they were eventually removed from the pharmaceutical market in the 1970s. *H. italicum* shows a remarkable infraspecific variation in its phytochemical profile, even without its various subspecies,[7] and we have found that several commercial samples of the plant are totally devoid of pyrone derivatives. It is therefore unsurprising that, in the lack of a proper standardization, the early *Helichyrsum* pharmaceutical products were doomed to failure.

(12) Ohtani, I.; Kusumi, T.; Kashman, Y.; Kakisawa, H. *J. Am. Chem. Soc.* **1991**, *113*, 4092−4096.

(13) Lehnert, W.; Junker, A. *Clin. Chim. Acta* **1980**, *104*, 47−51.

(14) Liu, H.; Olsen, C.; Christensen, S. B. *J. Nat. Prod.* **2004**, *67*, 1439−1440.

(15) Bowen, D. M.; DeGraw, J. I.; Shah, V. R.; Bonner, W. A. *J. Org. Chem.* **1963**, *6*, 315−319.

(16) (a) Bohlmann, F.; Zdero, C. *Tetrahedron Lett.* **1970**, *41*, 3575−3576. (b) Haensel, R.; Cybulski, B.; Mericli, A. H.; Bohlmann, F.; Zdero, C. *Phytochemistry* **1980**, *19*, 639−644.

(17) Emsley, J. *Chem. Soc. Rev.* **1980**, *9*, 91−124.

(18) Crassipin A (Socolsky, C.; Rates, S. M. K.; Stein, A. C.; Asakawa, Y.; Bardon, A. *J. Nat. Prod.* **2012**, *75*, 1007−1017.) and myrtucommulone A (Appendino, G.; Bianchi, F.; Minassi, A.; Sterner, O.; Ballero, M.; Gibbons, S. *J. Nat. Prod.* **2002**, *65*, 334−338) exemplify phloroglucinyl heterodimers showing, respectively, two distinct sets of signals or very broad spectra in their NMR spectra at room temperature.

(19) Smirnov, V. V.; Fasil'ev, V. N.; Preobrazhenskaia, N. E.; Zhmura, L. V. *Mikrobiol. Zh.* **1990**, *52*, 56−59.

(20) Marshall, N. J; Piddock, L. J. V. *Microbiologia* **1997**, *13*, 285−300.

(21) Shiu, W. K. D.; Gibbons, S. *Phytochemistry* **2006**, *67*, 2568−2572.

(22) Minassi, A.; Cicione, L.; Koeberle, A.; Bauer, J.; Laufer, S.; Werz, O.; Appendino, G.; Appendino, G. *Eur. J. Org. Chem.* **2012**, 772−779.

(23) Rosa, A.; Pollastro, F.; Atzeri, A.; Appendino, G.; Melis, M. P.; Deiana, M.; Incani, A.; Loru, D.; Dessi, M. A. *Chem. Phys. Lipids* **2011**, *164*, 24−32.

(24) Gibbons, S.; Udo, E. E. *Phytother. Res.* **2000**, *14*, 139−140.

(25) Kaatz, G. W.; Seo, S. M.; Ruble, C. A. *Antimicrob. Agents Chemother.* **1993**, *37*, 1086−1094.

(26) Ross, J. I.; Farrell, A. M.; Eady, E. A; Cove, J. H.; Cunliffe, W. J. *J. Antimicrob. Chemother.* **1989**, *24*, 851−862.

(27) Richardson, J. F.; Reith, S. *J. Hosp. Infect.* **1993**, *25*, 45−52.

(28) Cox, R. A.; Conquest, C.; Mallaghan, C.; Marples, R. R. *J. Hosp. Infect.* **1995**, *29*, 87−106.

JOURNAL OF NATURAL PRODUCTS

Article

pubs.acs.org/jnp

Structural Characterization and Antimicrobial Evaluation of Atractyloside, Atractyligenin, and 15-Didehydroatractyligenin Methyl Ester

Federico Brucoli,* Maria T. Borrello, Paul Stapleton, Gary N. Parkinson, and Simon Gibbons

UCL School of Pharmacy, London, WC1N 1AX, U.K.

Supporting Information

ABSTRACT: We report the first complete structure elucidation of the *ent*-kaurane diterpenoid glycoside atractyloside (**1**) by means of NMR and X-ray diffractometry techniques. Extensive one- and two-dimensional NMR experiments were employed to assign the proton and carbon signals of **1**, and crystallography experiments established the configurations of all stereogenic centers. Furthermore, we present a novel semisynthetic route for the preparation of the highly cytotoxic aglycone derivative of **1**, 15-didehydroatractyligenin methyl ester (**3**). All compounds were tested for their antibiotic activity against *Enterococcus faecalis*, *Escherichia coli*, and several strains of *Staphylococcus aureus*, including fluoroquinolone-resistant (SA1199B) and two epidemic MRSA (EMRSA-15 and -16) strains. Compound **3** exhibited moderate activity against all of the *Staph. aureus* strains with an MIC value of 128 mg/L.

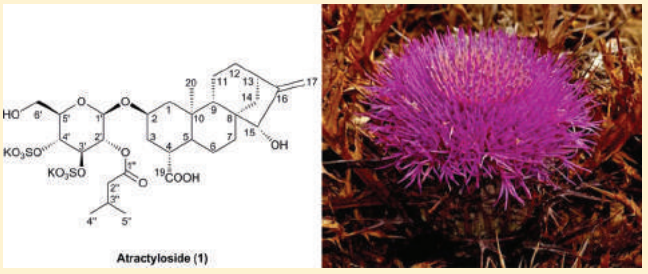

Atractylis gummifera L. (Asteraceae) is a thistle that grows throughout the Mediterranean region and is widely known for its acute toxicity.[1,2] Accidental ingestion of *A. gummifera* rhizomes still remains a cause of human poisoning, particularly during the spring or winter, when the content of the active plant principles, atractyloside (**1**) and its C-4 dicarboxylic acid derivative, carboxyatractyloside, are higher.[3,4] Atractyloside (**1**) was first isolated by Lefranc in 1868 from the roots of *A. gummifera*,[5] and several other atractyloside analogues, which all contain its aglycone derivative atractyligenin (**2**), were recently discovered in *Callilepsis laureola*,[6] *Widelia glauca*,[7] and species of various coffee plants (*Coffea arabica* and *Coffea robusta*).[8,9] The glucoside atractyloside consists of the tetracyclic *ent*-kaurane diterpene genin **2** attached through a β-linkage to the anomeric carbon of the D-(+)-glucose residue. Only one hydroxy group is free in the carbohydrate moiety (C-6′), while the others are either linked to a residue of isovaleric acid (C-2′) or transformed into two sulfate moieties (C-3′ and C-4′) (Figure 1).[10−12]

The mechanism of action of atractyloside and carboxyatractyloside has been elucidated and involves the inhibition of oxidative phosphorylation in the mitochondria of hepatocytes and proximal tubular epithelial cells.[13] These glucosides block the transport of adenosine diphosphate (ADP) into mitochondria by inhibiting the adenine nucleotide translocator (ANT) and impairing ATP production in the cell.[14,15] Atractyligenin (**2**) exerts similar, albeit weaker, biological activity compared to **1** and is about 150-fold less toxic,[13] suggesting that the glucose moiety and disulfuric and isovaleric acid residues increase the inhibitory effect on ATP production. Atractyloside (**1**) and atractyligenin (**2**) exhibit modest antiproliferative activity

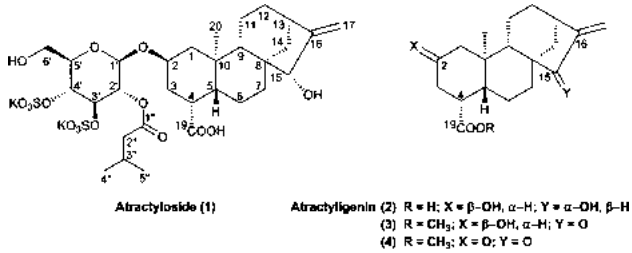

Figure 1. Structures of atractyloside (**1**), atractyligenin (**2**), and 15-didehydro- (**3**) and 2,15-di(didehydro)-atractyligenin methyl ester (**4**) derivatives.

against murine melanoma and metastatic (B-16)[16] and human chronic myelogenous leukemia (K-562)[17] cell lines, respectively. NMR structure elucidation of atractyloside (**1**) has been only partially achieved to date, and previous ^{1}H NMR spectroscopic data of **1** in DMSO-d_6 at 100 MHz reported only signals of H-1′, H-2′, H-3′, and H-4′ of the glucosyl moiety, *ent*-kaurane H_2-1, H-2, H_2-3, and H-4, *exo*-methylene H_2-17 (2H), and methyl CH_3-20 (3H).[7,13] Furthermore, NMR spectroscopy studies on the interactions of atractyloside with the mitochondrial ANT carrier reported incomplete carbon and no proton resonance assignments for **1**.[18] On the other hand, early resonance assignments made for carboxyatractyloside might provide a general reference for structure elucidation of the carbon skeleton of **1**.[19]

Received: January 27, 2012
Published: May 17, 2012

More recently, some naturally occurring and semisynthetic tetracyclic *ent*-kaurane diterpenoids, structurally related to **1** and **2**, have attracted attention due to their interesting anticancer, antibacterial, and anti-inflammatory activity.[20−22] In particular, a semisynthetic derivative of atractyloside (**1**), 15-didehydroatractyligenin methyl ester (**3**), exhibited significantly higher cytotoxicity against selected cancer cell lines compared to **1** and **2** (Figure 1).[22] This compound (**3**) contains in its molecular framework an *exo*-methylene group (C-16−C-17) conjugated with a carbonyl residue (C-15) and may exert its biological activity by acting as a Michael-type acceptor compound, with the α,β-unsaturated carbonyl system serving as the alkylating center.[23]

In this paper, we present the first complete structural characterization of **1** by NMR spectroscopy and X-ray crystallography. Results from ^{1}H and ^{13}C NMR spectra and COSY, NOESY, HSQC, and HMBC experiments were analyzed and employed to assign all carbon and proton signals of **1**. Crystallography experiments allowed evaluation of the atomic spatial arrangement of three independent molecules of **1** in the non-centrosymmetric space group $C\ 2\ 2\ 2_1$ and the determination of their absolute structures and configurations.

We also report some synthetic modification of the atractyloside structure including a novel semisynthetic route for the preparation of the highly cytotoxic derivative **3** starting from **1**. Selective oxidation of the 15-hydroxy group of **1** afforded compound **3** in good yield and purity, with an intact C-2 hydroxy group. The presence of a free hydroxy group in the molecule is a prerequisite for coupling with different residues, including various carbohydrate moieties, to improve its biological activity. The hydroxy group could also be amenable to enzymatic transformation within the cell or could be available to hydrogen-bond with H-acceptors of protein/DNA base pairs.

Finally, compounds **1**−**3** were evaluated for their antimicrobial activities against a number of Gram-positive cocci, including *Enterococcus faecalis* and different strains of methicillin- (MRSA) and antibiotic-resistant *Staphylococcus aureus*, and Gram-negative bacilli such as *Escherichia coli*.

RESULTS AND DISCUSSION

Synthetic modification of the atractyloside structure started with the hydrolysis of its glycosidic bond under basic conditions to give atractyligenin (**2**) (Scheme 1). The genin was characterized by NMR spectroscopy, and the assignments of its proton and carbon signals served as a reference in the NMR structure elucidation of **1** (Table 1).

Next, attention was focused on the synthesis of the 15-didehydroatractyligenin derivative **3**. Previous attempts to prepare **3** from atractyligenin methyl ester were partially efficient. Direct oxidation of the latter with MnO_2 led to a mixture of 15-didehydro- (**3**) and 2,15-di(didehydro)-atractyligenin methyl ester (**4**) derivatives (Figure 1).[21] A novel synthetic route for the preparation of **3** was developed, and selective oxidation of the C-15 hydroxy group was achieved utilizing the carbohydrate moiety of **1** as a protective group for the C-2 hydroxy group (Scheme 1). Methylation of **1** at C-19 using (trimethylsilyl)diazomethane ($TMSCH_2N_2$) gave atractyloside methyl ester **5**. The ^{1}H NMR spectrum of **5** showed the presence of both methyl ester and carbohydrate proton signals, indicating that it still comprised both the sugar and *ent*-kaurane moieties. At this stage, the original strategy would involve oxidation of the C-15 hydroxy group with the Dess-Martin

Scheme 1[a]

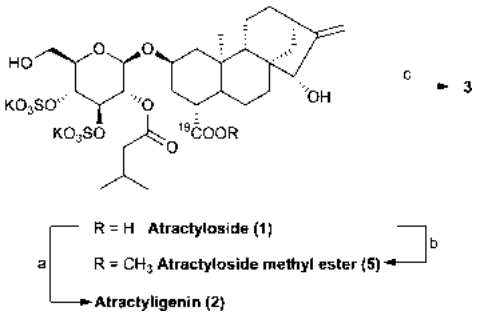

[a]Reagents and conditions: (a) 20% KOH in H_2O, 100 °C, 6 h; (b) $TMSCH_2N_2$, THF/MeOH (4:1 v/v), −78 °C to rt, 3 h; (c) DMP, CH_2Cl_2, 0 °C to rt, 3 h.

periodinane (DMP) and enzymatic or acidic cleavage of the glycosidic bond to give **3**. However, the use of an excess of DMP not only oxidized the C-15 hydroxy group but also cleaved the glycosidic bond, gratifyingly affording the 15-didehydro derivative **3** in two synthetic steps. The ^{1}H and ^{13}C NMR spectra of **3** showed the methyl ester signal at δ_H 3.67, the two broad methylene singlets at δ_H 5.95 and 5.26, which were shifted downfield compared to **1** and **2**, and the C-15 carbonyl at δ_C 210.2, confirming the completion of the reaction.

The unexpected oxidative cleavage of the glycosidic bond might take place as a side-reaction during the quenching of the oxidation reaction with concentrated aqueous NaOH solution. A possible mechanism is shown in Scheme 2. After oxidation of the C-15 alcohol group of **5**, the 15-oxokaurenoic and glucose residues were still joined by a glycosidic bond in **6**. Attack of the heterocyclic oxygen of **6** to iodinane (DMP) led to the formation of complex **7** with loss of an acetate ligand. This unstable intermediate (**7**) might be susceptible to cleavage of the pyranose ring by hydroxide ion and hydrolysis of residues R_2 and R_3 at C-2′, C-3′, and C-4′ to give **8**. Deprotonation at the C-1′ proton by an acetate ion would subsequently afford the pyranose derivative **9**, iodinane, and acetic acid. Finally, intramolecular esterification yielded δ-gluconolactone **10** and the 15-oxo derivative **3**. The proposed mechanism was corroborated by the presence of traces of δ-gluconolactone in the ^{1}H NMR spectrum of the $CHCl_3$ extracts of the neutralized aqueous solution after workup. No anomeric proton signals were detected in this spectrum.

The main challenge in determining the structure of atractyloside (**1**) by NMR spectroscopy was posed by the overlapping signals of nine protons pertaining to its *ent*-kaurane residue. The ^{1}H NMR spectrum of **1** in DMSO-d_6 at 500 MHz showed crowded regions at δ_H 1.56−1.49 (spin system A) and δ_H 1.38−1.28 (spin system B), integrating for four and five protons, respectively. Two-dimensional heteronuclear NMR experiments showed correlations between the A and B system protons and six carbon signals, including five methylene groups and one methine carbon. ^{1}H−^{13}C HSQC−DEPT135 experiments revealed that the methylene carbon signals at δ_C 17.5, 32.1, and 34.7 correlated with two protons each in systems A and B. These carbon signals were assigned to C-11, C-12, and C-7, respectively. The methylene carbon signal at δ_C 24.9 correlated with one multiplet at δ_H 1.78−1.73 (1H) and to one A spin system proton and was assigned to C-6. The methylene signal at δ_C 35.7 correlated with the overlapped doublet at δ_H 1.70 and with one B system proton and was assigned to C-14.

Table 1. ^{1}H and ^{13}C NMR Data for Compounds 1−3

	1[a]		2[b]		3[c]	
position	δ_H (J in Hz)	δ_C	δ_H (J in Hz)	δ_C	δ_H (J in Hz)	δ_C
1	2.18−2.15 m Hα, 0.64 t (11.9) Hβ	46.9, CH_2	2.20−2.15 m Hα, 0.73−0.67 m Hβ	50.4, CH_2	2.19 ddd (12.2, 4.5, 1.7) Hα, 0.73 t (11.7) Hβ	48.6, CH_2
2	4.06−4.00 m, overlapped	72.4, CH[d]	4.20−4.13 m	65.1, CH	4.25 ddd (15.8, 11.2, 4.5)	64.4, CH
3	2.23 dd (2.19, 1.75), 1.07 ddd (5.41, 5.30, 4.74)	34.2, CH_2	2.40−2.35 m, 1.27−1.23 m	38.3, CH_2	2.44−2.40 m, 1.26−1.24 m (2H)	37.6, CH_2
4	2.57 bs	45.5, CH_2	2.65 bs	44.9, CH	2.70 ddd (10.4, 5.2, 1.9)	43.7, CH_2
5	1.38−1.28 m (5H)	48.3, CH	1.54−1.46 m (4H)	NA[e]	1.55−1.52 m (2H)	48.4, CH
6	1.78−1.73 m, 1.56−149 m (4H)	24.9, CH_2	1.98−1.88 m, 1.71−1.61 m (4H)	26.7, CH_2	1.70−1.66 m (3H), 1.87−1.78 m (2H)	24.5, CH_2
7	1.56−149 m (4H), 1.38−1.28 m (5H)	34.7, CH_2	1.71−1.61 m (4H), 1.54−1.46 m (4H)	36.2, CH_2	1.94−1.89 m, 1.36−1.32 m	33.3, CH_2
8		47.1, C		NA[e]		52.2, C
9	0.97 d (7.9)	52.3, CH	1.06 d (7.5)	54.5, CH	1.26 − 1.24 m (2H)	50.9, CH
10		42.8, C		41.8, C		40.9, C
11	1.56−1.49 m (4H), 1.38−1.28 m (5H)	17.5, CH_2	1.71−1.61 m (4H), NA[e]	19.2, CH_2	1.70−1.66 m (3H), 1.55−1.52 m (2H)	18.3, CH_2
12	1.56−1.49 m (4H), 1.38−1.28 m (5H)	32.1, CH_2	1.71−1.61 m (4H), NA[e]	33.6, CH_2	1.87−1.79 m (2H), 1.70−1.66 m (3H)	32.1, CH_2
13	2.61 bs	41.4, CH	2.71 bs	43.7, CH	3.04 m (1H)	38.1, CH
14	1.70 d (10.9), 1.38−1.28 m (5H)	35.7, CH_2	1.90−1.87 m, 1.42−1.38 dd (4.9, 4.8)	37.2, CH_2	2.34 d (11.9), 1.42−1.37 m	36.7, CH_2
15	3.63−3.61 m	81.1, CH	3.77 s	83.6, CH		210.2, C=O
16		159.5, C		160.3, C		149.3, C
17	5.06 bs, 4.96 bs	107.6, CH_2	5.19 bs, 5.08 bs	109.1, CH_2	5.95 bs, 5.26 bs	114.9, CH_2
19		176.2, C=O		179.1, C=O		175.3, C=O
20	0.89 d (2.63, 3H)	16.3, CH_3	1.01 s (3H)	17.3, CH_3	0.96 bs (3H)	16.3, CH_3
OCH_3					3.67 bs (3H)	51.4, CH_3
1′	4.55 d (7.8)	98.9, CH				
2′	4.64 t (8.0)	72.2, CH[d]				
3′	4.31 t (8.3)	77.0, CH				
4′	4.02 t (8.5), overlapped	73.1, CH				
5′	3.45−3.42 (m)	75.8, CH				
6′	3.67−3.64 (m), 3.59−3.54 (m)	61.2, CH_2				
1″		170.8, C=O				
2″	2.14 d (2.33), 2.12 d (1.98)	42.7, CH_2				
3″	1.96 sept (6.7)	24.8, CH				
4″, 5″	0.87 d (2.5, 6H)	22.13, 22.17, CH_3				

[a]Recorded in DMSO-d_6, 500 and 125 MHz. [b]Recorded in methanol-d_4, 400 and 100 MHz. [c]Recorded in $CDCl_3$, 400 and 100 MHz. [d]Assignments may be interchanged. [e]Carbon signals C-5 and C-8 of genin **2** were previously recorded at δ_C 49.9 and 48.6, respectively.[7] NA = not assigned.

dx.doi.org/10.1021/np300080w | J. Nat. Prod. 2012, 75, 1070−1075

Scheme 2. Proposed Mechanism for the Oxidative Cleavage of the Glycosidic Bond of 6

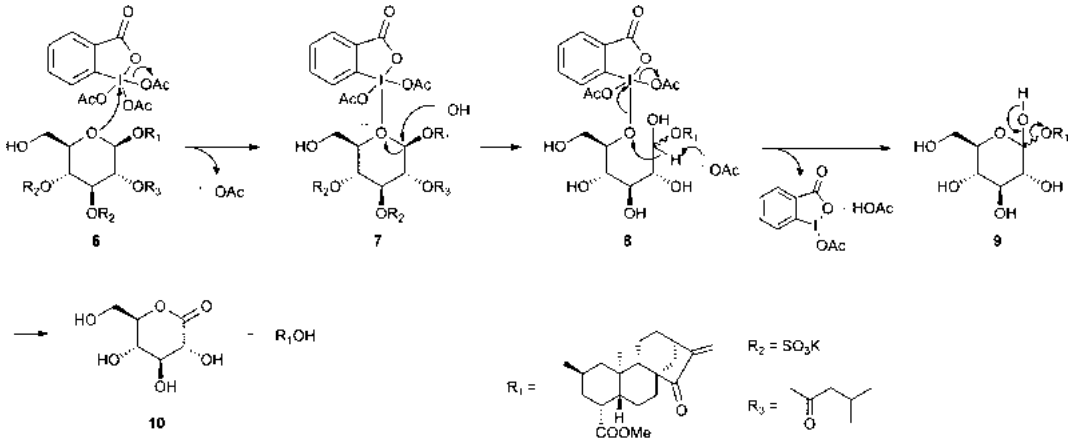

Finally, the methine carbon signal at δ_C 48.3 correlated with the remaining proton of spin system B and was assigned to C-5. Carbon assignment was followed by the identification of the A and B spin system protons. It was found that spin system A comprised H_2-6 (1H), H_2-7 (1H), H_2-11 (1H), and H_2-12 (1H), whereas spin system B included H-5 (1H), H_2-7 (1H), H_2-11 (1H), H_2-12 (1H), and H_2-14 (1H).

At this stage, the low-field region of the ^{1}H NMR spectrum of atractyloside was investigated and glucose-proton signals at δ_H 4.55 (d, J = 7.8 Hz), 4.31 (t, J = 8.3 Hz), and 3.45−3.42 (m) were assigned to H-1′, H-3′, and H-5′, respectively (Table 1). Superimposed signals at δ_H 4.06−4.00 (m, 2H) and three multiplets at δ_H 3.67−3.64 (1H), 3.63−3.61 (1H), and 3.59−3.54 (1H) were analyzed using long-range (HMBC) and through-bond (HSQC) heteronuclear correlation experiments.

Two triplets, δ_H 4.64 (J = 8.0 Hz, 1H) and 4.02 (J = 8.5 Hz, slightly overlapped) correlated with three carbon signals at δ_C 72.2, 72.4, and 73.1. The triplet at δ_H 4.64 was assigned to H-2′ due to its ^2J long-range correlations (HMBC) with C-3′ (δ_C 77.0) and C-1′ (δ_C 98.9) and a ^3J correlation with C-1″ (δ_C 170.8) of the isovaleric residue (Figure 2). Furthermore, the

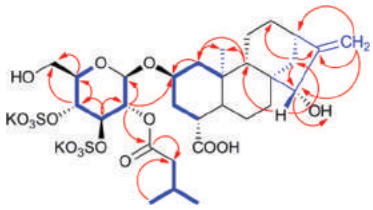

Figure 2. ^{1}H−^{1}H COSY (blue lines) correlations and key HMBC (red arrows) for **1**.

triplet at δ_H 4.02, which was overlapped with the H-2 signal, was assigned to H-4′ of the carbohydrate unit of **1**. Further sets of connectivities (HSQC) were observed between one methylene carbon signal at δ_C 61.2 and two multiplets at δ_H 3.67−3.64 and 3.59−3.54 and between the methine carbon signal at δ_C 81.1 and the multiplet at δ_H 3.63−3.61. This multiplet (δ_H 3.63−3.61) also showed HMBC correlations with C-9 (δ_C 52.3) and C-14 (δ_C 35.7) and was assigned to H-15, whereas the carbon signal at δ_C 61.2 was assigned to C-6′ due to its long-range correlations with H-4′ and H-5′ (Figure 2). Final assignment of proton resonances of the isovaleric acid residue completed the first structure elucidation of atractyloside **1** by NMR spectroscopy (Table 1).

X-ray crystallographic analysis allowed determination of the configurations of (−)-atractyloside, and the resulting ORTEP drawings are presented in Figure 3a,b. The crystallographic experiments established the configuration 2*R**, 4*R**, 5*R**, 8*R**, 9*S**, 10*R**, 13*R**, 15*S**, 1′*S**, 2′*R**, 3′*R**, 4′*R**, and 5′*R**. Moreover, observation of the stick model in Figure 3b revealed that the perhydrophenanthrene portion of **1** has little conformational flexibility. The cyclohexane rings A, B, and C all adopt a chair conformation, with the A and B rings being *trans* fused and B and C rings *cis* fused. The cyclopentane D ring is in turn fused to the C ring to form a bicyclo[3.2.1]-octane cage with the methylene and hydroxy groups sticking out from the periphery of the molecule. The α-oriented C-19 carboxylic and C-20 methyl residues of the *ent*-kaurane moiety and the β-oriented C-2−O-5−C-1′ bridge are also clearly evident in Figure 3b.

Interestingly, it was also observed that the crystal asymmetric unit of atractyloside contained three equivalent molecules coordinated to six metal ions. As a result, three sets of positional parameters and bond distances/angles were obtained, and these data could be employed, at a later stage, to aid in the determination of the most thermodynamically favorable conformation of **1**. This could further lead to in silico molecular modeling studies on the interaction of atractyloside with its biological target and to the synthesis of analogues with improved efficacy.

Compounds **1**−**3** were evaluated in vitro for their antimicrobial activity against *E. coli*, *Ent. faecalis*, and several strains of *Staph. aureus*, some of which were multidrug- and methicillin-resistant (MRSA), and minimum inhibitory concentration (MIC) values were determined. Only compound **3** exhibited moderate antibiotic activity (128 mg/L) against a susceptibility testing control strain (ATCC 29523), a fluoroquinolone-resistant derivative (SA1199B), and two epidemic-MRSA (EMRSA-15 and -16) isolates of *Staph. aureus*.

EXPERIMENTAL SECTION

General Experimental Information. Optical rotations were determined on a Bellingham and Stanley polarimeter ADP 220. Infrared spectra were acquired on a Perkin-Elmer FT-IR spectrometer (Spectrum 1000), and absorbance frequencies are reported in reciprocal centimeters (cm^{-1}). ^{1}H and ^{13}C NMR spectra were acquired using Bruker Avance 400 and 500 NMR spectrometers. Chemical shifts are reported in parts per million (ppm) with the solvent resonance as the internal standard, and coupling constants (J) are quoted in hertz (Hz). Spin multiplicities are described as s

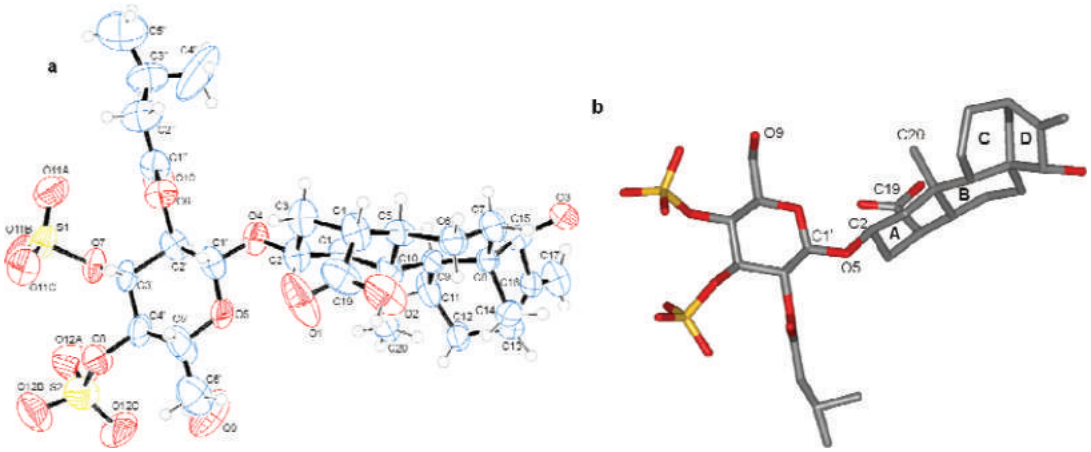

Figure 3. ORTEP[24] representations of one molecule of atractyloside (**1**): (a) with thermal ellipsoids drawn at 50% probability, hydrogen atoms drawn as spheres modeled with idealized geometry, and (b) in a stick model. Only non-hydrogen atoms are given.

(singlet), bs (broad singlet), d (doublet), dd (doublet of doublets), ddd (doublet of doublets of doublets), t (triplet), q (quadruplet), sept (septet), and m (multiplet). LC-MS analyses were carried out on a Phenomenex Monolithic C_{18} reversed-phase column (50 × 4.6 mm) with a flow rate of 3 mL min^{-1} and a linear gradient of B (5−95%) over 5 min. Eluent A: H_2O/0.1% formic acid; eluent B: CH_3CN/0.1% formic acid. TLC was performed on Merck silica gel 60 F_{254} aluminum sheets. TLC system 1: silica gel, EtOAc/acetone/H_2O:HOAc, 5:3:1:1, sprayed with a vanillin/H_2SO_4 solution prepared by dissolving 15 g of vanillin in 250 mL of EtOH with 0.01% concentrated H_2SO_4. TLC system 2: Si gel, $CHCl_3$/MeOH/HOAc, 8:2:0.5. Preparative TLC was performed on Merck silica gel 60 F_{254}, 2 mm, 20 × 20 cm plates. All chemicals were purchased from Fisher Scientific, Sigma Aldrich, and Merck Chemicals and used without further purification. Atractyloside potassium salt (**1**) was purchased from Enzo Life Science (batch no. P4432) and Sigma Aldrich and characterized prior to synthetic modification.

Chemistry. *Characterization of atractyloside potassium salt (1):* amorphous solid; TLC (system 1) R_f 0.45 (purple); $[\alpha]_D^{20}$ −52.5 (*c* 0.2, H_2O); IR ν_{max} (golden gate) cm^{-1} 3454, 2930, 1709, 1705, 1247, 1031, 909, 795; ^1H NMR and ^{13}C NMR (DMSO-d_6) see Table 1; ESIMS *m*/*z* (negative mode) 725 $[M - H]^-$, 645 $[M - SO_3 - H]^-$, 362, 322.

Synthesis of Atractyligenin (2). Atractyloside potassium salt (**1**) (0.056 mmol, 45 mg) was added to a solution of KOH (1 g, 0.018 mol) in H_2O (5 mL). The reaction mixture was allowed to stir at reflux (100 °C) for 6 h. After acidification with 10% HCl to pH = 3, the genin was extracted with EtOAc (3 × 10 mL) and dried over $MgSO_4$, and the solvent was evaporated under reduced pressure to yield 15 mg (0.047 mmol, 84%) of a white residue. The product was judged pure by analysis of TLC, LC-MS, NMR, and IR spectra. TLC (system 2): R_f 0.17; $[\alpha]_D^{20}$ −145 (*c* 0.2, EtOH); IR ν_{max} (golden gate) cm^{-1} 3420, 1701, 1658, 910; ^1H NMR and ^{13}C NMR (MeOD) see Table 1; ESIMS *m*/*z* (negative mode) 319 $[M - H]^-$.

Synthesis of Atractyloside Methyl Ester (5). To a solution of atractyloside potassium salt (**1**) (100 mg, 0.124 mmol) in a mixture of dry THF/MeOH (4:1, 5 mL) was added $TMSCH_2N_2$ (93 μL, 0.186 mmol, 2.0 M in Et_2O) dissolved in 0.5 mL of dry MeOH over a period of 5 min at −40 °C (MeCN/dry ice cooling bath). The reaction mixture was allowed to reach room temperature and then stirred for a further 3 h. The mixture was filtered on a pad of Si gel and eluted with MeOH (15 mL). The solvent was evaporated under reduced pressure to yield 48 mg of **5** as a white solid (0.058 mmol, 47.5%), which was judged pure by analysis of TLC, LC-MS, NMR, and IR spectra. $[\alpha]_D^{20}$ −40.0 (*c* 0.1, MeOH); TLC (system 1) R_f 0.54 (pink); ^1H NMR (400 MHz, MeOD) δ_H 5.17 (bs, 1H), 5.07 (bs, 1H), 4.92−4.87 (m, 1H), 4.71 (d, *J* = 8.0 Hz, 1H), 4.59−4.54 (m, 2H), 4.32 (t, *J* = 9.4 Hz, 1H), 4.26−4.21 (m, 1H), 3.94 − 3.83 (m, 2H), 3.76 (s, 1H), 3.66 (s, 3H), 3.56−3.50 (m, 1H), 2.71 (bs, 1H), 2.45 (d, *J* = 11.1 Hz, 1H), 2.34−2.29 (m, 1H), 2.28 (d, *J* = 7.2 Hz, 2H), 2.08 (sept, *J* = 6.8 Hz, 1H), 1.87−1.78 (m, 2H), 1.69−1.56 (m, 4H), 1.46−144 (m, 4H), 1.41−1.39 (m, 2H), 1.38−1.35 (m, 2H), 1.26−1.22 (m, 2H), 1.05 (d, *J* = 7.1 Hz, 1H), 0.96 (dd, *J* = 6.7, 2.1 Hz, 6H), 0.90 (s, 3H), 0.77 (t, *J* = 11.9 Hz, 1H); ^{13}C NMR (400 MHz, MeOD) δ_C 177.0, 174.1, 160.4, 109.1, 83.6, 79.9, 77.4, 76.3, 75.4, 73.5, 73.3, 64.4, 61.7, 54.5, 51.8, 50.6, 46.8, 44.8, 44.6, 43.7, 41.6, 37.3, 36.2, 35.5, 33.6, 30.7, 26.4, 24.8, 23.0, 19.2, 17.2; ESIMS *m*/*z* (negative mode) 739 $[M - H]^-$, 659 $[M - SO_3 - H]^-$, 368; HR-ESIMS (*m*/*z*) 739.2299 $[M - H]^-$ (calcd for $C_{31}H_{46}O_{16}S_2$, 739.2306).

Synthesis of 15-Didehydroatractyligenin Methyl Ester (3). To a solution of atractyloside methyl ester (**1**) (47.7 mg, 0.058 mmol) in dry CH_2Cl_2 (10 mL) was added neat Dess-Martin periodinane reagent (90.75 mg, 0.213 mmol) in one portion at 0 °C. The reaction mixture was allowed to reach room temperature and stirred under a nitrogen atmosphere for 3 h. The reaction was quenched with 1.5 M NaOH (5 mL), allowed to stir for a further 45 min at room temperature, and extracted with EtOAc (3 × 5 mL). The combined organic fractions were washed with 1.5 M NaOH (3 × 5 mL) and brine (2 × 5 mL), dried over $MgSO_4$, and evaporated under reduced pressure to yield a white solid. Purification by preparative TLC ($CHCl_3$−0.4% MeOH, R_f = 0.34) afforded **3** as a white, crystalline solid (10 mg, 0.030 mmol, 52%): $[\alpha]_D^{20}$ −171.4 (*c* 0.1, $CHCl_3$); IR ν_{max} (golden gate) cm^{-1} 3430, 3063, 2940, 1710, 1670, 1650, 1435, 1270, 1201, 1195, 1050, 938; ^1H NMR and ^{13}C NMR ($CDCl_3$) see Table 1; ESIMS *m*/*z* (positive mode) 333 $[M + H]^+$.

X-ray Diffractometry. Large, rod-shaped crystals of atractyloside (**1**) were grown by recrystallization from DMSO under oil drops over several days at 12 °C. Data were collected at 105 K on a single flash-frozen crystal processed and scaled using CrysalisPro.[25] The structure was solved by direct methods using SIR92[26] and refined using SHELXL97[27] from 10 377 independent reflections. All non-hydrogen atoms were refined by full-matrix, least-squares with anisotropic temperature factors, with hydrogen atoms positioned using normal geometry.

Crystallographic data of atractyloside (1): colorless crystal, $C_{30}S_2H_{44}K_2O_{16}$, M_r = 802.13, solvent O_5, orthorhombic, space group *C* 2 2 2_1, *a* = 22.9830(10) Å, *b* = 42.3640(22) Å, *c* = 24.0500(11) Å, $\alpha = \beta = \gamma = 90°$ *V* = 1130.57(16) $Å^3$, *Z* = 8, Cu Kα radiation, three atractyloside molecules in each ASU, crystal dimensions = 0.40 × 0.05 × 0.04 mm.

Data collection: Xcalibur microfocus NovaT X-ray diffractometer, 20 588 measured reflections, 14 053 independent reflections, 10 377 reflections with $I > 2\sigma(I)$, R_{int} = 0.045, av $I/\sigma(I)$ = 14.7.

Refinement: $R[F^2 > 2\sigma(F^2)]$ = 0.0141, $wR(F^2)$ = 0.358, *S* = 1.48, 14 053 reflections, 1392 parameters, H-atom parameters constrained, $\Delta\rho_{max}$ =1.11 e $Å^{-3}$, $\Delta\rho_{min}$ = −0.89 e $Å^{-3}$.

Crystallographic data in this paper have been deposited with the Cambridge Crystallographic Data Centre (deposition number: CCDC

873675). Copies of the data can be obtained, free of charge, on application to the Director, CCDC, 12 Union Road, Cambridge CB2 1EZ, UK (fax: +44-(0)1223-336033 or e-mail: deposit@ccdc.cam.ac.uk).

Biological Assay. *Antibacterial Assay.* Unless otherwise stated, all chemicals were obtained from Sigma-Aldrich Company Ltd., UK. Cation-adjusted Mueller-Hinton broth was obtained from Oxoid and was adjusted to contain 20 and 10 mg/L of Ca^{2+} and Mg^{2+}, respectively. The *Staphylococcus aureus* strains used in this study included ATCC 25923, SA-1199B, EMRSA-15, and EMRSA-16. ATCC 25923 is a standard laboratory strain sensitive to antibiotics. SA-1199B overexpresses the NorA MDR efflux pump. EMRSA-15 and EMRSA-16 are epidemic strains in the UK. *Enterococcus faecalis* NCTC 12697 and *Escherichia coli* NCTC 10418 are antimicrobial susceptibility testing control strains and were obtained from The National Collection of Type Cultures (London, United Kingdom). *Staph. aureus*, *E. coli*, and *Ent. faecalis* strains were cultured on nutrient agar (Oxoid) and incubated for 24 h at 37 °C prior to MIC determination. An inoculum density of 5×10^5 colony forming units of each bacterial strain was prepared in normal saline (9 g/L) by comparison with a 0.5 MacFarland turbidity standard. The inoculum (125 μL) was added to all wells, and the microtiter plate was incubated at 37 °C for the corresponding incubation time. For MIC determination, 20 μL of a 5 mg/mL methanolic solution of 3-[4,5-dimethylthiazol-2-yl]-2,5-diphenyltetrazolium bromide was added to each of the wells and incubated for 20 min. Bacterial growth was indicated by a color change from yellow to dark blue. The MIC was recorded as the lowest concentration at which no growth was observed.

■ ASSOCIATED CONTENT

Supporting Information

$^1H-^{13}C$ HSQC–DEPT135 spectra showing spin systems A and B and the glucose moiety region of atractyloside in DMSO-d_6. This material is available free of charge via the Internet at http://pubs.acs.org.

■ AUTHOR INFORMATION

Corresponding Author

*Tel: +44 207 753 5800; +44 207 753 4876. E-mail: federico.brucoli@pharmacy.ac.uk; f.brucoli@ucl.ac.uk.

Notes

The authors declare no competing financial interest.

■ ACKNOWLEDGMENTS

Prof. F. Ajello is thanked for her support throughout the project.

■ REFERENCES

(1) Daniele, C.; Dahamna, S.; Firuzi, O.; Sekfali, N.; Saso, L.; Mazzanti, G. *J. Ethnopharmacol.* **2005**, *97*, 175–181.
(2) Georgiou, M.; Biol, D.; Sianidou, L.; Hatzis, T.; Papadatos, J.; Koutselinis, A. *Clin. Toxicol.* **1988**, *26*, 487–493.
(3) Fassina, G.; Contessa, A. R.; Toth, C. E. *B. Soc. Ital. Biol. Sper.* **1962**, *133*, 346–348.
(4) Hamouda, C.; Hedhili, A.; Zhioua, M.; Amamou, M. *Vet. Hum. Toxicol.* **2004**, *46*, 144–146.
(5) Lefranc, E. *C. R.* **1868**, *67*, 954–961.
(6) Popat, A.; Shear, N. H.; Malkiewicz, I.; Stewart, M. J.; Steenkamp, V.; Thomson, S.; Neuman, M. G. *Clin. Biochem.* **2001**, *34*, 229–236.
(7) Schteingart, C. D.; Pomilio, A. B. *J. Nat. Prod.* **1984**, *47*, 1046–1047.
(8) Pegel, K. H. *Chem. Eng. News* **1981**, *59*, 4.
(9) Ames, B. N. *Science* **1983**, *221*, 1256–1264.
(10) Ajello, T.; Piozzi, A.; Quilico, F.; Sprio, V. *Gazz. Chim. Ital.* **1963**, *93*, 867–915.
(11) Piozzi, F.; Quilico, A.; Ajello, T.; Sprio, V.; Melera, A. *Tetrahedron* **1966**, *22*, 515–529.
(12) Piozzi, F. In *Atractyloside: Chemistry, Biochemistry and Toxicology*; Piccin Medical Books: Padova, Italy, 1978; pp 13–32.
(13) Vignais, P. M.; Vignais, P. V.; Defaye, G. In *Atractyloside: Chemistry, Biochemistry and Toxicology*; Piccin Medical Books: Padova, Italy, 1978; pp 39–68.
(14) Roux, P.; Le Saux, A.; Fiore, C.; Schwimmer, C.; Dianoux, A. C.; Trezeguet, V.; Vignais, P. V.; Lauquin, G. J.; Brandolin, G. *Anal. Biochem.* **1996**, *234*, 31–37.
(15) Pebay-Peyroula, E.; Dahout-Gonzalez, C.; Kahn, R.; Trézéguet, V.; Lauquin, G. J. M.; Brandolin, G. *Nature* **2003**, *426*, 39–44.
(16) Camarda, L.; Di Stefano, V.; Schillaci, D. *Pharmazie* **2002**, *57*, 374–376.
(17) D'Ancona, S.; Magon, M.; Milanesi, C.; Santi, E. *Fitoterapia* **1989**, *60*, 509–517.
(18) Kedrov, A.; Hellawell, A. M.; Klosin, A.; Broadhurst, R. B.; Kunji, E. R. S.; Müller, D. J. *Structure* **2010**, *18*, 39–46.
(19) Macleod, J. K.; Gaul, K. L.; Oelrichs, P. B. *Aust. J. Chem.* **1990**, *43*, 1533–1539.
(20) Lee, S.; Shamon, L. A.; Chai, H. B.; Chagwedera, T. E.; Besterman, J. M.; Farnsworth, N. R.; Cordell, G. A.; Pezzuto, J. M.; Kinghorn, A. D. *Chem.-Biol. Interact.* **1996**, *99*, 193–204.
(21) Hanson, J. R. *Nat. Prod. Rep.* **1984**, *1*, 533–544.
(22) Rosselli, S.; Bruno, M.; Maggio, A.; Bellone, G.; Chen, T. H.; Bastow, K. F.; Lee, K. H. *J. Nat. Prod.* **2007**, *70*, 347–352.
(23) Lee, K. H.; Hall, I. H.; Mar, E. C.; Starnes, C. O.; ElGebaly, S. A.; Waddell, T. G.; Hadgraft, R. I.; Ruffner, C. G.; Weidner, I. *Science* **1977**, *196*, 533–536.
(24) Ortep-3 for Windows. Farrugia, L. J. *J. Appl. Crystallogr.* **1997**, *30*, 565.
(25) *CrysAlis PRO*; Agilent Technologies UK Ltd: Yarnton, England, 2011.
(26) Altomare, A.; Cascarano, G.; Giacovazzo, C.; Guagliardi, A. *J. Appl. Crystallogr.* **1993**, *26*, 343–350.
(27) Sheldrick, G. M.; Schneider, T. R. *Macromol. Crystallogr. Part B* **1997**, *277*, 319–343.

International Journal of Antimicrobial Agents 39 (2012) 124–129

Contents lists available at SciVerse ScienceDirect

International Journal of Antimicrobial Agents

journal homepage: http://www.elsevier.com/locate/ijantimicag

An antibacterial from *Hypericum acmosepalum* inhibits ATP-dependent MurE ligase from *Mycobacterium tuberculosis*

Khadijo Osman[a,b], Dimitrios Evangelopoulos[b,c], Chandrakala Basavannacharya[b], Antima Gupta[b], Timothy D. McHugh[c], Sanjib Bhakta[b,**], Simon Gibbons[a,*]

[a] *Department of Pharmaceutical and Biological Chemistry, The School of Pharmacy, University of London, 29–39 Brunswick Square, Bloomsbury, London WC1N 1AX, UK*
[b] *Institute of Structural and Molecular Biology, Department of Biological Sciences, Birkbeck, University of London, Malet Street, Bloomsbury, London WC1E 7HX, UK*
[c] *Centre for Clinical Microbiology, Department of Infection, Royal Free Campus, University College London, London NW3 2PF, UK*

ARTICLE INFO

Article history:
Received 27 June 2011
Accepted 21 September 2011

Keywords:
Hypericum acmosepalum
Hyperenone A
Hypercalin B
Staphylococcus aureus
Tuberculosis
Peptidoglycan
MurE ligase

ABSTRACT

In a project to characterise new antibacterial chemotypes from plants, hyperenone A and hypercalin B were isolated from the hexane and chloroform extracts of the aerial parts of *Hypericum acmosepalum*. The structures of both compounds were characterised by extensive one- and two-dimensional nuclear magnetic resonance (NMR) spectroscopy and were confirmed by mass spectrometry. Hyperenone A and hypercalin B exhibited antibacterial activity against multidrug-resistant strains of *Staphylococcus aureus*, with minimum inhibition concentration ranges of 2–128 mg/L and 0.5–128 mg/L, respectively. Hyperenone A also showed growth-inhibitory activity against *Mycobacterium tuberculosis* H37Rv and *Mycobacterium bovis* BCG at 75 mg/L and 100 mg/L. Neither hyperenone A nor hypercalin B inhibited the growth of *Escherichia coli* and both were non-toxic to cultured mammalian macrophage cells. Both compounds were tested for their ability to inhibit the ATP-dependent MurE ligase of *M. tuberculosis*, a crucial enzyme in the cytoplasmic steps of peptidoglycan biosynthesis. Hyperenone A inhibited MurE selectively, whereas hypercalin B did not have any effect on enzyme activity.

1. Introduction

In recent years, drug resistance in *Mycobacterium tuberculosis* and other clinically relevant bacterial pathogens such as meticillin-resistant *Staphylococcus aureus* (MRSA) has emerged as a major threat to public health, with severe economic and social implications [1,2]. MRSA is still one of the most widespread and virulent nosocomial pathogens in the world [3] and is usually resistant to multiple antibiotics, making infection difficult to treat, and accounts for an increased proportion of staphylococcal infections amongst hospitalised patients in countries where it has become established. Despite new advances in antibiotic development, with agents such as linezolid, daptomycin and quinupristin/dalfopristin appearing over the last decade [4], MRSA infections still remain of considerable concern owing to resistance to some of these new drugs [5,6].

Tuberculosis (TB) is caused predominantly by *M. tuberculosis*, an obligate aerobic pathogen that divides at an extremely slow rate. The World Health Organization estimates that 2 billion people have latent TB whilst another 2 million people die of TB each year worldwide [7]. Although TB is generally treatable, the exponential emergence of extensively drug-resistant or completely drug-resistant TB strains is a current global health emergency where there is virtually no treatment available [8]. Therefore, new antibacterial agents with novel modes of action are urgently needed to meet the challenge posed by these resistant variants.

The peptidoglycan biosynthesis pathway is a validated target for the development of antibacterial agents, including the classical β-lactam, cephalosporin and glycopeptide antibacterials [9]. The peptidoglycan layer of the cell wall serves as a base for the lipid-rich capsule. Peptidoglycan (or murein) is the polymeric mesh of the bacterial cell wall that plays a vitally important role in protecting bacteria against osmotic lysis. Peptidoglycan biosynthesis can be separated into two phases, comprising six intracellular enzymatic steps and three steps that occur outside of the plasma membrane [10]. Amongst the cytoplasmic steps involved in the biosynthesis of peptidoglycan, four ATP-dependent ligases (MurC, MurD, MurE and MurF) catalyse the assembly of its peptide moiety by successive additions of L-alanine, D-glutamate, a diamino acid [usually *meso*-diaminopimelic acid (*m*-DAP) or L-lysine] and D-alanine–D-alanine to UDP *N*-acetylmuramic acid (MurNAc) [11]. Although most antimicrobials target steps in the later stage of cell

* Corresponding author. Tel.: +44 207 753 5913; fax: +44 207 753 5909.
** Corresponding author. Tel.: +44 207 631 6355; fax: +44 207 631 6246.
E-mail addresses: s.bhakta@bbk.ac.uk (S. Bhakta), simon.gibbons@pharmacy.ac.uk (S. Gibbons).

0924-8579/$ – see front matter © 2011 Elsevier B.V. and the International Society of Chemotherapy. All rights reserved.
doi:10.1016/j.ijantimicag.2011.09.018

wall biosynthesis, the earlier steps in peptidoglycan biosynthesis have recently received renewed attention in terms of novel therapeutic targets [12]. To date, only fosfomycin, which targets MurA (NAG enolpyruvate transferase), has been developed as an antibacterial agent targeting early biosynthesis of cell wall peptidoglycan [10,11]. The enzymes involved in the peptidoglycan biosynthetic pathway are characteristic of Eubacteria and are absent in humans. These enzymes are therefore excellent targets for anti-infective drug development.

Although most antibiotics in clinical use have been obtained from microorganisms, an interest in plant antibacterials has re-emerged during the last three decades. Of the known plant species (estimated at 250 000), only a very small fraction has been investigated for the presence of antibacterial compounds and an even smaller number of these phytochemicals have been subjected to a modern rigorous pharmacological evaluation of their antibacterial properties.

Species of the plant genus *Hypericum* are used in traditional medicine for their therapeutic value [13]. *Hypericum perforatum* L. (commonly known as St John's Wort) is the most investigated member of the genus both from the perspective of chemical constituents and biological activity [14]. It has been used extensively in herbal medicine as an antidepressant [14], for various skin treatments such as eczema, wounds and burns, as well as in disorders of the alimentary tract, amongst others [14].

Hypericum acmosepalum is a shrub of 0.6–2 m in height with deep-yellow petals that are sometimes tinged red. It is cultivated as an ornamental shrub in many parts of the world, but particularly in Great Britain [15]. Previous studies on *H. acmosepalum* are limited, with some ethnobotanical usage by the Yao People of Yunnan Province in China [16]. Here we describe the isolation, structural elucidation and antibacterial action of two natural products from *H. acmosepalum*. Their ability to inhibit the ATP-dependent MurE ligase enzyme from *M. tuberculosis* [10], a pivotal enzyme in peptidoglycan biosynthesis, was also assessed.

2. Materials and methods

2.1. Bacterial strains

A standard *S. aureus* strain (ATCC 25923) as well as a clinical isolate (XU212) that possesses the Tet(K) efflux pump and is also an MRSA strain were obtained from Dr Edet Udo (Kuwait University) [17]. Epidemic MRSA types 15 and 16 (EMRSA-15 and EMRSA-16) were provided by Dr Paul Stapleton (The School of Pharmacy, University of London, UK). Strain SA-1199B that overexpresses the NorA multidrug resistance efflux pump was donated by Prof. Glenn W. Kaatz (Wayne State University, Detroit, MI) [18]. Strain RN4220 that has the MsrA macrolide efflux pump was a generous gift from Dr Jon Cove (University of Leeds, UK) [19]. *Mycobacterium bovis* BCG (ATCC 35734) and RAW 264.7 (a mouse leukaemic monocyte macrophage cell line) were obtained from Prof. Siamon Gordon (Sir William Dunn School of Pathology, University of Oxford, Oxford, UK). *Mycobacterium tuberculosis* H37Rv (ATCC 9360) was purchased from the Health Protection Agency (Porton Down, Salisbury, UK).

2.2. Isolation of compounds

Hypericum acmosepalum was collected from the National *Hypericum* Collection at the Royal Botanic Gardens, Kew (Ardingly, UK) in August 2005. The authenticity of this species has been verified by Dr N.K.B. Robson. Voucher specimens of these collections have been deposited at the Department of Pharmaceutical and Biological Chemistry (SG-2005-2/6) (School of Pharmacy, University of London, London, UK). Dried and powdered material (500 g) of *H. acmosepalum* was extracted sequentially in a Soxhlet apparatus (Fisher Scientific, Loughborough, UK) using 3.5 L of organic solvents of increasing polarity (hexane, chloroform and methanol). Vacuum-liquid chromatography (VLC) (Silica gel 60 $PF_{254+366}$; Merck, Darmstadt, Germany) was performed on 6.3 g of the hexane extract with an increasingly polar gradient of 10% increments, from 100% hexane to 100% ethyl acetate, yielding 12 fractions. Thin-layer chromatography (TLC) of Fraction 6 showed a major compound that was subjected to LH-20 Sephadex column chromatography (Sigma Aldrich, Gillingham, UK) to give 12 fractions by elution with hexane, chloroform and chloroform–methanol mixtures. Fractions 6, 7 and 8 eluted with 30% hexane and in chloroform were combined yielding pure compound **1** (94 mg). The chloroform extract (8.3 g) was fractionated by VLC with an increasingly polar gradient of 10% from 100% hexane to 100% ethyl acetate, yielding 12 fractions. Fractions 6 and 7 showing a similar TLC profile were combined (2.5 g) and were further separated using Sephadex column chromatography using the same method described above. Fractions 2 and 3 eluted with 35% hexane in chloroform from Sephadex were combined (160 mg) and further separated by preparative TLC silica plates (20 mm × 20 mm, $60F_{254}$; Merck) using hexane–ethyl acetate–acetic acid (85:15:2) to give compound **2** (25 mg).

Table 1
Nuclear magnetic resonance (NMR) [500 MHz (^{1}H) and 125 MHz (^{13}C)] data for hyperenone-A (**2**) in $CDCl_3$.

Position	^{1}H δ ppm (J)	^{13}C δ ppm
2		157.1
3		111.7
4		181.4
5	6.61	111.5
6		162.9
1		131.1
2′, 6′	7.70 m	125.4
3′, 5′	7.48 m	129.3
4′	7.47 m	131.0
1″		39.0
2″	6.25 dd (17.2, 10.4)	148.5
3″	4.90 d (17.2)4.95 d (10.4)	108.5
4″/5″	1.50	27.7
MeO	4.06	56.2

2.2.1. Compound ***1*** *(hypercalin B)*

Pale yellow amorphous solid. Electrospray ionisation mass spectrometry (ESI-MS) $[M+H]^+$ m/z 519, calculated for $C_{33}H_{43}O_5$. Ultraviolet (UV) ($CHCl_3$) λ_{max} (log ε): 360 (4.09), 285 (3.56), 244 (3.81) nm. Infrared (IR) vapour maximum (V_{max} thin film) cm^{-1}: (3370, 3060, 2960, 2920, 28 260). Proton (^{1}H) and carbon (^{13}C) nuclear magnetic resonance (NMR) spectroscopic data were in close agreement with those of hypercalin B isolated from *Hypericum calycinum* [20].

2.2.2. Compound ***2*** *(hyperenone A)*

Yellow oil. High-resolution ESI-MS $[M+H]^+$ m/z 271.1396 calculated for $C_{17}H_{19}O_3$. UV ($CHCl_3$) λ_{max} (log ε): 236 (4.12), 276 (4.07) nm. IR V_{max} (thin film) cm^{-1}: (1651, 1614, 1580). ^{1}H and ^{13}C NMR spectroscopic data (Table 1).

2.3. Structure elucidation

One-dimensional (1D) and two-dimensional (2D) NMR spectra were recorded on an Avance 500 MHz spectrometer (Bruker, Coventry, UK). Chemical shift values (δ) were reported in parts per million (ppm). Samples were dissolved in deuterated chloroform. IR spectra were recorded on a Nicolet 360 FT-IR spectrophotometer (Thermo Fisher Scientific, Loughborough, UK), and UV spectra on a Thermo Electron Corporation Helios spectrophotometer (Thermo

Fisher Scientific). Mass spectra were recorded on a Micromass Q-TOF Global Tandem Mass Spectrometer (Waters Corp., Manchester, UK).

2.4. Minimum inhibitory concentration (MIC) determination against Staphylococcus aureus

Prior to antibacterial bioassay, strains were subcultured freshly on Mueller–Hinton agar medium (Oxoid Ltd., Basingstoke, UK) and incubated for 24 h at 37 °C prior to MIC determination. Control antibiotics norfloxacin, tetracycline, vancomycin, erythromycin and ciprofloxacin were also used. Mueller–Hinton broth (Oxoid Ltd.) was adjusted to contain 20 mg/L Ca^{2+} and 10 mg/L Mg^{2+}. An inoculum density of 5×10^5 colony-forming units/mL of each *S. aureus* strain was prepared in normal saline (9 g/L) by comparison with a 0.5 McFarland turbidity standard. The inoculum (125 μL) was added to all wells of a microtitre plate and the plate was incubated at 37 °C for 18 h. For MIC determination, 20 μL of a 5 mg/mL methanolic solution of 3-(4,5-dimethylthiazol-2-yl)-2,5-diphenyltetrazolium bromide (MTT) was added to each of the wells and was incubated for 20 min. Bacterial growth was indicated by a colour change from yellow to dark blue. The MIC was recorded as the lowest concentration at which no growth was observed.

2.5. Minimum inhibitory concentration determination against mycobacteria

Mycobacterium bovis BCG was grown at 37 °C in an incubator in 100 mL of Middlebrook 7H9 broth medium supplemented with 10% (v/v) albumin–dextrose–catalase (Difco, Oxford, UK) and 0.05% Tween 80 in roller bottles with rotation at 2 rpm until mid-exponential phase [optical density at 600 nm (OD_{600}) = 1.0]. *Mycobacterium tuberculosis* H37Rv was grown at 37 °C in an incubator as a standing culture in 30 mL universals in Middlebrook 7H9 broth medium supplemented with 10% (v/v) oleic acid–albumin–dextrose–catalase (OADC) (Difco) and 0.05% Tween 80 until mid-exponential phase (1 McFarland turbidity standard).

For quality control of the mycobacterial cultures, *M. bovis* BCG was stained with a modified Ziehl–Neelsen staining protocol using a Tb-color kit (Bund Deutscher Hebammen Laboratory, Karlsruhe, Germany) according to the manufacturer's procedure, and *M. tuberculosis* H37Rv was grown on a blood agar plate to detect contamination. MICs against mycobacteria were determined using the spot culture growth inhibition assay as described previously [21]. An aliquot of 5 mL of Middlebrook 7H10 (BD Biosciences, Oxford, UK) supplemented with 0.2% glycerol and 10% OADC was added to a six-well plate along with compounds at concentrations of 100, 75, 50, 25, 10 and 0 mg/L in a 5 μL solution of dimethyl sulphoxide (DMSO). Afterwards, 5 μL of an appropriately diluted mid-log phase of 10^5 cells/mL was carefully dispensed into the centre of each well. A well with no compound containing 0.1% DMSO was used as a negative control. The MIC was determined after 2 weeks of incubation at 37 °C. A frontline antitubercular drug, isoniazid (INH), was also used as a positive control.

2.6. Escherichia coli JM109 killing curves

A seed culture of *E. coli* JM109 was grown up to mid-log phase (OD_{600} = 1.9). Then, 1 mL of the seed culture was mixed with 100 mL of fresh Luria–Bertani medium and 5 mL was distributed into 25-mL volume glass culture tubes (Brand GmbH, Wertheim, Germany) containing either the inhibitors used in this study (final concentration 200 mg/L) or DMSO (final concentration 0.1%). These cultures were then grown at 37 °C in a shaking incubator rotating at 180 rpm. The glass tubes were placed into the cell holder of a spectrophotometer (Biochrom WPA CO8000; Biochrom, Cambridge, UK) and the OD_{600} was measured every 30 min until the culture reached stationary phase. INH was taken as a positive control and the experiment was performed in triplicate.

2.7. Cytotoxicity assay

Mouse macrophage cells (RAW 264.7) were cultured in 5 mL of complete RPMI 1640 medium supplemented with 10% foetal bovine serum and 1% L-glutamine in a 25 cm^2 vented, screw-cap cell culture flask (Flowgen Bioscience Ltd., Hessle, UK) and incubated at 37 °C with a supply of 5% CO_2. For use in cytotoxicity assay, cells were detached using 5 mL of lidocaine–ethylene diamine tetraacetic acid (EDTA) for 10 min at room temperature, followed by banging the side of the flask against the palm of the hand, and diluted with an equal volume of fresh media. Cells were then centrifuged at 1000 rpm for 5 min at room temperature, washed twice with 1× phosphate-buffered saline, re-suspended in complete RPMI media, counted and diluted to adjust to 10^5 cells/mL. Then, 100 μL of cells were seeded to each well of a 96-well plate containing final concentrations (3.125–200 mg/L) of inhibitors and controls that had been pre-plated by serial dilution [22]. DMSO and INH were used as negative and positive controls, respectively, and the experiment was performed in triplicate. Following 48 h of incubation at 37 °C in 5% CO_2, medium was replaced and supplemented with 30 μL of freshly prepared 0.01% resazurin solution. A change in colour from blue to pink indicating the viability of cells was observed after 16 h incubation at 37 °C in 5% CO_2. For quantitative analysis, the fluorescence intensity was measured by excitation at 560 nm and emission at 590 nm using a fluorescence microtitre plate reader (BMG Labtech GmbH, Ortenberg, Germany).

2.8. Inhibition of ATP-dependent MurE ligase activity from Mycobacterium tuberculosis

The MurE enzyme activity assay [11] was set up using 100 ng of MurE enzyme in the presence of 25 mM Bis–Tris–propane/HCl (pH 8.5), 5 mM $MgCl_2$, 250 μM ATP, 100 μM UDP-MurNAc-L-Ala–D-Glu and 4% DMSO (enzyme reaction) at 37 °C. The compounds were dissolved in DMSO at concentrations of 100, 500 and 1000 μM. The reaction was initiated by the addition of 1 mM *m*-DAP. After 30 min, 12.5 μL of gold-lock reagent with accelerator was added to terminate the reaction. After 5 min, a stabiliser was added and the reaction was left for 30 min at room temperature (25 °C) for colour development. The assay was performed in a final volume of 50 μL in a half-area Costar microtitre plate (Applied Biosystems, Carlsbad, CA). Inorganic phosphate binds to the gold-lock reagent to form a complex with an absorption maximum of 635 nm. MurE activity was estimated through phosphate release by measuring the absorbance of the reaction mixtures at 635 nm after 30 min. Absorbance values were corrected for background absorbance of the reaction mixtures and for any non-enzymatic hydrolysis of ATP in the absence of the enzyme (control reaction). Percent inhibition was calculated using a negative control (0%) and enzyme reaction (100% activity). All assays were performed in triplicate.

3. Results

3.1. Structural elucidation of compounds

Examination of the ^{13}C spectra of compound **1** revealed similarities with other hypercalin derivatives previously isolated from *H. calycinum*, and the NMR data were in good agreement with those of hypercalin B [20]. Compound **2** was obtained as a yellow oil whose molecular formula was $C_{17}H_{18}O_3$ as established by high-resolution mass spectrometry showing an $[M+H]^+$ ion at *m*/*z* 271.1396. Its IR spectrum indicated the presence of a carbonyl (1651 cm^{-1}) and

Table 2
Minimum inhibitory concentrations (MICs) of compounds and control antibiotics against *Staphylococcus aureus* strains.

Agent	MIC (mg/L)					
	SA-1199B	EMRSA-15	EMRSA-16	RN4220	XU212	ATCC 25923
Compound **1**	0.5	128	64	16	2	16
Compound **2**	2	64	128	32	32	16
Norfloxacin	32	1	256	0.5	16	2
Tetracycline	0.25	0.25	0.25	0.25	64	0.25
Erythromycin	0.25	>128	>128	64	>128	0.25
Ciprofloxacin	8	8	16	0.25	1	0.25

benzene ring (1614 and 1580 cm^{-1}), which was confirmed by the ^{13}C NMR data (Table 1). The ^{13}C NMR spectra exhibited 17 signals, which by ^{1}H NMR and ^{13}C Dept-135 experiments corresponded to six quaternary carbons, seven methines, one methylene, two methyls and one methoxy group. Five aromatic hydrogens at δ 7.70 m, 7.48 m and 7.47 m in the ^{1}H NMR spectrum (Table 1) indicated the presence of a monosubstituted benzene ring. The ^{1}H and ^{13}C resonances of this moiety were assigned by close inspection of the heteronuclear multiple quantum coherence (HMQC) spectrum as δ 7.70 (H-2′, 6′) with δ 125.4 (C-2′, 6′), δ 7.48 (H-3′, 5′) with δ 129.3 (C-5′) and δ 7.47 (H-4′) with δ 131.0 (C-4′). Careful analysis of the heteronuclear multiple bond coherence (HMBC) spectrum revealed that the aromatic singlet at δ 6.61 (H-5) showed a ^{2}J correlation to the carbonyl at 181.4 (C-4), a quaternary carbon at 157.1 (C-2) and a ^{3}J correlation to the quaternary carbons at 111.5 (C-5) and 131.1 (C-1′).

This indicated that the aromatic ring was attached to a benzene ring at C-1′. The signals at 4.90 (1H, dd, 13.5, 0.5 Hz) and 1.50 (6-H) were indicative of a 1,1-dimethylprop-2-enyl side chain in the molecule. The assignment of all ^{1}H and ^{13}C resonances as well as the moiety of the attachment of 1,1-dimethylprop-2-enyl side chain at C-2 was achieved by the HMBC experiment. In addition, a methoxy group at δ 4.06 demonstrated a ^{3}J correlation to a quaternary carbon at 162.9 and confirmed its placement at C-3. These data together with analysis of the COSY spectrum revealed compound **2** to be hyperenone A (Fig. 1), which was previously isolated from *Hypericum mysorense* Heyne, but its ^{13}C data were not reported [23]. Here we publish the ^{13}C NMR data for hyperenone A for the first time based on extensive 1D- and 2D-NMR experiments (Table 1).

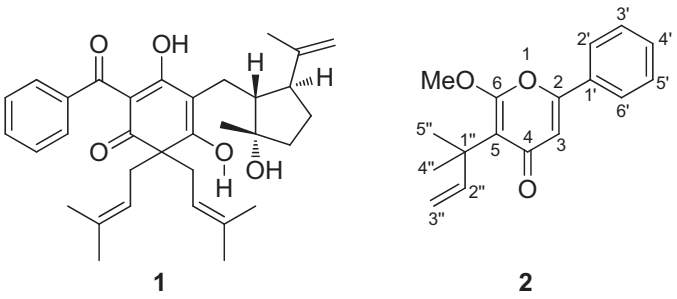

Fig. 1. Structures of hypercalin B (**1**) and hyperenone A (**2**).

3.2. Effect of both compounds on Staphylococcus aureus

Compounds **1** and **2** were tested for their ability to inhibit the growth of *S. aureus* strains. Both of the compounds showed significant antibacterial activity, with a range of MIC values from 0.5 mg/L to 128 mg/L (Table 2).

3.3. Growth inhibition of Mycobacterium spp.

Both compounds were evaluated for their antibacterial activity against *M. tuberculosis* H37Rv and *M. bovis* BCG on solid agar media at different concentrations (10, 25, 50, 75 and 100 mg/L) in a six-well plate. Compound **1** was found to be inactive for both species, whilst compound **2** was active with MIC values >75 mg/L for both species. At 100 mg/L, compound **2** showed complete growth inhibition, whereas at 75 mg/L reduced growth was observed compared with the negative control (Fig. 2).

3.4. Escherichia coli JM109 killing curves

To evaluate whether the compounds' selectivity affected slow-growing mycobacteria in comparison with fast-growing bacteria, whole-cell experiments were carried out. Comparative time measurement of *E. coli* growth after exposure to a high concentration of

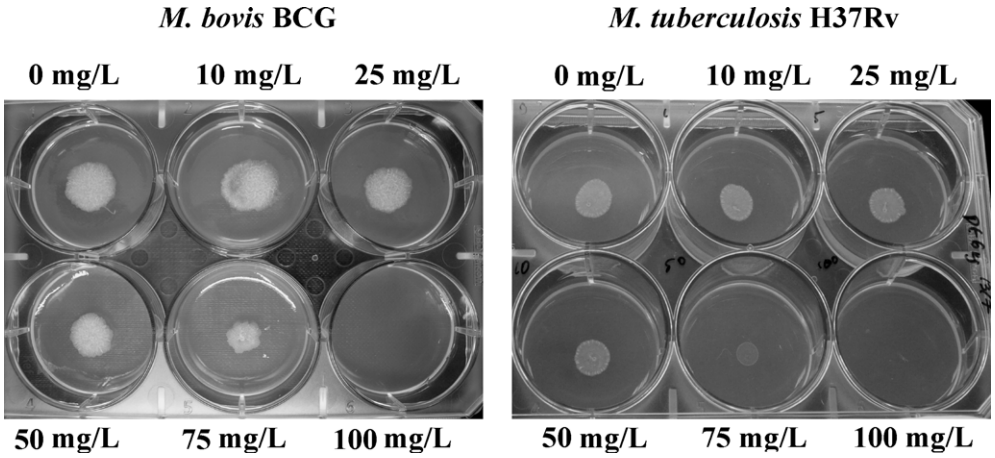

Fig. 2. Effect of compound **2** on the growth of mycobacterial species using a spot culture growth inhibition assay. Approximately 500 *Mycobacterium bovis* BCG and *Mycobacterium tuberculosis* H37Rv cells were spotted on solidified Middlebrook 7H10 agar containing different concentrations of compound **2** in a six-well plate. Pictures were taken using a digital camera after 14 days of inoculation.

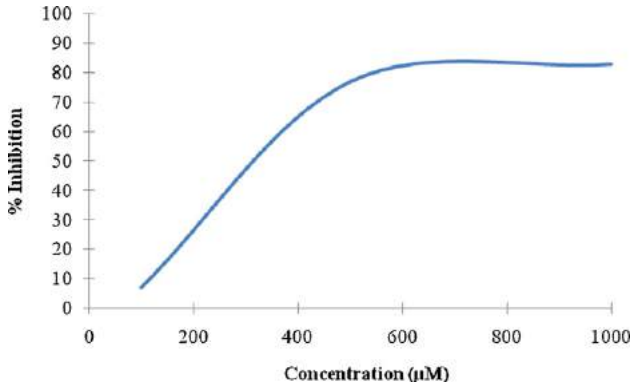

Fig. 3. Effect of compound **2** on MurE enzyme activity. The *x*-axis represents the different concentrations of the compound tested in the assay and the *y*-axis represents the percent inhibition at different concentrations of the compound. The assay was performed in triplicate.

compounds, typically 200 mg/L, was determined by measuring the OD_{600}. Compounds **1** and **2** were inactive against Gram-negative *E. coli* JM109.

3.5. Macrophage RAW 264.7 cytotoxicity

To determine whether the isolated compounds were toxic to mammalian cells, a cytotoxicity assay using RAW 264.7 cells at a serially diluted range of assay concentrations (3.125–200 mg/L) was performed and the cell viability was calculated. The result revealed that 100% eukaryotic cell viability was observed either up to 50 mg/L of compound **1** or up to 100 mg/L of compound **2** (Supplementary Fig. 1).

3.6. Mycobacterium tuberculosis MurE enzyme inhibition

Inhibition of recombinant *M. tuberculosis* MurE was assayed under different concentrations of isolated compounds using the colorimetric detection of phosphate, which has been shown to be stoichiometrically coupled to *m*-DAP ligation [10,24]. Compound **1** did not inhibit MurE, whilst compound **2** showed 7%, 77% and 83% inhibition at 100, 500 and 1000 μM concentrations, respectively, having a 50% inhibitory concentration (IC_{50}) of 320 μM (Fig. 3).

4. Discussion

The *Hypericum* genus is a valuable source of new phytochemicals and antibacterial compounds [13]. Compounds isolated from this group of plants have been shown to demonstrate antistaphylococcal activity [25,26] as well as many other biological activities such as antifungal properties [27]. Compound **1**, which was previously isolated from *H. calycinum*, exhibited in vitro growth inhibitory activity against the Co-115 human colon carcinoma cell line [20]. Compound **2** was previously isolated from *H. mysorense*. Here we show for the first time significant activity of these compounds with MIC values of 0.5–128 mg/L and 2–128 mg/L, respectively, against a panel of *S. aureus* strains, some of which are meticillin-resistant and multidrug-resistant (MDR) (Table 2). With the exception of EMRSA-15, compound **1** was slightly more active against all of the *S. aureus* strains compared with compound **2**. The strains included SA-1199B, a MDR strain that overexpresses the NorA efflux mechanism, the best characterised antibiotic pump in this species. SA-1199B also possesses a gyrase mutation that, in addition to NorA, confers a high level of resistance to certain fluoroquinolones. Against this strain, both compound **1** (MIC = 0.5 mg/L) and compound **2** (MIC = 2 mg/L) were more active than the control antibiotic norfloxacin (MIC = 32 mg/L). For MDR strain XU212, which possesses the Tet(K) efflux transporter and is resistant to both tetracycline and meticillin, compound **1** showed better inhibitory activity (MIC = 2 mg/L) compared with the positive control antibiotics (Table 2). Both compounds **1** and **2** showed moderate activity against a standard *S. aureus* strain (ATCC 25923) as well as RN4220, which possesses the MsrA macrolide efflux pump, but were less active than the control antibiotics. Compound **1** was slightly more active against EMRSA-16 compared with EMRSA-15, one of the major EMRSA strains occurring in UK hospitals. In addition, compound **2** (MIC = 2 mg/L) was marginally more active against SA-1199B than the fluoroquinolone ciprofloxacin control (MIC = 8 mg/L).

The in vitro antibacterial activity of compounds **1** and **2** did not inhibit the growth of *E. coli* and both were non-toxic to mammalian cells. Compound **2** was evaluated against the pathogenic *M. tuberculosis* H37Rv and the vaccine strain *M. bovis* BCG (Fig. 2) and was shown to be active at 100 mg/L for both species. Compounds with a higher degree of lipophilicity may play an important role in antimycobacterial activity. The mycobacterial cell wall contains lipophilic substances such as mycolic acid, thus lipophilic compounds would therefore have the advantage of better penetration through the cell wall to inhibit the growth of mycobacteria.

There is an ongoing effort to find inhibitors of Mur enzymes involved in peptidoglycan biosynthesis to target different bacterial diseases. Phosphonates, phosphinates and sulphonamides are amongst the inhibitors of MurC, MurD, MurE and MurF. Sova et al. [28] evaluated a series of phosphorylated hydroxyethylamines as a new type of small-molecule inhibitor of Mur ligases and found that the IC_{50} values of these inhibitors were in the micromolar range, making them a promising starting point for the development of multiple inhibitors of Mur ligases as potential antibacterial agents. Towards identifying the inhibitors of these enzymes, compounds extracted from *H. acmosepalum* were tested against MurE of *M. tuberculosis*. Of the two compounds tested, compound **2** showed a good dose-dependent inhibition of MurE enzyme activity. Although the precise antibacterial mode of action of compound **2** remains unknown, it is possible that its activity could be due to MurE enzyme inhibition. However, this hypothesis needs further investigation. Availability of the three-dimensional structure of MurE of *M. tuberculosis* facilitates further optimisation of this compound to improve its potency through fragment-based screening or docking studies [10,24]. This increases the chance of developing a natural product into a potential antimycobacterial compound with a novel mechanism of action.

To conclude, here we report the antibacterial activity of compounds **1** and **2** against a panel of *S. aureus*, *M. tuberculosis* H37Rv and *M. bovis* BCG bacteria. In addition, both of the compounds were non-cytotoxic to mammalian cells. Furthermore, compound **2** demonstrated specific dose-dependent inhibition of MurE enzyme activity of *M. tuberculosis*. As there is a lack of antibacterial compounds targeting Mur ligase enzymes, further research in this respect is required. The antibacterial activity of these compounds represents a promising starting point for further development.

Acknowledgments

The authors thank the Bloomsbury College Studentships for KO's graduate research studies. They are grateful to Dr Chris Clennett (Royal Botanic Gardens, Kew at Wakehurst Place, Ardingly, UK) for the plant material.

Funding: Funding for this study was received from the UK Medical Research Council (MRC, UK) for a New Investigators Research Grant to SB (grant reference no. GO801956) and UNESCO-L'ORÉAL for a co-sponsored international fellowship to AG.

Competing interests: None declared.

Ethical approval: Not required.

Appendix A. Supplementary data

Supplementary data associated with this article can be found, in the online version, at doi:10.1016/j.ijantimicag.2011.09.018.

References

[1] Graffunder EM, Venezia RA. Risk factors associated with nosocomial methicillin-resistant *Staphylococcus aureus* (MRSA) infection including previous use of antimicrobials. J Antimicrob Chemother 2002;49:999–1005.
[2] Koul A, Arnoult E, Lounis N, Guillemont J, Andries K. The challenge of new drug discovery for tuberculosis. Nature 2011;469:483–90.
[3] Crowcroft NE, Catchpole M. Mortality from methicillin-resistant *Staphylococcus aureus* in England and Wales: analysis of death certificates. BMJ 2002;325:1390–1.
[4] Wesson KM, Lerner DS, Silverberg NB, Weinberg JM. Linezolid, quinupristin/dalfopristin, and daptomycin in dermatology. Dis Mon 2004;50:395–406.
[5] Meka VG, Gold HS. Antimicrobial resistance to linezolid. Clin Infect Dis 2004;39:1010–15.
[6] Skiest DJ. Treatment failure resulting from resistance of *Staphylococcus aureus* to daptomycin. J Clin Microbiol 2006;44:655–6.
[7] World Health Organization. WHO report 2008. Global tuberculosis control 2008: surveillance, planning, financing. Geneva, Switzerland: WHO; 2008. WHO/HTM/TB/2008.393.
[8] Crick DC, Brennan PJ. Antituberculosis drug research. Curr Opin Anti-infect Invest Drugs 2000;2:154–63.
[9] Brown ED, Wright GD. New targets and screening approaches in antimicrobial drug discovery. Chem Rev 2005;105:759–74.
[10] Turk S, Kovac A, Boniface A, Bostock JM, Chopra I, Blanot D, et al. Discovery of new inhibitors of the peptidoglycan biosynthesis enzymes MurD and MurF by structure-based virtual screening. Bioorg Med Chem 2009;17:1884–9.
[11] Basavannacharya C, Robertson G, Munshi T, Keep NH, Bhakta S. ATP-dependent MurE ligase in *Mycobacterium tuberculosis*: biochemical and structural characterization. Tuberculosis (Edinb) 2010;90:16–24.
[12] Spiegelman MK. New tuberculosis therapeutics: a growing pipeline. J Infect Dis 2007;196(Suppl. 1):S28–34.
[13] Rocha L, Marston A, Potterat O, Auxiliadora M, Kaplan C, Stoeckli-Evans H, et al. Antibacterial phloroglucinols and flavonoids from *Hypericum brasiliense*. Phytochemistry 1995;40:1447–52.
[14] Barnes J, Anderson LA, Phillipson JD. St John's Wort (*Hypericum perforatum* L.): a review of its chemistry, pharmacology and clinical properties. J Pharm Pharmacol 2001;53:583–600.
[15] Demirci B, Baser KHC, Crockett SL, Khan IA. Analysis of the volatile constituents of Asian *Hypericum* L. (Clusiaceae, Hyperidoideae) species. J Essent Oil Res 2005;17:659–63.
[16] Long C-L, Li R. Ethnobotanical studies on medicinal plants used by red-headed Yao People in Jinping, Yunnan Province, China. J Ethnopharmacol 2004;90:389–95.
[17] Gibbons S, Udo EE. The effect of reserpine, a modulator of multidrug efflux pumps, on the in vitro activity of tetracycline against clinical isolates of methicillin-resistant *Staphylococcus aureus* (MRSA) possessing the *tet*(K) determinant. Phytother Res 2000;14:139–40.
[18] Kaatz GW, Seo SM, Ruble CA. Efflux-mediated fluoroquinolone resistance in *Staphylococcus aureus*. Antimicrob Agents Chemother 1993;37:1086–94.
[19] Ross JI, Cove JH, Farrell AM, Eady EA, Cunliffe WJ. Characterisation and molecular cloning of the novel macrolide streptogramin B determinant from *Staphylococcus epidermidis*. J Antimicrob Chemother 1989;24:851–62.
[20] Decosterd LA, Stoeckli-Evans H, Chapuis JC, Sordat B, Hostettmann K. New cell growth-inhibitory cyclohexadienone derivatives from *Hypericum calycinum* L. Helvet Chim Acta 1989;70:1833–45.
[21] Evangelopoulos D, Bhakta S. Rapid methods for testing inhibitors for mycobacterial growth. In: Gillespie SH, McHugh TD, editors. Antibiotic resistance protocols. 2nd ed. London, UK: Humana Press; 2010. p. 193–201.
[22] Guzman JD, Gupta A, Evangelopoulos D, Basavannacharya C, Pabon LC, Plazas EA, et al. Anti-tubercular screening of natural product from Colombian plants: 3-methoxynordomesticine, an inhibitor of MurE ligase of *Mycobacterium tuberculosis*. J Antimicrob Chemother 2010;65:2101–7.
[23] Kikuchi T, Kadota S, Matsuda S, Tanaka K, Namba T. Studies on the constituents of medicinal and related plants in Sri Lanka. II. Isolation and structure of new gamma-pyrone and related compounds from *Hypericum mysorense* Heyne. Chem Pharm Bull (Tokyo) 1985;33:557–64.
[24] Basavannacharya C, Moody PR, Munshi T, Cronin N, Keep NH, Bhakta S. Essential residues for the enzyme activity of ATP-dependent MurE ligase from *Mycobacterium tuberculosis*. Protein Cell 2010;1:1011–22.
[25] Rabanal RM, Arias A, Prado B, Hernández-Pérez M, Sánchez-Mateo CC. Antimicrobial studies on three species of *Hypericum* from the Canary Islands. J Ethnopharmacol 2002;81:287–92.
[26] Gibbons S, Ohlendorf V, Johnsen I. The genus *Hypericum*—a valuable resource of anti-staphylococcal leads. Fitoterapia 2002;73:300–4.
[27] Cakir A, Kordali S, Zengin H, Izumi S, Hirata T. Composition and antifungal activity of essential oils isolated from *Hypericum hyssopifolium* and *Hypericum heterophyllum*. Flavour Fragr J 2004;19:62–8.
[28] Sova M, Kovac A, Turk S, Hrast M, Blanot D, Gobec S. Phosphorylated hydroxyethylamines as novel inhibitors of the bacterial cell wall biosynthesis enzymes MurC to MurF. Bioorg Chem 2009;37:217–22.

JOURNAL OF NATURAL PRODUCTS

ARTICLE

pubs.acs.org/jnp

Antibacterial Acylphloroglucinols from *Hypericum olympicum*

Winnie K. P. Shiu, M. Mukhlesur Rahman, Jonathan Curry, Paul Stapleton, Mire Zloh, John P. Malkinson, and Simon Gibbons*

Department of Pharmaceutical and Biological Chemistry, The School of Pharmacy, University of London, 29-39 Brunswick Square, London WC1N 1AX, U.K.

Supporting Information

ABSTRACT: New antibacterial acylphloroglucinols (**1**−**5**) were isolated and characterized from the aerial parts of the plant *Hypericum olympicum* L. cf. *uniflorum*. The structures of these compounds were confirmed by extensive 1D- and 2D-NMR experiments to be 4,6-dihydroxy-2-*O*-(3″,7″-dimethyl-2″,6″-octadienyl)-1-(2′-methylbutanoyl)benzene (**1**), 4,6-dihydroxy-2-*O*-(7″-hydroxy-3″,7″-dimethyl-2″,5″-octadienyl)-1-(2′-methylbutanoyl)benzene (**2**), 4,6-dihydroxy-2-*O*-(6″-hydroxy-3″,7″-dimethyl-2″,7″-octadienyl)-1-(2′-methylbutanoyl)benzene (**3**), 4,6-dihydroxy-2-*O*-(6″-hydroperoxy-3″,7″-dimethyl-2″,7″-octadienyl)-1-(2′-methylbutanoyl)benzene (**4**), and 4,6-dihydroxy-2-*O*-(6″,7″-epoxy-3″,7″-dimethyloct-2″-enyl)-1-(2′-methylbutanoyl)benzene (**5**). These new natural products have been given the trivial names olympicins A−E (**1**−**5**). All compounds were evaluated against a panel of methicillin-resistant *Staph. aureus* and multidrug-resistant strains of *Staph. aureus*. Compound **1** exhibited minimum inhibitory concentrations (MICs) of 0.5−1 mg/L against the tested *Staph. aureus* strains. Compounds **2** to **5** were also shown to be active, with MICs ranging from 64 to 128 mg/L. Compound **1** was synthesized using a simple four-step method that can be readily utilized to give a number of structural analogues of **1**.

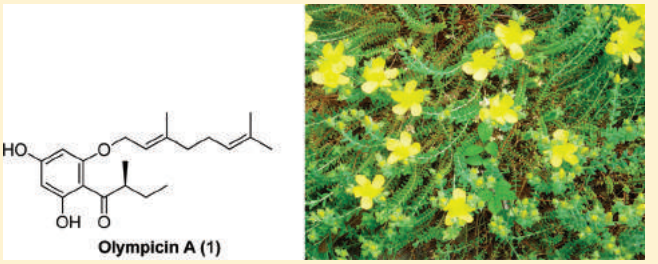

The widespread interest in the use of *Hypericum perforatum* (St. John's Wort) in mild to moderate depression has attracted much attention in investigating the bioactive metabolites from other species in the *Hypericum* genus. The acylphloroglucinol hyperforin is the best characterized acylphloroglucinol from this genus in terms of its bioactivity and has been shown to be the major antibacterial constituent in *H. perforatum*[1] and active against *Staph. aureus* and MRSA strains at concentrations as low as 0.1 mg/L.[2] Other acylphloroglucinol derivatives with antibacterial activities have been isolated and characterized from this genus.[3,4] Notable among these acylphloroglucinols are the antibacterial drummondins from *Hypericum drummondii*, which are filicinic acid derivatives displaying MIC values as low as 0.39 mg/L.[5] This study is part of ongoing research in our group to identify antibacterial metabolites from various *Hypericum* species.

These levels of activity, coupled with interesting acylphloroglucinol chemistry, which is often complex, prompted us to screen a range of *Hypericum* species collected from the UK National Collection at the Royal Botanic Gardens Kew at Wakehurst Place.[8] This led to the isolation and evaluation of the antibacterial properties of a series of new acylphloroglucinol natural products (**1**−**5**) from *Hypericum olympicum*. This species is a small herb with typical yellow *Hypericum* flowers.

The simplicity of compound **1**, coupled with its level of activity against a range of methicillin-resistant *Staph. aureus* (MRSA) and multidrug-resistant (MDR) strains of *Staph. aureus*, shows the value of this class as antibacterial drug leads, which could be further developed into antibiotics to treat resistant strains.

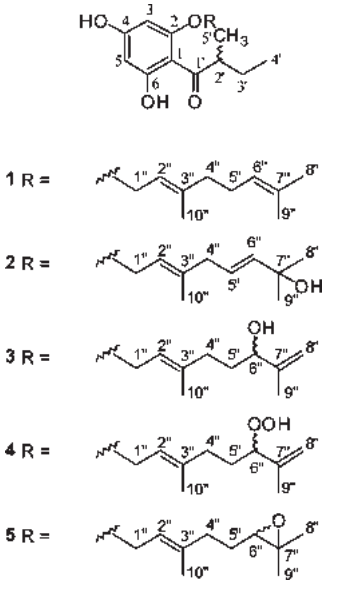

Special Issue: Special Issue in Honor of Gordon M. Cragg

Received: April 19, 2011

dx.doi.org/10.1021/np2003319 | *J. Nat. Prod.* XXXX, XXX, 000–000

Table 1. ^{1}H (500 MHz) and ^{13}C NMR (125 MHz) Spectroscopic Data and $^{1}H-^{13}C$ Long-Range Correlations for 1−3 Recorded in $CDCl_3$

	1				2				3			
position	^{1}H (J, Hz)	^{13}C	^{2}J	^{3}J	^{1}H (J, Hz)	^{13}C	^{2}J	^{3}J	^{1}H (J, Hz)	^{13}C	^{2}J	^{3}J
1		105.0				105.9				105.9		
2		162.6				162.4				162.4		
3	5.92 d (2.5)	91.5	C-4	C-1, C-5	5.90 d (2)	91.7	C-4	C-1, C-5	5.92 d (2)	91.6		C-1
4		161.9				162.1				161.9		
5	5.98 d (2.5)	96.5	C-6	C-1, C-3	5.99 d (2)	96.6	C-6	C-1, C-3	5.98 d (2)	96.6		C-3
6		167.5				167.5				167.6		
1′		210.4				210.3				210.3		
2′	3.66 m	46.1			3.63 m	46.1			3.64 m	46.1		
3′	1.37 m, 1.80 m	26.8			1.37 m, 1.80 m	26.9			1.37 m, 1.80 m	26.8		
4′	0.89 t (7.5)	11.8	C-3′	C-2′	0.88 t (7.5)	11.9	C-3′	C-2′	0.88 t (7.5)	11.9	C-3′	C-2′
5′	1.12 d (6.5)	16.6	C-2″	C-1′, C-3′	1.12 d (7)	16.7	C-2′	C-1′, C-3′	1.12 d (6.5)	16.7	C-2′	C-1′, C-3′
1″	4.57 d (6.5)	65.7	C-2″	C-3, C-3″	4.58 d (6.5)	65.6	C-2″	C-3″	4.57 d (6.5)	65.6		C-3″
2″	5.51 m	118.2		C-4″, C-10″	5.30 m	119.6			5.53 dt	118.7		
3″		142.3				140.5				141.9		
4″	2.13 m	39.5	C-3″, C-5″	C-2″, C-6″	2.81 d (6.5)	42.2	C-3″, C-5″	C-2″, C-6″	2.15 m	35.5		
5″	2.10 m	26.3	C-4″, C-6″	C-3″	5.68 m	128.4			1.75	26.8	C-4″	C-3″
6″	5.10 m	123.6			5.66 d (15)	135.9			4.08 t (6.5)	75.5		
7″		132.0				82.2				147.2		
8″	1.62 s	17.7	C-7″	C-6″, C-9″	1.35 s	24.3	C-7″	C-6″, C-8″	4.95 s, 4.87 t	111.4		C-6″
9″	1.69 s	25.7	C-7″	C-6″, C-8″	1.35 s	24.3	C-7″	C-6″, C-8″	1.76 s	16.7	C-7″	C-6″, C-8″
10″	1.74 s	16.7	C-3″	C-2″, C-4″	1.74 s	16.8	C-3″	C-2″	1.74 s	17.6	C-3″	C-2″, C-4″
4-OH	5.32 bs											
6-OH	14.02 s		C-1	C-2, C-6	14.00 s		C-6	C-1, C-5	13.99 s			C-1, C5

RESULTS AND DISCUSSION

Compound **1** was isolated as a pale yellow oil from the *n*-hexane extract of *H. olympicum* L. cf. *uniflorum*. The HR-ESIMS indicated an $[M - H]^-$ ion at *m/z* 345, suggesting a molecular formula of $C_{21}H_{30}O_4$. The ^{1}H and ^{13}C NMR data (Table 1) were indicative of an acylphloroglucinol with a terpene substituent. The ^{1}H NMR spectrum showed two signals for hydroxy groups, one of which was highly deshielded and hydrogen-bonded (δ 14.02) and the other of which appeared as a broad singlet at δ 5.32. Other signals observed in the ^{1}H NMR spectrum included two *meta*-coupled aromatic protons (δ 5.98 d, *J* = 2.5 Hz; 5.92 d, *J* = 2.5 Hz), two olefinic protons (δ 5.51 m; 5.10 m), one methine (δ 3.66 m), four methylene groups, three methyl singlets (δ 1.74, 1.69, 1.62), one methyl doublet (δ 1.12, *J* = 6.5 Hz), and one methyl triplet (δ 0.89, *J* = 7.5 Hz). The ^{13}C NMR spectrum displayed signals for six aromatic carbons, three of which were highly deshielded, implying that these carbons were attached to electron-withdrawing groups. The pattern of these signals suggested a 1,3,5-trihydroxybenzene (phloroglucinol) structure. In the HMBC spectrum the hydrogen-bonded proton showed a ^{2}J correlation with the carbon to which it was directly attached (δ 167.5, C-6) and ^{3}J correlations with an aromatic methine carbon (δ 96.5, C-5) and a quaternary aromatic carbon (δ 105.0, C-1), confirming the position of the hydroxy group. The other aromatic hydrogen at δ 5.92 was then placed at C-3, as it was *meta*-coupled to H-5. This was further confirmed by HMBC correlations between this proton and C-1, C-5, and a deshielded carbon (δ 161.9, C-4). The second hydroxy group was therefore placed between the aromatic protons at C-4.

The substituent at C-1 included a methine multiplet (δ 3.66, H-2′), a methylene multiplet (δ 1.37, 1.80, H_2-3′), a methyl triplet (δ 0.89, H_3-4′), and a methyl doublet (δ 1.12, H_3-5′). In the COSY spectrum, the methylene (H_2-3′) was coupled to the methyl triplet (H_3-4′), and the methine multiplet (H-2′) was coupled to the methyl doublet (H_3-5′). The HMBC spectrum revealed cross-peaks between this methyl doublet and C-2′, C-3′, and a carbonyl carbon (δ 210.4, C-1′), which could interact with the hydroxy group at C-6 via a hydrogen bond and be responsible for the downfield resonance of this hydroxy group. This confirmed the 2-methylbutanoyl side-chain at C-1.

The final substituent at C-2 included an oxymethylene group (δ 4.57 d, *J* = 6.5 Hz, C-1″), which showed long-range $^{1}H-^{13}C$ correlations with a deshielded aromatic carbon (δ 162.6, C-2) and two carbons associated with an olefinic group (δ 118.2, C-2″; δ 142.3, C-3″). In the HMBC spectrum, an olefinic proton (δ 5.51 m) at C-2″ was coupled to the carbon of a methyl moiety (δ 16.7, C-10″) and to a methylene carbon (δ 39.5, C-4″) via three bonds. This methylene group (δ 2.13 m, H-4″) showed ^{2}J correlations with C-3″ and C-5″ (δ 26.3) and ^{3}J correlations with C-2″ and C-6″ (δ 123.6). Two methyl singlets (δ 1.62, 1.69) were coupled to C-6″ and a quaternary carbon associated with this olefinic carbon (δ 132.0, C-7″), therefore completing the substituent at C-2. This side-chain consisted of 10 carbons, including two olefinic and three methyl groups, and was characteristic of a geranyl group. The COSY and NOESY spectra also

dx.doi.org/10.1021/np2003319 |J. Nat. Prod. XXXX, XXX, 000–000

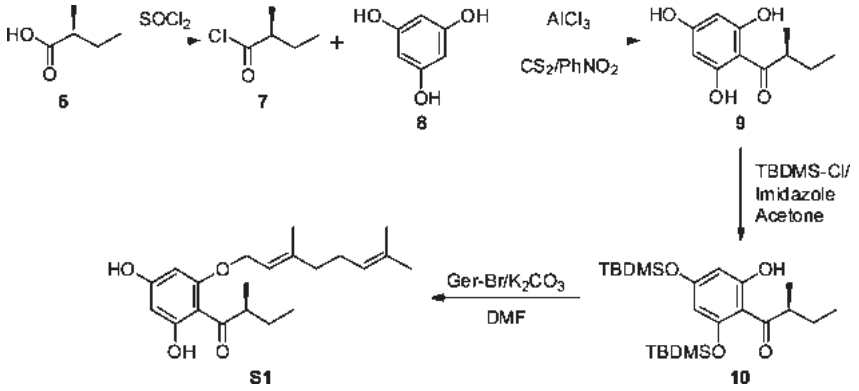

Figure 1. Synthesis of compound **S1**.

provided evidence for the geranyl side-chain. Both double bonds were assigned the *trans*-configuration on the basis of the nature of the biosynthesis of a geranyl side-chain from two isoprene units. This was also supported by an NOE correlation between H-2″ and H_2-4″. The ^{1}H and ^{13}C NMR data on the geranyloxy side-chain showed good agreement with reported data.[7]

The position of the *O*-geranyl substituent was assigned as *ortho* to the 2-methylbutanoyl group on the basis of the HMBC correlations as described and also the observation that the *meta*-coupled aromatic protons were nonequivalent. The configuration at the C-2′ stereogenic center can be identified by comparing the specific rotation of this compound with that of the synthetic compound **S1**, which was synthesized from (+)-(*S*)-2-methylbutanoic acid (Figure 1). The specific rotations for **1** and **S1** were found to be $[\alpha]_D^{22}$ +6.0 (*c* 0.25, $CHCl_3$) and $[\alpha]_D^{22}$ +6.0 (*c* 0.30, $CHCl_3$), respectively. The data implied that the stereogenic center in the natural product **1** was of the *S*-configuration. Compound **1** was therefore identified as the new natural product (*S*)-4,6-dihydroxy-2-*O*-(3″,7″-dimethyl-2″,6″-octadienyl)-1-(2′-methylbutanoyl)benzene and given the trivial name olympicin A. A patent was filed for this compound for its application as a potential antibacterial agent.[8]

Compound **2** was isolated as a pale yellow oil from the CH_2Cl_2 extract of *H. olympicum* L. cf. *uniflorum*. High-resolution ESIMS gave an $[M + H]^+$ ion at *m/z* 363, indicating a molecular formula of $C_{21}H_{30}O_5$. The ^{1}H and ^{13}C NMR spectroscopic data (Table 1) were similar to those of compound **1**. The ^{1}H NMR signals indicated the presence of a 2-methylbutanoyl phloroglucinol nucleus with one highly deshielded hydrogen-bonded hydroxy group (δ 14.00), two *meta*-coupled aromatic protons (δ 5.90 d, *J* = 2 Hz, H-3; 5.99 d, *J* = 2 Hz, H-5), one methine multiplet (δ 3.63, H-2′), one methylene (δ 1.37 m, 1.80 m, H_2-3′), one methyl triplet (δ 0.88, *J* = 7.5 Hz, H_3-4′), and one methyl doublet (δ 1.12, *J* = 7.5 Hz, H_3-5′). The ^{13}C NMR signals were again indicative of a phloroglucinol moiety with six aromatic carbons, comprising three deshielded quaternary carbons (δ 167.5, C-6; 162.4, C-2; 162.1, C-4), one quaternary carbon at δ 105.9 (C-1), and two methines at δ 96.6 (C-5) and 91.7 (C-3). The presence of a carbonyl carbon (δ 210.3, C-1′), one methine (δ 46.1, C-2′), one methylene (δ 26.9, C-3′), and two methyl carbon signals (δ 11.9, C-4′; 16.7, C-5′) again suggested a 2-methylbutanoyl side-chain in **2**. The structure of the 2-methylbutanoyl-phloroglucinol nucleus was further confirmed by HMBC correlations, which were described earlier in the structural elucidation of compound **1**.

The remaining signals in the ^{1}H NMR spectrum included three olefinic protons (δ 5.30 m, H-2″; 5.68 m, H-5″; 5.66 d, *J* = 15 Hz, H-6″), two methylene doublets including one shifted downfield at δ_H 4.58 (*J* = 6.5 Hz, H_2-1″) and one at δ 2.81 (*J* = 6.5 Hz, H_2-4″), two equivalent methyl groups integrating to six protons (δ 1.35 s, H_3-8″, H_3-9″), and an additional methyl singlet (δ 1.74, H_3-10″). The remaining signals in the ^{13}C NMR spectra included one quaternary olefinic carbon (δ 140.5, C-3″), three olefinic methines (δ 119.6, C-2″; 128.4, C-5″; 135.9, C-6″), an oxygenated quaternary carbon (δ 82.2, C-7″), two methylenes (δ 65.6, C-1″; 42.2, C-4″), two equivalent methyl carbons at δ 24.3 (C-8″, C-9″), and a further methyl carbon at δ 16.8 (C-10′). An oxymethylene (δ 4.58 d, H_2-1″) was coupled to the olefinic proton at δ 5.30 (H-2″) in the COSY spectrum. It also displayed ^{1}H−^{13}C ^2J correlation to the olefinic carbon at δ 119.6 (C-2″) and ^3J correlation to a quaternary olefinic carbon (δ 140.5, C-3″) to which a methyl group (δ 1.74 s, H_3-10″) was directly attached. The C-10″ methyl group was correlated to a methylene carbon at δ_C 42.2 (C-4″) in the HMBC spectrum, thus placing the methylene group (δ 2.81 d, H_2-4″) next to C-3″. This methylene doublet in turn displayed ^{1}H−^{13}C correlations to four olefinic carbons, confirming its position between the two olefinic bonds. An olefinic multiplet at δ_H 5.68 (H-5″) was placed between the methylene group (H_2-4″) and the olefinic doublet (δ 5.66, H-6″), as they showed correlations in the COSY spectrum. The splitting of the olefinic multiplet (δ 5.68, H-5″) was due to the fact that the signal was split by both the neighboring methylene (H_2-4″) and the C-6″ olefinic proton. The olefinic proton at H-6″ appeared as a clear doublet because the signal was only split by the neighboring H-5″. The large coupling constant between H-5″ and H-6″ (*J* = 15 Hz) indicated that these two protons were in a *trans*-configuration. The equivalent methyl groups (δ 1.35 s, 6 H, H_3-8″, H_3-9″) at the terminus of the side-chain were directly attached to a quaternary carbon (δ 82.2, C-7″), which was shifted downfield by a hydroxy group directly attached to this carbon. This connection was supported by HMBC correlations between the methyl singlet and C-7″ and the olefinic carbon at C-6″. This completed the structural elucidation of compound **2**. The specific rotation of this compound was found to be $[\alpha]_D^{22}$ +5.8 (*c* 0.22, $CHCl_3$), which might again imply that C-2′ was of an *S*-configuration (synthetic compound **S1**, $[\alpha]_D^{22}$ +6.0 (*c* 0.30, $CHCl_3$)). Compound **2** was therefore identified as 4,6-dihydroxy-2-*O*-(7″-hydroxy-3″,7″-dimethyl-2″,5″-octadienyl)-1-(2′-methylbutanoyl)-benzene, assigned as olympicin B, and is described here for the first time.

Compound **3** was isolated as a pale yellow oil from the CH_2Cl_2 extract of *H. olympicum*. The HR-ESIMS gave an $[M - H]^-$ ion

dx.doi.org/10.1021/np2003319 |*J. Nat. Prod.* XXXX, XXX, 000–000

Table 2. ^{1}H (500 MHz) and ^{13}C NMR (125 MHz) Spectroscopic Data and $^{1}H-^{13}C$ Long-Range Correlations of **4** and **5** Recorded in $CDCl_3$

	4				5				
position	^{1}H (*J*, Hz)	^{13}C	^{2}J	^{3}J	position	^{1}H (*J*, Hz)	^{13}C	^{2}J	^{3}J
1		105.9			1		105.5		
2		162.4			2		162.3		
3	5.91 d (2.5)	91.7		C-1, C-5	3	6.02 d (2.5)	92.7		C-1, C-5
4		162.0			4		162.8		
5	5.98 d (2.5)	96.6	C-6	C-1, C-3	5	5.98 d (2.5)	96.8		C-3
6		167.5			6		167.6		
1′		210.3			1′		210.0		
2′	3.63 m	46.1			2′	3.63 m	46.1		
3′	1.35 m, 1.80 m	26.8			3′	1.38 m, 1.81 m	26.5		
4′	0.88 t (7.5)	11.9	C-3′	C-2′	4′	0.90 t (7.5)	12.0	C-3′	C-2′
5′	1.11 d (6)	16.6	C-2′	C-1′, C-3′	5′	1.1 d (7)	16.6	C-2′	C-1′, C-3′
1″	4.58 d (6.5)	65.6	C-2″	C-3″	1″	4.67 m	66.4		
2″	5.52 m	119.2			2″	5.50 m	121.9		
3″		141.2			3″		138.5		
4″	2.21 m	35.2			4″	2.30 m	37.0		
5″	1.75 m	26.8			5″	1.65 m, 1.90 m	26.5		
6″	4.32 t	89.0			6″	2.77 dt	65.1		
7″		143.3			7″		59.1		
8″	5.02 s, 5.05 t	114.6		C-6″, C-9″	8″	1.31 s	18.9	C-7″	C-6″, C-9″
9″	1.75 s	17.2	C-7″	C-6″, C-8″	9″	1.34 s	24.6	C-7″	C-6″, C-8″
10″	1.75 s	16.6	C-3″	C-2″, C-4″	10″	1.76 s	16.0	C-3″	C-2″, C-4″
4-OH	5.32 bs				1-OH	13.95 s			C-1, C-5
6-OH	13.99 s		C-6	C-1, C-5	5-OH	6.90 bs			

at *m/z* 361, suggesting a molecular formula of $C_{21}H_{30}O_5$. The ^{1}H and ^{13}C NMR spectroscopic data (Table 3) were again similar to those of compound **1**. The common signals in the ^{1}H NMR spectrum included one highly deshielded hydrogen-bonded hydroxy group (δ 13.99, 6-OH), two *meta*-coupled aromatic protons (δ 5.92 d, *J* = 2 Hz, H-3; 5.98 d, *J* = 2 Hz, H-5), one methine (δ 3.64 m, H-2′), one methylene (δ 1.37 m, 1.80 m, H_2-3′), one methyl triplet (δ 0.88 t, *J* = 7.5 Hz, H_3-4′), and one methyl doublet (δ 1.12 d, *J* = 6.5 Hz, H_3-5′). In the ^{13}C NMR spectrum, signals suggesting a (2-methylbutanoyl)phloroglucinol nucleus were again seen, including three deshielded quaternary aromatic carbons (δ 167.6, C-6; 162.4, C-2; 161.9, C-4), one quaternary aromatic carbon (δ 105.9, C-1), two methine aromatic carbons (δ 91.6 C-3; 96.6, C-5), one carbonyl carbon (δ 210.3, C-1′), one methine (δ 46.1, C-2′), one methylene (δ 26.8, C-3′), and two methyl carbons (δ 11.9, C-4′; 16.7, C-6′). HMBC correlations further confirmed the structure of the (2-methylbutanoyl)phloroglucinol nucleus and were similar to those described in the structural elucidation of compound **1**.

The ^{1}H NMR signals for the side-chain at the 2-*O* position consisted of four methylenes, including one shifted downfield (δ 4.57 d, *J* = 6.5 Hz, H_2-1″) and an *exo*-methylene (δ 4.87 t, 4.95 s, H_2-8″), one olefinic proton (δ 5.53 dt, H-2″), one deshielded methine triplet (δ 4.08, *J* = 6.5 Hz, H-6″), and two methyl singlets (δ 1.76, H_3-9″; 1.74, H_3-10″). Ten carbons were accountable for this side-chain, again indicative of a geranyl moiety. These included two methines (δ 118.7, C-2″; 75.5, C-6″), four methylenes (δ 65.6, C-1″; 35.5, C-4″; 26.8, C-5″; 111.4, C-8″), two quaternary olefinic carbons (δ 141.0, C-3″; 147.2, C-7″), and two methyl carbons (δ 16.7, C-9″; 17.6, C-10″).

The oxymethylene group showed HMBC correlations with an olefinic carbon at δ 118.7 (C-2″) and COSY correlations to the olefinic proton associated with this carbon (δ 5.53). A methyl singlet at δ 1.74 (H_3-10″) showed HMBC correlations with C-2″, an olefinic carbon to which it was directly attached (δ 141.9, C-3″), and to a methylene carbon at δ 35.5 (C-4″). The methylene protons at C-4″ were coupled to another methylene group (δ 1.75 m), which was coupled to a methine triplet (δ 4.08, *J* = 6.5 Hz, H-6″), as shown in the COSY spectrum. This triplet was shifted downfield and was attached to a carbon at δ 75.5 (C-6″), indicating that a hydroxy group should be attached here, and this was supported by the mass spectrum. The remaining methyl group (δ 1.76) was placed at C-7″, as it exhibited a ^{2}J HMBC correlation to a quaternary carbon at δ 143.3 (C-7″) and ^{3}J correlations to the oxygenated methine carbon (C-6″) and to an olefinic carbon at δ 111.4 (C-8″) bearing two *exo*-methylene protons. The specific rotation of **3** was $[\alpha]_D^{22}$ +2.5 (*c* 0.41, $CHCl_3$). Although it showed the same direction of rotation as **S1**, the configuration of **3** could not be determined, as two stereogenic centers were present in this compound. Compound **3** was therefore identified as the new natural product 4,6-dihydroxy-2-*O*-(6″-hydroxy-3″,7″-dimethyl-2″,7″-octadienyl)-1-(2′-methylbutanoyl)benzene and was given the trivial name olympicin C.

Compound **4** was isolated as a pale yellow oil from the CH_2Cl_2 extract of *H. olympicum* L. cf. *uniflorum*. High-resolution ESIMS gave an $[M - H]^-$ ion at *m/z* 377, indicating a molecular formula

dx.doi.org/10.1021/np2003319 |*J. Nat. Prod.* XXXX, XXX, 000–000

Table 3. MIC (μM) Values of Compound 1 and Control Antibiotics against *Staph. aureus*, *Mycobacterium* species, *P. aeruginosa*, and *Salmonella enterica* serovar Typhimurium

strain	control	control (μM)	compound **1** (μM)
S. aureus			
SA-1199B	norfloxacin	100	2.9
XU212	tetracycline	288	2.9
RN4220	erythromycin	349	2.9
ATCC25923	norfloxacin	3.1	2.9
EMRSA-15	oxacillin	79	1.45
EMRSA-16	oxacillin	1276	2.9
Mycobacterium			
M. smegmatis ATCC 14468	isoniazid; ethambutol	14.6; 2.4	11.6
M. fortuitum ATCC 6841	isoniazid; ethambutol	29.2; 2.4	23.2
M. smegmatis MC^2 2700	isoniazid; ethambutol	14.6; 2.4	11.6
M. phlei ATCC 11758	isoniazid; ethambutol	14.6; 2.4	11.6
P. aeruginosa			
K 1119	norfloxacin	6.2	>1 mM
K 767	norfloxacin	6.2	>1 mM
S. enterica serovar Typhimurium			
L 354	tetracycline	2.3	>1 mM
L 10	tetracycline	2.3	>1 mM

of $C_{21}H_{30}O_6$. The ^{1}H and ^{13}C NMR data (Table 2) for compound **4** were similar to those of compound **3**. The characteristic ^{1}H NMR features of a (2-methylbutanoyl)phloroglucinol were again seen in this compound, including one highly deshielded hydrogen-bonded hydroxy group (δ 13.99, 6-OH), two *meta*-coupled aromatic protons (δ 5.91 d, J = 2.5 Hz, H-3; 5.98 d, J = 2.5 Hz, H-5), one methine (δ 3.63 m, H-2′), one methylene (δ 1.35 m, 1.80 m, H$_2$-3′), one methyl triplet (δ 0.88, J = 7.5 Hz, H$_3$-4′), and one methyl doublet (δ 1.11, J = 6 Hz, H$_3$-5′). Signals in the ^{13}C NMR spectrum accounting for a (2-methylbutanoyl)phloroglucinol nucleus consisted of three deshielded quaternary aromatic carbons (δ 167.5, C-6; 162.3, C-3; 162.0, C-4), one quaternary aromatic carbon (δ 105.9, C-1), two aromatic methine carbons (δ 91.7, C-3; 96.6, C-5), one carbonyl carbon (δ 210.3, C-1′), one methine (δ 46.1, C-2′), one methylene (δ 26.8, C-3′), and two methyl carbons (δ 11.9, C-4′; 16.6, C-5′). The connection of these protons and carbons was made through HMBC studies and was identical to those seen in the structural elucidation of compound **1**.

The ^{1}H NMR signals for the side-chain at the 2-*O* position consisted of four methylenes, including an oxymethylene (δ 4.58 d, J = 6.5 Hz, H$_2$-1″) and an *exo*-methylene (δ 5.02 s, 5.05 t, H$_2$-8″), one olefinic proton (δ 5.52 dt, H-2″), one deshielded methine triplet (δ 4.32, J = 6.5 Hz, H-6″), and two overlapping methyl singlets (δ 1.75, 6H, H$_3$-9″, H$_3$-10″). Ten carbon signals were observed in the ^{13}C NMR spectrum for this side-chain, including two methines (δ 89.0, C-6″; 119.2, C-2″), four methylenes (δ 65.6, C-1″; 35.2, C-4″; 26.8, C-5″; 114.6, C-8″), two quaternary olefinic carbons (δ 141.2, C-3″; 143.3, C-7″), and two methyl carbons (δ 17.2, C-9″; 16.6 C-10″). These signals were indicative of a geranyl derivative and were again similar to those of compound **3**.

The oxymethylene group (δ 4.58, H$_2$-1″) exhibited HMBC correlations with two carbons at δ_C 119.2 (C-2″) and 141.2 (C-3″) and COSY correlation with the olefinic proton at C-2″. The methyl singlet at δ 1.74 (H-10″) showed a ^2J HMBC correlation to the olefinic carbon to which it was directly attached (C-3″) and ^3J HMBC correlations to C-2″ and a methylene carbon at δ 35.2 (C-4″). The methylene protons at C-4″ (2.21 m) were coupled to another methylene group (δ 1.75 m, H-5″), which was coupled to a methine triplet (δ 4.32, H-6″), as shown in the COSY spectrum. This triplet was shifted downfield and was attached to a carbon at δ 89.0 (C-6″), indicating that an electron-withdrawing group with a stronger deshielding effect than a hydroxy group was present at this carbon (δ_C 75.5 for hydroxy-bearing C-6″ in compound **3**). This chemical shift was characteristic of a hydroperoxy-bearing methine. The molecular formula for this compound ($C_{21}H_{30}O_6$) indicated that it had an extra oxygen when compared to that of compound **3** ($C_{21}H_{30}O_5$). The remaining methyl group (δ_H 1.75, H-9″) was placed at C-7″ (δ_C 143.3), as the methyl singlet showed HMBC correlations to this carbon, the hydroperoxy-bearing carbon (C-6″), and the *exo*-methylene carbon at δ_C 114.6 (C-8″). This was further confirmed by HMBC correlations between the *exo*-methylene group and C-6″ and C-9″. This completed the structural elucidation of compound **4**. Like **S1** and other acylphloroglucinols isolated from *H. olympicum* L. cf. *uniflorum*, the specific rotation of compound **4** showed a positive value ($[\alpha]_D^{22}$ +2.7 (c 0.32, $CHCl_3$)). However, two stereogenic centers (C-2′ and C-6″) were present in **4**, and thus the configuration at each stereogenic center could not be determined by direct comparison with the specific rotation of **S1**. A further experiment using a starch-iodide test strip (Fisher) was conducted to confirm the presence of the hydroperoxide group in this compound. A starch-iodide test strip was dipped into a $CHCl_3$ solution of compound **4** (approximately 2 mg/mL) and showed a positive color reaction (light brown). $CHCl_3$ was used as a negative control and did not result in any color change. A $CHCl_3$ solution of mCPBA (20 mg/mL) was used as a positive control, and it turned the test strip dark blue. When a lower concentration of mCPBA was used (approximately 2 mg/mL), the test strip turned light brown, implying that the color change was dependent on the concentration of the hydroperoxide present. Compound **4** was therefore identified as 4,6-dihydroxy-2-*O*-(6″-hydroperoxy-3″,7″-dimethyl-2″,7″-octadienyl)-1-(2′-methylbutanoyl)benzene (olympicin D) and is reported here for the first time.

Compound **5** was isolated as a pale yellow oil from the CH_2Cl_2 extract of *H. olympicum* L. cf. *uniflorum*. The molecular formula of compound **5** was $C_{21}H_{30}O_5$, indicated by an $[M + H]^+$ ion at m/z 363 in the high-resolution ESIMS. The ^{1}H NMR spectrum (Table 2) revealed signals typical of a (2-methylbutanoyl)phloroglucinol, including a broad signal accounting for a hydroxy group (δ 6.90, 4-OH), two *meta*-coupled aromatic protons (δ 6.02 d, J = 2.5, H-3; 5.98 d, J = 2.5, H-5), a methine multiplet (δ 3.63, 1H, H-2′), and a methylene group (δ 1.38 m, 1.81 m, H$_2$-3′). More interestingly, duplication of the following signals was observed: a highly deshielded hydrogen-bonded singlet (δ 13.95, 6-OH), a methyl triplet (δ 0.90, J = 7.5, H$_3$-4′), and a methyl doublet (δ 1.13, J = 7, H$_3$-5′). The carbon signals corresponding to the phloroglucinol nucleus included three deshielded aromatic carbons (δ 167.6, C-6; 162.3, C-2; 162.8, C-4), a quaternary aromatic carbon (δ 105.5, C-1), and two aromatic methines (δ 92.7, C-3; 96.8, C-5). Duplication of the signals in the ^{13}C NMR spectrum was also observed for the 2-methylbutanoyl side-chain: a carbonyl carbon (δ 210.1 and 210.0, C-1′), a methine

dx.doi.org/10.1021/np2003319 |*J. Nat. Prod.* XXXX, XXX, 000–000

(δ 46.09 and 46.12, C-2′), a methylene (δ 26.93 and 26.96, C-3′), and two methyl carbons (δ 11.96 and 12.00, C-4′; 16.52 and 16.55, C-5′). The HMBC correlations observed for the acylphloroglucinol nucleus of this compound were identical to those of compound **1** and were as described previously. The duplication of NMR signals was indicative of the presence of two rotamers, and this phenomenon has been observed in some natural products, including acylphloroglucinols.[9] In the case of acylphloroglucinols, two isomers in rotameric forms were possible: one with the acyl chain above the plane of the phloroglucinol and the other below the plane. Molecular modeling calculation was carried out for this compound. Since two relatively stable conformations were possible, two different energy minima were expected. However, there was only one energy minimum observed in the calculation.

The ^{1}H NMR signals for the side-chain at the 2-*O* position included three methylenes (δ 4.67 m, H_2-1″; 2.30 m, H_2-4″; 1.65 m, 1.90 m, H_2-5″), one olefinic proton (δ 5.50 m, H-2″), one deshielded oxymethine (δ 2.77 dt, H-6″), and three methyl singlets (δ 1.34 s, H_3-8″; 1.31 s, H_3-9″; 1.76 s, H_3-10″). Ten carbon signals were observed in the ^{13}C NMR spectrum for this side-chain, including three methylenes (δ 66.4, C-1″; 37.0, C-4″; 26.5, C-5″), an olefinic carbon (δ 121.9, C-2″), an oxymethine (δ 65.1, C-6″), and three methyl carbons (δ 24.6, C-8″; 18.9, C-9″; 16.0, C10″).

Due to the small quantity of the compound, signals in the HMBC spectrum were very weak. The COSY spectrum and the structures of the other related derivatives isolated from this plant played an important role in the structural elucidation of this compound. As with the other acylphloroglucinols, the oxymethylene group (δ 4.67 m, H_2-1″) was placed at C-2 of the acylphloroglucinol. The oxymethylene protons showed a COSY correlation with the olefinic proton (δ 5.50 m, H-2″), thus placing the olefinic proton at C-2″. The methyl group shifted downfield at δ_H 1.76 (H_3-10″) showed a ^2J HMBC correlation to a quaternary olefinic carbon at δ 138.5 (C-3″) and ^3J HMBC correlations to C-2″ and a methylene carbon at δ 37.0 (C-4″). The methylene protons at C-4″ (δ 2.30 m) showed a COSY correlation to a further methylene group (δ 1.65 m, 1.90 m, C-5″), which was coupled to an oxymethine, as revealed by the COSY spectrum (δ 2.77 dt, H-6″). The remaining methyl groups at δ 1.34 (H_3-8″) and 1.31 (H_3-9″) showed HMBC correlations to δ 18.9 (C-9″) and 24.6 (C-8″), respectively, indicating that the methyl groups were geminal to each other. These methyl groups also correlated to a quaternary carbon at δ 59.1 (C-7″) and the oxymethine carbon (C-6″). The ^{13}C NMR chemical shifts of C-6″ and C-7″ were indicative of an epoxy moiety,[10] and the ^{1}H and ^{13}C NMR data of this side-chain showed close agreement with the corresponding substituent of 6′,7′-epoxygeranyloxypsoralen.[10] Again, this compound showed a positive specific rotation ($[\alpha]_D^{22}$ +2.6 (*c* 0.19, $CHCl_3$)). However, due to the presence of two stereogenic centers (C-2′ and C-6″) in the molecule, the configuration at the stereocenter could not be determined by direct comparison with that of S1. Compound **5** was therefore identified as the new 4,6-dihydroxy-2-*O*-(6″,7″-epoxy-3″,7″-dimethyloct-2″-enyl)-1-(2′-methylbutanoyl)benzene and was given the trivial name olympicin E.

Olympicin A (**1**) displayed exceptional activity against all of the *Staph. aureus* strains tested, with MIC values ranging from 0.5 to 1 mg/L (Table 3). It was more active than the control antibiotics against the MDR and epidemic strains and as active as norfloxacin with the standard susceptibility testing strain (ATCC 25923). The activity of olympicin A seemed to be unaffected by the MDR mechanisms, as shown by the fairly consistent MIC values against the different effluxing strains. It was also active against four *Mycobacterium* strains at MIC values ranging from 4 to 8 mg/L, but was not as active as the control antibiotics. Olympicin A was not active against any of the Gram-negative species at 512 mg/L. This may result from the impermeability of the outer membrane of the Gram-negative bacteria, which prevents the influx of chemicals from the surrounding environment into the cells, or may be due to the different efflux pumps these bacteria express.

Compounds **2**−**5** (olympicins B−E) were moderately active against the *Staph. aureus* strains, with MICs ranging from 64 to 128 mg/L. The simple nature of olympicin A and the ease of its synthesis, coupled with its activity toward Gram-positive strains of *Staph. aureus*, some of which are effluxing and methicillin-resistant, make this chemotype worthy of further evaluation, and synthetic efforts are underway to optimize its antibacterial action. The need for new topical antibacterials, particularly those used in the decolonization of MRSA from patients, offers a potential use for these simple acylphloroglucinols, particularly given the resistance occurring to conventional agents such as mupirocin and fusidic acid.

EXPERIMENTAL SECTION

General Experimental Procedures. Optical rotations were measured on a Bellingham and Stanley ADP 200 polarimeter. UV spectra were recorded on a Thermo Electron Corporation Helios spectrophotometer, and IR spectra were recorded on a Nicolet 360 FT-IR spectrophotometer. NMR spectra were recorded on a Bruker AVANCE 500 MHz spectrometer. Chemical shift values (δ) are reported in ppm, relative to appropriate internal solvent standard, and *J* values are given in Hz. Mass spectra were recorded on a Finnigan MAT 95 high-resolution, double-focusing, magnetic sector mass spectrometer. Accurate mass measurement was achieved using voltage scanning of the accelerating voltage. This was nominally 5 kV, and an internal reference of heptacosa was used. Resolution was set between 5000 and 10 000.

Plant Material. The aerial parts of *H. olympicum* L. cf. *uniflorum* N. Robson (accession number 1969-31184) were collected from the Royal Botanic Garden at Wakehurst Place, Surrey, which forms part of the National *Hypericum* Collection.

Extraction and Isolation. Dried, powdered plant material (937 g) was sequentially extracted with 3.5 L of *n*-hexane, CH_2Cl_2, and MeOH using a Soxhlet apparatus. The *n*-hexane and CH_2Cl_2 extracts were active at a concentration of 32 and 16 mg/L, respectively, whereas the MeOH extract was active at 512 mg/L. The *n*-hexane extract (15.2 g) was fractionated by VLC (silica gel $PF_{254+366}$; Merck) using a step-gradient solvent system from 100% *n*-hexane to 100% EtOAc with a 10% increment and a final MeOH wash. VLC fractions 6 to 8 were active against SA-1199B with an MIC value of 64 mg/L. They displayed similar TLC profiles and were combined (total of 842.0 mg). The combined fraction was separated by Sephadex LH-20 (Amersham Biosciences) chromatography, giving five fractions eluted with $CHCl_3$/MeOH (1:1) and one fraction eluted with MeOH. The fraction eluted with MeOH (80.9 mg) was active at an MIC of 1 mg/L. Compound **1** (29.1 mg) was isolated from this fraction using preparative TLC (silica; toluene/EtOAc/HOAc, 80:18:2, R_f = 0.62, yield 0.0031%).

A portion (2.5 g) of the CH_2Cl_2 extract was applied to a Sephadex LH-20 column, giving five fractions eluted with $CHCl_3$/MeOH (1:1) and one fraction eluted with MeOH. Fractions 4 to 6 exhibited excellent antibacterial activity at 0.5 mg/L. They showed similar TLC profiles and

dx.doi.org/10.1021/np2003319 |*J. Nat. Prod.* XXXX, XXX, 000–000

were combined, giving 62.0 mg. The combined fraction was directly purified by p-TLC (silica; toluene/EtOAc/HOAc, 75:23:2), yielding compounds **2** (4.2 mg, R_f = 0.48, yield 0.00045%), **3** (3.8 mg, R_f = 0.44, yield 0.00041%), and **4** (1.8 mg, R_f = 0.34, yield 0.00019%). Sephadex fraction 3 (140.8 mg) was active at 512 mg/L. It was further separated by SPE on a silica gel column using a step-gradient system from 100% *n*-hexane to 100% EtOAc. SPE fraction 8 (17.8 mg), which was eluted with 70% EtOAc in *n*-hexane, was purified by p-TLC (silica; toluene/EtOAc/HOAc, 75:23:2), yielding compound **5** (1.3 mg, R_f = 0.57, yield 0.00013%). All compounds gave an orange color reaction with vanillin-H_2SO_4 spray on a TLC plate.

*4,6-Dihydroxy-2-O-(3″,7″-dimethyl-2″,6″-octadienyl)-1-(2′-methylbutanoyl)benzene (**1**), olympicin A:* pale yellow oil; $[\alpha]_D^{22}$ +6.0 (*c* 0.25, $CHCl_3$); UV ($CHCl_3$) λ_{max} (log ε) 240 (4.05), 289 (4.35) nm; IR ν_{max} (thin film) cm^{-1} 3348, 2968, 2931, 1624, 1593, 1448, 1377, 1216, 1162, 1099, 826; ^1H NMR and ^{13}C NMR ($CDCl_3$) see Table 1; HR-ESIMS (*m*/*z*) 345.2056 $[M - H]^-$ (calcd for $C_{21}H_{30}O_4$, 345.2071).

*4,6-Dihydroxy-2-O-(7″-hydroxy-3″,7″-dimethyl-2″,5″-octadienyl)-1-(2′-methylbutanoyl)benzene (**2**), olympicin B:* pale yellow oil; $[\alpha]_D^{22}$ +5.8 (*c* 0.12, $CHCl_3$); UV ($CHCl_3$) λ_{max} (log ε) 240 (4.26), 290 (3.62) nm; IR ν_{max} (thin film) cm^{-1} 3338, 2967, 2934, 2873, 1620, 1594, 1448, 1217; ^1H NMR and ^{13}C NMR ($CDCl_3$) see Table 1; HR-ESIMS (*m*/*z*) 363.2168 $[M + H]^+$ (calcd for $C_{21}H_{30}O_5$, 363.2172).

*4,6-Dihydroxy-2-O-(6″-hydroxy-3″,7″-dimethyl-2″,7″-octadienyl)-1-(2′-methylbutanoyl)benzene (**3**), olympicin C:* pale yellow oil; $[\alpha]_D^{22}$ +2.5 (*c* 0.41, $CHCl_3$); UV ($CHCl_3$) λ_{max} (log ε) 240 (4.44), 288 (4.90) nm; IR ν_{max} (thin film) cm^{-1} 3357, 1734, 1653, 1558, 1540, 1506, 1457; ^1H NMR and ^{13}C NMR ($CDCl_3$) see Table 1; HR-ESIMS (*m*/*z*) 363.2163 $[M + H]^+$ (calcd for $C_{21}H_{30}O_5$, 363.2172).

*4,6-Dihydroxy-2-O-(6″-hydroperoxy-3″,7″-dimethyl-2″,7″-octadienyl)-1-(2′-methylbutanoyl)benzene (**4**), olympicin D:* pale yellow oil; $[\alpha]_D^{22}$ +2.7 (*c* 0.32, $CHCl_3$); UV ($CHCl_3$) λ_{max} (log ε) 240 (4.05), 289 (4.35) nm; IR ν_{max} (thin film) cm^{-1} 3397, 2970, 2928, 1622, 1594, 1456, 1217; ^1H NMR and ^{13}C NMR ($CDCl_3$) see Table 2; HR-ESIMS (*m*/*z*) 379.2120 $[M + H]^+$ (calcd for $C_{21}H_{30}O_6$, 379.2121).

*4,6-Dihydroxy-2-O-(6″,7″-epoxy-3″,7″-dimethyloct-2″-enyl)-1-(2′-methylbutanoyl)benzene (**5**), olympicin E:* pale yellow oil; $[\alpha]_D^{22}$ +2.6 (*c* 0.19, $CHCl_3$); UV ($CHCl_3$) λ_{max} (log ε) 240 (4.05), 289 (3.68) nm; IR ν_{max} (thin film) cm^{-1} 3376, 2970, 2934, 1622, 1593, 1447, 1217; ^1H NMR and ^{13}C NMR ($CDCl_3$) see Table 2; HR-ESIMS (*m*/*z*) 363.2181 $[M + H]^+$ (calcd for $C_{21}H_{30}O_5$, 363.2166).

Synthesis of Compound 1. *(S)-2-Methylbutanoyl Chloride (**7**) (ref* 11*).* (*S*)-2-Methylbutanoic acid (**6**; 10 g, 97.91 mmol) and $SOCl_3$ (10.71 mL, 146.9 mmol, 1.5 equiv) were heated together at 80 °C under reflux for 2 h. Distillation of the reaction mixture afforded (*S*)-2-methylbutanoyl chloride (10.63 g, 88.21 mmol, 90%): colorless liquid; $[\alpha]_D^{22}$ +10.1 (*c* 0.54, $CHCl_3$); bp 119−120 °C; ^1H NMR and ^{13}C NMR ($CDCl_3$) see Supporting Information.

*(S)-2-Methyl-1-(2,4,6-trihydroxyphenyl)butan-1-one (**9**) (ref* 12*).* $AlCl_3$ (46.43 g, 351.8 mmol, 4.1 equiv) was added to a stirred suspension of phloroglucinol (**8**; 10.81 g, 85.8 mmol, 1 equiv) in CS_2 (50 mL). Nitrobenzene (40 mL) was added to the solution over 30 min. The solution was heated under reflux at 55 °C for 30 min. A solution of **7** (10.34 g, 85.8 mmol) dissolved in 5 mL of nitrobenzene was added to the reaction mixture over 30 min, followed by heating for another 30 min. The reaction mixture was allowed to cool with stirring and then poured into an ice−water bath (400 mL). Then 100 mL of 3 M HCl was added. The organic solvents were removed under reduced pressure, and the oily residue containing the acylphloroglucinol was extracted into Et_2O. After the removal of the Et_2O, the crude product was purified by VLC using silica. The fraction eluting with 6:4 *n*-hexane/EtOAc was identified to be the title compound, isolated as a pale yellow oil (9.71 g, 46.19 mmol, 54%): $[\alpha]_D^{22}$ +8.5 (*c* 0.35, $CHCl_3$); UV ($CHCl_3$) λ_{max} (log ε) 240 (4.17), 290 (3.97) nm; IR ν_{max} (thin film) cm^{-1} 3297, 1628, 1602, 1222; ^1H NMR and ^{13}C NMR ($CDCl_3$), see Supporting Information; HR-ESIMS (*m*/*z*) 209.0813 $[M - H]^-$ (calcd for $C_{11}H_{14}O_4$, 209.0814).

*(S)-1-(2,4-Bis[(tert-butyldimethylsilyl)oxy]-6-hydroxyphenyl)-2-methylbutan-1-one (**10**) (ref* 13*).* Acylphloroglucinol **9** (9.71 g, 46.19 mmol) was dissolved in 150 mL of dry acetone. Imidazole (3.43 g, 138.6 mmol, 3 equiv) was added to the solution, and the reaction mixture stirred for 5 min before the addition of TBDMS-Cl (14.61 g, 97.0 mmol, 2.1 equiv). The reaction mixture was stirred for 2 h at room temperature. The reaction mixture was diluted with $CHCl_3$ and washed with 1 M HCl (150 mL). The solvent was removed under reduced pressure, and the crude product purified by VLC over silica gel to afford TBDMS-protected phloroglucinol **10** in the fraction eluted with 9:1 *n*-hexane/EtOAc. The title compound was isolated as a pale yellow oil (16.4 g, 37.26 mmol, 81%): $[\alpha]_D^{22}$ +4.9 (*c* 0.39, $CHCl_3$); UV ($CHCl_3$) λ_{max} (log ε) 239 (4.26), 290 (4.23) nm; IR ν_{max} (thin film) cm^{-1} 3276, 2973, 1688, 1572, 1531, 1256, 1131, 1072, 850; ^1H NMR and ^{13}C NMR ($CDCl_3$), see Supporting Information; HR-ESIMS (*m*/*z*) 437.2554 $[M - H]^-$ (calcd for $C_{23}H_{42}O_4Si_2$, 437.2549).

*(S)-4,6-Dihydroxy-2-O-(3″,7″-dimethyl-2″,6″-octadienyl)-1-(2′-methylbutanoyl)benzene (**S1**), Olympicin A (ref* 13*).* TBDMS-protected acylphloroglucinol **10** (6.6 g, 15.0 mmol) was dissolved in 100 mL of dry DMF, to which anhydrous K_2CO_3 was added (3.1 g, 22.5 mmol, 1.5 equiv). The mixture was stirred for approximately 5 min before the addition of geranyl bromide (3.43 mL, 18 mmol, 1.2 equiv). The mixture was heated at 80 °C for 3 h with stirring. The reaction mixture was poured over H_2O and extracted with $CHCl_3$. The solvent in the organic layer was removed under reduced pressure. The crude product was purified by chromatography over silica gel by VLC. Compound **S1** was eluted with 9:1 *n*-hexane/EtOAc, and removal of the solvents under reduced pressure yielded the title compound as a pale yellow oil. All spectral data were identical to those of the natural product **1**, and the overall yield was 1.6%.

Antibacterial Assay with *Staphylococcus aureus*. Unless otherwise stated, all chemicals were obtained from Sigma-Aldrich Company Ltd., UK. Cation-adjusted Mueller-Hinton broth was obtained from Oxoid and was adjusted to contain 20 and 10 mg/L of Ca^{2+} and Mg^{2+}, respectively. The *Staph. aureus* strains used in this study included ATCC 25923, SA-1199B, RN4220, XU212, EMRSA-15, and EMRSA-16. ATCC 25923 is a standard laboratory strain sensitive to antibiotics.[14] SA-1199B overexpresses the NorA MDR efflux pump.[15] RN4220 possesses the MsrA macrolide efflux protein.[16] XU212 is a Kuwaiti hospital isolate that is a MRSA strain possessing the TetK tetracycline efflux pump.[14] EMRSA-15[17] and EMRSA-16[18] are epidemic strains in the U.K. *Mycobacterium* species used in this study included the fast-growing species *M. smegmatis* ATCC14468, *M. fortuitum* ATCC6841, and *M. phlei* ATCC11758. All were obtained from the National Collection of Type Cultures (NCTC). *M. smegmatis* $MC^2$2700, which possesses the *M. tuberculosis* fatty acid synthase I gene (Fas 1), was obtained from Zimhony et al.[19] Two wild-type Gram-negative bacteria were used in this study, namely, *Pseudomonas aeruginosa* K767 and *Salmonella typhimurium* L354, and both were obtained from the NCTC.

Staph. aureus, *P. aeruginosa*, and *S. typhimurium* strains were cultured on nutrient agar (Oxoid) and incubated for 24 h at 37 °C prior to MIC determination. *Mycobacterium* species were cultured on Columbia agar (Oxoid) supplemented with 7% defibrinated horse blood (Oxoid) and were subcultured and incubated for 72 h at 37 °C prior to the assay. An inoculum density of 5×10^5 colony forming units of each bacterial strain was prepared in normal saline (9 g/L) by comparison with a 0.5 MacFarland turbidity standard. The inoculum (125 μL) was added to all wells, and the microtiter plate was incubated at 37 °C for the corresponding incubation time. For MIC determination, 20 μL of a 5 mg/mL methanolic solution of 3-[4,5-dimethylthiazol-2-yl]-2,5-diphenyltetrazolium bromide (MTT) was added to each of the wells and incubated for 20 min. Bacterial growth was indicated by a color change

dx.doi.org/10.1021/np2003319 |*J. Nat. Prod.* XXXX, XXX, 000–000

from yellow to dark blue. The MIC was recorded as the lowest concentration at which no growth was observed.[14]

■ ASSOCIATED CONTENT

Supporting Information. This material is available free of charge via the Internet at http://pubs.acs.org.

■ AUTHOR INFORMATION

Corresponding Author

*Tel: +44 207 753 5913. Fax: +44 207 753 5964. E-mail: simon.gibbons@pharmacy.uk.

■ ACKNOWLEDGMENT

We thank the School of Pharmacy for the award of an EPSRC DTA to W.K.P.S.

■ DEDICATION

Dedicated to Dr. Gordon M. Cragg, formerly Chief, Natural Products Branch, National Cancer Institute, Frederick, Maryland, for his pioneering work on the development of natural product anticancer agents.

■ REFERENCES

(1) Bystrov, N. S.; Chernov, B. K.; Dobrynin, V. N.; Kolosov, M. N. *Tetrahedron Lett.* **1975**, *32*, 2791–2794.
(2) Schempp, C. M.; Pelz, K.; Wittmer, A.; Schöpf, E.; Simon, J. C. *Lancet* **1999**, *353*, 2129.
(3) Shiu, W. K. P.; Gibbons, S. *Phytochemistry* **2006**, *67*, 2568–2572.
(4) Gibbons, S.; Moser, E.; Hausmann, S.; Stavri, M.; Smith, E.; Clennett, C. *Phytochemistry* **2005**, *66*, 1472–1475.
(5) Jayasuriya, H.; Clark, A. M.; McChesney, J. D. *J. Nat. Prod.* **1991**, *54*, 1314–1320.
(6) Gibbons, S.; Ohlendorf, B.; Johnsen, I. *Fitoterapia* **2002**, *73*, 300–304.
(7) Hu, L.; Khoo, H. C. W.; Vittal, J. J.; Sim, K. Y. *Phytochemistry* **2000**, *53*, 705–709.
(8) Shiu, W. K. P.; Malkinson, J. P.; Gibbons, S. U.K. Patent GB0718023.5, 2007.
(9) Appendino, G.; Bianchi, F.; Minassi, A.; Sterner, O.; Ballero, M.; Gibbons, S. *J. Nat. Prod.* **2002**, *65*, 334–338.
(10) Row, E. C.; Brown, S. A.; Stachulski, A. V.; Lennard, M. S. *Bioorg. Med. Chem.* **2006**, *14*, 3865–3871.
(11) Begley, M. J.; Crombie, L.; Jones, R. C. F.; Palmer, C. J. *J. Chem. Soc., Perkin Trans. 1* **1987**, *1*, 353–357.
(12) Crombie, L.; Jones, R. C. F.; Palmer, C. J. *J. Chem. Soc., Perkin Trans. 1* **1987**, *1*, 317–331.
(13) Liu, A.; Dillon, K.; Campbell, R. M.; Cox, D. C.; Huryn, D. M. *Tetrahedron Lett.* **1996**, *22*, 3785–3788.
(14) Gibbons, S.; Udo, E. E. *Phytother. Res.* **2000**, *14*, 139–140.
(15) Kaatz, G. W.; Seo, S. M.; Ruble, C. A. *Antimicrob. Agents Chemother.* **1993**, *44*, 1404–1406.
(16) Ross, J. L.; Farrell, A. M.; Eady, E. A.; Cove, J. H.; Cunliffe, W. J. *J. Antimicrob. Chemother.* **1989**, *24*, 851–862.
(17) Richardson, J. F.; Reith, S. *J. Hosp. Infect.* **1993**, *25*, 45–32.
(18) Cox, R. A.; Conquest, C.; Mallaghan, C.; Marples, R. R. *J. Hosp. Infect.* **1995**, *29*, 87–106.
(19) Zimhony, O.; Vilcheze, C.; Jacobs, W. R. *J. Bacteriol.* **2004**, *186*, 4051–4055.

dx.doi.org/10.1021/np2003319 |*J. Nat. Prod.* XXXX, XXX, 000–000

Antimycobacterials from natural sources: ancient times, antibiotic era and novel scaffolds

Juan D. Guzman[1,2], Antima Gupta[1], Franz Bucar[3], Simon Gibbons[2], Sanjib Bhakta[1]

[1]Institute of Structural and Molecular Biology, Department of Biological Sciences, Birkbeck, University of London, London WC1E 7HX, UK, [2]Department of Pharmaceutical and Biological Chemistry,The School of Pharmacy, University of London, 29-39 Brunswick Square, London WC1N 1AX, UK, [3]Department of Pharmacognosy, Institute of Pharmaceutical Sciences, Karl Franzens University Graz, Universitatsplatz 4, A-8010 Graz, Austria

TABLE OF CONTENTS

1. ABSTRACT

Mycobacteria are a group of aerobic, non-motile, acid fast bacteria that have a characteristic cell wall composed of a mycolyl-arabinogalactan-peptidoglycan complex. They display different phenotypic attributes in their growth, color and biochemistry. Tuberculosis (TB) is defined as the infection with *Mycobacterium tuberculosis* complex and was declared a global health emergency principally because of the appearance of multidrug-resistant strains and the associated risk of infection in immune-compromised population. There is an urgent clinical need for novel, potent and safe anti-TB drugs. Natural products have been used since antiquity for treating diverse complaints and novel pharmacophores are discovered every year. Two of the most potent used antimycobacterials, the rifamycins and streptomycin, were first detected in *Streptomyces* bacteria. Plants are also the source of an exquisite variety of antimicrobials that can lead to useful therapeutics in the future. In this review, natural preparations used since antiquity for treating tuberculosis are described, together with a rapid view of the 20th century antibiotic development against TB. Finally a summary of the most potent recent natural antimycobacterials is displayed.

2. INTRODUCTION

It has been hypothesized that mycobacteria existed in the Jurassic geological period (1-2), however the imperfection of the fossil register and the difficulty of observing microorganisms in petrifications make the probable date of appearance of mycobacteria purely speculative. DNA from the *Mycobacterium tuberculosis* complex has been found in the bones of an extinct long-horned bison in Wyoming dating from 18,000 years ago (3). In Egyptian (4000 BC) and in Peruvian human mummies (1000 BC) mycobacterial DNA characteristic of the tuberculosis complex has also been found (4-5). Tuberculosis (TB) has been a dreadful disease since human history incipiency appearing in all geographical populations at all times. We should not forget the disastrous outbreak at the end of 19th century which may recall us today on the necessity of having a constant alertness towards the disease. Many famous writers, philosophers and poets (John Keats, Franz Kafka, Edgar Allan Poe, George Orwell, Karl Marx), artists (Paul Gauguin, Amadeo Modigliani), composers (Frederic Chopin, Carl PE Bach), and political leaders (Simon Bolivar, Cardinal Richelieu, King Tutankhamen of Egypt) succumbed to the disease (6). It was also the source of inspiration for literature, arts and

other human activities, and the pieces "The Magical Mountain" by Thomas Mann or the painting "Misery" by Cristobal Rojas clearly evidence this relation.

Today we encounter *Mycobacterium* species persisting in fish, amphibians, reptiles, birds, and mammals and their ubiquity in organisms as well as in the soil and the water, reflect their ancient past (7). It is possible that through their evolution, mycobacteria had to face nutrient depletion or poisonous environments and we can hypothesize that their complex cell wall is the consequence of such an overwhelming paleo-environment. Recently *Streptomyces* and *Mycobacterium* species were found to have a similar lifecycle (8) and perhaps *Streptomyces* developed the production of antibiotics as an alternative tactic to overcome highly competitive microbial environments. Mycobacteria is one of the most unsusceptible microorganisms against chemical injury, and the impermeability, thickness and low fluidity of its cell wall extensively contributes to its natural resistance against chemical agents (9).

The *M. tuberculosis* complex is a set of evolutionary closely related slow growing mycobacterial species, all containing the mobile insertion sequence IS6610 in their genome (10), and causing TB disease in humans and other mammals. TB is nowadays a growing global health problem since the numbers of human cases are increasing all around the planet. For 2009 the World Health Organization reported more than 9.4 million new cases and more than 1.6 million deaths (11). The main factors aggravating the issue are the massive appearance of drug resistant strains of *M. tuberculosis*: multi-drug resistant (MDR), resistant to isoniazid and rifampicin, and extensively-drug resistant (XDR), resistant to isoniazid, rifampicin, any fluoroquinolone and at least one second-line injectable drug, and HIV co-infection (12). Although there is an increasing funding trend for TB drug research (13) it is not clear whether there are enough novel chemical entities entering the pipeline to assure a new full chemotherapeutic regimen in the next decade (14-15). Novel drugs must comply with three conditions: safety, potency sufficient to shorten treatment and prevent rapid emergence of resistance, and absence of interaction with antiretroviral therapy. To achieve these goals several pharmaceutical companies (GlaxoSmithKline, Sanofi-Aventis, AstraZeneca, Bayer, Novartis) have entered in collaboration with academics from universities and small companies (FASgen Inc, Lupin Limited, Otsuka, Sequella Inc, Cumbre Pharmaceuticals) with the financial help of the TB Alliance (consortium sponsored by the Bill and Melinda Gates Foundation), for establishing the dynamic partnership necessary for urgently developing a new, effective and safe chemotherapy of TB.

3. ANCIENT TIMES

M. tuberculosis has infected *Homo sapiens* from the very beginning of human history (16). "Phthisis" (wasting) was the Greek name of the disease and "consumption" is a French-derived word (originally from the Latin word "consumere") which translates one of the features of the disease: the depletion of the body (17). In ancient Egypt, Greece and in the Roman Empire, the use of natural scents and essential oils was widespread, used often for baths and cleaning purposes and these practices can be considered as the beginning of aromatherapy. The Egyptians used cedar-wood oil and natural resins and ointments in a mixture known as "cedrium" for embalming and protecting the corpses from microorganisms and preventing the deleterious effects of oxygen and water (18). The Greek and the Roman civilizations inherited the medicinal legacy of the Egyptians and they increased our knowledge of medicinal plants enormously, notably with Pedanius Dioscorides´ (40-90 AD) famous book *De Materia Medica*. These ancient civilizations were also well aware of terrible diseases.

Hippocrates (460-376 BC) described phthisis as being almost always fatal, and recommended a special diet based on milk, wine and bread (19). Aristotle (384-322 BC) deducted the contagious nature of phthisis and Pliny (23-79 AD) attributed curative properties to pine forests (20). Propolis, the resinous material produced by bees from plant exudates, was used in ancient Greece for treating infections including tuberculosis (21), however its efficacy is still not conclusive (22).

Historically garlic (*Allium sativum*) has been one of the most useful natural medicines ever described and it has been employed by several ancient civilizations for different purposes (23). In ancient Greece, Rome, India and China it was used for treating infections and respiratory ailments, among other applications. More recently it has been proved that garlic inhibits the growth of almost all species of mycobacteria (24). Diallylthiosulfinate or allicin (1) (Figure 1, Table 1) is the phytochemical responsible for the antimicrobial action of garlic and it is generated by the enzyme alliin lyase from *S*-allylcysteine-*S*-oxide (alliin) when garlic cloves are crushed (25). However due to the instability of allicin further degradation products like ajoenes, vinyldithiin and sulfides (26) have to be taken into account when estimating the *in vitro* and *in vivo* activity of allicin. The minimum inhibitory concentration (MIC) of allicin has been reported to be 25 mg/L against both susceptible and isoniazid-resistant strains (27). RNA synthesis in *Salmonella typhimurium* was demonstrated to be inhibited by allicin (Figure 5) (28). Moreover allicin was shown to be toxic for mammalian phagocytic cells at a concentration higher than 100 μM, but at a lower concentration it decreases the expression of endogenous antigen for *M. tuberculosis* 85B together with TNF-γ, acting at the mRNA level (29-30). These results show that allicin has a dual action, acting directly on the microorganism by inhibiting its growth but also exerting an immunomodulatory action on the host. Furthermore other types of interesting antimycobacterials have been isolated from *Allium* species, such as the pyridine-*N*-oxides (31).

Chocolate, known also as "the food of the Gods", is obtained from the roasted seeds of the South American shrub *Theobroma cacao* (Sterculiaceae). The drink obtained from the slight roasting of the seeds is said to have healing properties that can alleviate those who are suffering

Table 1. Antimycobacterial data (MIC, SI) and targets of promising natural scaffolds and antibiotics

Natural product class	Compound	Antimycobacterial data		Molecular antimycobacterial target	References
		MIC on *M. tuberculosis* or specified (mg/L)	Selectivity index in relation to mammalian cells (SI = GIC_{50} / MIC)		
	Allicin (1)	25	0.65	RNA synthesis inhibition	(27, 29)
	Licochalcone A (2)	20	nd	Unknown	(41)
	Glabridin (3)	30	nd	Unknown	(42)
	Caespitate (4)	100	nd	Unknown	(46)
	(*E*)-phytol (5)	2	nd	Unknown	(48)
	Lawsone (6)	100	nd	Unkownn	(51)
	(*3R,8S,9Z*)-Falcarindiol (7)	8 Mb	0.6	Unknown	(54)
	Berberine (8)	25 Ms	nd	Exact mechanism unknown	(59, 61)
Antibiotics	Benzylpenicillin (9)	> 512 Mf	nd	Peptidoglycan biosynthesis inhibition	(77)
	Streptomycin (10)	1	nd	16S rRNA of 30S ribosomal subunit	(85)
	Kanamycin (11)	2	nd	16S rRNA of 30S ribosomal subunit	(93)
	Amikacin (12)	0.75	nd	16S rRNA of 30S ribosomal subunit	(97)
	Cycloserine (13)	25	nd	Alanine racemase (Alr) and L-ala:D-ala ligase (Ddl)	(105)
	Rifampicin (14)	0.25	nd	B-subunit of RNA polymerase (RpoB)	(114)
	Capreomycin (15)	2	nd	70S ribosomal subunit	(118)
	Clarithromycin (16)	8	nd	50S ribosomal subunit	(128)
Lipids, sterols and triterpenoids	(*R/S*)-2-methoxydecanoic acid (17)	44	1.5	Unknown	(161)
	2-octadecynoic acid (18)	2.5 Mb	nd	Unknown	(163)
	Micromolide (19)	1.5	63	Unknown	(166)
	24,25-Epoxycyclo-artan-3-one (20)	8	9	Unknown	(168)
	3-Epi-lupeol (21)	4	15	Unknown	(172)
	Saringosterol-24-epimers (22)	0.125	1024	Unknown	(173)
	Stigmast-5,22-dien-3β-ol-7-one (23)	4	95	Unknown	(174)
Terpenoids	Dehydrocostus lactone (24)	2	nd	Unknown	(183)
	12-Demethyl-multicauline (25)	0.46	nd	Unknown	(186)
Phenolics	7-Methyljuglone (26)	0.5	30	Micothiol disulfide reductase (Mtr)	(189-192)
	Engelhardione (27)	0.2	nd	Unknown	(199)
	Bakuchiol (28)	20 Mb	nd	Unknown	(202)
	Preussomerin (29)	3	6	Unkown	(206)
Alkaloids	Ascididemin (30)	0.1	0.4	Mycobactin biosynthesis (MtbB)	(209-210)
	Sampangine (31)	0.2 Mi	24	Unknown	(212)
	Evocarpine (32)	2 Ms	nd	Unknown	(214)
	Hirsutellone A (33)	0.78	64	Unknown	(216)
	6-Hydroxy-manzamine E (34)	0.4	11	Unknown	(217)

Mb *M. bovis* BCG; Mi *M. intracellulare*; Ms *M. smegmatis*; Mf *M. fortuitum*. nd *no data*

from tuberculosis (32). There is no information about the antimycobacterial activity of the pyrones, pyrazines, furans and other products formed during the roasting of the cocoa beans; however a report in 2008 showed that roasted cocoa beans have radical scavenging (antioxidant) and antibacterial activities (33).

In Ayurvedic medicine, two plants have been used since antiquity for treating tuberculosis: *Tylophora asthmatica* (Asclepiadaceae) and *Ocimum sanctum* (Lamiaceae) (34). Leaves of *Tylophora asthmatica* also recorded as *Tylophora indica*, are a major source of phenanthroindolizine alkaloids (35) however reports of the anti-tubercular activity of this type of alkaloid have not been found, probably because they have not been tested or because they are inactive. *Ocimum sanctum* is known by the local communities as "Tulsi" or holy basil and the extract of this plant has shown inhibition of *M. tuberculosis* growth, but again no active compound has yet been isolated (36). Another plant widely used in traditional Ayurvedic medicine is *Adathoda vasica* (Acanthaceae) known as "Vasaka" for curing bronchitis, leprosy, tumors, fever, gonorrhea and tuberculosis among other ailments (37). The water extract of the leaves of this plant was shown to have antimycobacterial activity but a detailed phytochemical evaluation is lacking (38). "Mandukaparni" or "Gotu Kola" are names given to the Ayurvedic rejuvenator plant *Centella asiatica* (Apiaceae) which has been recommended for tuberculosis, leprosy, diarrhea, inflammation, and psoriasis among several ailments (39). Asiaticoside and other triterpene glycosides have been isolated from the roots of *Centella asiatica*, and there is one report of its inhibitory activity against *M. leprae* and *M. tuberculosis* (40), showing an MIC value greater than 16 mg/L with no mention of cytotoxicity. Licorice or *Glycyrrhiza glabra* (Fabaceae) is another old traditional herb described in Ayurveda, both as a medicinal and as a flavoring resource. Licochalcone A (2) was isolated from Chinese licorice roots and was initially thought to be responsible for the antimycobacterial activity of the plant, having an MIC less than 20 mg/L against species of the *M. tuberculosis* complex (41). However, later it was found that another phytochemical with an interesting antimycobacterial profile could also contribute to the antimycobacterial properties of

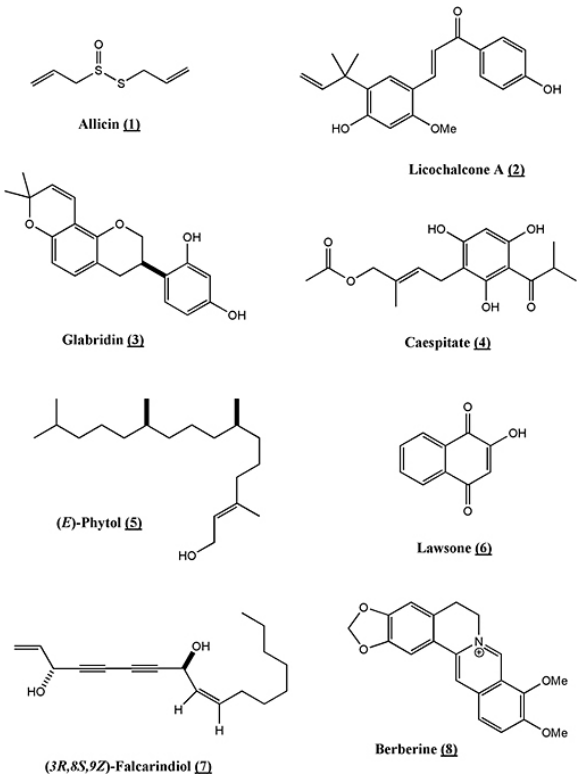

Figure 1. Chemical structure of some active antimycobacterial natural products obtained from ancient medicinal plants.

this plant. This compound, glabridin (3), was isolated from the ethyl acetate extract of the roots of *Glycyrrhiza glabra* collected in India and it showed an MIC of 30 mg/L against *M. tuberculosis* $H_{37}Rv$ (42).

Traditionally in Africa, species of the genus *Helichrysum* (Asteraceae) have been used for the treatment of respiratory disorders and tuberculosis (43-44). Whilst some compounds have been isolated from these species, none have shown potent inhibition of mycobacterial growth (45). Until now, the most active compound found in *Helichrysum caespititium* is caespitate (4) which has an MIC value of 100 mg/L against *M. tuberculosis* (46). In a review of the plants used in South African traditional medicine for treating mycobacterial infections, several species of the *Helichrysum* genus are reported to be used for treating coughs and TB (47). Interestingly the Asteraceae family is recorded to have prominent application for coughs, chest and respiratory complaints related to TB symptomatology and therefore the Asteraceae species should be considered for bio-guided phytochemical studies. The infusion of the leaves of the Kenyan shrub *Leucas volkenssii* (Lamiaceae) has been used as a remedy for asthma, bronchitis and other lung diseases. A bioguided phytochemical study showed the presence of several lipophilic components with very potent inhibition of mycobacterial growth. In particular (*E*)-phytol (5) showed an MIC value of 2 mg/L against *M. tuberculosis* $H_{37}Rv$ in a radiorespirometric assay (48). The leaves of *Lawsonia inermis* (Lythraceae) produce a dye known as "Henna" which has been widely used for body art since antiquity and was reported as a treatment for leprosy (49). An infusion of the leaves is able to reduce the number of lesions by 30% in relation to the control, notably in the kidneys and liver, in guinea pigs infected with *M. tuberculosis* (50). The phytochemicals assumed to be responsible for the activity are of quinoid nature such as lawsone (6) which has demonstrated an MIC value close to 100 mg/L against *M. tuberculosis* (51). The antimycobacterial activity of naphthoquinones has motivated a deeper research focusing on the determination of the chemical features essential for their activity, leading to active derivatives which will be discussed later.

In China, during the 28th Century BC, Shen Nong wrote a book titled "Pen-T´sao" (translated as "The Herbal") describing hundreds of herbal medicines and poisons mostly tested directly on himself (52). The herb known as "Bai-Zhi" corresponds to *Angelica dahurica* (Apiaceae) used for the relief of headaches, colds and infections (53). An active polyacetylene known as (3*R*,8*S*)-falcarindiol (7) has been isolated from the roots of this plant, displaying an MIC value as low as 8 mg/L against *M. fortuitum* (54) and *M. bovis* BCG. Moreover falcarindiol has also a marked mammalian cytotoxicity of the same order of magnitude as the antibacterial activity (55), therefore preventing its use as antimicrobial. The molecular target of falcarindiol is still unknown although several studies point to an induction of anti-oxidant enzymes at low concentrations which are beneficial but with a reversion of the effect at higher concentrations (56-57). The rhizome of *Coptis chinensis* (Ranunculaceae) know as "Huang Lian" which means "yellow connection" is a very bitter root that has been extensively used for treating diarrhea, nausea, insomnia, and cleaning abscesses, furuncles, burns and other lesions (58). The active principle found in the "Huang Lian" rhizome is the quaternary alkaloid berberine (8), which has an MIC of 25 mg/L against fast-growing *M. smegmatis* but has a higher MIC against pathogenic mycobacteria such as *M. avium* (MIC 50 mg/L) and *M. bovis* BCG (MIC 200 mg/L) (59). Berberine is a compound with multiple biological activities, acting as immunomodulatory being able to activate macrophages (60), it also intercalates in DNA (61) and it prevents the adherence of microorganisms to the cells (62).

During the obscure period of the Middle Ages (5th to 15th Century) very little advance of biosciences was achieved. The clergy kept the knowledge of the herbs in the convents and also the majority of medieval people were analphabet. By the turn of the 16th Century and the introduction of liberal Renaissance ideas notably in the arts, coupled to the discovery of a new continent, logical and scientific thinking started to appear again. South American *Cinchona* bark and Ipecacuanha root were transported to Europe for treating malaria and dysentery respectively. Dysentery was a common problem in the days of unsanitary urban settings in which people would throw dirty water and rubbish into the streets. Some scientific spirits tried to demystify the real world by inventing novel instruments and postulating novel theories to explain it.

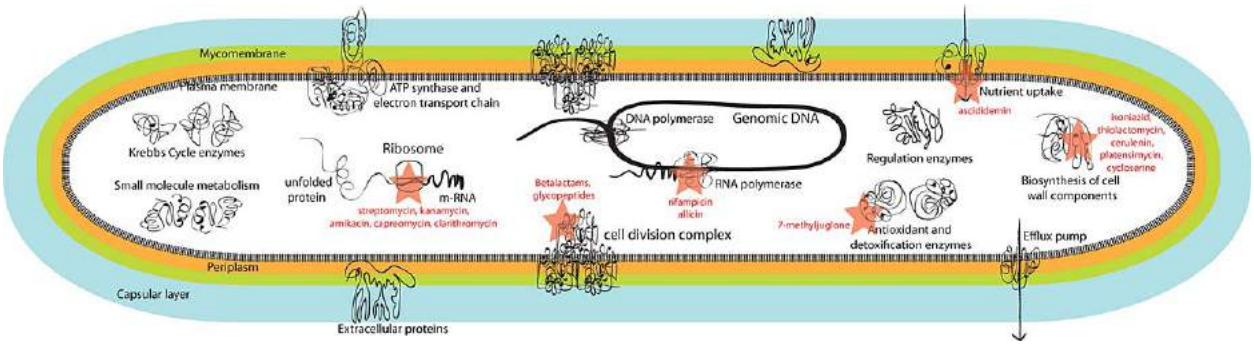

Figure 5. Mycobacterial cell diagram showing the principal biochemical pathways and natural product inhibitors.

Notably the experimental sciences: physics with Galileo Galilei (1564-1672), Johannes Kepler (1571-1630) and Isaac Newton (1643-1727) and chemistry with Robert Boyle (1627-1691), Antoine Lavoisier (1743-1794) and Jacob Berzelius (1779-1848) started to shape the thinking of academics in Europe, providing novel ideas for structuring a modern view of the world.

4. DISCOVERY OF ANTIBIOTICS

Louis Pasteur (1822-1895) was a French chemist, microbiologist, immunologist and biotechnologist who brilliantly tackled many important problems of the biosciences of the epoch. Amongst his most important achievements are the foundation of chemical stereochemistry, the introduction of the germ theory of diseases, the demonstration of microbial fermentation and the setting of the first vaccines against virus and bacteria (63). Together with Antony van Leeuwenhoek (1632-1723), the first to observe under the microscope "animalcules" or microorganisms, Louis Pasteur is considered the father of microbiology. Later Joseph Lister (1827-1912), an English surgeon, was convinced by the experiments of his French contemporary, of the necessity of an aseptic technique in surgery and he was the first physician to use antiseptic (64). Lister used carbolic acid, which is known today as phenol, and he described it, in 1867, as a "volatile organic compound which appears to exercise a peculiarly destructive influence upon low forms of life" (65). The word "antibiosis" was used for the first time in 1889 by Pasteur´s pupil Paul Vuillemin (1861-1932) for describing the action of one organism against another one in mixed cultures (66). The pioneer work of chemotherapy can be ascribed to Paul Ehrlich (1854-1915) who was the first to notice that certain dyes colored selectively certain animal and bacterial cells while others did not. He realized that it may be possible to produce chemical compounds (dye like) known as "magic bullets" that selectively kill the bacterium while not killing the humans infected with the bacterium (67). With the help of Sahachiro Hata (1873-1938), the team chemically modified several dyes and salvarsan-606, an organo-arsenical compound, was successfully identified as a compound able to kill *Treponema pallidum*, the spirochaete bacterium that cause syphilis, without harming the host (68). This was the start of the chemotherapeutic era.

Undoubtedly a major breakthrough in the history of Medicine was the demonstration of the bacterial etiology of TB in Berlin in 1882 by the German physician Robert Koch (1843-1910) (69). He proposed "Koch´s Postulates" which are in fact a rational experimental design for proving that a bacterium is the cause of a disease (70). The first postulate establishes that in every case of the disease, the infecting organisms must be present. It must be possible also to isolate the microorganism causing the disease from a host carrying the disease and to grow it in pure culture. Then it must be shown that after inoculation of the pure culture on a healthy susceptible host, the disease appears. Finally the organism causing the disease must be re-isolated from the experimentally infected host. Although the French military physician Jean-Antoine Villemin (1827-1892) had already demonstrated that TB was contagious using rabbits (71), it was Robert Koch who isolated, cultured and stained *M. tuberculosis*. He successfully inoculated guinea pigs and re-isolated the mycobacterial strain from the organs of the sick animals. Finally Koch was the first to prepare tuberculin, an extracellular protein mixture extracted from cultures of *M. tuberculosis*, which he claimed erroneously to be the cure of TB as a vaccine (72), but which was shown to be a very useful diagnostic test developed years later by Clemens von Pirquet (1874-1929) and established finally by Charles Mantoux (1877-1947).

Although Ehrlich´s salvarsan was effective in curing spirochaetal infection it was also considerably toxic and undesirable side effects were common (73). However it was used globally as the only cure for syphilis until the advent of the first antibiotic. In 1928, the Scottish microbiologist Alexander Fleming (1881-1955) discovered a lysogenic effect on an abandoned Petri dish of staphylococci contaminated by the fungi *Penicillium notatum*, when returning from a holiday. By analytical observation, he hypothesized that the fungi produced a chemical which diffused slowly on the plate and attempted to isolate the potent compound. The substance was soluble in ethanol but not in water, discarding the possibility of a lysogenic protein such as lysozyme (74). Ernst Chain (1906-1979) and Howard Florey (1898-1968) were able to isolate around 1940, a mildly pure brown penicillin sample from a fermented culture of the fungi. It was however Gerhard Domagk (1895-1964) and his team who experimentally obtained the first agent active against

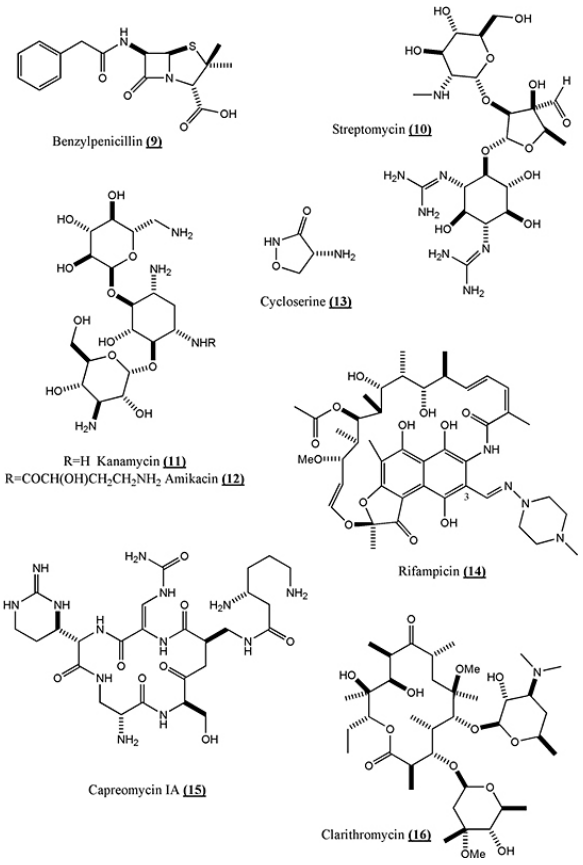

Figure 2. Antibiotics used in the treatment of mycobacterial diseases (except benzylpenicillin) developed from natural products discovered in the antibiotic era.

streptococci (the microbes causing bacterial sore throat) and staphylococci. Synthesized in 1932 by I.G. Farbenindustrie, the so called "Prontosil Rubrum", was the first sulfonamide ever used on patients, and it saved 6-year old Domagk´s daughter, Hildegard, from arm amputation following a streptococcal infection (75). From natural sources, other antimicrobials were soon discovered such as gramicidin and tyrocidine isolated by the French microbiologist René Dubos (1901-1982) from cultures of the soil inhabitant *Bacillus brevis* (76). However these compounds were either inactive against *M. tuberculosis* or the concentration needed to kill the bug was so high that toxicity hindered their use.

The penicillins, cephalosporins, carbapenems and monobactams are arguably the most important group of antibiotics, characterized by the presence of the fused β-lactam which prevent the final crosslinking and polymerization steps of the biosynthesis of peptidoglycan (Figure 5). Benzylpenicillin or penicillin G (9) (Figure 2, Table 1) was the first naturally occurring β-lactam to be discovered, however it has a weak activity against mycobacteria (>512 mg/L for *M. fortuitum*) (77) due to the fact that mycobacteria produce chromosomally encoded β-lactamases (78). It has been suggested therefore that a mixture of a β-lactamase inhibitor (clavulanic acid) together with a β-lactam might be useful for treatment of TB and other mycobacterial diseases (79-81) however conclusive clinical studies are still expected. Clavulanic acid has been hypothesized to have also a direct effect on the cell wall facilitating the entry of β-lactams to the periplasmic space (82).

The first natural product to be successfully used for curing TB patients was streptomycin (10), an aminoglycoside isolated from *Streptomyces griseus* by Selman Waksman (1888-1973) and Albert Schatz (1922-2005) at Rutgers University in 1943 (83). The word "antibiotic" was clarified by Waksman to delimit the group of "chemical substances, produced by microorganisms, which have the capacity to inhibit the growth of and even to destroy bacteria and other microorganisms" (66). Waksman places emphasis on the selective character of the antibiotics, some of them been able only to kill a specific type of microorganisms while others have a wider spectrum of activity. In March 1944, streptomycin was tested on animals by Merck & Co in the Mayo Clinic and in 1946 the UK Medical Research Council performed a randomized trial of streptomycin on young individuals with acute, bacteriologically proven pulmonary TB, achieving cure rates of 100% (84). The impact of streptomycin was seen as miraculous particularly on children with TB meningitis; however the joy was soon eclipsed as many children relapsed after a few months of treatment. It was evident that *M. tuberculosis* had become resistant to streptomycin. The MIC of streptomycin for susceptible *M. tuberculosis* strains is between 1-2 mg/L and between 25-50 mg/L for resistant strains; with 30 mg/L being the critical concentration, defined as the concentration able to inhibit 95% of the wild-type strains while not inhibiting the resistant strains (85). A study by the British bacteriologist Dennis Mitchison (born in 1919) showed that streptomycin-resistant variants appeared in populations of *M. tuberculosis* that had never been exposed to the drug with a discontinuous distribution (86). At low populations (less than 10^6 cells), all the bacteria were susceptible to 2 mg/L of streptomycin, however when the population reached 10^9 cells, several hundreds of cells were able to grow at 10 mg/L of streptomycin and around 1-2 cells at a concentration of 100 or 1000 mg/L of streptomycin. These bacterial populations are commonly found in TB lesions and therefore in monotherapy, resistance develops quite rapidly. It is recognized today that the molecular target of streptomycin is the small ribosomal unit known as S12 codified by the *rpsL* gene, which contains several mutations in streptomycin resistant strains of *M. tuberculosis* (87).

In 1940, Frederick Bernheim discovered that the TB bacillus doubled the uptake of oxygen when sodium salicylate was present in the media (88). We have to remind the reader that salicin is the glycoside of salicylic alcohol, occurring naturally in many *Salix* species (Salicaceae). Bernheim published a second paper disclosing that 2,3,5-triiodobenzoate and nicotinic acid inhibited the growth of *M. tuberculosis* (89). It was the Swedish chemist Jörgen Lehmann (1898-1989) who, after reading the 1940 paper of Bernheim, realized that this meant that salicylic-type

structures had some specific effect "on the internal workings of the tuberculosis bacterium – something that might be significant for its very life" (67). Allied with the small Swedish pharmaceutical company Ferrosan, he predicted that the presence of an amino group in the *para* position of the carboxylic acid of salicylic acid would have an inhibitory effect of TB bacillus. By December 1943, with minute amounts of the drug, Lehman confirmed that he was indeed correct (67). The MIC of *p*-aminosalicylic acid is 0.3-1 mg/L against *M. tuberculosis* $H_{37}Rv$, and it has proven to be a very effective second-line anti-TB agent despite its irritant and nauseous side effects (90).

After the Second World War, Japan organized the "Japan Antibiotics Research Association" in order to recruit experts in microbiology, fermentation and natural product chemistry for the manufacture of penicillin (91). In the golden era of antibiotics (1950-1965), several Japanese groups started exploratory research in microbial products disclosing a vast array of antibiotic classes such as colistin (1950), variotin (1951), trichomycin (1952) gramicidin J (1952), kitasamycin (1953) and the mikamycins (1956). In 1957 Hamao Umezawa (1914-1986) isolated kanamycin (11) from *Streptomyces kanamyceticus* (92) and was soon established as the drug of choice for treatment of streptomycin-resistant TB. The MIC of kanamycin against *M. tuberculosis* $H_{37}Rv$ is close to 2 mg/L and it inhibits protein synthesis by tightly binding to 16S rRNA of the 30S ribosomal unit (Figure 5) (93). Kanamycin-resistant strains have an MIC value of more than 200 mg/L and this resistance can be caused by three different mechanisms: enzymatic aminoglycoside modification, specific methylation of the rRNA or mutation in the 16S rRNA codifying gene *rrs* (94). The clinical adverse reactions of aminoglycosides are typically nephrotoxicity and ototoxicity caused by a perturbation of the membrane function of the cells, leading to damage of the renal tubule and the vestibule followed by hearing loss (95). Amikacin (12) a semisynthetic derivative of kanamycin was synthesized in 1972, in order to generate an analog of kanamycin with activity towards kanamycin-resistant strains (96). *N*-acetylation, *O*-phosphorylation and *O*-adenylation are mechanisms for the enzymatic modification of aminoglycosides rendering them inactive, and amikacin was developed in order to prevent *N*-acylation. Amikacin has an MIC between 0.5-1 mg/L against *M. tuberculosis* $H_{37}Rv$ and has been shown to be superior to kanamycin with a bactericidal activity at 2 mg/L (97). It has also been demonstrated that all amikacin-resistant strains are resistant to kanamycin, but not all kanamycin-resistant strains are resistant to amikacin supposing a more difficult step for the bacteria to become resistant to amikacin (98). A typical mutation conferring resistance to both kanamycin and amikacin occurs in the *rrs* gene, replacing adenine in position 1401 for guanine.

It is not clear whether the German group supervised by Gerhard Domagk or the North American team at Squibb and Hoffman-La-Roche were the first to test the activity of the isomers of nicotinic acid (99). Based on early observations that nicotinamide (vitamin B3) had anti-tubercular properties, researchers worldwide were exploring this particular class of nitrogen heterocycle simultaneously (100). Both pyrazinamide and isoniazid were developments of the same chemical lead. Although Roche and Squibb held the patent for isoniazid, they did not retain the exclusive rights and granted production licenses to reliable pharmaceutical companies in order to increase the coverage and the supply of the drug all over the world (101). Today it is recognized that isoniazid is the most popular anti-tubercular agent, for *M. tuberculosis* is extremely sensitive to this synthetic chemical, admittedly as a consequence of a pleiotropic effect (102-103). It has been demonstrated that flavonols can significantly reduce isoniazid resistance in rapid growing mycobacteria (104).

Almost at the same time, another interesting antitubercular compound made its appearance. Cycloserine (13) was isolated in 1952 from *Streptomyces orchidaceus* by Commercial Solvents Corp. This isoxazolidinone has wide spectrum of activity against Gram-positive and Gram-negative bacteria and particularly against mycobacteria. Cycloserine inhibits two enzymes alanine racemase (Alr) and D-alanine D-alanine ligase (Ddl) of the peptidoglycan biosynthesis pathway (105). The MIC of cycloserine is 25 mg/L against the $H_{37}Rv$ strain. Despite being an efficient agent, its severe toxicity has limited its widespread use and it is included as a second line drug (106). There are also other antibiotics acting on the cytoplasmic steps of the biosynthesis of peptidoglycan. Fosfomycin is an inhibitor of the MurA ligase of *Escherichia coli*, forming an adduct with a cysteine residue of the protein (107). In the MurA of *M. tuberculosis*, the critical residue is an aspartic acid and it is assumed that *Mycobacterium* has innate resistance to fosfomycin. Another interesting antibiotic is bacitracin which has a more pronounced inhibitory effect on *M. smegmatis* than *M. tuberculosis* (108). It functions by sequestering undecaprenol phosphate by forming a complex together with a bound divalent metal cation, therefore preventing its binding with a phosphatase and finally inhibiting peptidoglycan biosynthesis (109).

Streptomyces mediterranei was initially obtained from a pine forest soil sample near Nice in 1959 in France by Lepetit Research Laboratories (110). The name of the derived antibiotic rifamycin was coined from a French popular movie of the time "Rififi", perhaps translating the difficult and complex isolation and characterization of the active products. The isolated rifamycins A, B, C, D and E were separated according their mobility in paper chromatography (111). The naturally occurring rifamycin B can be oxidized reversibly to rifamycin O which then loses a glycolic acid molecule liberating rifamycin S, which is very active (112). However these naturally occurring rifamycins have poor solubility in water and low absorption, and therefore cannot be administered orally. Several hundred rifamycin analogues were prepared by Lepetit and Ciba and it was found that the introduction of a formyl group (or another unsaturated substituent) in position 3 usually increased the antibacterial activity of the initial rifamycin. In 1966 rifampicin (14) was finally formulated as an oral, safe and effective anti-TB drug (111). Rifampicin acts on the β-unit of RNA polymerase (Figure 5) codified by *rpoB*, preventing DNA translation to

RNA. Crystals of the *Thermus aquaticus* RNA polymerase bound to rifampicin were obtained by the soaking technique and showed that rifampicin binds to a deep pocket within the DNA/RNA channel around 12 Å from the active site, therefore preventing elongation of the RNA polymer (113). The MIC of rifampicin is 0.1-0.4 mg/L for *M. tuberculosis* $H_{37}Rv$ (114). Almost all of the mutations conferring rifampicin resistance occur on rpoB (> 98%) notably in the region from 513 to 531 amino acids which provide high levels of resistance. There are other analogues of rifampicin such as rifabutin and rifapentine, but resistant *M. tuberculosis* strains can show cross-resistance, rendering these compounds ineffective (115).

Capreomycin (15) is a cyclic pentapeptide antibiotic isolated by Herr and collaborators from *Streptomyces capreolus* in 1960 (116). It is a water soluble compound with close chemical and biological properties to viomycin and the tuberactomycin antibiotics (117). Commercially available capreomycin occurs as a mixture of closely related IA and IB differing by the presence of serine in capreomycin IA instead of alanine in IB. The MIC of capreomycin IA is 2 mg/L against *M. tuberculosis* $H_{37}Rv$ and it is also active against *M. avium* complex species (118). The importance of capreomycin resides on its ability to inhibit the growth of multi-drug resistant strains and non-replicative forms (119). Although the exact mechanism of action is still unknown, it is clear that it interacts with the ribosome by inhibiting translation and therefore protein synthesis. By using microarrays, the translational response of *M. tuberculosis* was studied, and the results showed that several genes are up-regulated following capreomycin exposure, notably the genes related to information pathways involved in the translational system, most encoding ribosomal proteins and t-RNA or r-RNA (120). The *tlyA* gene, although not essential, is thought to codify for a protein able to alter ribosomal proteins and plays a role in *M. tuberculosis* resistance to capreomycin (121). This antibiotic has the same toxicity profile as the aminoglycosides causing ototoxicity and nephrotoxicity, but can also cause renal tubulopathy characterized by alkalosis (122). Another interesting glycopeptide is vancomycin, which shows an MIC of 40 mg/L against the $H_{37}Rv$ strain and is thought to act by a pleiotropic mechanism, because several biochemical pathways are induced after exposure to inhibitory and sub-MIC levels of the antibiotic (123).

Pikromycin was the first macrolide antibiotic extracted from a natural source. It was isolated from *Streptomyces venezuelae*, taken from a Venezuelan soil sample in 1947. This species of *Streptomyces* also produces the important antibiotic chloramphenicol (124). The term "macrolide" was introduced in 1957 by Robert B. Woodward (1917-1979) as a shortcut of macrolactone glycoside to designate a class of polyketide antibiotics composed by a macrolactone ring bound with one or several aminosugar units (125). Pikromycin is a 14-membered macrolide reported for the first time in 1950 having weak activity against Gram-positive bacteria (126). Two years later, McGuire and collaborators isolated erythromycin A from *Saccharopolyspora erythraea* with an increased activity against Gram-positive and Gram-negative bacteria including *Legionella pneumophila*, *Mycoplasma pneumoniae* and *Chlamydia* spp (127). The second generation of macrolides was developed for increasing the bioavailability and pharmacokinetic profile of erythromycin (125). Clarithromycin (16) was prepared by a short sequence of chemical transformations from erythromycin, providing modifications that confer greater resistance towards acid-catalyzed inactivation. It has also increased lipophilicity which enhances tissue penetration and has been therefore effective against intracellular pathogens such as *Heamophilus influenzae* and *M. tuberculosis*. Clarithromycin shows an MIC value of 8 mg/L against the $H_{37}Rv$ strain (128), however there are reports of much weaker activity of clarithromycin against clinical isolates, with MIC values above 64 mg/L (129). In general clarithromycin is much more active against *M. avium* (MIC 8 mg/L), *M. kansasii* (MIC 0.5 mg/L) and *M. ulcerans* (MIC 2 mg/L) (130). Presently there is an increasing interest in developing further the macrolide class for increasing its potency specifically against *M. tuberculosis* (131-132).

There are several antibiotics that display inhibition on lipid biosynthesis of *M. tuberculosis* and this pathway may be important for future TB drug development. Thiolactomycin, isolated in 1982 from a *Nocardia* species (133), has shown an MIC of approximately 26 mg/L for the $H_{37}Rv$ strain (134). The mechanism of action has been reported to be by inhibition of β-ketoacyl-ACP synthases, KasA and KasB, which are necessary enzymes for the biosynthesis of mycolic acids. Cerulenin was initially obtained from *Cephalosporium caerulens* in 1963 and this compound demonstrated antimycobacterial activity, having an MIC value between 3.0-6.25 mg/L against *M. tuberculosis*, 1.5 mg/L against *M. smegmatis*, and 12.5 mg/L against *M. kansasii* (135). Different lipidic patterns were observed in treated cells of *M. bovis* BCG, *M. avium* and *M. smegmatis* in comparison with the controls, revealing that cerulenin acts on lipid biosynthesis. Platensimycin is another interesting antibiotic acting on lipid biosynthesis discovered in 2006 from *Streptomyces platensis* (136). By using an antisense method for comparing the level of RNA expression of fatty acid biosynthesis genes against controls after exposure to a wide range of natural extracts, Merck Co. found that an extract from a soil sample from Africa contained amounts of an active amide named platensimycin (137). The MIC of this compound against *M. tuberculosis* $H_{37}Rv$ is around 12 mg/L and it acts by inhibiting β-ketoacyl-ACP synthases just as thiolactomycin (138).

5. NOVEL ANTIMYCOBACTERIAL SCAFFOLDS FROM NATURAL SOURCES

In this part of the review we focus our attention on the natural products that are potent enough (MIC < 5 mg/L) to be considered as hits for generating novel antimycobacterial leads, displaying also an acceptable selectivity towards *M. tuberculosis* $H_{37}Rv$ (SI >10). Several bioguided studies have appeared in the literature showing inhibitory data for the isolated natural products, but only a

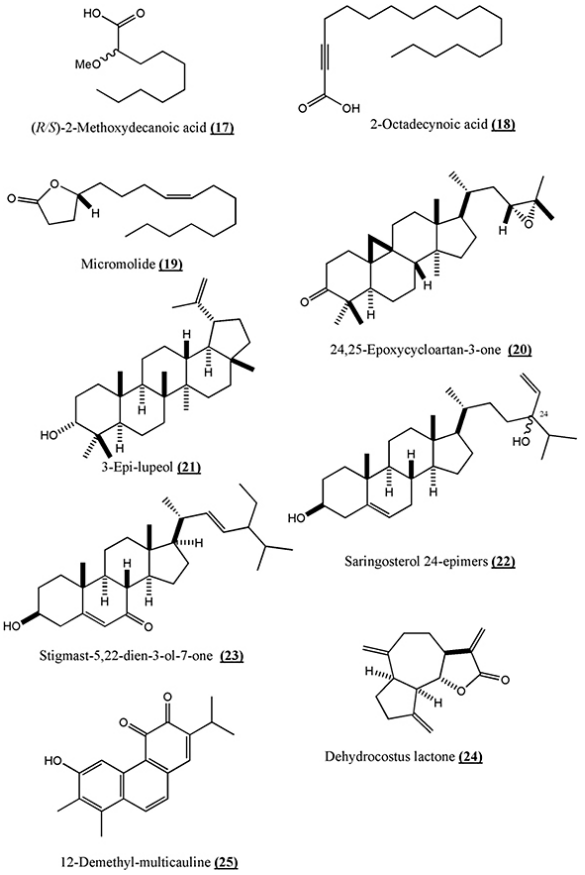

Figure 3. Fatty acids, lipids and terpenoidal natural products with antimycobacterial activity.

small fraction contains information about the non-specific toxicity towards mammalian cells. We insist on the fact that the MIC values only show the potency of the compound against bacterial viability but do not demonstrate selectivity. There are many chemicals which are highly toxic for both prokaryotic and eukaryotic cells and conversely there are other compounds which are mildly active as antibacterials yet having very low or no toxicity towards mammalian cells. These compounds would be easily ignored in a screening where only the MIC value is considered for compound selection and further development. Thus the determination of the half growth inhibitory concentration (GIC_{50}) against mammalian cells on early stages of drug discovery is likely to increase the impact of the first-time reported hits. An excellent review from 2005, emphasizes the importance of determining the cytotoxicity as early as possible (139). Many papers include the MIC of potent antimycobacterial compounds but lack the cytoxicity information, making the examination and comparison of hits a rather flawed and non-standardized procedure. A commentary from 2001 established that a promising hit should show a selectivity index (SI), defined as the ratio between the GIC_{50} on mammalian cells and the MIC on pathogenic mycobacteria, of more than 10 (140). That means that a preliminary hit must be selectively active against mycobacteria at least one order of magnitude in comparison with the degree they affect mammalian cells. Isoniazid is until now an "unbeatable" control, as it has a selectivity index superior to 40,000 (141). The 2001 commentary also encourages rapid determination of the viability of *Mycobacterium* inside the macrophages treated by inhibitors, in order to have a better picture of the intracellular action of the compound, the effective killing concentration inside the cell, and the transport mechanisms from the exterior to the interior of the mammalian cells (140).

There are few reviews on the antimycobacterial activity of natural products, some focusing on certain type or origin of metabolites such as terpenoids (142), marine natural products (143) and alkaloids (144) while others specialize on the coverage of plant metabolites (145) and others include many classes of natural products (146-148).

Mycobacteria has a complex and well-organized system for lipid acquisition and trafficking, being able to capture lipids from the host and utilize them as carbon source and energy (149-151). Around one tenth of all the functional genes of the genome of *M. tuberculosis* are related to lipids (152). Many mycobacterial proteins acting on lipid substrates have been predicted from the genome, involved in fatty acids degradation (118 open reading frames (ORFs)), lipid biosynthesis (65 ORFs), esterases and lipases (38 ORFs) and fatty acid transport (2 ORFs). Therefore it is not surprising that several lipid-like molecules have been found to have an inhibitory effect on the growth of *M. tuberculosis*.

There are early reports of the inhibitory action of oleic acid on TB bacilli from 1926 to 1950 by Boissevain, Platonov, Bergstrom, Dubos and others (153). In 1948, Sattler and Youmans noted that the wetting agent Tween 80 was able to inhibit the growth of *M. tuberculosis* specially when the inoculum size was small (154). The effect can be reversed if oleic acid is eliminated from impure Tween 80 or if albumin is added to the medium. As Tween 80 can be hydrolyzed by the bacteria to produce minute amounts of oleic acid, it can have inhibitory effects in the absence of albumin. By 1977 it was found that a free carboxylic acid was required for antimycobacterial activity, being their esters inactive (155). The most bactericidal fatty acid was found to be myristic acid (C14:0). Against rapid growing mycobacteria such as *M. aurum*, *M. parafortuitum*, *M flavescens* and *M. gilvum*, lauric acid (C12:0) was found to have an MIC value close to 6.25 mg/L (156). It has been demonstrated that activated macrophages release around six times more fatty acids than their normal non-activated macrophages, suggesting that macrophages can perform antimycobacterial functions without phagocytosis (157). Against mycobacteria belonging to the *M. avium* complex, the fatty acids lauric (C12:0), oleic (C18:1) and linolenic (C18:3) have comparable potency (158). When using a bioguided isolation method, one has to be aware that fatty acids frequently occur in lipophilic extracts and therefore dereplication procedures of active lipophilic extracts is recommended for avoiding isolating already known active components.

Interestingly ozonized sunflower oil (Oleozon) was found to have antibacterial properties with an MIC of

950 mg/L against *M. tuberculosis* $H_{37}Rv$ and other mycobacteria (159). The concentration may seem high in comparison with potent antibiotics but it must be remembered that the mixture is simple culinary oil and it has therefore little toxicity. The presumed mechanism of action of these fatty acids is by insertion into the mycolic or phospholipid layers of the bacterial cell walls, therefore altering their permeability and function (156).

The structural type of 2-methoxyfatty acids obtained from marine symbiotic sponges such as the Caribbean *Callyspongia fallax* were discovered to possess antimycobacterial properties (160-161). In a synthetic approach the C_8-C_{14} 2-methoxyfatty acids were prepared and demonstrated activity in the order $C_{10}>C_{12}>C_{14}>C_8$, with 2-methoxydecanoic acid (17) (Figure 3, Table 1) showing an MIC of 40-48 mg/L against the $H_{37}Rv$ strain having an SI above 1.5 (161-162). Interestingly the close relative 2-alkyne fatty acids displayed higher antimycobacterial activity (163). The proposed mechanism of action is inhibition of mycobacterial fatty acid biosynthesis and degradation when toxic levels of the compound are attained, but paradoxically, at non-toxic levels, the alkyne fatty acids may be used for the bacteria to synthesize their mycolic acids. The most active, 2-octadecynoic acid (18) displayed an MIC value of 1.2 mg/L and 2.5 mg/L against *M. smegmatis* mc^2155 and *M. bovis* BCG respectively. Unfortunately there is no mention of the cytotoxicity of the alkyne fatty acids. Other natural fatty acids and lipids have been reported as inhibitors of mycobacterial growth such as the oropheic acids from *Mitrephora glabra* (Annonaceae) (164), or maracin and maracen from the bacterium *Sorangium cellulosum* (165) both with MICs around 12 mg/L but again lacking cytotoxicity data.

From the stem bark of the Vietnamese tree *Micromelum hirsutum* (Rutaceae), the lactone derived from oleic acid, micromolide (19) was isolated and shown to be a potent inhibitor of *M. tuberculosis* growth with an MIC of 1.5 mg/L against the $H_{37}Rv$ strain (166). The selectivity index was calculated to be 63 and it is considered quite a good lead for an unmodified natural product. A report from 2008 published the stereoselective synthesis of the enantiomers of micromolide and several analogue structures with polar groups in the acyclic side chain (167). The data showed that all of the derivatives prepared were less active than the parent compound, indicating that the stereochemistry of the double bond and the lipophilicity of the side chain are the main structural factors contributing to the antimycobacterial activity. The alkenyl unsaturated motif is a particular chemical feature of several natural antimycobacterials suggesting that lipophilic chains of natural products are essential for activity, probably because it allows to diffuse and cross the mycobacterial cell wall.

Another group of important antimycobacterial natural products related to the lipids is the class formed by sterols and triterpenes. The first potent phytochemicals of this class to be identified were the cycloartanes isolated from *Borrichia frutescens* (Asteraceae), an herb occurring in the saline coastal marshes in the USA (168). In that early paper, the MIC of 24,25-epoxycycloartan-3-one (20) was reported to be 8 mg/L against *M. tuberculosis* $H_{37}Rv$, having a selectivity index close to 9 in epithelial kidney cells from the African green monkey (Vero cells). In 1999, two papers describing anti-TB natural products of this class appeared from the same research group (169-170). From the aerial parts of the Kenyan plant *Ajuga remota* (Lamiaceae), ergosterol-5,8-endoperoxide was isolated as a colorless powder showing an MIC of 1 mg/L against the virulent $H_{37}Rv$ strain. Hydroxykulactone, isolated as colorless oil, showed an MIC of 4 mg/L against the same virulent strain. However there is no data regarding the toxicity on mammalian cells and therefore it is difficult to assess whether they have any specificity towards mycobacteria or they are cytotoxic compounds. The Caribbean sea sponge *Svenzea zeai* (Dictyonellidae) contains two *abeo*-sterols named parguesterols which are active against mycobacteria having an MIC value between 8 and 12 mg/L with an SI between 6.5 and 4.3 in relation to Vero cells (171). 3-Epilupeol (21) obtained from the medicinal Chinese flowers of *Chrysanthemum morifolia* (Asteraceae) was found to be a growth inhibitor of the $H_{37}Rv$ strain with an MIC value of 4 mg/L and a SI of 15 against Vero cells (172), constituting a promising scaffold for future development. From the Chilean brown algae *Lessonia nigrescens* (Laminariales), the sterol saringosterol (22) was found to be impressively selective against *M. tuberculosis* having an MIC of 0.125 mg/L for the 24*R* epimer and 1.0 mg/L for the 24*S* epimer, with a very low toxicity ($IC_{50}>128$ mg/L) against Vero cells (173). The calculated SI is above 1024 for the 24*R* epimer and 128 for the 24*S* epimer, evidencing very high mycobacterial specificity for an unmodified natural product and constituting therefore a very interesting lead for further development. Surprisingly after 10 years of the publication of this hit, there are no reports on the evaluation of the compound in a more real setting such as *ex vivo* or *in vivo* models of TB infection. There is no data pertaining to its pharmacodynamic or pharmacokinetic profile or data on its mechanism of action or even the activity of chemical analogues. In order to increase the impact of this hit, several questions still need to be addressed. The stigmastane sterols from *Thallia multiflora* (Maranthaceae) have also been found to be potent and selective antimycobacterials. Stigmast-5-en-3β-ol-7-one, stigmast-4-ene-6β-ol-3-one, stigmast-5,22-dien-3β-ol-7-one (23) and stigmast-4,22-dien-6β-ol-3-one have MIC values between 1 and 4.2 mg/L and showed selectivity indexes above 95 against Vero cells (174). There are other active interesting steroidal natural products such as aegicerin ($H_{37}Rv$ MIC 1.6-3.2 mg/L) isolated from the Peruvian plant *Clavijera procera* (Theophrastaceae) (175) and the steroidal endoperoxides from *Ruprechtia trifolia* (Polygonaceae) (176) both having potent metabolites but lacking cytotoxicity information.

Essential oils are volatile extracts obtained by steam distillation typically from aromatic plants, and they are mainly composed of monoterpenoids (177). The components of essential oils have shown inhibitory effects but these apolar substances also display toxic effects such as phototoxicity, abortive and cancerogenic activities (178-

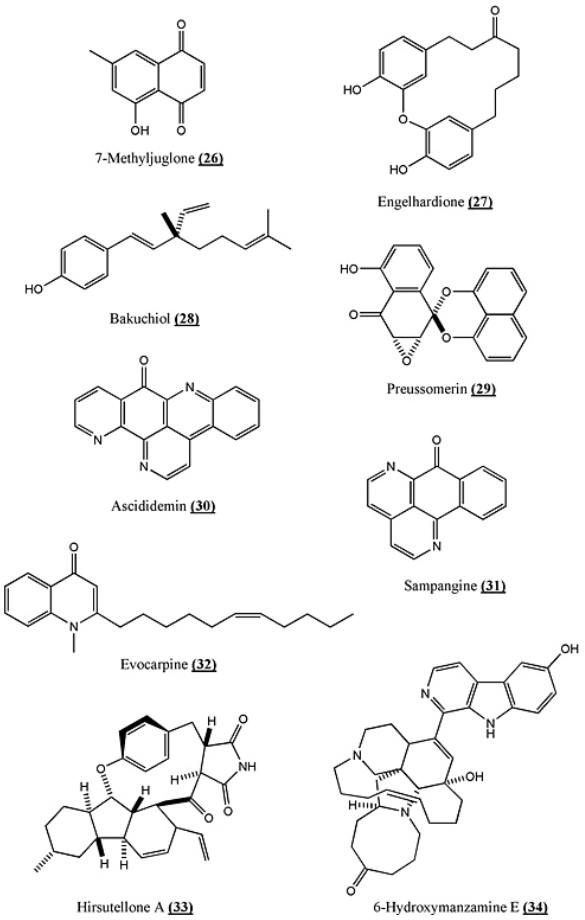

Figure 4. Phenolic and alkaloidal natural products with potent antimycobacterial activity.

180). Among the sesquiterpenoids there are structures with mild activity (MIC~50 mg/L) such as the sesquiterpene lactones costunolide and parthenolide which are also cytotoxic (181-182). The sesquiterpene lactone dehydrocostus lactone (24) from *Saussurea lappa* (Asteraceae) was found to have a significant MIC value around 2 mg/L against *M. tuberculosis* $H_{37}Rv$ (183) but is also cytotoxic with an GIC_{50} between 2.5 and 3.5 mg/L against the cancer line cells HepG2, HeLa and OVCAR-3 (184). 11α-hydroxycinnamosmolide, isolated from the South African plant *Warburgia salutaris* (Canellaceae) showed an MIC value of 40 mg/L against *M. bovis* BCG and inhibited mycobacterial *N*-acetyl-transferase enzyme (185). From the roots of Turkish *Salvia multicaulis* (Lamiaceae), several diterpenoids with antimycobacterial activity have been isolated (186). The quinones 12-demethylmulticauline (25), 2-demethylmultiorthoquionone and 12-methyl-5-dehydroacetylhorminone showed MIC values of 0.46 mg/L, 1.2 mg/L and 0.89 mg/L against the $H_{37}Rv$ strain respectively. However there is no mention about the cytotoxicity of these diterpenoids. From the berries of Turkish *Juniperus excelsa* (Cupressaceae), the diterpenoid sclareol was found to inhibit *M. tuberculosis* $H_{37}Rv$ growth at 6 mg/L (187) however in another paper, it was found to be toxic having the ability to arrest the cell cycle in human breast cancer cells (188).

Several naphthoquinones isolated mainly from *Euclea* species (Ebenaceae) have been found to be inhibitors of *M. tuberculosis* growth (189-190). The activity of 2-hydroxynaphthoquinone (lawsone) has already been discussed earlier in this review. The MIC values of plumbagin, crassiflorone and diospyrone have been determined on *M. tuberculosis* $H_{37}Rv$, being inferior to 5 mg/L (191), however no information of the mammalian cytotoxicity was given. In a report from 2007, lawsone (6), menadione and juglone showed an MIC below or equal to 5 mg/L, but the compounds were cytotoxic against Vero cells, showing a SI below 2 (192). Nonetheless the research team also synthesized several analogue structures finding that 7-methyljuglone (26) (Figure 4, Table 1) displayed a potent 0.5 mg/L MIC against the $H_{37}Rv$ strain and had an SI of around 30. The researchers also found that the naphthoquinones had some affinity for the mycothiol disulfide reductase of *M. tuberculosis*, an enzyme necessary for maintaining the balance of mycothiol, the Actinomycete analogue of glutathione necessary for surviving under exogenous and endogenous oxidative stress (Figure 5) (193-195). Quite a few analogues of plumbagin have been recently synthesized, some of which show promising anti-TB activity but the cytotoxicity information is lacking (196). The lapachones (α and β-pyran naphthoquinones) are interesting antimycobacterial natural products isolated from *Tabebuia* species (Bignoniaceae) and several analogues have been developed with interesting properties but the relative toxicity of these compounds is still unknown (197). Some terpenoid quinones have also been isolated from *Plectranthus* species and they displayed antitubercular activity however the selectivity index was calculated to be below 10 (198).

From the roots of the Asian plant *Engelhardia roxbhurgiana* (Juglandaceae) several secondary metabolites with antitubercular properties were isolated (199). A diphenyl ether ketone named engelhardione (27) has been reported to have an MIC of 0.2 mg/L against the virulent laboratory strain of *M. tuberculosis* but there is no information about its cytotoxicity. Other antimycobacterial metabolites have been obtained from this plant such as 3-methoxyjuglone ($H_{37}Rv$ MIC 0.2 mg/L), 4-hydroxytetralone ($H_{37}Rv$ MIC 4.0 mg/L) and engelharquinone (90-221387 MIC 30 mg/L) but again no information about the specificity was provided (200).

Lipophilic phenols such as 6-paradol and 6-shogaol have shown inhibitory activity against *M. chelonei*, *M. smegmatis*, *M. intracellulare* and *M. xenopi*, having an MIC value between 10 and 15 mg/L but there is no mention about toxicity on mammalian cells (201). Bakuchiol (28) isolated from the seeds of *Psoralea corilifolia* (Papilionaceae) was found to be active against *M. aurum* and *M. bovis* BCG with an MIC of 16 mg/L and 21 mg/L respectively but inactive against *M. smegmatis* showing an MIC above 400 mg/L (202). However in another study the GIC_{50} of this phenol against the human cancer lines AGS and HeLa was 1.5 mg/L and 1.8 mg/L respectively (203).

Phloroglucinol derivatives have also been reported to display inhibition of the growth of mycobacteria. The drummondins D-F isolated from *Hypericum drummondii* (Hypericaceae) showed inhibitory activity towards *M. smegmatis* with MIC values between 1.56 and 3.12 mg/L (204). This class of compound has also been reported to have cytotoxic effects on leukemia and tumoral cell lines with a GIC_{50} in the same order of magnitude (205).

From the lichen fungus *Microsphaeropsis* spp. collected in Thailand, various preussomerins have been isolated and found to inhibit the growth of mycobacteria. Preussomerin (29) was reported to display an MIC value between 1.56 and 3.12 mg/L against *M. tuberculosis* $H_{37}Ra$, having a SI close to 6 (206). Osthrutin is a geranyl coumarin isolated from *Peucedanum ostruthium* (Apiaceae) that has significant antimycobacterial activity against fast growing mycobacteria such as *M. aurum*, *M. smegmatis*, *M. phlei* and *M. fortuitum* (207).

The pentacyclic aromatic pyridoacridone alkaloid, ascididemin (30) is a natural product isolated from marine tunicate *Didemnum* spp (208). The MIC of this compound against *M. tuberculosis* $H_{37}Rv$ is an astonishing 0.1 mg/L however the GIC_{50} on Vero cells is even lower (0.04 mg/L), making the compound less active for *M. tuberculosis* than for mammalian cells (209). This example shows the importance of the toxicity assay when evaluating compounds for growth inhibition against bacteria. An analogue tetraquinone of ascididemin with a dimethylamino-ethenyl chain has a much higher mycobacterial specificity showing an MIC of 0.39 mg/L with a SI of 15 in relation to Vero cells. Using microarray experiments it was found that this compound induces mycobactin biosynthetic genes (210) indicating that the compound interferes with iron uptake (Figure 5) which was confirmed by an increase in the MIC when the mycobacteria was grown in a medium containing an excess of iron, and a decrease of the MIC when the mycobactin gene (*mtbB*) was deleted. The aza-oxoaporphine alkaloid sampangine (31), isolated from the aromatic Ylang-ylang tree *Cananga odorata* (Annonaceae) (211) has been reported to display an MIC value of 0.2 mg/L against *M. intracellulare* (212). The GIC_{50} of sampangine was established to be 4.76 mg/L on Vero cells, having therefore a selectivity index of 23.8 (213). From the unripe fruit of *Evodia rutaecarpa* (Rutaceae) a new class of lipophilic quinolones was reported to have antimycobacterial activity (214). In particular the alkaloid (32) showed an MIC of 2 mg/L against rapid growing *M. smegmatis*, *M. fortuitum* and *M. phlei*. The aporphine alkaloids are also interesting antimycobacterial skeletons, and recently 3-methoxynordomesticine hydrochloride was found to have an MIC value around 5 mg/L against *M. tuberculosis* $H_{37}Rv$ and *M. bovis* BCG (215). The alkaloid inhibited the MurE ligase of *M. tuberculosis* and displayed a selectivity index close to 12 in relation to murine macrophages RAW264.7 cells.

Hirsutellone alkaloids isolated from the pathogenic fungi *Hirsutella nivea* have been found to be potent antimycobacterials (216). Hirsutellone A (33) displayed an MIC of 0.78 mg/L against *M. tuberculosis* $H_{37}Ra$ strain, showing a GIC_{50} higher than 50 mg/L against Vero cell, therefore recording a promising SI above 64. Another interesting alkaloid scaffold is related to the manzamines which have been isolated from the Indonesian sponge *Acanthostrongylophora* sp. The alkaloid 6-hydroxymanzamine E (34) had a potent antitubercular activity with an MIC value of 0.4 mg/L against *M. tuberculosis* $H_{37}Rv$ and a GIC_{50} of 4.3 mg/L on Vero cells, evidencing a selectivity index of 10.75 (217).

6. PERSPECTIVE

Several interesting antimycobacterial hits have been discovered in natural products screening projects such as the saringosterol epimers, micromolide, sampangine and the hirsutellones which share high potency and selectivity towards mycobacteria. These hits should be studied thoroughly for their mechanism of action, for their inhibitory activity on *ex vivo* or *in vivo* infection assays, as well as for structure-activity relationships. Determining their mechanism of action provides a starting point for the elaboration of analogues by rational design, and could also unlock previously neglected antimicrobial molecular targets. It should also be said that chemical biodiversity screening programmes and bioprospection projects should be kept running if we aim to maintain fueling the anti-TB drug pipeline.

Minute amount of bioactive metabolites in their natural sources is often a limitation for detailed biological evaluation. Therefore synthetic procedures should be developed in early stages of lead identification research, as this enables the generation not only of higher amounts of bioactive material but also analogue structures, precursors and derivatives which allow chemical space exploration and identification of essential pharmacophore scaffolds.

7. ACKNOWLEDGEMENTS

The authors of this manuscript acknowledge the researchers who contributed to the antimycobacterial screening of natural products all around the world. We are also thankful to the support from the Medical Research Council, UK (G0801956) to SB, the Austrian Science Fund (FWF) to FB, SG and SB, and TB Drug Discovery-UK (www.tbd-uk.org.uk). AG is sponsored by UNESCO-L'Oreal International Fellow and JDG by Colfuturo and Bloomsbury Colleges (University of London).

8. REFERENCES

1. J. Hayman: *Mycobacterium ulcerans*: an infection from Jurassic time? *Lancet* 324(8410), 1015-1016 (1984)

2. J. Hayman: A hypothesis refuted: *Mycobacterium ulcerans* is of recent evolution. *Lancet Infect Dis* 5(6), 327-328 (2005)

3. B. M. Rothschild, L. D. Martin, G. Lev, H. Bercovier, G. Bar-Gal, C. Greenblatt, H. Donoghue, M. Spigelman and

D. Brittain: *Mycobacterium tuberculosis* complex DNA from an extinct bison dated 17,000 years before the present. *Clin Infect Dis* 33(3), 305-311 (2001)

4. W. L. Salo, A. C. Aufderheide, J. Buikstra and T. A. Holcomb: Identification of *Mycobacterium tuberculosis* DNA in a pre-Columbian Peruvian mummy. *Proc Natl Acad Sci U S A* 91(6), 2091-2094 (1994)

5. A. R. Zink, C. Sola, U. Reischl, W. Grabner, N. Rastogi, H. Wolf and A. G. Nerlich: Characterization of *Mycobacterium tuberculosis* complex DNAs from Egyptian mummies by spoligotyping. *J Clin Microbiol* 41(1), 359-367 (2003)

6. A. S. Weissfeld: Infectious diseases and famous people who succumbed to them. *Clin Microbiol News* 31(22), 169-172 (2009)

7. J. Eisenstadt and G. S. Hall: Microbiology and classification of mycobacteria. *Clin Dermatol* 13(3), 197-206 (1995)

8. N. Scherr and L. Nguyen: *Mycobacterium* versus *Streptomyces*-we are different, we are the same. *Curr Opin Microbiol* 12(6), 699-707 (2009)

9. V. Jarlier and H. Nikaido: Mycobacterial cell wall: Structure and role in natural resistance to antibiotics. *FEMS Microbiol Lett* 123(1-2), 11-18 (1994)

10. D. Thierry, M. D. Cave, K. D. Eisenach, J. T. Crawford, J. H. Bates, B. Gicquel and J. L. Guesdon: IS6110, an IS-like element of *Mycobacterium tuberculosis* complex. *Nucl Acids Res* 18(1), 188 (1990)

11. WHO: Global tuberculosis control. In: *WHO report* World Health Organization, (2010)

12. R. G. Neel, N. Paul, D. Keertan, H. S. Schaaf, Z. Matteo, S. Dick van, J. Paul and B. Jaime: Multidrug-resistant and extensively drug-resistant tuberculosis: a threat to global control of tuberculosis. *Lancet* 375(9728), 1830-1843 (2010)

13. TAG: Report on tuberculosis research funding trends (2005-2008). In: Treatment Action Group, New York, USA, (2009)

14. M. Casenghi, S. T. Cole and C. F. Nathan: New approaches to filling the gap in tuberculosis drug discovery. *PLoS Med* 4(11), e293 (2007)

15. M. Zhenkun, L. Christian, M. Helen, J. N. Andrew and W. Xiexiu: Global tuberculosis drug development pipeline: the need and the reality. *Lancet* 375(9731), 2100-2109 (2010)

16. T. Wirth, F. Hildebrand, C. Allix-Béguec, F. Wölbeling, T. Kubica, K. Kremer, D. van Soolingen, S. Rüsch-Gerdes, C. Locht, S. Brisse, A. Meyer, P. Supply and S. Niemann: Origin, spread and demography of the *Mycobacterium tuberculosis* complex. *PLoS Pathog* 4(9), e1000160 (2008)

17. T. M. Daniel: The history of tuberculosis. *Respir Med* 100(11), 1862-1870 (2006)

18. J. Koller, U. Baumer, Y. Kaup, M. Schmid and U. Weser: Effective mummification compounds used in pharaonic Egypt: Reactivity on bone alkaline phosphatase. *Z Naturforsch* 58(5), 462-480 (2003)

19. M. Christodoulaki, G. Moschaki, M. Kalloniatou, G. Tsoukalas, A. Kanitsakis, D. Athanasopoulos, S. Blazaki, S. Fiotaki and I. Tsoukalas: Tuberculosis according to Hippocrates. *Paediatr Respir Rev* 7, S294-S294 (2006)

20. J. M. Steger and T. L. Barret: Cutaneous tuberculosis. In: *Military dermatology*. Ed R. Zaijtchuk & R. F. Bellamy. Walter Reed Medical Army Center, Washington, USA, (1994)

21. S. Castaldo and F. Capasso: Propolis, an old remedy used in modern medicine. *Fitoterapia* 73, S1-S6 (2002)

22. Z. Yildirim, S. Hacievliyagil, N. O. Kutlu, N. E. Aydin, M. Kurkcuoglu, M. Iraz and R. Durmaz: Effect of water extract of Turkish propolis on tuberculosis infection in guinea-pigs. *Pharmacol Res* 49(3), 287-292 (2004)

23. R. S. Rivlin: Historical perspective on the use of garlic. *J Nutr* 131(3), 951S-954 (2001)

24. E. C. Delaha and V. F. Garagusi: Inhibition of mycobacteria by garlic extract (*Allium sativum*). *Antimicrob Agents Chemother* 27(4), 485-486 (1985)

25. J. E. Lancaster and H. A. Collin: Presence of alliinase in isolated vacuoles and of alkyl cysteine sulphoxides in the cytoplasm of bulbs of onion (*Allium cepa*). *Pl Sci Lett* 22(2), 169-176 (1981)

26. D. Lawson Larry: Garlic: A review of its medicinal effects and indicated active compounds. In: *Phytomedicines of Europe*. American Chemical Society, 14, 176-209 (1998)

27. P. Ratnakar and P. Murthy: Purification and mechanism of action of antitubercular principle from garlic (*Allium sativum*) active against isoniazid susceptible and resistant *Mycobacterium tuberculosis* H37Rv. *Ind J Clin Biochem* 10(1), 34-38 (1995)

28. R. S. Feldberg, S. C. Chang, A. N. Kotik, M. Nadler, Z. Neuwirth, D. C. Sundstrom and N. H. Thompson: In vitro mechanism of inhibition of bacterial cell growth by allicin. *Antimicrob Agents Chemother* 32(12), 1763-1768 (1988)

29. N. Hasan, N. Yusuf, Z. Toossi and N. Islam: Suppression of *Mycobacterium tuberculosis* induced reactive oxygen species (ROS) and TNF-α mRNA expression in human monocytes by allicin. *FEBS Lett* 580(10), 2517-2522 (2006)

30. N. Hasan, M. U. Siddiqui, Z. Toossi, S. Khan, J. Iqbal and N. Islam: Allicin-induced suppression of *Mycobacterium tuberculosis* 85B mRNA in human monocytes. *Biochem Biophys Res Commun* 355(2), 471-476 (2007)

31. G. O'Donnell, R. Poeschl, O. Zimhony, M. Gunaratnam, J. B. C. Moreira, S. Neidle, D. Evangelopoulos, S. Bhakta, J. P. Malkinson, H. I. Boshoff, A. Lenaerts and S. Gibbons: Bioactive Pyridine-N-oxide Disulfides from Allium stipitatum. *J Nat Prod* 72(3), 360-365 (2008)

32. C. d. Ledesma: Chocolate: or, and Indian drinke. Translated by James Wandsworth in 1652. Stinson Brand Innovation, London, UK (2009)

33. C. Summa, J. McCourt, B. Cämmerer, A. Fiala, M. Probst, S. Kun, E. Anklam and K.-H. Wagner: Radical scavenging activity, anti-bacterial and mutagenic effects of Cocoa bean Maillard reaction products with degree of roasting. *Mol Nutr Food Res* 52(3), 342-351 (2008)

34. R. P. Samy, P. N. Pushparaj and P. Gopalakrishnakone: A compilation of bioactive compounds from Ayurveda. *Bioinformation* 3(3), 100-10 (2008)

35. W. Gao, A. P.-C. Chen, C.-H. Leung, E. A. Gullen, A. Fürstner, Q. Shi, L. Wei, K.-H. Lee and Y.-C. Cheng: Structural analogs of tylophora alkaloids may not be functional analogs. *Bioorg Med Chem Lett* 18(2), 704-709 (2008)

36. T. Naserpour, A. Mohagheghi, S. Shahraki, M. Naderi and B. Sharafi: Anti-tuberculosis effect of *Ocimum sanctum* extracts in in vitro and macrophage culture. *J Med Sci* 6(3), 348-351 (2006)

37. K. P. Sampath, D. Bhowmik, Chiranjib, P. Tiwari and R. Kharel: Indian traditional herbs *Adhatoda vasica* and its medicinal application. *J Chem Pharm Res*, 2(1), 240-245 (2010)

38. R. Gupta, B. Thakur, P. Singh, H. B. Singh, V. D. Sharma, V. M. Katoch and S. V. S. Chauhan: Anti-tuberculosis activity of selected medicinal plants against multi-drug resistant *Mycobacterium tuberculosis* isolates. *Indian J Med Res* 131, 809-813 (2010)

39. M. Ullah, S. Sultana, A. Haque and S. Tasmin: Antimicrobial, cytotoxic and antioxidant activity of *Centella asiatica*. *Europ J Sci Res* 30(2), 260-264 (2009)

40. S. Medda, N. Das, S. B. Mahata, P. R. Mahadevan and M. K. Basu: Glycoside-bearing liposomal delivery systems against macrophage-associated disorders involving *Mycobacterium leprae* and *Mycobacterium tuberculosis*. *Indian J Biochem Biophys* 32(3), 147-151 (1995)

41. A. Friis-Møller, M. Chen, K. Fuursted, S. B. Christensen and A. Kharazmi: In Vitro antimycobacterial and antilegionella activity of licochalcone A from Chinese licorice roots. *Planta Med* 68(05), 416-419 (2002)

42. V. K. Gupta, A. Fatima, U. Faridi, A. S. Negi, K. Shanker, J. K. Kumar, N. Rahuja, S. Luqman, B. S. Sisodia, D. Saikia, M. P. Darokar and S. P. S. Khanuja: Antimicrobial potential of *Glycyrrhiza glabra* roots. *J Ethnopharm* 116(2), 377-380 (2008)

43. N. Lall and J. J. M. Meyer: In vitro inhibition of drug-resistant and drug-sensitive strains of *Mycobacterium tuberculosis* by ethnobotanically selected South African plants. *J Ethnopharm* 66(3), 347-354 (1999)

44. A. C. U. Lourens, A. M. Viljoen and F. R. van Heerden: South African *Helichrysum* species: A review of the traditional uses, biological activity and phytochemistry. *J Ethnopharm* 119(3), 630-652 (2008)

45. N. Lall, A. A. Hussein and J. J. M. Meyer: Antiviral and antituberculous activity of *Helichrysum melanacme* constituents. *Fitoterapia* 77(3), 230-232 (2006)

46. Meyer, J. J. M., Lall, N., Mathekga and A. D. M.: In vitro inhibition of drug-resistant and drug-sensitive strains of *Mycobacterium tuberculosis* by *Helichrysum caespititium*. Foundation for Education, Science and Technology, Pretoria, South Africa (2002)

47. L. J. McGaw, N. Lall, J. J. M. Meyer and J. N. Eloff: The potential of South African plants against *Mycobacterium* infections. *J Ethnopharm* 119(3), 482-500 (2008)

48. M. S. Rajab, C. L. Cantrell, S. G. Franzblau and N. H. Fischer: Antimycobacterial activity of (E)-phytol and derivatives: A preliminary structure-activity study. *Planta Med* 64(01), 2-4 (1998)

49. G. Chaudhary, S. Goyal and P. Poonia: *Lawsonia inermis* Linnaeus: a phytopharmacological review. *Int J Pharm Sci Drug Res* 2(2), 91-98 (2010)

50. V. K. Sharma: Tuberculostatic activity of henna (*Lawsonia inermis* Linn.). *Tubercle* 71(4), 293-295 (1990)

51. C. Courreges, L. Rajabi and T. Primm: *Drug development against mycobacteria*. University of Texas. Department of Biological Sciences. El Paso, Texas, USA (2003)

52. L. B. Kan: Introduction to Chinese medical literature. *Bull Med Libr Assoc* 53, 60-70 (1965)

53. Y. Xingrong, F. Bingyi, S. Fang, Q. Jinlin, L. Quan, W. Shuqian, H. Werner, C. Yinfu and Z. Xinsheng: Encyclopedic reference of traditional Chinese medicine. Springer-Verlag, Heidelberg, Germany (2003)

54. D. Lechner, M. Stavri, M. Oluwatuyi, R. Pereda-Miranda and S. Gibbons: The anti-staphylococcal activity

of *Angelica dahurica* (Bai Zhi). *Phytochemistry* 65(3), 331-335 (2004)

55. L. Meot-Duros, S. Cérantola, H. Talarmin, C. Le Meur, G. Le Floch and C. Magné: New antibacterial and cytotoxic activities of falcarindiol isolated in *Crithmum maritimum* L. leaf extract. *Food Chem Toxicol* 48(2), 553-557 (2010)

56. J. F. Young, L. P. Christensen, P. K. Theil and N. Oksbjerg: The polyacetylenes falcarinol and falcarindiol affect stress responses in myotube cultures in a biphasic manner. *Dose-Response* 6(3), 239-51 (2008)

57. T. Ohnuma, T. Komatsu, S. Nakayama, T. Nishiyama, K. Ogura and A. Hiratsuka: Induction of antioxidant and phase 2 drug-metabolizing enzymes by falcarindiol isolated from *Notopterygium incisum* extract, which activates the Nrf2/ARE pathway, leads to cytoprotection against oxidative and electrophilic stress. *Arch Biochem Biophys* 488(1), 34-41 (2009)

58. J. Chen and T. Chen: Heat clearing herbs Huang Lian. In: *Chinese medical herbology and pharmacology*. AOM Press. (2004)

59. E. J. Gentry, H. B. Jampani, A. Keshavarz-Shokri, M. D. Morton, D. Vander Velde, H. Telikepalli, L. A. Mitscher, R. Shawar, D. Humble and W. Baker: Antitubercular natural products: Berberine from the roots of commercial *Hydrastis canadensis* powder. Isolation of inactive 8-oxotetrahydrothalifendine, canadine, β-hydrastine, and two new quinic acid esters, hycandinic acid esters-1 and -2. *J Nat Prod* 61(10), 1187-1193 (1998)

60. K. Yoshio, I. Akihiro, F. Mitsuru, F. Haruo, N. Chiaki and K. Nomoto: Activation of peritoneal macrophages by berberine-type alkaloids in terms of induction of cytostatic activity. *Int J Immunopharmacol* 6(6), 587-592 (1984)

61. G. S. Kumar, D. Debnath, A. Sen and M. Maiti: Thermodynamics of the interaction of berberine with DNA. *Biochem Pharmacol* 46(9), 1665-1667 (1993)

62. D. Sun, S. N. Abraham and E. H. Beachey: Influence of berberine sulfate on synthesis and expression of Pap fimbrial adhesin in uropathogenic *Escherichia coli*. *Antimicrob Agents Chemother* 32(8), 1274-1277 (1988)

63. S. Mahadevan: The legend of Louis Pasteur. *Resonance* 12(1), 15-22 (2007)

64. R. Brand: Biographical sketch: Baron Joseph Lister, FRCS, 1827–1912. *Clin Orthop Relat Res* 468(8), 2009-2011 (2010)

65. B. Lister: The classic: On the antiseptic principle in the practice of surgery. *Clin Orthop Relat Res* 468(8), 2012-2016 (2010)

66. S. A. Waksman: What Is an antibiotic or an antibiotic substance? *Mycologia* 39(5), 565-569 (1947)

67. F. Ryan: Tuberculosis: the greatest story never told. Swift Publishers, Worcestershire, UK (1992)

68. S. H. E. Kaufmann: Paul Ehrlich: founder of chemotherapy. *Nat Rev Drug Discov* 7(5), 373-373 (2008)

69. D. S. Barnes: Historical perspectives on the etiology of tuberculosis. Elsevier, Kidlington, UK (2000)

70. J. Tyagi: The timeless legacy of Robert Koch. *Resonance* 11(9), 20-28 (2006)

71. L. Landouzy: The cinquantenary of the experimental demonstration, at the académie de médecine by A. Villemin, of the specific and contagious virulence of tuberculosis. *Dublin J Med Sci* 141(3), 193-202 (1916)

72. D. S. Burke: Of postulates and peccadilloes: Robert Koch and vaccine (tuberculin) therapy for tuberculosis. *Vaccine* 11(8), 795-804 (1993)

73. F. Bosch and L. Rosich: The contributions of Paul Ehrlich to pharmacology: A tribute on the occasion of the centenary of his Nobel prize. *Pharmacology* 82(3), 171-179 (2008)

74. K. Brown: Penicillin man. Alexander Fleming and the antibiotic revolution. Sutton Publishing, Gloucestershire, UK (2004)

75. F. Jones and S. Ricke: Observations on the history of the development of antimicrobials and their use in poultry feeds. *Poult Sci* 82(4), 613-617 (2003)

76. R. J. Dubos, R. D. Hotchkiss and A. F. Coburn: The effect of gramicin and tyrocidine on bacterial metabolism. *J Biol Chem* 146(2), 421-426 (1942)

77. L. Fattorini, G. Orefici, S. H. Jin, G. Scardaci, G. Amicosante, N. Franceschini and I. Chopra: Resistance to beta-lactams in *Mycobacterium fortuitum*. *Antimicrob Agents Chemother* 36(5), 1068-1072 (1992)

78. H. H. Kwon, H. Tomioka and H. Saito: Distribution and characterization of [beta]-lactamases of mycobacteria and related organisms. *Tuber Lung Dis* 76(2), 141-148 (1995)

79. Utrup, L. J., Moore, T. D., Actor, P., Poupard and J. A.: Susceptibilities of nontuberculosis mycobacterial species to amoxicillin-clavulanic acid alone and in combination with antimycobacterial agents. *Antimicrob Agents Chemother* 39(7), 1454-1457 (1995)

80. I. Dinçer, A. Ergin and T. Kocagöz: The vitro efficacy of β-lactam and β-lactamase inhibitors against multidrug resistant clinical strains of *Mycobacterium tuberculosis*. *Int J Antimicrob Agents* 23(4), 408-411 (2004)

81. J.-E. Hugonnet and J. S. Blanchard: Irreversible inhibition of the *Mycobacterium tuberculosis* β-lactamase by clavulanate. *Biochemistry* 46(43), 11998-12004 (2007)

82. A. R. Flores, L. M. Parsons and Pavelka, Martin S., Jr: Genetic analysis of the β-lactamases of *Mycobacterium tuberculosis* and *Mycobacterium smegmatis* and susceptibility to β-lactam antibiotics. *Microbiology* 151(2), 521-532 (2005)

83. W. Kingston: Streptomycin, Schatz v. Waksman, and the balance of credit for discovery. *J Hist Med Allied Sci* 59(3), 441-462 (2004)

84. J. Crofton: The MRC randomized trial of streptomycin and its legacy: a view from the clinical front line. *J Roy Soc Med* 99(10), 531-4 (2006)

85. A. Meier, P. Sander, K. Schaper, M. Scholz and E. Bottger: Correlation of molecular resistance mechanisms and phenotypic resistance levels in streptomycin-resistant Mycobacterium tuberculosis. *Antimicrob Agents Chemother* 40(11), 2452-2454 (1996)

86. D. A. Mitchison: The segregation of streptomycin-resistant variants of Mycobacterium tuberculosis into groups with characteristic levels of resistance. *J Gen Microbiol* 5(3), 596-604 (1951)

87. B. Springer, Y. G. Kidan, T. Prammananan, K. Ellrott, E. C. Bottger and P. Sander: Mechanisms of streptomycin resistance: Selection of mutations in the 16S rRNA gene conferring resistance. *Antimicrob Agents Chemother* 45(10), 2877-2884 (2001)

88. F. Bernheim: The effect of salicylate on the oxygen uptake of the tubercle bacillus. *Science* 92(2383), 204 (1940)

89. A. K. Saz and F. Bernheim: The effect of 2,3,5, triiodobenzoate and various other compounds ont he growth of tubercle bacillus. *J Pharmacol Exp Ther* 73(1), 78-84 (1941)

90. P. B. Woolley: The use of antrenyl in gastro-intestinal irritation due to PAS compounds. *Brit J Tuber Dis Chest 51*(4), 382-384 (1957)

91. J. Kumazawa and M. Yagisawa: The history of antibiotics: The Japanese story. *J Infect Chemother* 8(2), 125-133 (2002)

92. H. Umezawa: Kanamycin: its discovery. Ann N Y Acad Sci 76 (The Basic and Clinical Research of the New Antibiotic, Kanamycin), 20-26 (1958)

93. TBAlliance: Kanamycin. *Tuberculosis* 88(2), 117-118 (2008)

94. Y. Suzuki, C. Katsukawa, A. Tamaru, C. Abe, M. Makino, Y. Mizuguchi and H. Taniguchi: Detection of kanamycin-resistant Mycobacterium tuberculosis by identifying mutations in the 16S rRNA gene. *J Clin Microbiol* 36(5), 1220-1225 (1998)

95. E. J. Begg and M. L. Barclay: Aminoglycosides - 50 years on. *Br J Clin Pharmac* 39(6), 597-603 (1995)

96. H. Kawaguchi: Discovery, chemistry, and activity of amikacin. *J Infect Dis* 134, Supplement, 242-248 (1976)

97. TBAlliance: Amikacin. *Tuberculosis* 88(2), 87-88 (2008)

98. L. Jugheli, N. Bzekalava, P. de Rijk, K. Fissette, F. Portaels and L. Rigouts: High level of cross-resistance between kanamycin, amikacin, and capreomycin among *Mycobacterium tuberculosis* isolates from Georgia and a close relation with mutations in the rrs gene. *Antimicrob Agents Chemother* 53(12), 5064-5068 (2009)

99. W. McDermott: The story of INH. *J Infect Dis* 119(6), 678-83 (1969)

100. M. F. Murray: Nicotinamide: An oral antimicrobial agent with activity against both *Mycobacterium tuberculosis* and human immunodeficiency virus. *Clin Infect Dis* 36(4), 453-460 (2003)

101. J. A. Aeschlimann: Isoniazid - victim of a limited market. *Ind Eng Chem* 52(1), 22-23 (1960)

102. Y. Zhang, S. Dhandayuthapani and V. Deretic: Molecular basis for the exquisite sensitivity of *Mycobacterium tuberculosis* to isoniazid. *Proc Natl Acad Sci U S A* 93(23), 13212-13216 (1996)

103. C. Vilchèze and J. W. Jr.: The mechanism of isoniazid killing: clarity through the scope of genetics. *Ann Rev Microbiol* 61(1), 35-50 (2007)

104. D. Lechner, S. Gibbons and F. Bucar: Modulation of isoniazid susceptibility by flavonoids in *Mycobacterium*. *Phytochem Lett* 1(2), 71-75 (2008)

105. TBAlliance: Cycloserine. *Tuberculosis* 88(2), 100-101 (2008)

106. J. Simeon, M. Fink, T. M. Itil and D. Ponce: d-Cycloserine therapy of psychosis by symptom provocation. *Compr Psychiatry* 11(1), 80-88 (1970)

107. D. H. Kim, W. J. Lees, K. E. Kempsell, W. S. Lane, K. Duncan and C. T. Walsh: Characterization of a Cys115 to Asp substitution in the *Escherichia coli* cell wall biosynthetic enzyme UDP-GlcNAc enolpyruvyl transferase (MurA) that confers resistance to inactivation by the antibiotic fosfomycin. *Biochemistry* 35(15), 4923-4928 (1996)

108. M. Rieber, T. Imaeda and I. M. Cesari: Bacitracin action on membranes of mycobacteria. *J Gen Microbiol* 55(1), 155-159 (1969)

109. F. Drabløs, D. G. Nicholson and M. Rønning: EXAFS study of zinc coordination in bacitracin A. *Biochem Biophys Acta* 1431(2), 433-442 (1999)

110. S. Scheindlin: The fight against tuberculosis. *Mol Intervent* 6(3), 124-130 (2006)

111. P. Sensi: History development of rifampin. *Rev Infect Dis* 5(3), S402 (1983)

112. W. Wehrli and M. Staehelin: Actions of the rifamycins. *Bacteriol Rev* 35(3), 290-309 (1971)

113. E. A. Campbell, N. Korzheva, A. Mustaev, K. Murakami, S. Nair, A. Goldfarb and S. A. Darst: Structural mechanism for rifampicin inhibition of bacterial RNA polymerase. *Cell* 104(6), 901-912 (2001)

114. TBAlliance: Rifampin. *Tuberculosis* 88(2), 151-154 (2008)

115. D. L. Williams, L. Spring, L. Collins, L. P. Miller, L. B. Heifets, P. R. J. Gangadharam and T. P. Gillis: Contribution of rpoB mutations to development of rifamycin cross-resistance in *Mycobacterium tuberculosis*. *Antimicrob Agents Chemother* 42(7), 1853-1857 (1998)

116. E. B. Herr and M. O. Redstone: Chemical and physical characterization of capreomycin. *Ann N Y Acad Sci* 135, 940-946 (1966)

117. S. Nomoto, T. Teshima, T. Wakamiya and T. Shiba: The revised structure of capreomycin. *J Antibio* 30(11), 955-959 (1977)

118. TBAlliance: Capreomycin. *Tuberculosis*, 88(2), 89-91 (2008)

119. L. Heifets, J. Simon and V. Pham: Capreomycin is active against non-replicating *M. tuberculosis*. *Ann Clin Microbiol Antimicrob* 4(1), 6 (2005)

120. L. M. Fu and T. M. Shinnick: Genome-wide exploration of the drug action of capreomycin on *Mycobacterium tuberculosis* using Affymetrix oligonucleotide GeneChips. *J Infect* 54(3), 277-284 (2007)

121. C. E. Maus, B. B. Plikaytis and T. M. Shinnick: Mutation of tlyA confers capreomycin resistance in *Mycobacterium tuberculosis*. *Antimicrob Agents Chemother* 49(2), 571-577 (2005)

122. G. Di Perri and S. Bonora: Which agents should we use for the treatment of multidrug-resistant *Mycobacterium tuberculosis*? *J Antimicrob Chemother* 54(3), 593-602 (2004)

123. R. Provvedi, F. Boldrin, F. Falciani, G. Palu and R. Manganelli: Global transcriptional response to vancomycin in *Mycobacterium tuberculosis*. *Microbiology* 155(4), 1093-1102 (2009)

124. V. S. Malik: Plasmid and chloramphenicol production in *Streptomyces venezuelae*. *Biotechnol Lett* 2(10), 455-457 (1980)

125. L. Katz and G. W. Ashley: Translation and protein synthesis: Macrolides. *Chem Rev* 105(2), 499-528 (2005)

126. Z. Ma and P. A. Nemoto: Discovery and development of ketolides as a new generation of macrolide antimicrobial agents. *Curr Med Chem - Anti-Infect Agents* 1, 15-34 (2002)

127. Gasc, J.-C., D'ambrieres, S. G., Lutz, A., Chantot and J.-F.: New ether oxime derivatives of erythromycin A a structure-activity relationship study. *J Antibio* 44(3), 313-330 (1991)

128. TBAlliance: Clarithromycin. *Tuberculosis* 88(2), 92-95 (2008)

129. C. Truffot-Pernot, N. Lounis, J. Grosset and B. Ji: Clarithromycin is inactive against *Mycobacterium tuberculosis*. *Antimicrob Agents Chemother* 39(12), 2827-2828 (1995)

130. F. Portaels, H. Traore, K. De Ridder and W. M. Meyers: In vitro susceptibility of *Mycobacterium ulcerans* to clarithromycin. *Antimicrob Agents Chemother* 42(8), 2070-3 (1998)

131. K. Falzari, Z. Zhu, D. Pan, H. Liu, P. Hongmanee and S. G. Franzblau: In vitro and in vivo activities of macrolide derivatives against *Mycobacterium tuberculosis*. *Antimicrob Agents Chemother* 49(4), 1447-1454 (2005)

132. J. Z. Zhaohai, K. Olga, P. Dahua, P. Valentina, Y. Gengli, L. Yinghui, L. Huiwen, H. Saweon, W. Yuehong, W. Baojie, L. Wenzhong and G. F. Scott: Structure-activity relationships of macrolides against *Mycobacterium tuberculosis*. *Tuberculosis* 88, S49-S63 (2008)

133. T. Noto, S. Miyakawa, H. Oishi, H. Endo and H. Okazaki: Thiolactomycin, a new antibiotic. III. In vitro antibacterial activity. *J Antibio* 35(4), 401-410 (1982)

134. L. Kremer, J. D. Douglas, A. R. Baulard, C. Morehouse, M. R. Guy, D. Alland, L. G. Dover, J. H. Lakey, W. R. Jacobs, P. J. Brennan, D. E. Minnikin and G. S. Besra: Thiolactomycin and related analogues as novel antimycobacterial agents targeting KasA and KasB condensing enzymes in *Mycobacterium tuberculosis*. *J Biol Chem* 275(22), 16857-16864 (2000)

135. N. M. Parrish, F. P. Kuhajda, H. S. Heine, W. R. Bishai and J. D. Dick: Antimycobacterial activity of cerulenin and its effects on lipid biosynthesis. *J Antimicrob Chemother* 43(2), 219-226 (1999)

136. S. B. Singh, H. Jayasuriya, J. G. Ondeyka, K. B. Herath, C. Zhang, D. L. Zink, N. N. Tsou, R. G. Ball, A. Basilio, O. Genilloud, M. T. Diez, F. Vicente, F. Pelaez, K. Young and J. Wang: Isolation, structure, and absolute stereochemistry of platensimycin, a broad spectrum antibiotic discovered using an antisense differential sensitivity strategy. *J Am Chem Soc* 128(36), 11916-11920 (2006)

137. S. B. Singh, K. B. Herath, J. Wang, N. Tsou and R. G. Ball: Chemistry of platensimycin. *Tetrahedron Lett* 48(31), 5429-5433 (2007)

138. A. K. Brown, R. C. Taylor, A. Bhatt, K. Fütterer and G. S. Besra: Platensimycin activity against mycobacterial β-ketoacyl-ACP synthases. *PLoS ONE* 4(7), e6306 (2009)

139. G. F. Pauli, R. J. Case, T. Inui, Y. Wang, S. Cho, N. H. Fischer and S. G. Franzblau: New perspectives on natural products in TB drug research. *Life Sci* 78(5), 485-494 (2005)

140. I. Orme: Search for new drugs for treatment of tuberculosis. *Antimicrob Agents Chemother* 45(7), 1943-1946 (2001)

141. M. J. Hearn and M. H. Cynamon: Design and synthesis of antituberculars: preparation and evaluation against *Mycobacterium tuberculosis* of an isoniazid Schiff base. *J Antimicrob Chemother* 53(2), 185-191 (2004)

142. Cantrell, C. L., Franzblau, S. G., Fischer and N. H.: Antimycobacterial plant terpenoids. *Planta Med* 67(8), 685-694 (2001)

143. G. M. König, A. D. Wright and S. G. Franzblau: Assessment of antimycobacterial activity of a series of mainly marine derived natural products. *Planta Med* 66(04), 337-342 (2000)

144. N. Kishore, B. B. Mishra, V. Tripathi and V. K. Tiwari: Alkaloids as potential anti-tubercular agents. *Fitoterapia* 80(3), 149-163 (2009)

145. S. M. Newton, C. Lau and C. W. Wright: A review of antimycobacterial natural products. *Phytother Res* 14(5), 303-322 (2000)

146. B. R. Copp: Antimycobacterial natural products. *Nat Prod Rep* 20(6), 535-557 (2003)

147. B. R. Copp and A. N. Pearce: Natural product growth inhibitors of *Mycobacterium tuberculosis*. *Nat Prod Rep* 24(2), 278-297 (2007)

148. A. S. Negi, J. K. Kumar, S. Luqman, D. Saikia and S. P. S. Khanuja: Antitubercular potential of plants: A brief account of some important molecules. *Med Res Rev* 30(4), 603-645 (2010)

149. W. L. Beatty, E. R. Rhoades, H.-J. Ullrich, D. Chatterjee, J. E. Heuser and D. G. Russell: Trafficking and release of mycobacterial lipids from infected macrophages. *Traffic* 1(3), 235-247 (2000)

150. D. G. Russell, H. C. Mwandumba and E. E. Rhoades: *Mycobacterium* and the coat of many lipids. *J Cell Biol* 158(3), 421-426 (2002)

151. M.-J. Kim, H. C. Wainwright, M. Locketz, L.-G. Bekker, G. B. Walther, C. Dittrich, A. Visser, W. Wang, F.-F. Hsu, U. Wiehart, L. Tsenova, G. Kaplan and D. G. Russell: Caseation of human tuberculosis granulomas correlates with elevated host lipid metabolism. *EMBO Mol Med* 2(7), 258-274 (2010)

152. S. T. Cole, R. Brosch, J. Parkhill, T. Garnier, C. Churcher, D. Harris, S. V. Gordon, K. Eiglmeier, S. Gas, C. E. Barry, F. Tekaia, K. Badcock, D. Basham, D. Brown, T. Chillingworth, R. Connor, R. Davies, K. Devlin, T. Feltwell, S. Gentles, N. Hamlin, S. Holroyd, T. Hornsby, K. Jagels, A. Krogh, J. McLean, S. Moule, L. Murphy, K. Oliver, J. Osborne, M. A. Quail, M. A. Rajandream, J. Rogers, S. Rutter, K. Seeger, J. Skelton, R. Squares, S. Squares, J. E. Sulston, K. Taylor, S. Whitehead and B. G. Barrell: Deciphering the biology of *Mycobacterium tuberculosis* from the complete genome sequence. *Nature* 393(6685), 537-544 (1998)

153. K. Minami: Bactericidal action of oleic acid for tubercle bacilli: I. quantitative and analytical survey of the action. *J Bacteriol* 73(3), 338-344 (1957)

154. T. H. Sattler and G. P. Youmans: The effect of "Tween 80," bovine albumin, glycerol, and glucose on the growth of *Mycobacterium tuberculosis* var. hominis (H37Rv). *J Bacteriol* 56(2), 235-43 (1948)

155. E. Kondo and K. Kanai: The relationship between the chemical structure of fatty acids and their mycobactericidal activity. *Jpn J Med Sci Biol* 30(4), 171-178 (1977)

156. H. Saito, H. Tomioka and T. Yoneyama: Growth of group IV mycobacteria on medium containing various saturated and unsaturated fatty acids. *Antimicrob Agents Chemother* 26(2), 164-169 (1984)

157. G. R. Hemsworth and I. Kochan: Secretion of antimycobacterial fatty acids by normal and activated macrophages. *Infect Immun* 19(1), 170-177 (1978)

158. H. Saito and H. Tomioka: Susceptibilities of transparent, opaque, and rough colonial variants of *Mycobacterium avium* complex to various fatty acids. *Antimicrob Agents Chemother* 32(3), 400-402 (1988)

159. L. A. Sechi, I. Lezcano, N. Nunez, M. Espim, Dupr, I., A. Pinna, P. Molicotti, G. Fadda and S. Zanetti: Antibacterial activity of ozonized sunflower oil (Oleozon). *J Appl Microbiol* 90, 279-284 (2001)

160. N. M. Carballeira and M. Pagán: New methoxylated fatty acids from the Caribbean sponge *Callyspongia fallax*. *Journal of Natural Products*, 64(5), 620-623 (2001)

161. N. Carballeira, H. Cruz, C. Kwong, B. Wan and S. Franzblau: 2-Methoxylated fatty acids in marine sponges: Defense mechanism against mycobacteria? *Lipids* 39(7), 675-680 (2004)

162. N. M. Carballeira: New advances in fatty acids as antimalarial, antimycobacterial and antifungal agents. *Prog Lipid Res* 47(1), 50-61 (2008)

163. H. R. Morbidoni, C. Vilchèze, L. Kremer, R. Bittman, J. C. Sacchettini and W. R. Jacobs: Dual inhibition of mycobacterial fatty acid biosynthesis and degradation by 2-alkynoic acids. *Chem Biol* 13(3), 297-307 (2006)

164. C. Li, D. Lee, T. N. Graf, S. S. Phifer, Y. Nakanishi, S. Riswan, F. M. Setyowati, A. M. Saribi, D. D. Soejarto, N. R. Farnsworth, I. I. I. J. O. Falkinham, D. J. Kroll, A. D. Kinghorn, M. C. Wani and N. H. Oberlies: Bioactive constituents of the stem bark of *Mitrephora glabra*. *J Nat Prod* 72(11), 1949-1953 (2009)

165. M. Herrmann, B. Böhlendorf, H. Irschik, H. Reichenbach and G. Höfle: Maracin and maracen: New types of ethynyl vinyl ether and α-chloro divinyl ether antibiotics from *Sorangium cellulosum* with specific activity against mycobacteria. *Angew Chem Int Ed* 37(9), 1253-1255 (1998)

166. C. Ma, R. J. Case, Y. Wang, H.-J. Zhang, G. T. Tan, N. Van Hung, N. M. Cuong, S. G. Franzblau, D. D. Soejarto, H. H. S. Fong and G. F. Pauli: Anti-tuberculosis constituents from the stem bark of *Micromelum hirsutum*. *Planta Med* 71(03), 261-267 (2005)

167. H. Yuan, R. He, B. Wan, Y. Wang, G. F. Pauli, S. G. Franzblau and A. P. Kozikowski: Modification of the side chain of micromolide, an anti-tuberculosis natural product. *Bioorg Med Chem Lett* 18(19), 5311-5315 (2008)

168. C. L. Cantrell, T. Lu, F. R. Fronczek, N. H. Fischer, L. B. Adams and S. G. Franzblau: Antimycobacterial cycloartanes from *Borrichia frutescens*. *J Nat Prod* 59(12), 1131-1136 (1996)

169. C. L. Cantrell, M. S. Rajab, S. G. Franzblau and N. H. Fischer: Antimycobacterial triterpenes from *Melia volkensii*. *J Nat Prod* 62(4), 546-548 (1999)

170. C. L. Cantrell, M. S. Rajab, S. G. Franzblau, F. R. Fronczek and N. H. Fischer: Antimycobacterial ergosterol-5,8-endoperoxide from *Ajuga remota*. *Planta Med* 65(08), 732-734 (1999)

171. X. Wei, A. D. Rodríguez, Y. Wang and S. G. Franzblau: Novel ring B abeo-sterols as growth inhibitors of *Mycobacterium tuberculosis* isolated from a Caribbean Sea sponge, *Svenzea zeai*. *Tetrahedron Lett* 48(50), 8851-8854 (2007)

172. T. Akihisa, S. G. Franzblau, M. Ukiya, H. Okuda, F. Zhang, K. Yasukawa, T. Suzuki and Y. Kimura: Antitubercular activity of triterpenoids from *Asteraceae* flowers. *Biol Pharm Bull* 28(1), 158-160 (2005)

173. G. A. Wächter, S. G. Franzblau, G. Montenegro, J. J. Hoffmann, W. M. Maiese and B. N. Timmermann: Inhibition of *Mycobacterium tuberculosis* growth by saringosterol from *Lessonia nigrescens*. *J Nat Prod* 64(11), 1463-1464 (2001)

174. M.-T. Gutierrez-Lugo, Y. Wang, S. G. Franzblau, E. Suarez and B. N. Timmermann: Antitubercular sterols from *Thalia multiflora* Horkel ex Koernicke. *Phytother Res* 19(10), 876-880 (2005)

175. R. Rojas, L. Caviedes, J. C. Aponte, A. J. Vaisberg, W. H. Lewis, G. Lamas, C. Sarasara, R. H. Gilman and G. B. Hammond: Aegicerin, the first oleanane triterpene with wide-ranging antimycobacterial activity, isolated from *Clavija procera*. *J Nat Prod* 69(5), 845-846 (2006)

176. G. M. Woldemichael, S. G. Franzblau, F. Zhang, Y. Wang and B. N. Timmermann: Inhibitory effect of sterols from *Ruprechtia triflora* and diterpenes from *Calceolaria pinnifolia* on the growth of *Mycobacterium tuberculosis*. *Planta Med* 69(07), 628-631 (2003)

177. A. M. Janssen, J. J. C. Scheffer and A. B. Svendsen: Antimicrobial activities of essential oils. *Pharm World Sci* 9(4), 193-197 (1987)

178. A. Woolf: Essential oil poisoning. *Clin Toxicol* 37(6), 721-727 (1999)

179. R. Singh, O. Koul, P. J. Rup and J. Jindal: Toxicity of some essential oil constituents and their binary mixtures against Chilo partellus (Lepidoptera: Pyralidae). *Int J Trop Insect Sci* 29(02), 93-101 (2009)

180. J. G. Bueno-Sanchez, J. R. Martínez-Morales, E. E. Stashenko and W. Ribon: Anti-tubercular activity of eleven aromatic and medicinal plants occurring in Colombia. *Biomédica* 29, 51-60 (2009)

181. N. H. Fischer, T. Lu, C. L. Cantrell, J. Castaneda-Acosta, L. Quijano and S. G. Franzblau: Antimycobacterial evaluation of germacranolides *Phytochemistry*,49(2), 559-564 (1998)

182. T. S. Tiuman, T. Ueda-Nakamura, D. A. Garcia Cortez, B. P. Dias Filho, J. A. Morgado-Diaz, W. de Souza and C. V. Nakamura: Antileishmanial activity of parthenolide, a sesquiterpene lactone isolated from *Tanacetum parthenium*. *Antimicrob Agents Chemother* 49(1), 176-182 (2005)

183. C. L. Cantrell, I. S. Nuñez, J. Castañeda-Acosta, M. Foroozesh, F. R. Fronczek, N. H. Fischer and S. G. Franzblau: Antimycobacterial activities of dehydrocostus lactone and its oxidation products. *J Nat Prod* 61(10), 1181-1186 (1998)

184. C.-M. Sun, W. Syu, Jr., M.-J. Don, J.-J. Lu and G.-H. Lee: Cytotoxic sesquiterpene lactones from the root of *Saussurea lappa*. *J Nat Prod* 66(9), 1175-1180 (2003)

185. V. E. Madikane, S. Bhakta, A. J. Russell, W. E. Campbell, T. D. W. Claridge, B. G. Elisha, S. G. Davies, P. Smith and E. Sim: Inhibition of mycobacterial arylamine N-acetyltransferase contributes to antimycobacterial activity of *Warburgia salutaris*. *Bioorg Med Chem* 15(10), 3579-3586 (2007)

186. A. Ulubelen, G. Topcu and C. B. Johansson: Norditerpenoids and diterpenoids from *Salvia multicaulis* with antituberculous activity. *J Nat Prod* 60(12), 1275-1280 (1997)

187. G. Topçu, R. Erenler, O. Çakmak, C. B. Johansson, C. Çelik, H.-B. Chai and J. M. Pezzuto: Diterpenes from the berries of *Juniperus excelsa*. *Phytochemistry* 50(7), 1195-1199 (1999)

188. K. Dimas, M. Papadaki, C. Tsimplouli, S. Hatziantoniou, K. Alevizopoulos, P. Pantazis and C. Demetzos: Labd-14-ene-8,13-diol (sclareol) induces cell cycle arrest and apoptosis in human breast cancer cells and enhances the activity of anticancer drugs. *Biomed Pharmacother* 60(3), 127-133 (2006)

189. L. J. McGaw, N. Lall, T. M. Hlokwe, A. L. Michel, J. J. M. Meyer and J. N. Eloff: Purified compounds and extracts from *Euclea* species with antimycobacterial activity against *Mycobacterium bovis* and fast-growing mycobacteria. *Biol Pharm Bull* 31(7), 1429-1433 (2008)

190. J. L. d. Silva, A. R. Mesquita and E. A. Ximenes: In vitro synergic effect of γ-lapachone and isoniazid on the growth of *Mycobacterium fortuitum* and *Mycobacterium smegmatis*. *Mem Inst Oswaldo Cruz* 104, 580-582 (2009)

191. V. Kuete, J. G. Tangmouo, J. J. Marion Meyer and N. Lall: Diospyrone, crassiflorone and plumbagin: three antimycobacterial and antigonorrhoeal naphthoquinones from two *Diospyros* spp. *Int J Antimicrob Agents* 34(4), 322-325 (2009)

192. A. Mahapatra, S. P. N. Mativandlela, B. Binneman, P. B. Fourie, C. J. Hamilton, J. J. M. Meyer, F. van der Kooy, P. Houghton and N. Lall: Activity of 7-methyljuglone derivatives against *Mycobacterium tuberculosis* and as subversive substrates for mycothiol disulfide reductase. *Bioorg Med Chem* 15(24), 7638-7646 (2007)

193. D. Sareen, G. L. Newton, R. C. Fahey and N. A. Buchmeier: Mycothiol is essential for growth of *Mycobacterium tuberculosis* Erdman. *J Bacteriol* 185(22), 6736-6740 (2003)

194. N. A. Buchmeier, G. L. Newton and R. C. Fahey: A mycothiol synthase mutant of *Mycobacterium tuberculosis* has an altered thiol-disulfide content and limited tolerance to stress. *J Bacteriol* 188(17), 6245-6252 (2006)

195. M. Rawat and Y. Av-Gay: Mycothiol-dependent proteins in actinomycetes. *FEMS Microbiol Rev* 31, 278-292 (2007)

196. R. Mathew, A. K. Kruthiventi, J. V. Prasad, S. P. Kumar, G. Srinu and D. Chatterji: Inhibition of mycobacterial growth by plumbagin derivatives. *Chem Biol Drug Des* 76(1), 34-42 (2010)

197. S. B. Ferreira, F. d. C. d. Silva, F. A. F. M. Bezerra, M. C. S. Lourenço, C. R. Kaiser, A. C. Pinto and V. F.
207. A. Schinkovitz, S. Gibbons, M. Stavri, M. J. Cocksedge and F. Bucar: Ostruthin: An antimycobacterial coumarin from the roots of *Peucedanum ostruthium*. *Planta Med* 69(04), 369-371 (2003)

208. J. I. Kobayash, J.-F. Cheng, H. Nakamura, Y. Ohizumi, Y. Hirata, T. Sasaki, T. Ohta and S. Nozoe: Ascididemin, a novel pentacyclic aromatic alkaloid with potent antileukemic activity from the okinawan tunicate sp. *Tetrahedron Lett* 29(10), 1177-1180 (1988)

Ferreira: Synthesis of α- and β-pyran naphthoquinones as a new class of antitubercular agents. *Arch Pharm* 343(2), 81-90 (2010)

198. P. Rijo, M. F. Simões, A. P. Francisco, R. Rojas, Robert H. Gilman, Abraham J. Vaisberg, B. Rodríguez and C. Moiteiro: Antimycobacterial metabolites from *Plectranthus*: royleanone derivatives against *Mycobacterium tuberculosis* strains. *Chem Biodivers* 7(4), 922-932 (2010)

199. W.-Y. Lin, C.-F. Peng, I.-L. Tsai, J.-J. Chen, M.-J. Cheng and I.-S. Chen: Antitubercular constituents from the roots of *Engelhardia roxburghiana*. *Planta Med* 71(02), 171-175 (2005)

200. C.-C. Wu, C.-F. Peng, I.-L. Tsai, M. H. Abd El-Razek, H.-S. Huang and I.-S. Chen: Secondary metabolites from the roots of *Engelhardia roxburghiana* and their antitubercular activities. *Phytochemistry* 68(9), 1338-1343 (2007)

201. A. M. Galal: Antimicrobial activity of 6-paradol and related compounds. *Pharm Biol* 34(1), 64-69 (1996)

202. S. M. Newton, C. Lau, S. S. Gurcha, G. S. Besra and C. W. Wright: The evaluation of forty-three plant species for in vitro antimycobacterial activities; isolation of active constituents from *Psoralea corylifolia* and *Sanguinaria canadensis*. *J Ethnopharm* 79(1), 57-67 (2002)

203. C.-Z. Wu, S. S. Hong, X. F. Cai, N. T. Dat, J.-X. Nan, B. Y. Hwang, J. J. Lee and D. Lee: Hypoxia-inducible factor-1 and nuclear factor-[kappa]B inhibitory meroterpene analogues of bakuchiol, a constituent of the seeds of *Psoralea corylifolia*. *Bioorg Med Chem Lett* 18(8), 2619-2623 (2008)

204. H. Jayasuriya, A. M. Clark and J. D. McChesney: New antimicrobial filicinic acid derivatives from *Hypericum drummondii*. *J Nat Prod* 54(5), 1314-1320 (1991)

205. H. Jayasuriya, J. D. McChesney, S. M. Swanson and J. M. Pezzuto: Antimicrobial and cytotoxic activity of rottlerin-type compounds from *Hypericum drummondii*. *J Nat Prod* 52(2), 325-331 (1989)

206. P. Seephonkai, M. Isaka, P. Kittakoop, P. Palittapongarnpim, S. Kamchonwongpaisan, M. Tanticharoen and Y. Thebtaranonth: Evaluation of antimycobacterial, antiplasmodial and cytotoxic activities of preussomerins isolated from the lichenicolous fungus *Microsphaeropsis* sp. BCC 3050. *Planta Med* 68(01), 45-48 (2002)
209. B. R. Copp, H. C. Christiansen, B. S. Lindsay and S. G. Franzblau: Identification of heteroarylenamines as a new class of antituberculosis lead molecules. *Bioorg Med Chem Lett* 15(18), 4097-4099 (2005)

210. H. I. M. Boshoff, T. G. Myers, B. R. Copp, M. R. McNeil, M. A. Wilson and C. E. Barry: The transcriptional responses of *Mycobacterium tuberculosis* to inhibitors of metabolism. *J Biol Chem* 279(38), 40174-40184 (2004)

211. J. U. M. Rao, G. S. Giri, T. Hanumaiah and K. V. J. Rao: Sampangine, a new alkaloid from *Cananga odorata*. *J Nat Prod* 49(2), 346-347 (1986)

212. K. Y. Orabi: Microbial models of mammalian metabolism. Sampangines. *Stud Nat Prod Chem* 23, 3-49 (2000)

213. I. Muhammad, D. C. Dunbar, S. Takamatsu, L. A. Walker and A. M. Clark: Antimalarial, cytotoxic, and antifungal alkaloids from *Duguetia hadrantha*. *J Nat Prod* 64(5), 559-562 (2001)

214. M. Adams, A. A. Wube, F. Bucar, R. Bauer, O. Kunert and E. Haslinger: Quinolone alkaloids from *Evodia rutaecarpa*: a potent new group of antimycobacterial compounds. *Int J Antimicrob Agents* 26(3), 262-264 (2005)

215. J. D. Guzman, A. Gupta, D. Evangelopoulos, C. Basavannacharya, L. C. Pabon, E. A. Plazas, D. R. Muñoz, W. A. Delgado, L. E. Cuca, W. Ribon, S. Gibbons and S. Bhakta: Anti-tubercular screening of natural products from Colombian plants: 3-methoxynordomesticine, an inhibitor of MurE ligase of *Mycobacterium tuberculosis*. *J Antimicrob Chemother* 65(10), 2101-2107 (2010)

216. M. Isaka, N. Rugseree, P. Maithip, P. Kongsaeree, S. Prabpai and Y. Thebtaranonth: Hirsutellones A-E, antimycobacterial alkaloids from the insect pathogenic fungus *Hirsutella nivea* BCC 2594. *Tetrahedron* 61(23), 5577-5583 (2005)

217. K. V. Rao, N. Kasanah, S. Wahyuono, B. L. Tekwani, R. F. Schinazi and M. T. Hamann: Three new manzamine alkaloids from a common Indonesian sponge and their activity against infectious and tropical parasitic diseases. *J Nat Prod* 67(8), 1314-1318 (2004)

Key Words: Antimycobacterials, TB, natural products, antibiotics, MIC, SI, Review

Send correspondence to: Sanjib Bhakta, Department of Biological Sciences, Birkbeck College, Malet Street, London. WC1E 7HX., UK, Tel: 4402076316355, Fax: 4402076316246, E-mail: s.bhakta@bbk.ac.uk

J Antimicrob Chemother 2011; **66**: 1766–1772
doi:10.1093/jac/dkr203 Advance Access publication 28 May 2011

Journal of Antimicrobial Chemotherapy

Interaction of *N*-methyl-2-alkenyl-4-quinolones with ATP-dependent MurE ligase of *Mycobacterium tuberculosis*: antibacterial activity, molecular docking and inhibition kinetics

Juan David Guzman[1,2], Abraham Wube[3], Dimitrios Evangelopoulos[1,4], Antima Gupta[1], Antje Hüfner[5], Chandrakala Basavannacharya[1], Md. Mukhleshur Rahman[2], Christina Thomaschitz[3], Rudolf Bauer[3], Timothy Daniel McHugh[4], Irene Nobeli[1], Jose M. Prieto[2], Simon Gibbons[2], Franz Bucar[3]† and Sanjib Bhakta[1]*†

[1]*Department of Biological Sciences, Institute of Structural and Molecular Biology, Birkbeck College, University of London, Malet Street, London WC1E 7HX, UK;* [2]*Department of Pharmaceutical and Biological Chemistry, The School of Pharmacy, University of London, 29–39 Brunswick Square, London WC1N 1AX, UK;* [3]*Department of Pharmacognosy, Institute of Pharmaceutical Sciences, Karl Franzens University Graz, Universitätsplatz 4, A-8010 Graz, Austria;* [4]*Department of Medical Microbiology, Royal Free Hospital, University College London, Rowland Hill Street, London NW3 2PF, UK;* [5]*Department of Pharmaceutical Chemistry, Institute of Pharmaceutical Sciences, Karl Franzens University Graz, Universitätsplatz 1, A-8010 Graz, Austria*

*Corresponding author. Tel: +44-20-7631-6355/+44-20-7079-0799; Fax: +44-20-7631-6246; E-mail: s.bhakta@bbk.ac.uk
†These authors made an equal contribution to the study.

Received 7 February 2011; returned 18 March 2011; revised 18 April 2011; accepted 27 April 2011

Objectives: The aim of this study was to comprehensively evaluate the antibacterial activity and MurE inhibition of a set of *N*-methyl-2-alkenyl-4-quinolones found to inhibit the growth of fast-growing mycobacteria.

Methods: Using the spot culture growth inhibition assay, MICs were determined for *Mycobacterium tuberculosis* H_{37}Rv, *Mycobacterium bovis* BCG and *Mycobacterium smegmatis* mc^2155. MICs were determined for *Mycobacterium fortuitum*, *Mycobacterium phlei*, methicillin-resistant *Staphylococcus aureus*, *Escherichia coli* and *Pseudomonas aeruginosa* using microplate dilution assays. Inhibition of *M. tuberculosis* MurE ligase activity was determined both by colorimetric and HPLC methods. Computational modelling and binding prediction of the quinolones in the MurE structure was performed using Glide. Kinetic experiments were conducted for understanding possible competitive relations of the quinolones with the endogenous substrates of MurE ligase.

Results: The novel synthetic *N*-methyl-2-alkenyl-4-quinolones were found to be growth inhibitors of *M. tuberculosis* and rapid-growing mycobacteria as well as methicillin-resistant *S. aureus*, while showing no inhibition for *E. coli* and *P. aeruginosa*. The quinolones were found to be inhibitory to MurE ligase of *M. tuberculosis* in the micromolar range (IC_{50} ~40–200 μM) when assayed either spectroscopically or by HPLC. Computational docking of the quinolones on the published *M. tuberculosis* MurE crystal structure suggested that the uracil recognition site is a probable binding site for the quinolones.

Conclusions: *N*-methyl-2-alkenyl-4-quinolones are inhibitors of mycobacterial and staphylococcal growth, and show MurE ligase inhibition. Therefore, they are considered as a starting point for the development of increased affinity MurE activity disruptors.

Keywords: 4-quinolones, Mur ligase inhibitors, *M. tuberculosis*

Introduction

Tuberculosis (TB) is a contagious disease caused by infection with species belonging to the *Mycobacterium tuberculosis* complex.[1] This slow-growing acid-fast bacterium exerts a tremendous impact on current global health.[2] *Staphylococcus aureus* is also a major concern, as this pathogen is the most common cause of bacterial infection worldwide[3] and methicillin-resistant *S. aureus* (MRSA) strains remain difficult to treat,[4] despite the approval of agents such as linezolid, quinupristin/dalfopristin and daptomycin over the last decade. Infection with drug-resistant *M. tuberculosis* strains is extremely serious, prolonging

treatment time, decreasing the probability of cure and increasing the cost of treatment.[5] The current anti-TB chemotherapy must be administered for 6 months for drug-susceptible strains and for ≥2 years for multidrug-resistant (MDR) or extensively drug-resistant (XDR) infections. Outbreaks of drug-resistant pathogens are more and more frequent everywhere, and it would be catastrophic if these pathogens develop total drug resistance.[6,7] Novel chemical entities are therefore required for treating drug-resistant strains. They must be potent enough to reduce the length of treatment and to prevent the emergence of resistance, but they must also be safer than second-line drugs and not interfere with antiretroviral therapy.[8] Screening for novel mechanisms of action seems a reasonable strategy to develop inhibitors against MDR, XDR and totally drug-resistant strains of *M. tuberculosis*, as the resulting compounds may have a disrupting effect on pathways or enzymes that have never been targeted before.

Natural products are a primordial source of bioactive chemical scaffolds that have been therapeutically exploited for a large number of diseases.[9] Plants and microorganisms have developed many successful secondary metabolites for protection against microbial infection. Antibiotics are, by definition, produced by microorganisms[10] and are one of the most valuable antimicrobial classes, as they gained bacteria-killing competence by targeting essential biochemical pathways through centuries of microbial evolution. β-Lactams, glycopeptides, bacitracin, fosfomycin and cycloserine are all antibiotics targeting the peptidoglycan biosynthetic pathway.[11] Peptidoglycan is an essential bacterial cell wall polymer that is responsible for cell shape and serves as containment for cytoplasmic pressure. Because it is a well-validated pathway, there is growing interest in developing small molecule inhibitors that target novel proteins of this biosynthetic route.[12] Mycobacterial peptidoglycan is the sustaining mesh that supports the mycolyl-arabinogalactan complex and is therefore considered an indispensable building block.[13] Mur ligases are cytoplasmic enzymes that perform the biosynthesis of uridine-diphosphate-*N*-acetylmuramyl-L-Ala-D-Glu-*m*-DAP-D-Ala-D-Ala (UDP-MurNAc-pentapeptide) from uridine-diphosphate-*N*-acetylglucosamine (UDP-NAcGlc).[14] ATP-dependent Mur ligases C, D, E and F are able to sequentially add the amino acids forming the pentapeptide chain, and have been shown to act by a similar mechanism to folylpolyglutamate synthetase.[15] The MurE ligase of *M. tuberculosis* preferentially adds *meso*-diaminopimelic acid (*m*-DAP) to the γ-carboxyl group of glutamic acid in UDP-MurNAc-L-Ala-D-Glu.[16,17] Natural product inhibitors have been already reported by us[18] and increasing efforts are being made to develop specific inhibitors of this enzyme.

The approach used in this work was to comprehensively evaluate the bioactivity of five synthetic evocarpine-related quinolones. The compounds belonging to this class have been shown to be effective inhibitors of rapid-growing *Mycobacterium* species.[19] *N*-methyl-2-alkenyl-4-quinolones were tested against slow- and rapid-growing mycobacterial species (*M. tuberculosis* H_{37}Rv, *Mycobacterium bovis* BCG, *Mycobacterium smegmatis*, *Mycobacterium fortuitum* and *Mycobacterium phlei*). The antibacterial activity was also recorded against two epidemic strains of commonly prevalent MRSA (EMRSA-15 and -16) and two Gram-negative bacteria and the cytotoxicity was evaluated against murine macrophages, in order to assess the specificity of the quinolones in whole cell experiments. In our in-house MurE screening programme of potential inhibitors, these quinolones were shown to inhibit *M. tuberculosis* MurE ligase activity when assayed colorimetrically. This finding was further confirmed by HPLC quantification of UDP-MurNAc-tripeptide, the product of the MurE reaction. The quinolones were computationally modelled and docked into the published *M. tuberculosis* MurE protein X-ray structure (PDB:2wtz) to propose a probable binding site. The docking results and the competition experiments of quinolone **2** with MurE ligands suggest that they bind to a specific hydrophobic pocket close to the uracil-binding site that could be exploited to generate a novel class of antimycobacterials.

Materials and methods

Reagents

Isoniazid, norfloxacin, kanamycin, resazurin, Tween 80, glycerol, *m*-DAP, ATP, bis-trispropane, magnesium chloride, Luria–Bertani broth, Mueller–Hinton broth, RPMI-1640, L-glutamine, heat-inactivated fetal calf serum, DMSO and ammonium formate were purchased from Sigma–Aldrich. Middlebrook 7H9, Middlebrook 7H10, and oleic acid, albumin, dextrose and catalase supplement (OADC) were obtained from BD Diagnostics. The MurE substrate UDP-MurNAc-L-Ala-D-Glu was purchased from the BaCWAN synthetic facility (University of Warwick, UK).

Synthesis of *N*-methyl-2-alkenyl-4-quinolones 1–5

The *N*-methyl-2-alkenyl-4-quinolones **1**–**5** were obtained using a synthetic route recently reported.[19] The quinolone alkaloids with a *cis*-unsaturated aliphatic side chain (**1** and **2**) were prepared by the reaction of *cis*-unsaturated methyl ketones with *N*-methyl isatoic acid anhydride in the presence of lithium diisopropylamide (LDA). *Trans*-α,β-unsaturated methyl ketones were used to prepare alkaloids **3**–**5** using the same type of condensation with *N*-methyl isatoic acid anhydride in the presence of LDA. The identity of the quinolone alkaloids and their corresponding intermediates was confirmed by analysis of 1D- and 2D-NMR spectroscopy and liquid chromatography–electrospray ionization–mass spectrometry data. Spectroscopic data of quinolones **1**–**5** are provided as Supplementary data at *JAC* Online.

Bacterial strains and cells

M. tuberculosis H_{37}Rv (ATCC 27294), *M. bovis* BCG (ATCC 35734), *M. smegmatis* mc^2155 (ATCC 700084), *M. fortuitum* (ATCC 6841), *M. phlei* (ATCC 11758), *Escherichia coli* JM109 (ATCC 53323), *Pseudomonas aeruginosa* (ATCC 25668) and murine RAW264.7 macrophages (ATCC TIB71) were used in this study. EMRSA-15 and -16 were gifts from Dr Paul Stapleton (School of Pharmacy, University of London, UK). Competent *E. coli* BL21(DE3)pLysS cells (New England Biolabs, UK) were used for overproducing MurE ligase of *M. tuberculosis* H_{37}Rv.

Drug susceptibility

The spot culture susceptibility assay for *M. tuberculosis* H_{37}Rv, *M. bovis* BCG and *M. smegmatis* mc^2155 species was performed as described previously.[20] Briefly, Middlebrook 7H9 mycobacterial cultures were serially diluted to 10^5 cfu/mL. A 5 μL aliquot of the diluted culture (~500 viable cells) was spotted onto 5 mL of solidified Middlebrook 7H10 agar medium, supplemented with 10% (v/v) OADC in a six-well plate containing various concentrations of compounds **1**–**5**. A negative control containing only DMSO was included in each plate. A six-well plate containing various concentrations of isoniazid was also used as a positive control. Following incubation at 37°C for 2 weeks for slow growers and 3 days for *M.*

smegmatis, the MIC was determined as the concentration at which there was no visible mycobacterial growth. Microdilution-based methods using Mueller–Hinton broth for *S. aureus*, and Luria–Bertani broth for *E. coli* and *P. aeruginosa* were employed for the MIC determination of the quinolones.[18] Kanamycin and norfloxacin were used as positive controls. Susceptibilities of *M. fortuitum* and *M. phlei* were assessed as reported previously[21] in a microdilution assay in cation-adjusted Mueller–Hinton broth using isoniazid as a positive control.

Cytotoxicity towards RAW264.7 macrophages

RAW264.7 macrophages (National Collection of Type Cultures) were maintained in RPMI-1640 medium supplemented with 2 mM L-glutamine and 10% heat-inactivated fetal calf serum, in a humidified incubator containing 5% CO_2, at 37°C, and passaged twice before the assay. The cell suspension was adjusted to 5×10^5 cells/mL and the assay was performed in 96-well cell culture flat-bottom plates (Costar 3596; VWR) in triplicate. Firstly, 2 μL of the 10 g/L stock solution of compounds **1**–**5** was added to 200 μL of RPMI-1640 medium in the first row and then 2-fold serially diluted. In each well, 100 μL of diluted macrophage cells was added. After 48 h of incubation, the monocytes were washed twice with PBS and fresh RPMI-1640 medium was added. The plates were then revealed with 30 μL of a freshly prepared and filter-sterilized aqueous 0.01% resazurin solution, and incubated overnight at 37°C. The following day, fluorescence was measured at 590 nm with excitation at 560 nm using a Fluostar Optima microplate reader (BMG LABTECH).

MurE ligase inhibition assay

The MurE protein of *M. tuberculosis* was overexpressed in *E. coli* BL21(DE3)pLysS and purified as previously reported.[17,18] The phosphate colorimetric detection method was performed for the preliminary screen of the small molecules. Additionally, *M. tuberculosis* MurE inhibition was assayed using HPLC analysis. A solution containing 25 mM bis-trispropane buffer (pH 8.5), 5 mM $MgCl_2$, 100 μM UDP-MurNAc-dipeptide, 250 μM ATP and 1 mM *m*-DAP was prepared in water as the enzyme–substrate mixture. Quinolones **1**–**5** were dissolved in DMSO at a concentration of 25, 8.3, 2.5, 0.83, 0.25 and 0.083 mM, and 2 μL was dispensed into 0.5 mL Eppendorfs. MurE enzyme was added to the enzyme–substrate mixture at a final concentration of ∼40 nM, and 48 μL of the mixture was rapidly added to each Eppendorf and incubated at 37°C for 30 min. The reaction was stopped by denaturing the protein at 100°C using a block heater for 10 min. The content was centrifuged for homogenization at 4000 rpm for 30 s and then transferred to 200 μL glass inserts (Supelco) fitted to HPLC vials that were analysed directly by HPLC (Agilent 1100 series) using an octadecylsilane RP-18 column (4.6 mm×250 mm×5 μm, Jones chromatography) eluting isocratically with a buffer of 50 mM ammonium formate (pH 4.0) and at a flow rate of 0.5 mL/min. The products of the reaction were detected at 268 nm and 220 nm simultaneously using a diode array detector system. A calibration curve was constructed for the tripeptide and confirmed a good linearity ($R^2=0.9978$) of the signal at 268 nm to the concentration of UDP-MurNAc-tripeptide. Activity controls at 0% (without enzyme) and 100% (with enzyme) were included.

Docking the MurE protein structure

The protein was prepared using the protein preparation wizard of the Maestro software (Schrödinger Software Suite 2009) from the PDB:2wtz file downloaded from the RCSB Protein Data Bank web site (http://pdb.org/pdb/explore/explore.do?structureId=2wtz). Chain B was selected and the peptide plane of Thr-298 was rotated to prevent overlapping with His-307. All of the residues were left charged as expected at a working pH of 8.5, except for Glu-198, which was set uncharged. The modified residue *N*6-carboxylysine-262 was appropriately recognized. The docking grid was built as a centroid of 30 Å, choosing the residues fundamental for the binding of the substrate according to the PDBsum LigPlot diagram,[22] such as Ala-69, Thr-85, Thr-86, Thr-195, Glu-198, Ser-222 and His-248. The ligands **1**–**5** were drawn using Chemdraw, converted into sdf format with BabelGUI and, lastly, were all processed using LigPrep at pH 8.5 ± 1.0. Docking was performed with Glide[23] using standard precision scoring and varying amide bond conformations.

Kinetic competition assays

Different concentrations of **2** (1000, 300, 100, 30 and 0 μM) were prepared separately with different concentrations of the MurE substrates: UDP-MurNAc-dipeptide (300, 100, 30, 10 and 3 μM); *m*-DAP (300, 100, 30, 10 and 3 μM); and ATP (300, 100, 30, 10 and 3 μM). The formation of the UDP-MurNAc-tripeptide product was followed by HPLC after 30 min of reaction. The conditions of the reaction and the analytical system were exactly the same as those described earlier for the HPLC inhibition assay. The experiments were performed in duplicate, and the total amount formed was calculated from the area under the peak (retention time ∼7 min) using the calibration curve and divided by the time (30 min) to obtain the velocity in μM/min.

Results

Bacterial growth inhibition and cytotoxicity

All of the synthesized *N*-methyl-2-alkenyl-4-quinolones (**1**–**5**) (Figure 1a) were significantly active in susceptibility testing on rapid-growing mycobacteria. They also showed growth inhibition of slow-growing mycobacteria (*M. tuberculosis* H_{37}Rv and *M. bovis* BCG), having an MIC value between 5 and 25 mg/L (Table 1). The quinolones were more active against rapid-growing species, showing an MIC value between 0.5 and 10 mg/L. The growth of the highly problematic EMRSA strains was also notably inhibited, revealing MIC values in the range of 0.5–4 mg/L. Moreover, the quinolones did not show any significant inhibition at 50 mg/L for *E. coli*, behaving similarly to the control, isoniazid. The MIC values of **1**–**5** for *E. coli* were >1000 mg/L and for *P. aeruginosa* they were >256 mg/L. These compounds were moderately cytotoxic towards macrophage RAW264.7 cells, having a 50% growth inhibition concentration (GIC_{50}) of between 24 and 112 mg/L (Table 1). The selectivity index (SI), defined as the GIC_{50} value divided by the MIC, varied between 1.0 and 5.6 for *M. tuberculosis*, but was much higher for *S. aureus* (SI: 9.75–112).

M. tuberculosis MurE ligase inhibition

MurE ligase activity in the presence of compounds was assayed by HPLC quantification of the product (UDP-MurNAc-L-Ala-D-Glu-*m*-DAP) formed after 30 min and by the phosphate colorimetric detection method. Clearly, all of quinolones **1**–**5** showed inhibition of MurE [Figures 1b and S1 (Figure S1 is available as Supplementary data at *JAC* Online)], displaying an IC_{50} value of 95–207 μM when determined by HPLC and of 36–72 μM when analysed by the phosphate detection colorimetric method (Table 1). Quinolone **2** was the most active MurE inhibitor, with an IC_{50} value of 95 μM, as can be inferred from the chromatograms at different concentrations of the inhibitor (Figure 1b). The difference between the MurE inhibition values determined

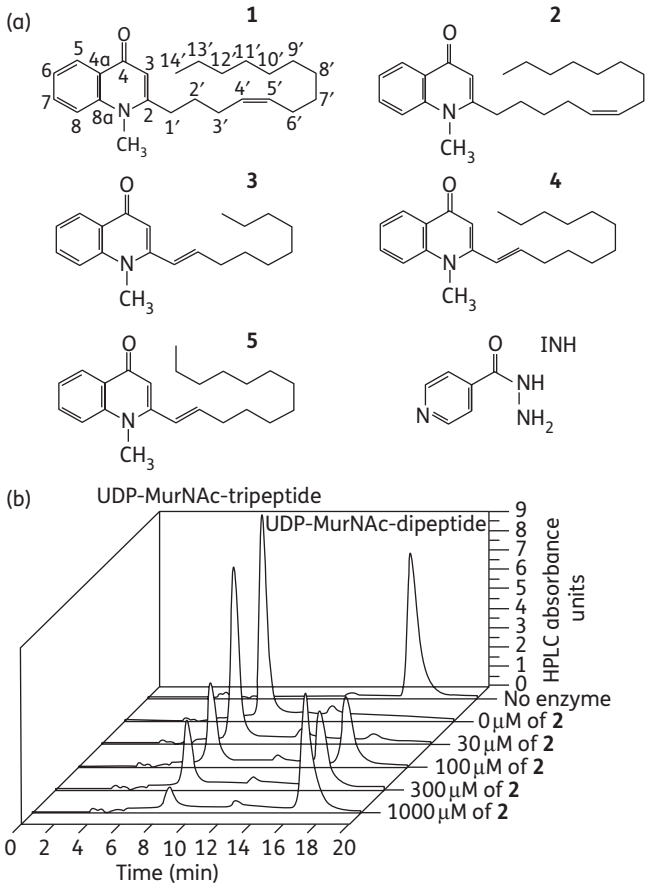

Figure 1. Structure of *N*-methyl-2-alkenyl-4-quinolones **1**–**5** and isoniazid (INH), and HPLC MurE inhibitory activity of quinolone **2**. (a) Chemical structure of the synthesized quinolones showing the modifications on the alkenyl chain. (b) HPLC chromatograms at 268 nm of the product (UDP-MurNAc-tripeptide) and the substrate (UDP-MurNAc-dipeptide) of the reaction catalysed by *M. tuberculosis* MurE in the presence of different concentrations of quinolone **2**.

by the phosphate and HPLC methods had a consistent value for all of the quinolones.

Docking of the quinolones in the MurE structure

The MurE substrate UDP-MurNAc-L-Ala-D-Glu used as a self-dock test[23] was effectively docked in the same orientation as the published MurE-substrate crystal structure (PDB:2wtz), displaying a GlideScore of −9.92 kcal/mol. The root mean square distance of the heavy atoms of the UDP-MurNAc-L-Ala-D-Glu substrate in the docked and crystal structures was 3.09 Å, indicating a good preparation of the protein and adequate docking parameters. Our results suggested that all of the quinolones interacted in a similar fashion to a pocket located near the uracil recognition site (Figure 2a) of the Rossmann fold in domain 1 of MurE.[14] According to the calculated hydrophilicity surface of the protein (Figure 2b), the quinolone was attracted to the lipophilic patches on the protein surface. The GlideScore for quinolones **1**–**5** was in the range of −2.46 to −4.51 kcal/mol, with quinolone **4** having the highest score in absolute value. This range indicated a rather weak binding, as can be observed in the orientations with a single hydrogen bond participating in the interaction (via the hydroxyl group of Thr-176 to the tertiary nitrogen atom of the quinolone in Figure 2c).

Kinetic competition between the quinolones and MurE substrates

The velocity of formation of the MurE product in the presence of quinolone **2** displayed a dependence on the concentration of the UDP-MurNAc-dipeptide substrate. At a high concentration of UDP-MurNAc-dipeptide (300 and 100 μM), the velocity decreased with an increase in the concentration of the quinolone (Figure 3a). For these two concentrations, the fitted lines converge to a point of intersection, therefore indicating competitive inhibition between the UDP-MurNAc-dipeptide and the quinolone.[24] However, at a low concentration of UDP-MurNAc-dipeptide (30, 10 and 3 μM), the velocity of MurE product formation was independent of the concentration of the quinolone. For the two other substrates, namely ATP (Figure 3b) and *m*-DAP (Figure 3c), the change in the velocity was less drastic when varying the concentration of the quinolone, and the curves had the same tendency without converging to a point of intersection, indicating uncompetitive inhibition.[24]

Discussion

Initially isolated as the active antimycobacterial entities from the fruits of the traditional Chinese medicinal tree *Evodia rutaecarpa* (Rutaceae),[25] the *N*-methyl-2-alkenyl-4-quinolone chemotype was further exploited by synthetic methods in order to explore chemical variation and improve activity.[19] A group of these chemical entities, which showed the highest activity on rapidly growing mycobacteria, were selected for a comprehensive biological evaluation. We found that these compounds were growth inhibitors of mycobacterial species and the highly problematic EMRSA strains, being also inhibitors of the MurE ligase of *M. tuberculosis*. The MIC indicated that these compounds are notable antibacterials, particularly against EMRSA-15 and -16, which are regularly encountered in UK hospitals.[26] The macrophage SI in relation to the H_{37}Rv strain for the quinolones was considerably low (SI < 10);[27] however, the SI in relation to EMRSA-15 and -16 was much higher (SI range 9.75–112), indicating a promising selectivity. Moreover, the compounds did not show inhibition of *E. coli* growth up to a high dose and they are probably innocuous to bacterial gut flora. It was also noted that the cytotoxicity was reduced when the linear alkenyl chain was extended, suggesting an interesting relation for differential selectivity.

The 4-quinolone nucleus is a specific class of compound that has attracted and continues to attract significant interest from the pharmaceutical industry, principally because of the impact of the fluoroquinolones, which inhibit both DNA gyrase and topoisomerase IV,[28] and the anticancer 2-phenyl-4-quinolones targeting tubulin.[29] In comparison to the fluoroquinolones, the compounds of the present study lack a carboxyl group at position C-3, which is considered to be essential for DNA gyrase inhibition,[30] and therefore a further mechanism of action must be assumed. Moreover, this class of chemicals may also be

Table 1. MICs for different species of bacteria, GIC_{50} and SI for macrophage cells and MurE IC_{50} of the synthetic quinolones **1**–**5**

	MIC in mg/L (μM)							Murine macrophages		*M. tuberculosis* MurE	
						S. aureus				IC_{50} (μM)	
Compound	*M. tuberculosis* $H_{37}Rv$	*M. bovis* BCG	*M. smegmatis* mc^2155	*M. fortuitum*	*M. phlei*	EMRSA-15	EMRSA-16	GIC_{50} (mg/L)	SI	phosphate-based method	HPLC method
1	25 (70.7)	10 (28.3)	10 (28.3)	0.5 (1.41)	0.5 (1.4)	1 (2.8)	0.5 (1.4)	24±9	1.0	52±22	159±6
2	10 (28.3)	10 (28.3)	10 (28.3)	1 (2.83)	1 (2.8)	1 (2.8)	0.5 (1.4)	39±12	3.9	36±16	95±9
3	25 (84.0)	25 (84.0)	5 (16.8)	2 (6.72)	1 (3.4)	4 (13.4)	2 (6.72)	39±11	1.6	70±25	207±6
4	10 (30.7)	5 (15.3)	5 (15.3)	1 (3.06)	0.5 (1.5)	2 (6.12)	2 (6.12)	40±7	4.0	72±23	187±8
5	20 (58.9)	10 (29.4)	10 (29.4)	1 (2.94)	1 (2.9)	2 (5.8)	1 (2.9)	112±10	5.6	52±20	140±5
Isoniazid	0.1 (0.73)	0.1 (0.73)	5 (18.5)	1 (3.65)	4 (15)	ND	ND	>500	>5000	>1000	>1000

ND, not determined.
The MIC of norfloxacin was 0.5 and 256 mg/L for EMRSA-15 and -16, respectively.
The SI was calculated by dividing the GIC_{50} by the MIC for *M. tuberculosis* $H_{37}Rv$.
IC_{50} and GIC_{50} values are shown ±SD.

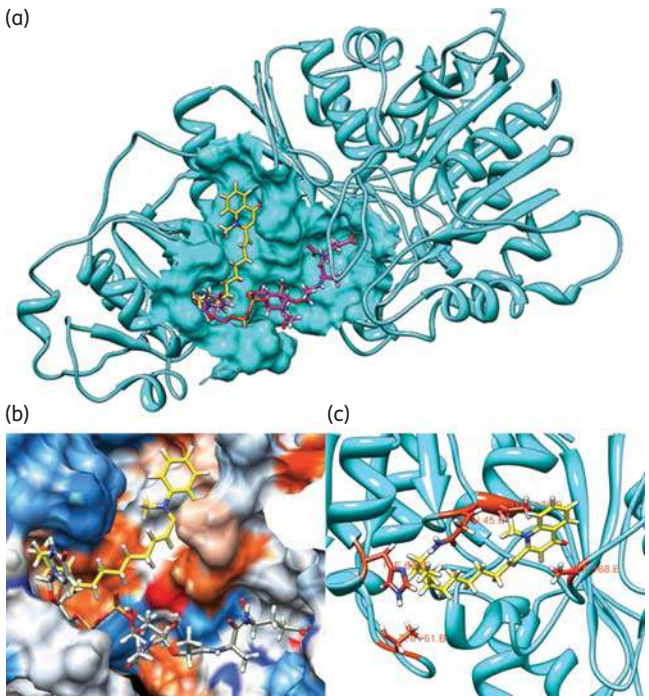

Figure 2. Lowest GlideScore docking pose of quinolone **4** interacting with MurE (PDB:2wtz) of *M. tuberculosis*.[17] (a) Presumed binding pocket of the quinolones (in yellow) near the uracil recognition site of UDP-MurNAc-dipeptide (in magenta). (b) Protein surface showing the high hydrophobicity (in red) of the quinolone binding pocket calculated using UCSF Chimera software.[34] (c) MurE residues that may interact with the quinolones: Thr-176, Ala-168, Gln-45, His-66 and Thr-61. This figure appears in colour in the online version of *JAC*, and in black and white in the print version of *JAC*.

exploited for the discovery and development of bacterial Mur ligase inhibitors. Using both colorimetric and HPLC methods, it was found that the compounds reproducibly inhibited *in vitro* the ligase activity of MurE from *M. tuberculosis*. Comparing **1** and **2**, a slight influence on MurE inhibition was observed for the position of the double bond in the alkenyl chain. Furthermore, the percentage of inhibition when determined using the phosphate colorimetric method was slightly higher than when compared with the HPLC method, probably because of a small decoupling between phosphatase and ligase activities.

For the computational prediction of the binding of potential ligands to a protein, it is advisable to use a 3D structural model of atomic resolution,[31] typically below 2 Å. However, in the absence of structures of MurE from *M. tuberculosis* below 2 Å resolution, we used the available published model at 3 Å as a preliminary basis for assessing probable binding sites. Interestingly, quinolones **1**–**5** were predicted to bind to a hydrophobic pocket located near the uridine recognition site in domain 1 of the enzyme. The GlideScore was low (∼−4 kcal/mol) in comparison with general reported values for inhibitors (∼−10 kcal/mol);[32] however, considering the weak interactions between the quinolones and the protein, it is not surprising to observe low GlideScore values. This also indicates that there is space for improvement in the search for chemical and steric complementarities, and the possibility of using this lipophilic cavity for rational drug design. We hypothesize that the aliphatic lipophilic chain of **1**–**5** interacts with the buried hydrophobic residues of MurE ligase, probably inducing a change in the conformation that prevents binding to UDP-MurNAc-dipeptide. In order to gain further evidence of this possibility, a kinetic competition experiment showed that at a low concentration of the dipeptide, the velocity of the reaction was unaltered by the concentration of the inhibitor. At low concentration of the dipeptide substrate, the majority of the enzyme was free and,

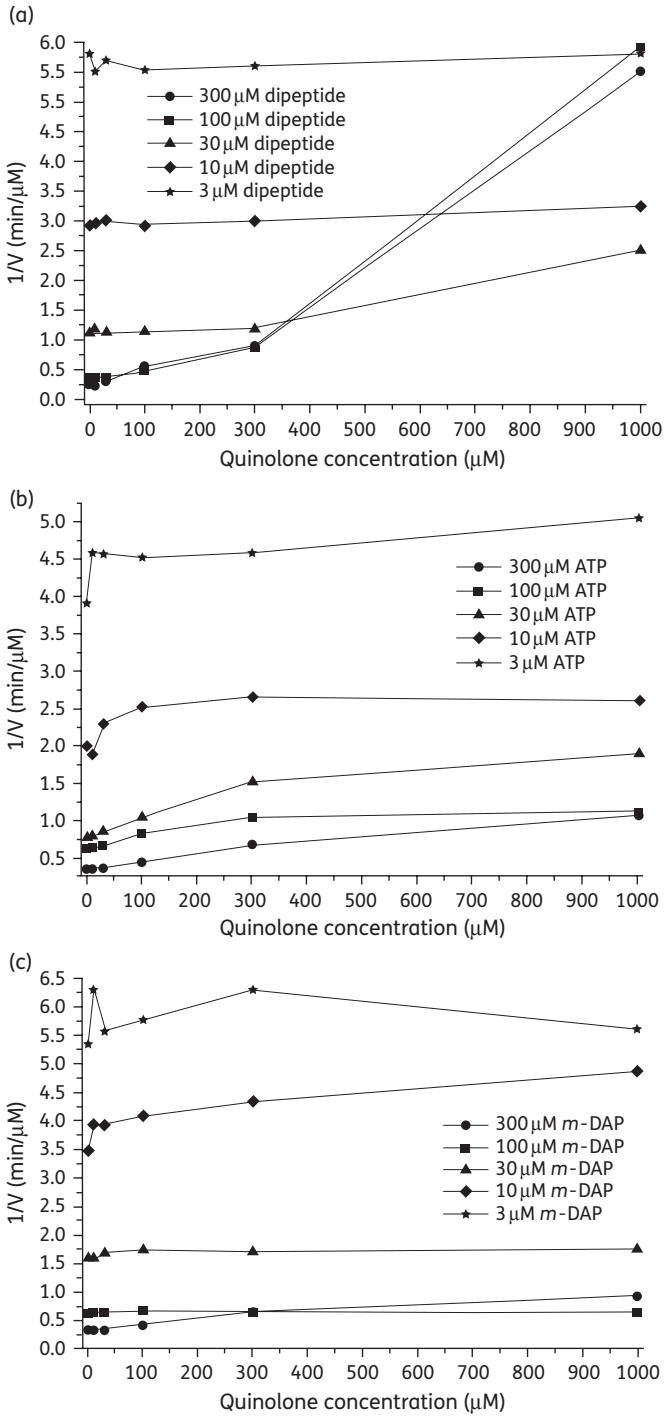

Figure 3. Dixon plots of the activity of the MurE enzyme assayed by HPLC. (a) Plot of the inverse of the velocity of UDP-MurNAc-tripeptide formation versus the concentration of quinolone **2**, for different concentrations of UDP-MurNAc-dipeptide. (b) Plot of the inverse of the velocity of UDP-MurNAc-tripeptide formation versus the concentration of quinolone **2**, for different concentrations of ATP. (c) Plot of the inverse of the velocity of UDP-MurNAc-tripeptide formation versus the concentration of quinolone **2**, for different concentrations of *m*-DAP.

therefore, according to our results, the conformation of the free MurE enzyme has low interaction with the quinolones. However, when the concentration of the dipeptide substrate was high, most of the enzyme formed the enzyme–substrate complex, which, in agreement with the induced-fit theory,[33] has a different protein conformation. Our results suggested that this induced-fit enzyme–substrate conformation of MurE interacted with the quinolones and when this conformation occurred, inhibition of ligase activity took place. This novel type of MurE inhibitor can be included as a starting point in virtual and fragment screening MurE projects that may help in the detection of structure–activity relationships. Structural modifications of a particularly interesting MurE inhibitor pharmacophore can potentially lead to potent and selective antibacterials in the near future.

Acknowledgements

We thank Dr Philip Lowden (Birkbeck College, London, UK) for support in the HPLC analysis.

Funding

This work was supported by the Medical Research Council, UK (grant G0801956) and the Austrian Science Fund (FWF): project P21152-B18. Colfuturo and Bloomsbury Colleges contributed towards J. D. G.'s research study.

Transparency declarations

None to declare.

Supplementary data

The spectroscopic data of the quinolones **1**–**5** and Figure S1 are available as Supplementary data at *JAC* Online (http://jac.oxfordjournals.org/).

References

1 Cole ST. Comparative and functional genomics of the *Mycobacterium tuberculosis* complex. *Microbiology* 2002; **148**: 2919–28.

2 WHO. *Global Tuberculosis Control, WHO Report*. Geneva: WHO, 2010.

3 DeLeo FR, Otto M, Kreiswirth BN *et al*. Community-associated meticillin-resistant *Staphylococcus aureus*. *Lancet* 2010; **375**: 1557–68.

4 Howden BP, Ward PB, Charles PGP *et al*. Treatment outcomes for serious infections caused by methicillin-resistant *Staphylococcus aureus* with reduced vancomycin susceptibility. *Clin Infect Dis* 2004; **38**: 521–8.

5 Ormerod LP. Multidrug-resistant tuberculosis (MDR-TB): epidemiology, prevention and treatment. *Br Med Bull* 2005; **73–4**: 17–24.

6 Walsh FM, Amyes SGB. Microbiology and drug resistance mechanisms of fully resistant pathogens. *Curr Opin Microbiol* 2004; **7**: 439–44.

7 Velayati AA, Farnia P, Masjedi MR *et al*. Totally drug-resistant tuberculosis strains: evidence of adaptation at the cellular level. *Eur Resp J* 2009; **34**: 1202–3.

8 Ginsberg AM, Spigelman M. Challenges in tuberculosis drug research and development. *Nat Med* 2007; **13**: 290–4.

9 Newman DJ, Cragg GM. Natural products as sources of new drugs over the last 25 years. *J Nat Prod* 2007; **70**: 461–77.

10 Waksman SA. What is an antibiotic or an antibiotic substance? *Mycologia* 1947; **39**: 565–9.

11 Silver LL. Does the cell wall of bacteria remain a viable source of targets for novel antibiotics? *Biochem Pharmacol* 2006; **71**: 996–1005.

12 Bugg TDH, Braddick D, Dowson CG *et al*. Bacterial cell wall assembly: still an attractive antibacterial target. *Trends Biotechnol* 2011; **29**: 167–73.

13 Hett EC, Rubin EJ. Bacterial growth and cell division: a mycobacterial perspective. *Microbiol Mol Biol Rev* 2008; **72**: 126–56.

14 Smith CA. Structure, function and dynamics in the mur family of bacterial cell wall ligases. *J Mol Biol* 2006; **362**: 640–55.

15 Bertrand JA, Fanchon E, Martin L *et al*. 'Open' structures of MurD: domain movements and structural similarities with folylpolyglutamate synthetase. *J Mol Biol* 2000; **301**: 1257–66.

16 Basavannacharya C, Moody P, Munshi T *et al*. Essential residues for the enzyme activity of ATP-dependent MurE ligase from *Mycobacterium tuberculosis*. *Protein Cell* 2010; **1**: 1011–22.

17 Basavannacharya C, Robertson G, Munshi T *et al*. ATP-dependent MurE ligase in *Mycobacterium tuberculosis*: biochemical and structural characterisation. *Tuberculosis* 2010; **90**: 16–24.

18 Guzman JD, Gupta A, Evangelopoulos D *et al*. Anti-tubercular screening of natural products from Colombian plants: 3-methoxynordomesticine, an inhibitor of MurE ligase of *Mycobacterium tuberculosis*. *J Antimicrob Chemother* 2010; **65**: 2101–7.

19 Wube AA, Hüfner A, Thomaschitz C *et al*. Design, synthesis and antimycobacterial activities of 1-methyl-2-alkenyl-4(1H)-quinolones. *Bioorg Med Chem* 2011; **19**: 567–79.

20 Evangelopoulos D, Bhakta S. Rapid methods for testing inhibitors of mycobacterial growth. In: *Antibiotic Resistance Protocols, Methods in Molecular Biology*. New York: Humana Press, 2010; 279.

21 Schinkovitz A, Gibbons S, Stavri M *et al*. Ostruthin: an antimycobacterial coumarin from the roots of *Peucedanum ostruthium*. *Planta Med* 2003; **69**: 369–71.

22 Wallace AC, Laskowski RA, Thornton JM. LIGPLOT: a program to generate schematic diagrams of protein–ligand interactions. *Protein Eng* 1995; **8**: 127–34.

23 Friesner RA, Banks JL, Murphy RB *et al*. Glide: a new approach for rapid, accurate docking and scoring. 1. Method and assessment of docking accuracy. *J Med Chem* 2004; **47**: 1739–49.

24 Cornish-Bowden A. *Fundamentals of Enzyme Kinetics*. London: Portland Press, 2004.

25 Adams M, Wube AA, Bucar F *et al*. Quinolone alkaloids from *Evodia rutaecarpa*: a potent new group of antimycobacterial compounds. *Int J Antimicrob Agents* 2005; **26**: 262–4.

26 Richardson JF, Reith S. Characterization of a strain of methicillin-resistant *Staphylococcus aureus* (EMRSA-15) by conventional and molecular methods. *J Hosp Infect* 1993; **25**: 45–52.

27 Orme I. Search for new drugs for treatment of tuberculosis. *Antimicrob Agents Chemother* 2001; **45**: 1943–6.

28 Drlica K, Zhao X. DNA gyrase, topoisomerase IV, and the 4-quinolones. *Microbiol Mol Biol Rev* 1997; **61**: 377–92.

29 Xia Y, Yang Z-Y, Morris-Natschke SL *et al*. Recent advances in the discovery and development of quinolones and analogues as antitumor agents. *Curr Med Chem* 1999; **6**: 179–94.

30 Chu DT, Fernandes PB. Structure–activity relationships of the fluoroquinolones. *Antimicrob Agents Chemother* 1989; **33**: 131–5.

31 Krovat EM, Steindl T, Langer T. Recent advances in docking and scoring. *Current Computer-Aided Drug Design* 2005; **1**: 93–102.

32 Umamaheswari A, Pradhan D, Hemanthkumar M. Virtual screening for potential inhibitors of homology modeled *Leptospira interrogans* MurD ligase. *J Chem Biol* 2010; **3**: 175–87.

33 Herschlag D. The role of induced fit and conformational changes of enzymes in specificity and catalysis. *Bioorg Chem* 1988; **16**: 62–96.

34 Pettersen EF, Goddard TD, Huang CC *et al*. UCSF Chimera—a visualization system for exploratory research and analysis. *J Comput Chem* 2004; **25**: 1605–12.

JOURNAL OF NATURAL PRODUCTS

ARTICLE

pubs.acs.org/jnp

Dolabellanes with Antibacterial Activity from the Brown Alga *Dilophus spiralis*

Efstathia Ioannou,[†] Antonio Quesada,[‡] M. Mukhlesur Rahman,[§] Simon Gibbons,[§] Constantinos Vagias,[⊥,†] and Vassilios Roussis*[,†]

[†]Department of Pharmacognosy and Chemistry of Natural Products, School of Pharmacy, University of Athens, Panepistimiopolis Zografou, Athens 15771, Greece

[‡]Department of Didactics of Sciences, University of Jaén, PO 23071, Jaén, Spain

[§]Department of Pharmaceutical and Biological Chemistry, School of Pharmacy, University of London, 29-39 Brunswick Square, London WC1N 1AX, U.K.

Supporting Information

ABSTRACT: Seventeen diterpenes featuring the dolabellane skeleton (**1**−**17**) were isolated from the organic extracts of the brown alga *Dilophus spiralis*. Seven compounds are new natural products (**1**, **3**, **5**, **6**, **11**, **14**, **15**) and eight are structurally revised (**2**, **4**, **7**−**10**, **12**, **13**), among which three are reported for the first time from a natural source (**4**, **9**, **10**). The structure elucidation and the assignment of the relative configurations of the isolated natural products were based on detailed analyses of their spectroscopic data. The structure of metabolite **10** was confirmed by single-crystal X-ray diffraction analysis, whereas the absolute configurations of compounds **2**, **4**−**10**, **12**, and **13** were determined using the modified Mosher's method on the semisynthetic product **18** and chemical interconversions. The antibacterial activities of compounds **1**−**18** were evaluated against six strains of *Staphylococcus aureus*, including multidrug- and methicillin-resistant variants.

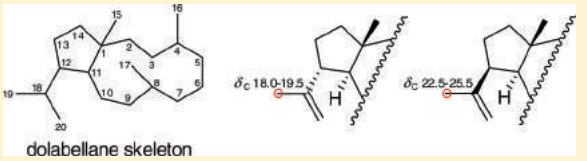

Brown algae of the family Dictyotaceae are widely distributed in the tropical and subtropical waters of the world, found mainly in the Atlantic, Pacific, and Indian Oceans, the Caribbean and Mediterranean Seas, and the Sea of Japan. They have been the subject of extensive studies in the last five decades, having yielded almost 500 new secondary metabolites to date. The majority of these natural products are sesquiterpenes and diterpenes of normal or mixed biosynthesis, often exhibiting antibacterial, antiviral, cytotoxic, algicidal, antifouling, antifeedant, and/or ichthyotoxic activity.[1,2]

In the course of our continuing research aimed at the isolation of bioactive natural products from marine organisms found along the coastlines of Greece, we undertook a thorough investigation of the chemical composition of *Dilophus spiralis* (Montagne) Hamel (syn. *ligulatus*). Previously, we reported the isolation and structural characterization of five new dolastanes, one new 2,6-*cyclo*-xenicane, and several known metabolites from *D. spiralis*.[3,4] Herein, we describe the isolation and structure elucidation of 17 dolabellanes (**1**−**17**) from the same algal specimens and the evaluation of their antibacterial activities against six strains of *Staphylococcus aureus*, some of which are resistant, via multidrug efflux. Seven compounds are new natural products (**1**, **3**, **5**, **6**, **11**, **14**, **15**) and eight are structurally revised (**2**, **4**, **7**−**10**, **12**, **13**), among which three are reported for the first time from a natural source (**4**, **9**, **10**).

RESULTS AND DISCUSSION

Specimens of the brown alga *D. spiralis*, collected on Elafonissos Island, Greece, were exhaustively extracted with CH_2Cl_2 and MeOH, and the organic extracts were subsequently subjected to a series of chromatographic separations to allow for the isolation of compounds **1**−**17**.

Compounds **1**−**3**, isolated as oils, displayed molecular ion peaks at *m*/*z* 286 (EIMS), corresponding to $C_{20}H_{30}O$. The absorption band at 1735 cm^{-1} in their IR spectra indicated the presence of a carbonyl group, while their ^{13}C NMR spectra revealed 20 carbon signals, which were assigned to five quaternary carbon atoms, four methines, seven methylenes, and four methyls, as determined by DEPT experiments. The structural elements displayed in the ^1H and ^{13}C NMR spectra of **1**−**3** (Tables 1 and 2) included four methyl groups on quaternary carbons ($\delta_{H/C}$ 0.91/17.5, 1.48/15.8, 1.54/18.1, and 1.77/18.2 for **1**; $\delta_{H/C}$ 1.09/18.3, 1.51/15.7, 1.53/16.5, and 1.70/22.8 for **2**; $\delta_{H/C}$ 0.93/21.9, 1.66/23.5, 1.63/17.2, and 1.76/25.0 for **3**), one 1,1-disubstituted double bond ($\delta_{H/C}$ 4.81, 4.93/113.5, δ_C 144.7 for **1**; $\delta_{H/C}$ 4.64, 4.91/112.1, δ_C 144.7 for **2**; $\delta_{H/C}$ 4.58, 4.91/113.3, δ_C 148.0 for **3**), two trisubstituted double bonds ($\delta_{H/C}$ 4.70/122.8, δ_C 134.6 and $\delta_{H/C}$ 4.86/125.3, δ_C 136.1 for **1**; $\delta_{H/C}$ 5.12/122.8, δ_C 136.6 and $\delta_{H/C}$ 4.84/128.3, δ_C 133.0 for **2**; $\delta_{H/C}$ 4.69/122.4, δ_C 137.4 and $\delta_{H/C}$ 5.13/125.4, δ_C 134.9 for **3**), and a ketone functionality (δ_C 221.8 for **1**; δ_C 222.8 for **2**; δ_C 226.3 for **3**). Because the carbonyl group and the three carbon−carbon double bonds accounted for four of the six degrees of unsaturation,

Received: September 16, 2010
Published: December 29, 2010

dx.doi.org/10.1021/np1006586 | *J. Nat. Prod.* 2011, 74, 213–222

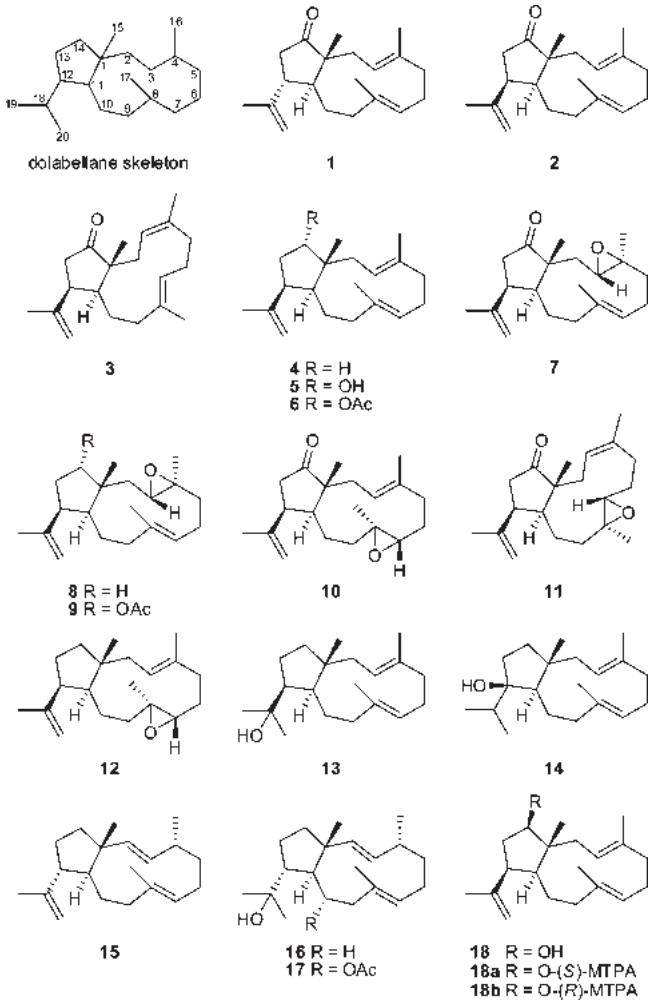

the molecular structures of **1**−**3** were determined as bicyclic. Analyses of their 2D NMR spectra resulted in the establishment of the same planar structure, suggesting that the three compounds were stereoisomers. Specifically, the long-range coupling between H_3-19 and H_2-20 observed in the COSY spectrum indicated the presence of an isopropenyl group, whereas the correlations of C-18 with H-12 and H_3-19, as well as of C-12 with H_3-19 and H_2-20 in the HMBC spectrum, fixed its position. The cross-peaks of H-11/H-12 and H-12/H_2-13 observed in the COSY spectrum, in combination with the HMBC correlations of C-1, C-12, and C-14 with H-11 and H_2-13, identified the five-membered ring. Furthermore, the correlations of C-3 and C-4 with H_2-2, H_2-5, and H_3-16, of C-7 and C-8 with H_2-6, H_2-9, and H_3-17, and of C-1 and C-11 with H_2-2 and H_2-10 displayed in the HMBC spectrum, in conjunction with the COSY correlations of H_2-2/H-3, H_2-5/H_2-6, H_2-6/H-7, H_2-9/H_2-10, and H_2-10/H-11, concluded the assignment of the 11-membered ring. Finally, the HMBC correlations of H_3-15 with C-1, C-11, and C-14 placed the aliphatic methyl on C-1. The relative configurations of the stereogenic centers and the geometries of the double bonds of metabolites **1**−**3** were assigned on the basis of interactions observed in their NOESY spectra. The NOE enhancements of H-11/H_3-19, H-12/H_3-15, H-12/H-20β, and H_3-19/H-20α evident in the NOESY spectrum of **1** suggested the *trans* fusion of the two rings and indicated that H-12 was *trans*- and *cis*-oriented relative to H-11 and H_3-15, respectively. The geometries of the Δ^3 and Δ^7 double bonds were determined as 3*E*,7*E* on the basis of the NOE interactions of H-2α/H_3-16, H-2β/H-3, H-3/H_3-15, H-7/H-9β, and H-9α/H_3-17. This was further supported by the fact that C-16 and C-17 resonated at lower frequencies (δ_C 15.8 and 18.1, respectively). In contrast, the intense NOE enhancement of H-11/H-12 displayed in the NOESY spectra of **2** and **3**, in conjunction with the observed NOE cross-peaks of H-2α/H-11, H-2β/H_3-15, H-12/H-20α, and H_3-19/H-20β for **2** and of H-3/H-11, H-3/H-13α, H-12/H-13α, H-12/H_3-19, H-13β/H-20β, H_3-15/H-20β, and H_3-19/H-20α for **3**, suggested the *trans* fusion of the two rings and the *cis*- and *trans*-orientation of H-12 in relation to H-11 and H_3-15, respectively. The geometries of the Δ^3 and Δ^7 double bonds in **2** were determined as 3*E*,7*E* on the basis of the NOE interactions of H-2α/H_3-16, H-2α/H_3-17, H-2β/H-3, H-3/H-7, and H-3/H_3-15, as in the case of **1**, which was further supported by the fact that C-16 and C-17 resonated at lower frequencies (δ_C 15.7 and 16.5, respectively). However, the geometries of the Δ^3 and Δ^7 double bonds in **3** were determined as *Z* and *E*, respectively, on the basis of the NOE cross-peaks of H-3/H_3-16, H_2-6/H_3-17, H-7/H-9β, H-7/H-10β, and H-10β/H_3-15. This was further verified by the fact that C-16 and C-17 resonated at higher (δ_C 23.5) and lower (δ_C 17.2) frequencies, respectively. On the basis of the above-mentioned data, metabolite **1** was identified as (1*R*,3*E*,7*E*,11*S*,12*R*)-14-oxo-3,7,18-dolabellatriene, **2** as its epimer at C-12, and **3** as the geometrical isomer of **2** at Δ^3. The spectroscopic and physical characteristics of **2** were identical to those of a previously reported dolabellane, although its structure was established as that of compound **1**.[5,6] A closer examination of the details of that work revealed that the relative configuration of C-12 had been erroneously assigned, based on rather tenuous evidence prior to the introduction of 2D NMR experiments. Possible reasons for the misassignment of the relative configuration of C-12 might include a misinterpretation of the results of the lanthanide-induced shift experiments used to determined the relative orientation of H_3-15 and the isopropenyl group and the fact that the relative orientation of H-11 and H-12 was established on the basis of their coupling constant alone without the use of NOE correlations.

Compound **4**, obtained as a yellowish oil, displayed a profile closely resembling those of metabolites **1**−**3**. Its spectroscopic and physical characteristics were the same as those of a semisynthetic product reported in the literature, whose structure had been mistakenly assigned, concerning the relative configuration of C-12, on the basis of the original misassignment regarding compound **2**.[7] Indeed, the NOE enhancements of H-2α/H-11, H-2β/H_3-15, H-11/H-12, H-12/H-20α, and H_3-19/H-20β, as in the case of **2**, suggested the *trans* fusion of the two rings and indicated that H-12 was *cis*- and *trans*-oriented relative to H-11 and H_3-15, respectively. Thus, metabolite **4** was identified as the 14-deoxo derivative of **2**, reported for the first time as a natural product.

Compound **5**, isolated as a colorless oil, had the molecular formula $C_{20}H_{32}O$, as calculated from the HRFABMS measurements. Analysis of the spectroscopic data of **5** (Tables 1 and 2) showed a high degree of similarity with metabolite **4**. In agreement with the molecular formula, it was clear that the difference was the presence of one hydroxy group. This was verified from the signals of an oxygenated methine ($\delta_{H/C}$ 3.90/81.8) evident in the ^{1}H and ^{13}C NMR spectra, as well as the absorption band at 3370 cm^{-1} in the IR spectrum. The hydroxy group was placed at C-14 due to the heteronuclear correlations of C-14 with H-11, H-12, H_2-13, and H_3-15. The relative configurations of the stereogenic centers C-1, C-11, and C-12 and the geometries of

dx.doi.org/10.1021/np1006586 |*J. Nat. Prod.* 2011, 74, 213–222

Table 1. ^{1}H NMR Data (400 MHz, $CDCl_3$) of Compounds 1, 3−6, and 18

position		1 (J in Hz)		3 (J in Hz)		4 (J in Hz)		5 (J in Hz)		6 (J in Hz)		18 (J in Hz)
2	α	2.35, dd (14.6, 6.6)		1.95, m	α	2.19, m	α	2.23, m	α	2.30, m	α	2.10, m
	β	1.93, dd (14.6, 6.6)			β	1.67, m	β	1.72, m	β	1.66, m	β	1.79, m
3		4.70, dd (6.6, 6.6)		4.69, dd (11.6, 2.9)		5.13, dd (11.4, 4.4)		5.10, dd (10.8, 3.8)		5.09, dd (11.1, 4.0)		5.09, dd (8.4, 6.4)
5	a	2.08, m	a	2.29, m	a	2.22, m	a	2.19, m	a	2.21, m		2.12, m
	b	2.01, m	b	1.78, m	b	2.05, m	b	2.05, m	b	2.08, m		
6	a	2.17, m		2.19, m	a	2.28, m	a	2.28, m	a	2.27, m	a	2.22, m
	b	2.11, m			b	2.03, m	b	2.03, m	b	2.05, m	b	2.08, m
7		4.86, dd (7.5, 7.5)		5.13, dd (7.7, 7.7)		4.84, m		4.87, dd (10.8, 1.8)		4.86, m		4.83, dd (9.8, 4.2)
9	α	2.03, m	α	2.15, m	a	2.11, m	a	2.10, m	a	2.11, m	a	2.05, m
	β	1.75, m	β	1.80, m	b	1.88, m	b	1.77, m	b	1.85, m	b	1.87, m
10	a	1.49, m	α	1.62, m	a	1.31, m	a	1.34, m	a	1.33, m	a	1.36, m
	b	1.37, m	β	1.18, m	b	1.23, m	b	1.23, m	b	1.22, m	b	1.18, m
11		1.99, m		2.55, ddd (8.9, 7.9, 1.5)		1.74, m		1.93, m		1.92, m		1.84, m
12		2.53, ddd (11.3, 11.3, 7.9)		2.87, dd (8.9, 8.9)		2.61, ddd (10.0, 6.8, 6.8)		2.90, ddd (9.9, 7.6, 7.6)		2.85, ddd (9.5, 7.4, 7.4)		2.56, ddd (12.4, 7.8, 6.4)
13	a	2.36, dd (18.5, 7.9)	α	2.31, dd (18.2, 8.9)	a	1.64, m	a	1.95, m	a	2.02, m	α	1.99, ddd (12.4, 6.4, 6.4)
	b	2.23, dd (18.5, 11.3)	β	2.48, d (18.2)	b	1.56, m	b	1.65, m	b	1.64, m	β	1.64, ddd (12.4, 12.4, 9.8)
14					a	1.52, m		3.90, dd (6.3, 6.3)		4.91, dd (6.0, 4.2)		3.72, dd (9.8, 6.4)
					b	1.42, m						
15		0.91, s		0.93, s		1.06, s		1.03, s		1.10, s		0.96, s
16		1.48, s		1.66, s		1.51, s		1.52, s		1.52, s		1.50, s
17		1.54, s		1.63, s		1.51, s		1.53, s		1.51, s		1.49, s
19		1.77, s		1.76, s		1.70, s		1.70, s		1.72, s		1.71, s
20	α	4.81, brs	α	4.91, brs	α	4.64, brs	α	4.63, brs	α	4.64, brs	α	4.68, brs
	β	4.93, brs	β	4.58, brs	β	4.82, brs	β	4.82, brs	β	4.85, brs	β	4.87, brs
OAc										2.03, s		

the double bonds at C-3 and C-7 were established by analysis of the key correlations displayed in the NOESY spectrum of **5**, in accordance with those of **4**. The NOE enhancements of H-2β/H-14 and H-14/H_3-15 suggested a *cis*-relationship between H-14 and H_3-15 and determined the relative configuration of C-14 as *S**. Therefore, metabolite **5** was identified as the 14*S*-hydroxy derivative of **4**.

Compound **6**, with the molecular formula $C_{22}H_{34}O_2$, as deduced from the HRFABMS measurements, was obtained as a colorless oil. Its ^{1}H and ^{13}C NMR spectra (Tables 1 and 2) were rather similar to those of **5**, with the most prominent difference being the replacement of the hydroxy group by an acetoxy group. The shift of H-14 to higher frequencies (δ_H 4.91), in conjunction with the presence of an acetoxy group, as suggested by an ester carbonyl (δ_C 171.0) and an acetoxy methyl ($\delta_{H/C}$ 2.03/21.2), was indicative of the acetylation of the hydroxy group at C-14. The correlations observed in the homo- and heteronuclear experiments supported the proposed structure of **6** as the acetyl derivative of **5**. The relative configuration and the geometry of the double bonds of **6**, found in accordance with those of **5**, were established by analysis of its NOESY spectrum.

Compounds **7**−**9**, obtained as oils, exhibited spectroscopic and physical characteristics consistent with those of dolabellanes already reported in the literature, whose structures had been incorrectly assigned, concerning the relative configuration of C-12, on the basis of the original misassignment regarding compound **2**.[5,6] Inspection of the NOESY spectra of **7**−**9** revealed cross-peaks of H-2α/H-12, H-2β/H-3, H-3/H_3-15, H-11/H-12, H-12/H-20α, and H_3-19/H-20β, thus determining the same relative configurations for C-1, C-11, and C-12 as in **2**−**6**. Metabolite **9** is reported for the first time as a natural product.

Compounds **10** and **11**, isolated as white crystals and a colorless oil, respectively, displayed molecular ion peaks at *m*/*z* 302 (EIMS), corresponding to $C_{20}H_{30}O_2$. The structural elements displayed in the ^{1}H and ^{13}C NMR spectra of **10** and **11** (Tables 3 and 4) exhibited a high degree of similarity with those of metabolite **7**. In agreement with the molecular formula, it was obvious that they were both isomers of the latter. Analyses of their 2D NMR spectra resulted in the establishment of the same planar structure, implying that **10** and **11** were stereoisomers. In this case, the trisubstituted double bond remained between carbons C-3 and C-4, as in **1**−**3**, whereas the epoxide function was placed between carbons C-7 and C-8, on the basis of the HMBC correlations of C-5, C-6, C-8, and C-9 with H-7 and both C-7 and C-8 with H_2-6, H_2-9, and H_3-17. The relative configuration and the geometry of the double bond of both metabolites were assigned on the basis of interactions observed in their NOESY spectra. The intense NOE enhancement of H-11/H-12 established the same relative

dx.doi.org/10.1021/np1006586 |J. Nat. Prod. 2011, 74, 213–222

Table 2. ^{13}C NMR Data (50 MHz, $CDCl_3$) of Compounds 1, 3−6, and 18

position	1		3		4		5		6		18	
1	53.0,	C	50.6,	C	46.5,	C	48.3,	C	49.2,	C	48.9,	C
2	35.2,	CH_2	38.0,	CH_2	43.4,	CH_2	35.0,	CH_2	35.2,	CH_2	40.0,	CH_2
3	122.8,	CH	122.4,	CH	125.8,	CH	124.2,	CH	124.4,	CH	124.5,	CH
4	134.6,	C	137.4,	C	134.5,	C	135.4,	C	135.4,	C	134.9,	C
5	39.3,	CH_2	31.7,	CH_2	39.9,	CH_2	39.9,	CH_2	39.8,	CH_2	39.8,	CH_2
6	25.0,	CH_2	25.2,	CH_2	24.4,	CH_2	24.4,	CH_2	24.9,	CH_2	24.6,	CH_2
7	125.3,	CH	125.4,	CH	127.3,	CH	126.8,	CH	127.3,	CH	127.2,	CH
8	136.1,	C	134.9,	C	133.9,	C	134.4,	C	133.9,	C	134.1,	C
9	37.1,	CH_2	36.0,	CH_2	37.7,	CH_2	36.8,	CH_2	37.3,	CH_2	38.2,	CH_2
10	29.9,	CH_2	23.8,	CH_2	24.4,	CH_2	26.3,	CH_2	24.4,	CH_2	24.1,	CH_2
11	43.3,	CH	41.7,	CH	41.8,	CH	42.0,	CH	41.8,	CH	41.4,	CH
12	49.9,	CH	41.4,	CH	51.0,	CH	46.0,	CH	47.1,	CH	44.4,	CH
13	42.0,	CH_2	47.1,	CH_2	28.5,	CH_2	37.6,	CH_2	35.0,	CH_2	37.7,	CH_2
14	221.8,	C	226.3,	C	42.1,	CH_2	81.8,	CH	83.3,	CH	80.3,	CH
15	17.5,	CH_3	21.9,	CH_3	24.3,	CH_3	22.3,	CH_3	22.6,	CH_3	16.9,	CH_3
16	15.8,	CH_3	23.5,	CH_3	15.6,	CH_3	15.5,	CH_3	15.6,	CH_3	15.7,	CH_3
17	18.1,	CH_3	17.2,	CH_3	16.7,	CH_3	17.7,	CH_3	17.0,	CH_3	16.4,	CH_3
18	144.7,	C	148.0,	C	146.9,	C	146.4,	C	145.7,	C	145.6,	C
19	18.2,	CH_3	25.0,	CH_3	23.5,	CH_3	23.3,	CH_3	23.3,	CH_3	23.3,	CH_3
20	113.5,	CH_2	113.3,	CH_2	111.2,	CH_2	112.4,	CH_2	112.2,	CH_2	112.1,	CH_2
OAc									171.0,	C		
OAc									21.2,	CH_3		

Table 3. ^{1}H NMR Data (400 MHz, $CDCl_3$) of Compounds 9−11 and 13−15

position	9 (J in Hz)	10 (J in Hz)	11 (J in Hz)	13 (J in Hz)	14 (J in Hz)	15 (J in Hz)
2	α 1.41, dd (14.2, 11.0)	α 2.15, m	2.15, m	a 2.11, m	a 2.09, m	5.20, d (15.9)
	β 1.78, dd (14.2, 2.4)	β 1.83, dd (13.1, 3.9)		b 1.67, m	b 1.73, m	
3	2.89, dd (11.0, 2.4)	5.38, dd (11.4, 3.9)	4.73, m	4.98, dd (7.2, 7.2)	4.93, m	5.13, dd (15.9, 7.8)
4						2.03, m
5	α 2.14, m	2.27, m	a 2.53, m	2.08, m	2.08, m	a 1.52, m
	β 1.24, m		b 1.88, dd (14.0, 7.4)			b 1.34, m
6	α 2.32, m	α 1.56, m	a 2.03, m	a 2.13, m	a 2.14, m	a 2.12, m
	β 2.16, m	β 1.90, m	b 1.44, m	b 2.10, m	b 2.10, m	b 2.08, m
7	5.03, brd (10.7)	2.72, brd (10.0)	2.88, m	4.86, dd (6.7, 6.7)	4.95, m	4.98, dd (9.8, 5.4)
9	α 2.00, m	α 2.01, m	a 2.02, m	2.12, m	a 2.11, m	α 1.99, m
	β 2.19, m	β 1.28, m	b 1.55, m		b 1.83, m	β 1.57, m
10	a 1.39, m	1.42, m	α 1.51, m	1.50, m	a 1.64, m	a 1.42, m
	b 1.28, m		β 1.37, m		b 1.27, m	b 1.23, m
11	1.95, m	2.14, m	2.52, m	1.52, m	1.67, m	1.37, m
12	2.77, ddd (11.7, 7.0, 7.0)	2.94, ddd (7.9, 7.7, 7.7)	2.89, m	1.72, m		2.27, m
13	a 2.03, m	2.40, m	a 2.54, m	a 1.65, m	a 1.68, m	a 1.76, m
	b 1.57, m		b 2.29, dd (18.4, 9.0)	b 1.33, m	b 1.42, m	b 1.50, m
14	4.84, dd (7.1, 3.2)			a 1.44, m	a 1.57, m	a 1.72, m
				b 1.37, m	b 1.43, m	b 1.41, m
15	1.29, s	1.08, s	0.96, s	0.97, s	0.97, s	0.85, s
16	1.23, s	1.64, s	1.67, s	1.54, s	1.48, s	0.91, d (6.8)
17	1.56, s	1.27, s	1.33, s	1.53, s	1.55, s	1.46, s
18					1.85, m	
19	1.70, s	1.73, s	1.79, s	1.21, s	0.93, d (6.8)	1.70, s
20	α 4.63, brs	α 4.69, brs	α 4.95, brs	1.23, s	0.97, d (6.6)	α 4.68, brs
	β 4.87, brs	β 4.96, brs	β 4.61, brs			β 4.70, brs
OAc	2.01, s					

dx.doi.org/10.1021/np1006586 |J. Nat. Prod. 2011, 74, 213–222

Table 4. ^{13}C NMR Data (50 MHz, $CDCl_3$) of Compounds 9−11 and 13−15

position	9		10		11		13		14		15	
1	46.7,	C	52.8,	C	50.1,	C	46.7,	C	44.5,	C	45.1,	C
2	35.6,	CH_2	37.1,	CH_2	38.0,	CH_2	38.7,	CH_2	41.8,	CH_2	136.5,	CH
3	63.9,	CH	122.1,	CH	122.8,	CH	124.6,	CH	124.2,	CH	132.7,	CH
4	62.0,	C	136.9,	C	137.5,	C	133.0,	C	133.8,	C	38.5,	CH
5	38.8,	CH_2	37.9,	CH_2	27.7,	CH_2	39.5,	CH_2	39.0,	CH_2	35.3,	CH_2
6	24.2,	CH_2	23.6,	CH_2	25.1,	CH_2	24.9,	CH_2	24.3,	CH_2	27.8,	CH_2
7	126.5,	CH	64.9,	CH	62.5,	CH	126.5,	CH	124.4,	CH	127.2,	CH
8	133.8,	C	61.2,	C	62.2,	C	135.3,	C	135.9,	C	133.2,	C
9	37.1,	CH_2	36.2,	CH_2	35.0,	CH_2	39.2,	CH_2	37.7,	CH_2	40.5,	CH_2
10	23.2,	CH_2	23.3,	CH_2	23.7,	CH_2	31.5,	CH_2	23.0,	CH_2	24.9,	CH_2
11	42.0,	CH	41.9,	CH	42.5,	CH	41.7,	CH	45.6,	CH	55.1,	CH
12	47.7,	CH	43.3,	CH	40.9,	CH	60.2,	CH	87.3,	C	54.1,	CH
13	34.3,	CH_2	42.0,	CH_2	46.9,	CH_2	26.4,	CH_2	30.5,	CH_2	27.3,	CH_2
14	83.1,	CH	222.3,	C	224.7,	C	41.1,	CH_2	39.5,	CH_2	39.8,	CH_2
15	22.5,	CH_3	18.0,	CH_3	21.3,	CH_3	23.2,	CH_3	24.3,	CH_3	20.7,	CH_3
16	15.9,	CH_3	15.9,	CH_3	23.8,	CH_3	16.4,	CH_3	15.6,	CH_3	22.6,	CH_3
17	16.3,	CH_3	19.1,	CH_3	21.7,	CH_3	16.5,	CH_3	17.4,	CH_3	16.6,	CH_3
18	145.0,	C	144.6,	C	147.0,	C	73.3,	C	35.0,	CH	147.5,	C
19	22.8,	CH_3	23.4,	CH_3	25.2,	CH_3	26.5,	CH_3	18.7,	CH_3	18.5,	CH_3
20	112.1,	CH_2	113.4,	CH_2	114.2,	CH_2	30.8,	CH_3	17.9,	CH_3	110.4,	CH_2
OAc	170.9,	C										
OAc	21.2,	CH_3										

configurations for C-1, C-11, and C-12 as in **7**. The NOE interactions of H-3/H-7, H-7/H_3-15, H-11/H_3-17, and H_3-16/H_3-17 for **10** and the cross-peaks of H-7/H-10β, H-10β/H_3-15, H-11/H_3-17, and H_3-16/H_3-17 for **11** suggested that the oxygenated methine H-7 was *cis*- and *trans*-oriented relative to H_3-15 and H_3-17, respectively, and established the relative configuration of C-7 and C-8 as 7*S**,8*S**. The geometry of the double bond at C-3 was established as *E* in **10** on the basis of the NOE enhancements of H-2α/H_3-16, H-2β/H-3, and H-3/H_3-15, which was further supported by the fact that C-16 resonated at lower frequencies (δ_C 15.9). On the contrary, the geometry of the Δ^3 double bond was established as *Z* in **11** on the basis of the NOE enhancements of H-3/H-11 and H-3/H_3-16, which was further verified by the fact that C-16 resonated at higher frequencies (δ_C 23.8). Thus, the geometrical isomers **10** and **11** were identified as positional isomers of **7**. The proposed structure of **10** was confirmed by single-crystal X-ray diffraction analysis (Figure 1).[8] The spectroscopic and physical characteristics of compound **10** were identical to those of a semisynthetic product reported in the literature, whose structure had been erroneously assigned concerning the relative configuration of C-12 on the basis of the original misassignment regarding compound **2**, while the relative configurations of C-7 and C-8 were not established.[5]

Compound **12**, obtained as a yellowish oil, possessed spectroscopic and physical characteristics congruent with those of a previously reported dolabellane, whose structure had been incorrectly assigned concerning the relative configuration of C-12 due to the overlap of H-7 and H-12 and the misinterpretation thereafter of the NOE correlations observed.[9] The NOE enhancements of H-2α/H_3-16, H-2β/H-3, H-3/H-7, H-3/H_3-15, H-7/H_3-15, H-11/H-12, H-12/H-20α, and H_3-19/H-20β, more easily distinguishable in 1D NOE experiments, indicated the same relative configurations for C-1, C-7, C-8, C-11, and C-12 and the geometry of the Δ^3 double bond as in the case of **10**.

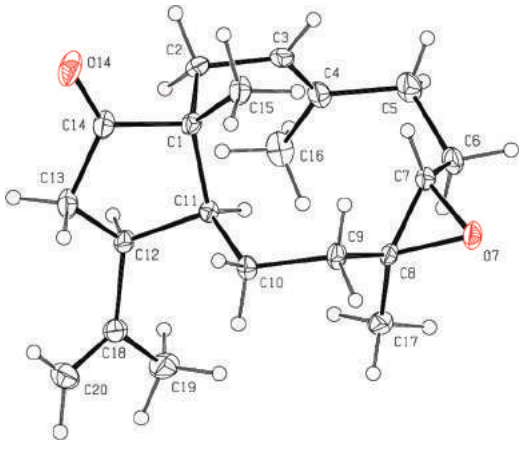

Figure 1. ORTEP drawing of compound **10**. Displacement ellipsoids are shown at 30% probability.

Compound **13**, isolated as a colorless oil, displayed spectroscopic and physical characteristics identical to those of a previously reported dolabellane, whose structure had been erroneously assigned, concerning the relative configuration of C-12, on the basis of the original misassignment regarding compound **2**.[7] As in the case of metabolites **2**−**12**, the NOE enhancement of H-11/H-12 indicated the same relative configurations for C-1, C-11, and C-12.

Compound **14**, with the molecular formula $C_{20}H_{34}O$, as deduced from the HRFABMS measurements, was obtained as a colorless oil. The structural characteristics evident in the ^1H and ^{13}C NMR spectra included three singlet methyls ($\delta_{H/C}$ 0.97/24.3, 1.48/15.6, and 1.55/17.4), two doublet methyls

dx.doi.org/10.1021/np1006586 |*J. Nat. Prod.* 2011, 74, 213–222

Scheme 1. Chemical Interconversions Performed[a] Correlating Compounds 2, 4−10, 12, 13, and 18

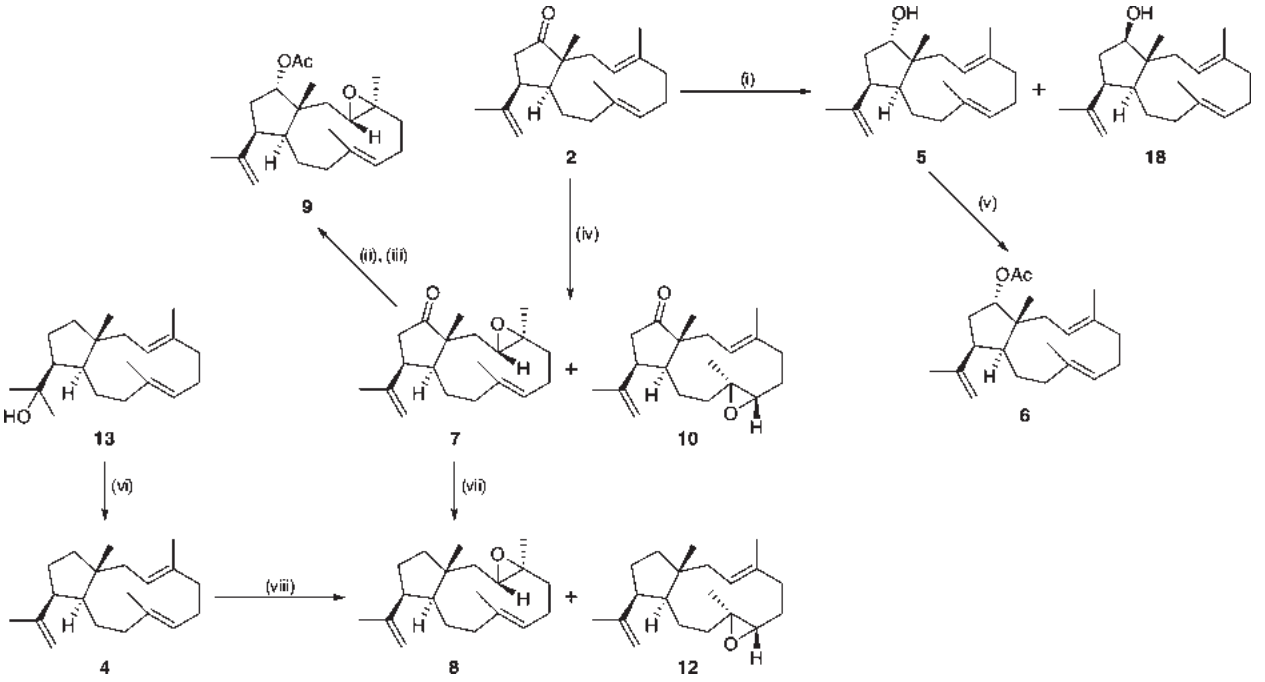

[a] Reagents and conditions: (i) $NaBH_4$, MeOH, 1 h; (ii) $NaBH_4$, EtOH, 2 h; (iii) Ac_2O, pyridine, overnight; (iv) *m*-CPBA, benzene, 45 min; (v) Ac_2O, pyridine, 70 °C, 16 h; (vi) $POCl_3$, pyridine, 0 °C, 20 min; (vii) $N_2H_4 \cdot H_2O$, $N_2H_4 \cdot 2HCl$, TEG, 130 °C, 1.5 h, KOH, 170 °C, 2 h; (viii) *m*-CPBA, benzene, 30 min.

($\delta_{H/C}$ 0.93/18.7 and 0.97/17.9), two trisubstituted double bonds ($\delta_{H/C}$ 4.93/124.2, δ_C 133.8 and $\delta_{H/C}$ 4.95/124.4, δ_C 135.9), and an oxygenated quaternary carbon (δ_C 87.3). The spectroscopic data of **14** (Tables 3 and 4) closely resembled those of **13**. In this case, the hydroxy group was placed at C-12, as indicated by the HMBC correlations of C-12 with H-11, H_2-13, H_3-19, and H_3-20 and the COSY cross-peaks of H-18 with both H_3-19 and H_3-20. The geometries of the Δ^3 and Δ^7 double bonds were determined as 3*E*,7*E* due to the fact that C-16 and C-17 resonated at lower frequencies (δ_C 15.6 and 17.4, respectively). On the basis of the interaction of H-11/H_3-19 observed in the NOESY spectrum, measured in C_6D_6 because there was partial overlapping of key NMR signals in $CDCl_3$, the relative configurations of C-1, C-11, and C-12 were established as 1*R**,11*R**,12*R**.

Compound **15**, obtained as a colorless oil, displayed an ion peak at *m*/*z* 272.2495 (HRFABMS), corresponding to $C_{20}H_{32}$ and consistent with $[M]^+$. Analysis of the spectroscopic data of **15** (Tables 3 and 4) showed a high degree of similarity with metabolite **4**, and with an identical molecular formula, it was obvious that the two were isomers. In the ^1H NMR spectrum three singlet methyls (δ_H 0.85, 1.46, and 1.70), one doublet methyl (δ_H 0.91), an exomethylene group (δ_H 4.68 and 4.70), and three olefinic methines (δ_H 4.98, 5.13, and 5.20) were evident, suggesting that the difference between the two molecules was the replacement of a trisubstituted double bond by a 1,2-disubstituted one. The 1,2-disubstituted double bond was placed between C-2 and C-3 on the basis of the COSY cross-peaks of H-2/H-3, H-3/H-4, H-4/H_2-5, and H-4/H_3-16 and the correlations of C-1 and C-15 with H-2, as well as of C-3, C-4, and C-5 with H_3-16. Inspection of the NOESY spectrum of **15** revealed the interaction of H-12/H_3-15, which led to the

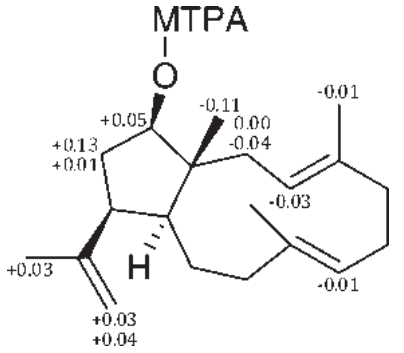

Figure 2. $\Delta\delta_{S-R}$ values (ppm) for the C-14 MTPA derivatives of **18** in $CDCl_3$.

determination of the relative configurations of C-1, C-11, and C-12 as 1*R**,11*S**,12*R**. Furthermore, the NOE enhancements of H-2/H-11, H-2/H_3-16, H-11/H_3-17, H-3/H-7, and H-3/H_3-15 established the relative configuration of C-4 as *R** and the geometries of the double bonds at C-2 and C-7 as 2*E*,7*E*. The latter conclusion was also supported by the large coupling constant of H-2/H-3 (15.9 Hz) and the fact that C-17 resonated at lower frequencies (δ_C 16.6).

Reduction of metabolite **2** yielded both epimeric alcohols at C-14 (**5** and **18**), while acetylation of metabolite **5** afforded **6**. Furthermore, epoxidation of metabolite **4** yielded monoepoxides **8** and **12** (Scheme 1). Semisynthetic compounds **5**, **6**, **8**, and **12** were identical in all respects to the natural products, whereas **18** was not detected as a natural product during the chromatographic separations. In the previous reports on compounds **2**, **4**, **7**−**10**, and **13**, several chemical interconversions were used to

dx.doi.org/10.1021/np1006586 |*J. Nat. Prod.* 2011, 74, 213–222

Table 5. Antibacterial Activities[a] of Compounds 1−18

compound	ATCC 25923	EMRSA-15	EMRSA-16	RN4220	SA1199B	XU212
1	inactive[b]	inactive[b]	inactive[b]	inactive[b]	inactive[b]	inactive[b]
2	inactive[b]	inactive[b]	16	inactive[b]	128	inactive[b]
3	inactive[b]	inactive[b]	inactive[b]	inactive[b]	inactive[b]	inactive[b]
4	64	128	16	128	128	128
5	128	64	8	64	32	64
6	inactive[b]	inactive[b]	inactive[b]	inactive[b]	inactive[b]	inactive[b]
7	inactive[b]	inactive[b]	inactive[b]	128	inactive[b]	inactive[b]
8	inactive[b]	inactive[b]	32	inactive[b]	inactive[b]	inactive[b]
9	32	128	32	64	64	128
10	inactive[b]	inactive[b]	inactive[b]	inactive[b]	inactive[b]	inactive[b]
11	inactive[b]	inactive[b]	inactive[b]	inactive[b]	inactive[b]	inactive[b]
12	inactive[b]	128	4	inactive[b]	inactive[b]	inactive[b]
13	32	32	8	64	32	64
14	8	8	8	8	16	16
15	inactive[b]	inactive[b]	inactive[b]	inactive[b]	inactive[b]	inactive[b]
16	64	64	16	64	64	64
17	inactive[b]	inactive[b]	64	inactive[b]	inactive[b]	inactive[b]
18	4	2	2	4	2	4
norfloxacin	0.5	0.5	128	0.5	32	8

[a] Expressed as MIC (in μg/mL). [b] MIC > 128 μg/mL.

correlate them, and it was proven that the relative configurations of the asymmetric centers C-1, C-11, and C-12 remained unchanged (Scheme 1).[5,7] In the present study it was shown using the observed NOE enhancements that the relative configuration of C-12 of these compounds should be inverted, a fact that was also verified through the single-crystal X-ray diffraction analysis of **10**. The absolute configuration of **18** was determined by application of a modified Mosher's method.[10] When **18** was treated with (*R*)- and (*S*)-MTPA chloride, the secondary hydroxy group at C-14 reacted to give the (*S*)- and (*R*)-MTPA derivatives (**18a** and **18b**), respectively. The ^{1}H NMR chemical shifts of **18a** and **18b** were assigned by analysis of ^{1}H NMR, HSQC, and COSY spectra. The calculation of the $\Delta\delta_{S-R}$ values, shown in Figure 2, clearly defined the absolute configuration of C-14 as *R* and, subsequently, on the basis of its relative configuration, established the absolute configuration of **18** as depicted. Because compounds **2**, **4**−**10**, **12**, **13**, and **18** were clearly correlated through the chemical interconversions described above, the absolute configurations of **2**, **4**−**10**, **12**, and **13** are also as shown. The absolute configurations of metabolites **1**, **3**, **11**, **14**, and **15** were not determined, but on the basis of biogenetic considerations they are expected to be the same.

In addition to metabolites **1**−**15**, two known natural products were isolated and identified as (1*R*,2*E*,4*R*,7*E*,11*S*,12*R*)-18-hydroxy-2,7-dolabelladiene (**16**) and (1*R*,2*E*,4*R*,7*E*,10*S*,11*S*,12*R*)-10-acetoxy-18-hydroxy-2,7-dolabelladiene (**17**) by comparison of their spectroscopic and physical characteristics with those reported in the literature.[11] Even though the absolute configurations of **16** and **17** were not established, they are expected to be the same as those of **1**−**15** on the basis of a common biogenetic route. Furthermore, the ^{1}H and ^{13}C NMR chemical shifts for compounds **4**, **9**, **10**, and **13** are presented in Tables 1−4, supplementing the relevant literature, since only a few characteristic ^{1}H NMR resonances were available.

Comprehensive examination of the spectroscopic data for compounds **1**−**12**, **15**, and **18**, as well as for other previously described dolabellanes featuring an isopropenyl group,[12,13] revealed that the chemical shift of C-19 is very characteristic of the orientation of methine H-12 relative to H-11 and H_3-15. Specifically, when H-12 is *cis*- and *trans*-oriented in relation to H-11 and H_3-15, respectively, C-19 resonates at higher frequencies (δ_C 22.5 to 25.5), whereas when H-12 is *trans*- and *cis*-oriented relative to H-11 and H_3-15, respectively, C-19 resonates at lower frequencies (δ_C 18.0 to 19.5).

Compounds **1**−**18** were evaluated for their antibacterial activities against a panel of six strains of *Staphylococcus aureus*. These included a standard laboratory strain (ATCC 25923), two epidemic MRSA strains (EMRSA-15 and EMRSA-16), a macrolide-resistant variant (RN4220), and two multi-drug-resistant effluxing strains (SA1199B and XU212). According to the results of the antibacterial activity assessment (Table 5), the most active compound against all tested bacterial strains was the semisynthetic alcohol **18**, with MIC values in the range 2−4 μg/mL. Interestingly, metabolite **5**, which is the epimer of **18** at C-14, exhibited moderate activity against strain EMRSA-16 with a MIC value of 8 μg/mL, but only weak activity against the other strains, with MIC values ranging from 32 to 128 μg/mL. Metabolite **14** was moderately active against all tested strains, with MIC values in the range 8−16 μg/mL, while compounds **2**, **4**, **12**, **13**, and **16** displayed moderate activity only against strain EMRSA-16, with MIC values between 4 and 16 μg/mL, but weak or no activity against the other strains. Thus, it seems that strain EMRSA-16 is fairly susceptible to dolabellane diterpenes. It is worth noting that the majority of the dolabellanes that demonstrated antibacterial activity against the tested strains possessed a hydroxy group, whereas the presence of a ketone functionality at C-14 rendered the dolabellanes inactive.

EXPERIMENTAL SECTION

General Experimental Procedures. Optical rotations were measured on a Perkin-Elmer model 341 polarimeter with a 1 dm cell.

UV spectra were obtained on a Shimadzu UV-160A spectrophotometer. IR spectra were obtained on a Paragon 500 Perkin-Elmer spectrometer. NMR spectra were recorded on Bruker AC 200 and Bruker DRX 400 spectrometers. Chemical shifts are given on a δ (ppm) scale using TMS as internal standard. The 2D experiments (HSQC, HMBC, COSY, NOESY) were performed using standard Bruker pulse sequences. High-resolution mass spectrometric data were provided by the University of Notre Dame, Department of Chemistry and Biochemistry, Notre Dame, IN, USA. Low-resolution EI mass spectra were measured on a Hewlett-Packard 5973 mass spectrometer. Column chromatography separations were performed with Kieselgel 60 (Merck). HPLC separations were conducted using a CECIL 1100 Series liquid chromatography pump equipped with a GBC LC-1240 refractive index detector, using the following columns: (i) Spherisorb S10W (Phase Sep, 25 cm × 10 mm), (ii) Econoshpere Silica 10u (Grace, 25 cm × 10 mm), and (iii) Chiralcel OD 10 μm (Daicel Chemical Industries Ltd., 25 cm × 10 mm). TLC was performed with Kieselgel 60 F_{254} (Merck aluminum support plates), and spots were detected after spraying with 15% H_2SO_4 in MeOH reagent and heating at 100 °C for 1 min. The lyophilization was carried out in a Freezone 4.5 freeze-dry system (Labconco).

Plant Material. Specimens of *Dilophus spiralis* were collected by hand on Elafonissos Island (GPS coordinates 36°30′ N, 22°58′ E), south of Peloponnese, Greece, at a depth of 0.1−1 m, in April 2004. A voucher specimen of the alga has been deposited at the Herbarium of the Department of Pharmacognosy and Chemistry of Natural Products, University of Athens (ATPH/MO/159).

Extraction and Isolation. Specimens of the freeze-dried alga (272 g) were exhaustively extracted with CH_2Cl_2 and subsequently with MeOH at room temperature. Evaporation of the solvents in vacuo afforded two dark green oily residues. The CH_2Cl_2 residue (9.2 g) was subjected to vacuum column chromatography on silica gel, using cyclohexane with increasing amounts of EtOAc, followed by EtOAc with increasing amounts of MeOH as the mobile phase, to yield 15 fractions (A1−A15). Fractions A1 (100% cyclohexane, 131.4 mg) and A2 (10% EtOAc in cyclohexane, 18.3 mg) were separately and repeatedly purified by normal-phase HPLC, using *n*-hexane (100%) as eluent, to afford **4** (39.6 mg) and **15** (0.9 mg). Fraction A3 (20% EtOAc in cyclohexane, 1.17 g) was further fractionated by gravity column chromatography on silica gel, using cyclohexane with increasing amounts of EtOAc as the mobile phase, to yield 21 fractions (A3a−A3u). Fraction A3b (1% EtOAc in cyclohexane, 355.7 mg) was subjected to gravity column chromatography on silica gel, using cyclohexane with increasing amounts of CH_2Cl_2, followed by CH_2Cl_2 with increasing amounts of EtOAc as the mobile phase, to afford 11 fractions (A3b1−A3b11). Fractions A3b8 (100% CH_2Cl_2, 55.6 mg) and A3b9 (50% EtOAc in CH_2Cl_2, 195.6 mg) were separately purified by normal-phase HPLC, using cyclohexane/EtOAc (99:1) and subsequently *n*-hexane/EtOAc (99:1) as eluent, to yield **2** (185.6 mg), **3** (2.8 mg), and **6** (1.9 mg). Fractions A3c (1% EtOAc in cyclohexane, 162.9 mg) and A3d (1% EtOAc in cyclohexane, 55.3 mg) were separately purified by normal-phase HPLC, using *n*-hexane/EtOAc (98:2 and subsequently 99:1) as eluent, to afford **1** (1.1 mg), **2** (96.5 mg), **3** (1.5 mg), **8** (29.1 mg), and **14** (0.8 mg). Fractions A3i (2% EtOAc in cyclohexane, 81.7 mg) and A3j (2% EtOAc in cyclohexane, 28.2 mg) were purified separately by normal-phase HPLC, using cyclohexane/EtOAc (95:5) as eluent, to yield **16** (21.2 mg). Fraction A3l (10% EtOAc in cyclohexane, 81.9 mg) was subjected to gravity column chromatography on silica gel, using cyclohexane with increasing amounts of EtOAc as the mobile phase, to afford 10 fractions (A3l1−A3l10). Fraction A3l6 (6% EtOAc in cyclohexane, 7.6 mg) was purified by normal-phase HPLC, using cyclohexane/EtOAc (90:10) as eluent, to yield **5** (1.4 mg). Fraction A4 (30% EtOAc in cyclohexane, 3.58 g) was further fractionated by vacuum column chromatography on silica gel, using cyclohexane with increasing amounts of EtOAc, followed by EtOAc with increasing amounts of MeOH as the mobile phase, to afford nine fractions (A4a−A4i). Fraction A4b (10% EtOAc in cyclohexane, 46.1 mg) was purified by normal-phase HPLC, using cyclohexane/EtOAc (98:2) as eluent, to yield **1** (0.4 mg), **2** (12.8 mg), **8** (2.2 mg), **12** (0.4 mg), and **13** (1.2 mg). Fraction A4c (20% EtOAc in cyclohexane, 812.3 mg) was subjected to gravity column chromatography on silica gel, using cyclohexane with increasing amounts of EtOAc, followed by EtOAc with increasing amounts of MeOH as the mobile phase, to afford 23 fractions (A4c1−A4c23). Fractions A4c2 (1% EtOAc in cyclohexane, 174.3 mg), A4c3 (1% EtOAc in cyclohexane, 129.8 mg), and A4c4 (1% EtOAc in cyclohexane, 9.9 mg) were separately purified by normal-phase HPLC, using *n*-hexane/EtOAc (97:3) and subsequently *n*-hexane/2-propanol (99.5:0.5) as eluent, to yield **1** (1.4 mg), **2** (144.8 mg), **3** (2.7 mg), **8** (2.4 mg), and **12** (7.8 mg). Fractions A4c10 (2% EtOAc in cyclohexane, 17.0 mg), A4c11 (3% EtOAc in cyclohexane, 10.8 mg), A4c12 (5% EtOAc in cyclohexane, 18.7 mg), A4c13 (7% EtOAc in cyclohexane, 47.0 mg), A4c14 (10% EtOAc in cyclohexane, 46.6 mg), A4c15 (12% EtOAc in cyclohexane, 138.5 mg), A4c16 (20% EtOAc in cyclohexane, 13.3 mg), and A4c17 (20% EtOAc in cyclohexane, 24.7 mg) were separately purified by normal-phase HPLC, using cyclohexane/EtOAc (90:10) and subsequently *n*-hexane/2-propanol (90:10, 87:13, and 82:18) as eluent, to afford **5** (16.3 mg), **7** (27.2 mg), **9** (13.6 mg), **10** (17.6 mg), **11** (5.2 mg), and **16** (0.9 mg). The MeOH residue (32.8 g) was subjected to vacuum column chromatography on silica gel, using cyclohexane with increasing amounts of EtOAc, followed by EtOAc with increasing amounts of MeOH as the mobile phase, to yield 14 fractions (B1−B14). Fraction B1 (10% EtOAc in cyclohexane, 51.0 mg) was purified by normal-phase HPLC, using *n*-hexane (100%) as eluent, to afford **4** (13.3 mg). Fraction B3 (20% EtOAc in cyclohexane, 361.0 mg) was repeatedly purified by normal-phase HPLC, using cyclohexane/EtOAc (90:10) and subsequently *n*-hexane/2-propanol (86:14 and 83:17) as eluent, to yield **2** (3.3 mg), **5** (9.0 mg), **9** (5.4 mg), **11** (3.8 mg), **16** (2.4 mg), and **17** (0.9 mg).

*(1R,3E,7E,11S,12R)-14-Oxo-3,7,18-dolabellatriene (**1**):* colorless oil; $[\alpha]_D^{20}$ −76 (*c* 0.09, $CHCl_3$); UV ($CHCl_3$) λ_{max} (log ε) 245.5 (2.96) nm; IR (thin film) ν_{max} 2971, 2916, 1735, 1275 cm^{-1}; ^1H NMR data, see Table 1; ^{13}C NMR data, see Table 2; EIMS 70 eV *m*/*z* (rel int %) 286 (22), 271 (22), 253 (10), 243 (6), 228 (6), 213 (9), 203 (7), 189 (43), 175 (23), 161 (22), 147 (28), 135 (42), 121 (42), 107 (85), 91 (87), 79 (79), 67 (100), 53 (53); HRFABMS *m*/*z* 286.2303 $[M]^+$ (calcd for $C_{20}H_{30}O$, 286.2297).

*(1R,3Z,7E,11S,12S)-14-Oxo-3,7,18-dolabellatriene (**3**):* yellowish oil; $[\alpha]_D^{20}$ −98 (*c* 0.09, $CHCl_3$); UV ($CHCl_3$) λ_{max} (log ε) 241.8 (2.28) nm; IR (thin film) ν_{max} 2958, 2920, 1734, 1454 cm^{-1}; ^1H NMR data, see Table 1; ^{13}C NMR data, see Table 2; EIMS 70 eV *m*/*z* (rel int %) 286 (11), 271 (15), 253 (3), 243 (6), 229 (4), 217 (7), 203 (8), 189 (28), 175 (19), 163 (55), 150 (75), 135 (100), 121 (39), 107 (57), 93 (57), 81 (49), 67 (48), 55 (34); HRFABMS *m*/*z* 287.2366 $[M + H]^+$ (calcd for $C_{20}H_{31}O$, 287.2375).

*(1R,3E,7E,11S,12S)-3,7,18-Dolabellatriene (**4**):* yellowish oil; $[\alpha]_D^{20}$ +41.0 (*c* 0.10, $CHCl_3$); UV ($CHCl_3$) λ_{max} (log ε) 243.8 (2.57) nm; IR (thin film) ν_{max} 2930, 2854, 1645, 1454 cm^{-1}; ^1H NMR data, see Table 1; ^{13}C NMR data, see Table 2; EIMS 70 eV *m*/*z* (rel int %) 272 (38), 257 (26), 243 (4), 229 (33), 215 (10), 203 (12), 189 (35), 175 (43), 161 (54), 147 (63), 135 (75), 121 (90), 107 (93), 93 (100), 81 (73), 79 (72), 67 (67), 55 (47); HRFABMS *m*/*z* 272.2493 $[M]^+$ (calcd for $C_{20}H_{32}$, 272.2504).

*(1R,3E,7E,11S,12S,14S)-14-Hydroxy-3,7,18-dolabellatriene (**5**):* colorless oil; $[\alpha]_D^{20}$ +44 (*c* 0.06, $CHCl_3$); UV ($CHCl_3$) λ_{max} (log ε) 244.0 (2.48) nm; IR (thin film) ν_{max} 3370, 2936, 2360, 1290 cm^{-1}; ^1H NMR data, see Table 1; ^{13}C NMR data, see Table 2; EIMS 70 eV *m*/*z* (rel int %) 288 (5), 270 (12), 255 (22), 227 (17), 213 (12), 201 (15), 191 (38), 173 (25), 163 (41), 145 (51), 135 (76), 121 (81), 107 (94), 95 (86), 81 (100), 67 (64), 55 (69); HRFABMS *m*/*z* 288.2479 $[M]^+$ (calcd for $C_{20}H_{32}O$, 288.2453).

dx.doi.org/10.1021/np1006586 |*J. Nat. Prod.* 2011, 74, 213–222

(1R,3E,7E,11S,12S,14S)-14-Acetoxy-3,7,18-dolabellatriene (***6***): colorless oil; $[\alpha]_D^{20}$ +29 (*c* 0.07, $CHCl_3$); UV ($CHCl_3$) λ_{max} (log ε) 241.4 (2.27) nm; IR (thin film) ν_{max} 2967, 2920, 1734, 1538 cm^{-1}; ^1H NMR data, see Table 1; ^{13}C NMR data, see Table 2; EIMS 70 eV *m/z* (rel int %) 330 (1), 315 (1), 288 (1), 270 (50), 255 (46), 241 (8), 227 (31), 213 (17), 201 (20), 187 (32), 173 (42), 159 (55), 145 (69), 133 (93), 119 (100), 105 (69), 91 (67), 81 (54), 67 (42), 55 (43); HRFABMS *m/z* 330.2535 $[M]^+$ (calcd for $C_{22}H_{34}O_2$, 330.2559).

(1R,3S,4S,7E,11S,12S,14S)-14-Acetoxy-3,4-epoxy-7,18-dolabelladiene (***9***): yellowish oil; $[\alpha]_D^{20}$ +47.8 (*c* 0.25, $CHCl_3$); UV ($CHCl_3$) λ_{max} (log ε) 243.0 (2.18) nm; IR (thin film) ν_{max} 2962, 2907, 1734, 1243 cm^{-1}; ^1H NMR data, see Table 3; ^{13}C NMR data, see Table 4; EIMS 70 eV *m/z* (rel int %) 346 (1), 328 (8), 286 (61), 271 (28), 268 (27), 253 (25), 243 (19), 228 (33), 213 (29), 201 (41), 187 (51), 173 (47), 159 (62), 145 (79), 133 (100), 119 (92), 105 (96), 91 (81), 79 (49), 67 (25), 55 (31); HRFABMS *m/z* 346.2488 $[M]^+$ (calcd for $C_{22}H_{34}O_3$, 346.2508).

(1R,3E,7S,8S,11S,12S)-7,8-Epoxy-14-oxo-3,18-dolabelladiene (***10***): colorless crystals; $[\alpha]_D^{20}$ −66.4 (*c* 0.19, $CHCl_3$); UV ($CHCl_3$) λ_{max} (log ε) 241.5 (2.24) nm; IR (thin film) ν_{max} 2966, 2925, 2859, 1733, 1457 cm^{-1}; ^1H NMR data, see Table 3; ^{13}C NMR data, see Table 4; EIMS 70 eV *m/z* (rel int %) 302 (39), 284 (78), 269 (41), 241 (19), 233 (14), 227 (16), 215 (31), 205 (24), 187 (57), 173 (45), 163 (92), 159 (57), 150 (58), 145 (63), 135 (90), 119 (75), 105 (94), 91 (100), 79 (69), 67 (58), 55 (50); HRFABMS *m/z* 303.2325 $[M + H]^+$ (calcd for $C_{20}H_{31}O_2$, 303.2324).

(1R,3Z,7S,8S,11S,12S)-7,8-Epoxy-14-oxo-3,18-dolabelladiene (***11***): colorless oil; $[\alpha]_D^{20}$ −13.0 (*c* 0.25, $CHCl_3$); UV ($CHCl_3$) λ_{max} (log ε) 242.5 (2.16) nm; IR (thin film) ν_{max} 2935, 1733, 1275 cm^{-1}; ^1H NMR data, see Table 3; ^{13}C NMR data, see Table 4; EIMS 70 eV *m/z* (rel int %) 302 (14), 284 (63), 269 (22), 256 (11), 241 (15), 215 (25), 205 (20), 187 (58), 173 (40), 163 (96), 159 (55), 150 (53), 145 (68), 135 (80), 119 (80), 105 (97), 91 (100), 79 (68), 67 (55), 55 (49); HRFABMS *m/z* 303.2330 $[M + H]^+$ (calcd for $C_{20}H_{31}O_2$, 303.2324).

(1R,3E,7E,11R,12R)-12-Hydroxy-3,7-dolabelladiene (***14***): colorless oil; $[\alpha]_D^{20}$ +16 (*c* 0.09, $CHCl_3$); UV ($CHCl_3$) λ_{max} (log ε) 242.5 (2.23) nm; IR (thin film) ν_{max} 3330, 2958, 2877, 1276 cm^{-1}; ^1H NMR data, see Table 3; ^{13}C NMR data, see Table 4; ^1H NMR (400 MHz, C_6D_6) δ 5.03 (1H, m, H-3), 5.02 (1H, m, H-7), 2.15 (1H, m, H-9a), 2.14 (1H, m, H-2a), 2.09 (2H, m, H-6), 2.05 (2H, m, H-5), 1.90 (1H, ddd, 13.8, 12.3, 1.9 Hz, H-9b), 1.80 (1H, dd, 14.9, 5.2 Hz, H-2b), 1.75 (1H, m, H-18), 1.71 (1H, m, H-10a), 1.67 (1H, m, H-11), 1.64 (1H, m, H-14a), 1.54 (1H, m, H-13a), 1.53 (3H, s, H-17), 1.46 (3H, s, H-16), 1.39 (1H, m, H-14b), 1.30 (1H, m, H-13b), 1.29 (1H, m, H-10b), 1.07 (3H, s, H-15), 0.93 (3H, d, 6.7 Hz, H-20), 0.88 (3H, d, 6.8 Hz, H-19); EIMS 70 eV *m/z* (rel int %) 290 (1), 272 (12), 257 (10), 247 (3), 229 (25), 216 (4), 201 (5), 189 (18), 175 (9), 161 (30), 149 (20), 135 (100), 121 (71), 107 (54), 93 (49), 81 (31), 67 (27), 55 (20); HRFABMS *m/z* 290.2629 $[M]^+$ (calcd for $C_{20}H_{34}O$, 290.2610).

(1R,2E,4R,7E,11S,12R)-2,7,18-Dolabellatriene (***15***): colorless oil; $[\alpha]_D^{20}$ −21 (*c* 0.03, $CHCl_3$); UV ($CHCl_3$) λ_{max} (log ε) 242.2 (2.53) nm; IR (thin film) ν_{max} 2948, 2920, 1538 cm^{-1}; ^1H NMR data, see Table 3; ^{13}C NMR data, see Table 4; EIMS 70 eV *m/z* (rel int %) 272 (32), 257 (25), 243 (5), 229 (68), 215 (10), 201 (13), 190 (25), 175 (73), 161 (47), 147 (71), 133 (60), 121 (67), 107 (100), 93 (83), 81 (74), 67 (57), 55 (50); HRFABMS *m/z* 272.2495 $[M]^+$ (calcd for $C_{20}H_{32}$, 272.2504).

Reduction of 2. Compound **2** (48.0 mg) was treated with $NaBH_4$ (50.0 mg) in MeOH (10 mL) and left under constant stirring at room temperature for 1 h. The reaction was quenched by the addition of H_2O (3 mL), and the mixture was evaporated in vacuo. The residue was purified by normal-phase HPLC, using cyclohexane/EtOAc (90:10) as eluent, to obtain **5** (7.3 mg) and **18** (31.2 mg).

(1R,3E,7E,11S,12S,14R)-14-Hydroxy-3,7,18-dolabellatriene (***18***): colorless oil; $[\alpha]_D^{20}$ +12.0 (*c* 0.10, $CHCl_3$); UV ($CHCl_3$) λ_{max} (log ε) 244.0 (2.31) nm; IR (thin film) ν_{max} 3389, 2926, 2360, 1279 cm^{-1}; ^1H NMR data, see Table 1; ^{13}C NMR data, see Table 2; EIMS 70 eV *m/z* (rel int %) 288 (8), 270 (14), 255 (12), 245 (6), 227 (13), 220 (14), 205 (12), 189 (21), 173 (17), 163 (56), 149 (40), 135 (79), 121 (78), 107 (92), 95 (84), 81 (100), 67 (63), 55 (70); HRFABMS *m/z* 288.2426 $[M]^+$ (calcd for $C_{20}H_{32}O$, 288.2453).

Epoxidation of 4. A solution of *m*-chloroperbenzoic acid (20.0 mg) in benzene (1 mL) was added dropwise to a solution of compound **4** (20.0 mg) in benzene (2 mL), and the mixture was left under constant stirring at room temperature for 30 min. The reaction was quenched by the addition of 10% Na_2SO_3 (3 mL), and the mixture was partitioned between the aqueous and the organic layer. The organic layer was washed with 5% $NaHCO_3$ and subsequently H_2O. After evaporation of the organic layer in vacuo, the residue was purified by normal-phase HPLC, using *n*-hexane/2-propanol (99.75:0.25) as eluent, to afford **8** (6.3 mg) and **12** (5.9 mg).

Acetylation of 5. Compound **5** (2.8 mg) was treated with Ac_2O (1 mL) in pyridine (1 mL) and left under constant stirring at 70 °C for 16 h. The reaction was quenched by the addition of H_2O (1 mL), and the mixture was evaporated in vacuo. The residue was purified by normal-phase HPLC, using cyclohexane/EtOAc (99:1) as eluent, to obtain **6** (2.3 mg).

Preparation of MTPA Derivatives of 18. Compound **18** (3.3 mg) was treated with (*R*)-MTPA chloride (5 μL) in freshly distilled dry pyridine (1 mL) and left under constant stirring at room temperature for 16 h. The reaction was quenched by the addition of H_2O (1 mL) and CH_2Cl_2 (3 mL), and the mixture was partitioned between the aqueous and the organic layer. After evaporation of the organic layer in vacuo, the residue was purified by normal-phase HPLC, using cyclohexane/EtOAc (95:5) as eluent, to give the (*S*)-MTPA derivative (**18a**, 3.2 mg). The (*R*)-MTPA derivative (**18b**, 2.4 mg) was prepared with (*S*)-MTPA chloride and purified in the same manner.

(S)-MTPA Derivative of ***18*** (***18a***): ^1H NMR (400 MHz, $CDCl_3$) δ 7.53 (2H, m, Ar-H), 7.39 (3H, m, Ar-H), 5.07 (1H, dd, 9.2, 6.0 Hz, H-3), 4.97 (1H, dd, 9.1, 7.1 Hz, H-14), 4.89 (1H, brs, H-20a), 4.79 (1H, dd, 9.5, 4.1 Hz, H-7), 4.66 (1H, brs, H-20b), 3.55 (3H, s, OMe), 2.65 (1H, m, H-12), 2.24 (1H, m, H-6a), 2.18 (1H, m, H-5a), 2.17 (1H, m, H-2α), 2.15 (1H, m, H-13β), 2.08 (1H, m, H-6b), 2.07 (1H, m, H-5b), 2.02 (1H, m, H-9a), 1.90 (1H, m, H-2β), 1.89 (1H, m, H-9b), 1.88 (1H, m, H-11), 1.81 (1H, m, H-13α), 1.70 (3H, s, H-19), 1.50 (3H, s, H-16), 1.47 (3H, s, H-17), 1.34 (1H, m, H-10a), 1.16 (1H, m, H-10b), 0.83 (3H, s, H-15).

(R)-MTPA Derivative of ***18*** (***18b***): ^1H NMR (400 MHz, $CDCl_3$) δ 7.51 (2H, m, Ar-H), 7.39 (3H, m, Ar-H), 5.10 (1H, dd, 9.3, 6.6 Hz, H-3), 4.92 (1H, dd, 8.9, 7.0 Hz, H-14), 4.86 (1H, brs, H-20a), 4.80 (1H, dd, 8.5, 3.7 Hz, H-7), 4.62 (1H, brs, H-20b), 3.52 (3H, s, OMe), 2.65 (1H, ddd, 13.3, 7.1, 7.1 Hz, H-12), 2.24 (1H, m, H-6a), 2.21 (1H, m, H-2α), 2.17 (1H, m, H-5a), 2.14 (1H, m, H-13β), 2.08 (1H, m, H-6b), 2.07 (1H, m, H-5b), 2.02 (1H, m, H-9a), 1.90 (1H, m, H-2β), 1.89 (1H, m, H-9b), 1.88 (1H, m, H-11), 1.68 (1H, m, H-13α), 1.67 (3H, s, H-19), 1.51 (3H, s, H-16), 1.47 (3H, s, H-17), 1.34 (1H, m, H-10a), 1.16 (1H, m, H-10b), 0.94 (3H, s, H-15).

Single-Crystal X-ray Analysis of 10. Compound **10** crystallized after slow evaporation of a saturated solution of EtOAc/$CHCl_3$ (1:1) as colorless blocks. Single-crystal X-ray diffraction data were collected at 120 K on a Nonius Kappa CCD diffractometer with graphite-monochromated Mo Kα radiation (λ = 0.71073 Å) using the Nonius Collect Software. The space group was determined on the basis of the systematic absences and confirmed by the successful structure solution and refinement. The structure was solved by direct methods and refined based on F^2 using the WINGX package. All non-hydrogen atoms were refined with anisotropic thermal parameters, whereas all hydrogen atoms were located in the calculated positions and refined in a rigid group model.

In the absence of atoms with significant anomalous scattering, the absolute configuration of **10** was indeterminate.

Crystallographic Data of ***10***: $C_{20}H_{30}O_2$, M = 302.4, 0.52 × 0.24 × 0.22 mm, T = 120(2) K, orthorhombic, space group $P2_12_12_1$(#19) with a = 7.7877(11) Å, b = 13.9979(13) Å, c = 15.5830(16) Å, V = 1698.73(3) Å^3, Z = 4, Z' = 1, D_{calcd} = 1.183 Mg/m^3, μ = 0.074 mm^{-1}, F(000) = 664, $2\theta_{max}$ = 55.00°, 16 541 collected reflections, 3866 independent reflections (R_{int} = 0.0467), R_1 = 0.0450, wR_2 = 0.0939, GoF = 0.994 for 2997 reflections (201 parameters) with $I > 2\sigma(I)$, R_1 = 0.0722, wR_2 = 0.1080, GoF = 0.994 for all 3866 reflections, max./min. residual electron density +0.182/−0.179 e Å^3.

Evaluation of Antibacterial Activity. Standard strain ATCC 25923 and strain XU212, which possesses the gene encoding the TetK tetracycline efflux protein, were provided by Dr. E. Udo. Strain SA1199B, which possesses the gene encoding the NorA quinolone efflux protein, was a generous gift of Prof. G. W. Kaatz. Strain RN4220, which possesses the gene encoding the MsrA macrolide efflux protein, was provided by Dr. J. Cove. The epidemic methicillin-resistant strains EMRSA-15 and EMRSA-16 were obtained from Dr. P. Stapleton. All strains were cultured on nutrient agar and incubated for 24 h at 37 °C prior to the determination of minimum inhibitory concentration (MIC) values. Compounds **1**−**18** were dissolved in DMSO and subsequently diluted in Mueller-Hinton broth (MHB) to give a starting concentration of 512 μg/mL. Bacterial inocula equivalent to the 0.5 McFarland turbidity standard were prepared in normal saline for each strain and diluted to a final inoculum density of 5 × 10^5 cfu/mL. MHB supplemented with 10 mg/L Mg^{2+} and 20 mg/L Ca^{2+} (125 μL/well) was dispensed into wells 1−11 of each row of 96-well microtiter plates. The compound solution (125 μL) was added to the first well of each row and was serially diluted across the row, leaving well 11 empty for growth control. The final volume was dispensed into well 12, which being free of MHB or inoculum served as the sterility control. The inoculum (125 μL/well) was added to wells 1−11 of each row, and the microtiter plates were incubated for 18 h at 37 °C. The lowest concentration at which no bacterial growth was observed was recorded as the MIC. The observation was confirmed by the addition of a 5 mg/mL methanolic solution of 3-(4,5-dimethylthiazol-2-yl)-2,5-diphenyltetrazolium bromide (MTT, 20 μL/well) and further incubation for 20 min at 37 °C. Bacterial growth was indicated by a color alteration from yellow to dark blue. Norfloxacin was used as a positive control. The highest concentration of DMSO remaining after dilution (3.125% v/v) caused no inhibition of bacterial growth. All samples were tested in triplicate. Culture media were obtained from Oxoid, whereas all other chemicals were obtained from Sigma-Aldrich.

■ ASSOCIATED CONTENT

Ⓢ Supporting Information. ^{1}H and ^{13}C NMR spectra of compounds **1**−**18**, NOESY spectra of compounds **1**−**15** and **18**, NMR data in tabular form of compounds **2**, **7**, **8**, and **12**, and CIF data for the crystal structure of metabolite **10**. This material is available free of charge via the Internet at http://pubs.acs.org.

■ AUTHOR INFORMATION

Corresponding Author

*To whom correspondence should be addressed. Tel/Fax: +30-210-7274592. E-mail: roussis@pharm.uoa.gr.

Notes

⊥Deceased on May 12, 2010.

■ ACKNOWLEDGMENT

This study was partially supported by a "Kapodistrias" grant from the University of Athens.

■ REFERENCES

(1) Blunt, J. W.; Copp, B. R.; Munro, M. H. G.; Northcote, P. T.; Prinsep, M. R. *Nat. Prod. Rep.* **2010**, *27*, 165−237, and earlier reviews in this series.

(2) *MarinLit Database*; Department of Chemistry, University of Canterbury: http://www.chem.canterbury.ac.nz/marinlit/marinlit.shtml.

(3) Ioannou, E.; Quesada, A.; Vagias, C.; Roussis, V. *Tetrahedron* **2008**, *64*, 3975–3979.

(4) Ioannou, E.; Zervou, M.; Ismail, A.; Ktari, L.; Vagias, C.; Roussis, V. *Tetrahedron* **2009**, *65*, 10565–10572.

(5) Amico, V.; Oriente, G.; Piattelli, M.; Tringali, C.; Fattorusso, E.; Magno, S.; Mayol, L. *Tetrahedron* **1980**, *36*, 1409–1414.

(6) Piattelli, M.; Tringali, C.; Neri, P.; Rocco, C. *J. Nat. Prod.* **1995**, *58*, 697–704.

(7) Amico, V.; Currenti, R.; Oriente, G.; Piattelli, M.; Tringali, C. *Phytochemistry* **1981**, *20*, 848–849.

(8) Crystallographic data (excluding structure factors) for compound **11** have been deposited with the Cambridge Crystallographic Data Centre as supplementary publication no. CCDC 759848. Copies of the data can be obtained, free of charge, on application to CCDC, 12 Union Road, Cambridge CB2 1EZ, UK (fax: +44-(0)1223-336033 or e-mail: deposit@ccdc.cam.ac.uk).

(9) Duran, R.; Zubia, E.; Ortega, M. J.; Salva, J. *Tetrahedron* **1997**, *53*, 8675–8688.

(10) Seco, J. M.; Quiñoá, E.; Riguera, R. *Chem. Rev.* **2004**, *104*, 17–117.

(11) Ireland, C.; Faulkner, D. J. *J. Org. Chem.* **1977**, *42*, 3157–3162.

(12) Ramírez, M. C.; Toscano, R. A.; Arnason, J.; Omar, S.; Cerda-García-Rojas, C. M.; Mata, R. *Tetrahedron* **2000**, *56*, 5085–5091.

(13) Wang, Y.; Harrison, L. J.; Tan, B. C. *Tetrahedron* **2009**, *65*, 4035–4043.

J Antimicrob Chemother 2010; **65**: 2101–2107
doi:10.1093/jac/dkq313 Advance Access publication 18 August 2010

Journal of Antimicrobial Chemotherapy

Anti-tubercular screening of natural products from Colombian plants: 3-methoxynordomesticine, an inhibitor of MurE ligase of *Mycobacterium tuberculosis*

Juan D. Guzman[1–4], Antima Gupta[1], Dimitrios Evangelopoulos[1], Chandrakala Basavannacharya[1], Ludy C. Pabon[2], Erika A. Plazas[2], Diego R. Muñoz[2], Wilman A. Delgado[2], Luis E. Cuca[2], Wellman Ribon[3]†, Simon Gibbons[4] and Sanjib Bhakta[1]*

[1]*Department of Biological Sciences, Institute of Structural and Molecular Biology, Birkbeck College, University of London, London WC1E 7HX, UK;* [2]*Departamento de Química, Facultad de Ciencias, Universidad Nacional de Colombia, Carrera 30 No. 45–03, Bogotá, Colombia;* [3]*Subdirección de Investigación, Instituto Nacional de Salud, Calle 26 No. 51–20, Bogotá, Colombia;* [4]*Department of Pharmaceutical and Biological Chemistry, The School of Pharmacy, University of London, London WC1N 1AX, UK*

*Corresponding author. Tel: +44-(0)207-631-6355 (office)/+44-(0)207-079-0799 (lab); Fax: +44-(0)207-631-6246; E-mail: s.bhakta@bbk.ac.uk
†Present address: Escuela de Bacteriología y Laboratorio Clínico, Facultad de Salud, Universidad Industrial de Santander, Carrera 32 No. 29–31, Bucaramanga, Colombia.

Received 22 April 2010; returned 14 June 2010; revised 6 July 2010; accepted 22 July 2010

Objectives: New anti-mycobacterial entities with novel mechanisms of action are clinically needed for treating resistant forms of tuberculosis. The purpose of this study was to evaluate anti-tubercular activity and selectivity of seven recently isolated natural products from Colombian plants.

Methods: MICs were determined using a liquid medium growth inhibition assay for *Mycobacterium tuberculosis* H_{37}Rv and both solid and liquid media growth inhibition assays for *Mycobacterium bovis* BCG. *Escherichia coli* growth inhibition and mammalian macrophage cell toxicity were evaluated to establish the degree of selectivity of the natural product against whole cell organisms. Enzymatic inhibition of ATP-dependent MurE ligase from *M. tuberculosis* was assayed using a colorimetric phosphate detection method. The most active compound, 3-methoxynordomesticine hydrochloride, was further investigated on *M. bovis* BCG for its inhibition of sigmoidal growth, acid-fast staining and viability counting analysis.

Results: Aporphine alkaloids were found to be potent inhibitors of slow-growing mycobacterial pathogens showing favourable selectivity and cytotoxicity. In terms of their endogenous action, the aporphine alkaloids were found inhibitory to *M. tuberculosis* ATP-dependent MurE ligase at micromolar concentrations. A significantly low MIC was detected for 3-methoxynordomesticine hydrochloride against both *M. bovis* BCG and *M. tuberculosis* H_{37}Rv.

Conclusions: Considering all the data, 3-methoxynordomesticine hydrochloride was found to be a potent anti-tubercular compound with a favourable specificity profile. The alkaloid showed MurE inhibition and is considered an initial hit for exploring related chemical space.

Keywords: TB, aporphine alkaloids, MurE inhibitors

Introduction

Tuberculosis (TB) is an ancient and contagious disease caused by infection with *Mycobacterium tuberculosis* complex.[1,2] It causes characteristic necrotic and caseotic lesions, notably in the lungs, but it may also affect the skin, lymph nodes, brain and almost every other organ. More than 9.3 million new cases and 1.8 million deaths were notified globally in 2008 according to the latest WHO report.[3] TB was declared to be a global health emergency because of the increase in HIV co-infection and the appearance of multidrug-resistant and extensively drug-resistant strains (MDR- and XDR-TB).[4] A TB burden also occurs as a consequence of low compliance due to the long and complex TB regimen and the lack of treatment or adapted treatment derived from the absence of appropriate health programmes.[5,6] New anti-mycobacterial entities with novel mechanisms of action are clinically needed for treating resistant forms of TB. A global effort among all sectors of society is required for controlling the burden of TB.[7]

Natural products are crucial sources of new antimicrobials because of their amazing chemical diversity and their validation

through centuries of evolution.[8,9] It is usual for plants (or microbes) to fight against environmental infections using their chemical arsenal of secondary metabolites and therefore many types of different structures have been reported to display an antimicrobial function.[10,11] Colombian Lauraceae, Magnoliaceae and Piperaceae species have been recently studied as sources for bioactive metabolites that might be useful in agricultural and medicinal applications. Ethno-medicinal *Ocotea macrophylla* Kunth (Lauraceae),[12] endangered *Dugandiodendron argyrotrichum* Lozano (Magnoliaceae),[13,14] spicy *Piper hispidum* Kunth[15] and aromatic *Piper eriopodon* CDC (Piperaceae) were included in this study for evaluating the anti-tubercular activity of some of their constitutive natural products.

The strategy used in this investigation was to screen the purified natural compounds for growth inhibition against two slow-growing mycobacteria (*Mycobacterium bovis* BCG and *M. tuberculosis* H_{37}Rv) and against gut bacteria (*Escherichia coli*) and mammalian macrophages (RAW264.7), in order to gain an idea of their mycobacterial specificity in whole cell experiments. Given the availability of recently characterized ATP-dependent MurE ligase from *M. tuberculosis*[16] of the peptidoglycan biosynthetic pathway, the activity of the enzyme was recorded in the presence of the natural products. The gene encoding for this enzyme occurs as a single copy in the *M. tuberculosis* genome[17] and was found to be essential for bacterial growth and survival.[18,19] Furthermore, a detailed study in *M. bovis* BCG involving the growth curve, acid-fast staining and viability counting was undertaken for the most active compound. To the best of our knowledge, this is the first instance in which a natural product is reported to have inhibitory activity against MurE ligase from any organism.

Materials and methods

Natural products and organisms

Natural products **1** and **2** were previously isolated from *O. macrophylla*,[12] **4** and **5** from *D. argyrotrichum*[13,14] and **6** from *P. hispidum*.[15] In this study, compound **3** was obtained in 75% yield by HCl treatment from compound **1** in ethanol and column chromatography on silica gel with CH_2Cl_2-AcOEt (97:3). ^{1}H and ^{13}C NMR spectroscopy and the two-dimensional techniques of correlation spectroscopy (COSY), heteronuclear multiple quantum coherence (HMQC) and heteronuclear multiple bond coherence (HMBC) were used to assign unambiguously the signals at δ 10.49 (1H, s) and 9.67 (1H, s) to the diastereoisomeric hydrogens on the positively charged nitrogen atom. The absolute configuration of C-6a was assigned as (*S*) due to a negative Cotton effect at 280 nm and a positive effect at 240 nm in the circular dichroism spectrum. The exact mass of the compound was determined by high-resolution electrospray ionization mass spectrometry in positive mode, obtaining the pseudo-molecular ion $[M+H]^+$ at 343.1440 *m/z*, corresponding to a molecular formula of $C_{19}H_{20}NO_5$. Compound **7** was obtained abundantly from an ethanolic extract of the leaves of *P. eriopodon* CDC. Briefly, 60 g of ethanolic extract from 1.2 kg of dried leaves was fractioned using Soxhlet extraction with petroleum ether, chloroform and methanol. The petroleum extract (30 g) was subjected to flash chromatography on silica gel, eluting with a toluene/ethyl acetate gradient. Fraction 3 was further purified by column chromatography on silica gel eluting with petroleum ether/toluene (4:6) to obtain 5.7 g of pure gibbilimbol-B (**7**). The chemical structure was identified by analysis of the ^{1}H and ^{13}C NMR spectra, which correlated exactly with reported data.[20] Boldine was purchased from Sigma-Aldrich.

M. tuberculosis H_{37}Rv (ATCC 27294), *M. bovis* BCG (ATCC 35734), *E. coli* JM109 (ATCC 53323), *Pseudomonas putida* KT2442 (ATCC 47054), *Staphylococcus aureus* (ATCC 25923) and murine RAW264.7 macrophages (ATCC TIB71) were used in this study.

Recombinant MurE overexpression and purification

M. tuberculosis MurE (Rv2158c) was overexpressed in *E. coli* BL21(DE3)-pLysS and purified using a reported protocol.[16] Briefly, transformed *E. coli* pSBC1 was grown in 1 L of Luria-Bertani broth in the presence of kanamycin until the optical density at 600 nm (OD_{600}) reached 0.6 and expression was induced with 1 mM IPTG at 20°C for 18 h. The cells were harvested, resuspended in lysis buffer and lysed by sonication on ice.[16] The cytoplasmic extract was separated from cell debris by ultracentrifugation and loaded onto an Ni^{2+}-NTA affinity column pre-equilibrated with lysis buffer. Elution with 100 mM imidazole and concentration by molecular weight filtration (10 kDa cut–off) afforded 8 mg of recombinant MurE.

Liquid culture-based microplate assay

The method employed was adapted from reported protocols.[21,22] Briefly, 200 mg of bacilli from a 14–28 day culture of *M. tuberculosis* H_{37}Rv in Löwenstein-Jensen slopes was diluted (1:10) in sterile water and further diluted (1:100) in Middlebrook 7H9 (BD Diagnostics) broth supplemented with 10% oleic acid/albumin/dextrose/catalase supplement (OADC; BD Diagnostics) and 0.2% glycerol. The same dilution procedure was performed for *M. bovis* BCG from a liquid culture having a cell density of 10^8 cfu/mL. The final cell density added to the microplates was 10^5 cfu/mL. From a sterile DMSO stock of the compounds at 50 g/L, a solution in liquid medium was prepared at 512 mg/L (final concentration of DMSO 0.5%). Rifampicin was included as a positive control at 8 mg/L. To a 96-well microplate, 100 μL of liquid medium was added and then the compounds were serially diluted 2-fold. An aliquot of 100 μL of the inoculum was added and the plates were sealed. Agitation was carried out manually every day, and after 6 days of incubation at 37°C the plates were carefully uncovered and 22 μL of a freshly prepared mixture (10:12) of 5 g/L methyl thiazolyl tetrazolium (MTT) and 20% Tween-80 was added. For *M. bovis* BCG, 30 μL of freshly prepared aqueous solution containing 0.05% resazurin and 0.1% Tween-80 was added to each well. Results were observed the next day after incubation at 37°C.

Solid plate-based spot culture growth inhibition assay

The spot culture growth inhibition assay was performed as reported elsewhere.[23] An aliquot of 5 mL of Middlebrook 7H10 (BD Diagnostics) supplemented with 0.2% glycerol and 10% OADC was added to a six-well microplate along with 5 μL of natural compounds in a solution of DMSO at a concentration of 50, 25, 10, 5, 1 and 0 g/L. Isoniazid was included at 1, 0.5, 0.2, 0.1, 0.05 and 0 g/L. Afterwards, 5 μL of an appropriately diluted mid-log phase (10^6 cfu/mL) *M. bovis* BCG culture was carefully dispensed into the centre of each well. Results were observed after 2 weeks of incubation at 37°C.

Antibacterial assay against E. coli, P. putida and S. aureus

A seed culture of *E. coli* JM109 was prepared in Luria-Bertani broth and grown overnight at 37°C with shaking at 200 rpm. Then to each tube 5 mL of a 100× diluted culture (10^6 cfu/mL) and 20 μL of the compounds at 50 g/L stock concentration were added to make a final concentration of 200 mg/L. Controls of isoniazid and kanamycin at the same concentration and two negative controls (with and without DMSO, final concentration 0.1%) were included. The cells were incubated with agitation at

200 rpm and OD_{600} was measured each hour up to the stationary phase. The MICs against *E. coli*, *P. putida* and *S. aureus* were determined in duplicate using a microdilution resazurin technique from 512 to 1 mg/L of the natural products following the CLSI (formerly NCCLS) guidelines.[24] Kanamycin was used as a positive control for Gram-negative bacteria and norfloxacin for Gram-positive bacteria.

Mammalian macrophage cytotoxicity assay

RAW264.7 macrophages were maintained in RPMI medium and passaged twice before the assay. The cells were detached using lidocaine–EDTA and mechanical tapping. Cell viability for macrophages was performed using a trypan blue assay and the cell density was adjusted to 10^5 cells/mL with RPMI. To a 96-well microplate, 2 μL aliquots of the 10 g/L natural product stocks in DMSO were added. Then 200 μL of RPMI was added to the first row and serially diluted 2-fold. Finally, 100 μL of diluted macrophage cells was added. After 48 h of incubation, the cells were washed with PBS twice. Fresh RPMI medium was added and then the plates were revealed with 30 μL of freshly prepared 0.01% resazurin solution.[25] A positive control of digitonin was used in the assay. The plates were incubated overnight and the next day spectrofluorometric detection was performed at 590 nm after excitation at 560 nm. The assay was carried out in duplicate on different days. In addition, microscopic observation of treated and untreated cells was performed at ×400 magnification.

M. tuberculosis MurE activity inhibition assay

M. tuberculosis MurE activity was assayed as reported previously.[16] The assay mixture contained 25 mM bis-trispropane buffer at pH 8.5, 5 mM $MgCl_2$, 100 μM UDP-MurNAc-dipeptide (BaCWAN, University of Warwick, UK), 250 μM ATP and 1 mM *meso*-diaminopimelic acid. The compounds were dissolved in DMSO at concentrations of 25, 8.3, 2.5, 0.83, 0.25 and 0.083 mM and 2 μL aliquots were added to half area 96-well plates. The reaction was initiated by the addition of MurE enzyme at a final concentration of 40 nM to the assay mixture, 48 μL of the mixture was added to each well and the plate was incubated at 37°C for 30 min. Phosphate release was determined in triplicate using the Pi ColorLock Gold kit (Innova Biosciences) reagents. Isoniazid was included as negative control at the same concentrations. A control reaction was performed with all the components except the enzyme. Absorbance at 635 nm was measured and percentage inhibition was calculated using a negative control (0% activity) and enzyme reaction (100% activity).

M. bovis BCG growth curve, acid-fast staining and viability counting

To roller bottles, 100 mL of Middlebrook 7H9 containing 0.2% glycerol, 0.05% Tween-80 and 10% albumin/dextrose/catalase supplement (ADC; BD Diagnostics) was added. Compound **3** dissolved in DMSO was added to the roller bottles at final concentrations of 5, 2.5, 1 and 0 mg/L. A 1:100 inoculation from a first-passage *M. bovis* BCG culture in supplemented 7H9 was performed and the bottles were incubated at 37°C, rolling at 2 rpm. OD_{600} measurements were taken every 24 h for 2 weeks using an appropriate blank. Serial 10-fold dilutions in Middlebrook 7H9 were performed from 1.2 OD_{600} culture until 10^{-10} dilution; 100 μL aliquots of these dilutions were spread in duplicate on fresh Middlebrook 7H10 medium supplemented with 0.2% glycerol and 10% OADC. Counting of single colonies allowed calculation of initial viable bacterial density. To two pairs of glass slides, 50 μL of liquid culture was added and the slides were dried at 110°C for 20 min. The fixed slides were stained with a Tb-color Staining Kit (Merck) using fuchsin, EtOH–HCl and malachite green, and they were observed under the microscope at ×1000 magnification.

Results

Growth inhibition of Mycobacterium spp.

Natural products **1**–**7** (Figure 1) were screened for growth inhibition against *M. tuberculosis* H_{37}Rv in liquid medium and *M. bovis* BCG in solid and liquid media (Table 1). Interestingly, anti-tubercular activity was more pronounced for the polar and mildly acidic alkaloid **3** (MIC ≤ 5 mg/L) when compared with more basic compound **1** (MIC ≥ 25 mg/L) and *N*-methoxycarbonyl-substituted **2** (MIC ≥ 50 mg/L). The diastereoisomeric *erythro* and *threo* mixture of austrobailignan-6 (**5**) showed inhibition of mycobacterial growth in liquid and solid media and the *meso* and *threo* mixture of dihydroguaiaretic acid (**4**) was inactive (Table 1). 2′,4′,6′-Trimethoxydihydrochalcone (**6**) showed partial inhibition at 50 mg/L and, interestingly, gibbilimbol-B (**7**) completely inhibited *M. bovis* BCG growth in solid medium at 25 mg/L with significant effects at 10 mg/L. Boldine, a natural aporphine alkaloid structurally related to 3-methoxynordomesticine, was shown to be inactive, having an MIC greater than 50 mg/L.

Antibacterial activity on E. coli, P. putida and S. aureus

To appraise whether the compounds selectively affected slow-growing mycobacteria in comparison with fast growing bacteria, whole-cell experiments were performed. Comparative time measurement of *E. coli* growth after exposure to high concentrations of compounds, typically 200 mg/L, was evaluated by measuring OD_{600} (Figure 2a). Potent anti-tubercular alkaloids **1**–**3** showed a similar profile (among the alkaloids **1**–**3**, only **3** is shown in Figure 2a), and weakly affected *E. coli* growth at concentrations at least 20 times their MIC on mycobacteria. Diastereoisomeric mixture **4** inhibited *E. coli* growth, as deduced by the small OD_{600} difference between the start and the end of the experiment. Diastereoisomers **5**, dihydrochalcone **6** and phenol **7** were moderate growth inhibitors of *E. coli*. Using the microdilution technique, all the natural compounds were inactive against Gram-negative (*E. coli* and *P. putida*) and Gram-positive bacteria (*S. aureus*) except phenol **7**, which significantly inhibited the growth of *S. aureus* (J. D. Guzman, D. R. Muñoz, W. A. Delgado, L. E. Cuca, S. Gibbons and S. Bhakta, unpublished results).

Macrophage RAW264.7 cytotoxicity

Growth inhibitory concentration 50 (GIC_{50}) was calculated for all of the natural compounds (Table 1). Microscopic slides of RAW264.7 cells at a concentration of 50 mg/L were observed. Viability in the presence of **1**–**3** demonstrated moderate cytotoxicity. For the alkaloids, the selectivity index ($SI = GIC_{50}/MIC$) showed a value ranging from 0.5 to 12, compound **3** being the most specific (SI = 12). Microscopic observation showed that **1** did not affect macrophages at 50 mg/L, although **3** showed some growth inhibition at the same concentration. Moreover, macrophages were strongly susceptible to flavonoid **6** and moderately susceptible to phenol **7** and lignans **4** and **5** (Table 1).

M. tuberculosis MurE inhibition

Overexpressed and purified recombinant *M. tuberculosis* protein MurE was assayed under different concentrations of natural products using colorimetric detection of phosphate, which has been

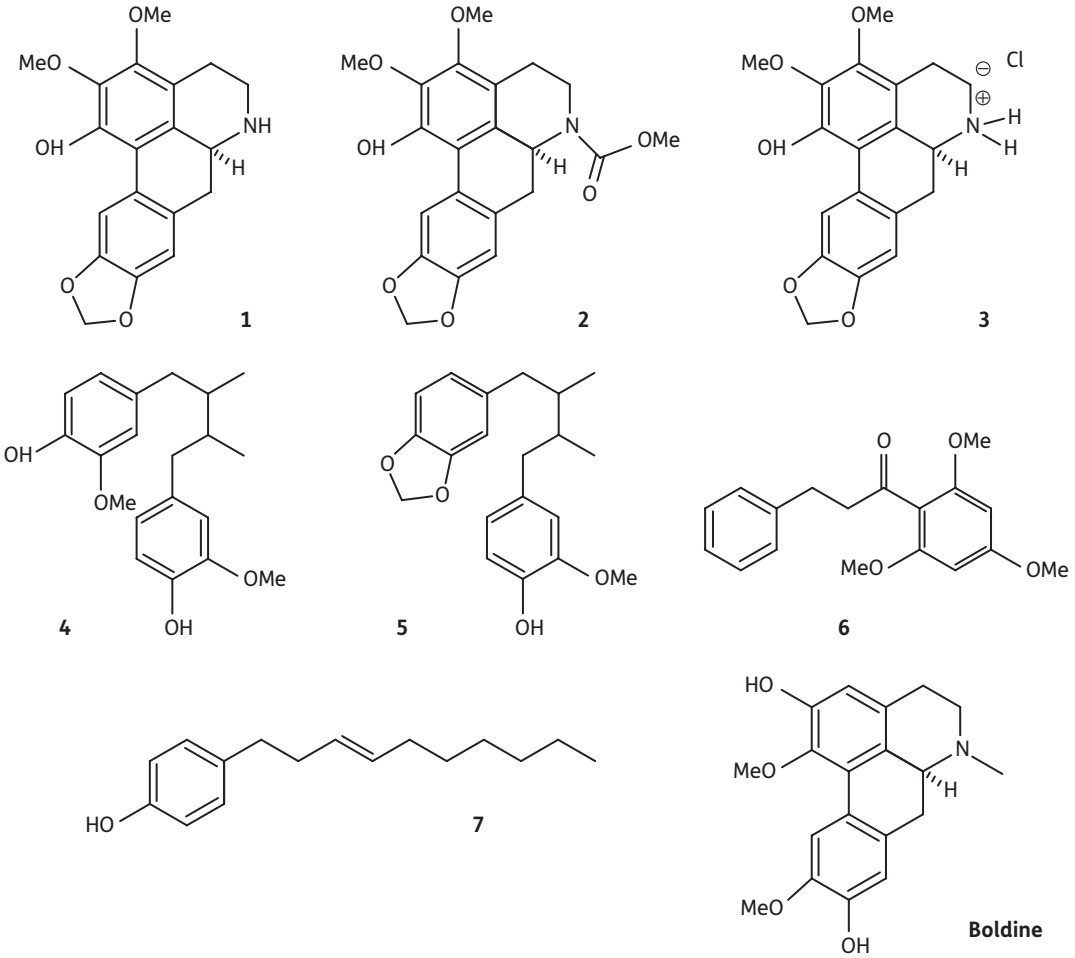

Figure 1. Chemical structures of 3-methoxynordomesticine (**1**), *N*-methoxycarbonyl-3-methoxynordomesticine (**2**), 3-methoxynordomesticine hydrochloride (**3**), dihydroguaiaretic acid *meso* and *erythro* diastereoisomers (**4**), austrobailignan-6 *threo* and *erythro* diastereoisomers (**5**), 2′,4′,6′-trimethoxydihydrochalcone (**6**), gibbilimbol-B (**7**) and boldine.

Table 1. MICs, GIC_{50}, SI and MurE IC_{50} of natural compounds **1**–**7**

	MIC (mg/L)					
		M. bovis BCG				
Natural products	*M. tuberculosis* $H_{37}Rv$, MTT microtitre assay[21]	spot culture growth inhibition assay[23]	resazurin microtitre assay[22]	GIC_{50} for RAW264.7 (mg/L)	SI[a]	IC_{50} for *M. tuberculosis* MurE (μM) [mg/L]
1	64	25	64	62±5	0.97	67±11 [22.9]
2	128	50	256	67±7	0.52	75±15 [30.0]
3	4	5	16	47±6	12	57±14 [19.5]
4	>128	>50	256	43±13	<0.34	>1000 [>330]
5	128	50	128	45±6	0.35	286±33 [93.9]
6	>128	>50	>256	10±8	<0.078	>1000 [>300]
7	128	25	128	36±8	0.28	184±16 [42.8]
Isoniazid	0.125	0.05	0.0625	>500	>4000	>1000 [>137]
Rifampicin	0.25	ND	ND	ND	ND	>500 [>411]

ND, not determined.
[a]The SI was calculated by dividing the GIC_{50} for RAW264.7 by the MIC for *M. tuberculosis* $H_{37}Rv$.

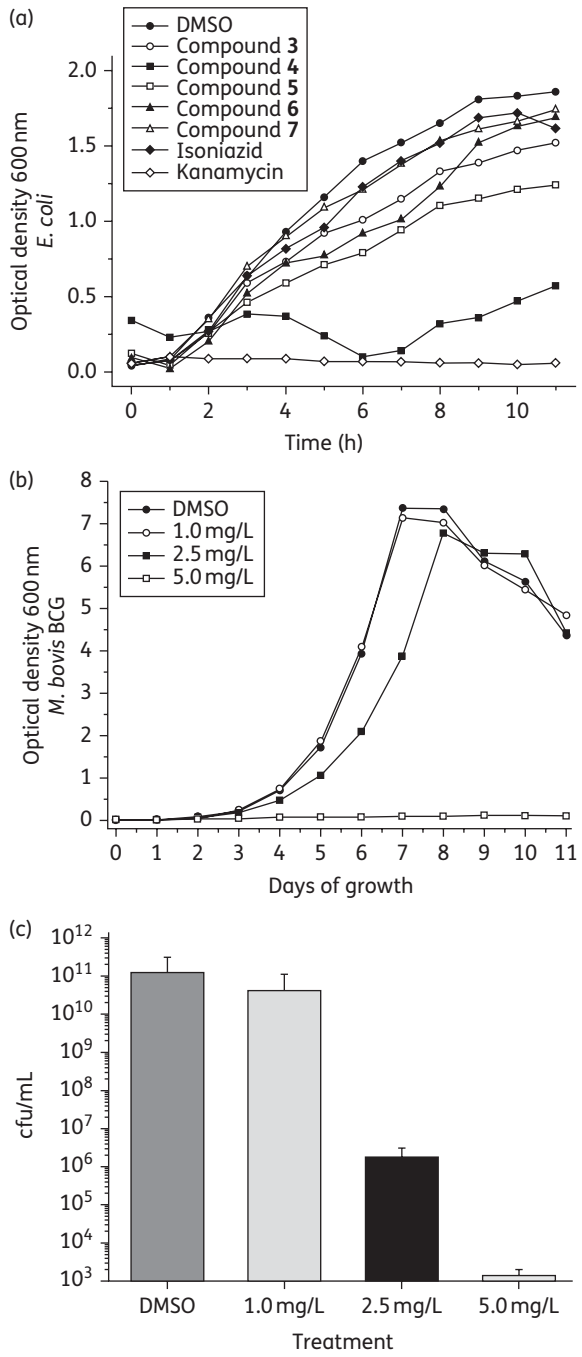

Figure 2. Antimicrobial activity of natural products (**3**–**7**) against *E. coli* and effect of 3-methoxynordomesticine hydrochloride (**3**) on liquid culture of *M. bovis* BCG. (a) Growth curve of *E. coli* at 200 mg/L of the natural compounds. (b) Growth curve of the bacilli under four different concentrations (0, 1.0, 2.5 and 5.0 mg/L) of **3**. (c) Bar diagram showing the number of cfu/mL of liquid culture under different concentrations of **3**. Error bars show the SD of the mean.

shown to be stoichiometrically coupled to *meso*-diaminopimelic acid ligation.[16] A consistent MurE inhibition was observed for aporphine alkaloids **1**–**3**, all having IC_{50} values of less than 100 μM (Table 1). Boldine was not inhibitory to MurE even at higher concentrations ($IC_{50} > 1$ mM). Natural products **5** and **7** showed moderate MurE inhibition and compounds **4** and **6** were inactive. Known anti-TB drugs were also tested against MurE inhibition, but none showed activity (isoniazid and rifampicin were included as controls).

Alteration in mycobacterial growth curve, acid-fast staining and viability counting

The growth curve of *M. bovis* BCG in the presence of different concentrations of 3-methoxynordomesticine hydrochloride (**3**) corroborated the high activity (MIC < 5 mg/L) observed in liquid and solid culture (Figure 2b). After five days of growth (OD ~ 1.2) cells were acid-fast stained and counted for viability. Not a single acid-fast cell was observable in the 5 mg/L treated sample. Alkaloid **3** decreased by more than 7-log the number of colony forming units (Figure 2c) at 5.0 mg/L, indicating a bactericidal effect.

Discussion

The *in vitro* growth of bacteria on solid and in liquid media represents two different physiological states of the microorganism. In solid medium mycobacteria grow more slowly than in liquid medium and the bacilli are restricted to a surface as opposed to a liquid medium, where there is aeration and constant movement. Differences between the activity of the compounds or antibiotics may exist in liquid and solid media. In this work, apolar natural products such as compounds **4**, **5** and **7** showed significant differences in their MIC in liquid and solid culture for the same species, *M. bovis* BCG. Moreover, in liquid medium the MIC was presumably overestimated because of precipitation and hence reduced availability of the compounds in Middlebrook 7H9 and LB broth. We must also consider the longer incubation time for slow-growing mycobacteria, which may increase the amount of precipitation for compounds with low solubility in aqueous medium. On the other hand, the alkaloids **1**–**3** showed a similar effect in liquid and solid media. There are also reports of interaction of some natural compounds with the MTT viability indicator, especially for flavonoids.[26] In this work dihydrochalcone **6** reduced the viability indicator MTT in the absence of bacterial cells, introducing some ambiguity to the MIC determination, hence subsequently a solid agar-based screening was appropriately introduced.

The aporphine alkaloids **1**–**3** were found to be selective inhibitors of slow-growing mycobacteria. Anti-mycobacterial activity has previously been reported for structurally related piperolactam and cepharadione aporphine alkaloids,[27] suggesting a promising anti-tubercular hit in related chemical space. Moreover, a recent paper has reported anti-inflammatory activity of alkaloid **1** and, interestingly, also recorded a low antimicrobial effect (MIC > 256 mg/L) against *E. coli*, *S. aureus* and *Candida albicans*,[28] supporting mycobacterial selectivity for this metabolite. Interestingly, the closely related alkaloid boldine was ineffective as a MurE inhibitor as well as not showing any effect on the *in vitro* growth inhibition of slow-growing mycobacteria, indicating that substitution in the aryl rings and/or nitrogen atom is essential for the anti-tubercular activity of aporphines. Dibenzylbutane lignan **5** was a moderate inhibitor of slow-growing

mycobacteria, and related chemical structures have displayed anti-tubercular activity,[29] but are in some way cytotoxic as they also inhibit DNA topoisomerases.[30] All diastereomers of dihydroguaiaretic acid **4** have shown potent antimicrobial activity[31] and this study confirmed this observation. Flavonoid **6** did not show significant inhibition of mycobacteria or *E. coli*, but was surprisingly toxic to macrophages. Gibbilimbol-B **7** had anti-mycobacterial properties, but lacked selectivity. O-arylated catechol analogues of **7** have been reported as potent inhibitors of the mycolic acid biosynthetic InhA enzyme, a recognized target of isoniazid.[32]

To our understanding, this is the first report of MurE ligase inhibition by natural products. The IC_{50} of the aporphine alkaloids fell in the micromolar range and these initial hits may be exploited in the future for constructing increased affinity ligands. The fact that the MurE IC_{50} of the aporphine alkaloids has the same order of magnitude as the GIC_{50} on macrophages reveals that further structural improvement is needed in order to make the alkaloids less toxic while increasing their affinity for the enzyme. A synthetic route for these alkaloids has already been described[28] and consequently it is possible to generate closely related analogues by varying a single chemical functionality in order to gain structure–activity information. More detailed studies involving fragment screening, inhibition kinetics and structural molecular approaches are envisaged for augmenting the impact of these hits. Additionally, we must consider the analysis of muropeptides[33] in treated bacilli at the sub-MIC of the inhibitors for confirming pathway interference as the mode of action of these alkaloids. We believe that the unique upper leaflets (mycolyl-arabinogalactan) covalently bound to the lower polymeric mesh (peptidoglycan) in the asymmetrical model proposed by Minnikin and collaborators[34] are most likely to disappear when lower layers are attacked; thus, inhibitors of a key peptidoglycan biosynthesis step have the potential to be developed into a novel anti-TB chemotherapy.

Acknowledgements

We are thankful to Professor Siamon Gordon (Sir William Dunn School of Pathology, University of Oxford) and Professor Edith Sim (Department of Pharmacology, University of Oxford) for kindly providing RAW264.7 macrophage cell line and *P. putida* culture stocks, respectively, for this study. We acknowledge Professor Nicholas H. Keep and Dr Philip Lowden for valuable discussions. J. D. G. is grateful to Dr Fernando Echeverri for the project 'Searching for anti-tubercular compounds in Colombian flora', which motivated further research in the field.

Funding

This work was supported by the MRC, UK (grant reference number G0801956; to S. B.). A Bloomsbury Colleges studentship and Colfuturo contributed towards J. D. G.'s research study.

Transparency declarations

None to declare.

References

1 Cole ST. Comparative and functional genomics of the *Mycobacterium tuberculosis* complex. *Microbiology* 2002; **148**: 2919–28.

2 Donoghue HD, Lee OY-C, Minnikin DE *et al*. Tuberculosis in Dr Granville's mummy: a molecular re-examination of the earliest known Egyptian mummy to be scientifically examined and given a medical diagnosis. *Proc R Soc Lond B Biol Sci* 2010; **277**: 51–6.

3 WHO. *Global Tuberculosis Control: A Short Update to The 2009 Report*. Geneva: WHO, 2009.

4 Brewer TF, Heymann SJ. To control and beyond: moving towards eliminating the global tuberculosis threat. *J Epidemiol Community Health* 2004; **58**: 822–5.

5 Hehenkamp A, Hargreaves S. Tuberculosis treatment in complex emergencies: South Sudan. *Lancet* 2003; **362**: s30–s1.

6 Lienhardt C, Ogden JA. Tuberculosis control in resource-poor countries: have we reached the limits of the universal paradigm? *Trop Med Int Health* 2004; **9**: 833–41.

7 Casenghi M, Cole ST, Nathan CF. New approaches to filling the gap in tuberculosis drug discovery. *PLoS Med* 2007; **4**: 1722–5.

8 Gonzalez-Lamothe R, Mitchell G, Gattuso M *et al*. Plant antimicrobial agents and their effects on plant and human pathogens. *Int J Mol Sci* 2009; **10**: 3400–19.

9 Bednarek P, Osbourn A. Plant-microbe interactions: chemical diversity in plant defense. *Science* 2009; **324**: 746–8.

10 Gibbons S. Anti-staphylococcal plant natural products. *Nat Prod Rep* 2004; **21**: 263–77.

11 Copp BR, Pearce AN. Natural product growth inhibitors of *Mycobacterium tuberculosis*. *Nat Prod Rep* 2007; **24**: 278–97.

12 Pabon LC, Cuca LE. Aporphine alkaloids from *Ocotea macrophylla* (Lauraceae). *Quim Nova* 2010; **33**: 875–9.

13 Guzman JD, Isaza JH, Cuca LE. Fragmentacion diastereoespecifica en NCI de dos lignanos dibencilbutanicos de la corteza de *Dugandiodendron argyrotrichum* (Magnoliaceae). *Rev Prod Nat* 2008; **2**: 6–12.

14 Guzman JD, Cuca LE. Metabolitos secundarios aislados de *Dugandiodendron argyrotrichum* Lozano (Magnoliaceae). *Rev Col Quim* 2008; **37**: 275–88.

15 Plazas EA, Delgado W, Cuca LE. Flavonoides aislados de las inflorescencias de *Piper hispidum* Kunth (Piperaceae) y derivados acetilados. *Rev Col Quim* 2008; **37**: 135–44.

16 Basavannacharya C, Robertson G, Munshi T *et al*. ATP-dependent MurE ligase in *Mycobacterium tuberculosis*: biochemical and structural characterisation. *Tuberculosis* 2010; **90**: 16–24.

17 Cole ST, Brosch R, Parkhill J *et al*. Deciphering the biology of *Mycobacterium tuberculosis* from the complete genome sequence. *Nature* 1998; **393**: 537–44.

18 Jana M, Luong T-T, Komatsuzawa H *et al*. A method for demonstrating gene essentiality in *Staphylococcus aureus*. *Plasmid* 2000; **44**: 100–4.

19 Anishetty S, Pulimi M, Pennathur G. Potential drug targets in *Mycobacterium tuberculosis* through metabolic pathway analysis. *Comput Biol Chem* 2005; **29**: 368–78.

20 Orjala J, Mian P, Rali T *et al*. Gibbilimbols A–D, cytotoxic and antibacterial alkenylphenols from *Piper gibbilimbum*. *J Nat Prod* 1998; **61**: 939–41.

21 Mshana RN, Tadesse G, Abate G *et al*. Use of 3-(4,5-dimethylthiazol-2-yl)-2,5-diphenyl tetrazolium bromide for rapid detection of rifampin-resistant *Mycobacterium tuberculosis*. *J Clin Microbiol* 1998; **36**: 1214–9.

22 Palomino JC, Martin A, Camacho M *et al*. Resazurin microtiter assay plate: simple and inexpensive method for detection of drug resistance in *Mycobacterium tuberculosis*. *Antimicrob Agents Chemother* 2002; **46**: 2720–2.

23 Evangelopoulos D, Bhakta S. Rapid methods for testing inhibitors of mycobacterial growth. In: *Antibiotic Resistance Protocols, Methods in Molecular Biology*. London: Humana Press, 2010; 193–201.

24 National Committee for Clinical Laboratory Standards. *Methods for Dilution Antimicrobial Susceptibility Tests for Bacteria That Grow Aerobically—Fifth Edition: Approved Standard M7-A5*. NCCLS, Wayne, PA, USA, 1999.

25 Gupta A, Bhakta S, Kundu S *et al*. Fast-growing, non-infectious and intracellularly surviving drug-resistant *Mycobacterium aurum*: a model for high-throughput antituberculosis drug screening. *J Antimicrob Chemother* 2009; **64**: 774–81.

26 Talorete T, Bouaziz M, Sayadi S *et al*. Influence of medium type and serum on MTT reduction by flavonoids in the absence of cells. *Cytotechnology* 2006; **52**: 189–98.

27 Mata R, Morales I, Perez O *et al*. Antimycobacterial compounds from *Piper sanctum*. *J Nat Prod* 2004; **67**: 1961–8.

28 Nimgirawath S, Udomputtimekakul P, Taechowisan T *et al*. First total syntheses of (±)-isopiline, (±)-preocoteine, (±)-oureguattidine and (±)-3-methoxynordomesticine and the biological activities of (±)-3-methoxynordomesticine. *Chem Pharm Bull* 2009; **57**: 368–76.

29 Rivero-Cruz I, Acevedo L, Guerrero J *et al*. Antimycobacterial agents from selected Mexican medicinal plants. *J Pharm Pharmacol* 2005; **57**: 1117–26.

30 Li G, Lee C-S, Woo M-H *et al*. Lignans from the bark of *Machilus thunbergii* and their DNA topoisomerases I and II inhibition and cytotoxicity. *Biol Pharm Bull* 2004; **27**: 1147–50.

31 Kawaguchi Y, Yamauchi S, Masuda K *et al*. Antimicrobial activity of stereoisomers of butane-type lignans. *Biosci Biotech Biochem* 2009; **73**: 1806–10.

32 Lu H, Tonge PJ. Inhibitors of FabI, an enzyme drug target in the bacterial fatty acid biosynthesis pathway. *Accounts Chem Res* 2008; **41**: 11–20.

33 Mahapatra S, Crick DC, McNeil MR *et al*. Unique structural features of the peptidoglycan of *Mycobacterium leprae*. *J Bacteriol* 2008; **190**: 655–61.

34 Minnikin DE, Kremer L, Dover LG *et al*. The methyl-branched fortifications of *Mycobacterium tuberculosis*. *Chem Biol* 2002; **9**: 545–53.

Structure and Antibacterial Activity of Brominated Diterpenes from the Red Alga *Sphaerococcus coronopifolius*

by **Vangelis Smyrniotopoulos**[a]), **Constantinos Vagias**[a]), **Mukhlesur M. Rahman**[b]), **Simon Gibbons**[b]), and **Vassilios Roussis***[a])

[a]) Department of Pharmacognosy and Chemistry of Natural Products, School of Pharmacy, University of Athens, Panepistimiopolis Zografou, GR-Athens 15771 (phone/fax: +30-210-7274592; e-mail: roussis@pharm.uoa.gr)

[b]) Centre for Pharmacognosy and Phytotherapy, The School of Pharmacy, University of London, 29-39 Brunswick Square, London WC1N 1AX, UK

Four new tetracyclic brominated diterpenes, **1**–**4**, were isolated from the organic extract of *Sphaerococcus coronopifolius*, collected from the rocky coasts of Corfu Island. The structures of the new natural products, as well as their relative configurations, were elucidated on the basis of extensive spectral analyses, including 2D-NMR experiments. The isolated metabolites were evaluated for their antibacterial activity against a panel of bacteria including multidrug-resistant (MDR) and methicillin-resistant *Staphylococcus aureus* (MRSA) with *MIC* values in the range of 16–128 μg/ml.

Introduction. – The increasing problem of bacterial resistance to antibiotic therapy and the growing number of pathogens resistant to several classes of antimicrobial drugs has resulted in rising worldwide concern. Multidrug-resistant (MDR) and methicillin-resistant *Staphylococcus aureus* (MRSA) has been a cause of hospital-acquired infections, posing an increasing threat, as not only can the organism survive for long periods in the environment, but it can colonize the skin, nose, and throat of patients and healthcare staff, and is readily spread by direct contact [1].

The red alga *Sphaerococcus coronopifolius* is an unusual prolific source of an extended variety of interesting diterpenes having di-, tri-, or tetracyclic skeletons, often rearranged, most of which contain one or more Br-atoms [2–4]. A number of halogenated metabolites have been suggested to function as chemical defense against marine herbivores [5–7], and some of them have been proven to possess insecticidal [8], antibacterial [9], antifungal [10], and antiviral activities [11].

In the course of our ongoing investigations toward the isolation of bioactive metabolites from marine organisms of the Greek seas [12–14], we recently studied the chemical composition of the red alga *S. coronopifolius*, collected from the west coast of Corfu Island. In this report, we describe the isolation and structure elucidation of four new diterpenes, **1**–**4**, with a bromotetrasphaerol C-skeleton [15], all of which were obtained from the organic extract of *S. coronopifolius*. The structures of the new metabolites were elucidated by extensive spectroscopic analyses, and their relative configurations were established by NOESY experiments.

All compounds were evaluated for antibacterial activity against a panel of *Staphylococcus aureus* strains including multidrug-resistant (MDR) and methicillin-

resistant *Staphylococcus aureus* (MRSA) using a microtitre plate-based minimum inhibitory concentration (*MIC*) assay. The metabolites were found to possess significant activities in comparison to the standard antibiotic norfloxacin.

Results and Discussion. – 1. *Isolation and Structure Elucidation*. The red seaweed *S. coronopifolius* was collected in Palaiokastritsa Bay on the west side of Corfu Island. Extensive chromatographic purification of the CH_2Cl_2/MeOH algal extract afforded compounds **1**–**4**.

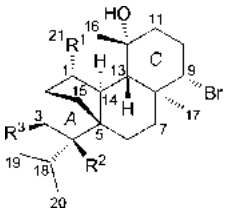

	R¹	R²	R³
1	MeO	H	H
2	H	OH	H
3	H	H	OH
4	H	H	Br

Compound **1** was isolated as a colorless oil. The molecular formula $C_{21}H_{35}BrO_2$ was deduced from HR-FAB-MS in combination with the NMR data (*Table 1*). The CI-MS ions at *m*/*z* 349/351 with relative intensities 1.2/1.0 ($[M+H-MeOH-H_2O]^+$) indicated the presence of one Br-atom, a MeO, and a OH group. In the IR spectrum, the broad band at $\tilde{\nu}_{max}$ 3478 cm^{-1} supported the presence of a OH group, while the peak at $\tilde{\nu}_{max}$ 1097 cm^{-1} indicated the presence of an ether moiety in the molecule. The ^{13}C-NMR and DEPT spectra exhibited 21 signals corresponding to three quaternary C-atoms, and seven CH, six CH_2, and five Me groups. The ^{1}H- and ^{13}C-NMR spectra displayed resonances for two Me groups (δ(H/C) 0.94/23.5; 1.02/23.7) of an i-Pr group linked to a CH group (δ(H/C) 1.74–1.83/29.9) attached on another CH group (δ(H/C) 1.20–1.26/52.4), two aliphatic *singlet* Me groups (δ(H/C) 1.09/16.2 and δ(H/C) 1.37/29.3), one O-bearing Me group (δ(H/C) 3.09/55.5), one O-bearing CH group (δ(H/C) 3.42/89.1), one halomethine (δ(H/C) 3.95/69.1) and three aliphatic CH groups (δ(H/C) 2.22–2.26/36.9, 1.20/54.6 and 1.74/40.4), and six aliphatic CH_2 groups (δ(H/C) 1.53–1.63, 1.44/27.8; 1.94, 1.21–1.27/27.0; 1.85, 1.11/38.6; 2.48, 2.00/30.7; 1.66, 1.50–1.60/43.9 and δ(H/C) 1.80–1.84, 0.98–1.02/42.1). With four degrees of unsaturation, the structure was suggested to contain four rings. All protonated C-atoms and their H-atoms were assigned by the COSY and HSQC experiments. The structure elucidation was assisted by analyses of the HMBC spectra. The correlation in the HMBC experiments, of both Me(19) and Me(20) (δ(H) 0.94 and 1.02) with C(4) (δ(C) 52.4), confirmed the position of the i-Pr group. The correlations of C(1) (δ(C) 89.1) with the MeO H-atoms Me(21) (δ(H) 3.09) established C(1) as the point of attachment of the MeO group. The position of the aliphatic CH_2(15) was secured between C(2) and the quaternary C-atom C(5), as depicted from the correlations of C(5) (δ(C) 50.9) with H_α–C(6) (δ(H) 1.94), H–C(14) (δ(H) 1.74), and H_b–C(15) (δ(H) 0.98–1.02), of H_a–C(15) (δ(H) 1.80–1.84) with C(1) (δ(C) 89.1), C(2) (δ(C) 36.9), C(3) (δ(C) 27.8), C(4) (δ(C) 52.4), and C(6) (δ(C) 27.0), of H_b–C(15) (δ(H) 0.98–1.02) with C(1) (δ(C) 89.1) and C(6) (δ(C) 27.0), and of C(15) (δ(C) 42.1) with H–C(14) (δ(H) 1.74). The Br-atom was positioned at C(9), as indicated by the correlations of C(9) (δ(C) 69.1) with H_α–C(11) (δ(H) 1.66), H–C(13) (δ(H) 1.20), and Me(17) (δ(H) 1.09).

Moreover, the correlations between Me(16) (δ(H) 1.37) with C(12) (δ(C) 72.6), C(13) (δ(C) 54.6), and C(11) (δ(C) 43.9), and of Me(17) (δ(H) 1.09) with C(8) (δ(C) 40.9), C(7) (δ(C) 38.6), C(9) (δ(C) 69.1), and C(13) (δ(C) 54.6), confirmed the positions of the Me groups linked to quaternary C-atoms. Comparison of the NMR data of **1** with reported values for bromotetrasphaerol [15] led to the assignment of the structure as 1-methoxybromotetrasphaerol. The relative configuration of **1** was assigned on the basis of NOESY experiments. The strong NOE correlations of H–C(9)/H_β–C(7), H–C(9)/H–C(13), H–C(9)/H_β–C(10), H_β–C(7)/H_a–C(15), H_a–C(15)/H–C(1), and H–C(13)/H–C(1) established the relative configuration at C(1), C(2), C(5), C(9), and C(13). The strong NOE correlations of Me(17)/H_α–C(10), Me(17)/H_α–C(6), Me(20)/H_α–C(6), H–C(14)/Me(20), and H–C(14)/Me(17) determined the configuration at C(4), C(8), and C(14). The NOE correlations of Me(16)/H–C(1) and Me(16)/Me(21) confirmed the equatorial configuration of Me(16). The large coupling-constant values of the H-atom pairs H_α–C(6)/H_β–C(7), H–C(9)/H_α–C(10), and H–C(13)/H–C(14) supported their *trans*-diaxial configuration, establishing the chair conformation of the rings *B* and *C*. In view of the above-mentioned data, metabolite **1** was assigned as (1*S**)-1-methoxybromotetrasphaerol.

Compound **2**, purified by means of HPLC, was isolated as a white amorphous solid. A combination of its ^{13}C-NMR data (*Table 1*) and HR-FAB-MS measurements suggested the molecular formula $C_{20}H_{33}BrO_2$. The CI-MS peaks at *m*/*z* 349/351 with relative intensities of 1.2/1.0 ($[M+H-2\ H_2O]^+$), at *m*/*z* 287 ($[M+H-HBr-H_2O]^+$), and at *m*/*z* 269 ($[M+H-HBr-2\ H_2O]^+$), indicated the presence of one Br-atom and two OH groups. The ^{13}C-NMR spectrum of **2** exhibited signals for 20 C-atoms with the multiplicities of the C-atom signals determined from the DEPT spectra as: four *singlet*s, five *doublet*s, seven *triplet*s, and four *quadruplet*s. Strong IR absorptions at $\tilde{\nu}_{max}$ 3468 cm^{-1} and ^{13}C-NMR signals at δ(C) 73.0 (C(12)) and δ(C) 82.5 (C(4)) indicated the presence of two tertiary OH groups. Among the other C-atoms, one was brominated, resonating at δ(C) 68.4 (C(9)). Furthermore, the ^{1}H-NMR spectra revealed signals due to a halomethine H-atom at δ(H) 3.96 (H–C(9)), two Me groups of an i-Pr group at δ(H) 0.96 (Me(19)) and 1.07 (Me(20)) coupled to a CH group at δ(H) 1.96 (H–C(18)), and two *singlet* Me groups at δ(H) 1.16 (Me(16)) and 1.14 (Me(17)). The structure elucidation was assisted by analyses of the HMBC spectra. Comparison of the NMR data of **2** with reported values for bromotetrasphaerol [15] showed close similarities and led to the assignment of the structure as the 4-OH isomer of bromotetrasphaerol. The correlation in the HMBC spectra, between Me(19) (δ(H) 0.96) and Me(20) (δ(H) 1.07) with C(4) (δ(C) 82.5), confirmed the position of the i-Pr group on the quaternary C-atom C(4) bearing one of the OH groups. The relative configuration of **2** was elucidated on the basis of NOESY experiments and was deduced to be the same as in **1** and bromotetrasphaerol [15]. The NOE correlations of H_α–C(6)/Me(19) and Me(19)/H–C(14) established the configuration at C(4). In view of the above-mentioned data, metabolite **2** was named (4*R**)-4-hydroxy-1-deoxybromotetrasphaerol.

Compound **3**, purified by means of HPLC, was isolated as a colorless oil. Both ^{13}C-NMR data and HR-FAB-MS measurements supported the molecular formula $C_{20}H_{33}BrO_2$. The CI-MS peaks at *m*/*z* 349/351 with relative intensities 1.2/1.0 ($[M+H-2\ H_2O]^+$), at *m*/*z* 287 ($[M+H-HBr-H_2O]^+$), and at *m*/*z* 269 ($[M+H-HBr-2$

Table 1. *NMR Data*[a]) *of Compounds* **1** *and* **2**

Position	**1**				**2**			
	δ(H)	NOESY	δ(C)	HMBC (C→H)	δ(H)	NOESY	δ(C)	HMBC (C→H)
1	3.42 (*t*, *J* = 2.5)	2, 13, 15a, 16, 21	89.1	3α, 3β, 13, 14, 15a, 15b, 21	1.49–1.57 (*m*, H_a) 1.49–1.57 (*m*, H_b)	16	43.8	3β, 15a, 3α/15b
2	2.22–2.26 (*m*)	1, 3α, 3β, 21	36.9	17a	2.00–2.04 (*m*)		34.5	15a, 15b
3	1.53–1.63 (*m*, H_β) 1.44 (*ddd*, *J* = 12.4, 5.4, 2.5, H_α)	2, 4 2, 19, 20, 21	27.8	17a	1.50–1.58 (*m*, H_β) 1.43–1.51 (*m*, H_α)	 19	49.1	15a
4	1.20–1.26 (*m*)	3β	52.4	17a, 19, 20			82.5	3α, 3β, 15a, 19, 20
5			50.9	6α, 14, 15b			55.4	2, 7β, 14, 15a, 3α/15b
6	1.94 (*td*, *J* = 14.1, 4.6, H_α) 1.21–1.27 (*m*, H_β)	17, 20	27.0	4, 14, 15a, 15b	1.83 (*ddd*, *J* = 13.7, 13.7, 4.1, H_α) 1.68 (*ddd*, *J* = 13.7, 3.2, 3.2, H_β)	20 7α	21.9	7β, 14
7	1.85 (*ddd*, *J* = 12.8, 4.6, 2.5, H_α) 1.11 (*ddd*, *J* = 14.1, 12.8, 4.2, H_β)	 9, 15a	38.6	6β, 13, 17	1.88–1.94 (*m*, H_α) 1.13–1.20 (*m*, H_β)	6β, 9 9, 15a	38.6	9, 17
8			40.9	14, 17			41.1	6β, 7α, 9, 10α, 14, 17
9	3.95 (*dd*, *J* = 12.8, 4.2)	7β, 10β, 11β, 13	69.1	11α, 13, 17	3.96 (*dd*, *J* = 12.9, 4.1)	7α, 7β, 10β, 11β, 13	68.4	10α, 11, 17
10	2.48 (*tdd*, *J* = 13.3, 12.8, 4.6, H_α) 2.00 (*dtd*, *J* = 13.3, 4.2, 2.9, H_β)	17 9	30.7		2.46 (*dq*, *J* = 6.4, 12.9, H_α) 2.00–2.09 (*m*, H_β)	11α, 17 9	30.8	11
11	1.66 (*ddd*, *J* = 14.5, 4.6, 2.9, H_α) 1.50–1.60 (*m*, H_β)	 9	43.9	16	1.57–1.61 (*m*, H_β) 1.56–1.60 (*m*, H_α)	9 10α	43.6	10α, 16
12			72.6	16			73.0	10β, 11, 16
13	1.20 (*d*, *J* = 11.2)	1, 9	54.6	14, 16, 17	1.12 (*d*, *J* = 10.5)	9, 15a	56.4	11, 16, 17
14	1.74 (*dt*, *J* = 11.2, 2.5)	17, 20	40.4	15b	1.85–1.93 (*m*)	20	32.2	6β, 13, 15a, 15b
15	1.80–1.84 (*m*, H_a) 0.98–1.02 (*m*, H_b)	1, 7β	42.1	14	1.64 (br. *d*, *J* = 9.6, H_a) 1.47 (br. *d*, *J* = 9.6, H_b)	7β, 13	40.0	1, 3α, 14
16	1.37 (*s*)	1, 21	29.3		1.16 (*s*)	1	32.7	
17	1.09 (*s*)	6α, 10α, 14	16.2	9, 13	1.14 (*s*)	10α	17.4	9, 13
18	1.74–1.83 (*m*)		29.9	19, 20	1.96 (*sept*, *J* = 6.7)	19	34.2	19, 20
19[b])	0.94 (*d*, *J* = 6.6)	3α	23.5	18, 20	0.96 (*d*, *J* = 6.7)	3α, 18	19.3	18, 20
20[b])	1.02 (*d*, *J* = 6.6)	3α, 6α, 14	23.7	18, 19	1.07 (*d*, *J* = 6.7)	6α, 14	18.2	18, 19
21	3.09 (*s*)	1, 2, 3α, 16	55.5					

[a]) ^{1}H- (400 MHz) and ^{13}C-NMR (50.3 MHz) spectra recorded in $CDCl_3$ (δ(H) 7.24, δ(C) 77.0), chemical shifts are expressed in ppm and *J* values in Hz.
[b]) Assignments may be interchanged.

$H_2O]^+$), indicated the presence of one Br-atom and two OH groups. The presence of OH groups in the molecule was also supported by the intense and broad IR band at $\tilde{\nu}_{max}$ 3407 cm^{-1}. The ^{13}C-NMR spectrum of **3** (*Table 2*) exhibited signals for 20 C-atoms, with the multiplicities of the C-atoms determined from the DEPT spectra, as: three quaternary C-atoms, seven CH groups, six CH_2 groups, and four Me groups. Among the C-atoms, one was brominated, resonating at δ(C) 68.4 (C(9)), and two were O-bearing, resonating at δ(C) 81.1 (C(3)) and δ(C) 73.0 (C(12)). The ^{1}H-NMR spectra displayed signals for one O-bearing CH group at δ(H) 3.44 (H–C(3)), one halomethine at δ(H) 3.95 (H–C(9)), two Me groups of an i-Pr group at δ(H) 1.05 (Me(19)) and 1.08 (Me(20)) attached to a CH group at δ(H) 1.65 (H–C(18)), and two uncoupled Me groups at δ(H) 1.17 (Me(16)) and 1.11 (Me(17)), one of which was linked to an O-bearing C-atom. With four degrees of unsaturation, the structure was suggested to contain four rings. The NMR-data comparison of **3** with those of **1**, **2**, and bromotetrasphaerol [15] showed minor differences only in ring A, suggesting that metabolite **3** was the 3-hydroxy-1-deoxy derivative of bromotetrasphaerol. The position of the secondary OH group at C(3) was established from correlations of C(3) (δ(C) 81.1) with H-atoms CH_2(1) (δ(H) 1.48–1.56), H–C(4) (δ(H) 0.94), and H_a–C(15) (δ(H) 1.74), as well as of H–C(3) (δ(H) 3.44) with C-atoms C(1) (δ(C) 38.9), C(5) (δ(C) 51.3), and C(18) (δ(C) 28.7), observed in the HMBC spectrum. The relative configuration of **3** was again assigned by NOE experiments. The NOE correlations of H–C(3)/H–C(1), H–C(3)/H–C(18), and H–C(3)/Me(19) led the relative configuration at C(3) (*Fig.*). Accordingly, the structure of metabolite **3** was established as (3*S**)-3-hydroxy-1-deoxy-bromotetrasphaerol.

Compound **4** was isolated, after purification by HPLC, as a colorless oil. The molecular formula $C_{20}H_{32}Br_2O$ was deduced from HR-FAB-MS data in combination with the NMR data (*Table 2*). The CI-MS ions at *m*/*z* 429/431/433 with relative intensities 1.5/2.0/1.0 ($[M+H-H_2O]^+$), at *m*/*z* 349/351 with relative intensities 1.2/1.0 ($[M+H-HBr-H_2O]^+$), and at *m*/*z* 269 ($[M+H-2\ HBr-H_2O]^+$) indicated the presence of two Br-atoms and a OH group. In the IR spectrum, the intense broad band at 3475 cm^{-1} supported the presence of a OH group. The ^{13}C-NMR exhibited 20 signals corresponding to three quaternary C-atoms, seven CH groups, six CH_2 groups, and four Me groups. The ^{1}H- and ^{13}C-NMR spectra showed strong similarities with those of **3**, and the only difference was signals indicating the presence of two halomethines (δ(H/C) 3.73/60.1 and δ(H/C) 3.94/68.0), instead of one brominated and one O-bearing CH group. Due to the overlap of diagnostic signals in the $CDCl_3$ ^{1}H-NMR spectrum, the ^{1}H-NMR, COSY, HSQC, HMBC, and NOESY experiments were also recorded in C_6D_6. Comparison of the NMR data of **4** with those of **3**, led to the assignment of the structure as 3-bromo-1-deoxybromotetrasphaerol. The correlations of C(3) (δ(C) 60.1) with CH_2(1) (δ(H) 1.10–1.14), H–C(4) (δ(H) 1.82), and CH_2(15) (δ(H) 1.51–1.58), as well as of H–C(3) (δ(H) 3.56) with C(1) (δ(C) 41.7), C(15) (δ(C) 41.0), and C(18) (δ(C) 29.3) in the HMBC experiments secured the position of the additional brominated CH(3) group. The relative configuration of **4** was assigned on the basis of NOESY experiments, and was deduced to be the same as of **3**, as indicated by the observed NOE correlations (*Table 2*). In view of the above-mentioned data, metabolite **4** was identified as (3*S**)-3-bromo-1-deoxybromotetrasphaerol.

Table 2. *NMR Data*[a]) *of Compounds* **3** *and* **4**

Position	**3**				**4**				
	δ(H)	NOESY	δ(C)	HMBC (C→H)	δ(H)	δ(H)[b])	NOESY	δ(C)	HMBC (C→H)
1	1.48–1.56 (*m*, H_a) 1.48–1.56 (*m*, H_b)	3, 16	38.9	2, 3, 13, 14, 15b	1.57–1.67 (*m*, H_a) 1.57–1.67 (*m*, H_b)	1.10–1.14 (*m*, H_a) 1.10–1.14 (*m*, H_b)	3, 14, 16	41.7	3, 13, 15
2	1.88–1.94 (*m*)		43.6	1, 4, 15a, 15b	2.26–2.32 (*m*)	2.20 (br. *s*)	15	46.2	1, 15
3	3.44 (br. *s*)	1, 18, 19	81.1	1, 4, 15a	3.73 (*dd*, *J*=3.7, 2.1)	3.56 (*dd*, *J*=3.7, 2.1)	1, 18, 19	60.1	1, 4, 15
4	0.94 (*dd*, *J*=9.1, 2.9)	6β, 15b	64.6	2, 6α, 15a, 15b, 19, 20	1.82 (*dd*, *J*=9.1, 3.7)	1.82 (*dd*, *J*=9.1, 3.7)	15	65.3	2, 6α, 14, 15, 18, 19, 20
5			51.3	3, 4, 6α, 6β, 7α, 15a, 15b				53.6	2, 4, 6α, 6β, 7α, 14, 15
6	1.96 (*ddd*, *J*=14.1, 12.8, 4.1, H_α) 1.43–1.51 (*m*, H_β)	17 4, 15b	26.0	7α, 14, 15a	1.92 (*ddd*, *J*=14.1, 12.4, 3.7, H_α) 1.48–1.56 (*m*, H_β)	1.78 (*ddd*, *J*=14.1, 12.4, 3.7, H_α) 1.28 (*dt*, *J*=14.1, 3.7, H_β)	17, 20 7α, 15	25.8	4, 7α, 7β, 14
7	1.86 (*ddd*, *J*=12.8, 4.1, 3.3, H_α) 1.15–1.25 (*m*, H_β)	17 9, 15a	39.0	6α, 6β, 9, 17	1.84–1.90 (*m*, H_α) 1.15–1.25 (*m*, H_β)	1.93 (*dt*, *J*=12.4, 3.7, H_α) 0.93 (*td*, *J*=12.4, 3.7, H_β)	6β, 17	38.8	6α, 6β, 9, 13, 17
8			41.1	6β, 7α, 10β, 17			9, 13, 15	41.0	7β, 9, 13, 17
9	3.95 (*dd*, *J*=12.8, 4.1)	7β, 10β, 13	68.4	10α, 11, 13/17	3.94 (*dd*, *J*=13.0, 4.1)	3.63 (*dd*, *J*=12.4, 3.7)	7β, 10β, 13	68.0	10α, 11, 13, 17
10	2.46 (*tdd*, *J*=12.8, 12.4, 6.6, H_α) 2.04 (*dtd*, *J*=12.8, 4.1, 3.3, H_β)	17 9	30.8	11	2.38–2.50 (*m*, H_α) 2.05 (*dtd*, *J*=13.7, 4.1, 3.4, H_β)	2.44 (*dq*, *J*=7.0, 12.4, H_α) 1.90 (*dq*, *J*=12.4, 3.7, H_β)	11, 17 9	30.7	9, 16
11	1.54–1.62 (*m*, H_a) 1.54–1.62 (*m*, H_b)	16	43.5	10α, 16	1.54–1.61 (*m*, H_a) 1.54–1.61 (*m*, H_b)	0.97–1.03 (*m*, H_a) 0.97–1.03 (*m*, H_b)	10α	43.6	10α, 16
12			73.0	11, 16				72.9	11, 14, 16
13	1.10 (*d*, *J*=10.4)	9	56.0	1, 7α, 11, 16, 17	1.08–1.12 (*m*)	0.45 (*d*, *J*=10.8)	7β, 9, 15, 16	55.8	1, 11, 14, 16, 17
14	1.80 (*ddd*, *J*=10.4, 7.9, 4.1)	17	30.9	1, 2, 4, 6β, 13, 15a, 15b	1.84–1.90 (*m*)	1.64 (*dd*, *J*=10.8, 6.2)	17, 18	31.0	1, 2, 4, 6β, 13, 15
15	1.74 (br. *d*, *J*=10.4, H_a) 1.25 (br. *d*, *J*=10.4, H_b)	7β 4, 6β	40.1	1	1.84–1.90 (*m*, H_a) 1.49–1.57 (*m*, H_b)	1.51–1.58 (*m*, H_a) 1.51–1.58 (*m*, H_b)	2, 4, 6β, 7β, 13	41.0	1, 3
16	1.17 (*s*)	1, 11	32.8		1.15 (*s*)	0.64 (*s*)	1, 13	32.8	13
17	1.11 (*s*)	6α, 7α, 10α, 14	17.0	9, 13	1.10 (*s*)	1.20 (*s*)	6α, 7α, 10α, 14	16.9	7β, 9, 13
18	1.65 (*dsept*, *J*=9.1, 6.6)	3	28.7	3, 4, 19, 20	1.65–1.77 (*m*)	1.33–1.43 (*m*)	3, 14, 19, 20	29.3	3, 4, 19, 20
19[c])	1.05 (*d*, *J*=6.6)	3	23.4	18, 20	1.10 (*d*, *J*=6.6)	1.05 (*d*, *J*=6.6)	3, 18	22.9	4, 18, 20
20[c])	1.08 (*d*, *J*=6.6)		23.8	18, 19	1.09 (*d*, *J*=6.6)	0.96 (*d*, *J*=6.6)	6α, 18	24.0	4, 18, 19

[a]) ^{1}H- (400 MHz) and ^{13}C-NMR (50.3 MHz) spectra recorded in $CDCl_3$ (δ(H) 7.24, δ(C) 77.0), chemical shifts are expressed in ppm and *J* values in Hz. [b]) ^{1}H-NMR (400 MHz) recorded in C_6D_6 (δ(H) 7.16), chemical shifts are expressed in ppm and *J* values in Hz. [c]) Assignments may be interchanged.

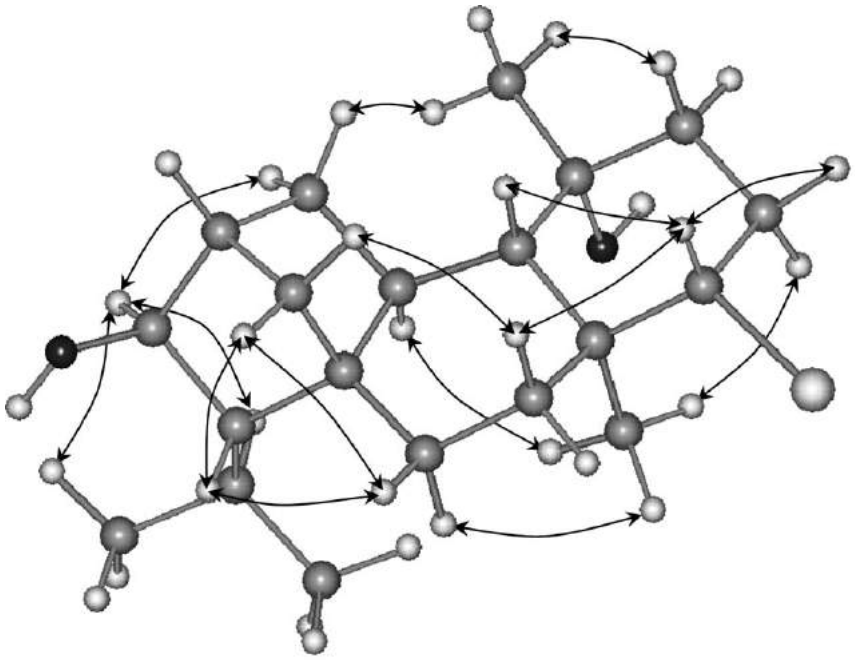

Figure. *NOE Correlations and relative configuration for compound* **3**

2. *Antibacterial Activity.* Metabolites **1**–**4** were evaluated for their antibacterial activity against a panel of *Staphylococcus aureus* strains. These included a multidrug-resistant (MDR) variant (SA1199B), a macrolide-resistant strain (RN4220), a tetracycline-effluxing strain (XU212) which was also methicillin-resistant (MRSA), and two epidemic MRSA strains (*Table 3*). The minimum inhibitory concentrations (*MIC*s) of **2**–**4** were found to be in the range of 16–128 μg/ml. The metabolites exhibited activities which were 4- to 16-times stronger than the standard antibiotic, norfloxacin, against EMRSA-16 (which expresses mecA and is resistant to methicillin). Compounds possessing additional OH groups, *i.e.*, **2** and **3**, showed higher activity than compounds bearing an additional bromine, *i.e.*, **4**, or a MeO group, *i.e.*, **1**. The minor

Table 3. MIC*s of Compounds* **1**–**4** *and a Standard Antibiotic* (Norfloxacin) *in μg/ml against MDR and Methicillin Resistant* Staphylococcus aureus

	SA1199B (NorA) MultiDrug Resistant	RN4220 (MsrA) Macrolide Resistant	EMRSA-15 (mecA) Epidemic Methicillin Resistant	ATCC 25943	XU212 (TetK, mecA) Tetracycline, Methicillin Resistant	EMRSA-16 (mecA) Epidemic Methicillin Resistant
1	128	–	–	128	128	16
2	64	64	64	64	64	32
3	64	64	32	64	64	32
4	64	128	64	64	128	64
Nor	32	1	0.5	0.5	8	256

structural alterations in these tetracyclic brominated diterpenes that cause significant variations in their antibacterial activity make these preliminary results a stimulus for further structure–activity investigations.

This study was partially supported by the *FP-39 EPAN* program of the *Greek Secretariat for Research and Technology*, and a '*Kapodistrian*' program of the University of Athens.

Experimental Part

General. Vacuum liquid chromatography (VLC): Kieselgel *60* (*Merck*). Gravity column chromatography (GCC): Kieselgel *60 H* (*Merck*). TLC: Kieselgel *60* F_{254} aluminum support plates (*Merck*), spots detected after spraying with 15% H_2SO_4 in MeOH reagent and charring. HPLC: *Agilent 1100* model equipped with refractive-index detector and a *Kromasil 100 C18 5u* 25 cm × 8 mm HPLC column. Optical rotations: *Perkin-Elmer* model *341* polarimeter with a 10-cm cell. UV Spectra: *Shimadzu UV-160A* spectrophotometer, in spectroscopic-grade $CHCl_3$. IR Spectra: *Paragon 500 Perkin-Elmer* spectrophotometer. NMR Spectra: *Bruker AC 200* and *Bruker DRX 400* spectrometers; chemical shifts are given on a δ [ppm] scale with TMS as internal standard; the 2D experiments (^{1}H,^{1}H-COSY, HSQC, HMBC, NOESY) were performed using standard *Bruker* microprograms. The structure in the *Figure* was generated and optimized (energy: 55.18 kcal) by HyperChem™ 7.0 molecular-modeling and simulation software (force field: MM+; optimization algorithm: *Polak-Ribiere*). CI-MS: *Thermo DSQ* Mass Detector using Direct Exposure Probe (DEP) and CH_4 as the CI gas; HR-MS: by the University of Notre Dame, Department of Chemistry and Biochemistry, Indiana, USA.

Plant Material. *S. coronopifolius* was collected by SCUBA diving in Palaiokastritsa Bay at the west coast of Corfu Island, Greece, at a depth of 10–15 m in May, 2002. A specimen is deposited with the Herbarium of the Laboratory of Pharmacognosy and Chemistry of Natural Products, University of Athens (ATPH/MO/201).

Extraction and Isolation. *S. coronopifolius* was initially freeze-dried (291.4 g dry weight) and then exhaustively extracted with CH_2Cl_2/MeOH 3:1 at r.t. The combined extracts were concentrated to give a dark green residue (8.20 g), which was later subjected to VLC on SiO_2, using cyclohexane with increasing amounts (10%) of AcOEt and finally MeOH as mobile phase. *Fr. IIa* (20% AcOEt in cyclohexane; 4.01 g) was subjected to GCC, using cyclohexane with increasing amounts (2%) of AcOEt as mobile phase. The MeCN-soluble portion (173.4 mg) of *Fr. XIb* (50% AcOEt in cyclohexane) (199.6 mg) was subjected to reversed-phase HPLC, using MeCN as mobile phase to yield pure compounds **1** (2.2 mg), **2** (4.1 mg), **3** (3.8 mg), and **4** (2.2 mg).

(1S)-1-Methoxybromotetrasphaerol* (=*(1S*,2S*,3S*,4S*,5R*,8S*,9S*,12S*,13S*)-8-Bromo-2-methoxy-5,9-dimethyl-13-(1-methylethyl)tetracyclo[10.2.1.0^{3,12}.0^{4,9}]pentadecan-5-ol*; **1**). Colorless oil. $[\alpha]_D^{20}$ = +12.0 (c = 2.0, $CHCl_3$). UV ($CHCl_3$): 247 (2.80), 414 (2.61), 325 (2.32), 671 (2.18). IR ($CHCl_3$): 3440, 2936. ^{1}H- and ^{13}C-NMR: *Table 1*. CI-MS: 399/401 (1:1, $[M+H]^+$), 381/383 (4:5, $[M+H-H_2O]^+$), 365/367 (1:1), 349/351 (10:9, $[M+H-H_2O-MeOH]^+$), 319 (7, $[M+H-HBr]^+$), 301 (43, $[M+H-H_2O-HBr]^+$), 287 (22, $[M+H-MeOH-HBr]^+$), 269 (100, $[M+H-H_2O-MeOH-HBr]^+$), 253 (19), 199 (12), 120 (31), 81 (21). HR-FAB-MS: 397.1760 ($[M-H]^+$, $C_{21}H_{34}{}^{79}BrO_2^+$; calc. 397.1742).

(4R)-4-Hydroxy-1-deoxybromotetrasphaerol* (=*(1R*,3S*,4S*,5R*,8S*,9S*,12R*,13R*)-8-Bromo-5,9-dimethyl-13-(1-methylethyl)tetracyclo[10.2.1.0^{3,12}.0^{4,9}]pentadecane-5,13-diol*; **2**). White amorphous solid. $[\alpha]_D^{20}$ = −14.3 (c = 3.4, $CHCl_3$). UV ($CHCl_3$): 247 (2.67). IR ($CHCl_3$): 3468, 2942. ^{1}H- and ^{13}C-NMR: *Table 1*. CI-MS: 367/369 (3:2, $[M+H-{}_2O]^+$), 349/351 (11:9, $[M+H-2\ H_2O]^+$), 287 (18, $[M+H-H_2O-HBr]^+$), 269 (100, $[M+H-2\ H_2O-HBr]^+$), 213 (5), 199 (6), 161 (11), 121 (19), 91 (9). HR-FAB-MS: 367.1652 ($[M-OH]^+$, $C_{20}H_{32}{}^{79}BrO^+$; calc. 367.1636).

(3S)-3-Hydroxy-1-deoxybromotetrasphaerol* (=*(1R*,3S*,4S*,5R*,8S*,9S*,12R*,13S*,14S*)-8-Bromo-5,9-dimethyl-13-(1-methylethyl)tetracyclo[10.2.1.0^{3,12}.0^{4,9}]pentadecane-5,14-diol*; **3**). Colorless oil. $[\alpha]_D^{20}$ = −5.1 (c = 3.2, $CHCl_3$). UV ($CHCl_3$): 247 (2.71). IR ($CHCl_3$): 3408, 2942. ^{1}H- and ^{13}C-NMR: *Table 2*. CI-MS: 367/369 (7:6, $[M+H-H_2O]^+$), 349/351 (18:15, $[M+H-2\ H_2O]^+$), 305

(4, $[M+H-HBr]^+$), 287 (30, $[M+H-H_2O-HBr]^+$), 269 (100, $[M+H-2\ H_2O-HBr]^+$), 213 (6), 199 (9), 134 (17), 121 (19), 91 (10). HR-FAB-MS: 383.1575 ($[M-H]^+$, $C_{20}H_{32}{}^{79}BrO_2^+$; calc. 383.1586).

(3S)-3-Bromo-1-deoxybromotetrasphaerol* (=*(1R*,3S*,4S*,5R*,8S*,9S*,12R*,13S*,14S*)-8,14-Dibromo-5,9-dimethyl-13-(1-methylethyl)tetracyclo[10.2.1.0^{3,12}.0^{4,9}]pentadecan-5-ol*; **4**). Colorless oil. $[\alpha]_D^{20} = -3.5$ ($c=2.0$, $CHCl_3$). UV ($CHCl_3$): 248 (3.02), 287 (2.25), 296 (2.14). IR ($CHCl_3$): 3475, 2957. ^{1}H- and ^{13}C-NMR: *Table 2*. CI-MS: 429/431/433 (3:4:2, $[M+H-H_2O]^+$), 367/369 (10:8, $[M+H-HBr]^+$), 349/351 (40:37, $[M+H-H_2O-HBr]^+$), 287 (27, $[M+H-2\ HBr]^+$), 269 (100, $[M+H-H_2O-2\ HBr]^+$), 213 (7), 161 (9), 134 (11), 121 (16), 81 (12). HR-FAB-MS: 429.0783 ($[M-OH]^+$, $C_{20}H_{31}{}^{79}Br_2^+$; calc. 429.0792).

Bacterial Strains and Antibiotic. A standard *S. aureus* strain ATCC 25923 and a clinical isolate (XU212), which possesses the TetK efflux pump and is also a MRSA strain, were obtained from Dr. *E. Udo* [16]. Strain RN4220, which has the MsrA macrolide efflux pump, was provided by Dr. *J. Cove* [17]. EMRSA-15 [18] and EMRSA-16 [19] were obtained from Dr. *P. Stapleton*. Strain SA1199B, which over-expresses the NorA MDR efflux pump, was the gift of Prof. *G. Kaatz* [20]. Norfloxacin was obtained from the *Sigma Chemical Co. Mueller–Hinton* broth (*MHB*; Oxoid) was adjusted to contain 20 mg/l Ca^{2+} and 10 mg/l Mg^{2+}.

Antibacterial Assay. Overnight cultures of each strain were made up in 0.9% saline to an inoculum density of 5×10^5 cfu by comparison with a *McFarland* standard. Norfloxacin was dissolved in DMSO and then diluted in MHB to give a starting concentration of 512 μg/ml. Using Nunc 96-well microtitre plates, 125 μl of MHB were dispensed into wells 1–11. 125 μl of the test compound or the appropriate antibiotic were dispensed into well 1 and serially diluted across the plate, leaving well 11 empty for the growth control. The final volume was dispensed into well 12, which, being free of MHB or inoculum, served as the sterile control. Finally, the bacterial inoculum (125 μl) was added to wells 1–11, and the plate was incubated at 37° for 18 h. A DMSO control (3.125%) was also included. All *MIC* values were determined in duplicate. The *MIC* value was determined as the lowest concentration at which no growth was observed. A methanolic soln. (5 mg/ml) of 3-(4,5-dimethylthiazol-2-yl)-2,5-diphenyl-2*H*-tetrazolium bromide (MTT; *Lancaster*) was used to detect bacterial growth by a color change from yellow to blue.

REFERENCES

[1] D. Patel, I. Madan, *Occup. Med.* **2000**, *50*, 392.
[2] V. Smyrniotopoulos, A. Quesada, C. Vagias, D. Moreau, C. Roussakis, V. Roussis, *Tetrahedron* **2008**, *64*, 5184.
[3] V. Smyrniotopoulos, C. Vagias, M. M. Rahman, S. Gibbons, V. Roussis, *J. Nat. Prod.* **2008**, *71*, 1386.
[4] S. Etahiri, V. Bultel-Poncé, C. Caux, M. Guyot, *J. Nat. Prod.* **2001**, *64*, 1024, and refs. cit. therein.
[5] N. A. Paul, R. de Nys, P. D. Steinberg, *Mar. Ecol.: Prog. Ser.* **2006**, *306*, 87.
[6] D. Davyt, R. Fernandez, L. Suescun, A. W. Mombrú, J. Saldaña, L. Domínguez, M. T. Fujii, E. Manta, *J. Nat. Prod.* **2006**, *69*, 1113.
[7] R. de Nys, S. A. Dworjanyn, P. D. Steinberg, *Mar. Ecol.: Prog. Ser.* **1998**, *162*, 79.
[8] K. A. El Sayed, D. C. Dunbar, T. L. Perry, S. P. Wilkins, M. T. Hamann, J. T. Greenplate, M. A. Widemann, *J. Agric. Food Chem.* **1997**, *45*, 2735.
[9] C. S. Vairappan, M. Suzuki, T. Abe, M. Masuda, *Phytochemistry* **2001**, *58*, 517.
[10] M. V. D'Auria, L. G. Paloma, L. Minale, A. Zampella, C. Debitus, J. Perez, *J. Nat. Prod.* **1995**, *58*, 121.
[11] S. Sakemi, T. Higa, C. W. Jefford, G. Bernardinelli, *Tetrahedron Lett.* **1986**, *27*, 4287.
[12] E. Ioannou, A. Quesada, C. Vagias, V. Roussis, *Tetrahedron* **2008**, *64*, 3975.
[13] I. Kontiza, M. Stavri, M. Zloh, C. Vagias, S. Gibbons, V. Roussis, *Tetrahedron* **2008**, *64*, 1696.
[14] M. Kladi, C. Vagias, M. Stavri, M. M. Rahman, S. Gibbons, V. Roussis, *Phytochem. Lett.* **2008**, *1*, 31.
[15] F. Cafieri, E. Fattorusso, L. Mayol, *Tetrahedron* **1986**, *42*, 4273.
[16] S. Gibbons, E. E. Udo, *Phytother. Res.* **2000**, *14*, 139.
[17] J. I. Ross, A. M. Farrell, E. A. Eady, J. H. Cove, W. J. Cunliffe, *J. Antimicrob. Chemother.* **1989**, *24*, 851.

[18] J. F. Richardson, S. Reith, *J. Hosp. Infect.* **1993**, *25*, 45.
[19] R. A. Cox, C. Conquest, C. Mallaghan, R. R. Maples, *J. Hosp. Infect.* **1995**, *29*, 87.
[20] G. W. Kaatz, S. M. Seo, C. A. Ruble, *Antimicrob. Agents Chemother.* **1993**, *37*, 1086.

Received October 17, 2008

Constituents of Cinnamon Inhibit Bacterial Acetyl CoA Carboxylase

Authors Glen Meades, Jr.[1], Rachel L. Henken[2], Grover L. Waldrop[1], Md. Mukhlesur Rahman[3], S. Douglass Gilman[2], Guy P. P. Kamatou[4], Alvaro M. Viljoen[4], Simon Gibbons[3]

Affiliations
[1] Division of Biochemistry and Molecular Biology, Louisiana State University, Baton Rouge, Louisiana, USA
[2] Department of Chemistry, Louisiana State University, Baton Rouge, Louisiana, USA
[3] Department of Pharmaceutical and Biological Chemistry, The School of Pharmacy, University of London, London, UK
[4] Department of Pharmaceutical Sciences, Faculty of Science, Tshwane University of Technology, Pretoria, South Africa

Key words
- *Cinnamomum zeylanicum*
- Lauraceae
- *trans*-cinnamaldehyde
- acetyl-CoA carboxylase
- carboxyltransferase

Abstract

Cinnamon bark (*Cinnamomum zeylanicum*) is used extensively as an antimicrobial material and currently is being increasingly used in Europe by people with type II diabetes to control their glucose levels. In this paper we describe the action of cinnamon oil, its major component, *trans*-cinnamaldehyde, and an analogue, 4-hydroxy-3-methoxy-*trans*-cinnamaldehyde against bacterial acetyl-CoA carboxylase in an attempt to elucidate the mechanism of action of this well-known antimicrobial material. These natural products inhibited the carboxyltransferase component of *Escherichia coli* acetyl-CoA carboxylase but had no effect on the activity of the biotin carboxylase component. The inhibition patterns indicated that these products bound to the biotin binding site of carboxyltransferase with *trans*-cinnamaldehyde having a K_i value of 3.8 ± 0.6 mM. The inhibition of carboxyltransferase by 4-hydroxy-3-methoxy-*trans*-cinnamaldehyde was analyzed with a new assay for this enzyme based on capillary electrophoresis. These results explain, in part, the antibacterial activity of this well-known antimicrobial material.

received Dec. 7, 2009
revised February 22, 2010
accepted March 4, 2010

Bibliography
DOI http://dx.doi.org/10.1055/s-0030-1249778
Published online April 8, 2010
Planta Med 2010; 76: 1570–1575 © Georg Thieme Verlag KG Stuttgart · New York · ISSN 0032-0943

Correspondence
Simon Gibbons
Department of Pharmaceutical and Biological Chemistry
The School of Pharmacy
University of London
29–39 Brunswick Square
London WC1N 1AX
United Kingdom
Phone: + 44 20 77 53 59 13
simon.gibbons@pharmacy.ac.uk

Introduction

Sri Lankan cinnamon or sweet cinnamon (*Cinnamomum zeylanicum* Breyne) is one of the most ancient medicinal plant materials and is mentioned in the Bible [1]. The Greek physician Dioscorides mentions the use of cinnamon as an anti-inflammatory preparation and in combination with honey for use as an antibacterial material to remove spots from the skin [2].

Powdered cinnamon bark has recently gained popularity in Europe as a Herbal Medicinal Product (HMP), particularly amongst patients with type II diabetes, and this has led to a number of recent articles on its use [3–8]. Sweet cinnamon bark is rich in an essential oil which constitutes 0.5–2.5% w/w, and this oil is produced in considerable quantity for the flavor and fragrance markets. The European Pharmacopeia states that cinnamon oil should be comprised of 55–75% of *trans*-cinnamaldehyde with less than 0.5% of coumarin, which is also present in other species of *Cinnamomum* such as Chinese cinnamon (*Cinnamomum cassia* Blume, syn. *C. aromaticum*), which is less valuable and less commercially important than the oil of the bark of sweet cinnamon.

Cinnamon oil and the main constituent of the oil, *trans*-cinnamaldehyde (**1**), have been studied intensively for their many pharmacological effects, which include antifungal activity [9,10], antibacterial activity [11–13], food preservation [14], antityrosinase activity [15], anti-inflammatory action [16], potential in slowing the onset of Alzheimer's disease [17], and the regulation of glucose and fatty acid metabolism [18–20].

Here we show that cinnamon oil and its main component, *trans*-cinnamaldehyde, inhibit bacterial acetyl-CoA carboxylase (ACC), and that these findings may, in part, explain the activity of these agents against bacteria and other microbes.

Materials and Methods

Materials

Coupling enzymes and substrates for the assay of *E. coli* biotin carboxylase and carboxyltransferase were from Sigma. *trans*-Cinnamaldehyde (> 99% by GC) and 4-hydroxy-3-methoxy-cinnamaldehyde (98%) were obtained from Sigma-Aldrich and cinnamon oil (batch number CIN0006/1000) was obtained from Botanicals and Natural Products, Ltd. Moiramide B was a gift from Pfizer. Nor-

floxacin (98% by TLC) was obtained from Sigma-Aldrich and 3-[4,5-dimethylthiazol-2-yl]-2,5-diphenyltetrazolium bromide was obtained from MTT. Tris Buffer was from Acros Organics.

Bacterial strains and chemicals

Methicillin-resistant *Staphylococcus aureus* (MRSA) strain XU212, a clinical isolate [21] which possesses the TetK efflux pump, and the standard ATCC25923 strain was obtained from Dr. E. Udo. Strain RN4220, which has the MsrA macrolide efflux protein, was provided by J. Cove [22]. EMRSA-15 and EMRSA-16 [23] were obtained from Dr. Paul Stapleton. Strain SA1199B, which overexpresses the NorA MDR efflux pump, was the gift of Professor Glenn W. Kaatz [24]. Mueller-Hinton broth (MHB; Oxoid) was adjusted to contain 20 mg/L Ca^{2+} and 10 mg/L Mg^{2+}.

GC-MS analysis of the cinnamon oil

The oil was analyzed by GC-MS on an Agilent 6890 N GC system coupled directly to a 5973 mass spectrometer. A volume of 1 microliter was injected using a split ratio (200 : 1) with an autosampler at 24.79 psi and an inlet temperature of 250 °C. The GC system was equipped with an HP-Innowax polyethylene glycol column of dimensions 60 m × 250 µm with an internal diameter of 0.25 µm film thickness. The oven temperature program was 60 °C for the first 10 minutes, rising to 220 °C at a rate of 4 °C/min and held for 10 min, and then rising to 240 °C at a rate of 1 °C/min. Helium was used as carrier gas at a constant flow of 1.2 mL/min. Spectra were obtained by electron impact at 70 eV, scanning from 35 to 550 *m/z*. The percentage compositions of the individual components were obtained from electronic integration measurements using flame ionization detection (FID, 250 °C). *n*-Alkanes were used as reference points in the calculation of relative retention indices (RRI). The identification of the compounds was carried out using NIST®, Mass Finder® and Flavour® libraries by comparing mass spectra and retention indices.

Antibacterial assays

Overnight cultures of each strain were made up in 0.9% saline to an inoculum density of 5×10^5 cfu by comparison with a MacFarland standard. Norfloxacin was dissolved in DMSO and then diluted in MHB to give a starting concentration of 512 µg/mL. Using Nunc 96-well microtiter plates, 125 µL of MHB were dispensed into wells 1–11. A volume of 125 µL of the test compound or the antibiotic norfloxacin was dispensed into well 1 and serially diluted across the plate, leaving well 11 empty for the growth control. The final volume was dispensed into well 12, which being free of MHB or inoculum, served as the sterile control. Finally, the bacterial inoculum (125 µL) was added to wells 1–11, and the plate was incubated at 37 °C for 18 h. A DMSO control (3.125%) was also included. All MICs were determined in duplicate. The MIC was determined as the lowest concentration at which no growth was observed. A methanolic solution (5 mg/mL) of 3-[4,5-dimethylthiazol-2-yl]-2,5-diphenyltetrazoliium bromide was used to detect bacterial growth by a color change from yellow to blue.

Assay of *E. coli* biotin carboxylase

Biotin carboxylase from *E. coli* was isolated from a strain of *E. coli* that was engineered to overexpress the gene (*accC*) coding for the enzyme [25]. The activity of the purified enzyme was determined by measuring the production of ADP using a coupled enzyme assay of pyruvate kinase and lactate dehydrogenase as described by Blanchard et al. [25].

Assay of *E. coli* carboxyltransferase

The carboxyltransferase component of *E. coli* ACC was isolated from a strain of *E. coli* that was engineered to overexpress the genes (*accA* and *accD*) coding for the enzyme [26]. The activity of the enzyme was determined in the reverse direction using a coupled enzyme assay where the production of acetyl-CoA was coupled to the citrate synthase-malate dehydrogenase reactions requiring NAD^+ reduction [26]. The cinnamon constituents did not inhibit either of the coupling enzymes.

Data analysis

Data for competitive and uncompetitive inhibition were fitted to equations 1 and 2, respectively, using the programs of Cleland [27]. In equations 1 and 2, v is the initial velocity, V_{max} is the maximal velocity, A is the substrate concentration, I is the concentration of inhibitor, K_m is the Michaelis constant, and K_i is the inhibition constant.

$$v = V_{max} \cdot A/[K_m(1 + I/K_i) + A] \quad (1)$$

$$v = V_{max} \cdot A/[K_m + A(1 + I/K_i)] \quad (2)$$

Capillary electrophoresis assay of *E. coli* carboxyltransferase

Capillary electrophoretic separations were performed using a P/ACE MDQ with 32 Karat version 5.0 software from Beckman Coulter, Inc. This instrument was equipped with a D_2 lamp and a photodiode array detector. Electropherograms for this work were plotted at a wavelength of 260 nm. The enzyme assay was performed off-line, and a sample of the reaction mixture was injected hydrodynamically for 0.5 s at 5 psi. The separation was performed in 50.0 mM Tris Buffer, pH 8.85 with an applied voltage of 20.0 kV (322 V/cm) resulting in a current of 4.4 µA. The fused silica capillary was purchased from Polymicro with an inner diameter of 50 µm and a 360 µm outer diameter. The total length of the capillary was 62 cm with a 50-cm length to the detection window. The detection window was made by removing a short section, less than 5 mm, of the polyimide coating from the capillary with a MicorSolv CE window maker.

Results and Discussion

Whilst there is a plethora of literature concerning the use of cinnamon and its corresponding volatile oil as an antimicrobial substance, there is surprisingly little known about the mechanism of the antibacterial action of the oil or the major natural products. We therefore set out to investigate the oil (CO), its main constituent, *trans*-cinnamaldehyde (CA) (**1**) and the related commercially available natural product analogue, 4-hydroxy-3-methoxy-*trans*-cinnamaldehyde (**2**) (coniferaldehyde), as potential inhibitors of acetyl-CoA carboxylase (**Fig. 1**). A commercially available batch of cinnamon oil was analyzed using GC-MS and the composition and chromatogram are given in **Table 1** and **Fig. 2**, respectively. These show the characteristic major constituent *trans*-cinnamaldehyde, which is consistently present in the bark of sweet cinnamon (*Cinnamomum zeylanicum*) and along with the absence of coumarin is a diagnostic feature of this crude plant drug.

We first investigated the activity of the three components against a panel of *Staphylococcus aureus* strains with all three natural products displaying antibacterial activity with minimum inhibitory concentration (MIC) values ranging from 64–512 mg/L (**Ta-**

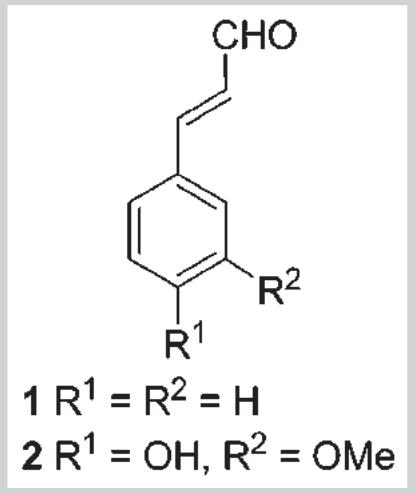

Fig. 1 Structures of *trans*-cinnamaldehyde (**1**) and 4-hydroxy-3-methoxy-*trans*-cinnamaldehyde (**2**).

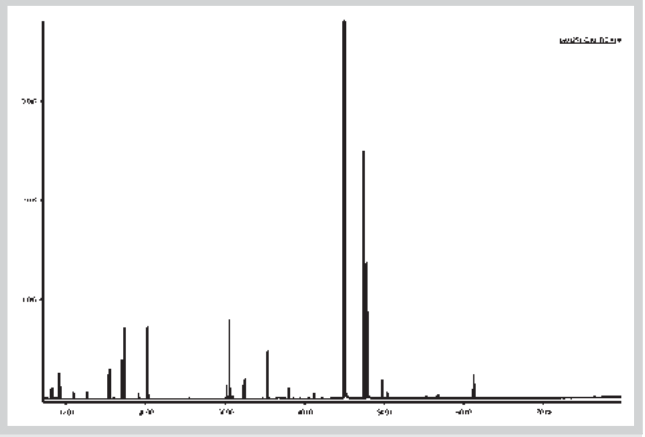

Fig. 2 GC chromatogram of the cinnamon oil used in this study.

Table 1 Relative retention indices and percentage area of cinnamon oil.

RRI	Compounds	% area
1000	Decane	0.2
1018	α-Pinene	0.4
1061	Camphene	0.1
1104	β-Pinene	0.1
1161	α-Phellandrene	0.6
1194	Limonene	0.9
1202	1,8-Cineole	1.6
1244	γ-Terpinene	0.1
1272	*p*-Cymene	1.4
1531	Dihydrolinalool	0.1
1534	Benzaldehyde	0.4
1545	Linalool	2.4
1556	*trans*-*p*-Menth-2-en-1-ol	0.1
1601	B-Caryophyllene	0.3
1603	Terpinen-4-ol	0.5
1701	α-Terpineol	1.4
1794	Benzenepropanal	0.7
1847	Geraniol	0.1
1889	Benzyl alcohol	0.1
1955	Benzene-2-propenyl	0.1
2067	*E*-Cinnamaldehyde	70.9
2170	Cinnamyl acetate	9.1
2186	Eugenol	5.4
2298	Cinnamyl alcohol	0.4
2587	2-Methyl-naphthalen-1-ol	0.2
2798	Benzyl benzoate	1.3
		98.9

ble 2). These strains included a standard laboratory strain (ATCC 25923) and several strains which are clinical isolates and resistant to several antibiotics such as the multidrug-resistant SA 1199B (fluoroquinolone-effluxing), XU212 (tetracycline-effluxing) and EMRSA-15 and 16, the two most prevalent epidemic methicillin-resistant strains from UK hospitals [23]. Given the activity of *trans*-cinnamaldehyde (**1**) it is likely that it is the major compound responsible for antibacterial action in cinnamon oil, demonstrating the highest activity against EMRSA-16 with an MIC of 64 mg/L. To investigate the possible mechanism of action for the antibacterial activity of *trans*-cinnamaldehyde (**1**) we examined the effect of cinnamon oil (CO), *trans*-cinnamaldehyde (CA) (**1**) and 4-hydroxy-3-methoxy-*trans*-cinnamaldehyde (**2**) on the activity of the antibiotic target acetyl-CoA carboxylase.

Acetyl-CoA carboxylase (ACC) catalyzes the first committed step in fatty acid biosynthesis in all animals, plants and bacteria. The enzyme requires the cofactor biotin and utilizes a two-step reaction sequence shown in **Fig. 3**.

In the first half-reaction, biotin carboxylase catalyzes the ATP-dependent carboxylation of biotin. In the next reaction, catalyzed by the carboxyltransferase subunit, the carboxyl group is transferred to acetyl-CoA to make malonyl-CoA. *In vivo*, biotin is covalently attached to the biotin carboxyl carrier protein (designated as enzyme-biotin in **Fig. 3**). In bacteria each of the three components of ACC are separate proteins where biotin carboxylase and carboxyltransferase retain their enzymatic activity after purification and will utilize free biotin as a substrate in place of the carrier protein [28]. In eukaryotes, all three functions of ACC are combined within a single polypeptide.

The biotin carboxylase component of *E. coli* ACC was not inhibited by the cinnamon oil, *trans*-cinnamaldehyde, or the cinnamaldehyde analogue 4-hydroxy-3-methoxy-*trans*-cinnamaldehyde.

In contrast to the biotin carboxylase component, the carboxyltransferase component of *E. coli* ACC was inhibited by all three materials tested. To test the inhibitory properties of cinnamaldehyde (**1**) and the cinnamon oil, a coupled enzyme assay was used where the reduction of NAD^+ can be measured based on the absorbance at 340 nm [26]. The reaction is run in the non-physiological direction, which means that malonyl-CoA and biocytin are the substrates. Biocytin is an analogue of biotin where lysine is attached to the valeric acid carboxyl group. Biocytin has utility in place of biotin for the coupled enzyme assay as it is more reactive [26].

Using this assay, both cinnamaldehyde and cinnamon oil exhibited competitive inhibition with respect to biocytin and, therefore, presumably bind in the biotin binding site (**Fig. 4A, B**). Due to the high absorbance of both **1** and **2** at 340 nm, the kinetics at only one concentration of inhibitor could be measured (i.e., higher concentrations of **1** and cinnamon oil masked the absorbance due to NADH production). The K_i for **1** was 3.8 ± 0.6 mM. By GC-MS, the *trans*-cinnamaldehyde (CA) constitutes 70.9% of the cinnamon oil by mass. Therefore, the Ki for **1** in the context of CO was calculated to be 5.6 ± 0.8 mM which is very close to the K_i value determined for pure *trans*-cinnamaldehyde. In contrast to biocytin, both **1** and cinnamon oil exhibited uncompetitive inhibition with respect to malonyl-CoA (**Fig. 4C, D**). The

Table 2 Minimum inhibitory concentrations of *trans*-cinnamaldehyde (**1**), cinnamon oil (CO), 4-hydroxy-3-methoxycinnamaldehyde (**2**) and norfloxacin in mg/L against multidrug-resistant (MDR) and methicillin-resistant *Staphylococcus aureus* strains. Resistance mechanisms for each strain are given in parentheses.

Compounds	SA 1199B (NorA)	RN4220 (MsrA)	EMRSA-15 (mecA)	ATCC 25 943	XU212 (TetK)/(mecA)	EMRSA-16 (mecA)
1	128	128	256	126	128	64
CO	256	128	256	256	256	128
2	256	256	512	256	256	128
Norfloxacin	32	1	0.5	0.5	8	256

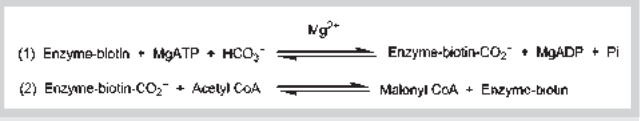

Fig. 3 Two-step reaction catalyzed by acetyl-CoA carboxylase.

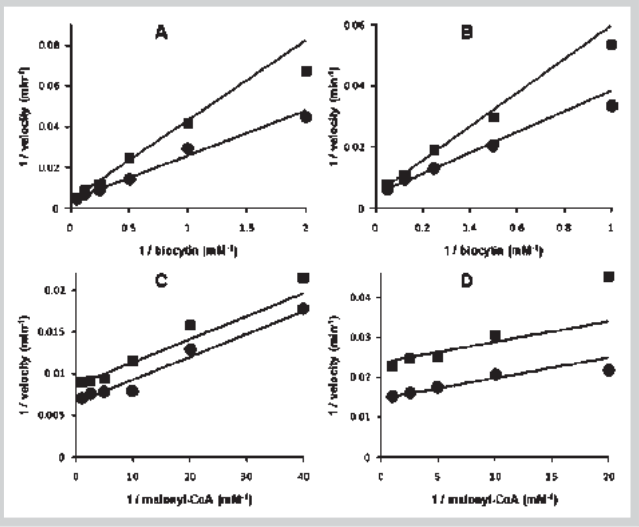

Fig. 4 Inhibition of carboxyltransferase by *trans*-cinnamaldehyde (**A, C**) and cinnamon oil (**B, D**). When malonyl-CoA was the variable substrate (**A, B**), biocytin was held constant at 2.0 mM, and when biocytin was the variable substrate (**C, D**), malonyl-CoA was held constant at 0.1 mM. The points are the reciprocal of the experimental velocities, and the lines are derived from the best fit of the data to either competitive inhibition (Equation 1) (**A, B**) or uncompetitive inhibition (Equation 2) (**C, D**). Circles represent no inhibitor present; squares represent the presence of either 2.0 mM cinnamaldehyde (**A, C**) or 0.8 µg/mL cinnamon oil (**B, D**).

uncompetitive inhibition pattern with respect to malonyl-CoA is consistent with *trans*-cinnamaldehyde (**1**) which is also present in cinnamon oil binding in the biocytin binding site, given that carboxyltransferase has an ordered addition of substrates with malonyl-CoA binding first [26, 29]. Since *trans*-cinnamaldehyde binds in the biocytin binding site, malonyl-CoA must have previously bound to the enzyme before *trans*-cinnamaldehyde can bind and inhibit turnover. Therefore, only at a saturating level of malonyl-CoA (i.e., the y intercept) do the cinnamon derivatives exhibit inhibition, whereas at a very low level of malonyl-CoA (i.e., the slope) the cinnamon derivatives do not bind, and no change is observed. As a positive control, the known carboxyltransferase inhibitor moiramide B [38] was used to exhibit inhibition of activity in the same assay used to determine inhibition by **1**. Carboxyltransferase in the presence of 600 nM moiramide B shows 19% activity compared to uninhibited enzyme, and 0.9% activity with 6 µM moiramide B present.

It is important to note that the inhibition of carboxyltransferase by *trans*-cinnamaldehyde was not irreversible. The inhibition of carboxyltransferase could have been the result of covalent modification of essential residues on the enzyme by the aldehyde group of **1**. This could feasibly occur through a classical "Michael-type" addition to the double bond which is alpha to the aldehyde. However, when 2 mM of cinnamaldehyde were incubated with carboxyltransferase, the activity was found not to decrease with time for a period of 30 min. The lack of a time dependence suggested that inhibition of carboxyltransferase by *trans*-cinnamaldehyde is not due to covalent modification but instead is simple reversible binding to the biocytin binding site. Moreover, if **1** inhibited by randomly modifying amino acids in the enzyme then biotin carboxylase would have been just as susceptible as carboxyltransferase.

The *trans*-cinnamaldehyde analogue 4-hydroxy-3-methoxy-*trans*-cinnamaldehyde (**2**) (coniferaldehyde) could not be analyzed using the conventional coupled enzyme assay described above because of its strong absorbance at 340 nm, which interferes with the absorbance of NADH from the coupled reaction. Therefore, to determine if **2** inhibited carboxyltransferase, an assay using capillary electrophoresis was developed. Capillary electrophoresis is a separation technique based on differences in the ratio of charge to hydrodynamic radius for analytes in a conductive solution. Capillary electrophoresis can be used to analyze enzyme kinetics and perform assays both on- and off-column [30, 31]. In this work the assay was performed off-column by sampling the reaction mixture at intervals. Reaction mixtures of 20 µM malonyl-CoA, 4 mM biocytin, and 114 µg/mL ACC were sampled and analyzed at 0, 30, 60, and 90 min in both the absence and presence of 20 µM of the inhibitor 4-hydroxy-3-methoxy-*trans*-cinnamaldehyde. The mixture was sufficiently separated such that malonyl-CoA, acetyl-CoA and 4-hydroxy-3-methoxy-*trans*-cinnamaldehyde, when included, were baseline resolved in less than 10 min. The reaction progress can be monitored by the increase in the acetyl-CoA product peak and the depletion of the substrate peak, malonyl-CoA, as seen in ◉ **Fig. 5**, which shows the reaction progress in the absence of 4-hydroxy-3-methoxy-*trans*-cinnamaldehyde. When this inhibitor was present in the reaction mixture, less product formation and less substrate depletion were observed (◉ **Fig. 6**) compared to reactions without the inhibitor. These results indicate that 4-hydroxy-3-methoxy-*trans*-cinnamaldehyde is also an inhibitor of the carboxyltransferase component of *E. coli* ACC.

At first glance it is not immediately apparent why *trans*-cinnamaldehyde would inhibit the carboxyltransferase component of ACC. However, if this inhibition is examined from the context of enzyme structure, it becomes obvious why it inhibits. Carboxyltransferase belongs to the crotonase superfamily of enzymes whose members all catalyze reactions that generate enolate

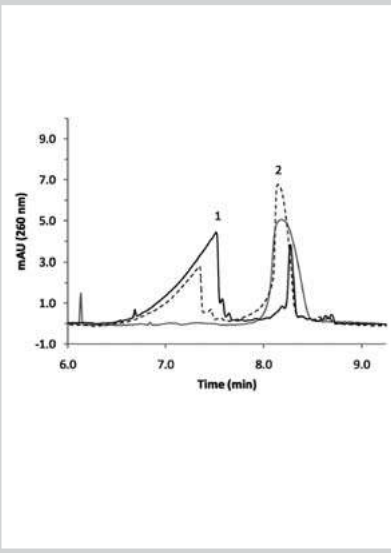

Fig. 5 Electropherograms of reaction mixture without inhibitor at times 0 (grey trace), 30 (dash), and 60 min (black) showing the increase of (1) acetyl-CoA product peak and the decrease of the (2) malonyl-CoA substrate. At each time interval a sample of the reaction mixture was injected for 5.0 s at 0.5 psi into the column, which contained a separation buffer of 50 mM Tris, pH ;8.85 and was separated with a 20.0 kV applied voltage.

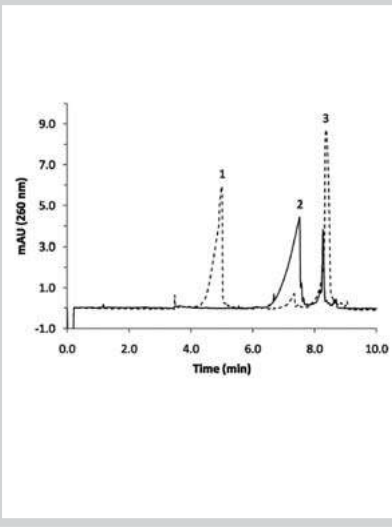

Fig. 6 Electropherograms of reaction mixtures with (dash) and without (black) inhibitor after 60 min incubation. 1.4-hydroxy-3-methoxy-*trans*-cinnamaldehyde (inhibitor), 2. acetyl-CoA (product), 3. malonyl-CoA (substrate). A sample of the reaction mixture was injected for 5.0 s at 0.5 psi into the column, which contained a separation buffer of 50.00 mM Tris, pH 8.85 and was separated with a 20.0 kV applied voltage.

anion intermediates [32, 33]. In carboxyltransferase the transfer of the carboxyl group from carboxybiotin to acetyl-CoA involves formation of enolate or enolate-like anions for both carboxybiotin and acetyl-CoA. To this end, both the α and β subunits of carboxyltransferase have evolved tertiary folds that stabilize oxyanions. Acetyl-CoA binds to the β subunit, while carboxybiotin binds to the α subunit, and the tertiary structure of both the α and β subunits contain a similar α/β spiral core of two β-sheets surrounded by α-helices, suggesting a gene duplication event. Within the spiral core of both the α and β subunits of carboxyltransferase are oxyanion holes formed by main chain amides from glycine residues [34]. The inhibition patterns indicate that *trans*-cinnamaldehyde (**1**) binds to the biotin/biocytin binding site. The binding is likely to involve the interaction of the carbonyl oxygen of **1** with the oxyanion hole in the α subunit.

Further support for this mechanism of inhibition of carboxyltransferase comes from the fact that other members of the crotonase superfamily of enzymes utilize cinnamaldehyde derivatives as substrates. For example, hydroxycinnamoyl-CoA hydratase lyase plays a role in the microbial degradation of phenolic compounds by catalyzing the conversion of feruloyl-CoA into vanillin [35]. Moreover, the crystal structure of enoyl-CoA hydratase (i.e., crotonase) was solved with 4-(*N,N*-dimethylamino)-cinnamoyl-CoA bound in the active site [36]. The three-dimensional structures of both of these enzymes showed that the carbonyl oxygen of the thioester, which is equivalent to the carbonyl oxygen in the cinnamon derivatives used in this study, bound in the oxyanion hole. Thus, the ability of other members of the crotonase superfamily of enzymes to bind structural analogues of *trans*-cinnamaldehyde certainly makes the observation of cinnamaldehyde binding weakly to carboxyltransferase not unexpected and also suggests a possible mechanism of interaction.

The finding that cinnamon inhibits bacterial growth and the carboxyltransferase subunit of *E. coli* ACC does have implications for pharmaceutical development. Both the biotin carboxylase [37] and carboxyltransferase [38] subunits have been shown to be targets for antibiotic development. In fact, the natural product moiramide B inhibits carboxyltransferase with a K_i value of 5 nM and has structural features similar to those of cinnamaldehyde [38]. However, moiramide B was too toxic for pharmaceutical use. Cinnamaldehyde derivatives on the other hand could be used as an initial lead for fragment-based drug design. Fragment-based drug design has been used recently with increasing success to develop pharmaceuticals [39]. The basic approach involves identifying small molecules (< 250 Da) that bind weakly to a target molecule, and then through an iterative process of synthetic modification and structure determination a more potent derivative of the initial fragment is developed. *trans*-Cinnamaldehyde could therefore be a promising starting fragment especially considering that it is nontoxic.

References

1 The King James Bible, Exodus, 30: 23–26
2 *Farrell KT.* Spices, condiments and seasonings. New York: The AVI Publisher Co.; 1985
3 *Mishra A, Bhatti R, Singh A, Ishar MPS.* Ameliorative effect of the cinnamon oil from *Cinnamomum zeylanicum* upon early stage diabetic nephropathy. Planta Med 2010; 76: 412–417
4 *de Luis DA, Aller R, Romero E.* Cinnamon as possible treatment of diabetes mellitus type 2. Med Clin (Barc) 2008; 131: 279
5 *Ammon HP.* Cinnamon in type 2 diabetics. Med Monatsschr Pharm 2008; 31: 179–183
6 *Baker WL, Gutierrez-Williams G, White CM, Kluger J, Coleman CI.* Effect of cinnamon on glucose control and lipid parameters. Diabetes Care 2008; 31: 41–43
7 *Dugoua JJ, Seely D, Perri D, Cooley K, Forelli T, Mills E, Koren G.* From type 2 diabetes to antioxidant activity: a systematic review of the safety and efficacy of common and cassia cinnamon bark. Can J Physiol Pharmacol 2007; 85: 837–847
8 *Suppapitiporn S, Kanpaksi N, Suppapitiporn S.* The effect of cinnamon cassia powder in type 2 diabetes mellitus. J Med Assoc Thai 2006; 89 (Suppl. 3): S200–S205
9 *Inouye S, Uchida K, Nishiyama Y, Hasumi Y, Yamaguchi H, Abe S.* Combined effect of heat, essential oils and salt on fungicidal activity against *Trichophyton mentagrophytes* in a foot bath. Nippon Ishinkin Gakkai Zasshi 2007; 48: 27–36
10 *Pozzatti P, Scheid LA, Spader TB, Atayde ML, Santurio JM, Alves SH. In vitro* activity of essential oils extracted from plants used as spices against fluconazole-resistant and fluconazole-susceptible *Candida* spp. Can J Microbiol 2008; 54: 950–956
11 *Prabuseenivasan S, Jayakumar M, Ignacimuthu S. In vitro* antibacterial activity of some plant essential oils. BMC Complement Altern Med 2006; 6: 39
12 *Shahverdi AR, Monsef-Esfahani HR, Tavasoli F, Zaheri A, Mirjani R.* trans-Cinnamaldehyde from *Cinnamomum zeylanicum* bark essential oil reduces the clindamycin resistance of *Clostridium difficile in vitro*. J Food Sci 2007; 72: S055–S058

13 *Wong SY, Grant IR, Friedman M, Elliott CT, Situ C.* Antibacterial activities of naturally occurring compounds against *Mycobacterium avium* subsp. *paratuberculosis*. Appl Environ Microbiol 2008; 74: 5986–5990
14 *Mosqueda-Melgar J, Raybaudi-Massilia RM, Martín-Belloso O.* Combination of high-intensity pulsed electric fields with natural antimicrobials to inactivate pathogenic microorganisms and extend the shelf-life of melon and watermelon juices. Food Microbiol 2008; 25: 479–491
15 *Marongiu B, Piras A, Porcedda S, Tuveri E, Sanjust E, Meli M, Sollai F, Zucca P, Rescigno A.* Supercritical CO_2 extract of *Cinnamomum zeylanicum*: chemical characterization and antityrosinase activity. J Agric Food Chem 2007; 55: 10022–10027
16 *Kim DH, Kim CH, Kim MS, Kim JY, Jung KJ, Chung JH, An WG, Lee JW, Yu BP, Chung HY.* Suppression of age-related inflammatory NF-kappaB activation by cinnamaldehyde. Biogerontology 2007; 8: 545–554
17 *McCarty MF.* Toward prevention of Alzheimers disease – potential nutraceutical strategies for suppressing the production of amyloid beta peptides. Med Hypotheses 2006; 67: 682–697
18 *Kannappan S, Jayaraman T, Rajasekar P, Ravichandran MK, Anuradha CV.* Cinnamon bark extract improves glucose metabolism and lipid profile in the fructose-fed rat. Singapore Med J 2006; 47: 858–863
19 *O'Keefe JH, Gheewala NM, O'Keefe JO.* Dietary strategies for improving post-prandial glucose, lipids, inflammation, and cardiovascular health. J Am Coll Cardiol 2008; 51: 249–255
20 *Qin B, Polansky MM, Sato Y, Adeli K, Anderson RA.* Cinnamon extract inhibits the postprandial overproduction of apolipoprotein B48-containing lipoproteins in fructose-fed animals. J Nutr Biochem 2009; 20: 901–908
21 *Gibbons S, Udo EE.* The effect of reserpine, a modulator of multidrug efflux pumps, on the *in vitro* activity of tetracycline against clinical isolates of methicillin resistant *Staphylococcus aureus* (MRSA) possessing the tet(K) determinant. Phytother Res 2000; 14: 139–140
22 *Ross JI, Farrell AM, Eady EA, Cove JH, Cunliffe WJ.* Characterisation and molecular cloning of the novel macrolide-streptogramin B resistance determinant from *Staphylococcus epidermidis*. J Antimicrob Chemother 1989; 24: 851–862
23 *Richardson JF, Reith S.* Characterization of a strain of methicillin-resistant *Staphylococcus aureus* (EMRSA-15) by conventional and molecular methods. J Hosp Infect 1993; 25: 45–52
24 *Kaatz GW, Seo SM, Ruble CA.* Efflux-mediated fluoroquinolone resistance in *Staphylococcus aureus*. Antimicrob Agents Chemother 1993; 37: 1086–1094
25 *Blanchard CZ, Lee YM, Frantom PA, Waldrop GL.* Mutations at four active site residues of biotin carboxylase abolish substrate-induced synergism by biotin. Biochemistry 1999; 38: 3393–3400
26 *Blanchard CZ, Waldrop GL.* Overexpression and kinetic characterization of the carboxyltransferase component of acetyl-CoA carboxylase. J Biol Chem 1998; 273: 19140–19145
27 *Cleland WW.* Statistical analysis of enzyme kinetic data. Methods Enzymol 1979; 63: 103–138
28 *Cronan JE, Waldrop GL.* Multi-subunit acetyl-CoA carboxylases. Prog Lipid Res 2002; 41: 407–435
29 *Levert KL, Waldrop GL.* A bisubstrate analog inhibitor of the carboxyltransferase component of acetyl-CoA carboxylase. Biochem Biophys Res Commun 2002; 291: 1213–1217
30 *Glatz Z.* Determination of enzymatic activity by capillary electrophoresis. J Chromatogr B 2006; 841: 23–37
31 *Chantiwas R, Yan X, Gilman SD.* Biological applications of microfluidics. Hoboken: John Wiley & Sons; 2008: 135–170
32 *Holden HM, Benning MM, Haller T, Gerlt JA.* The crotonase superfamily: divergently related enzymes that catalyze different reactions involving acyl coenzyme A thioesters. Acc Chem Res 2001; 34: 145–157
33 *Hamed RB, Batchelar ET, Clifton IJ, Schofield CJ.* Mechanisms and structures of crotonase superfamily enzymes – how nature controls enolate and oxyanion reactivity. Cell Mol Life Sci 2008; 65: 2507–2527
34 *Bilder P, Lightle S, Bainbridge G, Ohren J, Finzel B, Sun F, Holley S, Al-Kassim L, Spessard C, Melnick M, Newcomer M, Waldrop GL.* The structure of the carboxyltransferase component of acetyl-CoA carboxylase reveals a zinc-binding motif unique to the bacterial enzyme. Biochemistry 2006; 45: 1712–1722
35 *Leonard PM, Brzozowski AM, Lebedev A, Marshall CM, Smith DJ, Verma CS, Walton NJ, Grogan G.* The 1.8 Å resolution structure of hydroxycinnamoyl-coenzyme A hydratase-lyase (HCHL) from *Pseudomonas fluorescens*, an enzyme that catalyses the transformation of feruloyl-coenzyme A to vanillin. Acta Crystalllogr D 2006; D62: 1494–1501
36 *Bahnson BJ, Anderson VE, Petsko GA.* Structural mechanism of enoyl-CoA hydratase: Three atoms from single water are added in either an E1cb stepwise or concerted fashion. Biochemistry 2002; 41: 2621–2629
37 *Miller JR, Dunham S, Mochalkin I, Banotai C, Bowman M, Buist S, Dunkle B, Hanna D, Harwood HJ, Huband MD, Karnovsky A, Kuhn M, Limberakis C, Liu JY, Mehrens S, Mueller WT, Narasimhan L, Ogden A, Ohren J, Prasad JVNV, Shelly JA, Skerlos L, Sulavik M, Thomas VH, VanderRoest S, Wang L, Wang Z, Whitton A, Zhu T, Stover CK.* A class of selective antibacterials derived from a protein kinase inhibitor pharmacophore. PNAS 2009; 106: 1737–1742
38 *Freiberg C, Brunner NA, Schiffer G, Lampe T, Pohlmann J, Brands M, Raabe M, Häbich D, Ziegelbauer KJ.* Identification and characterization of the first class of potent bacterial acetyl-CoA carboxylase inhibitors with antibacterial activity. J Biol Chem 2004; 279: 26066–26073
39 *Congreve M, Chessari G, Tisi D, Woodhead AJ.* Recent developments in fragment-based drug discovery. J Med Chem 2008; 51: 3661–3680

Ioniols I and II, Tetracyclic Diterpenes with Antibacterial Activity, from *Sphaerococcus coronopifolius*

by **Vangelis Smyrniotopoulos**[a]), **Constantinos Vagias**[a]), **Mukhlesur M. Rahman**[b]), **Simon Gibbons**[b]), and **Vassilios Roussis***[a])

[a]) Department of Pharmacognosy and Chemistry of Natural Products, School of Pharmacy, University of Athens, Panepistimiopolis Zografou, GR-Athens 15771 (phone/fax: +30-210-7274592; e-mail: roussis@pharm.uoa.gr)

[b]) Centre for Pharmacognosy and Phytotherapy, The School of Pharmacy, University of London, 29-39 Brunswick Square, UK-London WC1N1AX

Two naturally occurring diterpenes featuring unprecedented tetracyclic skeletons, ioniols I and II (**1** and **2**, resp.), along with two previously reported metabolites **3** and **4**, were isolated from the organic extract of *Sphaerococcus coronopifolius* collected from the rocky coasts of Corfu island in the Ionian Sea. The structures of the new natural products, as well as their relative configuration, were elucidated on the basis of extensive spectral analysis, including 2D-NMR experiments. The isolated metabolites were evaluated for their antibacterial activity against a panel of *Staphylococcus aureus* strains, which included multidrug-resistant (MDR) and methicillin-resistant *Staphylococcus aureus* (MRSA) strains.

Introduction. – The cosmopolitan bright-red alga *S. coronopifolius*, generally growing on rocks in shallow areas, has yielded a number of interesting brominated diterpenes of diverse molecular architectures [1–3]. In the past, several halogenated metabolites have been suggested to function as chemical defense against marine herbivores, and some of them have been proven to possess antibacterial [4], insecticidal [5], antifungal [6], and antiviral activities [7].

Bacterial resistance poses a major challenge for the development of new antimicrobial agents, because infections from bacteria such as *Staphylococcus aureus* have again become a serious threat in developed countries. These bacteria form chronic, biofilm-based infections, which are challenging because bacterial cells living as biofilms are more tolerant to antibiotics than their planktonic counterparts [8].

In the course of our ongoing investigations toward the isolation of bioactive metabolites from marine organisms of the Greek seas [9][10], we recently studied the chemical composition of the red alga *S. coronopifolius*, collected from the West coast of Corfu island [11]. Herein, we describe the isolation and structure elucidation of two new isomeric brominated diterpenes, **1** and **2**, respectively, which feature unprecedented tetracyclic ring systems, along with the already described metabolites **3** (bromotetrasphaerol) [12], and **4** (coronopifoliol) [13], from the organic extract of *S. coronopifolius*. The molecular structures of the novel compounds, named ioniols I and II (**1** and **2**, resp.), were established by 1D- and 2D-NMR, IR, UV, and high-resolution mass spectral measurements.

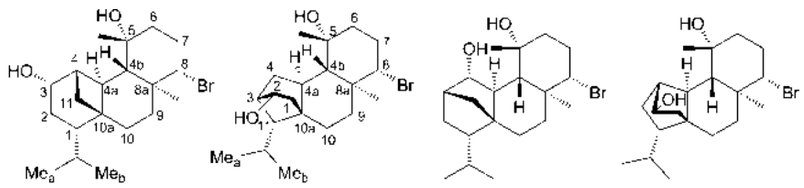

1 **2** **3** **4**

All compounds were evaluated for antibacterial activity against a panel of *Staphylococcus aureus* strains including multidrug-resistant (MDR) and methicillin-resistant *Staphylococcus aureus* (MRSA) using a microtiter plate based minimum inhibitory concentration (*MIC*) assay. Metabolites **2** and **4** were found to possess highly significant activity in comparison with the standard antibiotic, norfloxacin.

Results and Discussion. – *S. coronopifolius* seaweeds were collected in Palaiokastritsa bay on the West side of Corfu island, and the CH_2Cl_2/MeOH extract of the freeze-dried algae were subjected to a series of gravity column chromatography fractionations on silica gel using mixtures of cyclohexane/AcOEt as mobile phase, as well as reversed-phase high pressure liquid chromatography (HPLC) separations, using MeCN as eluent, to yield compounds **1**–**4** in pure form.

Metabolite **1** was isolated as a white amorphous solid, with $[\alpha]_D^{20} = -44.2$ ($c = 4.8$, $CHCl_3$). The HR-FAB-MS measurements suggested the molecular formula $C_{20}H_{33}BrO_2$ (*m*/*z* 288.2445 ($[M - OH - Br]^+$)), and the $[M + H - 2\,H_2O]^+$ peaks in the CI-MS spectrum, at *m*/*z* 349 and 351 with relative intensities 29 : 27, indicated the presence of one Br atom and two OH groups in the molecule. The presence of OH groups was supported by the intense and broad IR band at ν_{max} 3358 cm^{-1}. The ^{13}C-NMR spectrum of **1** (*Table 1*) showed 20 resolved resonances, with the multiplicities of the C-atom signals determined from the DEPT spectra, corresponding to three quaternary C, seven CH, six CH_2 groups, as well as four Me groups. The ^{1}H- and ^{13}C-NMR spectra ($CDCl_3$) of **1** confirmed the presence of a Br–CH group (δ(H/C) 4.03/68.7), an O-bearing CH group (δ(H/C) 4.14/72.8), and of an O-bearing quaternary C-atom (δ(C) 72.9). The four degrees of unsaturation required by the molecular formula had to be accounted for by four rings. Due to overlapping of some diagnostic signals in the ^{1}H-NMR spectrum of **1** in $CDCl_3$ the ^{1}H-NMR, COSY, HSQC, HMBC, and NOESY experiments were also recorded in C_6D_6. Partial structures from C(9) to C(10) (**A**), C(6) to C(8) (**B**), also present in other previously reported metabolites of *S. coronopifolius*, and substructure **C** were clearly revealed by the analysis of the ^{1}H-NMR, COSY, TOCSY, and HSQC spectra of **1** (*Fig. 1*). Complementary HMBCs (*Table 1*) allowed to confirm the structure of these fragments. Detailed analysis of the H- and C-atom chemical shifts and of the correlations observed in the HMBC spectra indicated the position of the three quaternary C-atoms that connect segments **A**, **B**, and **C**, thus confidently establishing the gross structure shown for **1**. In particular, the strong correlations of C(4b), C(5), and C(6) with Me–C(5) showed that units **B** and **C** were connected through the OH-bearing quaternary C-atom C(5). The connection of the partial structures through the fully substituted C-atom C(8a) was determined from the

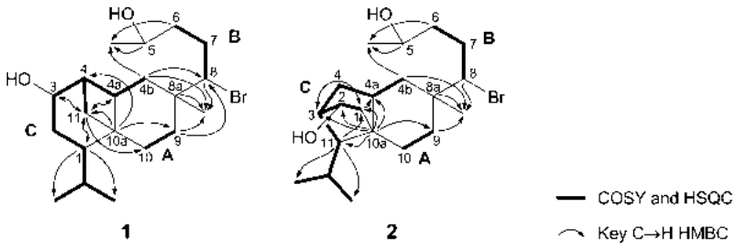

Fig. 1. *Partial Structures of* **1** *and* **2**

HMBC cross peaks of C(4b), C(8), C(8a), and C(9) with Me–C(8a), as well as from the correlations of C(9) and C(4b) with H–C(8). The remaining quaternary C-atom C(10a) had to be linked to C(1), C(4a), C(10), and C(11) as depicted from the correlations of C(10a) with H-atoms H–C(1), CH_2(2), H–C(4), H_α–C(9) and H_a–C(11), as well as of C(1), C(3), C(4), and C(10) with H_a–C(11), of C(1), C(3), and C(10) with H_b–C(11), and of C(11) with H–C(1), H–C(3), H–C(4), H–C(4a), and H_α–C(10). The relative configurations for the nine stereogenic centers of the tetracyclic framework were assigned primarily on the basis of the ^{1}H-NMR coupling constants and NOESY experiments. The NOE correlations observed (*Table 1*, *Fig. 2*) between H–C(8)/H–C(4b), H–C(8)/H_β–C(7), H–C(8)/H_β–C(9), H_β–C(9)/H–C(4b), H_β–C(9)/H_a–C(11), H–C(4b)/H_a–C(11), Me–C(5)/H–C(4), Me–C(5)/H–C(4b), Me–C(5)/H_α–C(6) and Me–C(5)/H_β–C(6), established the relative configuration at C(4), C(4b), C(5), C(8), and C(10a). Moreover, H_b–C(11) exhibited strong NOE correlations to both H–C(3) and H–C(1), showing the homofacial orientation of the isopropyl side chain at C(1) and the OH group at C(3). The strong correlations between Me–C(8a)/H–C(4a), Me–C(8a)/H_α–C(9), and Me–C(8a)/H_α–C(7) determined the relative configuration at C(4b) and C(8a). The large coupling constants of the H-atom pairs H_β–C(9)/H_α–C(10) (13.2 Hz), H_α–C(7)/

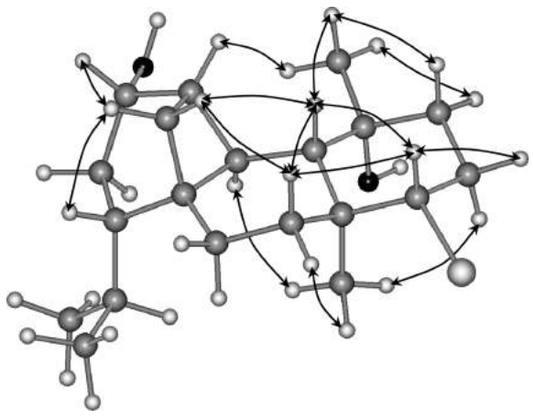

Fig. 2. *NOE Correlations and relative configuration for compound* **1**

Table 1. *NMR Data*[a]) *of Ioniol I* (**1**). ^{1}H-NMR at 400 MHz, ^{13}C-NMR at 50.3 MHz; chemical shifts are expressed in ppm and *J* values in Hz.

	δ(H)	δ(H)[b])	NOESY	δ(C)	HMBC (C→H)
H−C(1)	1.56–1.62 (*m*)	1.45 (*ddd*, *J* = 11.2, 6.4, 2.9)	H_b−C(11), Me_b−C−C(1)	48.4	CH_2(2), H_α−C(10), H_a−C(11), H_b−C(11), H−C−C(1), Me_a−C−C(1), Me_b−C−C(1)
H_a−C(2)	2.11–2.17 (*m*)	1.48–1.56 (*m*)		27.6	H−C(4), H−C−C(1)
H_b−C(2)	1.54–1.66 (*m*)	1.48–1.56 (*m*)			
H−C(3)	4.14 (*td*, *J* = 7.5, 1.6)	3.87 (*td*, *J* = 7.3, 1.5)	H−C(4), H_b−C(11)	72.8	CH_2(2), H−C(4a), H_a−C(11), H_b−C(11)
H−C(4)	2.09–2.15 (*m*)	1.89–1.97 (*m*)	H−C(3), H−C(4b), Me−C(5)	45.4	H−C(4b), H_a−C(11)
H−C(4a)	2.08–2.14 (*m*)	2.14 (*dd*, *J* = 10.2, 5.4)	Me−C(8a), Me_a−C−C(1)	31.5	H−C(1), H−C(3), H−C(4b), H_b−C(11)
H−C(4b)	1.49 (*d*, *J* = 9.9)	1.08 (*d*, *J* = 10.2)	H−C(4), H−C(8), H_β−C(9), H_a−C(11), Me−C(5)	51.8	H−C(4), H−C(4a), H_α−C(6), H−C(8), H_α−C(9), Me−C(5), Me−C(8a)
C(5)	–	–	–	72.9	H−C(4b), H_α−C(6), H_β−C(7), Me−C(5)
H_α−C(6)	1.62–1.69 (*m*)	1.34 (*ddd*, *J* = 13.7, 4.4, 2.4)	Me−C(5)	42.5	H_α−C(7), Me−C(5)
H_β−C(6)	1.50–1.56 (*m*)	1.10 (*ddd*, *J* = 13.7, 13.2, 4.4)	H_β−C(7), Me−C(5)		
H_α−C(7)	2.48 (*dq*, *J* = 4.6, 13.3)	2.62 (*dq*, *J* = 4.4, 13.2)	Me−C(8a)	30.5	
H_β−C(7)	2.01–2.08 (*m*)	1.97 (*dddd*, *J* = 13.2, 4.4, 3.9, 2.4)	H_β−C(6), H−C(8)		
H−C(8)	4.03 (*dd*, *J* = 13.3, 3.8)	3.79 (*dd*, *J* = 13.2, 3.9)	H−C(4b), H_β−C(7), H_β−C(9)	68.7	H−C(4b), H_α−C(6), H_α−C(7), H_β−C(7), Me−C(8a)
C(8a)	–	–	–	39.1	H−C(4b), H−C(8), H_α−C(9), Me−C(8a)
H_α−C(9)	1.91 (*ddd*, *J* = 13.3, 4.6, 2.5)	2.08 (*ddd*, *J* = 13.2, 4.4, 2.4)	H_α−C(10), H_β−C(10), Me−C(8a)	36.9	H−C(4b), H−C(8), H_β−C(10), Me−C(8a)
H_β−C(9)	1.32 (*td*, *J* = 13.3, 4.6)	1.18 (*td*, *J* = 13.2, 3.9)	H−C(4b), H−C(8), H_β−C(10), H_a−C(11)		
H_α−C(10)	1.59–1.66 (*m*)	1.56 (*ddd*, *J* = 14.2, 13.2, 4.4)	H_α−C(9), H−C−C(1), Me−C(8a)	24.0	H_a−C(11), H_b−C(11)
H_β−C(10)	0.89–0.95 (*m*)	0.77 (*ddd*, *J* = 14.2, 3.9, 2.4)	H_α−C(9), H_β−C(9)		
C(10a)	–	–	–	43.3	H−C(1), CH_2(2), H−C(4), H_α−C(9), H_α−C(10), H_β−C(10), H_a−C(11)

Table 1 (cont.)

	δ(H)	δ(H)[b])	NOESY	δ(C)	HMBC (C→H)
H_a−C(11)	2.42 (*dd*, *J*=10.0, 7.9)	2.22 (*dd*, *J*=9.8, 7.3)	H−C(4b), H_β−C(9)	34.5	H−C(1), H−C(3), H−C(4), H−C(4a), H_α−C(10)
H_b−C(11)	0.65 (*dd*, *J*=10.0, 5.4)	0.48 (*dd*, *J*=9.8, 5.4)	H−C(1), H−C(3)		
Me−C(5)	1.12 (*s*)	0.95 (*s*)	H−C(4), H−C(4b), H_α−C(6), H_β−C(6)	31.1	
Me−C(8a)	1.05 (*s*)	1.28 (*s*)	H−C(4a), H_α−C(7), H_α−C(9), H_α−C(10)	15.9	H−C(4b), H−C(8), H_β−C(9)
H−C−C(1)	2.00–2.09 (*m*)	1.89–1.97 (*m*)	H_α−C(10), Me_a−C−C(1), Me_b−C−C(1)	27.5	CH_2(2), Me_a−C−C(1), Me_b−C−C(1)
Me_a−C−C(1)[c])	0.91 (*d*, *J*=6.6)	0.93 (*d*, *J*=6.8)	H−C(4a), H−C−C(1)	15.9	Me_b−C−C(1)
Me_b−C−C(1)[c])	0.88 (*d*, *J*=6.6)	0.84 (*d*, *J*=6.8)	H−C(1), H−C−C(1)	22.7	Me_a−C−C(1)

[a]) Measured in $CDCl_3$ (δ(H) 7.24, δ(C) 77.0). [b]) Measured in C_6D_6 (δ(H) 7.16). [c]) Positions may be interchanged.

H–C(8) (13.2 Hz), H_β–C(6)/H_α–C(7) (13.2 Hz) and H–C(4a)/H–C(4b) (10.2 Hz) supported their *trans*-diaxial configuration, establishing chair conformations for the corresponding rings. In view of the above-mentioned data, ioniol I (**1**) was assigned as the shown structure.

The structural characterization of metabolite **2** was carried out in an analogous manner. Ioniol II (**2**) was isolated as a colorless oil, with $[\alpha]_D^{20} = +1.4$ ($c = 2.8$, $CHCl_3$), possessing the same molecular formula as that of **1** (HR-FAB-MS: m/z 383.1570 ($[M-H]^+$)), and similar MS and IR spectra, indicating the presence of the same functional groups, as was also confirmed by the ^{1}H- and ^{13}C-NMR data ($CDCl_3$) of **2** (*Table 2*). These showed signals for a Br–CH group (δ(H/C) 3.98/68.6), an O-bearing CH group (δ(H/C) 3.55/73.5), and an O-bearing quaternary C-atom (δ(C) 73.4). Analyses of the COSY, HSQC, and HMBC spectra resulted in the unambiguous assignment of all H- and C-atoms in the molecule. The NMR data of **2** showed close similarities with those of **1** and **4** [13] suggesting the same C-atom skeleton and the same relative configuration except for substructure **C** (*Fig. 1*). The HMBCs of C(4), C(10a), and C(11) with H–C(2), of C(3), C(4a), C(10a), and C(11) with H_a–C(1), and the correlation of C(2) with H_b–C(1), confidently established the gross structure for metabolite **2**. The relative configuration of **2** was elucidated on the basis of the NOESY experiments. The NOE correlations observed (*Table 2*, *Fig. 3*) between H–C(2)/H_β–C(4), H–C(2)/H_a–C(1), H_a–C(1)/H–C(4b), H_b–C(1)/H–C(11), and H_b–C(1)/H_β–C(10) established the configuration at C(2), C(3), C(10a), and C(11). Accordingly, the structure of **2** was elucidated as ioniol II.

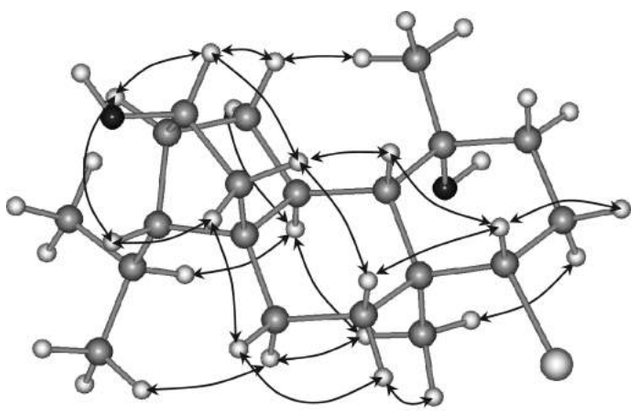

Fig. 3. *NOE Correlations and relative configuration for compound* **2**

The co-occurrence of compounds **1** and **2** with the previously described **3** and **4** in the same organism indicated the possibility that they all derive from the common metabolite bromosphaerol [12][14], as illustrated in the proposed biogenetic pathway (*Scheme*). Ioniol I (**1**) can biogenetically be derived from bromosphaerol (**I**) [14] by a nucleophilic attack of the C=C bond on the Br–CH_2 C-atom, and a subsequent nucleophilic substitution by a H_2O molecule on the tetracyclic intermediate carboca-

Table 2. *NMR Data of Ioniol II* (**2**). ^{1}H-NMR at 400 MHz, ^{13}C-NMR at 50.3 MHz; recorded in $CDCl_3$ (δ(H) 7.24, δ(C) 77.0); chemical shifts are expressed in ppm and *J* values in Hz.

	δ(H)	NOESY	δ(C)	HMBC (C→H)
H_a–C(1)	2.34 (*dd*, *J* = 14.1, 7.4)	H–C(2), H–C(4b), H_β–C(9)	42.9	H–C(3), H–C(4a), H_α–C(10), H_β–C(10)
H_b–C(1)	0.94 (br. *d*, *J* = 14.1)	H_β–C(10), H–C(11)		
H–C(2)	3.55 (br. *d*, *J* = 7.4)	H_a–C(1), H–C(3), H_β–C(4)	73.5	H_b–C(1), H–C(11), H_β–C(4)
H–C(3)	1.99 (br. *d*, *J* = 5.8)	H–C(2), H–C(11)	47.1	H_a–C(1), H_α–C(4), H_β–C(4), H–C(4a), H–C(11)
H_α–C(4)	1.80 (*ddd*, *J* = 13.3, 10.8, 5.8)	H–C(4a)	30.6	H–C(2), H–C(4a), H–C(11)
H_β–C(4)	0.85–0.93 (*m*)	H–C(2), Me–C(5)		
H–C(4a)	2.17 (*ddd*, *J* = 11.2, 10.8, 7.0)	H_α–C(4), Me–C(8a), H–C–C(11)	35.3	H_a–C(1), H_b–C(1), H–C(3), H–C(4b), H–C(11)
H–C(4b)	1.24 (*d*, *J* = 11.2)	H_a–C(1), H–C(8)	51.4	H–C(4a), H_α–C(9), CH_2(6), Me–C(5), Me–C(8a)
C(5)	–	–	73.4	CH_2(6), H_β–C(7), Me–C(5)
H_a–C(6)	1.57–1.63 (*m*)		43.7	H_α–C(7), Me–C(5)
H_b–C(6)	1.57–1.63 (*m*)			
H_α–C(7)	2.46 (*dddd*, *J* = 13.2, 12.9, 10.8, 7.4)	Me–C(8a)	30.8	CH_2(6)
H_β–C(7)	2.03 (*dq*, *J* = 13.2, 3.7)	H–C(8)		
H–C(8)	3.98 (*dd*, *J* = 12.9, 3.7)	H–C(4b), H_β–C(7), H_β–C(9)	68.6	CH_2(6), H_α–C(7), Me–C(8a)
C(8a)	–	–	42.0	H_β–C(10), Me–C(8a)
H_α–C(9)	1.78 (*ddd*, *J* = 13.3, 3.7, 3.3)	H_β–C(10), Me–C(8a)	38.8	Me–C(8a)
H_β–C(9)	1.11 (*ddd*, *J* = 13.7, 13.3, 3.3)	H_a–C(1), H–C(8)		
H_α–C(10)	1.89 (*ddd*, *J* = 13.7, 13.3, 3.7)	Me–C(8a), Me_b–C–C(11)	27.3	
H_β–C(10)	1.42 (*dt*, *J* = 13.3, 3.3)	H_b–C(1), H_α–C(9)		
C(10a)	–	–	49.6	H_a–C(1), H–C(2), H–C(3), H–C(4a), H–C(11), H_α–C(9)
H–C(11)	1.46 (br. *d*, *J* = 9.1)	H_b–C(1), H–C(3)	54.5	H_a–C(1), H–C(2), Me_a–C–C(11), Me_b–C–C(11)
Me–C(5)	1.19 (*s*)	H_β–C(4)	33.8	
Me–C(8a)	1.20 (*s*)	H_α–C(7), H_α–C(9), H_α–C(10), H–C(4a)	15.7	H–C(4b), H–C(8), H_β–C(9)
H–C–C(11)	1.70 (*dsept.*, *J* = 9.1, 6.6)	H–C(4a)	24.0	H–C(11), Me_a–C–C(11), Me_b–C–C(11)
Me_a–C–C(11)[a])	0.90 (*d*, *J* = 6.6)		23.4	H–C(11), Me_b–C–C(11)
Me_b–C–C(11)[a])	0.99 (*d*, *J* = 6.6)	H_α–C(10)	23.9	H–C(11), Me_a–C–C(11)

[a]) Positions may be interchanged.

Scheme. *Proposed Biogenetic Origin of* **1**–**4**

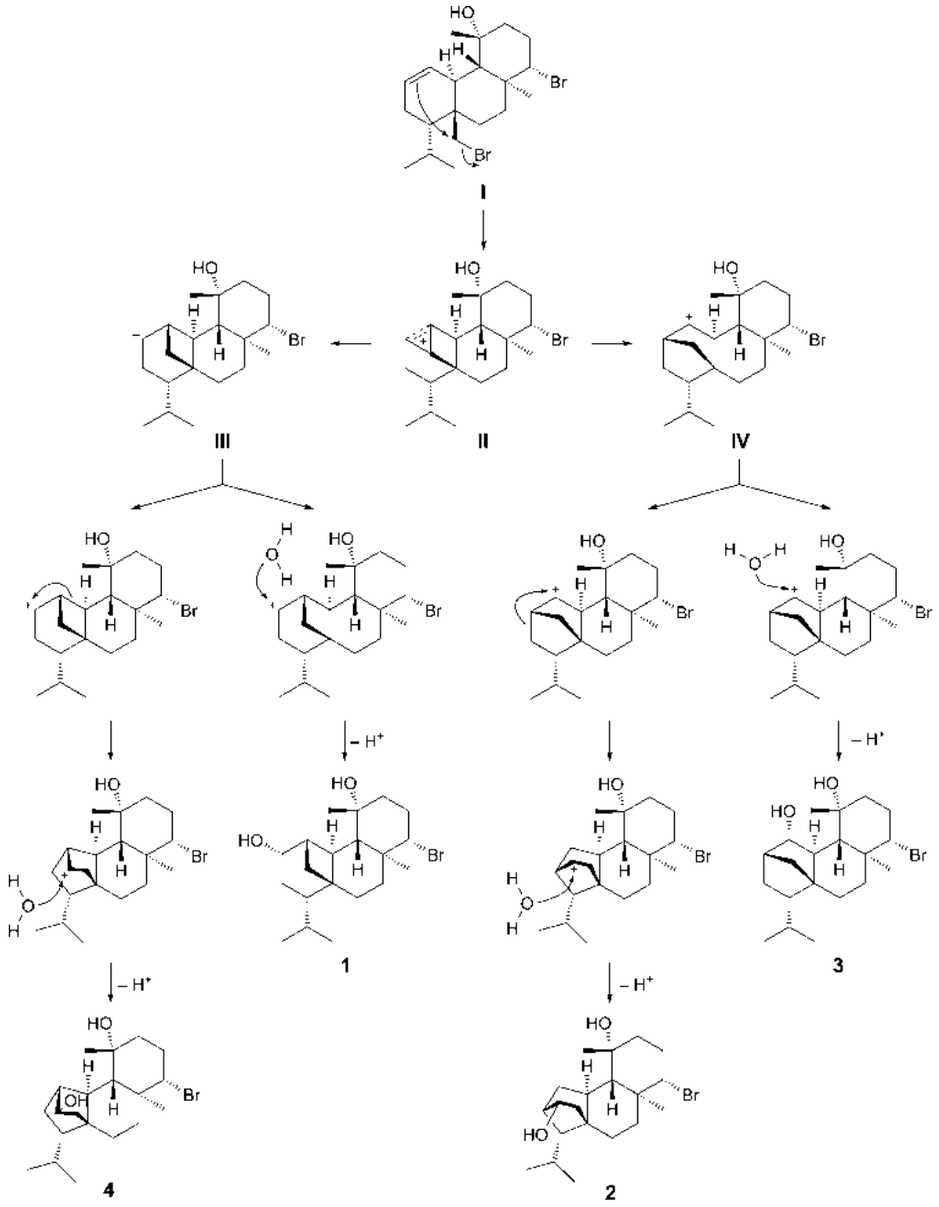

tion **III**. Rearrangement of **III** and addition of H_2O can yield coronopifoliol (**4**) [13]. Carbocation **II** may rearrange to **IV** that by addition of H_2O generates bromotetrasphaerol (**3**) [12]. Alternatively, the intermediate carbocation **IV** can produce ioniol II (**2**) by a rearrangement.

Metabolites **1**–**4** were evaluated for their antibacterial activity against a panel of *Staphylococcus aureus* strains. These included a multidrug-resistant (MDR) variant (SA1199B), a macrolide-resistant strain (RN4220), a tetracycline-effluxing strain (XU212) which was a clinical isolate and methicillin-resistant (MRSA), and two epidemic MRSA strains (EMRSA-15 and -16) (*Table 3*). The minimum inhibitory concentrations (*MIC*s) of **2** and **4** were found to be in the range of 16–64 μg/ml. Metabolites **2**, **3**, and **4** exhibited activities close to those of the standard antibiotic, norfloxacin, against SA-1199B (which expresses NorA), while **2** and **4** exhibited activities 8 to 16 times stronger than norfloxacin, against EMRSA-16 (which expresses mecA and is resistant to methicillin). The minor structural alterations in these tetracyclic brominated diterpenes that cause significant variations in their antibacterial activity make these preliminary results a stimulus for further structure–activity investigations.

Table 3. MIC*s of Compounds* **1**–**4** *and a Standard Antibiotic* (norfloxacin) *in* μg/*ml against MDR and Methicillin Resistance* Staphylococcus aureus

Strains	SA1199B (NorA) Multidrug Resistant	RN4220 (MsrA) Macrolide Resistant	EMRSA-15 (mecA) Epidemic Methicillin Resistant	ATCC 25943	XU212 (TetK, mecA) Tetracycline, Methicillin Resistant	EMRSA-16 (mecA) Epidemic Methicillin Resistant
1	–	–	–	–	–	–
2	64	32	64	64	32	32
3	32	–	128	–	–	–
4	32	32	32	64	16	16
Norfloxacin	32	1	0.5	0.5	8	256

Experimental Part

General. Vacuum liquid chromatography (VLC): Kieselgel *60* (SiO_2; *Merck*). Gravity column chromatography (GCC): Kieselgel *60 H* (*Merck*). Thin layer chromatography (TLC): Kieselgel *60* F_{254} aluminum support plates (*Merck*); spots were detected after spraying with 15% H_2SO_4 in MeOH reagent and charring. HPLC Separations: *Agilent 1100* model equipped with refractive index detector and a *Kromasil 100 C18* 5μ (250 × 8 mm) HPLC reversed-phase column. Optical rotations: *Perkin-Elmer* model *341* polarimeter with a 10 cm cell. UV Spectra: in spectroscopic grade $CHCl_3$ on a *Shimadzu UV-160A* spectrophotometer. IR Spectra: *Paragon 500 Perkin-Elmer* spectrophotometer. NMR Spectra: *Bruker AC 200* and *Bruker DRX 400* spectrometers; chemical shifts are given on a δ [ppm] scale using TMS as internal standard; 2D experiments (COSY, HSQC, HMBC, NOESY) were performed using standard *Bruker* microprograms. The structures in *Figs. 2* and *3* were generated and optimized (energy: 81.07 and 58.35 kcal/mol, resp.) by 'HyperChem™ 7.0' molecular modelling and simulation software (force field: MM+; optimisation algorithm: Polak-Ribiere). High-resolution mass spectral data were provided by the University of Notre Dame, Department of Chemistry and Biochemistry, Indiana, USA. CI-MS: *Thermo DSQ* Mass Detector using Direct Exposure Probe (DEP) and CH_4 as the CI gas.

Plant Material. *S. coronopifolius* was collected by SCUBA diving in Palaiokastritsa bay at the West coast of Corfu island, Greece, at a depth of 10–15 m in May of 2002. A specimen was deposited with the Herbarium of the Laboratory of Pharmacognosy and Chemistry of Natural Products, University of Athens (ATPH/MO/201).

Extraction and Isolation. *S. coronopifolius* was initially freeze-dried (291.4 g dry weight) and then exhaustively extracted with a mixture of CH_2Cl_2/MeOH (3:1) at r.t. The combined extracts were concentrated to give a dark green residue (8.20 g), which was later subjected to VLC on SiO_2, using a 10% step gradient of cyclohexane/AcOEt elution sequence. *Fr. IIa* (20% AcOEt in cyclohexane; 4.01 g) was subjected to GCC, using a 2% step gradient of cyclohexane/AcOEt. The MeCN-soluble portion (173.4 mg) of *Fr. XIb* (50% AcOEt in cyclohexane; 199.6 mg) was subjected to reversed-phase HPLC, using MeCN as mobile phase to yield pure compounds **1** (4.8 mg), **2** (3.4 mg), **3** (15.3 mg), and **4** (10.9 mg).

Ioniol I (=(*1*R*,*3*R*,*4*R*,*4a*R*,*4b*R*,*5*S*,*8*R*,*8a*R*,*10a*R*)*-8-Bromododecahydro-5,8a-dimethyl-1-(1-methylethyl)-1*H*-4,10a-methanophenanthrene-3,5-diol*; **1**). White amorphous solid. $[\alpha]_D^{20} = -44.2$ (c = 4.8, $CHCl_3$). UV ($CHCl_3$): 248 (1.99). IR ($CHCl_3$): 3358 (OH), 2946, 1456, 758. ^{1}H- and ^{13}C-NMR: *Table 1*. CI-MS: 367, 369 (13:12, $[M+H-H_2O]^+$), 349, 351 (29:27, $[M+H-2\,H_2O]^+$), 305 (6, $[M+H-HBr]^+$), 287 (68, $[M+H-HBr-H_2O]^+$), 269 (100, $[M+H-HBr-2\,H_2O]^+$). HR-FAB-MS: 288.2445 ($[M-OH-Br]^+$, $C_{20}H_{32}O^+$; calc. 288.2453).

Ioniol II (=(*2*R*,*3*S*,*4a*R*,*4b*R*,*5*S*,*8*R*,*8a*R*,*10a*S*,*11*S*)*-8-Bromododecahydro-5,8a-dimethyl-11-(1-methylethyl)-1*H*-3,10a-methanophenanthrene-2,5-diol*; **2**). Colorless oil. $[\alpha]_D^{20} = +1.4$ (c=2.8, $CHCl_3$). UV ($CHCl_3$): 248 (2.84), 671 (1.22). IR ($CHCl_3$): 3397 (OH), 2952, 2861, 752. ^{1}H- and ^{13}C-NMR: *Table 2*. CI-MS: 367, 369 (4:3, $[M+H-H_2O]^+$), 349, 351 (16:15, $[M+H-2\,H_2O]^+$), 287 (22, $[M+H-HBr-H_2O]^+$), 269 (100, $[M+H-HBr-2\,H_2O]^+$). HR-FAB-MS: 383.1570 ($[M-H]^+$, $C_{20}H_{32}^{79}BrO_2^+$; calc. 383.1586).

Bacterial Strains and Antibiotic. A standard laboratory *S. aureus* strain (ATCC 25923) and a clinical isolate (XU212), which possesses the TetK efflux pump and is also an MRSA strain, were obtained from Dr. *E. Udo* [15]. Strain RN4220 which has the MsrA macrolide efflux pump was provided by Dr. *J. Cove* [16]. EMRSA-15 [17] and EMRSA-16 [18] were obtained from Dr. *P. Stapleton*. Strain SA1199B which over-expresses the NorA MDR efflux pump was a gift of Prof. *G. Kaatz* [19]. Norfloxacin was obtained from the *Sigma Chemical Co. Mueller–Hinton* broth (MHB; *Oxoid*) was adjusted to contain 20 mg/l Ca^{2+} and 10 mg/l Mg^{2+}.

Antibacterial Assay. Overnight cultures of each strain were made up in 0.9% saline to an inoculum density of 5×10^5 cfu by comparison with a *McFarland* standard. Norfloxacin was dissolved in DMSO and then diluted in MHB to give a starting concentration of 512 μg/ml. Using Nunc 96-well microtitre plates, 125 μl of MHB were dispensed into wells *1–11*. 125 μl of the test compound or the appropriate antibiotic were dispensed into well *1* and serially diluted across the plate leaving well *11* empty for the growth control. The final volume was dispensed into well *12*, which being free of MHB or inoculum served as the sterile control. Finally, the bacterial inoculum (125 μl) was added to wells *1–11*, and the plate was incubated at 37° for 18 h. A DMSO control (3.125%) was also included. All *MIC*s were determined in duplicate. The *MIC* was determined as the lowest concentration at which no growth was observed. A MeOH soln. (5 mg/ml) of 3-(4,5-dimethylthiazol-2-yl)-2,5-diphenyltetrazolium bromide (MTT; *Lancaster*) was used to detect bacterial growth by a color change from yellow to blue.

This study was partially supported by the FP-39 EPAN program of the Greek Secretariat for Research and Technology.

REFERENCES

[1] V. Smyrniotopoulos, A. Quesada, C. Vagias, D. Moreau, C. Roussakis, V. Roussis, *Tetrahedron* **2008**, *64*, 5184.
[2] V. Smyrniotopoulos, C. Vagias, M. M. Rahman, S. Gibbons, V. Roussis, *J. Nat. Prod.* **2008**, *71*, 1386.
[3] S. Etahiri, V. Bultel-Poncé, C. Caux, M. Guyot, *J. Nat. Prod*. **2001**, *64*, 1024, and refs. cited therein.
[4] C. S. Vairappan, M. Suzuki, T. Abe, M. Masuda, *Phytochemistry* **2001**, *58*, 517.

[5] K. A. El Sayed, D. C. Dunbar, T. L. Perry, S. P. Wilkins, M. T. Hamann, J. T. Greenplate, M. A. Wideman, *J. Agric. Food Chem.* **1997**, *45*, 2735.
[6] M. V. D'Auria, L. G. Paloma, L. Minale, A. Zampella, C. Debitus, J. Perez, *J. Nat. Prod.* **1995**, *58*, 121.
[7] S. Sakemi, T. Higa, C. W. Jefford, G. Bernardinelli, *Tetrahedron Lett*. **1986**, *27*, 4287.
[8] T. Bjarnsholt, M. Givskov, *Curr. Infect. Dis. Rep.* **2008**, *10*, 22.
[9] E. Ioannou, A. Quesada, C. Vagias, V. Roussis, *Tetrahedron* **2008**, *64*, 3975.
[10] I. Kontiza, M. Stavri, M. Zloh, C. Vagias, S. Gibbons, V. Roussis, *Tetrahedron* **2008**, *64*, 1696.
[11] V. Smyrniotopoulos, C. Vagias, M. M. Rahman, S. Gibbons, V. Roussis, *Chem. Biodiversity* **2010**, *7*, 186.
[12] F. Cafieri, E. Fattorusso, L. Mayol, C. Santacroce, *Tetrahedron* **1986**, *42*, 4273.
[13] F. Cafieri, E. Fattorusso, L. Mayol, C. Santacroce, *J. Org. Chem.* **1985**, *50*, 3982.
[14] S. de Rosa, S. de Stefano, P. Scarpelli, N. Zavodnik, *Phytochemistry* **1988**, *27*, 1875.
[15] S. Gibbons, E. E. Udo, *Phytother. Res.* **2000**, *14*, 139.
[16] J. I. Ross, A. M. Farrell, E. A. Eady, J. H. Cove, W. J. Cunliffe, *J. Antimicrob. Chemother.* **1989**, *24*, 851.
[17] J. F. Richardson, S. Reith, *J. Hosp. Infect.* **1993**, *25*, 45.
[18] R. A. Cox, C. Conquest, C. Mallaghan, R. R. Maples, *J. Hosp. Infect.* **1995**, *29*, 87.
[19] G. W. Kaatz, S. M. Seo, C. A. Ruble, *Antimicrob. Agents Chemother.* **1993**, *37*, 1086.

Received November 17, 2008

Notes

Antibacterial Diterpenes from *Plectranthus ernstii*

Michael Stavri,[†] Alan Paton,[‡] Brian W. Skelton,[§] and Simon Gibbons*[,†]

Centre for Pharmacognosy and Phytotherapy, The School of Pharmacy, University of London, 29-39 Brunswick Square, London WC1N 1AX, U.K., Herbarium, Royal Botanic Gardens, Kew, Richmond, Surrey, TW9 3DS, U.K., and Chemistry M313, School of Biomedical, Biomolecular & Chemical Sciences, University of Western Australia, Crawley, 6009, Western Australia, Australia

Received September 16, 2008

Three new diterpenoids including two pimaranes (**1** and **2**) and a labdane (**3**) were isolated from the whole herb of *Plectranthus ernstii*. The structures of these compounds were determined as *rel*-15(ζ),16-epoxy-7α-hydroxypimar-8,14-ene (**1**) and *rel*-15(ζ),16-epoxy-7-oxopimar-8,14-ene (**2**), and compound **3** was elucidated as 1*R*,11*S*-dihydroxy-8*R*,13*R*-epoxylabd-14-ene on the basis of single-crystal X-ray structural analysis. Compound **1** exhibited moderate antistaphylococcal activity against a range of multidrug-resistant (MDR) and methicillin-resistant (MRSA) strains of *Staphylococcus aureus* with a minimum inhibitory concentration (MIC) of 32 μg/mL. All three diterpenes exhibited antimycobacterial activity against three strains of rapidly growing mycobacteria with MIC values ranging from 8 to 128 μg/mL.

Plectranthus ernstii Codd. belongs to the Lamiaceae family, and the genus has been shown to be a rich source of diterpenes, particularly of the abietane, labdane, and neoclerodane classes,[1−3] and while the phytochemistry of the genus has been reviewed,[4] this particular species does not appear to have been phytochemically studied before. Many *Plectranthus* species are used as ornamentals but also have economic and medicinal value, particularly in infectious disease.[5,6] Medicinal uses include the treatment of a range of ailments, particularly digestive, skin, infective, and respiratory problems.[7] *P. ernstii* is a South African species and exists in several forms including "Oribi",[8] which is cultivated widely in the UK as an attractive house plant with pale blue spur-like flowers and aromatic leaves. The ability of many *Plectranthus* species to produce antibacterial metabolites, particularly of the diterpene class, prompted us to investigate the chemistry and antibacterial activity of extracts from this species. This paper details the characterization of two new pimarane diterpenes (**1** and **2**) and a labdane diterpene (**3**).

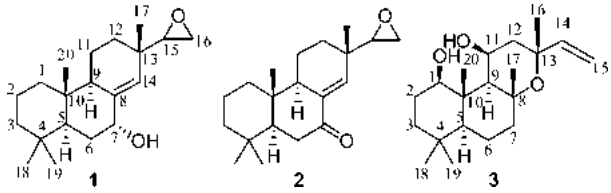

All of the isolated compounds were evaluated against a panel of methicillin- and multidrug-resistant (MDR) *Staphylococcus aureus* strains and selected species of rapidly growing mycobacteria (RGM).

The aerial parts of *P. ernstii* were dried and extracted in a Soxhlet apparatus. Compound **1** was isolated as a white, amorphous powder from the *n*-hexane extract. The ^{1}H and ^{13}C NMR spectra (Table 1) provided signals that were characteristic of a pimarane diterpene.[9,10] By inspection of the HMBC and COSY spectra it could be determined that compound **1** had connectivities of a pimarane diterpene. From the HMBC data, a *geminal* pair of methyl groups (H_3-18 and H_3-19) exhibited a ^2J correlation to a quaternary carbon, C-4, as well as ^3J correlations to C-3 (CH_2) and C-5, a methine carbon. COSY correlations between H_2-3 and H_2-2 and also between H_2-2 and H_2-1 were also observed. A methyl singlet (C-20) showed a ^2J correlation to C-10 and ^3J correlations to C-1 (CH_2) and two methine carbons (C-5 and C-9), therefore completing ring A of the pimarane skeleton. The methine hydrogen H-9, located at the ring junction of rings B and C, provided ^2J correlations to a methylene carbon (C-11) and an olefinic quaternary carbon (C-8, $\delta_C = 141.7$) as well as a ^3J correlation to the olefinic partner C-14 ($\delta_C = 130.2$). The olefinic hydrogen of this carbon (H-14, $\delta_H = 5.43$) provided a ^3J correlation to a downfield methine carbon positioned at C-7. Due to the downfield appearance of this carbon, a hydroxy group was placed here. H-7 exhibited a COSY correlation with a methylene group (H_2-6), confirming its assignment, and also a ^3J correlation to C-5, completing ring B of the pimarane. The olefinic hydrogen, H-14, also exhibited a ^2J HMBC correlation to C-13 along with ^3J correlations to C-12 (CH_2) and C-15, an oxymethine carbon. A ^2J HMBC correlation between H_2-12 and C-11 as well as a COSY coupling between these two sets of methylene hydrogens completed ring C. A methyl singlet (C-17) exhibited a ^2J HMBC correlation to C-13 along with ^3J correlations to C-12, C-14, and C-15, fixing this methyl group here in accordance with a pimarane skeleton. The oxymethine resonance H-15 gave a COSY coupling to an oxymethylene pair of hydrogens (H_2-16). The HRESIMS of **1** suggested a pseudomolecular formula of $C_{20}H_{33}O_2$ $[M + H]^+$ (305.2487). In addition to the hydroxy group at C-7, this indicated that C-15 and C-16 were also linked together by an epoxide bridge.

The relative configuration of **1** was determined by inspection of the ^{1}H and NOESY spectra. H-7 appeared as a triplet in the ^{1}H NMR spectrum with a coupling constant of 2.5 Hz, indicating that this hydrogen should be in an equatorial position (β-oriented) and therefore the hydroxy group should be axial (α-oriented). An NOE between the olefinic hydrogen H-14 and the oxymethine proton H-15 implied that this epoxide moiety should be in an equatorial position (α) with the methyl group at position 17 in an axial and β-orientation. A further NOESY correlation between H-14 and H-7 supported the previous assignment of this hydrogen as equatorial

* To whom correspondence should be addressed. Tel: +44-207-753-5913. Fax: +44-207-753-5909. E-mail: simon.gibbons@pharmacy.ac.uk.
[†] University of London.
[‡] Royal Botanic Gardens, Kew.
[§] University of Western Australia.

10.1021/np800581s CCC: $40.75
Published on Web 05/15/2009

Table 1. ^{1}H and ^{13}C NMR Data (500 and 125 MHz, $CDCl_3$) for Compounds **1**−**3**[a]

	1		**2**		**3**	
position	^{1}H	^{13}C	^{1}H	^{13}C	^{1}H	^{13}C
1	1.08 dt (3.5, 12.5)	39.1	1.11 dt (4.5, 13.0)	38.8	3.48 dd (4.5,11.0)	78.8
	1.71 m		1.79 m			
2	1.45 m	18.9	1.45 m	18.6	1.63 m	28.9
			1.58 m		1.73 m	
3	1.22 m	42.0	1.51 m	41.7	1.26 m	39.5
	1.44 m				1.39 dt (3.5, 13.5)	
4		32.8		33.1		32.8
5	1.57 m	46.9	1.47 m	50.0	0.83 m	55.7
6	1.58 m	29.3	2.28 dd (13.5, 18.5)	37.4	1.47 m	44.0
	1.79 m		2.57 m		1.85 m	
7	4.20 t (2.5)	73.2		200.5	1.49 m	20.2
					1.64 m	
8		141.7		137.3		75.4
9	2.13 m	46.5	2.05 m	51.2	1.54 d (5.5)	55.1
10		38.4		36.0		43.7
11	1.47 m	17.7	1.45 m	18.3	4.37 dt (6.0, 9.0)	65.6
			1.76 m			
12	1.35 dt (3.5, 13.0)	30.9	1.42 m	30.5	2.02 dd (9.0, 14.0)	40.3
	1.43 m		1.57 m		2.27 dd (8.5, 14.0)	
13		34.4		36.0		73.0
14	5.43 bs	130.2	6.61 bs	140.9	5.89 dd (10.5, 17.0)	147.1
15	2.80 dd (2.5, 4.0)	59.8	2.85 dd (2.5, 3.5)	59.0	4.95 dd (1.5, 11.0)	111.2
					5.19 dd (1.5, 17.0)	
16	2.56 dd (2.5, 4.5)	43.9	2.56 m	43.8	1.24 s	32.1
	2.66 t (4.5)		2.66 t (4.0)			
17	1.02 s	22.8	1.06 s	22.7	1.16 s	13.6
18	0.91 s	33.4	0.87 s	32.6	0.85 s	32.8
19	0.86 s	21.9	0.90 s	21.1	0.80 s	21.1
20	0.76 s	14.0	0.83 s	13.9	1.48 s	27.8

[a] Coupling constants (Hz) in parentheses.

(β). Compound **1** is therefore assigned as *rel*-15(ζ),16-epoxy-7α-hydroxypimar-8,14-ene and is reported here for the first time.

Compound **2** was isolated from the *n*-hexane extract and exhibited signals similar to those of compound **1**, indicating the presence of a further pimarane diterpene. The HRESIMS of **2** differed from that of **1** by a loss of two hydrogens with an *m*/*z* 303.2320 $[M + H]^+$, indicating a pseudomolecular formula of $C_{20}H_{31}O_2$. The appearance of a quaternary carbon at $\delta_C = 200.5$ (C-7) provided evidence for the presence of a ketonic carbonyl. The *geminal* pair of methyls (H_3-18 and H_3-19) yielded HMBC signals to a methylene group (CH_2-3), to a quaternary carbon ($\delta_C = 33.1$, C-4) to which they were directly attached, and to a methine carbon (C-5). The methine hydrogen (H-5) associated with this carbon provided correlations to both hydrogens of a downfield methylene ($\delta_H = 2.28$ and 2.56, H_2-6), placing this group here. A ^2J HMBC correlation between H_2-6 and C-7 enabled the positioning of the ketonic carbonyl to be assigned at C-7. This was further confirmed by a ^3J HMBC correlation between the olefinic proton H-14 ($\delta_H = 6.61$) and C-7. The remaining resonances of compound **2** were highly similar to those of **1** (Table 1), and again NOESY correlations supported the assignment of identical configurations at C-5, C-9, C-10, and C-13. Compound **2** was therefore assigned as *rel*-15(ζ),16-epoxy-7-oxopimar-8,14-ene and is reported here for the first time. Compounds **1** and **2** are structurally related to pimarane diterpenes isolated from *Salvia mellifera* that possess an intact 15−16 double bond.[11]

Compound **3** was isolated as a colorless oil from the *n*-hexane extract and yielded ^{1}H and ^{13}C NMR signals indicative of a labdane diterpene. By inspection of the HMBC and COSY spectra it could be shown that compound **3** had the connectivities typical of a labdane diterpene.[5] By inspection of the HMBC and DEPT-135 data a methyl singlet (CH_3-20) provided a ^2J correlation to C-10 and ^3J correlations to C-5 and C-9 (both CH) and an oxymethine carbon (C-1). The hydrogen directly attached to this carbon appeared as a double doublet ($J = 4.5$, 11.0 Hz), placing it in an axial orientation. This hydrogen coupled to two hydrogens of a methylene group (C-2), which in turn coupled to a second group of methylene protons (CH_2-3). From the HMBC spectrum, a pair of *geminal* methyl groups exhibited a ^2J correlation to C-4 and ^3J correlations to C-3 and C-5, therefore completing ring A. The methine signal, H-5, exhibited a COSY correlation to a methylene group (H_2-6), which in turn coupled to a second methylene group (H_2-7). A fourth methyl singlet (C-17) provided a ^2J correlation to an oxygen-bearing quaternary carbon (C-8) as well as ^3J correlations to C-7 and C-9, thus completing ring B of the labdane diterpene nucleus. A fifth methyl singlet (C-16) exhibited a ^2J correlation to a second oxygen-bearing quaternary carbon (C-13) as well as ^3J correlations to a methylene group (C-12) and an olefinic carbon (C-14). The olefinic hydrogen associated with this carbon (H-14) provided COSY couplings to both hydrogens of an *exo*-methylene group (H_2-15), completing the olefin moiety. The methine hydrogen at C-9 coupled to a deshielded proton (H-11, $\delta_H = 4.37$) and together with the downfield appearance of C-11 indicated that a hydroxy group should be placed here. The molecular weight determined by HRESIMS (*m*/*z* 323.2597 $[M + H]^+$) meant that ring C of the labdane should be completed by an ether linkage between the two oxygen-bearing quaternary carbons C-8 and C-13. From the coupling constant of H-1 of 11.0 Hz this hydrogen must be axial and α-oriented, placing the hydroxy group in an equatorial position (β). Two 1,3 interactions between H-1 and H-5 and H-5 and H-9 placed these hydrogens in an α-orientation (axial). An NOE between the H_3-18 and both hydrogens of H_2-3 placed this group in an equatorial position (α). A 1,3 interaction between the axial proton of H_2-2 and H_3-19 placed this methyl group in a β-orientation. NOEs between H_3-19 and H_3-20 as well as H_3-20 and H_3-17 placed these methyl groups cofacial in a β-orientation. A 1,3 interaction between H_3-17 and H_3-16 also placed this group on the same face (β), leaving the olefin moiety to be α-oriented (equatorial). A large coupling constant for H-11 (9.0 Hz) would indicate that H-11 should be axial (β), leaving the hydroxy group to be α-oriented (equatorial). However, given the presence of several bulky substituents on ring C, a number of conformations could be adopted. To resolve this issue and assign configuration at C-11 and all of the stereogenic centers, single-crystal X-ray structural analysis

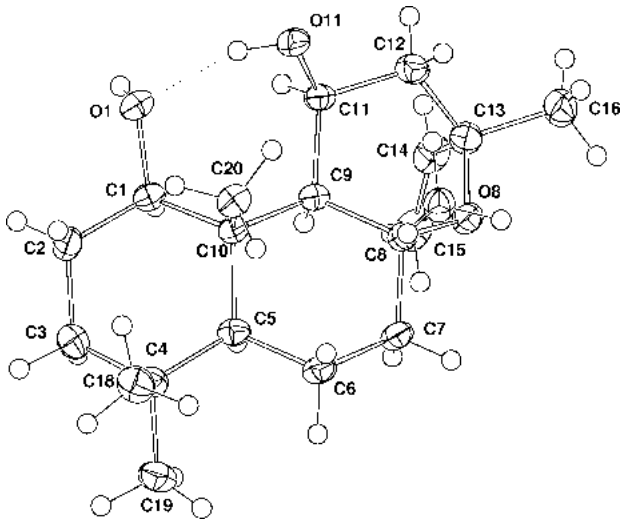

Figure 1. Molecular structure and numbering scheme of **3**. The non-hydrogen atom ellipsoids are shown at the 50% probability level.

Table 2. Minimum Inhibitory Concentrations of Compounds **1**−**3** in μg/mL

strain	**1**	**2**	**3**	Nor[a]	Eryth[b]	Tet[c]	Eth[d]
S. aureus SA-1199B (NorA)	32	[e]	[e]	32			
S. aureus RN4220 (MsrA)	32	[e]	[e]		128		
S. aureus XU-212 (TetK, mecA)	32	[e]	[e]			128	
S. aureus EMRSA-15	32	[e]	[e]	2			
S. aureus ATCC 25923	32	[e]	[e]	0.5			
Mycobacterium fortuitum	16	128	128				4
Mycobacterium phlei	8	64	128				2
Mycobacterium smegmatis	16	128	128				0.5

[a] Norfloxacin. [b] Erythromycin. [c] Tetracycline. [d] Ethambutol. [e] Not active at 128 μg/mL.

was conducted and **3** was crystallized from EtOAc (Figure 1). This indicated that the hydroxy at C-11 is actually β-oriented and that the C ring of **3** is a twist boat conformer. Compound **3** is therefore assigned as 1*R*,11*S*-dihydroxy-8*R*,13*R*-epoxylabd-14-ene and is reported here for the first time. Both the 1*R* and 11*S* hydroxy analogues of compound **3** have been reported from *Rhizophora apiculata*[12] and *Juniperus oxycedrus*,[13] respectively.

Certain diterpenes, such as totarol, have been shown to possess multifaceted activities as potent antibacterials with minimum inhibitory concentration values of 2 μg/mL and at the same time behaving as efflux pump inhibitors.[14] Several pimarane diterpenes have also been reported as bacterial resistance modifying agents.[15] All three compounds were therefore tested for antimycobacterial activity against a panel of fast-growing mycobacteria (Table 2), with **1** showing the greatest activity, ranging from 8 to 16 μg/mL, whereas compounds **2** and **3** demonstrated only weak activity. Compound **1** also exhibited moderate antistaphylococcal activity against multidrug-resistant (MDR) and methicillin-resistant (MRSA) strains of *Staphylococcus aureus* with a minimum inhibitory concentration (MIC) of 32 μg/mL. Surprisingly the simple change from 7-hydroxy (**1**) to 7-oxo (**2**) resulted in a loss of antistaphylococcal activity, presumably as a result of increased lipophilicity and poorer uptake. The activity against effluxing and MRSA strains is noteworthy, and the use of standardized extracts containing these components could find utility as topical antibacterial preparations, particularly given their lipophilicity and the need for replacements for mupirocin and fusidic acid creams, to which resistance is arising.

Experimental Section

General Experimental Procedures. Optical rotations were measured on a Bellingham and Stanley ADP 200 polarimeter. IR spectra were recorded on a Nicolet 360 FT-IR spectrophotometer and UV spectra on a Thermo Electron Corporation Helios spectrophotometer. NMR spectra were recorded on a Bruker AVANCE 500 MHz spectrometer. Chemical shift values (δ) were reported in parts per million (ppm) relative to appropriate internal solvent standard, and coupling constants (*J* values) are given in hertz. Mass spectra were recorded on a Finnigan MAT 95 high-resolution, double-focusing, magnetic sector mass spectrometer. Accurate mass measurement was achieved using voltage scanning of the accelerating voltage. This was nominally 5 kV, and an internal reference of heptacosa was used. Resolution was set between 5000 and 10 000.

Plant Material. *Plectranthus ernstii* was purchased from Oakland Nurseries (Burton-on-the-Wolds, Loughborough, UK). The material was identified by A.P., and a voucher specimen (MS/SG/07/2006/PE) is deposited at the Centre for Pharmacognosy and Phytotherapy.

Extraction and Isolation. The whole herb of *P. ernstii* (275 g) was air-dried, coarsely powdered, and sequentially extracted with *n*-hexane (3.5 L), $CHCl_3$ (3.5 L), and MeOH (3.5 L) in a Soxhlet apparatus. The *n*-hexane extract (8.7 g) was adsorbed onto silica gel (13 g) and subjected to vacuum-liquid chromatography (VLC) on silica gel (130 g) eluting with *n*-hexane containing 10% increments of EtOAc to give 12 fractions (200 mL each). VLC fraction 5 (6:4 *n*-hexane−EtOAc) was further fractioned by solid-phase extraction (SPE) on a normal-phase column (silica, 60 g). Fraction 5, eluted with 8:2 hexane−EtOAc (50 mL), was then fractioned by reversed-phase SPE (C_{18}, 60 g) eluting with H_2O containing 10% increments of MeOH (50 mL) to give 11 fractions. Preparative TLC of fraction 10 on a reversed-phase TLC plate using a 9:1 MeCN−H_2O system afforded compound **1** (4.9 mg). Compound **3** was isolated by reversed-phase preparative TLC of SPE fraction 9 using a 95:5 MeCN−H_2O system. This afforded 41.9 mg of **3**. VLC fraction 4 of the *n*-hexane extract was subjected to SPE on a silica normal-phase column (60 g) eluting with 9:1 *n*-hexane−EtOAc (50 mL). Fraction 2 was then further fractioned by SPE in reversed-phase mode (C_{18}, 60 g) eluting with H_2O containing 10% increments of MeOH (50 mL) to give 11 fractions. Preparative TLC of SPE fraction 10 using an 8:2 MeCN−H_2O system yielded compound **2** (6.9 mg).

Antibacterial Assay. *Staphylococcus aureus* ATCC 25923 was the generous gift of E. Udo (Kuwait University, Kuwait). *S. aureus* RN4220 containing plasmid pUL5054, which carries the gene encoding the MsrA macrolide efflux protein, was provided by J. Cove.[16] *S. aureus* XU-212, possessing the TetK tetracycline efflux protein, was provided by E. Udo.[17] SA-1199B, which overexpresses the *norA* gene encoding the NorA MDR efflux protein, was provided by G. Kaatz.[18] *Mycobacterium* species were acquired from the NCTC. All *S. aureus* strains were cultured on nutrient agar and incubated for 24 h at 37 °C prior to minimum inhibitory concentration (MIC) determination. Mycobacterial strains were grown on Columbia Blood agar (Oxoid) supplemented with 7% defibrinated horse blood (Oxoid) and incubated for 72 h at 37 °C. Bacterial inocula equivalent to the 0.5 McFarland turbidity standard were prepared in normal saline and diluted to give a final inoculum density of 5×10^5 cfu/mL. The inoculum (125 μL) was added to all wells, and the microtiter plate was incubated at 37 °C for 18 h. The MIC was recorded as the lowest concentration at which no bacterial growth was observed as previously described.[10]

***rel*-15(ζ),16-Epoxy-7α-hydroxypimar-8,14-ene (1):** white, amorphous powder; $[\alpha]^{16}_D$ −84 (*c* 0.047, $CHCl_3$); UV λ_{max} (log ε) ($CHCl_3$) 241 (2.61); IR (film) ν_{max} 3526 (br), 2924, 2867, 1456, 1387, 1369, 1024, 787 cm^{-1}; HRESIMS *m/z* 305.2487 $[M + H]^+$ (calcd for $C_{20}H_{33}O_2$ *m/z* 305.2475); ^1H and ^{13}C NMR data, Table 1.

***rel*-15(ζ),16-Epoxy-7-oxopimar-8,14-ene (2):** white, amorphous powder; $[\alpha]^{16}_D$ −43 (*c* 0.092, $CHCl_3$); UV λ_{max} (log ε) ($CHCl_3$) 248 (3.97); IR (film) ν_{max} 2961, 2920, 2864, 1684, 1616, 1457, 1388, 1262, 1218 cm^{-1}; HRESIMS *m/z* 303.2320 $[M + H]^+$ (calcd for $C_{20}H_{31}O_2$ *m/z* 303.2318); ^1H and ^{13}C NMR data, Table 1.

1*R*,11*S*-Dihydroxy-8*R*,13*R*-epoxylabd-14-ene (3): colorless oil; $[\alpha]^{16}_D$ +18 (*c* 1.21, $CHCl_3$); UV λ_{max} (log ε) ($CHCl_3$) 242 (2.14); IR (film) ν_{max} 3324 (br), 2938, 2864, 1456, 1369, 1067, 998, 755 cm^{-1}; HRESIMS *m/z* 323.2597 $[M + H]^+$ (calcd for $C_{20}H_{35}O_3$ *m/z* 323.2581); ^1H and ^{13}C NMR data, Table 1.

X-ray Crystallographic Data of 3. **3**·H_2O: $C_{20}H_{34}O_3$, H_2O, M = 340.49, monoclinic, a = 6.8213(1) Å, b = 12.9640(1) Å, c = 11.3897(1) Å, β = 104.690(1)°, V = 974.28(2) Å^3, T = 100(2) K, space group $P2_1$, specimen: 0.23 × 0.20 × 0.06 mm^3, μ = 0.624 mm^{-1}, D_c (Z = 2) = 1.161 g cm^{-3}, λ(Cu Kα) = 1.54178 Å, $T_{min/max}$ = 0.80, $2\theta_{max}$ = 134.4°. A total of 12 963 reflections were collected, of which 3441 were unique (R_{int} = 0.0195); R_1 = 0.030, wR_2 = 0.083, S = 0.94;

$|\Delta\rho_{max}| = 0.20$ e·Å^{-3}. Data collection was by means of an Oxford Diffraction Gemini diffractometer. Following multiscan absorption corrections the structure was determined and refined by full-matrix refinement on F^2 using the SHELXL 97[19] program. Hydroxy and water molecule H atoms were located and refined without restraints. The remaining hydrogen atoms were placed in calculated positions and refined as part of riding models. The absolute configuration was determined by refinement of the Flack absolute structure parameter, $x = 0.09(12)$, and is as shown in Figure 1. (Full X-ray crystallographic data are available as Supporting Information.) Crystallographic data for the structure **3** (CCDC-702204) reported in this paper have been deposited with the Cambridge Crystallographic Data Centre. Copies of the data can be obtained, free of charge, via the Internet at http://www.ccdc.cam.ac.uk/conts/retrieving.html (or from the CCDC, 12 Union Road, Cambridge CB2 1EZ, U.K.; fax: +44 1223 336033; e-mail: deposit@ccdc.cam.ac.uk).

Acknowledgment. We thank the Engineering and Physical Sciences Research Council for the award of a postdoctoral scholarship to M.S.

Supporting Information Available: This material is available free of charge via the Internet at http://pubs.acs.org.

References and Notes

(1) Rijo, P.; Gaspar-Marques, C.; Simões, M. F.; Duarte, A.; Apreda-Rojas, M. C.; Cano, F. H.; Rodríguez, B. *J. Nat. Prod.* **2002**, *65*, 1387–1390.
(2) Oliveira, P. M.; Ferreira, A. A.; Silveira, D.; Alves, R. B.; Rodrigues, G. V.; Emerenciano, V. P.; Raslan, D. S. *J. Nat. Prod.* **2005**, *68*, 588–591.
(3) Gaspar-Marques, C.; Rijo, P.; Simões, M. F.; Duarte, M. A.; Rodríguez, B. *Phytomedicine* **2006**, *13*, 267–271.
(4) Abdel-Mogib, M.; Albar, H. A.; Batterjee, S. M. *Molecules* **2002**, *7*, 271–301.
(5) Rijo, P.; Simões, M. F.; Rodríguez, B. *Magn. Reson. Chem.* **2005**, *43*, 595–598.
(6) Rabe, T.; Van Staden, J. *S. Afr. J. Bot.* **1998**, *64*, 62–65.
(7) Lukhoba, C. W.; Simmonds, M. S.; Paton, A. J. *J. Ethnopharmacol.* **2006**, *103*, 1–24.
(8) Van Jaarsveld, E. *The Southern African Plectranthus*; Fernwood Press: Simon's Town, 2006.
(9) Na, G. X.; Wang, T. S.; Yin, L.; Pan, Y.; Guo, Y. L.; LeBlanc, G. A.; Reinecke, M. G.; Watson, W. H.; Krawiec, M. *J. Nat. Prod.* **1998**, *61*, 112–115.
(10) Gkinis, G.; Ioannou, E.; Quesada, A.; Vagias, C.; Tzakou, O.; Roussis, V. *J. Nat. Prod.* **2008**, *71*, 926–928.
(11) Luis, J. G.; Andres, L. S. *Nat. Prod. Lett.* **1999**, *14*, 25–30.
(12) Saxena, E.; Garg, H. S. *Nat. Prod. Lett.* **1994**, *4*, 149–54.
(13) De Pascual Teresa, J.; San Feliciano, A.; Miguel del Corral, M. J. *An. Quim.* **1975**, *71*, 110–11.
(14) Smith, E. C. J.; Kaatz, G. W.; Seo, S. M.; Wareham, N.; Williamson, E. M.; Gibbons, S. *Antimicrob. Agents Chemother.* **2007**, *51*, 4480–4483.
(15) Gibbons, S.; Oluwatuyi, M.; Veitch, N. C.; Gray, A. I. *Phytochemistry* **2003**, *62*, 83–87.
(16) Ross, J. I.; Farrell, A. M.; Eady, E. A.; Cove, J. H.; Cunliffe, W. J. *J. Antimicrob. Chemother.* **1989**, *24*, 851–862.
(17) Gibbons, S.; Udo, E. E. *Phytother. Res.* **2000**, *14*, 139–140.
(18) Kaatz, G. W.; Seo, S. M.; Ruble, C. A. *Antimicrob. Agents Chemother.* **1993**, *37*, 1086–1094.
(19) Sheldrick, G. M. *SHELXL 97: A Program for Crystal Structure Solution and Refinement*; University of Göttingen: Göttingen, Germany, 1997.

NP800581S

Bioactive Pyridine-*N*-oxide Disulfides from *Allium stipitatum*[¶]

Gemma O'Donnell,[†] Rosemarie Poeschl,[†] Oren Zimhony,[‡] Mekala Gunaratnam,[§] Joao B. C. Moreira,[§] Stephen Neidle,[§] Dimitrios Evangelopoulos,[⊥] Sanjib Bhakta,[⊥] John P. Malkinson,[∥] Helena I. Boshoff,[△] Anne Lenaerts,[○] and Simon Gibbons*[,†]

Centre for Pharmacognosy and Phytotherapy, The School of Pharmacy, University of London, 29-39 Brunswick Square, London WC1N 1AX, U.K., Infectious Diseases Division, Kaplan Medical Center, The Hebrew University, Jerusalem, Rehovot, Israel, CRUK Biomolecular Structure Group, The School of Pharmacy, University of London, London WC1N 1AX, U.K., School of Biological and Chemical Sciences, Birkbeck College, University of London, Malet Street, London WC1E 7HX, U.K., Department of Pharmaceutical and Biological Chemistry, The School of Pharmacy, University of London, 29-39 Brunswick Square, London WC1N 1AX, U.K., Tuberculosis Research Section, Laboratory of Immunogenetics, National Institute of Allergy and Infectious Diseases, Rockville, Maryland 20852, and Department of Microbiology, Immunology and Pathology, Colorado State University, 200 West Lake Street, Building 1682, Ft. Collins, Colorado 80523-4629

Received September 11, 2008

From *Allium stipitatum*, three pyridine-*N*-oxide alkaloids (**1**−**3**) possessing disulfide functional groups were isolated. The structures of these natural products were elucidated by spectroscopic means as 2-(methyldithio)pyridine-*N*-oxide (**1**), 2-[(methylthiomethyl)dithio]pyridine-*N*-oxide (**2**), and 2,2′-dithio-bis-pyridine-*N*-oxide (**3**). The proposed structure of **1** was confirmed by synthetic *S*-methylthiolation of commercial 2-thiopyridine-*N*-oxide. Compounds **1** and **2** are new natural products, and **3** is reported for the first time from an *Allium* species. All compounds were evaluated for activity against fast-growing species of *Mycobacterium*, methicillin-resistant *Staphylococcus aureus*, and a multidrug-resistant (MDR) variants of *S. aureus*. Compounds **1** and **2** exhibited minimum inhibitory concentrations (MICs) of 0.5−8 μg/mL against these strains. A small series of analogues of **1** were synthesized in an attempt to optimize antibacterial activity, although the natural product had the most potent in vitro activity. In a whole-cell assay at 30 μg/mL, **1** was shown to give complete inhibition of the incorporation of ^{14}C-labeled acetate into soluble fatty acids, indicating that it is potentially an inhibitor of fatty acid biosynthesis. In a human cancer cell line antiproliferative assay, **1** and **2** displayed IC_{50} values ranging from 0.3 to 1.8 μM with a selectivity index of 2.3 when compared to a human somatic cell line. Compound **1** was evaluated in a microarray analysis that indicated a similar mode of action to menadione and 8-quinolinol by interfering with the thioredoxin system and up-regulating the production of various heat shock proteins. This compound was also assessed in a mouse model for in vivo toxicity.

The genus *Allium* is a rich source of bioactive natural products and a prolific producer of sulfur-containing metabolites. Common garlic (*Allium sativum* L.) has a long history of use as an antibacterial material, and the major active principle, allicin, was isolated and characterized in the 1940s.[1−3] Garlic was even used clinically in the United States and known as Russian penicillin.[4] We have been investigating extracts of bulbs from the Liliaceae and Alliaceae families for their ability to produce antibacterial compounds.[5,6] The rationale is that it is highly likely that plants produce defensive antimicrobial compounds in their subterranean organs, given the richness of soil in terms of its microbial content. Soil is rich in filamentous bacteria such as *Streptomyces* and *Mycobacterium*, and it is conceivable that plants have evolved defensive secondary metabolites with activity against these genera. A number of species of the genus *Allium* have also been used medicinally in Tajikistan and Uzbekistan for various uses including the promotion of wound healing.[7]

There is a pressing need for new classes of antibacterials to deal with emerging threats such as extensively drug-resistant (XDR) tuberculosis and multidrug resistance (MDR) increasingly associated with clinically relevant bacteria such as *Staphylococcus aureus*. Plants are a relatively untapped source of antibacterial compounds, and some of the examples in the literature are striking, in terms of their preliminary in vitro potency.[8,9] However, many of these studies lack depth in terms of their biological evaluation, and in the majority of cases there is little evaluation of mammalian cell cytotoxicity or determination of potential mode of action. Unfortunately there have been only a small number of new antibacterial substances based on new carbon skeletons developed over the last 10 years, and these include daptomycin, a lipopeptide, arguably from a well-known class of natural product, and linezolid, a totally new oxazolidinone class derived synthetically. Limited reports of resistance to these new agents have been reported,[10,11] and therefore new classes of antibacterials would be valuable. There are several compelling reasons to evaluate plants as a source of new antibacterial agents. First, given the structural dissimilarity that exists between many plant antibacterials and conventional antibiotics such as tetracyclines, fluoroquinolones, and macrolides, it is possible that these phytochemical antibacterials exert their effects through new modes of action. Second, there are countless examples of ethnomedical usage of plant extracts to treat topical and systemic bacterial infections in many systems of traditional medicine.[12]

Given the need for new antibacterial substances and the pressing problems of bacterial MDR, we have evaluated *Allium stipitatum* Regel, which is grown horticulturally in Europe for its beautiful spherical flowers with tightly packed umbels. Herein, we describe the isolation, structure elucidation, and in-depth in vitro and in vivo biological evaluation of new antibacterial pyridine-*N*-oxide disulfides isolated from the bulbs of this species.

Results and Discussion

Compound **1** was isolated as a colorless waxy solid from the chloroform extract of *A. stipitatum*. The high-resolution ESIMS indicated a $[M + H]^+$ ion at *m/z* 174 and a $[M + Na]^+$ ion at *m/z*

[¶] Dedicated to Dr. David G. I. Kingston of Virginia Polytechnic Institute and State University for his pioneering work on bioactive natural products.

* To whom correspondence should be addressed. Tel: +44 207 753 5913; +44 207 753 5909. E-mail: simon.gibbons@pharmacy.ac.uk.

[†] Centre for Pharmacognosy and Phytotherapy, The School of Pharmacy, University of London.

[‡] The Hebrew University.

[§] CRUK Biomolecular Structure Group, The School of Pharmacy, University of London.

[⊥] Birkbeck College, University of London.

[∥] Department of Pharmaceutical and Biological Chemistry, The School of Pharmacy, University of London.

[△] National Institute of Allergy and Infectious Diseases, Rockville, MD.

[○] Colorado State University.

10.1021/np800572r CCC: $40.75
Published on Web 12/18/2008

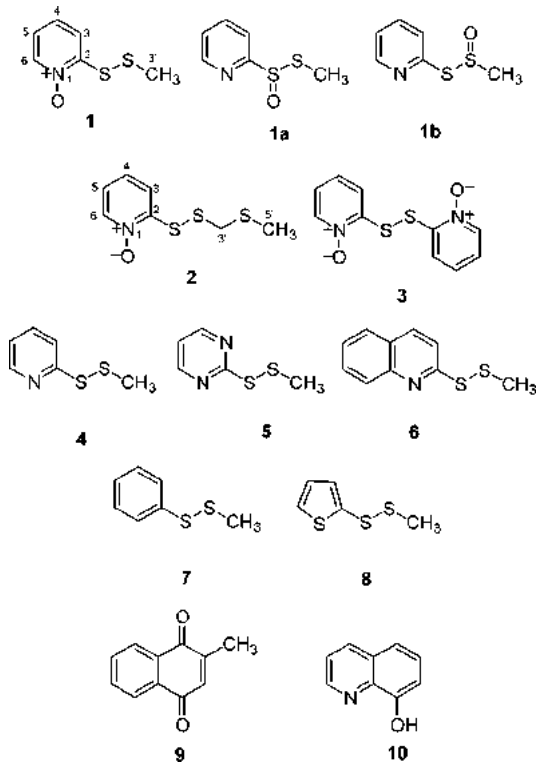

196, suggesting a molecular formula of $C_6H_8NOS_2$, and the spectrum also gave the isotope pattern for two sulfur atoms. The compound displayed a positive reaction with Dragendorff's reagent when analyzed by normal-phase TLC, indicating that it may be an alkaloidal natural product.

The ^{1}H spectrum (Table 1) displayed a deshielded methyl singlet at δ 2.50 and four hydrogens indicative of an ABCD aromatic system. The ^{13}C NMR and DEPT-135 spectra (Table 1) showed four methine aromatic carbons at δ 140.5−123.4, a deshielded quaternary carbon at δ 153.4, and a methyl carbon at δ 22.1. Given the deshielded nature of one of the hydrogens (δ 8.35, H-6) and that the coupling constant for this resonance was typical for a hydrogen α to the nitrogen of a pyridine,[13] compound **1** could be shown to be a pyridine ring-containing natural product. The aromatic hydrogens of this system were identified by correlations observed in the COSY spectrum. Specifically, a double-doublet of H-3 (δ 8.07; J = 8.0, 1.5 Hz) coupled to an H-4 triplet (δ 7.67; J = 7.5 Hz), which coupled to a second triplet of H-5 (δ 7.38; J = 7.0 Hz), and finally coupled to the α H-6 doublet (δ 8.35; J = 6.5 Hz).

A methyl group appeared as a singlet at δ 2.50 displaying no couplings to the remaining hydrogens and suggesting that it was isolated from the aromatic nucleus. Its downfield appearance in the ^{1}H spectrum at 2.50 ppm indicated that it was slightly deshielded and was attached to a heteroatom such as one of the sulfur atoms. A weak correlation (^4J) in the HMBC spectrum from the methyl hydrogens to the quaternary carbon C-2 suggested it was in the terminal position on a disulfide side-chain α to the nitrogen. Furthermore, a NOE was also evident in the NOESY spectrum from the methyl hydrogens to H-3. The aromatic hydrogen H-3 was deshielded due to its positioning β to the nitrogen of the pyridine ring and α to the disulfide side-chain. From the molecular formula of **1**, this left the placement of one oxygen atom in the structure of **1**. This posed a dilemma, as there were three structural possibilities that could exist without appreciably great differences in terms of their NMR spectroscopic data. For example, the placement of the oxygen atom on the nitrogen would give a pyridine-*N*-oxide natural product (structure **1**). However, placement of the oxygen could also occur at the sulfur directly attached to the aromatic ring (**1a**) or to the sulfur to which the methyl group was attached (**1b**), resulting in thiosulfinate natural products that occur widely in the genus *Allium* and include the well-known example allicin.[14] This was resolved by the synthesis of compound **1** by the simple method of Kitson and Loomes.[15] Briefly, commercially available 2-thiopyridine-*N*-oxide was treated with base and reacted with *S*-methyl methanethiosulfonate, resulting in *S*-methylthiolation of the thiol to generate 2-(methyldithio)pyridine-*N*-oxide, which was identical in terms of its spectroscopic and biological data with compound **1**. Pyridine-*N*-oxides have not been described from the genus *Allium* previously, and this is the first report of this compound as a natural product. The compound is, however, the subject of two Japanese patents.[16,17] These describe the use of **1** for the disinfection of seeds against *Pyrenophora graminea*[16] and the use of this compound as an antibacterial against a number of bacteria including *Staphylococcus aureus, Pyricularia oryzae*, and *Aspergillus niger*.[17]

Compound **2** was isolated as a yellow oil from the chloroform extract. The high-resolution ESIMS indicated a $[M + H]^+$ ion at m/z 220 and a $[M + Na]^+$ ion at m/z 242, suggesting a molecular formula of $C_7H_{10}NOS_3$, differing from compound **1** by CH_2S. The ESIMS gave an isotope pattern for three sulfur atoms. The compound also displayed a positive reaction with Dragendorff's reagent when analyzed by normal-phase TLC, and the NMR data were very similar to those of **1**. The ^{1}H spectrum (Table 1) also revealed the presence of four aromatic hydrogens with chemical shifts and coupling patterns similar to those for **1**, again indicative of a substituted pyridine-*N*-oxide. A deshielded methyl singlet (δ 2.29) and a methylene singlet (δ 4.02) were evident. The ^{13}C NMR and DEPT-135 spectra indicated the presence of four aromatic methine carbons at δ 140.3−123.8, a quaternary aromatic carbon at δ 153.5, a methylene at δ 44.9, and a methyl at δ 15.7 (Table 1). The methyl singlet was again slightly deshielded (2.29 ppm), indicating that it was attached to a sulfur atom. The deshielded nature of the methylene resonance at 4.02 ppm was also suggestive of attachment to at least one heteroatom, although oxygen could be ruled out due to the upfield nature of the carbon resonance (44.0 ppm). The downfield appearance of this resonance could be explained by attachment to two sulfur atoms. A correlation was evident in the HMBC spectrum from the methyl hydrogens to this methylene carbon. A ^4J correlation from the methylene hydrogens to the quaternary carbon of C-2 was also evident, and this was analogous to the ^4J correlation seen in compound **1**. These data suggested that a 2-(methylthio)methyldithio side-chain (R−S−S−CH_2−S−CH_3) was present in compound **2** and would account for the additional CH_2S seen in the molecular formula of **2**, when compared to **1**. Both the methyl and methylene hydrogens displayed NOE correlations to the H-2 aromatic hydrogen in the NOESY spectrum. This is the first time the isolation and NMR data have been described for 2-[(methylthiomethyl)dithio]pyridine-*N*-oxide and the first reported isolation of the compound as a natural product.

Compound **3** was isolated as an orange oil from the chloroform extract. The ESIMS indicated a $[M + H]^+$ ion at m/z 253 and an $[M + Na]^+$ ion at m/z 275, suggesting a molecular formula of $C_{10}H_8N_2O_2S_2$. The only signals in the ^{1}H spectrum were two doublet and two triplet aromatic hydrogens, again supportive of a 1,2,3,4 splitting pattern. The ^{13}C, DEPT-135, and HMQC spectra revealed four methine aromatic carbons and a quaternary aromatic carbon, indicating that **3** is a dimeric analogue of **1**, but lacking the methyl group. The presence of a monosubstituted pyridine ring system was characterized through HMBC correlations. The H-4 triplet (δ 7.41; J = 7.0 Hz) and the H-6 doublet (δ 8.46; J = 6.0 Hz) displayed ^3J correlations to the quaternary carbon C-2 (δ 147.3). Furthermore, the coupling constant of H-6 was again indicative of a hydrogen α to the nitrogen of a pyridine ring. H-3 displayed a ^3J correlation to C-5 (δ 123.5), and H-5, in turn, displayed a ^3J correlation to C-3 (δ 121.8) and a ^2J correlation to C-6 (δ 138.5). This completed the assignment of the pyridine-*N*-oxide ring. Analysis of the ESIMS data suggested that compound **3** is a dimer with a disulfide chain

Table 1. ^{1}H, ^{13}C, and HMBC NMR Data for **1** and **2**

	1				**2**			
no.	^{1}H	^{13}C	^{2}J	^{3}J	^{1}H	^{13}C	^{2}J	^{3}J
2		153.4				153.5		
3	8.07 dd (1.5, 8.0)	123.4		C-5	8.09 dd (1.5, 8.5)	140.3		C-5
4	7.67 t (1.0, 8.5)	130.6	C-3	C-2, C-6	7.64 t (1.5, 8.5)	130.4	C-3, C-5	C-2, C-6
5	7.38 t (1.5, 7.0)	123.9	C-6	C-3	7.37 t (2.0, 8.0)	123.8	C-6	C-3
6	8.35 d (6.5)	140.5	C-3, C-5	C-2, C-4	8.34 d (7.0)	124.0	C-5	C-2, C-4
3′	2.50	22.1	C-2		4.02 s	44.9		C-2
5′					2.29 s	15.7		C-7

Table 2. Minimum Inhibitory Concentration (MIC) Values of Compounds (μg/mL)

	1	**2**	**3**	**4**	**5**	**6**	**7**	**8**	Nor[a]	Ox[b]	Eth[c]	Iso[d]
M. fortuitum	8	8	16	8	8	4	>128	>128	–[e]	–[e]	2	0.25
M. smegmatis	8	4	16	8	8	8	64	64	–[e]	–[e]	32	0.25
M. smegmatis (mc^2 2700)	8	4	–[e]	–[e]	–[e]	–[e]	–[e]	–[e]	–[e]	–[e]	–[e]	–[e]
M. phlei	2	2	16	16	16	8	>128	>128	–[e]	–[e]	2	128
S. aureus (SA−1199B)	2	1	1	2	2	4	128	128	32	0.25	–[e]	–[e]
S. aureus (XU212)	1	1	1	4	4	4	>128	>128	16	128	–[e]	–[e]
S. aureus (EMRSA-15)	0.5	0.5	0.5	2	2	4	>128	>128	0.5	32	–[e]	–[e]

[a] Norfloxacin. [b] Oxacillin. [c] Ethambutol. [d] Isoniazid. [e] Not tested (−).

linking two pyridine-*N*-oxide rings in a symmetrical C-2−C-2′ linkage. This compound has been previously isolated from a basidiomycete mushroom of the *Cortinarius* genus,[18] and the observed NMR data are in accordance with this report.

A series of methyl sulfide analogues were prepared and with the natural products they were assayed against a panel of bacteria (Table 2). Compounds **1**−**6** were highly active (MIC < 4 μg/mL) against the three *Staphylococcus aureus* strains. These included a multidrug-resistant strain that overexpresses the NorA efflux transporter (SA1199B); a tetracycline-effluxing strain that is also a MRSA (XU212); and EMRSA-15, one of the major epidemic strains of MRSA responsible for bacteraemias in U.K. hospitals.[19] The levels of activity of the natural products against this EMRSA strain are particularly noteworthy at 0.5 μg/mL. The natural products were also marginally more active than the synthetic compounds against the fast-growing mycobacteria (FGM) (Table 2) with MIC values in the range 2−16 mg/mL. Compounds **7** and **8** were either inactive or only marginally active, indicating that the presence of the disulfide moiety is not the only factor responsible for activity. It is possible that this disulfide is strongly "activated" by the presence of electron-withdrawing functional groups such as pyridine, pyridine-*N*-oxide, pyrimidine, and quinoline, whereas phenyl and thiophene are poorly electron-withdrawing and therefore have little effect on the "reactivity" of the disulfide bond.

Both compounds **1** and **2** were evaluated against *Mycobacterium bovis* BCG and *Mycobacterium tuberculosis* H37Rv (Figure 1) and were shown to be highly active. Compound **1** is bactericidal against nonreplicating cells of *M. tuberculosis*, with a concentration of 1.25 μg/mL, resulting in a 99% decrease in viable counts of anaerobically adapted cells after one week of exposure.[20] To investigate the macromolecular processes that were affected by treatment with this disulfide, we analyzed the effects on translation and fatty acid synthesis. The disulfide structure stimulated us first to test the effect of **1** on protein biosynthesis; however, application of **1** at 10−20-fold of the MIC followed by incubation with ^{35}S methionine yielded no effect of **1** on ^{35}S methionine incorporation into protein. Therefore, protein biosynthesis is not affected by **1**. We next investigated the ability of **1** to inhibit the incorporation of labeled acetate into soluble fatty acids. Replicating *M. smegmatis* bacilli were treated with **1** at a concentration of 30 μg/mL for 2 h before adding [1-^{14}C] acetate for another 2 h followed by soluble lipid extraction (which yields mostly fatty acids) and comparison of the counts per minute to the untreated control as previously described.[21] Incubation with **1** resulted in complete inhibition of acetate incorporation into soluble lipids, indicating that this natural product may inhibit fatty acid synthesis. The primary possibility for this finding is that **1** inhibits FAS-I, which should be next tested by an in vitro assay. The antibacterial activity against *S. aureus* (which synthesizes fatty acids through a FAS-II system) then may be due to inhibition of a FAS-II enzyme. Other possibilities that could explain the observed results are inhibition of the enzyme acetyl-CoA carboxylase AccD1, which mediates the formation of malonyl CoA,[22] or inhibition of the acyl-CoA condensation reaction with malonyl-AcpM in a reaction catalyzed by mtFabH.[23,24] However, the possibility that the observed arrest in fatty acid synthesis is a nonspecific result of a generalized toxic effect can not be excluded.

Microarray analysis of RNA extracted from cells treated with **1** revealed that transcriptional profiles elicited were similar to the profiles generated during treatment of cells with compounds such as menadione (**9**) and 8-quinolinol (**10**) that result in oxidative stress. Genes that characterized the response to compound **1**, menadione, and 8-quinolinol included the thioredoxin system components encoded by *trxB2* and *trxC* as well as several genes associated with the heat shock response such as *clpB*, *sigH*, *dnaJ*, *dnaK*, and *hsp*. Other genes that have been found to be up-regulated during treatment of *M. tuberculosis* at high temperatures[25] were also up-regulated, including *Rv0331*, *Rv3463*, *Rv3054c*, and *Rv1334-Rv1335*. These results suggest that compound **1** possibly generates damaged proteins and other oxidative stress signals as part of its mechanism of action.

Compound **1** was also evaluated in vivo, including efficacy in a mouse model of TB infection. The maximum tolerated dose (MTD) was determined using an escalating single dose of drug given to mice by oral gavage. Acute adverse effects were observed at doses of 100 and 300 mg/kg. No adverse effects, reactions, or toxicity was observed at oral doses of 30 mg/kg (Table 3). Subsequently, the efficacy of **1** was evaluated in mice at a dose of 30 mg/kg administered via oral gavage in infected GKO C57BL/6 mice.[26] Compound **1** was found to be inactive in that it did not effectively reduce the bacterial numbers in the lungs and spleens with respect to the untreated controls at the dose tested (Table 4).

Both compounds **1** and **2** showed significant activity in antiproliferative assays using MCF7 breast carcinoma and A549 non-small-cell lung carcinoma cancer cells, as well as human colon adenocarcinoma HT29 cells (Table 5). They showed greater selectivity to a human normal fibroblast cell line than the established clinical anticancer agent cisplatin, indicating their potential for anticancer activity, although at this stage no information is available on their mechanism of action.

It is possible that compound **1**, in being an *N*-oxide, is rapidly excreted, and this would presumably be the main route of metabolism of the parent pyridine methyldisulfide (**4**). Compound

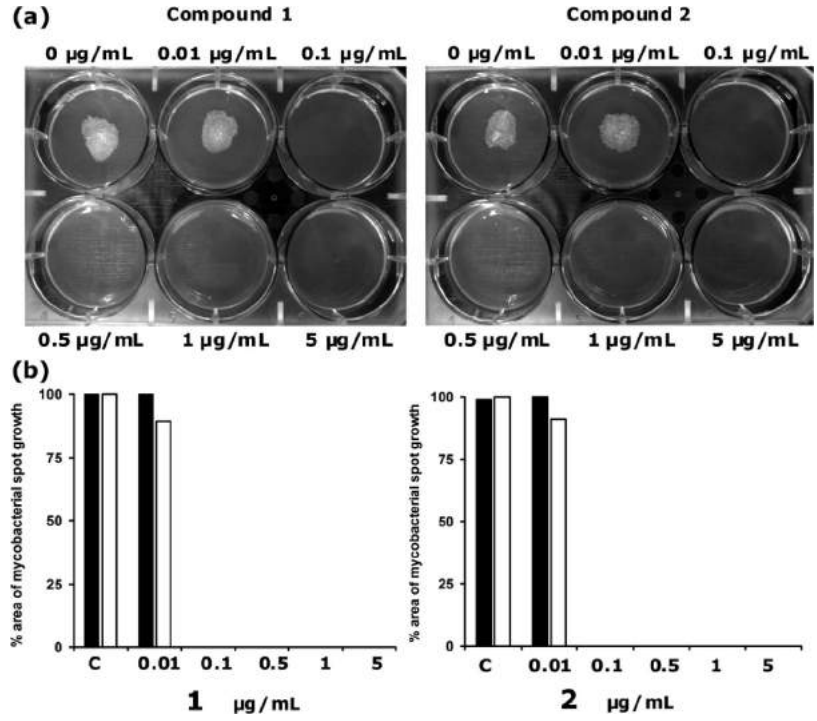

Figure 1. Effect of **1** and **2** on the growth of mycobacteria. (a) Growth of *M. bovis* BCG on solid agar at 37 °C in the presence of different concentrations of compounds **1** and **2**. The MIC values of compounds **1** and **2** are both 0.1 μg/mL (a) Approximately 10^3 *M. bovis* BCG cells were spotted on solidified Middlebrook 7H10 agar containing different concentrations of **1** and **2** (0.01, 0.1, 0.5, 1, and 5 μg/mL) in a six-well plate. Pictures of cultures that grew as spots were taken on the 14th day of inoculation using a BioDoc-ItTM imaging system. (b) *M. tuberculosis* H37Rv was grown in the presence of similar concentrations of **1** and **2** as in (a) above. A comparison of inhibitory effects of **1** and **2** on *M. bovis* BCG (black bars) versus *M. tuberculosis* H37Rv (open bars) is illustrated on the bar graphs.

Table 3. In Vivo Toxicity Data of **1** after 3-day Dosing in Mice

dose (mg/kg)	days Rx	% survival + comments
300	3	1/5 lethality after 2 days of dosing, 1/5 additional lethality after 3 days of dosing
100	3	transient lethargy after dosing
30	3	no adverse effects

Table 4. Bacterial Numbers in Lungs and Spleens of *Mycobacterium tuberculosis*-Infected Mice at the Start of Treatment (15 days after aerosol infection) and after 9 Days of Drug Treatment (24 days after aerosol infection)

		$\log_{10}$ CFU ± SEM	
treatment regimen	dose	lung	spleen
day 15, start of treatment (pretreatment controls)	−	6.08 ± 0.06	4.00 ± 0.19
day 24, untreated controls	−	8.13 ± 0.11	6.35 ± 0.13
day 24, isoniazid	25	5.33 ± 0.10	2.16 ± 0.26
day 24, **1**	30	8.17 ± 0.11	6.17 ± 0.29

4 displays a similar level of antibacterial activity to **1** and **2** and is also likely to possess toxicity to mammalian cell lines. An investigation of the activity of **4** in a mouse model of infection and in a xenograft antitumor assay would be worthwhile to gauge the in vivo utility of this class of compound.

Experimental Section

General Experimental Procedures. UV spectra were recorded on a Thermo Electron Corporation Helios spectrophotometer, and IR spectra were recorded on a Nicolet 360 FT-IR spectrophotometer. NMR spectra were recorded on a Bruker AVANCE 500 MHz spectrometer. Chemical shift values (δ) are reported in parts per million (ppm) relative to appropriate internal solvent standard, and coupling constants (J values) are given in Hz. Mass spectra were recorded on a Finnigan MAT 95 high-resolution, double-focusing, magnetic sector mass spectrometer. Accurate mass measurement was achieved using voltage scanning of the accelerating voltage. This was nominally 5 kV, and an internal reference of heptacosa was used. Resolution was set between 5000 and 10 000.

Plant Material. The fresh bulbs of *Allium stipitatum* were purchased from Gee Tee Garden Products, Spalding, Lincolnshire, U.K., and a voucher specimen (GO'D/017B) has been deposited in their herbarium.

Extraction and Isolation. A 4.43 kg quantity of macerated bulbs was extracted exhaustively with hexane, chloroform, and methanol to form three extracts with MIC values of 16, 8, and >512 μg/mL against *Mycobacterium fortuitum*. The chloroform extract (4.9 g) was separated on silica gel by VLC, eluting 11 fractions (200 mL) with hexane and 10% increments of ethyl acetate, followed by one 100% chloroform fraction (300 mL) and a final 100% methanol wash (500 mL). The final fraction (13) exhibited an MIC of 8 μg/mL against *M. fortuitum*. Then, 1000 mg of VLC fraction 13, eluted in the 100% methanol wash, was subjected to reversed-phase preparative HPLC (Waters XTerra Prep MS C_{18} column, 10 μM, 19 × 300 mm, 100% water to 100% acetonitrile from 2 to 15 min, 50 mL/min) to yield three peaks, eluting at 10.4 (**3**, 361.1 mg), 12.8 (**1**, 250.5 mg), and 14.8 min (**2**, 72.1 mg).

2-(Methyldithio)pyridine-*N*-oxide (1): colorless, waxy solid; UV (MeOH) λ_{max} (log ε) 239.0 (4.37) nm; IR (film) ν_{max} 3410 (br), 3090, 1463, 1419, 1260, 1220, 1138, 1079, 836, 760 cm^{-1}; ^1H and ^{13}C NMR ($CDCl_3$, 500 and 125 MHz), see Table 1; HRESIMS *m/z* 174.0043 [M + H]$^+$ (calcd for $C_6H_8NOS_2$ 174.0042).

2-[(Methylthiomethyl)dithio]pyridine-*N*-oxide (2): yellow oil; UV (MeOH) λ_{max} (log ε) 239.0 (4.18), 204.0 (4.00) nm; IR (film) ν_{max} 3386 (br), 3096, 2916, 1418, 1259, 1221, 836, 760 cm^{-1}; ^1H and ^{13}C NMR ($CDCl_3$, 500 and 125 MHz), see Table 1; HRESIMS *m/z* 219.9931 [M + H]$^+$, 241.9751 [M + Na]$^+$ (calcd for $C_7H_{10}NOS_3$ 219.9919).

2,2′-Dithio-bis-pyridine-*N*-oxide (dipyrithione, 3): yellow oil; UV (MeOH) λ_{max} (log ε) 266.0 (4.17), 240.5 (3.73) nm; IR (film) ν_{max} 3420, 1647, 1558, 1379, 1022, 1000, 822, 760 cm^{-1}; ^1H and ^{13}C NMR (methanol-d_4) in agreement with those published;[18] HRESIMS *m/z* 253.0102 [M + H]$^+$ (calcd for $C_{10}H_9N_2S_2O_2$ 253.0105).

Synthesis of Methyl Disulfides. Aromatic thiols (2-thiopyridine, 2-thiopyrimidine, 2-thioquinoline, thiobenzene, and 2-thiothiophene) and *S*-methyl methanethiosulfonate were purchased from Sigma-Aldrich, Gillingham, U.K. The method of Kitson and Loomes[15] was

Table 5. Short-Term Cytotoxicity Data for Compounds **1**, **2**, and Cisplatin (IC_{50}) in Human Breast, Lung, and Colorectal Cancer Cell Lines and Normal Human Fibroblast Cell Line[a,b]

	human breast cancer (MCF7)	human lung cancer (A549)	human colorectal cancer (HT29)	lung fibroblast (WI38)	selectivity index (WI38IC_{50}/ MCF7 IC_{50})
1	0.35	0.22	1.84	0.8	2.3
2	0.39	0.78	[c]	0.89	2.3
cisplatin	0.76	2.47	3.27	1	1.4

[a] Data expressed in μM. [b] Cells were exposed to compounds for 96 h and stained with sulforhodamine B. [c] Not determined.

adapted as follows. The appropriate thiol (2.5 mmol) was dissolved in water (5 mL) containing NaOH (0.10 g, 2.5 mmol, 1 equiv). *S*-Methyl methanethiosulfonate (0.315 g, 2.5 mmol, 1 equiv) was then added, and the solution stirred for 1 h at room temperature. The cloudy suspension formed was extracted with dichloromethane (20 mL). The resulting dichloromethane solution was then dried with anhydrous sodium sulfate, filtered, and concentrated under reduced pressure to afford the pure disulfide.

2-(Methyldithio)pyridine (4): pale yellow oil; UV (MeOH) λ_{max} (log ε) 283.0 (3.66), 237.5 (3.93), 201.0 (3.82) nm; IR (film) ν_{max} 1571, 1559, 1444, 1415, 1307, 1274, 1143, 1112, 1082, 1042, 985, 953, 755, 716 cm^{-1}; ^1H NMR (500 MHz, methanol-d_4) δ 8.39 (1H, dt, $J = 5.2$, 4.8 Hz), 7.77 (2H, m), 7.17 (1H, dt, $J = 9.6$, 8.4 Hz), 2.47 (3H, s); ^{13}C NMR (125 MHz, methanol-d_4) 161.2 (s), 150.6 (d), 139.2 (d), 122.3 (d), 120.8 (d), 23.4 (q); HRESIMS *m/z* 158.0103 $[M + H]^+$ (calcd for $C_6H_7NS_2$ 158.0098).

2-(Methyldithio)pyrimidine (5): yellow oil; UV (MeOH) λ_{max} (log ε) 238.5 (3.94) nm; IR (film) ν_{max} 1558, 1546, 1372, 1189, 1166, 955, 800, 770, 741 cm^{-1}; ^1H (500 MHz, methanol-d_4) δ 8.66 (2H, d, $J =$ 4.8 Hz), 7.26 (t, $J = 5.2$, 4.8 Hz), 2.54 s (3H, s); ^{13}C NMR (125 MHz, methanol-d_4) δ 172.4 (s), 159.4 (d), 119.6 (d), 23.0 (q); HRESIMS *m/z* 159.0051 $[M + H]^+$ (calc for $C_5H_6N_2S_2$ 159.0051).

2-(Methyldithio)quinoline (6): yellow oil; UV (MeOH) λ_{max} (log ε) 334.0 (3.84), 325.0 (3.79), 250.5 (4.39), 212.0 (4.62) nm; IR (film) υ_{max} 1615, 1582, 1553, 1492, 1447, 1291, 1137, 1103, 1087, 952, 939, 851, 815, 778, 744 cm^{-1}; ^1H NMR (500 MHz, $CDCl_3$) δ 8.12 (1H, d, $J = 8.8$ Hz), 8.02 (1H, d, $J = 8.4$ Hz), 7.87 (1H, d, $J = 8.8$ Hz), 7.79 (1H, d, $J = 8.4$ Hz), 7.71 (1H, t, $J = 8.4$ Hz), 7.50 (1H, t, $J = 8.0$ Hz), 2.56 (3H, s); ^{13}C NMR (125 MHz, $CDCl_3$) δ 160.4 (s), 148.3 (s), 137.1 (d), 130.3 (d), 128.5 (d), 127.9 (d), 126.4 (s), 126.2 (d), 117.3 (d), 23.5 (q); HRESIMS *m/z* 208.0256 $[M + H]^+$ (calcd for $C_{10}H_{10}NS_2$ 208.0255).

2-(Methyldithio)benzene (7): pale yellow oil; UV (MeOH) λ_{max} (log ε) 239.0 (3.56), 205.0 (3.56) nm; IR (film) ν_{max} 1576, 1475, 1437, 1305, 1136, 1067, 1022, 951, 735, 686 cm^{-1}; ^1H NMR (500 MHz, $CDCl_3$) δ 7.43 (2H, dd, $J = 5.2$, 1.2 Hz), 7.25 (1H, dd, $J = 3.6$, 1.2 Hz), 7.00 (2H, dd, $J = 5.2$, 3.6 Hz), 2.55 (3H, s); ^{13}C NMR (125 MHz, $CDCl_3$) δ 137.1 (s), 129.2 (d), 127.7 (d), 127.0 (d), 23.1 (q); ESIMS *m/z* 156 $[M + H]^+$ (calcd for $C_7H_8S_2$ 156).

2-(Methyldithio)thiophene (8): orange oil; UV (MeOH) λ_{max} (log ε) 311.5 (3.80), 240.0 (3.40), 203.5 (3.94) nm; IR (film) ν_{max} 1397, 1327, 1303, 1250, 1214, 1133, 1083, 1023, 987, 950, 846, 742, 699 cm^{-1}; ^1H NMR (500 MHz, $CDCl_3$) δ 7.55 (1H, dd, $J = 8.4$, 1.2 Hz), 7.35 (1H, t, $J = 8.0$ Hz), 7.26 (1H, bd, $J = 7.2$ Hz), 2.46 (3H, s); ^{13}C NMR (125 MHz, $CDCl_3$) δ 136.6 (s), 134.2 (d), 131.0 (d), 127.8 (d), 23.3 (q); ESIMS *m/z* 142 $[M + H]^+$ (calcd for $C_6H_6S_2$ 142).

Antibacterial Assay with Fast-Growing *Mycobacterium* species and *Staphylococcus aureus*. *Mycobacterium* species were acquired from the NCTC, Salisbury, U.K. Strains were grown on Columbia blood agar (Oxoid) supplemented with 7% defibrinated horse blood (Oxoid) and incubated for 72 h at 37 °C prior to minimum inhibitory concentration (MIC) determination. *S. aureus* strains were the generous gift of Dr. Edet Udo (XU212), Prof. Glenn W. Kaatz (SA1199B), and Dr. Paul Stapleton (EMRSA-15). Antibacterial assays were performed as previously described.[5,27] Ethambutol and isoniazid were used as positive controls for the mycobacteria, and norfloxacin and oxacillin were used as positive controls for the staphylococci.

Determination of MIC Value in *M. bovis* BCG and in *M. tuberculosis* Using Spot-Culture Growth Inhibition Assays. *M. bovis* BCG was cultured at 37 °C in an incubator with rotation at two revolutions per minute in Middlebrook 7H9 broth supplemented with 10% (v/v) albumin-dextrose-catalase (ADC; Difco) and 0.05% Tween 80 until the midexponential phase (OD_{600} of 1.0). *M. tuberculosis* H37Rv was grown at 37 °C in an incubator as standing culture in 30 mL unbreakable universals containing Middlebrook 7H9 broth supplemented with 10% (v/v) oleic acid-albumin-dextrose-catalase (OADC; Difco) and 0.05% Tween 80 with occasional stirring until the midexponential phase (OD_{600} of 0.6) was attained. For the quality control of the mycobacterial cultures, they were stained each time with a modified Ziehl-Neelsen staining protocol using a Tb-color kit, Bund Deutscher Hebammen Laboratory (Karlsruhe, Germany), followed by bright field microscopy.

To measure anaerobic cidal activity of the compounds, *M. tuberculosis* H37Rv (ATCC27294) was cultured in a self-generated oxygen-depletion model as described by Wayne[28] using 19.5 × 145 mm tubes with a magnetic stirrer. Tubes were sealed with Teflon-lined caps and subsequently with paraplast and incubated for 3 weeks at 37 °C on a magnetic stirrer. The tubes were opened in an anaerobic chamber and diluted 10-fold into anaerobic Dubos medium, and 1 mL volumes were treated with various concentrations of the compound in 24-well plates. Control cultures were treated with DMSO. Positive and negative drug controls were metronidazole and isoniazid, respectively. The plates were sealed in anaerobic bags and incubated for 7 days at 37 °C. Serial dilutions were subsequently plated on 7H11 Middlebrook agar to monitor bacterial survival.

For the spot-culture growth inhibition assay,[20] bacilli in the culture were serially diluted in order to give a final concentration of 10^3 cells/mL. Then, 5 μL of the diluted culture was spotted onto 5 mL of Middlebrook 7H10 agar medium, supplemented with 10% (v/v) OADC in a six-well plate containing various concentrations of compounds **1** and **2**, and incubated at 37 °C for 14 days. A well with no compound as a positive control was also used. MIC was determined as the lowest concentration at which there is no growth.

Sulforhodamine B Short-Term Cytotoxicity Assay. Short-term growth inhibition was measured using the SRB assay as described previously.[29] Briefly, cells were seeded (4000 cells/wells) into the wells of 96-well plates in DMEM and incubated overnight at 37 °C and 5% CO_2 to allow the cells to attach. Subsequently, cells were exposed to freshly made solutions of compounds at increasing concentrations of 0.1 to 25 μM in quadruplicate and incubated for a further 96 h. Following this, the cells were fixed with ice-cold trichloroacetic acid (TCA) (10% w/v) for 30 min and stained with 0.4% SRB dissolved in 1% acetic acid for 15 min. All incubations were carried out at room temperature. The IC_{50} value, the concentration required to inhibit cell growth by 50%, was determined from the mean absorbance at 540 nm for each drug concentration expressed as a percentage of the control for untreated well absorbance.

Microarray Analysis. *M. tuberculosis* H37Rv (ATCC 27294) was grown in 7H9 Middlebrook medium supplemented with 0.2% glycerol, 0.5% bovine serum albumin fraction V, 0.05% Tween 80, 0.08% NaCl, and 0.2% glucose to an OD_{650nm} of 0.3 and was treated with either 2, 5, or 10 μg/mL of compound **1** or an equivalent amount of DMSO for 6 h before harvesting cells for RNA isolation. RNA was isolated and labeled cDNA synthesized, and microarray hybridizations and microarray analysis were performed as described by Boshoff et al.[30] Genes that were predictive for various treatment groups were determined by a class prediction software developed by Tibshirani et al.[31]

Maximum Tolerated Dose (MTD). C57BL/6 female mice were orally administered (by gavage) a single dose of drug at 30, 100, or 300 mg/kg, using three mice per dose. Mice were observed postadministration at 4 and 6 h and then twice daily for the duration of the study (1 week).

Evaluation of in Vivo Efficacy against *M. tuberculosis*. Eight- to 10-week-old female specific-pathogen-free C57BL/6-Ifngtm1ts mice (gamma interferon gene-disrupted [GKO] mice) were purchased from Jackson Laboratories, Bar Harbor, ME. Mice were infected via low-dose aerosol exposure to *M. tuberculosis* Erdman using a Middlebrook aerosol generation device (Glas-Col Inc., Terre Haute, IN), and the short-course mouse model was performed as described previously. One day postinfection, three mice were sacrificed to verify the uptake of

50 to 100 CFU of bacteria per mouse. Negative control mice remained untreated. An isoniazid (INH) control group (isoniazid administered via oral gavage at 25 mg/kg/day) was included in each study. Each treatment group consisted of five mice. Treatment was started 14 days postinfection and continued for nine consecutive days. Five infected mice were killed at the start of treatment as pretreatment controls. Drugs were administered daily by oral gavage using 0.5% methyl cellulose (200 μL volume).

Statistical Analysis. The viable counts were converted to logarithms, which were then evaluated by a one-way ANOVA test, followed by a multiple comparison analysis of variance by a one-way Tukey test (SigmaStat software program). Differences were considered significant at the 95% level of confidence.

Acknowledgment. We thank the Engineering and Physical Sciences Research Council for the award of a doctoral scholarship to G.O. CRUK is thanked for support to M.G. and S.N. This work was funded, in part, by the Division of Intramural Research of NIH, NIAID.

References and Notes

(1) Cavallito, C. J.; Buck, J. S.; Suter, C. M. *J. Am. Chem. Soc.* **1944**, *66*, 1950–1951.
(2) Cavallito, C. J.; Bailey, J. H. *J. Am. Chem. Soc.* **1944**, *66*, 1952–1954.
(3) Cavallito, C. J.; Bailey, J. H.; Buck, J. S. *J. Am. Chem. Soc.* **1945**, *67*, 1032–1033.
(4) Bolton, S. G.; Null, G.; Troetel, W. M. *J. Am. Pharm. Assoc.* **1982**, *22*, 40–43.
(5) O'Donnell, G.; Bucar, F.; Gibbons, S. *Phytochemistry* **2006**, *67*, 178–182.
(6) O'Donnell, G.; Gibbons, S. *Phytother. Res.* **2007**, *21*, 653–657.
(7) Keusgen, M.; Fritsch, R. M.; Hisoriev, H.; Kurbonova, P. A.; Khassanov, F. O. *J. Ethnobiol. Ethnomed.* **2006**, *2*, 18.
(8) Gibbons, S. *Planta Med.* **2008**, *74*, 594–602.
(9) Gibbons, S. *Nat. Prod. Rep.* **2004**, *21*, 263–277.
(10) Bennett, J. W.; Murray, C. K.; Holmes, R. L.; Patterson, J. E.; Jorgensen, J. H. *Diagn. Microbiol. Infect. Dis.* **2008**, *60*, 437–40.
(11) Schulte, B.; Heininger, A.; Autenrieth, I. B.; Wolz, C. *Epidemiol. Infect.* **2007**, *25*, 1–3.
(12) Smith, J. E.; Tucker, D.; Watson, K.; Lloyd Jones, G. *J. Ethnopharmacol.* **2007**, *112*, 386–393.
(13) Zhu, J.; Wang, M.; Wu, W.; Ji, Z.; Hu, Z. *Phytochemistry* **2002**, *61*, 699–704.
(14) Naznin, M. T.; Akagawa, M.; Okukawa, K.; Maeda, T.; Morita, N. *Food Chem.* **2008**, *106*, 1113–1119.
(15) Kitson, T. M.; Loomes, K. M. *Anal. Biochem.* **1985**, *146*, 429–430.
(16) Nakayama, K.; Hisada, Y.; Yamashita, N. *Jap. patent, JP 61056104*, 1986.
(17) *Sumitomo Chemical Co., Ltd. Jap. patent, JP 59163368,* 1984.
(18) Nicholas, G. M.; Blunt, J. W.; Munro, M. H. G. *J. Nat. Prod.* **2001**, *64*, 341–344.
(19) Johnson, A. P.; Aucken, H. M.; Cavendish, S.; Ganner, M.; Wale, M. C. J.; Warner, M.; Livermore, D. M.; Cookson, B. D. *J. Antimicrob. Chemother.* **2001**, *48*, 143–144.
(20) Madikane, V. E.; Bhakta, S.; Russell, A. J.; Campbell, W. E.; Claridge, T. D.; Elisha, B. G.; Davies, S. G.; Smith, P.; Sim, E. *Bioorg. Med. Chem.* **2007**, *15*, 3579–3586.
(21) Zimhony, O.; Cox, J. S.; Welch, J. T.; Vilchèze, C.; Jacobs, W. R., Jr. *Nat. Med.* **2000**, *6*, 1043–1047.
(22) Gande, R.; Dover, L. G.; Krumbach, K.; Besra, G. S.; Sahm, H.; Oikawa, T.; Eggeling, L. *J. Bacteriol.* **2007**, *189*, 5257–5264.
(23) Choi, K. H.; Kremer, L.; Besra, G. S.; Rock, C. O. *J. Biol. Chem.* **2000**, *275*, 28201–28207.
(24) He, X.; Reynolds, K. A. *Antimicrob. Agents Chemother.* **2002**, *46*, 1310–1318.
(25) Stewart, G. R.; Wernisch, L.; Stabler, R.; Mangan, J. A.; Hinds, J.; Laing, K. G.; Young, D. B.; Butcher, P. D. *Microbiology* **2002**, *148*, 3129–3138.
(26) Lenaerts, A. J. M.; Gruppo, V.; Brooks, J. V.; Orme, I. M. *Antimicrob. Agents Chemother.* **2003**, *47*, 783–785.
(27) Gibbons, S.; Udo, E. E. *Phytother. Res.* **2000**, *14*, 139–140.
(28) Wayne, L. G. In *Mycobacterium Tuberculosis Protocols*; Parish, T., Stoker, N. G., Eds.; Humana Press: Totowa, NJ, 2001; pp 247−270.
(29) Moore, M. J.; Schultes, C. M.; Cuesta, J.; Cuenca, F.; Gunaratnam, M.; Tanious, F. A.; Wilson, W. D.; Neidle, S. *J. Med. Chem.* **2006**, *49*, 582–599.
(30) Boshoff, H. I.; Myers, T. G.; Copp, B. R.; McNeil, M. R.; Wilson, M. A.; Barry, C. E., III *J. Biol. Chem.* **2004**, *279*, 40174–40184.
(31) Tibshirani, R.; Hastie, T.; Narashiman, B.; Chu, G. *Proc. Natl. Acad. Sci. U.S.A.* **2002**, *99*, 6567–6572.

NP800572R

Antibacterial Cannabinoids from *Cannabis sativa*: A Structure−Activity Study

Giovanni Appendino,*[,†,‡] Simon Gibbons,*[,⊥] Anna Giana,[†,‡] Alberto Pagani,[†,‡] Gianpaolo Grassi,[§] Michael Stavri,[⊥] Eileen Smith,[⊥] and M. Mukhlesur Rahman[⊥]

Dipartimento di Scienze Chimiche, Alimentari, Farmaceutiche e Farmacologiche, Università del Piemonte Orientale, Via Bovio 6, 28100 Novara, Italy, Consorzio per lo Studio dei Metaboliti Secondari (CSMS), Viale S. Ignazio 13, 09123 Cagliari, Italy, Centre for Pharmacognosy and Phytotherapy, The School of Pharmacy, University of London, 29-39 Brunswick Square, London WC1N 1AX, U.K., and CRA-CIN Centro di Ricerca per le Colture Industriali, Sede distaccata di Rovigo, Via Amendola 82, 45100 Rovigo, Italy

Received May 1, 2008

Marijuana (*Cannabis sativa*) has long been known to contain antibacterial cannabinoids, whose potential to address antibiotic resistance has not yet been investigated. All five major cannabinoids (cannabidiol (**1b**), cannabichromene (**2**), cannabigerol (**3b**), Δ^9-tetrahydrocannabinol (**4b**), and cannabinol (**5**)) showed potent activity against a variety of methicillin-resistant *Staphylococcus aureus* (MRSA) strains of current clinical relevance. Activity was remarkably tolerant to the nature of the prenyl moiety, to its relative position compared to the *n*-pentyl moiety (abnormal cannabinoids), and to carboxylation of the resorcinyl moiety (pre-cannabinoids). Conversely, methylation and acetylation of the phenolic hydroxyls, esterification of the carboxylic group of pre-cannabinoids, and introduction of a second prenyl moiety were all detrimental for antibacterial activity. Taken together, these observations suggest that the prenyl moiety of cannabinoids serves mainly as a modulator of lipid affinity for the olivetol core, a *per se* poorly active antibacterial pharmacophore, while their high potency definitely suggests a specific, but yet elusive, mechanism of activity.

Several studies have associated the abuse of marijuana (*Cannabis sativa* L. Cannabinaceae) with an increase in opportunistic infections,[1] and inhalation of marijuana has indeed been shown to interfere with the production of nitric oxide from pulmonary macrophages, impairing the respiratory defense mechanisms against pathogens and causing immunosuppression.[2] The association of *C. sativa* with a decreased protection against bacterial infections is paradoxical, since this plant has long been known to contain powerful antibacterial agents.[3] Thus, preparations from *C. sativa* were investigated extensively in the 1950s as highly active topical antiseptic agents for the oral cavity and the skin and as antitubercular agents.[3] Unfortunately, most of these investigations were done at a time when the phytochemistry of *Cannabis* was still in its infancy, and the remarkable antibacterial profile of the plant could not be related to any single, structurally defined and specific constituent. Evidence that pre-cannabidiol (**1a**) is a powerful plant antibiotic was, nevertheless, obtained,[4] and more recent investigations have demonstrated, to various degrees, antibacterial activity for the nonpsychotropic cannabinoids cannabichromene (CBC, **2**),[5] cannabigerol (CBG, **3b**),[6] and cannabidiol (**1b**),[7] as well as for the psychotropic agent Δ^9-tetrahydrocannabinol (THC, **4b**).[7] These observations, and the inactivity of several noncannabinoid constituents of *C. sativa* as antibacterial agents, suggest that cannabinoids and their precursors are the most likely antibacterial agents present in *C. sativa* preparations.[8] However, differences in bacterial strains and end-points make it difficult to compare the data reported in these scattered studies, and the overall value of *C. sativa* as an antibacterial agent is therefore not easy to assess.

There are currently considerable challenges with the treatment of infections caused by strains of clinically relevant bacteria that show multidrug-resistance (MDR), such as methicillin-resistant *Staphylococcus aureus* (MRSA) and the recently emerged and extremely drug-resistant *Mycobacterium tuberculosis* XDR-TB. New antibacterials are therefore urgently needed, but only one new class of antibacterial has been introduced in the last 30 years.[9] Despite the excellent antibacterial activity of many plant secondary metabolites[10] and the ability of some of them to modify the resistance associated with MDR strains[11] and efflux pumps,[12] plants are still a substantially untapped source of antimicrobial agents.

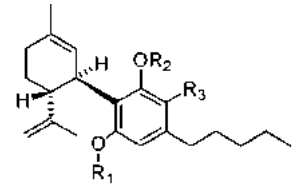

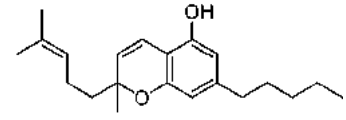

2

	R_1	R_2	R_3
1a	H	H	COOH
1b	H	H	H
1c	Ac	Ac	H
1d	Me	H	H
1e	Me	Me	H
1f	H	H	COOMe
1g	H	H	$COOCH_2CH_2Ph$

These considerations, as well as the observation that cross-resistance to microbial and plant antibacterial agents is rare,[10] make *C. sativa* a potential source of compounds to address antibiotic resistance, one of the most urgent issues in antimicrobial therapy. To obtain structure−activity data and define a possible microbiocidal cannabinoid pharmacophore, we investigated the antibacterial profile of the five major cannabinoids, of their alkylation and acylation products, and of a selection of their carboxylic precursors (pre-cannabinoids) and synthetic positional isomers (abnormal cannabinoids).

Results and Discussion

The antibacterial cannabinoid chemotype is poorly defined, as is the molecular mechanism of its activity. Since many simple phenols show antimicrobial properties, it does not seem unreasonable to assume that the resorcinol moiety of cannabinoids serves as the antibacterial pharmacophore, with the alkyl, terpenoid, and carboxylic appendices modulating its activity. To gain insight into

* To whom correspondence should be addressed. Tel: +39 0321 373744 (G.A.); +44 207 753 5913 (S.G.). Fax: +39 0321 375621 (G.A.); +44 207 753 5909 (S.G.). E-mail: appendino@pharm.unipmn.it (G.A.); simon.gibbons@pharmacy.ac.uk (S.G.).

† Università del Piemonte Orientale.

‡ Consorzio per lo Studio dei Metaboliti Secondari.

⊥ University of London.

§ Centro Ricerca Colture Industriali.

10.1021/np8002673 CCC: $40.75
Published on Web 08/06/2008

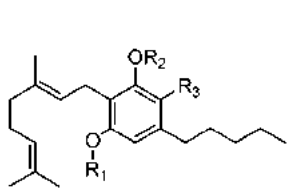

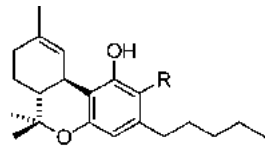

	R_1	R_2	R_3
3a	H	H	COOH
3b	H	H	H
3c	Ac	Ac	H
3d	Me	H	H
3e	Me	Me	H
3f	H	H	COOMe
3g	H	H	$COOCH_2CH_2Ph$

	R
4a	COOH
4b	H

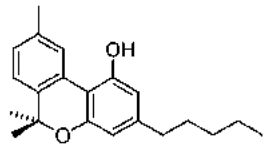

5

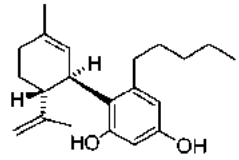

6

the microbiocidal cannabinoid pharmacophore, we have investigated how the nature of the terpenoid moiety, its relative position compared to the *n*-pentyl group, and the effect of carboxylation of the resorcinyl moiety are translated biologically, assaying the major cannabinoids and a selection of their precursors and regioisomeric analogues against drug-resistant bacteria of clinical relevance. Within these, we have selected a panel of clinically relevant *Staphylococcus aureus* strains that includes the (in)famous EMRSA-15, one of the main epidemic methicillin-resistant strains,[13] and SA-1199B, a multidrug-resistant strain that overexpresses the NorA efflux mechanism, the best characterized antibiotic efflux pump in this species.[14] SA-1199B also possesses a gyrase mutation that, in addition to NorA, confers a high level of resistance to certain fluoroquinolones. A macrolide-resistant strain (RN4220),[15] a tetracycline-resistant line overexpressing the TetK efflux pump (XU212),[16] and a standard laboratory strain (ATCC25923) completed the bacterial panel.

Δ^9-Tetrahydrocannabinol (THC, **4b**), cannabidiol (CBD, **1b**), cannabigerol (CBG, **3b**), cannabichromene (CBC, **2**), and cannabinol (CBN, **5**) are the five most common cannabinoids.[17] They could be obtained in high purity (>98%) by isolation from strains of *C. sativa* producing a single major cannabinoid (THC, CBD, CBG), by total synthesis (CBC),[6] or by semisynthesis (CBN).[18] Their antimicrobial properties are listed in Table 1. All compounds showed potent antibacterial activity, with MIC values in the 0.5−2 μg/mL range. Activity was exceptional against some of these strains, in particular the multidrug-resistant (MDR) SA-1199B, which has a high level of resistance to certain fluoroquinolones. Also noteworthy is the potent activity demonstrated against EMRSA-15 and EMRSA-16, the major epidemic methicillin-resistant *S. aureus* strains occurring in U.K. hospitals.[13,19] These activities compare highly favorably with the standard antibiotics for these strains. The potent activity against strains possessing the NorA and TetK efflux transporters suggests that cannabinoids are not substrates for the most common resistance mechanisms to current antibacterial agents, making them attractive antibacterial leads.

Given their nonpsychotropic profiles, CBD (**1b**) and CBG (**3b**) seemed especially promising, and were selected for further structure−activity studies. Thus, acetylation and methylation of their phenolic hydroxyls (compounds **1c**−**e** and **3c**−**e**, respectively) were both detrimental for activity (MIC >100 μg/mL), in accordance with the essential role of the phenolic hydroxyls in the antibacterial properties. However, in light of the potent activity of the monophenols CBC (**2**), THC (**4b**), and CBN (**5**), it was surprising that monomethylation of the diphenols CBD (**1b**) and CBG (**3b**) was so poorly tolerated in terms of antibacterial activity.

Cannabinoids are the products of thermal degradation of their corresponding carboxylic acids (pre-cannabinoids).[17] Investigation of the antibacterial profile of the carboxylated versions of CBD, CBG, and THC (compounds **1a**, **3a**, and **4a**, respectively) showed a substantial maintenance of activity. On the other hand, methylation of the carboxylic group (compounds **1f** and **3f**, respectively) caused a marked decrease of potency, as did esterification with phenethyl alcohol (compounds **1g** and **3g**, respectively). This operation is associated with a potentiation of the antibacterial properties of phenolic acids, as exemplified by phenethyl caffeate (CAPE), the major antibacterial from propolis, compared to caffeic acid.[20] Remarkably, the synthetic abnormal cannabinoids abn-CBD (**6**)[21] and abn-CBG (**7**)[22] showed antibacterial activity comparable to, although slightly less potent than, their corresponding natural products, while olivetol (**10**) showed modest activity against all six strains, with MICs of 64−128 μg/mL, and resorcinol (**11**) did not exhibit any activity even at 256 μg/mL. Thus, the pentyl chain and the monoterpene moiety greatly enhance the activity of resorcinol.

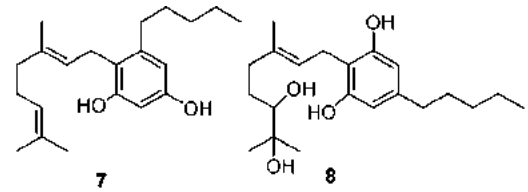

7 **8**

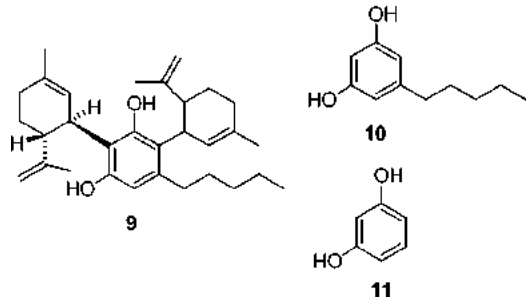

9 **10** **11**

Taken together, these observations show that the cannabinoid antibacterial chemotype is remarkably tolerant to structural modification of the terpenoid moiety and its positional relationship with the *n*-pentyl chain, suggesting that these residues serve mainly as modulators of lipid affinity, and therefore cellular bioavailability. This view was substantiated by the marked decrease of activity observed when the antibacterial activity of CBG (**3b**) was compared to that of its polar analogue carmagerol (**8**).[23] The results against the resistant strains confirm this suggestion, and it is likely that the increased hydrophilicity caused by the addition of two hydroxyls greatly reduces the cellular bioavailability by substantially reducing membrane permeability. Conversely, the addition of a further prenyl moiety, as in the bis-prenylated cannabinoid **9**,[21] while increasing membrane solubility, may result in poorer aqueous solubility and therefore a lower intracellular concentration, similarly leading to a substantial loss of activity. A single unfunctionalized terpenyl moiety seems therefore ideal in terms of lipophilicity balance for the antibacterial activity of olivetol derivatives. The great potency of cannabinoids suggests a specific interaction with a bacterial target, whose identity is, however, still elusive.

Given the availability of *C. sativa* strains producing high concentrations of nonpsychotropic cannabinoids, this plant represents an interesting source of antibacterial agents to address the problem of multidrug resistance in MRSA and other pathogenic bacteria. This issue has enormous clinical implications, since MRSA

Table 1. MIC (μg/mL) Values of Cannabinoids and Their Analogues toward Various Drug-Resistant Strains of *Staphylococcus aureus*[a,b]

compound	SA-1199B	RN-4220	XU212	ATCC25923	EMRSA-15	EMRSA-16
1a	2	2	2	2	2	2
1b	1	1	1	0.5	1	1
2	2	2	1	2	2	2
3a	4	2	4	4	2	4
3b	1	1	1	1	2	1
3f	64	[c]	64	[c]	[c]	[c]
4a	8	4	8	4	8	4
4b	2	1	1	1	2	0.5
5	1	1	1	1	1	[c]
6	1	1	1	1	1	1
7	2	1	0.5	1	2	[c]
8	32	32	16	16	16	32
10	64	64	64	128	64	64
norfloxacin	32	1	4	1	0.5	128
erythromycin	0.25	64	>128	0.25	>128	>128
tetracycline	0.25	0.25	128	0.25	0.125	0.125
oxacillin	0.25	0.25	128	0.125	32	>128

[a] Compounds **1c**−**g**, **3c**−**e**, **3g**, and **9** exhibited MIC values of >128 μg/mL for all organisms in which they were evaluated. [b] Compound **11** exhibited MIC values of >256 μg/mL for all organisms in which they were evaluated. [c] Not tested.

is spreading throughout the world and, in the United States, currently accounts for more deaths each year than AIDS.[24] Although the use of cannabinoids as systemic antibacterial agents awaits rigorous clinical trials and an assessment of the extent of their inactivation by serum,[25] their topical application to reduce skin colonization by MRSA seems promising, since MRSA resistant to mupirocin, the standard antibiotic for this indication, are being detected at a threatening rate.[26] Furthermore, since the cannabinoid anti-infective chemotype seems remarkably tolerant to modifications in the prenyl moiety, semipurified mixtures of cannabinoids could also be used as cheap and biodegradable antibacterial agents for cosmetics and toiletries, providing an alternative to the substantially much less potent synthetic preservatives, many of which are currently questioned for their suboptimal safety and environmental profile.[27]

Experimental Section

General Experimental Procedures. IR spectra were obtained on a Shimadzu DR 8001 spectrophotometer. ^{1}H NMR (300 MHz) and ^{13}C NMR (75 MHz) spectra were obtained at room temperature with a JEOL Eclipse spectrometer. The spectra were recorded in $CDCl_3$, and the solvent signals (7.26 and 77.0 ppm, respectively) were used as reference. The chemical shifts (δ) are given in ppm, and the coupling constants (J) in Hz. Silica gel 60 (70−230 mesh) and Lichroprep RP-18 (25−40 mesh) were used for gravity column chromatography. Reactions were monitored by TLC on Merck 60 F_{254} (0.25 mm) plates and were visualized by UV inspection and/or staining with 5% H_2SO_4 in ethanol and heating. Organic phases were dried with Na_2SO_4 before evaporation. All known cannabinoids were identified according to their physical and spectroscopic data.[28] Semisynthetic cannabinoids **1c**−**f**, and **3c**−**f** were prepared and identified according to their corresponding literature references.[22,29,30] Synthetic [abnormal (**6**,[21] **7**[6]) and polyprenyl (**9**)[21]] cannabinoids were synthesized and characterized according to the literature.

Plant Material. The three strains of *Cannabis sativa* used for the isolation of THC, CBD, and CBG came from greenhouse cultivation at CRA-CIN, Rovigo (Italy), where voucher specimens are kept for each of them, and were collected in September 2006. The isolation and manipulation of all cannabinoids were done in accordance with their legal status (License SP/101 of the Ministero della Salute, Rome, Italy).

Isolation of Cannabinoids (1b, 3b, 4b). The powdered plant material (100 g) was distributed in a thin layer on cardboard and heated at 120 °C for 2 h in a ventilated oven to affect decarboxylation, then extracted with acetone (ratio solvent to plant material 3:1, ×3). The residue (6.5 g for the CBD chemotype, 4.1 g for the CBG chemotype, 7.4 g for the THC chemotype) was purified by gravity column chromatography on silica gel (ratio stationary phase to extract 6:1) using a petroleum ether−ether gradient. Fractions eluted with petroleum ether−ether (9:1) afforded **1b** (628 mg, 0.63%, from the CBD chemotype) and **3b** (561 mg, 0.56%, from the CBG chemotype), precipitated from hot hexane to obtain white powders. Crude THC (3.2 g, 3.2%, from the THC chemotype) was obtained as a greenish oil, part of which (400 mg) was further purified by RP-18 flash chromatography with methanol−water (1:1) as eluant, affording **4b** as a colorless oil (315 mg).

Isolation of Pre-cannabinoids (1a, 3a, 4a). The powdered plant material (100 g) was extracted with acetone (ratio solvent to plant material 5:1, ×3). After removal of the solvent, the residue (7.7 g for the CBD chemotype, 4.9 g for the CBG chemotype, 7.9 g for the THC chemotype) was fractionated by vacuum chromatography on RP-18 silica gel (ratio stationary phase to extract 5:1) using methanol−water (75:25) as eluant. Fractions of 100 mL were taken, and those containing pre-cannabinoids were pooled, concentrated to ca. half-volume at 30 °C, saturated with NaCl, and extracted with EtOAc. After removal of the solvent, the residue was further purified by gravity column chromatography on silica gel (ratio stationary phase to crude compound 5:1) using a petroleum ether−EtOAc gradient (from 8:2 to 5:5) to afford 1.59 g (1.6%) of **1a** from the CBD chemotype, 0.93 g (0.93%) of **3a** from the CBG chemotype, and 2.1 g (2.1%) of **4a** from the THC chemotype. All pre-cannabinoids were obtained as white foams that resisted crystallization.

Synthesis of CBC (2) and CBN (5). CBG (**2**) was synthesized from olivetol,[6] and CBN was prepared from THC (**6**) by aromatization with sulfur.[18]

Mitsunobu Esterification of Pre-cannabinoids (synthesis of 3g as an example). To a cooled (ice bath) solution of **3a** (360 mg, 1.1 mmol) in dry CH_2Cl_2 (4 mL) were added sequentially phenethyl alcohol (92 μL, 0.76 mmol, 0.75 molar equiv), triphenylphosphine (TPP) (220 mg, 0.84 mmol, 0.80 molar equiv), and diisopropyldiazodicarboxylate (DIAD) (228 μL, 1.1 mmol, 1 molar equiv). At the end of the addition, the cooling bath was removed, and the reaction was stirred at room temperature. After 16 h, the reaction was worked up by evaporation, and the residue was dissolved in toluene and cooled at 4 °C overnight to remove most of the TPPO-dihydroDIAD adduct. The filtrate was evaporated and purified by gravity column chromatography on silica gel (10 g, petroleum ether as eluant) to afford 126 mg (32%) of **3g**. Under the same reaction conditions, the yield of **1g** from **1a** was 26%.

Pre-cannabigerol Phenethyl Ester (3g): colorless foam; IR ν^{KBr}_{max} 3746, 3513, 3313, 1715, 1589, 1421, 1274, 1164, 980, 804, 690 cm^{-1}; ^{1}H NMR (300 MHz, $CDCl_3$) δ 12.08 (1H, s), 7.25 (5H, m), 6.02 (1H, s), 5.98 (1H, s), 5,25 (1H, br t, J = 7.0 Hz), 5.01 (1H, br t, J = 6.5 Hz), 4.56 (2H, t, J = 6.6 Hz), 3.40 (2H, d, J = 7.3 Hz), 3.1 (2H, t, J = 6.6 Hz), 2.7 (2H, t, J = 6.6 Hz), 2.05 (4H, m), 1.79 (3H, s), 1.65 (3H, s), 1.57 (3H, s), 1.24 (6H, m), 0.88 (3H, t, J = 7.1 Hz); ^{13}C NMR (75 MHz, $CDCl_3$) δ 172.1 (s), 162.7 (s), 159.5 (s), 148.8 (s), 139.1 (s), 137.4 (d), 132.1 (s), 128.8 (d), 126.8 (d), 125.9 (d), 121.5 (d), 111.5 (s), 110.8 (s), 65.8 (t), 39.8 (t), 36.6 (t), 35.0 (t), 32.0 (t), 31.5 (t), 26.5 (t), 25.8 (q), 22.2 (t), 17.8 (q), 16.3 (q), 14.2 (q); CIMS m/z [M + H] 465 [$C_{30}H_{40}O_4$ + H].

Pre-cannabidiol Phenethyl Ester (1g): colorless oil; IR (KBr) ν_{max} 3587, 3517, 3423, 3027, 1642, 1499, 1425, 1274, 1172, 1143, 980, 894 cm^{-1}; ^{1}HNMR (300 MHz, $CDCl_3$) δ 12.13 (1H, s), 6.23 (5H, m), 6.48 (1H, s), 6.19 (1H, s), 5,55 (1H, s), 4.52 (3H, m), 4.4 (1H, s), 4.08 (1H, br s), 3.08 (2H, t, $J = 7.0$ Hz), 2.7 (2H, m), 2.11 (1H, m), 1.78 (3H, s), 1.71 (3H, s), 1.5 (4H, m), 1.28 (6H, m), 0.88 (3H, t, $J = 6.9$ Hz); ^{13}C NMR (75 MHz, $CDCl_3$) δ 172.2 (s), 171.5 (s), 163.5 (s), 160.0 (s), 148.8 (s), 147.0 (s), 145.9 (s), 140.2 (s), 137.4 (s), 128.7 (d), 126.7 (d), 124.0 (d), 114.4 (t), 112.3 (d), 105.8 (s), 65.6 (t), 46.6 (d), 39.1 (t), 37.0 (d), 31.9 (d), 31.5 (t), 27.8 (t), 25.3 (q), 22.6 (t), 21.9 (t), 18.5 (q), 14.1 (q); CIMS *m/z* [M + H] 463 [$C_{30}H_{38}O_4$ + H].

Bacterial Strains and Chemicals. A standard *S. aureus* strain (ATCC 25923) and a clinical isolate (XU212), which possesses the TetK efflux pump and is also a MRSA strain, were obtained from E. Udo.[16] Strain RN4220, which has the MsrA macrolide efflux pump, was provided by J. Cove.[30] EMRSA-15[13] and EMRSA-16[19] were obtained from Paul Stapleton. Strain SA-1199B, which overexpresses the NorA MDR efflux pump, was the gift of Professor Glenn Kaatz.[14] Tetracycline, norfloxacin, erythromycin, and oxacillin were obtained from Sigma Chemical Co. Oxacillin was used in place of methicillin as recommended by the NCCLS. Mueller-Hinton broth (MHB; Oxoid) was adjusted to contain 20 mg/L Ca^{2+} and 10 mg/L Mg^{2+}.

Antibacterial Assays. Overnight cultures of each strain were made up in 0.9% saline to an inoculum density of 5×10^5 cfu by comparison with a MacFarland standard. Tetracycline and oxacillin were dissolved directly in MHB, whereas norfloxacin and erythromycin were dissolved in DMSO and then diluted in MHB to give a starting concentration of 512 μg/mL. Using Nunc 96-well microtiter plates, 125 μL of MHB was dispensed into wells 1−11. Then, 125 μL of the test compound or the appropriate antibiotic was dispensed into well 1 and serially diluted across the plate, leaving well 11 empty for the growth control. The final volume was dispensed into well 12, which being free of MHB or inoculum served as the sterile control. Finally, the bacterial inoculum (125 μL) was added to wells 1−11, and the plate was incubated at 37 °C for 18 h. A DMSO control (3.125%) was also included. All MICs were determined in duplicate. The MIC was determined as the lowest concentration at which no growth was observed. A methanolic solution (5 mg/mL) of 3-[4,5-dimethylthiazol-2-yl]-2,5-diphenyltetrazoliium bromide (MTT; Lancaster) was used to detect bacterial growth by a color change from yellow to blue.

References and Notes

(1) Caiffa, W. T.; Vlahov, D.; Graham, N. M. H.; Astemborski, J.; Solomon, L.; Nelson, K. E.; Munoz, A. *Am. J. Resp. Crit. Care Med.* **1994**, *150*, 1593–1598.
(2) Roth, M. D.; Whittaker, K.; Salehi, K.; Tashkin, D. P.; Baldwin, G. C. *J. Neuroimmunol.* **2004**, *147*, 82–86.
(3) (a) Krjci, Z. *Lekarske Listy* **1952**, *7*, 500–503; *Chem. Abstr.* **1952**, *48*, 78326. (b) Ferenczy, L.; Gracza, L.; Jakobey, I. *Naturwissenschaften* **1958**, *45*, 188. (c) Krejci, Z. *Pharmazie* **1958**, *13*, 155–156. (d) Rabinovich, A. S.; Aizenman, B. L.; Zelepukha, S. I. *Mikrobiol. Zh* **1959**, *21*, 40–48. (PubMed ID 14435632). (e) Turner, C. E.; Elsohly, M. A.; Boeren, E. G. *J. Nat. Prod.* **1980**, *43*, 169–243.
(4) Schultz, O. E.; Haffner, G. A. *Z. Naturforsch.* **1959**, *14b*, 98–100.
(5) Turner, C. E.; Elsohly, M. A. *J. Clin. Pharmacol.* **1981**, *21*, 283S–291S.
(6) Elsohly, H. N.; Turner, C. E.; Clark, A. M.; Elsohly, M. A. *J. Pharm. Sci.* **1982**, *71*, 1319–1323.
(7) Van Klingeren, B.; Ten Ham, M. *Lab. Chemother. Natl. Inst. Public Health* **1976**, *42*, 9–12; *Chem. Abstr.* **1976**, *85*, 14622.
(8) Molnar, J.; Csiszar, K.; Nishioka, I.; Shoyama, Y. *Acta Microb. Hung.* **1986**, *33*, 221–231.
(9) Barrett, C. T.; Barrett, J. F. *Curr. Opin. Biotechnol.* **2003**, *14*, 621–626.
(10) Gibbons, S. *Nat. Prod. Rep.* **2004**, *21*, 263–277.
(11) Stavri, M.; Piddock, L. J. V.; Gibbons, S. *J. Antimicrob. Chemother.* **2007**, *59*, 1247–1260.
(12) Smith, E. C. J.; Kaatz, G. W.; Seo, S. M.; Wareham, N.; Williamson, E. M.; Gibbons, S. *Antimicrob. Agents Chemother.* **2007**, *51*, 4480–4483.
(13) Richardson, J. F.; Reith, S. J. *Hosp. Infect.* **1993**, *25*, 45–52.
(14) Kaatz, G. W.; Seo, S. M.; Ruble, C. A. *Antimicrob. Agents Chemother.* **1993**, *37*, 1086–1094.
(15) Ross, J. I.; Farrell, A. M.; Eady, E. A.; Cove, J. H.; Cunliffe, W. J. *J. Antimicrob. Chemother.* **1989**, *24*, 851–862.
(16) Gibbons, S.; Udo, E. E. *Phytother. Res.* **2000**, *14*, 139–140.
(17) (a) Mechoulam, R.; McCallum, N. K.; Burstein, S. *Chem. Rev.* **1976**, *76*, 75–112. (b) Elsohly, M. A.; Slade, D. *Life Sci.* **2005**, *78*, 539–548.
(18) (a) Ghosh, R.; Todd, A. R.; Wilkinson, S. *J. Chem. Soc.* **1940**, 1393–1396. (b) Bastola, K. P.; Hazekamp, A.; Verpoorte, R. *Planta Med.* **2007**, *73*, 273–275.
(19) Cox, R. A.; Conquest, C.; Mallaghan, C.; Maples, R. R. *J. Hosp. Infect.* **1995**, *29*, 87–106.
(20) Castaldo, S.; Capasso, F. *Fitoterapia* **2002**, *73*, S1−S6.
(21) Razdan, R. K.; Dalzell, H. C.; Handrick, G. R. *J. Am. Chem. Soc.* **1974**, *96*, 5860–5865.
(22) Baek, S. H.; Srebnik, M.; Mechoulam, R. *Tetrahedron Lett.* **1985**, *26*, 1083–1086.
(23) Appendino, G. Unpublished results.
(24) Bancroft, E. A. *J. Am. Med. Assoc.* **2007**, *298*, 1803.
(25) Mechoulam, R.; Gaoni, Y. *Tetrahedron* **1965**, *21*, 1223–1229.
(26) Simor, A. E.; Stuart, T. L.; Louie, L.; Watt, C.; Ofner-Agostini, M.; Gravel, D.; Mulvey, M.; Loeb, M.; McGeer, A.; Bryce, E.; Matlow, A. *Antimicrob. Agents Chemother.* **2007**, *51*, 3880–3886.
(27) McGrath, K. G. *Eur. J. Cancer Prev.* **2003**, *12*, 479–485.
(28) Hazekamp, A.; Peltenburg, A.; Verpoorte, R.; Giroud, C. *J. Liq. Chromatogr. Rel. Technol.* **2005**, *28*, 2361–2382.
(29) Vailancourt, V.; Albizati, K. F. *J. Org. Chem.* **1992**, *57*, 3627–3631.
(30) Mechoulam, R.; Gaoni, Y. *Tetrahedron* **1965**, *21*, 1223–1229.

NP8002673

PHYTOTHERAPY RESEARCH
Phytother. Res. **23**, 99–103 (2009)
Published online 11 August 2008 in Wiley InterScience
(www.interscience.wiley.com) **DOI**: 10.1002/ptr.2568

Antibacterial Iridoid Glucosides from *Eremostachys laciniata*

Masoud Modaressi[1], Abbas Delazar[1], Hossein Nazemiyeh[1], Fatemeh Fathi-Azad[1], Eileen Smith[2], M. Mukhlesur Rahman[2], Simon Gibbons[2], Lutfun Nahar[3] and Satyajit D. Sarker[3]*

[1]School of Pharmacy, Drug Applied Research Center, Tabriz University of Medical Sciences, Tabriz, Iran
[2]Centre for Pharmacognosy and Phytochemistry, The School of Pharmacy, University of London, 29–39 Brunswick Square, London WC1N 1AX, UK
[3]School of Biomedical Sciences, University of Ulster, Cromore Road, Coleraine BT52 1SA, Co. Londonderry, Northern Ireland, UK

***Eremostachys laciniata* (L) Bunge (family: Lamiaceae alt. Labiatae; subfamily: Lamioideae) is one of the 15 endemic Iranian herbs of the genus *Eremostachys*. A decoction of the roots and flowers of *E. laciniata* has traditionally been taken orally for the treatment of allergies, headache and liver diseases. Three antibacterial iridoid glucosides, phloyoside I (1), phlomiol (2) and pulchelloside I (3) have been isolated from the rhizomes of this plant. The structures of these compounds were elucidated unequivocally by a series of 1D and 2D NMR analyses. The antibacterial activity and brine shrimp toxicity of these compounds were assessed using the resazurin microtitre assay and the brine shrimp lethality assay, respectively. All three iridoid glycosides 1–3 exhibited from low to moderate levels (MIC = 0.05–0.50 mg/mL) of antibacterial activity. Of these compounds, compound 3 was the most active, and displayed antibacterial activity against 9 of 12 different strains tested. The most noteworthy activity of 3 was against *Bacillus cereus*, penicillin-resistant *Escherichia coli*, *Proteus mirabilis* and *Staphylococcus aureus* with an MIC value of 0.05 mg/mL. Copyright © 2008 John Wiley & Sons, Ltd.**

Keywords: Eremostachys laciniata; Lamiaceae; iridoid; phloyoside I; pulchelloside I; phlomiol; antibacterial; chemotaxonomy.

INTRODUCTION

Eremostachys laciniata (L) Bunge (family: Lamiaceae alt. Labiatae; subfamily: Lamioideae), a perennial herb with a thick root and pale purple or white flowers, is one of the 15 endemic Iranian species of the genus *Eremostachys*, and is also grown in other countries of the Middle-East Asia, Western Asia and Caucasus (GRIN Database, 2008; Mozaffrian, 1996). A decoction of the roots and flowers of *E. laciniata* has traditionally been taken orally for the treatment of allergies, headache and liver diseases (Said *et al.*, 2002). A previous phytochemical study on *E. laciniata* revealed the presence of various mono- and sesquiterpenes in its essential oils (Navaei and Mirza, 2006). The crude extract of this plant was reported to possess a free-radical-scavenging property (Erdemoglu *et al.*, 2006). As part of our on-going studies on the plants of the Iranian flora (Nazemiyeh *et al.*, 2008, 2007; Delazar *et al.*, 2007a, 2007b, 2006a, 2006b, 2006c, 2006d, 2005, 2004a, 2004b), we now report on the isolation, structure elucidation and bioactivity of three iridoid glucosides, phloyoside I (**1**), phlomiol (**2**) and pulchelloside (**3**) from the rhizomes of *E. laciniata*.

* Correspondence to: S. D. Sarkar, School of Biomedical Sciences, University of Ulster, Cromore Road, Coleraine BT52 1SA, Co. Londonderry, Northern Ireland, UK.
E-mail: S.Sarker@ulster.ac.uk

MATERIALS AND METHODS

General experimental procedures. UV spectra were obtained in methanol using a Hewlett-Packard 8453 UV/vi spectrophotometer in MeOH. NMR spectra were recorded in CD_3OD on a Bruker DRX 500 MHz NMR spectrometer (500 MHz for ^1H and 125 MHz for ^{13}C) using the residual solvent peaks as an internal standard. MS analyses were performed on a Finnigan MAT95 spectrometer. HMBC spectra were optimized for a long range $J_{H\text{-}C}$ of 9 Hz and a NOESY experiment was carried out with a mixing time of 0.8 s.

Plant material. The rhizomes of *Eremostachys laciniata* (L) Bunge were collected during September–October 2005 from Ajabshir county in East Azarbaijan province in Iran (37° 36′ 46.7″ N latitude, 46° 11′ 15.6″ E longitude and altitude 1900 m above sea level). A voucher specimen (TUM-ADE 0204) has been retained in the herbarium of the Faculty of Pharmacy, Tabriz University of Medical Science, and in the herbarium of the Plant and Soil Science Department, University of Aberdeen, Scotland (ABD).

Extraction and isolation of compounds. The dried and ground rhizomes of *E. laciniata* (100 g) were Soxhlet-extracted, successively, with *n*-hexane, dichloromethane and methanol (1.1 L each). The MeOH extract (2 g) was subjected to Sep-Pack fractionation using a step gradient of MeOH–water mixture (10:90, 20:80, 40:60, 60:40, 80:20 and 100:0). The preparative reversed-phase HPLC analysis (Shim-Pak ODS column 10 μm,

Received 12 February 2008
Revised 18 March 2008
Accepted 20 March 2008

Table 1. ^{1}H NMR (500 MHz, coupling constant *J* in Hz in parentheses) and ^{13}C NMR (125 MHz in parentheses) data of iridoid glucosides 1–3

	Chemical shift (δ_H) in ppm			Chemical shift (δ_C) in ppm		
Position	**1**	**2**	**3**	**1**	**2**	**3**
1	5.83 s	5.83 s	5.67 d (2.0)	93.1	93.9	95.0
3	7.49 s	7.45 s	7.45 s	153.7	154.2	153.6
4	–	–	–	115.0	114.4	114.9
5	–	–	–	64.9	70.1	68.6
6	3.55 d (9.0)	4.18 d (4.5)	3.67*	79.7	77.2	82.9
7	3.82 d (9.0)	3.66 d (4.5)	3.43 dd (7.0, 10.0)	83.7	80.5	83.3
8	–	–	1.35 m	74.9	78.5	37.8
9	2.47 s	2.51 s	1.96 dd (2.0, 12.0)	57.6	56.9	53.9
10	1.02 s	1.39 s	1.37 d (6.5)	17.2	22.3	16.1
11	–	–	–	168.4	168.8	168.5
11-OMe	3.74 s	3.73 s	3.73 s	52.0	51.7	51.8
1′	4.59 d (8.0)	4.60 d (8.0)	4.58 d (8.0)	99.7	99.5	100.0
2′	3.19 dd (8.0, 9.0)	3.20 bt (8.0)	3.19 bt (8.0)	74.4	74.4	74.4
3′	3.38 bt (9.0)	3.38*	3.38*	77.4	77.5	77.4
4′	3.28*	3.28*	3.28*	71.7	71.6	71.6
5′	3.32*	3.29*	3.29*	78.4	78.4	78.5
6′	3.90 dd (2.0, 11.5)	3.90 bd (12.0)	3.90 dd (2.0, 11.5)	62.9	62.6	62.7
	3.66 dd (6.0, 11.5)	3.67*	3.68*			

Spectra obtained in CD_3OD.
All assignments were confirmed by ^{13}C DEPT135, COSY, NOESY, HMBC and HSQC experiments.

250 mm × 21.2 mm; mobile phase: 0–70 min gradient 4%–9% ACN in water; flow-rate: 20 mL/min, detection at 248 nm) of the 10% methanol Sep-Pack fraction afforded three iridoid glucosides, phloyoside I (**1**, 13.2 mg, t_R = 12.3 min) (Kasai *et al.*, 1994), phlomiol (**2**, 6.7 mg, t_R = 13.6 min) (Zhang *et al.*, 1991) and pulchelloside I (**3**, 6.7 mg, t_R = 16.6 min) (Milz and Rimpler, 1978; El-Hela *et al.*, 2000). All compounds **1–3** were identified unequivocally by a series of 1D and 2D NMR experiments, notably, ^{1}H, ^{13}C, ^{13}C DEPT, ^{1}H-^{1}H COSY, ^{1}H-^{1}H NOESY, ^{1}H-^{13}C HMQC and ^{1}H-^{13}C HMBC (Table 1; Fig. 1) and HR-ESIMS analysis. The spectroscopic data of the known compounds were also compared with the respective published data.

*Phloyoside I (**1**).* White amorphous solid; 13.2 mg; UV λ_{max} (MeOH): 230 nm; HR-FABMS *m/z* 439.1451, $C_{17}H_{27}O_{13}$ requires 439.1452; ^{1}H NMR and ^{13}C NMR (Table 1).

*Phlomiol (**2**).* White amorphous solid; 6.7 mg; UV λ_{max} (MeOH): 230 nm; HR-FABMS *m/z* 439.1451, $C_{17}H_{27}O_{13}$ requires 439.1452; ^{1}H NMR and ^{13}C NMR (Table 1).

*Pulchelloside I (**3**).* White amorphous solid; 6.7 mg; UV λ_{max} (MeOH): 230 nm; HR-FABMS *m/z* 423.1503, $C_{17}H_{27}O_{12}$ requires 423.1502; ^{1}H NMR and ^{13}C NMR (Table 1).

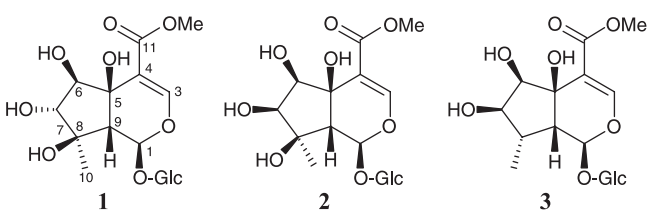

Figure 1. Structures of iridoid glycosides isolated from the rhizomes of *Eremostachys laciniata.*

Antibacterial activity. Antibacterial activity of **1–3** was assessed against 12 strains of Gram-positive and Gram-negative bacteria including *Bacillus cereus* (NCTC 9689), *Citrobacter freundii* (NCTC 9750), *Escherichia coli* (NCIMB 8110), *Escherichia coli* (NCIMB 4174), *Klebsiella aerogenes* (NCTC 9528), *Lactobacillus plantarum* (NCIMB 6376), *Micrococcus luteus* (NCIMB 9278), *Proteus mirabilis* (NCIMB 60), *Pseudomonas aeruginosa* (NCTC 6750), *Staphylococcus aureus* (NCTC 10788), *Staphylococcus aureus* (MRSA) (NCTC 11940), *Staphylococcus epidermidis* (NCIMB 8558) using the 96-well microtitre-plate-based serial dilution method, incorporating resazurin as an indicator of cell growth (Sarker *et al.*, 2007). Isosensitized nutrient broth was obtained from Oxoid, Basingstoke, Hampshire, England. Microtitre plates were from Serowel, Bibby sterilin, Stone, Staffs, UK. Eppendorf pipettes were purchased from Netheter-hinz-Gmbh, 22 331, Hamburg, Germany. Bacterial suspension (20 µL) in double strength nutrient broth at a concentration of 5×10^5 colony forming units (CFU)/mL was used. Test compounds (**1–3**) were dissolved in 10% aqueous DMSO to obtain a stock concentration of 1 mg/mL. Ciprofloxacin, a well-known broad-spectrum antibiotic, was used as a positive control. The minimum inhibitory concentration (MIC) was determined for each compound and compared with that of ciprofloxacin.

Brine shrimp lethality assay. Shrimp eggs were purchased from The Pet Shop, Kittybrewster Shopping Complex, Aberdeen, UK. The bioassay was conducted following the procedure described by Meyer *et al.* (1982). The eggs were hatched in a conical flask containing 300 mL artificial seawater. The flasks were well aerated with the aid of an air pump, and kept in a water bath at 29–30 °C. A bright light source was left on and the nauplii hatched within 48 h. The extracts were dissolved in 2% aq. DMSO to obtain a concentration of 1 mg/mL. These were serially diluted to obtain seven different

DOI: 10.1002/ptr

concentrations. A solution of each concentration (1 mL) was transferred into clean sterile universal vials with a pipette, and aerated sea-water (9 mL) was added. About 10 nauplii were transferred into each vial with a pipette. A check count was performed and the number alive after 24 h was noted. LD_{50} values were determined using the Probit analysis method (Finney, 1971). Podophylotoxin, a well known cytotoxic lignan, was used as a positive control.

RESULTS AND DISCUSSION

Reversed-phase preparative HPLC analysis of the methanol extract of the rhizomes of *E. laciniata* afforded three iridoid glucosides, which were identified unequivocally as phloyoside I (**1**), phlomiol (**2**) and pulchelloside I (**3**) on the basis of extensive 1D and 2D NMR data analyses.

All three compounds (**1–3**) showed spectroscopic characteristics, especially, UV and NMR signals (Table 1), assignable to iridoid glucoside skeletons with a carbomethoxy group at C-4, and a methyl at C-8 (Boros and Stermitz, 1991). The HR-FABMS spectra of **1–3**, *pseudo*-molecular ions $[M+1]^+$, respectively, at *m/z* 439.1451, 439.1451 and 423.1502, corresponding to the molecular formula, $C_{17}H_{26}O_{13}$, $C_{17}H_{26}O_{13}$ and $C_{17}H_{26}O_{12}$, respectively. In the ^1H and ^{13}C NMR spectra of **1** (Table 1), in addition to the signals associated with a β-D-glucosyl and carbomethoxy moieties, there were signals corresponding to C-8 methyl (δ_H 1.02 and δ_C 17.2), olefinic methine (δ_H 7.49 and δ_C 153.7, C-3), three oxymethines at C-1 (δ_H 5.83 and δ_C 93.1), C-6 (δ_H 3.55 and δ_C 79.7) and C-7 (δ_H 3,82 and δ_C 83.7), a methine at C-9 (δ_H 2.47 and δ_C 57.6) and two oxygenated quarternary carbons at C-5 (δ_C 64.9) and C-8 (δ_C 74.9). While a ^1H-^1H COSY45 displayed all ^1H-^1H scalar couplings within the molecule, an HMBC together with an HSQC confirmed the ^1H-^{13}C connectivities, and thus the structure of the molecule. The relative stereochemistry at the chiral centres in **1**, was established from the nOe interactions observed in the ^1H-^1H NOESY spectrum, especially, the strong nOe interactions between H-9 and H-7 established that both these protons were on the same face of the molecule. Thus, the identity of **1** was confirmed as phloyoside I, and the NMR data of **1** were comparable to the published data (Kasai *et al.*, 1994).

The ^1H and ^{13}C NMR data of **2** (Table 1) were similar to those of **1**, with a few minor differences which originated from the differences in relative stereochemistry at the chiral centres of both molecules. Using the nOe interactions observed in the ^1H-^1H NOESY spectrum, the identity of **2** was confirmed as phlomiol. The NMR data of **2** were comparable to the published data (Zhang *et al.*, 1991).

In the ^1H NMR spectrum of **3** (Table 1), all signals were similar to those observed in the case of compounds **1** and **2**, with the exceptions that the C-8 methyl signal (δ 1.37) appeared as a doublet, and an additional methine signal at δ 1.35 as a multiplet was observed. In the ^{13}C NMR spectrum (Table 1), the C-8 oxygenated quarternary signal was absent, and a methine signal (δ 37.8) was present instead. Finally, with the help of a ^1H-^1H COSY 45, ^1H-^{13}C HSQC, ^1H-^{13}C HMBC and ^1H-^1H NOESY, the identity of compound **3** was confirmed as puchelloside I. The NMR data of **3** were comparable to the published data (Milz and Rimpler, 1978; El-Hela *et al.*, 2000).

To our knowledge, this is first report on the occurrence of iridoid glucosides **1–3** in the rhizomes of *Eremostachys laciniata*. However, Calis *et al.* (2007b), recently reported in a conference abstract, the presence of compounds **1** and **2** in the aerial parts of *E. laciniata* growing in Turkey. Iridoid glycosides are of common occurrence in the genus *Phlomis* (Delazar *et al.*, 2004a; ISI Database, 2008; Combined Chemical Dictionary, 2008). Most recently, iridoid glycosides have also been reported from the genus *Eremostachys* (Delazar *et al.*, 2004a, Calis *et al.*, 2007a, 2007b), which is taxonomically close to *Phlomis*. Within the genus *Phlomis*, phloyoside I (**1**) was isolated previously from *P. rotata* and *P. younghusbandii*, and phlomiol (**2**) from *P. tuberosa*, *P. longifolia* and *P. younghusbandii* (ISI Database, 2008). However, pulchelloside I (**3**) was not previously reported either from the *Phlomis* or the *Eremmostachys*. Both the genera, *Eremostachys* and *Phlomis*, belong to the subtribe Lamieae of the family Lamiaceae (Azizian and Cutler, 1988; Delazar *et al.*, 2004a), and they are morphologically similar. Anatomical and cytological studies on the species of these genera also established this close affinity between these two genera. During the preliminary chemotaxonomic studies on the family Lamiaceae using flavonoids as the markers, some degrees of similarities between these genera were also identified (Delazar *et al.*, 2004a). Iridoids have been considered as valuable chemotaxonomic markers (Frederiksen *et al.*, 1999), and in fact, they have been employed successfully to describe chemotaxonomic relationships among the taxa within various families, e.g. Acanthaceae, Bigoniaceae, Cornaceae, Oleaceae and Rubiaceae (Delazar *et al.*, 2004a; ISI Database, 2008). Within the family Lamiaceae, iridoid glycosides have recently been employed as chemotaxonomic markers for the species of the genus *Lamium* (Alipieva *et al.*, 2003). Therefore, the co-occurrence of iridoid glycosides, especially **1** and **2**, in the closely related genera *Eremostachys* and *Phlomis* could be significant chemotaxonomically.

All three iridoid glycosides **1–3** exhibited (Table 2) from low to moderate levels (MIC = 0.05–0.50 mg/mL) of antibacterial activity. Among these compounds, compound **3** was the most active, and displayed antibacterial activity against 9 of 12 different strains tested. The most noteworthy activity of **3** was against *Bacillus cereus*, penicillin-resistant *Escherichia coli*, *Proteus mirabilis* and *Staphylococcus aureus* with an MIC value of 0.05 mg/mL. None of the compounds (**1–3**) exhibited any inhibitory activities against *Klebsiella aerogenes*, *Lactobacillus plantarum* and methicillin-resistant *Staphylococcus aureus*. The antibacterial activity profiles of compounds **1** and **2**, possibly owing to their structural similarities, were quite similar. The growth of *Escherichia coli*, penicillin resistant *Escherichia coli*, *Micrococcus luteus* and *Staphylococcus epidermidis* was inhibited only by compound **3**. All compounds were active against *Bacillus cereus*, *Citrobacter freundii*, *Proteus mirabilis*, *Pseudomonas aeruginosa* and *Staphylococcus aureus.*

The brine shrimp lethality assay (BSL) has been used routinely in the primary screening of the crude extracts as well as the isolated compounds to assess the toxicity towards brine shrimps, which could also provide an

DOI: 10.1002/ptr

Table 2. Antibacterial properties of iridoid glucosides 1–3

Bacterial strain	MIC in mg/mL			
	1	**2**	**3**	Ciprofloxacin
Bacillus cereus	0.50	0.50	0.05	2.5×10^{-8}
Citrobacter freundii	0.50	0.50	0.50	2.5×10^{-7}
Escherichia coli	–	–	0.25	2.5×10^{-7}
Escherichia coli (penicillin resistant)	–	–	0.05	2.5×10^{-6}
Klebsiella aerogenes	–	–	–	2.5×10^{-6}
Lactobacillus plantarum	–	–	–	2.5×10^{-7}
Micrococcus luteus	–	–	0.50	2.5×10^{-7}
Proteus mirabilis	0.50	0.10	0.05	2.5×10^{-8}
Pseudomonas aeruginosa	0.50	0.50	0.10	2.5×10^{-8}
Staphylococcus aureus	0.25	0.10	0.05	2.5×10^{-8}
Staphylococcus aureus (MRSA)	–	–	–	2.5×10^{-8}
Staphylococcus epidermidis	–	–	0.10	2.5×10^{-7}

indication of possible cytotoxic properties of the test materials (Meyer *et al.*, 1982). It has been established that the cytotoxic compounds usually show good activity in the BSL assay, and this assay can be recommended as a guide for the detection of antitumour and pesticidal compounds because of its simplicity and cost-effectiveness. In the BSL assay, none of these iridoid glycosides (**1–3**) showed any significant level of toxicity, and the LD_{50} values were >1.0 mg/mL, compared with 2.80 μg/mL of the positive control, podophyllotoxin.

Acknowledgement

We thank the EPSRC National Mass Spectrometry Service Centre (Department of Chemistry, University of Wales Swansea, Swansea, Wales, UK) for MS analyses. NMR studies were performed in the School of Pharmacy, University of London, UK.

REFERENCES

Alipieva KI, Taskova RM, Evstatieva LN, Handjieva NV, Popov SS. 2003. Benzoxazinoids and iridoid glucosides from four *Lamium* species. *Phytochemistry* **64**: 1413–1417.

Azizian D, Cutler DF. 1988. Anatomical, cytological and phytochemical studies on *Phlomis* L and *Eremostachys* Bunge (Labiatae). *Bot J Linn Soc* **85**: 249–281.

Boros CA, Stermitz FR. 1991. Iridoids. An updated review. Part II. *J Nat Prod* **54**: 1173–1246.

Calis I, Guvenc A, Armagan M, Koyuncu M, Gotfredsen CH, Jensen SR. 2007a. Iridoid glucosides from *Eremostachys moluccelloides* Bunge. *Helv Chim Acta* **90**: 1461–1466.

Calis I, Guvenc A, Armagan M, Koyuncu M, Gotfredsen CH, Jensen SR. 2007b. Secondary metabolites from *Eremostachys laciniata* (meeting abstract). *Planta Med* **73**: 942–942.

Combined Chemical Dictionary. 2008. Chapman & Hall/CRC Press LLC. URL: http://www.chemnetbase.com/

Delazar A, Biglari F, Nazemiyeh H *et al.* 2006a. GC-MS analysis of the essential oils, and the isolation of phenylpropanoid derivatives from the aerial parts of *Pimpinella aurea*. *Phytochemistry* **67**: 2176–2181.

Delazar A, Byres M, Gibbons S *et al.* 2004a. Iridoid glycosides from *Eremostachys glabra*. *J Nat Prod* **67**: 1584–1587.

Delazar A, Celik S, Gokturk RS, Unal O, Nahar L, Sarker SD. 2005. Two acylated flavonoids from *Stachys bombycina* and their free radical scavenging activity. *Die Pharmazie* **60**: 878–880.

Delazar A, Gibbons S, Kosari AR *et al.* 2006b. Flavonoid C-glycosides and cucurbitacin glycosides from *Citrullus colocynthis*. *DARU* **14**: 109–114.

Delazar A, Modarresi M, Shoeb M *et al.* 2006c. Eremostachiin: A new furanolabdane diterpene glycoside from *Eromostachys glabra*. *Nat Prod Res* **20**: 167–172.

Delazar A, Naseri M, Nahar L *et al.* 2007a. GC-MS analysis and antioxidant activities of essential oils of two cultivated *Artemisia* species. *Chem Nat Comp* **43**: 112–114.

Delazar A, Naseri M, Nazemiyeh H *et al.* 2007b. Flavonol 3-methyl ether glucosides and a tryptophylglycine dipeptide from *Artemisia fragrans* (Asteraceae). *Biochem Syst Ecol* **35**: 52–56.

Delazar A, Reid RG, Sarker SD. 2004b. GC-MS analysis of essential oil of the oleoresin from *Pistacia atlantica* var *mutica*. *Chem Nat Comp* **40**: 24–27.

Delazar A, Talischi B, Nazemiyeh Z, Rezazadeh H, Nahar L, Sarker SD. 2006d. Chrozophorin: a new acylated flavone glucoside from *Chrozophora tinctoria*. *Rev Bras Farmacogn (Braz J Pharmacogn)* **16**: 286–290.

El-Hela AA, Sowinski P, Krauze-Baranowska M. 2000. Iridoids and phenylethanoids of *Verbena bipinnatifida* Nutt. *Acta Pol Pharm* **57**: 65–68.

Erdemoglu N, Turan NN, Cakoco I, Sener B, Aydon A. 2006. Antioxidant activities of some Lamiaceae plant extracts. *Phytother Res* **20**: 9–13.

Finney DJ. 1971. *Probit Analysis*, 3rd edn. Cambridge University Press: Cambridge.

Frederiksen LB, Damtoft S, Jensen SR. 1999. Biosynthesis of iridoids lacking C-10 and the chemotaxonomic implications of their distribution. *Phytochemistry* **52**: 1409–1420.

GRIN Database. 2008. USDA, ARS, National Genetic Resources Program, Germplasm Resources Information Network – (GRIN) [Online Database], National Germplasm Resources Laboratory, Beltsville, Maryland. Available on-line at: http://www.ars-grin.gov/cgi-bin/npgs/html/taxon.pl?15378

ISI database. 2008. ISI Web of Knowledge, Thomson ISI, London. Available on-line at, http://wok.mimas.ac.uk/

Kasai R, Katagiri M, Ohtani K, Yamasaki K, Yang C-R, Tanak O. 1994. Iridoid glycosides from *Phlomis younghusbandii* roots. *Phytochemistry* **36**: 967–970.

Meyer BN, Ferrigni NR, Putnam JE, Jacobson JB, Nicholas DE, McLaughlin JL. 1982. Brine shrimp: a convenient bioassay for active plant constituents. *Planta Med* **45**: 31–34.

Milz S, Rimpler H. 1978. Pulchelloside-1, new iridoid from *Verbena pulchella* Sweet. *Tetrahedron Lett* **10**: 895–898.

Mozaffarian V. 1996. *A Dictionary of Iranian Plant Names*. Farhang Moaser: Tehran, 765.

Navaei MN, Mirza M. 2006. Chemical composition of the oil of *Eremostachys laciniata* (L.) Bunge from Iran. *Flav Fragr J* **21**: 645–646.

Nazemiyeh H, Delazar A, Ghahramani M-A, Talebpour A-H, Nahar L, Sarker SD. 2008. Phenolic glycosides from *Phlomis lanceolata* (Lamiaceae). *Nat Prod Commun* **3**: 53–56.

Nazemiyeh H, Maleki N, Mehmani F *et al.* 2007. Assessment of anti-inflammatory properties ethyl acetate extract of *Stachys schtschegleevii* Sosn. *DARU* **4**: 174–182.

Said O, Khalil K, Fulder S, Azaizeh H. 2002. Ethnopharmacological survey of medicinal herbs in Israel, the Golan Heights and the West Bank region. *J. Ethnopharmacol* **83**: 251–265.

Sarker SD, Nahar L, Kumarasamy Y. 2007. Microtitre plate-based antibacterial assay incorporating resazurin as an indicator of cell growth, and its application in the *in vitro* antibacterial screening of phytochemicals. *Methods* **42**: 321–324.

Zhang C-Z, Li C, Feng S-l, Shi J-G. 1991. Iridoid glucosides from *Phlomis rotata*. *Phytochemistry* **30**: 4156–4158.

Brominated Diterpenes with Antibacterial Activity from the Red Alga *Sphaerococcus coronopifolius*

Vangelis Smyrniotopoulos,[†] Constantinos Vagias,*[,†] M. Mukhlesur Rahman,[‡] Simon Gibbons,[‡] and Vassilios Roussis[†]

Department of Pharmacognosy and Chemistry of Natural Products, School of Pharmacy, University of Athens, Panepistimiopolis Zografou, Athens 15771, Greece, and Centre for Pharmacognosy and Phytotherapy, The School of Pharmacy, University of London, 29-39 Brunswick Square, London WC1N 1AX, U.K.

Received March 22, 2008

Four new brominated diterpenes (**1**, **2**, **4**, **5**), along with two previously reported metabolites (**3**, **6**), were isolated from the organic extract of *Sphaerococcus coronopifolius*, collected in Palaiokastritsa Bay at the west coast of Corfu Island. The structures of the new products, as well as their relative configuration, were established by means of spectroscopic data analyses, including 2D NMR experiments. The isolated metabolites were evaluated for their antibacterial activity against a panel of multidrug-resistant (MDR) and methicillin-resistant *Staphylococcus aureus* (MRSA) with MICs in the range 0.5−128 μg/mL.

Diterpenes are widespread metabolites in marine brown algae, but are much less common in Rhodophyta,[1] having been found mainly in species of the genus *Laurencia*[2] and in the unrelated species *Sphaerococcus coronopifolius*. Particularly, the latter yields an extended variety of interesting diterpenes having di-, tri-, or tetracyclic skeletons, often rearranged, most of which contain one or more bromine atoms.[3] These halogenated metabolites have been suggested to function as chemical defense against marine herbivores.[4–6] Moreover some of these halogenated metabolites have been proven to possess antimalarial,[3] insecticidal,[7] antibacterial,[8] antifungal,[9] and antiviral activities.[10]

In the course of our ongoing investigations toward the isolation of bioactive metabolites from marine organisms of the Greek seas,[11–13] we recently studied the chemical composition of the red alga *S. coronopifolius*, collected from the west coast of Corfu Island. In this paper we describe the isolation and structure elucidation of four new metabolites (**1**, **2**, **4**, and **5**), along with the already described metabolites **3**[14] and **6** (1*S*-hydroxy-1,2-dihydrobromosphaerol),[15] all of which were obtained from the organic extract of *S. coronopifolius*. The structures of the new metabolites were elucidated by extensive spectroscopic analyses and their relative configuration was determined by NOESY experiments. Moreover, detailed analyses of the 1D and 2D NMR spectra allowed the revision of the structure for metabolite **3** and the full assignment of the ^{13}C and ^{1}H data, which have not been reported before for **6**.

All compounds were evaluated for antibacterial activity against a panel of multidrug-resistant (MDR) and methicillin-resistant *Staphylococcus aureus* (MRSA) using a microtiter plate based minimum inhibitory concentration (MIC) assay. The metabolites, specifically **4** and **6**, were found to possess highly significant activity in comparison to the standard antibiotic norfloxacin.

Results and Discussion

S. coronopifolius was collected in Palaiokastritsa Bay on the west side of Corfu Island, and the CH_2Cl_2/MeOH extract of the freeze-dried alga was subjected to a series of gravity column chromatography fractionations on silica gel using mixtures of cyclohexane/EtOAc as mobile phase, as well as normal- and reversed-phase high-pressure liquid chromatography (HPLC) separations, using mixtures of *n*-hexane/$CHCl_3$ or CH_3CN, respectively, as eluent, to yield compounds **1**−**6** in pure form.

Compound **1** was isolated after purification by HPLC as a colorless oil. The molecular formula $C_{20}H_{32}Br_2O_2$ was deduced from the HRFABMS in combination with the NMR data (Table 1). The LRCI-MS ions at *m*/*z* 445/447/449 $[MH - H_2O]^+$, with relative intensities 1.4/2.0/1.0, and at *m*/*z* 347/349 $[MH - 2H_2O - HBr]^+$ with relative intensities 1.0/1.0 indicated the presence of two bromine atoms. In the IR spectrum, the intense and broad band at ν_{max} 3377 cm^{-1} indicated the presence of a hydroxyl group in the molecule. The ^{13}C NMR spectrum exhibited 20 signals, which by DEPT spectra corresponded to four quaternary carbons, six methines, six methylenes, and four methyls. The ^{1}H and ^{13}C NMR spectra displayed resonances for two methyls ($\delta_{H/C}$ 0.82/18.7; 0.97/24.8) of an isopropyl group linked to a methine ($\delta_{H/C}$ 1.75/25.9) bonded to another methine ($\delta_{H/C}$ 1.89/41.1), two methyls attached to quaternary carbons ($\delta_{H/C}$ 1.18/15.3 and 1.36/29.6), one oxygenated methine ($\delta_{H/C}$ 4.28/68.9), one halomethine ($\delta_{H/C}$ 3.97/67.7), one trisubstituted double bond ($\delta_{H/C}$ 6.45/133.0 and δ_C 137.2), one aliphatic methine ($\delta_{H/C}$ 1.88/51.2), one halomethylene ($\delta_{H/C}$ 3.81, 3.44/38.7), and five aliphatic methylenes ($\delta_{H/C}$ 1.85, 1.26/28.3; 1.85, 1.35/27.8; 1.87, 1.34/38.0; 1.61, 1.60/44.8; and 2.43, 2.00/29.8). With four degrees of unsaturation, the structure was expected to contain three rings in addition to the double bond. All protonated carbons and the corresponding protons were assigned by COSY and HMQC experiments. The NMR data comparison of **1** with reported values for bromosphaerodiol[16] suggested that metabolite **1** was its 2-hydroxy-$\Delta^{1,10}$ isomer. The correlation in the HMBC experiments, from H_3-19 and H_3-20 (δ_H 0.82 and 0.97) to C-4 (δ_C 41.1), confirmed the position of the isopropyl group. The hydroxyl group was positioned on C-2, as deduced from the correlations of C-2 (δ_C 68.9) with H-3α (δ_H 1.26) and of C-1 (δ_C 133.0) with H-2 (δ_H 4.28). Moreover, the strong correlations between C-1 (δ_C 133.0) and H-9 (δ_H 1.88) as well as the correlations of H-1 (δ_H 6.45) with C-3 (δ_C 28.3), C-9 (δ_C 51.2), and the quaternary carbon C-5 (δ_C 45.5) established the position of the olefinic proton at C-1. The correlation of H-17a (δ_H 3.81) with C-4 (δ_C 41.1), C-5 (δ_C 45.5), and C-6 (δ_C 27.8) and of H-17b (δ_H 3.44) with C-4 (δ_C 41.1), C-5 (δ_C 45.5), and C-10 (δ_C 137.2) secured the position of the bromomethyl group at C-5. The additional bromine atom was positioned on C-14, as concluded by the correlations of C-14 (δ_C 67.7) with H-9 (δ_H 1.88), H_2-12 (δ_H 1.61, 1.60), H-13α (δ_H 2.43), and H_3-15 (δ_H 1.26). Moreover, the correlations of H_3-15 (δ_H 1.18) with C-8 (δ_C 42.6), C-7 (δ_C 38.0), C-9 (δ_C 51.2), and C-14 (δ_C 67.7) and of H_3-16 (δ_H 1.36) with C-11 (δ_C 72.3), C-9 (δ_C 51.2), and C-12 (δ_C 44.8) confirmed the positions of the remaining methyl groups. The relative configuration of **1** was assigned on the basis

* Corresponding author. Tel: +30 210 7274592. Fax: +30 210 7274590. E-mail: vagias@pharm.uoa.gr.
[†] University of Athens.
[‡] University of London.

10.1021/np8001817 CCC: $40.75
Published on Web 07/03/2008

Table 1. NMR Data[a] of Compounds **1**−**3**

	1					**2**					**3**		
no.	^{1}H (δ)	m (J)	NOESY	^{13}C (δ)	HMBC (C→H)	^{1}H (δ)	m (J)	NOESY	^{13}C (δ)	HMBC (C→H)	^{1}H (δ)	m (J)	^{13}C (δ)
1	6.45	br s	2, 15, 16	133.0	2, 9	6.57	br s	2, 15, 16	129.0	9	6.46	br s	127.8
2	4.28	dd 10.0, 5.0	1, 3β, 4	68.9	3α, 3β/4	4.60	dd 10.4, 5.0	1, 3β, 4	81.9	3α, 4	4.61	br dd 10.4, 5.4	82.1
3	β 1.85	m	2	28.3	1, 4, 18	β 1.87	m	2	22.4	1, 4, 18	a 1.88	m	22.7
	α 1.26	m	19			α 1.49	m	19			b 1.47	m	
4	1.89	m	2, 17b	41.1	3α, 17a, 17b, 19, 20	1.94	m	2, 17b, 20	40.9	17a, 17b, 18, 19, 20	1.93	m	40.9
5				45.5	1, 3β/4, 17a, 17b, 18				45.7	1, 4, 9, 18, 3β/7α			46.1
6	α 1.85	m	15	27.8	7α, 17a	α 1.88	m	15	27.6		a 1.86	m	27.8
	β 1.35	m	17b, 18, 19			β 1.35	m	18			b 1.35	m	
7	α 1.87	m	14, 17a	38.0	6β, 15	α 1.86	m	9, 14, 17a	37.5	15	a 1.82	m	37.7
	β 1.34	m				β 1.27	m				b 1.39	m	
8				42.6	7β, 9, 15				42.6	9, 15			42.8
9	1.88	m	12β, 14, 16, 17a	51.2	1, 7α, 12, 15, 16	1.80	br s	7α, 12, 14, 17a	49.5	1, 15, 16	2.37	br s	45.8
10				137.2	9, 17b				138.5	9, 17b			139.6
11				72.3	9, 12, 16				74.1	9, 16			74.7
12	β 1.61	m	9, 14, 16 13α	44.8	13α, 16	3.36	dd 12.0, 4.2	9, 13β, 14, 16	75.9	13α, 13β, 16	3.40	dd 3.7, 2.5	78.1
	α 1.60	m											
13	α 2.43	tdd 13.2, 10.0, 7.4	12α, 15	29.8	12	α 2.40	td 12.4, 12.0	15	37.6		α 2.71	ddd 13.3, 13.3, 2.5	36.4
	β 2.00	dtd 13.2, 3.7, 3.3	14			β 2.20	dt 12.4, 4.2	12, 14			β 2.14	ddd 13.3, 4.2, 3.7	
14	3.97	dd 13.2, 3.7	7β, 9, 12β, 13β	67.7	9, 12, 13α, 15	3.91	dd 12.4, 4.2	7β, 9, 12, 13β	62.2	9, 13α, 13β, 15	4.44	dd 13.3, 4.2	62.4
15	1.18	s	1, 6α, 13α	15.3	9, 14	1.13	s	1, 6α, 13α	15.0	9	1.14	s	15.1
16	1.36	s	1, 9, 12β	29.6		1.41	s	1, 12	24.8		1.43	s	25.8
17	a 3.81	d 10.8	7β, 9	38.7	6α	a 3.78	d 11.2	7β, 9	38.2		a 3.91	d 11.2	38.5
	b 3.44	d 10.8	4, 6β, 18			b 3.46	d 11.2	4, 18			b 3.46	d 11.2	
18	1.75	br hept 6.6	6β, 17b, 19, 20	25.9	19, 20	1.78	br hept 6.6	6β, 17b, 19, 20	26.1	19, 20	1.79	m	26.0
19[b]	0.82	d 6.6	3α, 6β, 18	18.7	4, 18, 20	0.83	d 6.6	3α, 18	18.7	4, 18, 20	0.83	d 7.0	18.7
20[b]	0.97	d 6.6	18	24.8	4, 18, 19	0.99	d 6.6	4, 18	24.7	4, 18, 19	0.99	d 7.0	24.7

[a] ^{1}H (400 MHz) and ^{13}C NMR (50.3 MHz) recorded in $CDCl_3$ (δ_H 7.24, δ_C 77.0); chemical shifts are expressed in ppm and J values in Hz. [b] Positions can be interchanged.

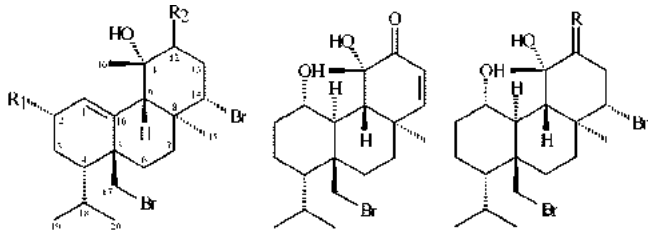

Figure 1. Metabolites isolated from *S. coronopifolius*.

of NOESY data. The strong NOE correlations between H-14/H-9, H-14/H-13β, H-14/H-7β, H-14/H-12β, H-12β/H-9, H-9/H_3-16, H-9/H-17a, H-17a/H-7β, H-17b/H-4, H-17b/H-6β, and H_3-16/H-12β determined the configuration at C-4, C-5, C-9, C-11, and C-14. The strong NOE correlations between H_3-15/H-13α and H-6α/H_3-15 established the configuration at C-8. The NOE correlations between H-2/H-3β and H-2/H-4 determined the configuration at C-4. The large coupling constant values of H-13α and H-14 supported the *trans*-diaxial orientation of these protons. In view of the above-mentioned data metabolite **1** was identified as 2*S*-hydroxyisobromosphaerol (Figure 1).

Compound **2** was purified by means of HPLC and isolated as a white solid. A combination of its NMR data (Table 1) and HRFABMS measurements suggested the molecular formula $C_{20}H_{32}Br_2O_4$. The LRCI-MS peaks at *m/z* 477/479/481 $[MH - H_2O]^+$, with relative intensities 1.1/2.0/1.0, and at *m/z* 459:461:463 $[MH - 2H_2O]^+$, with relative intensities 1.0/1.9/1.3, indicated the presence of two bromine atoms. The ^{13}C NMR spectrum of **2** exhibited signals for 20 carbon atoms with the multiplicities of the carbon signals determined from the DEPT spectra as four singlets, seven doublets, five triplets, and four quartets. Strong IR absorptions at ν_{max} 3422 cm^{-1} and ^{13}C NMR signals at δ_C 74.1 (C-11) and 75.9 (C-12) indicated the presence of hydroxyl groups. An additional oxygenated carbon resonated at lower fields [δ_C 81.9 (C-2)], characteristic for the presence of a hydroperoxy group. Among the other carbons, two were olefinic, resonating at δ_C 129.0 (C-1) and 138.5 (C-10), and two were brominated, resonating at δ_C 62.2 (C-14) and 38.2 (C-17). Furthermore, the ^1H NMR spectra revealed signals due to an olefinic proton at δ_H 6.57 (H-1), one halomethine proton at δ_H 3.91 (H-14), two halomethylene protons at δ_H 3.78 and 3.46 (H-17a and H-17b), two oxygenated methine protons at δ_H 4.60 (H-2) and 3.36 (H-12), two methyls of an isopropyl group at δ_H 0.83 (H_3-19) and 0.99 (H_3-20) attached to a methine at δ_H 1.78 (H-18), and two singlet methyls at δ_H 1.13 (H_3-15) and 1.41 (H_3-16). All protonated carbons and their protons were assigned on the basis their COSY and HMQC correlations. The structure elucidation was assisted by analyses of the HMBC experiments. Based on the correlations of C-2 (δ_C 81.9) with H-3α (δ_H 1.49) and H-4 (δ_H 1.94) and of H_2-13 methylene protons (δ_H 2.40 and 2.20) and H_3-16 (δ_H 1.41) with C-12 (δ_C 75.9), observed in the HMBC spectrum, the hydroperoxy- and hydroxymethines were placed at C-2 and C-12, respectively. The position of the olefinic bond between C-1 and C-10 was established from correlations of H-1 (δ_H 6.57) with C-3 (δ_C 22.4) and C-9 (δ_C 49.5), as well as from the correlations of C-1 (δ_C 129.0) and C-10 (δ_C 138.5) with H-9 (δ_H 1.80). The correlation of H_3-19 (δ_H 0.83) and H_3-20 (δ_H 0.99) with C-4 (δ_C 40.9) confirmed the position of the isopropyl group on C-4. The correlation of H-17a (δ_H 3.78) with C-4 (δ_C 40.9), H-17b (δ_H 3.46) with C-4 (δ_C 40.9) and C-10 (δ_C 138.5), and C-5 (δ_C 45.7) with H-1 (δ_H 6.57), H-4 (δ_H 1.94), H-9 (δ_H 1.80), and H-18 (δ_H 1.78) secured the position of the bromomethyl group on C-5. The position of the second bromine atom at C-14 was indicated by the correlation of C-14 (δ_C 62.2) with H_3-15 (δ_H 1.13) and H_2-13 (δ_H 2.40 and 2.20). Moreover the correlations of H_3-15 (δ_H 1.13) with C-8 (δ_C 42.6), C-7 (δ_C 37.5), C-9 (δ_C 49.5), and C-14 (δ_C 62.2) and of H_3-16 (δ_H 1.41) with C-11 (δ_C 74.1), C-9 (δ_C 49.5), and C-12 (δ_C 75.9) confirmed the positions of these methyl groups. Comparison of the NMR data of **2** with literature data showed a close similarity with those of the previously reported 2*S*,12*S*-dihydroxyisobromosphaerol.[14] The above-mentioned data led us to assign **2** as 2*S*-hydroperoxy-12*R*-hydroxyisobromosphaerol. The proposed structure was confirmed by NOESY correlations (Figure 2). The NOE correlations between H-14/H-9, H-14/H-13β, H-14/H-7β, H-14/H-12, H-13β/H-12, H-9/H-12, H-9/H-7β, H-9/H-17a, H-17a/H-7β, and H-17b/H-4 determined the configuration at C-4, C-5, C-9, C-14, and C-12. The NOE correlations between H_3-15/H-13α and H_3-15/H-6α determined the configuration at C-8. The absence of any correlation between H_3-15/H_3-16 and the NOE correlations between H_3-16/H-1 and H_3-16/H-12 confirmed the equatorial orientation of H_3-16. The NOE correlations between H-2/H-4, H-2/H-3β, and H-3α/H_3-19 and the absence of any correlation between H-2/H-3α established the configuration at the oxygenated carbon C-2. The large coupling constants of H-12, H-13α, and H-14 supported the axial orientation of these protons.

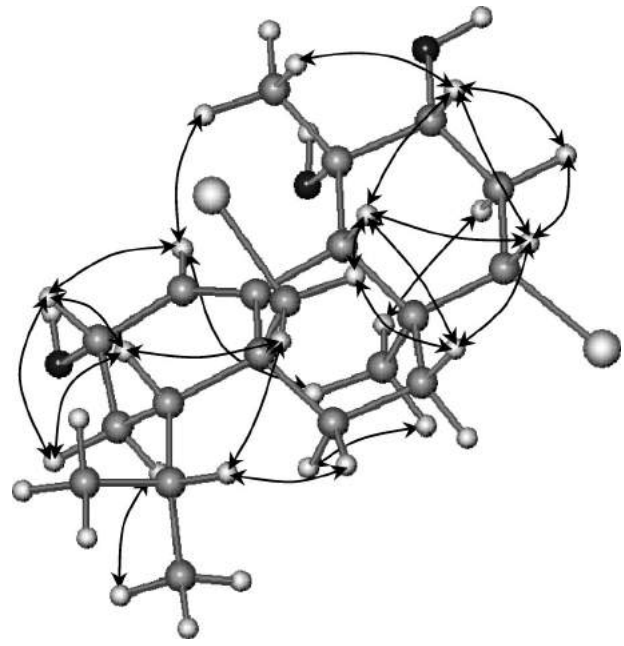

Figure 2. NOE correlations for compound **2**.

Compound **3** after purification by HPLC was isolated as a white solid. Comparison of its NMR (Table 1) and MS spectra with literature data showed them to be almost identical to those for 2*S*,12*S*-dihydroxyisobromosphaerol.[14] However, the fact that C-2 resonated downfield (δ_C 81.9) when compared with 2*S*-hydroxyisobromosphaerol (**1**) (C-2 signal at δ_C 68.9) was again indicative of the presence of a hydroperoxy group at C-2, as seen in **2**. Additionally, several ^{13}C and ^1H NMR chemical shifts were reassigned. On the basis of the above evidence, metabolite **3** was characterized as 2*S*-hydroperoxy-12*S*-hydroxyisobromosphaerol.

Compound **4** was purified by means of HPLC separations and was isolated as a colorless oil. Both ^{13}C NMR data and HRFABMS measurements supported the molecular formula $C_{20}H_{31}BrO_3$. The LREIMS showed $[M - H_2O]^+$ peaks at *m/z* 380/382 with intensities 1.0/1.0, indicating the presence of one bromine atom. The presence of a carbonyl group was evident from the intense IR band at 1698 cm^{-1}, while absorptions at ν_{max} 3468 cm^{-1} indicated the presence of hydroxyl groups in the molecule. The ^{13}C NMR spectrum of **4** (Table 2) exhibited signals for 20 carbons, with the multiplicities of the carbons determined from the DEPT spectra as four quaternary carbons, seven methines, five methylenes, and four methyls. Among

Table 2. NMR Data[a] of Compounds **4**−**6**

	4					**5**					**6**		
no.	^{1}H (δ)	m (J)	NOESY	^{13}C (δ)	HMBC (C→H)	^{1}H (δ)	m (J)	NOESY	^{13}C (δ)	HMBC (C→H)	^{1}H (δ)	m (J)	^{13}C (δ)
1	3.61	ddd 10.4, 10.4, 4.6	2β, 16	75.6	3α/9, 10	3.48	m	2β, 9, 16	74.8	2β, 3α, 3β, 9/10	3.99	m	67.3
2	β 2.00	m	1	29.2		β 1.99	m	1, 3β	29.0		a 1.91	m	34.0
	α 1.46	m	10, 19/20			α 1.46	m	b 1.52		m			
3	α 1.89	m	19/20	23.3		α 1.88	m	20	23.0	2α	a 1.66	m	18.8
	β 1.40	m	17b			β 1.42	m	2β, 4, 17b			b 1.50	m	
4	1.78	m		44.3	17a, 19, 20	1.78	m	3β, 17b	43.7	2β/6β, 17a, 19, 20	1.72	m	43.3
5				43.1	6a, 6b, 7				42.4	3α, 17b			43.9
6	a 1.92	m		27.4	7, 17b	β 1.96	m	7β, 17a, 19	27.6	17a, 17b	α 1.74	m	27.7
	b 1.80	m				α 1.73	m	15, 20			β 1.58	m	
7	a 1.64	m		34.0	6a, 6b, 14, 15	α 1.71	m	6β, 14, 17a	35.6	15	α 1.82	dt 13.4, 4.1	36.7
	b 1.64	m				β 1.31	m				β 1.21	ddd 13.4, 12.9, 4.1	
8				38.0	7, 13, 14, 15				42.4	13β, 14, 15			41.7
9	1.88	m	17a	50.0	7, 10, 14, 15, 16	1.67	m	1, 7β/16, 14, 17a	53.8	7α, 10, 14, 15, 16	1.60	d 10.2	52.3
10	1.86	m	2α, 15, 19/20	48.5	2β, 6a	1.67	m	15, 20	49.6	2α, 4, 6β, 9	2.27	dd 10.2, 9.9	46.1
11				84.2	10, 13, 16				83.9	9/10, 13α, 16			72.1
12				200.6	14,16				205.8	13α, 13β, 16	α 1.78	dt 14.3, 3.2	45.4
											β 1.59	m	
13	5.97	d 9.6		129.9		β 3.19	dd 18.4, 8.2	14, 16	47.0	14	α 2.42	qd 13.1, 3.3	30.0
						α 2.85	dd 18.4, 9.4	15			β 1.90	m	
14	6.88	d 9.6		153.9	15	4.29	dd 9.4, 8.2	7β, 9, 13β	54.8	13α, 13β, 15	3.98	m	69.9
15	0.99	s	10	24.9	7, 9	0.93	s	6α, 10, 13α	13.1	7β, 9, 14	1.31	s	14.5
16	1.35	s	1	27.7	9	1.32	s	1, 13β	25.6	9	1.36	s	32.3
17	a 3.79	d 10.4	9	38.8	6b, 10	a 3.73	d 10.2	6β, 7β, 9	38.0	10	a 3.96	d 10.5	40.9
	b 3.58	dd 10.4, 2.1	3β			b 3.53	dd 10.2, 2.0	3β, 4			b 3.49	br d 10.5	
18	1.70	br hept 6.6		26.1	19, 20	1.65	m		25.9	4, 19, 20	1.97	m	26.5
19[b]	0.98	d 6.6	(2α, 3α, 10)	21.3	20	0.97	d 6.6	6β	21.2	20	1.04	d 6.7	21.2
20[b]	0.95	d 6.6	(2α, 3α, 10)	26.0	19	0.95	d 6.6	3α, 10, 6α	26.0	19	1.01	d 6.7	25.5

[a] ^{1}H (400 MHz) and ^{13}C NMR (50.3 MHz) recorded in $CDCl_3$ (δ_H 7.24, δ_C 77.0); chemical shifts are expressed in ppm and J values in Hz. [b] Positions can be interchanged.

the carbons, one was a carbonyl, resonating at δ_C 200.6 (C-12), two were olefinic, resonating at δ_C 129.9 (C-13) and 153.9 (C-14), one was brominated, resonating at δ_C 38.8 (C-17), and two were oxygenated, resonating at δ_C 84.2 (C-11) and 75.6 (C-1). The proton resonances at δ_H 5.97 (H-13) and 6.88 (H-14) displayed in the ^{1}H NMR spectra defined the isolated AB system of an α,β-unsaturated ketone. Furthermore, the spectra displayed signals corresponding to one oxygenated methine proton at δ_H 3.61 (H-1), two halomethylene protons at δ_H 3.79 and 3.58 (H-17a and H-17b), two methyls of an isopropyl group at δ_H 0.98 (H_3-19) and 0.95 (H_3-20) bonded to a methine at δ_H 1.70 (H-18), and two methyls linked to quaternary carbons at δ_H 0.99 (H_3-15) and 1.35 (H_3-16). With five degrees of unsaturation, the structure was expected to contain three rings in addition to the carbonyl group and the double bond. All protonated carbons and their protons were assigned by COSY and HMQC experiments. The NMR data comparison of **4** with those of sphaerococcenol-A[17,18] suggested that metabolite **4** was its 1-hydroxy-1,2-dihydro derivative. On the basis of the correlations of carbonyl C-12 (δ_C 200.6) with H-14 (δ_H 6.88) and H_3-16 (δ_H 1.35), of H-13 (δ_H 5.97) with the quaternary carbons C-8 (δ_C 38.0) and C-11 (δ_C 84.2), and of H-14 (δ_H 6.88) with C-7 (δ_C 34.0), C-8 (δ_C 38.0), and C-9 (δ_C 50.0), observed in the HMBC spectrum, the carbonyl group was placed at C-12 and the double bond between C-13 and C-14. The correlations between H_3-19 and H_3-20 (δ_H 0.98 and 0.95) with C-4 (δ_C 44.3) confirmed the position of the isopropyl group on C-4. The correlation of H-17a (δ_H 3.79) with C-4 (δ_C 44.3), of H-17b (δ_H 3.58) with C-6 (δ_C 27.4), and of carbon C-17 (δ_C 38.8) with protons H-6a (δ_H 1.92) and H-10 (δ_H 1.86) secured the position of the bromomethyl group at C-5. The oxygenated methine was positioned at C-1, as concluded by the correlations of C-1 (δ_C 75.6) with H-9 (δ_H 1.88) and/or H-3α (δ_H 1.89) and H-10 (δ_H 1.86). Moreover the correlations of H_3-15 (δ_H 0.99) with C-8 (δ_C 38.0), C-7 (δ_C 34.0), C-9 (δ_C 50.0), and C-14 (δ_C 153.9) and of H_3-16 (δ_H 1.35) with C-11 (δ_C 84.2), C-9 (δ_C 50.0), and C-12 (δ_C 200.6) confirmed the positions of the remaining methyl groups. The relative configuration of **4** was assigned on the basis of the NOE experiments. The correlations between H-10/H_3-15 and H-10/(H_3-19 or H_3-20) and H-10/H-18, observed in the NOESY spectra, determined the configuration at C-4, C-8, and C-10. The NOE correlations between H-17a/H-9, H-17b/H-3β, and H-3α/(H_3-19 or H_3-20) determined the configuration at C-5 and C-9. The strong NOE correlations between H-1/H-2β, H-2α/H-10, and H-2α/(H_3-19 or H_3-20) established the configuration at C-1. The absence of any correlation between H_3-15/H_3-16 or H-10/H_3-16 and the strong NOE correlation between H_3-16/H-1 determined the configuration at C-11. According to the above observations, the structure of metabolite **4** was established as 1*S*-hydroxy-1,2-dihydrosphaerococcenol-A.

Compound **5** was isolated after purification by HPLC as a colorless oil. The molecular formula $C_{20}H_{32}Br_2O_3$ was deduced from HRFABMS data in combination with the NMR data (Table 2). The LRCI-MS ions at *m/z* 461/463/465 $[MH - H_2O]^+$, with relative intensities 1.0/2.3/1.3, and at *m/z* 381/383 $[MH - H_2O - HBr]^+$ with relative intensities 1.1/1.0 indicated the presence of two bromine atoms. In the IR spectrum, the broad band at 3414 cm^{-1} indicated the presence of a hydroxyl group, while the intense absorption at ν_{max} 1723 cm^{-1} suggested a carbonyl functionality in the molecule. The ^{13}C NMR exhibited 20 signals corresponding, as determined from the DEPT spectra, to four quaternary carbons, six methines, six methylenes, and four methyls. Among the carbons, one was carbonyl, resonating at δ_C 205.8 (C-12), two were brominated, resonating at δ_C 54.8 (C-14) and 38.0 (C-17), and two were oxygenated, resonating at δ_C 83.9 (C-11) and 74.8 (C-1). The ^{1}H NMR spectra displayed bands corresponding to one halomethine at δ_H 4.29 (H-14) and two halomethylene protons at δ_H 3.73 and 3.53 (H-17a and H-17b), one oxygenated methine proton at δ_H 3.48 (H-1), two methyls of an isopropyl group at δ_H 0.97 (H_3-19) and 0.95 (H_3-20) bonded to a methine at δ_H 1.65 (H-18), and two singlet methyls at δ_H 0.93 (H_3-15) and 1.32 (H_3-16). With four degrees of unsaturation, the structure was suggested to contain three rings besides the carbonyl group. All protonated carbons and their protons were assigned by COSY and HMQC experiments. The NMR data comparison of **5** with those of sphaerococcenol-A[17,18] suggested that metabolite **5** was its 14-bromo-1-hydroxy-1,2,13,14-tetrahydro derivative. On the basis of the correlations of carbonyl C-12 (δ_C 205.8) with H_2-13 (δ_H 3.19 and 2.85) and H_3-16 (δ_H 1.32), observed in the HMBC spectrum, the carbonyl group was placed on C-12. The correlations between H_3-19 and H_3-20 (δ_H 0.97 and 0.95) with C-4 (δ_C 43.7) confirmed the position of the isopropyl group on C-4. The correlation of H-17a (δ_H 3.73) with C-4 (δ_C 43.7) and C-6 (δ_C 27.6), of H-17b (δ_H 3.53) with C-6 (δ_C 27.6) and C-5 (δ_C 43.7), and of carbon C-17 (δ_C 38.0) with proton H-10 (δ_H 1.67) secured the position of the bromomethyl group on C-5. The position of the second bromine atom at C-14 was indicated by the correlation of C-14 (δ_C 54.8) with H_3-15 (δ_H 0.93) and H_2-13 (δ_H 3.19 and 2.85). The oxygenated methine was positioned on C-1, as concluded by the correlations of C-1 (δ_C 74.8) with H-2β (δ_H 1.99), H_2-3 (δ_H 1.88 and 1.42), and H-9 (δ_H 1.67), and/or H-10 (δ_H 1.67). Moreover the correlations of H_3-15 (δ_H 0.93) with C-8 (δ_C 42.4), C-7 (δ_C 35.6), C-9 (δ_C 53.8), and C-14 (δ_C 54.8) and of H_3-16 (δ_H 1.32) with C-11 (δ_C 83.9), C-9 (δ_C 53.8), and C-12 (δ_C 205.8) confirmed the positions of the methyl groups linked to quaternary carbon atoms. The relative configuration of **5** was assigned on the basis of the NOE experiments (Figure 3). The NOE correlations between H-14/H-7β, H-14/H-9, H-14/H-13β, H-9/H-17a, H-7β/H-17a, H-7β/H-6β, H-17a/H-6β, H-17b/H-3β, H-3α/H_3-20, H-3β/H-4, and 17b/H-4 determined the configuration at C-4, C-5, C-9, and C-14. The correlations between H_3-15/H-13α, H_3-15/H-6α, H_3-20/H-6α, H_3-20/H-10, and H_3-15/H-10, observed in the NOESY spectra, established the configuration at C-8 and C-10. Strong NOE correlations between H-1/H-2β, H-2β/H-3β, H-1/H-9, and H-1/H_3-16 determined the configuration at C-1. The strong NOE correlations between H_3-16/H-1 and H_3-16/H-13β determined the configuration at C-11. According to the above observations, metabolite **5** was named 14*S*-bromo-1*S*-hydroxy-1,2,13,14-tetrahydrosphaerococcenol-A.

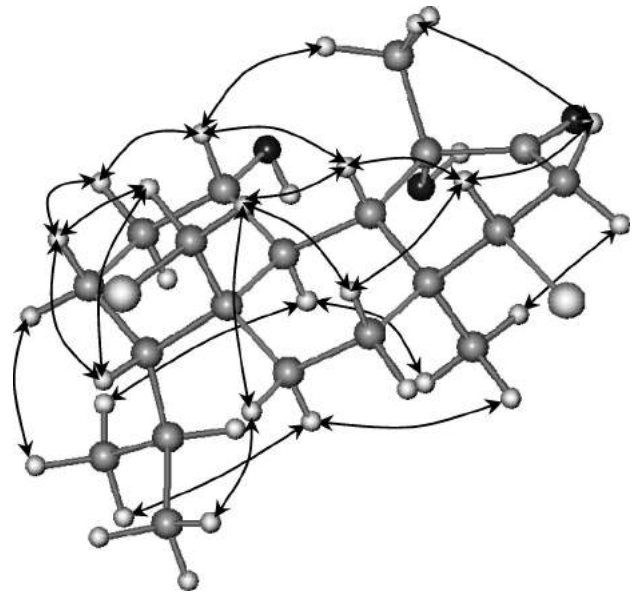

Figure 3. NOE correlations for compound **5**.

Compound **6**, after purification by HPLC, was isolated as a white solid and identified by comparison of its ^{1}H NMR and MS spectra with previously reported data as being 1*S*-hydroxy-1,2-dihydrobromosphaerol.[15] Extensive analyses of the ^{13}C NMR, COSY,

Table 3. MICs of Compounds **1**−**6** and a Standard Antibiotic (Norfloxacin) in μg/mL against MDR and Methicillin Resistant *Staphylococcus aureus*

compound	SA1199B	RN4220	EMRSA-15	ATCC 25943	XU212 (TetK)/	EMRSA-16
1	16	16	16	16	16	16
2	16−32	16	16	32	16	16
3	16	16	16	32	16	16
4	0.5	1	0.5	0.5	1	0.25
5	32	32	128	32	32−64	64
6	1−2	2	2	2	2	1−2
Nor	32	1	0.5	0.5	8	128

HSQC, HMBC, and NOESY spectra allowed full ^{13}C and ^{1}H NMR assignments for **6** (Table 2).

Metabolites **1**−**6** were evaluated for their antibacterial activity against a panel of multidrug-resistant (MDR) and methicillin-resistant *Staphylococcus aureus* strains (Table 3). The minimum inhibitory concentrations (MICs) of **1**−**6** were found to be in the range 0.5−128 μg/mL. Among the metabolites, the highest activity was exhibited by **4**, which was 64 and 512 times more active than the standard antibiotic norfloxacin against *Staphylococcus aureus* SA 1199B (overexpressing the NorA efflux protein) and EMRSA-16 (which expresses mecA and is resistant to methicillin), respectively. The second most potent compound was **6**, having MICs of 1−2 μg/mL. The presence of the α,β-unsaturated ketone moiety at C-12 may well account for the activity of metabolite **4**, with this compound being capable of undergoing Michael-type additions to this moiety via attack at C-14 by biological nucleophiles. In compound **5**, C-13 is conceivably acidic and the elements of HBr could readily eliminate, giving rise to an α,β-unsaturated ketone and generating compound **4** *in situ*. This may account for the antibacterial activity seen for compound **5**. The activity seen for compound **6** is intriguing, and perhaps the bromine atom enhances uptake of this compound. The minor structural alterations in these tricyclic brominated diterpenes that cause such significant variations in their antibacterial activity make these preliminary results a stimulus for further structure−activity investigations.

Experimental Section

General Experimental Procedures. Optical rotations were measured on a Perkin-Elmer model 341 polarimeter with a 10 cm cell. UV spectra were acquired in spectroscopic grade $CHCl_3$ on a Shimadzu UV-160A spectrophotometer. IR spectra were obtained using a Paragon 500 Perkin-Elmer spectrophotometer. NMR spectra were recorded using Bruker AC 200 and Bruker DRX 400 spectrometers. Chemical shifts are given on a δ (ppm) scale using TMS as internal standard. The 2D NMR experiments ($^{1}H-^{1}H$ COSY, HMQC, HMBC, NOESY) were performed using standard Bruker microprograms. The structures in Figures 2 and 3 were generated and optimized (energy: 41.00 and 60.42 Kkcal, respectively) by HyperChem 7.0 molecular modeling and simulation software (force field, MM+; optimization algorithm, Polak-Ribiere). High-resolution mass spectral data were provided by the University of Notre Dame, Department of Chemistry and Biochemistry, IN. Low-resolution electron impact or chemical ionization MS data were recorded on a Thermo DSQ mass detector using a direct exposure probe (DEP) and methane as the CI gas. Vacuum liquid chromatography (VLC) separation was performed with Kieselgel 60 (Merck), gravity column chromatography (GCC) was performed with Kieselgel 60H (Merck), thin-layer chromatography (TLC) was performed with Kieselgel 60 F_{254} aluminum support plates (Merck), and spots were detected after spraying with 15% H_2SO_4 in MeOH reagent and charring. HPLC separations were conducted using an Agilent 1100 model equipped with refractive index detector and a SupelcoSil 5u (250 × 10 mm) HPLC normal-phase column or a Kromasil 100 C18 5u (250 × 8 mm) HPLC reversed-phase column.

Plant Material. *S. coronopifolius* was collected by scuba diving in Palaiokastritsa Bay at the west coast of Corfu Island, Greece, at a depth of 10−15 m in May of 2002. A specimen is kept at the Herbarium of the Laboratory of Pharmacognosy and Chemistry of Natural Products, University of Athens (ATPH/MO/201).

Extraction and Isolation. *S. coronopifolius* was initially freeze-dried (291.4 g dry weight) and then exhaustively extracted with mixtures of CH_2Cl_2/MeOH (3:1) at room temperature. The combined extracts were concentrated to give a dark green residue (8.20 g), which was later subjected to VLC on silica gel, using cyclohexane with increasing amounts (10%) of EtOAc and finally MeOH as mobile phase. The CH_3CN-soluble portion (306.7 mg) of fraction IV_a (60% EtOAc in cyclohexane) (337.8 mg) was subjected to reversed-phase HPLC chromatography, using 100% CH_3CN as mobile phase. Peak V_b (retention time 9.4 min) (3.3 mg) was subjected again to reversed-phase HPLC chromatography, using CH_3CN as mobile phase, to yield pure compound **4** (1.1 mg), while peaks X_b (retention time 12.0 min) (21.0 mg) and XI_b (retention time 12.5 min) (86.3 mg) with similar repurification yielded pure compounds **3** (1.3 mg) and **2** (2.0 mg), respectively. The CH_3CN-soluble portion (323.4 mg) of fraction V_a (70% EtOAc in cyclohexane) (419.8 mg) was subjected to reversed-phase HPLC chromatography, using CH_3CN as mobile phase. Peaks IV_c (retention time 7.8 min) (8.9 mg) and $VIII_c$ (retention time 9.2 min) (11.1 mg) were subjected again to reversed-phase HPLC chromatography, using CH_3CN as mobile phase, to yield pure compounds **1** (1.4 mg) and **5** (1.3 mg), respectively, while peak XII_c (retention time 11.6 min) (48.1 mg) with HPLC normal-phase purification, using 70% $CHCl_3$ in *n*-hexane as mobile phase, yielded pure compound **6** (2.0 mg).

2*S*-Hydroxyisobromosphaerol (1): colorless oil; $[\alpha]^{20}_D$ +8.4 (*c* 2.70, $CHCl_3$); UV ($CHCl_3$) λ_{max} (log ε) 245 (2.51) nm; IR ($CHCl_3$) ν_{max} 3377, 2942, 2860 cm^{-1}; NMR data ($CDCl_3$), see Table 1; CIMS *m/z* (rel int %) 445:447:449 $[MH - H_2O]^+$ (1:2:1), 427:429:431 $[MH - 2H_2O]^+$ (1:2:1), 365:367 $[MH - HBr - H_2O]^+$ (12:9), 347:349 $[MH - HBr - 2H_2O]^+$ (14:15), 285 $[MH - 2HBr - H_2O]^+$ (22), 267 $[MH - 2HBr - 2H_2O]^+$ (100), 223 (7), 187 (8), 159 (18), 109 (6), 95 (18), 81 (19); HRFABMS *m/z* 461.0675 $[M - H]^+$ (calcd for $C_{20}H_{31}{}^{79}Br_2O_2$, 461.0691).

2*S*-Hydroperoxy-12*R*-hydroxyisobromosphaerol (2): white solid; $[\alpha]^{20}_D$ +6.6 (*c* 1.70, $CHCl_3$); UV ($CHCl_3$) λ_{max} (log ε) 247 (3.00) nm; IR ($CHCl_3$) ν_{max} 3422, 2936 cm^{-1}; NMR data ($CDCl_3$), see Table 1; CIMS *m/z* (rel int %) 477:479:481 $[MH - H_2O]^+$ (43:83:41), 459:461:463 $[MH - 2H_2O]^+$ (12:22:13), 443:445:447 $[MH - H_2O_2 - H_2O]^+$ (6:8:4), 397:399 $[MH - HBr - H_2O]^+$ (21:19), 379:381 $[MH - HBr - 2H_2O]^+$ (42:45), 363:365 $[MH - HBr - H_2O_2 - H_2O]^+$ (31:31), 345:347 (7:9), 337:339 (12:13), 317 (23), 299 $[MH - 2HBr - 2H_2O]^+$ (38), 283 $[MH - 2HBr - H_2O_2 - H_2O]^+$ (100), 265 (39), 239 (16), 201 (17), 159 (29), 95 (23), 83 (79); HRFABMS *m/z* 477.0621 $[M - OH]^+$ (calcd for $C_{20}H_{31}{}^{79}Br_2O_3$, 477.0640).

2*S*-Hydroperoxy-12*S*-hydroxyisobromosphaerol (3): white solid; $[\alpha]^{20}_D$ +3.1 (*c* 2.20, $CHCl_3$); NMR data ($CDCl_3$), see Table 1; EIMS 70 eV, *m/z* (rel int %) 476:478:480 $[M - H_2O]^+$ (2:6:3), 460:462:464 $[M - 2OH]^+$ (4:6:3), 445:447:449 $[M - 2OH - Me]^+$ (3:6:3), 429:431:433 $[M - 2OH - O - Me]^+$ (3:5:3), 415:417 $[M - Br]^+$ (2:2), 383:385 (36:34), 365:367 (26:27), 339:341 $[M - Br - OH - O - Me_2C]^+$ (24:21), 311 (13), 299 (41), 267 $[M - HBr - Br - H_2O_2 - 2OH]^+$ (7), 207 (17), 159 (31), 91 (34), 43 (100).

1*S*-Hydroxy-1,2-dihydrosphaerococcenol-A (4): colorless oil; $[\alpha]^{20}_D$ −32.7 (*c* 0.90, $CHCl_3$); UV ($CHCl_3$) λ_{max} (log ε) 247 (3.29) nm; IR ($CHCl_3$) ν_{max} 3468, 1698 cm^{-1}; NMR data ($CDCl_3$), see Table 2; EIMS 70 eV, *m/z* (rel int %) 380:382 $[M - H_2O]^+$ (4:4), 365:367 $[M - OH - O]^+$ (2:2), 301 $[M - Br - H_2O]^+$ (9), 283 $[M - Br - 2H_2O]^+$ (2), 273 $[M - CH_2Br - OH - Me]^+$ (100), 215 (7), 191 (58), 145 (16), 95 (69); HRFABMS (*m/z*): 381.1437 $[M - OH]^+$ (calcd for $C_{20}H_{31}{}^{79}BrO_2$, 381.1429).

14*S*-Bromo-1*S*-hydroxy-1,2,13,14-tetrahydrosphaerococcenol-A (5): colorless oil; $[\alpha]^{20}_D$ −6.6 (*c* 2.70, $CHCl_3$); UV ($CHCl_3$) λ_{max} (log ε) 247 (2.67) nm; IR ($CHCl_3$) ν_{max} 3414, 1723 cm^{-1}; NMR data ($CDCl_3$), see Table 2; CIMS *m/z* (rel int %) 461:463:465 [MH −

$H_2O]^+$ (1:2:1), 443:445:447 $[MH - 2H_2O]^+$ (2:4:2), 381:383 $[MH - HBr - H_2O]^+$ (44:40), 363:365 $[MH - HBr - 2H_2O]^+$ (17:20), 352:354 (29:32), 311 (22), 301 $[MH - 2HBr - H_2O]^+$ (100), 283 $[MH - 2HBr - 2H_2O]^+$ (61), 273 (45), 255 (23), 215 (28), 147 (29), 123 (25), 81 (38); HRFABMS (*m/z*) 460.0596 $[M - H_2O]^+$ (calcd for $C_{20}H_{30}{}^{79}Br_2O_2$, 460.0613).

1*S*-Hydroxy-1,2-dihydrobromosphaerol (6): white solid; $[\alpha]^{20}{}_D$ +5.1 (*c* 2.70, $CHCl_3$); NMR data ($CDCl_3$), see Table 2; CIMS *m/z* (rel int %) 447:449:451 $[MH - H_2O]^+$ (4:6:3), 429:431:433 $[MH - 2H_2O]^+$ (8:18:12), 367:369 $[MH - HBr - H_2O]^+$ (100:98), 349:351 $[MH - HBr - 2H_2O]^+$ (60:63), 335:337 $[MH - CH_3Br - 2H_2O]^+$ (10:8), 287 $[MH - 2HBr - H_2O]^+$ (53), 269 $[MH - 2HBr - 2H_2O]^+$ (46), 255 $[MH - CH_3Br - HBr - 2H_2O]^+$ (11), 203 (9), 175 (10), 147 (7), 105 (11), 83 (47).

Bacterial Strains and Antibiotic. A standard *S. aureus* strain ATCC 25923 and a clinical isolate (XU212), which possesses the TetK efflux pump and was an MRSA strain, were obtained from Dr. E. Udo.[19] Strain RN4220, which has the MsrA macrolide efflux pump, was provided by Dr. J. Cove.[20] EMRSA-15[21] and EMRSA-16[22] were obtained from Dr. Paul Stapleton. Strain SA1199B, which overexpresses the NorA MDR efflux pump, was the gift of Professor G. Kaatz.[23] Norfloxacin was obtained from the Sigma Chemical Co. Mueller-Hinton broth (MHB; Oxoid) was adjusted to contain 20 mg/L Ca^{2+} and 10 mg/L Mg^{2+}.

Antibacterial Assay. Overnight cultures of each strain were made up in 0.9% saline to an inoculum density of 5×10^5 cfu by comparison with a McFarland standard. Norfloxacin was dissolved in DMSO and then diluted in MHB to give a starting concentration of 512 μg/mL. Using Nunc 96-well microtiter plates, 125 μL of MHB was dispensed into wells 1−11. Then 125 μL of the test compound or the appropriate antibiotic was dispensed into well 1 and serially diluted across the plate, leaving well 11 empty for the growth control. The final volume was dispensed into well 12, which being free of MHB or inoculum served as the sterile control. Finally, the bacterial inoculum (125 μL) was added to wells 1−11, and the plate was incubated at 37 °C for 18 h. A DMSO control (3.125%) was also included. All MICs were determined in duplicate. The MIC was determined as the lowest concentration at which no growth was observed. A methanolic solution (5 mg/mL) of 3-[4,5-dimethylthiazol-2-yl]-2,5-diphenyltetrazoliium bromide (MTT; Lancaster) was used to detect bacterial growth by a color change from yellow to blue.

Acknowledgment. This study was partially supported by the FP-39 EPAN program of the Greek Secretariat for Research and Technology.

References and Notes

(1) Fenical, W. *Marine Natural Products*; Scheuer, P. J., Ed.; Academic Press: New York, 1978; Vol. 2, pp 174−245.
(2) Erickson, K. L. *Marine Natural Products: Chemical and Biological Perspectives*; Scheuer, P. J., Ed.; Academic Press: New York, 1983; Vol. 5, pp 131−257.
(3) Etahiri, S.; Bultel-Poncé, V.; Caux, C.; Guyot, M *J. Nat. Prod.* **2001**, *64*, 1024–1027, and references cited therein.
(4) Wright, A. D.; Goclik, E.; König, G. M. *J. Nat. Prod.* **2003**, *66*, 435–437.
(5) Davyt, D.; Fernandez, R.; Suescun, L.; Mombrú, A. W.; Saldaña, J.; Dominguez, L.; Fujii, M. T.; Manta, E. *J. Nat. Prod.* **2006**, *69*, 1113–1116.
(6) De Nys, R.; Wright, A. D.; König, G. M.; Sticher, O. *J. Nat. Prod.* **1993**, *56*, 887–883.
(7) El Sayed, K. A.; Dunbar, D. C.; Perry, T. L.; Wilkins, S. P.; Hamann, M. T. *J. Agric. Food Chem.* **1997**, *45*, 2735–2739.
(8) Caccamese, S.; Azzolina, R.; Duesler, E. N.; Paul, I. C.; Rinehart, K. L. *Tetrahedron Lett.* **1980**, *21*, 2299–2302.
(9) König, G. M.; Wright, A. D. *Planta Med.* **1997**, *63*, 186–187.
(10) Sakemi, S.; Higa, T.; Jefford, C. W.; Bernardinelli, G. *Tetrahedron Lett.* **1986**, *27*, 4287–4290.
(11) Kontiza, I.; Stavri, M.; Zloh, M.; Vagias, C.; Gibbons, S.; Roussis, V. *Tetrahedron* **2008**, *64*, 1696–1702.
(12) Kladi, M.; Vagias, C.; Papazafiri, P.; Furnari, G.; Serio, D.; Roussis, V. *Tetrahedron* **2007**, *63*, 7606–7611.
(13) Kontiza, I.; Abatis, D.; Malakate, K.; Vagias, C.; Roussis, V. *Steroids* **2006**, *71*, 177–181.
(14) Cafieri, F.; Ciminiello, P.; Fattorusso, E.; Mangoni, C. *Gazz. Chim. Ital.* **1990**, *120*, 139–142.
(15) Cafieri, F.; Ciminiello, P.; Santacroce, C.; Fattorusso, E. *Phytochemistry* **1982**, *21*, 2412–2413.
(16) Cafieri, F.; Ciminiello, P.; Fattorusso, E.; Santacroce, C. *Experientia* **1977**, *33*, 1549–1688.
(17) De Rosa, S.; De Stefano, S.; Scarpelli, P.; Zavodnik, N. *Phytochemistry* **1988**, *27*, 1875–1878.
(18) Fenical, W.; Finer, J.; Clardy, J. *Tetrahedron Lett.* **1976**, *17*, 731–734.
(19) Gibbons, S.; Udo, E. E. *Phytother. Res.* **2000**, *14*, 139–140.
(20) Ross, J. I.; Farrell, A. M.; Eady, E. A.; Cove, J. H.; Cunliffe, W. J. *J. Antimicrob. Chemother.* **1989**, *24*, 851–862.
(21) Richardson, J. F.; Reith, S. *J. Hosp. Infect.* **1993**, *25*, 45–52.
(22) Cox, R. A.; Conquest, C.; Mallaghan, C.; Maples, R. R. *J. Hosp. Infect.* **1995**, *29*, 87–106.
(23) Kaatz, G. W.; Seo, S. M.; Ruble, C. A. *Antimicrob. Agents Chemother.* **1993**, *37*, 1086–1094.

NP8001817

PHYTOTHERAPY RESEARCH
Phytother. Res. **22**, 681–684 (2008)
Published online 18 March 2008 in Wiley InterScience
(www.interscience.wiley.com) **DOI**: 10.1002/ptr.2408

Antimycobacterial Polyacetylenes from *Levisticum officinale*

Andreas Schinkovitz[1,2], Michael Stavri[3], Simon Gibbons[3] and Franz Bucar[1]*

[1]Institute of Pharmaceutical Sciences, Department of Pharmacognosy, Karl-Franzens-University, Graz, Austria
[2]Department of Medicinal Chemistry and Pharmacognosy, College of Pharmacy University of Illinois at Chicago, Chicago, IL, USA
[3]Centre for Pharmacognosy and Phytotherapy, The School of Pharmacy, University of London, UK

No conflicts of interest concerning financial matters or personal relationships exist between the authors and those who might bias this work. The present work is in part included the PhD thesis of A. Schinkovitz (University of Graz) but has not been published elsewhere previously.

The dichloromethane extract of the roots of *Levisticum officinale* L. (Apiaceae) exhibited significant antimycobacterial activity against *Mycobacterium fortuitum* and *Mycobacterium aurum* in a microtiter plate dilution assay and was further analysed following a bioassay-guided fractionation strategy. 3(*R*)-Falcarinol (3(*R*)-(-)-1,9-heptadecadien-4,6-diin-3-ol] and 3(*R*)-8(*S*)-falcarindiol [3(*R*)-8(*S*)-(+)-1,9-heptadecadien-4,6-diin-3,8-diol] could be identified as the active components in this extract. The minimal inhibitory concentration (MIC) of 3(*R*)-falcarinol against *M. fortuitum* and *M. aurum* was 16.4 μM while that of 3(*R*)-8(*S*)-falcarindiol was 30.7 μM against *M. fortuitum* and 61.4 μM against *M. aurum*, respectively. Previously, 3(*R*),8(*R*)-dehydrofalcarindiol was isolated from *Artemisia monosperma* and surprisingly this polyacetylene exhibited no antimycobacterial activity at 128 μg/mL. This indicates that the terminal methyl group is vital for retention of antimycobacterial activity. Reference antibiotics ethambutol and isoniazid exhibited an activity of 115.5 μM and 14.6 μM against *M. fortuitum*, and 3.4 μM and 29.2 μM against *M. aurum*, respectively. Copyright © 2008 John Wiley & Sons, Ltd.

Keywords: Levisticum; *Mycobacterium*; polyacetylene; falcarinol; falcarindiol.

INTRODUCTION

Causing 1.6 million deaths annually, tuberculosis and mycobacterial related diseases still represent a serious health problem. One third of the world's population is latently infected, of which 5–10% will develop a clinical disease. *Mycobacterium tuberculosis* represents the most prominent pathogen among mycobacteria but additionally rapidly growing mycobacteria are increasingly being recognized as human pathogens. In addition to *M. tuberculosis*, these rapidly growing species are capable of causing serious lung infections, particularly in immune comprised people such as HIV-positive individuals. Furthermore, they can infect skin, spleen, bones and kidney (Lakely *et al.*, 2001).

Plant extracts and their ingredients are known to exhibit significant antimycobacterial effects and therefore might be a valuable source of lead structures for the development of new antibiotics (Gautam *et al.*, 2007; Gibbons, 2005). In the course of our studies on antimycobacterial plant constituents (Schinkovitz *et al.*, 2003; Stavri *et al.*, 2005), the roots of *Levisticum officinale* L. (Apiaceae), which are traditionally used to treat lung disorders, were analysed.

* Correspondence to: Ao. Univ.-Prof. Dr Franz Bucar, Institute of Pharmaceutical Sciences; Department of Pharmacognosy, Karl-Franzens-University Graz; Universitaetsplatz 4/1A-8010 Graz, Austria.
E-mail: franz.bucar@uni-graz.at

MATERIAL AND METHODS

General experimental procedures. Optical rotation was measured on a Perkin Elmer 241 MC polarimeter in dichloromethane at 589 nm. ^{1}H NMR and ^{13}C NMR (125 MHz, $CDCl_3$) data were recorded on a Bruker AVANCE 500.

APCI mass spectra were recorded on a Finnigan Navigator instrument. GC-MS analysis was performed on an HP 5890 Series II Plus gas chromatograph with an HP-5MS column (0.25 mm i.d. × 30 m, film thickness: 0.5 μm) in combination with an HP 5989B mass spectrometer; carrier gas, helium 5.6 at a flow rate of 1.0 mL/min; injector temperature, 280 °C; detector temperature, 280 °C; heating program, 100 °C; heating rate, 8 °C/min up to 280 °C, constantly held for 20 min.

Column chromatography was performed on silica gel 60 (Merck, Darmstadt) and on Sephadex LH-20 (Pharmacia Biotech, Uppsala). TLC analyses were carried out on silica gel 60 F_{254} pre-coated plates (Merck, Darmstadt). Spots were visualized by spraying with vanillin–sulphuric acid reagent followed by heating for 5 min at 100 °C. Preparation and determination of Mosher's esters was conducted as previously described (Lechner *et al.*, 2004).

Plant material. Plant material was obtained as a commercial sample (Kottas, Vienna) and identity was verified by microscopy and TLC experiments. A voucher specimen is kept at the herbarium of the Institute of Pharmaceutical Sciences, Department of Pharmacognosy, University of Graz.

Received 19 September 2007
Accepted 29 September 2007

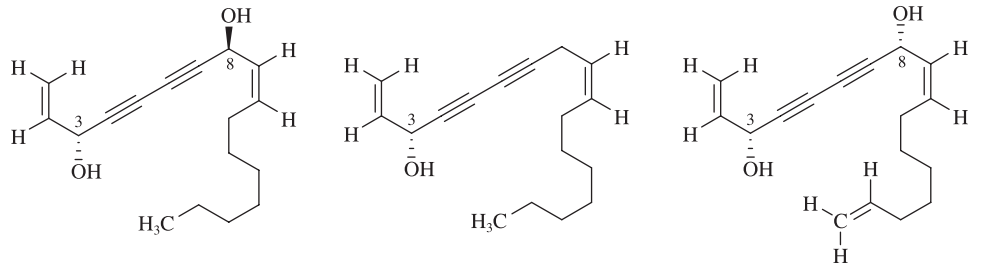

Figure 1. Polyacetylenes from *Levisticum officinale* and *Artemisia monosperma.*

Extraction and isolation. 650 g of dried roots was ground and underwent Soxhlet extraction giving 12.88 g of dichloromethane extract, 4 g of which was then separated on a silica gel 60 column (4 × 10 cm). The solvent composition was as follows: fr. 1–2 toluene/EtOEt/hexane/EtOAc (16:16:68:0.33 v/v), fr. 3–4 toluene/EtOEt/hexane/EtOAc (25:25:50:0.5), fr. 5–6 toluene/EtOEt/hexane/EtOAc (33:32:33:1), fr. 7–8 toluene/EtOEt/hexane (34:32:34) and fr. 9–10 methanol (100), flow rate 5 mL/min. Fractions were collected every 50 mL. Evaporated residues of fr. 4 and 8 exhibited significant antimycobacterial activity and were then separated on a Sephadex LH-20 column (1.3 × 62.5 cm), eluant dichloromethane/acetone (80:20), flow rate: 6 mL/min. 3(*R*)-falcarinol (**1**, 4.2 mg) was finally isolated from fr. 4 between 80 and 95 mL while 3(*R*)-8(*S*)-falcarindiol (**2**, 25.9 mg) was sampled between 117 and 130 mL from fr. 8. The purity of isolated compounds was monitored by TLC analysis, toluene/EtOEt/EtOAc (10:10:0.1 v/v). Both isolates gave a black coloration with vanillin–sulphuric acid reagent, R_f values: **1** = 0.9, **2** = 0.6.

Mycobacterial assay. *M. fortuitum* ATCC 6841 was obtained from the NCTC. *M. aurum* PI 104482 was obtained from the Pasteur Institute. The assay comprised a standard minimum inhibitory concentration (MIC) determination of test compounds in Ca^{2+} and Mg^{2+} adjusted Mueller-Hinton-Broth (MHB) (Gibbons and Udo, 2000). Plant extract and fractions were dissolved in DMSO and then diluted with MHB to particular concentrations. Reference antibiotics ethambutol (EMB) and isoniazid (INH) were used as positive controls and directly dissolved in MHB. The bacterial inoculum was prepared in normal saline (0.9%) by comparison with the 0.5 McFarland turbidity standard and further dilution to a final density of 5×10^5 cfu/mL. Mycobacterial strains were grown on Colombia blood agar (CBA) supplemented with 7% defibrinated horse blood (Oxoid, Hampshire). Dissolved plant extract, chromatographic fractions and antibiotics were serially diluted in a microtiter plate followed by the addition of 125 µL bacterial inoculum. The plate was incubated at 37 °C for 72 h (*M. fortuitum*) and 120 h (*M. aurum*) respectively. The MIC was recorded as the lowest concentration at which no bacterial growth could be observed. This was facilitated by the addition of 20 µL of a MTT (Sigma) solution (10 mg/mL in MeOH) to each well and incubated at 37 °C for 20 min. Bacterial growth was indicated by a blue coloration. Appropriate DMSO, growth and sterile controls were conducted.

RESULTS AND DISCUSSION

The dichloromethane extract from the roots of *L. officinale* exhibited significant antimycobacterial activity against *M. fortuitum* when tested in a microtiter plate dilution assay (MIC: 64 µg/mL). Further fractionation by CC on silica gel resulted in two active fractions both with an MIC of 32 µg/mL. Finally, using CC on Sephadex LH-20 two polyacetylenes, i.e. 3(*R*)-falcarinol (**1**) and 3(*R*)-8(*S*)-falcarindiol (**2**), Fig. 1, were obtained in a pure state, which represented the active principles of the dichloromethane extract of *L. officinale*. These natural products exhibited significant antimycobacterial activities against both species with the following MIC values: *M. fortuitum,* 30.4 µM (**1**) and 16.4 µM (**2**); *M. aurum*, 60.8 µM (**1**) and 16.4 µM (**2**). MICs of reference antibiotics were as follows: EMB: 115.5 µM (*M. fortuitum*) and 14.6 µM (*M. aurum*); INH: 3.4 µM (*M. fortuitum*) and 29.2 µM (*M. aurum*), respectively.

1 and **2** appeared as pale yellow oils. ^{1}H NMR analysis of **1** revealed an *exo*-cyclic methylene group indicated by olefinic signals at 5.25 and 5.48 ppm which showed a characteristic multiplet structure due to coupling with H-2 at 5.95 ppm (*ddd*). Another olefinic group was apparent due to multiplet signals at 5.39 and 5.52 ppm. Furthermore, the signal at 0.89 ppm showed a typical triplet structure associated with a chain ending methyl group. Both NMR and GC-MS data indicated the presence of falcarinol and are consistent with published data (Czepa and Hofmann, 2003). The optical rotation was determined as $[\alpha]_D^{22}$ – 33.1° (2.2 mg/mL, $CHCl_3$). Due to the negative rotation the absolute stereochemistry was assigned as 3 (*R*) in correspondence to the literature (Kobaisy *et al.*, 1997).

^{1}H NMR and ^{13}C NMR analysis of (**2**) revealed four quaternary carbons at δ_c: 79.9, 78.3 70.3 and 68.7 ppm, indicating a polyacetylene structure with two triple bonds. Signals in the ^{1}H and ^{13}C NMR spectra included a *cis*-double bond as well as two methine carbons bearing oxygen and three olefinic protons. The latter were coupled to each other in a ^{1}H-^{1}H COSY spectrum. The molecular weight was determined as $[M\text{-}H]^-$: 259 by APCI-MS in the negative ion mode. NMR and MS were consistent with the acetylene falcarindiol, which was previously published as a common component of Apiaceous plant roots (Furumi *et al.*, 1998; Lechner *et al.*, 2004). Stereochemical conformation of falcarindiol was analysed as 3(*R*)-8(*S*) by Mosher's

DOI: 10.1002/ptr

ester methodology according to the literature (Lechner *et al.*, 2004). The optical rotation was $[\alpha]_D^{22}$ + 243.8° (12.7 mg/mL, $CHCl_3$).

Polyacetylenes such as falcarinol and falcarindiol are widespread among the plant families of Apiaceae and Araliaceae (Kobaisy *et al.*, 1997). They exhibit a wide variety of different pharmacological effects including antibacterial, antifungal and antimycobacterial activities (Cichy *et al.*, 1984; Kobaisy *et al.*, 1997; Matsuura *et al.*, 1996; Stavri and Gibbons, 2005). Although the inhibitory effects of 3(*S*)-(+)-falcarinol, 3(*S*)-8(*S*)-(+)-falcarindiol and 3(*S*)-8(*R*)-falcarindiol against *M. tuberculosis* have been described previously, this is the first report on the antimycobacterial activity of 3(*R*)-(-)-falcarinol and its isolation from the roots of *L. officinale* (Kobaisy *et al.*, 1997; Lechner *et al.*, 2004). Santos *et al.* had reported the isolation of falcarinol from the roots *L. officinale*, however, the study did not provide stereochemical information on the compound (Santos *et al.*, 2005).

Interestingly, antimycobacterial properties of different stereoisomers of both falcarinol and falcarindiol had been observed, and it appears that the absolute stereochemistry does not have a significant impact on antimycobacterial activity and that stereoselective enzyme inhibition could be excluded as the active principle (Kobaisy *et al.*, 1997; Lechner *et al.*, 2004; Stavri *et al.*, 2005).

Further polyacetylenes with mycobactericidal properties are oplopandiol, oplopandiol acetate and 9,17-octadecadiene-12,14-diyne-1,11,16-triol (Kobaisy *et al.*, 1997).

So far the mechanism of antimycobacterial activities of polyynes remains unknown. Lipid membrane disruption, haemolysis of erythrocytes and destruction of clamydospores in *Mycocentrospora acerina* under the impact of falcarindiol has been observed previously (Garrod and Lewis, 1979). These observations indicate a possible interaction between bacterial cell wall components and polyynes, which might contribute to their antimycobacterial effect.

The study isolated and characterized 3(*R*),8(*R*)-(+)-dehydrofalcarindiol (**3**) (Fig. 1) from *Artemisia monosperma* (Stavri *et al.*, 2005), and this was tested against fast-growing strains of mycobacteria, including *M. fortuitum* and *M. aurum*, but this compound did not display any activity at 128 μg/mL. This is surprising given the high degree of similarity between this compound and falcarinol and falcarindiol. As the stereochemistry of alcohols in the chain seems to have little impact on antibacterial activity, it is highly likely that a terminal methyl group, which is present in falcarinol and falcarindiol (both active), and absent in dehydrofalcarindiol (inactive), is vital for antimycobacterial activity. Molecular modelling studies suggest that the presence of a hydrophobic group on the substituent of a polyacetylene moiety is crucial for antimicrobial activity (Zloh *et al.*, 2007). This indicates a specific mode of action for these compounds rather than a non-specific target such as membrane disruption. These compounds resemble unsaturated antibacterial fatty acids such as oleic and linoleic acids, which were recently shown to be active against fast-growing species of mycobacteria (Stavri *et al.*, 2004). Oleic and linoleic acids have been shown to inhibit unsaturated fatty acid biosynthesis in lactic acid bacteria (Weeks and Wakil, 1970) and it was hypothesized that the action of these polyacetylenes may be due to this mode of action.

Both falcarinol and falcarindiol exhibit significant *in vitro* cytotoxicity (Cunsolo *et al.*, 1993). Moreover, falcarinol but not falcarindiol was found to induce contact dermatitis even at a very low concentration (0.03%) (Hausen *et al.*, 1987; Machado *et al.*, 2002). Furthermore, no *in vivo* cytotoxicity in mice could be observed for falcarindiol up to a concentration of 25 mg/kg (Matsuda *et al.*, 1998). Additionally, intraperitoneal or oral application of falcarindiol in mice resulted in hepatoprotective effects due to a reduced serum GPT (glutamic–pyruvic transaminase) and GOT (glutamic–oxaloacetic transaminase) increase after D-galactosamine and lipopolysaccharide induced liver injury. While cicutoxin and aethusin, two polyacetylenic toxins from *Cicuta virosa*, caused a six-fold increase in the repolarization of giant cells RPD1 from *Lymnaea stagnalis* L., such an effect could not be observed for falcarinol and falcarindiol (Wittstock *et al.*, 1997). Both polyacetylenes are common in vegetables and part of our daily diet (Brandt and Christensen, 2000; Czepa and Hofmann, 2003) and their action as cancer protective agents has been discussed (Wang *et al.*, 2000). In summary the results indicate that polyacetylenes such as falcarinol and falcarindiol deserve further attention as potential sources of new antimycobacterial drugs. So far no antibiotic, using a polyyne structure as its active principle, has been developed. Without doubt polyynes are susceptible to oxidation and efficient drug delivery may be challenging. Nevertheless, further investigation should be performed on the elucidation of their mode of action in order to reveal new targets for new antimycobacterial antibiotics.

REFERENCES

Brandt K, Christensen P. 2000. Vegetables as Neutriceuticals – Falcarinol in carrots and other crops. In *Proceedings of Food and Cancer Prevention III Meeting: Dietary Anticancerogens and Antimutagens,* Johnson IT, Fenwick GR (eds). Royal Society of Chemistry: Cambridge, UK, 386–391.

Cichy M, Wray V, Hoefle G. 1984. New constituents of *Levisticum officinale* Koch. *Liebigs Ann Chem* **2**: 397–400.

Cunsolo F, Ruberto G, Amico V, Piattelli M. 1993. Bioactive metabolites from Sicilian marine fennel, *Crithmum maritimum*. *J Nat Prod* **56**: 1598–1600.

Czepa A, Hofmann T. 2003. Structural and sensory characterization of compounds contributing to the bitter off-taste of carrots (*Daucus carota* L.) and carrot puree. *J Agric Food Chem* **51**: 3865–3873.

Furumi K, Fujioka T, Fujii H *et al.* 1998. Novel antiproliferative falcarindiol furanocoumarin ethers from the root of *Angelica japonica*. *Bioorg Med Chem Lett* **8**: 93–96.

Garrod B, LE, Lewis BG. 1979. Studies on the mechanism of action of the antifungal compound falcarindiol. *New Phytol* **83**: 463–471.

Gautam R, Saklani A, Jachak SM. 2007. Indian medicinal plants as a source of antimycobacterial agents. *J Ethnopharmacol* **110**: 200–234.

Gibbons S. 2005. Plants as a source of bacterial resistance modulators and anti-infective agents. *Phytochem Rev* **4**: 63–78.

Gibbons S, Udo EE. 2000. The effect of reserpine, a modulator of multidrug efflux pumps, on the *in vitro* activity of

tetracycline against clinical isolates of methicillin resistant *Staphylococcus aureus* (MRSA) possessing the tet(K) determinant. *Phytother Res* **14**: 139–140.
Hausen BM, Broehan J, Koenig WA, Faasch H, Hahn H, Bruhn G. 1987. Allergic and irritant contact dermatitis from falcarinol and didehydrofalcarinol in common ivy (*Hedera helix* L.). *Contact Dermatitis* **17**: 1–9.
Kobaisy M, Abramowski Z, Lermer L *et al.* 1997. Antimycobacterial polyynes of Devil's Club (*Oplopanax horridus*), a North American native medicinal plant. *J Nat Prod* **60**: 1210–1213.
Lakely DL, Wright PW, Wallace RJ. 2001. Non-tuberculous mycobacteria. In *Tuberculosis: Current Concepts and Treatment,* Friedman LN (ed.). CRC Press: Boca Raton, 232–261.
Lechner D, Stavri M, Oluwatuyi M, Pereda-Miranda R, Gibbons S. 2004. The anti-staphylococcal activity of *Angelica dahurica* (Bai Zhi). *Phytochemistry* **65**: 331–335.
Machado S, Silva E, Massa A. 2002. Occupational allergic contact dermatitis from falcarinol. *Contact Dermatitis* **47**: 113–114.
Matsuda H, Murakami T, Kageura T *et al.* 1998. Hepatoprotective and nitric oxide production inhibitory activities of coumarin and polyacetylene constituents from the roots of *Angelica furcijuga*. *Bioorg Chem Lett* **8**: 2191–2196.
Matsuura H, Saxena G, Farmer SW, Hancock REW, Towers GHN. 1996. Antibacterial and antifungal polyyne compounds from *Glehnia littoralis*. *Planta Med* **66**: 256–259.
Santos PAG, Figueiredo AC, Oliveira MM *et al.* 2005. Growth and essential oil composition of hairy root cultures of *Levisticum officinale* W.D.J. Koch (lovage). *Plant Sci* **168**: 1089–1096.
Schinkovitz A, Gibbons S, Stavri M, Cocksedge MJ, Bucar F. 2003. Ostruthin: an antimycobacterial compound from the roots of *Peucedanum ostruthium*. *Planta Med* **69**: 369–371.
Stavri M, Ford CHJ, Bucar F *et al.* 2005. Bioactive constituents of *Artemisia monosperma*. *Phytochemistry* **66**: 233–239.
Stavri M, Gibbons S. 2005. The antimycobacterial constituents of Dill (*Anethum graveolens*). *Phytother Res* **19**: 938–941.
Stavri M, Schneider R, O'Donnell G, Lechner D, Bucar F, Gibbons S. 2004. The antimycobacterial components of hops (*Humulus lupulus*) and their dereplication. *Phytother Res* **18**: 774–776.
Wang CN, Shiao YJ, Kuo YH, Chen CC, Lin YL. 2000. Inducible nitric oxide synthase inhibitors from *Saposhnikovia divaricata* and *Panax quinquefolium*. *Planta Med* **66**: 644–647.
Weeks G, Wakil SJ. 1970. Studies on the control of fatty acid metabolism II. The inhibition of fatty acid synthesis in *Lactobacillus plantarum* by exogenous fatty acid. *J Biol Chem* **245**: 1913–1921.
Wittstock U, Lichtnow KH, Teuscher E. 1997. Effects of cicutoxin and related polyacetylenes from *Cicuta virosa* on neuronal action potentials. A comparative study on the mechanism of the convulsive action. *Planta Med* **63**: 120–124.
Zloh M, Bucar F, Gibbons S. 2007. Quantum chemical studies on structure activity relationship of natural product polyacetylenes. *Theor Chem Acc* **117**: 247–252.

DOI: 10.1002/ptr

Available online at www.sciencedirect.com
ScienceDirect
Tetrahedron 64 (2008) 1696–1702
Tetrahedron
www.elsevier.com/locate/tet

New metabolites with antibacterial activity from the marine angiosperm *Cymodocea nodosa*

Ioanna Kontiza [a], Michael Stavri [b], Mire Zloh [b], Constantinos Vagias [a], Simon Gibbons [b], Vassilios Roussis [a,*]

[a] *Department of Pharmacognosy and Chemistry of Natural Products, School of Pharmacy, University of Athens, Panepistimiopolis Zografou, Athens 15771, Greece*
[b] *Centre for Pharmacognosy and Phytotherapy, The School of Pharmacy, University of London, 29-39 Brunswick Square, London WC1N 1AX, UK*

Received 28 July 2007; received in revised form 19 November 2007; accepted 6 December 2007
Available online 8 December 2007

Abstract

Four new metabolites (**1**–**4**) have been isolated from the organic extract of the seagrass *Cymodocea nodosa*, collected at the coastal area of Porto Germeno, in Attica Greece. Compounds **1** and **2** belong to the structural class of diarylheptanoids, which have been found only once before in marine organisms [Kontiza, I.; Vagias, C.; Jakupovic, J.; Moreau, D.; Roussakis, C.; Roussis, V. *Tetrahedron Lett.* **2005**, *46*, 2845–2847]. Compound **3** is a new meroterpenoid, while compound **4**, to the best of our knowledge, is the first briarane diterpene isolated from seaweeds, and only the second analog of this class with a tricyclic skeleton. Furthermore metabolite **4** is the first brominated briarane diterpene. The structures and the relative stereochemistry of the new natural products were established by spectral data analyses. The new metabolites were submitted for evaluation of their antibacterial activity against multidrug-resistant (MDR) pathogens including methicillin-resistant (MRSA) strains of *Staphylococcus aureus*, as well as the rapidly growing mycobacteria, *Mycobacterium phlei*, *Mycobacterium smegmatis*, and *Mycobacterium fortuitum*.

Keywords: *Cymodocea nodosa*; Diarylheptanoids; Meroterpenoid; Briarane diterpene; Antibacterial activity

1. Introduction

The marine angiosperm *Cymodocea nodosa* (Ucria) Ascherson, significantly influences the local ecosystem by amplifying the primary substrate and by providing a spatially diverse nursery habitat structure and resources for algal and animal communities, many of which are commercially important.[2–4] *C. nodosa* is one of the six species in the Mediterranean Sea that are recognized as seagrasses. The seagrasses' contribution to global marine primary productivity and their role as 'structural' species in the marine biodiversity of coastal environments, have led to the inclusion of their habitat for protected ecosystems in the UNCED Action Paper (Agenda 21).

Despite the important ecological role of *C. nodosa* in the marine ecosystem, knowledge of its chemical content is limited. In particular, molecules frequently found in terrestrial plants such as caffeic acid, inositol, sucrose, monoglucoside of quercetin, monoglucoside of isoramnetin, cichoric acid, as well as polyamines like putrescine, spermidine, and spermine, have been reported as constituents of *C. nodosa* in the literature.[5–7] Furthermore, 24α-ethyl sterols and 24α-methyl sterols along with their 24β-epimers, cymodiene and cymodienol, the first diarylheptanoids isolated from marine organisms, comprise the total number of metabolites isolated from *C. nodosa*.[1,8] It is believed that *C. nodosa* originated from terrestrial ancestors and returned to the sea,[9,10] during the period of the ancient Tethys Sea, surrounded by Africa, Gondwanaland, and Asia, approximately 100 million years ago, thus explaining the 'terrestrial-like' chemical profile of the seagrass.

* Corresponding author.
E-mail address: roussis@pharm.uoa.gr (V. Roussis).

0040-4020/$ - see front matter © 2007 Elsevier Ltd. All rights reserved.
doi:10.1016/j.tet.2007.12.007

In the course of our ongoing research activities toward the isolation of bioactive metabolites from marine organisms from the Greek seas,[11,12] we were recently able to collect and analyze specimens of *C. nodosa* from the sandy marine plains of Porto Germeno near Athens. Herein, we report the isolation, structure elucidation, and antibacterial properties of two biphenyl compounds deoxycymodienol (**1**) and isocymodiene (**2**), the meroterpenoid nodosol (**3**), and the brominated briarane diterpene (1*S**,2*S**,3*S**,7*R**,8*S**,9*R**,11*R**,12*S**,14*R**)-7-bromo-tetradecahydro-12-hydroxy-1-isopropyl-8,12-dimethyl-4-methylenephenanthren-9,14-yl diacetate (**4**).

2. Results and discussion

C. nodosa specimens were collected and freeze dried during June of 2005 from the coastal area of Porto Germeno, and subsequently extracted exhaustively with a mixture of dichloromethane/methanol (3:1) to afford a brownish oily extract (27.1 g) that was subjected to fractionation with a combination of chromatographic techniques, such as vacuum liquid chromatography on silica gel (VLC), solid phase extraction (SPE), preparative TLC, and normal phase HPLC, to allow the isolation of (**1**) (2.3 mg), (**2**) (3.8 mg), (**3**) (2.3 mg), and (**4**) (1.2 mg) in pure form.

Compound **1** was isolated as a colorless oil. The $[M]^+$ ion at *m/z* 278.1298 observed in the high-resolution (HR) mass spectrum in combination with the ^{13}C NMR data indicated a molecular formula of $C_{19}H_{18}O_2$. The IR and UV bands at 1635 cm^{-1} and 295 nm, respectively, were characteristic for the presence of a benzene ring.[13,14] The presence of 16 aromatic/olefinic carbons in the ^{13}C NMR spectrum in combination with 11 degrees of unsaturation suggested a tricyclic structure. The 1D ^{13}C and DEPT NMR spectra revealed the presence of 3 methylene, 10 methine, and 6 quaternary carbons. Two deshielded carbons resonating at δ 150.0 and 150.9 ppm implied that they were each attached to an electronegative atom, such as oxygen. The doubly allylic protons at δ 3.50/3.25 ppm were coupled with the first proton of a diene system at δ 5.95 ppm. The spin system of the conjugated double bonds was clearly resolved by the $^1H-^1H$ COSY experiment, additionally showing the coupling of an allylic methylene (δ 2.88 and 2.40 ppm) with a second benzylic methylene (δ 2.60 and 2.88 ppm). The *E* and *Z* geometry of the double bonds is proposed on the basis of the coupling constants ($J_{2,3}$=15.5 Hz, $J_{4,5}$=11.0 Hz). Analysis of the 2D-heteronuclear experiments revealed the biphenyl system of two ABX aromatic spin systems. The observed long range heteronuclear correlations of H-1b with C-2′ and H-9, H-13 with C-7 (Table 1), the chemical shifts of the aromatic carbons, and the spectral similarities with metabolites alnusdiol and cymodienol (**5**) previously isolated from the tree *Alnus japonica* and from the seagrass *C. nodosa*, respectively,[15,1] confirmed the arrangement of the trisubstituted aromatic rings. On the basis of the above-mentioned data, along with conformational analysis performed using the Monte Carlo method and OPLS-AA force,[16,17] and the calculated ^1H and ^{13}C NMR shielding

Table 1
NMR data for deoxycymodienol (**1**) and isocymodiene (**2**)

Position	Deoxycymodienol (**1**)			Isocymodiene (**2**)			δ_H,[b] m, *J* (Hz)
	δ_H,[a] m, *J* (Hz)	δ_C[a]	HMBC[a]	δ_H,[a] m, *J* (Hz)	δ_C[a]	HMBC[a]	
1a	3.50, m	32.5	C-3	5.15, dd, 17.3, 1.6	115.6	C-2, C-3	5.12, dd, 17.3, 1.9
1b	3.25, m	32.5	C-2′	5.12, dd, 10.4, 1.6		C-2, C-3	5.01, dd, 10.4, 1.9
2	5.95, ddd, 7.9, 7.9, 15.5	136.5	C-1, C-3	5.97, ddd, 17.3, 10.4, 5.7	139.3	C-3	5.96, ddd, 17.3, 10.4, 5.7
3	6.78, dd, 15.5, 11.0	128.8	C-2	4.43, dd, 8.2, 5.7	42.1	C-1, C-2, C-4′, C-3′	4.65, dd, 8.2, 5.7
4	6.05, dd, 11.0, 10.7	128.1		5.53, dd, 10.7, 8.2	129.5	C-3, C-6	5.60, dd, 9.9, 8.2
5	5.40, m	131.8		5.60, ddd, 10.7, 7.6, 6.6	131.3	C-3	5.50, m
6a	2.88, m	28.2	C-7, C-5	2.40, ddd, 14.8, 7.6, 6.6	29.6	C-7, C-8, C-5, C-4	2.36, m
6b	2.40, m	28.2	C-7, C-5				
7a	2.60, m	31.7	C-6, C-8, C-5	2.58, m	34.7	C-6, C-8, C-13, C-9	2.48, m
7b	2.88, m	31.7	C-6, C-8, C-5				
8	—	129.7	—	—	133.9	—	—
9	7.21, d, 2.2	135.1	C-7, C-11, C-13	7.00, d, 8.5	129.5	C-7, C-13, C-11, C-10	6.89, d, 8.5
10	—	126.4	—	6.71, d, 8.5	115.2	C-8, C-11, C-12	6.71, d, 8.5
11	—	150.0	—	—	153.7	—	—
12	6.74, d, 8.1	114.7	C-10, C-11	6.71, d, 8.5	115.2	C-8, C-10, C-11	6.71, d, 8.5
13	6.97, dd, 2.2, 8.1	129.2	C-9, C-11, C-7	7.00, d, 8.5	129.5	C-7, C-9, C-12, C-11	6.89, d, 8.5
1′	—	133.8	—	—	154.0	—	—
2′	7.60, d, 2.5	139.7	C-1, C-3′, C-4′, C-6′	6.65, d, 0.9	114.6	C-4′, C-3, C-6′	6.88, d, 3.0
3′	—	126.2	—	—	130.1	—	—
4′	—	150.9	—	—	147.6	—	—
5′	6.63, d, 8.0	114.1	C-3′, C-4′	6.72 overlapped	117.1	C-3′, C-4′	6.50, d, 8.6
6′	7.04, dd, 2.5, 8.0	128.2	C-4′, C-2′	6.66 overlapped	112.4	C-4′, C-2′	6.57, dd, 8.6, 3.0
OH-C-4′	n.d.	—		n.d.	—		n.d.
OH-C-11	n.d.	—		4.67, br s	—	—	n.d.
OMe-C-1′	—	—		3.73, s	55.7	C-1′	3.36, s

[a] Measured in $CDCl_3$.
[b] Measured in C_6D_6, n.d.: not detected.

constants by pseudospectral methods[18] the structure of the (**1**) is diarylheptanoid deoxycymodienol proposed as shown in Figure 1. The calculated chemical shifts are: (a) for ^{1}H NMR: δ (ppm) 3.51 (H-1a), 2.90 (H-1b), 6.19 (H-2), 7.00 (H-3), 6.15 (H-4), 5.61 (H-5), 2.81 (H-6a), 2.51 (H-6b), 2.61 (H-7a), 2.91 (H-7b), 7.58 (H-9), 6.93 (H-12), 6.92 (H-13), 7.61 (H-2′), 6.72 (H-5′), 7.04 (H-6′); ^{13}C NMR: δ (ppm) 39.1 (C-1), 136.8 (C-2), 122.8 (C-3), 125.3 (C-4), 127.5 (C-5), 31.8 (C-6), 34.7 (C-7), 134.2 (C-8), 116.1 (C-9), 126.0 (C-10), 143.8 (C-11), 107.1 (C-12), 123.0 (C-13), 126.8 (C-1′), 135.2 (C-2′), 123.7 (C-3′), 149.2 (C-4′), 111.7 (C-5′), 124.4 (C-6).

Metabolite **2** was obtained as a colorless oil. The molecular formula deduced from the HRESIMS showing *m/z* 309.1485 ([M−H]$^-$) and ^{13}C NMR data was $C_{20}H_{22}O_3$. The intense absorbances in the IR spectrum at 3375 (broad band), 2922, and 1514 cm^{-1}, indicated the presence of an hydroxyl group, an *exo*-methylene double bond, and a benzene ring, respectively. Additionally, UV absorbances at 239 and 285 nm were indicative of the presence of a phenolic ring.[19] Seven overlapping aromatic protons along with five olefinic protons were observed in the ^{1}H NMR spectrum measured in $CDCl_3$. The ^{13}C NMR spectrum in combination with the DEPT spectrum revealed the presence of 5 quaternary, 11 tertiary, 3 secondary (one sp^2 and two sp^3), and 1 primary carbon. Additionally three quaternary carbons at δ 153.7, 154.0, and 147.6 ppm along with the primary carbon at δ 55.7 ppm, indicated the presence of phenolic rings and a methyl group. The significant spectral data similarities between metabolite **2** and the previously reported diarylheptanoid cymodiene,[1] drove us to the conclusion that they bear similar structures. When the ^{1}H NMR spectrum of **2** was recorded in C_6D_6, the shielding of aromatic protons led to a much better resolved set of peaks in the aromatic region. Two doublets at δ 6.89 and 6.71 (J=8.5 Hz) ppm each integrating for two protons, indicated a *para* substituted phenyl ring. The remaining aromatic signals required a 1,2,4-trisubstituted second aromatic ring. The spin system of the seven carbon chain linking the phenolic rings was clarified by the ^{1}H−^{1}H COSY correlations. The *Z* configuration of the second double bond (Δ_4) was deduced from the coupling constant of $J_{4,5}$=10.7 Hz. The heteronuclear correlation of the benzylic carbon at δ 34.7 ppm with the aromatic proton at δ 7.00 ppm secured the position of the disubstituted phenyl ring of metabolite **2**, and this new natural product is assigned the trivial name isocymodiene. The strong NOE effects (in C_6D_6) between the methoxy singlet and the *meta* coupled aromatic protons at δ 6.88 (d) and 6.57 (dd) ppm (Fig. 2), indicated the positions of the hydroxy and methoxy moieties on the second aromatic ring. All connectivities as presented above were confirmed by the HMBC data and are included in Table 1.

The HRFABMS ([M]$^+$ 228.1528) of metabolite **3**, a colorless oil, suggested a molecular formula of $C_{16}H_{20}O$. The ^{13}C NMR spectrum of **3** in $CDCl_3$ displayed 16 signals, including 12 signals in the aromatic/olefinic region. The resonances in the ^{1}H NMR spectrum at δ_H 4.79 (1H, br s), 5.09 (1H, br s), 5.03 (1H, d, J=17.5 Hz), and 4.98 (1H, d, J=10.6 Hz) ppm, in combination with the presence of two sp^2 secondary carbons at δ_C 110.8 and 115.8 ppm, as DEPT experiments indicated, confirmed the presence of two *exo*-methylene groups. The IR bands at 3400 and 1609 cm^{-1} suggested a phenolic ring, a fact that was also supported by the presence of an exchangeable signal at δ_H 4.59 ppm (br s). Two doublets at δ 6.70 (2H, d, J=8.8 Hz) and 7.33 (2H, d, J=8.8 Hz) ppm, indicated a *para* substituted phenyl ring. The seven degrees of unsaturation, in combination with the presence of a phenolic ring, two *exo*-methylene groups, and one trisubstituted double bond at δ_H 6.20 ppm (1H, s) and δ_C 122.7 ppm suggested a monocyclic skeleton for compound **3**. This evidence along with the existing literature,[20] drove us to the conclusion that metabolite **3** was a meroterpenoid. HMBC correlations between the chemically equivalent methyl groups at δ_H 1.22 ppm and the tertiary carbons at δ_C 42.8 and 149.0 ppm, fixed their position at the side chain. Furthermore the vinyl methyl at δ_H 1.77 ppm (3H, s) showed strong correlations with the tertiary carbons at δ_C 144.1 and 149.0 ppm, as well as with the secondary sp^2 carbon at δ_C 115.8 ppm, facts that secured the carbon sequence of the side chain. Meanwhile the strong NOE effects of the olefinic proton at δ_H 6.20 ppm and the vinyl methyl at δ_H 1.77 ppm with the aromatic proton at δ_H 7.33 ppm (Fig. 2), confirmed their proximity to the aromatic ring. Finally the *para* position of the hydroxyl group on the aromatic ring was clarified by its strong NOE correlation with the aromatic protons at δ_H 6.70 ppm and the chemical equivalence of the two pairs of aromatic protons as well as their *ortho* coupling (J=8.8 Hz) (Fig. 2). The new

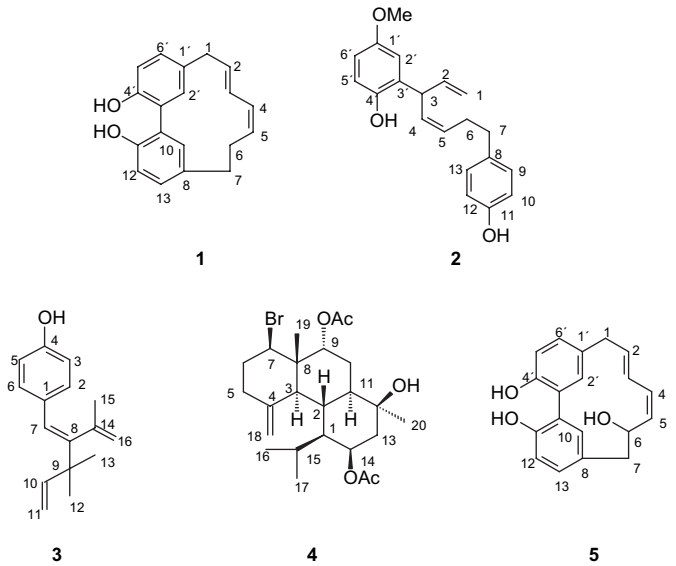

Figure 1. Metabolites isolated from *C. nodosa*.

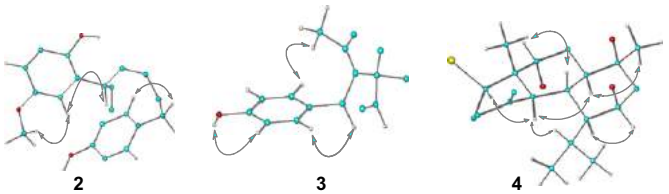

Figure 2. NOESY correlations of metabolites **2**–**4**.

Table 2
NMR data for nodosol (**3**) in $CDCl_3$

Position	δ_H, m, J (Hz)	δ_C	HMBC
1	—	130.7	
2	7.33, d, 8.8	129.9	C-4, C-6, C-3
3	6.70, d, 8.8	114.8	C-4, C-5, C-1
4	—	154.0	
5	6.70, d, 8.8	114.8	C-4, C-3, C-1
6	7.33, d, 8.8	129.9	C-4, C-2, C-5
7	6.20, s	122.7	C-6, C-2, C-8, C-14, C-9
8	—	149.0	
9	—	42.8	
10	5.91, dd, 17.5, 10.6	147.6	C-9, C-12, C-13
11a	5.03, d, 17.5	110.8	C-9, C-10
11b	4.98, d, 10.6	110.8	C-9, C-10
12	1.22, s	26.5	C-9, C-13, C-10
13	1.22, s	26.5	C-9, C-12, C-10
14	—	144.1	
15	1.77, s	24.7	C-16, C-8, C-14
16a	5.09, br s	115.8	C-8, C-9, C-15
16b	4.79, br s	115.8	C-8, C-9, C-15
OH-C-4	4.59, br s	—	C-4, C-3, C-5

meroterpenoid was named nodosol (**3**), and its spectral data are given in Table 2.

Metabolite **4** was purified by HPLC and was isolated as a colorless oil. Both ^{13}C NMR data and HRESIMS measurements supported the molecular formula $C_{24}H_{37}BrO_5$. The presence of one bromine atom was indicated by the EIMS exhibiting $[M-AcO]^+$ peaks at *m/z* 424 and 426 with intensities of 1:1. Furthermore the fragment at *m/z* 285, corresponding to $[M-2AcO-Br]^+$, in combination with a strong band in the IR spectrum at 1734 cm^{-1}, indicated the presence of two acetoxy groups. The ^{13}C NMR spectrum along with the DEPT experiments showed the presence of five quaternary, eight methine, five methylene, and six methyl carbon atoms. Among them, two were olefinic at δ_C 145.0 ppm (quaternary) and 109.4 ppm (secondary), suggesting the presence of an *exo*-methylene group, four of them were contributing to the two acetoxy groups (δ_C 21.2, 169.8, 21.7, and 169.6 ppm), and finally four were resonating in the chemical shift region of oxygenated/halogenated carbons (δ_C 75.6, 72.3, 71.0, and 59.0 ppm). Additionally the ^1H NMR spectrum revealed the presence of three oxygenated or halogenated methines at δ_H 5.05 (dd, J=3.8, 1.6 Hz), 5.31 (br s), and 4.37 (dd, J=12.1, 4.9 Hz) ppm, two secondary methyl groups at δ_H 0.58 (d, J=6.8 Hz) and 0.89 (d, J=6.8 Hz) ppm forming an isopropyl group and two methyls at δ_H 1.05 (s) and 0.85 (s) ppm situated on quaternary carbons. The presence of two acetoxy groups was also confirmed by two singlets at δ_H 2.11 and 2.06 ppm, each of them integrating for three protons, while the two broad singlets at δ_H 4.95 (1H) and 4.76 (1H) ppm were associated with the *exo*-methylene group. The NMR data of this compound (Table 3) were similar to those of briarane diterpenes, which have been isolated in the past from *Pennatulacea* and *Gorgonacea* octocorals, and a Mediterranean nudibranch.[21,22]

The six degrees of unsaturation, combined with the presence of one *exo*-methylene group and two acetoxy groups, suggested that compound **4** should be tricyclic. The HMBC

Table 3
NMR data for compound **4** in $CDCl_3$

Position	δ_H, m, J (Hz)	δ_C	HMBC	NOESY
1α	1.24, m	55.6	C-2, C-3, C-16, C-11	H-13α, H-3α, H-14α
2β	2.27, m	31.2	C-3, C-1	H-16, H-19
3α	2.00, m	47.7	C-7, C-1, C-18, C-4	H-11α, H-7α, H-1α, H-6α
4	—	145.0		
5α	2.11, m	35.7	C-3, C-7, C-18, C-4	
5β	2.29, m		C-3, C-7, C-4	H-19, H-6β
6α	2.34, m	38.3	C-7, C-5, C-8, C-18, C-4	H-3α
6β	2.08, m		C-5	H-5β
7α	4.37, dd, 12.1, 4.9	59.0		H-3α, H-6α, H-6β
8	—	44.2		
9β	5.05, dd, 3.8, 1.6	75.6	C-11	H-10β, H-19
10α	1.92, ddt, 14.8, 3.8, 3.8	23.5		H-11α
10β	1.74, ddd, 14.8, 14.8, 1.6		C-12	H-9β
11α	1.37, m	47.6		H-1α, H-3α, H-20, H-10α
12	—	72.3		
13α	1.60, dd, 14.9, 3.5	44.9	C-20	H-20
13β	2.01, m		C-14, C-1	H-20
14α	5.31, br s	71.0	C-12, C-2	H-13α, H-1α, H-13β, H-16, H-17
15	1.80, m	27.1	C-14, C-1	
16	0.58, d, 6.8	18.7	C-1, C-17	H-2β, H-18a, H-14α
17	0.89, d, 6.8	25.2	C-1, C-15, C-16	H-2β, H-14α
18a	4.76, s	109.4	C-3, C-4, C-6	H-2β, H-19, H-16
18b	4.95, s		C-3, C-6	H-5β
19	0.85, s	16.1	C-8, C-9, C-3, C-7	H-9β, H-10β, H-2β
20	1.05, s	27.8	C-11, C-12, C-13	H-11α, H-13α
MeCOO on C-14	2.06, s	21.7	C═O (C-14)	H-17
MeCOO on C-14	—	169.6		
MeCOO on C-9	2.11, s	21.2	C═O (C-9)	H-7α
MeCOO on C-9	—	169.8		

experiment revealed correlations between H_3-19 and C-8, C-3, C-7, and C-9, confirming the ring fusion between C-8 and C-3 as expected in briarane diterpenes. However, the cross peaks between H-11 and C-1 observed in the HMBC spectrum (see Table 3), in combination with the correlation between H-2 and H-11, which was shown in the $^1H-^1H$ COSY spectrum, along with the multiplicities of C-2 and C-11, suggested a bond between these carbons. This is the second naturally occurring briarane diterpene possessing such a ring fusion and the first case of a brominated briarane.[23] The relative stereochemistry for compound **4** was determined on the basis of the NOESY spectrum and $^1H-^1H$-coupling constants. In particular NOE enhancements between H_3-19 and H-9 possessing an equatorial configuration as its coupling constant (J=3.8, 1.6 Hz) suggested, confirmed their cis (β) configuration. Furthermore, observed NOE effects between H-3α and H-11α, H-7α, H-1α along with the NOE interactions between H-11α/H_3-20, H-1α/H-14α and H-14α/H-13α proved their cis (α) configuration and confirmed the trans-fusion of the rings at C-8/C-3 and C-11/C-2 (Fig. 2). Compound **4** is a new briarane diterpene named (1*S**,2*S**,3*S**,7*R**,8*S**,9*R**,11*R**,12*S**,14*R**)-7-bromo-tetradecahydro-12-hydroxy-1-isopropyl-8,12-dimethyl-4-methylenephenanthren-9,14-yl diacetate (**4**).

Metabolites (**1**–**5**) isolated from *C. nodosa* were assayed for evaluation of their antibacterial activity against multidrug-resistant (MDR) and methicillin-resistant strains of *Staphylococcus aureus* (MRSA) as well as rapidly growing mycobacteria, including *Mycobacterium phlei*, *Mycobacterium smegmatis*, and *Mycobacterium fortuitum*, which are used as an alternative screening model to *Mycobacterium tuberculosis* for evaluation of antitubercular drugs.[24] These species have obvious advantages over *M. tuberculosis* since they can be handled in class 2 microbiological laboratories and are fast growing strains, with a completion time for one assay of 72 h. The observed activity ranged from weak to strongly active. In general compounds **1**–**3** were found to be more active against MDR strains than against the standard *S. aureus* strain ATCC 25923. Specifically nodosol (**3**) was the most active compound in the assays (Table 4) leading to a threefold lower minimum inhibitory concentration (MIC) in comparison with that of tetracycline against the effluxing strain XU212 possessing the Tetk pump. A twofold lower MIC compared to that of the fluoroquinolone norfloxacin was observed for nodosol (**3**) against strain SA1199B possessing the NorA MDR efflux transporter, which is resistant to certain fluoroquinolones. The same metabolite (**3**) against RN4220, which possesses the MsrA macrolide efflux protein and is resistant to erythromycin, exhibited a fourfold lower MIC compared to that of erythromycin. The meroterpenoid bakuchiol isolated from the seeds of *Psoralea corylifolia*,[25] which shows similarities in its structure with nodosol (**3**), has exhibited in the past strong activity against different strains of *Streptococcus*.[26] During this study we had the opportunity to re-isolate the diarylheptanoid cymodienol (**5**), which has previously been shown to be cytotoxic against cancer cell lines A549 and NSCLC-N6-L16[1] and we have evaluated its antibacterial activity (Table 4). Deoxycymodienol (**1**) was slightly more active compared to cymodienol (**5**) against all examined strains. Isocymodiene (**2**) exhibited strong to moderate activity against MDR and MRSA strains of *S. aureus*. Compound **4** did not show any inhibition against any of the examined strains of *S. aureus*. In view of the constantly increasing number of fatal incidences attributed to MRSA[27] and the reported resistance to vancomycin and linezolid in MRSA,[28,29] further investigations in the diarylheptanoid and meroterpenoid chemical classes as antistaphylococcal leads should be continued.

Among the compounds tested, nodosol (**3**) displayed the most potent inhibitory activity with MIC value of 16 μg/ml against *M. fortuitum*, *M. phlei*, and *M. smegmatis* (Table 5). Cymodienol (**5**) has an additional hydroxyl group compared to metabolite **1** and showed no activity against *M. fortuitum*, which in comparison with the observed MIC (64 μg/ml) of deoxycymodienol (**1**) against the same strain, supports the hypothesis that polarity seems to influence the in vitro antimycobacterial activity previously reported in the literature.[30,31] Higher lipophilicity may hold a key role in the antimycobacterial activity, due to the lipophilic nature of the mycobacterial cell wall. In contrast to this against *M. phlei*, deoxycymodienol (**1**) exhibited a fourfold higher MIC in comparison to cymodienol (**5**). Isocymodiene (**2**) showed moderate activity against *M. fortuitum* and *M. phlei* with an MIC of 32 μg/ml. To the best of our knowledge this is the first report of antimycobacterial activity of diarylheptanoids. The simple structures of the meroterpenoid nodosol (**3**) and the diarylheptanoids, cymodienol (**5**), deoxycymodienol (**1**), and isocymodiene (**2**), make them feasible targets for the synthesis and chemical

Table 4
Minimum inhibitory concentrations (MIC)[a] of metabolites **1**–**5** against strains of *S. aureus*

Metabolite	Strain (resistance mechanism)					
	SA1199B (NorA)	RN4220 (MsrA)	XU212 (TetK, mecA)	ATCC 25923	EMRSA-15	CD-1281 (TetK)
1	32	32	32	32	n.t.	n.t.
5	64	64	64	64	64	64
2	32	64	64	64	n.t.	n.t.
3	16	16	16	16	16	16
4	>128	>128	>128	n.t.	n.t.	n.t.
Norfloxacin	32			0.5	0.5	
Erythromycin		128				
Tetracyclin			128			32

[a] All MICs (μg/ml) were determined in duplicate, n.t.: not tested.

Table 5
Minimum inhibitory concentrations (MIC)[a] of metabolites **1**–**5** against fast growing species of *Mycobacterium*

Metabolite	Strain		
	M. smegmatis	*M. fortuitum*	*M. phlei*
1	n.t.	64	64
5	128	>128	16
2	n.t.	32	32
3	16	16	16
4	n.t.	>128	>128
Ethambutol	0.5	8	2

[a] All MICs (μg/ml) were determined in duplicate, n.t.: not tested.

modification that can lead to optimization of their antibacterial activity.

3. Experimental section

3.1. General experimental procedures

Optical rotations were measured using a Perkin–Elmer model 341 polarimeter and a 10 cm cell. UV spectra were determined in spectroscopic grade CH_2Cl_2 and $CHCl_3$ on a Shimadzu UV-160A spectrophotometer. IR spectra were obtained using a Paragon 500 Perkin–Elmer spectrophotometer. NMR spectra were recorded using a Bruker AC 200, Bruker DRX 400, and Bruker Avance 500 MHz spectrometers. Chemical shifts are given on a δ (ppm) scale using TMS as internal standard. The 2D experiments ($^1H-^1H$ COSY, HMQC, HMBC, and NOESY) were performed using standard Bruker microprograms. High-resolution mass spectral data were provided by the University of Notre Dame, Department of Chemistry and Biochemistry, Notre Dame, Indiana, USA. EIMS data were recorded on a Hewlett Packard 5973 Mass Selective Detector. VCC separation was performed with Kieselgel 60H (Merck), TLC was performed with Kieselgel $60F_{254}$ aluminum support plates (Merck) and spots were detected with 15% H_2SO_4 in MeOH reagent. HPLC separation was conducted using a Pharmacia LKB 2248 model equipped with a refractive index detector RI GBC LC-1240 and a Spherisorb HPLC normal phase column, 25 cm×10 mm, S10W, 64,340 plates/meter.

3.2. Plant material

The seagrass was collected by hand at Porto Germeno in Corinthiakos Gulf in Greece, at a depth of 0.5–1 m during the summer of 2005. A voucher specimen is kept at the Herbarium of the Pharmacognosy Laboratory, University of Athens.

3.3. Extraction and isolation

The organism was initially freeze dried (1.16 kg dry weight) and then exhaustively extracted at room temperature with mixtures of CH_2Cl_2/MeOH (3:1). The organic extract, after vacuum evaporation of the solvents, afforded a brownish oily residue (27.1 g). The crude extract was subjected to VLC on silica gel using cyclohexane with increasing amounts of EtOAc and finally MeOH as eluants. Fractions eluted with 20% (A), 22% (B), 24% (C), and 32% (D) of EtOAc in cyclohexane were further purified. Fraction C was subjected to VLC on silica gel starting from 100% cyclohexane with increasing amounts of EtOAc. The fraction eluted with 50% EtOAc was further purified with reverse phase SPE, Phenomenex Strata silica (10 g/60 ml giga tubes) using a step gradient system from 100% H_2O to 100% MeOH, yielding 11 fractions. The fraction eluted with 100% MeOH contained compound **1** in pure form (2.3 mg). Fraction D was further purified by HPLC (column Spherisorb; S10W 25 cm×10 mm), using as mobile phase of cyclohexane/EtOAc (85:15) to yield pure compound **2** (3.8 mg), which had a retention time of 37.1 min (flow rate 2 ml/min). Fraction B was further purified with SPE, using a reverse-phase column (Phenomenex Strata silica, 10 g/60 ml giga tubes) starting from 100% H_2O with increasing amounts of MeOH. The fraction eluted with 100% MeOH was subjected to preparative TLC, using as mobile phase of cyclohexane/EtOAc (80:20) to finally afford compound **3** (2.3 mg) (R_f: 0.30). Finally fraction A was subjected again to VLC on silica gel using cyclohexane with increasing amounts of EtOAc. The fraction eluted with 30% EtOAc (A1) was subjected to normal phase HPLC, column Spherisorb; S10W 25 cm×10 mm), using as mobile phase cyclohexane/EtOAc (78:22), to yield pure compound **4** (1.2 mg), which had a retention time of 29.0 min (flow rate 2 ml/min).

3.3.1. Compound *1*

Colorless oil; UV (CH_2Cl_2) λ_{max} (log ε) 254.0 (0.39), 295.0 (0.10); IR (film) ν_{max} 3354, 2930, 1716, 1635, 1576, 1507, 1235 cm^{-1}; HREIMS: *m/z* $[M]^+$; 278.1298 ($C_{19}H_{18}O_2$, calcd 278.1302); NMR data (500 MHz; $CDCl_3$), see Table 1.

3.3.2. Compound *2*

Colorless oil; $[\alpha]_D^{25}$ +0.35 (*c* 0.06, CH_2Cl_2); UV ($CHCl_3$) λ_{max} (log ε) 285.0 (0.84), 239.0 (0.97), 229.0 (0.61); IR (film) ν_{max} 3375, 2922, 2851, 1716, 1643, 1514, 1202 cm^{-1}; HRESIMS: *m/z* $[M-H]^-$; 309.1485 ($C_{20}H_{21}O_3$, calcd 309.1496); NMR data (500 MHz; $CDCl_3$ and 500 MHz; C_6D_6) see Table 1.

3.3.3. Compound *3*

Colorless oil; UV (CH_2Cl_2) λ_{max} (log ε) 250 (3.7), 260.5 (3.8), 272.5 (2.8), 295.0 (2.7); IR (film) ν_{max} 3400, 2965, 1609, 1509 cm^{-1}; HRFABMS *m/z* 228.1528 $[M]^+$ ($C_{16}H_{20}O$, calcd 228.1514); NMR data (500 MHz; $CDCl_3$), see Table 2.

3.3.4. Compound *4*

Colorless oil; $[\alpha]_D^{25}$ +3.5 (*c* 0.06 CH_2Cl_2); UV (CH_2Cl_2) λ_{max} (log ε) 233 (2.2), 218 (2.7); IR (film) ν_{max} 2927, 1734 cm^{-1}; HRESIMS *m/z* 502.2163 $[M+NH_4]^+$ ($C_{24}H_{41}^{79}BrNO_5$, calcd 502.2155); NMR data (400 MHz; $CDCl_3$), see Table 3; EIMS 70 eV, *m/z* (rel int.): 424 $[M-AcO]^+$ (10), 366 (15), 285 $[M-2AcO-Br]^+$ (90), 267 $[M-2AcO-Br-H_2O]^+$ (60), 43 (100).

3.4. Bacterial strains

Ethambutol was used as a positive control for the mycobacterial strains, while for *S. aureus* strains the control antibiotics

norflorxacin, tetracycline, and erythromycin were employed. All antibiotics were obtained from the Sigma Chemical Co., *S. aureus* standard strain ATCC 25923 and tetracycline-resistant strain XU212, which is also an MRSA strain were provided by Dr. Edet Udo.[32] Strain SA1199B was provided by Professor Glenn Kaatz.[33] Strain RN4220 was provided by Dr. J. Cove.[34] Epidemic MRSA strain EMRSA-15, which accounts for the majority of MRSA bacteraemia in UK hospitals,[35] was obtained from Dr Paul Stapleton (ULSOP). Finally strain CD-1281 was generously provided as gift from Professor C. Dowson (University of Warwick, UK). Mycobacterial species were acquired from the NCTC.

3.5. Determination of MIC

S. aureus strains were cultured on nutrient agar and incubated for 24 h at 37 °C prior to MIC determination, while *Mycobacterium* strains were grown on Columbia blood agar (Oxoid) supplemented with 7% defibrinated Horse blood (Oxoid) and incubated for 72 h at 37 °C prior to MIC determination. Bacterial inocula equivalent to the 0.5 McFarland turbidity standard were prepared in normal saline and diluted to give a final inoculum density of 5×10^5 cfu/ml. Using Nunc 96-well microtitre plates, 125 μl of Mueller–Hinton broth (MHB) (Oxoid) were dispensed into wells 1–11. Test compound (125 μl) or the appropriate antibiotic were dispensed into well 1 and serially diluted across the plate leaving well 11 empty for the growth control. The final volume was dispensed into well 12, which being free of MHB or inoculum served as the sterile control. The inoculum (125 μl) was added to all wells and the microtitre plate was incubated at 37 °C for 72 h for *M. fortuitum*, *M. smegmatis*, and *M. phlei* and for 18 h for *S. aureus* strains. The MIC was recorded as the lowest concentration at which no bacterial growth was observed and this was enhanced by the addition of 20 μg/ml methanolic solution of 3-[4,5-dimethylthiazol-2-yl]-2,5-diphenyltetrazolium bromide (MTT; Sigma) to each of the wells followed by incubation at 37 °C for 20 min. A blue coloration indicated growth. No growth resulted in the well remaining yellow, as previously described.[32] Mueller–Hinton broth was adjusted to contain 20 and 10 mg/l of Ca^{2+} and Mg^{2+}, respectively.

Acknowledgements

Financial support by the 01ED146 PENED program from the Greek General Secretariat for Research and Technology is gratefully acknowledged.

References and notes

1. Kontiza, I.; Vagias, C.; Jakupovic, J.; Moreau, D.; Roussakis, C.; Roussis, V. *Tetrahedron Lett.* **2005**, *46*, 2845–2847.
2. Rismondo, A.; Curiel, D.; Marzocchi, M.; Scattoli, M. *Aquat. Bot.* **1997**, *58*, 55–64.
3. Cebrián, J.; Duarte, C. M.; Marbà, N. *J. Exp. Mar. Biol. Ecol.* **1996**, *204*, 103–111.
4. Guidetti, P.; Bussotti, S. *Ocean. Acta* **2000**, *23*, 759–770.
5. Cariello, L.; Zanetti, L.; De Stefano, S. *Comp. Biochem. Physiol.* **1979**, *62B*, 159–161.
6. Drew, E. A. *New Phytol.* **1978**, *81*, 249–264.
7. Marián, F. D.; Garcia-Jimenez, P.; Robaina, R. R. *Aquat. Bot.* **2000**, *68*, 179–184.
8. Sica, D.; Piccialli, V.; Massulo, A. *Phytochemistry* **1984**, *23*, 2609–2611.
9. Waycott, M.; Les, D. H. *Seagrass Biology: Proceedings of an International Workshop*; Kuo, J., Phillips, R. C., Walker, D. I., Kirkman, H., Eds.; University of Western Australia: Perth, 1996; pp 71–78.
10. Larkum, A. W. D.; den Hartog, C. *Biology of Seagrasses*; Larkum, A. W. D., Mc Comb, A. J., Shepherd, S. A., Eds.; Elsevier: Amsterdam, 1989; pp 112–156.
11. Iliopoulou, D.; Mihopoulos, N.; Vagias, C.; Papazafiri, P.; Roussis, V. *J. Org. Chem.* **2003**, *68*, 7667–7674.
12. Iliopoulou, D.; Vagias, C.; Galanakis, D.; Argyropoulos, D.; Roussis, V. *Org. Lett.* **2002**, *4*, 3263–3266.
13. Fuchino, H.; Satoh, T.; Shimizu, M.; Tanaka, N. *Chem. Pharm. Bull.* **1998**, *46*, 166–168.
14. Morihara, M.; Sakurai, N.; Inque, T.; Kawai, K.; Nagai, M. *Chem. Pharm. Bull.* **1997**, *45*, 820–823.
15. Nomura, M.; Tokoroyama, T.; Kubota, T. *Phytochemistry* **1981**, *20*, 1097–1104.
16. Kolossvary, I.; Guida, W. C. *J. Am. Chem. Soc.* **1996**, *118*, 5011–5019.
17. Jorgensen, W. L.; Maxwell, D. S.; Tirado-Rives, J. *J. Am. Chem. Soc.* **1996**, *118*, 11225–11236.
18. Cao, Y.; Beachy, M. D.; Braden, D. A.; Morrill, L. A.; Ringnalda, M. N.; Friesner, R. A. *J. Chem. Phys.* **2005**, *122*, 224116.
19. Kanada, N.; Kinghorn, D.; Farnsworth, R.; Tuchinda, P.; Udchachon, J.; Santisuk, T.; Reutrakul, V. *Phytochemistry* **1990**, *29*, 3366–3368.
20. Jiangning, L. G.; Xinchu, W.; Hou, W.; Qinghua, L.; Kaishun, B. *Food Chem.* **2005**, *91*, 287–292.
21. Hanson, J. R. *Nat. Prod. Rep.* **2004**, *21*, 785–793.
22. Zhang, W.; Guo, Y. W.; Mollo, E.; Cimino, G. *Helv. Chim. Acta* **2004**, *87*, 2341–2345.
23. Bowden, B. F.; Coll, J. C.; Vasilescu, I. M. *Aust. J. Chem.* **1989**, *42*, 1705–1726.
24. Gibbons, S.; Fallah, F.; Wright, C. W. *Phytother. Res.* **2003**, *17*, 434–436.
25. Mehta, G.; Nayak, U. R.; Sukh, D. *Tetrahedron* **1973**, *29*, 1119–1125.
26. Katsura, H.; Tsukiyama, R. I.; Suzuki, A.; Kobayashi, M. *Antimicrob. Agents Chemother.* **2001**, *45*, 3009–3013.
27. Enright, M. C. *Lancet* **2006**, *367*, 705–706.
28. Appelbaum, P. C.; Bozdogan, B. *Clin. Lab. Med.* **2004**, *24*, 381–402.
29. Tsiodras, S.; Gold, H. S.; Sakoulas, G.; Eliopoulos, G. M.; Wennersten, C.; Venkataraman, L.; Moellering, R. C.; Ferraro, M. J. *Lancet* **2001**, *358*, 207–208.
30. Haemers, A.; Leysen, D. C.; Bollaert, W.; Zhang, M.; Pattyn, S. R. *Antimicrob. Agents Chemother.* **1990**, *34*, 496–497.
31. Wube, A. A.; Bucar, F.; Gibbons, S.; Asres, K. *Phytochemistry* **2005**, *66*, 2309–2315.
32. Gibbons, S.; Udo, E. E. *Phytother. Res.* **2000**, *14*, 139–140.
33. Kaatz, G. W.; Seo, S. M.; Ruble, C. A. *Antimicrob. Agents Chemother.* **1993**, *37*, 1086–1094.
34. Ross, J. I.; Farrell, A. M.; Eady, E. A.; Cove, J. H.; Cunliffe, W. J. *J. Antimicrob. Chemother.* **1989**, *24*, 851–862.
35. Johnson, A. P.; Aucken, H. M.; Cavendish, S.; Ganner, M.; Wale, M. C. J.; Warner, M.; Livermore, D. M.; Cookson, B. D. *J. Antimicrob. Chemother.* **2001**, *48*, 143–144.

Chemical and Antibacterial Constituents of *Skimmia anquetelia*

Rajni Kant Sharma[1], **Devendra Singh Negi**[1], **Simon Gibbons**[2], **Hideaki Otsuka**[3]

[1] Department of Chemistry, HNB Garhwal University, Srinagar (Garhwal), Uttarakhand, India

[2] Centre for Pharmacognosy and Phytotherapy, The School of Pharmacy, University of London, London, U.K.

[3] Department of Pharmacognosy, Graduate School of Biomedical Sciences, Hiroshima University, Hiroshima, Japan

Abstract

Investigation of the leaves of *Skimmia anquetelia* (Rutaceae) led to the isolation of a new coumarin glucoside 7,8-dihdroxy-6-[3′-β-D-glucopyranosyloxy-2′(ξ)-hydroxy-3'-methylbutyl]-coumarin (**1**) together with five known coumarins: 6-(2,3-dihydroxy-3-methylbutyl)-7-methoxycoumarin (**2**), skimmin (**3**), osthol (**4**), esculetin (**5**) and scopuletin (**6**). The antibacterial activity of compounds **1** and **3** was also investigated against the plant bacterial pathogens *Agrobacterium tumifaciens*, *Pseudomonas syringae* and *Pactobacterium carotovorum*. Structures were determined on the basis of analyses of spectral evidence including 1D, 2 D NMR (COSY, HMQC, HMBC and NOESY) and mass spectroscopy.

Key words

Skimmia anquetelia · Rutaceae · coumarin glycosides · antibacterial activity

Supporting information available online at http://www.thieme-connect.de/ejournals/toc/plantamedica

The genus *Skimmia* is known to be a rich source of essential oils, coumarins and alkaloids and is widely distributed throughout the world [1], [2], [3]. *Skimmia anquetelia* is an aromatic, evergreen, glabrous shrub (ver. *nairpatti*) found in the subalpine region of the Garhwal Himalayas [4]. Previously some feed-deterrent and antitumor constituents have been reported from *Skimmia* species [5], [6]. In an examination of the constituents of *S. anquetelia*, a new coumarin glycoside along with five known coumarins has been isolated from the leaves. The present paper deals with the isolation, structure elucidation of the new coumarin glycoside **1** (**Fig. 1**) and the *in vitro* antibacterial activity of compounds **1** and **3** against plant pathogens.

The HR-ESI-MS of compound **1** revealed an *m/z* of 442.1722 corresponding to $C_{20}H_{26}O_{11}$ ($[M]^+$). A positive color test with alcoholic ferric chloride suggested the presence of a phenolic hydroxy group. The IR spectrum revealed absorption bands at 3470 for hydroxy and 1725 cm^{-1} for a lactonic carbonyl function. The ^{1}H-NMR spectrum of compound **1** substantiated the presence of a 3,4 unsubstituted coumarin nucleus. The ^{1}H-NMR spectrum revealed signals for 26 protons. Two downfield proton doublets at $\delta = 7.90$ ($J = 9.5$ Hz) and 6.19 ($J = 9.5$ Hz) were characteristic for H-4 and H-3 of a coumarin nucleus [9]. The assignment of these olefinic protons was also confirmed by a COSY spectrum in which H-3 ($\delta = 6.19$) showed a coupling with H-4 ($\delta = 7.90$). A sharp singlet at $\delta = 6.99$ was assigned to H-5 of the coumarin nucleus and this was further supported by the presence of a correlation between this hydrogen and H-4 in the NOESY spectrum. Two double-doublets at $\delta = 3.17$ and 3.38 were assigned to C-1′ methylene protons which showed vicinal coupling with H-2′. This H-2′ hydrogen ($\delta = 4.78$) resonated as a double doublet, due to vicinal coupling with both H-1′ hydrogens. Two methyl groups appeared as singlets at $\delta = 1.28$ and 1.24. A doublet resonating at 4.45 ($J = 8$ Hz) was assigned to an anomeric hydrogen of a sugar moiety with a β (axial) configuration. The ^{13}C-NMR spectrum of **1** along with the DEPT 135 spectrum revealed the presence of twenty carbons including two methylene, nine methine, two methyl and seven quaternary carbons. Downfield ^{13}C-NMR signals at $\delta = 145.2$ and 111.0 were assigned to the C-3 and C-4 olefinic carbons. Two methylene signals resonating at $\delta = 60.1$ and 29.7 could be ascribed to C-6″ and C-1′. The downfield shift of C-2′ ($\delta = 89.8$) was due to the presence of a hydroxy substituent. The nature of the side chain and the sugar position was investigated by COSY and HMBC correlation techniques (**Fig. 1**). The COSY spectrum showed that H-2′ was vicinally

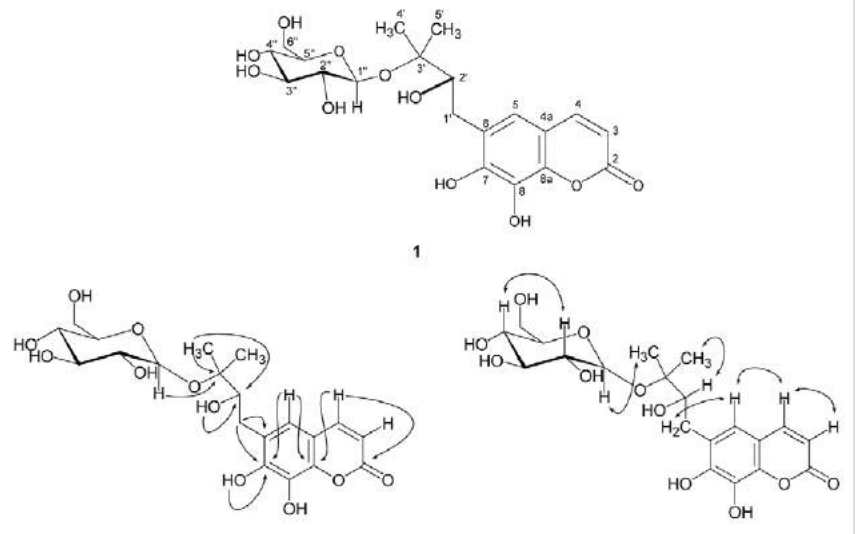

Fig. 1 Chemical structure, selected HMBC correlations (single-headed arrow) and NOESY correlations (double-headed arrow) for **1**.

coupled to CH_2 – 1′ methylene protons resonating at δ = 3.17. Inspection of the HMBC spectrum revealed a correlation between CH_2 – 1′ with C-6 suggesting that side chain must be positioned at the C-6 position of the coumarin nucleus. Other HMBC correlations are given in **Table 1**. The EI-MS of **1** gave a molecular ion peak at *m/z* = 442. The base peak was observed at *m/z* = 263 due to loss of a sugar moiety [M^+ – Glu – H]. Other fragments at *m/z* = 425 were due to the loss of a hydroxy group and at *m/z* = 246 [M^+ – Glu – H_2O] were also observed. Acid hydrolysis of **1** gave the aglycone and the sugar was identified as D-glucose by co-TLC with an authentic sample. The final placement of the glucose could be made by inspection of the HMBC spectrum. A correlation between H-1″ and C-3′ revealed that the glucose must be attached at position C-3′. On the basis of the above data the structure of **1** was established as 7,8-dihdroxy-6-[3′-*β*-D-glucopyranosyloxy-2′(*ξ*)-hydroxy-3′-methylbutyl]-coumarin and designated as skimminan.

The structural determination of the known coumarins **2** – **6** was made by comparison of the spectroscopic data with literature data (UV, IR, NMR and MS) for 6-(2,3-dihydroxy-3-methylbutyl)-7-methoxycoumarin **2** [7], skimmin **3** [8], osthol **4**, esculetin **5** and scopuletin **6** [3].

The antibacterial activity of the methanolic extract and compounds **1** and **3** was evaluated *in vitro* by using the disc diffusion method [9] with the three Gram-negative microorganisms as given in **Table 2**. Compound **1** showed antibacterial activity against the plant bacterial pathogens *Agrobacterium tumifaciens* MTCC 609, *Pseudomonas syringae* MTCC 1604 and *Pactobacterium carotovorum* MTCC 1428 whereas skimmin was found to be active against *A. tumifaciens* MTCC 609 only at a high concentration of 200 μg/disc.

Materials and Methods

IR spectra were determined on Perkin Elmer-157 instrument. The NMR spectra were recorded on Bruker AVANCE 500 (^{1}H 500 MHz; ^{13}C 125 MHz) and Jeol ARX (^{1}H 400 MHz; ^{13}C 100 MHz) spectrometers, with TMS as internal standard and deuterated DMSO-d_6, $CDCl_3$ or C_5D_5N as solvent. MS were taken at 70 eV on Micromass Quattro II and the Jeol SX-102 spectrometers. TLC was performed over plates made of silica gel G (Merck) and by spraying with sulphuric acid/water (5 : 95) followed by heating.

The plant material was collected from Tungnath Chopta, Chamoli, Uttarakhand, India at altitude of 3000 – 3200 meter in October 2004 and identified by Prof R. D. Gaur, a taxonomist from the Department of Botany HNB Garhwal University. The voucher specimen (8892 GUH) is deposited in the herbarium of the Department of Botany, HNB Garhwal University, Srinagar, 246 174, Uttarakhand, India.

In vitro antibacterial studies were carried out with disc diffusion method against three Gram-negative plant pathogens, *Pseudomonas syringae* MTCC 1604, *Agrobacterium tumifaciens* MTCC 609 and *Pactobacterium carotovorum* MTCC 1428 procured from IMTECH, India. The extract and compounds were dissolved in methanol and DMSO (Merck) and tested at concentration of 200 μg/disc. Pure solvent was used as negative control. *P. syringae* and *P. carotovorum* were grown in Nutrient Agar (HiMEDIA) while *A. tumifaciens* was grown in Trypticase Soy Agar media (HiMEDIA). Tetracycline hydrochloride (HiMEDIA) 30 μg and gentamicin sulphate (HiMEDIA) 10 μg were tested as positive controls. The experiments were repeated three times and results were expressed as average values.

Table 1 ^{1}H-, ^{13}C- and 2D-NMR data of **1** in DMSO-d_6

Position	δ_H (J = in Hz)	δ_C	COSY	HMBC	
				^{2}J	^{3}J
2	–	160.4	–	–	–
3	6.19 (d, *J* = 9.5)	111.0	4	C-2	C-4, 4a
4	7.90 (d, *J* = 9.5)	145.2	3	C-5	C-8, 8a, 2
5	6.99 s	114.1	–	C-4 ◦	C-4, 7, 8a
6	–	125.5	–	–	–
7	–	151.2	–	–	–
8	–	128.2	–	–	–
4a	–	113.0	–	–	–
8a	–	143.8	–	–	–
1′	3.38 (dd, *J* = 8.5, 14)	29.7	2′	C-2′, 6	C-5, 7
	3.18 (dd, *J* = 9, 14)				
2′	4.78 (dd, *J* = 3, 9)	89.9	1′	C-3′	C-6, 7
3′	–	48.6	–	–	–
4′	1.28 s	23.3	–	C-3″	C-2″
5′	1.24	21.8	–	–	C-2′
1″	4.45 (d, *J* = 8)	97.3	2″	C-2″	C-3″
2″	2.88 (dd, *J* = 5, 8.5)	73.5	1″, 3″	C-3″, 1″	–
3″	3.17 (t, *J* = 9.5)	76.4	4″	C-4″	C-5″
4″	3.05 (d, *J* = 9.5)	76.9	3″	C-3″	–
5″	4.03 (ddd, *J* = 5, 9.5)	70.0	4″, 6″	–	C-3″
6″	3.34 (dd, *J* = 5, 10.5)	60.1	5″	–	C-4′
	3.38 (d, *J* = 2, 10.5)				
OH-8	9.58	–	–	–	–
OH-7	4.81	–	–	C-6, 7′	–
OH-2′	4.84	–	–	C-1′	–

Table 2 *In vitro* antibacterial activities of *S. anquetelia* extract and compound **1** and **3** against plant bacterial pathogens (200 μg/disc)

Particular	Zone of inhibition (mm)[a*]		
	A. tumifaciens MTCC 609	*P. syringae* MTCC 1 604	*P. carotovorum* MTCC 1 428
Methanol extract[b*]	12.6 ± 0.8	8.4 ± 1.2	9.1 ± 0.3
Skimminan[b*] **1**	9.3 ± 0.5	9.1 ± 1.0	7.0 ± 0.2
Skimmin[b*] **3**	7.4 ± 0.3	Nil	Nil
Positive control	25.0 ± 0.3	22.0 ± 0.1	24.0 ± 0.8

[a*] Inhibition zone including the diameter of the paper disc (5 mm).

[b*] (200 μg/disc).

Values for zone of inhibition are presented as means of three replicate ± S.D. Nil = no zone inhibition.

The air-dried powdered leaves of *S. anquetelia* (3.4 kg) were exhaustively extracted with 90% ethanol (5 × 1000 mL, 24 h). The extract (134.2 g) obtained after removal of solvent under vacuum was partitioned with hexane to afford a hexane-soluble fraction F001 (26.4 g) and methanol-soluble fraction F002 (84.7 g). After removal of the solvent from the methanolic fraction, F002 was chromatographed over silica gel (800 g) and eluted with mixtures of $CHCl_3$/MeOH as eluents to give eight fractions F003 – F010 (98 : 2, 0.8 L; 96 : 4, 0.4 L; 92 : 8, 0.4 L; 9 : 1, 0.4 L; 88 : 12, 0.2 L; 85 : 15, 0.5 L; 88 : 12, 0.4 L; 4 : 1, 0.3 L; Frs of n-hexane/EtOAc mixtures (9 : 1, 0.4 L; 85 : 15, 0.6 L; Frs of 25 mL) yielding **2** (20 mg), **4** (48 mg), **5** (34 mg) and **6** (41 mg). Fraction F005 (248 mg, 0.4 L) was rechromatographed on silica gel (60 g) with $CHCl_3$/MeOH (92 : 8, 0.6 L; Frs of 20 mL) to afford crude compound (102 mg) again washed with MeOH to result in **3** (82 mg). Fraction F006 (357 mg, 0.4 L) was rechromatographed with $CHCl_3$/MeOH mixtures (9 : 1, 0.3 L; 88 : 12, 0.2 L; 85 : 15, 0.4 L; Frs of 10 mL) and yielded **1** (112 mg; 85 : 15, 0.4 L) as crude crystals that were further recrystallized in acetone to give **1** (98 mg).

Skimminan {7,8-dihdroxy-6-[3′-β-D-glucopyranosyloxy-2′(ξ)-hydroxy-3′-methylbutyl]-coumarin, **1**}: $C_{20}H_{24}O_{11}$, yellow crystals, m. p. 228 °C. IR (KBr): ν = 3478, 1725, 1594, 1326, 834 cm^{-1}; HR-ESI-MS: *m/z* = 442.1722, calcd. 442.1475; EI-MS: *m/z* (% int.) = 442 (48), 425 (8), 288 (23), 263 (100), 245 (6); ^{1}H- and ^{13}C-NMR data of **1** are listed in ▶ **Table 1**.

Acknowledgements

We are grateful to Kailash. N. Bhardwaj, Microbiology Section, Department of Botany, HNB Garhwal University, Srinagar (Garhwal), India for evaluation of antibacterial activity. Thanks are also due to DST, Govt. of India for financial support.

References

1 *Wu TS.* Alkaloids and coumarins of *Skimmia reevesiana.* Phytochemistry 1987; 26: 873 – 5
2 *Rahman AU, Sultana N, Choudhary MI, Shah PM, Khan MR.* Isolation and structural studies on the chemical constituents of *Skimmia laureola.* J Nat Prod 1998; 61: 713 – 7
3 *Razdan TK, Harkar S, Qadri B, Qurishi MA, Khuroo MA.* Lupene derivatives from *Skimmia laureola.* Phytochemistry 1988; 27: 1890 – 2
4 *Gaur RD.* Flora of the district Garhwal Northwest Himalaya, 1st edition. Srinagar: Trans Media Publication; 1999: 381 – 2
5 *Escoubas P, Fukushi Y, Lajide L, Mizutani J.* A new method for fast isolation of antifeedant compounds from complex mixture. J Chem Ecol 1992; 18: 1819 – 32
6 *Hashi M.* Antitumour effects and anticomplementary effects of tree polysaccharides. Bulletin of the Forestry and Forest Products Research Institute, Ibaraki 1991; 360: 121 – 48
7 *Joshi P, Shukla YN, Bhakuni DS, Dhar MM.* 6-(2,3-dihydroxy-3-methylbutyl)-7-methoxycoumarin, a new coumarin from *Micromelum pubescens.* Indian J Chem 1975; 13: 772 – 4.
8 *Reisch J, Achenbach SH.* A furocoumarin glucoside from stembark of *Skimmia japonica.* Phytochemistry 1992; 31: 4376 – 7
9 *Jorgensen JH, Turnidge JD, Wahington JA.* Antibacterial susceptibility tests: dilution and disc diffusion method. In: Hurray PR, editor. Manual of clinical microbiology Washington: ASM Press; 1999: 1526 – 43

received July 15, 2007
revised December 7, 2007
accepted December 10, 2007

Bibliography
DOI 10.1055/s-2008-1034281
Planta Med 2008; 74: 175–177

Published online January 31, 2008
ISSN 0032-0943

Correspondence
Dr. Devendra Singh Negi
Department of Chemistry
P.B. No. 75,
HNB Garhwal University
Srinagar (Garhwal)
Uttarakhand-246 174
India
Phone: +91-1370-267-994
Fax: +91-1346-252-174
devendra_negi@yahoo.com

PHYTOTHERAPY RESEARCH
Phytother. Res. **22**, 1356–1360 (2008)
Published online 20 June 2008 in Wiley InterScience
(www.interscience.wiley.com) **DOI**: 10.1002/ptr.2501

Antibacterial terpenes from the oleo-resin of *Commiphora molmol* (Engl.)

M. Mukhlesur Rahman[1], Mark Garvey[2], Laura J.V. Piddock[2] and Simon Gibbons[1]*

[1]Centre for Pharmacognosy and Phytotherapy, the School of Pharmacy, University of London, 29–39 Brunswick Square, London WC1N 1AX, UK
[2]Antimicrobial Agents Research Group, Division of Immunity and Infection, the Medical School, University of Birmingham, Birmingham, B15 2TT, UK

Two octanordammaranes, mansumbinone (1) and 3,4-*seco*-mansumbinoic acid (2), and two sesquiterpenes, β-elemene (3) and T-cadinol (4) have been isolated from the oleo-resin of *Commiphora molmol* (Engl.). The structures of these compounds were established unambiguously by a series of 1D and 2D-NMR analyses. We have also unambiguously assigned all ^{1}H and ^{13}C NMR resonances for 2 and revised its ^{13}C data. The crude extract of the oleo-resin of *C. molmol* displayed potentiation of ciprofloxacin and tetracycline against *S. aureus*, several *Salmonella enterica* serovar Typhimurium strains and two *K. pneumoniae* strains. The antibacterial activity of terpenes 1–4 was determined against a number of *Staphylococcus aureus* strains: SA1199B, ATCC25923, XU212, RN4220 and EMRSA15 and minimum inhibitory concentration (MIC) values were found to be in the range of 4–256 μg/ml. The highest activity was observed by the *seco*-A-ring octanordammarane 2 with an MIC of 4 μg/ml against SA1199B, a multidrug-resistant strain which over-expresses the NorA efflux transporter, the major characterized antibiotic pump in this species. This activity compared favorably to the antibiotic norfloxacin with an MIC of 32 μg/ml. Compound 2 also displayed weak potentiation of ciprofloxacin and tetracycline activity against strains of *Salmonella enterica* serovar Typhimurium SL1344 and L10. Copyright © 2008 John Wiley & Sons, Ltd.

Keywords: Commiphora molmol; Burseraceae; octanordammaranes; 3,4-*seco*-mansumbinoic acid; Antibacterial; *Staphylococcus aureus*; MRSA; *Salmonella enterica* ser. Typhimurium.

INTRODUCTION

Infections cause by multidrug- and methicillin-resistant *Staphylococcus aureus* (MRSA) are cause for some concern in the clinical environment. In the UK, MRSA has been headline news for the past few years, resulting in considerable public awareness of the potentially lethal consequences of an MRSA infection. According to the latest data from the Office for National Statistics in England and Wales there has been a dramatic increase in the number of death certificates that cite MRSA, with 1211 citations in 2001 rising to 2083 in 2005 (Office for National Statistics, 2007). Despite the release of agents such as linezolid, daptomycin and synercid, the ability of MRSA to acquire resistance necessitates further antibacterial discovery. As part of a continuing project to characterize new anti-staphylococcal agents (Smith *et al.*, 2007; Shiu and Gibbons, 2006), we have conducted bioassay-guided fractionation of the oleo-resin of *Commiphora molmol.*

Commiphora molmol Engl. (syn. *Commiphora myrrha* Holmes, *Balsamodendron myrrha*; (Burseraceae)) is a thorny shrub or small tree of approximately 3 m in height that is indigenous to the desert areas of Somalia, Ethiopia and parts of Kenya (van Wyk and Wink, 2004). The oleo-gum resin (oleo-resin) exudes from fissures or incisions in the bark and is collected as irregular masses. Myrrh is used as an aromatic for perfumes, funerals, and insect repellent. It is also used as an antiseptic and anti-inflammatory for the topical treatment of mouth and throat infections, including gingivitis and other gum diseases, tonsillitis and mouth ulcers (van Wyk and Wink, 2004). From the phytochemical perspective, myrrh is known to produce a number of sesquiterpenes from its essential oil (Brieskorn and Noble, 1983; El Ashry *et al.*, 2003; Marongiu *et al.*, 2005; Morteza-Semnani *et al.*, 2001; Zhu *et al.*, 2003).

Although bacteria can be multi-drug resistant (MDR) via multiple mechanisms of resistance, one single mechanism is particularly important i.e. the constitutive over-expression of chromosomally encoded efflux pumps (Piddock, 2006). As efflux pumps exist in antibiotic susceptible and resistant bacteria they are potential targets for novel non-antibiotic therapeutics. Inhibitors of various efflux pump systems have been described in the literature and typically these are plant alkaloids, but as yet no product has been marketed for use in human medicine (Lomovskaya and Bostain, 2006).

As a part of an effort to characterize new antibacterials with activity against effluxing MDR strains of *Staphylococcus aureus* and Enterobacteriaceae, we report the isolation of four terpenes (**1**–**4**) from the oleo-resin from the stems of *Commiphora molmol* (Engl.) as well as their anti-staphylococcal activity against a panel of drug-resistant *Staphylococcus aureus* strains. We have also unambiguously assigned all ^{1}H and ^{13}C NMR resonances for compound **2** and revised its ^{13}C data.

* Correspondence to: Professor Simon Gibbons, Centre for Pharmacognosy and Phytotherapy, the School of Pharmacy, University of London, 29–39 Brunswick Square London WC1N 1AX, UK.
E-mail: simon.gibbons@pharmacy.ac.uk

Received 12 December 2007
Accepted 29 December 2007

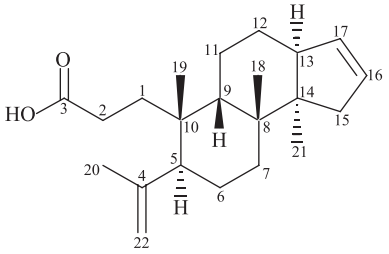

2

MATERIALS AND METHODS

General. NMR spectra were recorded on a Bruker AVANCE 500 MHz spectrometer. Chemical shifts values (δ) were reported in parts per million (ppm) relative to the appropriate internal solvent standard and coupling constants (J values) are given in Hertz. Vacuum-liquid chromatography (VLC) was carried out using Merck Si gel 60 H. TLC and preparative-TLC were conducted on normal-phase Merck Si gel 60 PF_{254} plates. Spots on TLC and PTLC plates were visualized after spraying with 1% vanillin-H_2SO_4 followed by heating at 110 °C for 5–10 min.

Plant material. The oleo-resin of *C. molmol* (Batch No. 19214; Origin North Africa) was purchased from Proline Botanicals, UK, in October 2006.

Extraction and isolation. 100 g of dried, ground resin of *C. molmol* was extracted with $CHCl_3$ at room temperature. The $CHCl_3$ extract (10.8 g) was fractionated by VLC on Silica gel 60H using a mobile phase of petroleum ether, EtOAc and MeOH in order of increasing polarity. The eluates were combined together on the basis of TLC analysis. Preparative TLC (100% hexane; double development) on the VLC fraction eluted with 5% EtOAc in petroleum ether afforded **3** (4.2 mg). VLC fractions eluted with 10–12.5% EtOAc in petroleum ether were further subjected to preparative-TLC (mobile phase, Toluene:EtOAc:Acetic Acid = 95:4:1, double development) to yield **1** (8.3 mg) and **4** (7.5 mg). Compound **2** (10.4 mg) was isolated from the VLC eluted with 20–25% EtOAc in petroleum ether followed by preparative TLC (mobile phase, Toluene: EtOAc:Acetic Acid = 90:9:1, double development).

Bacterial strains. The antibacterial assay was performed against a panel of multi-drug and methicillin-resistant strains of *Staphylococcus aureus*. *S. aureus* standard strain ATCC 25923 and tetracycline-resistant strain XU212 which possesses the TetK tetracycline efflux protein were provided by Dr Edet Udo (Gibbons and Udo, 2000). Strain SA-1199B which over-expresses the norA gene encoding the NorA MDR efflux pump was provided by Professor Glenn Kaatz (Kaatz *et al.*, 1993). Strain RN4220 which possesses the MsrA macrolide efflux protein was provided by Dr Jon Cove (Ross *et al.*, 1989). EMRSA-15 (Richardson and Reith, 1993) was the generous gift of Dr Paul Stapleton.

In addition, ten strains of *Salmonella enterica* serovar Typhimurium strains were used (Table 2). The strains consisted of *S.* Typhimurium L3, which was isolated from a patient prior to a course of ciprofloxacin, four post-therapy strains (L10–L18) were MDR (Piddock *et al.*, 2000); SL1344 isolated from calves (Wray and Sojka, 1986); two laboratory mutants of *S.* Typhimurium in which the *tolC* or *acrB* genes had been disrupted (Eaves *et al.*, 2004). In addition, one strain of *Staphylococcus aureus* (NCTC 8532), two strains of *Klebsiella pneumoniae* (NCTC 10896; NCTC 9633), one strain of *Enterobacter cloacae* (NCTC 10005), one strain of *Serratia marcescens* (NCTC 2847), one strain of *Providentia stuarti* (NCTC 10318), one strain of *Pseudomonas aeruginosa* (NCTC 10662) and two strains of *Escherichia coli* (NCTC 10418 and NCTC 10538) were used. All strains were grown on Iso-Sensitest medium (Unipath) aerobically at 37 °C for 18–24 h. All strains were stored on Protect™ beads (Technical Service Consultants, Lancashire, UK) at −80 °C.

Minimum inhibitory concentration (MIC) assay. The MIC of each antibiotic and disinfectant +/– the oleo-resin of *Commiphora molmol* or 3,4-*seco*-mansumbinoic acid (**2**) for each strain of Gram-negative bacteria was determined by the agar doubling dilution method according to the guidelines of the BSAC (Andrews, 2001). All antibiotics and disinfectants were made up and used according to the manufacturer's instructions: chloramphenicol, ciprofloxacin, norfloxacin, nalidixic acid and tetracycline (Sigma-Aldrich Company Ltd, Dorset, UK); triclosan (Gift from Ciba, Switzerland).

The MIC of each antibiotic and disinfectant +/– the plant extract *Commiphora molmol* for each strain of Gram-negative bacteria was also determined by the micro-broth dilution following the BSAC recommended protocol (Andrews, 2001).

All 5 *S. aureus* strains were cultured on nutrient agar (Oxoid) and incubated for 24 h at 37 °C prior to MIC determination. Norfloxacin was purchased from the Sigma Chemical Co. Mueller-Hinton broth (MHB; Oxoid) was adjusted to contain 20 and 10 mg/l of Ca^{2+} and Mg^{2+}, respectively. An inoculum density of 5×10^5 cfu of each of the test organisms was prepared in normal saline (9 g/l) by comparison with a 0.5 MacFarland standard. MHB (125 µl) was dispensed into 10 wells of a 96 well microtitre plate (Nunc, 0.3 ml volume per well). A stock solution of norfloxacin was prepared by dissolving the antibiotic in DMSO (Sigma) and dilution in MHB to give a final concentration of 0.625%. A DMSO control was included in all assays.

Compounds were serially diluted into each of the wells followed by the addition of the bacterial inoculum and the microtitre plate was incubated at 37 °C for 18 h. The MIC recorded the lowest concentration at which no growth was observed. This was facilitated by the addition of 20 µl of a 5 mg/ml methanolic solution of 3-[4,5-dimethylthiazol-2-yl]-2,5-diphenyltetrazolium bromide (MTT; Sigma) to each of the wells and incubation for 20 minutes. A blue colouration indicated bacterial growth.

All MICs were determined on at least three independent occasions.

RESULTS AND DISCUSSION

Chemistry

VLC fractionation of a chloroform extract of the oleo-resin from the stems of *Commiphora molmol* (Engl.)

Table 1. ^{1}H NMR (500 MHz), ^{13}C NMR (125 MHz) and HMBC (500 MHz) data of 2 in $CDCl_3$

Position	^{1}H	^{13}C	HMBC (H→C)	
			^{2}J	^{2}J
1	1.63, *m*	34.5	–	–
2	2.42, *m*	28.4	–	–
3	–	179.9	–	–
4	–	147.7	–	–
5	2.00, *dd*, *J* = 12.4, 2.7 Hz	51.2	C-4	C-7, C-19, C-20, C-22
6	1.38, *m*	25.0	–	–
7	1.65, *m*	34.4	–	–
8	–	39.8	–	–
9	1.88, *m*	41.7	–	C-5, C-12, C-19
10	–	39.5	–	–
11	1.73, *m*	22.6	–	–
12	1.46, *m*	24.0	–	–
13	2.77, *br d*, *J* = 12.4 Hz	47.9	–	C-16
14	–	53.6	–	–
15	2.38, *m*	40.2	–	–
16	5.67, *m*	130.2	C-15, C-17	C-13, C-14
17	5.60, *m*	134.2	C-13, C-16	C-14, C-15
18	1.08, *s*	17.2	–	C-7, C-9, C-14
19	0.88, *s*	20.2	C-10	C-1, C-5, C-9
20	1.75, *s*	23.4	C-4	C-5, C-22
21	1.03, *s*	18.1	C-14	C-13, C-8
22	4.69, *d*, *J* = 1.5 Hz 4.89, *d*, *J* = 1.5 Hz	113.7	C-4	C-5, C-20

yielded two octanordammaranes and two sesquiterpenes. By comparing the spectral data to those previously reported, the compounds were identified as β-elemene (**3**) (Adio *et al.*, 2004), T-cadinol (**4**) (Claeson *et al.*, 1991) and mansumbinone (**1**) (Provan and Waterman, 1986). The remaining octanordammarane was identified as 3,4-*seco*-mansumbinoic acid (**2**). Although the ^{1}H and ^{13}C NMR data of **2** was reported previously by Provan and Waterman (1986), there was ambiguity in the assignment of several carbon chemical shifts. A series of 1D and 2D NMR data including COSY, NOESY, HMQC and HMBC has enabled us to revise its ^{13}C NMR data here.

The ^{1}H NMR (500 MHz, $CDCl_3$, Table 1) of **2** showed the presence of an *exo*-methylene (4.69, *d*, *J* = 1.5 Hz; 4.89, *d*, *J* = 1.5 Hz), two olefinic hydrogens (5.60, *m*; 5.67, *m*), four methyl groups (0.88, *s*; 1.03, *s*; 1.08, *s*; 1.75, *s*) and a group of unresolved methine and methylene hydrogens. The ^{13}C NMR (125 MHz, $CDCl_3$, Table 1) of **2** exhibited a total of 22 carbons including a carboxylic acid (δ_C 179.9). The DEPT135 experiment revealed the presence of 8 methylene carbons including an *exo*-methylene at 113.7 ppm. In the HMBC spectrum (Table 1), a common ^{3}J correlation by two methyl groups resonating at 0.88 and 1.75 and the *exo*-methylene protons to a methine carbon at 51.2 ppm confirmed its assignment as C-5. Again, C-9 was assigned at 41.7 ppm by ^{3}J correlations from the methyl hydrogens at 1.08 (Me-18) and 0.88 (Me-19). The carbon chemical shifts of C-5 and C-9 were previously reported (Provan and Waterman, 1986) at 41.4 and 51.0, respectively, which we have revised here.

Provan and Waterman (1986) assigned the carbon chemical shifts of Me-19 and Me-20 at 19.9 and 23.1 and reported these to be interchangeable. However, we can confirm the assignment of Me-19 and Me-20 at 20.2 and 23.4, respectively. This was achieved by analysis of the HMBC spectra which revealed ^{3}J connectivities by both H-5 and H-9 to a methyl carbon at 20.2 (Me-19) and another ^{3}J correlation by H-5 and the *exo*-methylene protons to a carbon at 23.4 (Me-20). The assignments of C-16 and C-17 at 129.8 and 133.9 were also reported to be interchangeable by Provan and Waterman (1986). We were able to resolve this ambiguity by careful analysis of the HMBC (Table 1) and COSY spectra. A ^{3}J correlation between the hydrogens of methyl-21 and C-13 enabled assignment of H-13 (δ_H = 2.77, *br d*) *via* the HMQC spectrum. H-13 exhibited a COSY correlation to H-17 (δ_H 5.60) and its associated carbon resonance could be discerned by analysis of the HMQC spectrum (C-17; δ_C 134.2). H-17 was also coupled to H-16 (δ_H 5.67) and we were again able to identify C-16 on the basis of direct correlation observed in the HMQC spectrum (δ_C 130.2). We were therefore able to unambiguously revise the assignment of carbons C-16 and C-17 to 130.2 and 134.2, respectively. The chemical shifts of the remaining carbon resonances of **2** were almost identical to those described by Provan and Waterman (1986). Therefore, compound **2** was identified as 3,4-*seco*-mansumbinoic acid previously isolated from *Commiphora incisa*. Among these four compounds, this is the first time report of isolation of **1** and **2** from *C. molmol*.

Anti-staphylococcal activity

All compounds were assessed for their *in vitro* anti-staphylococcal activity in a MIC assay (Table 2). Among the sesquiterpenes and octanordammaranes, the most pronounced anti-staphylococcal activity was exhibited by compound **2**. Its highest potency was observed against the multi-drug-effluxing strain SA 1199B (MIC 4 μg/ml) and was found to be eight times more potent

DOI: 10.1002/ptr

Table 2. MICs of antibiotics and terpenes +/– CM to *S. Typhimurium*, *K. pneumoniae* and *S. aureus*.

				MIC μg/ml^{-1}								
Strain	Species	Description	Reference	cip	cip (+CM)	nor	nor (+CM)	tet	tet (+CM)	1	2	3	4
L354	*S.* Typhimurium	SL1344, commonly used UK strain	Wray & Sojka, 1978	0.03	0.03	0.25	0.25	2	2	nd	0.015	nd	nd
14028s	*S.* Typhimurium	Commonly used wild-type strain	Type strain	0.03	0.03	0.12	0.12	4	**2**	nd	nd	nd	nd
LT2	*S.* Typhimurium	Commonly used wild-type strain	Type strain	0.03	0.03	0.12	0.12	4	**2**	nd	nd	nd	nd
L3	*S.* Typhimurium	Human pre-therapy clinical isolate, susceptible	Piddock *et al.*, (2000)	0.03	**0.015**	0.06	0.06	1	1	nd	nd	nd	nd
L10	*S.* Typhimurium	Human post-therapy clinical isolate, *acrAB*$^{++}$	Piddock *et al.*, (2000)	0.25	**0.12**	0.5	0.5	16	**8**	nd	0.12	nd	nd
L12	*S.* Typhimurium	Human post-therapy clinical isolate	Piddock *et al.*, (2000)	0.5	0.5	2	2	8	**4**	nd	nd	nd	nd
L13	*S.* Typhimurium	Human post-therapy clinical isolate	Piddock *et al.*, (2000)	0.5	**0.25**	2	2	16	**8**	nd	nd	nd	nd
L18	*S.* Typhimurium	Human post-therapy clinical isolate, *acrAB*$^{++}$	Piddock *et al.*, (2000)	0.5	0.5	2	2	32	**16**	nd	nd	nd	nd
L108	*S.* Typhimurium	L354 *tolC::aph*	Buckley *et al.*, (2006)	0.008	0.008	0.06	**0.03**	1	1	nd	nd	nd	nd
L643	*S.* Typhimurium	L354 *acrB::aph*	Eaves *et al.*, (2004)	0.008	0.008	0.03	0.03	2	**1**	nd	nd	nd	nd
F77	*S. aureus*	NCTC 8532 type strain	Type strain	0.25	**0.12**	1	**0.5**	4	**2**	nd	nd	nd	nd
ATCC 25923	*S. aureus*	Commonly used wild-type strain	Type strain	nd	nd	1	nd	nd	nd	128	64	256	256
XU212	*S. aureus*	TetK tetracycline efflux protein	Gibbons and Udo, 2000	nd	nd	16	nd	nd	nd	64	32	128	128
SA-1199B	*S. aureus*	NorA MDR efflux pump	Kaatz *et al.*, 1993	nd	nd	32	nd	nd	nd	64	4	128	256
RN4220	*S. aureus*	MsrA macrolide efflux protein	Ross *et al.*, 1989	nd	nd	2	nd	nd	nd	256	16	64	64
EMRSA-15	*S. aureus*	Epidemic methicillin-resistant strain	Richardson and Reith, 1993	nd	nd	1	nd	nd	nd	128	16	128	64
H42	*K. pneumoniae*	NCTC 10896 type strain	Type strain	0.12	**0.06**	2	**0.5**	8	**4**	nd	nd	nd	nd
H43	*K. pneumoniae*	NCTC 9633 type strain	Type strain	0.25	**0.12**	2	**1**	8	**4**	nd	nd	nd	nd

Bold represents a reduction in the MIC of the antibiotic on the addition of *Commiphora molmol*. Cip, ciprofloxacin; nor, norfloxacin; tet, tetracycline. (+CM) = 200 μg/ml of *Commiphora molmol* added. *acrAB*$^{++}$, over-expression of the genes *acrAB*. nd, not determined.

DOI: 10.1002/ptr

than the control antibiotic norfloxacin. It is possible that this metabolite is a fatty acid mimic, possessing a carboxylic acid function due to the formation of the *seco*-A-ring moiety and **2** may interfere with biosynthesis of essential fatty acids.

Antibacterial activity for Gram-negative bacteria

The wild-type strains of *S.* Typhimurium (L354, 14028s and LT2) showed the typical susceptibility of this species to all agents tested (Table 2).

The oleo-resin of *C. molmol* (200 μg ml^{-1}) reduced the MIC of ciprofloxacin by 2-fold for the human pre-therapy isolate (L3), two of the post-therapy MDR strains (L10 and L13), *S. aureus* NCTC 8532 and *K. pneumoniae* NCTC 10896 and 9633 (Table 2). The oleo-resin of *C. molmol* had no affect on the MIC of ciprofloxacin on any of the other strains of Enterobacteriaceae tested (data not shown).

The oleo-resin of *C. molmol* (200 μg ml^{-1}) reduced the MIC of norfloxacin by 2-fold for the two laboratory mutants with the *tolC* (L108) or *acrB* (L643) genes disrupted; however it had no effect on any other of the *S.* Typhimurium strains. The oleo-resin reduced the MIC of norfloxacin by four 2-fold for *S. aureus* and the two *K. pneumoniae* strains (Table 2). However, no affect was observed on the MIC of norfloxacin on any of the other strains of Enterobacteriaceae tested (data not shown).

The oleo-resin of *C. molmol* (200 μg ml^{-1}) had a broader affect with tetracycline compared to the other agents tested (Table 2). The MIC of tetracycline was reduced by 2-fold in the presence of the oleo-resin (200 μg ml^{-1}) for the wild-type *S.* Typhimurium strains 14028s and LT2, the post therapy human isolates, L10, L12, L13 and L18, L643 with *acrB* disrupted, the *S. aureus* strain F77 and the two *K. pneumoniae* strains H42 and H43 (Table 2). As previously observed for norfloxacin, no affect was observed on the MIC of tetracycline on any of the other strains of Enterobacteriaceae tested (data not shown).

Out of the four compounds isolated from the oleo-resin of *C. molmol* only compound **2** displayed a weak 2-fold potentiation of ciprofloxacin and tetracycline against *S.* Typhimurium strains SL1344 and L10 (Table 2). No other Enterobacteriaceae were affected (data not shown).

Acknowledgement

We thank the Leverhulme Trust for the award of postdoctoral fellowships to M. M. Rahman and M. Garvey (Grant No. F/00094AR).

REFERENCES

Adio AM, Paul C, Kloth P, Konig WA. 2004. Sesquiterpenes of the liverwort *Scapania undulata*. *Phytochemistry*. **65**: 199–206.

Andrews JM. 2001. The development of the BSAC standardized method of disc diffusion testing. *J. Antimicrob Chemother*. **48**: 29–42.

Brieskorn CH, Noble P. 1983. Two furanoeudesmanes from the essential oil of myrrh. *Phytochemistry* **22**: 187–189.

Claeson P, Andensson R, Samuelsson G. 1991. T-Cadinol – a pharmacologically active constituent of scented myrrh – introductory pharmacological characterization and high-field ^{1}H-NMR and ^{13}C-NMR data. *Planta Med* **57**: 352–356.

El Ashry ESH, Rashed N, Salama OM, Saleh A. 2003. Components, therapeutic value and uses of myrrh. *Pharmazie* **58**: 163–168.

Eaves DJ, Ricci V, Piddock LJV. 2004. Expression of acrB, acrF, acrD, marA, and soxS in *Salmonella enterica* serovar Typhimurium: role in multiple antibiotic resistance. *Antimicrob Agents Chemother* **48**: 1145–1150.

Gibbons S, Udo EE. 2000. The effect of reserpine, a modulator of multidrug efflux pumps, on the in vitro activity of tetracycline against clinical isolates of methicillin-resistant *Staphylococcus aureus* (MRSA) possessing the tet(K) determinant. *Phytother Res* **14**: 139–140.

Kaatz GW, Seo SM, Ruble CA. 1993. Efflux-mediated fluoroquinolone resistance in *Staphylococcus aureus*. *Antimicrob Agents Chemother* **37**: 1086–1094.

Lomovskaya O, Bostian KA. 2006. Practical applications and feasibility of efflux pump inhibitors in the clinic-a vision for applied use. *Biochem Pharmacol* **71**: 910–918.

Marongiu B, Piras A, Porcedda S, Scorciapino A. 2005. Chemical composition of the essential oil and supercritical CO_2 extract of *Commiphora myrrha* (Nees) Engl. and of *Acorus calamus* L. *J Agric Food Chem* **53**: 7939–7943.

Morteza-Semnani K, Saeedi M. 2003. Constituents of the Essential Oil of *Commiphora myrrha* (Nees) Engl. var. *molmol*. *J Essent Oil Res* **15**: 50–51.

Office for National Statistics, 2007. Deaths involving MRSA and *Clostridium difficile* continue to rise. *Health Statistics Quarterly*, 22 February 1–3.

Piddock LJV. 2006. Clinically relevant chromosomally encoded multidrug resistance efflux pumps in bacteria. *Clin Microbiol Rev* **19**: 382–402.

Piddock LJV, White DG, Gensberg K, Pumbwe L, Griggs DJ. 2000. Evidence for an efflux pump mediating multiple antibiotic resistance in *Salmonella enterica* serovar Typhimurium. *Antimicrob Agents Chemother* **44**: 3118–3121.

Provan GJ, Waterman PG. 1986. Chemistry of the Burseraceae – the mansumbinanes – octanordammaranes from the resin of *Commiphora incise*. *Phytochemistry* **25**: 917–922.

Richardson JF, Reith S. 1993. Characterization of a strain of methicillin-resistant *Staphylococcus aureus* (EMRSA-15) by conventional and molecular methods. *J Hosp Infect* **25**: 45–52.

Ross JI, Farrell AM, Eady EA, Cove JH, Cunliffe WJ. 1989. Characterisation and molecular cloning of the novel macrolide streptogramin B resistance determinant from *Staphylococcus epidermidis*. *J Antimicrob Chemother* **24**: 851–862.

Shiu WKP, Gibbons S. 2006. Anti-staphylococcal acylphloroglucinols from *Hypericum beanii*. *Phytochemistry* **67**: 2568–2572.

Smith ECJ, Williamson EM, Kaatz GW, Gibbons S. 2007. Antibacterials and modulators from immature cones of *Chamaecyparis lawsoniana*. *Phytochemistry* **68**: 210–217.

Van Wyk B-E, Wink M. 2004. *Medicinal plants of the world an illustrated scientific guide to important medicinal plants and their uses*. Timber Press: Portland, Oregon.

Wray C, Sojka WJ. 1986. The serological responses of calves to live *Salmonella* dublin vaccine – a comparison of different serological tests. *J Biol Stand* **12**: 277–282.

Zhu N, Kikuzaki H, Sheng S, Sang S, Rafi MM, Wang M, Nakatani N, DiPaola RS, Rosen RT, Ho C-T. 2001. Furanosesquiterpenoids of *Commiphora myrrha*. *J Nat Prod* **64**: 1460–1462.

Available online at www.sciencedirect.com
ScienceDirect
Phytochemistry Letters 1 (2008) 49–53
PHYTOCHEMISTRY LETTERS
www.elsevier.com/locate/phytol

2β-Acetoxyferruginol—A new antibacterial abietane diterpene from the bark of *Prumnopitys andina*

Eileen C.J. Smith [a], Neale Wareham [b], Mire Zloh [c], Simon Gibbons [a,*]

[a] *Centre for Pharmacognosy and Phytotherapy, The School of Pharmacy, University of London, 29-39 Brunswick Square, London WC1N 1AX, UK*
[b] *Stiefel International R&D, Whitebrook Park, 68 Lower Cookham Road, Maidenhead, Berkshire SL6 8XY, UK*
[c] *Department of Pharmaceutical and Biological Chemistry, The School of Pharmacy, University of London, 29-39 Brunswick Square, London WC1N 1AX, UK*

Received 8 November 2007; received in revised form 12 December 2007; accepted 16 December 2007
Available online 1 February 2008

Abstract

As part of an on-going project to isolate antibacterial compounds from rare conifer species, a new abietane diterpene, 2β-acetoxyferruginol was isolated from the stem bark of *Prumnopitys andina*. Molecular modelling studies were conducted to explain some of the NOEs observed in the A-ring of this compound and to support assignment of relative stereochemistry. This new compound had antibacterial activity at 8 μg/ml against two effluxing strains of *Staphylococcus aureus*, but interestingly was inactive at 128 μg/ml against a wild-type strain and against a methicillin-resistant (MRSA) clinical isolate. We have previously demonstrated that ferruginol is active against these four *S. aureus* stains and therefore the results indicate that the presence of the acetoxy group has a detrimental effect on antibacterial activity against certain strains. 2β-Acetoxyferruginol was also assayed against *Propionibacterium acnes* and was active at 4 μg/ml.

Keywords: *Prumnopitys andina*; Diterpene; Antibacterial; *Staphylococcus aureus*; *Propionibacterium acnes*

1. Introduction

The needles, cones, oleoresin and bark of conifers have been used in traditional medicine by many cultures (Diğrak, Ilçim, & Alma, 1999; Langenheim, 2003; Ritch-Krc, Turner, & Towers, 1996), and are known to be a rich source of diterpenes, many of which have antibacterial properties. Multidrug-resistant staphylococci have become a major health risk and the need for new antibacterials is becoming increasingly urgent. As part of an on-going project to isolate antibacterial compounds from conifers, a new antibacterial abietane diterpene, 2β-acetoxyferruginol, was isolated from the stem bark of the rare conifer *Prumnopitys andina* Poepp. ex Endl. (Podocarpaceae). This species is indigenous to Chile and is also known as Chilean conifer or ''Ileuque'' by the indigenous Mapuche peoples of Chile (Mill & Quinn, 2001).

Compound **1** (Fig. 1) was isolated by bioassay-guided fractionation. The compound was tested against four strains of *Staphylococcus aureus*: one possessing the TetK efflux pump specific for tetracyclines; another strain overexpressing the multidrug-resistance transporter NorA; a wild-type ATCC strain and the epidemic methicillin-resistant hospital isolate EMRSA-15. The compound was also assayed against a standard strain of *Propionibacterium acnes* which is thought to be one of the major causative agents in the skin condition acne (Bojar & Holland, 2004). The minimum inhibitory concentrations (MICs) of the new diterpene are shown in Table 2 together with the MICs for ferruginol (Fig. 1) which we have previously tested against these same strains of *S. aureus* (Smith, Williamson, Wareham, Kaatz, & Gibbons, 2007) and which has been isolated from *P. andina* by Flores et al. (2002) who also evaluated ferruginol against standard strains.

2. Results and discussion

Bioassay-guided fractionation led to the isolation of compound **1** as a pale yellow oil. The GC–MS data indicated a molecular ion with a large peak at $[M]^+$ 344 *m/z* suggesting a possible formula of $C_{22}H_{32}O_3$. Examination of the ^{13}C NMR spectrum confirmed the presence of 22 carbons with signals at

* Corresponding author. Tel.: +44 207 7535913; fax: +44 207 7535909.
E-mail address: simon.gibbons@pharmacy.ac.uk (S. Gibbons).

1874-3900/$ – see front matter
doi:10.1016/j.phytol.2007.12.006

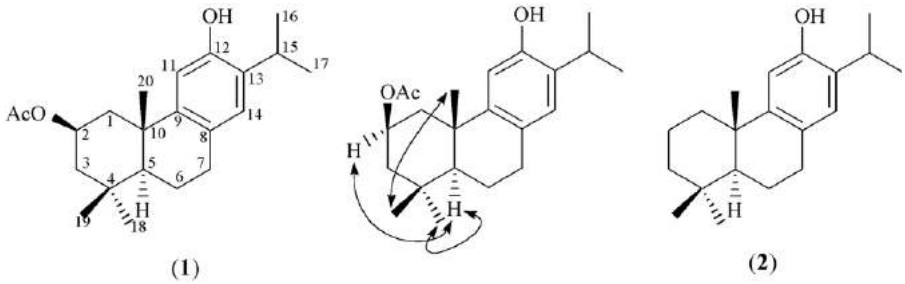

Fig. 1. 2β-Acetoxyferruginol (**1**) with key NOESY correlations and ferruginol (**2**).

170.6 and 70.7 ppm characteristic for the carbonyl carbon of an ester and for a carbon bound to an oxygen atom, respectively. From the IR spectrum, peaks at 1707 and 1247 cm^{-1} were indicative of an ester group with a broad absorption at 3403 cm^{-1} attributed to an hydroxyl group. Further observation of the mass spectrum revealed a small peak at $[M–Me]^+$ 329 *m/z* probably resulting from the loss of a methyl and a larger peak at 284 *m/z* probably due to loss of acetic acid $[M–AcOH]^+$. The base peak at 269 *m/z* was attributable to the loss of acetic acid and a methyl group $[M - AcOH - Me]^+$.

The ^1H NMR spectrum (Table 1) was characteristic of an abietane diterpene with a septet at δ 3.09 integrating for one hydrogen, suggesting the methine hydrogen of an isopropyl group and two methyl doublets at δ 1.20 and δ 1.22 completing this group. Signals at δ 150.8 in the carbon spectrum and at δ 4.46 in the proton spectrum were indicative of a phenolic hydroxyl group, with two singlets at δ 6.56 and δ 6.81 in the proton spectrum indicating *para* aromatic hydrogens. The ^1H and ^{13}C NMR spectra were very similar to those of the abietane diterpene ferruginol (**2**) (Wenkert et al., 1976).

Correlations seen in the HMBC experiment further substantiated that compound **1** was an abietane. From the HMBC spectrum, the isopropyl methine H-15 exhibited a ^2J correlation to C-13 and ^3J correlations to C-12 and C-14, with the methyl groups of the isopropyl (C-16, C-17) also showing ^3J correlations to C-13, which placed the isopropyl group at position 13 on the C-ring. H-11 exhibited a ^2J correlation to C-12 which bore the phenolic OH group and ^3J correlations to the aromatic carbons C-8 and C-13. The H-14 methine showed ^3J correlations to the isopropyl methine carbon (C-15) and to C-7 and also to the aromatic carbons C-9 and C-12. The position of carbon 6 was confirmed by the H_2-6 methylene which showed

Table 1
^1H (500 MHz) and ^{13}C (125 MHz) NMR spectral data and ^1H–^{13}C long-range correlations of **1** recorded in $CDCl_3$

Position	^1H (*J* in Hz)	^{13}C	^2J	^3J
1	1.81 d (4.5) 2.43 m	41.6	C-2, C-10	C-5, C-20
2	5.20 m	70.7		
3	1.46 dd (15.0 4.0) 1.83 ddd (14.5, 4.0, 1.5)	43.2		
4		32.7		
5	1.42 dd (12.0, 2.0)	49.3	C-6, C-10	C-19, C-20
6	1.73 m 1.88 m	19.0	C-5, C-7	C-8, C-10
7	2.76 ddd (17.0, 11.5, 7.0) 2.85 br dd (16.5, 6.0)	29.7	C-6, C-8	C-5, C-9, C-14
8		126.7		
9		148.3		
10		37.0		
11	6.56 s	111.3	C-12	C-8, C-10, C-13
12		150.8	C-12	C-11, C-13
13		131.7		
14	6.81 s	126.6		C-7, C-9, C-12, C-15
15	3.09 sept	27.0	C-13, C-16, C-17	C-12, C-14
16	1.20 d (7.0)	22.5[a]	C-15	C-13
17	1.22 d (7.0)	22.7[a]	C-15	C-13
18	0.97 s	33.6	C-4	C-3, C-5, C-19
19	1.07 s	23.3	C-4	C-3, C-5, C-18
20	1.34 s	26.8	C-10	C-1, C-5, C-9
21		170.6		
22	2.04 s	21.7	C-21	
OH(12)	4.46 s			

[a] Interchangeable values.

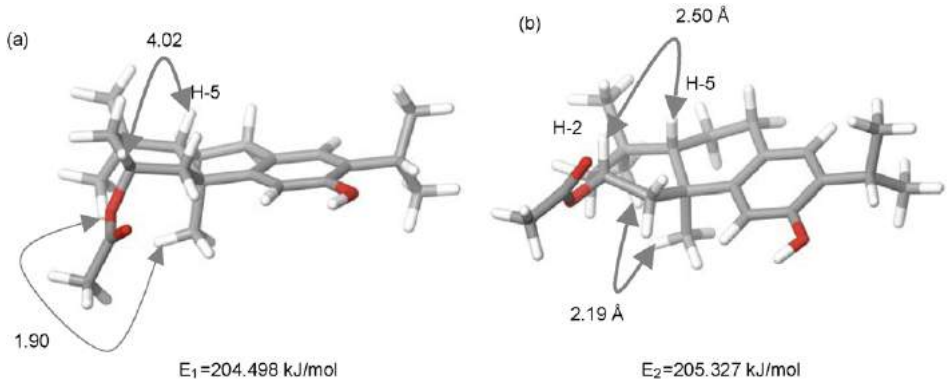

Fig. 2. Examples of low energy structures of 2β-acetoxyferruginol obtained by a conformational search with their total energies: (a) lowest energy conformer and (b) next lowest energy conformation. Arrows depict the distances that correspond to NOESY correlations.

^2J correlations to C-5 and C-7 and ^3J correlations to C-8 and C-10.

On the A-ring, two methyl groups attributed to C-18 and C-19 displayed ^2J connectivities to a quaternary carbon (C-4) and ^3J connectivities to C-3 and C-5. The H-5 methine in turn exhibited ^2J correlations to C-6 and C-10 and ^3J correlations to C-19 and C-20 methyl carbons. CH_3-20 displayed a ^2J correlation to C-10 at the A/B ring junction and ^3J correlations to C-1, C-5 and C-9. It could be seen from the carbon spectrum that an acetoxy group was attached to C-2 whose position was determined from $^1H \rightarrow {}^1H$ connectivities observed in the COSY spectrum. Couplings were detected between the C-2 methine and the methylene groups at C-1 and C-3. Carbon 1 also exhibited ^2J correlations (C-2, C-10) and ^3J correlations (C-5, C-20) in the HMBC experiment.

The relative stereochemistry of **1** was determined by NOE correlations observed in the NOESY spectrum (Fig. 1) and the observed coupling constants for H-5 in the ^1H spectrum. The H-5 methine had a large axial coupling (J = 12.0 Hz) to the axial H-6 proton and a small coupling (J = 2.0 Hz) to the H-6 equatorial proton. From the NOESY spectrum, a through space interaction was observed between the H_3-20 and H_3-19 methyls indicating that they were on the same face of the molecule. This relative stereochemistry was assigned a (β) orientation as reported in the literature for ferruginol (Wenkert et al., 1976). The methine proton H-5, assigned as (α), showed a NOE correlation to the CH_3-18 methyl group which would also have an (α) orientation. These data determined the A/B ring junction as *trans*. An NOE correlation between the H-2 and H-5 protons indicated that proton H-2 would have an (α) orientation suggesting a conformation for the A-ring that brings the two protons in close proximity (Fig. 1). This established that the acetoxy group at C-2 would have a relative (β) orientation and the compound was identified as a new abietane diterpene, 2β-acetoxyferruginol. Molecular modelling has confirmed the assignment of relative stereochemistry (Fig. 2), by observed distances between H-2 and H-5 for two different conformations of 4.02 and 2.50 Å. Both conformations can exist in solution simultaneously, where the rotation of acetoxy group changes the conformation of the A-ring and the energy difference between them is less than 1 kJ/mol. In both configurations the distance between H-2 and H-5 would lead to the appearance of a cross-peak in the NOESY spectrum.

The isolated compound, 2β-acetoxyferruginol was active only against the effluxing strains of *S. aureus* (8 μg/ml) in comparison with ferruginol which was active against all four strains at MIC values of 4–16 μg/ml (Table 2). This was a surprising result, since we have tested many diterpenes isolated from conifers against these strains and they have either been active against all strains or inactive against all strains. This is the first instance where a compound had activity against some strains but not against others. Strain XU212 has the TetK efflux pump and strain SA1199B over-expresses the NorA multidrug-resistance transporter. Both pumps are members of the major facilitator superfamily of efflux pumps and have 12 membrane-spanning helices (Marshall & Piddock, 1997). It is possible that 2β-acetoxyferruginol may bind to the pump substrate or to the pump itself; it may affect the conformation of the pump, or it could act at the level of transcription or translation and is therefore inactive against the wild-type and MRSA strains which do not express TetK or over-express NorA. However, this would imply that the mechanism of action of 2β-acetox-

Table 2
MICs (μg/ml) for 2β-acetoxyferruginol (**1**), ferruginol (**2**) and standard antibiotics (resistance mechanism)

Compound	ATCC 25923	XU212 (TetK)	SA1199B (NorA)	EMRSA-15 (*mecA*)	*Propionibacterium acnes* ATCC 6919
2β-Acetoxyferruginol (**1**)	>128	8	8	>128	4
Ferruginol (**2**)	8	8	4	16	4
Tetracycline	0.25	128	0.25	0.125	
Norfloxacin	1	16	32	0.5	
Oxacillin	0.125	128	0.25	32	
Clindamycin					0.125

yferruginol differs from that of ferruginol which is active against all four *S. aureus* strains. Another possibility is that the effluxing strains XU212 and SA1199B are susceptible to 2β-acetoxyferruginol due to a loss of fitness which can occur when a bacterium acquires a beneficial plasmid or over-expresses a particular protein. In the case of strain XU212, the *tetK* gene is carried on a plasmid which, once acquired confers resistance to tetracyclines, but in SA1199B the multidrug resistance mechanism is by over-expression of the indigenous NorA transporter due to increased transcription of the gene (Kaatz, Seo, & Ruble, 1993). Hence, the mechanisms by which these two strains have acquired resistance are not the same. In the case of EMRSA-15, methicillin-resistant strains have acquired the *mecA* gene which encodes the penicillin binding protein PBP2′. This gene is carried on the staphylococcal cassette chromosome (SCC) which also contains recombinase genes involved in the integration of *mecA* into the bacterial chromosome (Hiramatsu, Cui, Kuroda, & Ito, 2001). It might be expected that acquisition of resistance to methicillin could also lead to some loss in fitness.

It has often been suggested that phenolic compounds have a common mode of antibacterial action which is likely to be by disruption of the cell membrane, and that the effectiveness of such a compound is related to its ability to cross the bacterial cell membrane, which is determined by its lipophilic characteristics. The results seen for 2β-acetoxyferruginol (**1**), which was active against two effluxing strains of *S. aureus* but inactive against a wild-type and an MRSA strain, when compared with ferruginol which was active against all four strains, suggests that other factors may be involved.

3. Experimental

3.1. Extraction and isolation

The stem bark of *P. andina* was supplied by Bedgebury Pinetum, Goudhurst, Kent and a voucher specimen was placed in the herbarium at the School of Pharmacy (voucher specimen no. ECJS/020).

124 g of ground stem bark were sequentially extracted using 1 L of solvents of increasing polarity: hexane, chloroform, acetone, methanol. The active methanol fraction was subjected to preparative reverse-phase HPLC using an XTerra™ MS C_{18} 300 × 19 mm 10 μm column (www.waters.com). Elution commenced with 100% H_2O (0.1% acetic acid) going in a gradient to 100% methanol (0.1% acetic acid) over 25 min and was then held for 2 min. Seven fractions were collected; fraction 6 yielded compound **1** (2.6 mg) and fraction 7 yielded ferruginol (**2**) (Fig. 1).

3.2. Structure elucidation

GC–MS analysis was carried out using an Agilent 6890 GC coupled to an Agilent 5973 mass selective detector. An HP-5ms capillary column of 30 m length with a diameter of 250 μm was used with a non-polar stationary phase of 5% phenylmethylsiloxane and a film thickness of 0.25 μm. Samples were introduced into the system using split injection with a split ratio of between 5:1 and 10:1 and an injector temperature of 250 °C. Helium was used as the carrier gas at an average linear velocity of 50 cm/s. The initial oven temperature was 50 °C and the temperature was increased after 5 min at a rate of 5 °C to a maximum of 300 °C. The MS was run in EI mode.

1D and 2D NMR spectra were recorded on a Bruker AVANCE 500 MHz spectrometer and processed using XWin NMR 3.5 software. Samples were dissolved in deuterated-chloroform which was also used as the internal solvent standard and referenced to 7.26 ppm.

3.3. Molecular modelling

Molecular modelling calculations were carried out using Macromodel 9.11 (Mohamadi et al., 1990) and MMFFs force field (Cramer & Truhlar, 1995). The solvent effects of chloroform on the conformation were considered implicitly using the generalised Born/surface area continuum (GB/SA) method (Still, Tempczyk, Hawley, & Hendrickson, 1990) with a constant dielectric function ($\varepsilon = 1$). An extended non-bonded cutoff (van der Waals: 8 Å; electrostatics: 20 Å) was used. The conformational search was achieved by torsional sampling as implemented in Macromodel.

3.4. Antibacterial assay

A standard *S. aureus* strain ATCC 25923 and a clinical isolate (XU212), which possesses the TetK efflux pump, were obtained from Dr. E. Udo (Gibbons & Udo, 2000). Strain SA1199B which over-expresses the NorA MDR efflux pump was provided by Professor Glenn Kaatz. The clinical isolate EMRSA-15 (Richardson & Reith, 1993) was obtained from Dr. Paul Stapleton. *S. aureus* minimum inhibitory concentration (MIC) assays were carried out as previously described (Smith, Williamson, Zloh, & Gibbons, 2005). *P. acnes* standard strain ATCC 6919 was obtained from Oxoid (Basingstoke, UK). *P. acnes* inocula were prepared from a 72 h culture grown anaerobically on blood agar. MIC assays were carried out as for *S. aureus* but using anaerobe basal broth (Oxoid, Basingstoke, UK) and microtitre plates were incubated for 72 h under anaerobic conditions at 37 °C. The MICs for *P. acnes* were read visually and determined as the lowest concentration with an absence of turbid bacterial growth.

3.5. 2β-Acetoxyferruginol (*1*)

Pale yellow oil; λ_{max} (log ε): 287.0 (3.47) nm; IR: υ_{max} (thin film) cm^{-1}: 3403, 2958, 1707, 1418, 1379, 1247, 1186, 1028; ^1H NMR and ^{13}C NMR ($CDCl_3$): see Table 1; HR-ESIMS (*m/z*): 367.2251 $(M + Na]^+$ (calc. for $C_{22}H_{32}O_3Na$, 367.2249).

Acknowledgements

We thank Stiefel International R&D Ltd. for post-doctoral funding to E. Smith. The Engineering and Physical Sciences Research Council is thanked for a multi project equipment

grant (Grant No. GR/R47646/01). We also thank Bedgebury Pinetum, Goudhurst, Kent, UK for the supply of conifer material.

References

Bojar, R. A., & Holland, K. T. (2004). Acne and *Propionibacterium acnes*. *Clin. Dermatol., 22*, 375–379.

Cramer, C. J., & Truhlar, D. G. (1995). In K. B. Lipkowitz & D. B. Boyd (Eds.), *Rev. comp. ch.*. Vol. 6 (pp.1–72). New York: VCH.

Diğrak, M., Ilçim, A., & Alma, M. H. (1999). Antimicrobial activities of several parts of *Pinus brutia*, *Juniperus oxycedrus*, *Abies cilicia*, *Cedrus libani* and *Pinus nigra*. *Phytother. Res., 13*, 584–587.

Flores, C., Alarcon, J., Becerra, J., Bittner, M., Hoeneisen, M., & Silva, Y. M. (2002). Extractable compounds of native trees chemical and biological study I: Bark of *Prumnopytis andina* (Podocarpaceae) and *Austrocedrus chilensis* (Cupressaceae). *Bol. Soc. Chil. Qumm., 47*, 151–157.

Gibbons, S., & Udo, E. E. (2000). The effect of reserpine, a modulator of multidrug efflux pumps, on the *in vitro* activity of tetracycline against clinical isolates of methicillin resistant *Staphylococcus aureus* (MRSA) possessing the *tet*(K) determinant. *Phytother. Res., 14*, 139–140.

Hiramatsu, K., Cui, L., Kuroda, M., & Ito, T. (2001). The emergence and evolution of methicillin-resistant *Staphylococcus aureus*. *Trends Microbiol., 9*, 486–493.

Kaatz, G. W., Seo, S. M., & Ruble, C. A. (1993). Efflux-mediated fluoroquinolone resistance in *Staphylococcus aureus*. *Antimicrob. Agents Chemother., 37*, 1086–1094.

Langenheim, J. H. (2003). *Plant resins: Chemistry, evolution, ecology and ethnobotany.* Portland, Oregon, USA: Timber Press Inc.. (pp. 453–456).

Marshall, N. J., & Piddock, L. J. V. (1997). Antibacterial efflux systems. *Microbiologica, 13*, 285–300.

Mill, R. R., & Quinn, C. J. (2001). *Prumnopitys andina* reinstated as the correct name for ''Ileuque'', the Chilean conifer recently renamed *P. spicata* (*Podocarpaceae*). *Taxon, 50*, 1143–1154.

Mohamadi, F., Richards, N., Guida, W., Liskamp, R., Lipton, M., Caulfield, C., et al. (1990). MacroModel—an integrated software system for modeling organic and bioorganic molecules using molecular mechanics. *J. Comput. Chem., 11*, 440–467.

Richardson, J. F., & Reith, S. (1993). Characterisation of a strain of methicillin-resistant *Staphylococcus aureus* (EMRSA-15) by conventional and molecular methods. *J. Hosp. Infect., 25*, 45–52.

Ritch-Krc, E. M., Turner, N. J., & Towers, G. H. N. (1996). Carrier herbal medicine: An evaluation of the antimicrobial and anticancer activity in some frequently used remedies. *J. Ethnopharmacol., 52*, 151–156.

Smith, E., Williamson, E., Zloh, M., & Gibbons, S. (2005). Isopimaric acid from *Pinus nigra* shows activity against multidrug-resistant and EMRSA strains of *Staphylococcus aureus*. *Phytother. Res., 19*, 538–542.

Smith, E. C. J., Williamson, E. M., Wareham, N., Kaatz, G. W., & Gibbons, S. (2007). Antibacterials and modulators of bacterial resistance from the immature cones of *Chamaecyparis lawsoniana*. *Phytochemistry, 68*, 210–217.

Still, W. C., Tempczyk, A., Hawley, R. C., & Hendrickson, T. (1990). Semianalytical treatment of solvation for molecular mechanics and dynamics. *J. Am. Chem. Soc., 112*, 6127–6129.

Wenkert, E., Buckwalter, B. L., Burfitt, I. R., Gašic, M. J., Gottlieb, H. E., Hagaman, E. W., et al. (1976). Carbon-13 nuclear magnetic resonance spectroscopy of naturally occurring substances. In G. C. Levy (Ed.), *Topics in Carbon-13 NMR spectroscopy* (pp. 98–100). John Wiley & Sons Inc.. (Chapter 2).

Inhibitory Activities of Lichen-Derived Compounds against Methicillin- and Multidrug-Resistant *Staphylococcus aureus*

Tetsuo Kokubun[1], Winnie Ka Po Shiu[2], Simon Gibbons[2]

Abstract

The inhibitory effects of selected phenolic lichen substances were tested against a panel of methicillin- and multidrug-resistant *Staphylococcus aureus*. Depsidones with long alkyl chains on both of the aromatic rings were consistently active against the strains tested, comparable to or better than the level of clinically used antibacterial drugs. A similar level of activity was also observed for rhizocarpic acid. The previously described cytotoxic pentacyclic compound hybocarpone was by far the most active, exhibiting minimum inhibitory concentrations (MICs) of 4 – 8 μg/mL (8.13 – 16.3 μM) against a range of multidrug efflux pump expressing strains of *S. aureus*.

Supporting information available online at http://www.thieme-connect.de/ejournals/toc/plantamedica

Letter

Methicillin-resistant *Staphylococcus aureus* (MRSA) and multidrug-resistant (MDR) variants of this species are necessitating the search for new classes of anti-staphylococcal agents. MDR strains are of particular concern as they over-express efflux mechanisms, for example, the TetK efflux pump, which export particular classes of antibiotic, or true MDR pumps such as the NorA system which has broad substrate specificity and extrudes fluoroquinolones, detergents and dyes [1]. New antibacterials are therefore needed which are opaque to these mechanisms of resistance or which exert their antibacterial action by a new mode of action, therefore increasing the potential lifetime of the antibacterial class. As part of a continuing project to characterise new antibacterial templates from plants, we have been evaluating a range of lichen natural products which display moderate to good activity against MRSA and effluxing strains.

Lichens are best recognised as a microecological form of fungi, where fungal and algal partners form symbiotic relationships [2]. As many as 18,000 species of mainly Ascomycetes (i.e., approx. 40% of all known Ascomycetes) are known to form lichens [2]. They produce a number of secondary metabolites collectively known as lichen substances that are virtually unique to this group of fungi. The majority of lichen substances are believed to be produced by the fungal partners which account for approximately 80 to 90% of the body mass; however, available evidence suggests that the algae may influence the overall chemical profile of the resultant lichens [3]. Currently over 800 compounds are known, yet with the exception of a very small number of compounds and whole lichen extracts, lichen substances are generally poorly studied and are a relatively untapped resource for medicinal use [3], [4]. The biggest challenge that underlines this is the supply problem and the relative inaccessibility to a large quantity of material with a constant chemical profile [3]. Artificial culturing on various media has been achieved but lichen growth is generally slow so that it requires several months to years before a compound can be extracted [5], [6].

We have examined selected lichen substances for their activity against strains of MRSA, including two hospital isolates, exhibiting resistance to existing antibacterial drugs. The lichen substances were obtained from naturally growing lichen thalli collected from various parts of the UK as detailed below.

The experiment was conducted in two stages. In the initial testing, compound **1** – **5** (Fig. **1**) were examined against the multidrug-resistant SA-1199B, which over-expresses the NorA MDR efflux transporter that confers resistance to certain fluoroquinolones including norfloxacin (Table **1**). These compounds have previously been tested in other laboratories using various species and strains of bacteria and exhibited various degrees of activity [7], [8], [9], [10]. Evernic acid **2** showed very weak activity, as opposed to the reported result on this compound [9]. This discrepancy may be attributed to the different assay methods employed (paper disk diffusion), beside the presumed susceptibility of the previous strain. The activity of physcion (**1**) (inactive at 256 μg/mL, equivalent to 901 μM) is consistent with the reported MIC of 320 μg/mL (1128 μM) [7]. The β-orcinol depsidone (**4**) was found to be inactive at the maximum concentration attainable for the compound in the test system (512 μg/mL, 1320 μM).

The most encouraging result was obtained with lobaric acid (**5**), which has one C_5-alkyl chain on each of the aromatic rings. To explore and confirm that this structural feature is a requirement of activity, two further compounds with a similar overall structure were included in the following stage of the testing, in addition to rhizocarpic acid (**8**) and hybocarpone (**9**), for which there has been no report on antimicrobial activity, and usnic acid (**10**). The MICs of compounds **5** – **10** (Fig. **1**) against 5 further strains of *S. aureus*, including two epidemic MRSA strains in the UK (EMRSA-15 and -16) are presented in Table **1**.

Lobaric acid (**5**) displayed an MIC of 8 μg/mL (17.5 μM) against SA-1199B which is consistent with the previous determination, but it was less effective against all the other strains including the standard norfloxacin-susceptible strain ATCC 25923. The three depsidones **5** – **7** showed similar activities to each other. The weaker activity of 3-hydroxyphysodic acid (**7**) when compared to physodic acid (**6**) may be due to the difference in the partition coefficients, being less lipophilic and bioavailable. The effect of a free carboxylic acid moiety on activity, resulting in an increase in acidity, possibly has a minimal effect. There does not

Affiliation: [1] Royal Botanic Gardens, Kew, Richmond, Surrey, UK · [2] The School of Pharmacy, University of London, Brunswick Square, London, UK (ULSOP)

Correspondence: Dr. Tetsuo Kokubun · Sustainable Uses Group · Jodrell Laboratory · Royal Botanic Gardens · Kew · Richmond · Surrey TW9 3DS · UK · Phone: +44-208-332-5318 · Fax: +44-208-332-5310 · E-mail: t.kokubun@kew.org

Received: July 24, 2006 · **Accepted:** November 20, 2006

Bibliography: Planta Med 2007; 73: 176–179 © Georg Thieme Verlag KG Stuttgart · New York · DOI 10.1055/s-2006-957070 · Published online December 21, 2006 · ISSN 0032-0943

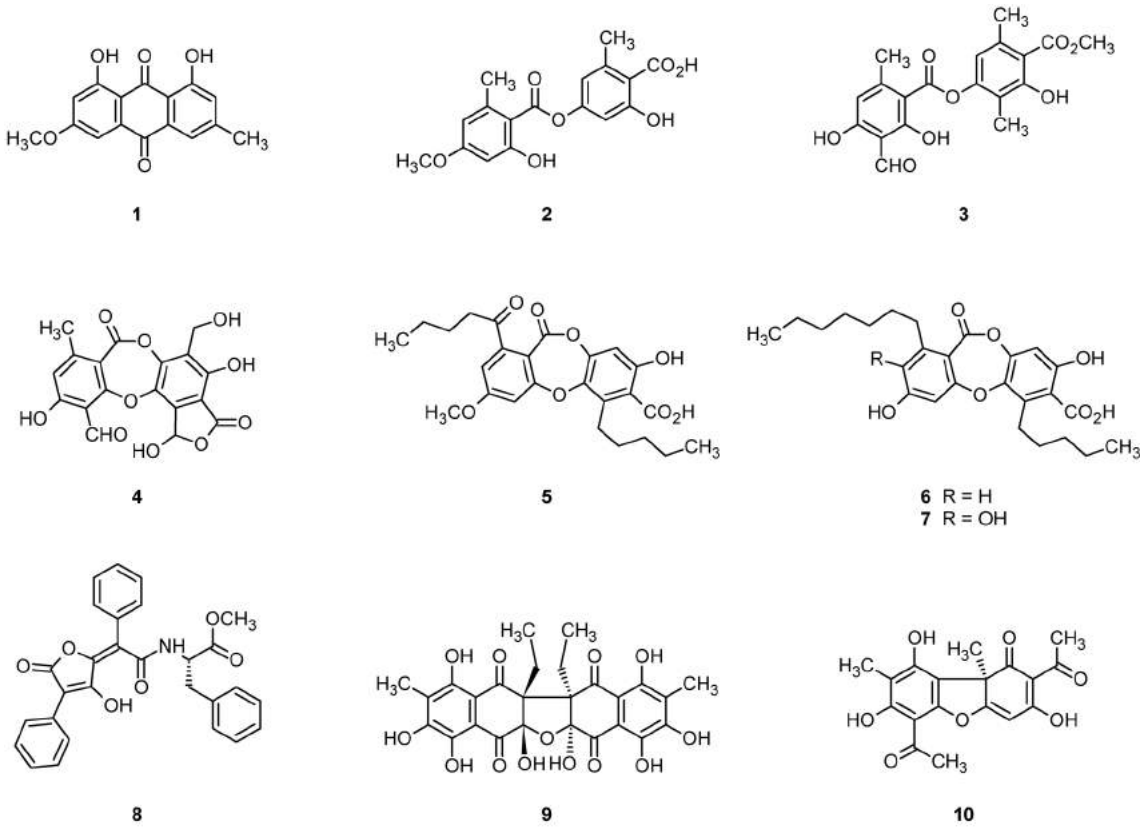

Fig. **1** Chemical structures of the tested lichen compounds **1** – **10**.

Table **1** Antibacterial activities of lichen substances against strains of *Staphylococcus aureus*

Compounds	*Minimum inhibitory concentration in µg/mL and in (µM)*[a]					
	ATCC 25923[b]	*SA-1199B (NorA)*[c]	*XU212 (TetK, mecA)*[d]	*RN4220 (MsrA)*[e]	*EMRSA-15*[f]	*EMRSA-16*[f]
Norfloxacin	1 (3.13)	32 (100)	–	–	–	–
Tetracycline	–	–	128 (288)	–	–	–
Erythromycin	–	–	–	128 (175)	–	–
Oxacillin	–	–	–	–	32 (79.8)	512 (1 277)
Physcion (**1**)	–	–[g]	–	–	–	–
Evernic acid (**2**)	–	128 (386)	–	–	–	–
Atranorin (**3**)	–	128 (314)	–	–	–	–
Salazinic acid (**4**)	–	–[h]	–	–	–	–
Lobaric acid (**5**)	64 (140)	8 (17.5)[i]	32 (70.1)	32 (70.1)	64 (140)	32 (70.1)
Physodic acid (**6**)	32 (68.0)	16 (34.0)	32 (68.0)	32 (68.0)	32 (68.0)	32 (68.0)
3-Hydroxyphysodic acid (**7**)	64 (132)	64 (132)	128 (263)	32 (65.8)	64 (132)	64 (132)
Rhizocarpic acid (**8**)	32 (68.2)	64 (136)	64 (136)	32 (68.2)	32 (68.2)	32 (68.2)
Hybocarpone (**9**)	4 (8.13)	8 (16.3)	8 (16.3)	4 (8.13)	4 (8.13)	8 (16.3)
(*R*)-(+)-Usnic acid (**10**)	16 (46.5)	8 (23.3)	16 (46.5)	8 (23.3)	16 (46.5)	16 (46.5)

[a] All MIC's were determined in duplicate. (–: not tested).
[b] A standard *S. aureus* strain.
[c] Possesses the NorA multi-drug resistant efflux pump and is resistant to certain fluoroquinolones.
[d] Possesses the TetK tetracycline efflux protein and is resistant to tetracycline. The *mec*A gene confers resistance to methicillin.
[e] Possesses the MsrA macrolide efflux protein and is resistant to macrolides including erythromycin.
[f] Two epidemic MRSA strains in the UK.
[g] Inactive at 256 µg/mL (901 µM).
[h] Inactive at 512 µg/mL (1320 µM).
[i] An average of four replicates.

seem to be a clear structure-activity relationship among the free acids (**2**, **5**–**7**) and ester/lactone (**3**, **4**) in the depside/depsidone series.

Rhizocarpic acid (**8**) showed a similar level of activity (MICs 32 to 64 μg/mL, 68.2 to 136 μM) to the alkylated depsidones. It is interesting to note that methyl pulvinate (= vulpinic acid), which possesses a methoxy group in place of methyl phenylalaninato-amide, gave an MIC (defined as EC_{99}) of 64 μg/mL against *Mycobacterium tuberculosis* H_{37}Rv (ATCC 7294), without significant mammalian cytotoxicity (KB cells, IC_{50} > 20 μg/mL) [11].

Usnic acid (**10**) was effective against a range of MRSA and MDR strains in addition to the mupirocin-resistant strain [12]. Meanwhile, the pentacyclic naphthazarin dimer hybocarpone (**9**) exhibited the strongest activity against all strains tested (MIC 4 to 8 μg/mL, 8.13 to 16.3 μM). Most strikingly, its activity was, like **10**, the least variable between strains with or without various over-expressing efflux proteins. This is an important finding as it suggests that these compounds are opaque to the efflux mechanisms expressed by the strains of *Staphylococcus aureus* tested. This feature would be a valuable property in a new class of antibacterial agents. It has been speculated that **9** acts on the DNA replication system through intercalation [13]. Further work is required to clarify the precise mode of action of this compound.

Lichens are a generally neglected source of useful and interesting compounds unless the supply is plentiful. Our antibacterial data for these compounds, particularly those for compound **9** against effluxing and methicillin-resistant variants of *Staphylococcus aureus* suggest that they are worthy of further study as prototype anti-staphylococcal agents.

Materials and Methods

The selection of lichen species for sourcing the substances was guided by the reported occurrence and an additional screening for the abundance of the compounds using an HPLC-DAD-ESI-MS set-up [14], [15], [16], [17], [18]. Hybocarpone (**9**), a cytotoxic compound only known from a cultured mycobiont of the lichen *Lecanora hybocarpa*[19], has for the first time been isolated from a naturally growing lichen as described below. The following materials were used for compound isolation: *Evernia prunastri* (L.) Ach. (Parmeliaceae), Polesden Lacey, Surrey, accession number K(M)125231 (evernic acid **2**); *Flavoparmelia caperata* (L.) Hale (Parmeliaceae), Egham, Surrey, K(M)128230 (salazinic acid **4**); *Hypogymnia physodes* (L.) Nyl. (Parmeliaceae), Kew, Surrey, K(M)139607 (physodic acid **6**, 3-hydroxyphysodic acid **7**); *Lecanora albescens* (Hoffm.) Branth & Rostr. (Lecanoraceae), Kew, Surrey, K(M)139619 (*R*-(+)-usnic acid **10**); *Lecanora conizaeoides* Nyl. ex Cromb. (Lecanoraceae), Kew, Surrey, K(M)128228 (hybocarpone **9**); *Lepraria lobificans* Nyl. (*Familiae incertae*), Kew, Surrey, K(M)128235 (atranorin **3**); *Psilolechia lucida* (Ach.) M.Choisy (Micareaceae), Egham, Surrey, K(M)128236 (rhizocarpic acid **8**); *Stereocaulon dactylophyllum* Flörke (Stereocaulaceae), Sutherland, Scotland, K(M)139596 (lobaric acid **5**); *Xanthoria parietina* (L.) Th.Fr. (Teloschistaceae), Egham, Surrey, K(M)128229 (physcion **1**). The representative specimens of the above have all been deposited in the mycological herbarium of the Royal Botanic Gardens, Kew [K(M)]. Generally, compounds were extracted from the lichen thalli with Me_2CO at room temperature, followed by purification using normal and reverse phase chromatography and repeated recrystallisation with appropriate solvents. The identities of the isolated compounds were confirmed by comparison with the published data [m.p. (uncorrected), UV, ESI-MS both in positive and negative modes, optical rotation, and 1D ^1H (400 MHz) and ^{13}C (100 MHz), and 2D NMR experiments (Bruker Avance 400; Bruker; Coventry, UK)] [19], [20]. The purities of all the isolated compounds in the crystalline forms were ensured by analytical HPLC and NMR. The full details of compound isolation and spectral data are obtainable from the author of correspondence.

Crude Me_2CO extracts were analysed using a Waters Separations Module 2695 coupled to a photodiode array detector (Waters 2996) and an orthogonal quadrupole mass spectrometer (Waters-Micromass ZQ) in tandem (Waters; Herts, UK), all controlled by MassLynx software (v 4.0). An ESCi multiprobe was used but the atmospheric pressure chemical ionisation mode was turned off during the analyses.

HPLC-DAD conditions: Genesis C_{18} column (250 × 4.6 mm i.d., dp 4 μm; Jones Chromatography; Mid Glamorgan, UK), 30 °C, solvent system A = MeOH-HOAc (49 : 1), B = H_2O-HOAc (49 : 1); gradient 50 – 100% A over 20 min, 100% A for 15 min; flow rate: 1 mL/min; injection volume 20 μL. DAD conditions: 200 – 500 nm (resolution 3.6 nm).

ESI-MS conditions: split ratio: 1 : 9. The acquisition times were set to 0.4 sec for both positive and negative modes, and the change-over time of 0.1 sec was allowed between the modes. Scan range: 150 – 1000; vapouriser 450 °C; N_2 flow (desolvation) 500 L/h; source temperature 120 °C; capillary voltage 2.5 kV; cone voltage 20.0 V; RF lens voltage 1.0 V.

Isolation of hybocarpone (**9**): air-dried lichen (96.4 g) was extracted with 4 × 800 mL Me_2CO. The solid residue of this extract was re-extracted with $CHCl_3$. The MeOH-soluble portion (85.4 mg) of the $CHCl_3$-extract was chromatographed over a silica gel column (ø37 × 55 mm, 40 – 63 μm) with toluene-EtOAc-HCO_2H (5 : 4:1, v/v/v). Fractions containing **9** (elution volume 105 – 150 mL) were combined and further purified by semi-preparative HPLC: Genesis C_{18}, 250 × 10 mm i.d., 30 °C; solvent system A = MeOH-HOAc (49 : 1), B = H_2O-HOAc (49 : 1); linear gradient 50 – 100% A over 20 min, 100% A for 5 min; flow rate: 4.0 mL/min. Hybocarpone eluted at 20.4 – 21.2 min, yielding yellow amorphous solid (8.1 mg). The physico-chemical data (m.p., retention times, UV absorption spectra and ESI-MS both in positive and negative modes) of **9** and all other isolated compounds are available in the Supporting Information.

S. aureus ATCC 25923 is a standard strain and is sensitive to commonly used antibiotics. XU212 which possesses the TetK tetracycline efflux protein and *mec*A gene is resistant to both tetracycline and methicillin [21]. These two strains were provided by E. Udo. Strain SA-1199B which overexpresses the *nor*A gene encoding the NorA multidrug-resistant (MDR) efflux pump was provided by G. Kaatz [1]. The NorA efflux pump confers resistance to quaternary ammonium antiseptics and certain fluoroqui-

nolones including norfloxacin. Strain RN4220 which possess the MsrA macrolide efflux protein and hence resistant to erythromycin was provided by J. Cove [21]. The epidemic methicillin-resistant strains EMRSA-15 and EMRSA-16 are hospital isolates [22], [23], and were obtained from P. Stapleton (ULSOP).

All *S. aureus* strains were cultured on nutrient agar (Oxoid; Basingstoke, UK) and incubated for 24 h at 37 °C prior to MIC determination. Control antibiotics norfloxacin, tetracycline, erythromycin and oxacillin were obtained from Sigma Chemical Co (St. Louis, MO, USA). Mueller-Hinton broth (MHB; Oxoid) was adjusted to contain 20 and 10 mg/L of Ca^{2+} and Mg^{2+}, respectively. Tetracycline and oxacillin were dissolved directly in MHB. Norfloxacin, erythromycin and the test compounds were first dissolved in dimethyl sulfoxide (DMSO) and then diluted in MHB. The starting concentration of control antibiotics was 256 μg/mL. Depending on the amount of test compounds available, the starting concentrations of the test compounds were either 256 or 512 μg/mL. An aliquot of MHB (125 μL) was first dispensed into wells 1 – 11 of the 96-well microtitre plate (Nunc Fisher Scientific; Leicester, UK), then 125 μL of the test compound or the control antibiotic were dispensed into well 1 which was serially diluted across the plate to well 10. Since well 11 served as the growth control, the final 125 μL were dispensed into well 12. Bacterial inocula equivalent to the 0.5 McFarland turbidity standard were prepared in normal saline and diluted to give a final inoculum density of 5×10^5 cfu/mL. Inoculum (125 μL) was added to wells 1 to 11 of the microtitre plate only, and well 12 served as the sterile control which was free of bacteria. The microtitre plate was incubated at 37 °C for 18 h. All MICs were determined in duplicate. For MIC determination, 20 μL of a 5 mg/mL methanolic solution of 3-[4,5-dimethylthiazol-2-yl]-2,5-diphenyltetrazolium bromide (MTT; Sigma) were added to each of the wells and incubated for 20 min. Bacterial growth was indicated by a colour change from yellow to dark blue. The MIC was recorded as the lowest concentration at which no growth was observed [21].

Acknowledgements

Dr. M. B. Aguirre-Hudson of the Mycology Section, Jodrell Laboratory, RBG Kew, is thanked for her expert advice on the collection, identification and referencing of the lichen materials. We also thank Dr. N. C. Veitch for running NMR experiments.

References

[1] Kaatz GW, Seo SM, Ruble CA. Efflux-mediated fluoroquinolone resistance in *Staphylococcus aureus*. Antimicrob Agents Chemother 1993; 37: 1086 – 94

[2] Lutzoni F, Pagel M, Reeb V. Major fungal lineages are derived from lichen symbiotic ancestors. Nature 2001; 411: 937 – 40

[3] Boustie J, Grube M. Lichens – a promising source of bioactive secondary metabolites. Plant Genet Resour 2005; 3: 273 – 87

[4] Huneck S. New results on the chemistry of lichen substances. In: Herz W, Falk H, Kirby GW, Moore RE, editors: Progress in the chemistry of organic natural products; Wien: Springer Verlag; 2001: 1 – 276

[5] Yoshimura I, Kurokawa T, Kinoshita Y, Yamamoto Y, Miyawaki H. Lichen substances in cultured lichens. J Hattori Bot Lab 1994; 76: 249 – 61

[6] Stocker-Wörgötter E, Elix JA. Experimental studies of lichenized fungi: formation of rare depsides and dibenzofurans by the cultured mycobiont of *Bunodophoron patagonicum* (Sphaerophoraceae, lichenized Ascomycota). Bibl Lichenol 2004; 88: 659 – 69

[7] Manojlovic NT, Solujic S, Sukdolak S. Antimicrobial activity of an extract and anthraquinones from *Caloplaca schaereri*. Lichenologist 2002; 34: 83 – 5

[8] Manojlovic NT, Solujic S, Sukdolak S, Krstic LJ. Isolation and antimicrobial activity of anthraquinones from some species of the lichen genus *Xanthoria*. J Serb Chem Soc 2000; 65: 555 – 60

[9] Lawrey JD. Lichen secondary compounds – evidence for a correspondence between antiherbivore and antimicrobial function. Bryologist 1989; 92: 326 – 8

[10] Ingólfsdóttir K, Chung GAC, Skúlason VG, Gissurarson SR, Vilhelmsdóttir M. Antimycobacterial activity of lichen metabolites *in vitro*. Eur J Pharm Sci 1998; 6: 141 – 4

[11] König GM, Wright AD, Franzblau SG. Assessment of antimycobacterial activity of a series of mainly marine derived natural products. Planta Med 2000; 66: 337 – 42

[12] Lauterwein M, Oethinger M, Belsner K, Peters T, Marre R. *In-vitro* activities of the lichen secondary metabolites vulpinic acid, (+)-usnic acid, and (–)-usnic acid against aerobic and anaerobic microorganisms. Antimicrob Agents Chemother 1995; 39: 2541 – 3

[13] Nicolaou KC, Gray DLF. Total synthesis of hybocarpone and analogues thereof. A facile dimerization of naphthazarins to pentacyclic systems. J Am Chem Soc 2004; 126: 607 – 12

[14] Culberson CF. Chemical and botanical guide to lichen products. Chapel Hill: The University of North Carolina Press; 1979

[15] Culberson CF. Supplement to "Chemical and botanical guide to lichen products". Bryologist 1970; 73: 177 – 377

[16] Culberson CF, Culberson WL, Johnson A. Second supplement to "Chemical and botanical guide to lichen products". St Louis: Missouri Botanical Garden; 1977

[17] Feige GB, Lumbsch HT, Huneck S, Elix JA. Identification of lichen substances by a standardized high-performance liquid chromatographic method. J Chromatogr 1993; 646: 417 – 27

[18] Yoshimura I, Kinoshita Y, Yamamoto Y, Huneck S, Yamada Y. Analysis of secondary metabolites from lichen by high performance liquid chromatography with a photodiode array detector. Phytochem Anal 1994; 5: 197 – 205

[19] Ernst-Russell MA, Elix JA, Chai CLL, Willis AC, Hamada N, Nash III TH. Hybocarpone, a novel cytotoxic naphthazarin derivative from mycobiont cultures of the lichen *Lecanora hybocarpa*. Tetrahedron Lett 1999; 40: 6321 – 4

[20] Huneck S, Yoshimura I. Identification of lichen substances. Berlin: Springer Verlag; 1996: 1 – 493

[21] Gibbons S, Udo EE. The effect of reserpine, a modulator of multidrug efflux pumps, on the in vitro activity of tetracycline against clinical isolates of methicillin resistant *Staphylococcus aureus* (MRSA) possessing the tet(K) determinant. Phytother Res 2000; 14: 139 – 40

[22] Ross JI, Farrell AM, Eady EA, Cove JH, Cunliffe WJ. Characterisation and molecular cloning of the novel macrolide-streptogramin B resistance determinant from *Staphylococcus epidermidis*. J Antimicrob Chemother 1989; 24: 851 – 62

[23] Richardson JF, Reith S. Characterization of a strain of methicillin-resistant *Staphylococcus aureus* (EMRSA-15) by conventional and molecular methods. J Hosp Infect 1993; 25: 45 – 52

[24] Cox RA, Conquest C, Mallaghan C, Marples RR. A major outbreak of methicillin-resistant *Staphylococcus aureus* caused by a new phage-type (EMRSA-16). J Hosp Infect 1995; 29: 87 – 106

Available online at www.sciencedirect.com
ScienceDirect
Phytochemistry 68 (2007) 210–217
PHYTOCHEMISTRY
www.elsevier.com/locate/phytochem

Antibacterials and modulators of bacterial resistance from the immature cones of *Chamaecyparis lawsoniana*

Eileen C.J. Smith [a], Elizabeth M. Williamson [b], Neale Wareham [c], Glenn W. Kaatz [d], Simon Gibbons [a,*]

[a] *Centre for Pharmacognosy and Phytotherapy, The School of Pharmacy, University of London, 29-39 Brunswick Square, London WC1N 1AX, UK*
[b] *Department of Pharmacy, University of Reading, Whiteknights, Reading, Berks RG6 6AJ, UK*
[c] *Stiefel International R&D, Whitebrook Park, 68 Lower Cookham Road, Maidenhead, Berkshire SL6 8XY, UK*
[d] *Department of Internal Medicine, Division of Infectious Diseases, School of Medicine, Wayne State University and the John D. Dingell Department of Veterans Affairs Medical Center, Detroit, MI 48201, USA*

Received 13 July 2006; received in revised form 29 September 2006
Available online 15 November 2006

Abstract

As part of an on-going project to characterize compounds from immature conifer cones with antibacterial or modulatory activity against multidrug-resistant (MDR) strains of *Staphylococcus aureus*, eight compounds were isolated from the cones of *Chamaecyparis lawsoniana*. The active compounds were mainly diterpenes, with minimum inhibitory concentrations ranging from 4 to 128 μg/ml against MDR effluxing *S. aureus* strains and two epidemic methicillin-resistant (EMRSA) clinical isolates. The compounds extracted were the diterpenes ferruginol, pisiferol and its epimer 5-epipisiferol, formosanoxide, *trans*-communic acid and torulosal, the sesquiterpene oplopanonyl acetate and the germacrane 4β-hydroxygermacra-1(10)-5-diene. Some of these compounds also exhibited modulatory activity in potentiating antibiotic activity against effluxing strains and ferruginol, used at a sub-inhibitory concentration, resulted in an 80-fold potentiation of oxacillin activity against strain EMRSA-15. An efflux inhibition assay using an *S. aureus* strain possessing the MDR NorA efflux pump resulted in 40% inhibition of ethidium bromide efflux at 10 μM ferruginol (2.86 μg/ml). We report the ^{1}H and ^{13}C NMR data for the *cis* A/B ring junction epimer of pisiferol which we have named 5-epipisiferol. We also unambiguously assign all ^{1}H and ^{13}C NMR resonances for *trans*-communic acid.

Keywords: *Chamaecyparis lawsoniana*; Diterpene; MRSA; Antibacterial; Multidrug-resistant; Efflux pump; Modulator; Ferruginol

1. Introduction

Multidrug-resistant (MDR) staphylococci have become a major health risk, in terms of both nosocomial and community-acquired infections. Methicillin-resistant *Staphylococcus aureus* (MRSA) has been headline news in the UK for the past few years, resulting in considerable public awareness of the potentially lethal consequences of an MRSA infection. The latest figures released by the Office for National Statistics reveal that in England and Wales, the number of death certificates citing MRSA has risen from 669 in 2000 to 1,168 in 2004 (Office for National Statistics, 2006).

Some *S. aureus* strains exert their resistance by means of an efflux pump in the cell membrane, examples being TetK which effluxes certain tetracyclines and the MDR pump NorA which removes certain fluoroquinolones and other compounds including quaternary ammonium compounds (QACs). In this study, compounds were isolated from the immature cones of *Chamaecyparis lawsoniana* and assayed for anti-staphylococcal activity against a standard ATCC strain and five drug-resistant clinical isolates. These included a strain which not only has the TetK pump but is also an MRSA strain; two other effluxing strains, one

* Corresponding author. Tel.: +44 207 7535913; fax: +44 207 7535909.
E-mail address: simon.gibbons@pharmacy.ac.uk (S. Gibbons).

0031-9422/$ - see front matter © 2006 Elsevier Ltd. All rights reserved.
doi:10.1016/j.phytochem.2006.10.001

with the MsrA macrolide pump, the other strain with NorA; and the epidemic MRSA strains EMRSA-15 and EMRSA-16 which account for the majority of MRSA bacteraemias in UK hospitals (Johnson et al., 2001).

Chamaecyparis lawsoniana (Murray) Parlatore, also known as Lawson's Cypress or Port-Orford cedar is a native tree of North America. It is found in coastal and mountainous regions of southwest Oregon and northern California (Vidaković, 1991). There is very little reported on the use of *Chamaecyparis* species in traditional medicine. The Southern Kwakiutl Indians of British Columbia used the leaves, branch tips and bark of *C. nootkatensis* to treat sores, arthritis and rheumatism (Turner, 1979), but the Salish people of British Columbia consider that illness could result from inhaling the strong odour of *Chamaecyparis* (Turner, 1988). However, all species have hard, aromatic wood which is highly prized and has been used by Native American peoples to make bows, canoe paddles and dishes (Turner, 1979). In Japan, the wood of *C. obtusa* is valued for use in the construction of important buildings such as temples and shrines and is also considered to have hygienic properties for use as counter tops in sushi bars (Koyama et al., 1997).

Several species of *Chamaecyparis* have been shown to possess insecticidal activity. Termiticidal activity has been reported for the heartwood of *C. lawsoniana* (McDaniel, 1989) and seed extracts of this species exhibited juvenilising activity against the yellow mealworm beetle *Tenebrio molitor* (Jacobson et al., 1975). Antibacterial properties have been cited for *Chamaecyparis* (Johnson et al., 2001; Xiao et al., 2001;Yatagai and Nakatani, 1994) and Debiaggi et al. (1988) reported that an ethanolic extract of the leaves of *C. lawsoniana* had antiviral activity against *Herpes simplex* virus type 2. However, this is the first report of antibacterial compounds from the immature cones of *C. lawsoniana*. Our rationale for studying immature cones is that conifers invest considerable resources into cone production as, unlike angiosperms, the female gametophyte (cone) is formed with a food supply before fertilisation takes place. This is very wasteful of resources as some cones will not be fertilised, and together with the fact that some coniferous cones can take three years to ripen, it was considered likely that immature cones would contain protective compounds against microbial attack.

Anti-staphylococcal activity has been previously demonstrated for many of the isolated compounds (Politi et al., 2003;Xiao et al., 2001;Muhammad et al., 1995;Kobayashi et al., 1988), but here we report their activity against clinically relevant MDR and MRSA clinical isolates, and report for the first time the resistance modifying activity of some of these compounds against virulent *S. aureus* strains. Furthermore, we report the full ^{1}H and ^{13}C NMR data for 5-epipisiferol and *trans*-communic acid. 5-Epipisiferol has previously been synthesized (Matsumoto et al., 1983) and was also reported as 20-hydroxyferruginol (Son et al., 2005), but here we unambiguously assign the stereochemistry as the 5-epimer of pisiferol.

2. Results and discussion

Structure elucidation of the isolated compounds was conducted by extensive spectroscopic studies using 1D and 2D NMR and mass spectroscopy. The data were compared with and were in close agreement with the literature for ferruginol (Wenkert et al., 1976), pisiferol (Yatagai et al., 1978), formosanoxide (Hsu et al., 1995), 4β-hydroxygermacra-1(10)-5-diene (Cornwell et al., 2001;Feliciano et al., 1995), *trans*-communic acid (Yamamoto et al., 1997;Muhammad et al., 1995;Fang et al., 1989), torulosal (Su et al., 1994) and oplopanonyl acetate (De Bruyn et al., 1990). The ^{1}H and ^{13}C NMR data for 5-epipisiferol are presented in Table 1. The ^{1}H spectra for pisiferol and 5-epipisiferol revealed a large coupling for the H-5 methine to the axial H-6 proton ($J = 12.5$ and 12.0, respectively). In the *trans* A/B ring junction of pisiferol, proton H-5 was axial and relatively α with respect to ring A, but in 5-epipisiferol the position of this hydrogen was equatorial and relatively (β) with respect to ring A but axial with respect to the B ring. The relative stereochemistry of pisiferol was assigned by correlations seen in the NOESY spectrum (Fig. 1). A correlation between the H_2-20 methylene protons and the H_3-19 methyl group established that they were on the same face of the molecule and were assigned an axial (β) orientation as described in the literature (Yatagai et al., 1978). Further NOE signals between proton H-5 and the CH_3-18 methyl and between H-5 and proton H-6b and the axial proton of the H-7 methylene suggested an alpha orientation and a *trans* A/B ring junction. For 5-epipisiferol, the NOESY data indicated a *cis* A/B ring junction. This was deduced by through space interactions between the H-20b methylene proton and the H-5 proton which in turn had a correlation to the H_3-19 methyl indicating that these protons were all on the same face of the molecule. These groups were assigned a relative (β) configuration and we therefore describe the compound as 5-epipisiferol, an epimer of pisiferol.

All compounds were assessed for antibacterial activity in a minimum inhibitory concentration (MIC) assay (Table 2). The phenolic diterpenes ferruginol, pisiferol, 5-epipisiferol and the labdane diterpene *trans*-communic acid had the greatest activity at 4–16 μg/ml. The stereochemistry at the A/B ring junction of pisiferol and 5-epipisiferol (Fig. 1) did not affect activity as both epimers had MICs of 8–16 μg/ml against all strains. However, the presence of an ether bridge linking C-7 and C-20, seen in formosanoxide (Fig. 1), destroyed anti-staphylococcal activity, since this compound was inactive at 512 μg/ml against the two strains tested. 4β-hydroxygermacra-1(10)-5-diene displayed modest antibacterial activity at 128–256 μg/ml. The sesquiterpene oplopanonyl acetate was inactive at 128 μg/ml, as was torulosal, except against strain EMRSA-16 where its MIC was 128 μg/ml. It is interesting that nearly all the active compounds had a higher MIC against EMRSA-15 than for strain EMRSA-16. This was surprising, since the MIC for oxacillin against EMRSA-15 is only 32 μg/ml

Table 1
^{1}H (500 MHz) and ^{13}C NMR (125 MHz) spectral data for 5-epipisiferol and *trans*-communic acid in $CDCl_3$

5-Epipisiferol			*trans*-Communic acid		
Position	^{1}H (*J* in Hz)	^{13}C	Position	^{1}H (*J* in Hz)	^{13}C
1	1.52 *m*	41.8	1	1.05 *m*	38.0
	1.84 *m*			2.16 *m*	
2	1.44 *m*	18.7	2	1.52 *m*	19.1
3	1.24 *m*	42.4	3	1.14 *dd* (13.5, 4.0)	39.2
	1.41 *d* (2.5)			1.86 *m*	
4		34.4	4		44.1
5	2.64 *dd* (12.0, 2.5)	58.0	5	1.34 *dd* (12.0, 2.5)	56.2
6	1.26 *m*	24.3	6	1.96 *m*	25.8
	1.99 *m*		7	1.91 *m*	38.5
7	2.66 *m*	35.4		2.39 *m*	
	2.73 *m*		8		147.9
8		133.0	9	1.76 *s*	56.4
9		135.5	10		40.3
10		71.6	11	2.13 *m*	23.3
11	6.66 *s*	118.8		2.36 *m*	
12 (OH)	5.99 *s*	151.6	12	5.39 *t* (6.5)	133.9
13		133.4	13		133.4
14	6.90 *s*	126.6	14	6.31 *dd* (17.5,11.0)	141.6
15	3.17 *q*	26.6	15	4.86 *d* (11.0)	109.9
16	1.21[a] *d* (7.0)	22.5[a]		5.03 *d* (17.5)	
17	1.19[a] *d* (7.0)	22.8[a]	16	1.73 *s*	11.8
18	0.91 *s*	21.7	17	4.45 *s*	107.7
19	0.88 *s*	32.2		4.82 *s*	
20	2.55 *d* (14.0)	51.0	18	1.23 *s*	29.0
	3.00 *d* (14.0)		19		182.5
			20	0.64 *s*	12.8

[a] Interchangeable values.

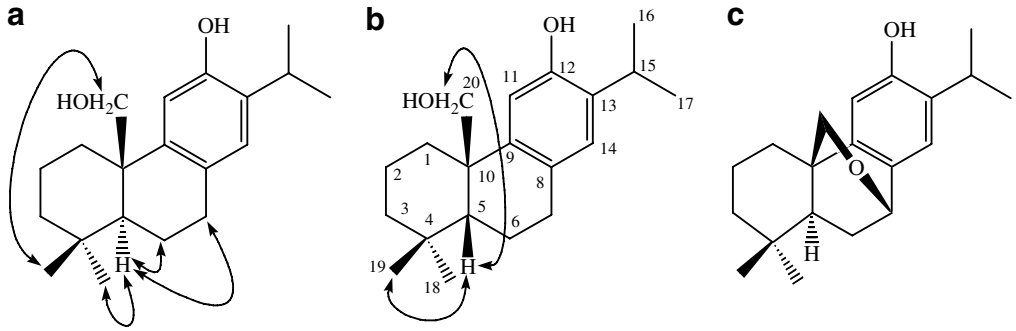

Fig. 1. Pisiferol (a), 5-epipisiferol (b) (selected NOEs) and formosanoxide (c).

compared with 512 μg/ml against strain 16. EMRSA-16 is resistant to norfloxacin whereas strain 15 is sensitive, and it also has a two fold greater resistance to erythromycin. It is possible that acquisition of resistance to many antibiotics has resulted in a loss in fitness, making EMRSA-16 more susceptible to some compounds or types of compounds than EMRSA-15. Another possibility is that EMRSA-15 may possess an as yet uncharacterized mechanism of resistance, or some efflux of compounds may occur, accounting for the higher MICs seen for this strain compared with EMRSA-16.

There was no significant variation in the anti-staphylococcal activity of a compound between the six strains. For example, there were no instances where a compound had a high activity against the standard ATCC 25923 strain, but considerably reduced or even no activity against the resistant strains. If a compound had activity against one *S. aureus* strain, it was active against all strains tested. With the exception of ferruginol (Fig. 2), which had a four-fold higher activity against EMRSA-15 than strain 16, none of the compounds had more than a twofold difference in activity between strains. This was a surprising result which may reflect that the active compounds were mainly diterpenes, some with a very similar structure and with the same functional groups and possibly the same mode of action. However, *trans*-communic acid (Fig. 2), which had good activity compared with the standard antibiotics, is a labdane diterpene and does not possess a phenolic hydroxyl group as found in the active abietanes. Our previous work on isopimaric acid (Smith et al., 2005) isolated

Table 2
MICs (μg/ml) of isolated compounds and standard antibiotics against a standard ATCC strain and five clinical isolates of *S. aureus* (resistance mechanism)

Compound	ATCC 25923	XU212 (TetK)/ (*mecA*)	SA1199B (NorA)	RN4220 (MsrA)	EMRSA-15 (*mecA*)	EMRSA-16 (*mecA*)
Ferruginol	8	8	4	8	16	4
Formosanoxide	>512	>512	–	–	–	–
4β-Hydroxygermacra-1(10)-5-diene	128	128	256	128	256	128
Oplopanonyl acetate	>128	>128	>128	>128	>128	>128
Pisiferol	16	16	16	8	8	8
5-Epipisiferol	8	16	8	16	16	8
Torulosal	>128	>128	>128	>128	>128	128
trans-Communic acid	16	16	8	8	16	8
Tetracycline	0.25	128	0.25	0.25	0.125	0.125
Norfloxacin	1	16	32	2	0.5	128
Erythromycin	0.25	4,096	0.25	128	2,048	4,096
Oxacillin	0.125	128	0.25	0.25	32	512

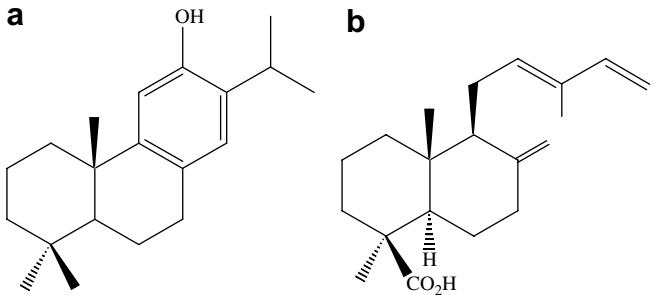

Fig. 2. Ferruginol (a) and *trans*-communic acid (b).

from the cones of *Pinus nigra*, and commercially obtained abietic acid, although not as active (MICs 32–64 μg/ml), still displayed the same trend, that if they were active against one strain, they were active against all strains at approximately the same MIC value. This suggests there may be a common mode of action for each compound against all strains, for example membrane perturbation is often suggested as the antibacterial action for phenolic diterpenes. However, research by Clarkson et al. (2003) demonstrated that ferruginol did not affect erythrocyte morphology even at high concentration (100 μg/ml), therefore the mode of antibacterial action of these diterpenes is unlikely to be merely membrane lysis or disruption. It is possible that these compounds have a mode of action which clinically relevant isolates have not previously encountered.

Oplopanonyl acetate and torulosal were tested in combination with the MDR inhibitor reserpine against the effluxing strains XU212 and SA1199B. This was conducted to assess whether these inactive compounds had antibacterial activity when the efflux pump was inhibited, as seen with several compounds tested by Tegos et al. (2002). However, the presence of an efflux inhibitor had no effect and both compounds remained inactive at 128 μg/ml.

4β-Hydroxygermacra-1(10)-5-diene and compounds with no anti-staphylococcal activity in the MIC assay were tested in the modulation assay at 10 μg/ml and active compounds were assayed at half MIC. Ferruginol was the most active compound in the modulation assays (Table 3) and displayed a similar activity to the control reserpine against the effluxing strain XU212 possessing the TetK pump, causing a fourfold reduction in the MIC of tetracycline. Against strain SA1199B which has the NorA pump, a twofold potentiation of norfloxacin activity was observed in the presence of ferruginol, whereas reserpine caused an eightfold increase in norfloxacin activity, reducing its MIC from 32 to 4 μg/ml. The plant alkaloid reserpine inhibits the NorA and TetK pumps of *S. aureus* (Markham et al., 1999). However, unlike reserpine, ferruginol also potentiated the activity of erythromycin against a strain possessing the MsrA efflux pump. No inhibitor of this pump has so far been reported.

Ferruginol showed excellent potentiation of oxacillin activity against the epidemic MRSA strain EMRSA-15,

Table 3
MICs (μg/ml) of standard antibiotics in the presence and absence of ferruginol and 5-epipisiferol

Compound	XU212 tetracycline	XU212 oxacillin	SA1199B norfloxacin	RN4220 erythromycin	EMRSA-15 oxacillin	EMRSA-16 oxacillin
Ferruginol	128 (**32**)	256 (**32**)	32 (**16**)	128 (**32**)	32 (**0.40**)	–[a]
5-Epipisiferol	128 (**32**)	–	–[a]	–[a]	–[a]	–[a]
Reserpine	128 (**32**)	256 (**256**)	32 (**4**)	128 (**128**)	–	–
Epicatechin gallate	–	256 (**0.16**)	–	–	32 (**0.32**)	256 (**0.32**)

Figures in bold denote MICs in the presence of the test compound. Reserpine was assayed @ 20 μg/ml; epicatechin gallate @ 10 and 4 μg/ml against EMRSA-15 and EMRSA-16, respectively.

[a] A concentration of half MIC inhibited the growth control; a concentration of one quarter MIC was inactive.

comparable with the activity for the epicatechin gallate control against the same strain. An 80-fold reduction in the MIC for oxacillin was achieved, restoring oxacillin sensitivity in this resistant strain. This potentiation of antibiotic activity by ferruginol against MRSA and effluxing strains of *S. aureus* has not been previously reported. However, similar activity has been demonstrated against mycobacteria. Mossa et al. (2004) reported the antimycobacterial activity of ferruginol at 5 μg/ml and its fourfold potentiation of isonaizid activity at half MIC against several species of mycobacteria.

5-Epipisiferol also potentiated the activity of tetracycline, causing a fourfold reduction in its MIC against strain XU212. This is an interesting result since pisiferol was inactive in the modulation assays, which suggests that the stereochemistry at the A/B ring junction is important for modulatory activity but does not affect the antibacterial activity of the epimers.

Some compounds which had antibacterial activity at low MICs, when tested in the modulation assay at half MIC, inhibited the growth control but were inactive at one quarter MIC. This reflects the intrinsic twofold variability in results achieved for MIC assays. The results suggest that there is a narrow window of modulatory activity for these compounds. This may be partly due to the fact that compounds which were active in the modulation assay also had antibacterial activity and, when used at half MIC, there might still be some antibacterial activity. This was in comparison with reserpine which has no anti-staphylococcal activity even at 512 μg/ml and its potentiation of tetracycline and norfloxacin activity would not be due to additive effects.

An efflux inhibition assay (Fig. 3) supported the modulation results for ferruginol, showing that the presence of ferruginol resulted in a reduction in efflux of ethidium bromide (EtBr) in SA1199B, a strain which overexpresses the NorA pump (Kaatz et al., 1993). Ferruginol (10 μM) resulted in a 40% inhibition of efflux, with 50% inhibition occurring at around 17 μM. These two values correspond to 2.86 μg/ml and 4.86 μg/ml, respectively. Fifty per cent inhibition of efflux occurred at the MIC value for ferruginol against this strain and, as the antibacterial activity of ferruginol would have an effect at this concentration, the experiment was stopped at 30 μM ferruginol. The results suggest that ferruginol is likely to be a weak efflux pump inhibitor. In the modulation assay, ferruginol at half its MIC value (2 μg/ml), resulted in a twofold reduction in the MIC of norfloxacin against SA1199B. Reserpine reduced the MIC of norfloxacin from 32 to 4 μg/ml which suggested that the pump was not completely inhibited and that there was still some residual efflux occurring. The presence of other efflux pumps for which norfloxacin and EtBr are substrates, but which are not inhibited by reserpine or affected by ferruginol could also be responsible for some efflux of compounds (Kaatz et al., 2000).

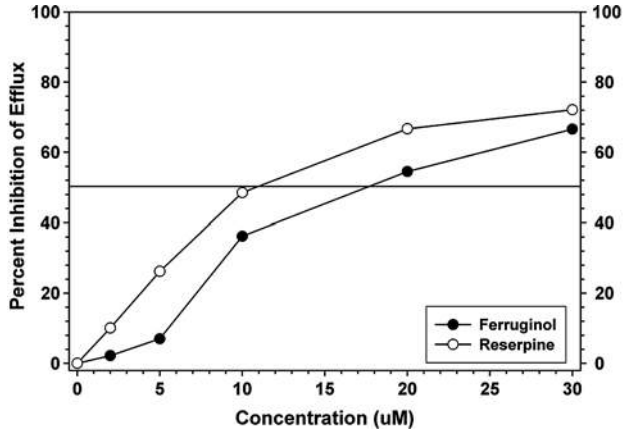

Fig. 3. Ethidium efflux inhibition assay against SA1199B, which overexpresses the NorA efflux pump.

Work by Shiota et al. (1999) on the polyphenols epicatechin gallate (ECG) and epigallocatechin gallate (EGCG) showed that ECG reduced the MIC of oxacillin against MRSA strains by 250–500-fold. Epigallocatechin gallate (EGCG), which differs from ECG only by an extra hydroxyl group on the B-ring, had much lower activity, resulting in a 4–64-fold reduction in oxacillin MIC. It is interesting that an extra phenolic hydroxyl on EGCG should have such an effect on modulatory activity, suggesting that either the position of the hydroxyl groups is important or that the increase in hydrophilicity afforded by the extra hydroxyl was sufficient to affect the activity. Research carried out by our group (Gibbons et al., 2004a) on these two compounds showed that in the antibacterial MIC assays, conversely, EGCG has a 2–16-fold greater anti-staphylococcal activity than ECG which suggests that potentiation of antibiotic activity is by a different mechanism from antibacterial activity. An efflux inhibition assay also revealed the surprising result that at low concentration, ECG increases efflux of EtBr, but at high concentration inhibits efflux. Ferruginol demonstrated good modulatory activity in restoring oxacillin sensitivity in strain EMRSA-15, but against the MRSA isolate XU212 which is also an effluxing strain possessing the TetK pump, the potentiation of oxacillin activity was modest in comparison. Here, ferruginol only resulted in an eightfold reduction in the MIC of oxacillin from 256 to 32 μg/ml, which is not sufficient to restore oxacillin sensitivity (MIC $\geqslant$ 4 μg/ml). Against SA1199B (NorA) and RN4220 (MsrA), ferruginol only caused a two and fourfold potentiation of the activity of norfloxacin and erythromycin, respectively. One possibility for this lower activity is that ferruginol may be a substrate for the efflux pumps; however, it is likely that the modulatory mode of action against effluxing strains differs from that against MRSA strains. The efflux pump inhibitor reserpine had no effect on oxacillin activity against strain XU212, which suggests that oxacillin is not a substrate for the TetK pump. However, ECG reduced the MIC of oxacillin from 256 to 0.16 μg/ml. Shiota et al. (1999) suggested that ECG acts on the penicillin binding protein PBP2′ encoded by the *mecA* gene. This conclusion was also reached by

Nicolson et al. (1999) who suggested that modulators of methicillin activity act by inhibition of *de novo* synthesis of PBP2′. If this is the case, then the mode of action in potentiating antibiotic activity against effluxing strains and MRSA strains must be different. It has recently been reported (Tian, 2006) that ECG inhibits animal fatty acid synthase and this enzyme could also be a target of ECG activity in bacteria. It is possible that the modest increases in antibiotic activity against effluxing strains were due to an additive effect as the compounds are antibacterial, although used at sub-inhibitory concentrations. The efflux inhibition experiments on ferruginol however, do indicate that this compound is a weak inhibitor of efflux.

In searching the literature for NMR data on *trans*-communic acid, there were inconsistencies in some of the ^{13}C data published (Yamamoto et al., 1997;Muhammad et al., 1995;Fang et al., 1989). Here we have revised the ^{13}C NMR data for *trans*-communic acid based on extensive 1D and 2D data (Table 1). This data is in close agreement to that reported by Muhammad et al., differing only in the assignment of the signals for C-1 and C-3 which we have revised.

3. Experimental

3.1. General experimental procedures

GC–MS analysis was carried out using an Agilent 6890 GC coupled to an Agilent 5973 mass selective detector. An HP-5 ms capillary column of 30 m length with a diameter of 250 μm was used with a non-polar stationary phase of 5% phenylmethylsiloxane and a film thickness of 0.25 μm. Samples were introduced into the system using split injection with a split ratio of between 5:1 and 10:1 and an injector temperature of 250 °C. Helium was used as the carrier gas at an average linear velocity of 50 cm/s. The initial oven temperature was 50 °C and the temperature was increased after 5 min at a rate of 5 °C to a maximum of 300 °C. The MS was run in EI mode.

NMR spectra were recorded on a Bruker AVANCE 500 MHz spectrometer. Chemical shift values (δ) are reported in parts per million (ppm) relative to an appropriate internal solvent standard and coupling constants (J values) are given in Hertz.

3.2. Plant material

Immature cones of *C. lawsoniana* were identified and supplied by Dr Caroline Priestley. A voucher specimen (ECJS/001) was placed in the herbarium at the Centre for Pharmacognosy and Phytotherapy.

3.3. Extraction and isolation

Four hundred grams of immature cones were chopped and placed in a Soxhlet apparatus. Sequential extraction started with hexane, followed by $CHCl_3$, acetone and, finally MeOH. Vacuum liquid chromatography (VLC) on 8 g of hexane extract yielded 12 fractions. Elution commenced with 100% hexane going to 100% EtOAc in 10% increments, finishing with an EtOAc/MeoH 50:50 wash. MIC assays identified the most active fraction (4) and solid phase extraction (SPE) was performed on 450 mg of this fraction. A Phenomenex Strata Sl-1 silica column (10 g/60 ml giga tubes) was used and elution commenced with 100% petroleum spirit, followed by a gradient of 5% increments of Et_2O to 70:30 petroleum spirit/Et_2O. The Et_2O increments were then increased to 40%, 60% and 80%, finally eluting with 100% Et_2O. PTLC was performed on 50 mg of fraction 3, using four analytical silica plates (petroleum spirit/toluene 80:20, 1 development; petroleum spirit/Et_2O 90:10, 2 developments) to give 25 mg ferruginol. SPE fractions 7–11 were run on three analytical silica plates (hexane/Et_2O/EtOAc 80:15:5, 2 developments), which yielded *trans*-communic acid (5.5 mg). Two hundred milligrams of VLC fraction 6 were loaded onto a LH-20 sephadex column (200 mg per column run) and eluted with $CHCl_3$, followed by CH_2Cl_2, CH_2Cl_2/MeOH 50:50, finishing with 100% MeOH. PTLC (hexane/Et_2O/EtOAc 80:15:5, 3 developments) on pooled fractions 12–17 gave oplopanonyl acetate (15.1 mg) and torulosal (10.3 mg). Using the same solvent system (4 developments), fractions 36–42 yielded pisiferol (6.2 mg), formosanoxide (4.2 mg) and 5-epipisiferol (14.9 mg). VLC fraction 3 (390 mg) was run on PTLC to yield 6.2 mg 4β-hydroxygermacra-1(10)-5-diene.

3.4. Antibacterial assay and modulation assay

A standard *S. aureus* strain ATCC 25923 and a clinical isolate (XU212), which possesses the TetK efflux pump and is also an MRSA strain, were obtained from E. Udo (Gibbons and Udo, 2000). Strain RN4220 which has the MsrA macrolide efflux pump was provided by J. Cove (Ross et al., 1989). EMRSA-15 (Richardson and Reith, 1993) and EMRSA-16 (Cox et al., 1995) were obtained from Paul Stapleton. Glenn Kaatz provided strain SA1199B which over-expresses the NorA MDR efflux pump (Kaatz et al., 1993). Minimum inhibitory concentration (MIC) and modulation assays were carried out as previously described (Smith et al., 2005).

3.5. Efflux inhibition assay

Ferruginol was assayed at varying concentrations against SA1199B (NorA) for potential to reduce the efflux of ethidium bromide (EtBr) which is a substrate for the NorA MDR pump. EtBr fluorescence will decrease over time as it is effluxed from the cell, the potential of a compound to inhibit efflux can be determined by the strength of the fluorescent signal which remains in the cell. The efflux inhibition was carried out as previously described (Kaatz et al., 2000).

Acknowledgements

We thank Stiefel International R&D Ltd. for the award of a studentship and post-doctoral funding to E. Smith. The Engineering and Physical Sciences Research Council is thanked for a multi project equipment grant (Grant No. GR/R47646/01).

References

Clarkson, C., Campbell, W.E., Smith, P., 2003. In vitro antiplasmodial activity of abietane and totarane diterpenes isolated from *Harpagophytum procumbens* (Devil's Claw). Planta Medica 69, 720–724.

Cornwell, C.P., Reddy, N., Leach, D.N., Wyllie, S.G., 2001. Germacradienols in the essential oils of the Myrtaceae. Flavour and Fragrance Journal 16, 263–273.

Cox, R.A., Conquest, C., Mallaghan, C., Maples, R.R., 1995. A major outbreak of methicillin-resistant *Staphylococcus aureus* caused by a new phage type (EMRSA-16). Journal of Hospital Infection 29, 87–106.

Debiaggi, M., Pagani, L., Cereda, P.M., Landini, P., Romero, E., 1988. Antiviral activity of *Chamaecyparis lawsoniana* extract: study with *Herpes simplex* virus type 2. Microbiologica 11, 55–61.

De Bruyn, A., De Pooter, H.L., De Buyck, L., Jans, A.W.H., Budesinsky, M., Sedmera, P., 1990. Identification of oplopanonyl acetate isolated from *Chamaecyparis pisifera*. Magnetic Resonance in Chemistry 28 (12), 1030–1039.

Fang, J.M., Hsu, K.C., Cheng, Y.S., 1989. Terpenoids from leaves of *Calocedrus formosana*. Phytochemistry 28 (4), 1173–1175.

Gibbons, S., Moser, E., Kaatz, G.W., 2004a. Catechin gallates inhibit multidrug resistance (MDR) in *Staphylococcus aureus*. Planta Medica 70, 1240–1242.

Gibbons, S., Udo, E.E., 2000. The effect of reserpine, a modulator of multidrug efflux pumps, on the *in vitro* activity of tetracycline against clinical isolates of methicillin resistant *Staphylococcus aureus* (MRSA) possessing the *tet*(K) determinant. Phytotherapy Research 14, 139–140.

Hsu, K.C., Fang, J.M., Cheng, Y.S., 1995. Diterpenes from pericarps of *Chamaecyparis formosensis*. Journal of Natural Products 58 (10), 1592–1595.

Jacobson, M., Redfern, R.E., Mills, G.D., 1975. Naturally occurring insect growth regulators part 2 screening of insect and plant extracts as insect juvenile hormone mimics. Lloydia 38 (6), 455–472.

Johnson, A.P., Aucken, H.M., Cavendish, S., Ganner, M., Wale, M.C.J., Warner, M., Livermore, D.M., Cookson, B.D., 2001. Dominance of EMRSA-15 and -16 among MRSA causing nosocomial bacteraemia in the UK: analysis of isolates from the European Antimicrobial Resistance Surveillance System (EARSS). Journal of Antimicrobial Chemotherapy 48, 143–144.

Kaatz, G.W., Seo, S.M., O'Brien, L., Wahiduzzaman, M., Foster, T.J., 2000. Evidence for the existence of a multidrug efflux transporter distinct from NorA in *Staphylococcus aureus*. Antimicrobial Agents and Chemotherapy 44 (5), 1404–1406.

Kaatz, G.W., Seo, S.M., Ruble, C.A., 1993. Efflux-mediated fluoroquinolone resistance in *Staphylococcus aureus*. Antimicrobial Agents and Chemotherapy 37 (5), 1086–1094.

Kobayashi, K., Nishino, C., Fukushima, M., Shiobara, Y., Kodama, M., 1988. Antibacterial activity of pisiferic acid and its derivatives against gram-negative and gram-positive bacteria. Agricultural and Biological Chemistry 52 (1), 77–83.

Koyama, S., Yamaguchi, Y., Tanaka, S., Motoyoshiya, J., 1997. A new substance (Yoshixol) with an interesting antibiotic mechanism from wood oil of Japanese traditional tree (Kiso-Hinoki), *Chamaecyparis obtusa.*. General Pharmacology 28 (5), 797–804.

Markham, P.N., Westhaus, E., Klyachko, K., Johnson, M.E., Neyfakh, A.A., 1999. Multiple novel inhibitors of the NorA multidrug transporter of *Staphylococcus aureus*. Antimicrobial Agents and Chemotherapy 43, 2404–2408.

Matsumoto, T., Endo, Y., Okimoto, M., 1983. The synthesis of (+)-pisiferol and (+)-pisiferal. Bulletin of the Chemical Society of Japan 56, 2018–2022.

McDaniel, C.A., 1989. Major termiticidal components of heartwood of Port-Orford cedar, *Chamaecyparis lawsoniana* (A. Murr.). Parl. Material und Organismen 24 (1), 1–16.

Mossa, J.S., El-Feraly, F.S., Muhammad, I., 2004. Antimycobacterial constitutents from *Juniperus procera, Ferula communis* and *Plumbago zeylanica* and their *in vitro* synergistic activity with isonicotinic acid hydrazide. Phytotherapy Research 18, 934–937.

Muhammad, I., Mossa, J.S., Al Yahya, M.A., Ramadan, A.F., El-Feraly, F.S., 1995. Further antibacterial diterpenes from the bark and leaves of *Juniperus procera* Hochstex Endl. Phytotherapy Research 9, 584–588.

Nicolson, K., Evans, G., O'Toole, P.W., 1999. Potentiation of methicillin activity against methicillin-resistant *Staphylococcus aureus* by diterpenes. FEMS Microbiology Letters 179, 233–239.

Office for National Statistics, 2006. Report: Deaths involving MRSA: England and Wales 2000–2004. Health Statistics Quarterly 29, 63–68.

Politi, M., Braca, A., De Tommasi, N., Morelli, I., Manunta, A., Battinelli, L., Mazzanti, G., 2003. Antimicrobial diterpenes from the seeds of *Cephalotaxus harringtonia* var. *drupacea*. Planta Medica 69, 468–470.

Richardson, J.F., Reith, S., 1993. Characterisation of a strain of methicillin-resistant *Staphylococcus aureus* (EMRSA-15) by conventional and molecular methods. Journal of Hospital Infection 25, 45–52.

Ross, J.I., Farrell, A.M., Eady, E.A., Cove, J.H., Cunliffe, W.J., 1989. Characterisation and molecular cloning of the novel macrolide streptogramin B resistance determinant from *Staphylococcus epidermidis*. Journal of Antimicrobial Chemotherapy 24, 851–862.

San Feliciano, A., Medarde, M., Gordaliza, M., Lucas, M.J., 1995. Structure elucidation of germacrane alcohols from *Juniperus communis* subsp. *Hemisphaerica*. Journal of Natural Products 58 (7), 1059–1064.

Shiota, S., Shimizu, M., Mizushima, T., Ito, H., Hatano, T., Yoshida, T., Tsuchiya, T., 1999. Marked reduction in the minimum inhibitory concentration (MIC) of beta-lactams in methicillin-resistant *Staphylococcus aureus* produced by epicatechin gallate, an ingredient of green tea (*Camellia sinensis*). Biological & Pharmaceutical Bulletin 22, 1388–1390.

Smith, E., Williamson, E., Zloh, M., Gibbons, S., 2005. Isopimaric acid from *Pinus nigra* shows activity against multidrug-resistant and EMRSA strains of *Staphylococcus aureus*. Phytotherapy Research 19, 538–542.

Son, K.H., Oh, H.M., Choi, S.K., Han, D.C., Kwon, B.M., 2005. Antitumor abietane diterpenes from the cones of *Sequoia sempervirens*. Bioorganic & Medicinal Chemistry Letters 15, 2019–2021.

Su, W.C., Fang, J.M., Cheng, Y.S., 1994. Labdanes from *Cryptomeria japonica*. Phytochemistry 37 (4), 1109–1114.

Tegos, G., Stermitz, F.R., Lomovskaya, O., Lewis, K., 2002. Multi-drug pump inhibitors uncover remarkable activity of plant antimicrobials. Antimicrobial Agents and Chemotherapy 46, 3133–3141.

Tian, W.X., 2006. Inhibition of fatty acid synthase by polyphenols. Current Medicinal Chemistry 13 (8), 967–977.

Turner, N.J., 1988. Ethnobotany of coniferous trees in Thompson and Lillooet Interior Salish of British Columbia. Economic Botany 42 (2), 177–194.

Turner, N.J., 1979. The ethnobotany of the Southern Kwakiutl Indians of British Columbia. Economic Botany 27, 257–310.

Vidaković, M., 1991. Conifers Morphology and Variation. Grafički Zavod Hrvatske, Zagreb, Croatia.

Wenkert, E., Buckwalter, B.L., Burfitt, I.R., Gašic, M.J., Gottlieb, H.E., Hagaman, E.W., Schell, F.M., Wovkulich, P.M., 1976. Carbon-13 nuclear magnetic resonance spectroscopy of naturally occurring substances. In: Levy, George C. (Ed.), Topics in Carbon-13 NMR Spectroscopy. John Wiley & Sons Inc., pp. 98–100 (Chapter 2).

Xiao, D., Kuroyanagi, M., Itani, T., Matsuura, H., Udayama, M., Murakami, M., Umehara, K., Kawahara, N., 2001. Studies on constituents from *Chamaecyparis pisifera* and antibacterial activity of diterpenes. Chemical and Pharmaceutical Bulletin 49 (11), 1479–1481.

Yamamoto, H., Asano, N., Sawano, C., Sone, T., Gasha, T., Ono, Y., 1997. Diterpenes isolated from the resin of the resinous stem canker of Japanese Cypress, *Chamaecyparis obtusa*. Mokuzai Gakkaishi 43, 558–565.

Yatagai, M., Nakatani, N., 1994. Antimite, antifly, antioxidative and antibacterial activities of pisiferic acid and its congeners. Mokuzai Gakkaishi 40, 1355–1362.

Yatagai, M., Shirato, T., Hayashi, Y., Fukuhara, N., Takahashi, T., 1978. Pisiferic acid, a new phenolic diterpene carboxylic acid from *Chamaecyparis pisifera* S. et Z. Mokuzai Gakkaishi 24, 267–269.

PHYTOTHERAPY RESEARCH
Phytother. Res. **21**, 653–657 (2007)
Published online 10 April 2007 in Wiley InterScience
(www.interscience.wiley.com) **DOI**: 10.1002/ptr.2136

Antibacterial Activity of Two Canthin-6-one Alkaloids from *Allium neapolitanum*

Gemma O'Donnell and Simon Gibbons*

Centre for Pharmacognosy and Phytotherapy, The School of Pharmacy, University of London, 29–39 Brunswick Square, London WC1N 1AX, UK

The emergence of multidrug-resistant strains of many human pathogens has led to an urgent need for the discovery and development of new antimicrobial agents. As part of an ongoing investigation into the antibacterial properties of the Alliaceae, the isolation of 1 (canthin-6-one), 2 (8-hydroxy-canthin-6-one) and 3 (5(ζ)-hydroxy-octadeca-6(*E*)-8(*Z*)-dienioc acid)) from *A. neapolitanum*, a perennial bulbous herb found in open pastures of the Mediterranean is reported. Compounds 1 and 2 were isolated by Sephadex LH-20 from fractions exhibiting a positive reaction with Dragendorff's reagent on TLC, compound 3 was isolated after HPLC purification of Sephadex fractions. Structures were elucidated by extensive 1D and 2D NMR experiments and are in accordance with published data, however, the ^{13}C NMR data for compound 2 and the ^{1}H and ^{13}C NMR data for compound 3 are reported here for the first time. Canthin-6-one alkaloids are well-known constituents of the Simaroubaceae and Rutaceae, and display a wide range of biological activities. These metabolites are reported as constituents of the Alliaceae here for the first time, and displayed minimum inhibitory concentrations (MICs) in the range 8–32 μg/mL against a panel of fast-growing *Mycobacterium* species and 8–64 μg/mL against multidrug-resistant (MDR) and methicillin-resistant (MRSA) strains of *Staphylococcus aureus*. Compound 3 displayed antimycobacterial activity in the range of 16–32 μg/mL.

Keywords: Allium neapolitanum; antibacterial; canthin-6-one; *Mycobacterium*; *Staphylococcus aureus.*

INTRODUCTION

The genus *Allium* is represented by 550 species distributed in the temperate, tropical or often semi-arid regions of the world. Many species are cultivated for culinary, medicinal and ornamental use. *Allium sativum* (garlic) has been widely studied for its pharmaceutical properties with allicin being identified as the major antibacterial component in the 1940s (Cavallito *et al.*, 1944a; 1944b; 1945). Garlic is popularly known as 'Russian penicillin' and was of clinical use in the treatment of tuberculosis (TB) patients in the early 20th century (Bolton *et al.*, 1982). The World Health Organization (WHO) has estimated that 8 million people each year become infected with TB and approximately 2 million die (WHO, 2000). The disease was declared a global emergency in 1993 with HIV/AIDS induced immunosuppression being a major factor in the acceleration of mycobacterial infection. There has also been a rise in infection caused by non-tuberculous mycobacteria (Falkinham, 1996) and the recovery of fast-growing strains from patients with cystic fibrosis is becoming more common (Bange *et al.*, 1999). In recent decades, single-drug and multi-drug resistant strains of non-tuberculous mycobacteria have been documented resulting in an urgent need for new antimycobacterial agents with novel modes of action. As part of a project to identify antimycobacterial natural products from the subterranean parts of the Liliales, the bioassay-guided fractionation of the chloroform extract of *A. neapolitanum* against fast-growing strains of *Mycobacterium* is reported. The isolation of a number of flavonoids and flavonoid glycosides has been reported from this perennial bulbous herb (Carotenuto *et al.*, 1997).

MATERIALS AND METHODS

Instruments and reagents. NMR spectra were recorded on a Bruker Avance 500 MHz spectrometer. Chemical shift values (δ) were reported in parts per million (ppm) relative to appropriate internal solvent standard and coupling constants (J values) are given in Hertz. Mass spectra were recorded on a Finnigan MAT 95 high resolution, double focusing, magnetic sector mass spectrometer. Accurate mass measurement was achieved using voltage scanning of the accelerating voltage. This was nominally 5 kV and an internal reference of heptacosa was used. Resolution was set between 5000 and 10 000. IR spectra were recorded on a Nicolet 360 FT-IR spectrophotometer and UV spectra on a Thermo Electron Corporation Helios spectrophotometer.

Plant material. The fresh bulbs of *A. neapolitanum* were obtained from Gee Tee Garden Products,

* Correspondence to: Dr S. Gibbons, Centre for Pharmacognosy and Phytotherapy, The School of Pharmacy, University of London, 29–39 Brunswick Square, London WC1N 1AX, UK.
E-mail: simon.gibbons@pharmacy.ac.uk
Contract/grant sponsor: Engineering and Physical Sciences Research Council; contract/grant number: GR/R47646/01.
Contract/grant number: GR/S30269/01.

Received 1 February 2007
Accepted 12 February 2007

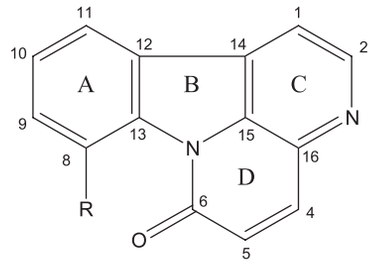

1; R = H

2; R = OH

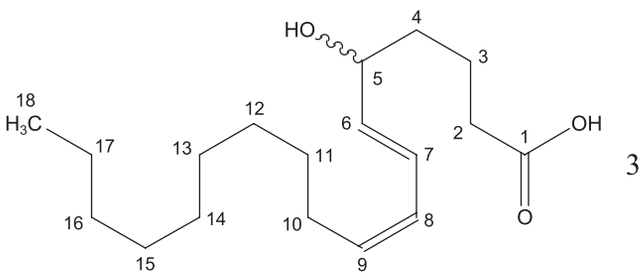

3

Lincolnshire, UK, and a herbarium specimen (GO'D/013B) was deposited at the Centre for Pharmacognosy and Phytotherapy.

Extraction and isolation. 6.3 kg of macerated bulb material underwent cold extraction with hexane, chloroform and methanol (3 L). The chloroform extract (3.4 g) was subjected to vacuum liquid chromatography (VLC) on silica gel eluting with hexane and 10% increments of ethyl acetate to yield 12 fractions. The fractions eluted with 30% and 20% hexane exhibited MIC values of 32 µg/mL against *Mycobacterium fortuitum* and, combined, underwent a further fractionation by Sephadex (LH-20) eluting fractions with 95% methanol to yield compounds **1** (13.6 mg) and **2** (4.4 mg). Sephadex fraction 2 underwent a final purification with reversed-phase preparative HPLC (5–95% acetonitrile, 50 mL/min) to yield compound **3** (16.3 mg).

Antibacterial assay. *Mycobacterium fortuitum*, *M. smegmatis*, *M. abscessus* and *M. phlei* were acquired from the NTCC. *M. smegmatis* $mc^2$2700, which expresses the *M. tuberculosis* FASI gene, was provided by O. Zimhony (Zimhony *et al.*, 2004). Strains were grown on Columbia blood agar (Oxoid) supplemented with 7% defibrinated horse blood (Oxoid) and incubated for 72 h (120 h for *M. abscessus*) at 37 °C prior to minimum inhibitory concentration (MIC) determination. *S. aureus* strains were cultured on nutrient agar and incubated for 24 h at 37 °C. Strain XU212, which possesses the TetK tetracycline efflux protein, was a generous gift from E. Udo (Gibbons and Udo, 2000). SA-1199B, which overexpresses the norA gene encoding the NorA MDR efflux protein was provided by G. Kaatz (Kaatz, 1993). EMRSA-15 which possesses the mecA gene was provided by Dr Paul Stapleton, ULSOP. Bacterial inocula equivalent to the 0.5 McFarland turbidity standard were prepared in normal saline and diluted to give a final inoculum density of 5×10^5 cfu/mL. The inoculum (125 µL) was added to all wells and the microtitre plate was incubated at 37 °C for 24 h for *S. aureus* strains and 72 h for *M. fortuitum*, *M. smegmatis* and *M. phlei.* For *M. abcessus* the plate was incubated for 120 h. The MIC was recorded as the lowest concentration at which no bacterial growth was observed as previously described (Gibbons and Udo, 2000).

Ethambutol and isoniazid were used as positive controls for the mycobacterial strains and norfloxacin was used for *S. aureus*.

Canthin-6-one (1). Amorphous yellow solid; λ_{max} (log ε): 398.0 (3.97), 383.0 (3.95), 319.5 (4.19), 240.0 (4.64) nm; IR ν_{max} (thin film) cm^{-1}: 2917, 2358, 1652, 1600, 1436; HR-MS (*m/z*): 221.0755 $[M + H]^+$ (calc. For $C_{14}H_8ON_2$, 220.0636).

8-Hydroxy-canthin-6-one (2). Amorphous yellow solid; λ_{max} (log ε): 381.5 (3.76), 374.0 (3.66), 364.0 (3.93), 318.0 (3.90), 295.5 (3.77), 292.5 (3.77), 261.0 (3.90) nm; IR ν_{max} (thin film) cm^{-1}: 3286 (br), 3060, 1669, 1632, 1434, 1333, 1142, 844, 794, 749; ^{1}H NMR and ^{13}C NMR ($CDCl_3$): see Table 1; HR-MS (*m/z*): 237.0664 $[M + H]^+$ (calc. For $C_{14}H_8O_2N_2$, 236.0585).

5(ζ)-Hydroxy-octadeca-6(*E*)-8(*Z*)-dienioc acid (3). Colourless oil; $[\alpha]24_D$ 0° (c 0.65, MeOH). UV (MeOH): λ_{max}: (log ε) 276.0 (3.45), 232.0 (4.22) nm. IR (film) υ_{max}: 2928, 2856, 1707, 987 cm^{-1}; ^{1}H-NMR and ^{13}C-NMR (MeOD): Table 2; HR-MS (*m/z*): 295.2267 [M]- (calc. for $C_{18}H_31O_3$, 295.2273).

RESULTS AND DISCUSSION

Bioactivity guided isolation of the active chloroform extract (16 µg/mL) yielded compound **1** as a yellow solid, which displayed a positive reaction to Dragendorff's reagent on analysis by TLC. High-resolution ESI-MS showed the $[M + H]^+$ ion at *m/z* 221.0755 indicating a molecular formula of $C_{14}H_8N_2O$. The ^{1}H and ^{13}C-NMR data were in accordance with the published data for canthin-6-one previously isolated from *Ailanthus altissima* (Koike and Ohmoto, 1985).

Compound **2** was isolated as a yellow solid and assigned a molecular formula of $C_{14}H_8N_2O_2$ $[M + H]^+$ (237.0664) with HRESI-MS. A positive reaction was also observed with Dragendorff's reagent, and the ^{1}H-NMR data (Table 1) were in close agreement with the published literature for 8-hydroxy-canthin-6-one previously isolated from *Ailanthus excelsa* (Cordell *et al.*, 1978). However, the full NMR data for this metabolite were not reported so a full analysis of the resonances of **2** was undertaken. The ^{1}H and ^{13}C-NMR data were similar to those for compound **1**; however, ring A was seen to be an ABC tri-substituted aromatic system and a deshielded hydroxyl singlet was present at δ 11.95 in the ^{1}H-NMR spectrum. In addition to the hydroxyl group, the ^{1}H-NMR data for compound **2** displayed seven signals in the aromatic region (δ 7.10–8.90). Three protons, two doublets (δ 7.58 and δ 7.23) and one triplet (δ 7.45) were equivalent to an ABC aromatic system as seen through COSY correlations. Two further *ortho* coupled aromatic systems were also evident; one indicative of a *cis* double-bond adjacent to a carbonyl group at δ 8.18 and δ 7.10 (J = 10.0 Hz) and the other consistent with positioning next to an aromatic nitrogen δ 8.90 and δ 8.00 (J = 5.0 Hz). In addition to seven

Table 1. ^{1}H (500 MHz) and ^{13}C NMR (125 MHz) spectral data and ^{1}H-^{13}C long-range correlations of 2 recorded in $CDCl_3$

No	^{1}H	^{13}C	^{2}J	^{3}J
1	8.00 *d* (5.0)	117.0		
2	8.90 *d* (5.0)	147.2		
4	8.18 *d* (10.0)	141.3		C-6, C-15
5	7.10 *d* (10.0)	127.0		C-16
6	–	160.7		
8	–	146.8		
9	7.23 *d* (8.0)	119.6	C-10	C-11
10	7.45 *t* (8.0)	128.7		C-8, C-12
11	7.58 *d* (7.5)	113.4	C-10, C-12	C-9, C-14
12	–	126.9		
13	–	141.4		
14	–	127.5		
15	–	131.6		
16	–	136.9		
OH	11.95 *s*	–		C-9

Table 2. ^{1}H (500 MHz) and ^{13}C NMR (125 MHz) spectral data and ^{1}H-^{13}C long-range correlations of 3 recorded in MeOD

No.	^{1}H	^{13}C	^{2}J	^{3}J
1	–	177.8		
2	2.27 *t* (7.5)	35.1	C-1	
3	1.60 *m*	26.3		C-1
4	1.53 *m*	38.5		
	1.47			
5	4.09 *dd* (13.0, 6.5)	73.4	C-4, C-6	C-3, C-7
6	5.62 *dd* (15.0, 7.0)	137.3	C-5	C-4, C-8
7	6.50 *dd* (15.4, 11.0)	126.5	C-8	C-5, C-9
8	5.98 *t* (11.0)	129.4	C-7	C-6, C-10
9	5.41 *dt* (15.0, 10.5, 7.5)	132.9	C-10	C-7, C-11
10	2.20 *dd* (13.0, 7.5)	28.4	C-9, C-11	C-8
11	1.39 *m*	30.7		C-9
12–15	1.31 *m*	30.7		
16	1.31 *m*	33.0		
17	1.31 *m*	23.7		
18	0.91 *t* (7.0)	14.0	C-17	C-16

methine carbons, the ^{13}C-NMR spectrum revealed the presence of six aromatic quaternary carbons (δ 113.4–147.2), and one deshielded signal consistent with a carbonyl carbon (δ 160.7).

Ring A was defined as an ABC aromatic system by COSY correlations. The doublet at δ 7.23 (H-9; J = 8.0 Hz) displayed a COSY correlation to the triplet at δ 7.45 (H-10; J = 8.0 Hz) which in turn coupled to the doublet at δ 7.58 (H-11; J = 7.5 Hz). H-10 displayed a ^{3}J HMBC correlation to the hydroxylated quaternary carbon C-8 (δ 146.8) and H-10 displayed a ^{3}J correlation to C-12 (δ 126.9).

Ring C was consistent with an *ortho* coupled pair of hydrogens (H-1, δ 8.00 and H-2, δ 8.90; J = 5.0 Hz) positioned on a pyridine ring. H-1 displayed an HMBC correlation to the quaternary carbon C-15 (δ 131.6), completing the assignment of ring B, while H-2 showed an HMBC correlation to the C-14 quaternary (δ 127.5). The only NOESY correlation present was between H-1 and H-11 concluding the β-carboline skeleton of the cantin-6-one structure. The D ring was finally assigned as a pyridone through further HMBC correlations. H-4 and H-5 (δ 8.18 and δ 7.10) gave a coupling constant of 10.0 Hz suggesting they were positioned α and β to a carbonyl carbon and a ^{3}J HMBC correlation between H-4 to C-6 (δ 160.7) confirmed this. Furthermore ^{3}J correlations between H-4 and C-15 (δ 131.6), and H-5 to C-16 (δ 136.9) revealed the quaternary carbons of the C→D ring junction. The remaining quaternary carbon C-13 was assigned by comparison with the published literature for canthin-6-one (Koike and Ohmoto, 1985). The ^{13}C NMR data have not been published previously for this metabolite and are reported here for the first time.

Compound **3** was isolated as a colourless oil and assigned a molecular formula of $C_{18}H_{31}O_3$ $[M + H]^-$ (295.2267) with HRESI-MS. The ^{1}H-NMR data (Table 2) were reminiscent of a monohydroxylated unsaturated fatty acid recently described by Stavri *et al.* (2006).

A deshielded methylene triplet at δ 2.27 (H-2; J = 7.5 Hz) displayed a strong ^{2}J correlation to a carbonyl carbon (δ 177.8) of the carboxylic acid. A weaker ^{3}J correlation was evident from a second downfield methylene (δ 1.60 m) positioned β to the carbonyl carbon. Non-equivalent methylene hydrogens at δ 1.53 (C-4) displayed a ^{2}J correlation to C-3 (δ 26.3). An oxymethine

DOI: 10.1002/ptr

Table 3. MICs of 1, 2 and 3 and standard antibiotics in μg/mL

Strain	1	2	3	Ethambutol	Isoniazid	Norfloxacin
M. fortuitum ATCC 6841	16	16	32	4	0.25	ξ
M. smegmatis ATCC 14468	8	16	32	0.25	2	ξ
M. smegmatis mc^{2}2700	8	2	16	0.25	2	ξ
M. phlei ATCC 11758	8	8	16	0.5	2	ξ
M. abcessus ATCC 19977	16	32	ξ	128	128	ξ
S. aureus 1199B	8	16	>128	ξ	ξ	32
S. aureus XU212	8	8	>128	ξ	ξ	16
S. aureus EMRSA-15	32	64	>128	ξ	ξ	0.5

ξ, not tested.

hydrogen (H-5; δ 4.09) displayed ^2J correlations to the methylene of C-4 (δ 38.5) and to an olefinic carbon at C-6 (δ 137.3). ^3J correlations from H-5 to the C-3 methylene (δ 26.3) and the C-7 olefinic carbon (δ 137.3) were also evident.

The olefinic hydrogens were ordered through COSY correlations. The double doublet of H-6 (δ 5.62; J = 15.0, 7.0 Hz) coupled to the double doublet of H-7 (δ 6.50; J = 15.5, 11.0 Hz) through a large coupling constant which signified a *trans* configuration. H-7 then coupled to a triplet of H-8 (δ 5.98; J = 11.0 Hz) which in turn displayed a coupling to a doublet of triplets of H-9 (δ 5.41; J = 10.5, 7.5 Hz). The coupling constant between H-8 and H-9 was smaller than that for the H-7/H-8 double bond suggesting a *cis* configuration. H-9 displayed a further coupling to a methylene at δ 2.20 (H-10) which coupled to a methylene at δ 1.39 (H-11) and finally into a methylene envelope at δ 1.31. ^2J and ^3J correlations from H-9 to C-10 (δ 28.4) and C-11 (δ 30.7), respectively, confirmed this. The terminal methyl exhibited a COSY coupling to the methylene envelope and ^2J and ^3J HMBC correlations into methylene carbons at δ 23.7 and δ 33.0, respectively.

The specific optical rotation data (α = 0.00; c = 0.65, MeOH) was inconclusive for the stereochemical assignment of C-5. This is in accordance with the findings of Stavri *et al.* (2006) where it was suggested that the racemate could be due to a non-enzymatic hydrolysis of a 2-3 double bond to afford 3(ζ)-hydroxy-octadeca-4(E)-6(Z)-dienoic acid (a 4-5 double bond in the case of compound **3**) resulting in the non-specific orientation of the hydroxyl group.

The ^{1}H and ^{13}C-NMR data were very similar to those for 3(ζ)-hydroxy-octadeca-4(E)-6(Z)-dienoic acid isolated from *Scrophularia deserti* (Stavri *et al.*, 2006) and this is the first time the NMR data for 5(ζ)-hydroxy-octadeca-6(E)-8(Z)-dienoic acid have been reported.

Compounds **1** and **2** exhibited the most pronounced antibacterial activity with MIC values of 8–64 μg/mL against the *S. aureus* strains and 2–32 μg/mL against a range of fast-growing *Mycobacterium* species (Table 3). The antimycobacterial activity compared favourably with the control antibiotic isoniazid against *M. smegmatis* (mc^{2}2700), *M. phlei* and *M. abscessus*. The MIC values for **1** and **2** were comparable against most bacterial strains tested, however, **2** displayed enhanced activity against the *M. smegmatis* (mc^{2}2700) strain expressing the *M. tuberculosis* FASI gene, when compared with that for **1**. Furthermore, the activity of **2** was greater against *M. smegmatis* (mc^{2}2700) than *M. smegmatis* (ATCC 14468) suggesting that the C-8 hydroxyl substituent may play a role in the inhibition of FASI. This is an intriguing target for new antimycobacterial agents as mycobacterial FASI is a unique but important enzyme in mycolic acid synthesis (Zimhony *et al.*, 2004). In addition, these compounds are planar and it may also be deduced that the mode of action could be through DNA intercalation. Canthin-6-one type alkaloids are well known constituents of the Simaroubaceae and Rutaceae and antimicrobial activity, particularly from the genus *Zanthoxylum*, is well reported (Islam and Ashan, 1997; Thouvenel *et al.*, 2003). This is the first reported isolation of these natural products from the Alliaceae and may be of chemotaxonomic value. Compound **3** displayed activity in the range 16–32 μg/mL against the fast-growing *Mycobacterium* species but no activity at the concentrations tested against the *S. aureus* strains. These data are consistent with those reported for the antibacterial activity of 3(ζ)-hydroxy-octadeca-4(E)-6(Z)-dienoic acid (Stavri *et al.*, 2006) suggesting that the position of the olefinic and hydroxyl groups may have little influence on the antibacterial activity.

Acknowledgement

We thank the Engineering and Physical Sciences Research Council (grant numbers GR/R47646/01 and GR/S30269/01) for funding. No conflict of interest exists.

REFERENCES

Bange F-C, Kirschner P, Böttger S. 1999. Recovery of mycobacteria from patients with cystic fibrosis. *J Clin Microbiol* **37**: 3761–3763.

Bolton SG, Null G, Troetel WM. 1982. The medical uses of garlic – fact and fiction. *J Am Pharm Assoc* **22**: 40–43.

Carotenuto A, Fattorusso E, Lanzotti V, Magno S, De Feo V, Cicala C. 1997. The flavonoids of *Allium neapolitanum*. *Phytochemistry* **44**: 949–957.

Cavallito CJ, Bailey JH. 1944a. Allicin, the antibacterial principle of *Allium sativum*. II. Determination of the chemical structure. *J Am Chem Soc* **66**: 1952–1954.

Cavallito CJ, Bailey JH, Buck JS. 1945. The antibacterial principle

of *Allium sativum* III. Its precursor and 'essential oil of garlic'. *J Am Chem Soc* **67**: 1032–1033.
Cavallito CJ, Buck JS, Suter CM. 1944b. Allicin, the antibacterial principle of *Allium sativum*. I. Isolation, physical properties and antibacterial action. *J Am Chem Soc* **66**: 1950–1951.
Cordell GA, Ogura M, Farnsworth NR. 1978. Alkaloid constituents of *Ailanthus excelsa* (Simaroubaceae). *Lloydia* **41**: 166–168.
Falkinham JO. 1996. Epidemiology of infection by nontuberculous mycobacteria. *Clin Microbiol Rev* **9**: 177–215.
Gibbons S, Udo EE. 2000. The effect of reserpine, a modulator of multidrug efflux pumps, on the *in vitro* activity of tetracycline against clinical isolates of methicillin resistant *Staphylococcus aureus* (MRSA) possessing the *tet*(K) determinant. *Phytother Res* **14**: 139–140.
Islam SKN, Ashan M. 1997. Biological activities of the secondary metabolites isolated from *Zieria smithii* and *Zanthoxylum elephantiasis* on microorganisms and brine shrimps. *Phytother Res* **11**: 64–66.
Kaatz GW. 1993. Efflux-mediated fluoroquinolone resistance in *Staphylococcus aureus*. *Antimicrobial Agents Chemother* **37**: 1086–1094.
Koike K, Ohmoto T. 1985. Carbon-13 nuclear magnetic resonance study of canthin-6-one alkaloids. *Chem Pharm Bull* **33**: 5239–5244.
Stavri M, Mathew KT, Gibbons S. 2006. Antimicrobial constituents of *Scrophularia deserti*. *Phytochemistry* **67**: 1530–1533.
Thouvenel C, Gantier J-C, Duret P *et al.* 2003. Antifungal compounds from *Zanthoxylum chiloperone* var. *angustifolium*. *Phytother Res* **17**: 678–680.
World Health Organization. 2000. WHO Tuberculosis Fact Sheet No. 104. WHO: Geneva.
Zimhony O, Vilchèze C, Jacobs Jr WR. 2004. Characterization of *Mycobacterium smegmatis* expressing the *Mycobacterium tuberculosis* fatty acid synthase I (*fasI*) gene. *J Bacteriol* **186**: 4051–4055.

Theor Chem Acc (2007) 117: 247–252
DOI 10.1007/s00214-006-0148-7

REGULAR ARTICLE

Mire Zloh · Franz Bucar · Simon Gibbons

Quantum chemical studies on structure activity relationship of natural product polyacetylenes

Received: 24 June 2005 / Accepted: 10 November 2005 / Published online: 22 June 2006

Abstract An extract of the roots of *Levisticum officinale* L. (Apiaceae) exhibited significant antimycobacterial activity against *Mycobacterium fortuitum*, where diacetylene compounds were identified as the active components in this extract. In contrast, polyacetylenes isolated from different sources surprisingly exhibited no anti-mycobacterial activity. Additionally, a whole series of furanocoumarin ethers of the polyacetylene falcarindiol exhibited anti-proliferative properties. We have studied the relationship between the electronic properties and biological activity of these structurally related compounds and a good qualitative correlation between predicted lipophilic parameters and activity has been established.

Keywords Antimycobacterial activity · Polyacetylenes · Falcarindiol · log *P*

1 Introduction

Polyacetylene natural products are widespread in the plant families Asteraceae and Apiaceae exhibit many biological activities. Some of these compounds are highly poisonous such as cicutoxin from water hemlock (*Cicuta virosa*). Recently, the toxicity of these compounds has been shown to be due to their ability to bind to GABA-gated Cl^- channels of GABA receptors, and these channels play an important role in the acute toxicity of these compounds [1].

Certain diacetylenes have been found to have antimycobacterial [2], anti-staphylococcal [3], and anti-proliferative activities [4]. Polyacetylenes are also synthesized *de novo* as phytoalexins [5] and it is highly likely that these compounds are produced by plants as part of their chemical defense against microbes in their environment.

Our interest in this class of natural product started with the evaluation of members of the plant family Apiaceae with a view to discover and characterize new classes of antibacterial agents from plants [3,6,7]. Certain compounds, particularly falcarindiol display moderate bacterial, and mammalian cytotoxicity and are active against multi-drug resistant (MDR) strains of *Staphylococcus aureus* which is a continuing problem in the clinical setting. We have characterized a number of these agents to date and have noticed that simple changes to the polyacetylene core dramatically influence biological activity.

Significant antimycobacterial activity against *Mycobacterium fortuitum* was attributed to the active components 3(*R*)-falcarinol [3(*R*)-(-)-1,9-heptadecadien-4,6-diin-3-ol] (panaxynol) **1** and 3(*R*)-8(*S*)-falcarindiol [3(*R*)-8(*S*)-(+)-1,9-heptadecadien-4,6-diin-3,8-diol] **2** from an extract of the roots of *Levisticum officinale* L. (Apiaceae) [6]. 3(*R*),8(*R*)-dehydrofalcarindiol **3** and 1,3 *R*,8 *R*-trihydroxydec-9-en-4,6-yne **4** were inactive, while a whole series of polyacetylenes exhibited inhibitory activity against MK-1 cell growth (panaxynol **1**, (9Z)-l,9-heptadecadiene-4,6-diyne-3,8,11-triol **5**, 8-acetoxy-heptadeca-1,9-diene-4,6-diyne-8-ol **6**, and japoangelols A, B, C and D **7**, **8**, **9** and **10**, respectively) [8].

This paper describes an evaluation of the calculated molecular properties of a series of polyacetylenes (Scheme 1) in an attempt to explain differences in bioactivity, particularly as cytotoxic agents against bacterial and mammalian cell lines.

M. Zloh (✉)
Department of Pharmaceutical and Biological Chemistry,
The School of Pharmacy,
University of London,
29/39 Brunswick Square,
London, WC1N 1AX, UK
E-mail: mire.zloh@ulsop.ac.uk

F. Bucar
Department of Pharmacognosy,
Institute of Pharmaceutical Sciences,
University of Graz,
Universitaetsplatz 4/I,
8010 Graz, Austria

S. Gibbons
Centre for Pharmacognosy and Phytotherapy,
The School of Pharmacy,
University of London,
29/39 Brunswick Square,
London, WC1N 1AX, UK

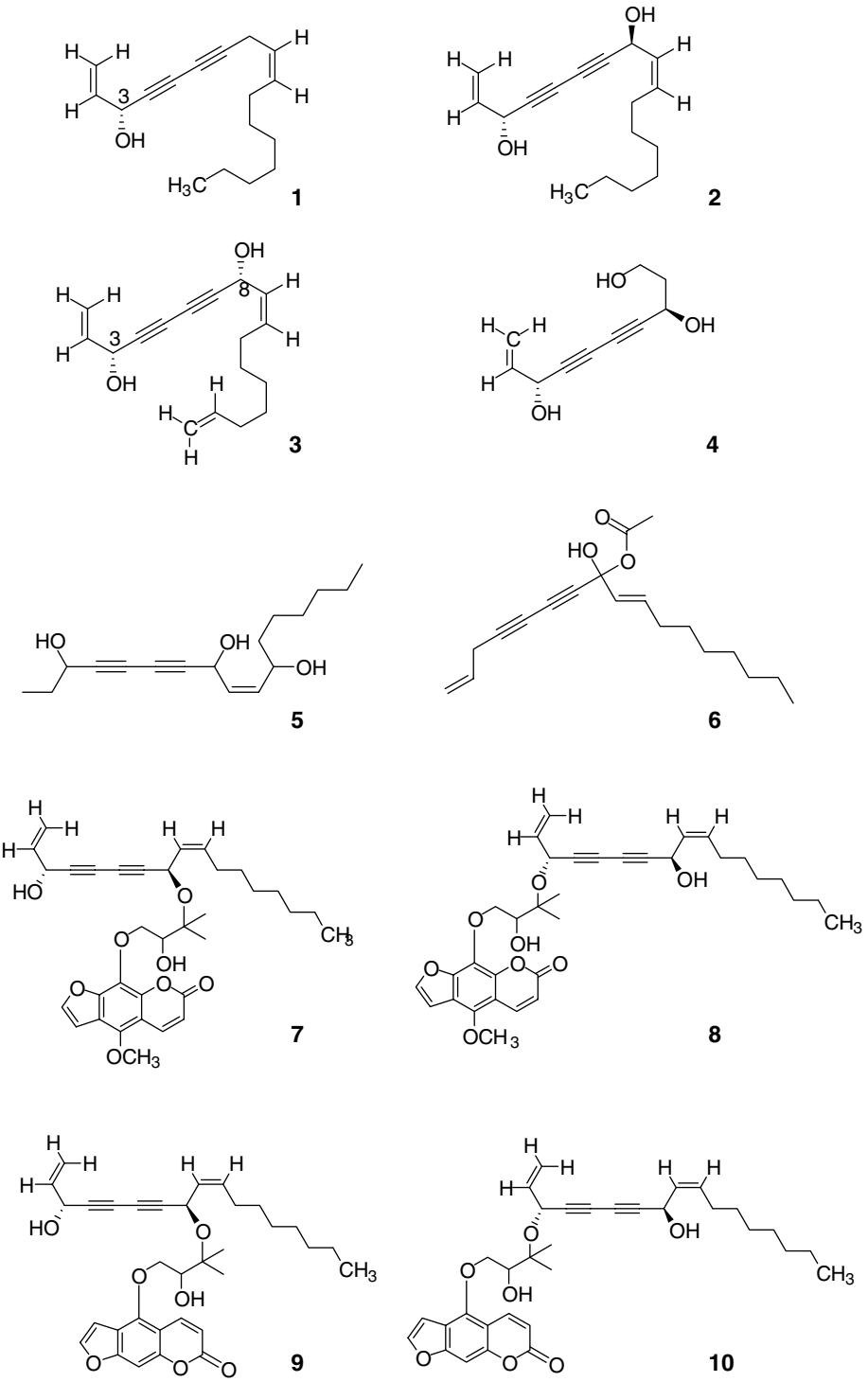

Scheme 1

2 Computational methods

2.1 Model building and conformational analysis

The initial structures of a series of polyacetylenes were built and saved as mol2 files by Chemoffice Ultra 7.0.0 [9]. These structures were imported into MacroModel [10], atom and bond types were adjusted and minimized with the MMFFs force field parameters [11]. The generalized Born/surface area (GB/SA) continuum solvent model for H_2O [12] implemented in MacroModel was used to simulate an aqueous environment, with a constant dielectric function ($\varepsilon = 1$). An extended non-bonded cutoff (van der Waals 8 Å; electrostatics 20 Å) was used.

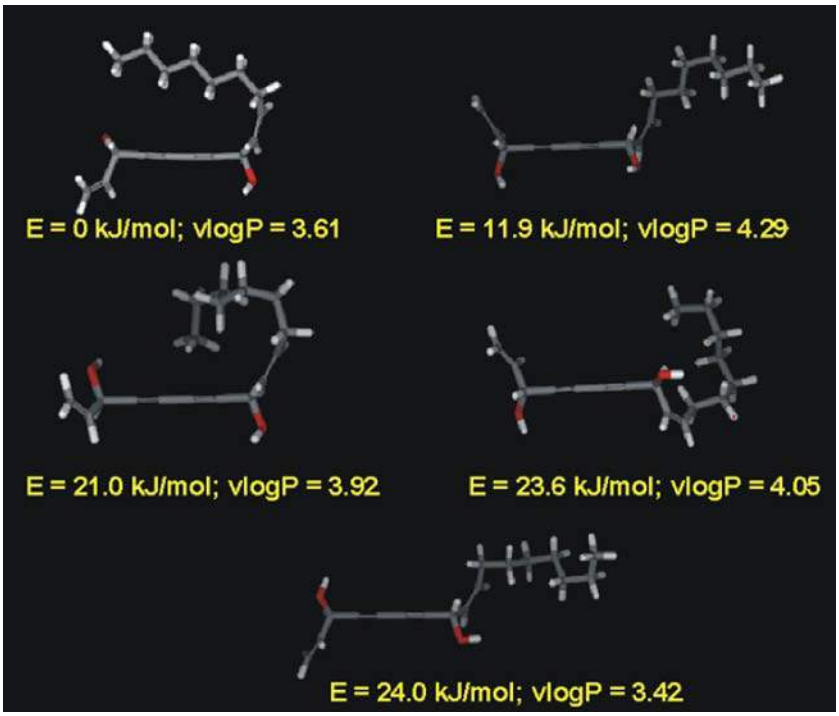

Fig. 1 The representative structures of **2** with the virtual log P (v log P) and relative energies (E) calculated using the HF/3-21G(d) basis set

Using the optimized structures, a systematic conformational search on each molecule was performed. All compounds used 500 step Monte Carlo conformational analysis, with the energy cut off generally set to $\Delta E = 10$ kJ/mol above the lowest energy conformation. The ensembles of generated structures were clustered and analyzed using the cluster analysis program Xclusterl [12]. Representative structures for each molecule were selected and subjected to *ab initio* calculation using Gamess US software and HF/3-21G(d) basis set [13].

2.2 Calculation of molecular properties

Molecular lipophilicity potential (MLP) is a structure–property descriptor that visualizes the lipophilic properties of the molecule on its three-dimensional (3D) surface and was calculated by projecting the Broto–Moreau lipophilicity atomic constants on the molecular surface [14]. The virtual log P, Broto log P and lipole, of all single molecules and complexes were evaluated by VegaZZ software [15,16].

The correlations between different calculated values and activities were examined by the Gretl software package [17].

3 Results and discussions

The conformational, electronic, and molecular properties were studied to examine the possible relationship between structure and broad cytotoxic activity on several different targets, although the mechanism of action of polyacetylenes is still not known.

The conformational space of all compounds was examined using a Monte Carlo conformational search and five representative structures were fully optimized using an HF/3-31G(d) basis set. This produced a set of stable structures for each compound, with some conformations that could be adopted. The conformational flexibility of molecule **2** is shown in Fig. 1 as an example, and the energies calculated by the *ab initio* method are given relative to the most stable conformation. It was noticed that lipole and virtual log P depend on the conformation of a molecule, and the predicted values of virtual log P (v log P) from **2** are also depicted in Fig. 1. The virtual log P varies in a wide range from 3.42 to 4.29, and depends on the spatial arrangement of the terminal double bond and the hydrocarbon chain. The lowest value of virtual log P was observed when those two moieties are in a *trans* conformation, while the *cis* arrangement will result in high virtual log P values. The arrangement of other groups of the molecule will contribute to the variations of the virtual log P within extremes. Since it is not known which conformation is bioactive, the average values of lipole and virtual log P were used in further calculation. The most stable conformation was selected from five representative conformations of each molecule and used in calculation of other molecular descriptors used in this study.

3.1 Antibacterial activity of polyacetylenes

The molecular properties of the set of molecules with known antibacterial activity are shown in the Table 1. Although this set is small, a trend was observed in which the antibacterial

Table 1 Calculated molecular descriptors log *P*, HOMO, LUMO, their difference, dipole moment, and antibacterial activity against *Mycobacterium fortuitum* from [1,2]

Molecule	log *P*	lipole	Virtual logp *P*	HOMO(eV)	LUMO(eV)	Difference(eV)	Dipole(Db)	LogMIC(exp)	LogMIC (calc)
1	4.762	6.530	5.180	−9.2286	3.550	12.779	2.044	4.80	4.59
2	3.409	4.206	3.860	−9.3744	3.318	12.693	1.731	4.19	4.41
3	03.172	4.717	3.736	−9.3204	3.413	12.733	4.529	<3.30	3.37
4	−0.249	2.073	0.232	−9.6066	3.208	12.814	3.319	<3.15	3.06

MIC is defined as a molar minimum inhibitory concentration

Table 2 Calculated molecular descriptors log *P*, HOMO, LUMO, their difference, dipole moment, and inhibitory activity against MK-1 cell growth from [3]

Molecule	log *P*	lipole	Virtual logp *P*	HOMO(eV)	LUMO(eV)	Difference(eV)	Dipole(Db)	LogMIC(exp)	LogMIC (calc)
1	4.762	6.530	5.180	−9.2286	3.550	12.779	2.044	5.92	5.71
5	2.293	3.337	3.049	−9.5526	3.1185	12.671	2.198	5.10	4.98
6	3.672	3.809	4.804	−9.2961	3.4209	12.717	1.836	4.97	5.07
2	3.409	4.206	3.860	−9.3744	3.3183	12.693	1.731	4.91	5.17
7	8.705	2.010	7.330	−8.5428	1.7469	10.290	6.068	4.83	4.75
8	8.705	1.843	6.528	−8.1135	1.9953	10.109	11.075	4.90	4.69
9	8.564	3.323	8.090	−8.7156	1.6902	10.406	7.465	4.87	5.07
10	8.564	2.389	7.251	−8.6886	1.7199	10.409	8.493	4.81	4.84

MIC is defined as a molar minimum inhibitory concentration

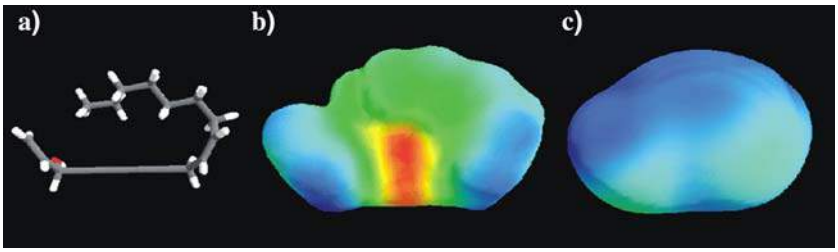

Fig. 2 **a** Lowest energy conformation of **1**, **b** map of electrostatic potential, **c** map of lipophilicity potential

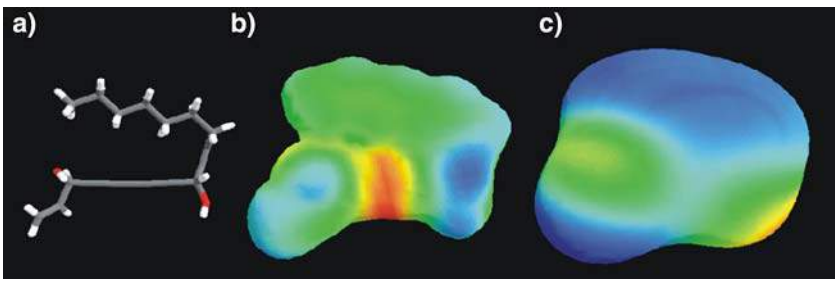

Fig. 3 **a** Lowest energy conformation of **2**, **b** map of electrostatic potential, **c** map of lipophilicity potential

activity decreases with the decreasing log *P*. This is expected since it is known that the log *P* is usually correlated with a biological activity [18]. It was also found that biological activity could be correlated to predict dipole moments. The correlations were tested using the Mixed Approach method [19] and regression analysis. Results of the regression analysis are shown in Eq. (1).

$$\text{LogMIC} = 4.3(\pm 0.6) + 0.21(\pm 0.09) \times \log P - 0.35(\pm 0.15) \times \text{Dipole} \quad (1)$$

$$n = 4,\ r = 0.94,\ F = 8.45,\ s = 0.77,$$

where *n* is number of molecules, *r* is correlation, *F* is Fisher's significance factor and *s* is the standard deviation. It has to be considered that the data set is small and this result might not be statistically significant. Although the fit is good (Table 1), these correlations should be treated with caution, especially since the small difference in log *P* between **2** and **3** does not fully explain the different activity. Therefore maps of electrostatic and lipophilicity potential were compared for

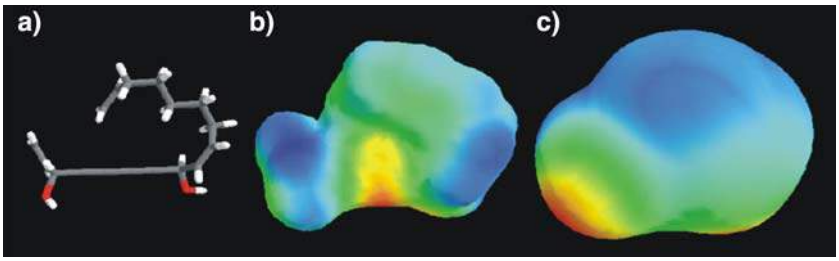

Fig. 4 **a** Lowest energy conformation of **3**, **b** map of electrostatic potential, **c** map of lipophilicity potential

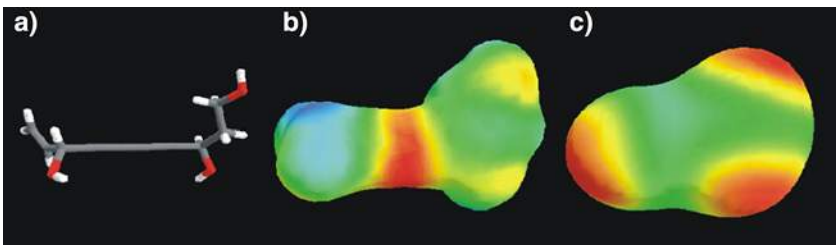

Fig. 5 **a** Lowest energy conformation of **4**, **b** map of electrostatic potential, **c** map of lipophilicity potential

molecules **1**–**4** (Figs. 2, 3, 4, 5, respectively). It is noticeable that the polarity and the lipophilicity of the substituents on the diacetylene moiety are different for all molecules. The higher polarity of the surface of the substituent may explain the lower antimicrobial activity of the molecule. Since the mechanism of cytotoxicity of the polyacetylene class is not known, we can hypothesize that the hydrophobic interaction between substituents on the polyacetylene structure and the target in the cell could play an important role for antibacterial activity.

3.2 Anti-proliferative properties

A separate study on a series of polyacetylene compounds was carried out to determine their inhibitory activity against MK-1 cell growth [8]. Molecular properties were calculated for each and correlated with their anti-proliferative activity. A correlation was observed between activity and calculated lipole. This suggests that the activity might depend on drug influx into cells [20]. Additionally, a correlation was observed between activity and LUMO energy. A similar correlation between the anti-proliferative activity and the E_{LUMO} was observed for bispyridinium compounds in the inhibition of choline kinase and the equation for predicting activity has given excellent results [21]. The mechanism of action was explained by the occurrence of either charge transfer or bipolar interactions. We believe that a similar mechanism could be involved in inhibition of MK-1 cell growth, since a correlation between activity and LUMO energies was observed. These correlations were tested using regression analysis and the results are given as Eq. (2).

$$\mathrm{LogMIC} = 4.4(\pm 0.25) + 0.24(\pm 0.083) \times \mathrm{lipole} - 0.06(\pm 0.15) \times \mathrm{LUMO}$$

$$n = 8,\ r = 0.76,\ F = 7.92,\ s = 0.22. \tag{2}$$

These findings do not have statistical significance and there is a problem to accurately calculate activities of most molecules, however it has predicted the activity of the highly potent molecule **1**. Therefore, these correlations should be used as qualitative indicators, rather than quantitative predictions of anti-proliferative activities.

Although it has been found that compound **3** is not active against bacteria, the log P and the LUMO energy value is similar to those of anti-proliferative compounds. Therefore, we have decided on the basis of this study to evaluate the anti-proliferative activity of **3**, for which we are awaiting results.

4 Conclusions

Molecular modeling analysis of a series of the polyacetylene compounds has allowed us to correlate molecular properties with experimental antibacterial and anti-proliferative data. Although the datasets are small for a full QSAR study, based on the reasoning described above, we have concluded that antimicrobial activity correlates well with the calculated log P and with the presence of a hydrophobic group on the substituent of the polyacetylene moiety. The anti-proliferative activity increases with increasing lipole in a series of polyacetylene compounds. A good correlation was also observed between activity and LUMO energies, suggesting that charge transfer might be involved in the mechanism of action. The preliminary QSAR study indicated that it is not possible to quantitatively predict activities, but a fairly good qualitative tendency between experimental activities and calculated values for molecular properties was found for this series of polyacetylenic natural products.

References

1. Uwai K, Ohashi K, Takaya Y, Ohta T, Tadano T, Kisara K, Shibusawa K, Sakakibara R, Oshima Y (2000) J Med Chem 43:4508–4515
2. Kobaisy M, Abramowski Z, Lermer L, Saxena G, Hancock REW, Towers GHN, Doxsee D, Stokes RW (1997) J Nat Prod 60:1210
3. Lechner D, Stavri M, Oluwatuyi M, Pereda-Miranda R, Gibbons S (2004) Phytochemistry 64:331
4. Bernart MW, Cardellina JH II, Balaschak MS, Alexander MR, Shoemaker RH, Boyd MR (1996) J Nat Prod 59:748
5. Elgersma DM, Liem JI (1989) Physiol Mol Plant P 34:545
6. Schinkovitz A, Stavri M, Gibbons S, Bucar F (2005) Fitoterapia (submitted)
7. Stavri M, Mathew KT, Gibson T, Williamson RT, Gibbons S (2004) J Nat Prod 67:892
8. Furumi K, Fujioka T, Fujii H, Okabe H, Nakano Y, Matsunaga H, Katano M, Mori M, Mihashi K (1998) Bioorg Med Chem Lett 8:93
9. ChemOffice Ultra 2002 (2001) nCambridgeSoft
10. Mohamadi F, Richards N, Guida W, Liskamp R, Lipton M, Caulfield C, Chang G, Hendrickson T, Still W (1990) J Comput Chem 11:440
11. Cramer CJ, Truhlar DG (1995) In: Lipkowitz KB, Boyd DB (eds) Rev Comp Chem, VCH, New York 6:1
12. Still WC, Tempczyk A, Hawley RC, Hendrickson T (1990) J Am Chem Soc 112:6127
13. Schmidt MW, Baldridge KK, Boatz JA, Elbert ST, Gordon MS, Jensen JH, Koseki S, Matsunaga N, Nguyen KA, Su SJ, Windus TL, Dupuis M, Montgomery JA (1993) J Comput Chem 14:1347
14. Gaillard P, Carrupt PA, Testa B, Boudon A (1994) J CAMD 8:83
15. Pedretti A, Villa L, Vistoli G (2002) J Mol Graph 21:47
16. Pedretti A, Villa L, Vistoli G (2003) Theor Chem Acc 109:229
17. Gretl 1.3.2 "GNU regression, econometrics and time-series library"
18. Cubini H (1995) In: Burger's medicinal chemistry and drug discovery, vol 1. Interscience, New York
19. Buchwald P, Bodor N (1998) Curr Med Chem 5:353
20. Mälkiä A, Murtomäki L, Urtti A, Kontturi K (2004) Eur J Pharm Sci 23:13
21. Campos J, del Carmen Núñez M, Rodríguez V, Entrena A, Hernández-Alcoceba R, Fernández F, Lacal JC, Gallo MA, Espinosa A (2001) Eur J Med Chem 36:215

Pharmaceutical Biology
2008, Vol. 46, No. 4, pp. 250–253

informa
healthcare

A Naturally Occurring Inhibitory Agent from *Hypericum sampsonii* with Activity Against Multidrug-Resistant *Staphylococcus aureus*

Zhi Yong Xiao,[1] Winnie Ka Po Shiu,[2] Yi Han Zeng,[1] Qing Mu,[1] and Simon Gibbons[2]

[1]School of Pharmacy, Fudan University, Shanghai, People's Republic of China; [2]Centre for Pharmacognosy and Phytotherapy, The School of Pharmacy, University of London, London, United Kingdom

Abstract

Bioassay-directed fractionation employing a multidrug-resistant (MDR) strain of *Staphylococcus aureus* resulted in the isolation of an antibacterial prenyl substituted xanthone derivative (**1**) named hyperixanthone A from the root of *Hypericum sampsonii* Hance (Hyperiaceae). Compound **1** showed promising inhibitory activity against the norfloxacin-resistant *S. aureus* strain SA-1199B at a minimum inhibitory concentration (MIC) of 2 μg/mL (4.3 μM), wheres the positive standard antibacterial drug norfloxacin showed an MIC of 32 μg/mL (100 μM). This strain overexpresses the NorA multidrug efflux transporter, the major characterized drug pump in *Staphylococcus aureus*. The activity of this compound against an effluxing strain of *S. aureus* is reported here for the first time. Compound **1**, together with 1,7-dihydroxyxanthone (**2**) and 2-hydroxyxanthone (**3**), were obtained by silica gel column chromatography, and their structures were determined by means of extensive NMR and MS spectra.

Keywords: Hyperiaceae, *Hypericum*, *Hypericum sampsonii* Hance, Hyperixanthone A, multidrug-resistant (MDR) *S. aureus*, norfloxacin-resistant *S. aureus*, xanthone.

Introduction

Multidrug-resistant *Staphylococcus aureus* infections, particularly those caused by methicillin-resistant *S. aureus* (MRSA), have been a major threat to public health in hospitals and the community in the past decade. Despite the new advances in antibiotic development, MRSA infections remain a considerable concern due to the few agents that can be used in their treatment. In 2002, MRSA strains fully resistant to vancomycin were isolated in the United States (CDC, 2002). Resistance to linezolid has also been reported in some patients followed by prolonged antibiotic treatment in the United States (Peeters & Sarria, 2005). Therefore, there is an urgent need to develop new classes of antibiotics to fight the problem of drug resistance. In the search for antibacterial compounds from plants with activity against multidrug-resistant (MDR) *Staphylococcus aureus*, a number of species of the genus *Hypericum* have been investigated because of their ability to produce extracts with antibacterial activity toward MDR strains (Gibbons et al., 2002; Mu et al., 2006).

Our previous research in this area has led to the isolation and characterization of a number of antibacterial acylphloroglucinol natural products (Gibbons et al., 2002, 2005). In this paper, we have evaluated a Chinese species, *Hypericum sampsonii* Hance (Hyperiaceae) of this group against a multidrug-resistant strain of *Staphylococcus aureus*. The lower MIC (64 μg/mL) of the root ethanoll extract against SA-1199B, a NorA overexpressing strain, prompted us to isolate the active constituents. This led to the isolation of the major active prenylated substituted xanthone derivative (**1**), hyperixanthone A (Fig. 1), which exhibited a minimum inhibitory concentration of 2 μg/mL (4.3 μM) against SA-1199B.

Materials and Methods

Plant and chromatography material

Hypericum sampsonii was collected in September 2005 from Chalin County in Hunan province, China. The plant

Accepted: August 30, 2007.

Address correspondence to: Qing Mu, Yi Xue Yuan Road 138, Box 254, School of Pharmacy, Fudan University, Shanghai 200032, People's Republic of China; Email:muqing2000@yahoo.com

DOI: 10.1080/13880200701739405

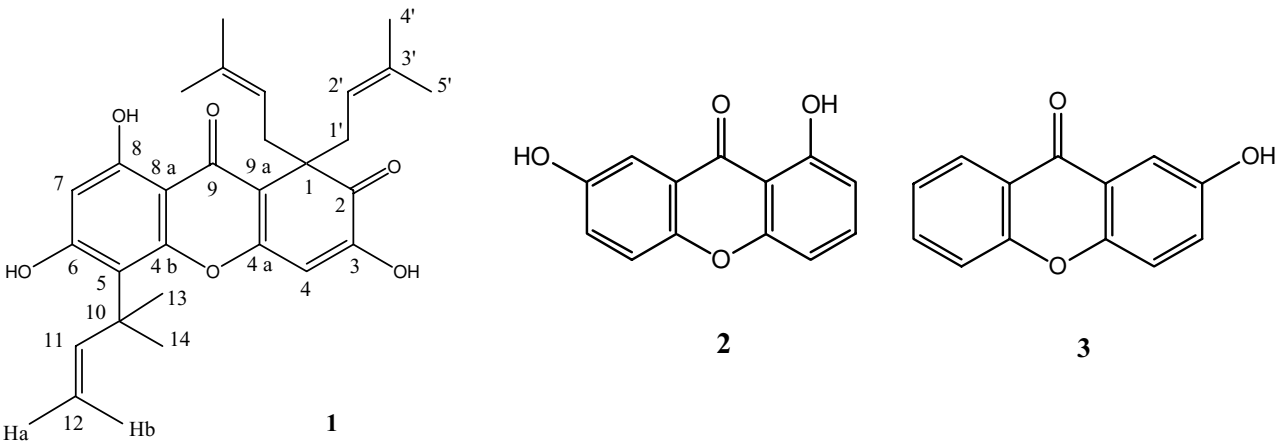

Figure 1. Structures of compounds **1**, **2**, and **3**.

was identified by Dr. Zhang Wen-Ju, Associate Professor at the Center of Biodiversity of the Biology School, Fudan University, China. Voucher specimens (no. HS-001) have been deposited at the Natural Medicinal Chemistry Laboratory of the School of Pharmacy, Fudan University. The silica TLC (thin-layer chromatography) precoated plates and silica resin (200–300 mesh) for column chromatography were made in the Qingdao Marine Chemical Plant (QingDao, China).

Extraction and isolation

Air-dried and powdered (16 mesh) roots of the plant (1.1 kg) were extracted with 95% EtOH, affording 90 g of extract. This ethanol extract (90 g) was fractionated into various solvents of increasing polarity to afford the petroleum ether (40 g), methanol (13 g), and watersoluble fractions. The petroleum ether–soluble fraction was subjected to column chromatography over silica gel, eluting with a gradient from petroleum ether to ethyl acetate and final wash with methanol to afford 15 fractions (Fr. 1 to Fr. 15). Fraction 4 was re-chromatographed on a silica gel column with petroleum ether–acetone to yield **1** (100 mg). Fractions 7 and 8 were subjected to silica gel column chromatography using chloroform-acetone as eluent to give **2** (43 mg) and **3** (46 mg), respectively (Fig. 1).

Minimum inhibitory concentration (MIC) assay

SA-1199B was cultured on nutrient agar (Oxoid, Cambridge, UK) and incubated for 24 h at 37°C prior to MIC determination. The origin of SA-1199B is as described in Kaatz et al. (1993). MICs were determined in duplicate by the microdilution assay as previously described (Gibbons & Udo, 2000). The control antibiotic norfloxacin was obtained from Sigma Chemical Co (Cambridge, UK). Mueller-Hinton broth (MHB; Oxoid) was adjusted to contain 20 and 10 mg/L of Ca^{2+} and Mg^{2+}, respectively. An inoculum density of 5×10^5 CFU of *S. aureus* strain SA-1199B was prepared in normal saline (9 g/L) by comparison with an 0.5 MacFarland turbidity standard. The inoculum (125 μL) was added to all wells and the microtiter plate was incubated at 37°C for 18 h. For MIC determinations, 20 μL of a 5 mg/mL methanol solution of 3-[4,5-dimethylthiazol-2-yl]-2,5-diphenyltetrazolium bromide (MTT; Sigma) was added to each of the wells and incubated for 20 min. Bacterial growth was indicated by a color change from yellow to dark-blue. The MIC was recorded as the lowest concentration at which no growth was observed (Gibbons & Udo, 2000).

Results and Discussion

Compound **1** was isolated as yellow oil and gave rise to a molecular ion peak at m/z 464 in its Electron Ionization Mass Spectrometry (EIMS) spectrum, which corresponded with a molecular formula $C_{28}H_{32}O_6$. The IR spectrum for **1** showed the presence of a phenolic hydroxyl group (3347 cm^{-1}), a conjugated carbonyl group (1663 cm^{-1}), and an aromatic ring (1558, 1450 cm^{-1}).

The ^{1}H NMR spectrum of **1** (Table 1) showed signals for a hydrogen-bonded hydroxyl (δ 13.42), two free hydroxyl groups (δ 7.14, s, OH-6; δ 7.01, s, OH-3), and two singlet aromatic protons at δ 6.48 (H-4) and δ 6.29 (H-7). Further signals in the ^{1}H spectrum could be assigned to the presence of two identical isoprenyl substituents (C1′ to C5′), and a further 1,1-dimethyl-prop-2-enyl group (C10 to C14). In addition, the ^{13}C NMR data indicated the presence of two carbonyl carbons (δ 201.2, C-2; δ 179.7, C-9), one aliphatic quaternary carbon (δ 55.8, C-1), and 10 aromatic carbons. In the HMBC spectrum, cross-peaks were observed between the protons of H_3-13/14 and H-11 and the carbon of C-5, indicating that the 1,1-dimethyl-prop-2-enyl side chain was at C-5 (Fig. 2). The above data revealed that isolate

Table 1. NMR spectral data of compound **1** ($CDCl_3$, *J*, Hz, 400 MHz).

Position	H	C	HMBC	Position	H	C	HMBC
1		55.8		11	6.44 dd (10.6, 17.6)	149.0	5, 10, 13, 14
2		201.2		12	5.39 d (10.6)	113.5	10, 11
3		158.6			5.48 d (17.6)		
4	6.48 s	108.1	2, 3, 4a, 9, 9a	13	1.69 s	28.1	5, 10, 11
4a		151.8		14	1.69 s	28.0	5, 10, 11
4b		154.8		1′	2.81 dd (7.8, 13.7)	37.8	1, 2, 2′, 3′, 9a
5		109.2		1′	3.42 dd (7.1, 13.7)		1, 2, 2′, 3′, 9a
6		161.3		2′	4.66 m	117.7	1, 1′, 4′, 5′
7	6.29 s	101.6	5, 6, 8, 8a, 9	3′		135.3	
8		161.1		4′	1.49 s	25.7	1′, 2′, 3′, 5′
8a		105.7		5′	1.51 s	17.9	1′, 2′, 3′, 4′
9		179.7		8-OH	13.42s		7, 8, 8a
9a		116.2		6-OH	7.14s		5, 6, 7
10		40.9		3-OH	7.01s		2, 3, 4, 4a

was 1,2-dihydro-3,6,8-trihydroxy-1,1-*bis*(3-methyl-but-2-enyl)-5-(1,1-dimethylprop-2-enyl)-xanthen-2,9-dione (**1**), previously isolated from *H. erectum* Thunb. (Hyperiaceae, ex Guttiferae), and the NMR spectral data are in close agreement with those published (An et al., 2002) and later named as hyperixanthone A in this paper.

Compound **2** was obtained as yellow needles. The Electrospray Ionization Mass Spectrometry (ESI-MS) of **2** suggested a molecular formula of $C_{13}H_8O_4$ $[M+H]^+$ (229.1). The ^{13}C NMR spectrum displayed 13 signals in the aromatic region, including a signal for carbonyl carbon. The Distortionless Enhancement by Polarization Transfer (DEPT) 135 spectrum showed six positive signals, indicating that seven quaternary carbons were present and that methylene groups were absent. These signals were characteristic for a xanthone. The ^1H NMR spectrum revealed three aromatic protons in an ABD spinning system with resonances at δ 7.54 (d, $J_{ortho} = 9.0$ Hz, H-5), δ 7.36 (dd, $J = 2.7$, 9.0 Hz, H-6), and δ7.43 (d, $J = 2.7$ Hz, H-8) and three aromatic protons in an ABC spinning system with resonances at δ 7.04 (dd, $J = 0.8$, 8.2 Hz, H-2), δ 7.70 (t, $J = 8.2$ Hz, H-3), and δ 6.78 (dd, $J = 0.8$, 8.2 Hz, H-4). Compound **2** was identified as 1,7-dihydroxyxanthone, and the NMR data for this compound were in close agreement with that in the literature (Lin et al., 1996; Shiu & Gibbons, 2006).

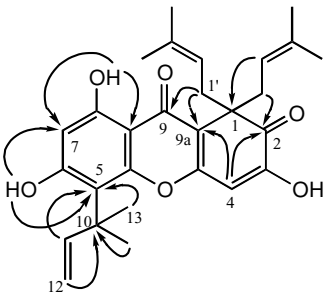

Figure 2. Key HMBC correlations of hyperixanthone A (**1**).

Compound **3** was obtained as yellow needles, and the ESI-MS of **3** suggested a molecular formula of $C_{13}H_8O_3$ $[M+H]^+$ (213.1). The ^1H and ^{13}C data for **3** were in close agreement with those published for 2-hydroxyxanthone (Luz Cardona, 1982).

All compounds were tested for their ability to inhibit the growth of SA-1199B. Compound **1** showed significant antibacterial activity with a MIC of 2 μg/mL (4.3 μM), and this compares well with the positive control norfloxacin, which gave an MIC of 32 μg/mL (100 μM), whereas compounds **2** and **3** were inactive. The greater degree of lipophilicity (and membrane solubility) for **1** may account for its antibacterial activity compared with **2** and **3**. Xanthones are an underexploited class of antibacterial agent, and the fact that **1** demonstrates activity against an effluxing strain may indicate that this large molecule may not be a substrate for the NorA efflux pump. This characteristic would make prenylated xanthones worthy of further investigation as anti-staphylococcal drug leads.

*1,2-Dihydro-3,6,8-trihydroxy-1,1-bis(3-methylbut-2-enyl)-5-(1,1-dimethylprop-2-enyl)-xanthen-2,9-dione (hyperixanthone A; **1**)*

Yellow oil. Positive EI-MS *m/z* (rel. int.): 464 $[M]^+$ (4), 395 (100), 396 (32.7), 353 (31.8). IR (KBr) ν_{max} 3347, 1663, 1640, 1594, 1558, 1502, 1450 cm^{-1}; UV ($CHCl_3$) λ_{max} (logε) 330 (2.95), 298 (3.27), 243 (3.29), 222 (3.05) nm; ^1H,^{13}C,^1H-^1H COSY, HMQC, and HMBC spectra of compound **4** are in close agreement with An et al. (2002).

*1,7-Dihydroxyxanthone (**2**)*

Yellow needles, m.p. 236–238°C. ESI-MS *m/z*: 229.1 $[M+H]^+$. The ^1H NMR data are in good agreement with

those reported by Lin et al. (1996).[13]C NMR (400 MHz, $CDCl_3$): δ181.6 (C-9), 160.9 (C-1), 155.8 (C-4a), 154.1 (C-7), 149.3 (C-4b), 137.1 (C-3), 125.6 (C-6), 120.4 (C-8a), 119.3 (C-5), 109.6 (C-2), 107.8 (C-8, 8b), 107.1 (C-4).

*2-Hydroxyxanthone (**3**)*

Yellow amorphous powder, m.p. 238–239°C. ESI-MS m/z: 213.1 $[M+H]^+$, IR, UV, and ^{1}H NMR data are in close agreement with those reported by Luz Cardona (1982). ^{13}C NMR (400 MHz, $CDCl_3$): δ175.9 (C-9), 155.6 (C-4b), 153.9 (C-2), 149.2 (C-4a), 135.2 (C-6), 125.9 (C-8), 124.6 (C-3), 123.9 (C-7), 121.7 (C-8b), 120.4 (C-8a), 119.5 (C-4), 118.1 (C-5), 108.5 (C-1).

Acknowledgments

We are grateful for financial support from the National Science Foundation of China (30472068) and the Initiating Finance for Returnee of the Education Ministry of China (2006).

References

An TY, Hu LH, Chen ZL (2002): A new xanthone derivative from *Hypericum erectum*. *Chin Chem Lett 13*: 623–624.

CDC (2002): Staphylococcus areus resistant to vancomycin. *U.S. Morbidity and Mortality Weekly Reports 51*: 565–567.

Gibbons S, Moser E, Hausmann S, Stavri M, Smith E, Clennett C (2005): An anti-staphylococcal acylphloroglucinol from *Hypericum foliosum*. *Phytochemistry 66*: 1472–1475.

Gibbons S, Ohlendorf B, Johnsen I (2002): The genus *Hypericum* — a valuable resource of anti-staphylococcal leads. *Fitoterapia 73*: 300–304.

Gibbons S, Udo EE (2000): The effect of reserpine, a modulator of multidrug efflux pumps, on the *in vitro* activity of tetracycline against clinical isolates of methicillin resistant *Staphylococcus aureus* (MRSA) possessing the tet(K) determinant. *Phytother Res 14*: 139–140.

Kaatz GW, Seo SM, Ruble CA (1993): Efflux-mediated fluoroquinolone resistance in staphylococcus aureus. *Antimicrobial Agents and Chemotherapy 37*: 1086–1094.

Lin CN, Chung MI, Liou SJ, Lee TH, Want JP (1996): Synthesis and anti-inflammatory effects of xanthone derivatives. *J Pharm Pharmacol 48*: 532–538.

Luz Cardona M, Seoane E (1982): Xanthone constituents of *Hypericum ericoides*. *J Nat Prod 45*: 134–136.

Mu Q, Gibbons S, Stavri M, Smith E, Zhou FS, Hu CQ (2006): Antibacterial effects of *Hypericum ascyron* and *H. japonicum* against multidrug-resistant (MDR) *Staphylococcus aureus*. *Pharm Biol 44*: 157–159.

Peeters MJ, Sarria JC (2005): Clinical characteristics of linezolid resistant *Staphylococcus aureus* infections. *Am J Med Sci 330*: 102–104.

Shiu WKP, Gibbons S (2006): Anti-staphylococcal acylphloroglucinols from *Hypericum beanie*. *Phytochemistry 67*: 2568–2572.

Available online at www.sciencedirect.com
ScienceDirect
Phytochemistry 67 (2006) 2568–2572
PHYTOCHEMISTRY
www.elsevier.com/locate/phytochem

Anti-staphylococcal acylphloroglucinols from *Hypericum beanii*

Winnie Ka Po Shiu, Simon Gibbons *

Centre for Pharmacognosy and Phytotherapy, The School of Pharmacy, University of London, 29-39 Brunswick Square, London WC1N 1AX, UK

Received 21 July 2006; received in revised form 25 September 2006

Abstract

As part of an ongoing project to investigate the anti-staphylococcal properties of the *Hypericum* genus, an acylphloroglucinol, 1,5-dihydroxy-2-(2′-methylpropionyl)-3-methoxy-6-methylbenzene (**1**), was isolated from the dichloromethane extract of the aerial parts of *H. beanii* (Guttiferae), together with a minor related acylphloroglucinol 1,5-dihydroxy-2-(2′-methylbutanoyl)-3-methoxy-6-methylbenzene (**2**) as a mixture in a 5:2 ratio. The known compounds 1,7-dihydroxyxanthone (**3**), stigmasterol, catechin and shikimic acid were also isolated from this plant. The structures of the compounds were characterized by extensive 1- and 2D NMR spectroscopy and mass spectrometry. The minimum inhibitory concentration (MIC) values the acylphloroglucinol mixture and (**3**) against a panel of multidrug-resistant strains of *Staphylococcus aureus* ranged from 16–32 μg/ml to 128–256 μg/ml, respectively.

Keywords: *Hypericum beanii*; Guttiferae; Acylphloroglucinol; Phloroglucinol; Xanthone; MRSA; *Staphylococcus aureus*; Antibacterial; MDR

1. Introduction

Multidrug-resistant *Staphylococcus aureus* (MRSA) infections, particularly those caused by methicillin-resistant *S. aureus*, have been a major threat to public health in hospitals and the community in the past decade. In the UK, the number of MRSA infections rose by nearly 5% between 2003 and 2004 (White, 2004). The current treatment of MRSA infections in the UK includes the glycopeptides vancomycin (Vancocin®) and teicloplanin (Targocid®), the oxazolidinone linezolid (Zyvox®), and a combination of the streptogramins, quinupristin and dalfopristin (Synercid®) (British National Formulary, 2006). Despite the new advances in antibiotic development, MRSA infections remain a considerable concern owing to the anticipated resistance to these new drugs. In 2002, MRSA strains fully resistant to vancomycin were isolated in the US (Morbidity Mortality Weekly Report, 2002). Resistance to linezolid has also been reported in some patients followed by prolonged antibiotic treatment in the US (Peeters and Sarria, 2005). Therefore, there is an urgent need to develop new classes of antibiotics to fight the problem of drug resistance.

The genus *Hypericum* (Guttiferae) is known to produce antibacterial metabolites, including the major antibacterial principal hyperforin from *Hypericum perforatum* (Schempp et al., 1999), hyperbrasilols from *Hypericum brasiliense* (Rocha et al., 1995, 1996) and drummondins from *Hypericum drummondii* (Jayasuriya et al., 1991). Hyperforin is an acylphloroglucinol, which consists of a phloroglucinol skeleton substituted with complex isoprene side-chains and a simple 2-methylpropanoyl group. Its antibacterial activity against penicillin-resistant *S. aureus* (PRSA) and MRSA is exceptional, with minimum inhibitory concentration (MIC) values ranging from 0.1 to 1 μg/ml (Schempp et al., 1999). These findings prompted us to investigate the antistaphylococcal activity of 34 *Hypericum* species collected from the National *Hypericum* collection at the Royal Botanic Gardens at Wakehurst Place, UK (Gibbons et al., 2002). The chloroform extract of *Hypericum beanii* was one of the most active species against *S. aureus* in the preliminary evaluation. This is the first report on the phytochemistry and anti-staphylococcal activity of this species.

* Corresponding author. Tel.: +44 207 7535913; fax: +44 207 7535909.
E-mail address: simon.gibbons@pharmacy.ac.uk (S. Gibbons).

0031-9422/$ - see front matter © 2006 Elsevier Ltd. All rights reserved.
doi:10.1016/j.phytochem.2006.09.037

2. Results and discussion

Fractionation of the dichloromethane extract of the aerial parts of *H. beanii* led to the isolation of a mixture of a major compound (**1**) and a minor related compound (**2**) in a ratio of 5:2. HR ESI-TOF-MS of the mixture suggested molecular formulae of $C_{12}H_{17}O_4$ $[MH]^+$ (225.1129) (**1**) and $C_{13}H_{19}O_4$ $[MH]^+$ (239.1280) (**2**). Due to the similarity in polarity and size of these compounds, it was not possible to further purify (**1**) and (**2**). This problem was also experienced in isolating phloroglucinol derivatives from *Hypericum papuanum* by Winkelmann et al. (2000). The ^1H NMR spectrum (Table 1) showed the presence of one aromatic proton (δ_H 6.02, 1H), one methoxyl group (δ_H 3.86, 3H), one septet (δ_H 3.79, 1H), one deshielded methyl singlet (δ_H 1.97) and two overlapping methyl doublets (δ_H 1.14, 6H, $J = 7$ Hz). Six aromatic carbon signals were observed in the ^{13}C spectrum, indicating the presence of an aromatic ring. The three signals with chemical shifts of approximately 160 ppm implied that they were attached to an electron-withdrawing group, for example a hydroxyl group or a methoxyl group as they were deshielded. These carbon resonances were typical for a phloroglucinol (1,3,5-trihydroxylated benzene) (Gibbons et al., 2005). Assuming a phloroglucinol in the HMBC spectrum, the aromatic proton (H-4) coupled to four aromatic quaternary carbons (C-2, C-3, C-5 and C-6), two of which were oxygen-bearing (Fig. 1a). This proton was placed between the two oxygen-bearing carbons (C-3 and C-5). The methoxyl group was then placed next to the aromatic proton at C-3. This was confirmed by HMBC studies which showed correlations between the aromatic proton and the methoxyl group to an oxygen-bearing carbon (δ_C 162.1, C-3). A correlation between H-4 and the methoxyl in the NOESY spectrum also provided evidence that these groups were *ortho* to each other. The deshielded methyl group showed ^1H–^{13}C correlations in the HMBC spectrum with three aromatic carbons, one to which it was directly attached (C-6, δ_C 105.0) and two oxygen-bearing quaternary carbons (C-1, δ_C 166.1 and C-5, δ_C 162.2). This group was therefore placed at position 6 of the 1,3,5-trihydroxylated benzene.

The final substituent at position 2 included a methine septet which was coupled to the six-hydrogen methyl doublet in the COSY spectrum, indicating the presence of an isopropyl side chain. In the HMBC spectrum correlations were observed between the methyl doublets and the methine (^2J), methyl (^3J) and the carbonyl carbon (^3J, δ_C 211.4). This indicated that the isopropyl group was part of a 2′-methylpropionyl group. In the NOESY spectrum, cross-peaks were seen between the methoxyl group and the methyl groups of the isopropyl group. This correlation implied that the methoxyl group must be attached to a carbon next to the 2′-methylpropionyl-bearing carbon in the aromatic ring. Compound **1** was therefore identified as 1,5-dihydroxy-2-(2′-methylpropionyl)-3-methoxy-6-methylbenzene.

A minor compound **2** was isolated with compound **1**. The ^1H and ^{13}C data were almost identical with those of **1** with the exception of the side-chain at C-2 (Table 1). In the same ^1H spectrum, a methyl doublet (δ_H 1.16), a methine multiplet (δ_H 3.68, 0.4H), a methylene multiplet (δ_H 1.38 and δ1.81) and a methyl triplet (δ_H 0.92, 1.5H) were observed. In the COSY spectrum, the methyl triplet was coupled to the methylene which was coupled to the methine. The methine was also coupled to the methyl doublet. In the HMBC spectrum, this methyl doublet showed correlations to the methine (^2J), methylene (^3J) and a carbonyl (^3J) carbon (Fig. 1b). The methyl triplet exhibited ^1H–^{13}C correlations to the methylene (^2J) and methine (^3J). This confirmed the presence of the 2-methylbutanoyl side-chain in compound **2**. This side-chain was also found in the acylphloroglucinol isolated from *Hypericum foliosum* by our group (Gibbons et al., 2005). The NMR data for this side-chain showed a close agreement with those obtained by Gibbons et al. (2005). The molecular formula

Table 1
^1H (500 MHz) and ^{13}C NMR (125 MHz) spectral data and ^1H–^{13}C long-range correlations of **1** and **2** recorded in CD_3OD

1					**2**			
Position	^1H	^{13}C	^2J	^3J	^1H	^{13}C	^2J	^3J
1	–	166.1			–	166.1		
2	–	105.0			–	105.0		
3	–	162.1			–	162.1		
4	6.02	91.2	C3, C5	C2, C6	6.02	91.2	C3, C5	C2, C6
5	–	162.2			–	162.2		
6	–	105.0			–	105.0		
7	1.97	7.41	C6	C1, C5	1.97	7.41	C6	C1, C5
1′	–	211.4			–	211.2		
2′	3.79 *m*	40.5			3.68 *m*	47.3		
3′	1.14 *d* (7)	19.8	C2′	C1′, C4′	1.38 *m*, 1.81 *m*	28.3		
4′	1.14 *d* (7)	19.8	C2′	C1′, C3′	0.92 *t* (7.5)	12.4	C3′	C2′
5′	–	–	–	–	1.17 *d* (6)	17.2	C2′	C1′, C3′
3-OCH_3	3.86	55.9		C3	3.86	55.9		C3

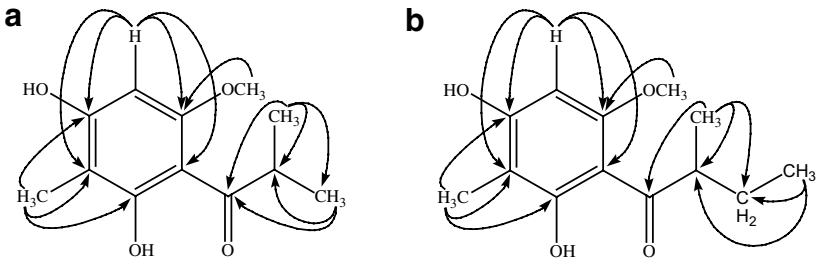

Fig. 1. Key HMBC correlations for **1** (a) and **2** (b).

of **2** differed to that of **1** by an addition of a CH_2 as suggested by mass spectrometry. Compound **2** was therefore identified as 1,5-dihydroxy-2-(2′-methylbutanoyl)-3-methoxy-6-methylbenzene and is described here for the first time.

Repeated chromatography on the DCM extract yielded compound **3** as a yellow oil. HR ESI-MS of **3** suggested a molecular formula of $C_{13}H_8O_4$ $[M+H]^+$ (229.0506). The ^{13}C NMR spectrum displayed 13 signals in the aromatic region, including a signal for carbonyl carbon. The DEPT-135 spectrum showed 6 positive signals, indicating that 7 quaternary carbons were present and that methylene groups were absent. These signals were characteristic for a xanthone. The ^1H NMR spectrum revealed 3 aromatic protons in the ABD system with resonances at δ7.45 (*d*, $J_{ortho} = 9.0$ Hz, H-5), δ7.33 (*dd*, $J = 3.0$, 9.0 Hz, H-6) and δ7.54 (*d*, $J_{meta} = 3.0$ Hz, H-8) and 3 aromatic protons in an ABC system with resonances at δ 6.75 (*dd*, $J = 0.5$, 7.8 Hz, H-2), δ 7.64 (*t*, $J = 8.3$ Hz, H-3) and δ 6.97 (*dd*, $J = 1.0$, 8.5 Hz, H-4). Compound **3** was identified as 1,7-dihydroxyxanthone. The NMR data for this compound were in close agreement with that in the literature (Lin et al., 1996).

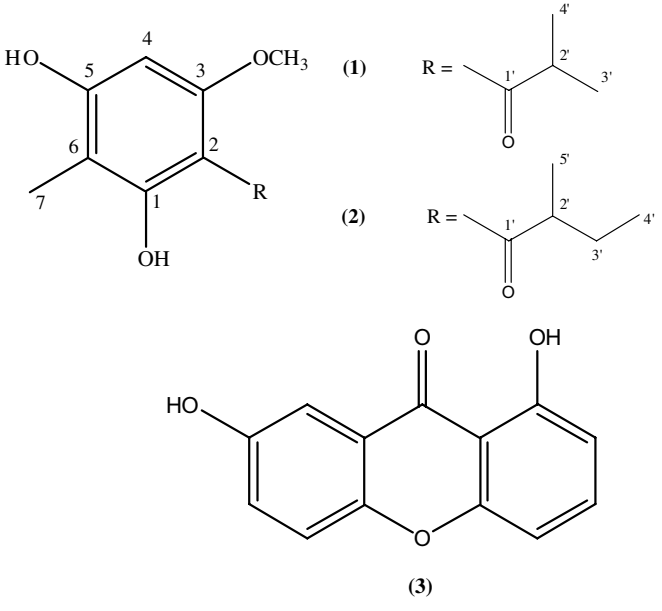

Fractionation of the hexane fraction led to the isolation of stigmasterol. Fractionation of the acetone fraction led to the isolation of catechin and shikimic acid. The structures of these compounds were elucidated from 1D and 2D NMR experiments and their molecular formula confirmed by HR ESI-MS. The data for these compounds are in agreement with that published (Forgo and Kover, 2004; Foo et al., 1996; Hall, 1964). These metabolites were inactive against *S. aureus*.

The mixture of compounds **1** and **2** was active against the tested *S. aureus* strains with MIC values of 16–32 μg/ml (Table 2). It was more active against multi-drug resistant strains XU212 and RN4220 than the standard *S. aureus* strain ATCC 25923. XU212, which possesses the TetK efflux transporter, and is resistant to both tetracycline and methicillin. RN4220 carries the MsrA macrolide efflux protein and is resistant to erythromycin. The activity of the mixture against SA-1199B was comparable to that of norfloxacin, the control antibiotic. SA-1199B possesses the NorA efflux protein which confers resistance to certain fluoroquinolones and quaternary ammonium antiseptics. Compound **3** exhibited weak anti-staphylococcal activity against all the tested strains with MIC values of 128–256 μg/ml. It had a similar activity against RN4220 as erythromycin. However, it was less active than the control antibiotics against other strains. Both compounds **1** and **2** are small molecules with simple structures and moderate anti-staphylococcal activity which could be enhanced. Derivatives of these compounds could be readily synthesized to investigate the structure–activity relationship of the acylphloroglucinol class of compounds.

Table 2
MICs of **1** and **2**, **3** and standard antibiotics in μg/ml

Strain (MDR efflux protein)	**1** and **2**	**3**	Norfloxacin	Tetracycline	Erythromycin
ATCC 25923	32	256	1	–	–
SA-1199B (NorA)	32	256	32	–	–
XU212 (TetK)	32	256	–	128	–
RN4220 (MsrA)	16	128	–	–	128

3. Experimental

3.1. General experimental procedures

NMR spectra were recorded on a Bruker AVANCE 500 MHz spectrometer. Chemical shifts values (δ) were reported in parts per million (ppm) relative to the appropriate internal solvent standard and coupling constants (J values) were given in Hertz. IR spectra were recorded on a Nicolet 360 FT-IR spectrophotometer and UV spectra on a Thermo Electron Corporation Helios spectrophotometer. Accurate mass spectrum of mixture **1** and **2** was obtained using a micrOTOF spectrometer. Mass spectra of all other compounds were recorded on a Finnigan MAT 95 high resolution, double focusing, magnetic sector mass spectrometer. Accurate mass measurement was achieved using voltage scanning of the accelerating voltage. This was nominally 5 kV and an internal reference of heptacosa was used. Resolution was set between 5000 and 10,000.

3.2. Plant material

The aerial parts of *H. beanii* were collected from the Royal Botanic Garden at Wakehurst Place in Surrey in August 2003 (Accession No. 1988-8790). A voucher specimen was deposited in the herbarium at the Centre for Pharmacognosy and Phytotherapy at the University of London School of Pharmacy.

3.3. Extraction and isolation

Air-dried, powdered aerial parts of *H. beanii* (650 g) were extracted exhaustively in a Soxhlet apparatus with solvents (3 l) of increasing polarity (hexane, dichloromethane, acetone and methanol). LH-20 Sephadex chromatography of the dichloromethane extract (5.7 g) eluted with dichloromethane yielded five different fractions by combining fractions showing similar TLC profile and one fraction with a final methanol wash. The fraction eluted with methanol was subjected to reverse phase solid phase extraction (SPE; Phenomenex Strata silica, 10 g/60 ml giga tubes) using a step gradient system with 10% increments from 100% water to 100% methanol, yielding 11 fractions. The fraction eluted with 100% methanol was further separated by preparative thin-layer chromatography (pTLC) using toluene–ethylacetate–acetic acid (TEA 80:18:2), yielding a mixture of compounds **1** and **2** (1.7 mg) and **3** (1.6 mg). The mixture of **1** and **2** and compound **3** had R_f values of 0.70 and 0.75, respectively.

3.4. Bacterial strains

S. aureus standard strain ATCC 25923 and tetracycline-resistant strain XU212 which possesses the TetK tetracycline efflux protein were provided by Gibbons and Udo (2000). Strain SA-1199B which overexpresses the norA gene encoding the NorA MDR efflux pump was provided by Kaatz et al. (1993). Strain RN4220 which possess the MsrA macrolide efflux protein was provided by Ross et al. (1989).

3.5. Minimum inhibitory concentration (MIC) assay

All strains were cultured on nutrient agar (Oxoid) and incubated for 24 h at 37 °C prior to MIC determination. Control antibiotics norflorxacin, tetracycline and erythromycin were obtained from Sigma Chemical Co. Mueller-Hinton broth (MHB; Oxoid) was adjusted to contain 20 and 10 mg/l of Ca^{2+} and Mg^{2+}, respectively. An inoculum density of 5×10^5 cfu of each *S. aureus* strain was prepared in normal saline (9 g/l) by comparison with a 0.5 MacFarland turbidity standard. The inoculum (125 µl) was added to all wells and the microtitre plate was incubated at 37 °C for 18 h. For MIC determination, 20 µl of a 5 mg/ml methanolic solution of 3-[4,5-dimethylthiazol-2-yl]-2,5-diphenyltetrazolium bromide (MTT; Sigma) was added to each of the wells and incubated for 20 min. Bacterial growth was indicated by a colour change from yellow to dark blue. The MIC was recorded as the lowest concentration at which no growth was observed (Gibbons and Udo, 2000).

3.6. 1,5-Dihydroxy-2-(2′-methylpropionyl)-3-methoxy-6-methylbenzene (*1*)

Pale yellow oil; UV (MeOH) λ_{max} (log ε): 293 (4.0), 206 (4.3) nm; IR ν_{max} (thin film) cm^{-1}: 3650, 1655, 1560, 1543, 1458, 1026; ^1H NMR and ^{13}C NMR (MeOD): see Table 1; HR ESI-TOF-MS (m/z): 225.1129 $[MH]^+$ (calc. for $C_{12}H_{17}O_4$, 226.1200).

3.7. 1,5-Dihydroxy-2-(2′-methylbutanoyl)-3-methoxy-6-methylbenzene (*2*)

Pale yellow oil; UV (MeOH) λ_{max} (log ε): 293 (4.0), 206 (4.3) nm; IR ν_{max} (thin film) cm^{-1}: 3650, 1655, 1560, 1543, 1458, 1026; ^1H NMR and ^{13}C NMR (MeOD): see Table 2; HR ESI-TOF-MS (m/z): 239.1280 $[MH]^+$ (calc. for $C_{13}H_{19}O_4$, 240.1356).

Acknowledgement

The Engineering and Physical Sciences Research Council is thanked for a multi project equipment grant (Grant No. GR/R47646/01).

References

British National Formulary, 2006. 51th ed. BMJ Publishing Group, Royal Pharmaceutical Society of Great Britain.

Foo, L.Y., Newman, R., Waghorn, G., McNabb, W.C., Ulyatt, M.J., 1996. Proanthocyanidins from *Lotus corniculatus*. Phytochemistry 41, 617–624.

Forgo, P., Kover, K.E., 2004. Gradient enhanced selective experiments in the ^{1}H NMR chemical shift assignment of the skeleton and side-chain resonances of stigmasterol, a phytosterol derivative. Steroids 69, 43–50.

Gibbons, S., Udo, E.E., 2000. The effect of reserpine, a modulator of multidrug efflux pumps, on the in vitro activity of tetracycline against clinical isolates of methicillin resistant *Staphylococcus aureus* (MRSA) possessing the tet(K) determinant. Phytotherapy Research 14, 139–140.

Gibbons, S., Moser, E., Hausmann, S., Stavri, M., Smith, E., Clennett, C., 2005. An anti-staphylococcal acylphloroglucinol from *Hypericum foliosum*. Phytochemistry 66, 1472–1475.

Gibbons, S., Ohlendorf, B., Johnsen, I., 2002. The genus *Hypericum* – a valuable resource of anti-Staphylococcal leads. Fitoterapia 73, 300–304.

Hall, L.D., 1964. The conformations of cyclic compounds in solution I. Shikimic acid. Journal of Organic Chemistry 29, 297–299.

Jayasuriya, H., Clark, A.M., McChesney, J.D., 1991. New antimicrobial filicinic acid derivatives from *Hypericum drummondii*. Journal of Natural Products 54, 1314–1320.

Kaatz, G.W., Seo, S.M., Ruble, C.A., 1993. Efflux-mediated fluoroquinolone resistance in *Staphylococcus aureus*. Antimicrobial Agents and Chemotherapy 37, 1086–1094.

Lin, C.N., Chung, M.I., Liou, S.J., Lee, T.H., Want, J.P., 1996. Synthesis and anti-inflammatory effects of xanthone derivatives. Journal of Pharmacy and Pharmacology 48, 532–538.

Peeters, M.J., Sarria, J.C., 2005. Clinical characteristics of linezolid-resistant Staphylococcus aureus infections. The American Journal of Medical Sciences 330, 102–104.

Rocha, L., Marston, A., Potterat, O., Kaplan, M.A.C., Stoeckli-Evans, H., Hostettmann, K., 1995. Antibacterial phloroglucinols and flavonoids from *Hypericum brasiliense*. Phytochemistry 40, 1447–1452.

Rocha, L., Marston, A., Potterat, O., Kaplan, M.A.C., Hostettmann, K., 1996. More phloroglucinols from *Hypericum brasiliense*. Phytochemistry 42, 185–188.

Ross, J.I., Farrell, A.M., Eady, E.A., Cove, J.H., Cunliffe, W.J., 1989. Characterisation and molecular cloning of the novel macrolide-streptogramin B resistance determinant from *Staphylococcus epidermidis*. Journal of Antimicrobial Chemotherapy 24, 851–862.

Schempp, C.M., Pelz, K., Wittmer, A., Schopf, E., Simon, J.C., 1999. Antibacterial activity of hyperforin from St. John's Wort, against multiresistant *Staphylococcus aureus* and Gram-positive bacteria. Lancet 353, 2129.

Vancomycin-resistant: *Staphylococcus aureus* – Pennsylvania, 2002. Morbidity Mortality Weekly Report 51, 902.

White, C., 2004. MRSA infections rose by 5% between 2003 and 2004. British Medical Journal 329, 131.

Winkelmann, K., Heilmann, J., Zerbe, O., Rali, T., Sticher, O., 2000. New Phloroglucinol derivatives from *Hypericum papuanum*. Journal of Natural Products 63, 104–108.

Available online at www.sciencedirect.com
SCIENCE DIRECT
Phytochemistry 67 (2006) 1530–1533
PHYTOCHEMISTRY
www.elsevier.com/locate/phytochem

Antimicrobial constituents of *Scrophularia deserti*

Michael Stavri [a], K.T. Mathew [b], Simon Gibbons [a,*]

[a] *Centre for Pharmacognosy and Phytotherapy, The School of Pharmacy, University of London, 29-39 Brunswick Square, London WC1N 1AX, UK*
[b] *The Herbarium, Department of Biological Sciences, Kuwait University, P.O. Box 5969, Safat 13060, Kuwait*

Received 20 April 2006; received in revised form 4 May 2006
Available online 23 June 2006

Abstract

A study of the chemistry and antibacterial activity of *Scrophularia deserti* led to the isolation of eight compounds, including the metabolite 3(ζ)-hydroxy-octadeca-4(*E*),6(*Z*)-dienoic acid (**1**). The known compounds ajugoside (**2**), scropolioside B (**3**), 6-*O*-α-L-rhamnopyranosylcatalpol (**4**), buddlejoside A_8 (**5**), scrospioside A (**6**), laterioside (**7**) and 3*R*-1-octan-3-yl-3-*O*-β-D-glucopyranoside (**8**) were also isolated. Compounds **1**–**3** exhibited moderate antibacterial activity against strains of multidrug and methicillin-resistant *Staphylococcus aureus* (MRSA) and a panel of rapidly growing mycobacteria with minimum inhibitory concentration (MIC) values ranging from 32 to 128 μg/ml.

Keywords: *Scrophularia*; Antimicrobial; Iridoids; *Staphylococcus aureus*; Multidrug-resistance; Mycobacterium

1. Introduction

The Scrophulariaceae, also known as the figwort family, comprise approximately 5100 species belonging to 268 genera (Mabberley, 1997). Phytochemically this family is a rich source of iridoid glycosides, especially from the genera *Buddleja*, *Scrophularia* and *Verbascum* (Ahmed et al., 2003; Miyase et al., 1991; Seifert et al., 1989). *Scrophularia deserti* Del. is the most common figwort found in Kuwait and is fairly abundant in areas where limestone underlies the sand (Shuaib, 1995). This plant can mainly be found growing in the Saharo-Arabian and adjacent Irano-Turanian territories, including Egypt, Palestine, Jordan, Syria, Iraq, Saudi Arabia, Bahrain, Iran as well as in Kuwait (Daoud and Al-Rawi, 1985). *S. deserti* is used in traditional medicine as an antipyretic, a remedy for kidney diseases and for tumours and lung cancer (Ahmed et al., 2003). In an investigation to evaluate antibacterial plant natural products, extracts of the whole plant of *S. deserti* were studied. This paper details the characterisation of a new hydroxylated unsaturated fatty acid (**1**), which exhibited moderate antibacterial activity. A further six known compounds all belonging to the iridoid glycoside natural product class were isolated, two of which (**2** and **3**) were shown to possess anti-staphylococcal activity. These compounds were evaluated against a panel of methicillin and multidrug-resistant *Staphylococcus aureus* strains and rapidly growing mycobacteria.

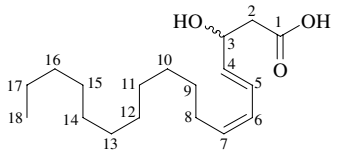

(**1**)

2. Results and discussion

Compound **1** was isolated as a colourless oil from the hexane extract following vacuum liquid chromatography

* Corresponding author. Tel.: +44 207 753 5913; fax: +44 207 753 5909.
E-mail addresses: simon.gibbons@pharmacy.ac.uk, simon.gibbons@ulsop.ac.uk (S. Gibbons).

0031-9422/$ - see front matter © 2006 Elsevier Ltd. All rights reserved.
doi:10.1016/j.phytochem.2006.05.011

Table 1
^{1}H (500 MHz) and ^{13}C (125 MHz) spectral data and ^{1}H and ^{13}C long-range correlations of compound **1** recorded in $CDCl_3$

Position	^{1}H	^{13}C	^{2}J	^{3}J
1	–	179.1		
2	1.52 *m*	37.2	C-3	
3	4.17 *dd* (13.0, 6.5)	72.9	C-2, C-4	C-5
4	5.67 *dd* (15.5, 7.0)	135.7	C-3	C-2, C-6
5	6.49 *dd* (15.5, 11.0)	125.8	C-6	C-3, C-7
6	5.97 *t* (11.0)	127.8	C-5	C-4, C-8
7	5.44 *dt* (11.0, 8.0)	132.8	C-8	C-5, C-9
8	2.18 *m*	27.6	C-7	C-6
9	1.39 *m*	25.1		C-7
10–13	1.31 *m*	28.9		
14	1.31 *m*	28.8		
15	1.31 *m*	29.3		
16	1.31 *m*	31.8		
17	1.31 *m*	22.6		
18	0.88 *t* (7.0)	14.0	C-17	C-16

(VLC) and multiple development preparative thin layer chromatography (p-TLC). HRCIMS revealed the M^+ ion at $m/z = 296.2324$ (calc. for $C_{18}H_{32}O_3$: 296.2352). The ^{1}H and ^{13}C NMR data (Table 1) indicated the presence of four olefinic protons, an oxymethine group, a carbonyl carbon, a methylene envelope, two downfield methylene groups and finally a methyl group.

The HMBC spectrum showed a ^{2}J correlation between a downfield methylene (δ_H 1.52 *m*, H_2-2) towards the carbonyl carbon (δ_C 179.1, C-1) of the carboxyl group. These methylene protons also showed a COSY correlation to the oxymethine proton, placing this oxymethine at C-3 (δ_H 4.17 *dd*, $J = 13.0$, 6.5 Hz, δ_C 72.9) and β to the carbonyl carbon of the carboxyl group. This oxymethine proton in turn showed a COSY coupling to an olefinic proton (δ_H 5.67 *dd*, $J = 15.5$, 7.0 Hz, H-4). Furthermore, H-4 coupled to the olefinic proton, H-5 (δ_H 6.49 *dd*, $J = 15.5$, 11.0 Hz) and the large coupling constant shown between H-4 and H-5 ($J = 15.5$ Hz) indicated that these protons were *trans*-orientated. The H-5 olefin also coupled to a third olefinic proton H-6 (δ_H 5.97 *t*, $J = 11.0$ Hz) which in turn coupled to a final olefinic hydrogen, H-7 (δ_H 5.44 *dt*, $J = 11.0$, 8.0 Hz). As H-6 appeared as a triplet in the ^{1}H spectrum, with a smaller coupling constant ($J = 11.0$ Hz), this suggested that H-6 and H-7 were *cis*-orientated. H-7, gave a COSY and HMBC correlation to a methylene group (δ_H 2.18 *m*, H_2-8). In the COSY spectrum this then coupled to the methylene envelope at δ_H 1.31 ppm, indicating the beginning of the alkyl chain. The alkyl chain was found to consist of 10 methylene groups and a terminal methyl group based on the result of mass spectrometry for this compound. This terminal methyl group coupled into the methylene envelope in the COSY spectrum. An attempt was made to assign the absolute stereochemistry at the C-3 position for compound **1** using Mosher's ester methodology, but unfortunately this was not possible due to the unstable nature of the compound. The optical rotation for **1** was zero and it is likely that **1** is racemic. This would make sense if **1** is biosynthesized through a non-enzymatic hydrolysis of a 2–3 double bond where attack by a water molecule from both faces of the olefin would lead to a racemate. However, 3(ζ)-hydroxy-octadeca-4(*E*),6(*Z*)-dienoic acid (**1**) is new and the full NMR data are reported here for the first time (Table 1).

Compound **2** was isolated from the chloroform extract as a colourless oil. The 1D and 2D NMR data enabled the structure of this compound to be elucidated as the known iridoid glucoside, ajugoside (Guiso et al., 1974, Bianco et al., 1981). The first report of ajugoside, by Guiso et al. (1974), was represented with the hydroxyl at position 6 in an α-orientation. However, subsequent analysis of the ^{13}C NMR data of iridoid glucosides (Chaudhuri et al., 1980), including ajugol and myoporoside and their acyl-derivatives (Damtoft et al., 1982), indicated that the configuration of the hydroxyl at position 6 should in fact be reversed to a β-orientation.

Compound **3** was isolated as a white amorphous solid from the chloroform extract. By comparison of the ^{1}H and ^{13}C NMR data with the literature, the structure of **3** was confirmed as scropolioside B (Calis et al., 1988).

6-*O*-α-L-rhamnopyranosylcatalpol (**4**), buddlejoside A_8 (**5**), scrospioside A (**6**), laterioside (**7**) and 3*R*-1-octan-3-yl-3-*O*-β-D-glucopyranoside (**8**) were also isolated and characterised by direct comparison with the literature (Hosny and Rosazza, 1998, Seifert et al., 1989, Miyase et al., 1991, Pachaly et al., 1994, Pardo et al., 1998, Yamamura et al., 1998).

Three of the eight compounds isolated from this plant exhibited antimicrobial activity. A panel of *S. aureus* strains, including one possessing the NorA multidrug-resistance efflux pump was tested along with a panel of rapidly growing mycobacteria. The unsaturated and hydroxylated fatty acid, 3(ζ)-hydroxy-octadeca-4(*E*),6(*Z*)-dienoic acid (**1**), exerted an anti-staphylococcal and antimycobacterial activity against all the strains tested with MIC values ranging from 32 to 128 μg/ml (Table 2).

The antibacterial activity of unsaturated fatty acids, such as 3(ζ)-hydroxy-octadeca-4(*E*),6(*Z*)-dienoic acid (**1**), against both *S. aureus* (Knapp and Melly, 1986, Kabara et al., 1972) and also mycobacteria (Saito et al., 1983) has long been known. However, it has only recently been deciphered that these compounds exert their antibacterial effect by inhibiting an enzyme or enzymes of Type II fatty acid synthesis (FAS) (Zheng et al., 2005). The enzyme FabI, an enoyl-acyl carrier protein reductase catalysing the final step in chain elongation, has been identified as a target for bacterial inhibition (Zheng et al., 2005, Heath et al., 2001, Payne et al., 2001). A series of hydroxylated unsaturated fatty acids have been reported as potent acetyl CoA carboxylase inhibitors (Watanebe et al., 1999) further indicating that these compounds interfere with fatty acid synthesis. Type II FAS differs from that found in mammalian cells (Type I FAS) therefore the differences between the two systems allows these enzymes to be used as a potential target for drug development. Further work to identify the

Table 2
MICs of **1**, **2** and **3** and standard antibiotics

Bacteria	**1**	**2**	**3**	Norfloxacin	Ethambutol
Staphylococcus aureus 1199B (NorA)	64	32	ξ	32	–
Staphylococcus aureus EMRSA-15	128	ξ	ξ	2	–
Staphylococcus aureus ATCC 25923	128	128	128	0.5	–
Mycobacterium fortuitum ATCC 6841	32	ξ	ξ	–	4
Mycobacterium phlei ATCC 11758	32	ξ	ξ	–	2
Mycobacterium aurum Pasteur Institute 104482	32	ξ	ξ	–	1
Mycobacterium smegmatis ATCC 14468	32	ξ	ξ	–	0.5

ξ = not active at 128 μg/ml; –, not tested.

actual enzyme being inhibited within FAS II needs to be performed.

Compound **2** exhibited weak anti-staphylococcal activity against *S. aureus* ATCC 25923 (Table 2) which has been reported previously (Ezer et al., 1995) and compound **3** was also shown to exert a similar effect against this strain. Interestingly, compound **2** exhibited a 4-fold greater anti-staphylococcal activity against the multidrug-resistant strain *S. aureus* 1199B, which codes for the NorA efflux pump transporter. Further work to identify more active iridoids and to elucidate the molecular target of this natural product class would appear to be worthwhile.

3. Experimental

3.1. General experimental procedures

NMR spectra were recorded on a Bruker AVANCE 500 MHz spectrometer. Chemical shifts (δ) were reported in parts per million (ppm) relative to appropriate internal solvent standard. Coupling constants (J values) are given in Hertz. Mass spectra were recorded on Finnigan Mat 95. IR spectra were recorded on a Nicolet 360 FT-IR spectrophotometer and UV recordings were made on a Perkin–Elmer Lambda 15 UV/VIS spectrophotometer.

3.2. Plant material

A collection of the plant sample was made at Wadi Al-Batin, in north-western Kuwait, bordering Iraq, in February 1999. A voucher specimen (KTM 4226, collected by K.T. Mathew and S. Gibbons on 19/2/1999) is deposited at the Kuwait University Herbarium (KTUH).

3.3. Extraction and isolation

The whole plant was air-dried for 3 days and ground to a fine powder. The powdered plant material (450 g) was sequentially extracted in a Soxhlet apparatus with hexane, chloroform and methanol (3 l each). Vacuum liquid chromatography (VLC) of the hexane extract (5.1 g) on silica gel using a step-gradient of 10% EtOAc in hexane followed by a methanol wash yielded 12 fractions. Fraction 7 (310 mg) was then subjected to LH-20 Sephadex column chromatography, eluting with dichloromethane followed by a methanol wash to give four fractions. Sephadex fraction 4 (58 mg) was then loaded onto four reverse phase TLC plates and developed twice with a 60:40 ACN-H_2O + AcOH (two drops) system to yield 15 mg of compound **1** (R_F: 0.21). VLC of the chloroform extract (10.5 g) using the same method described above again gave 12 fractions. Fraction 12 (1.5 g) was then fractioned further by LH-20 Sephadex column chromatography again using the same method as above to give 11 fractions. Solid phase extraction (C-18, SPE) of Sephadex fraction 10 (500 mg) using a step-gradient of 10% methanol in water yielded 11 fractions. SPE fractions 3 and 4 were combined (72 mg) and compound **2** was isolated by p-TLC using a 95:15 EtOAc–methanol + AcOH (two drops) solvent system. This afforded 27 mg of compound **2** (R_F: 0.32). Applying the same SPE protocol to Sephadex fraction 9 (425 mg) gave 11 fractions. Multiple development p-TLC in the normal phase mode (silica) of SPE fraction 9 (26 mg) using a 95:10 EtOAc–methanol + AcOH (two drops) (two developments) solvent system resulted in the isolation of compound **3** (10 mg; R_F: 0.44).

3.4. Antibacterial assay

S. aureus strain ATCC 25923 was a gift from E. Udo (Kuwait University, Kuwait), *S. aureus* strain SA-1199B, which overexpresses the *norA* gene encoding the NorA MDR efflux protein was a generous gift from G. Kaatz (Kaatz et al., 1993). Strain EMRSA-15 was provided by P. Stapleton. *Mycobacterium fortuitum* ATCC 6841, *Mycobacterium smegmatis* ATCC 14468, *Mycobacterium phlei* ATCC 11758 and *Mycobacterium aurum* Pasteur Institute 104482 were obtained from NTCC. The strains of *S. aureus* were cultured on nutrient agar and incubated for 24 h at 37 °C prior to MIC determination whilst the panel of rapidly growing mycobacteria were cultured on Columbia Blood agar (Oxoid) supplemented with 7% defibrinated Horse blood (Oxoid). *M. fortuitum*, *M. phlei* and *M. smegmatis* were incubated for 72 h and *M. aurum* for 120 h prior to MIC determination. Bacterial inocula equivalent to 5×10^5 cfu/ml were prepared in normal saline using the 0.5 McFarland turbidity standard followed by dilution. The MIC was recorded as the lowest concentration at which no bacterial growth was observed (Gibbons

and Udo, 2000). Norfloxacin was used as a positive control against all *S. aureus* strains and ethambutol was used as a positive control against all the mycobacterial strains. Growth and sterile controls were also performed.

3.5. 3(ζ)-Hydroxy-octadeca-4(E),6(Z)-dienoic acid (1)

Colourless oil. $[\alpha]_D^{24}$ 0° (*c* 0.2, $CHCl_3$). UV ($CHCl_3$): λ_{max}: (log ε) 275 (2.90), 243 (3.56) nm. IR (film) υ_{max}: 3359, 2928, 2855, 1709, 1412, 1248, 985 cm^{-1}; ^1H NMR and ^{13}C NMR ($CDCl_3$): see Table 1; HR-CIMS (*m*/*z*): 296.2324 $[M]^+$ (calc. for $C_{18}H_{32}O_3$, 296.2352).

Acknowledgement

The University of London School of Pharmacy is thanked for the award of a Doctoral scholarship to Michael Stavri.

References

Ahmed, B., Al-Rehaily, A.J., Al-Howiriny, T.A., El-Sayed, K.A., Ahmad, M.S., 2003. Scropolioside-D_2 and Harpagoside-B: two new iridoid glycosides from *Scrophularia deserti* and their antidiabetic and antiinflammatory activity. Biological and Pharmaceutical Bulletin 26, 462–467.

Bianco, A., Caciola, P., Guiso, M., Iavarone, C., Trogolo, C., 1981. Iridoids. XXXI. Carbon-13 nuclear magnetic resonance spectroscopy of free iridoid glucosides in water-d2 solution. Gazzetta Chimica Italiana 111, 201–206.

Calis, I., Gross, G.A., Winkler, T., Sticher, O., 1988. Isolation and structure elucidation of two highly acylated iridoid diglycosides from *Scrophularia scopolii*. Planta Medica 54, 168–170.

Chaudhuri, R.K., Afifi-Yazar, F.U., Sticher, O., 1980. ^{13}C NMR spectroscopy of naturally occurring iridoid glucosides and their acylated derivatives. Tetrahedron 36, 2317–2326.

Damtoft, S., Jensen, S.R., Nielsen, B.J., 1982. Structural revision of ajugol and myoporoside. Tetrahedron Letters 23, 1215–1216.

Daoud, H.S., Al-Rawi, A., 1985. The Flora of Kuwait, vol. 1. KPI Publishers, London.

Ezer, N., Akcos, Y., Rodriguez, B., Abbasoglu, U., 1995. An iridoid glucoside from *Sideritis libanotica* Labill. subsp. Linearis (Bentham) Bornm., and its antimicrobial activity. Hacettepe Universitesi Eczacilik Fakultesi Dergisi 15, 15–21.

Gibbons, S., Udo, E.E., 2000. The effect of reserpine, a modulator of multidrug efflux pumps, on the in vitro activity of tetracycline against clinical isolates of methicillin-resistant *Staphylococcus aureus* (MRSA) possessing the tet(K) determinant. Phytotherapy Research 14, 139–140.

Guiso, M., Marini-Bettolo, R., Agostini, A., 1974. Iridoids – XIII: ajugoside and ajugol: structure and configuration. Gazzetta Chimica Italiana 104, 25–33.

Heath, R.J., White, S.W., Rock, C.O., 2001. Lipid biosynthesis as a target for antibacterial agents. Progress in Lipid Research 40, 467–497.

Hosny, M., Rosazza, J.P.N., 1998. Gmelinosides A-L, twelve acylated iridoid glycosides from *Gmelina arborea*. Journal of Natural Products 61, 734–742.

Kaatz, G.W., Seo, S.M., Ruble, C.A., 1993. Efflux-mediated fluoroquinolone resistance in *Staphylococcus aureus*. Antimicrobial Agents and Chemotherapy 37, 1086–1094.

Kabara, J.J., Swieczkowski, D.M., Conley, A.J., Truant, J.P., 1972. Fatty acids and derivatives as antimicrobial agents. Antimicrobial Agents and Chemotherapy 2, 23–28.

Knapp, H.R., Melly, M.A., 1986. Bactericidal effects of polyunsaturated fatty acids. Journal of Infectious Diseases 154, 84–94.

Mabberley, D.J., 1997. The Plant Book. Cambridge University Press, Cambridge, UK.

Miyase, T., Akahori, C., Kohsaka, H., Ueno, A., 1991. Acylated iridoid glycosides from *Buddleja japonica* HEMSL. Chemical and Pharmaceutical Bulletin 39, 2944–2951.

Pachaly, P., Barion, J., Sin, K.S., 1994. Isolation and analysis of new iridoids from roots of *Scrophularia korainensis*. Pharmazie 49, 150–155.

Pardo, F., Perich, F., Torres, R., Delle Monache, F., 1998. Phytotoxic iridoid glucosides from the roots of *Verbascum thapsus*. Journal of Chemical Ecology 24, 645–653.

Payne, D.J., Warren, P.V., Holmes, D.J., Ji, Y., Lonsdale, J.T., 2001. Bacterial fatty-acid biosynthesis: a genomic-driven target for antibacterial drug discovery. Drug Discovery Today 6, 537–544.

Saito, H., Tomioka, H., Watanabe, T., Yoneyama, T., 1983. Mycobacteriocins produced by rapidly growing mycobacteria are Tween-hydrolyzing esterases. Journal of Bacteriology 153, 1294–1300.

Seifert, K., Lien, N.T., Schmidt, J., Johne, S., Popov, S.S., Porzel, A., 1989. Iridoids from *Verbascum pulverulentum*. Planta Medica 55, 470–473.

Shuaib, L., 1995. Wildflowers of Kuwait. Stacey International, London.

Watanebe, J., Kawabata, J., Kasai, T., 1999. 9-Oxooctadeca-10,12-dienoic acids as acetyl-CoA carboxylase inhibitors from Red Pepper (*Capsicum annuum* L.). Bioscience, Biotechnology and Biochemistry 63, 489–493.

Yamamura, S., Ozawa, K., Ohtani, K., Kasai, R., Yamasaki, K., 1998. Antihistaminic flavones and aliphatic glycosides from *Mentha spicata*. Phytochemistry 48, 131–136.

Zheng, C.J., Yoo, J.S., Lee, T.G., Cho, H.Y., Kim, Y.H., Kim, W.G., 2005. Fatty acid synthesis is a target for antibacterial activity of unsaturated fatty acids. Federation of European Biochemical Societies 579, 5157–5162.

Available online at www.sciencedirect.com
SCIENCE DIRECT
Phytochemistry 67 (2006) 178–182
PHYTOCHEMISTRY
www.elsevier.com/locate/phytochem

Phytochemistry and antimycobacterial activity of *Chlorophytum inornatum*

Gemma O'Donnell [a], Franz Bucar [b], Simon Gibbons [a,*]

[a] *Centre for Pharmacognosy and Phytotherapy, The School of Pharmacy, University of London, 29–39 Brunswick Square, London WC1N 1AX, UK*
[b] *Institute of Pharmaceutical Sciences, Universitätsplatz 4/I, Karl-Franzens Universität, A-8010 Graz, Austria*

Received 27 July 2005; received in revised form 19 October 2005
Available online 15 December 2005

Abstract

In a project to investigate plant derived natural products from the Liliaceae with activity against fast-growing strains of mycobacteria, we have identified two new metabolites from *Chlorophytum inornatum*. The active principle, a new homoisoflavanone (**1**) was identified as 3-(4′-methoxybenzyl)-7,8-methylenedioxy-chroman-4-one. The metabolite assigned as 7-(1′-hydroxyethyl)-2-(2″-hydroxyethyl)-3,4-dihydrobenzopyran (**2**) was characterised by extensive 1- and 2D NMR spectroscopy. The antimycobacterial activity of this plant was mainly due to the homoisoflavonoid which exhibited minimum inhibitory values ranging from 16–256 μg/ml against four strains of fast-growing mycobacteria.

Keywords: *Chlorophytum inornatum*; Homoisoflavanone; Liliaceae; *Mycobacterium*; Antibacterial; Mycobacteria

1. Introduction

At present there is a real need for new classes of antibacterials to deal with emerging resistant strains, particularly in the genera *Mycobacterium* and *Staphylococcus*. The genus *Mycobacterium* is responsible for tuberculosis (TB) and other infections caused by fast-growing mycobacteria (FGM) such as *M. abscessus* (Scholze et al., 2005). These FGM species are notoriously difficult to treat and cause infections in children with cystic fibrosis (Sermet-Gaudelus et al., 2003). Multidrug-resistance in some species of FGM (Sander et al., 2000) and TB causing species (Colangeli et al., 2005) has been encountered and it is likely that these mechanisms will be more clinically relevant in the future. There is therefore a requirement for new classes of antibacterials which have activity against these strains. In a project to meet these needs, we have been screening plants of the Liliales, particularly of the Alliaceae and Liliaceae families. These groups produce bulbs as part of their reproductive system and our rationale is that such bulbs are in contact with actinomycetes in the soil and will have evolved an antimicrobial defence against these filamentous bacteria. Members of the actinomycete genus *Mycobacterium* are commonly present in soil and it is possible that such an antimicrobial defence may be useful to find leads against species of this group. Allicin, the major antimicrobial principle of the garlic group (*Allium*), has been extensively studied for its antibacterial properties some considerable time ago (Cavallito et al., 1944; Cavallito and Bailey, 1944; Cavallito et al., 1945). Garlic has also been used clinically to treat patients with TB in the early part of the 20th Century (Bolton et al., 1982) and is popularly known as 'Russian penicillin'.

These findings prompted us to conduct an evaluation of other less well chemically and biologically characterised members of the Liliaceae and Alliaceae groups and a collection of the subterranean parts of the poorly studied species *Chlorophytum inornatum* Ker Gawl. (Liliaceae) was made in Ghana. There is little phytochemical data available on this genus although *C. comosum*, a popular houseplant known as the spider plant or grass lily, along with

* Corresponding author. Tel.: +44 207 7535913; fax: +44 207 7535909.
E-mail address: simon.gibbons@ulsop.ac.uk (S. Gibbons).

0031-9422/$ - see front matter © 2005 Elsevier Ltd. All rights reserved.
doi:10.1016/j.phytochem.2005.10.023

other members of the genus, is of ethnobotanical use in areas of Africa and India (Tabuti et al., 2003 and Tandon et al., 1992). In southern Chinese folk medicine *C. comosum* is also used in the treatment of bronchitis, fractures and burns (Mimaki et al., 1996).

Here we report on the bioassay-guided fractionation of extracts of *C. inornatum* against fast-growing strains and on new phytochemistry of this species.

2. Results and discussion

Antibacterial activity was concentrated in the hexane extract (512 μg/ml) and bioassay-guided fractionation led to the isolation of compound **1** as a white solid. The molecular formula of compound **1** was assigned as $C_{18}H_{16}O_5$ on the basis of high-resolution ESI-MS $[M+H]^+$ (313.1085). The ^1H NMR spectrum (Table 1) displayed a chemical shift pattern indicative of a 3-benzyl-4-chromanone type homoisoflavanone skeleton previously isolated from the Liliaceae and Hyacinthaceae (Anh et al., 2003; Adinolfi et al., 1984). Analysis of the 1D and 2D NMR spectra revealed the presence of methylenedioxy and methoxyl substituents on the aromatic A and B rings, respectively. Two doublets (δ 6.87 and 7.17, $J = 8.5$ Hz) integrating for two protons each were typical for an aromatic AA′BB′ system for ring B, with a strong HMBC signal between the *para* substituted methoxyl (δ 3.81) and C-4′ (δ 158.4). Correlations observed in the NOESY spectrum from the methoxyl to the aromatic protons H-3′ and H-5′ (δ 6.87) further confirmed this arrangement. Two coupled proton doublets of ring A (δ 7.61 and 6.62) showed an *ortho* coupling ($J = 8.0$ Hz), while the HMBC correlation between the proton at δ 7.61 and the C-4 carbonyl (δ 192.1) identified the protons as H-5 and H-6, respectively. The difference between the ^1H chemical values for H-5 and H-6 can be attributed to the observations that H-5 is β to the C-4 carbonyl and that there is likely to be a *peri* through space deshielding interaction between H-5 and this carbonyl moiety.

The methylenedioxy group was positioned at C-7 and C-8 by HMBC correlations for the methylenedioxy protons to the aromatic quaternary carbons C-7 and C-8. This positioning was further confirmed by HMBC correlations from H-5 to the carbonyl at C-4 and the quaternary carbon C-4a. Furthermore, H-6 displayed HMBC correlations to C-7 and C-8. The COSY spectrum showed a $–CH_2–CH–CH_2–$ system reminiscent of a homoisoflavanone with C-2, C-3 and C-9 assigned through comparison with the literature (Adinolfi et al., 1984) and confirmed by 2D NMR experiments. This system was accordingly linked to the B ring through HMBC correlations from H_2-9 to the aromatic carbons C-2′ and C-6′. The compound was therefore determined to be 3-(4′-methoxybenzyl)-7,8-methylenedioxychroman-4-one, and is described here for the first time. Measurement of the specific optical rotation of **1** gave a result of +18.9°. Comparison with the results for homoisoflavanones with an *R* configuration described in Amschler et al. (1996) ([α] = −46.2 and −38.0) implied an *S* configuration for compound **1** (see Fig. 1).

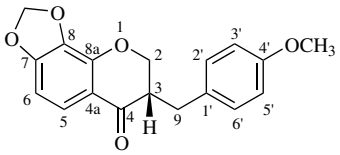

(**1**)

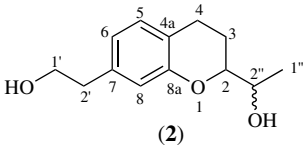

(**2**)

Fractionation of the chloroform extract led to the isolation of a new metabolite, compound **2**. HRESI-MS of compound **2** suggested a molecular formula of $C_{13}H_{18}O_3$ $[M-H]^+$ (221.1168). The ^1H NMR spectrum (Table 2)

Table 1
^1H (500 MHz) and ^{13}C NMR (500 MHz) spectral data and ^1H–^{13}C long-range correlations of **1** recorded in $CDCl_3$

Position	^1H	^{13}C	^2J	^3J	^4J
2a	4.42 *dd* (11.5, 4.0)	70.0		C-4, C-9	C-4a
2b	4.26 *dd* (11.5, 7.0)		C-3	C-4, C-9	C-4a
3	2.86 *m*	48.1	C-9		
4	–	192.1			
4a	–	145.5			
5	7.61 *d* (8.0)	123.1	C-4a	C-4, C-7	
6	6.62 *d* (8.0)	103.5	C-7	C-8	C-8a
7	–	154.0			
8	–	134.4			
8a	–	117.3			
9a	2.72 *dd* (14.0, 10.5)	31.8	C-3	C-2, C-4, C-2′, C-6′	
9b	3.19 *dd* (14.0, 4.5)		C-3	C-2, C-4, C-2′, C-6′	
1′	–	130.0			
2′/6′	7.17 *d* (8.5)	130.1	C-1′, C-3′	C-9, C-4′, C-6′	C-5′
3′/5′	6.87 *d* (8.5)	114.1	C-2′, C-4′	C-1′, C-5′	C-6′
4′	–	158.4			
O–CH_2–O	6.09 *d* (1.0)	102.7		C-7, C-8	
OMe (4′)	3.81 *s*	55.3		C-4′	

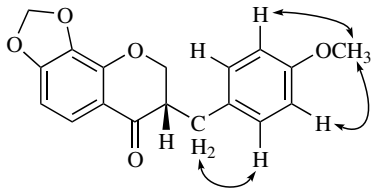

Fig. 1. Key NOESY correlations for compound **1**.

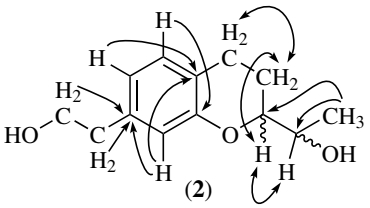

Fig. 2. Key HMBC (single headed arrows) and COSY (double headed arrows) correlations for compound **2**.

revealed three aromatic resonances at δ 6.67 (*d*, $J_{ortho} = 8.0$ Hz, H-5), δ 6.65 (*d*, $J_{meta} = 2.0$ Hz, H-8) and δ 6.52 (*dd*, $J = 2.0$, 8.0 Hz, H-6) reminiscent of an ABD trisubstituted ring system. Further resonances included two oxygenated methine multiplets (δ 4.40 and 3.75), an oxygenated methylene triplet (δ 3.67, $J = 7.5$ Hz), two benzylic methylene triplets (δ 2.66, $J = 7.0$ Hz and 2.55, $J = 8.5$ Hz), two one-proton multiplets corresponding to a further methylene by HMQC analysis (δ 2.25 and 2.07) and a methyl doublet (δ 1.21, $J = 6.5$ Hz) completing the ^{1}H signals for compound **2**. HMBC correlations from the protons of the oxygenated methylene (δ 3.67, H-1′) to a methylene carbon at δ 39.7 (C-2′) and a quaternary aromatic carbon at δ 131.8 were suggestive of an hydroxyethyl substituent attached to an aromatic ring. This was further confirmed by a NOESY correlation between the methylene protons (CH_2-2′) and the aromatic protons (H-6 and H-8). This was supported by HMBC correlations between the protons of this methylene and C-7 (^2J) and C-6 and C-8 (^3J). H-5 gave a strong HMBC correlation (Fig. 2) to C-8a which was a deshielded aromatic quaternary carbon with a resonance reminiscent of an oxygen bearing carbon (δ 146.1).

The remaining resonances could be linked by analysis of the COSY spectrum (Fig. 2). A methyl doublet (H-1″, δ 1.21) displayed a single correlation to the first of the oxygenated methines at δ 3.75 (H-2″), which in turn coupled to the second oxygenated methine at δ 4.40 (H-2). H-2 subsequently coupled to a methylene (H_2-3, δ 2.25 and 2.07), which showed a final coupling to a deshielded methylene triplet of H-4 (δ 2.55), whose resonance was typical for a benzylic methylene and similar to that of CH_2-2′. This methylene must be attached at C-4a, *ortho* to C-5 as this is the only remaining free position on the aromatic core. The data were similar to other natural product benzopyran derivatives (Seeram et al., 1998) and we propose that a link between the oxygen at C-8a (neighbouring C-8) and C-2 is formed to give a substituted benzopyran derivative. From HRESI-MS this would mean that hydroxyl groups must be placed at C-1′ and C-2″. Theoretical ^{1}H NMR resonances were calculated using ChemDraw Ultra and are given in Table 2. These resonances show close correlation with experimental data, particularly for H-4, H-1′, H-2′, H-1″ and H-2″ and even the aromatic resonances have the same trend in magnitude. The main discrepancy is for H-2 (4.40 exp, 3.76 theoret.) and we propose that this is due to the deshielding effect of the hydroxyl at C-2″, resulting in a more deshielded signal for H-2. Compound **2** is therefore assigned as 7-(1′-hydroxyethyl)-2-(2″-hydroxyethyl)-3,4-dihydrobenzopyran and its NMR data are described here for the first time.

Table 2
^{1}H (500 MHz) and ^{13}C NMR (500 MHz) spectral data and ^{1}H–^{13}C long-range correlations for **2**, recorded in MeOD

Position	^{1}H	^{13}C	^2J	^3J	^{1}H[a]
2	4.40 *m*	85.9	–	–	3.76
3	2.25 *m*, 2.07 *m*	25.0	C-4	–	2.00
4	2.55 *t* (8.5)	29.5	C-3	–	2.55
4a	–	144.9	–	–	–
5	6.67 *d* (8.0)	116.3	C-7	C-8a, C-4a	6.96
6	6.52 *dd* (2.0, 8.0)	121.2	C-5, C-7	–	6.63
7	–	131.8	–	–	–
8	6.65 *d* (2.0)	117.1	C-7	C-4a, C-6	6.58
8a	–	146.1	–	–	–
1′	3.67 *t* (7.0)	64.6	C-2′	C-7	3.86
2′	2.66 *t* (7.0)	39.7	C-1′, C-7	C-6, C-8	2.74
1″	1.21 *d* (6.5)	19.0	C-2″	C-2	1.21
2″	3.75 *m*	70.2	–	–	3.89

[a] Calculated using Chemdraw Ultra 7.0.

Further fractionation of the hexane extract led to the isolation stigmasterol-3-*O*-glycoside-6′-palmitate (Lavaud et al., 1994), a racemic mixture of [25*R*]-5α-spirostane-2α,3β-diol (gitogenin) and [25*S*]-5α-spirostane-2α,3β-diol (neogitogenin) (Mimaki et al., 1996) and 4-hydroxy-3-methoxy-benzaldehyde (vanillin). Further fractionation of the chloroform extract yielded *trans*-*N*-(4-hydroxyphenethyl)-feruloylamide (Muñoz et al., 1996). The structures were elucidated from 1D and 2D NMR experiments and compared against chemical shift resonances in the literature. The structure of stigmasterol-3-*O*-glycoside-6′-palmitate was further confirmed by hydrolysis and GC-MS of the derivatised hydrolysate.

Compound **1** exhibited MIC values of 16–256 μg/ml against a range of fast-growing *Mycobacterium* species, comparing favourably with the control antibiotics ethambutol and isoniazid against *M. phlei* and *M. aurum* (Table 3). This is the first report of the antimycobacterial activity of a homoisoflavanone. The simple structure makes this compound an attractive target for synthesis and derivatisation to optimise the antibacterial activity. Compound **2** displayed moderate activity against *M. aurum* (64 μg/ml), however showed no inhibition against any of the other fast growing mycobacterial strains tested (Table 3).

Table 3
MICs of **1** and standard antibiotics in μg/ml

Strain	1	2	Ethambutol	Isoniazid
M. fortuitum	128	–	2	0.25
M. smegmatis	256	–	32	0.25
M. phlei	16	–	2	128
M. aurum	32	64	16	>256

3. Experimental

3.1. General experimental procedures

NMR spectra were recorded on a Bruker AVANCE 500 MHz spectrometer. Chemical shift values (δ) are reported in parts per million (ppm) relative to appropriate internal solvent standard and coupling constants (J values) are given in Hertz. Mass spectra were recorded on a Finnigan MAT 95 high resolution, double focusing, magnetic sector mass spectrometer. Accurate mass measurement was achieved using voltage scanning of the accelerating voltage. This was nominally 5 kV and an internal reference of heptacosa was used. Resolution was set between 5000 and 10,000.

IR spectra were recorded on a Nicolet 360 FT-IR spectrophotometer and UV spectra on a Thermo Electron Corporation Helios spectrophotometer. Determination of specific optical rotation [α] was carried out using an ADP 200 Polarimeter, Bellingham and Stanley, with a 1 ml sample tube.

3.2. Plant material

The dried root material of *C. inornatum* was collected in Aburi, Ghana, in August 2003 and a herbarium specimen (ACH/114866J) was deposited at the Centre for Pharmacognosy and Phytotherapy.

3.3. Extraction and isolation

234.2 g of air-dried and powdered subterranean parts were extracted in a Soxhlet apparatus using sequential extraction by hexane (3 L), chloroform (3 L) and finally methanol (3 L). The hexane extract (5.68 g) was subjected to vacuum liquid chromatography (VLC) on silica gel (15 g) eluting with hexane containing 10% increments of ethyl acetate to yield 12 fractions. The fraction eluted in 60% hexane underwent further separation on reversed-phase SPE (Phenomenex Strata C18-E, 10 g/60 ml giga tubes) eluting with 100% MeOH. SPE fraction 1 exhibited an MIC of 16 μg/ml against *M. fortuitum* and was further fractionated by Sephadex (LH-20) and a final PTLC (Merck RP-18, 85% MeOH: 15% water) purification to yield compound **1** (5.3 mg).

The chloroform extract (8.78 g) underwent initial fractionation with Biotage flash chromatography on silica gel, eluting with hexane containing 10% increments of ethyl acetate to yield 12 fractions. The fraction eluted in 10% hexane was further separated by reversed-phase SPE eluting with 60% MeOH: 40% water. SPE fraction 1 was subsequently fractionated by PTLC (50% MeOH: 50% water) to yield compound **2** (1.6 mg).

3.4. Antibacterial assay

Mycobacterium species were acquired from the NCTC. Strains were grown on Columbia Blood agar (Oxoid) supplemented with 7% defibrinated Horse blood (Oxoid) and incubated for 72 h at 37 °C prior to minimum inhibitory concentration (MIC) determination. Bacterial inocula equivalent to the 0.5 McFarland turbidity standard were prepared in normal saline and diluted to give a final inoculum density of 5×10^5 cfu/ml. The inoculum (125 μL) was added to all wells and the microtitre plate was incubated at 37 °C for 72 h for *M. fortuitum*, *M. smegmatis* and *M. phlei*. For *M. aurum* the plate was incubated for 120 h. The MIC was recorded as the lowest concentration at which no bacterial growth was observed as previously described (Gibbons and Udo, 2000).

Ethambutol and isoniazid were used as positive controls.

3.5. 3-(4′-methoxybenzyl)-7,8-methylenedioxy-chroman-4-one (*1*)

Amorphous white solid; $[\alpha]^{21}D$ +18.9° (*c* 0.05, $CHCl_3$) λ_{max} (log ε): 242.5 (3.60), 290.0 (3.61) nm; IR ν_{max} (thin film) cm^{-1}: 3855.34, 3735.96, 2918.31, 2850.23, 2359.02, 1684.84, 1630.82, 1512.72, 1364.37, 1289.81, 1247.99, 1083.89, 1035.90, 773.15; ^1H NMR and ^{13}C NMR ($CDCl_3$): see Table 1; HR-MS (*m*/*z*): 313.1085 $[M + H]^+$ (calc. for $C_{18}H_{17}O_5$, 313.1071).

3.6. 7-(1′-hydroxyethyl)-2-(2″-hydroxyethyl)-3,4-dihydrobenzopyran (*2*)

Amorphous solid; $[\alpha]^{21}D$ +157.14° (*c* +0.11, MeOH) λ_{max}: 201.5, 280 (br band) nm; IR ν_{max} (thin film) cm^{-1}: 3344.18, 2930.08, 1570.34, 1516.19, 1423.57, 1270.75, 1219.38, 1129.49, 1051.84, 773.07, 663.16; ^1H NMR and ^{13}C NMR (MeOD): see Table 2; HR-MS (*m*/*z*): 221.1168 $[M - H]^+$ (calc. for $C_{13}H_{17}O_3$, 221.1177).

Acknowledgements

We thank the Engineering and Physical Sciences Research Council (Grant Nos. GR/R47646/01 and GR/S30269/01) for funding.

References

Adinolfi, M., Barone, G., Belardini, M., Lanzetta, R., Laonigro, G., Parrilli, M., 1984. 3-Benzyl-4-chromanones from *Muscari comosum*. Phytochemistry 23 (9), 2091–2093.

Amschler, G., Frahm, A.W., Hatzelmann, A., Kilian, U., Müller-Doblies, D., Müller-Dolbies, U., 1996. Constituents of *Veltheimia viridifolia*; I. Homoisoflavanones of the bulbs. Planta Medica 62, 534–539.

Anh, N.T.H., Sung, T.V., Porzel, A., Franke, K., Wessjohann, L.A., 2003. Homoisoflavonoids from *Ophiopogon japonicus* Ker-Gawler. Phytochemistry 62, 1153–1158.

Bolton, S.G., Null, G., Troetel, W.M., 1982. The medical uses of garlic – fact and fiction. J. Am. Pharm. Assoc. 22, 40–43.

Cavallito, C.J., Bailey, J.H., 1944. Allicin, the antibacterial principle of *Allium sativum*. II. Determination of the chemical structure. J. Am. Chem. Soc. 66, 1952–1954.

Cavallito, C.J., Buck, J.S., Suter, C.M., 1944. Allicin, the antibacterial principle of *Allium sativum*. I. Isolation, physical properties and antibacterial action. J. Am. Chem. Soc. 66, 1950–1951.

Cavallito, C.J., Bailey, J.H., Buck, J.S., 1945. The antibacterial principle of *Allium sativum*. III. Its precursor and essential oil of garlic. J. Am. Chem. Soc. 67, 1032–1033.

Colangeli, R., Helb, D., Sridharan, S., Sun, J., Varma-Basil, M., Hazbon, M.H., Harbacheuski, R., Megjugorac, N.J., Jacobs Jr., W.R., Holzenburg, A., Sacchettini, J.C., Alland, D., 2005. The *Mycobacterium tuberculosis iniA* gene is essential for activity of an efflux pump that confers drug tolerance to both isoniazid and ethambutol. Mol. Microbiol. 55, 1829–1840.

Gibbons, S., Udo, E.E., 2000. The effect of reserpine, a modulator of multidrug efflux pumps, on the in vitro activity of tetracycline against clinical isolates of methicillin resistant *Staphylococcus aureus* (MRSA) possessing the tet(K) determinant. Phytotherapy Res. 14, 139–140.

Lavaud, C., Massiot, G., Barrera, J.B., Moretti, C., LeMen-Oliver, L., 1994. Triterpene saponins from *Myrsine pellucida*. Phytochemistry 37 (6), 1671–1677.

Mimaki, Y., Kanmoto, T., Sashida, Y., Nishino, A., Satomi, Y., Nishino, H., 1996. Steroidal saponins from the underground parts of *Chlorophytum comosum* and their inhibitory activity on tumour promotor-induced phospholipids metabolism of HeLa cells. Phytochemistry 41, 1405–1410.

Muñoz, O., Piovano, M., Garbaino, J., Hellwing, V., Breitmaier, E., 1996. Tropane alkaloids from *Schizanthus litoralis*. Phytochemistry 43 (3), 709–713.

Sander, P., De Rossi, E., Boddinghaus, B., Cantoni, R., Branzoni, M., Bottger, E.C., Takiff, H., Rodriquez, R., Lopez, G., Riccardi, G., 2000. Contribution of the multidrug efflux pump LfrA to innate mycobacterial drug resistance. FEMS Microbiol. Lett. 193, 19–23.

Scholze, A., Loddenkemper, C., Grünbaum, M., Moosmayer, I., Offermann, G., Tepel, M., 2005. Cutaneous *Mycobacterium abscessus* infection after kidney transplantation. Nephrol. Dialysis Transplant. 20 (8), 1764–1765.

Seeram, N.P., Jacobs, H., McLean, S., Reynolds, W.F., 1998. A prenylated benzopyran derivative from *Peperomia clusifolia*. Phytochemistry 49 (5), 1389–1391.

Sermet-Gaudelus, I., Le Bourgeois, M., Pierre-Audigier, C., Offredo, C., Guillemot, D., Halley, S., Akoua-Koffi, C., Vincent, V., Sivadon-Tardy, V., Ferroni, A., Berche, P., Scheinmann, P., Lenoir, G., Gaillard, J.L., 2003. *Mycobacterium abscessus* and children with cystic fibrosis. Emerg. Infect. Dis. 9, 1587–1591.

Tabuti, J.R.S., Lye, K.A., Dhillion, S.S., 2003. Traditional herbal drugs of Bulamogi, Uganda: plants, use and administration. J. Ethnopharmacol. 88, 19–44.

Tandon, M., Shukla, Y.N., Thakur, R., 1992. 4-Hydroxyl-8,11-oxidoheneicosanol and other constituents from *Chlorophytum arundinaceum* roots. Phytochemistry 31 (7), 2525–2526.

Antibacterial Galloylated Alkylphloroglucinol Glucosides from Myrtle (*Myrtus communis*)

Giovanni Appendino,*[,†,‡] Lucia Maxia,[†,‡] Piergiorgio Bettoni,[†,‡] Monica Locatelli,[†,‡] Carola Valdivia,[⊥] Mauro Ballero,[‡] Michael Stavri,[§] Simon Gibbons,[§] and Olov Sterner*[,⊥]

Dipartimento di Scienze Chimiche, Alimentari, Farmaceutiche e Farmacologiche, Università del Piemonte Orientale, Viale Ferrucci 33, 28100 Novara, Italy, Consorzio per lo Studio dei Metaboliti Secondari (CSMS), Viale S. Ignazio 13, 09123 Cagliari, Italy, Centre for Pharmacognosy and Phytotherapy, The School of Pharmacy, University of London, 29−39 Brunswick Square, London WC1N 1AX, U.K., and Department of Organic Chemistry, Lund University, P.O. Box 124, 221 00 Lund, Sweden

Received November 9, 2005

An investigation of the polar glycosidic fraction from the leaves of myrtle afforded four galloylated nonprenylated phloroglucinol glucosides (**3a**−**d**) related to the endoperoxide hormone G3 (**4**) in terms of structure and biogenesis. Despite their close similarity, significant antibacterial activity was shown only by one of these compounds (**3b**, gallomyrtucommulone B), while the G3 hormone (**4**) was inactive.

Myrtle (*Myrtus communis* L., Myrtaceae) is nowadays better known as a culinary herb rather than a medicinal plant, but holds an important place in Western culture because of its mythological associations[1] and its medicinal use as an antiseptic and an anti-inflammatory agent.[2] Over the past few years, liqueurs prepared from the berries of myrtle have become popular,[3] while its leaves have been used as a hop substitute in beer[4] and as a cosmetic ingredient in products against hair dandruff.[5] This has led to a renewed and general interest in myrtle, especially for its cultivation, since the collection from wild plants is becoming insufficient to satisfy the growing demand.[3] From a phytochemical standpoint, myrtle contains unique compounds, as exemplified by a series of oligomeric nonprenylated phloroglucinols related to myrtucommulone A (**1**).[6] This compound shows outstanding antibacterial[6] and anti-inflammatory[7] properties, while powerful antioxidant activity was demonstrated for its lower homologue, semimyrtucommulone (**2**).[8]

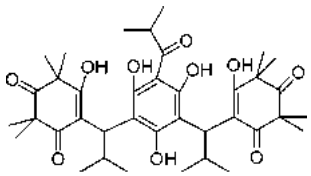

1

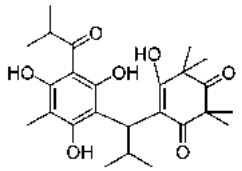

2

Apart from these constituents, the leaves of myrtle are a rich source of flavonoids, and especially of myricetin glycosides.[9] Myricetin can enhance glucose utilization and lower plasma glucose,[10] and antidiabetic properties have been traditionally attributed to myrtle in the folk medicine of various parts of the Mediterranean area.[11] We therefore became interested in the characterization of the glycosidic fractions of the leaves. Apart from large amounts (ca. 0.2% from the dried plant material) of myricetin rhamnopyranoside, a fraction containing galloylated glucosides was also obtained. When thoroughly purified, this fraction turned out to be made up of a series of closely related galloylated glucosides of alkylphloroglucinols, an unprecedented type of natural product and whose characterization is presented here.

Results and Discussion

A glycosidic fraction was obtained from an acetone extract of leaves by vacuum-liquid chromatography (VLC) on RP-18 silica gel. The galloylated fraction was next separated from myricetin rhamnopyranoside by gravity column chromatography on silica gel, eventually obtaining a yellow powder in ca. 0.08% yield from the dried leaves. The ^{1}H NMR spectrum of this fraction showed the resonances typical of gallic acid and of a 6-acylated glucosyl residue, and a cluster of olefinic and oxymethine singlets grouped around δ ca. 5.0 and 3.90. The fine splitting of all signals and the complexity of the upfield part of the spectrum suggested a mixture of related compounds. Preparative HPLC separation on normal-phase silica gel resolved the mixture into four peaks, corresponding to compounds **3a**−**d**, named gallomyrtucommulones A−D to emphasize their origin. Compounds **3a**−**d** showed closely related NMR spectra, but could be sorted out by mass spectrometry into two pairs, differing in their molecular weight (570 for **3a**,**b** and 568 for **3c**,**d**). The structure elucidation will be detailed for **3d**, the major constituent of the mixture. For the remaining compounds, only the interpretation of the spectroscopic differences into structural terms will be described.

Compound **3d** ($C_{27}H_{36}O_{13}$, HRMS) was obtained as an optically active yellowish powder. In the ^{1}H NMR spectrum (10% CD_3OD in $CDCl_3$, Table 1), the signals of a galloyl moiety (δ 7.07, s), as well as a glucose moiety acylated at the 6-hydroxyl (δ 4.52, m, H-1′; 3.25, dd, J = 8.0 and 7.8 Hz, H-2′; 3.45, m, H-3′; 3.42, m, H-4′; 3.48, m, H-5′; 4.53, m, H-6′a; 4.44, dd, J = 11.9, 4.7 Hz, H-6′b), an olefinic proton (δ 5.05, br s), an oxymethine (δ 3.81, s), two allylic methyls (δ 1.66 and 1.72, br s), and four quaternary methyls (δ 1.28, 1.28, 1.24, 1.17, s), were present. Apart from the protonated carbons corresponding to these resonances, the ^{13}C NMR spectrum (Table 2) showed a quaternary oxygenated carbon (δ 82.2, s), two ketone carbonyls (δ 215.4 and 211.4, s), and two quaternary carbons (δ 56.2 and 48.9, s). These signals were reminiscent of those observed in the endoperoxide G3 (**4**, Scheme 1), an antimalarial hormone constituent of various *Eucalyptus* species[12] that also occurs in myrtle.[6] Analysis of the HMBC correlations made it possible to evaluate the ^{1}H and ^{13}C NMR resonances in the dihydroxylated cyclohexadione structure **3d**. The *trans* configuration

* To whom correspondence should be addressed. Tel: +39 0321 375744 (G.A.); +46 70 5306649 (O.S.). Fax: +39 0321 375621 (G.A.); +46 46 2228209 (O.S.). E-mail: appendino@pharm.unipmn.it (G.A.); Olov.Sterner@organic.lu.se (O.S.).

† Università del Piemonte Orientale.

‡ Consorzio per lo Studio dei Metaboliti Secondari.

⊥ University of London.

§ Lund University.

10.1021/np050462w CCC: $33.50
Published on Web 01/20/2006

Table 1. ^{1}H NMR Data (500 MHz, 10% CD_3OD in $CDCl_3$) for Gallomyrtucommulones A (**3a**), B (**3b**), C (**3c**), and D (**3d**) [solvent signal of $CDCl_3$ (7.26 ppm) as reference, coupling constants (*J*) in Hz]

position	3a	3b	3c	3d
1	0.90 (d; 6.6)	0.88 (d; 6.6)	1.66 (s)	1.66 (s)
2	1.59 (m)	1.50 (m)		
3	0.73 (d; 6.6)	0.82 (d; 6.6)	1.66 (s)	1.72 (s)
4a	1.80 (dd; 6.4, 14.7)	1.89 (dd; 6.2, 14.7)	5.54 (br s)	5.05 (br s)
4b	1.28 (dd; 5.8, 14.7)	1.82 (dd; 5.0, 14.7)		
8		3.64 (s)		
10	3.73 (s)		3.70 (s)	3.81 (s)
11	1.22 (s)	1.32 (q)	1.22 (s)	1.28 (s)
12	1.21 (s)	1.07 (q)	1.19 (s)	1.24 (s)
13	1.18 (s)	1.15 (q)	1.18 (s)	1.17 (s)
14	1.15 (s)	1.09 (q)	1.18 (s)	1.28 (s)
1′	4.38 (d; 7.6)	4.36 (d; 7.8)	4.35 (d; 7.7)	4.52 (m)
2′	3.32 (m)	3.23 (m)	3.27 (m)	3.25 (dd; 8.0, 7.8)
3′	3.41 (m)	3.39 (m)	3.39 (m)	3.45 (m)
4′	3.38 (m)	3.40 (m)	3.37 (m)	3.42 (m)
5′	3.49 (m)	3.46 (m)	3.48 (m)	3.48 (m)
6′a	4.51 (dd; 1.6, 11.8)	4.55 (dd; 1.5, 11.9)	4.50 (dd; 1.5, 11.9)	4.53 (m)
6′b	4.37 (dd; 6.3, 11.8)	4.43 (dd; 5.3, 11.9)	4.36 ((dd; 5.3, 11.9)	4.44 (dd; 4.7, 11.9)
3″	7.03 (s)	7.06 (s)	7.02 (s)	7.07 (s)

Table 2. ^{13}C (125 MHz, 10% CD_3OD in $CDCl_3$) NMR Data for Gallomyrtucommulones A (**3a**), B (**3b**), C (**3c**), and D (**3d**) [solvent signal of $CDCl_3$ (77.0 ppm) as reference, multiplicities from HMQC experiments]

position	3a	3b	3c	3d
1	24.3 (q)	23.7 (q)	26.8 (q)	27.1 (q)
2	23.6 (d)	24.2 (d)	144.2 (s)	145.6 (s)
3	23.7 (q)	23.8 (q)	18.9 (q)	19.6 (q)
4	38.9 (t)	44.1 (t)	117.8 (d)	116.6 (d)
5	82.3 (s)	84.1 (s)	80.3 (s)	82.2 (s)
6	212.3 (s)	211.8 (s)	209.9 (s)	211.1 (s)
7	55.3 (s)	50.1 (s)	55.4 (s)	56.2 (s)
8	215.1 (s)	85.1 (d)	215.0 (s)	215.4 (s)
9	49.3 (s)	48.8 (s)	49.5 (s)	48.9 (s)
10	86.9 (d)	213.1 (s)	86.8 (d)	87.8 (d)
11	25.8 (q)	22.6 (q)	25.0 (q)	25.6 (q)
12	23.1 (q)	25.4 (q)	24.6 (q)	24.8 (q)
13	29.0 (q)	24.4 (q)	28.8 (q)	27.1 (q)
14	22.3 (q)	26.1 (q)	22.7 (q)	28.1 (q)
1′	105.8 (d)	103.1 (d)	104.7 (d)	105.0 (d)
2′	74.2 (d)	74.0 (d)	74.0 (d)	76.5 (d)
3′	76.5 (d)	76.5 (d)	76.3 (d)	74.0 (d)
4′	69.9 (d)	70.0 (d)	69.8 (d)	69.8 (d)
5′	74.1 (d)	74.0 (d)	74.1 (d)	74.0 (d)
6′	63.5 (t)	62.9 (t)	63.2 (t)	63.2 (t)
1″	167.0 (s)	166.9 (s)	167.0 (s)	167.0 (s)
2″	120.3 (s)	120.4 (s)	120.3 (s)	120.5 (s)
3″	109.2 (d)	109.2 (d)	109.2 (d)	109.3 (d)
4″	144.4 (s)	144.4 (s)	144.5 (s)	144.4 (s)
5″	137.7 (s)	137.6 (s)	137.6 (s)	137.6 (s)

of the glycol moiety was indicated by the observation of NOE correlations between the vinylic proton (H-4) and the methyl protons H-12 and H-14, while H-10 correlated with the 13-methyl. In **3c**, a compound having the same molecular weight as **3d**, the vinylic proton was not NOE correlated to any methyl, indicating not only a different configuration at C-5 but also a different conformation of the cyclohexadienone ring. Since the NMR spectra of **3c** and **3d** showed the same ^{1}H spin systems and ^{13}C multiplicities, these compounds were assigned as a pair of *cis/trans* isomers.

The other pair of compounds (**3a** and **3b**) showed a molecular weight two units higher than **3c** and **3d.** This and the lack of the vinyl protons and allyl methyls in the ^{1}H NMR spectrum suggested saturation of the isobutenyl group. However, the HMBC correlations showed a substantially different connectivity for the cyclohexadione moiety between **3a** and **3b**. Thus, **3a** was simply the hydrogenation product of **3d**, while in **3b** the oxymethine and the quaternary oxygenated carbons were "*para*" (1,4) and not "*ortho*"(1,2) related. In **3a**, H-3 correlated with the 12-methyl, and H-10 with the 11- and 13-methyls, supporting this configurational assignment. Due to the lack of diagnostic NOE effects, it was not possible to assign the relative configuration of **3b**. On the other hand, since the glucose and the cyclohexane domains are spectroscopically isolated, only

Scheme 1. Possible Biogenetic Derivation of Gallomyrtucommulones (**3a**−**d**) and G3 (**4**)[a]

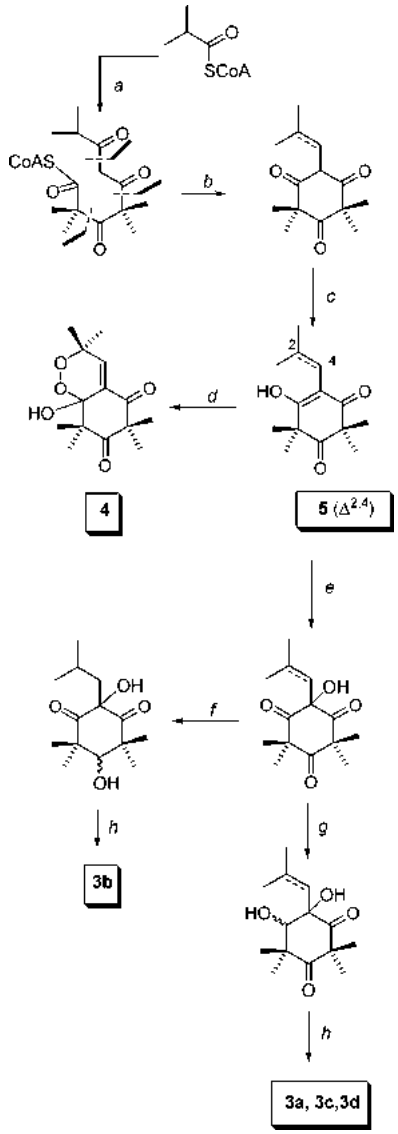

[a] Key: *a*: 3 × C2 elongation; *b*: intramolecular Claisen reaction; *c*: enolization; *d*: formal singlet oxygen cycloaddition; *e*: autoxidation; *f*: "*para*"-reduction; *g*: "*ortho*"-reduction; *h*: glucosidation and galloylation.

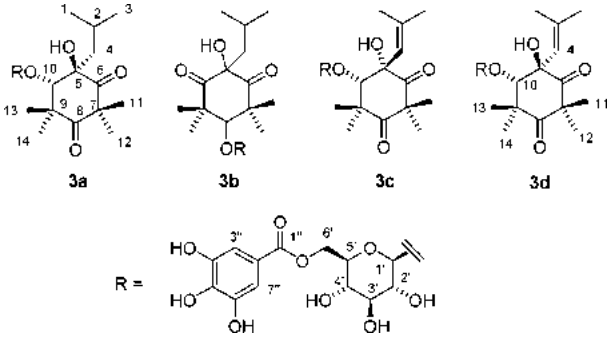

the relative configuration of the cyclohexadienone moiety of **3a**, **3c**, and **3d** could be assessed.

From a biogenetic standpoint, gallomyrtucommulones are presumably glycosidated polyketides, derived from an isobutyryl starter by three steps of C-2 homologation and two of geminal dimethylation (Scheme 1). After intramolecular Claisen cyclization and enolization, the enolic double bond is oxidized to a ketol, a known reaction for this type of compounds,[13] and then reduced and glycosidated. Compound **3c** (gallomyrtucommulone B) derives from a modification of this scheme, where the reduction step does not take place on one of the ketolic carbonyls, but on the "*para*" keto group. The endoperoxide hormone G3 (**4**) is presumably derived from the enolized trienone intermediate by reaction with a biological equivalent of singlet oxygen.

There is evidence that, under physiological conditions, the G-factors are present in plant tissues as inactive precursors, converted into the active hormones in response to damage or a biological stimulus. An oxidative deglucosidation would convert gallomyrtucommulones C and D (**3c** and **3d**) into the G3 precursor **5** (Scheme 1), making it of interest to evaluate the physiological relationship (if any) between G3 and these compounds. On the other hand, it was also interesting to investigate the antibacterial activity of gallomyrtucommulones, since powerful antibiotic activity has been shown for several phloroglucinols from myrtle.[6,15] All compounds were evaluated against a panel of resistant *Staphylococcus aureus* strains (Table 3), and these included MRSA strains XU212 (which also expresses the TetK efflux pump) and EMRSA-15 (which is an epidemic MRSA strain commonly encountered in the U.K.). Other isolates included the multidrug-resistant SA-1199B, which overexpresses the NorA MDR efflux transporter, and RN4220, which has a more specific macrolide efflux mechanism. Compounds **3c** and **3d** were inactive against the test panel of resistant staphylococci at a concentration of 256 μg/mL; however **3a** and **3b** had moderate antibacterial activities with minimum inhibitory concentration (MIC) values ranging from 64 to 256 μg/mL (Table 3). Compound **3b** showed significant (MIC =128 μg/mL) antibacterial activity against *Staphylococcus aureus* SA-1199B, but was ca. 4-fold less potent than the fluoroquinolone norfloxacin (MIC = 32 μg/mL), the reference compound for this type of activity. Compound **3b** was the most active analogue evaluated against RN4220, which expresses the MsrA macrolide transporter and is highly resistant to erythromycin (MIC > 128 μg/mL). Therefore, a surprising configurational dependence for the antibacterial activity of gallomyrtucommulones exists, an observation that suggests a specific biological target for these compounds. A similar dependence has been observed previously for myrtle phloroglucinols with respect to oligomerization.[6]

Taken together, the results of this study further qualify myrtle as a source of unique secondary metabolites. Nonprenylated acylphloroglucinols are common constituents of ferns,[16] but are otherwise very rare in higher plants, while alkylphloroglucinol glycosides are unknown as natural products.[17] It is therefore surprising that myrtle, despite the powerful and pleiotropic activity of its extracts and its medicinal, nutritional, and cultural relevance, has so long escaped the attention of phytochemists.

Table 3. Minimum Inhibitory Concentrations (MIC) of **3a** and **3b** (μg/mL)[a]

strain (resistance mechanism)	**3a**	**3b**	norfloxacin
ATCC 25923	128	64	1
SA-1199B (NorA)	256	128	32
RN4220 (MsrA)	128	128	2
XU212 (TetK, MecA)	256	128	4
EMRSA-15 (MecA)	128	128	0.5

[a] All MIC values were determined in duplicate.

Experimental Section

General Experimental Procedures. Optical rotations were determined on a Perkin-Elmer 192 polarimeter equipped with a sodium lamp (589 nm) and 10 cm microcell. IR spectra were obtained on a Shimadzu DR 8001 spectrophotometer. ^{1}H NMR (500 MHz) and ^{13}C NMR (125 MHz) spectra were obtained at room temperature with a Bruker DRX500 spectrometer with an inverse multinuclear 5 mm probehead equipped with a shielded gradient coil. The spectra were recorded in $CDCl_3$, and the solvent signals (7.26 and 77.0 ppm, respectively) were used as reference. The chemical shifts (δ) are given in ppm, and the coupling constants (J) in Hz. COSY, HMQC, and HMBC experiments were recorded with gradient enhancements using sine-shaped gradient pulses. For the 2D heteronuclear correlation spectroscopy the refocusing delays were optimized for $^1J_{CH} = 145$ Hz and $^nJ_{CH} = 10$ Hz. The raw data were transformed and the spectra were evaluated with the standard Bruker XWIN NMR software (rev. 010101). Mass spectra (HRESI) were recorded with a Micromass Q-TOF microinstrument. Silica gel 60 (70−230 mesh) and Lichroprep RP-18 (25−40 mesh) were used for gravity column chromatography. HPLC in isocratic mode was performed on a JASCO Herculite apparatus equipped with a UV detector set at 254 nm and using a 250 × 21.2 × 10 mm Chromasyl column.

Plant Material. *M. communis* L. was collected in April, 2003 near San Basilio (CA, Sardinia), and was identified by M. B. A voucher specimen (CAG 504) is deposited at the Dipartimento di Scienze Botaniche, Università di Cagliari.

Extraction and Isolation. Powdered, dried leaves (1156 g) were extracted with acetone at room temperature (2 × 5 L). The pooled extracts were filtered over Celite and concentrated to a small volume (bath temperature 35 °C). RP-18 silica gel (ca. 50 g) was then added, and evaporation was continued until a solid material was obtained. The latter was fractionated by VLC on RP-18 silica gel (bed size: 9 cm × 2 cm) using water−methanol mixtures. The fraction eluted with 1:1 methanol−water (4.4 g) contained a mixture of glycosides, which was fractionated by gravity column chromatography on silica gel (100 g, 1:1 petroleum ether−EtOAc as eluant) to afford 974 mg of a gallomyrtucommulone mixture and 2.185 g of myricetin rhamnopyranoside. A fraction (250 mg) of the gallomyrtucommulone mixture was purified by preparative HPLC to afford 12 mg of **3a**, 15 mg of **3b**, 11 mg of **3c**, and 25 mg of **3d**. The low final isolation yield was due to the difficulty of the separation and the fact that a baseline separation could not be achieved.

Gallomyrtucommulone A (3a): yellowish foam; $[\alpha]_D^{25}$ +56 (*c* 0.4, methanol); IR (KBr) ν_{max} 3356, 3320, 1654, 1557, 1354, 1287, 1210, 1151, 1071 cm^{-1}; ^{1}H and ^{13}C NMR, see Table 1; HRESIMS *m*/*z* 593.2198, calcd for $C_{27}H_{38}O_{13}$ + Na, 593.2210.

Gallomyrtucommulone B (3b): yellowish foam; $[\alpha]_D^{25}$ +44 (*c* 0.4, methanol); IR (KBr) ν_{max} 3350, 3315, 1648, 1558, 1350, 1289, 1221, 1151, 1039 cm^{-1}; ^{1}H and ^{13}C NMR, see Table 1; HRESIMS *m*/*z* 593.2208, calcd for $C_{27}H_{38}O_{13}$ + Na, 593.2210.

Gallomyrtucommulone C (3c): yellowish foam; $[\alpha]_D^{25}$ +38 (*c* 0.4, methanol); IR (KBr) ν_{max} 3352, 3321, 1641, 1513, 1287, 1217, 1154, 1079, cm^{-1}; ^{1}H and ^{13}C NMR, see Table 1; HRESIMS *m*/*z* 591.2061, calcd for $C_{27}H_{36}O_{13}$ + Na, 591.2054.

Gallomyrtucommulone D (3d): yellowish foam; $[\alpha]_D^{25}$ +31 (*c* 0.4, methanol); IR (KBr) ν_{max} 3356, 3320, 1647, 1658, 1351, 1284, 1221, 1156, 1069, cm^{-1}; ^{1}H and ^{13}C NMR, see Table 1; HRESIMS *m*/*z* 569.2211, calcd for $C_{27}H_{36}O_{13}$ + H, 569.2234.

Antibacterial Assays. *S. aureus* strain ATCC 25923 was the generous gift of E. Udo (Kuwait University, Kuwait). *S. aureus* RN4220 containing plasmid pUL5054, which carries the gene encoding the MsrA macrolide efflux protein, was provided by J. Cove.[18] Strain XU-212,

which possesses the TetK tetracycline efflux protein, was provided by E. Udo.[19] SA-1199B, which overexpresses the *norA* gene encoding the NorA MDR efflux protein, was provided by G. Kaatz.[20] EMRSA-15 is an epidemic strain of MRSA[21] and was the generous gift of P. Stapleton, School of Pharmacy, University of London. All *Staphylococcus aureus* strains were cultured on nutrient agar and incubated for 24 h at 37 °C prior to MIC determination. Bacterial inocula equivalent to the 0.5 McFarland turbidity standard were prepared in normal saline and diluted to give a final inoculum density of 5×10^5 cfu/mL. The inoculum (125 μL) was added to all wells, and the microtiter plate was incubated at 37 °C for 18 h. The MIC was recorded as the lowest concentration at which no bacterial growth was observed, as previously described.[19]

Acknowledgment. Financial support from MIUR (Fondi ex-40%, progetto Sostanze Naturali ed Analoghi Sintetici con Attività Antitumorale) is gratefully acknowledged.

References and Notes

(1) As a symbol of marital love, myrtle is one of the keys to two of the most famous and enigmatic paintings of the Renaissance, the *Venus of Urbino* by Titian and the *Two Court Ladies* by Carpaccio. (For a discussion, see: Romanelli, G. *Vittore Carpaccio. Le Due Dame Veneziane*; Silvana Editoriale: Cinisello Balsamo, 2003; pp 12−13)

(2) For a review, see: Diaz, A. M.; Aberger, A. *Fitoterapia* **1987**, *58*, 167−174. Myrtle is one of the oldest medicial plants, since its use to treat pain was already mentioned in the Ebers papyrus (ca. 1500 B.C.) (Metha, A. *Chem. Eng. News* **2005**, June 20, pp 46−47).

(3) Nuvoli, F. *Il Mirto della Sardegna*; Zonza Editore: Cagliari, Italy, 2004; pp 7−22.

(4) Also St. John's wort (*Hypericum perforatum* L.), another plant containing antibacterial phloroglucinols, has been used as a hop substitute for the production of beer (see: Buhner, S. H. *Sacred and Herbal Healing Beers*; Brewer Publications: Boulder, CO, 1998).

(5) Puybaret, C.; David, B.; Charveron, M.; Mamatas, S. FR 98-11619 19980917, 1990; *Chem. Abstr*. **1990**, *112*, 195230.

(6) Appendino, G.; Bianchi, F.; Minassi, A.; Sterner, O.; Ballero, M.; Gibbons, S. *J. Nat. Prod.* **2002**, *65*, 334−338.

(7) Feisst, C.; Franke, L.; Appendino, G.; Werz, O. *J. Pharmacol. Exp. Ther*. **2005**, *315*, 389−396.

(8) Rosa, A.; Deiana, M.; Casu, V.; Corona, G.; Appendino, G.; Bianchi, F.; Ballero, M., Dessì, A. *Free Radical Res*. **2003**, *37*, 1013−1019.

(9) Hinou, J.; Lakkas, N.; Philianos, S. *Plant. Méd. Phytothér*. **1988**, *22*, 98−103.

(10) Liu, J,-M.; Liou, S.-S.; Lan, T.-W.; Hsu, F.-L.; Cheng, J.-T. *Planta Med.* **2005**, *71*, 617−621.

(11) Elfellah, M. S.; Akhter, M. H.; Khan, M. T. *J. Ethnopahrmacol*. **1984**, *11*, 275−281.

(12) The G-factors are involved in plant resistance to frost and drought and also act as growth regulators (Ghisalberti, E. *Phytochemistry* **1996**, *41*, 7−22). For their antimalarial activity, see: Najjar, F.; Baltas, M.; Gorrichon, L.; Moreno, Y.; Tzedakis, T.; Vial, H.; André-Barrès, C. *Eur. J. Org. Chem*. **2003**, *17*, 3335−3343.

(13) Verotta, L.; Appendino, G.; Belloro, E.; Bianchi, F.; Sterner, O.; Lovati, M.; Bombardelli, E. *J. Nat. Prod*. **2002**, *65*, 433−438.

(14) Bolte, M. L.; Crow, W. D.; Yoshida, S. *Aust. J. Chem*. **1982**, *35*, 1431−1437.

(15) Antimycotic activity has been demonstrated for certain galloylated phenolic glucosides (De Leo, M.; Braca, A.; De Tommasi, N.; Norscia, I.; Morelli, I.; Battinelli, L.; Mazzanti, G. *Planta Med*. **2004**, *70*, 841−846).

(16) Murakami, T.; Tanaka, N. *Progress Chem. Org. Nat. Prod*. **1988**, *54*, 4−12.

(17) Glycosides of aromatic acylphloroglucinols are known (see for instance: Bohr, G.; Gerhäuser, C.; Knauft, J.; Zapp, J.; Becker, H. *J. Nat. Prod*. **2005**, *68*, 1545−1548).

(18) Ross, J. I.; Farrell, A. M.; Eady, E. A.; Cove, J. H.; Cunliffe, W. J. *J. Antimicrob. Chemother*. **1989**, *24*, 851−862.

(19) Gibbons, S.; Udo, E. E. *Phytother. Res.* **2000**, *14*, 139−140.

(20) Kaatz, G. W.; Seo, S. M.; Ruble, C. A. *Antimicrob. Agents Chemother*. **1993**, *37*, 1086−1094.

(21) Johnson, A. P.; Aucken, H. M.; Cavendish, S.; Ganner, M.; Wale, M. C. J.; Warner, M.; Livermore, D. M.; Cookson, B. D. *J. Antimicrob. Chemother.* **2001**, *48*, 143−144.

NP050462W

PHYTOTHERAPY RESEARCH
Phytother. Res. **19**, 938–941 (2005)
Published online in Wiley InterScience (www.interscience.wiley.com). **DOI**: 10.1002/ptr.1758

The Antimycobacterial Constituents of Dill (*Anethum graveolens*)

Michael Stavri and Simon Gibbons*

Centre for Pharmacognosy and Phytotherapy, The School of Pharmacy, University of London, 29–39 Brunswick Square, London WC1N 1AX, UK

As part of a project to characterize selected members of the Kuwaiti flora for their phytochemistry and antimycobacterial activity, a new furanocoumarin, 5-[4″-hydroxy-3″-methyl-2″-butenyloxy]-6,7-furocoumarin (3), was isolated from the whole herb of *Anethum graveolens*. The known compounds oxypeucedanin (1), oxypeucedanin hydrate (2) and falcarindiol (4) were also isolated from this plant. The structure of each compound was determined by interpretation of NMR and mass spectrometric data. The three known compounds exhibited antibacterial activity against a panel of rapidly growing mycobacteria with minimum inhibitory concentration (MIC) values in the range 2–128 μg/mL. Copyright © 2005 John Wiley & Sons, Ltd.

Keywords: Anethum graveolens; mycobacteria; furanocoumarins; polyacetylenes; antimycobacterial activity.

INTRODUCTION

Anethum graveolens L. is a member of the Apiaceae family and is more commonly known as dill. The plant is used both medicinally and as an aromatic herb and spice in cookery. The fruit of *A. graveolens* has been used for medicinal purposes to relieve digestive problems and also to stimulate milk for nursing mothers (Ishikawa *et al.*, 2002). Previous phytochemical studies have identified the monoterpene carvone to be the main constituent (50%–60%) of the essential oil (Ishikawa *et al.,* 2002). This monoterpene has a calming effect and is used in gripe water preparations (Heinrich *et al.*, 2004).

Over the past 15–20 years there has been a worldwide resurgence of tuberculosis (TB). *Mycobacterium tuberculosis* is the major cause of this disease, although *Mycobacterium bovis* and *Mycobacterium africanum* are also listed within the *M. tuberculosis* complex (Newton *et al.*, 2000; Wolinsky, 1992). Each year approximately 8 million people are infected with the tubercle bacilli, which causes around 3 million deaths, more than any other single bacterial infectious disease. The World Health Organization has estimated that between 2000 and 2020 nearly 1 billion people will be newly infected, 200 million will develop TB and 35 million will die from the disease (WHO, 2000). The emergence of multidrug resistant (MDR) strains of *M. tuberculosis* has resulted in an urgent need for new antimycobacterial drug leads to be identified for further development. As part of a continuing project to identify plant natural products as potential antimycobacterial drug leads, the extracts of *A. graveolens* were investigated.

* Correspondence to: Dr S. Gibbons, Centre for Pharmacognosy and Phytotherapy, The School of Pharmacy, University of London, 29–39 Brunswick Square, London WC1N 1AX, UK.
E-mail: simon.gibbons@ulsop.ac.uk
Contract/grant sponsor: Engineering and Physical Sciences Research Council; contract/grant number: GR/R47646/01.

MATERIALS AND METHODS

Plant material. *Anethum graveolens* was collected from Doha, Kuwait. The material was identified by S.G. and a voucher specimen is deposited at the Centre for Pharmacognosy and Phytotherapy, The School of Pharmacy, University of London.

Bacterial strains. *Mycobacterium fortuitum* ATCC 6841, *Mycobacterium smegmatis* ATCC 14468, *Mycobacterium phlei* ATCC 11758, *Mycobacterium aurum* Pasteur Institute 104482 and *Mycobacterium abscessus* ATCC 19977 were obtained from NTCC.

Antibacterial assay. The panel of rapidly growing mycobacteria were cultured on Columbia blood agar (Oxoid) supplemented with 7% defibrinated horse blood (Oxoid). *M. fortuitum*, *M. phlei* and *M. smegmatis* were incubated for 72 h, *M. abscessus* for 96 h and *M. aurum* for 120 h prior to MIC determination. Bacterial inocula equivalent to 5×10^5 cfu/mL were prepared in normal saline using the 0.5 McFarland turbidity standard followed by dilution. The MIC was recorded as the lowest concentration at which no bacterial growth was observed (Gibbons and Udo, 2000). Ethambutol was used as a positive control against all the mycobacterial strains. Growth and sterile controls were also performed.

General experimental procedures. NMR spectra were recorded on a Bruker AVANCE 500 MHz spectrometer. Chemical shift values (δ) were reported in parts per million (ppm) relative to the appropriate internal solvent standard. Coupling constants (J values) are given in Hertz. Mass spectra were recorded on a VG ZAB-SE instrument (FAB-EIMS) and a Finnigan navigator (ESIMS). IR spectra were recorded on a Nicolet 360 FT-IR spectrophotometer and UV spectra on a Perkin-Elmer Lambda 15 UV/Visible spectrophotometer. Optical rotations were measured on a Bellingham and Stanley ADP 200 polarimeter.

Received 9 July 2003
Accepted 28 October 2003

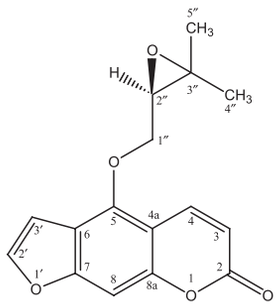

1

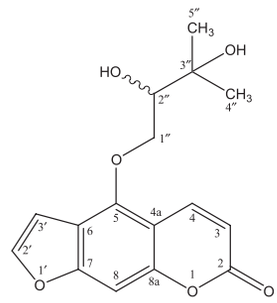

2

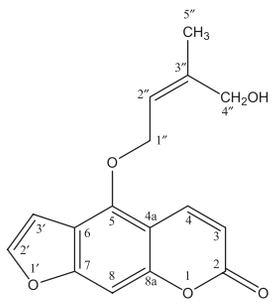

3

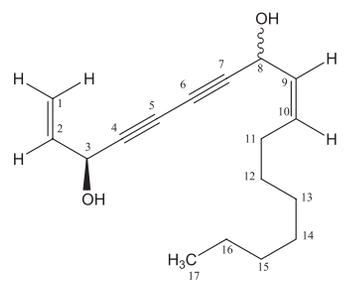

4

Extraction and isolation. The whole herb was air-dried for 3 days and ground to a powder. The powdered material (280 g) was sequentially extracted in a Soxhlet apparatus (3 L each) with hexane, chloroform and methanol. Vacuum liquid chromatography (VLC) of the hexane extract (8 g) was performed using a step-gradient system starting with hexane increasing to EtOAc by 10% increments followed by a methanol wash to yield 12 fractions. VLC fraction 6 (eluted with 1:1 hexane–EtOAc) was subjected to solid phase extraction (SPE) in normal phase mode. Preparative thin layer chromatography (PTLC) of fraction 5 (114 mg; 6:4 hexane–EtOAc) on reverse phase plates afforded compound **1** (35 mg). Compound **4** (8.8 mg) was isolated from VLC fraction 5 by normal phase SPE (eluting with 9:1 petroleum ether–chloroform), followed by PTLC of SPE fraction 5 (75:25:2 toluene–EtOAc–AcOH).

The chloroform extract (4.8 g) was subjected to VLC as described above. Normal phase SPE of VLC fraction 6 (143 mg; 1:1 hexane–EtOAc) using an isocratic system (8:2 hexane–EtOAc) yielded eight fractions. Fractions 4 and 5 were combined and multiple PTLC in reverse phase mode (65:35 methanol–water; 3 times) led to the purification of compound **2** (6.3 mg). LH-20 Sephadex chromatography of VLC fraction 8 (118 mg; eluted with 7:3 EtOAc–hexane) using dichloromethane yielded five fractions. Fraction 3 (18 mg) was subjected to multiple PTLC in normal phase mode (65:35:2; toluene–EtOAc–AcOH) and this afforded compound **3** (8.1 mg).

RESULTS AND DISCUSSION

The hexane and chloroform extracts both showed antimycobacterial activity against the screening model *Mycobacterium fortuitum*. Bioassay-guided fractionation led to the isolation and structure elucidation of the active components from this plant (oxypeucedanin [**1**], oxypeucedanin hydrate [**2**] and falcarindiol [**4**]).

The ^{1}H NMR spectrum of compound **1** showed characteristic signals for a furanocoumarin. This included signals for a pair of *cis* olefinic protons linked α and β to a carbonyl (δ_H 6.30 d, J = 10.0 Hz, H-3 and δ_H 8.19 dd, J = 10.0, 0.5 Hz, H-4) as well as signals for a pair of furan olefinic protons (δ_H 7.60 d, J = 2.0 Hz, H-2′ and δ_H 6.94 dd, J = 2.5, 1.0 Hz, H-3′). The ^{13}C NMR spectrum indicated the presence of 16 carbons, signifying that this furanocoumarin was prenylated.

The mass spectrum and NMR data for this compound were in close agreement with that published for the furanocoumarin oxypeucedanin, which was also previously isolated from the roots of *Angelica officinalis* (Harkar *et al.*, 1984). Measurement of a positive absolute rotation, $[\alpha]_D^{23}$ + 9.1° (*c* 1.755, $CHCl_3$), allowed **1** to be assigned as (*R*)-(+)-oxypeucedanin (Lemmich *et al.*, 1971).

Compound **2** was isolated as a colourless amorphous solid and a molecular formula of $C_{16}H_{16}O_6$ [M+H-H_2O]$^+$ (287.0) was assigned by ESI-MS. The ^{1}H and ^{13}C NMR spectra were very similar to that of **1** indicating the presence of another linear furanocoumarin. The ^{13}C NMR data for this compound were in close agreement with that published for oxypeucedanin hydrate, which was previously isolated from the roots of *Angelica officinalis* (Harkar *et al.*, 1984) and *Angelica dahurica* (Ishihara *et al.*, 2001). The ^{1}H NMR data (recorded in $CDCl_3$) for the furanocoumarin was also in close agreement with the literature, but differed with respect to the prenyl group. The downfield shift of the two methyl groups reported in this paper can be explained by a deshielding effect caused by the hydroxyl group at C-3″. The deshielding effect of this hydroxyl group must be equal for both the methyl groups. The hydroxyl group

Table 1. ^{1}H and ^{13}C NMR data and ^{1}H-^{13}C long-range correlations of compound 3 recorded in $CDCl_3$

Position	^{1}H	^{13}C	^{2}J	^{3}J
2	–	161.2		
3	6.30 d (9.5)	112.8	C-2	C-4a
4	8.16 d (10.0)	139.4		C-2, C-5, C-8a
4a	–	107.4		
5	–	148.6		
6	–	114.1		
7	–	158.1		
8	7.17 s	94.5	C-8a	C-6, C-4a
8a	–	152.7		
2′	7.61 d (2.5)	145.1		C-6, C-7
3′	6.96 dd (2.0, 0.5)	104.9	C-2′, C-6	C-7
1″	5.04 d (6.0)	68.9	C-2″	C-3″, C-5
2″	5.70 t (6.5)	122.1		
3″	–	141.4		
4″	4.20 s	61.9	C-3″	C-2″, C-5″
5″	1.90 s	21.4	C-3″	C-2″, C-4″

at C-2″ would also have a deshielding effect on the two methyl groups due to the close spatial proximity of these groups. Once more the deshielding effect of this hydroxyl group will be equal for both methyls as **2** was isolated as a racemic mixture. This would account for the methyl protons appearing as a 6H singlet at δ_H 1.70 in the ^{1}H NMR spectrum.

Compound **3** was the third furanocoumarin to be isolated from *A. graveolens*. A molecular formula of $C_{16}H_{14}O_5$ $[M]^+$ (286.0840) was established by HREIMS. The ^{1}H and ^{13}C NMR (Table 1) spectra once more provided evidence to indicate the presence of a 5-*O*-prenylated furanocoumarin. The signals for the furanocoumarin skeleton were identical to those of the previous compounds of this natural product class. The prenyl group was composed of two oxymethylenes (δ_H 5.04 d, H_2-1″ and δ_H 4.20 s, H_2-4″), an olefin (δ_H 5.70 t, H-2″, δ_C 122.1) and a methyl group (δ_H 1.90 s, H_3-5″). The ^{13}C spectrum also showed the presence of an olefinic quaternary carbon (δ_C 141.4, C-3″). All proton and carbon assignments were made by inspection of the HMQC and HMBC spectra acquired.

From the HMBC, H_2-1″ gave a ^{3}J correlation to C-5 placing this prenyl group here. The assignment of the carbon at position 5 was fixed by a ^{3}J correlation from the olefinic proton H-4 to C-5 (Table 1). A COSY signal between H_2-1″ and H-2″ placed the olefinic proton H-2″ next to the oxymethylene. Both the oxymethylene and olefin gave an HMBC signal to an olefinic quaternary carbon which could be assigned to position C-3″. The remaining oxymethylene and methyl groups appeared as singlets in the ^{1}H spectrum and each gave a ^{2}J correlation to C-3″ and so must be directly attached to this quaternary carbon. Due to the downfield nature of the H_2-4″ methylene protons (δ_H 4.20 s) an hydroxyl was placed here. H_3-5″ and H_2-4″ both gave allylic couplings to H-2″ in the COSY spectrum, as well as towards each other. These groups also showed *homo*-allylic correlations to H_2-1″, confirming the structure of the prenyl group.

The NOESY spectrum (Fig. 1) enabled the stereochemistry of the prenyl group to be ascertained. An NOE between H-2″ and methyl-5″ placed these

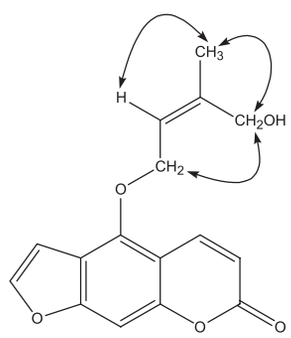

Figure 1. NOE correlations for **3**

protons on the same side of the molecule. This was further confirmed by a second NOE between H_2-1″ and H_2-4″. There has been no previous report of a linear furanocoumarin with this particular prenyl group attached at position 5 and so compound **3** is new.

Compound **4** was isolated as a pale yellow oil from the hexane extract. The ^{1}H and ^{13}C NMR spectra provided identical signals as for the C_{17} polyacetylene falcarindiol that was previously isolated by Lechner *et al.* (2004).

Due to a paucity of falcarindiol, the absolute stereochemistry at C-3 and C-8 could not be determined. However, a positive specific rotation ($[\alpha]_D^{23}$ + 72.6°) enabled two of the four stereoisomers to be dispelled leaving two possible stereoisomers. The literature describes 3*S*,8*S*-falcarindiol as having a positive specific rotation (Bernart *et al.*, 1996; Kobaisy *et al.*, 1997), whilst the 3*R*,8*S* stereoisomer has been described as having a negative specific rotation ($[\alpha]_D^{25}$ -130°) (Lechner *et al.*, 2004). The alternative laevoisomer must therefore be the 3*R*,8*R* enantiomer, which has previously been described as dextrorotatory (Lechner *et al.*, 2004). The dextrorotatory falcarindiol corresponds to the 3*S*,8*S* stereoisomer, therefore the alternative dextroisomer must be the 3*S*,8*R* stereoisomer. This enabled the stereochemistry of compound **4** at positions 3 and 8 to be assigned as either the 3*S*,8*S* or 3*S*,8*R* stereoisomer.

Table 2. Minimum inhibitory concentration (MIC) of compounds 1, 2 and 4 and ethambutol in μg/mL

Bacterial strain	**1**	**2**	**4**	Ethambutol
M. fortuitum ATCC 6841	128	128	4	4
M. phlei ATCC 11758	64	64	2	2
M. aurum Pasteur Institute 104482	32	32	4	0.5
M. smegmatis ATCC 14468	32	64	4	0.5
M. abscessus ATCC 19977	ξ	ξ	2	128

ξ, not tested.

Falcarindiol exhibited the greatest activity of the three active principles isolated with minimum inhibitory concentration (MIC) values in the range 2–4 μg/mL against a panel of rapidly growing mycobacteria (Table 2). Interestingly, 3*R*,8*R*-16,17-dehydrofalcarindiol showed no antimycobacterial activity against any of the rapidly growing mycobacteria tested (Stavri *et al*., 2005). This indicates that saturation at positions 16 and 17 of the molecule is crucial for activity.

Oxypeucedanin (**1**) and oxypeucedanin hydrate (**2**) also showed moderate antimycobacterial activity against the same panel of rapidly growing mycobacteria with MIC values in the range 32–128 μg/mL (Table 2). Coumarin natural products are known to exert their effects by inhibition of DNA gyrase. Novobiocin and coumermycin A_1 have been known to inhibit bacterial nucleic acid synthesis since the 1950s (Maxwell, 1997). Studies to elucidate the mechanism of action of coumarin antibiotics have revealed that they inhibit the ATP-dependent catalytic functions of DNA gyrase, such as DNA supercoiling and decatenation (Periers *et al.*, 2000). This is achieved by competitive inhibition of ATP binding (Periers *et al.*, 2000). The addition of a prenyl group to the furanocoumarin skeleton results in an increase in lipophilicity of the molecule, facilitating its passage through the thick membrane of these bacteria to its target site. Further studies on both the polyacetylene and coumarin natural product classes would appear to be worthwhile as drug leads given the rise in the number of infections caused by multidrug resistant mycobacterial species. 5-[4″-hydroxy-3″-methyl-2″-butenyloxy]-6,7-furocoumarin (**3**) White amorphous solid; UV ($CHCl_3$) λ_{max} (log ε) 305 (8.94), 266 (9.01), 258 (9.04), 255 (9.04); IR (thin film) ν_{max} cm^{-1}: 3631, 2936, 1541, 1507; ^1H NMR and ^{13}C NMR ($CDCl_3$): see Table 1. HREIMS (*m/z*): 286.0840 $[M]^+$ (calc. for $C_{16}H_{14}O_5$, 286.0841).

Acknowledgements

We thank the School of Pharmacy for a Doctoral Scholarship to Michael Stavri. We also thank the Engineering and Physical Sciences Research Council for funding (Grant No. GR/R47646/01).

REFERENCES

Bernart MW, Cardellina IJH, Balaschak MS, Alexander MR, Shoemaker RH, Boyd MR. 1996. Cytotoxic falcarinol oxylipins from *Dendropanax arboreus*. *J Nat Prod* **59**: 748–753.

Gibbons S, Udo EE. 2000. The effect of reserpine, a modulator of multidrug efflux pumps, on the *in vitro* activity of tetracycline against clinical isolates of methicillin resistant *Staphylococcus aureus* (MRSA) possessing the tet(K) determinant. *Phytother Res* **14**: 139–140.

Harkar S, Razdan TK, Waight ES. 1984. Steroids, chromone and coumarins from *Angelica officinalis*. *Phytochemistry* **23**: 419–426.

Heinrich M, Barnes J, Gibbons S, Williamson EM. 2004. *Fundamentals of Pharmacognosy and Phytotherapy*. Churchill Livingstone: London.

Ishihara K, Fukutake M, Asano T *et al.* 2001. Simultaneous determination of byak-angelicin and oxypeucedanin hydrate in rat plasma by column-switching high-performance liquid chromatography with ultraviolet detection. *J Chromatogr B* **753**: 309–314.

Ishikawa T, Kudo M, Kitajima J. 2002. Water-soluble constituents of Dill. *Chem Pharm Bull* **50**: 501–507.

Kobaisy M, Abramowski Z, Lermer L *et al.* 1997. Antimycobacterial polyynes of Devil's Club (*Oplopanax horridus*), a North American native medicinal plant. *J Nat Prod* **60**: 1210–1213.

Lechner D, Stavri M, Oluwatuyi M, Pereda-Miranda R, Gibbons S. 2004. The anti-staphylococcal activity of *Angelica dahurica* (Bai Zhi). *Phytochemistry* **65**: 331–335.

Lemmich J, Pedersen PA, Nielsen BE. 1971. Coumarins and terpenoids of the fruits of *Ligusticum seguieri*. *Phytochemistry* **10**: 3333–3334.

Maxwell A. 1997. DNA gyrase as a drug target. *Trends Microbiol* **5**: 102–109.

Newton SM, Lau C, Wright CW. 2000. A review of antimycobacterial natural products. *Phytother Res* **14**: 303–322.

Periers AM, Laurin P, Ferroud D *et al.* 2000. Coumarin inhibitors of gyrase B with *N*-propargyloxy-carbamate as an effective pyrrole bioisostere. *Bioorg Med Chem Lett* **10**: 161–165.

Stavri M, Ford CH, Bucar F *et al.* 2005. Bioactive constituents of *Artemisia monosperma*. *Phytochemistry* **66**: 233–239.

Wolinsky E. 1992. Mycobacterial diseases other than tuberculosis. *Clin Infect Dis* **15**: 1–12.

World Health Organization. 2000. *WHO Tuberculosis Fact Sheet* No. 104.

PHYTOTHERAPY RESEARCH
Phytother. Res. **19**, 538–542 (2005)
Published online in Wiley InterScience (www.interscience.wiley.com). **DOI**: 10.1002/ptr.1711

Isopimaric Acid from *Pinus nigra* shows Activity against Multidrug-resistant and EMRSA Strains of *Staphylococcus aureus*

Eileen Smith, Elizabeth Williamson, Mire Zloh and Simon Gibbons*

Centre for Pharmacognosy and Phytotherapy, The School of Pharmacy, University of London, 29-39 Brunswick Square, London WC1N 1AX, UK

The diterpene isopimaric acid was extracted from the immature cones of *Pinus nigra* (Arnold) using bioassay-guided fractionation of a crude hexane extract. Isopimaric acid was assayed against multidrug-resistant (MDR) and methicillin-resistant *Staphylococcus aureus* (MRSA). The minimum inhibitory concentrations (MIC) were 32–64 μg/mL and compared with a commercially obtained resin acid, abietic acid, with MICs of 64 μg/mL. Resin acids are known to have antibacterial activity and are valued in traditional medicine for their antiseptic properties. These results show that isopimaric acid is active against MDR and MRSA strains of *S. aureus* which are becoming increasingly resistant to antibiotics. Both compounds were evaluated for modulation activity in combination with antibiotics, but did not potentiate the activity of the antibiotics tested. However, the compounds were also assayed in combination with the efflux pump inhibitor reserpine, to see if inhibition of the TetK or NorA efflux pump increased their activity. Interestingly, rather than a potentiation of activity by a reduction in MIC, a two to four-fold increase in MIC was seen. It may be that isopimaric acid and abietic acid are not substrates for these efflux pumps, but it is also possible that an antagonistic interaction with reserpine may render the antibiotics inactive. ^{1}H-NMR of abietic acid and reserpine taken individually and in combination, revealed a shift in resonance of some peaks for both compounds when mixed together compared with the spectra of the compounds on their own. It is proposed that this may be due to complex formation between abietic acid and reserpine and that this complex formation is responsible for a reduction in activity and elevation of MIC. Copyright © 2005 John Wiley & Sons, Ltd.

Keywords: isopimaric acid; *Staphylococcus aureus*; MRSA; EMRSA; multidrug-resistance; MDR; efflux.

INTRODUCTION

Antibiotic resistance by pathogenic bacteria is a major problem both in hospitals and in the community. Methicillin-resistant *Staphylococcus aureus* (MRSA) is a primary nosocomial pathogen, potentially causing serious conditions such as bacteraemia, endocarditis and haemolytic pneumonia. Multi-drug resistant (MDR) strains of *S. aureus* are also becoming increasingly difficult to treat.

Many MDR strains of *S. aureus* are able to efflux antibiotics from the cell by means of a pump in the cytoplasmic membrane. Some of these pumps, such as NorA and QacA, are able to efflux a range of antibiotics, antiseptics and structurally unrelated compounds (Marshall and Piddock, 1997). Other pumps are more specific, for example TetK, which effluxes tetracycline and MsrA, the macrolide efflux pump. Isopimaric acid (IPA) which was isolated from *Pinus nigra* and a commercially obtained sample of abietic acid (AA) were assayed against strains possessing the TetK, MsrA and NorA efflux pumps.

* Correspondence to: Dr S. Gibbons, Centre for Pharmacognosy and Phytotherapy, The School of Pharmacy, University of London, 29-39 Brunswick Square, London WC1N 1AX, UK.
E-mail: simon.gibbons@ulsop.ac.uk
Contract/grant sponsor: Stiefel International R & D Ltd.
Contract/grant sponsor: Engineering and Physical Sciences Research Council; Contract/grant number: GR/R47646/01.

MRSA strains express their resistance via the *mecA* gene which encodes a lower-affinity penicillin binding protein PBP2′ which is absent in methicillin sensitive strains (Poole, 2004). Epidemic MRSA strains are a particular problem in hospitals. In England all acute NHS Trusts are now required to report instances of MRSA bacteraemia to the Department of Health's MRSA surveillance scheme (www.dh.gov.uk). The epidemic strains EMRSA-15 and 16 were the major strains found in MRSA bacteraemia isolates in a study from 26 UK hospitals (Johnson *et al.*, 2001). Here IPA and AA were tested against isolates of EMRSA-15 and EMRSA-16.

Compounds which potentiate antibiotic activity against MDR strains, even restoring antibiotic sensitivity in a resistant strain may be of value in treating virulent infections. IPA and AA were assayed in combination with antibiotics to test for their ability to potentiate antibiotic activity. Additionally, both compounds were tested in combination with the multidrug efflux pump inhibitor reserpine to ascertain if the pump inhibitor modulated their antibacterial activity.

Pine cones, foliage, bark and resin have been used in traditional medicine to treat rheumatism, and respiratory complaints and as general antiseptics (Leung and Foster, 1996). In this study, the immature cones of *Pinus nigra* (Arnold), known as European black pine, were investigated for activity against MDR and MRSA strains of *S. aureus*. The ecological rationale behind this study is that the cones are essential for plant reproduction

Received 21 February 2005
Accepted 14 April 2005

and it is highly likely that protective compounds have been biosynthesized in the immature cones. A previous study on a pine cone isolate from *P. nigra* showed anti-HIV activity (Eberhardt and Young, 1996).

Reported biological activities for IPA include activation of large-conductance calcium activated potassium channels in HEK cells (Imaizumi *et al.*, 2002). Furthermore, studies on rainbow trout revealed that it activates calcium release from intracellular stores (Rabergh *et al.*, 1999) and decreases intracellular pH of hepatocytes (Nikinmaa *et al.*, 1999). Additionally, IPA inhibits 12-*O*-tetradecanoylphorbol-13-acetate induced ornithine decarboxylase, an enzyme involved in tumorigenesis (Chang *et al.*, 2000). This diterpene also displays feeding deterrent properties against the gypsy moth (Raffa *et al.*, 2002).

MATERIALS AND METHODS

Plant material. Immature cones of *P. nigra* Arnold were collected from Great Paxton, Cambridgeshire. A voucher specimen was deposited in the herbarium at the School of Pharmacy.

Isolation of IPA. Sequential cold solvent extraction on 140 g immature cones yielded 4.2 g of an active crude hexane extract. Activity was tracked and determined by MIC assay, described below. The extract was subjected to vacuum liquid chromatography on silica gel and eluted with a step gradient with 10% increments from 100% hexane to 100% EtOAc. Biotage™ flash chromatography was performed on the active fraction 4, using a silica column and elution with a gradient in 20% increments from 100% hexane to 100% EtOAc. TLC identified similar fractions (9–12, 19–24, 27–47, 48–61, 62–79) which were then pooled. Finally, the active fraction (27–47) was further purified by preparative TLC (90:8:2 toluene:EtOAc:AcOH, two developments) which yielded a colourless crystalline solid. Abietic acid (70%) was obtained from Aldrich.

Bacterial strains. Strain XU212 which possesses the TetK tetracycline efflux pump and is also resistant to methicillin and erythromycin is a hospital isolate. XU212 and standard strain ATCC 25923 were obtained from E. Udo (Gibbons and Udo, 2000). Strain SA-1199B over-expresses the NorA MDR efflux pump and was provided by G. Kaatz (Kaatz *et al.*, 1993). RN4220 which has the MsrA macrolide efflux protein was provided by J. Cove (Ross *et al.*, 1989). The epidemic methicillin resistant strains EMRSA-15 and EMRSA-16 are hospital isolates (Richardson and Reith, 1993; Cox *et al.*, 1995) and were obtained from Paul Stapleton. All strains were cultured on nutrient agar (Oxoid) and incubated overnight at 37 °C prior to assay.

Minimum inhibitory concentration (MIC). Tetracycline, norfloxacin, erythromycin and oxacillin were obtained from Sigma Chemical Co. Oxacillin was used in place of methicillin as recommended by the NCCLS. Mueller-Hinton broth (MHB; Oxoid) was adjusted to contain 20 mg/L Ca^{2+} and 10 mg/L Mg^{2+}. NaCl (2%) was added to MHB for assays against EMRSA-15 and 16. Overnight cultures of each strain were made up in 0.9% saline to an inoculum density of 5×10^5 cfu by comparison with a MacFarland standard. Tetracycline and oxacillin were dissolved directly in MHB, whereas norfloxacin and erythromycin were dissolved in DMSO and then diluted in MHB to give a starting concentration of 512 μg/mL. Using Nunc 96-well microtitre plates, 125 μL of MHB were dispensed into wells 1–11. 125 μL of the test compound or the appropriate antibiotic were dispensed into well 1 and serially diluted across the plate leaving well 11 empty for the growth control. The final volume was dispensed into well 12, which being free of MHB or inoculum served as the sterile control. Finally, the bacterial inoculum (125 μL) was added to wells 1–11 and the plate was incubated at 37 °C for 18 h. A DMSO control (3.125%) was included. All MICs were determined in duplicate. The MIC was determined as the lowest concentration at which no growth was seen. A methanol solution (5 mg/mL) of 3-[4,5-dimethylthiazol-2-yl]-2,5-diphenyltetrazoliium bromide (MTT; Lancaster) was used to detect bacterial growth by a colour change from yellow to blue.

Modulation assays. To test for potentiation of antibiotic activity, IPA and AA were dissolved in DMSO, then diluted in MHB to give a final concentration of 10 μg/mL and 20 μg/mL, respectively. This IPA or AA containing MHB was then used in the MIC assay. For potentiation of tetracycline, norfloxacin and erythromycin activity, reserpine (Sigma) was used as a control at 20 μg/mL. For potentiation of oxacillin activity against EMRSA-15 and 16, epicatechin gallate (Sigma) was used as a control at 10 and 4 μg/mL, respectively.

To test for potentiation of IPA and AA activity, the compounds were assayed at a starting concentration of 512 μg/mL, in combination with reserpine at 20 μg/mL. This was undertaken to ascertain if the presence of an efflux pump inhibitor reduced their MICs against strains XU212 and SA-1199B. Both diterpenes were also assayed using EMRSA-15 and 16 in combination with epicatechin gallate at 10 and 4 μg/mL, respectively.

NMR spectroscopy and molecular modelling. 1D ^{1}H, 1D ^{13}C, 2D COSY, HMQC and HMBC NMR spectra were acquired on the Brüker Avance 500 MHz and spectra were processed using software package X-Win NMR 3.5. Reserpine, abietic acid and their mixture were dissolved in DMSO-d_6 and the spectra were acquired at 300K after overnight incubation at 310K. Chemical shifts were referenced to the residual DMSO methyl group signal at 2.5 ppm (^{1}H). Assignments of the ^{1}H spectra were achieved using standard assignment procedures. All NMR based calculations were carried out using Macromodel 8.1 (Schrödinger, Inc.) and Amber force field. A conformational search was performed using the GB/SA method with water as the solvent and the dielectric constant as 1 Db. Distance constraints between interacting hydrogen atoms were set to 3 Å. Resulting structures were further minimized for 1000 steps.

RESULTS AND DISCUSSION

The structure of the antibacterial compound from the hexane extract was determined by extensive 1 and 2D

Table 1. Minimum inhibitory concentrations (MICs) of isopimaric acid and abietic acid and standard antibiotics in μg/mL

Strain	IPA	AA	Tetracyline	Norfloxacin	Erythromycin	Oxacillin
XU212 (TetK)	32	64	128	16	4096	256
SA-1199B (NorA)	32	64	0.25	32	0.25	0.25
RN4220 (MsrA)	64	64	0.25	2	128	0.25
EMRSA-15	32	64	0.125	0.5	2048	32
EMRSA-16	64	64	0.125	128	4096	512
ATCC 25923	64	64	0.25	1	0.25	0.125

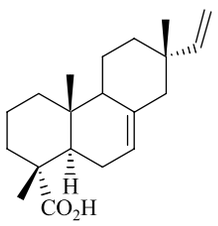

Figure 1. Isopimaric acid.

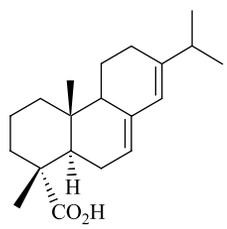

Figure 2. Abietic acid.

NMR spectroscopy and ESI mass spectrometry. Comparison of the data with the published literature (Wenkert and Buckwalter, 1972) confirmed the compound as isopimaric acid (Fig. 1).

IPA displayed activity against all of the effluxing strains (Table 1). Strain XU212 not only effluxes tetracycline but is also resistant to methicillin and erythromycin. IPA also exhibited activity against the epidemic MRSA strains. Both EMRSA strains are highly resistant to erythromycin with strain 16 also showing resistance to norfloxacin. IPA has previously been shown to be active against *S. aureus* (Hartmann *et al.*, 1981; Söderberg *et al.*, 1990) but here its activity was demonstrated against MDR and EMRSA strains for the first time.

Abietic acid (Fig. 2) was also active against all strains, although IPA had higher activity against three of the resistant strains. IPA was more active against two of the MDR strains with the TetK and NorA efflux pumps than against the standard ATCC strain. This finding has been noted in other studies (Lechner *et al.*, 2004; Tegos *et al.*, 2002) in which some isolated compounds have greater activity against MDR strains than against sensitive strains.

Isopimaric acid (10 μg/mL) and AA (20 μg/mL) were tested in combination with tetracycline, norfloxacin and erythromycin against XU212, SA-1199B and RN4220 respectively to determine whether either compound potentiated antibiotic activity against these effluxing strains. However, no reduction in MIC was seen for any of the antibiotics. The efflux pump inhibitor reserpine (20 μg/mL) was used as a positive control and caused a four-fold reduction in the MIC of tetracycline against XU212 and an eight-fold reduction in MIC for norfloxacin against SA-1199B, as seen previously (Gibbons *et al.*, 2003). Reserpine is not an inhibitor of the MsrA pump and did not reduce the MIC of erythromycin against RN4220.

The two diterpene acids were also tested for potentiation of oxacillin activity against EMRSA-15 and 16. Epicatechin gallate which potentiates the activity of oxacillin against both strains was used as a control. Again, neither IPA nor AA had any modulating activity.

IPA and AA were tested in combination with reserpine (20 μg/mL) against strains XU212 and SA-1199B, to determine whether inhibition of the efflux pumps present in these strains resulted in a reduction in MIC for these compounds.

Interestingly, the MICs for both IPA and AA increased in the presence of reserpine (Table 2). It was expected that the MICs would either decrease due to inhibition of the efflux pump, or, alternatively remain the same in the presence or absence of reserpine. Since the presence of an efflux pump inhibitor did not reduce the MICs, it is possible that neither compound is a substrate for the TetK or NorA efflux pump. However, the increase in MIC may be indicative of some interaction between the diterpene acids and reserpine, possibly causing antagonism. The effect was most pronounced against XU212. When in combination with reserpine, a four-fold increase in MIC for both compounds was seen.

IPA was tested against EMRSA-15 and AA against both EMRSA strains in combination with epicatechin

Table 2. MICs (μg/mL) for IPA and AA in the presence and absence of reserpine

Bacterium	IPA	AA	Tetracycline	Norfloxacin
XU212	32 (**128**)	64 (**256**)	128 (**32**)	–
SA1199B	32 (**64**)	64 (**128–256**)	–	32 (**4**)

Figures in bold denote MICs in the presence of reserpine.

Table 3. Reserpine and AA ^{1}H resonances which showed a change in chemical shift after mixing and overnight incubation

Reserpine	Reserpine + AA	Change in shift (ppm)	Hz	H
1.949	1.958	0.009	3.6	4a
2.847	2.856	0.009	3.6	6
2.876	2.883	0.007	2.8	5
3.011	3.024	0.013	5.2	7
4.342	4.361	0.019	7.6	13b
10.539	10.551	0.012	4.8	13
Abietic acid				
0.746	0.742	–0.004	–1.6	20
5.712	5.708	–0.004	–1.6	14

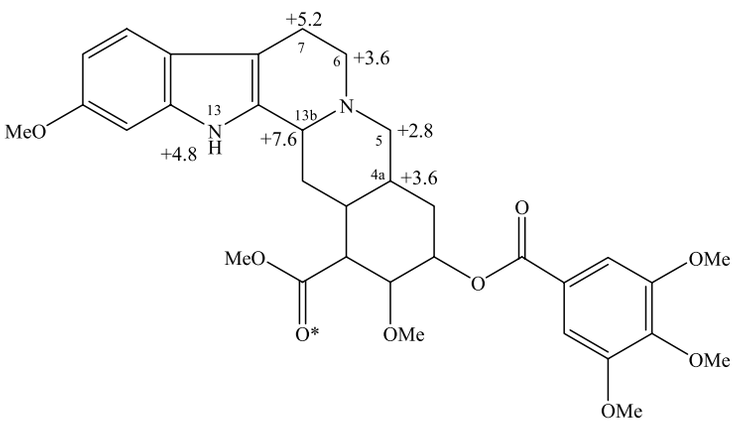

Figure 3. Structure of reserpine showing changes in chemical shifts in Hz (*depicts the oxygen atom involved in the proposed hydrogen bond formed between reserpine and abietic acid).

gallate to see if it potentiated their activity. However, the MICs were the same in both the presence and absence of epicatechin gallate. Therefore, unlike reserpine, there was no sign of a potential modulator having a negative effect.

It is possible that IPA and AA may form a complex with reserpine which affects the bio-availability of the compounds resulting in a reduction in activity shown by the increase in MIC. A study using molecular modelling (Zloh *et al.*, 2004) has suggested that MDR inhibitors may have affinity for the substrates of efflux pumps, possibly forming complexes with them. It is suggested that binding of an inhibitor to the pump substrate may facilitate its entry into the cell, after which the complex dissociates and the drug can exert its effect. It is possible that in some cases the inhibitor may bind the substrate too tightly, leading to a lack of or a very slow rate of dissociation which would lower the concentration of free drug and hence lower antibacterial activity.

^{1}H-NMR spectroscopy was undertaken to look for a potential interaction between AA and reserpine. AA and reserpine were incubated separately and in combination (1:1 molar ratio) in DMSO and left overnight in deuterated DMSO at 37 °C. ^{1}H-NMR spectra of the samples revealed a shift in resonance of some of the peaks for both compounds (Table 3, Fig. 3), although due to heavy overlap in the alkyl region of the mixture spectra some chemical shift changes could not be assigned. Changes of chemical shifts indicate that the environment of the affected hydrogen atoms has changed, most likely due to an interaction between molecules. Thus, the complex formation is possible where hydrogen atoms of abietic acid listed in Table 3 are in close proximity to reserpine hydrogen atoms (Table 3). These experimental results were used as a guide in molecular modelling of a reserpine–abietic acid complex (Fig. 4), showing the interaction between C and D rings of reserpine and abietic acid. The striking feature of the model is the

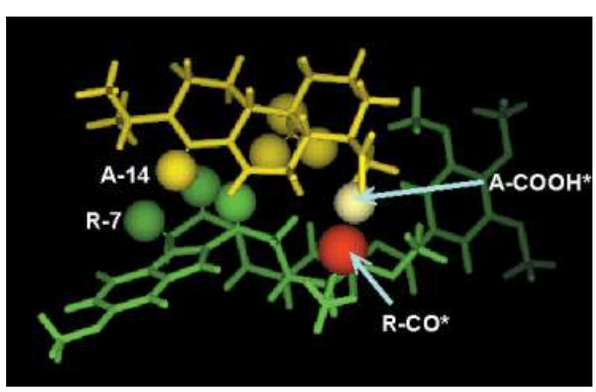

Figure 4. Molecular model of lowest energy reserpine (R) – abietic acid (A) complex. The interacting atoms were detected by changes in ^{1}H chemical shifts and are represented as a CPK model. *depicts the atoms involved in the proposed hydrogen bond formed between reserpine and abietic acid.

prediction of a hydrogen bond between the carboxylic acid of abietic acid and carbonyl group of reserpine (depicted with * in Fig. 3), that could be responsible for interaction between two molecules, consequently leading to a decrease in antimicrobial activity.

Isopimaric acid showed activity against two epidemic MRSA strains and three effluxing strains, one of which is also an MRSA strain. Studies on pimaranes from *Calceolaria pinifolia* have revealed activity as low as 2 μg/mL toward MRSA strains (Woldemichael *et al.*, 2003). IPA has a carboxyl group at C-19, however, their findings suggested that a C-19 oxymethylene group in pimaranes may contribute towards higher antibacterial activity rather than a carboxylic group in the same position.

Although IPA did not display any resistance modifying activity, other isopimaranes have been shown to moderately potentiate the activity of tetracycline and erythromycin against XU212 and RN4220, respectively, causing a two-fold reduction in MIC for these antibiotics (Gibbons *et al.*, 2003). These findings suggest that pimaranes and isopimaranes are worthy of further investigation in the search for new antibacterials and modulators of antibiotic activity.

Acknowledgements

Stiefel International R & D Ltd is thanked for the award of a studentship to E. Smith. We also thank the Engineering and Physical Sciences Research Council for funding (Grant No. GR/R47646/01).

REFERENCES

Chang LC, Song LL, Park EJ *et al.* 2000. Bioactive constituents of *Thuja occidentalis*. *J Nat Prod* **63**: 1235–1238.

Cox RA, Conquest C, Mallaghan C, Marples RR. 1995. A major outbreak of methicillin-resistant *Staphylococcus aureus* caused by a new phage-type (EMRSA-16). *J Hosp Infect* **29**: 87–106.

Department of Health. http://www.dh.gov.uk/PublicationsAndStatistics/Publications/PublicationsStatistics/PublicationsStatisticsArticle/fs/en?CONTENT_ID=4085951&chk=HBt2QD

Eberhardt TL, Young RA. 1996. Assessment of the anti-HIV activity of a pine cone isolate. *Planta Med* **62**: 63–65.

Gibbons S, Oluwatuyi M, Veitch NC, Gray AI. 2003. Bacterial resistance modifying agents from *Lycopus europaeus*. *Phytochemistry* **62**: 83–87.

Gibbons S, Udo EE. 2000. The effect of reserpine, a modulator of multidrug efflux pumps, on the *in vitro* activity of tetracycline against clinical isolates of methicillin resistant *Staphylococcus aureus* (MRSA) possessing the *tet*(K) determinant. *Phytother Res* **14**: 139–140.

Hartmann E, Renz B, Jung JA. 1981. Antimicrobial compounds in higher plants. Isolation, identification and antimicrobial activity of two resin acids from spruce bark. *J Phytopathol* **101**: 31–42.

Imaizumi Y, Sakamoto K, Yamada A *et al.* 2002. Molecular basis of pimarane compounds as novel activators of large-conductance Ca^{2+}-activated K^+ channel alpha-subunit. *Mol Pharmacol* **62**: 836–846.

Johnson AP, Aucken HM, Cavendish S *et al.* 2001. Dominance of EMRSA-15 and -16 among MRSA causing nosocomial bacteraemia in the UK: analysis of isolates from the European Antimicrobial Resistance Surveillance System (EARSS). *J Antimicrob Chemother* **48**: 143–144.

Kaatz GW, Seo SM, Ruble CA. 1993. Efflux-mediated fluoroquinolone resistance in *Staphylococcus aureus*. *Antimicrob Agents Chemother* **37**: 1086–1094.

Lechner D, Stavri M, Oluwatuyi M, Pereda-Miranda R, Gibbons S. 2004. The anti-staphylococcal activity of *Angelica dahurica* (Bai Zhi). *Phytochemistry* **65**: 331–335.

Leung AY, Foster S. 1996. *Encyclopaedia of Common Natural Ingredients Used in Food, Drugs and Cosmetics,* 2nd edn. John Wiley: New York; 502–503.

Marshall NJ, Piddock LJV. 1997. Antibacterial efflux systems. *Microbiologia* **13**: 285–300.

NCCLS – National Committee for Clinical Laboratory Standards 1998. M100-S8 *Performance Standards for Antimicrobial Susceptibility Testing*. Vol. 18 No. 1.

Nikinmaa M, Wickstrom C, Lilius H, Isomaa B, Rabergh C. 1999. Effects of resin acids on hepatocyte pH in rainbow trout *(Oncorhynchus mykiss)*. *Environ Toxicol Chem* **18**: 993–997.

Poole K. 2004. Resistance to β-lactam antibiotics. *Cell Mol Life Sci* **61**: 2200–2223.

Rabergh CM, Lilius H, Eriksson JE, Isomaa B. 1999. The resin acids dehydroabietic acid and isopimaric acid release calcium from intracellular stores in rainbow trout hepatocytes. *Aquat Toxicol* **46**: 55–65.

Raffa KF, Havill NP, Nordheim EV. 2002. How many choices can your test animal compare effectively? Evaluating a critical assumption of behavioural preference tests. *Oecologia* **133**: 422–429.

Richardson JF, Reith S. 1993. Characterization of a strain of methicillin-resistant *Staphylococcus aureus* (EMRSA-15) by conventional and molecular methods. *J Hosp Infect* **25**: 45–52.

Ross JI, Farrell AM, Eady EA, Cove JH, Cunliffe WJ. 1989. Characterisation and molecular cloning of the novel macrolide streptogramin B resistance determinant from *Staphylococcus epidermidis*. *J Antimicrob Chemother* **24**: 851–862.

Söderberg TA, Gref R, Holm S, Elmros T, Hallmans G. 1990. Antibacterial activity of rosin and resin acids *in vitro*. *Scand J Plast Reconstr Hand Surg* **24**: 199–205.

Tegos G, Stermitz FR, Lomovskaya O, Lewis K. 2002. Multi-drug pump inhibitors uncover remarkable activity of plant antimicrobials. *Antimicrob Agents Chemother* **46**: 3133–3141.

Wenkert E, Buckwalter BL. 1972. Carbon-13 nuclear magnetic resonance spectroscopy of naturally occurring substances. X. pimaradienes. *J Am Chem Soc* **94**: 4367–4369.

Woldemichael GM, Wächter G, Singh MP, Maiese WM, Timmermann BN. 2003. Antibacterial diterpenes from *Calceolaris pinifolia*. *J Nat Prod* **66**: 242–246.

Zloh M, Kaatz GW, Gibbons S. 2004. Inhibitors of multidrug resistance (MDR) have affinity for MDR substrates. *Bioorg Med Chem Lett* **14**: 881–885.

Available online at www.sciencedirect.com
SCIENCE DIRECT®
Phytochemistry 66 (2005) 1472–1475
PHYTOCHEMISTRY
www.elsevier.com/locate/phytochem

An anti-staphylococcal acylphloroglucinol from *Hypericum foliosum*

Simon Gibbons [a,*], Elisabeth Moser [a], Sebastian Hausmann [a], Michael Stavri [a], Eileen Smith [a], Christopher Clennett [b]

[a] *Centre for Pharmacognosy and Phytotherapy, The School of Pharmacy, University of London, 29-39 Brunswick Square, London WC1N 1AX, UK*
[b] *Royal Botanic Gardens, Wakehurst Place, Ardingly, Nr Haywards Heath, West Sussex RH17 6TN, UK*

Received 10 February 2005; received in revised form 5 April 2005
Available online 25 May 2005

Abstract

An investigation into the antibacterial properties of *Hypericum foliosum* Aiton. (Guttiferae) has led to the isolation of a new bioactive acylphloroglucinol natural product which by NMR spectroscopy and mass spectrometry was characterised as 1,3,5-trihydroxy-6-[2‴,3‴-epoxy-3‴-methyl-butyl]-2-[2″-methyl-butanoyl]-4-[3′-methyl-2″-butenyl]-benzene and is described here for the first time. This metabolite was evaluated against a panel of multidrug-resistant strains of *Staphylococcus aureus* and minimum inhibitory values ranged from 16 to 32 μg/ml.

Keywords: *Hypericum foliosum*; Acylphloroglucinol; Guttiferae; Antibacterial; MRSA; MDR; *Staphylococcus aureus*

1. Introduction

The genus *Hypericum* is a rich source of antibacterial metabolites of which hyperforin from *Hypericum perforatum* (St. John's Wort) is an exceptional example. Minimum inhibitory concentration (MIC) values for this natural product range from 0.1 to 1 μg/ml against penicillin-resistant *Staphylococcus aureus* (PRSA) and methicillin-resistant *S. aureus* (MRSA) strains (Schempp et al., 1999; Reichling et al., 2001). These results substantiate the use of St. John's Wort in several countries as a treatment for superficial burns and wounds that heal poorly (Reichling et al., 2001). Additionally, the possible use of this agent as an antibiotic is supported by the observation that no in vitro resistance has been observed at low concentrations and that even in strains with reduced susceptibility, no cross resistance with clinically used antibiotics could be detected (Hübner, 2003). Given the considerable need to find novel anti-staphylococcal compounds and the fact that surprisingly at present there are no single chemical entity plant-derived antibacterials used clinically, a molecule with hyperforin's activity may well become a development candidate.

Hyperforin is a member of the acylphloroglucinol group of natural products which are prolific within the Guttiferae family, although only a small number of species of *Hypericum* have been investigated for the antibacterial properties of these metabolites (Winkelmann et al., 2000, 2001; Gibbons, 2004). These natural products are based on an aromatic ring that in many cases has been reduced or has a keto-enol form. Many of these products are prenylated and/or farnesylated and possess simple acyl groups such as 2-methylpropanoyl which is found in hyperforin.

Our antibacterial studies on the *Hypericum* group started with an evaluation of 34 species and varieties collected from the national *Hypericum* collection at the Royal Botanic Gardens at Wakehurst Place, UK (Gibbons et al., 2002). This preliminary study revealed the potential of *Hypericum* metabolites as antibacterials

* Corresponding author. Tel.: +44 207 753 5913; fax: +44 207 753 5909.
E-mail address: simon.gibbons@ulsop.ac.uk (S. Gibbons).

0031-9422/$ - see front matter © 2005 Elsevier Ltd. All rights reserved.
doi:10.1016/j.phytochem.2005.04.024

and prompted us to make several large scale collections, one of which was *Hypericum foliosum* Aiton, a species which is classified under section *Androsaemum* and is endemic to the Azores (Robson, 1977). There is little phytochemical data on this species although the essential oil has been characterised (Santos et al., 1999). This paper details the isolation and characterisation of the main anti-staphylococcal constituent of this species.

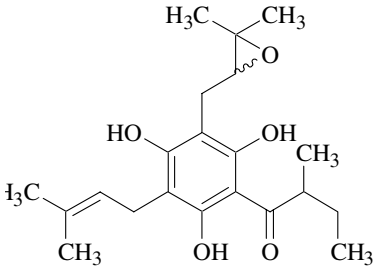

(**1**)

2. Results and discussion

Antibacterial activity was concentrated in the hexane extract of the aerial parts of *H. foliosum* and the MIC was 64 μg/ml, against *S. aureus* SA-1199B. This strain possesses the NorA multidrug efflux transporter which is the major characterised drug efflux pump in *S. aureus* and confers resistance to certain fluoroquinolones and quaternary ammonium antiseptics (Marshall and Piddock, 1997). Preparative HPLC of vacuum liquid chromatography fraction 4 (eluted with 30% EtOAc in hexane), the most active fraction (MIC = 32 μg/ml), led to the isolation of compound **1** as a yellow oil.

HRCI-MS of **1** suggested a molecular formula of $C_{21}H_{30}O_5$ $[M]^+$ (362.2079). The ^1H NMR spectrum (Table 1) provided signals for two highly deshielded hydrogen bonded hydroxyl groups (δ_H 14.26, 14.25) and an additional broad signal at δ_H 6.31 attributable to a proton of another hydroxyl group. Further signals for an olefin (δ_H 5.28 t, 1H), two methine protons (δ_H 3.81, 3.74), three methylene groups, four methyl singlets, one methyl doublet and one methyl triplet completed the ^1H resonances for **1** . The olefinic triplet was reminiscent of an olefinic proton of a prenyl (dimethyl allyl) substituent (Nayar and Bhan, 1972) and this was supported by HMBC correlations between the protons of two methyl groups (δ_H 1.84, 1.79) and the carbon associated with this olefin. The olefinic resonance also coupled to the protons of one of the methylene groups (δ_H 3.40 d, J = 7.2 Hz) further confirming the presence of a prenyl moiety. In the HMBC spectrum, the protons of this methylene coupled to three aromatic carbons, one to which it was directly attached (δ_C 105.6) and to two oxygen-bearing quaternary carbons. Hydroxyl groups were attached to these carbon atoms and key correlations were seen by the protons of these groups to carbons in the aromatic ring (Fig. 1). The carbon spectrum was indicative of a 1,3,5-trihydroxylated benzene with six quaternary carbons, three of which were deshielded due to the presence of hydroxyl substituents (Table 1). This was supported by the presence of two hydrogen-bonded and one non-hydrogen bonded OH groups in the ^1H spectrum. With the prenyl group attached at C-4 of this substituted benzene and the lack of aromatic protons, positions 2 and 6 of the aromatic nucleus must be substituted with further moieties. This was proved by inspection of the HMBC spectrum which showed correlations between the protons of a methylene group (δ_H 2.86, 2.61) and an aromatic quaternary carbon (C-6). In the COSY spectrum, these methylene protons cou-

Table 1
^1H (500 MHz) and ^{13}C NMR (125 MHz) spectral data and ^1H–^{13}C long-range correlations of **1** recorded in $CDCl_3$

Position	^1H	^{13}C	^2J	^3J
1	–	153.9		
2	–	*105.6		
3	–	163.0		
4	–	*105.7		
5	–	160.0		
6	–	97.8		
1′	3.40 *d* (7.2)	21.9	C-2′, C-4	C-3, C-5, C-3′
2′	5.28 *t* (7.2)	122.1		
3′	–	136.5		
4′	1.79 *s*	26.1	C-3′	C-2′, C-5′
5′	1.84 *s*	18.1	C-3′	C-2′, C-4′
1″	–	210.7		
2″	3.74 *m*	46.4		
3″	1.43 *m*, 1.85 *m*	27.1		
4″	0.91 *t* (7.6)	12.1	C-3″	C-2″
5″	1.17 *d* (6.6)	17.0	C-2″	C-1″, C-3″
1‴	2.61 *dd* (16.7, 5.4)	26.2	C-6	
	2.86 *dd* (16.7, 5.0)			
2‴	3.81 *bs*	68.9		
3‴	–	78.3		
4‴	1.39 *s*	24.9	C-3‴	C-2‴, C-5‴
5‴	1.42 *s*	22.1	C-3‴	C-2‴, C-4‴
1/3 - OH	*14.26 / *14.25	–		C-2/C-4
5 - OH	6.31 *bs*	–	C-5	C-4, C-6

Resonances denoted * may be interchangeable.

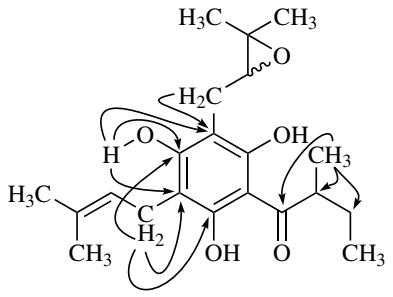

Fig. 1. Key HMBC correlations for compound **1**.

pled to a broad singlet of an oxymethine group with resonances attributable to an epoxide moiety (Asakawa et al., 1991). Two methyl singlets exhibited ^{3}J correlations to the carbon associated with this oxymethine and a ^{2}J correlation to an additional oxygen bearing portion of the epoxide to which the methyl groups were directly attached. This revealed the second substituent to be an epoxidised prenyl group and resonances for this portion are in close agreement to those found in the literature for epoxyprenyl groups which are directly attached to an aromatic ring and *ortho* to an hydroxyl (Asakawa et al., 1991).

Resonances for the final substituent included a methyl triplet which was coupled to a methylene group in the COSY spectrum. This methylene moiety further coupled to a methine proton which was coupled to by a methyl doublet. This methyl doublet exhibited correlations in the HMBC spectrum to the methine (^{2}J), methylene (^{3}J) and a ketonic carbon (^{3}J). These resonances completed the final substituent and identified it as a 2-methylbutanoyl moiety which is a side chain found in acylphloroglucinol natural products from *Hypericum papuanum* (Winkelmann et al., 2000). The point of attachment of this 2-methylbutanoyl moiety must be at C-2 of the aromatic ring allowing hydrogen-bonded deshielding of the hydroxyl groups at C-1 and C-3 via interaction with the carbonyl of the 2-methylbutanoyl group. Compound **1** is therefore assigned as the new acylphloroglucinol 1,3,5-trihydroxy-6-[2‴,3‴-epoxy-3‴-methyl-butyl]-2-[2″-methylbutanoyl]-4-[3′-methyl-2″-butenyl]-benzene and is described here for the first time. Acylphloroglucinols that are structurally related to **1** include adhumulone which possesses a central 1,3,5-trioxygenated ring system, two prenyl and one 2-methylbutanoyl substituents (Hermans-Lokkerbol and Verpoorte, 1994). Being the major component of the active fraction, compound **1** was tested for its ability to inhibit the growth of three effluxing strains and one standard strain of *S. aureus* and minimum inhibitory concentrations are given in Table 2.

Compound **1** was slightly more active against strains which possess efflux mechanisms of resistance (MIC = 16 μg/ml) when compared to a standard *S. aureus* ATCC 25923. XU212, in addition to possessing the TetK efflux transporter which confers resistance to tetracycline, is also a methicillin-resistant *S. aureus* (MRSA). SA-1199B possesses the NorA MDR efflux transporter which is resistant to certain fluoroquinolones and antiseptics and **1** was marginally more active than the fluoroquinolone norfloxacin. In the UK, the number of citations in death certificates that mention MRSA has dramatically risen during the 1990s and is a major clinical burden (Crowcroft and Catchpole, 2002). Given the dearth of novel classes of anti-staphylococcal agents, the occurrence of vancomycin resistance in MRSA (Appelbaum and Bozdogan, 2004) and the appearance of resistance to linezolid (Tsiodras et al., 2001), one of the newest anti-MRSA agents, further investigation of the acylphloroglucinol class as anti-staphylococcal leads is appropriate.

3. Experimental

3.1. General experimental procedures

NMR spectra were recorded on a Bruker AVANCE 500 MHz spectrometer. Chemical shift values (δ) were reported in parts per million (ppm) relative to appropriate internal solvent standard and coupling constants (J values) are given in Hertz. Mass spectra were recorded on a Finnigan MAT 95 high resolution, double focusing, magnetic sector mass spectrometer. Accurate mass measurement was achieved using voltage scanning of the accelerating voltage. This was nominally 5 kV and an internal reference of heptacosa was used. Resolution was set between 5000 and 10,000.

IR spectra were recorded on a Nicolet 360 FT-IR spectrophotometer and UV spectra on a Thermo Electron Corporation Helios spectrophotometer.

3.2. Plant material

H. foliosum was collected from the Royal Botanic Garden at Wakehurst Place in Surrey in May 2003, which forms part of the National *Hypericum* Collection (Accession No. 1984-5158). A voucher specimen has been deposited at the Centre for Pharmacognosy and Phytotherapy.

3.3. Extraction and isolation

Four hundred and fifty one grams of air-dried and powdered aerial parts were extracted in a Soxhlet apparatus using sequential extraction by hexane (3 l),

Table 2
MICs of **1** and standard antibiotics in μg/ml

Strain (resistance mechanism)	1	Norfloxacin	Erythromycin	Tetracycline
ATCC 25923	32	2	0.25	0.25
SA-1199B (NorA)	16	32	0.25	0.25
RN4220 (MsrA)	16	2	128	0.25
XU212 (TetK, *mecA*)	16	16	>256	128

All MICs were determined in duplicate.

chloroform (3 l) and finally methanol (3 l). The hexane extract (10.52 g) was subjected to vacuum liquid chromatography (VLC) on silica gel (15 g) eluting with hexane containing 10% increments of ethyl acetate to yield 12 fractions. The fraction eluted with 30% ethyl acetate was further purified by multiple preparative reverse-phase HPLC (four times on two coupled 40×100 mm 6 μm Nova-Pak HR C_{18} columns) using a gradient system from 100% water to 100% acetonitrile both containing 0.1% AcOH. This was performed by holding at 100% water for 2 min and linearly increasing to 100% acetonitrile at 15 min and maintaining this composition until 20 min. The flow rate was 50 ml/min and compound **1** (56.6 mg) had a retention time of 14.6 min.

3.4. Antibacterial assay

S. aureus strain ATCC 25923 was the generous gift of E. Udo (Kuwait University, Kuwait). *S. aureus* RN4220 containing plasmid pUL5054, which carries the gene encoding the MsrA macrolide efflux protein, was provided by J. Cove (Ross et al., 1989). Strain XU212, which possesses the TetK tetracycline efflux protein, was provided by E. Udo (Gibbons and Udo, 2000). SA-1199B, which overexpresses the *norA* gene encoding the NorA MDR efflux protein was provided by G. Kaatz (Kaatz et al., 1993). All *S. aureus* strains were cultured on nutrient agar and incubated for 24 h at 37 °C prior to MIC determination. Bacterial inocula equivalent to the 0.5 McFarland turbidity standard were prepared in normal saline and diluted to give a final inoculum density of 5×10^5 cfu/ml. The inoculum (125 μl) was added to all wells and the microtitre plate was incubated at 37 °C for 18 h. The MIC was recorded as the lowest concentration at which no bacterial growth was observed as previously described (Gibbons and Udo, 2000).

3.5. 1,3,5-Trihydroxy-6-[2‴,3‴-epoxy-3‴-methyl-butyl]-2-[2″-methyl-butanoyl]-4-[3′-methyl-2′-butenyl]-benzene (*1*)

Pale yellow oil; $[\alpha]_D^{21}$ $+80^\circ$ (*c* 0.075, $CHCl_3$); UV ($CHCl_3$) λ_{max} (log ε): 241 (3.47), 279 (3.50) nm; IR ν_{max} (thin film) cm^{-1}: 3852, 3170, 2974, 2924, 1716, 1635, 1540, 1123, 1050; ^1H NMR and ^{13}C NMR ($CDCl_3$): see Table 1; HRCI-MS (*m/z*): 362.2079 $[M]^+$ (calc. for $C_{21}H_{30}O_5$, 362.2093).

Acknowledgements

We thank the Engineering and Physical Sciences Research Council (Grant No. GR/R47646/01) and the Royal Society (RSRG 24268) for funding.

References

Appelbaum, P.C., Bozdogan, B., 2004. Vancomycin resistance in *Staphylococcus aureus*. Clinics in Laboratory Medicine 24, 381–402.

Asakawa, Y., Kondo, K., Takikawa, N.K., Tori, M., Hashimoto, T., Ogawa, S., 1991. Prenyl bibenzyls from the liverwort *Radula kojana*. Phytochemistry 30, 219–234.

Crowcroft, N.S., Catchpole, M., 2002. Mortality from methicillin-resistant *Staphylococcus aureus* in England and Wales: analysis of death certificates. British Medical Journal 325, 1390–1391.

Gibbons, S., Udo, E.E., 2000. The effect of reserpine, a modulator of multidrug efflux pumps, on the in vitro activity of tetracycline against clinical isolates of methicillin resistant *Staphylococcus aureus* (MRSA) possessing the tet(K) determinant. Phytotherapy Research 14, 139–140.

Gibbons, S., Ohlendorf, B., Johnsen, I., 2002. The genus *Hypericum* – a valuable resourceof anti-Staphylococcal leads. Fitoterapia 73, 300–304.

Gibbons, S., 2004. Anti-staphylococcal plant natural products. Natural Product Reports 21, 263–277.

Hermans-Lokkerbol, A.C.J., Verpoorte, R., 1994. Preparative separation and isolation of three α bitter acids from hop, *Humulus lupulus* L., by centrifugal partition chromatography. Journal of Chromatography A 664, 45–53.

Hübner, A.T., 2003. Treatment with *Hypericum perforatum* L. does not trigger decreased resistance in *Staphylococcus aureus* against antibiotics and Hyperforin. Phytomedicine 10, 206–208.

Kaatz, G.W., Seo, S.M., Ruble, C.A., 1993. Efflux-mediated fluoroquinolone resistance in *Staphylococcus aureus*. Antimicrobial Agents and Chemotherapy 37, 1086–1094.

Marshall, N.J., Piddock, L.J.V., 1997. Antibacterial efflux systems. Microbiologia 13, 285–300.

Nayar, M.N.S., Bhan, M.K., 1972. Coumarins and other constituents of *Hesperethusa crenulata*. Phytochemistry 11, 3331–3333.

Reichling, J., Weseler, A., Saller, R., 2001. A current review of the antimicrobial activity of *Hypericum perforatum* L. Pharmacopsychiatry 34 (Suppl. 1), S116–S118.

Robson, N.K.B., 1977. Studies in the genus *Hypericum* L. (Guttiferae) I. Infrageneric classification. Bulletin of the British Museum (Natural History) Botany 5, 118–119.

Ross, J.I., Farrell, A.M., Eady, E.A., Cove, J.H., Cunliffe, W.J., 1989. Characterisation and molecular cloning of the novel macrolide-streptogramin B resistance determinant from *Staphylococcus epidermidis*. Journal of Antimicrobial Chemotherapy 24, 851–862.

Santos, P.A.G., Figueiredo, A.C., Barroso, J.G., Pedro, L.G., Scheffer, J.J.C., 1999. Composition of the essential oil of *Hypericum foliosum* Aiton from five Azorean Islands. Flavour and Fragrance Journal 14, 283–286.

Schempp, C.M., Pelz, K., Wittmer, A., Schopf, E., Simon, J.C., 1999. Antibacterial activity of hyperforin from St. John's Wort, against multiresistant *Staphylococcus aureus* and Gram-positive bacteria. Lancet 353, 2129.

Tsiodras, S., Gold, H.S., Sakoulas, G., Eliopoulos, G.M., Wennersten, C., Venkataraman, L., Moellering, R.C., Ferraro, M.J., 2001. Linezolid resistance in a clinical isolate of *Staphylococcus aureus*. Lancet 358, 207–208.

Winkelmann, K., Heilmann, J., Zerbe, O., Rali, T., Sticher, O., 2000. New phloroglucinol derivatives from *Hypericum papuanum*. Journal of Natural Products 63, 104–108.

Winkelmann, K., Heilmann, J., Zerbe, O., Rali, T., Sticher, O., 2001. New prenylated bi- and tricyclic phloroglucinol derivatives from *Hypericum papuanum*. Journal of Natural Products 64, 701–706.

Available online at www.sciencedirect.com
SCIENCE DIRECT®
Phytochemistry 66 (2005) 2309–2315
PHYTOCHEMISTRY
www.elsevier.com/locate/phytochem

Sesquiterpenes from *Warburgia ugandensis* and their antimycobacterial activity

Abraham Abebe Wube [a], Franz Bucar [a,*], Simon Gibbons [b], Kaleab Asres [c]

[a] *Department of Pharmacognosy, Institute of Pharmaceutical Sciences, Karl-Franzens University Graz, Universitaetsplatz 4/1, A-8010 Graz, Austria*
[b] *Centre for Pharmacognosy and Phytotherapy, The School of Pharmacy, University of London, 29-39 Brunswick Square, London WC1N 1AX, UK*
[c] *Department of Pharmacognosy, The School of Pharmacy, Addis Ababa University, P.O. Box 1176, Addis Ababa, Ethiopia*

Received 3 May 2005; received in revised form 22 July 2005
Available online 8 September 2005

Abstract

The dichloromethane extract of the stem bark of *Warburgia ugandensis* afforded three new coloratane sesquiterpenes, namely: 6α,9α-dihydroxy-4(13),7-coloratadien-11,12-dial (**1**), 4(13),7-coloratadien-12,11-olide (**2**), and 7β-hydroxy-4(13),8-coloratadien-11,12-olide (**3**), together with nine known sesquiterpenes, i.e., cinnamolide-3β-acetate (**4**), muzigadial (**5**), muzigadiolide (**6**), 11α-hydroxymuzigadiolide (**7**), cinnamolide (**8**), 7α-hydroxy-8-drimen-11,12-olide (**9**), ugandensolide (**10**), mukaadial (**11**), ugandensidial (**12**), and linoleic acid (**13**). Their structures were assigned on the basis of 1D and 2D-NMR spectroscopic and GC-MS analysis.

The compounds were examined for their antimycobacterial activity against *Mycobacterium aurum*, *M. fortuitum*, *M. phlei* and *M. smegmatis*; and the active constituents showed MIC values ranged from 4 to128 μg/ml compared to the antibiotic drugs ethambutol (MIC ranged from 0.5 to 8 μg/ml) and isoniazid (MIC ranged from 1 to 4 μg/ml).

Keywords: *Warburgia ugandensis*; Canellaceae; Antimycobacterial activity; Drimane sesquiterpenes; Coloratane sesquiterpenes; 6α,9α-Dihydroxy-4(13),7-coloratadien-11,12-dial; 4(13),7-Coloratadien-12,11-olide; 7β-Hydroxy-4(13),8-coloratadien-11,12-olide

1. Introduction

Warburgia ugandensis Sprague (Canellaceae), which is commonly known as *zogdom* in Amharic, is characterized by its bitter and peppery taste. The stem bark has been widely used in East African ethnomedicine for the treatment of stomach-ache, constipation, toothache, cough, fever, muscle pains, weak joints and general body pains (Kokwaro, 1976; Watt and Breyer-Brandwijk, 1962). The Shinasha people in Ethiopia use the stem bark for the treatment of tuberculosis. Species of the genus *Warburgia* are known to be rich in sesquiterpenes of the drimane and coloratane skeletones (Kioy et al., 1990; Mashimbye et al., 1999), which have been shown to possess insect antifeedant, antimicrobial, antiulcer, molluscicidal (Kubo et al., 1983) and antifungal properties (Kubo and Taniguchi, 1988). Previous phytochemical investigation of *W. ugandensis* showed the presence of muzigadial, ugandensidal, pereniporin B, polygodial, mukaadial, warburganal, cinnamolide and 11α-hydroxymuzigadiolide in the stem bark; and ugandensolide, ugandensidial, warburgin and warburgiadione in the heart wood (Brooks and Draffan, 1969).

The drimanes, a group of sesquiterpenoides isolated from species of the genus *Warburgia*, are characterized by α,β-unsaturated carbonyl chromophores assembled around a *trans*-decalin ring system. As part of our search for antimycobacterial agents from Ethiopian medicinal plants, we identified three new and nine known sesquiterpenes along with a known unsaturated

* Corresponding author. Tel.: +43 316 380 5531; fax: +43 316 380 9860.
E-mail address: franz.bucar@uni-graz.at (F. Bucar).

0031-9422/$ - see front matter © 2005 Elsevier Ltd. All rights reserved.
doi:10.1016/j.phytochem.2005.07.018

fatty acid from the stem bark of *W. ugandensis* and evaluated their antimycobacterial activity against four rapidly growing species of mycobacteria.

There are several reports on the constituents of this plant, but no report has been found on their antimycobacterial activity.

2. Results and discussion

Compound **1** was obtained as colourless needles in *n*-hexane/CH_2Cl_2 (see Fig. 1). A molecular formula $C_{15}H_{20}O_4$ was determined by HRMS (*m/z*; measured 287.1264 $[M + Na]^+$; calc. 287.1259). In addition, a prominent peak at *m/z* 235 $[M - CHO]^+$ was present in the EI-MS spectrum, corresponding to a molecular formula $C_{15}H_{20}O_4$, which is in agreement with 15 carbon signals observed in the ^{13}C NMR spectrum. A broad band absorption at 3406 cm^{-1} in the IR spectrum suggested the presence of hydroxyl groups. In addition, the IR spectrum showed carbonyl absorptions at 1725, 1683 cm^{-1} and an olefinic absorption at 1640 cm^{-1}. An absorption maximum at 234 nm in the UV spectrum was also indicative of an α,β-unsaturated lactone. The ^1H NMR spectrum (Table 1) of **1** showed characteristic signals of a coloratadiene sesquiterpene ring system (Ying et al., 1995) with signals at δ 5.03 and 5.13 attributable to two exocyclic methylene protons, as well as a one proton doublet at δ 7.10 for H-7. A singlet at δ 0.96 and a doublet at 1.11 for two methyl groups were also observed in the ^1H NMR spectrum. The signals for H-13a and H-13b protons were unambiguously assigned based on NOE correlations observed between CH_3-14 and H-13a and between H-6β and H-13b in the NOESY spectrum. The signals at δ 9.50 and 9.65 were attributed to two aldehyde groups which were further confirmed by the carbonyl signals at δ 192.6 and

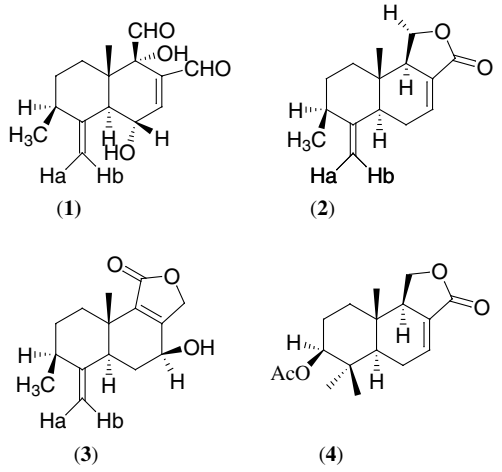

Fig. 1. The structure of compounds **1**–**4** isolated from *W. ugandensis* stem barks.

Table 1
^1H NMR spectral data for compounds **1**–**3**[a] (500 Hz, $CDCl_3$)

Proton	1	2	3
1α	1.02 (*dt*) (13.5, 4.0)	1.54 (*dt*) (13.5, 4.0)	1.47 (*dt*) (13.5, 4.0)
1β	2.05 (*m*)	1.65 (*td*) (13.5, 3.0)	2.58 (*m*)
2α	1.12 (*m*)	1.25 (*m*)	1.33 (*m*)
2β	1.73 (*m*)	1.70 (*td*) (13.0, 3.0)	1.80 (*m*)
3	2.00 (*m*)	2.05 (*m*)	2.11 (*m*)
5	2.65 (*d*) (10.0)	2.18 (*m*)	2.38 (*bd*) (13.0)
6α		2.35 (*m*)	1.92 (*m*)
6β	4.70 (*dd*) (10.0, 2.5)	2.32 (*m*)	1.99 (*m*)
7	7.10 (*d*) (2.5)	6.91 (*q*) (3.5)	4.54 (*d*) (4.0)
9		2.99 (*m*)	
11α	9.65 (*s*)	4.48 (*t*) (9.0)	
11β		4.02 (*t*) (9.0)	
12α	9.50 (*s*)		4.68 (*d*) (17.0)
12β			4.96 (*d*) (17.0)
13α	5.13 (*s*)	4.90 (*s*)	4.86 (*s*)
13β	5.03 (*s*)	4.73 (*s*)	4.62 (*s*)
14	1.11 (*d*) (6.5)	1.11 (*d*) (6.5)	1.10 (*d*) (7.0)
15	0.96 (*s*)	0.65 (*s*)	0.89 (*s*)
6-OH	1.59 (*bs*)		
7-OH			1.94 (*s*)
9-OH	4.07 (*bs*)		

Coupling constant values (in parentheses) are in Hz.
[a] Chemical shifts are in ppm relative to TMS.

200.5 in the ^{13}C spectrum. The remaining two broad singlets at δ 1.59 and 4.07 in the ^1H NMR spectrum, which did not exhibit any correlations in the HMQC spectrum, were assigned to two hydroxyl groups. The former was assigned to a hydroxyl group bonded to the tertiary carbon, C-6, whereas the downfield broad singlet at δ 4.07 was assigned to a hydroxyl group attached to the quaternary carbon, C-9. This was further supported by the downfield carbon resonances, δ 66.1 and 77.6, observed in the ^{13}C NMR spectrum of **1** for C-6 and C-9, respectively. The ^{13}C and DEPT analyses gave signals corresponding to two methyl, three methylene, six methine and four quaternary carbons further confirming the presence of a coloratane type sesquiterpene. Carbon resonances at δ 106.7, 139.3, 149.1 and 153.7 were assigned to four olefinic carbons, whereas carbon signals at δ 66.1 and 77.6 were assigned to methine and quaternary carbons bearing hydroxyl groups, respectively. The HMQC, HMBC and NOESY experiments allowed unambiguous assignment of the chemical shift values of the methylene protons at C-1 and C-2. Assignment of the relative stereochemistry of the two hydroxyl groups in **1** was accomplished by analyses of the coupling constants and NOESY spectrum. The proton H-6 showed NOE correlation (Fig. 2) to CH_3-15, thus H-6 occupied a position axial to the axial CH_3-15 group at C-10 leaving OH-6 α-oriented. This is in agreement with the observed coupling constants for H-6 ($J = 10.0$ Hz) with H-5 and ($J = 2.5$ Hz) with H-7. Similarly, a cross NOE peak was observed between the aldehyde proton H-11 and CH_3-15, indicating that the

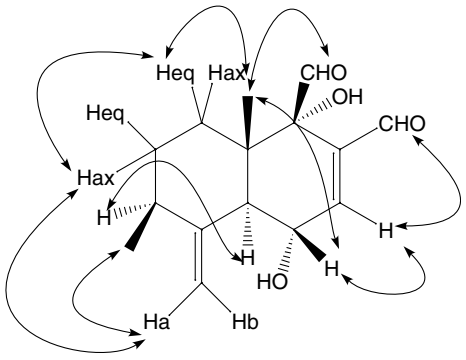

Fig. 2. NOE correlations in compounds **1**.

aldehyde at C-9 is located equatorial to the axial CH_3-15 leaving the hydroxyl at position 9 α-oriented. On the basis of these observations compound **1** was identified as 6α,9α-dihydroxy-4(13),7-coloratadien-11,12-dial.

Compound **2** was isolated as a white prism from CH_2Cl_2. A molecular formula of $C_{15}H_{20}O_2$ for **2** was deduced from the HRMS (*m/z*; measured 233.1542 $[M+H]^+$; calc. 233.1536). The EI-MS spectrum also gave *m/z* 232 $[M]^+$. The IR spectrum exhibited a strong absorption bands at 1757 and 1686 cm^{-1}, suggesting the presence of an α,β-unsaturated lactone and a band at 1639 cm^{-1} due to olefinic groups. The ^1H NMR spectrum of compound **2** differed from **1** in the absence of two aldehyde protons at C-11 and C-12. Instead, **2** exhibited mutually coupled methylene protons at δ 4.02 and 4.48 ($J = 9.0$ Hz), which were absent in **1**. The ^1H and ^{13}C NMR spectra were highly similar to that of **1**, except that **2** lacked the hydroxyl group at C-9 which was present in **1**. Of the two methyl signals observed in the ^1H NMR spectrum, the singlet at 0.65 was assigned to CH_3-15 and the doublet at δ 1.11 was assigned to CH_3-14. The protons of the latter methyl doublet gave HMBC correlation to the quaternary carbon C-4 and was therefore located at C-3. Three one proton multiplets at δ 2.05, 2.18 and 2.99 were assigned to the H-3, H-5 and H-9, respectively. The chemical shifts for the remaining methylene protons were assigned by a detailed analysis of HMQC and HMBC spectra. In the ^{13}C NMR spectrum, double bond carbon resonances at 127.0 (C-8) and 135.5 (C-7), and a lactone carbonyl carbon at 170.2 (C-12) suggested the presence of α,β-unsaturated lactone group (Table 2). The relative stereochemistry of the four asymmetric centres in the coloratadiene skeleton was determined by COSY and NOESY experiments (Fig. 3). Both the H-6α and H-6β resonances were seen to be coupled in the COSY spectrum to H-5 and H-7. The NOESY spectrum of **2** showed correlations between the protons of H-9 and H-5 and between the protons of H-9 and H-11α. These

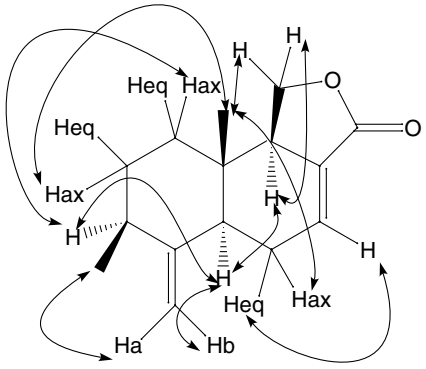

Fig. 3. Significant NOE correlations in compound **2**.

Table 2
^{13}C NMR and HMBC spectral data for compounds **1**–**4** (125.8 Hz, $CDCl_3$)

Carbon	**1**		**2**		**3**		**4**	
	δ	HMBC	δ	HMBC	δ	HMBC	δ	HMBC
1	31.7	H-15	39.7	H-15	33.7	H-15	36.9	H-2β, H-5, H-15
2	31.8	H-1α, H-1β	32.3	H-1α, H-1β, H-14	31.8	H-14	23.5	
3	38.8	H-13a, H-14	38.8	H-13a, H-14	38.5	H-13a, H-14	80.2	H-1α, H-2α, H-5 H-14H-13a, H-14
4	149.1	H-5, H-6, H-14	151.6	H-5, H-14	152.0	H-3α, H-5, H-14	37.7	H-14
5	50.4	H-7, H-13b, H-15	45.9	H-13b, H-15	44.2	H-6α, H-13b, H-15	49.4	H-1β, H-13b, H-14
6	66.1	H-5	26.9		31.5		24.7	H-5
7	153.7	H-6	135.5		62.3	H-6α	135.7	
8	139.3	H-12	127.0	H-11α	56.9	H-6α, H-12α, H-12β, 7-OH	127.2	
9	77.6	H-7, H-11. H-12, H-15	49.3	H-11α, H-11β, H-15	137.4	H-12α, H-12β, H-15	50.6	H-1α, H-5, H-11α, H-15
10	44.1	H-5, H-15	36.7	H-5, H-11β, H-15	36.8	H-6α, H-15	34.1	H-1α, H-2α, H-5, H-15
11	200.5		67.9		172.1		66.9	
12	192.6	H-7	170.2	H-11α	69.9		169.7	
13	106.7	H-5	105.5		104.7		27.6	H-5, H-14
14	18.2		18.6		18.1		15.9	H-3α, H-5 H-13
15	15.8	H-5	12.5	H-1α, H-5	16.4	H-1α	13.5	H-1α, H-5
CH_3–CO–							21.2	
CH_3–*C*O–							170.7	H-3, CH_3-CO

correlations require that H-9, H-5, and H-11α all be *cis* to each other, and therefore that the H-9 proton has an α-orientation. The ^{1}H–^{1}H coupling observed between H-9 and H_2-11 in the COSY spectrum confirmed the position of the methylene group to be at 11. The H-11β and H-11α protons were unambiguously distinguished by the NOESY spectrum, which displayed cross NOE peaks between the H-11β proton (δ 4.02) and the methyl H-15 protons (δ 0.65), as well as between the H-11α proton (δ 4.48) and the H-9α (δ 2.99) protons. The β-orientation of CH_3-14 was supported by a NOE cross-peak between CH_3-14 and one of the exocyclic methylene protons, Ha-13, at δ 4.90. This stereochemical assignment would be in agreement with that of other coloratadiene sesquiterpenes previously isolated from *Warburgia* species (Kioy et al., 1990; Rajab and Ndegwa, 2000). Therefore, the new compound **2** was established structurally as 4(13),7-coloratadien-12,11-olide.

Compound **3** was isolated as colorless prisms from CH_2Cl_2. A molecular formula $C_{15}H_{20}O_3$ was obtained from HRMS (*m*/*z*; measured 271.1302 $[M + Na]^+$; calc. 271.1310). Similarly, a prominent peak *m*/*z* 246 $[M - 2H]^+$ appeared in the EI-MS spectrum, corresponding to the molecular formula $C_{15}H_{20}O_3$, which was further supported by two methyl, five methylene, three methine, and five quaternary carbons signals observed in the ^{13}C and DEPT spectra. In addition, a fragment ion peak at *m*/*z* 215 indicated the facile loss of a hydroxyl group. The IR spectrum showed a hydroxyl stretch band at 3416 cm^{-1}, unsaturated lactone absorptions at 1735 and 1670 cm^{-1} and olefinic absorption at 1646 cm^{-1}. An absorption maximum at 230 nm in the UV spectrum was characteristic of a molecule possessing an unsaturated lactone structure. The ^{1}H NMR spectrum of **3** was very similar to that of **2** and exhibited two singlets at δ 4.62 and 4.86 that are typical of exocyclic methylene protons, and a three protons doublet at δ 1.10, which further characterized the compound as a rearranged drimane sesquiterpene in which one methyl group has migrated from C-4 to C-3. Furthermore, two one proton doublets at δ 2.38 and 4.54 were assigned to the H-5 and H-7, respectively. The doublets at δ 4.68 and 4.96 were unambiguously assigned to H-12α and H-12β, respectively, based on NOE correlations observed between H-12α and H-7 in the NOESY spectrum (Fig. 4). Similarly, the signals at δ 1.92 and 1.99 in the 1H NMR spectrum were ascribed to H-6α and H-6β, respectively, based on cross NOE peaks observed between H-6β and CH_3-15, and H-6β and H-13b. A broad singlet at 1.94 was attributed to a hydroxyl group at position 7. The position of the hydroxyl group at C-7 was determined by analysis of its HMBC spectrum, which showed a correlation between H-7 and C-8. This was also supported by the methine carbon resonance at δ 62.3 which suggested a hydroxyl substituted carbon, which was correlated in the HMBC to H-6 and thus assigned as C-7. The chemical shift values of the methyl protons at C-1 and C-2 were assigned based on HMQC, HMBC and NOESY experiments. When compared with the spectral data of **1**, the lack of two aldehyde groups was apparent from the ^{1}H NMR spectrum of **3**. The relative stereochemistry of the hydroxyl group was established by analysis of the NOESY spectrum. The H-7 resonance showed a NOESY correlation to H-5, which suggested an axial (α)-orientation for this H-7 proton, leaving the hydroxyl group with an equatorial (β)-orientation. These assignments were consistent with the coupling constant data ($J = 4.0$ Hz) for H-7. On the basis of these observations, the structure of **3** was assigned as 7β-hydroxy-4(13),8-coloratadien-11,12-olide.

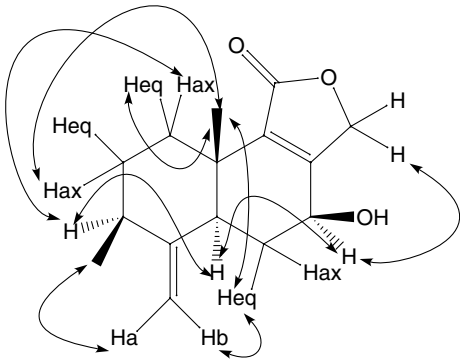

Fig. 4. Significant NOE correlations in compound **3**.

Compound **4** was obtained as colorless prisms from *n*-hexane–CH_2Cl_2 mixture. The EI-MS spectrum of **4** showed a molecular ion peak at *m*/*z* 291 $[M - H]^+$ and fragment ions at *m*/*z* 249 $[M - 43]^+$ and 232 $[M - 60]^+$ corresponding to the loss of an acetate and acetic acid groups, respectively. The IR spectrum displayed, in addition to α,β-unsaturated lactone at 1760 and 1683 cm^{-1}, the presence of an acetate group at 1731 cm^{-1}. The ^{1}H NMR data reported previously (Kioy et al., 1990; Ying et al., 1995) for this compound were highly similar to compound **4**, but the chemical shift values of each methylene proton were not assigned explicitly. Four three protons signals were observed in the ^{1}H NMR spectrum of **4**, of which the acetate methyl resonance appeared at δ 2.07. Of the remaining three methyl groups, the singlet at δ 0.84, which showed a HMBC correlation with the C-9 at δ 50.6, was located at C-10, while the remaining two methyl groups could be placed at C-4 on the basis of HMBC correlations. Although, the carbon resonances for C-1, C-6, C-13, C-15, C-12 and acetate carbonyl carbon reassigned by Ying et al. (1995) were very similar with the ^{13}C NMR spectrum of **4**, the carbon resonances for C-4 and C-10 still needed to be reversed as shown in the ^{13}C NMR and HMBC spectra (Table 2). The ^{13}C spectrum of **4** revealed resonances for C-7, C-8, C-9 and C-11 in close agreement with resonances for the corresponding carbons in **2**. The carbonyl carbon resonance of the ace-

tate group appeared at δ 170.7 and showed HMBC correlations with H-3 at δ 4.55, which indicated that the acetate group was attached at C-3. This was supported by the observation of NOE correlations between the CH_3–CO and CH_3-15. The HMBC spectrum showed connectivities between the H-11α proton (δ 4.41 *t*) and the carbonyl carbon of the lactone (δ 169.7), and between the H-3α proton (δ 4.55) and the carbonyl carbon of the acetate (δ 170.7), whereas the NOESY spectrum displayed NOE cross-peaks between the H-3α and H-5α protons, thus establishing the relative stereochemistry of the acetate group as β-oriented. Moreover, the acetate methyl proton (δ 2.07) showed an NOE correlation with the axial C-15 methyl protons (δ 0.84) but neither of the C-4 methyl protons (δ 0.94 and 1.00) showed an NOE with the H-3α proton. Although the optical rotation value determined for **4** was slightly different from previous report (Kioy et al., 1990), the above spectroscopic evidences strongly support the structural assignment of compound 4 as cinnamolide-3β-acetate. The full spectral data and unambiguous assignment of resonances are reported here for the first time.

Compounds **5**–**13** were identified as muzigadial, muzigadiolide, 11α-hydroxymuzigadiolide, cinnamolide, 7α-hydroxy-8-drimen-11,12-olide, ugandensolide, mukaadial, ugandensidial, and linoleic acid (*Z*, *Z*), respectively by spectroscopic analysis and comparison of their ^{1}H NMR, ^{13}C NMR, and mass spectral data with those in the literature (Kubo et al., 1976, 1983; Rajab and Ndegwa, 2000; Nakanishi and Kubo, 1977; Maurs et al., 1999). Although **9** has been reported from *Capsicodendron dinisii* (Mahmoud et al., 1980), this is the first time it has been found in the genus *Warburgia*. In addition, compound **13**, which is the constituent of most vegetable oils and animal fats, has been reported from the genus for the first time.

The antimycobacterial activity of the isolated compounds **1**–**13** was determined by the broth microtiter dilution method against fast growing strains of mycobacteria and their MICs are presented in Table 3.

Table 3
Antimycobacterial activity of compounds **1**–**13** and the antibiotic drugs[a]

Compound	MIC (μg/ml)			
	M. aurum	*M. fortuitum*	*M. phlei*	*M. smegmatis*
5	32	16	64	64
2	128	128	NA	128
6	128	128	64	128
3	NA	128	NA	NA
9	128	128	NA	NA
12	NA	128	NA	NA
13	4	8	4	16
Ethambutol	0.5	8	2	1
Isoniazid	4	1	4	4

[a] NA, not active; compounds **1**, **7**, **4**, **8**, **10**, and **11** showed no activity up to 128 μg/ml.

Among the compounds tested, compound **13** displayed the most potent inhibitory activity with MIC values of 4, 8, 4, 16 μg/ml against *M. aurum*, *M. fortuitum*, *M. phlei* and *M. smegmatis*, respectively. This is in agreement with previous reports (Stavri et al., 2004; Seidel and Taylor, 2004) about the antimycobacterial activity of linoleic acid. Interestingly, muzigadial (**5**) having the coloratadiene-dialdehyde structural feature displayed pronounced antimycobacterial activities with MICs ranging from 16 to 64 μg/ml. Previous studies done by Taniguchi et al. (1984) revealed that the dialdehyde moiety was responsible for the broad range of antimicrobial activity of muzigadial, which might have also contributed to enhancement of the antimycobacterial activity. In contrast, compound **1** having one more hydroxyl group compared to compound **5** showed no activity against the strains of mycobacteria in our assay. This suggests that compounds polarity seems to influence the in vitro antimycobacterial activity of drimane sesquiterpenes. Haemers et al. (1990) also reported that higher lipophilicity may play an important role in the antimycobacterial activity. This is due to the fact that the mycobacterial cell wall contains lipophilic substance such as mycolic acid, lipophilic compounds would therefore have the advantage of better penetration through the cell wall and inhibit the growth of mycobacteria. Among the sesquiterpene lactones compound **6** showed moderate activity, whereas the remaining sesquiterpenes failed to inhibit the growth of the four strains of mycobacteria up to 128 μg/ml. The use of *W. ugandensis* stem bark in Ethiopian folk medicine to treat tuberculosis can therefore be attributed to the presence of linoleic acid and the drimane sesquiterpenes.

3. Experimental

3.1. General experimental procedures

Melting points were determined with KOFLER microscope and are uncorrected. Optical rotations were measured on a Perkin–Elmer 241 MC polarimeter. Perkin–Elmer 881 infrared spectrophotometer was used in recording the IR. UV spectra were recorded on Shimadzu UV-160A spectrophotometer. Analytical TLC was performed on Merck silica gel 60 and plates were sprayed with 0.5% anisaldehyde sulphuric acid reagent. Semipreparative HPLC was performed using LiChrospher® RP-18 (10 μm, 250 × 10 mm i.d.) column and Hypercarb-S (100 × 4 mm i.d.), monitoring wavelength 214 nm. NMR spectra were recorded at 500 MHz for ^{1}H and 125 MHz for ^{13}C on a Bruker AVANCE 500 spectrometer. All spectra were measured in $CDCl_3$, except for compound **11** which was in pyridine-d_5. HRMS was determined with Micromass QTOF Ultima using the internal standard [Glu]-fibrinopeptide B which had

$[M + 2H]^{2+} = 785.8426$. Mass spectra were further obtained by EI-MS analysis on a 5890 Series II plus gas chromatograph interfaced to a 5989 B mass spectrometer (Hewlett-Packard). The analysis was performed on an HP5-MS (29 m × 0.25 mm i.d., 0.50 μm film thickness) fused silica capillary, carrier gas helium with a flow rate 1.0 ml/min; injection, interface and ion source temperatures: 250 °C and ionization at 70 eV. Strains of *M. aurum* (PI 104482), *M. fortuitum* (ATCC 6841), *M. phlei* (ATCC 19249) and *M. smegmatis* (ATCC 19420) were obtained from the American Type culture collection or the Pasteur Institute.

3.2. Plant material

Stem barks of *W. ugandensis* Sprague (Canellaceae) were collected from a single tree growing in Harena Forest, about 13 km from Dello Menna on the way to Goba, Ethiopia in April 2001 and identified by Mr. Melaku Wendafrash, the National Herbarium, Biology Department, Science Faculty, Addis Ababa University. A voucher specimen (collection No. 977) was deposited at the National Herbarium for further reference.

3.3. Extraction and isolation

The powdered stem barks of *W. ugandensis* (800 g) were extracted successively with *n*-hexane, dichloromethane and methanol in a Soxhlet apparatus. The dichloromethane extract was concentrated under vacuum to yield 35 g of yellowish residue, of which 25 g were subjected to vacuum column chromatography on silica gel eluting with *n*-hexane/EtOAc mixtures of increasing polarity and 18 fractions of 400 ml each were collected. Fractions 3 and 4 eluted with *n*-hexane/EtOAc (9:1) were combined and rechromatographed on silica gel eluting with *n*-hexane/EtOAc (95:5) and further purified on semi-prep. HPLC with Hypercarb S column using MeOH as eluent to yield **2** (5 mg). Fractions 5 and 6 eluted with *n*-hexane/EtOAc (8:2) were purified by semi-prep. HPLC using MeCN/H_2O (6:4 → 8:2) gradient elution for 50 min to afford **8** (9 mg). Fractions 7–13 were combined and applied to a Sephadex LH-20 column connected to a fraction collector using CH_2Cl_2 as eluent to give 120 subfractions of 15 ml each. Subfractions 111 and 112 afforded pure compound **7** (32 mg). Subfraction 14 gave **4** (60 mg) after multiple development on prep. TLC using *n*-hexane/EtOAc (7:3) as eluent. Subfractions 16–18 were further subjected to semi-prep. HPLC using MeCN/H_2O (44:56) isocratic elution for 70 min to give **5** (6 mg) and **12** (23 mg) at 56 and 66 min, respectively. Subfractions 49–54 were chromatographed on semi-prep. HPLC using MeCN/H_2O (45:55) isocratic elution to afford **1** (25 mg), **9** (4 mg) and **6** (10 mg) at 15, 35 and 41 min, respectively. Similarly, purification of subfractions 63 and 64 by semi-prep. HPLC eluting with MeCN/H_2O (45:55) isocratic system yielded **11** (24 mg), **3** (15 mg) and **10** (11 mg). Finally, compound **13** (35 mg) was purified from subfractions 33–37 by semi-prep. HPLC using MeCN/H_2O (25:75 → 9:1 for 30 min and MeCN/H_2O (9:1) isocratic system from 31 to 55 min.

3.4. Antimycobacterial assay

The antimycobacterial activities of the compounds were evaluated by the minimum inhibitory concentration assay method reported by Schinkovitz et al. (2003) in 96-well microtiter plates. The test compounds initially dissolved in DMSO were diluted in cation adjusted Mueller–Hinton broth (MHB) to give a concentration of 256 μg/ml. One hundred and twenty five microlitres of each test solution were added to each well containing 125 μl of MHB to achieve a starting concentration of 128 μg/ml. A twofold serial dilution of test solutions were prepared to get final concentrations ranging from 128 to 0.25 μg/ml. Mycobacterial strains were cultivated on Columbia blood agar supplemented with 7% defibrinated horse blood agar. Bacterial suspension with a turbidity of 0.5 on the MacFarland scale was made in 0.9% NaCl solution and diluted to give a final inoculum's density of 5×10^5 cfu/ml. After addition of 125 μl of bacterial inocula into all wells, except the blank the plates were incubated at 37 °C for 72 h. The lowest assay concentration of the test compounds that produce complete inhibition of the macroscopic growth (MIC) were detected by addition of 20 μl methanol solution of tetrazolium redox dye (MTT, 3.5 mg/ml) followed by incubation at 37 °C for 20 min. Tests were conducted three times in duplicate and ethambutol and isoniazid were used as positive controls.

3.5. 6α,9α-Dihydroxy-4(13),7-coloratadien-11,12-dial (*1*)

Colorless needles from *n*-hexane–CH_2Cl_2 mixture, m.p. 137–139 °C, $[\alpha]_D^{24}$ −40 (CH_2Cl_2; c1.6), UV$\lambda_{max}^{CH_2Cl_2}$ nm(log ε): 234(3.6), IR$\nu_{max}^{CH_2Cl_2}$ cm^{-1}: 3406(−OH), 1725 and 1683 (CH=CHO)), 1640 and 796 (exocyclic methylene), ^1H NMR (500 MHz, $CDCl_3$) see Table 1, ^{13}C NMR (125.8 MHz, $CDCl_3$) see Table 2, HRMS Found 287.1264 $[M + Na]^+$; $C_{15}H_{20}O_4Na$, calc. 287.1259, EI-MS (70 eV) *m/z* (rel. int.): 246 $[M - H_2O]^+$(5), 235 $[M - CHO]^+$(100), 217 $[M - CHO - H_2O]^+$(26), 189 $[M - CHO - H_2O - CO]^+$(40), 175 $[M - CHO - OH - Me - CO]^+$(35), 105(60), 91(73), 77 (66), 55(81), 41(93).

3.6. 4(13),7-Coloratadien-12,11-olide (*2*)

White prism from CH_2Cl_2, m.p. 85–87 °C, $[\alpha]_D^{24}$ +84.7 (CH_2Cl_2; c1.5), UV$\lambda_{max}^{CH_2Cl_2}$ nm(log ε): 231

(3.7), IR $\nu_{max}^{CH_2Cl_2}$ cm^{-1}: 1757 and 1686(CH=CHO), 1639 and 758 (exocyclic methylene), ^1H NMR (500 MHz, $CDCl_3$) see Table 1, ^{13}C NMR (125.8 MHz, $CDCl_3$) see Table 2, HRMS Found 233.1542 $[M+H]^+$; $C_{15}H_{21}O_2$, calc. 233.1536, EI-MS (70 eV) *m/z* (rel. int.): 232 $[M]^+$(22), 217 $[M-CH_3]^+$(17), 190 $[M-C_3H_6]^+$(10), 122(100), 107(58), 91(22), 41(12).

3.7. 7β-Hydroxy-4(13),8-coloratadien-11,12-olide (3)

Colorless prism from CH_2Cl_2, m.p. 139–142 °C, $[\alpha]_D^{25}$ + 242.1 (CH_2Cl_2; c1.9), UV $\lambda_{max}^{CH_2Cl_2}$ nm(log ε): 230 (3.3), IR $\nu_{max}^{CH_2Cl_2}$ cm^{-1}: 3414(−OH), 1735 and 1670 (CH=CHO)), 1646 and 786 (exocyclic methylene), ^1H NMR (500 MHz, $CDCl_3$) see Table 1, ^{13}C NMR (125.8 MHz, $CDCl_3$) see Table 2, HRMS Found 271.1302 $[M+Na]^+$; $C_{15}H_{20}O_3Na$, calc. 271.1310, EI-MS (70 eV) *m/z* (rel. int.): 230 $[M-H_2O]^+$(100), 215 $[M-H_2O-CH_3]^+$(55), 201 $[M-OH-2CH_3]^+$(25), 185(45), 171(83), 91(90), 77 (74), 41(77).

3.8. Cinnamolide-3β-acetate (4)

Colorless prism from *n*-hexane–CH_2Cl_2 mixture, m.p. 147–149 °C, $[\alpha]_D^{25}$ − 2.4(CH_2Cl_2; c1.3), UV $\lambda_{max}^{CH_2Cl_2}$ nm (log ε): 232.5(3.6), IR $\nu_{max}^{CH_2Cl_2}$ cm^{-1}: 1706 and 1683 (CH=CHO)), 1637 and 779 (exocyclic methylene), ^1H NMR (500 MHz, $CDCl_3$): δ 0.84 (3H, *s*, H-15), 0.94 (3H, *s*, H-13), 1.00 (3H, *s*, H-14), 1.42 (1H, *ddd*, *J* = 13.5, 4.0, H-1α), 1.48 (1H, *dd*, *J* = 10.5, 4.5 Hz, H-5), 1.64 (1H, *dt*, *J* = 13.5, 3.5 Hz, H-1β), 1.68 (1H, *ddd*, *J* = 12.5, 1.5 Hz, H-2β), 1.74 (1H, *ddd*, *J* = 13, 4 Hz, H-2α), 2.07 (3H, *s*, O–$COCH_3$), 2.22 (1H, *ddq*, *J* = 12.0, 3.5, 1.5 Hz, H-6β), 2.44 (1H, *dq*, *J* = 20, 5, 4.0 Hz, H-6α), 2.82 (1H, *m*, H-9α), 4.05 (1H, *t*, *J* = 9.0 Hz, H-11β), 4.41 (1H, *t*, *J* = 9.0 Hz, H-11α), 4.55 (1H, *dd*, *J* = 11.5, 4.5 Hz, H-3α), 6.89 (1H, *q*, *J* = 3.5 Hz, H-7), ^{13}C NMR (125.8 MHz, $CDCl_3$) see Table 2, EI-MS (70 eV) *m/z* (rel. int.): 291 $[M-H]^+$(5), 249 $[M-H-CH_3-CO]^+$(7), 232 $[M-CH_3-COOH]^+$(10), 217 $[M-CH_3-COOH-Me]^+$(8), 122(100), 107(65), 43(52).

Acknowledgements

A.A. Wube gratefully acknowledges the Austrian Academic Exchange Service (ÖAD) scholarship. One of us (SG) thanks the Engineering and Physical Sciences Research Council (Grant No. GR/R47646/01) for funding. We are grateful to Mrs. Elke Prettner, Department of Pharmaceutical Chemistry, Institute of Pharmaceutical Sciences, University of Graz, for IR, UV and Optical activity determination, and Mr. Melaku Wendafrash, The National Herbarium, Department of Biology, Addis Ababa University for identification of the plant material.

References

Brooks, C.J.W., Draffan, G.H., 1969. Sesquiterpenoids of *Warburgia* species. II. Ugandensolide and ugandensidial. Tetrahedron 25, 2887–2898.

Haemers, A., Leysen, D.C., Bollaert, W., Zhang, M., Pattyn, S.R., 1990. Influence of N substitution on antimycobacterial activity of ciprofloxacin. Antimicrob. Agents Chemother. 34, 496–497.

Kioy, D., Gray, A.I., Waterman, P.G., 1990. A comparative study of the stem bark drimane sesquiterpenes and leaf volatile oils of *Warburgia ugandensis* and *W. stuhlmannii*. Phytochemistry 29, 3535–3538.

Kokwaro, J.O., 1976. In: Medicinal Plants of East Africa. East African Literature Bureau, Nairobi, p. 45.

Kubo, I., Taniguchi, M., 1988. Polygodial, an antifungal potentiator. J. Nat. Prod. 51, 22–29.

Kubo, I., Lee, Yue-Wei, Pettei, M., Pilkiewicz, F., Nakanishi, K., 1976. Potent army worm antifeedants from the East African *Warburgia* plants. Chem. Commun. 24, 1013–1014.

Kubo, I., Matsumoto, T., Kakooko, A.B., Mubiru, N.K., 1983. Structure of mukaadial, a molluscicide from *Warburgia* plants. Chem. Lett. 7, 979–980.

Mahmoud, I.I., Kinghorn, A.D., Cordell, G.A., Farnsworth, N.R., 1980. Potential anticancer agents. XVI. Isolation of bicyclofarnesane sesquiterpenoids from *C. dinisii*. J. Nat. Prod. 43, 365–371.

Mashimbye, M.J., Maumela, M.C., Drewes, S.E., 1999. A drimane sesquiterpenoid lactone from *Warburgia salutaris*. Phytochemistry 51, 435–438.

Maurs, M., Azerad, R., Cortés, M., Aranda, G., Delahaye, M.B., Ricard, L., 1999. Microbial hydroxylation of natural drimenic lactones. Phytochemistry 52, 291–296.

Nakanishi, K., Kubo, I., 1977. Studies on warburganal, muzigadial and related compounds. Isr. J. Chem. 16, 28–31.

Rajab, M.S., Ndegwa, J.M., 2000. 11α-Hydroxymuzigadiolide, a novel drimane sesquiterpene from the stem bark of *Warburgia ugandensis*. Bull. Chem. Soc. Ethiop. 14, 45–49.

Schinkovitz, A., Gibbons, S., Stavri, M., Cocksedge, M.J., Bucar, F., 2003. Ostruthin: An antimycobacterial coumarin from *Peucedanum ostruthium*. Planta. Med. 69, 369–371.

Seidel, V., Taylor, P.W., 2004. In vitro activity of extracts and constituents of *Pelagonium* against rapidly growing mycobacteria. Int. J. Antimicrob. Agents 23, 613–619.

Stavri, M., Schneider, R., O'Donnell, G., Lechner, D., Bucar, F., Gibbons, S., 2004. The antimycobacterial components of hops (*Humulus lupulus*) and their dereplication. Phytother. Res. 18, 774–776.

Taniguchi, M., Adachi, T., Oi, S., Kimura, A., Katsumura, S., Isoe, S., Kubo, I., 1984. Structure–activity relationship of the *Warburgia* sesquiterpene dialdehydes. Agric. Biol. Chem. 48, 73–78.

Watt, J.M., Breyer-Brandwijk, M.G., 1962. Medicinal and Poisonous Plants of Southern and Eastern Africa. E. and S. Livingstone, London.

Ying, Bai-Ping, Peiser, G., Ji, Y., Mathias, K., Tutko, D., Hwang, Y., 1995. Phytotoxic sesquiterpenoids from *Canella winterana*. Phytochemistry 38, 909–915.

Anti-Staphylococcal and Cytotoxic Compounds from *Hyptis pectinata*

Mabel Fragoso-Serrano[1], Simon Gibbons[2], Rogelio Pereda-Miranda[1]

Abstract

Bioassay-guided fractionation of a $CHCl_3$ extract prepared from the Mexican medicinal plant *Hyptis pectinata* led to the isolation of four pyrones, pectinolides A – C (**1** – **3**) and H (**4**). Activity was tracked using cultured KB cells. Multidrug-resistant strains of *Staphylococcus aureus* were sensitive to pectinolide H (**4**; KB > 20 μg/mL) in the concentration range of 32 – 64 μg/mL. The absolute stereochemistry of this new compound was established as 5*S*-[(4*S*-acetyloxy)-(1*S*-hydroxy)-2*Z*-octenyl]-2(5*H*)-furanone on the basis of spectral, chiroptical data and chemical correlation with pectinolide A (**1**). Mosher ester derivatives were used with pectinolide B (**2**) for confirmation of the 3′-(*S*) absolute stereochemistry on the side chain chiral center of pectinolides A – C.

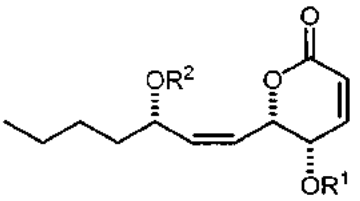

	R^1	R^2
1	Ac	Ac
2	Ac	H
3	H	Ac
5r	Ac	(R)-MTPA
5s	Ac	(S)-MTPA
6	H	H

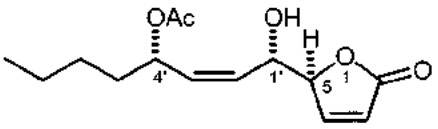

4

All Mexican medicinal members of the genus *Hyptis* (Lamiaceae) share three important therapeutic characteristics: they are used to treat gastrointestinal disturbances, as antiseptics for skin and eye infections, and as remedies in the treatment of rheumatism and muscular pain [1]. From the 16th century post-conquest accounts of the prehispanic herbolaria, "*De la Cruz-Badiano Codex*" [2] and "*Historia Plantarum Novae Hispaniae*" [3], we know that their employment goes back to ancient Mesoamerican civilizations as in the use of "*xoxouhcapahtli*" (bright green medicine) by the Aztecs [2]. The antiseptic qualities were the ethnobotanical clues on which we based our selection of plant material for chemical studies focused on the cytotoxic potential of crude extracts from several *Hyptis* species, correlating our results to their antimicrobial properties [1].

Formulations of *Hyptis pectinata* (L.) Poit., known as "hierba del burro" (donkey herb) by the contemporary Mexican rural population, are used in folk medicine as a multipurpose domestic remedy for the same illnesses as mentioned in the above referred colonial manuscripts as well as for treatment of fevers, rhinopharyngitis and lung congestions. The first report on the isolation of the antibacterial principle of this plant material was published by our group in the early 1990's when the $CHCl_3$-soluble extracts derived from the defatted whole plant afforded pectinolides A – C (**1** – **3**). Their antimicrobial activity against *Staphylococcus aureus* ATCC 6538 was comparable to that exhibited by clinical drug standards [4]. In the present project, a chemical reinvestigation of this same herb led to the isolation of a new compound, pectinolide H (**4**), which displayed a reasonably high potency against a panel of multidrug-resistant strains of *Staphylococcus aureus* (Table **1**).

Pectinolide H (**4**) exhibited a molecular formula of $C_{14}H_{20}O_5$ based on its HR-EI-MS data. NMR spectral evidence indicated that compound **4** is the γ-lactone diastereoisomer of pectinolide B (**2**). The characteristic resonance for the carbonyl group C-2 (δ = 172.5) as well as the vicinal coupling constant ($^3J_{H,H}$ = 6.0 Hz) for the vinylic protons on C-3 (δ = 6.2) and C-4 (δ = 7.5), as part of an ABX spin system with H-5 (δ = 5.2), indicated the presence of a pentenolide. The ^{13}C-NMR, HMQC and HMBC spectra of **4** fully supported the presence of a 4-(acetyloxy)-(1-hydroxy)-2-octenyl moiety at C-5. The discernible vicinal coupling constants $^3J_{H,H}$ = 11.0 Hz for the additional two sets of olefinic protons at C-2′(δ = 5.5) and C-3′(δ = 5.4) confirmed the *cis* configuration for the exocyclic double bond. The absolute stereochemistry of **4** was established as 5*S*-[(4*S*-acetyloxy)-(1*S*-hydroxy)-2*Z*-octenyl]-2(5*H*)-furanone on the basis of chemical correlation through acid hydrolysis with pectinolide A (**1**) as well as the interpretation of chiroptical data. The negative sign for the optical rotatory dispersion ($[\Phi]_D$: –110) [5] and circular dichroism [6] curves ($\Delta\varepsilon_{223}$: –18) was correlated with an (*S*) configuration at C-5. Mosher ester derivatives used with pectinolide B (**2**) (Table **2**) corroborated the C-3′-(*S*) absolute stereochemistry for compounds **1** – **3**.

Pectinolide H (**4**) displayed significant activity against two multidrug-resistant strains of *Staphylococcus aureus* (Table **1**). XU-212

Affiliation: [1] Departamento de Farmacia. Facultad de Química. Universidad Nacional Autónoma de México, Mexico City, Mexico · [2] Centre for Pharmacognosy and Phytotherapy. The School of Pharmacy, University of London, UK

Correspondence: Dr. Rogelio Pereda-Miranda · Departamento de Farmacia · Facultad de Química · Universidad Nacional Autónoma de México · Ciudad Universitaria · 04510 DF Mexico City · Mexico · Fax: +52-55-5622-5329 · E-mail: pereda@servidor.unam.mx

Received: July 12, 2004 · **Accepted:** October 24, 2004

Bibliography: Planta Med 2005; 71: 278–280 · © Georg Thieme Verlag KG Stuttgart · New York · DOI 10.1055/s-2005-837831 · ISSN 0032-0943

Table **1** Cytotoxic and anti-staphylococcal activities of compounds **1** – **4**

Compound	*ED_{50} (μg/mL)*	*MIC (μg/mL)*			
	KB	*ATCC 25923*	*XU-212*	*SA-1199B*	*EMRSA-15*
1	0.63	32	128	128	128
2	> 20	128	256	256	256
3	2.52	64	256	128	128
4	> 20	32	64	64	64
Ellipticine	0.10	–	–	–	–
Tetracycline	–	0.08	128	64	0.15

Table **2** ^{1}H NMR chemical shift data for diagnostic signals of the (*S*)- and (*R*)-MTPA-ester derivatives **5**

Proton chemical shifts ($\Delta\delta_H = \delta_S - \delta_R$)[a]								*C-3′ configuration*
H-1′	*$\Delta\delta_H$*	*H-2′*	*$\Delta\delta_H$*	*H-4′*	*$\Delta\delta_H$*	*H-7′*	*$\Delta\delta_H$*	
5.805		5.678		1.713		0.843		
	+0.033		+0.125		–0.083		–0.061	S
5.772		5.553		1.796		0.904		

[a] Data registered in $CDCl_3$ at 300 MHz [10].

is highly resistant to tetracycline via the presence of the TetK efflux protein and SA-1199B possesses the NorA efflux pump, which confers resistance to certain fluoroquinolones. Additionally, **4** was active against EMRSA-15, an epidemic strain of *S. aureus* which is methicillin-resistant (Table **1**). These results together with the lack of cytotoxicity for pectinolide H indicate potential as a model for designing new antibiotic leads with a γ-lactone pharmacophore. This compound represents the second report of a 2(5*H*)-furanone from *Hyptis* [7].

Material and Methods

Isolation procedures: The plant material was collected at Xalapa in Veracruz, Mexico. Voucher specimens (M-21853) are on deposit at the National Herbarium, Instituto de Biología, UNAM. The dried and finely powdered aerial parts of the plant (500 g) were extracted by maceration with $CHCl_3$ at room temperature, and the solvent removed under vacuum to yield 27 g of a crude extract. The fractionation was achieved by chromatography on a silica gel (350 g) column, using a $CHCl_3$-Me_2CO gradient elution system (9 : 1, 4 : 1, 2 : 1, 1 : 1, 800 mL each). A total of 80 fractions (40 mL) was collected, examined by TLC and combined to yield a cytotoxic pool (fractions 10 – 17) containing the mixture of **1** – **4** (3.7 g; KB, ED_{50} : 2.5 μg/mL). These compounds were purified by preparative HPLC, using a diode array detector (254 nm) on a Symetry C_{18} column (7 μm, 19 × 300 mm) with an isocratic elution of MeOH-H_2O (9 : 1), a flow rate of 3.0 mL/min, and sample injection of 500 μL (0.5 mg/mL), to yield 59 mg of peak 1, pectinolide A (**1**, t_R = 9.42 min), 7.1 mg of a mixture of **2** and **4** (peak II, t_R = 8.63 min) and 13.4 mg of peak III, pectinolide **C** (**3**, t_R = 6.36 min). A further purification of peak II by normal phase HPLC (μporasyl column, 10 μm, 19 × 150 mm) with hexane-EtOAc (3 : 2) as the mobile phase and a flow rate = 3 mL/min yielded 1.7 mg of **4** (pectinolide H, t_R = 14.5 min) and 2.4 mg of **2** (pectinolide B, t_R = 16.6 min). The known δ-lactones **1** – **3** were identical (NMR, TLC and HPLC) to standard samples [4]. Copies of the original spectra are obtainable from the author of correspondence.

Pectinolide H (**4**): Oil; ORD (*c* 0.24, $CHCl_3$) $[\alpha]_{589}^{25}$: –41, $[\alpha]_{578}^{25}$: –45, $[\alpha]_{546}^{25}$: –54, $[\alpha]_{436}^{25}$: –95, $[\alpha]_{365}^{25}$: –148; CD (*c* 0.02, MeOH): $\Delta\varepsilon$ (nm) = 0 (275), –1.5 (265), -18 (223), + 18 (204); ^{1}H NMR ($CDCl_3$, 300 MHz): δ = 7.55 (1H, dd, *J* = 6.0, 2.0 Hz, H-4), 6.22 (1H, dd, *J* = 6.0, 2.0 Hz, H-3), 5.53 (1H, dd, *J* = 11.0, 8.5 Hz, H-1′), 5.46 (1H, dd, *J* = 11.0, 6.0 Hz, H-2′), 5.39 (1H, ddd, *J* = 10.0, 7.5, 6.5 Hz, H-3′), 5.16 (1H, ddd, *J* = 5.0, 2.0, 2.0 Hz, H-5), 4.96 (1H, dddd, *J* = 8.5, 5.0, 3.5, 2.0 Hz, H-6), 3.60 (1H, d, *J* = 3.5 Hz, OH), 2.06 (3H, s, OAc), 1.70 (1H, m, H-4′a), 1.55 (1H, m, H-4′b), 1.35 (2H, m, H-5′), 1.30 (1H, m, H-6′), 0.92 (3H, t, *J* = 7.0 Hz, H-7′); ^{13}C NMR ($CDCl_3$, 125.7 MHz): δ = 176.5 (C, C-2), 171.8 (C, OAc), 153.3 (CH, C-4), 133.1 (CH, C-2′), 129.3 (CH, C-1′), 123.2 (CH, C-3), 84.1 (CH, C-5), 71.0 (CH, C-3′), 67.1 (CH, C-6), 33.6 (CH_2, C-4′), 27.1 (CH_2, C-5′), 22.4 (CH_2, C-6′), 21.3 (CH_3, OAc), 13.9 (CH_3, C-7′); FAB-MS: *m/z* = 251 $[M + H - H_2O]^+$; HR-EI-MS: *m/z* = 268.1312 $[M]^+$ (calcd. for $C_{14}H_{20}O_5$: 268.1310).

Hydrolysis of pectinolide A: Compound **1** (20 mg) was dissolved in MeOH (0.3 mL) and 1 N HCl (5 mL) and stirred for 10 h. Usual work-up of the reaction gave an oily residue which was separated by normal phase HPLC, using the same conditions mentioned for natural pectinolides, to afford the major products **2** (1 mg), **4** (1.5 mg) and **6** (0.6 mg, t_R = 35 min). Copies of the original spectra for **6** are obtainable from the author of correspondence.

Preparation of MTPA esters of pectinolide B: A solution (0.8 mg) of pectinolide B (**2**) in $CDCl_3$ (1 mL) was treated with 4-(dimethyl-

amino)pyridine (1 mg, previously heated at 70 °C) and (*R*)-(–)-α-methoxy-α-trifluoromethylphenylacetyl (MTPA) chloride (15 μL) in a dry NMR tube according to previously described protocols [8]. The reaction mixture was purified by HPLC (hexane-EtOAc, 3 : 2; flow rate = 3 mL/min) yielding 1.5 mg of the (*S*)-MTPA ester (**5s**). Treatment of compound **2** with (*S*)-(+)-MTPA chloride as described above yielded 1.4 mg of the (*R*)-MTPA ester (**5r**). Copies of the original spectra for derivatives **5s** and **5r** are obtainable from the author of correspondence.

Biological activity: Cytotoxicity was evaluated using cultured KB (nasopharyngeal carcinoma) cells according to previously described protocols [9]. The quantitative antimicrobial activity against *S. aureus* ATCC 25923, two multidrug-resistant strains [SA-1199B (NorA), XU-212 (TetK)] and one methicillin-resistant strain [EMRSA-15 (MecA)] was accomplished by the two-fold broth serial dilution technique in 96-well microtitre plates [10].

Acknowledgements

This research was partially supported by DGAPA, UNAM (IN 2142052) and The Royal Society.

References

[1] Pereda-Miranda R. Bioactive natural products from traditionally used Mexican plants. In: Arnason JT, Mata R, Romeo JT, editors. Phytochemistry of Medicinal Plants New York: Plenum Press, 1995: pp 83 – 112
[2] Emmart EW. The Badianus Manuscript (Codex Barberini, Latin 241), Vatican Library. An Aztec Herbal of 1552. Baltimore: The Johns Hopkins Press, 1940: p 268
[3] Varey S. The Mexican Treasury. The Writings of Dr. Francisco Hernández. Stanford: Stanford University Press, 2000: pp 200 – 1
[4] Pereda-Miranda R, Hernández L, Villavicencio MJ, Novelo M, Ibarra P. Structure and stereochemistry of pectinolides A – C, novel antimicrobial and cytotoxic 5,6-dihydro-α-pyrones from *Hyptis pectinata*. J Nat Prod 1993; 56: 583 – 93
[5] Tsuboi S, Sakamoto J, Yamashita H, Sakai T, Utaka M. Highly enantioselective synthesis of both enantiomers of γ-substituted butenolides by baker's yeast reduction and lipase-catalyzed hydrolysis. Total synthesis of (3A*S*,6a*S*)-ethisolide, whisky lactone, and (–)-avenaciolide. J Org Chem 1998; 63: 1102 – 8
[6] Snatzke G. Circular dichroism and optical rotatory dispersion. Principles and application to the investigation of the stereochemistry of natural products. Angew Chem 1968; 7: 14 – 25
[7] Boalino DM, Connolly JD, McLean S, Reynolds WF, Tinto WF. α-Pyrones and a 2(5*H*)-furanone from *Hyptis pectinata*. Phytochemistry 2003; 64: 1303 – 7
[8] Fragoso-Serrano M, González-Chimeo E, Pereda-Miranda R. Novel labdane diterpenes from the insecticidal plant *Hyptis spicigera*. J Nat Prod 1999; 62: 45 – 50
[9] Angerhofer CK, Guinaudeau H, Wongpanich V, Pezzuto JM, Cordell G. Antiplasmodial and cytotoxic activity of natural bisbenzylisoquinoline alkaloids. J Nat Prod 1999; 62: 59 – 66
[10] Lechner D, Stavri M, Oluwatuyi M, Pereda-Miranda R, Gibbons S. The anti-staphylococcal activity of *Angelica dahurica* (Bai Zhi). Phytochemistry 2004; 65: 331 – 5

Available online at www.sciencedirect.com
SCIENCE DIRECT®
Phytochemistry 66 (2005) 233–239
PHYTOCHEMISTRY
www.elsevier.com/locate/phytochem

Bioactive constituents of *Artemisia monosperma*

Michael Stavri [a], Christopher H.J. Ford [b], Franz Bucar [c], Bernhard Streit [c], Michael L. Hall [d], R. Thomas Williamson [d], K.T. Mathew [e], Simon Gibbons [a,*]

[a] *Centre for Pharmacognosy and Phytotherapy, The School of Pharmacy, University of London, 29–39 Brunswick Square, London WC1N 1AX, UK*
[b] *Department of Surgery, Faculty of Medicine, Kuwait University, P.O. Box 24923, Safat 13110, Kuwait*
[c] *Department of Pharmacognosy, Institute of Pharmaceutical Sciences, Karl-Franzens University, Universitätsplatz 4/I, A-8010 Graz, Austria*
[d] *Roche Carolina Inc., 6173 East Old Marion Highway, Florence, SC 29506-9330, USA*
[e] *The Herbarium, Department of Biological Science, Kuwait University, P.O. Box 5969, Safat 13060, Kuwait*

Received 27 October 2004
Available online 15 December 2004

Abstract

During a study on the chemistry and biological activity of Kuwaiti plants, new metabolites including 4,6-dihydroxy-3-[3′-methyl-2′-butenyl]-5-[4″-hydroxy-3″-methyl-2″-butenyl]-cinnamic acid (**1**), the 3*R*,8*R* stereoisomer of the C_{17} polyacetylene dehydrofalcarindiol (**2**) and a C_{10} polyacetylene glucoside (**3**) were characterised by spectroscopic means. Additionally, the previously characterised natural products 1,3*R*,8*R*-trihydroxydec-9-en-4,6-yne (**4**), spathulenol (**5**) and eriodyctiol-7-methyl ether (**6**) were also isolated.

Compounds **2**, **3**, and **4** were evaluated for their ability to inhibit the enzyme 12-lipoxygenase and **3** and **4** showed moderate activity at 30 μg/ml. Compound **2** was evaluated against a panel of colorectal and breast cancer cell lines and IC_{50} values ranged from 5.8 to 37.6 μg/ml. Against a panel of fast-growing mycobacteria and a standard ATCC strain of *Staphylococcus aureus*, compound **6** exhibited minimum inhibitory concentrations in the range of 64–128 μg/ml.

Keywords: *Artemisia monosperma*; Kuwait; 12-Lipoxygenase; *Mycobacterium*; *Staphylococcus aureus*, cytotoxic; polyacetylene

1. Introduction

The native flora of Kuwait consists of approximately 400 vascular plants (Daoud and Al-Rawi, 1985; Al-Rawi, 1987), with the family Asteraceae being the second largest taxon, particularly noticeable in the spring with their colourful flowers covering the entire desert. As part of a continuing study into the chemistry and biological activity of Kuwaiti plants (Gibbons et al., 1999; Gibbons et al., 2000; Stavri et al., 2004), we have studied *Artemisia monosperma* Del. (Asteraceae), a plant that has restricted distribution in Kuwait, being found growing along the Wadi-Al-Batin, a dry river bed running in a north-westerly direction along the border with Iraq. Previous phytochemical studies on this species have yielded polyyne, sesquiterpene (Stavri et al., 2004) and acetophenone natural products (Bohlmann and Ehlers, 1977). In this paper we detail the characterisation of three new metabolites (**1**–**3**) and the isolation of known metabolites including the sesquiterpene spathulenol, an hydroxylated polyyne and the flavonoid eriodyctiol-7-methyl ether. Where sufficient material permitted, compounds were evaluated for their activity in 12-lipoxygenase, antibacterial and cytotoxicity assays.

2. Results and discussion

Vacuum liquid chromatography of the chloroform extract of the aerial parts of *A. monosperma* led to the

* Corresponding author. Tel.: +44 207 7535913; fax: +44 207 7535909.
E-mail address: simon.gibbons@ulsop.ac.uk (S. Gibbons).

0031-9422/$ - see front matter © 2004 Elsevier Ltd. All rights reserved.
doi:10.1016/j.phytochem.2004.11.010

isolation of a colourless oil (**1**). HREIMS of **1** suggested a molecular formula of $C_{19}H_{24}O_5$ $[M]^+$ (332.1623). The ^1H NMR spectrum (Table 1) provided signals for four olefinic protons and one aromatic proton (δ_H 7.20). Two of the olefins were doublets and coupled to each other with large coupling constants indicative of a *trans* double bond (δ_H 7.70 d, J = 16.0 Hz, δ_H 6.30 d, J = 16.0 Hz). The remaining two olefins appeared as triplets with fine splitting and were reminiscent of the olefinic protons of prenyl (dimethyl allyl) substituents (δ_H 5.61, δ_H 5.31) (Nayar and Bhan, 1972). Three methyl singlets and two protons of an oxymethylene group also appearing as a singlet were detected in the ^1H NMR spectrum, confirming the presence of two prenyl groups. The ^{13}C NMR spectrum provided signals for 19 carbons, including 8 quaternary carbons of which two were oxygen bearing, 5 were olefinic/aromatic carbons and one was a carbonyl group (δ_C 172.1, C-9). With the presence of two prenyl substituents (10 carbons), a *trans* double bond and aromatic quaternary carbons, the NMR data indicated the presence of a prenylated *trans*-cinnamate structure.

Assuming a cinnamate moiety, it was possible by COSY, HMQC and HMBC spectra to unambiguously assign all resonances in the molecule and show that **1** was a diprenylated-dihydroxycinnamic acid. In the COSY spectrum, the *trans* olefin (H-8), coupled to its olefinic partner (H-7) and in the HMBC spectrum gave a ^2J correlation to a carboxyl carbonyl at C-9. The attachment of this three carbon chain to the aromatic ring was achieved by a ^3J correlation in the HMBC spectrum between H-8 and an aromatic quaternary carbon (C-1, δ_C 126.5). A further ^3J signal between H-7 and C-2 placed an aromatic methine group here. The proton associated with this aromatic methine carbon then provided ^3J signals to two oxygen-bearing quaternary aromatic carbons positioned at C-4 and C-6 of the aromatic ring. The molecular formula and downfield nature of the ^{13}C resonances for these carbons confirmed that hydroxyl groups should be placed at these positions. In the HMBC spectrum, H-2 also gave a ^3J signal to a methylene group (C-1′) of a prenyl moiety. This confirmed that one of the prenyl groups should be attached at C-3 of the aromatic ring. From the ^1H NMR spectrum, H-2 appeared as a small doublet (J = 3.5) which coupled to H_2-1′ in the COSY spectrum. Therefore the coupling constant of 3.5 Hz can be attributed to allylic coupling between H-2 and H_2-1′. The methylene protons (H_2-1′) coupled to an olefinic proton (H-2′) in the COSY spectrum and in the HMBC spectrum H_2-1′ also gave a ^3J correlation to an olefinic quaternary carbon (δ_C 135.9) placing this at C-3′. Two methyl groups (both at δ_H 1.80 s) gave ^2J signals to C-3′ placing these groups on this quaternary carbon and completing the first prenyl substituent. Further signals in the HMBC spectrum included those for H_2-1′ to C-3, the aromatic carbon to which it is attached and a ^3J signal to the oxygen-bearing aromatic quaternary carbon, C-4. The second prenyl group was placed at C-5 based on a ^2J correlation to this carbon from protons of a further methylene (H_2-1″). In the COSY spectrum H_2-1″ coupled to an olefinic proton (H-2″) and in the HMBC spectrum H_2-1″ provided a ^3J correlation to an olefinic quaternary carbon (C-3″). A methyl singlet (δ_H 1.80, H_3-5″) and a downfield methylene singlet (δ_H 4.08, H_2-4″) both gave ^2J HMBC correlations to C-3″, therefore these groups must be directly attached to this carbon. An hydroxyl was placed on the H_2-4″ methylene carbon, which would account for the downfield shift of both the ^1H and ^{13}C signals for this group. This completed resonances for the second prenyl moiety.

A sharp singlet at δ_H 3.96, had no correlation in the HMQC spectrum and must therefore be an hydroxyl group. This signal in the HMBC spectrum gave a ^2J correlation to an aromatic quaternary carbon (C-6), fixing its position. Both prenyl groups must be *ortho* with respect to C-4 as both methylene protons at H_2-1′ and H_2-1″ gave ^3J HMBC correlations to this carbon.

The structure of **1** was confirmed by correlations detected in the NOESY spectrum (Fig. 1). A correlation between H-2 and H_2-1′ placed these protons in close spatial proximity. A second NOE between H-2 and H-7 also meant these protons were in close association. Two key NOEs determined the stereochemistry of the second prenyl group. Firstly, an interaction between H_2-1″ and H_3-5″ placed these protons on the same face of this group (*cis*). A second NOE between the olefinic proton H-2″ and the oxymethylene protons H_2-4″ further confirmed the proposed stereochemistry of this prenyl group. Natural product **1** is therefore assigned as

Table 1
^1H (500 MHz) and ^{13}C NMR (125 MHz) spectral data and ^1H–^{13}C long-range correlations of **1** recorded in $CDCl_3$

Position	^1H	^{13}C	^2J	^3J
1	–	126.5		
2	7.20 *d* (3.5)	128.5		C-4, C-6, C-7, C-1′
3	–	127.7		
4	–	155.3		
5	–	127.2		
6	–	146.7		
7	7.70 *d* (16.0)	147.1	C-8	C-2, C-9
8	6.30 *d* (16.0)	114.2	C-9	C-1
9	–	172.1		
1′	3.37 *d* (7.0)	30.0	C-2′, C-3	C-3′, C-4
2′	5.31 *t* (7.0)	121.0	C-1′	C-4′, C-5′
3′	–	135.9		
4′	1.80 *s*	17.9	C-3′	C-2′, C-5′
5′	1.80 *s*	25.8	C-3′	C-2′, C-4′
1″	3.40 *d* (7.5)	28.5	C-2″, C-5	C-3″, C-4
2″	5.61 *t* (7.0)	122.8	C-1″	C-4″, C-5″
3″	–	137.1		
4″	4.08 *s*	68.5	C-3″	C-2″, C-5″
5″	1.80 *s*	13.8	C-3″	C-2″, C-4″
6-OH	3.96 *s*	–	C-6	

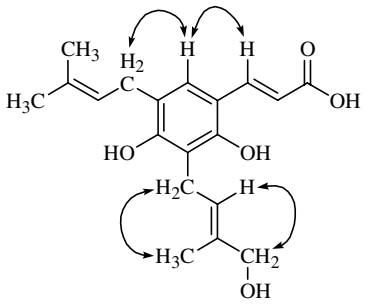

Fig. 1. Key NOE correlations for compound **1**.

4,6-dihydroxy-3-[3′-methyl-2′-butenyl]-5-[4″-hydroxy-3″-methyl-2″-butenyl]-cinnamic acid and is reported here for the first time.

Compound **2** was isolated as a pale yellow oil from the hexane extract. A molecular formula of $C_{17}H_{22}O_2$ was established by ESI-MS in the positive mode $[M + H]^+$ (259.0). The ^1H and ^{13}C NMR spectra were highly similar to those of falcarindiol, a widely occurring polyacetylenic natural product commonly found in the Apiaceae plant family and recently evaluated by us against multidrug-resistant strains of *Staphylococcus aureus* (Lechner et al., 2004). **2** differed from falcarindiol as it exhibited signals in the ^1H and ^{13}C NMR spectra (Table 2) indicating the presence of two vinyl groups. This accounted for the presence of an additional downfield methylene group at δ_H 2.05, (H_2-15). Four acetylenic carbons, two remaining olefins and two oxymethine groups were also present and similar to those found in falcarindiol, and by extensive 1 and 2-dimensional NMR studies (Table 2) we were able to show that compound **2** was the closely related metabolite, dehydrofalcarindiol. The data are in close agreement with those previously published (Bernart et al., 1996).

The absolute stereochemistry of **2** was determined by Mosher′s ester methodology (Seco et al., 2004), by esterifying the two hydroxyl groups attached to the chiral carbons with either *R*- or *S*-MPA (methoxyphenylacetic acid). The $\Delta\delta^{R,S}$ values ($\delta_R - \delta_S$) for H_2-1 (+0.19 and +0.15 ppm) and H-2 (+0.17 ppm) and also H-9 (+0.02 ppm) and H-10 (+0.10 ppm) were positive, indicating *R*-stereochemistry at both C-3 and C-8. This is the first report of the absolute stereochemistry of dehydrofalcarindiol as 3*R*,8*R*.

Natural product **3** was isolated as a pale yellow oil from the methanol extract by reverse-phase PTLC. A molecular formula of $C_{16}H_{22}O_8$ was assigned by ESI-MS $[M + Na]^+$ (365.1). The ^1H and ^{13}C NMR spectra (Table 2) provided resonances with similarity to **2** and almost identical to those found in 1,3*R*,8*R*-trihydroxy-dec-9-en-4,6-yne (**4**), a polyacetylenic natural product recently reported by us from this species (Stavri et al., 2004) but additional resonances were present for a hexose sugar. Signals for the aglycone moiety indicated the presence of an *exo*-methylene, an olefin, two oxymethine groups, a methylene and oxymethylene groups as well as four acetylenic quaternary carbons.

Table 2
^1H (500 MHz) and ^{13}C NMR (125 MHz) spectral data for **2** and **3** recorded in $CDCl_3$ and CD_3OD respectively

Position	^1H	^{13}C
2		
1	5.25 *dt* (10.5, 1.0)	117.3
	5.45 *dt* (17.0, 1.0)	
2	5.93 *ddd* (15.5, 10.5, 1.5)	135.8
3	4.93 *m*	63.5
4	–	78.3
5	–	70.3
6	–	68.7
7	–	79.8
8	5.20 *d* (8.5)	58.6
9	5.53 *ddt* (10.5, 8.5, 1.0)	127.8
10	5.61 *ddt* (10.5, 7.5, 1.0)	134.5
11	2.11 *m*	27.6
12	1.38 *m*	29.1
13	1.33 *m*	28.7
14	1.38 *m*	28.6
15	2.05 *m*	33.7
16	5.81 *ddt* (17.0, 10.0, 7.0)	139.0
17	4.95 *m*	114.3
	5.00 *dd* (17.5, 1.5)	
3		
1	3.73 *dt* (11.0, 6.0)	66.7
	3.99 *dt* (10.0, 6.0)	
2	1.97 *dd* (13.0, 7.0)	38.9
3	4.63 *t* (7.0)	60.0
4	–	82.0
5	–	68.9
6	–	70.1
7	–	79.5
8	4.88 *m*	63.8
9	5.91 *ddd* (17.0, 10.0, 5.5)	138.0
10	5.20 *dt* (10.0, 1.5)	116.6
	5.41 *dt* (17.0, 1.5)	
1′	4.27 *d* (7.5)	104.5
2′	3.17 *dd* (9.0, 8.0)	75.1
3′	3.35 *dd* (9.0, 8.0)	77.9
4′	3.28 *m*	71.6
5′	3.50 *m*	78.0
6′	3.68 *dd* (12.0, 5.0)	62.7
	3.87 *dd* (11.5, 1.5)	

In the COSY spectrum of **3**, the *exo*-cyclic methylene protons coupled to the olefin proton which also coupled to the first oxymethine signal (δ 4.88, C-8). This oxymethine then exhibited ^2J and ^3J correlations in the HMBC spectrum to two acetylenic carbons (C-7 and C-6). Further couplings in the COSY spectrum included those between the oxymethylene (C-1), methylene (C-2) and remaining oxymethine proton (δ 4.63, C-3) (Table 2), which resulted in a CH(O)-CH_2CH_2O system. In the HMBC spectrum the oxymethine resonance of this spin system also coupled to two acetylenic quaternary carbons (C-4 and C-5). The shielded nature of the two

triple bonds suggested that they must be conjugated and connected and this is a common feature in many acetylenes and was also seen with dehydrofalcarindiol (**2**). The deshielded nature of C-3 and C-8 and the ESIMS suggested that hydroxyl groups be placed at these positions. These data therefore confirmed that the aglycone is in fact 1,3,8-trihydroxydec-9-en-4,6-yne.

The hexose gave signals for four oxymethine groups, an oxymethylene and an anomeric carbon (δ_C 104.5) (Table 2). The COSY spectrum provided correlations between the anomeric proton (H-1′) and H-2′, H-2′ to H-3′, H-3′ to H-4′, H-4′ to H-5′ and H-5′ to the oxymethylene protons (H_2-6′). The coupling between the anomeric proton and H-2′ was large (7.5 Hz) as was the coupling between H-2′ and H-3′ (9.0 Hz). H-3′ appeared as a double doublet with a second coupling of 8.0 Hz indicating axial configuration for H-1′, H-2′, H-3′ and H-4′. An NOE between H-1′ and H-5′ indicated axial configuration for H-5′ and this was further confirmed by a second NOE between H-3′ and H-5′ and therefore the hexose was assigned as glucose. The point of attachment of the glucose moiety to the aglycone was shown to be at C-1 of the polyacetylene due to the presence of a ^3J correlation between the anomeric proton and the oxymethylene carbon (C-1) in the HMBC spectrum. Compound **3** is therefore assigned as 3(ζ),8(ζ)-dihydroxydec-9-en-4,6-yne-1-*O*-β-D-glucopyranoside. It is likely that the absolute stereochemistry of the hydroxyl groups at positions 3 and 8 is the same as that previously determined for the aglycone using Mosher's ester methodology, although the presence of glucose in the molecule has added to the difficulty in conducting the stereochemical analysis and therefore absolute configuration has not been assigned at these positions.

Compounds **4**, spathulenol (**5**) and eriodyctiol-7-methyl ether (**6**), were also isolated and characterised by direct comparison with the literature (Stavri et al., 2004; Inagaki and Abe, 1985; Wollenweber, 1981).

Acetylenic compounds are known to have activity against oxygenase enzymes (Resch et al., 2001; Liu et al., 1998) and compounds **2**, **3** and **4** were tested for their ability to inhibit 12-lipoxygenase (Table 3). This enzyme is implicated in many disorders including cancer, psoriasis, atherosclerosis, rheumatoid arthritis and epilepsy (Yoshimoto and Takahashi, 2002; Nie and Honn, 2002; Virmani et al., 2001; Müller, 1994). Compound **3** showed a moderate inhibitory dose dependent activity whereas **4** revealed an inverse dose activity relationship. The reason for this effect could not be elucidated during the present investigation. However, it has been shown previously that collagen or CRP (collagen-related peptide) mediated platelet 12-LOX product generation was potentiated by inhibition of PKC by the specific inhibitor chelerythrine (Coffey et al., 2004).

Table 3
12-Lipoxygenase inhibitory activity of **2**–**4**

Compound	Concentration (μg/ml)	% Inhibition[a]
2	10	0
2	30	0
3	10	8.11
3	30	25.81
4	10	32.17
4	30	18.15
Baicalein	10	56.23

[a] % inhibition is calculated by comparing 12(*S*)-HETE contents of samples containing the test compound versus control (solvent instead of inhibitor) using the following equation: % inhibition = {[12(*S*)-HETE]$_{control}$−[12(*S*)-HETE]$_{sample}$}/[12(*S*)−HETE]$_{control}$.

The 3(ζ),8(ζ) isomer of compound **2** has been shown to have cytotoxicity against human hepatocellular and epidermoid carcinoma cell lines with IC_{50} values of 9.3 and 29.8 μg/ml, respectively (Setzer et al., 1995). Compound **2** was therefore tested against a panel of colorectal and breast cancer cell lines (Table 4) to ascertain its IC_{50}. The greatest efficacy (lowest IC_{50} value) was seen with the breast cancer line MCF7, and COLO320DM was the most sensitive of the colorectal cell lines. Interestingly, this was the opposite of how this cell line responds to doxorubicin where it is highly resistant in comparison to LS174T and SKCO1.

All compounds were also evaluated against fast-growing strains of *Mycobacterium* and a standard ATCC strain of *S. aureus* (Table 5). Only eriodyctiol-7-methyl ether (**6**) was active against the bacteria tested, with moderate minimum inhibitory concentrations ranging from 64 to 128 μg/ml.

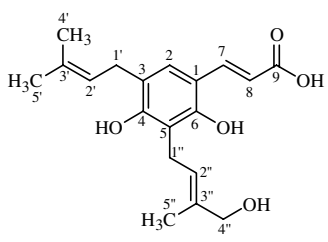

(**1**)

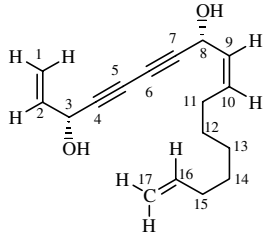

(**2**)

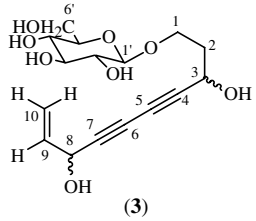

(**3**)

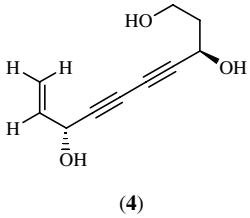

(**4**)

3. Experimental

3.1. General experimental procedures

NMR spectra were recorded on a Bruker AVANCE 500 MHz spectrometer. Chemical shift values (δ) were

Table 4
Cytotoxicity evaluation of compound **2**

Cell line	Type of cancer	Number of repeat assays	IC_{50} (μg/ml)[a]	Dilutions of DMSO causing toxicity	Doxorubicin IC_{50} (ng/ml)[c]
LS174T	Colorectal	3	14.8 (7.2)[b]	1/20–1/40	324 (100)[+]
SKCO1	Colorectal	3	13.3 (5.4)	1/20–1/40	28.5 (10)
COLO320DM	Colorectal	2	9.6	1/20–1/40	1163 (168)
WIDR	Colorectal	2	10.9	1/20–1/80	NT
MDA231	Breast	1	37.6	1/20–1/40	NT
MCF7	Breast	2	5.8	1/20–1/40	NT

NT, not tested.
[a] **2** was tested from 500 to 1.95 μg/ml and the DMSO control from 1/10 to 1/2560 dilutions to equate with the amount that would be present in the drug dilutions.
[b] Mean values with SDs in parentheses.
[c] Values for doxorubicin from previous studies (Ford et al., 2001).

Table 5
Antibacterial activity of **6**

Compound	*M. fortuitum* ATCC 6841	*M. phlei* ATCC 11758	*M. aurum* ATCC 23366	*M. smegmatis* ATCC 14468	*S. aureus* ATCC 25923
6	128	>128	64	128	128
Ethambutol	4	2	1	0.5	–
Isoniazid	0.5	2	2	2	–
Norfloxacin	–	–	–	–	0.5

–, Not tested

reported in parts per million (ppm) relative to appropriate internal solvent standard and coupling constants (*J* values) are given in Hertz. Mass spectra were recorded on VG ZAB-SE instrument (FAB-EIMS) and Finnigan navigator (ESIMS). IR spectra were recorded on a Nicolet 360 FT-IR spectrophotometer and UV spectra on a Perkin-Elmer Lambda 15 UV/Visible spectrophotometer.

3.2. Plant material

Artemisia monosperma was collected from the sandy gullies in north-western Kuwait that are bordered with sandstone ridges. These gullies open westwards into the plains of the Wadi Al-Batin that extend beyond the border into Iraq. The material was identified by K. T. M. A voucher specimen (KTM 4225, collected by K.T. Mathew and S. Gibbons on the 19th of February, 1999) is deposited at the Kuwait University Herbarium (KTUH).

3.3. Extraction and isolation

285 g of air-dried and powdered aerial parts were extracted in a Soxhlet apparatus using sequential extraction by hexane (3L), chloroform (3L) and finally methanol (3L). The chloroform extract (10 g) was subjected to vacuum liquid chromatography (VLC) on silica gel (15 g) eluting with hexane containing 10% increments of ethyl acetate to yield 12 fractions. The fraction eluted with 100% ethyl acetate was further purified by Sephadex LH-20 chromatography eluting with methanol. Final purification by multiple preparative TLC (2 times) (silica gel; toluene:EtOAc:AcOH, 30:68:2) afforded **1** (5.4 mg). Vacuum liquid chromatography of the hexane extract (10.0 g) on silica gel (15 g) eluting with hexane containing 10% increments of ethyl acetate yielded 12 fractions. The fraction eluted with 40% ethyl acetate was subjected to flash chromatography, eluting with hexane:ethyl acetate (8:2). Further purification by multiple PTLC (3 times) (silica gel; hexane: EtOAc; 8:2) afforded **2** (14 mg).

Vacuum liquid chromatography of the methanol extract (8.2 g) on silica gel (12 g) eluting with ethyl acetate containing 10% increments of methanol yielded 12 fractions. The fraction eluted with 70% ethyl acetate was further purified by C_{18} solid phase extraction (eluting with water:methanol; 8:2), followed by reverse phase PTLC (water:methanol; 7:3) afforded **3** (18 mg).

3.4. Preparation of Mosher's esters for compound 2

Compound **2** (5.26 mg) was dissolved in 525 μl of $CDCl_3$. 100 μl of this stock preparation was added to a vial containing 1.9 mg of *R*- or *S*-MPA, 16.3 mg of PS-carbodiimide resin (Argonaut Inc. Foster City CA, USA), 0.4 mg of DMAP and 0.75 mL of $CDCl_3$. The reaction mixtures were agitated overnight on a Turbula mixer. Each mixture was then applied to individual preconditioned silica solid phase extraction cartridges. The products were eluted from the cartridges using CH_2Cl_2 and evaporated to dryness under N_2.

3.5. 12-Lipoxygenase assay

The 12(*S*)-LOX inhibitory assay was conducted in vitro using human platelets as reported previously (Schneider et al., 2004). The platelets prepared from human blood were preincubated with reduced glutathione and the test compound or the positive control, baicalein. The suspensions were further incubated in the presence of arachidonic acid for 7 min and the reaction was terminated by adding 2 M HCl. 12(*S*)-HETE was quantified using a Correlate-EIA™-12(*S*)-HETE-kit (Assay Designs, Ann Arbor). The concentrations of 12(*S*)-HETE were calculated in relation to a standard 12(*S*)-HETE. The mean values of two measurements were taken and tests were conducted three times.

3.6. Cytotoxicity assay

The in vitro sensitivity of 6 human cancer cell lines (colorectal – LS174T, SKCO1, COLO320DM, WIDR: breast – MDA231, MCF7) to **2** was tested in an MTT assay, performed essentially as previously described (Ford et al., 2001). Cell lines were grown as monolayers in Eagle's MEM (MDA231, MCF7, WIDR, LS174T, SKCO1) or RPMI1640 (COLO320DM) containing 10% foetal calf serum and were maintained in culture as previously described (Ford et al., 1996). Briefly, cell lines were trypsinised and 10^4 cells plated into microplate wells, allowed a 24-h recovery, exposed to concentrations of **2** or equivalent dilutions of DMSO for 24 h followed by washing, a 24-h recovery period and then termination of the assay.

3.7. Antibacterial assay

Mycobacterium species were acquired from the NCTC. *S. aureus* strain ATCC25923 was the generous gift of E. Udo (Kuwait University, Kuwait). Mycobacterial strains were grown on Columbia Blood agar (Oxoid) supplemented with 7% defibrinated Horse blood (Oxoid) and incubated for 72 h at 37 °C prior to minimum inhibitory concentration (MIC) determination. *S. aureus* ATCC 25923 was cultured on nutrient agar and incubated for 24 h at 37 °C prior to MIC determination. Bacterial inocula equivalent to the 0.5 McFarland turbidity standard were prepared in normal saline and diluted to give a final inoculum density of 5×10^5 cfu/ml. The inoculum (125 μL) was added to all wells and the microtitre plate was incubated at 37 °C for 18 h for *S. aureus* and 72 h for *M. fortuitum*, *M. smegmatis* and *M. phlei*. For *M. aurum* the plate was incubated for 120 h. The MIC was recorded as the lowest concentration at which no bacterial growth was observed as previously described (Gibbons and Udo, 2000).

Ethambutol and isoniazid were used as positive controls for the mycobacterial strains and norfloxacin was used for *S. aureus*.

3.8. 4,6-Dihydroxy-3-[3′-methyl-2′-butenyl]-5-[4″-hydroxy-3″-methyl-2″-butenyl]-cinnamic acid (*1*)

Colourless oil; UV ($CHCl_3$) λ_{max} (log ε): 314 (8.15), 241 (7.86) nm; IR ν_{max} (thin film) cm^{-1}: 3328, 2915, 1684, 1635, 1473, 1270, 1199, 982; ^1H NMR and ^{13}C NMR ($CDCl_3$): see Table 1; HREI-MS (*m*/*z*): 332.1623 $[M]^+$ (calc. for $C_{19}H_{24}O_5$, 332.1623).

3.9. 3R,8R-Dehydrofalcarindiol (*2*)

Pale yellow oil; $[\alpha]_D^{25}$ + 39.8° (*c* 2.66, $CHCl_3$); UV ($CHCl_3$) λ_{max} (log ε): 284 (8.27), 268 (8.52), 254 (8.36), 244 (8.25) nm; IR ν_{max} (thin film) cm^{-1}: 3351, 2929, 2856, 2232, 2146, 1641, 1457, 1285, 993; ^1H NMR and ^{13}C NMR ($CDCl_3$): see Table 2; ESI-MS (*m*/*z*): 259.0 $[M + H]^+$.

3.10. 3(ζ),8(ζ)-Dihydroxydec-9-en-4,6-yne-1-O-β-D-glucopyranoside (*3*)

Pale yellow oil; $[\alpha]_D^{25}$ − 45.3° (*c* 0.75, CH_3OH); UV (CH_3OH) λ_{max} (log ε): 265 (7.97), 212 (8.06); IR ν_{max} (thin film) cm^{-1}: 3376, 2889, 1654, 1244, 1077, 1035; ^1H NMR and ^{13}C NMR (CD_3OD): see Table 2; HRESI-MS (*m*/*z*): 365.1190 $[M + Na]^+$ (calc. for $C_{16}H_{22}O_8Na$, 365.1212).

Acknowledgements

We thank the School of Pharmacy for a Doctoral Scholarship to Michael Stavri and the Engineering and Physical Sciences Research Council for funding (Grant No. GR/R47646/01). C.H.J.F. thanks Dr. B. Rego and Annie Mathew for assistance.

References

Al-Rawi, A., 1987. Flora of Kuwait, vol. 2. Alden Press, Oxford.

Bernart, M.W., Cardellina II, J.H., Balaschak, M.S., Alexander, M.R., Shoemaker, R.H., Boyd, M.R., 1996. Cytotoxic falcarinol oxylipins from *Dendropanax arboreus*. Journal of Natural Products 59, 748–753.

Bohlmann, F., Ehlers, D., 1977. Ein neues *p*-hydroxyacetophenonderivat aus *Artemisia monosperma*. Phytochemistry 16, 1450–1451.

Coffey, M.J., Jarvis, G.E., Gibbins, J.M., Coles, B., Barrett, N.E., Wylie, O.R.E., O'Donnell, V.B., 2004. Platelet 12-lipoxygenase activation via glycoprotein VI Involvement of multiple signaling pathways in agonist control of H(P)ETE synthesis. Circulation Research 94, 1598–1605.

Daoud, H.S., Al-Rawi, A., 1985. The Flora of Kuwait, vol. 1. KPI Publishers, London.

Ford, C.H.J., Tsaltas, G.C., Osborne, P.A., Addetia, K., 1996. Novel flow cytometric analysis of the progress and route of internalization of a monoclonal anti-carcinoembryonic antigen (CEA) antibody. Cytometry 23, 228–240.

Ford, C.H.J., Osborne, P.A., Rego, B.G., Mathew, A., 2001. Bispecific antibody targeting of doxorubicin to carcinoembryonic antigen-expressing colon cancer cell lines in vitro and in vivo. International Journal of Cancer 92, 851–855.

Gibbons, S., Mathew, K.T., Gray, A.I., 1999. A caffeic acid ester from *Halocnemum strobilaceum*. Phytochemistry 51, 465–467.

Gibbons, S., Denny, B.J., Ali-Amine, S., Mathew, K.T., Skelton, B.W., White, A.H., Gray, A.I., 2000. NMR spectroscopy, X-ray crystallographic, and molecular modeling studies on a new pyranone from *Haloxylon salicornicum*. Journal of Natural Products 63, 839–840.

Gibbons, S., Udo, E.E., 2000. The effect of reserpine, a modulator of multidrug efflux pumps, on the in vitro activity of tetracycline against clinical isolates of methicillin resistant *Staphylococcus aureus* (MRSA) possessing the tet(K) determinant. Phytotherapy Research 14, 139–140.

Inagaki, F., Abe, A., 1985. Analysis of ^{1}H and ^{13}C nuclear magnetic resonance spectra of spathulenol by two-dimensional methods. Journal of Chemical Society Perkin Transactions II, 1773–1778.

Lechner, D., Stavri, M., Oluwatuyi, M., Pereda-Miranda, R., Gibbons, S., 2004. The anti-staphylococcal activity of *Angelica dahurica* (Bai Zhi). Phytochemistry 65, 331–335.

Liu, J.H., Zschocke, S., Reininger, E., Bauer, R., 1998. Inhibitory effects of *Angelica pubescens biserrata* on 5-lipoxygenase and cyclooxygenase. Planta Medica 64, 525–529.

Müller, K., 1994. 5-Lipoxygenase and 12-lipoxygenase: attractive targets for the development of novel antipsoriatic drugs. Archiv der Pharmazie (Weinheim) 327, 3–19.

Nayar, M.N.S., Bhan, M.K., 1972. Coumarins and other constituents of *Hesperethusa crenulata*. Phytochemistry 11, 3331–3333.

Nie, D., Honn, K.V., 2002. Cyclooxygenase, lipoxygenase and tumor angiogenesis. Cellular and Molecular Life Sciences 59, 799–807.

Resch, M., Heilmann, J., Steigel, A., Bauer, R., 2001. Further phenols and polyacetylenes from the rhizomes of *Atractylodes lancea* and their anti-inflammatory activity. Planta Medica 67, 437–442.

Schneider, I., Gibbons, S., Bucar, F., 2004. Inhibitory activity of *Juniperus communis* on 12(*S*)-HETE production in human platelets. Planta Medica 70, 471–474.

Seco, J.M., Quinoa, E., Riguera, R., 2004. The assignment of absolute configuration by NMR. Chemical Reviews 104, 17–118.

Setzer, W.N., Green, T.J., Whitaker, K.W., Moriarity, D.M., Yancey, C.A., Lawton, R.O., Bates, R.B., 1995. A cytotoxic diacetylene from *Dendropanax arboreus*. Planta Medica 61, 470–471.

Stavri, M., Mathew, K.T., Gibson, T., Williamson, R.T., Gibbons, S., 2004. New constituents of *Artemisia monosperma*. Journal of Natural Products 67, 892–894.

Virmani, J., Johnson, E.N., Klein-Szanto, A.J.P., Funk, C.D., 2001. Role of platelet-type12-lipoxygenase in skin carcinogenesis. Cancer Letters 162, 161–165.

Wollenweber, E., 1981. Unusual flavanones from a rare American fern. Zeitschrift Fur Naturforschung 36, 604–606.

Yoshimoto, T., Takahashi, Y., 2002. Arachidonate 12-lipoxygenases. Prostaglandins and Other Lipid Mediators 68–69, 245–262.

Antimycobacterial Coumarins from the Sardinian Giant Fennel (*Ferula communis*)

Giovanni Appendino,*,† Enrico Mercalli,‡ Nicola Fuzzati,‡ Lolita Arnoldi,‡ Michael Stavri,§ Simon Gibbons,*,§ Mauro Ballero,⊥ and Andrea Maxia⊥

Dipartimento di Scienze Chimiche, Alimentari, Farmaceutiche e Farmacologiche, Università del Piemonte Orientale, Viale Ferrucci 33, 28100 Novara, Italy, Indena S.p.A., Via Don Minzoni 6, 20090 Settala (MI), Italy, Centre for Pharmacognosy and Phytotherapy, The School of Pharmacy, University of London, 29-39 Brunswick Square, London WC1N 1AX, U.K., and Dipartimento di Scienze Botaniche, Università di Cagliari, Viale Fra Ignazio 13, 09124 Cagliari, Italy

Received September 4, 2004

The structure of a new prenylated coumarin (*E*-ω-benzoyloxyferulenol, **1b**) from the Sardinian giant fennel (*Ferula communis*) has been confirmed by synthesis. The parent compound ferulenol (**1a**) showed submicromolar antimycobacterial activity, which was partly retained in **1b** and in the simplified synthetic analogue **3**, but diminished in its ω-hydroxy and ω-acetoxy derivatives (**1c** and **1d**, respectively). The outstanding activity of **1a**, its low toxicity, and the evidence for definite structure−activity relationships make this prenylated 4-hydroxycoumarin an interesting antibacterial chemotype worth further investigation.

The presence of two distinct chemotypes of giant fennel (*Ferula communis* L.; Apiaceae) has complicated the study of ferulosis, a hemorrhagic and often lethal intoxication of livestock pasturing in areas of Sardinia infested with this invasive species.[1] On the other hand, this chemical polymorphism has given phytochemists a unique opportunity to obtain large amounts of structurally unrelated bioactive compounds from the same species. Thus, while the poisonous chemotype is an excellent source of ferulenol (**1a**),[2] a hemorrhagic prenylated coumarin that shows also paclitaxel (Taxol) mimicry,[3] the potent phytoestrogen ferutinin (**2**) can be obtained in large amounts from the nonpoisonous chemotype.[4] Remarkably, the two chemotypes occupy distinct enclaves, and an extensive investigation failed to detect mixed populations.[5] The basis of this behavior remains unknown, but preliminary studies have shown distinct genetic diversities between the two chemotypes, which are otherwise morphologically indistinguishable.[6]

During the development of an expeditious HPLC procedure to fingerprint the two chemotypes, we noticed the presence of a minor compound having chromatographic behavior and a UV spectrum similar to those of ferulenol but with a higher molecular weight (+104 amu), corresponding to the introduction of a benzoyloxy group. From the mass fragmentation pattern, this moiety was located on one of the two ω-carbons of the prenyl group, but the low natural abundance and the close chromatographic behavior compared to ferulenol (**1a**), a major constituent of the extract, prevented its direct isolation.[7] To solve this matter, we planned to synthesize the *E*-isomer of the alleged structure (**1b**) from *E*-ω-hydroxyferulenol (**1c**), a compound easily available by isolation,[2] and compare the chromatographic and spectroscopic properties (UV, MS) of the synthetic compound with those of the unknown chromatographic peak.

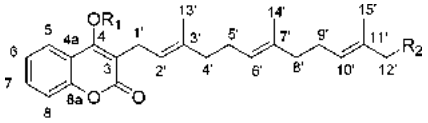

	R_1	R_2
1a	H	H
1b	H	OBz
1c	H	OH
1d	H	OAc
1e	Bz	OBz

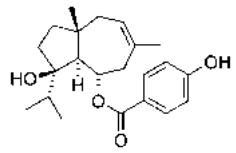

2

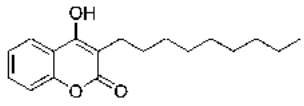

3

Diastereomerically pure *E*-ω-hydroxyferulenol (**1c**) was obtained, in 1.05% yield, along with ferulenol (**1a,** 0.55%) and its ω-acetoxy derivative (**1d**, 0.20%),[8] from a sample of giant fennel collected in southern Sardinia. The presence of *E,Z*-mixtures of ω-oxygenated ferulenols has been previously reported,[8] but in the sample under investigation, both ω-acetoxy and ω-hydroxyferulenol were obtained in a diastereomerically pure *E*-form. To prepare a compound with the alleged formula of the unknown peak, compound **1c** was treated with an excess of benzoyl chloride to afford the dibenzoate **1e**, which was then subjected to chemoselective deprotection. Opening of the lactone ring and decarboxylation to a prenylacetophenone[9] were not observed when a transamidation rather than a hydrolysis reaction was employed. Pyrrolidine is the standard base for the chemoselective transamidation of phenolic esters, but in our case, the two reaction products (**1b** and *N*-

* To whom correspondence should be addressed. Tel: +39 0321 375744 (G.A.); +44 207 753 5913 (S.G.). Fax: +39 0321 375631 (G.A.); +44 207 753 5909 (S.G.). E-mail: appendino@pharm.unipmn.it (G.A.); simon.gibbons@ulsop.ac.uk (S.G.).
† Università del Piemonte Orientale.
‡ Indena S.p.A.
§ University of London.
⊥ Università di Cagliari.

10.1021/np049706n CCC: $27.50
Published on Web 11/25/2004

Table 1. Minimum Inhibitory Concentrations (MIC, μg/mL) against Fast-Growing *Mycobacterium* Species of the Natural Coumarins **1a**−**1d**

species	ferulenol (**1a**)	**1b**	**1c**	**1d**	ethambutol	isoniazid
M. fortuitum	2	16	64	32	8	0.5
M. phlei	2	2	16	8	2	4
M. aurum	2	8	32	16	0.5	2
M. smegmatis	0.5	2	16	8	0.5	1

benzoylpyrrolidine) had very similar chromatographic mobility in a variety of solvents and could not be separated. The problem was solved by replacing pyrrolidine with ethylendiamine, which eventually afforded **1b** in overall 56% yield from **1c**. The NMR spectra confirmed the structure **1b** for the semisynthetic benzoate. Thus, when compared with *E*-ω-hydroxyferulenol (**1c**), a downfield shift ($\Delta\delta$ = +0.70) was observed for the allylic oxymethylene protons (H-12′a,b) in the ^{1}H NMR spectrum and diagnostic α- and γ-downfield (C-12′, C-10′; $\Delta\delta$ = 1.6 and 3.5, respectively) and β-upfield (C-11, $\Delta\delta$ = 4.1) shifts in the ^{13}C NMR spectrum.[10] Semisynthetic **1b** had a chromatographic mobility and UV and MS spectra indistinguishable from those of the unknown peak, suggesting that the two compounds are identical.

The antitubercular activity of ferulenol (**1a**) has been reported in preliminary form.[11] We have confirmed this antimycobacterial activity (Table 1), discovering excellent potency toward four strains of fast-growing mycobacteria, including *Mycobacterium fortuitum* ATCC 6841, which has been shown to be of use as an alternative screening model for potential antitubercular drugs.[12] The 12′-hydroxy-, 12′-benzoyloxy-, and 12′-acetoxy derivatives of ferulenol were also evaluated using these fast-growing strains. Introduction of a hydroxyl or an acetoxyl at position C-12′ (**1c** and **1d**, respectively) caused a marked reduction of potency, whereas a benzoyloxy group at C-12′ was better tolerated, fully restoring the antibacterial activity of the parent compound against *M. phlei* and *M. smegmatis* and, to a lesser extent, *M. fortuitum* and *M. aurum*. These observations indicate that a large and lipophilic group at C-12′ of ferulenol is tolerated.

Although ferulenol (**1a**) shows in vivo anticoagulant activity, its acute toxicity is low compared to warfarin.[13] Indeed, rather than with the presence of ferulenol, the toxicity of giant fennel seems better correlated with that of its ω-oxygenated derivatives. Thus, ferulenol could be detected in large amounts in samples of giant fennel coming from areas (Sicily, Crete, and continental Greece) where ferulosis is rare or unknown,[14] while the presence of ω-oxygenated derivatives is the hallmark of the plants coming from Sardinia and Morocco, where this intoxication is still widespread in livestock.[1,15]

Binding to tubulin seemingly underlies the cytotoxic activity of ferulenol (**1a**),[3] while as a 4-hydroxycoumarin derivative, its anticoagulant properties are due to inhibition of the enzyme vitamin K epoxide reductase.[16] Since neither protein is expressed in mycobacteria, a third and yet unknown antimicrobial target for ferulenol may exist, with possible divergences in the structure−activity requirements of the various molecular targets. In this context, it is interesting to remark that the structure of ferulenol combines two structural elements, the enolized β-dicarbonyl and the farnesyl moieties, individually present in two classes of antibacterial compounds.[17,18] Novobiocin, a coumarin that has limited use as a treatment for infections caused by Gram-positive bacteria, particularly resistant *Staphylococcus aureus* strains, also possesses a hydroxyl at C-4 and a substituent at C-3. This compound has been shown to inhibit mycobacterial DNA gyrase,[19] and it does not seem unreasonable to assume as a starting working hypothesis that ferulenol also exerts antimycobacterial effects via this mechanism.

When compared to the therapeutically used antimycobacterials such as isoniazid and ethambutol, the activity of ferulenol (**1a**) is promising, validating further work to evaluate the effects of its structural modification. Remarkably, antitubercular activity was substantially retained in a simpler analogue, 3-nonyl-4-hydroxycoumarin (**3**) (MIC = 3.5 μg/mL against *M. fortuitum*), a compound easily available by synthesis.[20] This observation shows that the isoprenoid features of the substituent at C-3 (methyl branches and double bonds) are redundant for the antimicrobial activity of ferulenol and suggests that this compound can serve as a basis for an analogue program aimed at defining the critical structure for antitubercular activity and its dissection from cytotoxic and anticoagulant properties.

Experimental Section

General Experimental Procedures. IR spectra were obtained on a Shimadzu DR 8001 spectrophotometer. The ^{1}H and ^{13}C NMR spectra were recorded at room temperature on a Varian INOVA 300 spectrometer, operating at 300 MHz for ^{1}H and 75 MHz for ^{13}C. Chemical shifts were referenced to the residual solvent signal. HRMS were recorded on a VG Prospect (Fisons) mass spectrometer. Mass spectral analyses were performed with a Finnigan MAT LCQ ion trap sammspectrometer equipped with both ESI and APCI interfaces. HPLC-DAD analyses were obtained on a system made up by a SpectraSYSTEM AS 3000 automatic sample injector module and a SpectraSYSTEM UV6000LP diode array detector (DAD). Silica gel 60 (70−230 mesh) was used for gravity column chromatography.

Plant Material. *F. communis* L. was collected in October 2001 near Cagliari, Sardinia, Italy, and identified by M.B. A voucher specimen (612A) is deposited at the Dipartimento di Scienze Botaniche, Università di Cagliari.

HPLC-DAD-UV Analysis of Giant Fennel Extracts. Powdered, dried roots (0.5 g) were treated with MeOH (150 mL) and extracted under sonication. After filtration, the extracts were analyzed on a Zorbax XDB column (250 × 4.6 mm) with a binary eluant system [0.1% HCOOH in water (solvent A) and 0.1% HCOOH in acetonitrile (solvent B)], starting with 55% A for 5 min and moving then to a linear gradient, from 55% A to 10% A in 40 min. The flow rate was 1.0 mL/min, and the injection volume 10 μL. For ESIMS detection, the following parameters were employed: (a) positive mode: capillary temp 250 °C; sheath gas flow 90 units; auxiliary gas flow 60 units; source voltage 4.8 kV; capillary voltage 19 kV; (b) negative mode: capillary temp 290 °C; sheath gas flow 80 units; auxiliary gas flow 40 units; source voltage 6.0 kV; capillary voltage 30 kV; vaporizer temperature 350 °C. The unknown peak identified as **1b** had a retention time of 36 min and UV maxima at 282 and 310 nm and presented an intense ion at *m/z* 365, attributable to the loss of benzoic acid from the pseudomolecular ion at *m/z* 487.

Isolation of ω-Hydroxyferulenol. A sample (450 g) of roots was powdered and extracted with acetone (3 × 3 L). The pooled extracts were evaporated to give 38 g of a brownish syrup, which was fractionated by gravity column chromatography (100 g silica gel, petroleum ether−EtOAc gradient) to give ferulenol (**1a**) (petroleum ether−EtOAc (9:1), 2.23 g, 0.55%), *E*-ω-acetoxyferulenol (**1d**) (petroleum ether−EtOAc 8:2, 0.82 g, 0.20%), and *E*-ω-acetoxyferulenol (**1c**) (petroleum ether−EtOAc (7:3), 4.2 g, 1.05%), identified by comparison (^{1}H NMR, TLC) with authentic standards.[8]

Synthesis of *E*-ω-Benzoyloxyferulenol (1b) from *E*-ω-Hydroxyferulenol (1c). (a) To a solution of **1c** (1.0 g, 2.6 mmol) in toluene (8 mL) were added benzoic acid (950 mg, 7.8 mmol, 3 molar equiv), dicyclohexylcarbodiimide (DCC) (1.6 g,

7.8 mmol, 3 molar equiv), and 4-(dimethylamino)pyridine (DMAP) (79 mg, 0.65 mmol, 0.25 molar equiv). After stirring overnight at room temperature, the reaction was worked up by filtration over alumina (ca. 5 g) to remove dicyclohexyl urea and the excess acid, and evaporation. The residue was further purified by filtration over silica gel (20 g) using petroleum ether−EtOAc (9:1) as eluant, to afford 1.3 g (82%) of crude **1e**. (b) To a solution of **1e** (583 mg, 0.96 mmol) in toluene (6 mL) was added an excess of ethylendiamine (320 μL, 288 mg, 4.8 mmol, 5 molar equiv), resulting in the formation of an orange color. After stirring at room temperature for 20 min, the reaction was worked up by dilution with EtOAc (10 mL) and washing with 2 N H_2SO_4 and brine. After drying (Na_2SO_4) and evaporation, the residue was purified by gravity column chromatography on silica gel (13 g, petroleum ether−EtOAc (9:1) as eluant), to afford 319 mg of **1b** (68% from **1d**, overall 56% from **1c**).

***E*-ω-Benzoyloxyferulenol (1b):** colorless syrup; UV (EtOH) λ_{max} (log ϵ) 282 (2.70), 310 (2.69) nm; IR (liquid film) ν_{max} 3300−2900 (broad), 1670, 1609, 1568, 1203, 1190, 1109, 1056, 757 cm^{-1}; ^1H NMR (300 MHz, $CDCl_3$) δ 8.03 (2H, Bz-AA′), 7.60 (1H, Bz-C), 7.50 2H, Bz-BB′), 7.94 (1H, dd, J = 7.9, 1.5 Hz, H-5), 7.60 (1H, m, H-7), 7.34 1H, t, J = 8.6 Hz, H-6), 7.32 (1H, m, H-8), 5.21 (1H, td, J = 8.4, 1.3 Hz, H-2′), 5.84 (1H, td, J = 8.2, 1.3 Hz, H-10′), 5.11 (1H, td, J = 8.0, 1.2 Hz, H-6′), 4.68 (2H, s, H-12′), 3.32 (2H, d, J = 7.0 Hz, H-1′), 2.10 (2H, m, H-5′), 2.10 (2H, m, H-9′), 2.03 (2H, m, H-8′), 2.01 (2H, m, H-4′), 1.80 (3H, d, J = 1.0 Hz, H-13′), 1.69 (3H, d, J = 0.9 Hz, H-15′), 1.59 (3H, d, J = 1.0 Hz, H-14′); ^{13}C NMR (75 MHz, MeOH-d_4) δ 166.7 (s, Bz), 165.0 (s, C-2), 160.7 (s, C-4), 152.4 (s, C-8a), 136.3 (s, C-3′), 134.3 (s, C-7′), 133.0 (d, Bz), 131.5 (d, C-7), 130.4 (s, C-11′), 130.1 (s, Bz), 129.4 (d, Bz), 129.3 (d, C-10′), 128.4 (d, Bz), 124.6 (d, C-6′), 124.0 (d, C-6), 123.0 (d, C-5), 121.0 (d, C-2′), 116.8 (s, C-4a), 116.3 (d, C-8), 105.3 (s, C-3), 70.4 (t, C-12′), 39.6 (t, C-4′), 38.9 (t, C-8′), 26.2 (t, C-9′), 26.1 (t, C-5′), 22.5 (t, C-1′), 15.3 (q, C-13′), 15.0 (q, C-14′), 12.9 (q, C-15′); HREIMS *m/z* 486.2419 $[M]^+$ (calcd for $C_{31}H_{34}O_5$, 486.2406); APCI+ MS-MS *m/z* 365 (35), 309 (100), 283 (80), 217 (45), 203 (49), 191 (55), 175 (32).

Synthesis of 3-Nonyl-4-hydroxycoumarin. To a cooled (ice bath) solution of 4-hydroxycoumarin (50 g, 30.8 mmol) in pyridine−piperidine (10:1, 800 mL) was added dropwise nonanoyl chloride (57.7 mL, 56.5 g, 32.1 mmol, 1.05 equiv) for ca. 5 min. At the end of the addition, the cooling bath was removed and the solution was allowed to warm to room temperature for 15 min and then refluxed for 48 h. After cooling, the reaction mixture was poured into crushed ice (ca. 200 g), and the orange suspension was acidified (pH 2) with 2 N H_2SO_4. The precipitate was collected by filtration, washed with water until neutral, dried, and crystallized from hot EtOH to afford 28.1 g (30%) of 3-nonanoyl-4-hydroxycoumarin. A portion of the latter (5 g, 26.3 mmol) was suspended in acetic acid (50 mL), heated to 100 °C (oil bath), and magnetically stirred until a clear solution was obtained. At this point, $NaBH_3CN$ (2.1 g, 33.8 mmol, 1.3 molar equiv) was added in small portions for ca. 10 min. At the end of the addition, the oil bath was removed, and the solution was stirred to room temperature for an additional 50 min. The reaction was then worked up by the addition of water, causing the formation of a bulky precipitate that was collected by filtration and repeatedly washed with water to afford 4.3 g (overall 27% from 4-hydroxycoumarin) of **3** as a white powder: mp 104 °C; IR (KBr) ν_{max} 3196, 1674, 1610, 1568, 1199, 1099, 1053, 914, 752 cm^{-1}; ^1H NMR (300 MHz, $CDCl_3$) δ 7.95 (1H, dd, J = 7.9, 1.5 Hz, H-5), 7.54 (1H, m, H-7), 7.34 (2H, m, H-6 and H-8), 2.67 (1H, t, J = 7.6 Hz, H-1′), 1.61 (2H, m, H-2′), 1.40−1.21 (12H, m, H-3′, H-4′, H-5′, H-6′, H-7′, H-8′), 0.85 (3H, t, J = 7.3 Hz, H-9); ^{13}C NMR (50 MHz, $CDCl_3$) δ 164.6 (s, C-2), 160.0 (s, C-4), 152.1 (s, C-8a), 131.4 (d, C-7), 124.0 (d, C-5 and C-6), 116.4 (d, C-8), 115.8 (s, C-4a), 105.6 (s, C-3), 31.7, 29.2, 28.4, 23.9, 22.5 (t, C-3′, C-4′, C-5′, C-6′, C-7′, C-8′), 14.0 (q, C-9′); CIMS (isobutanol) *m/z* 289 $[M + 1]^+$ $[C_{18}H_{24}O_3 + H]^+$.

Biological Assays. *Mycobacterium fortuitum* ATCC 6841 was obtained from Dr. Peter Lambert, Aston University, Birmingham, UK. *Mycobacterium smegmatis* ATCC 14468, *Mycobacterium phlei* ATCC 11758, and *Mycobacterium aurum* Pasteur Institute 104482 were obtained from Dr. Veronique Seidel, The School of Pharmacy, University of London. Bacteria were maintained on Columbia blood agar (Oxoid) supplemented with 5% defibrinated horse blood (Oxoid). This assay comprised a standard MIC determination[21,22] of test compound in Ca^{2+} and Mg^{2+} adjusted Mueller-Hinton broth (MHB). Compounds **1a**−**1d** were dissolved in DMSO and diluted out into MHB, to give a starting concentration of 512 μg/mL, which was then diluted across a 96-well microtiter plate in a 2-fold serial dilution to give a final concentration range from 512 to 1 μg/mL. Bacterial inocula equivalent to the 0.5 McFarland turbidity standard were prepared in normal saline and diluted to give a final inoculum density of 5×10^5 cfu/mL. The inoculum (125 μL) was added to all wells, and microtiter plates were incubated at 37 °C for 72 h for *M. fortuitum, M. smegmatis*, and *M. phlei*. For *M. aurum*, the plate was incubated for 120 h. The MIC was recorded as the lowest concentration at which no bacterial growth was observed. This was facilitated by the addition of 20 μL of MTT (Sigma 10 mg/mL in MeOH) to each well and incubation at 37 °C for 20 min, where bacterial growth was indicated by a blue coloration. Appropriate DMSO, growth, and sterile controls were carried out. Ethambutol and isoniazid were used as positive controls.

Acknowledgment. Financial support from MIUR (Fondi ex-40%, progetto Sostanze naturali ed analoghi sintetici con attività antitumorale) is gratefully acknowledged.

References and Notes

(1) For a review, see: Appendino, G. In *Virtual Activity, Real Pharmacology*; Verotta, L., Ed.; Research Signpost: Trivandrum, India, 1997; pp 1−15.
(2) Valle, M. G.; Appendino, G.; Nano, G. M.; Picci, V. *Phytochemistry* **1987**, *26*, 253−256.
(3) (a) Bocca, C.; Gabriel, L.; Bozzo, F.; Miglietta, A. *Planta Med.* **2002**, *68*, 1−3. (b) The anticoagulant dicoumarol can suppress tubulin dynamics and shows synergy with paclitaxel: Madari, H.; Panda, D.; Wilson, L.; Jacobs, R. S. *Cancer Res.* **2003**, *63*, 1214−1220.
(4) Appendino, G.; Cravotto, G.; Sterner, O.; Ballero, M. *J. Nat. Prod.* **2001**, *64*, 393−395.
(5) Sacchetti, G.; Appendino, G.; Ballero, M.; Loy, C.; Poli, F. *Biochem. Syst. Ecol.* **2003**, *31*, 527−534.
(6) Marchi, A.; Appendino, G.; Pirisi, I.; Ballero, M.; Loi, M. C. *Biochem. Syst. Ecol*. **2003**, *31*, 1397−1408.
(7) Arnoldi, L.; Ballero, M.; Fuzzati, N.; Mercalli, E.; Pagni, L. *Fitoterapia* **2004**, *75*, 342−354.
(8) (a) Appendino, G.; Tagliapietra, S.; Gariboldi, P.; Nano, G. M.; Picci, V. *Phytochemistry* **1998**, *27*, 3619−3624. (b) Surprisingly, giant fennel from Morocco has been reported to contain only the *Z*-isomer of ω-hydroxyferulenol: Lamnaouer, D.; Bodo, B.; Martin, M.-T.; Molho, D. *Phytochemistry* **1987**, *26*, 1613−1615.
(9) (a) Appendino, G.; Tagliapietra, S.; Cravotto, G.; Nano, G. M. *Gazz. Chim. Ital.* **1989**, 385−388. (b) Lamnaouer, D.; Khalti, F. B.-; Martin, M.-T.; Bodo, B. *Phytochemistry* **1994**, *36*, 1079−1080.
(10) The 15-methyl of *E*-ω-hydroxyferulenol (**1c**) undergoes a surprising γ-upfield shift upon benzoylation ($\Delta\delta$ = −0.8), as already observed for the acetylation (see ref 8).
(11) Al-Yahya, M. A.; Muhammad, I.; Mizra, H. H.; El-Feraly, F. S. *Phytother. Res.* **1998**, *12*, 335−339.
(12) Gillespie, S. H.; Morrissey, I.; Everett, D. *J. Med. Microbiol.* **2001**, *50*, 565−570.
(13) In male albino mice, the oral LD_{50} of ferulenol is 2.1 g/kg: Fraigui, O.; Lamnaouer, D.; Faouzi, M. A. *Vet. Human Toxicol*. **2002**, *44*, 5−7. As is common with coumarin anticoagulants, male animals were more sensitive to poisoning than females.
(14) Appendino, G. Unpublished results.
(15) Lamnaouer, D. *Therapia* **1999**, *54*, 747−751.
(16) Silverman, R. B. *J. Am. Chem. Soc.* **1981**, *103*, 3910−3915.
(17) Rajab, M. S.; Cantrell, C. L.; Franzblau, S. G.; Fischer, N. H. *Planta Med.* **1998**, *64*, 2−4.
(18) Porter, N. G.; Wilkins, A. L. *Phytochemistry* **1998**, *50*, 407−415.
(19) Chatterji, M.; Unniraman, S.; Mahadevan, S.; Nagaraja, V. *J. Antimicrob. Chemother.* **2001**, *48*, 479−485.
(20) Nutaitis, C. F.; Schultz, R. A.; Obaza, J.; Smith, F. X. *J. Org. Chem.* **1980**, *45*, 4606−4608.
(21) Gibbons, S.; Udo, E. E. *Phytother. Res.* **2000**, *14*, 139−140.
(22) Schinkovitz, A.; Gibbons, S.; Stavri, M.; Cocksedge, M. J.; Bucar, F. *Planta Med.* **2003**, *69*, 369−371.

NP049706N

REVIEW

NPR
www.rsc.org/npr

Anti-staphylococcal plant natural products

Simon Gibbons
Centre for Pharmacognosy and Phytotherapy, University of London School of Pharmacy, 29-39 Brunswick Square, London, UK WC1N 1AX

Received (in Cambridge, UK) 18th December 2003
First published as an Advance Article on the web 1st March 2004

Covering: 1995 to 2003

The occurrence of vancomycin-resistant *Staphylococcus aureus* (VRSA) and multidrug-resistant (MDR) strains of this organism necessitate the discovery of new classes of anti-staphylococcal drug leads. At present there are no single chemical entity plant derived antibacterials used clinically, and this biologically diverse group deserves consideration as a source of chemical diversity for two important reasons. Firstly, plants have exceptional ability to produce cytotoxic agents and, secondly, there is an ecological rationale that antibacterial natural products should be present or synthesised *de novo* following microbial attack to protect plants from invasive and pathogenic microbes in their environment. This review cites plant natural products that either modify resistance in *Staphylococcus aureus* or are antibacterial through bacteriostatic or bactericidal properties. The activities described here show that there are many potential new classes of anti-staphylococcal agents which should undergo further cytotoxicity, microbial specificity and preclinical *in vivo* studies to assess their potential.

Simon Gibbons was born in Gosport, England in 1966. He studied Chemistry at Kingston Polytechnic and completed a PhD in Phytochemistry under the supervision of Dr Sandy Gray and Professor Peter G. Waterman at the Department of Pharmaceutical Sciences, University of Strathclyde in 1994. He worked as a project chemist and research leader at the natural product biotech company Xenova before moving to the newly formed Faculty of Pharmacy at Kuwait University as Assistant Professor of Pharmaceutical Chemistry in 1997. In 1999 he moved to the University of London School of Pharmacy as Lecturer in Phytochemistry. His research is focused on the antibacterial and resistance modifying properties of plant derived natural products.

Simon Gibbons

1 Introduction

This review encompasses the literature from 1995 to 2003 on plant derived anti-staphylococcal compounds which act as either bacterial resistance modifying agents (RMAs) or have direct antibacterial action. For antibacterial compounds, only single chemical entities (SCEs) which have minimum inhibitory concentrations (MIC) of less than 64 μg ml^{-1} (or less than 5 μl ml^{-1} or 0.25% v/v for liquids) have been selected from the literature, and only examples where standard MIC determinations employing either broth or agar dilution methodologies are cited. These criteria have been applied so that direct comparison of activities can be made between compound classes. Extracts, whilst traditionally used in many systems of medicine to treat infections caused by bacteria, have been excluded from this review in an attempt to focus on the potential of plant derived SCEs.

The literature abounds with claims of natural products and extracts displaying antibiotic activity with many papers describing compounds with MIC values over 1 mg ml^{-1} (1000 μg ml^{-1}), which from a clinical perspective has little relevance. It is likely that a number of relatively inert substances may display antibacterial activity at this high concentration.

Resistance modifying agents are compounds which potentiate the activity of an antibiotic against a resistant strain. These compounds may for example, specifically target a resistance mechanism, such as the inhibition of multidrug resistance (MDR), *e.g.* inhibition of the NorA efflux mechanism in *Staphylococcus aureus*[1] or act in a synergistic fashion *via* an undescribed mechanism.

Staphylococcus aureus is a commensal organism that is commonly cited as being a major hospital-acquired pathogen.[2,3] Strains of this species that are resistant to β-lactams, notably the methicillin-resistant *Staphylococcus aureus* (MRSA) strains, have been described from clinical sources for over forty years.[4,5] It is the ability of this Gram-positive organism to acquire resistance to practically all useful antibiotics that is cause for considerable concern. Furthermore, in the UK there has been a significant increase in the number of death certificates which

DOI: 10.1039/b212695h

mention MRSA with 47 citations in 1993 rising to 398 in 1998.[6] The threat of untreatable multidrug-resistant bacteria has prompted a special report from the House of Lords[7] and a report on hospital-acquired infections by the National Audit Office.[8] The latter estimates that hospital-acquired infections and treatment of drug-resistant bacteria in the clinical setting cost the tax payer an estimated one billion pounds per annum.

The occurrence of a fully vancomycin resistant strain of MRSA in the US in 2002[9,10] indicates that the successful treatment of MRSA strains by the use of this glycopeptide antibiotic is not guaranteed. Linezolid (Zyvox®), a new member of the oxazolidinone group and the streptogramin quinupristin/dalfopristin mixture (Synercid®) are the newest anti-staphylococcal agents and have been heralded as a solution to MRSA infections. However, an isolated report of resistance to linezolid[11] in a clinical isolate of *Staphylococcus aureus* demonstrates that researchers should not be complacent in this area, and that there is a continual need for a pipeline of new agents to combat multidrug-resistant bacteria.

Abbreviations used in the review include SA (*Staphylococcus aureus*), SE (*Staphylococcus epidermidis*), MRSA (methicillin-resistant *Staphylococcus aureus*), MDR (multidrug-resistance) and MIC (minimum inhibitory concentration),

2 Resistance modifying agents (RMAs)

The concept of a compound that inhibits resistance in a bacterium which may be employed with a conventional antibiotic is well accepted and Augmentin® is an important example. This product, produced by GlaxoSmithKline, uses a combination of amoxicillin (a beta lactam antibiotic) and clavulanic acid, a microbially derived inhibitor of beta lactamases. The inhibitor greatly increases the stability of amoxicillin to degradation by beta lactamases[12] and the product is indicated for the treatment of patients with community-acquired pneumonia or acute bacterial sinusitis due to β-lactamase-producing pathogens.

Resistance modifying agents may also target and inhibit multidrug resistance (MDR) mechanisms. These are membrane proteins of varying substrate specificity which efflux antibiotics from the bacterial cell, resulting in a low intracellular ineffective concentration of the drug.[13] In combination with an antibiotic that is a substrate for these mechanisms, an inhibitor will increase the cellular concentration of the antibiotic therefore restoring its efficacy. It has also been shown that the use of such resistance modifying agents can also reduce the emergence of antibiotic resistant variants.[14]

2.1 Methicillin-resistance reversing agents

From the highly prolific group of Hamilton-Miller, much work on the ability of green tea and its constituents to inhibit methicillin-resistance in MRSA has been undertaken.[15,16] A patent[17] detailing the ability of 'compound P', which is also antibacterial (MIC = 280 μg ml^{-1}), to reverse methicillin-resistance has been described and the structure of this was revealed[18] as epicatechin gallate (**1**). This component appears to act by inhibiting the synthesis of penicillin binding protein 2′ (PBP2′) and is selective affecting only staphylococci that synthesise PBP2′. In the presence of a β-lactam antibiotic, epicatechin gallate renders MRSA strains sensitive, and an electron microscopy study has shown that **1** affects cell wall morphology of resistant strains whereas sensitive strains are unaffected. This highlights the potential of inhibiting the synthesis of PBP2′.

Diterpenes such as totarol (**2**) have also been shown to potentiate methicillin activity against MRSA *via* interference of PBP2′ expression.[19] When incorporated into the medium at 1 μg ml^{-1}, totarol caused at least an eight-fold increase in methicillin activity against an MRSA strain and totarol was antibacterial (MIC = 2 μg ml^{-1}) and inhibited respiration in *S. aureus*.

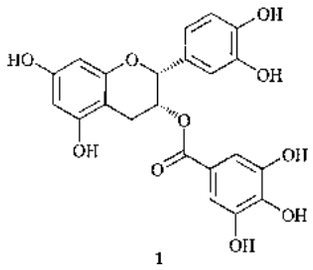

1

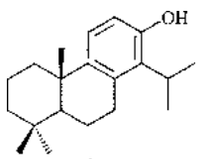

2

Two papers[20,21] from the Tsuchiya group on the effects of the hydrolysable tannins tellimagrandin I (**3**) and corilagin (**4**) show that these compounds work synergistically with oxacillin and that **4** reduces the MICs of various β-lactams but not other antimicrobial agents such as vancomycin, the fluoroquinolone ofloxacin or the macrolide erythromycin. The effects were seen against MRSA strains but not a methicillin-sensitive *Staphylococcus aureus* (MSSA) strain.[20] The authors suggest that the major action of this natural product is also by the inhibition of PBP2′ activity. In the presence of tellimagrandin I (**3**), the MICs of tetracycline against some strains of MRSA were also significantly reduced.[20]

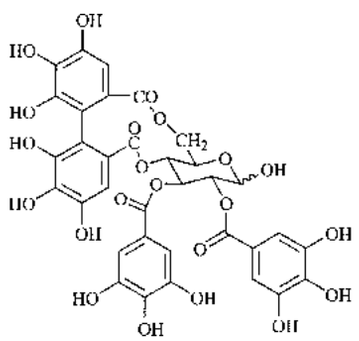

3

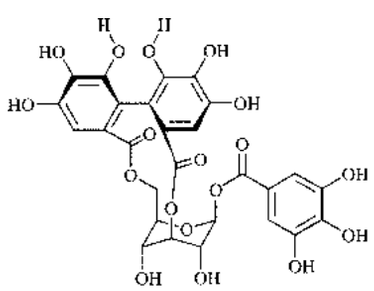

4

2.2 Modulators of multidrug resistance (MDR)

Some isopimarane diterpenes from *Lycopus europaeus* (Lamiaceae), typically **5**, have been shown to reduce the MICs of tetracycline and erythromycin by two-fold against strains possessing the Tet(K) and Msr(A) transporters which confer a high level of resistance to these antibiotics.[22] The MDR inhibitor reserpine (**6**) caused a four-fold reduction in the MIC of tetracycline although erythromycin activity was unaffected. The effects of (**6**) have been studied against a variety of multidrug-resistant MRSA and MSSA strains[23,24] and this compound

enhances the activity of tetracycline and norfloxacin against strains which possess efflux mechanisms such as the more specific Tet(K) protein and the MDR transporter NorA, the major drug efflux pump in this pathogen.[25] The NorA pump contributes significantly to decreased fluoroquinolone susceptibility. In one of these studies, reserpine reduced sparfloxacin, moxifloxacin and ciprofloxacin MICs up to four-fold in 11, 21 and 48 of 102 clinical isolates tested respectively.[24]

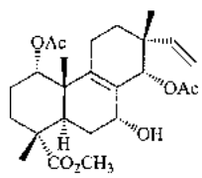

5

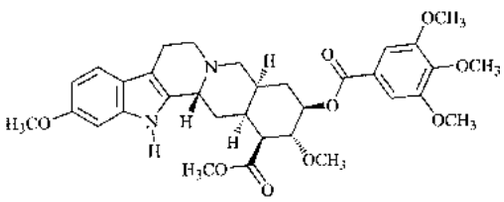

6

From the prolific groups of Stermitz and Lewis, a number of inhibitors of MDR in *S. aureus* have been described.[26–32] These workers studied the synergistic interaction between berberine (**7**), a plant antibacterial quaternary alkaloid produced by *Berberis fremontii* and another natural product, 5′-methoxyhydnocarpin (**8**) also present in this species.[26,27] Compound **8** potentiates the activity of berberine against strains possessing the NorA MDR transporter, and MDR-dependent efflux of berberine from cells was completely inhibited by this natural product. The authors postulate that the plant has evolved MDR inhibitors against MDR pumps in plant pathogens, and that in combination with latent antibacterial products (*e.g.* berberine), this offers an improved chemical defence. The flavonolignan silybin from the Milk thistle (*Silybum marianum*) of similar structure to **8**, and the porphyrin phaeophorbide A (**9**) (also from *Berberis fremontii*), have also been shown to be inhibitors of *S. aureus* MDR.[28,29] A key feature of these and many other MDR inhibitors is their large size and high degree of lipophilicity. These qualities are likely to be of importance for their solubility in the bacterial membrane and binding to the efflux transporters before inhibition can occur.

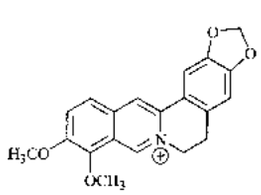

7

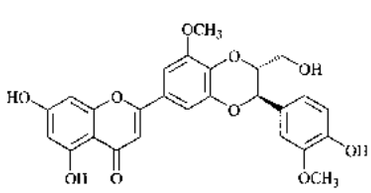

8

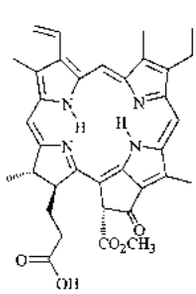

9

A number of methoxylated flavones[30] (**10**, **11**) and isoflavones[31] (**12**–**14**) that potentiate the activities of berberine and the synthetic fluoroquinolone antibiotic norfloxacin have been described. The first two flavones from Wormwood, *Artemisia annua* (Asteraceae) were earlier reported to potentiate the activity of the antimalarial artemisinin against the causative agent *Plasmodium falciparum,* and it is likely that in *S. aureus* (and possibly *P. falciparum*), these compounds exert their effects by inhibition of MDR pumps. Investigation of the isoflavones **12**–**14** from *Lupinus argenteus* has shown that they act as potentiators of berberine and linolenic acid antibacterial activity, the latter being present in this *Lupinus* species.

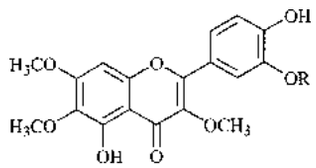

10 R = H
11 R = CH_3

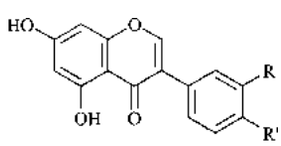

12 R = H, R′ = OH
13 R = R′ = OH
14 R = H, R′ = OMe

MDR pump inhibitors have even been described from popular horticultural taxa such as *Geranium* with some polyacylated neohesperidosides from *G. caespitosum*[32] for example **15**, showing potentiation activity of berberine by increasing berberine uptake by inhibition of MDR. Compound **15** was also shown to be only weakly cytotoxic against three leukaemia cell lines.

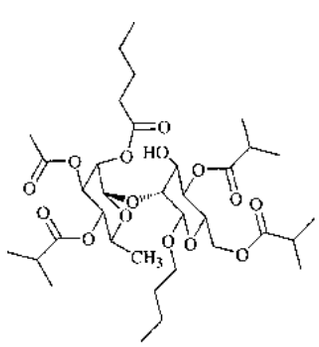

15

Salicylic acid (**16**), present in many plant species, has recently been shown to induce a reduction in the accumulation of the fluoroquinolone antibiotic ciprofloxacin and the MDR substrate ethidium.[33] Inactivation of NorA, the major MDR transporter in *S. aureus*, did not alter the ability of salicylate to induce increased ciprofloxacin and ethidium resistance.

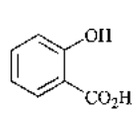

16

3 Antibacterial natural products

This section covers compounds which are directly antibacterial (cidal or static) and the section is broken down according to a general biogenetic source and an attempt has been made to

collate compounds according to structural similarity so that antibacterial activities can be compared according to class. Only the most active natural products from a literature source are mentioned and where mode of action is known this has been cited.

3.1 Monoterpenes

The tea tree (*Melaleuca alternifolia*, Myrtaceae) has long been regarded as a useful topical antiseptic agent in Australia[34] and there has been much research into the use of this oil as an antiseptic for nursing staff. The most active purified compounds from this oil include γ-terpinene, α-terpineol, terpinen-4-ol (**17**) and linalool (**18**) with MICs in the range of 0.125–0.25% v/v.[35–37] The most broad-spectrum of these being (**17**) with activity against Gram-negative bacteria.[36] It was also shown that non-oxygenated monoterpenes *e.g.* γ-terpinene and *p*-cymene reduce the efficacy of **17** by reducing its aqueous solubility.[37]

From *Artemisia asiatica*,[38] 1,8-cineole (**19**) was found to be the major anti-staphylococcal agent of the essential oil with an MIC of 2 μl ml^{-1}. This was also active against the Gram-negative species *Escherichia coli* and *Pseudomonas aeruginosa* (both MICs of 3 μl ml^{-1}) which in many cases are insensitive to plant antibacterials unless high concentrations are employed.

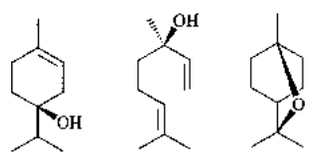

17 18 19

3.2 Sesquiterpenes

In a study to ascertain the active principles of a Nepalese medicinal plant used to treat sinus infections,[39] the guaianolide sesquiterpene lactone 6-*O*-isobutyroplenolin (arnicolide C) (**20**) was characterised as the most active against a methicillin-sensitive *Staphylococcus aureus* (MSSA) strain (MIC 38 μg ml^{-1}). The authors postulate that the activity depends on the presence of a *beta* unsubstituted cyclopentenone ring moiety and work by others[40] showed that saturation of this dramatically reduced activity. Interestingly, the antibacterial activity appears to be independent of an α-methylene-γ-lactone moiety, although this group is needed for significant antitumour activity. Furthermore, compound **20** was shown to be bactericidal and not bacteriostatic as bacteria grown in the presence of this product could not be recultured. The related guaianolide **21**, from *Artemisia gilvescens*[41] showed excellent potential against a clinical strain of MRSA (MIC, 1.95 μg ml^{-1}) and only moderate cytotoxicity toward a human colon carcinoma cell line

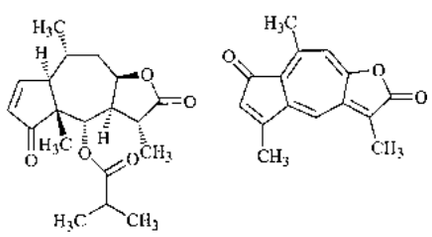

20 21

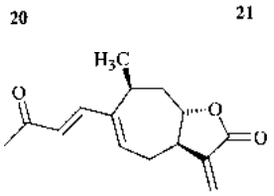

22

(IC_{50} = 16 μM) indicating that possibly this margin can be exploited. Xanthatin (**22**), exhibited species specific activity with only Gram-positive bacteria being affected and the authors profiled **22** against twenty MRSA and seven MSSA with MIC values being comparable for resistant and sensitive strains.[42]

Daucane sesquiterpenes with various aromatic ester moieties attached to them have been characterised from *Ferula* species, notably *F. hermonis*[43] (**23**, MIC, 6.25 μg ml^{-1}) and *F. kuhistanica* (**24**, MIC, 8–16 μg ml^{-1}).[44]

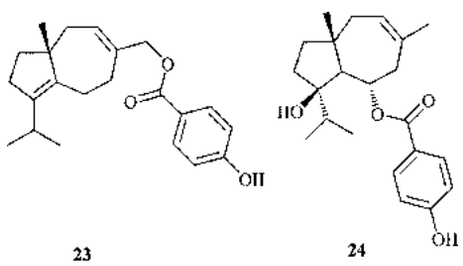

23 24

Sesquiterpene ester **24** was hydrolysed and the antibacterial activity of the hydrolysis products investigated. The sesquiterpene portion had greatly reduced activity (MIC, 125 μg ml^{-1}) and *p*-hydroxybenzoic acid was inactive indicating the importance of both moieties for overall activity.[44]

Much work has been conducted on myrrh (*Commiphora molmol*) antimicrobial properties[45] as these exudates are produced by trees belonging to the Burseraceae family, which secrete resins rich in terpenoids and carbohydrates that are probably produced by the tree as a defence against microbial and insect attack following damage. The furano *seco*-A-ring sesquiterpene curzerenone **25** was isolated along with other sesquiterpene mixtures as being responsible for the anti-staphylococcal activity (MIC = 0.7 μg ml^{-1}) and this compares very well with ciprofloxacin activity against the same strain (MIC = 0.12 μg ml^{-1}).[45] This may account for the use of myrrh in antiquity for treating wounds and as a local eye medication.[46]

Mansinone F (**26**) from *Ulmus davidiana* var. *japonica* exhibited superb activity *versus* 19 MRSA strains with MIC values in the range of 0.39–3.13 μg ml^{-1} and these compare favourably with vancomycin (0.39–1.56 μg ml^{-1}), the most widely used anti-MRSA antibiotic.[47] The authors mention that this structurally simple and unique *ortho*-naphthoquinone offers much potential as a new anti-MRSA lead and certainly this compound is amenable to synthetic modification and has potential as a template for analogue synthesis.

The aromatic sesquiterpene phenol, xanthorrizol (**27**),[48,49] had activity against SA and MRSA in the range of 16–32 μg ml^{-1} and this compound was shown to non-specifically inhibit DNA, RNA and protein synthesis[49] but a single oral dose did not protect mice infected with SA introduced intraperitoneally.

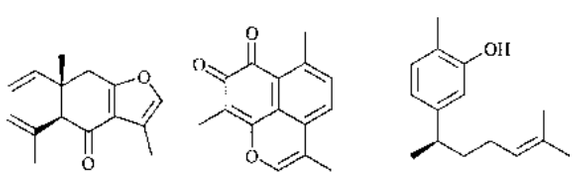

25 26 27

3.3 Diterpenes

This is one of the largest groups of plant derived natural products with anti-staphylococcal activity and certain plant taxa and diterpene classes are well represented. In particular, the genus *Salvia* from the Lamiaceae or mint plant family, is prolific and a recent important review covers the antibacterial and cardioactive properties of these species.[50]

From *Salvia blepharochlaena*,[51] the abietane diterpenes horminone (**28**) and 7-acetylhorminone (**29**) were active toward SA and *S. epidermidis* in the MIC range of 1.5–10 μg ml^{-1} and a similar level of activity is seen from 1-oxoferruginol (**30**) from *Salvia viridis*.[52]

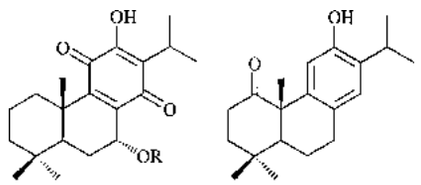

28 R = H
29 R = Ac

30

Salvia additionally produces isopimarane type diterpenes[53] *e.g.* **31** having comparable activity (9 μg ml^{-1})[54] to amikacin (16 μg ml^{-1}), ampicillin (8 μg ml^{-1}) and cefoperazone (16 μg ml^{-1}) which are commonly used to treat infections caused by Gram-positive bacteria. Abietane quinones from *Salvia prionitis*[55] and *S. lanigera*[56] (*e.g.* sanigerone, **32** MIC = 13 μg ml^{-1} against SA) highlight the potential of these compounds as lead structures. Sanigerone (**32**) is a *nor*-diterpene, presumably formed *via* oxidation of methyl-20 and decarboxylation resulting in the formation of an unusual aromatic B-ring abietane. Other taxa in the mint family excel at producing anti-staphylococcal compounds and these include *Plectranthus hereroensis*, which produces an acetylated abietane quinone (**33**, MIC = 31.2 μg ml^{-1})[57] related to horminone (**28**), and *P. elegans*[58] (**34** and **35**) with similar activities against Gram-positive bacteria, and causing inhibition of fungal spore germination (*Cladosporium cucumerinum*). The authors suggest that these compounds may have a role in the chemical defence of *Plectranthus.*[58]

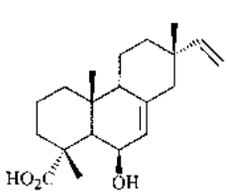

31

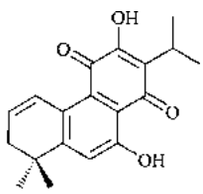

32

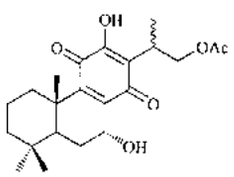

33

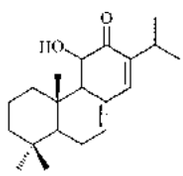

34

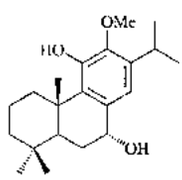

35

From *Dauphinia brevilabra* (Lamiaceae) the methoxylated abietic acid (**36**)[59] showed good potency of 1 μg ml^{-1} against a standard laboratory SA strain (NCTC 6751) with the same activity as chloramphenicol. Other reports of lamiaceous species producing antibacterial diterpenes include *Ballota saxatilis* subsp. *saxatilis* which yielded the furano-labdane diterpene ballonigrine (**37**) with moderate activity against SA and *S. faecalis* (25 μg ml^{-1}).[60]

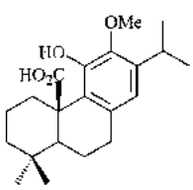

36

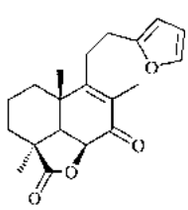

37

Coniferous plants (Pinopsida) are an interesting source of antibacterial leads, again being rich in abietane type diterpenes from *Cephalotaxus*[61] and *Chamaecyparis*[62] species, with MIC values below 15 μg ml^{-1} and there is potential to exploit this taxonomic group and the abietane diterpene class[63] providing that adequate dereplication can be carried out to avoid common and active natural products such as abietic acid itself.

The dehydroabietic acid (**38**) skeleton has been extensively investigated to determine structural effects on anti-staphylococcal and antifungal activity.[64] This study showed that simple derivatisation of dehydroabietic acid, for example, conversion of the acid to aldehyde or alcohol, improved activity and that removal of the isopropyl side chain from ring-C or the introduction of an alcohol or ketone at C-7 or C-12 could enhance activity depending on the organism. The stereochemistry of the A/B ring junction did not appear to display a significant role in antibacterial activity.

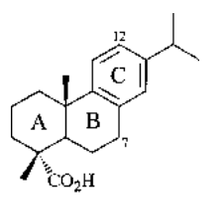

38

An excellent study has recently been conducted by Timmermann and co-workers[65] on the isopimarane **39**, using SA and MRSA strains and activity was also shown against *Bacillus subtilis* (MIC; 2, 2 and 4 μg ml^{-1} respectively). These authors showed that the presence of an oxymethylene group at C-19 is important to activity, since its replacement with a carboxylic acid reduces activity. This is mirrored in the above case of abietane diterpenes. Compound **39** rapidly and non-specifically inhibited uptake and incorporation of radio-labelled thymidine, uridine and amino acids at its MIC. The authors suggest that this may function by a membrane damaging effect although no specific mechanism is described. Using human red blood cells however, no haemolytic effect was observed until a concentration of 32 μg ml^{-1} was used. The compound was also evaluated *in vivo* for its ability, at a subcutaneous dose, to afford protection against SA infection but no protection was seen in a murine model.[65]

Work has been conducted on the totarane diterpene totarol (**40**) during the period of this review to ascertain mode of action[66] and structure activity relationships of derivatives.[67] This product originally comes from a coniferous plant *Podocarpus nagi,* and has activity against MRSA[68] and its activity is improved when tested in combination with other natural products.[69] The Kubo group[66] have demonstrated that **40** inhibits oxygen consumption and respiratory-driven proton translocation in whole cells, and oxidation of NADH in a membrane preparation. Amongst several key enzymes studied, NADH-cytochrome *c* reductase was inhibited whilst cytochrome *c* oxidase was not. The authors postulate that the site of respiratory inhibition of totarol was near CoQ in the bacterial electron transport chain.

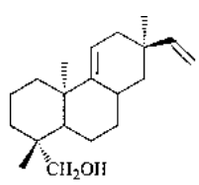

39

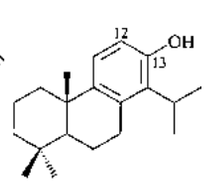

40

Modifications at C-12 and O-13 of totarol on antibacterial properties have been evaluated and in general a phenolic moiety

is essential for activity of <32 μg ml^{-1}. Derivatisation of C-12 was deleterious and totarol and its derivatives appear to be only active against Gram-positive species.[67]

Some of the rarer skeleta of diterpenes include the trachylobane class, typically **41** which has activity (both at 6.25 μg ml^{-1}) against SA and *Mycobacterium smegmatis,* a model for assessment of anti-tubercular drugs.[70] Again this compound is oxygenated at one of the methyl groups at C-4, which seems to be a regular feature of many antibacterial diterpenes. This is the case with beyerenoic acid (**42**) from the roots of *Viguiera hypargyrea* (Asteraceae) with activity toward SA and *Enterococcus faecalis* (MIC; 12 μg ml^{-1}) and this supports the use of these roots as a treatment of gastrointestinal disorders in Mexico.[71] *Fabiana densa* var. *ramulosa* is used in traditional medicine in Chile to treat coughs and illnesses of the lungs, and a bioassay-guided study led to the isolation of the succinate derivative **43** (MIC < 10 μg ml^{-1}),[72] which is structurally related to **42**.

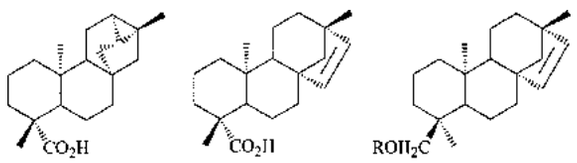

41 **42** **43** R = succinate

Continuing in the same theme of South American medicinal plants yielding useful anti-staphylococcal leads, Tincusi *et al.*, have investigated an oleoresin from Peruvian *Copaifera paupera* (Leguminosae). Diterpene **44** was active against SA and *S. epidermidis* at 5 and 10 μg ml^{-1} respectively and the control, cephotaxime had an MIC of 2.5 μg ml^{-1}.[73]

Investigation of essential oils of two *Helichrysum* species led to the characterisation of the cyclised labdane diterpene manoyl oxide (**45**) as having bacteriostatic activity against SA (MIC = 50 μg ml^{-1}).[74]

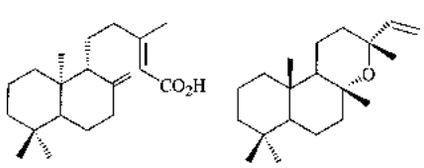

44 **45**

3.4 Triterpenes

All of the triterpenes reviewed are either acids or esters and the predominant skeleton is the Δ12-oleanene pentacycle. There are two *nor*-friedelane triterpenes (**46** and **47**) from *Crossopetalum gaumeri* with excellent potency toward *S. epidermidis* (0.54 and 1.11 μM respectively) when compared to chloramphenicol (12.4 μM).[75] These compounds are presumably formed *via* by decarboxylation of methyl-24 allowing unsaturation in rings A and B.

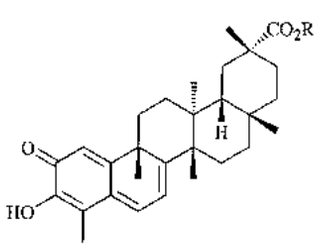

46 R = H
47 R = Me

Even simple compounds that are almost phytochemically ubiquitous such oleanolic acid (**48**) show appreciable anti-staphylococcal activity (MIC 8 and 16 μg ml^{-1}) against SA and

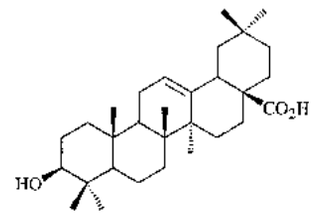

48

MRSA, and this compound was isolated from fractions with higher activity that contained polyphenolic components.[76] Esters of this skeleton, notably at the C-3 position such as **49** possessing a *trans-p*-coumarate, have been isolated and tested against SA and *Staphylococcus capitis* with 12.5 μg ml^{-1} MIC values[77] and even simple 29-oic acid derivatives possessing hydroxyl groups around the skeleton have similar activity such as maytenfolic acid (**50**).[78]

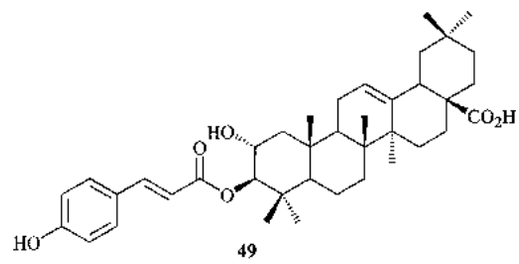

49

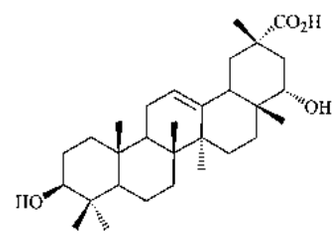

50

Triterpene glycosides are also represented and the acetylated rhamnoside oleanene (**51**)[79] and its corresponding aglycone have excellent potency *versus* SA with MICs at 6.25 and 3.13 compared to streptomycin at 0.78 μg ml^{-1}.

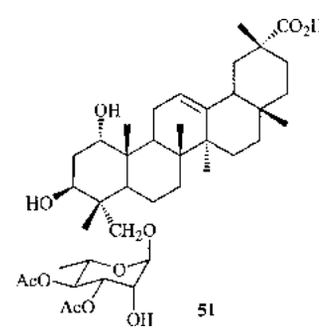

51

Muhammad *et al.*,[80] report an 11-ethoxy derivative (**52**) and a *seco*-A-ring oleanene, koetjapic acid (**53**), from *Maytenus undata* (Celastraceae) (MIC; 50 and 12.5 μg ml^{-1}; SA) and the *seco* compound is probably related to other oleananes present

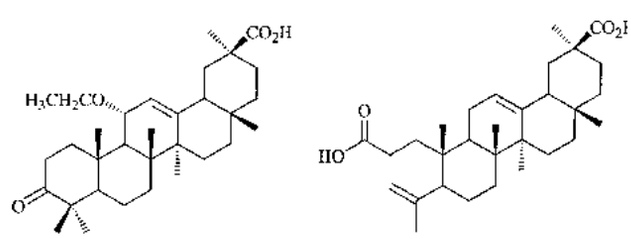

52 **53**

in the plant *via* a Baeyer–Villiger type oxidation. The prolific group of Timmermann and co-workers, have characterised from *Acalypha communis* (Euphorbiaceae), several active cycloartane type triterpenes[81] with **54** demonstrating activity against SA, MRSA and a vancomycin-resistant *Enterococcus faecium* at 32, 64 and 8 μg ml^{-1} compared to penicillin G at 0.06, 128 and 128 μg ml^{-1} respectively.

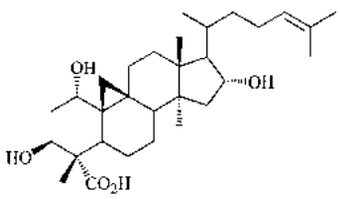

54

3.5 Phenylpropanoids and stilbenoids

In this section, natural products with the structural features of C_6–C_3 and C_6–C_2 moieties are covered and this includes the phenylpropanoids, coumarins, lignans and stilbene related compounds. Coumarins are known to have extensive antibacterial activity and there are microbially derived examples used clinically *e.g.* novobiocin, and these agents are thought to exert their effects by inhibition of bacterial DNA gyrase.[82] Osthol (**55**) from *Prangos pabularia*[83] is a 7-methoxylated, 8-prenylcoumarin with an MIC of 31.25 μg ml^{-1} towards a methicillin-resistant strain but was inactive against *E. coli* and *P. aeruginosa*, which is presumably due to poor penetration through the cell wall of the Gram-negative species. Compound **56**, bornyl coumarate, of mixed biosynthesis possessing both phenylpropanoid and monoterpene moieties, had excellent activity against a standard SA strain (0.6 μg ml^{-1}).[84] Presumably, the lipophilic monoterpene portion of the molecule allows membrane permeability of this compound and the phenolic coumarate may act as an ionophoric moiety. The *nor*-lignan (**57**)[85] from *Styrax ferrugineus* (Styracaceae), a plant which is used in Brazil to treat wound infections, was isolated with a series of other *nor*-lignans, some of which are glycosides, has an MIC of 10 μg ml^{-1} compared to chloramphenicol (SA, 5 μg ml^{-1}). This is a simple achiral metabolite and would be an excellent starting template to synthesise analogues to enhance potency.

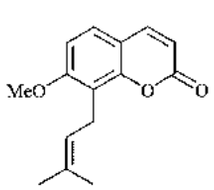

55

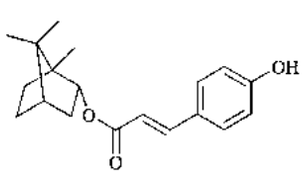

56

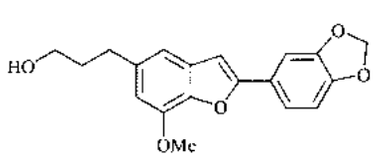

57

Other relatively simple examples include full lignans of the aryl tetralin class *e.g.* **58** and **59**, which are biosynthetically related to the cytotoxic podophyllotoxin group.[86] Both of these compounds were profiled using 18 strains of MRSA with values ranging from 4–32 μg ml^{-1} and interestingly these compounds are only active toward MRSA strains and not MSSA (methicillin-sensitive SA). This selectivity is intriguing and the authors are investigating the mechanism of how these agents

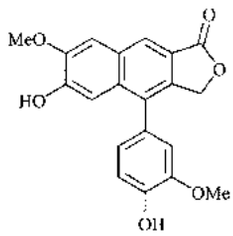

58

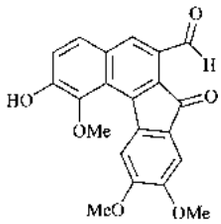

59

function. This highlights the value of screening metabolites against resistant and sensitive strains, particularly isolates of direct clinical relevance.

Marchantin A (**60**) from a Hungarian liverwort *Marchantia polymorpha*[87] has exceptional activity against a panel of both Gram-positive and Gram-negative bacteria (SA; MIC = 6.8 nM (!)) and as this compound is cyclic and has lipophilic and hydrophilic domains, it is possible that it functions by forming pores in cell membranes resulting in cell lysis. The exceptionally complex vaticaphenol A (**61**) (not a tempting synthetic target), is a resveratrol tetramer and was isolated employing bioassay-guided fractionation of extracts of the stem bark of *Vatica oblongifolia* ssp. *oblongifolia* (Dipterocarpaceae) from Sarawak.[88] This metabolite has moderate activity toward SA and *Mycobacterium smegmatis* (50 and 25 μg ml^{-1} respectively) but shows the best possible features of plant derived natural products being highly functional and chiral. The productive research group of Ilias Muhammad have isolated and characterised from *Machaerium multiflorum,* a series of highly unusual and rare stilbenoid-monoterpenes (*e.g.* **62**).[89,90] These agents are hexahydrobenzopyrans and these are the first reports of this type of compound from a higher plant other than the genus *Cannabis*, and **62** was active against SA and MRSA (5 and 4.5 μg ml^{-1} respectively).

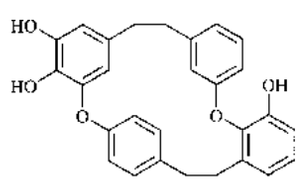

60

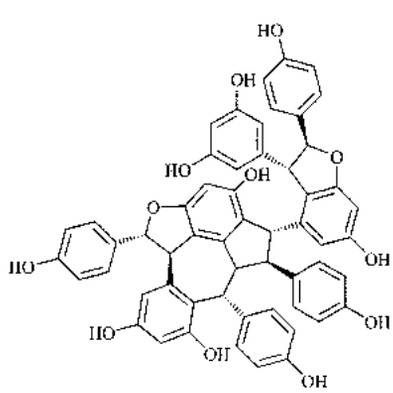

61

3.6 Simple phenols and tropolones

The leaves of *Piper gibbilimbum* (Piperaceae) is a scrambling shrub used in Papua New Guinea as an antiseptic to heal abscesses, ulceration of the skin and also to treat fevers. Fractionation of the petroleum extract of the leaves of this plant afforded several alkenylphenols (*e.g.* gibbilimbol B; **63**,

Table 1 Flavonoid anti-staphylococcal natural products

Compound	Subclass	Bacterium	MIC[a]	Compound	Subclass	Bacterium	MIC[a]
69	Chalcone[96,97]	SA	3.0	**78**	Flavanone-stilbene[107]	MRSA	3.13
70	Dihydrochalcone[98]	SA/MRSA	10/4.5	**79**	Isoflavanone[108]	SA	8.3
71	Flavone[99]	MRSA	3.9–15.6	**80**	Isoflav-2-one-4-ol (3-phenylcoumarin)[109]	SA	9.7
72	Flavone[99]	MRSA	62.5–125	**81**	Isoflavan[110]	MRSA	3.13
73	Flavanone[100]	SA	50	**82**	Isoflavan[97]	SA/MRSA	3.13/6.25
74	Flavanone[101]	SA/MRSA	1.56/1.56	**83**	Pterocarpan[111]	MRSA	3.13–6.25
75	Flavanone[102,103]	SA/MRSA	3.13–6.25	**84**	Pterocarpan[111]	MRSA	3.13–6.25
76	Flavanone[105]	SA/SE	5.0/5.0	**85**	Dimer[113]	SA	15.3
77	Flavanone[106]	SA/SE	1.8/1.8	**86**	Dimer[113]	MDR/MRSA	8

[a] In μg ml^{-1}; SA = *Staphylococcus aureus*; MRSA = methicillin-resistant *Staphylococcus aureus*; SE = *Staphylococcus epidermidis*; MDR = multidrug-resistant strain.

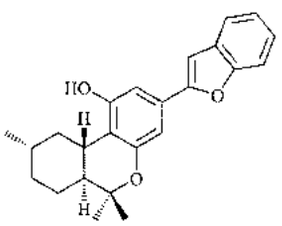

62

MIC = 2 μg ml^{-1}, SE) which were evaluated using Brine Shrimp and KB nasopharyngeal carcinoma cells (ED_{50} (**63**) 3.9 μg ml^{-1}).[91]

A semisynthetic study on derivatives of alkanin (**64**), which has been esterified by a range of alkyl substituents at position C-1′ was conducted employing vancomycin-resistant enterococci and MRSA.[92] The parent natural product (**64**) exhibited MIC values of 6.25 μg ml^{-1} against MSSA and MRSA but the semisynthetic small branched alkyl esters had greater potency (with the exception of aromatic esters).

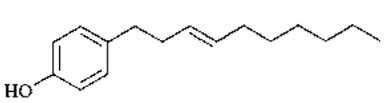

63

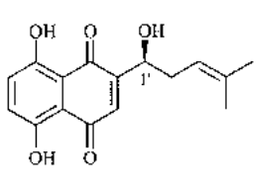

64

Tropolones such as 4-acetyltropolone (**65**) and hinokitiol (**66**) have been shown to have very low MICs against *S. epidermidis* (1.56 and 0.2 μg ml^{-1} respectively) and activity is suggested as being attributable to metal chelation between the carbonyl group at C-1 and hydroxyl at C-2 in both molecules.[93] Even simple acids and esters such as gallic acid (**67**) and ethyl gallate (**68**) have been evaluated for their anti-MRSA properties with MIC values recorded against 20 strains of MRSA and 7 strains of MSSA.[94] These compounds exhibited no activity toward *S. epidermidis* (MIC > 1000 μg ml^{-1}) and MIC values toward SA ranged from 15.7 to 62.5 μg ml^{-1}. The authors were prompted to investigate these natural products by work carried out by Kono *et al.*,[95] on the antimicrobial activity

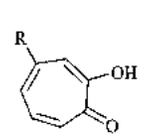

65 R = CHO
66 R = isopropyl

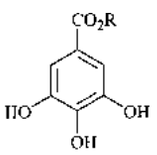

67 R = H
68 R = ethyl

of epicatechin gallate (**1**) against clinical isolates of MRSA, because epicatechin gallate can produce gallic acid through its hydrolysis.

3.7 Flavonoids

The activities of this group, which is one of the largest anti-staphylococcal (and broadly antibacterial) classes of metabolite, are reported in Table 1 where the subclass of flavonoid is also detailed.

Chalcone[96,97] and dihydrochalcone[98] flavonoids are represented by **69** and **70** and these, probably the simplest of flavonoids, have very respectable activities. The simplicity of these structures and the ease with which combinatorial libraries could be prepared from this template make them an attractive target, particularly licochalcone A (**69**) (originally isolated from liquorice), which would be amenable to a variety of prenyl and alkyl substitutions.

Even simple flavones[99] such as apigenin (**71**) and luteolin (**72**) exhibit good to moderate activities against SA and MRSA strains (3.9–62.5 μg ml^{-1}), and these compare with methicillin MIC values which, in some cases, were 1000 μg ml^{-1} against the same resistant strains.

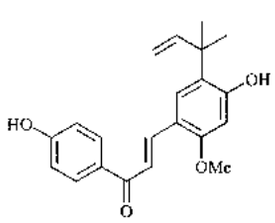

69

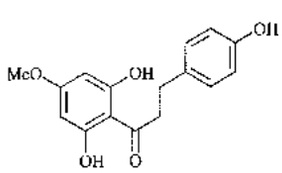

70

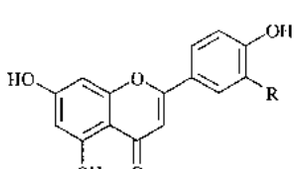

71 R = H
72 R = OH

It is the flavanones which are the most widely reported anti-staphylococcal flavonoids[100–106] and all of those reported here (**73**–**77**) possess either prenyl (sometimes more than one) or geranyl groups that presumably contribute to the lipophilicity and membrane solubility of these compounds. Of particular note[101] within this group is **74** with excellent potency toward standard and MRSA strains (Table 1). Sophoraflavanone G (**75**) is antibacterial[102] but also has strong synergism[103] in combination with vancomycin with a fractional inhibitory concentration (FIC) index of 0.16. This is a significant effect as FIC indices are an indicator of synergistic effects where FIC <0.5 relates to synergism.[104] This effect was also seen to a lesser extent with other antibiotics and the authors propose that a combination of **75** with vancomycin may contribute to better treatment of an MRSA infection. Flavanone **77** is related to sophoraflavanone G and isomeric with respect to the geranyl (lavandulyl) subunit[106] and an investigation on the impact of these monoterpene side chains on potency is valuable. Metabolite **78**, alopecurone B, is a flavanone-stilbene,[107] which when tested against 21 strains of MRSA, had potencies of between 3.13 and 6.25 μg ml^{-1} that compare highly favourably with methicillin (12.5–>100 μg ml^{-1}), gentamicin and erythromycin (both in the range 1.56–>100 μg ml^{-1}).

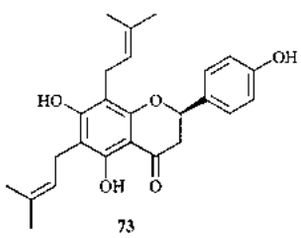

73

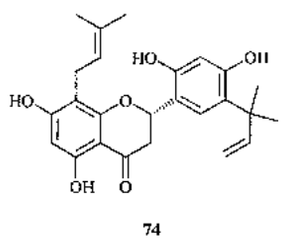

74

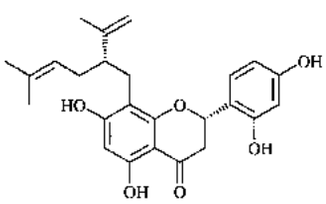

75

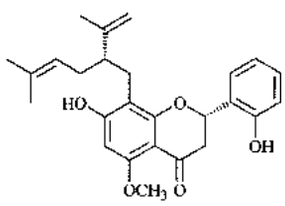

76

The genus *Erythrina* (Fabaceae) produces a number of prenylated isoflavonoids,[108–110] (*e.g.* **79**–**81**) and these are also present in *Glycyrrhiza* species[97] of the same family (*e.g.* **82**). Compound **80** is also a 3-phenylcoumarin and it has been postulated that these compounds exert their effects by inhibition of bacterial DNA gyrase.[82]

The pterocarpans (*e.g.* **83** and **84**), which are biosynthetically related to isoflavonoids and have similar anti-staphylococcal properties, occur within the same genera and species *e.g. Erythrina zeyheri*.[111] These metabolites are known to be phytoalexins which are antimicrobial natural products biosynthesised *de novo* following colonisation of plants by bacteria and fungi.[112] This ecological rationale for the presence of antibacterial products should certainly be exploited in lead discovery.

In Botswana and Zimbabwe, *Vahlia capensis* is widely used to treat eye infections and Majinda *et al.*,[113] have isolated an

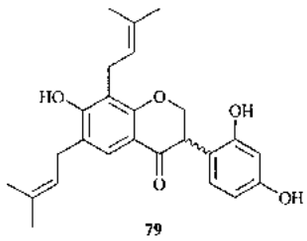

79

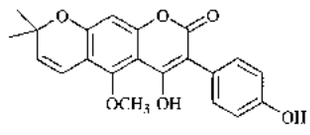

80

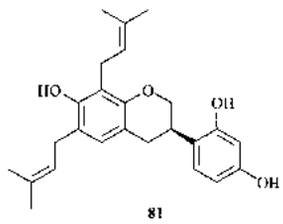

81

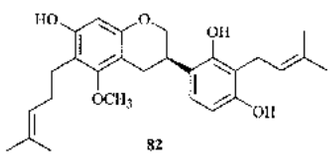

82

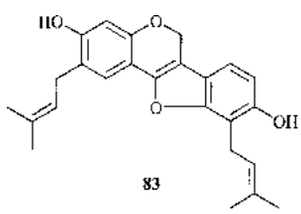

83

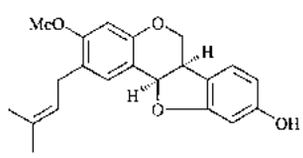

84

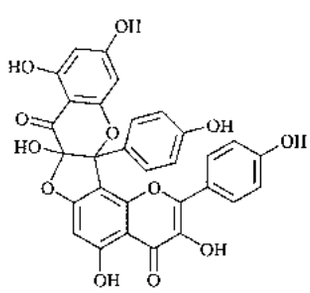

85

antibacterial flavonoid dimer (**85**) which may account for the traditional use of this species. The Washambaa people of the Western Usmabara Mountains of Tanzania use the yellow bark of *Ochna macrocalyx* for gastrointestinal disorders and from extracts of this species, a series of flavonoid dimers *e.g.* **86** have been isolated. This compound exhibited good activity (MICs = 8 μg ml^{-1})[114] against three SA strains which possess efflux mechanisms, one of which is the NorA MDR transporter, the major drug efflux pump in this species.

3.8 Alkaloids

There is excellent rationale that plant alkaloids should possess antibacterial activity, particularly given the number of cytotoxic drugs and templates from this source such as the vinca alkaloids (vincristine and vinblastine) and camptothecin and its synthetic derivatives (topotecan and irinotecan). From *Clausena heptaphylla* (Rutaceae), **87** has a broad spectrum of activity with MIC values of 3, 6 and 20 μg ml^{-1} against SA, *Escherichia coli* and *Pseudomonas aeruginosa*.[115] This activity toward the Gram-negative species, which are generally harder

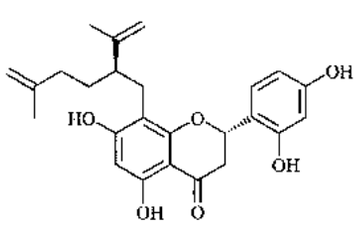

77

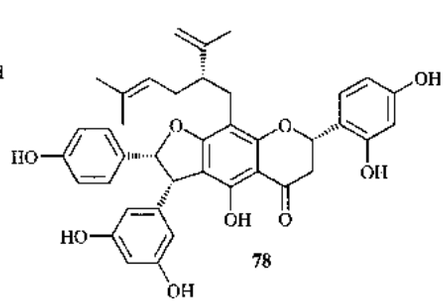

78

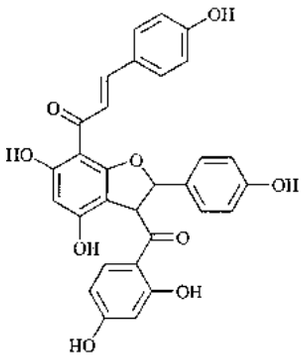

86

to find hits against, and the simple nature of this carbazole alkaloid is intriguing. From the same carbazole class, mahanine (**88**) showed a wide range of biological activities (MIC 12.5 μg ml^{-1}; SA), including cytotoxicity toward HL60 tumour cells (MIC_{100} = 4.0 μg ml^{-1}). Interestingly, this compound is also antimutagenic and in an Ames test was able to inhibit mutations caused by heterocyclic amines by 99% at a concentration of 20 μM, and no toxicity was seen against *Salmonella typhimurium* at this concentration.[116]

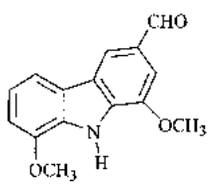

87

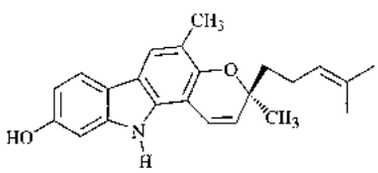

88

Cryptolepis sanguinolenta is widely used in West and Central Africa to treat infectious disease and the major active antimicrobial principle, cryptolepine (**89**) has been profiled using an extensive panel of Gram-negative, Gram-positive bacteria and yeasts. The MIC of the free base was less than 7.8 μg ml^{-1} whereas the hydrochloride salt was less active (60 μg ml^{-1}) toward *S. aureus.* This is unusual given the increased water solubility of the salt which may in fact be detrimental to cellular absorption (and hence reduced activity) of this indoloquinolizidine.[117] There are few examples of polymeric alkaloids in the literature and from *Calycodendron milnei* (Rubiaceae) a series of small polymers based on the pyrrolidinoindoline skeleton have been isolated.[118] One of these, isopsychotridine (**90**) (MIC; 5 μg ml^{-1}; SA), has five monomers joined together in which the first two monomer units are coupled through the alicyclic carbons C-3a to C-3a and further linkages are formed *via* bonds between the aromatic carbon C-7 and the C-3a carbon of another monomer. These agents also display antifungal, anti-yeast, anti-viral and cytotoxic activities.[118]

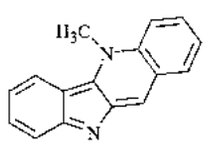

89

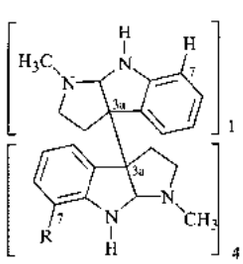

90

From the Clark group in Mississippi, an unusual azaanthraquinone (**91**) with an MIC of 6.25 μg ml^{-1} toward SA from *Mitracarpus scaber* (Rutaceae) has been characterised and compared with a commercially available synthetic sample.[119] Goldenseal (*Hydrastis canadensis*) is a widely used herbal product, especially in the United States for the treatment of a variety of gastric disorders.[120] It is a small perennial plant found in North American damp forests and is used by the Cherokee Indians as a disinfectant.[121] Extracts and isolated compounds from this species have been evaluated and the most active anti-staphylococcal compound is the quaternary ammonium alkaloid berberine (**7**) (MIC; 31 μg ml^{-1}; SA) which is present in the plant in high concentration (6%) and provides a rational basis for the traditional antibacterial use of Goldenseal.[122]

The Southern prickly ash (*Zanthoxylum clava-herculis,* Rutaceae), also produces quaternary alkaloids, and one of these chelerythrine (**92**), is the major anti-staphylococcal agent from this species. This agent has activity against a standard *S. aureus* ATCC 25923 strain (4 μg ml^{-1}) and toward three strains possessing the efflux mechanisms MsrA, TetK and NorA with MIC values of 8, 16 and 8 μg ml^{-1} respectively.[123] These activities compare well with the activities of erythromycin (64 μg ml^{-1}), tetracycline (256 μg ml^{-1}) and norfloxacin (32 μg ml^{-1}) against these resistant strains and indicate that chelerythrine may be a poorer substrate for these efflux systems than the antibiotics. Whilst chelerythrine in a known cytotoxin, it is possible that modification of the benzo[*c*]phenanthridine template could reduce the cytotoxicity and retain the antibacterial activity of this group toward effluxing strains.

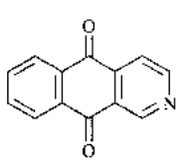

91

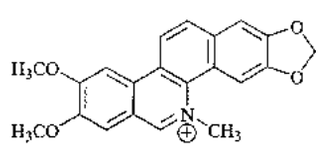

92

The final alkaloid to be reviewed is the aporphine **93** that comes from the annonaceous *Guatteria multivenia,* which has been evaluated against a series of yeasts (*C. albicans, Cryptococcus neoformans*) and SA and MRSA strains with MIC values of 2.0 μg ml^{-1} for the staphylococci.[124]

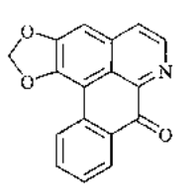

93

3.9 Polyketides and polyynes

An important paper published by Tegos *et al.*,[125] has shown that certain plant antimicrobials such as the polyketide derived rhein and plumbagin (**94**) have striking activity against MDR *S. aureus* and some Gram-negative bacteria when the MDR pumps within these species are disabled. The potentiation of activity is in some cases 100 to 2000-fold. This has great broad-spectrum potential. Furthermore, measurement of uptake of a plant metabolite (berberine) confirmed that disabling the MDRs strongly increased the level of penetration of the plant antimicrobial. The authors suggest that plants may have developed a way of delivering their antimicrobials into bacteria.

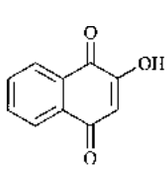

94

Again from the prolific research group of Alice M. Clark, the naphthopyrone **95**, from *Cassia quinquangulata*[126] has excellent potency toward SA and MRSA strains (MIC; 3.125 and 6.25 μg ml^{-1}) and the genus *Cassia* which includes the Senna species are prolific producers of polyketide derived naphtho- and anthraquinone phenolics and are certainly worth exploring further.

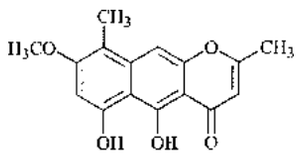

95

Xanthones (**96**–**99**) are metabolites commonly found in the Clusiaceae (Guttiferae) family and frequently occur as prenylated, geranylated or farnesylated products. Calozeyloxanthone, **96**, from *Calophyllum moonii* and *C. lankensis*[127] was profiled against 17 strains of SA (MIC; 4.1–8.1 μg ml^{-1}) comparing favourably with vancomycin (0.5–4 μg ml^{-1}) and this agent should certainly be further investigated using *in vivo* models. From another guttiferaceous plant, *Garcinia dioica,* rubraxanthone (**97**) has even better *in vitro* potency than vancomycin and is one of the most potent anti-MRSA agents from plants to date, having MIC values ranging from 0.313–1.25 μg ml^{-1} toward MRSA and MSSA strains.[128] The lipophilic nature of this compound is probably responsible for good bacterial uptake and the authors anticipate that these xanthones will have wide pharmaceutical uses. Further examples of this class include globulixanthones D and E (**98** and **99**)[129] (MIC; 8.0, 4.5 μg ml^{-1}; SA respectively) and the dimer (**99**) may well be a DNA intercalator having an interesting shape following rotation around C-5–C-8′ bond which may fit into a DNA groove.

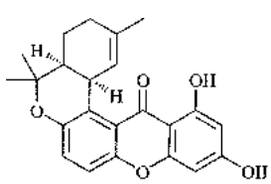

96

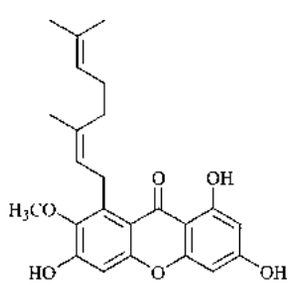

97

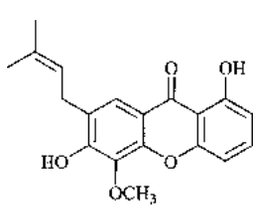

98

Simple C_6 compounds such as (3*E*)-hexenal display *S. aureus* bacteriostatic effects at low concentration (0.1–1 μg ml^{-1}),[130] and these compounds are part of the scent or 'green odour' of plant leaves and probably contribute to antimicrobial plant defence. Other straight-chain polyketides include the polyacetylenes which have wide distribution in several plant families (Asteraceae, Araliaceae and Apiaceae) and are in some cases produced as phytoalexins. The polyynes **100** and **101** from *Mitrephora celebica*[131] (Annonaceae) had moderate activity (MIC; 25 and 12.5 μg ml^{-1}, MRSA) and these acetylenic compounds are not commonly found in the Annonaceae. The authors remark that these acetylenic acids were unstable and decomposed to blue methanol insoluble products. Falcarindiol (**102**) is more stable, and two separate studies[132,133] one of which defined the absolute stereochemistry of this product using Mosher's ester methodology as 3(*R*),8(*S*),[133] have evaluated the anti-staphylococcal nature of this metabolite with activity toward three strains of MDR SA of between 8–16 μg ml^{-1} and epidemic MRSA strain-15 was also evaluated (MIC 32 μg ml^{-1}).

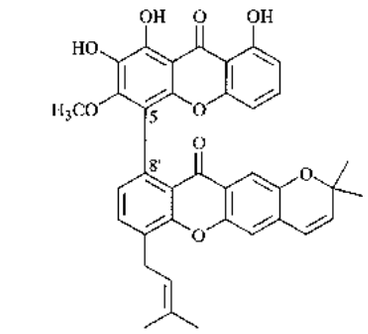

99

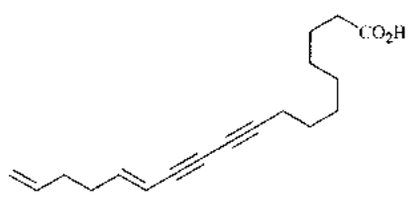

100

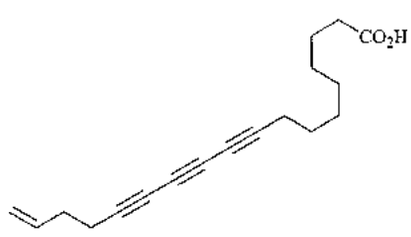

101

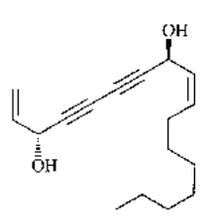

102

Verbalactone (**103**) from *Verbascum undulatum* is a cyclic lactone derived from the dimerization of two C_{10} hydroxylated fatty acids, and the stereochemistry of this compound was determined to be all (*R*) by base hydrolysis to afford the acids and then acid relactonisation to give the simple C_{10} lactone. The data of this was compared with known compounds.[134] This natural product has moderate activity (MIC 62.5 μg ml^{-1}, SA) and may function as a 'porin' former by localising in the bacterial membrane and causing cell lysis *via* formation of

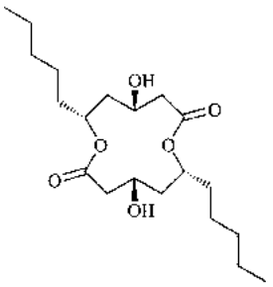

103

holes in the cell membrane. The final metabolite in this section, aculeatin D (**104**), comes from the ginger family (*Amomum aculeatum*, Zingiberaceae, MIC 8 μg ml^{-1}, SE)[135] and is a dispiro-ether with good cytotoxicity toward KB and L-6 cell lines (IC_{50} = 0.38 and 1 μg ml^{-1} respectively). Furthermore this metabolite was highly antiprotozoal towards *Plasmodium* and *Trypanosoma* species (IC_{50} 0.2–0.49 μg ml^{-1}) and the mechanism of cytotoxicity of this metabolite towards bacterial, mammalian and protozoal cells is unknown.

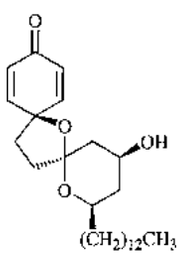

104

3.10 Sulfur containing products

Oils from the Garlic genus for example garlic itself (*Allium sativum,* Alliaceae) are rich in sulfur containing natural products (*e.g.* allicin) and are known to be strongly antimicrobial.[120] A series of diallyl sulfides, including diallyl tetrasulfide (**105**) have been evaluated[136] using SA and MRSA strains with MIC values of 0.5 and 2.0 μg ml^{-1} respectively. The pure compounds and the parent oils from garlic and Chinese leek (*Allium odorum*) were also active against *Candida* and *Aspergillus* species and are probably produced by *Allium* as latent antimicrobial substances. Ajoene (**106**), a common constituent of *Allium* species, occurs as both the *E* and *Z* isomers and is an inhibitor of platelet aggregation and has potential as a treatment for thrombosis. This metabolite also has anti-staphylococcal activity (bactericidal)[137] with an MIC value of 16 μg ml^{-1} and is additionally antibacterial to species of *Bacillus*, *Mycobacterium* and *Streptomyces*.

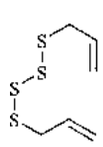

105

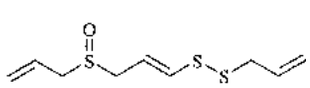

106

When induced by UVA irradiation, terthiophenes have antibiotic activity towards viruses, bacteria, fungi nematodes and eggs and larvae of insects.[138] In a study of nine terthiophenes, typified by **107**, Ciofalo *et al.*,[139] have shown that these compounds are highly active when irradiated (MIC = 0.022 μg ml^{-1} (!), SA, amikacin = 5 μg ml^{-1}) and are inactive at 10 μg ml^{-1} to *Pseudomonas aeruginosa*. This natural product exhibits an astounding level of potency toward *S. aureus* and whilst this activity must be initiated by UV light there may be opportunities to use this class as topical antibacterial agents. A far less

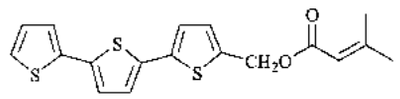

107

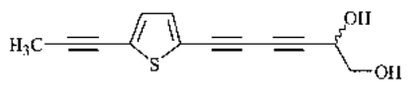

108

active thiophene-polyyne (**108**) from *Balsamorhiza sagittata* (MIC 25 μg ml^{-1} against MRSA) is also moderately potentiated by exposure to UV light for half an hour.[140]

3.11 Acylphloroglucinols

The acylphloroglucinols are natural products based on an aromatic ring that in many cases has been reduced or has a keto-enol form. The majority of these products are prenylated and/or farnesylated and possess simple acyl groups such as 2-methylpropanoyl which is found in hyperforin (**109**). This metabolite occurs in *Hypericum perforatum* (St John's Wort) and is commonly used as an herbal antidepressant product.[120] Much work has been done on the antibacterial evaluation of hyperforin and *in vitro* activity is exceptional with MIC values ranging from 0.1–1 μg ml^{-1} against penicillin-resistant SA (PRSA) and MRSA strains.[141,142] These results substantiate the use of St John's Wort in several countries as a treatment for superficial burns and wounds that heal poorly.[142] A recent paper describes that exposure of SA to hyperforin leads to a reduced sensitivity to this agent, although the author suggests that resistance cannot be acquired at the doses of which St John's Wort is given for antidepressant effects.[143] Furthermore, the potential use of this agent as an antibiotic is supported by the observation that no resistance occurred at low concentrations of hyperforin and that even in strains with reduced susceptibility, no cross resistance with clinically used antibiotics could be detected.[143] These findings highlight the potential of the acylphloroglucinol class as anti-staphylococcal drug-leads and although this compound is known to be unstable[144] even the degradation products, notably **110** and **111** that occur as a mixture, display moderate activity (50 μg ml^{-1}, SA).[145]

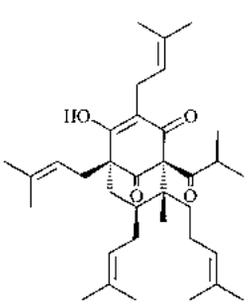

109

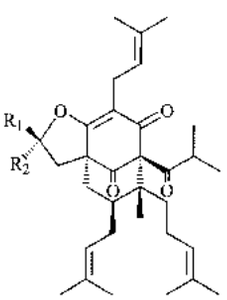

110 R_1 = H, R_2 = OH
111 R_1 = OH, R_2 = H

From the related species, *Hypericum papuanum,* a number of these interesting molecules have been characterised with antibacterial activity.[146,147]Compounds **112** and **113** are tautomeric isomers characterised as a mixture by NMR spectroscopy in the ratio of 4 : 3 respectively (MIC of mixture, 32 μg ml^{-1}, SE). The structure elucidation of these metabolites is not trivial due to the presence of tautomers and in some cases rotameric forms may also be present which can greatly complicate spectra. A

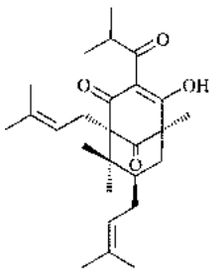

112

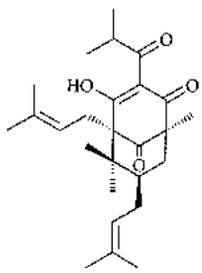

113

further tautomeric mixture from the same plant[147] is seen for **114** (only one form shown) with similar activity towards *S. epidermidis.*

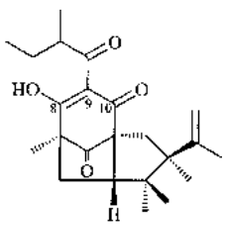

114

Traditional healers in the Free State province of South Africa use *Helichrysum caespititium* as a wound treatment in male circumcision rites and a bioassay-guided study of this species led to the isolation of **115** (MIC, 5 μg ml^{-1}, SA).[148] This compound also inhibited the growth of six fungi, including species of *Aspergillus, Cladosporium* and *Phytophthora,* at low concentration (0.5–5 μg ml^{-1}), indicating an ecological rationale for the presence of this metabolite.

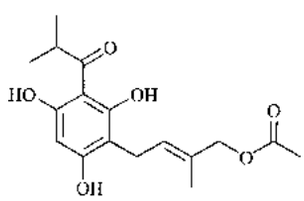

115

Another plant species used in the Mediterranean as an antiseptic is *Myrtus communis,* which produces myrtucommulone A (**116**). This was evaluated using a standard ATCC 25923 SA strain, MRSA possessing the TetK (tetracycline) efflux transporter and further efflux protein producing SA strains, and MIC values ranged from 0.5–2 μg ml^{-1}.[149] The MIC of **116** against SA-1199B which expresses the NorA MDR efflux pump was 1 μg ml^{-1} indicating that myrtucommulone A is not a substrate for this mechanism which would be advantageous in a new class of antibiotic-leads.

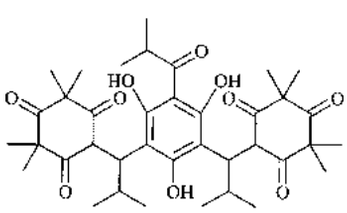

116

4 Summary

That no single chemical entity plant-derived anti-staphylococcal agents are used clinically is surprising given the enormous amount of literature on antibacterial extracts and their natural products. It is also puzzling given the use of herbal medicinal products to treat bacterial infections, for example cranberry juice in the management of urinary tract infections.[120,150]

The reasons for this are complex, but probably stem from pharmaceutical companies preferring to pursue microbially derived products, of which there are many first class drug examples which can be readily fermented with few re-supply issues. Additionally, pharmaceutical companies have neglected natural products preferring to utilise combinatorial chemistry libraries as a source of chemical diversity. Unfortunately such libraries lack the true chemical diversity that natural products display (extensive functional group chemistry and chirality) and these libraries are poor for discovery purposes but have potential in lead optimisation. A series of important recent reviews[151] have focused on this deficit and highlight the value of natural products as a screening resource and it is likely that pharmaceutical companies will once again turn their attention to plants, microbes and marine organisms.

Plant sources of antibacterials should not be overlooked as the anti-staphylococcal activities reported in this review are appreciable. Several of the examples such as the acylphloroglucinols and terthiophenes are exceptional and even concerns over re-supply issues could be overcome with access to materials by large-scale cultivation, failing an economically viable synthesis.

What is needed to progress these leads is further profiling against other Gram-positive and Gram-negative bacteria, particularly against resistant, clinically relevant species. In order to interest a pharmaceutical company partner to take on these compounds as development leads, mammalian cell cytotoxicity should be evaluated to see if the margin between bacterial and mammalian cell toxicity can be exploited and ideally small *in vivo* experiments should be conducted to gauge efficacy.

Pressure to find novel antibacterials with new modes of action will drive exploitation of plant sources as antimicrobials. The choice is logical given the ecological rationale that plants produce natural products as a chemical defence against microbes in their environment. Plants produce mammalian cytotoxic compounds *par excellence* and the successes of taxol and taxotere, camptothecin derivatives (topotecan, irinotecan), the vinca alkaloids and the podophyllotoxins to name some of the most successful clinically used anticancer drugs should be justification alone for the exploitation of this chemical pool.

The way is also open for the development of bacterial resistance modifying agents. These could readily mirror the successes seen with RMAs of human tumour resistance, for example inhibitors of p-glycoprotein, one of the major MDR mechanisms. There is also an ecological rationale for the production of natural products that modify microbial resistance. Tegos *et al.*,[125] speculate that plants may have evolved compounds which evade MDR mechanisms and that plant antimicrobials might be developed into broad spectrum antibiotics in combination with inhibitors of MDR. These MDR proteins are, in all probability, commonly found in nature (as efflux pumps to remove foreign toxic substances from the cell) as they are in clinical isolates of resistant pathogens. Further work on organisms which are environmentally relevant to plants is likely to show that these pumps are part of the normal removal of xenobiotics in both bacteria and fungi and it is likely that the compounds that inhibit these processes are also present in the same ecological niche.

5 References

1 S. Gibbons, M. Oluwatuyi and G. W. Kaatz, *J. Antimicrob. Chemother.*, 2003, **51**, 13.
2 T. M. Perl, *Am. J. Med.*, 1999, **106**, 26S–37S.
3 S. S. Rotun, V. McMath, D. J. Schoonmaker, P. S. Maupin, F. C. Tenover, B. C. Hill and D. M. Ackman, *Emerg. Infect. Dis.*, 1999, **5**, 147.

4 M. P. Jevons, *Br. Med. J.*, 1961, **1**, 124.
5 M. P. Jevons, A. W. Coe and M. T. Parker, *Lancet*, 1963, **1**, 904.
6 N. S. Crowcroft and M. Catchpole, *Br. Med. J.*, 2002, **325**, 1390.
7 *'Resistance to Antibiotics' Science and Technology – 7th Report to the House of Lords Committee*, The Stationery Office, London,1998.
8 The National Audit Office, *Report by the Comptroller and Auditor General.* (17th of February), The Stationery Office, London, 2000, pp. 6–121.
9 Public Health Dispatch, *Morbidity Mortality Weekly Rep.*, 2002, **51**, 902.
10 CDC, *Morbidity Mortality Weekly Rep.*, 2002, **51**, 565.
11 S. Tsiodras, H. S. Gold, G. Sakoulas, G. M. Eliopoulos, C. Wennersten, L. Venkataraman, R. C. Moellering and M. J. Ferraro, *Lancet*, 2001, **358**, 207.
12 S. Esposito and S. Noviello, *J. Chemother.*, 1990, **2**, 167.
13 N. J. Marshall and L. J. V. Piddock, *Microbiologia*, 1997, **13**, 285.
14 P. N. Markham, E. Westhaus, K. Klyachko, M. E. Johnson and A. A. Neyfakh, *Antimicrob. Agents Chemother.*, 1999, **43**, 2404.
15 T. S. Yam, J. M. Hamilton-Miller and S. Shah, *J. Antimicrob. Chemother.*, 1998, **42**, 211.
16 J. M. Hamilton-Miller and S. Shah, *FEMS Microbiol. Lett.*, 1999, **176**, 463.
17 J. M. Hamilton-Miller, 1995, Patent Application PCT GB/95/02107.
18 J. M. Hamilton-Miller and S. Shah, *J. Antimicrob. Chemother.*, 2000, **46**, 852.
19 K. Nicolson, G. Evans and P. W. O'Toole, *FEMS Microbiol. Lett.*, 1999, **179**, 233.
20 S. Shiota, M. Shimizu, T. Mizusima, H. Ito, T. Hatano, T. Yoshida and T. Tsuchiya, *FEMS Microbiol. Lett.*, 2000, **185**, 135.
21 M. Shimizu, S. Shiota, T. Mizushima, H. Ito, T. Hatano, T. Yoshida and T. Tsuchiya, *Antimicrob. Agents Chemother.*, 2001, **45**, 3198.
22 S. Gibbons, M. Oluwatuyi, N. C. Veitch and A. I. Gray, *Phytochemistry*, 2003, **62**, 83.
23 S. Gibbons and E. E. Udo, *Phytother. Res.*, 2000, **14**, 139.
24 F. J. Schmitz, A. C. Fluit, M. Luckefahr, B. Engler, B. Hofmann, J. Verhoef, H. P. Heinz, U. Hadding and M. E. Jones, *J. Antimicrob. Chemother.*, 1998, **42**, 807.
25 P. C. Hsieh, S. A. Siegel, B. Rogers, D. Davis and K. Lewis, *Proc. Natl. Acad. Sci. USA*, 1998, **95**, 6602.
26 F. R. Stermitz, P. Lorenz, J. N. Tawara, L. A. Zenewicz and K. Lewis, *Proc. Natl. Acad. Sci. USA*, 2000, **97**, 1433.
27 N. R. Guz and F. R. Stermitz, *J. Nat. Prod.*, 2000, **63**, 1140.
28 F. R. Stermitz, J. Tawara-Matsuda, P. Lorenz, P. Mueller, L. Zenewicz and K. Lewis, *J. Nat. Prod.*, 2000, **63**, 1146.
29 F. R. Stermitz, T. D. Beeson, P. J. Mueller, J. Hsiang and K. Lewis, *Biochem. Syst. Ecol.*, 2001, **29**, 793.
30 F. R. Stermitz, L. N. Scriven, G. Tegos and K. Lewis, *Planta Med.*, 2002, **68**, 1140.
31 C. Morel, F. R. Stermitz, G. Tegos and K. Lewis, *J. Agric. Food Chem.*, 2003, **51**, 5677.
32 F. R. Stermitz, K. K. Cashman, K. M. Halligan, C. Morel, G. P. Tegos and K. Lewis, *Bioorg. Med. Chem. Lett.*, 2003, **13**, 1915.
33 C. T. Price, G. W. Kaatz and J. E. Gustafson, *Int. J. Antimicrob. Agents*, 2002, **20**, 206.
34 I. B. Bassett, D. L. Pannowitz and R. S. Barnetson, *Med. J. Aust.*, 1990, **153**, 455.
35 A. Raman, U. Weir and S. F. Bloomfield, *Lett. Appl. Microbiol.*, 1995, **21**, 242.
36 C. F. Carson and T. V. Riley, *J. Appl. Bacteriol.*, 1995, **78**, 264.
37 S. D. Cox, C. M. Mann and J. L. Markham, *J. Appl. Microbiol.*, 2001, **91**, 492.
38 D. Kalemba, D. Kusewicz and K. Swiader, *Phytother. Res.*, 2002, **16**, 288.
39 R. S. Taylor and G. H. N. Towers, *Phytochemistry*, 1998, **47**, 631.
40 K. H. Lee, T. Ibuka, R. Y. Wu and T. A. Geissman, *Phytochemistry*, 1977, **16**, 1177.
41 K. Kawazoe, Y. Tsubouchi, N. Abdullah, Y. Takaishi, H. Shibata, T. Higuti, H. Hori and M. Ogawa, *J. Nat. Prod.*, 2003, **66**, 538.
42 Y. Sato, H. Oketani, T. Yamada, K. Singyouchi, T. Ohtsubo, M. Kihara, H. Shibata and T. Higuti, *J. Pharm. Pharmacol.*, 1997, **49**, 1042.
43 A. M. Galal, E. A. Abourashed, S. A. Ross, M. A. ElSohly, M. S. Al-Said and F. S. El-Feraly, *J. Nat. Prod.*, 2001, **64**, 399.
44 K. Tamemoto, Y. Takaishi, B. Chen, K. Kawazoe, H. Shibata, T. Higuti, G. Honda, M. Ito, Y. Takeda, O. K. Kodzhimatov and O. Ashurmetov, *Phytochemistry*, 2001, **58**, 763.
45 P. Dolara, B. Corte, C. Ghelardini, A. M. Pugliese, E. Cerbai, S. Menichetti and A. Lo Nostro, *Planta Med.*, 2000, **66**, 356.
46 A. O. Tucker, *Econ. Bot.*, 1986, **40**, 425.
47 D. Y. Shin, H. S. Kim, K. H. Min, S. S. Hyun, S. A. Kim, H. Huh, E. C. Choi, Y. H. Choi, J. Kim, S. H. Choi, W. B. Kim and Y. G. Suh, *Chem. Pharm. Bull. (Tokyo)*, 2000, **48**, 1805.
48 M. I. Aguilar, G. Delgado, M. L. Hernandez and M. L. Villarreal, *Nat. Prod. Lett.*, 2001, **15**, 93.
49 R. Mata, E. Martinez, R. Bye, G. Morales, M. P. Singh, J. E. Janso, W. M. Maiese and B. Timmermann, *J. Nat. Prod.*, 2001, **64**, 911.
50 A. Ulubelen, *Phytochemistry*, 2003, **64**, 395.
51 A. Ulubelen, S. Oksuz, G. Topcu, A. C. Goren and W. Voelter, *J. Nat. Prod.*, 2001, **64**, 549.
52 A. Ulubelen, S. Oksuz, U. Kolak, C. Bozok-Johansson, C. Celik and W. Voelter, *Planta Med.*, 2000, **66**, 458.
53 A. C. Goren, G. Topcu, S. Oksuz, G. Kokdil, W. Voelter and A. Ulubelen, *Nat. Prod. Lett.*, 2002, **16**, 47.
54 A. Ulubelen, S. Oksuz, G. Topcu, A. C. Goren, C. Bozok-Johansson, C. Celik, G. Kokdil and W. Voelter, *Nat. Prod. Lett.*, 2001, **15**, 307.
55 X. Chen, J. Ding, Y. M. Ye and J. S. Zhang, *J. Nat. Prod.*, 2002, **65**, 1016.
56 A. M. El-Lakany, *Pharmazie*, 2003, **58**, 75.
57 O. Batista, M. F. Simoes, A. Duarte, M. L. Valdeira, M. C. de la Torre and B. Rodriguez, *Phytochemistry*, 1995, **38**, 167.
58 J. E. Dellar, M. D. Cole and P. G. Waterman, *Phytochemistry*, 1996, **41**, 735.
59 J. E. Dellar, M. D. Cole and P. G. Waterman, *Biochem. Syst. Ecol.*, 1996, **24**, 83.
60 G. Çitoglu, M. Tanker, B. Sever, J. Englert, R. Anton and N. Altanlar, *Planta Med.*, 1998, **64**, 484.
61 M. Politi, A. Braca, N. De Tommasi, I. Morelli, A. Manunta, L. Battinelli and G. Mazzanti, *Planta Med.*, 2003, **69**, 468.
62 D. Xiao, M. Kuroyanagi, T. Itani, H. Matsuura, M. Udayama, M. Murakami, K. Umehara and N. Kawahara, *Chem. Pharm. Bull. (Tokyo)*, 2001, **49**, 1479.
63 D. Thangadurai, M. B. Viswanathan and N. Ramesh, *Pharmazie*, 2002, **57**, 714.
64 B. Gigante, A. M. Silva, M. J. Marcelo-Curto, S. S. Feio, J. Roseiro and L. V. Reis, *Planta Med.*, 2002, **68**, 680.
65 G. M. Woldemichael, G. Wachter, M. P. Singh, W. M. Maiese and B. N. Timmermann, *J. Nat. Prod.*, 2003, **66**, 242.
66 H. Haraguchi, S. Oike, H. Muroi and I. Kubo, *Planta Med.*, 1996, **62**, 122.
67 G. B. Evans and R. H. Furneaux, *Bioorg. Med. Chem.*, 2000, **8**, 1653.
68 H. Muroi and I. Kubo, *Biosci. Biotech. Biochem.*, 1994, **58**, 1925.
69 I. Kubo, H. Muroi and M. Himejima, *J. Nat. Prod.*, 1992, **55**, 1436.
70 J. R. Zgoda-Pols, A. J. Freyer, L. B. Killmer and J. R. Porter, *Fitoterapia*, 2002, **73**, 434.
71 A. Zamilpa, J. Tortoriello, V. Navarro, G. Delgado and L. Alvarez, *Planta Med.*, 2002, **68**, 281.
72 S. Erazo, M. Zaldivar, C. Delporte, N. Backhouse, P. Tapia, E. Belmonte, F. Delle Monarche and R. Negrete, *Planta Med.*, 2002, **68**, 361.
73 B. M. Tincusi, I. A. Jimenez, I. L. Bazzocchi, L. M. Moujir, Z. A. Mamani, J. P. Barroso, A. G. Ravelo and B. V. Hernandez, *Planta Med.*, 2002, **68**, 808.
74 V. Roussis, M. Tsoukatou, I. B. Chinou and A. Ortiz, *Planta Med.*, 1998, **64**, 675.
75 A. Ankli, J. Heilmann, M. Heinrich and O. Sticher, *Phytochemistry*, 2000, **54**, 531.
76 G. M. Woldemichael, M. P. Singh, W. M. Maiese and B. N. Timmermann, *Z. Naturforsch., C: Biosci.*, 2003, **58**, 70.
77 A. Braca, I. Morelli, J. Mendez, L. Battinelli, L. Braghiroli and G. Mazzanti, *Planta Med.*, 2000, **66**, 768.
78 K. Y. Orabi, S. I. Al-Qasoumi, M. M. El-Olemy, J. S. Mossa and I. Muhammad, *Phytochemistry*, 2001, **58**, 475.
79 D. R. Katerere, A. I. Gray, R. J. Nash and R. D. Waigh, *Phytochemistry*, 2003, **63**, 81.
80 I. Muhammad, K. A. El Sayed, J. S. Mossa, M. S. Al-Said, F. S. El-Feraly, A. M. Clark, C. D. Hufford, S. Oh and A. M. S. Mayer, *J. Nat. Prod.*, 2000, **63**, 605.
81 M. T. Gutierrez-Lugo, M. P. Singh, W. M. Maiese and B. N. Timmermann, *J. Nat. Prod.*, 2002, **65**, 872.
82 M. Chatterji, S. Unniraman, S. Mahadevan and V. Nagaraja, *J. Antimicrob. Chemother.*, 2001, **48**, 479.
83 Y. Tada, Y. Shikishima, Y. Takaishi, H. Shibata, T. Higuti, G. Honda, M. Ito, Y. Takeda, O. K. Kodzhimatov, O. Ashurmetov and Y. Ohmoto, *Phytochemistry*, 2002, **59**, 649.
84 W. N. Setzer, M. C. Setzer, R. B. Bates, P. Nakkiew, B. R. Jackes, L. Chen, M. B. McFerrin and E. J. Meehan, *Planta Med.*, 1999, **65**, 747.
85 P. M. Pauletti, A. R. Araujo, M. C. Young, A. M. Giesbrecht and V. D. Bolzani, *Phytochemistry*, 2000, **55**, 597.
86 K. Kawazoe, A. Yutani, K. Tamemoto, S. Yuasa, H. Shibata, T. Higuti and Y. Takaishi, *J. Nat. Prod.*, 2001, **64**, 588.
87 E. Kamory, G. M. Keseru and B. Papp, *Planta Med.*, 1995, **61**, 387.

88 J. R. Zgoda-Pols, A. J. Freyer, L. B. Killmer and J. R. Porter, *J. Nat Prod.*, 2002, **65**, 1554.
89 I. Muhammad, X. C. Li, D. C. Dunbar, M. A. ElSohly and I. A. Khan, *J. Nat. Prod.*, 2001, **64**, 1322.
90 I. Muhammad, X. C. Li, M. R. Jacob, B. L. Tekwani, D. C. Dunbar and D. Ferreira, *J. Nat. Prod.*, 2003, **66**, 804.
91 J. Orjala, P. Mian, T. Rali and O. Sticher, *J. Nat. Prod.*, 1998, **61**, 939.
92 C. C. Shen, W. J. Syu, S. Y. Li, C. H. Lin, G. H. Lee and C. M. Sun, *J. Nat. Prod.*, 2002, **65**, 1857.
93 Y. Morita, E. Matsumura, H. Tsujibo, M. Yasuda, T. Okabe, Y. Sakagami, Y. Kumeda, N. Ishida and Y. Inamor, *Biol. Pharm. Bull.*, 2002, **25**, 981.
94 Y. Sato, H. Oketani, K. Singyouchi, T. Ohtsubo, M. Kihara, H. Shibata and T. Higuti, *Biol. Pharm. Bull.*, 1997, **20**, 401.
95 K. Kono, I. Tatara, S. Takeda, K. Arakawa and Y. Hara, *Kansenshogaku Zasshi*, 1994, **68**, 1518.
96 R. Tsukiyama, H. Katsura, N. Tokuriki and M. Kobayashi, *Antimicrob. Agents Chemother.*, 2002, **46**, 1226.
97 T. Fukai, A. Marumo, K. Kaitou, T. Kanda, S. Terada and T. Nomura, *Fitoterapia*, 2002, **73**, 536.
98 A. S. Joshi, X. C. Li, A. C. Nimrod, H. N. ElSohly, L. A. Walker and A. M. Clark, *Planta Med.*, 2001, **67**, 186.
99 Y. Sato, S. Suzaki, T. Nishikawa, M. Kihara, H. Shibata and T. Higuti, *J. Ethnopharmacol.*, 2000, **72**, 483.
100 M. M. Rahman and A. I. Gray, *Phytochemistry*, 2002, **59**, 73.
101 N. P. Nanayakkara, C. L. Burandt Jr. and M. R. Jacob, *Planta Med.*, 2002, **68**, 519.
102 S. G. Dastidar, S. K. Mahapatra, K. Ganguly, A. N. Chakrabarty, Y. Shirataki and N. Motohashi, *In Vivo*, 2001, **15**, 519.
103 Y. Sakagami, M. Mimura, K. Kajimura, H. Yokoyama, M. Linuma, T. Tanaka and M. Ohyama, *Lett. Appl. Microbiol.*, 1998, **27**, 98.
104 N. Didry, L. Dubreuil and M. Pinkas, *Phytother. Res.*, 1993, **7**, 242.
105 M. Kuroyanagi, T. Arakawa, Y. Hirayama and T. Hayashi, *J. Nat. Prod.*, 1999, **62**, 1595.
106 Y. Deng, J. P. Lee, M. Tianasoa-Ramamonjy, J. K. Snyder, S. A. Des Etages, D. Kanada, M. P. Snyder and C. J. Turner, *J. Nat. Prod.*, 2000, **63**, 1082.
107 M. Sato, H. Tsuchiya, T. Miyazaki, M. Ohyama, T. Tanaka and M. Iinuma, *Lett. Appl. Microbiol.*, 1995, **21**, 219.
108 A. E. Nkengfack, J. C. Vardamides, Z. T. Fomum and M. Meyer, *Phytochemistry*, 1995, **40**, 1803.
109 A. K. Waffo, G. A. Azebaze, A. E. Nkengfack, Z. T. Fomum, M. Meyer, B. Bodo and F. R. van Heerden, *Phytochemistry*, 2000, **53**, 981.
110 H. Tanaka, T. Oh-Uchi, H. Etoh, M. Sako, F. Asai, T. Fukai, M. Sato, J. Murata and Y. Tateishi, *Phytochemistry*, 2003, **64**, 753.
111 H. Tanaka, M. Sato, S. Fujiwara, M. Hirata, H. Etoh and H. Takeuchi, *Lett. Appl. Microbiol.*, 2002, **35**, 494.
112 J. B. Harborne, *Introduction to Ecological Biochemistry*, Academic Press Publishers, London, 1994, 4th Edition.
113 R. R. Majinda, M. Motswaledi, R. D. Waigh and P. G. Waterman, *Planta Med.*, 1997, **63**, 268.
114 S. Tang, P. Bremner, A. Kortenkamp, C. Schlage, A. I. Gray, S. Gibbons and M. Heinrich, *Planta Med.*, 2003, **69**, 247.
115 A. Chakraborty, C. Saha, G. Podder, B. K. Chowdhury and P. Bhattacharyya, *Phytochemistry*, 1995, **38**, 787.
116 K. Nakahara, G. Trakoontivakorn, N. S. Alzoreky, H. Ono, M. Onishi-Kameyama and M. Yoshida, *J. Agric. Food Chem.*, 2002, **50**, 4796.
117 K. Cimanga, T. De Bruyne, A. Lasure, B. Van Poel, L. Pieters, M. Claeys, D. V. Berghe, K. Kambu, L. Tona and A. J. Vlietinck, *Planta Med.*, 1996, **62**, 22.
118 H. A. Saad, S. H. El-Sharkawy and W. T. Shier, *Planta Med.*, 1995, **61**, 313.
119 A. L. Okunade, A, M. Clark, C. D. Hufford and B. O. Oguntimein, *Planta Med.*, 1999, **65**, 447.
120 J. E. Barnes, L. A. Anderson and J. D. Phillipson, *Herbal Medicine: A Guide for Health Care Professionals*, Pharmaceutical Press, London, 2002, 2nd edition.
121 *Trease and Evans Pharmacognosy*, ed. W. C. Evans, W. B. Saunders Publishers, London, 2002, 15th Edition, p. 363.
122 F. Scazzocchio, M. F. Cometa, L. Tomassini and M. Palmery, *Planta Med.*, 2001, **67**, 561.
123 S. Gibbons, J. Leimkugel, M. Oluwatuyi and M. Heinrich, *Phytother. Res.*, 2003, **17**, 274.
124 Z. Zhang, H. N. ElSohly, M. R. Jacob, D. S. Pasco, L. A. Walker and A. M. Clark, *J. Nat. Prod.*, 2002, **65**, 856.
125 G. Tegos, F. R. Stermitz, O. Lomovskaya and K. Lewis, *Antimicrob. Agents Chemother.*, 2002, **46**, 3133.
126 X. C. Li, D. C. Dunbar, H. N. ElSohly, M. R. Jacob, A. C. Nimrod, L. A. Walker and A. M. Clark, *J. Nat. Prod.*, 2001, **64**, 1153.
127 H. R. Dharmaratne, W. M. Wijesinghe and V. J. Thevanasem, *J. Ethnopharmacol.*, 1999, **66**, 339.
128 M. Iinuma, H. Tosa, T. Tanaka, F. Asai, Y. Kobayashi, R. Shimano and K. Miyauchi, *J. Pharm. Pharmacol.*, 1996, **48**, 861.
129 A. E. Nkengfack, P. Mkounga, M. Meyer, Z. T. Fomum and B. Bodo, *Phytochemistry*, 2002, **61**, 181.
130 S. Nakamura and A. Hatanaka, *J. Agric. Food. Chem.*, 2002, **50**, 7639.
131 J. R. Zgoda, A. J. Freyer, L. B. Killmer and J. R. Porter, *J. Nat. Prod.*, 2001, **64**, 1348.
132 H. Matsuura, G. Saxena, S. W. Farmer, R. E. Hancock and G. H. N. Towers, *Planta Med.*, 1996, **62**, 256.
133 D. Lechner, M. Stavri, M. Oluwatuyi, R. Pereda-Miranda and S. Gibbons, *Phytochemistry*, 2004, **64**, 331.
134 P. Magiatis, D. Spanakis, S. Mitaku, E. Tsitsa, A. Mentis and C. Harvala, *J. Nat. Prod.*, 2001, **64**, 1093.
135 J. Heilmann, R. Brun, S. Mayr, T. Rali and O. Sticher, *Phytochemistry*, 2001, **57**, 1281.
136 S. M. Tsao and M. C. Yin, *J. Med. Microbiol.*, 2001, **50**, 646.
137 R. Naganawa, N. Iwata, K. Ishikawa, H. Fukuda, T. Fujino and A. Suzuki, *Appl. Environ. Microbiol.*, 1996, **62**, 4238.
138 J. Kagan, *Prog. Chem. Org. Nat. Prod.*, 1991, **56**, 87.
139 M. Ciofalo, S. Petruso and D. Schillaci, *Planta Med.*, 1996, **62**, 374.
140 H. Matsuura, G. Saxena, S. W. Farmer, R. E. Hancock and G. H. N. Towers, *Planta Med.*, 1996, **62**, 65.
141 C. M. Schempp, K. Pelz, A. Wittmer, E. Schopf and J. C. Simon, *Lancet*, 1999, **353**, 2129.
142 J. Reichling, A. Weseler and R. Saller, *Pharmacopsychiatry*, 2001, **34**(Suppl 1), S116.
143 A. T. Hübner, *Phytomedicine*, 2003, **10**, 206.
144 S. Trifunovic, V. Vajs, S. Macura, N. Juranic, Z. Djarmati, R. Jankov and S. Milosavljevic, *Phytochemistry*, 1998, **49**, 1305.
145 V. Vajs, S. Vugdelija, S. Trifunovic, I. Karadzic, N. Juranic, S. Macura and S. Milosavljevic, *Fitoterapia*, 2003, **74**, 439.
146 K. Winkelmann, J. Heilmann, O. Zerbe, T. Rali and O. Sticher, *J. Nat. Prod.*, 2001, **64**, 701.
147 K. Winkelmann, J. Heilmann, O. Zerbe, T. Rali and O. Sticher, *J. Nat. Prod.*, 2000, **63**, 104.
148 A. D. Mathekga, J. J. M. Meyer, M. M. Horn and S. E. Drewes, *Phytochemistry*, 2000, **53**, 93.
149 G. Appendino, F. Bianchi, A. Minassi, O. Sterner, M. Ballero and S. Gibbons, *J. Nat. Prod.*, 2002, **65**, 334.
150 A. Stapleton, *Infect. Dis. Clin. North Am.*, 2003, **17**, 457.
151 A. M. Rouhi, *Chem. Eng. News*, 2003, **81**, pp. 77, 93 and 104.

PHYTOTHERAPY RESEARCH
Phytother. Res. **18**, 774–776 (2004)
Published online in Wiley InterScience (www.interscience.wiley.com). **DOI**: 10.1002/ptr.1527

SHORT COMMUNICATION

The Antimycobacterial Components of Hops (*Humulus lupulus*) and their Dereplication

Michael Stavri[1], Ruth Schneider[1], Gemma O'Donnell[1], Doris Lechner[1], Franz Bucar[2] and Simon Gibbons[1]*

[1]Centre for Pharmacognosy and Phytotherapy, The School of Pharmacy, University of London, London, UK
[2]Institute for Pharmacognosy, University of Graz, Graz, Austria

Bioassay-guided fractionation of a hexane extract of strobile hops (*Humulus lupulus*) was undertaken to isolate and characterize the antimycobacterial constituents using the fast-growing mycobacterial species *Mycobacterium fortuitum*. Activity was associated with a low polarity fraction and ^{1}H NMR spectra indicated the presence of a fatty acid mixture with unsaturated components. GC-MS of the derivatives indicated the presence of palmitic, stearic and oleic acids with small quantities of lignoceric, arachidic, behenic and linoleic acids. These compounds were assessed against *M. fortuitum* and all saturated fatty acids were inactive at concentrations greater than 256 μg/ml, whereas the unsaturated fats oleic and linoleic acids displayed minimum inhibitory concentrations of between 4 and 16 μg/ml against the fast-growing species tested. The widespread occurrence of these components could render screening for antimycobacterials from natural sources highly problematic without adequate dereplication. We propose that GC-MS of derivatised components of lipophilic extracts be a first step before any antimycobacterial bioassay-guided study, as this technique is the method of choice for dereplication of fatty acids. Copyright © 2004 John Wiley & Sons, Ltd.

Keywords: Mycobacterium; antibacterial; unsaturated fatty acids; GC-MS; dereplication.

INTRODUCTION

In a continuing project to investigate plants for antimycobacterial activity, we evaluated extracts of strobile hops with a view to isolate and characterise the active constituents. An important review by Newton *et al*. (2000), covering antimycobacterial plant extracts led to this investigation and the primary literature cited in this review, which associated activity of an ethanol extract against *M. tuberculosis* (Gottshall *et al.*, 1949), did not detail the constituents responsible for activity. However, the antibacterial activity of hops has been described towards Gram-positive bacteria and fungi (Langezaal *et al*., 1992; Simpson and Smith, 1992) and thought to be due mainly to the presence of hop acids which are acylated phloroglucinol natural products of the humulone and lupulone type. The importance of hops to the brewing industry as a taste modifier and antibacterial agent is enormous and the effects of hops on beer spoilage bacteria have recently been reviewed (Sakamoto and Konings, 2003). The chemistry of hops is well documented (Verzele and De Keukeleire, 1991; Milligan *et al.*, 1999; Miranda *et al.*, 1999), presumably due to its use in the brewing industry, and herbal preparations of hops are gaining in popularity as sedatives, particularly in preparations to improve sleep patterns in combination with valerian.

* Correspondence to: Dr S. Gibbons, Centre for Pharmacognosy and Phytotherapy, The School of Pharmacy, University of London, 29-39 Brunswick Square, London WC1N 1AX, UK.
E-mail: simon.gibbons@ulsop.ac.uk

We were prompted by the lack of a report on this species describing the antibacterial agents responsible for antimycobacterial activity previously described. Extracts were prepared and screened in an *in vitro* assay using *Mycobacterium fortuitum* (ATCC 6841) which has been shown to be of use as an alternative screening model to *M. tuberculosis* for evaluating antitubercular drugs (Gillespie *et al*., 2001). This species has the obvious advantage over *M. tuberculosis* in that it can be handled in a class 2 microbiological laboratory and is a fast growing strain, leading to the completion of one assay within 72 h.

MATERIALS AND METHODS

Bacteria. *Mycobacterium fortuitum* ATCC 6841 was obtained from Dr Peter Lambert, Aston University. *Mycobacterium smegmatis* ATCC 14468, *Mycobacterium phlei* ATCC 11758 and *Mycobacterium aurum* Pasteur Institute 104482 were obtained from Dr Veronique Seidel, The University of Strathclyde.

Minimum Inhibitory Concentration Assay. *Mycobacterium fortuitum*, *Mycobacterium smegmatis Mycobacterium phlei* and *Mycobacterium aurum.* This assay comprised a standard minimum inhibitory concentration (MIC) determination (Gibbons and Udo, 2000) of test compound in Ca^{2+} and Mg^{2+} adjusted Mueller-Hinton Broth (MHB). Extracts and bands were first dissolved in DMSO and then diluted in MHB, to give a starting concentration of 512 μg/ml which was diluted out across a 96-well microtitre plate in a two-fold serial

Received 19 May 2004
Accepted 4 June 2004

dilution to give a final concentration range from 512–1 μg/ml. Mycobacterial strains were grown on Columbia Blood agar (Oxoid) supplemented with 7% defibrinated Horse blood (Oxoid). Bacterial inocula equivalent to the 0.5 McFarland turbidity standard were prepared in normal saline and diluted to give a final inoculum density of 5×10^5 cfu/ml. The inoculum (125 μL) was added to all wells and the microtitre plate was incubated at 37 °C for 72 h for *M. fortuitum*, *M. smegmatis* and *M. phlei.* For *M. aurum* the plate was incubated for 120 h. The MIC was recorded as the lowest concentration at which no bacterial growth was observed. This was facilitated by the addition of 20 μL of MTT (Sigma 10 mg/ml in MeOH) to each well and incubation at 37 °C for 20 min where bacterial growth was indicated by a blue colouration. Appropriate DMSO, growth and sterile controls were carried out. Ethambutol and isoniazid were used as positive controls.

Isolation. Strobile hops were obtained from the Herbal Apothecary (Syston, Leicester, UK, batch number 03540), and a voucher specimen (SG-2004-HL-1) has been deposited in the Centre for Pharmacognosy and Phytotherapy. Five hundred grams were powdered and extracted in a Soxhlet apparatus using hexane, dichloromethane and finally methanol (3 l each). Activity was associated with the hexane extract (minimum inhibitory concentration = 256 μg/ml). Nine grams of this extract were subjected to VLC on silica gel eluting with hexane and increasing polarity with 10% increments of ethyl acetate to give 11 fractions. A final wash with methanol gave fraction 12. Fraction 4 (eluted with 30% EtOAc in hexane; MIC = 128 μg/ml), was subjected to LH-20 Sephadex column chromatography eluting with dichloromethane (fractions 1–6) and finally with pure methanol to afford fraction 7. Fraction 7 was then subjected to multiple development preparative TLC (3 times; toluene:EtOAc:AcOH, 80:18:2) to afford three bands (**1–3**) with MIC values of 16, 256 and 512 mg/ml respectively. Pure fatty acid standards were obtained from the Sigma Chemical Company.

Derivatisation and GC-MS of band 1. Dried residue of band **1** was derivatised by adding a mixture of dimethylformamide-dimethylacetal/pyridine (1:1) and heating for 10 min at 60 °C. Thereafter the sample was directly used for GC-MS analysis by a 5890 Series II plus gas chromatograph interfaced to a 5989 B mass spectrometer (Hewlett-Packard). The analysis was performed on an HP-Innowax (59 m × 0.25 mm i.d., 0.25 μm film thickness) fused silica capillary. Temperature programme: 160 °C to 250 °C by 2 °C/min, 250 °C for 5 min, carrier gas helium, flow 1.0 ml/min; injector temperature: 250 °C, interface temperature: 250 °C; ionisation at 70 eV; ion source temperature 250 °C.

RESULTS AND DISCUSSION

At the outset of this study it seemed likely to us that activity would be associated solely with the hop acids, as the antibacterial effects were associated with a non-polar fraction of a hexane extract. Vacuum liquid chromatography on silica gel followed by gel filtration chromatography and finally preparative-TLC on silica gel led to the isolation of three bands, the least polar and most active of which (band **1**) had a minimum inhibitory concentration (MIC) of 16 μg/ml against *Mycobacterium fortuitum*. By analytical TLC **1** appeared as one spot, however ^{1}H NMR ($CDCl_3$, 400 MHz) indicated the presence of a mixture of fatty acids. Methyl triplets appearing in the spectrum at 0.8 and 0.9 ppm, a methylene envelope at 1.2 ppm, further deshielded methylene groups at δ 1.5, 2.0, 2.2, 2.7 ppm together with a multiplet at 5.3 ppm confirmed the presence of a mixture of fatty acids, some of which exhibited unsaturation. The integration indicated that these groups are present in differing proportions which further supported that this band contained a mixture of components. The final signal in the ^{1}H spectrum was a very broad singlet at 8.3 ppm suggestive of an exchangeable acidic proton which is characteristic for fatty acids in dry solvents.

Fatty acids are notoriously difficult to separate by conventional column and thin-layer chromatographies, particularly where a series of homologues may be present. Band **1** was therefore derivatised using DMF-DMA/pyridine and subjected to GC-MS in an attempt to identify the components (Fig. 1). The major components of this analysis were saturated and unsaturated fatty acids (Table 1). Palmitic, stearic and oleic acids

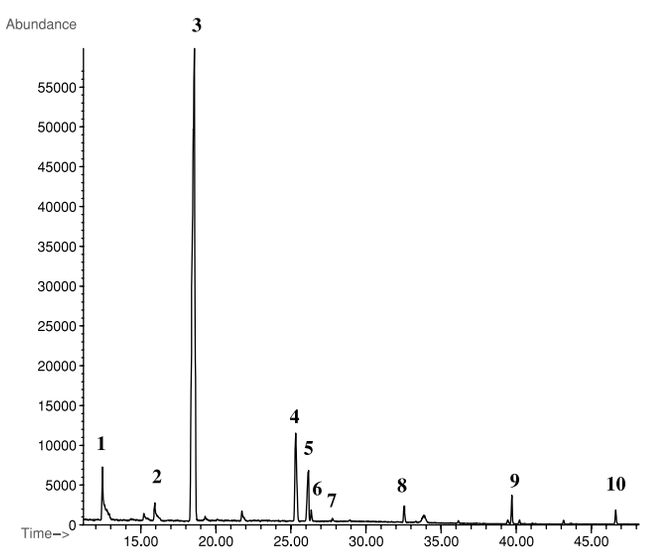

Figure 1. Selected ion chromatogram (m/z 74) obtained by GC-MS analysis of derivatised band **1**. Derivatisation to methyl esters by DMF-DMA/pyridine, fragment ion m/z 74 formed by McLafferty rearrangement is indicative for fatty acid methyl esters.

Table 1. GC-MS analysis of band 1 following derivatisation to methyl esters

Retention time (min)	Compound
12.47	**1** Myristic acid ME
15.94	**2** Nonanedioic acid dimethyl ester
18.57	**3** Palmitic acid ME
25.33	**4** Stearic acid ME
26.18	**5** Oleic acid ME
26.36	**6** C18:1 ME
27.78	**7** Linoleic acid ME
32.56	**8** Arachidic acid ME
39.80	**9** Behenic acid ME
46.64	**10** Lignoceric acid ME

Table 2. Minimum inhibitory concentrations (MIC) of fatty acids and standard antibiotics against fast growing species of Mycobacteria

Compound	*M. fortuitum*	*M. smegmatis*	*M. phlei*	*M. aurum*
Oleic acid	16	8	16	8
Linoleic acid	4	8	8	8
Palmitic acid	512	ξ	ξ	ξ
Ethambutol	4	0.5	2	1
Isoniazid	0.5	2	2	2

MIC of compounds in μg/ml. Stearic, arachidic, behenic and lignoceric acid were inactive at 512 μg/ml. ξ – Not tested.

were the most prominent and minor quantities of myristic, eicosanoic, behenic, lignoceric and linoleic acids and an unidentified unsaturated C18 (C18:1) acid was also present.

In an attempt to evaluate the antimycobacterial activity of these components, pure standards were acquired and tested against *Mycobacterium fortuitum*, our screening strain. All of the saturated acids were inactive at 256 μg/ml although oleic and linoleic acids had minimum inhibitory concentrations of 16 and 4 μg/ml respectively. This prompted us to test these compounds against other mycobacterial species namely *M. smegmatis*, *M. phlei* and *M. aurum* and MIC values were between 8 and 16 μg/ml for these strains (Table 2). Whilst these unsaturated fatty acids are known to be antibacterial (Dilika *et al.*, 2000) this is the first report of the antimycobacterial constituents of hops and it is pertinent to note that none of the other fractions tested in our assay exhibited appreciable activity less than 256 μg/ml.

Exogenous oleic and linoleic acids have been shown to inhibit fatty acid biosynthesis in *Lactobacillus plantarum* with the synthesis of unsaturated fatty acids being repressed more than saturated fat synthesis (Weeks and Wakil, 1970) although it is not certain that this effect is responsible for the antibacterial activity observed here. It has also been shown in *Helicobacter pylori* that oleic and linoleic acids are incorporated into cell mass and phospholipids and growth inhibition was associated with disruption of cell membranes (Khulusi *et al.*, 1995).

The antimycobacterial effects of Umkaloaba (*Pelargonium sidoides* and *Pelargonium reniforme*) a traditional treatment for TB used in South Africa has recently been demonstrated to be associated in part due to the presence of these simple unsaturated fatty acids (Seidel and Taylor, 2004).

The widespread occurrence of these practically ubiquitous compounds could complicate the search for new natural antimycobacterial substances and we propose that GC-MS be a first analytical step for evaluation of lipophilic antimycobacterial extracts. This would not of course rule out the possibility of the presence of other active antimycobacterial fat soluble natural products of which the terpenes are well represented (Cantrell *et al.*, 2001; Okunade *et al.*, 2004) but this approach could be used to prioritize extracts for large scale bioassay-guided fractionation.

REFERENCES

Cantrell CL, Franzblau SG, Fischer NH. 2001. Antimycobacterial plant terpenoids. *Planta Med* **67**: 685–694.

Dilika F, Bremner PD, Meyer JJ. 2000. Antibacterial activity of linoleic and oleic acids isolated from *Helichrysum pedunculatum*: a plant used during circumcision rites. *Fitoterapia* **71**: 450–452.

Gibbons S, Udo EE. 2000. The effect of reserpine, a modulator of multidrug efflux pumps, on the *in-vitro* activity of tetracycline against clinical isolates of methicillin resistant *Staphylococcus aureus* (MRSA) possessing the *tet*(K) determinant. *Phytother Res* **14**: 139–140.

Gillespie SH, Morrissey I, Everett D. 2001. A comparison of the bactericidal activity of quinolone antibiotics in a *Mycobacterium fortuitum* model. *J Med Microbiol* **50**: 565–570.

Gottshall RY, Lucas EH, Lickfeldt A, Roberts JM. 1949. The occurrence of antibacterial substances active against *Mycobacterium tuberculosis* in seed plants. *J Clin Invest* **28**: 920–921.

Khulusi S, Ahmed HA, Patel P, *et al.* 1995. The effects of unsaturated fatty acids on *Helicobacter pylori in vitro*. *J Med Microbiol* **42**: 276–282.

Langezaal CR, Chandra A, Scheffer JJ. 1992. Antimicrobial screening of essential oils and extracts of some *Humulus lupulus* L. cultivars. *Pharm Weekbl Sci* **14**: 353–356.

Milligan SR, Kalita JC, Heyerick A, *et al.* 1999. Identification of a potent phytoestrogen in hops (*Humulus lupulus* L.) and beer. *J Clin Endocrinol Metab* **84**: 2249–2252.

Miranda CL, Stevens JF, Helmrich A, *et al.* 1999. Antiproliferative and cytotoxic effects of prenylated flavonoids from hops (*Humulus lupulus*) in human cancer cell lines. *Food Chem Toxicol* **37**: 271–285.

Newton SM, Lau C, Wright CW. 2000. A review of antimycobacterial natural products. *Phytother Res* **14**: 303–322.

Okunade AL, Elvin-Lewis MPF, Lewis W. 2004. Natural antimycobacterial metabolites: current status. *Phytochemistry* **65**: 1017–1032.

Sakamoto K, Konings WN. 2003. Beer spoilage bacteria and hop resistance. *Int J Food Microbiol* **89**: 105–124.

Seidel V, Taylor PW. 2004. In vitro activity of extracts and constituents of *Pelargonium* against rapidly growing mycobacteria. *Int J Antimicrob Agents*, **23**: 613–619.

Simpson WJ, Smith AR. 1992. Factors affecting antibacterial activity of hop compounds and their derivatives. *J Appl Bacteriol* **72**: 327–334.

Verzele M, De Keukeleire D. 1991. *Chemistry and Analysis of Hop and Beer Bitter Acids* (*Developments in Food Science*). Elsevier: London.

Weeks G, Wakil SJ. 1970. Studies on the control of fatty acid metabolism. II. The inhibition of fatty acid synthesis in *Lactobacillus plantarum* by exogenous fatty acid. *J Biol Chem* **245**:1913–1921.

Available online at www.sciencedirect.com
SCIENCE DIRECT®
Phytochemistry 65 (2004) 331–335
PHYTOCHEMISTRY
www.elsevier.com/locate/phytochem

The anti-staphylococcal activity of *Angelica dahurica* (Bai Zhi)

Doris Lechner[a], Michael Stavri[a], Moyosoluwa Oluwatuyi[a], Rogelio Pereda-Miranda[b], Simon Gibbons[a,*]

[a]*Centre for Pharmacognosy and Phytotherapy, The School of Pharmacy, University of London, 29–39 Brunswick Square, London WC1N 1AX, UK*
[b]*Departmento de Farmacia, Facultad de Química, Universidad Nacional Autónoma de México, D.F. 04510, Mexico*

Received 11 September 2003; received in revised form 10 November 2003

Abstract

Bioassay-guided fractionation of a hexane extract prepared from the roots of the Chinese drug *Angelica dahurica* (Bai Zhi) led to the isolation of the polyacetylenic natural product falcarindiol (**1**). The absolute stereochemistry of this compound was confirmed by careful ^{1}H NMR analysis of its (*R*)- and (*S*)-Mosher ester derivatives as the 3(*R*), 8(*S*) isomer. Activity was tracked using a *Mycobacterium fortuitum* screening assay and the purified product was evaluated against multidrug-resistant and methicillin-resistant strains of *Staphylococcus aureus* (MRSA). The minimum inhibitory concentrations (MIC) of this metabolite ranged from 8 to 32 μg/ml highlighting the potential of the acetylene natural product class as antibiotic-lead compounds. These MIC values compare favourably with some of the newest agents in development for the treatment of MRSA infection and indicate that further evaluation of the antibiotic activity of acetylenes is warranted.

Keywords: Bai Zhi; *Angelica dahurica*; Apiaceae; Mosher's esters; Multidrug-resistance; *Staphylococcus aureus*; MDR; MRSA; Polyacetylenes

1. Introduction

Strains of *Staphylococcus aureus* express a series of multidrug resistance (MDR) efflux pumps such as Tet(K), Msr(A), Nor(A) and Qac(A) which confer resistance to a wide range of structurally unrelated antibiotics and antiseptics (Marshall and Piddock, 1997). These MDR pumps are part of an array of cytoplasmic membrane transport systems involved primarily in the uptake of essential nutrients, the excretion of toxic compounds and the maintenance of cellular homeostasis (Paulsen et al., 1996). In a continuing project to identify plant natural products with activity against MDR strains of *S. aureus*, extracts from the roots of *Angelica dahurica* (Apiaceae) were evaluated for in vitro antibacterial activity.

The plant is a perennial herb growing to 2.5 m with a hollow stem, large three-branched leaves and umbels bearing many white flower heads. It grows wild in thickets in China, Japan, Korea and Russia and the cultivated herb is mainly from central and eastern regions of China. The roots are known as Bai Zhi in traditional Chinese medicine, where they are classified as a sweat-inducing drug able to counter harmful external influences on the skin, such as cold, heat, dampness and dryness (Chevalier, 2001). Bai Zhi is also claimed to be effective in the treatment of acne, erythema, headache, toothache, sinusitis, colds and flu (Wagner, 1999).

2. Results and discussion

Antibacterial activity was associated with the hexane extract. Bioassay-guided fractionation by VLC and preparative thin-layer chromatography led to the isolation of the major active compound (**1**), which was a viscous pale yellow oil. Signals in the ^{13}C NMR spectrum for four quaternary carbons at δ_C 79.9, 78.3, 70.3 and 68.7 ppm were indicative of a polyacetylene natural product possessing two triple bonds. This was confirmed by a weak absorption in the IR spectrum at 2235

* Corresponding author. Tel.: +44-207-753-5913; fax: +44-207-753-5909.
E-mail address: simon.gibbons@ulsop.ac.uk (S. Gibbons).

0031-9422/$ - see front matter © 2004 Elsevier Ltd. All rights reserved.
doi:10.1016/j.phytochem.2003.11.010

cm^{-1}, which is also characteristic of an alkyne (Williams and Fleming, 1995). Further signals in the ^{1}H and ^{13}C NMR spectra included a *cis*-double bond, two methine protons bearing oxygen and three olefinic protons which were coupled to each other in a COSY spectrum. Two of these were part of an *exo*-cyclic methylene (δ_H 5.40 and 5.19). Negative ion mode APCI-MS revealed a peak at 259 $[M-H]^-$ and this with the NMR data indicated a molecular formula of $C_{17}H_{24}O_2$. These data were consistent with those published for the C_{17} polyacetylene falcarindiol (Fig. 1a), which is a common component of apiaceous plant roots (Furumi et al., 1998). The 3(*R*), 8(*S*) stereochemistry of falcarindiol was confirmed by Mosher's ester methodology (Rieser et al., 1992; Su et al., 2002; Ward and Rhee, 1991) and the (*S*)- and (*R*)-MTPA esters were prepared and chemical shifts in the H_2-1, H-2 and H-9/H-10 protons were measured for both derivatives (Fig. 1a). Using $\Delta_\delta = \delta_S - \delta_R$ methodology (Ohtani et al., 1991), for H_2-1 and H-2 protons a positive value for $\Delta_{\delta?}$ was observed for both sets of signals indicating that these groups should be place at R_1 in Fig. 1b and that R_2 would be the point of connection for the triple bond resulting in a 3(*R*) configuration for this stereogenic centre. For H-9 and H-10, Δ_δ was negative indicating that this *cis*-double bond should be placed at R_2 and that the absolute stereochemistry for C-8 corresponded to (*S*).

The literature also describes 3(*S*), 8(*S*)-falcarindiol (Bernart et al., 1996; Kobaisy et al., 1997) which has a positive specific rotation ($[\alpha]_D^{25} + 144.8$), whereas our isolate has a negative value. Whilst optical rotation is useful in characterizing known compounds, the presence of two chiral centres in a molecule could complicate the comparison with literature data. This investigation proves that the laevorotatory isolated falcarindiol corresponds to the 3(*R*), 8(*S*) diasteroisomer, whilst the alternative laevoisomer would represent the enantiomeric form of the previously described dextrorotatory natural product [i.e. 3(*R*), 8(*R*)]. Given the ease of preparation of Mosher's esters, the present application exemplifies the potential of this approach to confirm the stereochemical identity of novel and known natural products. This is particularly important where bioactivity studies are conducted and changes in absolute stereochemistry could dramatically alter biological activity. The use of a solid phase carbodiimide resin ensured that if the Mosher's acid chlorides, which are usually sufficiently reactive, are hydrolysed to the acids by the presence of extraneous amounts of moisture in the reaction solvent (i.e. dichloromethane or pyridine), the esters are still formed by the coupling action of the carbodiimide. These resins can then be conveniently removed by filtration.

Falcarindiol displayed low minimum inhibitory concentrations against a panel of methicillin-resistant and multidrug resistant (MDR) strains of *Staphylococcus aureus* (Table 1). Two of these strains (XU212 and RN4220) possess the TetK and MsrA transporters that export tetracycline and macrolide antibiotics respectively. Strain SA-1199B possesses the NorA MDR efflux mechanism, the major drug pump in this pathogen. Activity was also demonstrated against epidemic MRSA strain EMRSA-15 which was a clinical isolate initially isolated from hospitals in the Midlands and south-east of England (Richardson and Reith, 1993). Interestingly, falcarindiol was more active against the MDR strains than against the non-resistant ATCC strain. Whilst the anti-staphylococcal activity of 3(*S*), 8(*S*)-falcarindiol has been reported before (Kobaisy et al., 1997), this is the first report of the 3(*R*), 8(*S*) isomer possessing activity against MDR strains of this species. This result supports a recent study (Tegos et al., 2002), which demonstrated that certain plant natural products are more active against MDR than sensitive strains. Whilst falcarindiol has been shown to be mildly cytotoxic and has anti-inflammatory properties (Bernart et al., 1996; Liu et al., 1998) the activity exhibited here against MDR and methicillin-resistant *Staphylococcus aureus* indicates that the acetylene class of natural products should be further investigated as antibiotic leads. This is certainly worthwhile given the burden of drug-resistant mycobacterial and staphylococcal species

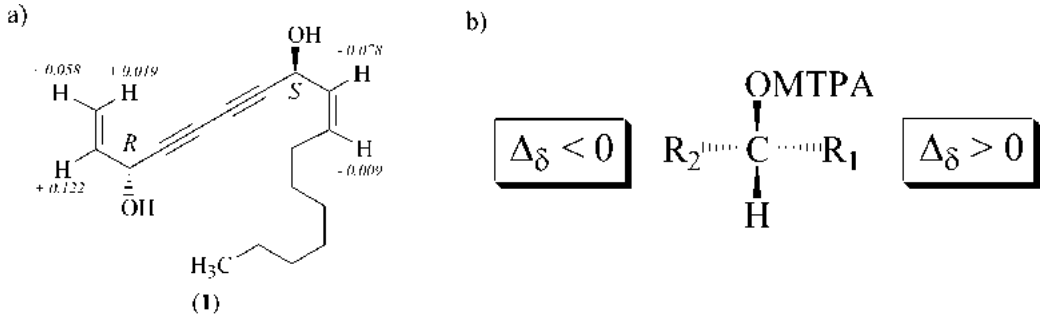

Fig. 1. (a) Structure of falcarindiol (**1**) depicting its 3-(*R*), 8-(*S*) absolute stereochemistry. The figures in italics are for Δ_δ where $\Delta_\delta = \delta_S - \delta_R$. δ_S and δ_R are the chemical shift values for a particular group of the (*S*) and (*R*) Mosher's esters of falcarindiol. (b) The Mosher's ester was (*R*)- or (*S*)-α-methoxy-α-trifluoromethylphenyl acetate (MTPA). When Δ_δ for a group of diagnostic resonances is positive then it must be placed at R_1. When Δ_δ for a group of diagnostic resonances is negative then the group must be placed at R_2.

Table 1
Minimum inhibitory concentrations (MIC) of falcarindiol and standard antibiotics in μg/ml

Bacterium	Falcarindiol	Norfloxacin	Tetracycline	Erythromycin	Ethambutol	Isoniazid
S. aureus SA-1199B (NorA)	8	32	32	2	[a]	[a]
S. aureus XU-212 (TetK)	16	8	256	[a]	[a]	[a]
S. aureus RN-4220 (MsrA)	16	64	64	64	[a]	[a]
S. aureus EMRSA-15 (MecA)	32	2	0.25	[a]	[a]	[a]
S. aureus ATCC 25923	32	0.5	0.5	0.25	[a]	[a]
M. fortuitum ATCC 6841	8	[a]	[a]	[a]	8	0.5

Resistance mechanism of staphylococcal strains in parentheses.
[a] Not tested.

which are difficult to treat and eradicate in both the clinical and community setting (Levy, 1998).

3. Experimental

3.1. General experimental procedures

Optical rotations were measured on a Bellingham and Stanley ADP 200 polarimeter. IR spectra were recorded on a Nicolet 360 FT-IR spectrophotometer. ^{1}H NMR (500 MHz) and ^{13}C NMR (125 MHz) spectra were recorded in $CDCl_3$ on a Bruker AVANCE 500 spectrometer. Chemical shifts values (δ) are reported in parts per million (ppm) relative to NMR solvent $CDCl_3$ ($\delta_H = 7.20$, $\delta_C = 77.0$). Coupling constants (J values) are given in Hertz. ^{1}H–^{1}H COSY, HMBC and HMQC experiments were recorded with gradient enhancements using sine shaped gradient pulses. APCI mass spectra were recorded on a Finnigan Navigator instrument. Vacuum liquid chromatography on Merck Silica gel 60 $PF_{254+366}$ was used for fractionation and isolation. TLC was performed using Kieselgel 60 F_{254} (Merck) pre-coated plates and spots were visualized by spraying with vanillin-sulphuric acid spray followed by heating.

3.2. Plant material

Air-dried roots of the plant were obtained from Kingham Herbs (Batch no. 863402001) and a voucher specimen (SG-2003-1) has been deposited at the Centre.

3.3. Bacterial strains

S. aureus RN4220 containing plasmid pUL5054, which carries the gene encoding the MsrA macrolide efflux protein, was provided by J. Cove (Ross et al., 1989). EMRSA-15 which possesses the *mecA* gene was provided by Dr. Paul Stapleton, ULSOP. Strain XU-212, which possesses the TetK tetracycline efflux protein, was provided by E. Udo (Gibbons and Udo, 2000). SA-1199B, which overexpresses the *norA* gene encoding the NorA MDR efflux protein was provided by G. Kaatz (Kaatz et al., 1993). *S. aureus* strains were cultured on nutrient agar (Oxoid) and *Mycobacterium fortuitum* was cultured on Columbia agar (Oxoid) supplemented with 5% defibrinated horse blood (Oxoid) and incubated for 24 and 72 h, respectively at 37 °C prior to MIC determination.

3.4. Minimum inhibitory concentration (MIC)

Tetracycline, norfloxacin, and erythromycin were obtained from Sigma Chemical Co. Mueller-Hinton broth (MHB; Oxoid) was adjusted to contain 20 and 10 mg/l of Ca^{2+} and Mg^{2+}, respectively. An inoculum density of 5×10^5 cfu of each of the test organisms was prepared in normal saline (9 g/l) by comparison with a MacFarland standard. MHB (125 μl) was dispensed into 10 wells of a 96-well microtitre plate (Nunc, 0.3 ml volume per well). Tetracycline and erythromycin were dissolved in MHB to give stock solutions. A stock solution of norfloxacin was prepared by dissolving the antibiotic in DMSO (Sigma) and dilution in MHB to give a final concentration of 0.625%. A DMSO control was included in all assays.

Antibiotics were serially diluted into each of the wells followed by the addition of the appropriate bacterial inoculum. The plate was incubated at 37 °C for 72 h (for *Mycobacterium fortuitum*) and 18 h (for *Staphylococcus aureus*) and the MIC recorded as the lowest concentration at which no growth was observed. This was facilitated by the addition of 20 μl of a 5 mg/ml methanolic solution of 3-[4,5-dimethylthiazol-2-yl]-2,5-diphenyltetrazolium bromide (MTT; Sigma) to each of the wells and incubation for 20 min. A blue colouration indicated bacterial growth.

3.5. Isolation of falcarindiol

The chopped dry roots (500 g) were ground and extracted sequentially in a Soxhlet apparatus with hexane (2.5 l) and dichloromethane (2.5 l) which when concentrated under vacuum gave 6.57 g and 2.05 g of extracts respectively. These were then screened for antibacterial

activity using an in vitro assay and the hexane extract was found to be active. 6.57 g of this were subjected to vacuum liquid chromatography (VLC) on silica gel by eluting with 200 ml hexane, and increasing polarity by 10% increments with EtOAc and finally a wash with methanol to yield 12 fractions.

Activity was traced to compound **1** which was isolated from VLC fraction 5 (hexane–EtOAc, 6:4) by PTLC using EtOAc–hexane (3:7, two developments) as a solvent system. Purity was monitored by TLC (EtOAc–hexane, 1:1) and **1** gave a black colouration on TLC with vanillin-sulphuric acid at R_f 0.47.

3.6. Preparation of Mosher's esters

Falcarindiol (18 mg) was dried under vacuum for 1 h and then two portions (4 mg each) were dissolved in dry CH_2Cl_2 (2 ml) containing 2 mg of dimethylaminopyridine (Sigma Chemical Co.). Eight equivalents of PS-carbodiimide resin (Argonaut Technologies Inc.) were added to each portion of falcarindiol. Six equivalents of either the (*S*) or the (*R*) isomer of α-methoxy-α-trifluoromethylphenylacetyl chloride (Sigma Chemical Co.) were added to a portion of falcarindiol which resulted in the formation of the (*R*) and (*S*) Mosher's esters of falcarindiol respectively. The reaction mixtures were stirred for 24 h, filtered to remove the PS-carbodiimide resin, concentrated under nitrogen and then redissolved in $CDCl_3$ (0.75 ml) and loaded into separate NMR tubes. NMR spectra were then recorded at 500 MHz and differences in the signals of protons that neighboured the chiral centres noted (Fig. 1a). The bulk effect on chemical shifts induced by esterification with the chiral reagents was calculated using $\Delta_\delta = \delta_S - \delta_R$ where δ_S and δ_R are the shifts (in ppm) of diagnostic protons neighbouring the chiral centres in falcarindiol of the (*S*) and (*R*) Mosher's esters, respectively. The positive and negative magnitudes of Δ_δ were interpreted using the model adapted by Kakisawa and collaborators (Ohtani et al., 1991) (Fig. 1b).

3.7. 3(R), 8(S)-falcarindiol (1)

Pale yellow oil; $[\alpha]_D^{25}$ −130 (MeOH, *c* 0.02); IR ν_{max} (thin film) cm^{-1}: 3393, 2925, 2855, 2235, 1735, 1718, 1457, 1375, 1228, 1216, 1034, 724; ^1H NMR ($CDCl_3$) δ: 0.82 (*t*, 6.9 Hz, 3H, H_3-17), 1.21 (*m*, 8H), 1.31 (*m*, 2H), 2.04 (*q*, 7.2 Hz, H_2-11), 4.88 (*d*, 5.4 Hz, H-3), 5.14 (*bd*, 8.2 Hz, H-8), 5.19 (*bd*, 10.1 Hz, H-1b), 5.41 (*bd*, 17.0 Hz, H-1a), 5.46 (*bd*, 8.8 Hz, H-9), 5.56 (*dt*, 11.0 and 7.6 Hz, H-10) and 5.87 (*ddd*, 17.0, 10.1 and 5.3 Hz, H-2); ^{13}C NMR ($CDCl_3$) δ: 14.1 (C-17), 22.6 (C-16), 27.7 (C-11), 29.1 (C-14), 29.1 (C-13), 29.2 (C-12), 31.8 (C-15), 58.6 (C-8), 63.4 (C-3), 68.7 (C-6), 70.2 (C-5), 78.2 (C-7), 79.8 (C-4), 117.3 (C-1), 127.6 (C-9), 134.6 (C-10), 135.8 (C-2); APCI-MS: *m*/*z* 259 $[M-H]^-$.

Acknowledgements

The EPSRC and the School of Pharmacy are thanked for the award of studentships to M. Oluwatuyi and M. Stavri, respectively. The Royal Society and Academia Mexicana de Ciencias are thanked for funding the visit of R. Pereda-Miranda to the University of London School of Pharmacy (Grant No. 15823).

References

Bernart, M.W., Cardellina, J.H. 2nd., Balaschak, M.S., Alexander, M.R., Shoemaker, R.H., Boyd, M.R., 1996. Cytotoxic falcarinol oxylipins from *Dendropanax arboreus*. Journal of Natural Products 59, 748–753.

Chevallier, A., 2001. Encyclopedia of Medicinal Plants. Dorling Kindersley Limited, London.

Furumi, K., Fujioka, T., Fujii, H., Okabe, H., Mihashi, K., Nakano, Y., Matsunaga, H., Katano, M., Mori, M., 1998. Novel antiproliferative falcarindiol furanocoumarin ethers from the root of *Angelica japonica*. Bioorganic Medicinal Chemistry Letters 8, 93–96.

Gibbons, S., Udo, E.E., 2000. The effect of reserpine, a modulator of multidrug efflux pumps, on the in-vitro activity of tetracycline against clinical isolates of methicillin resistant *Staphylococcus aureus* (MRSA) possessing the tet(K) determinant. Phytotherapy Research 14, 139–140.

Kaatz, G.W., Seo, S.M., Ruble, C.A., 1993. Efflux-mediated fluoroquinolone resistance in *Staphylococcus aureus*. Antimicrobial Agents and Chemotherapy 37, 1086–1094.

Kobaisy, M., Abramowski, Z., Lermer, L., Saxena, G., Hancock, R.E., Towers, G.H., Doxsee, D., Stokes, R.W., 1997. Antimycobacterial polyynes of Devil's Club (*Oplopanax horridus*), a North American native medicinal plant. Journal of Natural Products 60, 1210–1213.

Levy, S.B., 1998. The Challenge of Antibiotic Resistance. Scientific American 278, 46–53.

Liu, J.H., Zschocke, S., Reininger, E., Bauer, R., 1998. Inhibitory effects of *Angelica pubescens f. biserrata* on 5-lipoxygenase and cyclooxygenase. Planta Medica 64, 525–529.

Marshall, N.J., Piddock, L.J.V., 1997. Antibacterial efflux systems. Microbiologia 13, 285–300.

Ohtani, I., Kusumi, T., Kashman, Y., Kakisawa, H., 1991. High-field FT NMR application of Mosher's method. The absolute configurations of marine terpenoids. Journal of the American Chemical Society 113, 4092–4096.

Paulsen, I.T., Brown, M.H., Skurray, R.A., 1996. Proton-dependent multidrug efflux systems. Microbiology Reviews 60, 575–608.

Richardson, J.F., Reith, S., 1993. Characterization of a strain of methicillin-resistant *Staphylococcus aureus* (EMRSA-15) by conventional and molecular methods. Journal of Hospital Infection 25, 45–52.

Ross, J.I., Farrell, A.M., Eady, E.A., Cove, J.H., Cunliffe, W.J., 1989. Characterisation and molecular cloning of the novel macrolide-streptogramin B resistance determinant from *Staphylococcus epidermidis*. Journal of Antimicrobial Chemotherapy 24, 851–862.

Rieser, M.J., Hui, Y., Rupprecht, K.J., Kozlowski, J.F., Wood, K.V., McLaughlin, J.L., Hanson, P.R., Zhuang, Z., Hoye, T.R., 1992. Determination of absolute configuration of stereogenic carbinol centers in annonaceous acetogenins by ^1H and ^{19}F-NMR analysis of Mosher ester derivatives. Journal of the American Chemical Society 114, 10203–10213.

Su, B.N., Park, E.J., Mbwambo, Z.H., Santarsiero, B.D., Mesecar, A.D., Fong, H.H.S., Pezzuto, J.M., Kinghorn, A.D., 2002. New

chemical constituents of *Euphorbia quinquecostata* and absolute configuration assignment by a convenient Mosher ester procedure carried out in NMR tubes. Journal of Natural Products 65, 1278–1282.

Tegos, G., Stermitz, F.R., Lomovskaya, O., Lewis, K., 2002. Multidrug pump inhibitors uncover remarkable activity of plant antimicrobials. Antimicrobial Agents and Chemotherapy 46, 3133–3141.

Wagner, H., 1999. Arzneidrogen und ihre Inhaltsstoffe. Pharmazeutische Biologie Band 2. Wissenschaftliche Verlagsgesellschaft.

Ward, D.E., Rhee, C.K., 1991. A simple method for the microscale preparation of Mosher's acid chloride. Tetrahedron Letters 32, 7165–7166.

Williams, D.H., Flemming, I., 1995. Spectroscopic Methods in Organic Chemistry, fifth ed. McGraw Hill Publishers, London.

Pangelin, an Antimycobacterial Coumarin from *Ducrosia anethifolia*

Michael Stavri[1], K. T. Mathew[2], Franz Bucar[3], Simon Gibbons[1]

Abstract

The aerial parts of *Ducrosia anethifolia* afforded the monoterpene glucoside 8-debenzoylpaeoniflorin (**1**) and the prenylated furanocoumarin pangelin {5-[2″(*R*)-hydroxy-3″-methyl-3″-butenyloxy]furocoumarin} (**2**). Their structures were determined by extensive 1- and 2-dimensional NMR studies. Compound **2** demonstrated activity against a panel of fast growing mycobacteria, namely *Mycobacterium fortuitum, M. aurum, M. phlei* and *M. smegmatis* and minimum inhibitory concentration (MIC) values ranged from 64 – 128 μg/mL. Whilst compounds **1** and **2** have previously been reported as an antihyperglycaemic component from *Paeonia lactiflora,* and as a constituent of *Angelica pancici*, respectively, this is the first report of the full ^{1}H- and ^{13}C-NMR data for these natural products.

Plants are a comparatively untapped source of antimycobacterial agents and recent reviews indicate that there is great potential to find antibiotic leads from this source [1], [2], [3]. New antimycobacterial agents are urgently needed given the threat of multidrug resistant (MDR) tuberculosis and rare infections caused by fast growing species which in some cases resist treatment [4], [5].

As part of a continuing project to evaluate antimycobacterial plant natural products using a *Mycobacterium fortuitum* screening model, which has been used to characterise anti-tubercular drugs [6], we have investigated extracts of *Ducrosia anethifolia* (Apiaceae), an aromatic herb found along the Arabian Gulf coast of Kuwait. The oil from this plant has previously been investigated for antibacterial activity against Gram-positive bacteria and fungi, although no single antibacterial components have been isolated and characterised from this species [7]. Here we report the isolation and structure elucidation of the monoterpene glucoside 8-*O*-debenzoylpaeoniflorin (**1**) and the antimycobacterial prenylated furocoumarin pangelin (**2**).

Compound **1** was isolated as an amorphous solid from the hexane extract following VLC and preparative TLC (p-TLC). FABMS gave a base ion of 399 $[M + Na]^{+}$. Signals in the ^{1}H- and ^{13}C-NMR

Affiliation: [1] Centre for Pharmacognosy and Phytotherapy, The School of Pharmacy, University of London, London, U.K. · [2] The Herbarium, Department of Biological Science, Kuwait University, Safat, Kuwait · [3] Institute for Pharmacognosy, University of Graz, Graz, Austria

Correspondence: Dr. Simon Gibbons · Centre for Pharmacognosy and Phytotherapy · The School of Pharmacy · University of London · 29–39 Brunswick Square · London WC1N 1AX · U.K. · Phone: +44-207-753-5913 · Fax: +44-207-753-5909 · E-mail: simon.gibbons@ulsop.ac.uk

Received: March 10, 2003 · **Accepted:** June 19, 2003

Bibliography: Planta Med 2003; 69: 956–959 · © Georg Thieme Verlag Stuttgart · New York · ISSN 0032-0943

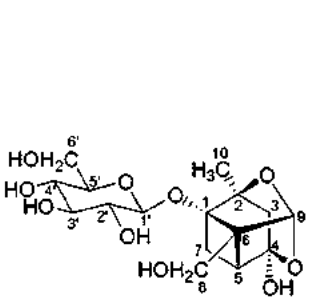

(1)

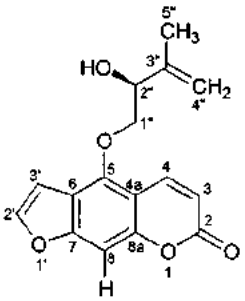

(2)

spectra (Table **1**) for an anomeric carbon (δ = 99.9), an oxymethylene and 4 oxymethine carbons indicated the presence of a hexose. A COSY spectrum further corroborated this with correlations between the anomeric (H-1′) and H-2′, H-3′ to H-4′, H-4′ to H-5′ and H-5′ finally to the H-6′ methylene protons. Whilst coupling between H-1′ and H-2′ was large (7.7 Hz) and H-2′ was a triplet (J = 7.7 Hz), indicating axial configuration for protons at positions 1′, 2′ and 3′, resonances for H-3′, H-4′ and H-5′ were superimposed and it was therefore not possible by NMR to ascertain if the hexose of **1** was a glucose or galactose. Compound **1** was therefore subjected to acid hydrolysis followed by GC-MS of the products which indicated that the hexose sugar was glucose. Additional signals in the ^{1}H- and ^{13}C-NMR for the remaining portion of the molecule included three methylene groups (one an oxymethylene), two methines, one methyl and four quaternary carbons supporting the assumption of a ten-carbon monoterpene moiety. These data were similar to those reported for pinane-type monoterpene glucosides from *P. albiflora* [8], [9]. Assuming a basic pinane skeleton for the monoterpene portion of **1**, it was possible to use HMBC spectroscopy to unambiguously assign all carbon resonances. Methyl-10 exhibited a *2J* correlation to an oxygen bearing quaternary (C-2) and *3J* correlations to C-3 (CH_2) and C-1, which was also correlated to by the anomeric proton of the glucose indicating the glucose was attached to this position. The protons of an oxymethylene group (C-8) also correlated to C-1, to a quaternary (C-6), to a methine (C-5) and to a highly deshielded acetal methine carbon (C-9) which is typical of the pinane glycosides of *Paeonia* species [8], [9]. The C-5 methine proton exhibited a *3J* correlation to C-1, a *2J* correlation to a highly deshielded quaternary carbon (C-4) and coupled to a methylene (C-7) in the COSY spectrum. This accounted for all ten carbons of the monoterpene skeleton. Additional couplings for the highly deshielded acetal proton (H-9) included correlations to C-2 and C-4 indicating that the acetal is formed between C-9 and these carbons. From the molecular weight and the deshielded nature of C-4 (δ = 106.4) an hydroxy group must be placed here. NOESY spectra showed a key correlation between the highly deshielded acetal proton, H-9, and between the H-8 oxymethylene protons indicating that they are on the same face of the pinane skeleton. Compound **1** is therefore assigned as the known monoterpene glucoside 8-debenzoylpaeoniflorin. Whilst this compound has been cited in the literature from *Paeonia lactiflora* as an antihyperglycaemic component by Hsu et al., [10], there has been no spectroscopic data recorded, despite this being alluded to by these authors as being present in cited references [8], [9]. The full NMR data is reported here for the first time (Table **1**).

The ^{1}H-NMR data for compound **2**, (Table **1**) were characteristic of a 5-*O*-substituted furocoumarin [11] and were in close agreement with that published for pangeline, previously isolated from *Angelica pancici* [12]. Full NMR spectroscopy including acquisition of HSQC and HMBC spectra led to the unambiguous assignment of all resonances and the ^{13}C-NMR data is presented here for the first time (Table **1**). Measurement of a positive absolute rotation confirmed the assignment of compound **2** as pangeline {5-[2″(*R*)-hydroxy-3″-methyl-3″-butenyloxy)-6,7-furocoumarin) [12].

Compound **2** was tested against a panel of fast-growing mycobacteria to investigate its effects on growth and minimum inhibitory concentrations (MIC) are presented in Table **2**. MIC values ranged from 64 – 128 μg/mL and the growth of all species tested was affected by **2**. Whilst these are moderate activities, there are few examples of antimycobacterial coumarin natural products [13], [14] and synthetic coumarins have been shown to exert their effects by inhibition of bacterial DNA gyrase [15]. Given the need to find compounds with activity against fast-growing strains, which are naturally resistant and difficult to treat, and given the burden of drug-resistant tuberculosis, further investigation of the antimycobacterial properties of coumarin natural products is worthwhile.

Materials and Methods

The aerial parts of the plant were collected from Khiran resort, Kuwait on the 20th of April 1999. A voucher specimen (K. T. Mathew and S. Gibbons 4557) is deposited at the Kuwait University Herbarium. The aerial parts were air-dried for 3 days and ground to a fine powder. The powdered plant material (500 g) was then extracted sequentially in a Soxhlet apparatus (3 litres each) with hexane, chloroform, acetone and finally methanol. Vacuum liquid chromatography (VLC) (Kieselgel 60) of the chloroform extract using a step gradient of 10% EtOAc increments in hexane, followed by a methanol wash gave 12 fractions. Fraction 12 was subjected to flash chromatography (SiO_2, 1 g, $CHCl_3$:MeOH, 1 : 1), followed by p-TLC ($CHCl_3$:MeOH; 8 : 2 + AcOH, 2 drops), to give compound **1** (14 mg), R_F: 0.19. The hexane extract (14.7 g) was subjected to VLC on Kieselgel 60 as described above. Fractions 7 – 11 were bulked (1 L), concentrated to a solid (1.5 g) and further fractionated by SiO_2 flash chromatography (eluting with hexane:EtOAc, 6 : 4). Fractions 41 – 65 (375 mL) were bulked and subjected to multiple development p-TLC (2 times) (EtOAc:hexane, 1 : 1), affording compound **2** (26 mg), R_F: 0.68.

NMR spectra were recorded on a Bruker Avance 400 spectrometer at 400 MHz. FAB-MS were recorded on a VG Analytical ZAB-SE instrument using MNOBA as matrix. Copies of the original spectra are obtainable from the author of correspondence.

8-O-Debenzoylpaeoniflorin (**1**): Colourless amorphous solid: $[\alpha]_D^{23}$: –12.8° (*c* 0.195, MeOH) {lit. [10]: $[\alpha]_D$: –9.6° (*c* 1.0, MeOH)}. IR (film): ν_{max} = 3344, 2925, 1386, 1075, 1049, 1011 cm^{-1}. ^{1}H- and ^{13}C-NMR (CD_3OD) are given in Table **1**. Positive FAB-MS: *m/z* = 399 $[M + Na]^+$ (100), 329 (30), 286 (35), 199 (47), 191 (30).

Table **1** NMR data for compounds **1** and **2** (400 MHz for ^{1}H and 100 MHz for ^{13}C. **1** recorded in CD_3OD and **2** recorded in $CDCl_3$)

	1			*2*	
Position	***^{1}H (J in Hz)***	***^{13}C***	***Position***	***^{1}H (J in Hz)***	***^{13}C***
1	–	89.4	2	–	161.0
2	–	87.3	3	6.30 d (9.6)	113.1
3	1.80, 2.16 ABq (12.5)	44.7	4	8.19 dd (9.6, 0.8)	139.0
4	–	106.4	4a	–	107.4
5	2.41 m	43.7	5	–	148.5
6	–	73.8	6	–	114.2
7	1.86, 2.40 ABq (10.0)	23.4	7	–	158.1
8	3.91, 4.00 ABq (12.4)	59.1	8	7.18 t (0.8)	94.8
9	5.25 s	102.3	8a	–	152.7
10	1.34 s	19.5	2′	7.61 d (2.4)	145.2
1′	4.60 d (7.7)	99.9	3′	6.98 dd (2.4, 0.8)	104.7
2′	3.24 t (7.7)	71.8	1″	4.42 dq (10.0, 7.2, 3.6)	75.7
3′	3.40 m	77.9	2″	4.55 m	74.3
4′	3.27 m	75.0	3″	–	143.4
5′	3.27 m	78.2	4″	5.21 m 5.08 m	113.4
6′	3.65, 3.85 m	62.9	5″	1.85 dt (0.8, 0.4)	18.7

Pangelin (**2**) Colourless amorphous solid: $[\alpha]_D^{23}$: + 63.5° (*c* 0.126, $CHCl_3$) {lit. [12]: $[\alpha]_D^{20}$: + 11° (*c* 0.3 %, $CHCl_3$)}. UV (MeOH): λ_{max} = 251, 311 nm. IR (film): ν_{max} = 3649, 2916, 1717, 1624, 1134 cm^{-1}. ^{1}H- and ^{13}C-NMR ($CDCl_3$) are given in Table **1**. Positive FAB-MS: *m/z* = 287 $[M + H]^+$ (100), 202 (73), 187 (14), 174 (16). The ^{1}H-NMR data and physical constants were identical with those of reference values [12].

Hydrolysis of 1 and GC-MS conditions: Compound **1** (1 mg) was refluxed with 2 mL of HCl (7 %) on a steam bath for 60 min. The hydrolysate was extracted 3 times with EtOAc. The sugar was identified in the remaining acidic solution which was evaporated to dryness under nitrogen. Trimethylsilyl (TMS) derivatives were analysed by GC/MS on a HP-5MS fused silica capillary (30 m, 0.25 mm I.D., 0.50 μm 5 % phenyl-95 % methylpolysiloxane film); carrier gas: helium 5.6, flow rate 0.8 mL/min, temperature programmed from 130 °C (1 min.), rate 5 °C/min to 230 °C; glucose R_t = 19.14 and 20.78 min; EI-MS (70 eV).

Mycobacterium fortuitum ATCC 6841 was obtained from Dr Peter Lambert, Aston University. *Mycobacterium smegmatis* ATCC 14468, *Mycobacterium phlei* ATCC 11758 and *Mycobacterium aurum* Pasteur Institute 104482 were obtained from Dr Veronique Seidel, The School of Pharmacy. Bacteria were maintained on Columbia Blood agar (Oxoid) supplemented with 5 % defibrinated Horse blood (Oxoid).

Table **2** Minimum inhibitory concentrations (MIC) in μg/mL of 2 and standard antibiotics against fast growing species of mycobacteria

***Mycobacterium* species**	***2***	***Ethambutol***	***Isoniazid***
Mycobacterium fortuitum ATCC 6841	128	8	0.5
Mycobacterium smegmatis ATCC 14468	64	0.25	2
Mycobacterium phlei ATCC 11758	64	1	2
Mycobacterium aurum Pasteur Institute 104482	64	1	2

The antimycobacterial assay comprised a standard MIC determination of test compound in Ca^{2+} and Mg^{2+} adjusted Mueller-Hinton Broth (MHB) as previously described [13], [16]. Appropriate solvent (DMSO), growth and sterile controls were carried out. Ethambutol and isoniazid were used as positive controls.

Acknowledgements

The University of London School of Pharmacy is thanked for the award of a PhD scholarship to Mr. M. Stavri.

References

[1] Cantrell CL, Franzblau SG, Fischer NH. Antimycobacterial plant terpenoids. Planta Medica 2001; 67: 685 – 94

[2] Newton SM, Lau C, Wright CW. A review of antimycobacterial natural products. Phytotherapy Research 2000; 14: 303 – 22

[3] Newton SM, Lau C, Gurcha SS, Besra GS, Wright CW. The evaluation of forty-three plant species for *in vitro* antimycobacterial activities; isolation of active constituents from *Psoralea corylifolia* and *Sanguinaria canadensis*. Journal of Ethnopharmacology 2002; 79: 57 – 67

[4] Raviglione MC, Gupta R, Dye CM, Espinal MA. The burden of drug-resistant tuberculosis and mechanisms for its control. Annals of the New York Academy of Science 2001; 953: 88 – 97

[5] Fujita N, Utani A, Matsumoto F, Matsushima H, Kakuta M, Hatamochi A, Shinkai H. Levofloxacin alone efficiently treated a cutaneous *Mycobacterium fortuitum* infection. Journal of Dermatology 2002; 29: 452 – 54

[6] Gillespie SH, Morrissey I, Everett D. A comparison of the bactericidal activity of quinolone antibiotics in a *Mycobacterium fortuitum* model. Journal of Medical Microbiology 2001; 50: 565 – 70

[7] Janssen AM, Scheffer JJ, Baerheim Svendsen A, Aynehchi Y. The essential oil of *Ducrosia anethifolia* (DC.) Boiss. Chemical composition and antimicrobial activity. Pharmaceutisch Weekblad Science 1984; 6: 157 – 60
[8] Kaneda M, Itaka Y, Shibata S. Chemical studies on the oriental plant drugs – XXXII The absolute structures of paeoniflorin, albiflorin, oxypaeoniflorin and benzoylpaeoniflorin isolated from Chinese paeony root. Tetrahedron 1972; 28: 4309 – 17
[9] Yamasaki K, Kaneda M, Tanaka O. Carbon-13 NMR spectral assignments of paeoniflorin homologues with the aid of spin-lattice relaxation time. Tetrahedron Letters 1976; 44: 3965 – 68
[10] Hsu F, Lai C, Cheng J. Antihyperglycaemic effects of paeoniflorin and 8-debenzylpaeoniflorin, glucosides from the root of *Paeonia lactiflora*. Planta Medica 1997; 63: 323 – 25
[11] Adebajo AC, Reisch J. Minor furocoumarins of *Murraya koenigii*. Fitoterapia 2000; 71: 334 – 7
[12] Ognyanov I, Botcheva D. Pangeline and angeloylpangeline – two new furocoumarins in the roots of *Angelica pancici* Vandas. Comptes Rendus de l'Academie Bulgare des Sciences 1971; 24: 315 – 8
[13] Schinkovitz A, Gibbons S, Stavri M, Cocksedge MJ, Bucar F. Ostruthin: An antimycobacterial coumarin from the roots of *Peucedanum ostruthium* Koch. Planta Medica 2003; 69: 369 – 71
[14] Al-Yayha MA, Muhammad I, Mirza HH, El-Feraly FS. Antibacterial constituents from the rhizomes of *Ferula communis*. Phytotherapy Research 1998; 12: 335 – 9
[15] Chatterji M, Unniraman S, Mahadevan1 S, Nagaraja V. Effect of different classes of inhibitors on DNA gyrase from *Mycobacterium smegmatis*. Journal of Antimicrobial Chemotherapy 2001; 48: 479 – 85
[16] Gibbons S, Udo EE. The effect of reserpine, a modulator of multidrug efflux pumps, on the *in-vitro* activity of tetracycline against clinical isolates of methicillin resistant *Staphylococcus aureus* (MRSA) possessing the *tet*(K) determinant. Phytotherapy Research 2000; 14: 139 – 40

PHYTOTHERAPY RESEARCH
Phytother. Res. **17**, 434–436 (2003)
Published online in Wiley InterScience (www.interscience.wiley.com). **DOI**: 10.1002/ptr.1284

SHORT COMMUNICATION

Cryptolepine Hydrochloride: A Potent Antimycobacterial Alkaloid Derived from *Cryptolepis sanguinolenta*

Simon Gibbons[1]*, Fatemeh Fallah[2]† and Colin W. Wright[2]

[1]Centre for Pharmacognosy and Phytotherapy, The School of Pharmacy, University of London, 29-39 Brunswick Square, London WC1N 1AX, UK
[2]School of Pharmacy, University of Bradford, West Yorkshire BD7 1DP, UK

The activity of cryptolepine hydrochloride, a salt of the main indoloquinoline alkaloid from the West African medicinal plant *Cryptolepis sanguinolenta*, was assessed against the fast growing mycobacterial species *Mycobacterium fortuitum*, which has recently been shown to be of use in the evaluation of antitubercular drugs. The low minimum inhibitory concentration (MIC) of this compound (16 μg/mL) prompted further evaluation against other fast growing mycobacteria namely, *M. phlei*, *M. aurum*, *M. smegmatis*, *M. bovis* BCG and *M. abcessus* and the MICs ranged over 2–32 μg/mL for these species. The strong activity of this agent, the need for new antibiotics with activity against *Mycobacterium tuberculosis*, coupled with the ethnobotanical use of *C. sanguinolenta* extracts to treat infections, highlight the potential of the cryptolepine template for development of antimycobacterial agents. Copyright © 2003 John Wiley & Sons, Ltd.

Keywords: Mycobacterium; antibacterial; cryptolepine; *Cryptolepis sanguinolenta*.

INTRODUCTION

There is still much opportunity to exploit the ethnopharmacological route to new drug leads (Heinrich and Gibbons, 2001), particularly in the discovery of antibiotic lead compounds, where there is a pressing need for new classes of antimycobacterial agents to manage infections caused by fast growing species. Additionally there is a requirement for new antibiotics to treat tuberculosis (TB) where multidrug-resistant (MDR) strains of *Mycobacterium tuberculosis* are implicated. Treatment of TB is protracted, and comprises a schedule of antimycobacterial drugs of which rifampicin, isoniazid, pyrazinamide and ethambutol are the core. Unfortunately, resistance to these agents is becoming increasingly common due to the emergence of strains which possess MDR mechanisms (Raviglione *et al.*, 2001).

Plants are an excellent source of antimycobacterial compounds (Newton *et al.*, 2000; Cantrell *et al.*, 2001; Newton *et al.,* 2002) but until recently there has been little pressure to develop natural products from plants as antitubercular leads, due to the susceptibility of strains to standard agents.

* Correspondence to: Dr S. Gibbons, Centre for Pharmacognosy and Phytotherapy, The School of Pharmacy, University of London, 29-39 Brunswick Square, London WC1N 1AX, UK.
E-mail: simon.gibbons@ulsop.ac.uk
† Present address: Department of Microbiology, Shaheed Beheshti University of Medical Sciences and Health Sciences, Tehran, Iran.

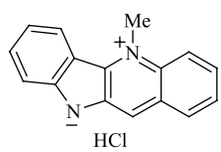

(1)

In a project to discover antimycobacterial plant derived natural products, cryptolepine hydrochloride (**1**) was screened in an *in vitro* assay using *Mycobacterium fortuitum* (ATCC 6841). This has recently been shown to be of use as an alternative screening model to *M. tuberculosis* for potential antitubercular drugs (Gillespie *et al.*, 2001), can be handled in a class II microbiological laboratory and is a fast growing strain with the assay being complete in 72 h. The current study with cryptolepine was driven because of the large number of ethnopharmacological uses for the producing species of the parent alkaloid, *Cryptolepis sanguinolenta*, which in West Africa is widely used particularly for the treatment of microbial infections and malaria (Silva *et al.*, 1996; Tona *et al.*, 1999).

Previous work on the antibacterial properties of this alkaloid have focused on diarrhoeal bacteria (Paulo *et al.*, 1994), *Escherichia coli* and yeasts (Sawyer *et al.*, 1995; 1997), antistaphylococcal activity (Boakye-Yiadom and Heman-Ackah, 1979), and one report on the activity of the free base and the hydrochloride against *Mycobacterium fortuitum* (Cimanga *et al.*, 1996) although there is no further evaluation of this compound against other species of mycobacteria. Cryptolepine has also recently been shown to intercalate into DNA at

Received 31 October 2002
Accepted 18 November 2002

Table 1. Minimum inhibitory concentrations (MIC) of cryptolepine hydrochloride and standard antibiotics against fast growing species of Mycobacteria

Mycobacterium species	Cryptolepine	Ethambutol	Isoniazid	Streptomycin sulphate
Mycobacterium fortuitum	16	8	0.5	–
Mycobacterium smegmatis	8	0.25	2	–
Mycobacterium phlei	4	1	2	–
Mycobacterium abcessus	32	128	32	–
Mycobacterium aurum	2	1	2	–
Mycobacterium bovis BCG	12.5	–	–	6.25

MIC of compounds in μg/mL.
– Not tested.

non-alternating cytosine-cytosine sites (Lisgarten *et al*., 2002) which may account for the cytotoxicity of this alkaloid.

MATERIALS AND METHODS

Isolation. Cryptolepine was isolated from *C. sanguinolenta* roots and crystallized as the hydrochloride salt as previously described (Wright *et al.*, 1996).

Bacteria. *Mycobacterium fortuitum* ATCC 6841 was obtained from Dr Peter Lambert, Aston University. *Mycobacterium smegmatis* ATCC 14468, *Mycobacterium phlei* ATCC 11758, *Mycobacterium abcessus* ATCC 19977 and *Mycobacterium aurum* Pasteur Institute 104482 were obtained from Dr Veronique Seidel, The School of Pharmacy. Intradermal BCG Vaccine BP (Evans Medical Ltd, Leatherhead, UK) was used as the source of *M. bovis* BCG, Copenhagen sub-strain 1077.

Minimum inhibitory concentration assay. *Mycobacterium fortuitum*, *Mycobacterium smegmatis*, *Mycobacterium phlei*, *Mycobacterium abcessus* and *Mycobacterium aurum* were assessed. This assay comprised a standard minimum inhibitory concentration (MIC) determination (Gibbons and Udo, 2000) of test compound in Ca^{2+} and Mg^{2+} adjusted Mueller-Hinton broth (MHB). Cryptolepine hydrochloride was dissolved in MHB, to give a starting concentration of 512 μg/mL which was then diluted out across a 96-well microtitre plate in a two-fold serial dilution to give a final concentration range of 512–1 μg/mL. Mycobacterial strains were grown on Columbia blood agar (Oxoid) supplemented with 7% defibrinated horse blood (Oxoid). Bacterial inocula equivalent to the 0.5 McFarland turbidity standard were prepared in normal saline and diluted to give a final inoculum density of 5×10^5 cfu/mL. The inoculum (125 μL) was added to all wells and the microtitre plate was incubated at 37 °C for 72 h for *M. fortuitum*, *M. smegmatis*, *M. phlei* and *M. abcessus*. For *M. aurum* the plate was incubated for 120 h. The MIC was recorded as the lowest concentration at which no bacterial growth was observed. This was facilitated by the addition of 20 μL of MTT (Sigma 10 mg/mL in MeOH) to each well and incubation at 37 °C for 20 min where bacterial growth was indicated by a blue colouration. Appropriate DMSO, growth and sterile controls were carried out. Ethambutol and isoniazid were used as positive controls. *M. bovis* BCG was cultured in 7H9 Middlebrook medium and activity against this organism was determined using a 96-well microtitre plate assay as previously reported for *M. aurum* (Newton *et al.*, 2002), in which bacterial growth was determined by measuring the optical densities of microtitre plate wells at 550 nm. Streptomycin sulphate was used as a positive control.

RESULTS AND DISCUSSION

Cryptolepine was tested against a panel of six species of fast growing mycobacteria and the results of minimum inhibitory concentrations are given in Table 1. Against the cattle tuberculosis causing *M. bovis,* cryptolepine hydrochloride had similar activity to that against the screening organism, *M. fortuitum* of 12.5 and 16 μg/mL, respectively. In a previous study in which both the hydrochloride salt and the free base were assessed against *M. fortuitum*, the salt was found to be almost ten-fold less active than the free base (60 vs 6.25 μg/mL) (Cimanga *et al*., 1996). Against *M. smegmatis* (**1**) was slightly more active than against *M. fortuitum* and *M. bovis* BCG.

Notably, antibiotic activity was most pronounced against *M. aurum* and *M. phlei* with the activities being comparable to those of the standard antibiotics ethambutol and isoniazid. Fast growing mycobacteria have been reported to cause peritoneal infections (Paul and Devarajan, 1998) and are highly problematic for patients with compromised immune systems, especially for those with AIDS. The activity of (**1**) against *M. aurum* and *M. bovis* BCG, which are slower growing species and more likely to be better models for *M. tuberculosis*, indicate that further evaluation against tuberculosis causing bacteria is warranted.

Cryptolepine is present in the roots of *C. sanguinolenta*, and as mycobacteria are part of the normal filamentous bacterial flora of soil, it is possible that this compound is produced as part of the plant chemical defence against these and other bacteria. Investigation of the roots of related species may well prove fruitful. The activity of cryptolepine hydrochloride is promising and our results indicate that further synthetic modification of the cryptolepine template is valuable, particularly if the broad cytotoxicity of this agent can be ameliorated whilst retaining the antimycobacterial activity.

REFERENCES

Boakye-Yiadom K, Heman-Ackah SM. 1979. Cryptolepine hydrochloride effect on *Staphylococcus aureus*. *J Pharm Sci* **68**: 1510–1514.

Cantrell CL, Franzblau SG, Fischer NH. 2001. Antimycobacterial plant terpenoids. *Planta Med* **67**: 685–694.

Cimanga K, De Bruyne T, Lasure A, *et al.* 1996. *In vitro* biological activities of alkaloids from *Cryptolepis sanguinolenta*. *Planta Med* **62**: 22–27.

Gibbons S, Udo EE. 2000. The effect of reserpine, a modulator of multidrug efflux pumps, on the *in-vitro* activity of tetracycline against clinical isolates of methicillin resistant *Staphylococcus aureus* (MRSA) possessing the *tet*(K) determinant. *Phytother Res* **14**: 139–140.

Gillespie SH, Morrissey I, Everett D. 2001. A comparison of the bactericidal activity of quinolone antibiotics in a *Mycobacterium fortuitum* model. *J Med Microbiol* **50**: 565–570.

Heinrich M, Gibbons S. 2001. Ethnopharmacology in drug discovery: an analysis of its role and potential contribution. *J Pharm Pharmacol* **53**: 425–432.

Lisgarten JN, Coll M, Portugal J, Wright CW, Aymami J. 2002. The antimalarial and cytotoxic drug cryptolepine intercalates into DNA at cytosine-cytosine sites. *Nat Struct Biol* **9**: 57–60.

Newton SM, Lau C, Gurcha SS, Besra GS, Wright CW. 2002. The evaluation of forty-three plant species for *in vitro* antimycobacterial activities; isolation of active constituents from *Psoralea corylifolia* and *Sanguinaria canadensis*. *J Ethnopharmacol* **79**: 57–67.

Newton SM, Lau C, Wright CW. 2000. A review of antimycobacterial natural products. *Phytother Res* **14**: 303–322.

Paul E, Devarajan P. 1998. *Mycobacterium phlei* peritonitis: a rare complication of chronic peritoneal dialysis. *Pediatr Nephrol* **12**: 67–68.

Paulo A, Pimentel M, Viegas S, *et al.* 1994. *Cryptolepis sanguinolenta* activity against diarrhoeal bacteria. *J Ethnopharmacol* **44**: 73–77.

Raviglione MC, Gupta R, Dye CM, Espinal MA. 2001. The burden of drug-resistant tuberculosis and mechanisms for its control. *Ann N Y Acad Sci* **953**: 88–97.

Sawyer IK, Berry MI, Brown MW, Ford JL. 1995. The effect of cryptolepine on the morphology and survival of *Escherichia coli*, *Candida albicans* and *Saccharomyces cerevisiae*. *J Appl Bacteriol* **79**: 314–321.

Sawyer IK, Berry MI, Ford JL. 1997. Effect of medium composition, agitation and the presence of EDTA on the antimicrobial activity of cryptolepine. *Lett Appl Microbiol* **25**: 207–211.

Silva O, Duarte A, Cabrita J, Pimentel M, Diniz A, Gomes E. 1996. Antimicrobial activity of Guinea-Bissau traditional remedies. *J Ethnopharmacol* **50**: 55–59.

Tona L, Ngimbi NP, Tsakala M, *et al.* 1999. Antimalarial activity of 20 crude extracts from nine African medicinal plants used in Kinshasa, Congo. *J Ethnopharmacol* **68**: 193–203.

Wright CW, Phillipson JD, Awe SO, *et al.* 1996. Antimalarial activity of cryptolepine and some other anhydronium bases. *Phytother Res* **10**: 361–363.

PHYTOTHERAPY RESEARCH
Phytother. Res. **17**, 274–275 (2003)
Published online in Wiley InterScience (www.interscience.wiley.com). **DOI**: 10.1002/ptr.1112

SHORT COMMUNICATION

Activity of *Zanthoxylum clava-herculis* Extracts against Multi-drug Resistant Methicillin-Resistant *Staphylococcus aureus* (mdr-MRSA)

Simon Gibbons*, Julia Leimkugel, Moyo Oluwatuyi and Michael Heinrich
Centre for Pharmacognosy and Phytotherapy, The School of Pharmacy, University of London, London, UK

In a continuing search for compounds with antibiotic activity against methicillin-resistant *Staphylococcus aureus* (MRSA) possessing multidrug efflux systems, we have demonstrated activity associated with extracts from Southern prickly ash bark, *Zanthoxylum clava-herculis*. Bioassay-guided isolation of an alkaloid extract led to the characterization of the benzo[c]phenanthridine alkaloid chelerythrine as the major active principle. This compound exhibited potent activity against strains of MRSA, which were highly resistant to clinically useful antibiotics *via* multidrug efflux mechanisms. Copyright © 2003 John Wiley & Sons, Ltd.

Keywords: Benzo[c]phenanthridine alkaloids; chelerythrine; efflux; MRSA; Nor(A); Msr(A); Tet(K); multidrug resistance; mdr.

INTRODUCTION

At present there are few available antibiotics that can be used to treat life-threatening infections caused by methicillin-resistant *Staphylococcus aureus* (MRSA) and unfortunately resistance to the main antibiotic used in its treatment, vancomycin, has become more frequent (Martin and Wilcox, 1997; Perl, 1999; Rotun *et al.*, 1999). Whilst the oxazolidinone and streptogramin type antibiotics have recently been heralded as a solution to MRSA infections, resistance to linezolid (an oxazolidinone) has recently been reported in vancomycin-resistant *Enterococcus faecium* (Gonzales *et al.*, 2001), and the possible occurrence of resistance to this agent in the Staphylococci is very likely to occur. The ability of MRSA to acquire resistance to the majority of therapeutically relevant antibiotics necessitates the requirement for new compounds that display broad-spectrum activity against multiply resistant isolates of this organism.

To meet this need, we have been screening plant extracts for activity against strains of MRSA which have multidrug efflux proteins as resistance mechanisms (Gibbons and Udo, 2000), and have shown that extracts from the bark of the Southern prickly ash, *Zanthoxylum clava-herculis*, demonstrated considerable activity against all of our resistant strains.

Previous phytochemical investigations on *Zanthoxylum clava-herculis* led to the isolation of a number of benzophenathridine and aporphine alkaloids, typically chelerythrine and magnoflorine (Waterman and Grundon, 1983). As far as we are aware, this is the first report of the activity of components of this species against efflux mediated multidrug resistant strains of MRSA.

* Correspondence to: Dr S. Gibbons, Centre for Pharmacognosy and Phytotherapy, The School of Pharmacy, London, WC1N 1AX, UK.
E-mail: simon.gibbons@ulsop.ac.uk

MATERIALS AND METHODS

Plant material

Powdered dry Southern prickly ash bark (3 kg) was obtained from the Herbal Apothecary, Syston, Leicester, batch No. 01962. A drug sample is deposited at the School of Pharmacy.

Bacterial strains

MRSA strain XU212 (tetracycline resistant) was cultured from clinical isolates of the Adan hospital (Kuwait). MRSA strains RN4220 (macrolide resistant) and 1199B and (fluoroquinolone-resistant) were provided by Drs Jon Cove and Glenn Kaatz respectively. *S. aureus* standard strain ATCC 25923 was obtained from the American Type Culture Collection. All strains were cultured on nutrient agar (Oxoid) prior to determination of minimum inhibitory concentration.

Determination of Minimum Inhibitory Concentration (MIC)

Mueller-Hinton broth (MHB) (Oxoid) was adjusted to contain 20 mg/L and 10 mg/L of Ca^{2+} and Mg^{2+} respectively. An inoculum density of 5×10^5 cfu of each of the test organisms was prepared in normal saline (9 g/L). MHB (125 µL) was dispensed into 10 wells of a 96 well microtitre plate (Nunc, 0.3 ml volume) and then 125 µL of test solution (2048 µg/ml) was serially diluted (2 fold) into each of the wells. 125 µL of inoculum was then added to each of the wells, which resulted in a test compound concentration range of 512 to 1 µg/ml. The plate was then incubated at 36 °C for 18 h and the MIC

Received 23 May 2001
Accepted 11 June 2001

Table 1. Minimum Inhibitory Concentrations (MIC'S) for test organisms

Bacterial Strain (mdr efflux system)	MIC (μg/ml) of antibiotic			
	Chelerythrine	Norfloxacin	Erythromycin	Tetracycline
RN4220 (Msr(A))	8	32	64	0.5
XU212 (Tet(K))	16	8	4096	256
1199-B (Nor(A))	8	64	2	32
ATCC 25923	4	16	0.25	0.5

was recorded as the lowest concentration at which no growth was observed. Standard antibiotics tetracycline, norfloxacin and erythromycin were obtained from the Sigma chemical company.

Extraction and isolation

The powdered bark (2 Kg) was suspended for one week in 80% methanol, 20% water (10 L). After filtration, the solvent was removed under vacuum. The crude extract was suspended in sulphuric acid (2%) and the pH was adjusted to pH = 1. This acidic solution was further purified by washing successively with hexane (300 ml) three times to remove fatty acids. The alkaloidal components were extracted from the aqueous phase with dichloromethane at pH 9 to yield 8.47 g of crude alkaloids. An additional portion of dried bark (500 g) was extracted sequentially with hexane, dichloromethane, methanol and water. All the crude extracts obtained were tested against *S. aureus* strain XU-212 of which the alkaloid extract was the most active (MIC = 32 μg/ml). The alkaloidal extract (8 g) was subjected to Biotage™ flash chromatography (Flash 75 S silica gel cartridge) eluting with hexane with increasing 10% amounts of ethyl acetate and finally 10% methanol in ethyl acetate. Each of the fractions were monitored for activity. The residue from the fraction eluted with 20% ethyl acetate in hexane displayed good activity (MIC = 32 μg/ml) and this was further purified by preparative TLC (silica gel, solvent BuOH 30%, ethyl acetate 50%, formic acid 5% and water 15%) to yield chelerythrine (4 mg) which was identified by comparison of spectroscopic data with an authentic sample (Sigma chemical Co.).

RESULTS AND DISCUSSION

Fractionation of the alkaloidal extract led to the isolation of the benzo[c]phenanthridine alkaloid chelerythrine as the major active natural product, and the minimum inhibitory concentration (MIC) of this compound was determined against our mdr strains and a standard ATCC strain (Table 1). Each of the strains with mdr efflux proteins were highly resistant to norfloxacin, tetracycline and erythromycin and showed cross resistance to these antibiotics. For example, the strain with the macrolide efflux system was highly resistant to norfloxacin in addition to erythromycin (Table 1). Chelerythrine displayed significant activity when compared to the standard antibiotics tetracycline, erythromycin and norfloxacin. Whilst chelerythrine is known to have inhibitory activity against yeast lipase (Grippa *et al.*, 1999), this is the first report describing activity against clinical strains of MRSA with multidrug efflux mediated mechanisms of resistance. Recently it has been shown that chelerythrine also acts as inhibitor of protein kinase C and induces apoptosis of human tumor cells while exhibiting only minimal toxicity in humans (Chmura *et al*., 2000).

New drug leads for antibiotics are greatly needed at present and it is possible that synthetic modification of the benzo[c]phenanthridine template could be carried out to reduce the general cytotoxicity of this class of natural products whilst retaining the anti-staphylococcal activity. The low MIC of chelerythrine may possibly indicate that it is not a substrate for efflux mechanisms present in MRSA, which would be advantageous in a new group of anti-staphylococcal agents.

REFERENCES

Chmura SJ, Dolan ME, Cha A, *et al.* 2000. *In vitro* and *in vivo* activity of protein kinase C inhibitor chelerythrine chloride induces tumor cell toxicity and growth delay in vivo. *Clin Cancer Res* **6**: 737 –742.

Gibbons S, Udo EE. 2000. The effect of reserpine, a modulator of multidrug efflux pumps, on the *in-vitro* activity of tetracycline against clinical isolates of methicillin resistant *Staphylococcus aureus* (MRSA) possessing the *tet*(K) determinant. *Phytother Res* **14**: 139–140.

Gonzales RD, Schreckenberger PC, Graham MB, *et al.* 2001. Infections due to vancomycin-resistant *Enterococcus faecium* resistant to linezolid. *Lancet* **357**(9263):1179

Grippa E, Valla R, Battinelli L. 1999. Inhibition of *Candida rugosa* lipase by berberine and structurally related alkaloids, evaluated by high-performance liquid chromatography. *Biotechnol Biochem* **63**: 1557–1562.

Martin R, Wilcox KR. 1997. Update: *Staphylococcus aureus* with reduced susceptibility to vancomycin, United States. *MMWR* **46** (35): 813–815.

Perl TM. 1999. The Threat of Vancomycin Resistance. *Am J Med* **106** (5A): 26S–37S.

Rotun SS, Schoomaker DJ, Maaupin PS, *et al.* 1999. *Staphylococcus aureus* with reduced susceptibility to vancomycin isolated from a patient with fatal bacteraemia. *Emerg Infect Dis* **5**: 147–149.

Waterman PG, Grundon MF (eds). 1983. (eds). *Chemistry and Chemical Taxonomy of the Rutales*. Academic Press: London.

Ostruthin: An Antimycobacterial Coumarin from the Roots of *Peucedanum ostruthium*

Andreas Schinkovitz[1], Simon Gibbons[2], Michael Stavri[2], Michael J. Cocksedge[3], Franz Bucar[1]

Abstract

Following a bioassay-guided fractionation, ostruthin (6-geranyl-7-hydroxycoumarin) was isolated from the roots of *Peucedanum ostruthium* Koch (Apiaceae) as a compound with pronounced *in vitro* activity against several species of rapidly growing Mycobacteria, namely *Mycobacterium abscesus, M. aurum, M. fortuitum, M. phlei* and *M. smegmatis*. Minimum inhibitory concentrations (MIC) ranged between 3.4 to 107.4 μM and were comparable to those of ethambutol and isoniazid. Imperatorin (8-isopent-2-enyloxy-6,7-furanocoumarin) showed no activity at concentrations up to 1.9 mM. Umbelliferone (7-hydroxycoumarin) was only weakly active (MIC = 0.79 mM).

From several plants traditionally used in the U.K. and CE Europe to cure tuberculosis, chronic lung diseases or other mycobacterial related diseases, *P. ostruthium* was selected by screening for antimycobacterial activity using *Mycobacterium fortuitum* in an *in vitro* assay. *M. fortuitum* is a pathogen capable of causing infections in the lung [1], cutaneous soft tissue [2] and has recently proven useful as a surrogate for *M. tuberculosis* as an antimycobacterial screening model [3]. The highest activity was found in the dichloromethane extract from the roots (MIC: 16 μg/mL), which was further separated. Ostruthin (**1**), a known constituent from *P. ostruthium* [4], was isolated as the active component after a two-step column separation. Imperatorin (**2**), another major compound in the active fraction, showed no activity at concentrations up to 1.9 mM. Compound **2** was identified by ^{1}H- and ^{13}C-NMR ($CDCl_3$) in comparison to [5]. The identity of **1** was verified by ^{1}H-NMR spectral data ($CDCl_3$) in correspondence to [6] and high resolution FAB-MS showing the M + H^+ ion at *m/z* = 299.1662, calculated for $C_{19}H_{23}O_3$: 299.1647. HPLC and GC-MS analysis were performed to prove the purity (> 99%). Compound **1** showed significant inhibitory activities against different strains of rapidly growing Mycobacteria, i.e., *M. aurum, M. fortuitum, M. phlei* and *M. smegmatis* with MIC values between 3.4 to 6.7 μM (see Table **1**). *M. abscessus* was less susceptible to **1** (MIC: 107.4 μM), but this was also true for isoniazid (INH) and

Affiliation: [1] Institute for Pharmacognosy, Karl-Franzens-University, Graz, Austria · [2] Centre for Pharmacognosy and Phytotherapy · [3] Department of Pharmaceutical and Biological Chemistry, The School of Pharmacy, University of London, U.K.

Correspondence: Ao. Univ.-Prof. Dr. Franz Bucar · Institute of Pharmacognosy · Karl-Franzens-University of Graz · Universitätsplatz 4/1 · 8010 Graz · Austria · E-mail: franz.bucar@uni-graz.at · Fax: +43-316-380-9860

Received: August 16, 2002 · **Accepted:** November 23, 2002

Bibliography: Planta Med 2003; 69: 369–371 · © Georg Thieme Verlag Stuttgart · New York · ISSN 0032-0943

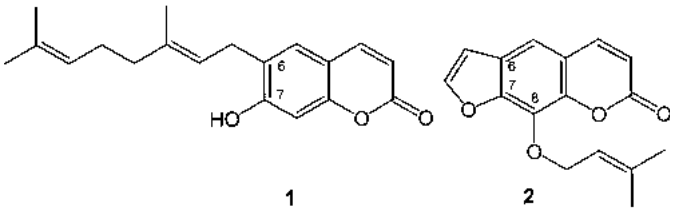

1 2

ethambutol (EMB) which were used as positive controls. The *in vitro* antimycobacterial activity of **1** was equivalent to those of INH and EMB, except for *M. smegmatis* which showed a higher susceptibility to EMB (MIC: EMB 0.6 μM; **1** 6.7 μM; INH 14.6 μM). In previous investigations, a number of crude plant extracts which are active against Mycobacteria have been found [7], [8], [9] but only in a few cases have the single active compounds been evaluated [7], [10], [11], and in the case of terpenoids, some structure-activity relationships have been established [12].

Antimicrobial activity has been previously demonstrated for a number of coumarins [13], however, this is the first report on the antimycobacterial properties of ostruthin. *P. ostruthium* is rich in linear furanocoumarins and other coumarins, some of which have shown insecticidal activities [14], [15]. Previously, the structure-activity relationship of some coumarins concerning the inhibition of formation of acid-fastness in Mycobacteria has been analysed [16] and a hydroxy group at C-7 was found to be essential. Interestingly, the simple monohydroxylated coumarin umbelliferone (7-hydroxycoumarin), was only weakly active against *M. fortuitum* (MIC: 0.79 mM). Furthermore the increased lipophilicity of ostruthin compared to simple hydroxycoumarins such as umbelliferone, which is due to the geranyl side chain, seems to play an important role, in agreement with [12]. Dabak and Zboril [17] showed that the inhibitory effect of ostruthin, its methyl ether and geraniol on succinic oxidase and succinate dehydrogenase was associated with the presence of an isoprenic side chain, as umbelliferone and other simple coumarins were without effect. Whether this activity of **1** is responsible for growth inhibition in Mycobacteria has not yet been investigated.

Our results indicate that coumarins with lipophilic side chains deserve further attention as potential sources for new antimycobacterial drugs.

Table **1** Antimycobacterial activity *in vitro* of ostruthin, ethambutol and isoniazid on different species of rapidly growing Mycobacteria

Species	Minimal inhibitory concentration (MIC)[a], µM		
	Ostruthin (1)	Ethambutol	Isoniazid
M. abscessus ATCC 19977	107.4	156.9	116.8
M. aurum PI 104482	3.4	4.9	4.6
M. fortuitum ATCC 6841	6.7	19.6	3.6
M. phlei ATCC 11758	6.7	4.9	7.3
M. smegmatis ATCC 14468	6.7	0.6	14.6

[a] MICs for *M. fortuitum* were recorded in triplicate all others were recorded in duplicate and are an average.

Material and Methods

Plant material was obtained as a commercial sample (Kottas, Vienna) and its identity was verified by microscopy and TLC referring to [18], [19] by one of the authors (F.B.). A voucher specimen is kept at the herbarium of the Institute of Pharmacognosy of the University of Graz (P.O.R-001)

Soxhlet extraction of the powdered roots (755 g) gave 90.24 g of dichloromethane extract (MIC : 16 μg/mL). 3.22 g of this were separated on a silica gel 60 column (4 × 10 cm). Solvent composition: fr.1 toluene/EtOEt/hexane/EtOAc (8 : 8 : 34 : 0.17) (MIC: 512 μg/mL), fr.2 toluene/EtOEt/hexane/EtOAc (12.5 : 12.5 : 25 : 0.5) (MIC: 128 μg/mL), fr.3 toluene/EtOEt/hexane/EtOAc (17 : 16 : 17 : 0.5) (MIC: 4 μg/mL), 5 mL/min and 200 mL each. Evaporated residue of fr. 3 was then separated on a Sephadex LH-20 column (1.8 × 30 cm), CH_2Cl_2/acetone 80 : 20, 5 mL/ min. Compound **1** (25 mg) was sampled between 375 – 415 mL, **2** (12 mg) between 305 – 345 mL. Column separation was accompanied by TLC analysis on silica gel 60 plates in toluene/EtOEt/EtOAc (50 : 50 : 1). Under UV light (365 nm) **1** appeared as a blue spot at R_F: 0.57, **2** showed green fluorescence at R_F: 0.67.

NMR spectra were recorded on a Bruker AM-250 spectrometer at 250 MHz and a Bruker AMX 500 at 500 and 125 MHz, respectively. Fast atom bombardment mass spectra were recorded on a VG Analytical ZAB-SE instrument using MNOBA as matrix. Accurate mass measurements were done by comparison with CsI or glycerol. Copies of the original spectra are obtainable from the author of correspondence. Analytical HPLC analysis was performed on a Lachrom D-7000 HPLC system (Merck-Hitachi) using a LiChrospher 100 RP-18 column (250 × 4 mm, 5 μm). Solvent composition was ACN/H_2O 40/60 changing to 100/0 within 30 min, flow rate 0.8 mL/min; temperature 22 °C. Ostruthin was detected at t_R: 22.14 min. GC-MS experiments were carried out on a HP 5890 Series II Plus gas chromatograph interfaced to a HP 5989B mass spectrometer on a HP-5MS column (ID: 0.25 mm, film thickness: 0.25 μm, length: 26 m).

M. fortuitum ATCC 6841 was obtained from Dr Peter Lambert, Aston University, U.K., *M. smegmatis* ATCC 14468, *M. phlei* ATCC 11758, *M. abscessus* ATCC 19977 and *M. aurum* Pasteur Institute 104482 were all obtained from the American Type Culture Collection or the Pasteur Institute.

The assay comprised a standard minimum inhibitory concentration (MIC) determination [20] of test compounds in Ca^{2+} and Mg^{2+} adjusted Mueller-Hinton broth (MHB). Plant extracts were dissolved in DMSO and diluted with MHB to particular concentrations. Positive controls EMB and INH were dissolved directly in MBH. Bacterial inocula equivalent to the 0.5 McFarland turbidity standard were prepared in normal saline and diluted to give a final inoculum density of 5×10^5 cfu/mL. Mycobacterial strains were grown on Columbia Blood agar (Oxoid) supplemented with 7% defibrinated Horse blood (Oxoid). The inoculum (125 μL) was added to all wells and the microtitre plate was incubated at 37 °C for 72 hours for *M. fortuitum, M. smegmatis, M. phlei* and *M. abscessus*. For *M. aurum* the plate was incubated for 120 hours. The MIC was recorded as the lowest concentration at which no bacterial growth was observed. This was facilitated by the addition of 20 μL of MTT (Sigma, 10 mg/mL in MeOH) to each

well and incubation at 37 °C for 20 minutes, where bacterial growth was indicated by a blue colouration. Appropriate DMSO, growth and sterile controls were carried out.

Acknowledgements

Financial support by The British Council, the Austrian Federal Ministry for Education, Science and Culture and the University of Graz is gratefully acknowledged.

References

[1] Griffith DE. Lung disease caused by rapidly growing Mycobacteria. Clin Pulm Med 1995; 2: 258 – 66
[2] Wallace RJ Jr, Swenson JM, Silcox VA, Good RC, Tschen JA, Stone MS. Spectrum of disease due to rapidly growing Mycobacteria. Rev Infect Dis 1983; 5: 657 – 79
[3] Tims KJ, Rathbone DL, Lambert PA, Attkins N, Cann SW, Billington DC. *Mycobacterium fortuitum* as a screening model for *Mycobacterium tuberculosis*. J Pharm Pharmacol 2000; 52 (Suppl): 135
[4] Khaled SA, Szendrei K, Novak I. Coumarin glycosides from *Peucedanum ostruthium*. Phytochemistry 1975; 14: 1461 – 2
[5] Masuda T, Takasugi M, Anetai M. Psoralen and other linear furanocoumarins as phytoalexins in *Glehnia littoralis*. Phytochemistry 1997; 47: 13 – 6
[6] Rashid MA, Armstrong JA, Gray AI, Waterman PG. Novel *C*-geranyl 7-hydroxycoumarins from the aerial parts of *Eriostemon tomentellus*. Z Naturforsch B: Chem Sci 1992; 47: 284 – 7
[7] Newton SM, Lau C, Wright CW. A review of antimycobacterial natural products. Phytother Res 2000; 14: 303 – 22
[8] Lall N, Meyer JJM. In vitro inhibition of drug–resistant and drug sensitive strains of *Mycobacterium tuberculosis* by ethnobotanically selected South African plants. J Ethopharmacol 1999; 66: 347 – 54
[9] Cantrell CL, Fischer NH, Urbatsch L, McGuire MS, Franzblau SG. Antimycobacterial crude plant extracts from South, Central, and North America. Phytomedicine 1998; 5: 137 – 43
[10] Rastogi N, Abaul J, Goh KS, Devallois A, Philogene E, Bourgeois P. Antimycobacterial activity of chemically defined natural substances from the Caribbean flora in Guadeloupe. FEMS Immunol Med Microbiol 1998; 20: 267 – 73
[11] König GM, Wright AD, Franzblau SG. Assessment of antimycobacterial activity of a series of mainly marine derived natural products. Planta Med 2000; 66: 337 – 42
[12] Cantrell CL, Franzblau SC, Fischer NH. Antimycobacterial plant terpenoids. Planta Med 2001; 67: 685 – 94
[13] Ojala T, Remes S, Haansuu P, Vourela H, Hiltunen R, Haahtela K, et al. Antimicrobial activity of some coumarin containing herbal plants growing in Finland. J Ethnopharmacol 2000; 73: 299 – 305
[14] Hadacek F, Mueller C, Werner A, Greger H, Proksch P. Analysis, isolation and insecticidal activity of linear furanocoumarins and other coumarin derivatives from *Peucedanum* (Apiaceae: Apioideae). J Chem Ecol 1994; 20: 2035 – 54
[15] Hiermann A, Schantl D, Schubert-Zsilavecz M. Coumarins from *Peucedanum ostruthium*. Phytochemistry 1996; 43: 881 – 3
[16] Kondo Y, Toida T, Kusano G, Imai J. Structure-activity relationships for the inhibition of formation of acid-fastness in mycobacterial organisms by coumarins and cinnamates. J Pharmacobio-Dyn 1980; 3: 41 – 5
[17] Dadak V, Zboril P. Antibiotic effect of natural coumarins. The effect of coumarins on succinate oxidation by non-phosphorylating enzyme preparation. Collect Czech Chem Commun 1967; 32: 4118 – 28
[18] Wagner H, Bladt S. Plant drug analysis. Springer, Berlin, Heidelberg, New York: 1996: pp. 140 – 2
[19] List PH, Hörhammer L, editors. Hagers Handbuch der pharmazeutischen Praxis. Springer, Berlin, Heidelberg, New York: 4th edition, Vol. 6, part A 1977: pp. 547
[20] Gibbons S, Udo EE. The effect of reserpine, a modulator of multidrug efflux pumps, on the *in vitro* activity of tetracycline against clinical isolates of methicillin resistant *Staphylococcus aureus* (MRSA) possessing the *tet*(K) determinant. Phytother Res 2000; 14: 139 – 40

ELSEVIER

Fitoterapia 73 (2002) 300–304

FITOTERAPIA

www.elsevier.com/locate/fitote

The genus *Hypericum*—a valuable resource of anti-Staphylococcal leads

Simon Gibbons[a,*], Birgit Ohlendorf[b], Inga Johnsen[b]

[a] *Centre for Pharmacognosy and Phytotherapy, The School of Pharmacy, University of London, 29-39 Brunswick Square, London WC1N 1AX, UK*

[b] *Ruprecht-Karls-Universität Heidelberg, Institut für Pharmazeutische Technologie und Biopharmazie, Im Neuenheimer Feld 366 D-69120 Heidelberg, Germany*

Received 22 February 2002; accepted 4 April 2002

Abstract

In the present study, extracts of 34 species and varieties of the genus *Hypericum* were screened for activity against a clinical isolate of methicillin-resistant *Staphylococcus aureus,* which in addition possessed a multidrug efflux mechanism conferring a high level of resistance to therapeutically useful antibiotics. Thirty-three of the 34 chloroform extracts showed significant activity in a disk diffusion assay, and five extracts had minimum inhibitory concentrations of 64 μg/ml, indicating that this genus has great potential to yield compounds with potent activity against multidrug-resistant bacteria.

Keywords: *Hypericum*; Antibacterial activity

1. Introduction

There is a considerable need for new classes of anti-microbial agents in order to counter the rapid increase in plasmid-determined, transmissible multidrug resistance (mdr). In particular, the occurrence and proliferation of mdr methicillin-resistant *Staphylococcus aureus* (MRSA) is cause for major concern in the clinical environment due to the few effective therapeutic agents that can be used against

* Corresponding author. Tel.: +44-207-753-5913; fax: +44-207-753-5909.
E-mail address: simon.gibbons@ulsop.ac.uk (S. Gibbons).

0367-326X/02/$ - see front matter
PII: S0367-326X(02)00082-5

this organism [1]. Intermediate resistance to vancomycin, one of the most widely used glycopeptides which is used to treat MRSA infections has arisen in Japan [2] and the USA [3,4]. Recent developments in anti-staphylococcal agents include the oxazolidinone (e.g. linezolid) and streptogramin [e.g. quinupristin/dalfostin (synercid)] type antibiotics, however, resistance to linezolid has recently been reported in vancomycin-resistant *Enterococcus faecium* [5], and the occurrence of resistance to this agent in the Staphylococci is highly likely. New classes of anti-MRSA compounds are, therefore, of significant importance if we are to avoid a similar situation to that of the glycopeptides, with no back up lead compounds to develop into agents with activity against multi-drug resistant bacterial strains.

Species of the genus *Hypericum* are known to produce strongly antibacterial compounds, typically prenylated phloroglucinol natural products such as hyperforin from *Hypericum perforatum* [6], the chinensins from *Hypericum chinense* [7], and filicinic acid derivatives from *Hypericum drummondii*, which show excellent anti-staphylococcal activity with sub 1 μg/ml minimum inhibitory concentrations (MIC) [8].

The activity of these natural products from *Hypericum* prompted us to collect 34 species and varieties of this group, extract and then screen them against a clinical isolate of MRSA possessing the multidrug efflux transporter Tet(K) [9] which was highly resistant to β-lactams, tetracyclines, macrolides and fluoroquinolones. Efflux mechanisms of resistance actively export many classes of antibiotics from the bacterial cell resulting in a low intracellular concentration of antimicrobial.

2. Experimental

2.1. Plant material

The aerial parts of all species studied were collected from the National Plant Collection of *Hypericum* at the Royal Botanic Gardens Kew at Wakehurst Place, and were shade dried at room temperature.

2.2. Preparation of extracts

Dried plant material (varying in dry mass from 0.3 to 3 g) was ground and extracted sequentially in chloroform and methanol (15 ml each). Extracts were filtered and blown down to dryness under nitrogen and stored at −80 °C prior to assay. Extract yields were in the range of 0.1–14%.

2.3. Antibacterial assays and bacteria

Disk diffusion assay. Mueller–Hinton agar (Oxoid) in Petri dishes was inoculated with a bacterial suspension (10^7 cfu/ml) and the excess suspension removed. Paper disks (5 mm Oxoid) were impregnated with test extracts at a concentration of 1 mg/disk, then laid onto the surface of the agar. An appropriate antibiotic control

disk (vancomycin, 5 μg/disk) was also placed onto the surface of the agar. The culture was then incubated for 18 h at 37 °C, and zones of inhibition appeared in the presence of antibacterial substances.

Minimum inhibitory concentration assay. This assay comprised a standard minimum inhibitory concentration (MIC) determination of test compound in Ca^{2+} and Mg^{2+} adjusted Mueller–Hinton Broth (MHB). Extracts were dissolved in DMSO and diluted in MHB, to give a starting extract concentration of 512 μg/ml which was then diluted out across a 96-well microtitre plate in a two-fold serial dilution to give a final concentration range from 512 to 1 μg/ml. The test organism was inoculated into each well at a density of 5×10^5 cfu/ml. The plate was incubated at 37 °C for 18 h and the MIC recorded as the lowest concentration at which no growth was observed. This was facilitated by the addition of 20 μl of MTT (Sigma 10 mg/ml in MeOH) to each well and incubation at 37 °C for 20 min where bacterial growth was indicated by a blue colouration. Appropriate DMSO, growth and sterile controls were carried out. Tetracycline was used as a positive control.

Bacteria. The test organism was a clinical isolate of MRSA (strain XU212) from the Adnan Hospital, Kuwait, possessing the previously characterised Tet(K) multidrug efflux mechanism [9].

3. Results and discussion

Thirty-three of the chloroform extracts and 32 of the methanol extracts exhibited good activity (zones of inhibition > 7 mm diameter) in the disk diffusion assay (Table 1). Several of the chloroform extracts exhibited large zones of inhibition (> 20 mm) when compared to vancomycin (zone of inhibition: 18 mm, 5 μg/disk). Whilst the concentration of 1 mg/disk is comparatively high, thin layer chromatography of these extracts indicated that they are complex, and it is highly likely that purification of the antibiotics from the extracts will result in compounds with very low MIC values. Where sufficient extract was available, chloroform extracts which exhibited inhibition zones greater than 13 mm, had minimum inhibitory concentrations determined against the Tet(K) producing multidrug resistant strain of MRSA (Table 2). The low minimum inhibitory concentrations of these extracts, when compared to conventional antibiotics (Table 2), highlight the potential of the genus *Hypericum* as an excellent source of anti-staphylococcal agents.

Previous systematic chemical studies on the anti-staphylococcal compounds from this genus has been limited, possibly due to the fact that when most of the research into new antibacterial agents from plants was conducted, there were a number of agents (e.g. vancomycin, teicoplanin) that could be used to treat resistant staphylococcal infections, and consequently there was little pressure to find new agents. A literature search on these species has shown that *Hypericum calycinum* produces xanthones [10] and chinensin-type [11] metabolites which have not been tested for antibacterial activity. However, *Hypericum hookerianum* extracts have recently been assessed for antibacterial activity [12].

Table 1
Antibacterial activities of *Hypericum* chloroform and methanol (in brackets) extracts against MRSA strain XU212[a]

Hypericum species	Inhibition zone in mm	*Hypericum* species	Inhibition zone in mm
H. acmosepalum	8 (12)	*H. kouytchense*	12 (7)
H. addingtonii	11 (9)	*H. lagarocladum*	14 (9)
H. androsaemum	9 (8)	*H. lancasteri*	11 (13)
H. arnoldianum	11 (13)	*H. maclarenii*	9 (12)
H. beanii	14 (11)	*H. maculatum* ssp. *maculatum*	0 (7)
H. bellum ssp. latisepalum	12 (13)	*H. moserianum*	12 (12)
H. calycinum	16 (12)	*H. olympicum 'citrinum'*	19 (6)
H. curvisepalum	9 (9)	*H. olympicum f. minus 'sulphureum'*	21 (12)
H. dummeri	13 (8)	*H. olympicum f. uniflorum*	19 (7)
H. foliosum	20 (7)	*H. patulum*	8 (12)
H. forrestii	13 (9)	*H. prolificum*	14 (11)
H. frondosum	16 (9)	*H. pseudohenryi*	11 (13)
H. hidecote	12 (8)	*H. reptans*	13 (9)
H. hircinum	12 (6)	*H. revolutum* ssp. *revolutum*	16 (8)
H. hircinum ssp. albimontanum	11 (13)	*H. stellatum*	10 (13)
H. hircinum ssp. majus	23 (0)	*H. subsessile*	10 (9)
H. hookerianum	9 (10)	*H. xylosteifolium*	7 (0)

Inhibition zones were measured as the diameter of the zone of inhibition. Zones were compared to vancomycin (5 μg/disk), which gave a zone of 18 mm in diameter. [a] XU212 is a clinical isolate of methicillin-resistant *Staphylococcus aureus* possessing the multidrug efflux transporter Tet(K).

Table 2
Minimum inhibitory concentrations (MIC) of selected chloroform extracts against MRSA strain XU212

Hypericum species	MIC (μg/ml)
H. beanii	256
H. calycinum	256
H. foliosum	64
H. hircinum ssp. majus	64
H. lagarocladu	128
H. olympicum f. minus 'sulphureum'	64
H. olympicum f. uniflorum	64
H. olympicum 'citrinum'	64
H. revolutum ssp .revolutum	128

MIC of standard antibiotics (μg/ml): tetracycline (128), erythromycin (4096), norfloxacin (8).

Whilst disk diffusion assays are a rapid way of detecting activity and may be used to track such activity through a separation process, a major drawback is the poor diffusability of lipophilic compounds through the media, resulting in small zones of inhibition [13]. Additionally, MIC values may be misleading due to the presence of low concentrations of highly active metabolites or high concentrations of poorly

active metabolites. Consequently, further chemistry is needed to assess these extracts.

These preliminary results highlight the potential of the genus *Hypericum* to produce anti-staphylococcal leads with good activity against a multidrug resistant strain. Bioassay-guided isolation is currently underway to characterise the antibacterial agents of this interesting taxon.

Acknowledgements

This work was funded by Royal Society Grant 21595. We are thankful to Mr Chris Clennett (Royal Botanic Gardens Kew at Wakehurst Place) for his help in the collection of plant material.

References

[1] Horikawa M, Noro T, Kamei Y. J Antibiot 1999;52:186.
[2] Hirimatsu K, Hanaki H, Ino T, Yabuta K, Oguri T, Tenover FC. J Antimicrob Chemother 1997;40:135.
[3] Martin R, Wilcox KR. MMWR 1997;46:813.
[4] Perl TM. Am J Med 1999;106:26S.
[5] Gonzales RD, Schreckenberger PC, Graham MB, Kelkar S, DenBesten K, Quinn JP. Lancet 2001;357:1179.
[6] Schempp CM, Pelz K, Wittmer A, Schopf E, Simon JC. Lancet 1999;353:2129.
[7] Nagai M, Tada M. Chem Lett 1987;1337.
[8] Jayasuriya H, Clark AM, McChesney JD. J Nat Prods 1991;54:1314.
[9] Gibbons S, Udo EE. Phytother Res 2000;14:139.
[10] Rath G, Potterat O, Mavi S, Hostettmann K. Phytochemistry 1996;43:513.
[11] Decosterd LA, Hoffmann E, Kyburz R, Bray D, Hostettmann K. Planta Med 1991;57:548.
[12] Mukherjee PK, Saritha GS, Suresh B. Fitoterapia 2001;72:558.
[13] Cole MD. Biochem Syst Ecol 1994;22:837.

Oligomeric Acylphloroglucinols from Myrtle (*Myrtus communis*)

Giovanni Appendino,*[,†] Federica Bianchi,[†] Alberto Minassi,[†] Olov Sterner,*[,‡] Mauro Ballero,[§] and Simon Gibbons[||]

DISCAFF, Università del Piemonte Orientale, Viale Ferrucci 33, 28100 Novara, Italy, Department of Organic and Bioorganic Chemistry, Lund University, P.O.B. 124, 221 00 Lund, Sweden, Dipartimento di Scienze Botaniche, Universitá degli Studi di Cagliari, Viale San Ignazio 13, 09123 Cagliari, Italy, and Centre for Pharmacognosy and Phytotherapy, The School of Pharmacy, University of London, London, WC1N 1AX England

Received September 7, 2001

The dimeric nonprenylated acylphloroglucinol semimyrtucommulone (**6**) was obtained from the leaves of myrtle (*Myrtus communis*) as a 2:1 mixture of two rotamers. The known trimeric phloroglucinol myrtucommulone A (**1**) was also isolated and characterized spectroscopically as a silylated cyclized derivative (**5**). Myrtucommulone A showed significant antibacterial activity against multidrug-resistant (MDR) clinically relevant bacteria, while semimyrtucommulone was less active.

Myrtle (*Myrtus communis* L., Myrtaceae) is the archetypal Mediterranean species, and its relevance in medicine, cuisine, and art as well as in religion and myth can hardly be overstated.[1] Current economic interest focuses on the berries and the leaves, which are used to make a popular liqueur and as a hop substitute for beer,[2] but several investigations have evidenced the strong antibacterial activity of myrtle leaf extracts,[3] supporting the use of this plant as an antiseptic in traditional Mediterranean medicine.[4] Phytochemical investigations spanning several decades afforded various monoterpenoids, flavonoids, and triterpenes,[5] but the identity of the antibacterial principle has long remained elusive. In the mid 1970s, Israeli scientists eventually reported the isolation of a phloroglucinol antibiotic from the leaves of myrtle. This compound was named myrtucommulone A (**1**) and was obtained as a

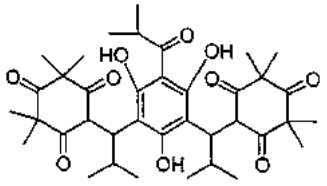

1

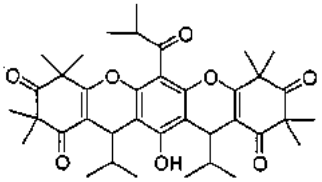

2

mixture of homologues and tautomers which was not amenable to a detailed NMR analysis.[6] Related compounds were also obtained,[6,7] and one of them, the dimer myrtucommulone B (**3**), has recently raised interest for the treatment of psoriatic disorders.[8] We present here the characterization of a new dimeric nonprenylated phloroglucinol from myrtle, the spectroscopic characterization of myrtucommulone A as a silylated cyclized derivative, and the disclosure of its significant activity against multidrug-resistant bacteria.

Results and Discussion

An acetone extract from the dried leaves of myrtle was fractionated by open CC to afford two phloroglucinol mixtures. The MS of the least polar and abundant (0.14%) fraction showed a cluster of five molecular ion peaks spaced by 14 mass units in an approximate ratio of 12:4:2:1:1, indicating a mixture of homologues. The NMR spectrum in a variety of solvents showed only unresolved peaks and was of little use for structure elucidation. Repeated crystallizations eventually removed the minor homologues and afforded a ca. 7:1 mixture (MS analysis) of two compounds, having EIMS and mp identical to those reported for myrtucommulone A (**1**).[6] The structure of this compound was established mainly on the basis of MS data,[6] with additional support from the acid-catalyzed cyclization to a bis-pyrane derivative (**2**) amenable to NMR investigation.[6b] The acidic treatment of our compound gave a complex mixture, and we tried therefore to confirm its identity with myrtucommulone A (**1**) using variable-temperature NMR experiments and an alternative derivatization strategy. Our compound proved too unstable for high-temperature NMR measurements. Thus, heating in DMSO at 80 °C for 24 h afforded a mixture of two compounds, a dimer (**4**) isomeric with myrtucommulone B (**3**) and a trimer related to the bis-dehydrated product **2**. In our hands, the two compounds could not be separated, and their structure was determined from the NMR analysis of the mixture. Owing to severe overlapping of many signals, it was not possible to fully characterize the trimeric product. However, the ^{13}C NMR spectrum showed that the central aromatic ring was not symmetric, thus suggesting an angular (cf. **5**) rather than a linear (**2**) structure. The formation of the dimer **4** was followed monitoring the upfield signal for H-5, while the substitution pattern of the benzene ring was established by HMBC correlations. The absence of a signals for 6-OH and 6′-OH and NOESY correlations between H-5 and 4-OH as well as the 14′-methyl supported a tricyclic structure, isomeric with myrtucommulone B, for **4**. It should be noted that the published NMR data for myrtucommulone B[6b] do not distinguish between structures **3** and

* To whom correspondence should be addressed. Tel (G.A.): +39 011 670 7684; (O.S.): +46 4622 28213. Fax (G.A.): + 39 011 670 7687; (O.S.): +46 4622 28213. E-mail (G.A.): appendin@pharm.unito.it; (O.S.): Olov.Sterner@orgk2.lth.se.

† DISCAFF, Università del Piemonte Orientale.

‡ Lund University.

§ Universitá degli Studi di Cagliari.

|| University of London.

10.1021/np010441b CCC: $22.00
Published on Web 02/19/2002

4, and the possibility that this compound might actually be reformulated as **4** should not be neglected. In this case, the facile transformation of **1** to **4** makes it possible that myrtucommulone B is an artifact of extraction and/or isolation.

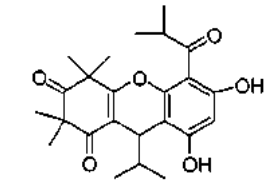

3

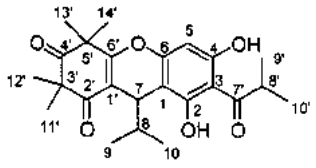

4

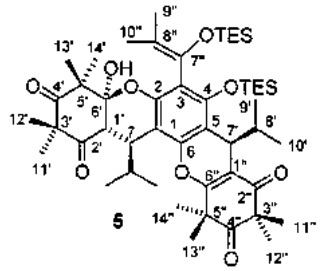

5

Acetylation and methylation of **1** gave complex mixtures, but silylation eventually delivered, in modest yield (23%), a derivative that maintained the carbon−carbon connectivity of the natural product and was amenable to spectroscopic analysis. The molecular formula of **5** ($C_{50}H_{78}O_9Si_2$) evidenced the presence of two −OTES groups, while careful analysis of the 2D NMR data settled unambiguously the structure and configuration. Surprisingly, the pentacyclic angular enol ether **5** was obtained in a configurationally unitary form and free from homologues. This structure is the one expected for a compound formed from the bisacetalization, the monodehydration, and the disilylation of a starting material having the bona fide formula of myrtucommulone A and is consequently complementing the previous structural identification based on the MS data. As to the site(s) of homologation of myrtucommulone A, the cluster of homologous peaks observed for the parent ion was also present in the mass peak resulting, after dehydration, from the α-cleavage of the isobutyryl group [M − C_3H_7 − H_2O], suggesting that homologation occurs at the isobutylidene bridge(s). The tautomeric composition of myrtucommulone A remains unknown. On the basis of previous studies of the prototropic equilibria in benzyl-substituted syncarpic acids,[9] several plausible tautomeric forms can be envisaged for myrtucommulone A, with formula **1** representing only one of the three possibilities where aromaticity of the central ring is maintained.

The more polar and abundant phloroglucinol **6**, named semimyrtucommulone, was obtained free from homologues. HRMS data established the molecular formula $C_{25}H_{34}O_7$, while the NMR spectra showed duplication of all resonances. The failure to evidence two compounds by HPLC techniques and the coalescence of the NMR signals at 90 °C indicated that **6** was a mixture of two tautomers or rotamers, in a ratio of ca. 2:1 at room temperature. The two sets of ^{1}H NMR signals showed the same proton spin systems (one isobutylidene group, one isopropyl, four methyls bound to nonprotonated aliphatic carbons, and one benzylic methyl), suggesting that the equilibrating species were rotamers rather than tautomers. Due to the high number of nonprotonated carbons, HMBC experiments were utilized extensively to correlate the ^{1}H and ^{13}C resonances and assemble them into the same dimeric phloroglucinol structure **6**. Again, correlations from the hydroxyl protons as well as from the methyl protons revealed the carbon skeleton of **6**. Silylation afforded a ca. 1:1 mixture of two isomeric cyclized derivatives, identified as **7** and **8**. HRMS experiments revealed the same elemental composition for these compounds. The unsaturation index, along with the NMR data, suggested that they are tricyclic derivatives, similar to compound **5**. NOESY correlations were used to distinguish between the two compounds. Thus, while the benzylic 11-methyl of **7** correlated with the methylene protons of both TES groups, in **8** the correlation with one of the TES groups was replaced by that with the 11-methyl. In addition, the signal for the hemiacetal proton in **8** was sufficiently resolved to give a NOESY correlation to the 14′-methyl and HMBC correlations to C-1′, C-5′, and C-6′. In both compounds, H-1′ gave NOESY correlations with the 12′-, 13′-, 9-, and 10-methyls, establishing the relative configuration. Remarkably, both compounds were configurationally pure, confirming the surprising capacity of oligomeric phloroglucinols to form polycyclic structures in a highly stereoselective way. Also noteworthy is the observation that, while the silylation of myrtucommulone A (**1**) yielded only one isomer, two isomers were instead formed from semimyrtucommulone (**6**). A possible explanation is that the phenolic hydroxyl in the linear trimeric assembly corresponding to **7** (that is, **2**) is sterically more encumbered than in the corresponding angular assembly like **5** (corresponding to **7**) and, thus, essentially unreactive with the bulky silylating agent. Acetylation of **6** gave one product (**6a**), identified by MS

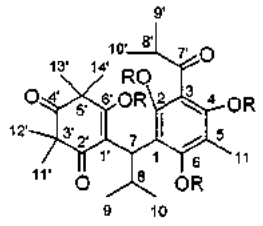

R
6 H
6a Ac

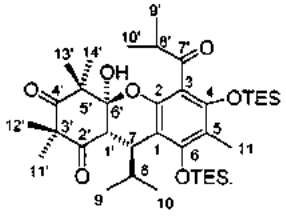

7

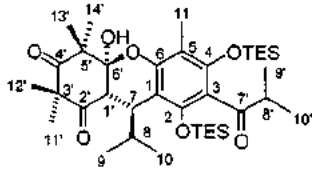

8

Table 1. Minimum Inhibitory Concentrations (MIC) of **1** and **6** against Various *Staphylococcus aureus* Strains

bacterial strain (MDR efflux system)	MIC (μg/mL)		
	1	**6**	tetracycline
RN4220 (Msr(A))[a]	0.5	32	0.5
XU212 (Tet(K))[b]	1	32	256
1199-B (Nor(A))[c]	1	32	32
ATCC 25923[d]	2	64	0.5

[a] Macrolides resistant. [b] Tetracyclines resistant. [c] Fluoroquinolones resistant. [d] Standard ATCC strain.

as a tetraacetate derivative of the natural product. The ^{1}H NMR spectrum taken at 500 MHz was poorly resolved, temperature dependent, and not suitable for structural identification. As expected for a dynamic equilibrium, a decrease of the instrumental frequency improved the resolution, and at 50 °C and 200 MHz most peaks of the ^{1}H NMR spectrum could be assigned. Since acetylation blocks prototropic equilibria, the detection of a dynamic process in the peracetyl derivative of **6** further confirmed that the duplication of the resonances in the NMR spectra of the natural product is due to a conformational process. The differences in NOESY pattern between the two rotamers of **6** could not be easily translated into definite arrangements around the bonds 1′−7 and 1−7, where hindered rotation seems most likely to occur. The discovery of a slow rotameric equilibrium in alkylidene-bridged phloroglucinyl−syncarpyl dimers makes factorial the problem of the characterization of **1**, suggesting that this compound, apart from the tautomeric equilibration typical of syncarpic acid derivatives,[8] can also undergo conformational equilibration.

A biological evaluation of **1** and **6** showed activity against clinically relevant microorganisms. The minimum inhibitory concentrations[10] of **1** and **6** were determined against strains of multidrug-resistant (MDR) *Staphylococcus aureus* which possessed efflux mechanisms of resistance to macrolides, tetracyclines, and fluoroquinolones via the Msr(A),[11] Tet(K),[12] and Nor(A)[13] transporters, respectively (Table 1). Myrtucommulone (**1**) showed a submicromolar or low micromolar activity against all the bacteria investigated, while semimyrtucommulone was 30−60-fold less active. Interestingly, the strains investigated were more susceptible to these agents than a standard ATCC strain, possibly indicating that these phloroglucinols are not substrates of multidrug efflux. Further work is underway to assess whether these compounds are inhibitors of these efflux mechanisms, which would also account for the potent activity observed against these MDR strains. Given the current shortage of efficient antibacterial agents against MDR bacteria, myrtucommulone A qualifies as a new and interesting lead for drug discovery.

The unifying feature of myrtle phloroglucinols is the presence of a fully substituted phloroglucinol core bound via isobutylidene bridge(s) to syncarpyl moiety(ies). The lack of prenylation sets these compounds apart from plant phloroglucinols,[14] while substitution at the phloroglucinol−syncarpyl bridge clearly distinguishes them from fern phloroglucinols.[15]

In conclusion, the leaves of myrtle provide access to unique chemical diversity, whose involvement in the antibacterial activity of the plant seems well established. Apart from the antibiotic properties, myrtle extracts show also powerful hypoglycemic activity[16] and can inhibit aryl hydrocarbon hydroxylase,[17] two activities of pharmacological interest in the realm of diabetes and chemoprevention. Further studies are, however, necessary to assess if also these properties can be traced back to the unique phloroglucinol constituents of the plant.

Experimental Section

General Experimental Procedures. IR spectra were recorded on a Shimadzu DR 8001 spectrophotometer. HRMS (EI, 70 eV) were taken on VG 7070 EQ and JEOL SX102 spectrometers. ^{1}H and ^{13}C NMR spectra were recorded with a Bruker DRX-500 spectrometer (500 and 125 MHz, respectively) equipped with a Bruker ARX500 spectrometer with an inverse multinuclear 5 mm probehead equipped with a shielded gradient coil. The ^{1}H NMR spectrum of **6a** was recored on a Bruker AM 200 spectrometer (200 MHz). The solvent signals ($CHCl_3$/$CDCl_3$ 7.26/77.0 ppm, DMSO-d_6 2.50/39.5 ppm) were used as internal reference. The chemical shifts (δ) are given in ppm, and the coupling constants (J) in Hz. COSY, HMQC, and HMBC experiments were recorded with gradient enhancements using sine-shaped gradient pulses. For the 2D heteronuclear correlation spectroscopy the refocusing delays were optimized for $^1J_{CH} = 145$ Hz and $^nJ_{CH} = 10$ Hz. The raw data were transformed and the spectra were evaluated with the standard Bruker XWIN-NMR software (rev. 010101). HRMS (EI, 70 eV) and CIMS were taken on a VG 7070 EQ spectrometer. HRFABMS were taken on a JEOL SX102 spectrometer. Silica gel 60 (70−230 mesh, Merck) and LiChroprep RP-18 (25−40 μM) were used for open-column chromatography (CC). A Waters Microporasil semipreparative column (0.8 × 30 cm) was used for HPLC, with detection by a Waters differential refractometer 340.

Plant Material. Various samples of *Myrtus communis* L. were collected in Sardinia during the years 1999−2001. The extraction and isolation procedure reported refers to a sample collected at Corongiu (Laconi, NU) on November 12, 2000. The plant was identified by M.B., and a voucher specimen (CAG 514) is deposited at the Dipartimento di Scienze Botaniche, Università di Cagliari.

Extraction and Isolation. Dried and powdered leaves (1 kg) were extracted with acetone at room temperature (4 × 3 L). Evaporation of the pooled extracts left a green gum, which was taken up in ethanol (1 L) and treated with an equal volume of 3% aqueous lead(II) acetate. After resting overnight, the solution was filtered over a bed of Celite (ca. 20 g), concentrated to ca. 500 mL, and diluted with water (500 mL). The mixture was extracted with EtOAc (4 × 300 mL), and the pooled organic phases were dried (Na_2SO_4) and evaporated to give 18 g (1.8%) of a green paste. A portion of this (15 g) was chromatographed on a Florisil column (250 g) packed with petroleum ether−EtOAc, 95:5, and eluted with a petroleum ether−EtOAc gradient. Fractions eluted with 9:1 petroleum ether−EtOAc gave a semisolid residue, which was washed with ether to afford 0.9 g of myrtucommulone A (**1**) as a yellow powder. Fractions eluted with 5:5 to 1:9 petroleum ether−EtOAc contained a mixture of myrtucommulone A and semimyrtucommulone and were further rechromatographed over Si gel (150 g, petroleum ether−EtOAc, 1:9) and then over RP-Si gel (30 g, MeOH−water, 8:2) to afford an additional 0.31 g of myrtucommulone A (overall yield 1.21 g, 0.12%) and 1.4 g (0.14%) of semimyrtucommulone (**6**).

Semimyrtucommulone (6): yellow powder, mp 147 °C; IR (KBr) ν_{max} 3501, 3517, 1707, 1614, 1470, 1385, 1289, 1157, 1020 cm^{-1}; ^{1}H NMR ($CDCl_3$) (major rotamer) δ 11.6 (1H, s, 4-OH), 10.5 (1H, s, 6′-OH), 5.46 (1H, s, 6-OH), 3.94 (1H, hept, J = 6.8 Hz, H-8′), 3.78 (1H, d, J = 11.0 Hz, H-7); 2.99 (1H, m, H-8); 2.09 (3H, s, H-11), 1.47 (3H, s, H-13′); 1.41 (3H, s, H-11′), 1.32 (3H, s, H-14′), 1.30 (3H, s, H-12′), 1.18 (6H, d, J = 6.8 Hz, H-9′ and H-10′), 0.83 (3H, d, J = 6.4 Hz, H-9), 0.72 (3H, d, J = 6.4 Hz, H-10); ^{13}C NMR ($CDCl_3$) (major rotamer) δ 212.7 (s, C-4′), 211.2 (s, C-7′), 203.2 (s, C-2′), 178.5 (s, C-6′), 161.6 (s, C-4), 160.8 (s, C-2), 156.0 (s, C-6), 114.2 (s, C-1′), 108.6 (s, C-1), 108.6 (s, C-5), 102.9 (s, C-3), 54.7 (s, C-3′), 48.9 (s, C-5′), 40.9 (d, C-7), 39.0 (d, C-8′), 26.5 (q, C-11′), 25.9 (q, C-13′), 25.8 (d, C-8), 24.8 (q, C-14′), 23.3 (q, C-12′), 22.0 (q, C-9), 21.8 (q,

C-10), 19.4 (q, C-9′), 19.3 (q, C-10′); HREIMS *m/z* 446.2288 $[M]^+$ (8) (calcd for $C_{25}H_{34}O_7$, 446.2304).

Thermal Degradation of Myrtucommulone (1). A sample of **1** in DMSO-d_6 was heated to 80 °C. The course of the degradation could be followed focusing on the upfield signal of H-5 (δ 6.24) and C-5 (δ 94.2) in the ^{1}H and ^{13}C NMR spectra, respectively. After 48 h the degradation was complete, and a mixture of isomyrtucommulone B (**4**) and a trimeric dehydration product was obtained. ^{1}H NMR data for **4**: ($CDCl_3$) δ 13.9 (1H, s, 2-OH), 11.2 (1H, s, 4-OH) 6.24 (1H, s, H-5), 4.12 (1H, d. J = 3.6 Hz, H-7), 3.91 (1H, hept., J = 6.8 Hz, H-8′), 1.85 (1H, m, H-8), 1.50 (3H, s, H-13′), 1.35 (3H, s, H-14′), 1.31 (3H, s, H-11′), 1.25 (3H, s, H-12′), 1.12 and 1.10 (2 × 3H, d, J = 6.8 Hz, H-9′ and H-10′), 0.69 (6H, d, J = 6.8 Hz, H-9 and H-10); ^{13}C NMR ($CDCl_3$) δ 211.5 (s, C-4′), 211.0 (s, C-7′), 196.9 (s, C-2′), 167.4 (s, C-6′), 162.4 (s, C-2), 159.7 (s, C-4), 156.5 (s, C-6), 110.9 (s, C-1′), 106.6 (s, C-3), 103.2 (s, C-1), 94.2 (d, C-5), 55.6 (s, C-3′), 46.8 (s, C-5′), 38.9 (d, C-8′), 35.0 (d, C-8), 31.2 (d, C-7), 25.2 (q, C-11′), 23.5 (q, C-12′), 25.0 (q, C-13′), 24.0 (q, C-14′), 19.2 (q, C-9), 18.8 (q, C-9′), 18.4 (q, C-10), 17.7 (q, C-10′).

Silylation of Myrtucommulone (1). To a suspension of **1** (200 mg) in dry CH_2Cl_2 (5 mL) were added an excess (20 molar equiv) of TES-Cl and imidazole. After stirring at room temperature overnight, the reaction was worked up by addition of Si gel 60 (1 g) and evaporation. The residue was purified twice by CC (Si gel, 5 g, petroleum ether−EtOAc, 95:5) to eventually afford 61 mg (23%) of **5** as an oil, along with 49 mg of recovered starting material. IR (liquid film) ν_{max} 3408, 1720, 1590, 1548, 1470, 1370, 1300, 1185, 1018 cm^{-1}; ^{1}H NMR ($CDCl_3$) δ 4.27 (1H, d, J = 3.3 Hz, H-7′), 4.17 (1H, dd, J = 5.9 and 3.6 Hz, H-7), 3.69 (1H, d, J = 5.9 Hz, H-1′), 2.71 (1H, s, 6′-OH), 2.57 (1H, m, H-8), 2.02 (1H, m, H-8′), 1.74 (3H, s, H-9″), 1.65 (3H, s, H-13″), 1.61 (3H, s, H-14″), 1.57 (3H, s, H-14′), 1.45 (3H, s, H-11″), 1.43 (3H, s, H-12′), 1.37 (3H, s, H-12″), 1.37 (3H, s, H-10″), 1.35 (3H, s, H-13′), 1.32 (3H, s, H-11′), 0.96 (2H, t, J = 8 Hz, 4-OTES), 0.94 (3H, d, J = 6.8 Hz, H-9), 0.89 (2H, t, J = 8 Hz, 7″-OTES), 0.83 (3H, d, J = 6.8 Hz, H-9′), 0.73 (3H, q, J = 8 Hz, 4-OTES), 0.67 (3H, d, J = 6.8 Hz, H-10), 0.61 (3H, d, J = 6.8 Hz, H-10′), 0.48 (3H, q, J = 8 Hz, 7″-OTES); ^{13}C NMR ($CDCl_3$) δ 214.2 (s, C-4′), 212.4 (s, C-4″), 205.4 (s, C-2′), 197.7 (s, C-2″), 168.6 (s, C-6″), 151.7 (s, C-4), 149.2 (s, C-6), 147.0 (s, C-2), 135.9 (s, C-7″), 117.9 (s, C-3), 112.4 (s, C-8″), 112.3 (s, C-1″), 109.6 (s, C-5), 108.8 (s, C-1), 98.9 (s, C-6′), 58.2 (s, C-3′), 56.1 (s, C-3″), 54.8 (s, C-5′), 47.6 (s, C-5″), 44.6 (d, C-1′), 34.1 (d, C-8′), 32.9 (d, C-7′), 31.6 (d, C-8), 29.7 (d, C-7), 27.3 (q, C-12′), 25.7 (q, C-13″), 25.4 (q, C-14″), 24.7 (q, C-11″), 24.6 (q, C-12″), 23.9 (q, C-14′), 21.7 (q, C-11′), 20.4 (q, C-10″), 20.4 (q, C-9′), 20.2 (q, C-9), 17.6 (q, C-13′), 16.9 (q, C-9″), 16.4 (q, C-10′), 15.8 (q, C-10), 6.8 and 6.7 (t, OTES), 5.4 and 5.1 (q, OTES); EIMS (70 eV) *m/z* 878 $[M]^+$ (2), 863 (3), 849 (19), 835 (100), 735 (13), 721 (12), 703 (9); diagnostic NOESY correlations H-1′/H-12′, H-1′/H-13′, H-1′/H-9, H-1′/H-10, H-9/13″-methyl, H-10/13″-methyl, H-7/14″-methyl; CIMS (NH_3) *m/z* 879 $[M + H]^+$ (73); HRFABMS (NaI added) *m/z* 901.5115 $[M + Na]^+$ (5) (calcd for $C_{50}H_{78}O_9Si_2Na$, 901.5082); HRFABMS (KBr added) *m/z* 917.4937 $[M + K]^+$ (10) (calcd for $C_{50}H_{78}O_9Si_2K$, 917.4821).

Acetylation of Semimyrtucommulone (6). To a solution of **6** (686 mg, mmol) in pyridine (4 mL) was added Ac_2O (4 mL). After stirring overnight at room temperature, the excess Ac_2O was quenched by the addition of MeOH (2 mL), and the reaction was worked up by dilution with 2 N H_2SO_4 and extraction with EtOAc. The organic phase was sequentially washed with 2 N H_2SO_4, water, saturated $NaHCO_3$, and brine. After drying (Na_2SO_4), removal of the solvent left a semisolid residue, which was purified by CC (15 g Si gel, petroleum ether−EtOAc, 95:5, as eluant) to afford, after crystallization from ether, 426 mg (45%) of **6a** as a white powder: mp 178 °C; IR (KBr) ν_{max} 1778, 1767, 1726, 1692, 1620, 1377, 1206, 1182, 1096, 1044 cm^{-1}; ^{1}H NMR ($CDCl_3$, 50 °C) δ 3.97 (1H, m, H-8′), 3.65 (1H, m, H-7); 2.86 (1H, m, H-8); 2.32, 2.30, 2.28, 2.24, 2.16 (each 3H, s, 4 × OAc and H-11), 1.37−1.22 (br m, H-11′, H-12′, H-13′, H-14′), 1.16 (6H, d, J = 7.0 Hz, H-9′ and H-10′), 0.85 (3H, d, J = 6.4 Hz, H-9), 0.67 (3H, d, J = 6.4 Hz, H-10); HREIMS *m/z* 614.2712 $[M]^+$ (2) (calcd for $C_{33}H_{42}O_{11}$, 614.2727).

Silylation of Semimyrtucommulone (6). To a solution of **6** (200 mg) in dry CH_2Cl_2 (5 mL) were added excess (12 molar equiv) TES-Cl and imidazole. After stirring at room temperature overnight, the reaction was worked up by addition of Si gel 60 (1 g) and evaporation. The residue was purified by CC (Si gel, 5 g, eluant petroleum ether−EtOAc, 95:5) to give a mixture of **7** and **8** (88 mg), which was further purified by HPLC (petroleum ether−EtOAc, 98:2) to afford 24 mg of **7** and 22 mg of **8** as colorless oils. Compound **7** was obtained as an oil: IR (liquid film) ν_{max} 3413, 1721, 1596, 1571, 1458, 1379, 1306, 1165, 1037 cm^{-1}; ^{1}H NMR ($CDCl_3$) δ 4.02 (1H, dd, J = 3.8 and 5.5 Hz, H-7), 3.52 (1H, d, J = 5.5 Hz, H-1′), 3.01 (1H, hept., J =7.0 Hz, H-8′), 2.44 (1H, m, H-8), 2.08 (3H, s, H-11), 1.79 (1H, brs, 6′-OH), 1.46 (3H, s, H-13′), 1.38 (3H, s, H-12′), 1.31 (3H, s, H-11′), 1.28 (3H, s, H-14′), 1.13 (3H, d, J = 7.0 Hz, H-9′), 1.12 (3H, d, J = 7.0 Hz, H-10′), 0.97 (3H, t, J = 8.1 Hz, 6-OTES), 0.91 (3H, t, J = 7.9 Hz, 4-OTES), 0.85 (2H, q, J = 8.1 Hz, 6-OTES), 0.84 (3H, d, J = 6.9 Hz, H-9), 0.67 (2H, q, J = 8 Hz, 4-OTES), 0.52 (3H, d, J = 6.8 Hz, H-10); ^{13}C NMR ($CDCl_3$) δ 215.0 (s, C-4′), 209.1 (s, C-7′), 205.7 (s, C-2′), 153.6 (s, C-2), 149.5 (s, C-4), 145.7 (s, C-6), 118.3 (s, C-3), 115.3 (s, C-5), 113.9 (s, C-1), 98.5 (s, C-6′), 58.0 (s, C-3′), 54.6 (s, C-5′), 45.7 (d, C-1′), 42.3 (d, C-8′), 30.9 (d, C-7), 30.3 (d, C-8), 27.2 (q, C-12′), 24.3 (q, C-13′), 21.9 (q, C-11′), 19.9 (q, C-9), 18.2 (q, C-9′), 18.1 (q, C-14′), 17.1 (q, C-10′), 16.0 (q, C-10), 11.6 (q, C-11), 6.7 (q, 6-OTES), 6.6 (q, 4-OTES), 5.5 (t, 6-OTES), 5.3 (t, 4-OTES); CIMS (NH_3): 675.4108 $[M + H]^+$ (100) (calcd for $C_{37}H_{63}O_7Si_2$, 675.4112), 645 (8%), 575 (17%), 561 (32%), 439 (24%), 325 (12%), 297 (10%). Compound **8** was also an oil: IR (liquid film) ν_{max} 3420, 1720, 1587, 1548, 1466, 1370, 1309, 1188, 1018 cm^{-1}; ^{1}H NMR ($CDCl_3$) δ 4.02 (1H, dd, J = 4.0 and 5.5 Hz, H-7), 3.62 (1H, d, J = 5.5 Hz, H-1′), 2.89 (1H, hept., J =7.0 Hz, H-8′), 2.60 (1H, brs, 6′-OH), 2.45 (1H, m, H-8), 2.03 (3H, s, H-11), 1.59 (3H, s, H-13′), 1.43 (3H, s, H-14′), 1.42 (3H, s, H-12′), 1.32 (3H, s, 11′), 1.10 (3H, d, J = 7.0 Hz, H-9′), 1.09, (3H, d, J = 7.0 Hz, H-10′), 0.91 (3H, t, J = 8.1 Hz, 6-OTES), 0.90 (3H, t, J = 7.9 Hz, 4-OTES), 0.84, (3H, d, J = 6.9 Hz, H-9), 0.80 (2H, q, J = 8 Hz, 6-OTES), 0.70 (2H, q, J = 8 Hz, 4-OTES), 0.52 (3H, d, J = 6.8 Hz, H-10; ^{13}C NMR ($CDCl_3$) δ 214.7 (s, C-4′), 209.0 (s, C-7′), 205.7 (s, C-2′), 149.7 (s, C-4), 149.4 (s, C-6), 148.4 (s, C-2), 122.0 (s, C-3), 113.0 (s, C-1), 112.4 (s, C-5), 98.2 (s, C-6′), 58.1 (s, C-3′), 54.4 (s, C-5′), 45.9 (d, C-1′), 42.2 (d, C-8′), 30.5 (d, C-7), 30.4 (d, C-8), 27.3 (q, C-12′), 24.3 (q, C-13′), 21.7 (q, C-11′), 19.9 (q, C-9), 18.3 (q, C-14′), 17.4 (q, C-9′), 17.2 (q, C-10′), 15.9 (q, C-10), 9.5 (q, C-11), 6.6 (q, 6-OTES), 6.6 (q, 4-OTES), 5.3 (t, 6-OTES), 5.0 (t, 4-OTES); CIMS (NH_3) *m/z* 675.4071 $[M + H]^+$ (100) (calcd for $C_{37}H_{63}O_7Si_2$, 675.4112), 659 (28), 645 (88), 561 (32), 543 (9), 493 (13), 463 (14), 439 (4), 325 (5), 297 (6), 237 (36).

Acknowledgment. We are grateful to Mrss. Sabrina Frongia and Silvia Turaglio and for their help throughout this investigation. We also thank also Dr. Luisella Verotta (University of Milano) for her helpful suggestions. This work was supported by EU (Contract ERB FAIR CT 1781) and MURST (Fondi 40%, Progetto Chimica dei Composti Organici di Interesse Biologico).

References and Notes

(1) See for instance: (a) Moldenke, H. N.; Moldenke, A. L. *Plants of the Bible*; Dover Publications: New York, 1952; pp 143−145. (b) Cattabiani, A. *Florario*; Mondadori: Milano, 1996; pp 348−353. (c) Brosse, J. *Les Arbres de France*; Librairie Plon: Paris, 1987; pp 136−140.
(2) Mulas, M.; Spano, D.; Biscaro, S.; Parpinello, L. *Ind. Bevande* **2000**, *29*, 494−498; *Chem. Abstr.* **2000**, *134*, 265512.
(3) Winter, A. G.; Willeke, L. *Naturwissenschaften* **1951**, *38*, 262−264.
(4) (a) Bruni, A.; Ballero, M.; Poli, F. *J. Ethnopharmacol.* **1997**, *57*, 97−124. (b) Uncini Manganelli, R. E.; Tomei, P. E. *J. Ethnopharmacol.* **1999**, 65, 181−202.
(5) For a review, see: Diaz, A. M.; Abeger, A. *Fitoterapia* **1987**, *58*, 167−174.

(6) (a) Rotstein, A.; Lifshitz, A.; Kashman, Y. *Isr. Antimicrob. Agents Chemother.* **1974**, *6*, 539−542. (b) Kashman, Y.; Rotstein, A.; Lifshitz, A. *Tetrahedron* **1974**, *30*, 991−997.
(7) Davidyuk, L. P.; Degtyareva, A. P.; Dmitriev, L. B.; Drozd, V. N.; Grandberg, I. I. *Izv. Timiryazevsk. S-kh. Akad.* **1989**, *6*, 164−169; *Chem. Abstr.* **1990**, *112*, 195230.
(8) Puybaret, C.; David, B.; Charveron, M.; Mamatas, S. FR 98-11619 19980917 1990; *Chem. Abstr.* **2000**, *132*, 339046.
(9) Birk, R. C.; Horn, D. H. S. *Austr. J. Chem.* **1965**, *18*, 1405.
(10) Gibbons, S.; Udo, E. E. *Phytother. Res.* **2000**, *14*, 139−140.
(11) Ross, J. I.; Eady, E. A.; Cove, J. H.; Cunliffe, W. J.; Baumberg, S.; Wootton, J. C. *Mol. Microbiol.* **1990**, *4*, 1207−1214.
(12) Guay, G. G.; Khan, S. A.; Rothstein, D. M. *Plasmid* **1993**, *30*, 163−166.
(13) Ng, E. Y. W.; Trucksis, M.; Hooper, D. C. *Antimicrob. Agents Chemother.* **1994**, *38*, 1345−1355.
(14) Ghisalberti, E. L. *Phytochemistry* **1996**, *41*, 7−22.
(15) Murakami, T.; Tanaka, N. In *Progress in the Chemistry of Organic Natural Products*; Herz, W., Grisebach, H., Kirby, G. W., Eds.; Springer: New York, 1988; Vol. 54, pp 4−12.
(16) Elfellah, M. S.; Akhter, M. H.; Khan, M. T. *J. Ethnopharmacol.* **1984**, *11*, 275−281.
(17) Alwan, A. H.; Al-Gaillany, K. A.; Naji, A. *Int. J. Crude Drug Res.* **1989**, *27*, 33−37.

NP010441B

Tetrahedron Letters 51 (2010) 5493–5496

Contents lists available at ScienceDirect

Tetrahedron Letters

journal homepage: www.elsevier.com/locate/tetlet

Structure elucidation of some highly unusual tricyclic *cis*-caryophyllane sesquiterpenes from *Marasmiellus troyanus*

Liam Evans [a,e], John Hedger [a], Gemma O'Donnell [b], Brian W. Skelton [c], Allan H. White [c], R. Thomas Williamson [d], Simon Gibbons [b,*]

[a] School of Biosciences, University of Westminster, London W1W 6UW, UK
[b] Department of Pharmaceutical and Biological Chemistry, The School of Pharmacy, University of London, 29-39 Brunswick Square, London WC1N 1AX, UK
[c] Chemistry, M313, SBBCS, University of Western Australia, Crawley, WA 6009, Australia
[d] Roche Carolina Inc. Florence, SC 29506 9330, USA
[e] Hypha Discovery Ltd., Brunel Science Park, Uxbridge UB8 3PQ, UK

ARTICLE INFO

Article history:
Received 23 June 2010
Revised 11 August 2010
Accepted 12 August 2010
Available online 17 August 2010

Keywords:
Caryophyllane
Marasmiellus troyanus
Basidiomycetes
Sesquiterpene

ABSTRACT

Three new unusual sesquiterpenes (**1**–**3**) were isolated from the tropical rainforest basidiomycete, *Marasmiellus troyanus* and their structure elucidation was achieved by NMR spectroscopy, single-crystal X-ray structural analysis and a modified Mosher's ester method to determine the absolute stereochemistry of compound **1**. These unusual metabolites are probably derived from the caryophyllane class of sesquiterpenes and a possible biosynthetic route to these compounds is proposed. These small natural products represent the best possible features of chemical diversity, being chiral and exhibiting extensive functional group chemistry highlighting the value of natural products as a screening resource for therapeutics discovery programmes.

Basidiomycetes are prolific producers of natural products derived from the terpenoidal biosynthetic pathways. In particular, their ability to produce a wide array of sesquiterpene,[1] diterpene,[2] sesterterpene[3] and triterpene[4] natural products, makes them a highly attractive target for those interested in screening for biologically active compounds as these classes are chiral and produce an exceptional diversity of functional group chemistry. As part of our continuing efforts to isolate and characterise a novel chemistries from fungi[5] and plants,[6] we herein describe the isolation[7] and structure elucidation of three highly unusual *cis*-caryophyllane sesquiterpenes from *Marasmiellus troyanus* Murr., a pan-tropical decomposer agaric ('gill fungus'), which forms troops of small white fruiting bodies on woody debris in rainforests.[8]

The first of these compounds (**1**) (Fig. 1) was subjected to full NMR spectroscopic investigation and single-crystal X-ray structural analysis (Fig. 2). HRESI-MS confirmed the molecular formula of $C_{15}H_{24}O_4$ by accurate mass measurement of the protonated adduct $[M+H]^+$, 269.1755 indicating a sesquiterpene. Full ^1H and ^{13}C NMR spectral analysis (Tables 1 and 2) together with HMBC spectra allowed the full unambiguous assignment of all resonances. In the HMBC spectrum, two geminally coupled methyl groups (δ 1.32 and 1.39) exhibited couplings to a quaternary carbon (δ_C 34.7), to a methine (δ_C 50.0) and to a methylene carbon (δ_C 36.2). In the COSY spectrum, the hydrogens of this methylene coupled to a methine hydrogen (3.03, m) which in turn coupled to the hydrogen of the methine carbon which was coupled to by the geminal methyl pair. This indicated a dimethyl-substituted cyclobutane moiety which is common among sesquiterpenes such as β-caryophyllane (**4**).[9] Assuming a caryophyllane-type skeleton (Fig. 1), the methine carbon at δ_C 50.0 was C-1 and H-1 (δ 2.87) coupled to a deshielded oxymethine hydrogen (δ 4.43, br d, H-2), which in turn coupled to a further deshielded oxymethine (H-3, δ 4.48). In the HMBC spectrum, the C-3 carbon was coupled to by the hydrogens of a methyl doublet (δ 1.20) which in turn coupled to the methine carbon to which it was directly attached (C-4, 2.28) and to a further methine carbon (C-5). The COSY spectra revealed couplings between H-5 and a deshielded oxymethylene group (δ 4.20, 4.25). A methyl singlet (C-15) exhibited a ^3J coupling to C-5, to a quaternary carbon to which it was directly attached (C-8) and to a carbonyl carbon (δ_C 181.6, C-7) and back into the cyclobutane ring by a coupling to C-9. The carbonyl carbon was also coupled to by the oxymethylene (H_2-6) hydrogens indicating a lactonic bridge between C-6 and C-7. In the ^1H NMR spectrum, two broad singlets were present which did not display any connectivity to carbons in the HMQC spectra indicating that they were hydroxyl groups. From the accurate mass measurement, four oxygen atoms were present supporting the inclusion of the lactone and the two hydroxyl moieties which should be placed at C-2 and C-3 due to the downfield nature of the ^1H and ^{13}C resonances at these positions. Given the

* Corresponding author. Tel.: +44 (0) 207 753 5913; fax: +44 (0) 207 753 5964.
E-mail address: simon.gibbons@pharmacy.ac.uk (S. Gibbons).

0040-4039/$ - see front matter © 2010 Elsevier Ltd. All rights reserved.
doi:10.1016/j.tetlet.2010.08.036

Table 1
^{1}H (500 MHz, mult, *J* in Hz) NMR assignments for **1**[a], **2**[b] and **3**[c]

No.	**1** δ_H	**2** δ_H	**3** δ_H
1	2.87, bt, 9.0	2.30 m	2.29, dt, 12, 2.5
2	4.43, br d, 10.5	5.19, d, 10.4	3.93, bt, 11.0
3	4.48, t, 5	—	3.66, dd, 9.0, 1.5
4	2.28, m	3.05, m	—
5	2.98, m	3.65, m	2.82, m 1.58, ddd, 11.0. 6.5, 4.5
6	4.20, bt, 9.0 4.25, bt, 8.0	4.46, t, 8.3 4.19, dd, 11.4, 8.6	3.98, m
7	—	—	—
8	—	—	—
9	3.03, m	2.89, m	3.37 m
10	1.75, m 1.95, m	1.93, t, 11.4 1.82, ddd, 10.6, 7.1, 3.5	1.94, ddd, 11.0. 9.0, 3.0 1.72, t, 10.5
11	—	—	—
12	1.39, s	1.36, s	1.25, s
13	1.32, s	1.26, s	1.12, s
14	1.20, d, 7.5	1.19, d, 7.3	0.88, s
15	1.77, s	1.05, s	5.08, dd, 3.0, 2.5 4.70, t, 2.5
OH-2	5.74, br s	6.51, br s	2.91, d, 9.0
OH-3	6.72, br s	—	4.32, d, 9.0
OH-7	—	—	5.65, s

[a] In $CDCl_3$.
[b] In C_5D_5N.
[c] In acetone-d_6.

Table 2
^{13}C NMR assignments (125 MHz) for **1**[a], **2**[b] and **3**[c]

Carbon	**1**	**2**	**3**
1	50.0	52.6	49.8
2	72.2	74.2	70.2
3	79.2	213.3	79.8
4	34.6	43.8	48.7
5	41.0	37.6	34.0
6	68.5	67.6	65.3
7	181.6	179.5	109.5
8	47.9	47.6	151.4
9	38.1	38.3	34.1
10	36.2	35.0	39.5
11	34.7	36.0	34.9
12	26.4	26.1	32.0
13	30.6	29.7	27.3
14	14.5	11.4	23.7
15	19.7	18.8	109.6

[a] In $CDCl_3$.
[b] In C_5D_5N.
[c] In acetone-d_6.

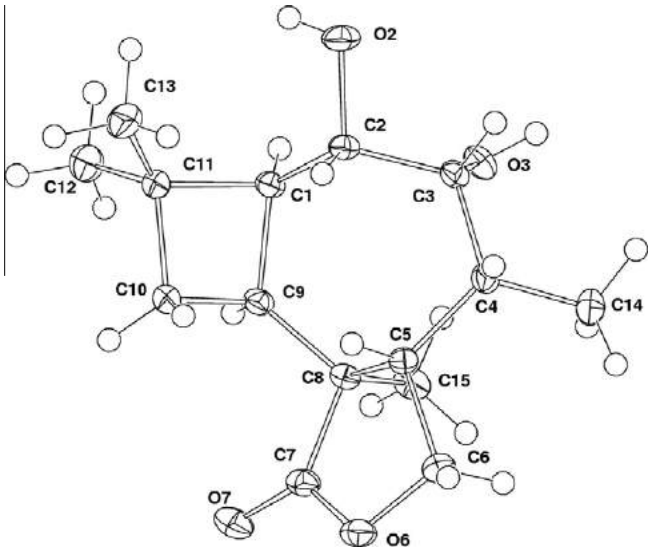

Figure 2. Molecular projection of **1** (50% probability amplitude displacement ellipsoids for C, O; arbitrary radii of 0.1 Å for H).

chiral nature of **1** and those seven-membered rings have a degree of flexibility, single-crystal X-ray structural analysis was conducted[10] to confirm the structure of **1** and to attempt to resolve the relative stereochemistry of this unusual compound. This showed that **1** was a cis-fused caryophyllane type sesquiterpene, confirmed the NMR spectral interpretation, and resolved the relative chemistry as depicted in Figures 1 and 2. For the assignment of the absolute configuration, Mosher's ester methodology[11] was considered but we were concerned that the presence of two vicinal diols at positions 2 and 3 could complicate the analysis. Fortunately the reaction of **1** with the *S* and *R* enantiomers of MPA gave only the 2-esters, presumably because the 3-carbinol is more sterically hindered, having hydroxyl and methyl groups as neighbours (Fig. 3). Shifts of H-1 and H-3 were diagnostic for an *S* chiral centre at C-2. The beauty of this methodology was that by resolving the absolute stereochemistry of one chiral centre, the relative configuration provided by the X-ray data then permitted unambiguous

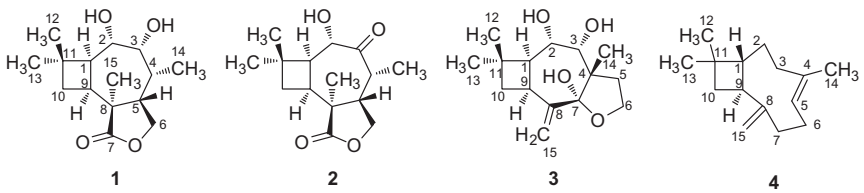

Figure 1. Structures of **1**–**4**.

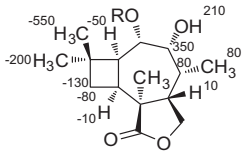

1

Figure 3. $\Delta\delta$ values [$\delta_R - \delta_S$] in ppb for *R*- and *S*-MPA esters of **1**.

assignment of the stereochemistry of all stereogenic centres as 1*S*, 2*S*, 3*R*, 4*R*, 5*S*, 8*S* and 9*S*. Compound **1** was therefore assigned as 2*S*,3*R*-dihydroxy-carophyllan-[5,8]-6,7-olide[12] and is described herein for the first time.

Compound **2** was submitted to full ^{1}H, ^{13}C, and 2-dimensional NMR analysis again permitting the unambiguous assignment of all resonances. Accurate mass measurement of **2** revealed a molecular formula of $C_{15}H_{22}O_4$ being two hydrogens less than that of **1**. The NMR data for **2** were highly similar to those for **1** (Tables 1 and 2) with the exception of a 3-keto group whose presence was confirmed by a ^{3}J HMBC correlation from methyl-14 to C-3 (δ 213.3) which would explain the difference in molecular formula compared to **1**. Compound **2** was therefore assigned as the 3-oxo derivative of **1**, 2*S*-hydroxy-3-oxo-carophyllan-[5,8]-6,7-olide[13] and is reported here for the first time.

Resonances for the final compound (**3**) were distinctly different from those for **1** and **2**, with the ester functional group being replaced with a hemiketal, methyl 15 being an exo-cyclic methylene and, from analysis of the HMBC spectra (Fig. 4), ring C of the tricycle was now found to be a [4,7] rather than a [5,8] linkage as seen in **1** and **2**.

Analysis of the HMBC and COSY spectra again allowed full unambiguous assignment of all ^{1}H and ^{13}C resonances (Tables 1 and 2 and Fig. 4). The geminal methyl pair of the cyclobutane again gave correlations to C-11, C-1 and C-10 and in the COSY spectrum H-1 coupled to H-2 which in turn coupled to H-3. In the HMBC spectrum, methyl-14 coupled to C-3, C-4, C-5 and C-7 which was a deshielded carbon (δ_C 109.5). In the COSY spectrum, the hydrogens of methylene C-5 coupled to a deshielded oxymethylene pair (C-6) which in the HMBC spectrum coupled through oxygen to C-7 indicating that a hemiketal group should be placed at C-7. For compound **3**, C-15 was an *exo*-methylene (rather than a methyl as seen in **1** and **2**) and in the HMBC spectrum the hydrogens of this group coupled to C-7, C-8 and C-9, completing all the resonances for **3**. Stereochemistries at carbons 1, 2, 3 and 9 were identical to those for **1** and **2**. In the NOESY spectrum, methyl-14 gave NOE correlations to H-3 and CH_2-15, suggesting that they were on the same face. A key NOE between the hydroxyl of the hemiketal at C-7 and the C-3 hydroxyl indicated an alpha orientation for the hemiketal hydroxyl and a trans B/C ring junction, which was also seen for compounds **1** and **2**. Compound **3** is therefore assigned as 2*S*,3*R*,7*S*-trihydroxy-carophyllan-[4,7]-6,8-oxide.[14]

These compounds are new members of the rare cis-fused caryophyllane class of sesquiterpene and the novel tricyclic nature has not been recorded previously. The nearest related natural products

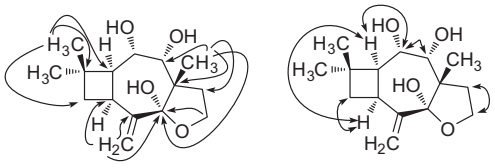

Figure 4. HMBC (single headed arrows) and COSY correlations (double headed arrows) for **3**.

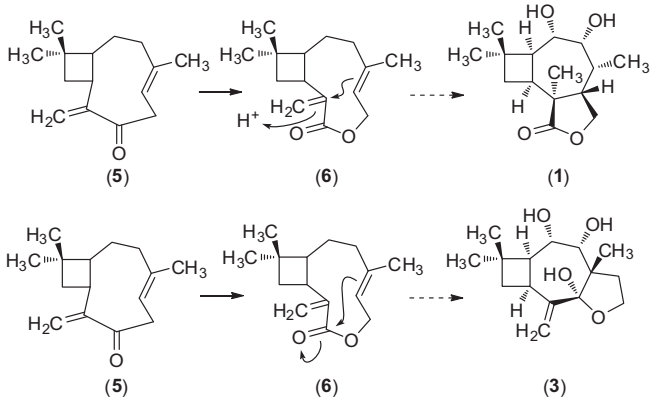

Scheme 1. Possible biosynthetic pathways of **1** and **3**.

are cis-fused caryophyllanes from the ectomycorrhizal fungus *Hebeloma longicaudum*.[15]

The biosynthesis of compounds **1** and **2** (Scheme 1) is likely to follow from a caryophyll-4,8(15)-diene precursor (**5**), which could undergo a Baeyer–Villiger type oxidation to afford the lactone (**6**). Subsequent attack of the exo-cyclic methylene by the 4,5 double bond would give [5,8] ring closure and would result in a stable tertiary carbocation at C-4. Oxidation at positions 2 and 3 would lead to metabolites **1** and **2**.

The biosynthesis of compound **3** is more problematic. Starting from the same lactone intermediate (**6**) as **1** and **2**, attack of the lactone carbonyl by the 4,5 double bond would result in a hemiketal at C-7 and a [4,7] B/C ring junction architecture. This would be less favourable, as in the formation of this 4–7 bond a carbocation would be generated on C-5 (rather than on C-4 above) and this would be a secondary and less stable carbocationic centre.

These novel and unusual natural products represent the best features of natural chemical diversity, being chiral and possessing extensive functional group chemistry. It is surprising that natural products of this type still remain un-tapped as a screening resource for pharmaceutical drug discovery. The lack of success of combinatorial chemistry to afford new drug entities[16] indicates that it is only a matter of time before pharmaceutical companies return to Basidiomycetes to exploit their chemical diversity for drug discovery.

Acknowledgement

S.G. thanks Emmanuel Samuel for running high-resolution mass spectrometry.

References and notes

1. (a) Luo, D. Q.; Wang, F.; Bian, X. Y.; Liu, J. K. *J. Antibiot.* **2005**, *58*, 456; (b) Schlegel, B.; Luhmann, U.; Kiet, T. T.; Leistner, E.; Grafe, U. *Pharmazie* **2002**, *57*, 778; (c) Morris, T. C.; Lira, R.; Gantzel, P. K.; Kelner, M. J.; Dawe, R. *J. Nat. Prod.* **2000**, *63*, 1557.
2. (a) Valdivia, C.; Kettering, M.; Anke, H.; Thines, E.; Sterner, O. *Tetrahedron* **2005**, *61*, 9527; (b) Kenmoku, H.; Kato, N.; Shimada, M.; Omoto, M.; Mori, A.; Mitsuhashi, W.; Sassa, T. *Tetrahedron Lett.* **2001**, *42*, 7439; (c) Mazur, X.; Becker, U.; Anke, T.; Sterner, O. *Phytochemistry* **1996**, *43*, 405.
3. Lauer, U.; Anke, T.; Sheldrick, W. S.; Scherer, A.; Steglich, W. *J. Antibiot.* **1989**, *42*, 875.
4. (a) de Silva, E. D.; van der Sar, S. A.; Santha, R. G.; Wijesundera, R. L.; Cole, A. L.; Blunt, J. W.; Munro, M. H. *J. Nat. Prod.* **2006**, *69*, 1245; (b) Tan, J.-W.; Dong, Z.-J.; Ding, Z.-H.; Liu, J.-K. *Z. Naturforsch [C]* **2002**, *57*, 963; (c) Quang, D. N.; Arakawa, Y.; Hashimoto, T.; Asakawa, Y. *Phytochemistry* **2005**, *66*, 1656.
5. Evans, L.; Hedger, J.; Brayford, D.; Stavri, M.; Smith, E.; O'Donnell, G.; Gray, A. I.; Griffith, G.; Gibbons, S. *Phytochemistry* **2006**, *67*, 2110.
6. (a) O'Donnell, G.; Poeschl, R.; Zimhony, O.; Gunaratnam, M.; Moreira, J. B. C.; Neidle, S.; Bhakta, S.; Malkinson, J. P.; Boshoff, H.; Lenaerts, A.; Gibbons, S. *J. Nat. Prod.* **2009**, *72*, 360; (b) Smith, E. C. J.; Kaatz, G. W.; Seo, S. M.; Wareham, N.; Williamson, E. M.; Gibbons, S. *Antimicrob. Agents Chemother.* **2007**, *51*, 4480; (c) Smith, E. C. J.; Wareham, N.; Zloh, M.; Gibbons, S. *Phytochem. Lett.* **2008**, *1*, 49.

7. A suspension of disrupted mycelium (2 ml) in sterilised water was added to each of twenty 1000 ml conical flasks, containing 200 ml of sterilised 2% potato dextrose broth (Difco). The flasks were shaken at 200 rpm for two weeks at 27 °C. The harvested filtrate was then extracted with Diaion HP20 resin (400 ml; Mitsubishi) which had previously been washed with HPLC grade methanol (Merck) and thoroughly conditioned with distilled water. The resin was removed, washed with distilled water (2 × 1000 ml) and eluted with HPLC grade methanol (2 × 1000 ml). The methanolic eluant was evaporated to dryness. Vacuum/liquid chromatography was used to purify the three products, **1**, **2** and **3**. Column eluant (4.2 g) was dissolved in chloroform (15 ml), to which was added silica gel (flash chromatography grade; BDH; 6 g) and evaporated. The slurry was applied to the top of a 60 mm diameter silica gel column. The column was eluted with 100 ml volumes of *n*-hexane/ethyl acetate mixtures, beginning with 100% *n*-hexane followed by sequential stepwise 10% increase in ethyl acetate, with a final elution of 10% methanol/ethyl acetate. On evaporating the column fractions, three were noticed to contain white needles within a yellow oil. Millilitre quantities of methanol, ethyl acetate, diethyl ether and chloroform were used to remove the oil and afford pure white needles of **1**. Compound **2** was eluted from the silica column with 80% ethyl acetate/*n*-hexane, **3** in 90% ethyl acetate/*n*-hexane and **1** with 10% methanol/ethyl acetate.
8. *Marasmiellus troyanus* was isolated from spore fall from a mature basidiocarp found on a dead liana, within the Rio Palenque Forest Reserve, Pichincha Province, Ecuador in 1986.
9. Marco, J. A.; Sanz, J. F.; Albiach, R. *Phytochemistry* **1992**, *31*, 2409.
10. $C_{15}H_{24}O_4$, $M = 268.3$ Orthorhombic, space group $P2_12_12_1$, $a = 5.8060(8)$, $b = 14.4068(10)$, $c = 16.7080(10)$ Å, $V = 1398$ Å^3. $D_c = 1.27_5$ cm^{-3}. $\mu_{Mo} = 0.091$ mm^{-1}; specimen: $0.43 \times 0.15 \times 0.12$ mm (no correction). Monochromatic MoKα radiation, $\lambda = 0.7107_3$ Å; T ca. 153 K; CCD instrument, ω-scans; 31882 reflections, merging to 2940 unique, $2840 > 2\sigma(I)$ ($2\theta_{max} = 65°$). $R_1 = 0.033$, $wR_2 = 0.087$ (weights $(\sigma^2(F_o^2) + (0.0538P)^2 + 0.1274P)^{-1}$ ($P = (F_o^2 + 2F_c^2)/3$)) x_{abs} not refined. $|\Delta\rho_{max}| = 0.33$ e Å^{-3}. O,H(2)···O(7) ($1/2 - x$, $1 - y$, $z - 1/2$) are 2.886(1), 2.2 (est.) Å and O, H(3)···O(2) ($1/2 + x$, $11/2 - y$, $1 - z$) 2.760(1), 2.0 (est.) Å. CCDC 638780.
11. Stavri, M.; Mathew, K. T.; Gibson, T.; Williamson, R. T.; Gibbons, S. *J. Nat. Prod.* **2004**, *67*, 892.
12. HR-ESI-MS $[M+H]^+$, 269.1755 $C_{15}H_{25}O_4$ requires 269.1747; $[\alpha]_D^{24}$ 35.7 (*c* 0.088 in methanol); IR ν_{max} (thin film) cm^{-1} = 3375, 2972, 2942, 1754, 1215, 1105, 1061 1048, 1012, 994, 692.
13. HR-ESI-MS $[M+H]^+$, 267.1593 $C_{15}H_{23}O_4$ requires 267.1591; $[\alpha]_D^{24}$ 102.2 (*c* 0.084 in methanol); IR ν_{max} (thin film) cm^{-1} = 3474, 2935, 1736, 1706, 1226, 1120, 1063, 1007, 991.
14. HR-ESI-MS $[M+H]^+$ 269.1750 $C_{15}H_{25}O_4$ requires 269.1753; $[\alpha]_D^{24}$ 23.7 (*c* 0.077 in methanol); IR ν_{max} (thin film) cm^{-1} = 3244, 2948, 1541, 1457, 1073, 997.
15. Wichlacz, M.; Ayer, W. A.; Trifonov, L. S.; Chakravarty, P.; Khasa, D. *Phytochemistry* **1999**, *51*, 873.
16. Kubinyi, H. *Nat. Rev. Drug Disc.* **2003**, *2*, 665.

Norlignans, Acylphloroglucinols, and a Dimeric Xanthone from *Hypericum chinense*

Wei Wang,[†] Yi Han Zeng,[†] Khadijo Osman,[‡] Kamlesh Shinde,[‡] Mukhlesur Rahman,[‡] Simon Gibbons,[‡] and Qing Mu*[,†]

School of Pharmacy, Fudan University, Shanghai, People's Republic of China, and Department of Pharmaceutical and Biological Chemistry, The School of Pharmacy, University of London, London WC1N 1AX, U.K.

Received July 2, 2010

Two new norlignans, hyperiones A (**1**) and B (**2**), three new acylphloroglucinols, aspidinol C (**3**) and hyperaspidinols A (**5**) and B (**6**), the known compound aspidinol D (**4**), and the symmetrical dimeric xanthone hyperidixanthone (**7**) were isolated from *Hypericum chinense*. Their structures were established by spectroscopic analysis. In an antibacterial assay using a panel of multidrug-resistant (MDR) strains, compounds **3** and **4** exhibited promising activity against the NorA efflux protein overexpressing MDR *Staphylococcus aureus* strain SA-1199B with a minimum inhibitory concentration (MIC) of 2 μg/mL (8.4 μM) and 4 μg/mL (16.8 μM), respectively. The positive control antibiotic norfloxacin showed activity at MIC 32 μg/mL (100 μM).

There is an urgent need to develop new classes of antibacterial agents to combat bacterial multidrug resistance (MDR), which can contribute to the failure of many classes of antibiotics in clinical therapy. Multidrug-resistant *Staphylococcus aureus* infections, particularly those caused by methicillin-resistant *S. aureus* (MRSA), have been a major threat to public health in hospitals and the community over the past decade. Despite the development of new compounds such as linezolid, MRSA infections remain a considerable concern due to the few agents that can be used in their treatment. In 2002, MRSA strains fully resistant to vancomycin were isolated in the United States.[1] Resistance to linezolid has also been reported in some patients followed by prolonged antibiotic treatment in the United States.[2] Therefore, there is a need to develop new classes of antibiotics to fight the problem of drug resistance. The genus *Hypericum* is a valuable source of naturally occurring inhibitors of bacterial growth, including compounds with activity against MDR and MRSA.[3] As part of our ongoing research on plant metabolites with activity against *S. aureus* antibiotic-resistant variants,[4] we have studied the chemistry and antibacterial activity of extracts of *Hypericum chinense* L. (Hypericaceae). This herb is widespread in China and has long been used for the treatment of fever, sepsis, acute laryngo-pharyngitis, conjunctivitis, hepatitis, and snake bite.[5] Former research on its chemical constituents resulted in the characterization of pharmacologically active compounds such as the antimicrobial compounds chinensins I and II,[6] the anti-HIV agents biyouyanagin A[7] and biyouyanagin B,[8] and several substituted xanthones.[9,10] A series of spiro-lactones, hyperolactones A−D, were also discovered.[8,11,12]

Our current phytochemical investigation of *H. chinense* has resulted in the isolation of two new norlignans (**1** and **2**), three new acylphloroglucinols (**3**−**6**), a known compound (**4**), and a symmetrical dimeric xanthone (**7**). Against a panel of multidrug-resistant strains, two acylphloroglucinols (**3** and **4**) showed promising activity against the NorA overexpressing MDR *Staphylococcus aureus* strain SA-1199B.

Results and Discussion

Powdered leaves of *H. chinense* were extracted with 95% EtOH, and the extract was separated into petroleum ether-soluble, EtOAc-soluble, and MeOH-soluble fractions. Repeated chromatography on the EtOAc-soluble fraction yielded compounds **1**−**6**, sesamin, and betulinic acid. Similarly, the EtOAc-soluble fraction of the roots afforded compound **7**.

Compound **1** was obtained as colorless oil. HREIMS (*m*/*z* 340.0950) indicated a molecular formula of $C_{19}H_{16}O_6$, which was supported by its ^{1}H and ^{13}C NMR spectra (Table 1). The ^{13}C NMR spectrum revealed a carbonyl [δ 196.7 (C-7)], which was coupled to two aromatic protons [δ 7.47 (d, J = 1.8 Hz, H-2) and 7.55 (dd, J = 8.2 Hz, J = 1.8 Hz, H-6)] in the HMBC spectrum. These aromatic hydrogens formed a piperonyl group with the remaining protons at δ 6.87 (d, J = 8.2 Hz, H-5) and the methylenedioxy protons downfield at δ 6.13 (s, OCH_2O-10). The two methylenedioxy protons correlated with the carbons at δ 148.3 (C-3) and 152.0 (C-4), confirming a 3,4-methylenedioxyphenyl (piperonyl) ketone system.[11] Similarly, another 3′,4′-methylenedioxyphenyl moiety was established by the ^{1}H and ^{13}C NMR, DEPT, and HMBC data. These two fragments were confirmed by the EIMS, which exhibited fragment ion peaks at *m*/*z* 149 (base peak) and 121, corresponding to the acylpiperonyl ion $[ArCO]^+$ and piperonyl ion $[Ar]^+$ fragments, generated due to bond cleavage at C-7/C-8 and C-1′/C-7′, respectively.[13]

The remaining bridge assignment was established as a tetrahydrofuran ring according to the NMR spectroscopic data. A signal at δ 4.86 (dd, J = 9.8 Hz, J = 5.8 Hz, H-7′), which in the HMBC spectrum was coupled to C-2′ and C-6′, was assigned to the benzylic oxygen-bearing carbon C-7′ (δ 82.0). The correlation between H-7′ and H-8′a (δ 2.51, m) and H-8′b (δ 2.30, m) shown in the ^{1}H−^{1}H COSY spectrum indicated a C-7′ and C-8′ (δ 38.3) linkage. The multiplet signals centered at δ 4.28 (H-9a) and 4.17 (H-9b) were assigned to the oxygen-bearing carbon C-9 (δ 70.3). The multiplet centered at δ 4.09 (m, H-8), assigned to C-8 at δ 47.0, displayed a correlation with C-7, C-9, and C-8′, indicating a tetrahydrofuran moiety of cyclo[C8−C9−O−C7′−C8′], with C-8 connected to the C-7 carbonyl and C-7′ to the phenyl ring at C-1′. This structure was therefore a norlignan compound with a $C_6C_3-C_2C_6$ skeleton. NOE experiments (Table 1) indicated a *cis*-configuration between H-8 and H-7′, which were both close to H-9a and H-8′a in space. Thus, the relative configuration of **1** was elucidated as shown, and this compound was given the trivial name hyperione A.

Compound **2** was obtained as a white, amorphous powder. The molecular formula $C_{19}H_{16}O_6$ was indicated by HREIMS, the same as that of **1**. Analyzing the NMR data, compound **2** was deduced to have the same planar structure as **1**. However, **1** and **2** showed different R_f values in TLC, and their ^{1}H NMR spectra revealed an obvious disparity in the splitting of H-9a, H-9b, and H-7′. Therefore, **2** was presumed to be a stereoisomer of **1** with the differences at the bridging tetrahydrofuran ring. In the ^{1}H NMR spectrum, an NOE between H-8 and H-7′ was observed. The H-8 proton showed no enhancement when H-7′ was irradiated, and *vice versa*. Furthermore, according to the NOE experiments, H-8 was close to

* To whom correspondence should be addressed. E-mail: muqing@fudan.edu.cn.
[†] Fudan University.
[‡] University of London.

10.1021/np1004483
Published on Web 11/02/2010

Table 1. NMR Spectroscopic Data for Hyperiones A (**1**) and B (**2**)

	1 ($CDCl_3$)				**2** (acetone-d_6)			
no.	δ_C, mult.		δ_H (J in Hz)	HMBC (C no.)	δ_C, mult.		δ_H (J in Hz)	HMBC (C no.)
1	131.1	C			132.1	C		
2	108.2	CH	7.47, d (1.8)	3, 4, 6, 7	108.7	CH	7.48, d (1.8)	3, 4, 6, 7
3	148.3	C			149.3	C		
4	152.0	C			152.9	C		
5	108.0	CH	6.87, d (8.2)	1, 3, 4	108.6	CH	6.98, d (8.2)	1, 3
6	124.7	CH	7.55, dd (8.2, 1.8)	2, 4, 7	125.7	CH	7.70, dd (8.2, 1.8)	2, 4, 7
7	196.7	C			198.1	C		
8[a]	47.0	CH	4.07, m	7, 9, 8′	46.9	CH	4.28, m	9
9	70.3	CH_2	(a) 4.28, m	7, 8, 7′, 8′	71.0	CH_2	(a) 4.40, t (8.2)	7, 8, 7′, 8′
			(b) 4.17, m	7, 8, 7′, 8′			(b) 3.95, dd (8.2, 6.3)	7
1′	135.1	C			137.5	C		
2′	106.7	CH	6.93, d (1.8)	4′, 6′, 7′	107.0	CH	6.92, d (1.6)	4′, 6′, 7′
3′	147.7	C			148.6	C		
4′	147.1	C			147.7	C		
5′	108.0	CH	6.76, d (7.8)	1′, 3′	108.5	CH	6.80, d (7.8)	1′, 3′
6′	119.7	CH	6.84, dd (7.8, 1.8)	2′, 4′, 7′	120.0	CH	6.87, dt (7.8, 1.6)	2′, 4′, 7′
7′[b]	82.0	CH	4.86, dd (9.8, 5.8)	2′, 6′	81.4	CH	4.83, t (7.8, 7.0)	2′, 6′
8′	38.3	CH_2	(a) 2.51, m	7, 8, 9, 7′	39.0	CH_2	(a) 2.60, m	7, 8, 9
			(b) 2.30, m	7, 7′			(b) 2.05, m	7′
10	101.9	OCH_2O	6.13, s	3, 4	103.1	OCH_2O	6.18, s	3, 4
9′	101.0	OCH_2O	5.96, s	3′, 4′	101.9	OCH_2O	5.99, s	3′, 4′

[a] NOE of H-8 (**1**): H-2, H-6, H-7′, H-9a, H-8′a; NOE of H-8 (**2**): H-2, H-6, H-8′b. [b] NOE of H-7 (**1**): H-2′, H-6′, H-8, H-9a, H-8′a; NOE of H-7 (**2**): H-2′, H-6′, H-8′a.

Table 2. NMR Spectroscopic Data of Aspidinols C (**3**) and D (**4**)

	3 (acetone-d_6)				**4** ($CDCl_3$)			
no.	δ_C, mult.		δ_H (J in Hz)	HMBC (C no.)	δ_C, mult.		δ_H (J in Hz)	HMBC (C no.)
1	104.7	C			104.4	C		
2	162.8	C			159.8	C		
3	103.4	C			103.5	C		
4	163.5	C			163.0	C		
5	90.2	CH	6.13, s	1, 3, 4, 6	91.6	CH	5.97, s	1, 3, 4, 6
6	160.2	C			161.1	C		
7	6.5	CH_3	1.91, s	2, 3, 4	7.1	CH_3	2.01, s	2, 3, 4, 5
8	55.0	OCH_3	3.81, s	4	55.6	OCH_3	3.82, s	4
1′	205.8[a]	C			210.5	C		
2′	52.6	CH_2	2.96, 2H, d (6.7)	1′, 3′, 4′, 5′	46.0	CH	3.75, m (6.7)	1′, 3′, 4′, 5′
3′	25.0	CH	2.24, m (6.7)	2′, 4′, 5′	27.0	CH_2	(a) 1.83, m	1′, 2′, 4′, 5′
							(b) 1.42, m	1′, 2′, 4′, 5′
4′	22.2	CH_3	0.94, d (6.7)	2′, 3′, 5′	12.0	CH_3	0.92, t (7.4)	2′, 3′
5′	22.2	CH_3	0.94, d (6.7)	2′, 3′, 4′	16.7	CH_3	1.18, dd (7.1, 1.2)	1′, 2′, 3′
2-OH			13.63, s	2, 3			13.62, s	
6-OH			10.12, s				9.67, s	

[a] Signal shown in $CDCl_3$ but overlapped in acetone-d_6.

H-8′b, while H-7′ to H-8′a, which confirmed a *trans*-configuration, and **2** was given the trivial name hyperione B.

In the isolation, a lignan was obtained and identified as sesamin by its NMR and X-ray data. Considering the reference,[11] hyperione B (**2**) was therefore presumed to be derived from sesamin by losing a $-CH_2-$ moiety in the plant, and the analogue hyperione A (**1**) could be derived from asarinin, an epimer of sesamin (Scheme S1, Supporting Information).

Aspidinol C (**3**), yellow crystals, had the molecular formula $C_{13}H_{18}O_4$ (by HREIMS). Six aromatic carbon signals (δ_C 163.5, 162.8, 160.2, 104.7, 103.4, 90.2) were displayed in its ^{13}C NMR spectrum (Table 2), in which three signals were downfield and over δ_C 160, implying a phloroglucinol skeleton. The ^1H NMR spectrum showed two hydroxy groups and a methoxy group, which were likely to be the three substituents of a phloroglucinol skeleton. This conclusion was confirmed by HMBC correlations (Figure 1a) between these groups and the corresponding aromatic quaternary carbons. The aromatic methyl (δ_H 1.91, s) was coupled to OH-bearing C-2 (δ_C 162.8) and C-3 (δ_C 103.4) and to OCH_3-bearing C-4 (δ_C 163.5) and was therefore placed at position 3. The only aromatic proton (δ_H 6.13, s) was coupled to C-1, C-3, C-4, and C-6, and therefore it was placed at position 5, *para* to C-2. The positions of these substituents were further supported by their NOE

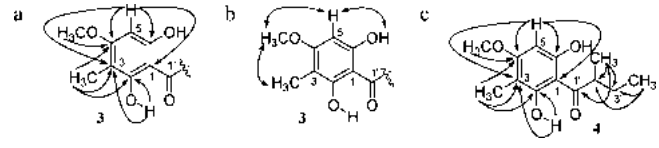

Figure 1. Key HMBC and NOE correlations: (a) key HMBC correlations of **3**; (b) key NOE correlations of **3**; (c) key HMBC correlations of **4**.

correlations (Figure 1b). The chain attached to C-1 included a carbonyl (C-1′), a methylene doublet (C-2), a methine septet (C-3), and a six-hydrogen methyl doublet (C-4 and C-5). The other aromatic hydroxyl group was placed at C-6 on the basis of its NOE spectrum (Figure 1b). Considering the coupling constant together with its $^1H-^1H$ COSY correlations, an isobutyl side chain was deduced [$-CH_2-CH-(CH_3)_2$]. In the HMBC spectrum, the methylene doublet was coupled to C-1′, and therefore an isopentanoyl chain was directly attached to C-1 of the phloroglucinol skeleton. The carbonyl group at C-1′ and the 2-OH formed an intramolecular H-bond. Furthermore, the base peak at m/z 181 $[M - C_4H_9]^+$ in the EIMS was attributable to the fragment generated from cleavage between C-1 and C-1′. Therefore, **3** was identified as 1-[2,6-dihydroxy-4-methoxy-3-methylphenyl]-3′-methylbutan-1′-one, a new

Table 3. NMR Spectroscopic Data of Hyperaspidinols A (**5**) and B (**6**)

	5 ($CDCl_3$)				**6** ($CDCl_3$)			
no.	δ_C, mult.		δ_H (J in Hz)	HMBC(C no.)	δ_C, mult.		δ_H (J in Hz)	HMBC (C no.)
1	108.1	C			107.6	C		
2	163.0	C			163.0	C		
3	112.1	C			112.1	C		
4	162.3	C			162.2	C		
5	104.0	C			104.0	C		
6	153.2	C			152.9	C		
7	206.9	C			211.7	C		
8	53.3	CH_2	(a) 3.14, dd (16.0, 5.7)	7, 9, 10, 11	45.8	CH_2	4.00, m	7, 9, 11
			(b) 2.83, dd (16.0, 7.7)	7, 9, 10, 11				
9	24.9	CH	2.20, m	8, 10, 11	27.7	CH	(a) 1.82, m	7, 10, 11
							(b) 1.35, m	7, 10, 11
10	22.7	CH_3	0.84, d (6.7)	8, 9, 11	11.5	CH_3	0.77, dd (7.8, 7.3)	8, 9
11	22.4	CH_3	0.81, d (6.7)	8, 9, 10	15.6	CH_3	1.12, dd (6.8, 2.4)	7, 8, 9, 10
12	8.4	CH_3	2.12, s	2, 3, 4, 5	8.5	CH_3	2.18, s	2, 3, 4
13	60.3	OCH	3.71, s	4	60.2	OCH_3	3.77, s	4
14	19.5	CH_2	(a) 2.95, d (17.0)	4, 5, 6, 15, 18	19.3	CH_2	(a) 3.01, dd (16.3, 2.0)	4, 5, 6, 15, 16, 18
			(b) 2.67, dd (17.0, 5.3)	4, 5, 6, 15, 16			(b) 2.74, dd (16.3, 6.8)	5, 6, 15, 16
15	44.3	CH	2.87, m	5, 16	44.5	CH	2.93, m	5, 14, 16
16	37.7	CH_2	(a) 2.40, m	15, 18	37.7	CH_2	(a) 2.47, m	15, 18
			(b) 1.84, m	14, 15, 17, 1″			(b) 1.88, m	14, 17, 1″
17	81.6	CH	5.24, dd (16.0, 7.7)	1″, 2″, 6″	81.8	CH	5.31, m	16, 1″, 2″, 5″
18	109.3	C			109.4	C		
1′	135.5	C			135.5	C		
2′	106.3	CH	7.01, d (1.8)	18, 4′, 6′	106.2	CH	7.08, d (1.5)	3′, 6′
3′	147.8	C			147.7	C		
4′	147.8	C			147.7	C		
5′	108.0	CH	6.79, d (7.5)	6′	107.9	CH	6.85, d (overlapped)	
6′	119.0	CH	7.00, dd (7.9, 1.8)	18, 2′, 4′	119.0	CH	7.06, dd (6.8, 1.5)	18, 2′, 3′, 4′
7′	101.3	CH	5.98, d (1.3)	3′, 4′	101.2	CH	6.03, s	3′, 4′
1″	135.1	C			135.1	C		
2″	106.6	OCH_2O	6.78, d (overlapped)	17, 4′, 6	106.5	OCH_2O	6.83, d (overlapped)	
3″	147.1	C			147.7	C		
4″	147.1	C			147.0	C		
5″	108.0	CH	6.70, d (7.9)	1″, 3″, 4″	107.9	CH	6.75, d (7.9)	
6″	119.4	CH	6.75, d (7.9)	17, 2″, 4″	119.4	CH	6.80, dd (7.9, 1.3)	
7″	101.0	OCH_2O	5.91, d (1.3)	3″, 4″	101.0	OCH_2O	5.96, s	3″, 4″
2-OH			13.87, s	1, 2, 3			13.80, s	1, 2, 3

compound of the acylphloroglucinol type, which was given the trivial name aspidinol C.

Compound **4** showed fragment ion peaks similar to those of **3** in the EIMS, and the base peak at 181. Its ^1H and ^{13}C NMR spectra indicated the same skeleton as **3**, with the exception of the C-1 side chain. The substituent at C-1 included a methine multiplet (C-2′), a methylene multiplet (C-3′), a methyl triplet (C-4′), and a methyl doublet (C-5′). By examining the coupling constants, the triplet methyl was placed next to the methylene. In the $^1H-^1H$ COSY spectrum, the methylene was coupled to the methine, which was coupled to the methyl doublet. In the HMBC spectrum the methylene multiplet was coupled to C-2′ and C-5′, while the methyl doublet was coupled to C-1′, C-2′, and C-3′. Therefore, a 2-methylbutanoyl side chain was deduced, which was directly attached to C-1 of the aspidinol skeleton to form an intramolecular hydrodren bond with the 2-OH. This compound was isolated from *Eucalyptus pulverulenta* in 1984.[14] Here we report its complete NMR assignments for the first time (Table 2) and have given it the trivial name aspidinol D.

Compound **5** was obtained as pale yellow oil. The HRESIMS ($[M + H]^+$ 561.21066, calcd for $C_{32}H_{33}O_9$ 561.21191) suggested a molecular formula of $C_{32}H_{32}O_9$, consistent with its ^1H and ^{13}C NMR spectroscopic data (Table 3). Further inspection of the spectra indicated signals similar to those of **1** and **3** combined, with signals reminiscent of an aspidinol skeleton (resembling that of **3**) and two methylenedioxyphenyl groups (resembling those in compound **1**). However, **5** was not a simple mixture of the two compounds mentioned above, but it was a complex single compound formed by combination of the two aspidinol moieties. This was supported by its TLC and HPLC chromatograms taken together with spectroscopic evidence from its HMBC spectrum.

Through careful examination of the ^1H and ^{13}C NMR and HMBC spectra, the carbons and protons of the aspidinol skeleton and two methylenedioxyphenyl groups were unambiguously assigned by direct reference to compounds **1** and **3**. The two protons H-5 and 6-OH in **3** were assumed to be substituted by alkyl groups in **5**, since no such signals were displayed in the ^1H NMR spectrum of **5**. The bridge between the three moieties deduced above consisted of two methylene groups (δ_C 37.7, 19.5), two methine groups (δ_C 81.6, 44.3), a quaternary carbon (δ_C 109.3), which were observed in the DEPT spectrum, and two oxygen atoms left according to the given molecular formula.

The $^1H-^1H$ COSY spectrum (Table 3) provided the evidence of how these saturated carbons were bonded: H-17 of a methine was coupled to H_2-16a/b, which were both coupled to H-15, with the latter coupling to H_2-14a/b. In the HMBC spectrum, H_2-14a/b were coupled to C-4, C-5, and C-6 of the aspidinol skeleton. The H-17 proton (δ_H 5.24, q), which was attached to an oxygen-bearing carbon, was coupled to three aromatic carbons (C-1′, C-2′, and C-6′) from one of the methylenedioxyphenyl groups. H-14b and H-16b, together with H-2′ and H-6′ from the other methylenedioxyphenyl group, were all coupled to a downfield quaternary carbon (δ_C 109.3, C-18), which, from its downfield nature, was attached to two oxygens (Figure 2a). Considering the degree of unsaturation as 17, the structure was deduced as shown. The ROESY spectrum elucidated a *cis*-configuration of H-15 and H-17. Compound **5** was therefore identified as a new acylphloroglucinol derivative, and it was given the trivial name hyperaspidinol A.

Compound **6** was obtained as pale yellow oil. The molecular formula of $C_{32}H_{33}O_9$ was assigned by the HRESIMS $[M + H]^+$, and its ^1H and ^{13}C NMR spectra closely resembled those of **5**. The spectroscopic data of the side chain resembled that of **4**, instead of

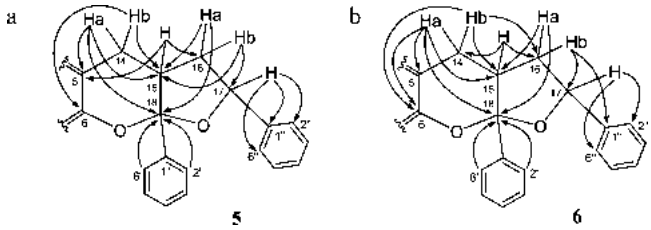

Figure 2. Key HMBC correlations: (a) key HMBC correlations of **5**; (b) key HMBC correlations of **6**.

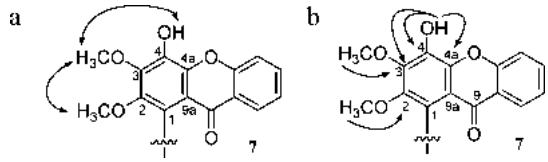

Figure 3. Key NOE and HMBC correlations: (a) key NOE correlations of **7**; (b) key HMBC correlations of **7**.

the isopentanoyl signals seen in compound **3**. Analysis of the HMBC spectra (Figure 2b) confirmed that the differences between **5** and **6** were solely due to the presence of a 2-methylbutanoyl side chain (in **6**) rather than a 3-methylbutanoyl side chain seen in **5**. The structure of compound **6** is, therefore, as shown, and it was named hyperaspidinol B.

Compound **7** was obtained as yellow crystals, and the molecular formula $C_{30}H_{22}O_{10}$ was determined by an accurate mass measurement of 542.1210 (calcd for $C_{30}H_{22}O_{10}$, 542.1213) in the HREIMS. The EIMS showed a molecular ion peak at *m*/*z* 542 $[M]^+$ and an obvious peak at *m*/*z* 271, which was presumably due to one-half of the molecule. The ^{1}H NMR spectrum showed four aromatic protons of one benzene ring, two methoxy groups, and one hydroxy group. The ^{13}C NMR data suggested a typical substituted xanthone skeleton[15] with two methoxy carbons and 12 aromatic carbons. These data indicated a structure consisting of two identical substituted xanthone moieties. Two methoxy groups and the one hydroxy group were attached to the substituted benzene ring, with the remaining free position (C-1) being the point of attachment to the other xanthone.

The locations of these substituents were supported by NOE experiments for the protons of compound **7** (Figure 3a). There existed a correlation between 2-OCH_3 and 3-OCH_3 (δ_H 3.43 and 3.95), respectively, in the NOE spectrum, and further radiation on the 3-OCH_3 resulted in an enhancement of the OH proton at δ_H 9.98 (4-OH). Therefore the 3-OCH_3 group (δ_H 3.95) had an *ortho* relationship with the other groups. The bond between the two xanthones was then expected to be either at C-1 or at C-4. The bonding position at C-1 was suggested by correlations between the 4-OH proton and C-3, C-4, and C-4a in the HMBC spectrum of **7**, and this linkage was further supported by the existence of C-9a at δ_C 115.8. This structure was also supported by its molecular ion (542 $[M]^+$) and the main fragment ions of cleavage in the EIMS (Figure 4). Compound **7** possessed a symmetrical dimeric xanthone skeleton and was therefore identified as 1-[4′-hydroxy-2′,3′-dimethoxy-1′-xanthonyl]-4-hydroxy-2,3-dimethoxyxanthone, with the trivial name hyperidixanthone.

Betulinic acid was also isolated and identified by comparing its MS and NMR data with those in the literature.[16,17]

The isolates were tested for antibacterial activity against several resistant *S. aureus* strains, and only **3** and **4**, with the simple aspidinol skeleton, showed promising activity against all of the strains. Compounds **5** and **6**, possessing a more complex skeleton, exhibited no inhibitory activity (Table 4). Among the tested strains, SA-1199B possesses the NorA efflux protein, which confers resistance to certain fluoroquinolones and quaternary ammonium antiseptics. Against this strain, both **3** (2 μg/mL, 8.4 μM) and **4** (4

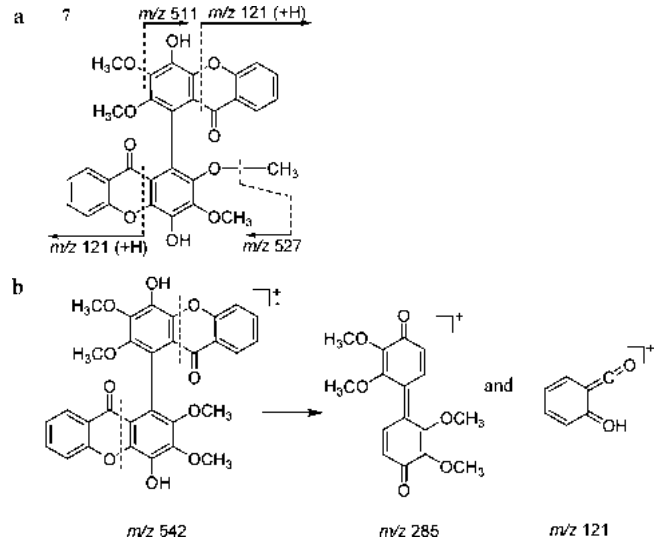

Figure 4. Generation of main fragment ions in the EIMS of **7**.

Table 4. MICs (μg/mL) of **3**, **4**, a Mixture of **5** and **6**, and Norfloxacin

compound	SA1199B	XU212	ATCC25943	RN4220	EMRSA-15	EMRSA-16
3	2	32	8	16	8	4
4	4	8	8	8	4	4
5 and **6**	>128	>128	>128	>128	>128	>128
norfloxacin	32	8	0.5	0.5	0.5	128

μg/mL, 16.8 μM) were more active than the control antibiotic norfloxacin (32 μg/mL, 100 μM). For MDR strain XU212, which possesses the TetK efflux transporter and is resistant to both tetracycline and methicillin, **4** showed inhibitory activity comparable to norfloxacin (8 μg/mL, 33.2 μM). A hospital epidemic MRSA,[18] EMRSA-16, was much more sensitive to **3** and **4** than to norfloxacin (Table 4). However, **3** and **4** showed moderate activity but were less active than the positive control antibiotic against the standard *S. aureus* strain ATCC 25923, the erythromycin-resistant strain RN4220 that carries the MsrA macrolide efflux protein, and the drug-resistant strain EMRSA-15.[19] These findings are encouraging, and further investigation of aspidinol as a template is suggested.

Experimental Section

General Experimental Procedures. Optical rotations were measured using a JASCO P-1020 polarimeter. IR spectra were recorded using an Avatar 360 ESP FTIR spectrophotometer, and UV spectra on a Hitachi U-2900 spectropolarimeter. ^{1}H and ^{13}C NMR spectra were obtained on a Varian Mercury Plus 400 MHz spectrometer. EIMS were obtained on an Agilent 5973N MSD spectrometer, and HREIMS on an IonSpec 4.7 T FTMS. Column chromatography (CC) was carried out with silica gel (10−40 μm, Qingdao Marine Chemical Plant). Fractions obtained from CC were monitored by TLC (silica gel plate HGF254, 10−40 μm, Qingdao Marine Chemical Plant, Yantai, China; RP-18 plates, E. Merck Co. Ltd.). The developed TLC plates were visualized by spraying with 20% H_2SO_4 followed by heating.

Plant Material. The dried whole herb of *Hypericum chinense* (8.5 kg) was purchased in Chaling County in Hunan Province, China, and separated into roots, stems, and leaves. A voucher specimen (No. HC-003) was deposited at the Natural Medicine Chemistry Laboratory of the School of Pharmacy, Fudan University. The plant was identified by Dr. Zhang Wen-Ju, Associate Professor at the Center of Biodiversity of the Biology School, Fudan University, China.

Extraction and Isolation. Dried leaves of *H. chinense* (2.26 kg) were chopped and then extracted with 95% ethanol (5 × 3.5 L) at 45 °C for 4 h to afford 437.8 g of extract. The extract was partitioned into petroleum ether (73.3 g), EtOAc (109.5 g), and MeOH fractions. The EtOAc fraction was subjected to CC over silica gel, eluting with a gradient from petroleum ether to EtOAc, and finally washed with MeOH to afford fractions 1−16. Fraction 7 (2.96 g) was rechromatographed

Chart 1

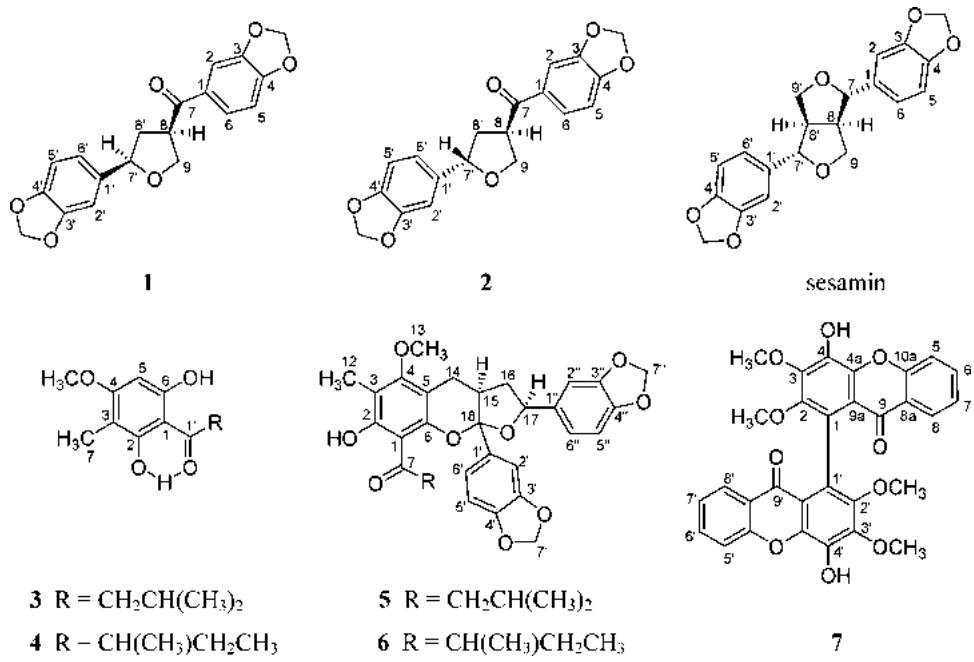

on a silica gel column eluting with petroleum−EtOAc to yield **1** (10.0 mg) and betulinic acid (20.0 mg). Fraction 6 was rechromatographed to yield **2** (19.0 mg), **3** (101.9 mg), and sesamin (32.8 mg). Compounds **4** (19.7 mg), **5** (3.0 mg), and **6** (6.7 mg) were obtained from fraction 4. Similarly, **7** (10.0 mg) was isolated from the roots of *H. chinense* (1.96 kg).

Bacterial Strains. *S. aureus* standard strain ATCC 25923 and tetracycline-resistant strain XU212, which possesses the TetK tetracycline efflux protein, were provided by Dr. Edet Udo.[20] Strain SA-1199B, which overexpresses the norA gene encoding the NorA MDR efflux pump, was the kind gift of Professor Glenn W. Kaatz.[21] Strain RN4220, which possesses the MsrA macrolide efflux protein, was provided by Dr. Jon Cove.[22]

Minimum Inhibitory Concentration (MIC) Assay. All strains were cultured on nutrient agar (Oxoid) and incubated for 24 h at 37 °C prior to MIC determination. The control antibiotic norfloxacin was obtained from Sigma Chemical Co. Mueller-Hinton broth (MHB; Oxoid) was adjusted to contain 20 and 10 mg/L of Ca^{2+} and Mg^{2+}, respectively. An inoculum density of 5×10^5 cfu of each *S. aureus* strain was prepared in normal saline (9 g/L) by comparison with a 0.5 McFarland turbidity standard. The inoculum (125 μL) was added to all wells, and the microtiter plate was incubated at 37 °C for 18 h. For MIC determination, 20 μL of a 5 mg/mL methanolic solution of 3-[4,5-dimethylthiazol-2-yl]-2,5-diphenyltetrazolium bromide (MTT; Sigma) was added to each of the wells and incubated for 20 min. Bacterial growth was indicated by a color change from yellow to dark blue. The MIC was recorded as the lowest concentration at which no growth was observed.

Hyperione A (1): colorless oil; $[\alpha]^{20}_D$ +195.6 (*c* 0.045, $CHCl_3$); UV (MeOH) λ_{max} (log ε) 307 (1.07), 276 (1.15), 229 (2.54), 207 (2.08) nm; IR (CH_2Cl_2) ν_{max} 1670, 1603, 1503, 1488, 1441, 1248 cm^{-1}; ^1H NMR, ^{13}C NMR, HMBC, and NOE data, see Table 1; EIMS *m/z* 340 $[M]^+$ (34), 310 (1), 177 (13), 164 (54), 149 (100), 121 (25), 65 (18), 63 (10); HREIMS *m/z* $[M]^+$ 340.0950 (calcd for $C_{19}H_{16}O_6$, 340.0947).

Hyperione B (2): white, amorphous powder; $[\alpha]^{20}_D$ +48.0 (*c* 0.050, acetone); UV (MeOH) λ_{max} (log ε) 308 (1.06), 276 (1.20), 230 (2.56), 207 (2.04) nm; IR (CH_2Cl_2) ν_{max} 1672, 1604, 1503, 1488, 1441, 1248 cm^{-1}; ^1H NMR, ^{13}C NMR, HMBC, and NOE data, see Table 1; EIMS *m/z* 340 $[M]^+$ (20), 310 (1), 177 (20), 164 (100), 149 (72), 121 (19), 65 (13), 63 (7); HREIMS *m/z* $[M]^+$ 340.0946 (calcd for $C_{19}H_{16}O_6$, 340.0947).

Aspidinol C (3): yellow crystals, mp 155−158 °C; UV ($CHCl_3$) λ_{max} (log ε) 330 (3.30), 288 (3.40), 267 (3.42), 243 (2.65) nm; IR (film) ν_{max} 3321, 2956, 1644, 1591, 1520, 1471, 1434, 1242, 1133, 794, 473 cm^{-1}; ^1H NMR, ^{13}C NMR, and HMBC, see Table 2; EIMS *m/z* 238 $[M]^+$ (25), 223 (14), 205 (4), 196 (4), 181 (100), 154 (6), 138 (2), 69 (4); HREIMS *m/z* $[M]^+$ 238.1207 (calcd for $C_{13}H_{18}O_4$, 238.1205).

Aspidinol D (4): yellow crystals, mp 95−97 °C; $[\alpha]^{20}_D$ −11.5 (*c* 0.400, $CHCl_3$); UV ($CHCl_3$) λ_{max} (log ε) 293 (3.26), 288 (3.33), 275 (3.26), 241 (2.10) nm; IR (film) ν_{max} 3387, 2963, 1635, 1585, 1412, 1229, 1145, 1097, 801 cm^{-1}; ^1H NMR, ^{13}C NMR, and HMBC data, see Table 2; EIMS *m/z* 238 $[M]^+$ (16), 223 (1), 181 (100), 138 (2), 69 (3), 65 (2), 55 (2), 41 (2).

Hyperaspidinol A (5): pale yellow oil; ^1H NMR, ^{13}C NMR, and HMBC data, see Table 3; ESI $[M + H]^+$ 561.2, $[M + Na]^+$ 583.1; HRESIMS *m/z* $[M + H]^+$ 561.21066 (calcd for $C_{32}H_{33}O_9$, 561.21191).

Hyperaspidinol B (6): pale yellow oil; IR ($CHCl_3$) ν_{max} 2924, 1612, 1504, 1489, 1442, 1248, 1125, 1038, 937, 811 cm-1; ^1H NMR, ^{13}C NMR, and HMBC data, see Table 3; ESI $[M + H]^+$ 561.2, $[M + Na]^+$ 583.1; HRESIMS *m/z* $[M + H]^+$ 561.21125 (calcd for $C_{32}H_{33}O_9$, 561.21191).

Hyperidixanthone (7): yellow crystals, mp 370−375 °C); UV (DMSO) λ_{max} (log ε) 315 (2.40), 281 (3.38), 270 (3.31) nm; IR (film) ν_{max} 3443, 2925, 1634, 1593, 1456, 1404, 1331, 1289, 1067, 951, 758 cm^{-1}; ^1H NMR (DMSO) δ_H (*J* in Hz) 9.96 (1H, s, OH-4/4′), 7.83 (1H, dd, 7.94, 1.83, H-8/8′), 7.79 (1H, dt, 7.80, 1.83, H-6/6′), 7.65 (1H, dd, 8.25, 0.70, H-5/5′), 7.32 (1H, dt, 7.18, 0.70, H-7/7′), 3.95 (3H, s, OCH_3-3/3′), 3.43 (3H, s, OCH_3-2/2′); ^{13}C NMR (DMSO) δ_C 175.7 (C-9/9′), 154.8 (C-10a/10a′), 146.5 (C-2/2′), 145.9 (C-3/3′), 143.9 (C-4a/4a′), 138.4 (C-4/4′), 134.8 (C-6/6′), 125.9 (C-8/8′), 123.9 (C-7/7′), 121.1 (C-8a/8a′), 117.7 (C-5/5′), 115.8 (C-9a/9a′), 109.7 (C-1/1′), 60.6 (OCH_3-3/3′), 60.0 (OCH_3−2/2′); EIMS *m/z* 542 $[M]^+$ (95), 527 $[M - CH_3]^+$ (5), 511 $[M - OCH_3]^+$ (100), 285 (71), 271 (24), 258 (25), 240 (23), 121 (9); HREIMS *m/z* $[M]^+$ 542.1210 (calcd for $C_{30}H_{22}O_{10}$, 542.1213).

Acknowledgment. This work was supported by the NSFC (30772630) and Royal Society International Joint Project/NSFC (JP091083, Sino-UK) and partly supported by National Drug Innovative Program of China (2009ZX09301-011). The authors are grateful to Ms. P. Yang and Ms. C. Y. Liu in Analysis Center, School of Pharmacy, Fudan University, for their technical support.

Supporting Information Available: Spectra of compounds **1**−**7** and Scheme S1 are available free of charge via the Internet at http://pubs.acs.org.

References and Notes

(1) Public Health Dispatch. *Morbidity and Mortality Weekly Reports* **2002**, *51*, 902.
(2) Peeters, M. J.; Sarria, J. C. *Am. J. Med. Sci.* **2005**, *330*, 102–104.
(3) Gibbons, S.; Ohlendorf, B.; Johnsen, I. *Fitoterapia* **2002**, *73*, 300–304.
(4) Xiao, Z. Y.; Mu, Q.; Shiu, W. K. P.; Zeng, Y. H.; Gibbons, S. *J. Nat. Prod.* **2007**, *70*, 1779–1782.

(5) *Glossary of National Herbs and Drugs*; Beijing People's Medical Publishing House: Beijing, 1978; Vol. II; p 396.
(6) Nagai, M.; Tada, M. *Chem. Lett.* **1987**, *16*, 1337–1340.
(7) Tanaka, N.; Okasaka, M.; Ishimaru, Y.; Takaishi, Y.; Sato, M.; Okamoto, M.; Oshikawa, T.; Ahmed, S. U.; Consentino, L. M.; Lee, K. H. *Org. Lett.* **2005**, *7*, 2997–2999.
(8) Tanaka, N.; Kashiwada, Y.; Kim, S. Y.; Hashida, W.; Sekiya, M.; Ikeshiro, Y.; Takaish, Y. *J. Nat. Prod.* **2009**, *72*, 1447–1452.
(9) Tanaka, N.; Takaishi, Y. *Phytochemistry* **2006**, *67*, 2146–2151.
(10) Tanaka, N.; Takaishi, Y. *Chem. Pharm. Bull.* **2007**, *55*, 19–21.
(11) Tada, M.; Nagai, M.; Okumura, C.; Osano, Y.; Matsuzaki, T. *Chem. Lett.* **1989**, 683–686.
(12) Aramaki, Y.; Chiba, K.; Tada, M. *Phytochemistry* **1995**, *38*, 1419–1421.
(13) Marchand, P. A.; Kato, M. J.; Lewis, N. G. *J. Nat. Prod.* **1997**, *60*, 1189–1192.
(14) Bolte, M. L.; Bowers, J.; Crow, W. D.; Paton, D. M.; Sakurai, A.; Takahashi, N.; Ujiie, M.; Yoshida, S. *Agric. Biol. Chem.* **1984**, *48*, 373–376.
(15) Westerman, P. W.; Gunasekera, S. P.; Uvais, M.; Sultanbawa, S.; Kazauskas, R. *Org. Magn. Reson.* **1977**, *9*, 613–636.
(16) Hsieh, T. J.; Lu, L. H.; Su, C. C. *Biophys. Chem.* **2005**, *114*, 13−20.
(17) Lu, J.; Kong, L. Y. *Mod. Chin. Med.* **2007**, *9*, 12–14.
(18) Cox, R. A.; Conquest, C.; Mallaghan, C.; Maples, R.R. *J. Hosp. Infect.* **1995**, *29*, 87–106.
(19) Richardson, J. F.; Reith, S. *J. Hosp. Infect.* **1993**, *25*, 45–52.
(20) Gibbons, S.; Udo, E. E. *Phytother. Res.* **2000**, *14*, 139–140.
(21) Kaatz, G. W.; Seo, S. M.; Ruble, C. A. *Antimicrob. Agents Chemother.* **1993**, *37*, 1086–1094.
(22) Ross, J. I.; Farrell, A. M.; Eady, E. A.; Cove, J. H.; Cunliffe, W. J. *J. Antimicrob. Chemother.* **1989**, *24*, 851–862.

NP1004483

Prenylated Benzophenone Peroxide Derivatives from *Hypericum sampsonii*

by **Zhi Yong Xiao**[a]), **Yi Han Zeng**[a]), **Qing Mu***[a]), **Winnie Ka Po Shiu**[b]), and **Simon Gibbons**[b])

[a]) School of Pharmacy, Fudan University, Zhangheng Road 826, Zhangjiang Pudong, Shanghai 200032, P. R. China (e-mail: muqing2000@yahoo.com)

[b]) Centre for Pharmacognosy and Phytotherapy, The School of Pharmacy, University of London, London, WC1N1AX, UK

Two new prenylated benzophenone peroxide derivatives, peroxysampsones A and B (**1** and **2**, resp.), together with a known compound, plukenetione C (**3**), were isolated from the roots of the Chinese medicinal plant *Hypericum sampsonii*, and their structures were elucidated by detailed spectral analysis. These compounds are the unusual peroxides of polyprenylated benzophenone derivatives, containing the unique caged moiety of 4,5-dioxatetracyclo[9.3.1.1^{9,13}.0^{1,7}]hexadecane-12,14,15-trione. In the biological test, peroxysampsone A (**1**) showed comparable activity with norfloxacin against a NorA over-expressing multidrug-resistant (MDR) strain of *Staphylococcus aureus* SA-1199B.

Introduction. – *Hypericum sampsonii* HANCE (Hyperiaceae) is a herbal medicine used in the treatment of blood stasis, to relieve swelling, and as an antitumor herb in China [1]. Due to its various bioactivities, the phytochemistry of this species has been investigated, and polyprenylated benzophloroglucinol derivatives and xanthones have been isolated from the plant [2]. Antibacterial screening tests have driven us to yielded constituents which inhibit a NorA over-expressing multidrug-resistant (MDR) *Staphylococcus aureus* strain SA-1199B from the root of *H. sampsonii* [3]. Our further phytochemical work on this species has led to the isolation of two new peroxides of polyprenylated benzophenone derivatives, which contained a unique caged dioxatetracyclic polyketone skeleton and were given the trivial names peroxysampsones A and B (**1** and **2**, resp.), together with a known analogue, plukenetione C (**3**; *Fig. 1*)[1]). Few peroxides of prenylated benzophenone derivatives have been isolated from guttiferous plants previously [4][5], and this is the first report of peroxides of prenylated benzophenone derivatives obtained from plants of the *Hypericum* genus.

Results and Discussion. – Peroxysampsone A (**1**) was obtained as an optically active colorless oil, $[\alpha]_D^{18} = +17.0$ ($c = 0.128$, $CHCl_3$). Its molecular formula, $C_{33}H_{42}O_8$, was established by HR-MALDI-MS peak at m/z 589.2772 ($[M+Na]^+$; calc. 589.2777). The IR spectrum showed strong bands for OH (3424 cm^{-1}) and C=O groups (1734, 1698, and 1666 cm^{-1}). The existence of an unsubstituted Bz group, three non-conjugated ketone C=O groups (δ(C) 204.3, 205.1, and 208.3), eight Me groups together with an olefinic H-atom (δ(H) 5.10 (br. *t*, 7.0)) revealed that the compound **1** was an analogue

[1]) Arbitrary atom numbering. For systemic names, see *Exper. Part.*

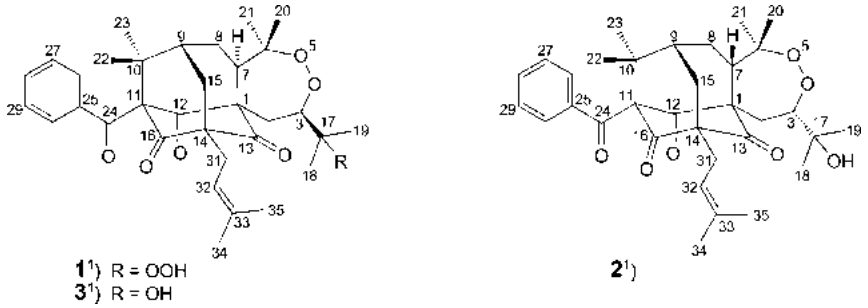

Fig. 1. *Structures of peroxysampsones A and B* (**1** and **2**, resp.), *and plukenetione C* (**3**).

of prenylated benzophenone derivative from the plant of *H. sampsonii* [2][3a]. By careful comparison of the ^{1}H-NMR spectral data (*Table 1*) with those of known prenylated benzophenone derivatives, compound **1** was found to be almost identical, with respect to the ^{1}H-NMR data, with plukenetione C (**3**) [5], a metabolite previously obtained from *Clusia plukenetii* belonging to plants of the Guttiferae family, except for resonances attributable to an O–CH group (δ(H) 4.95 (*dd*, J=2.7, 11.7, H–C(3)) in **1**, while δ(H) 4.56 (*dd*, J=2.9, 11.6, H–C(3)) in **3**). The peaks at *m*/*z* 492 ([M–$(CH_3)_2COO$]$^+$), and 459 ([$M-(CH_3)_2COO-O_2$]$^+$) in the EI-MS due to the loss of O_2 also provided persuasive evidence for the presence of a peroxide [6]. The high similarity between **1** and **3** was also supported by the ^{13}C-NMR-spectral data, with slight differences in the resonances of C(3) and C(17) (*Table 1*). Tracing the connectivities from the geminal dimethyl group at C(10) by means of 2D-NMR data, compound **1** was established as possessing the same skeletal moiety as **3**, *i.e.*, 4,5-dioxatetracyclo[9.3.1.1^{9,13}.0^{1,7}]hexadecane-12,14,15-trione, corresponding to the partial formula of $C_{30}H_{35}O_6$. An extra O-atom in the residual formula ($C_3H_7O_2$ in **1** and C_3H_7O in **3**), as well as the downfield quaternary C-atom (δ(C) 84.2 (C(17)) in **1** and 73.1 (C(17)) in **3**) necessitated the placement of a OOH rather than a OH group at C(17) as seen in **3**. The existence of the OOH group in peroxysampsone A (**1**) was verified by the positive reaction between the MeOH solution of **1** and wet paper with KI-starch. The relative configuration of peroxysampsone A was determined as **1** by ROESY spectra (*Fig. 2*).

Peroxysampsone B (**2**) was isolated as an optically active colorless oil, $[\alpha]_D^{20} = -41.2$ (c=0.042, $CHCl_3$), with the following spectral characteristics: IR (film) 3567, 3436, 1736, 1701, 1700 cm^{-1}, and UV ($CHCl_3$) 247 (3.91), 212 (3.08), 210 (3.08) nm. The features of a prenylated benzophenone skeleton were shown in the ^{1}H- and ^{13}C-NMR data of **2** (*Table 2*). Its molecular formula of $C_{33}H_{42}O_7$, the same as plukenetione C (**3**), was established by the HR-MALDI-MS peak at *m*/*z* 573.2823 ([M+Na]$^+$). Further analysis of its 2D-NMR spectral data (*Table 2*) revealed that compound **2** was an isomer of plukenetione C (**3**).

The differences in relative configuration occurred at C(3) and C(7) in the peroxide ring. The presence of a correlation H–C(7)/H–C(3) and H–C(7)/H$_b$–C(15) in the ROESY spectra of **2** (*Fig. 2*) led to the assignment of the H$_\beta$–C(3) and H$_\beta$–C(7),

Table 1. *NMR Data for Peroxysampsone A* (**1**) *and Plukenetione C* (**3**)[1]). δ in ppm, J in Hz.

	1			**3**	
	δ(H)	δ(C)	HMBC (H→C)	δ(H)	δ(C)
C(1)		66.4			66.5
CH_2(2)	1.56 (*dd*, *J*=2.7, 14.9, H_α)	30.8	12, 1, 7	1.54 (*dd*, *J*=2.9, 14.7)	31.0
	3.53 (*dd*, *J*=11.7, 14.9, H_β)		12, 1, 3, 13, 17	3.54 (*dd*, *J*=11.6, 14.7)	
CH(3)	4.95 (*dd*, *J*=2.7, 11.7)	85.6	2, 19, 18	4.56 (*dd*, *J*=2.9, 11.6)	88.8
C(6)		88.5			88.4
CH(7)	2.78 (*dd*, *J*=8.2, 11.0)	42.5	12, 1, 6, 8, 13, 21, 20	2.77 (*dd*, *J*=8.0, 11.0)	42.4
CH_2(8)	2.42 (*m*, H_α)	31.4	1, 7, 9, 15	2.40 (*m*)	31.4
	1.52 (*m*, H_β)		6, 7, 9	1.50 (*m*)	
CH(9)	2.10 (*m*)	44.3	11, 7, 8, 15, 14, 10, 23, 22	2.10 (*m*)	44.3
C(10)		50.3			50.3
C(11)		81.8			81.7
C(12)		208.3			208.0
C(13)		205.1			205.1
C(14)		68.4			68.4
CH_2(15)	2.58 (*dd*, *J*=5.1, 14.1, H_a)	41.6	8, 9, 14, 16, 13, 31	2.55 (*dd*, *J*=7.0, 14.3)	41.6
	1.86 (*dd*, *J*=0.8, 14.1, H_b)		8, 9, 14, 10, 31	1.87 (*d*, *J*=14.3)	
C(16)		204.3			204.4
C(17)		84.2			73.1
Me(18)	1.17 (*s*)	20.5	3, 17, 19	1.13 (*s*)	24.9
Me(19)	1.20 (*s*)	21.4	3, 17, 18	1.07 (*s*)	25.9
Me(20)	1.09 (*s*)	17.7	6, 7, 21	1.08 (*s*)	17.8
Me(21)	1.30 (*s*)	28.2	6, 7, 20	1.29 (*s*)	28.2
Me(22)	1.48 (*s*)	24.9	11, 9, 10, 23	1.48 (*s*)	24.9
Me(23)	1.36 (*s*)	22.6	11, 9, 10, 22	1.35 (*s*)	22.6
C(24)		192.1			192.1
C(25)		134.7			134.6
CH(26)	7.16 (*dt*, *J*=2.5, 8.4)	128.8	24, 28, 30	7.15 (*dt*, *J*=2.0, 8.4)	128.8
CH(27)	7.30 (*dt*, *J*=2.0, 8.0)	128.0	25, 29	7.28 (*dt*, *J*=1.8, 8.2)	128.0
CH(28)	7.41 (*m*)	132.4	26, 30	7.41 (*t*, *J*=8.0)	132.4
CH(29)	7.30 (*dt*, *J*=2.0, 8.0)	128.0	25, 27	7.28 (*dt*, *J*=1.8, 8.2)	128.0
CH(30)	7.16 (*dt*, *J*=2.5, 8.4)	128.8	24, 26, 28	7.15 (*dt*, *J*=2.0, 8.4)	128.8
CH_2(31)	2.60 (*d*, *J*=7.0)	29.7	15, 14, 16, 13, 32, 33, 34	2.59 (*d*, *J*=7.0)	29.7
CH(32)	5.10 (br. *t*, *J*=7.0)	118.7	32, 35, 34	5.09 (br. *t*, *J*=7.0)	118.8
C(33)		135.3			135.3
Me(34)	1.69 (*s*)	26.1	32, 33, 35	1.68 (*s*)	26.0
Me(35)	1.69 (*s*)	18.1	32, 33, 34	1.68 (*s*)	18.1

which differed from H_α–C(3) and H_α–C(7) in the structures **1** or **3** shown in *Fig. 2*. Thus, peroxysampsone B (**2**) corresponds to 3,7-epiplukenetione C.

Compound **3** was also obtained as an optically active colorless oil, $[\alpha]_D^{18} = +27.5$ (c = 0.272, $CHCl_3$), and its structure was determined as plukenetione C by comparison of its spectral data with those in the literature [5]. Its relative configuration was determined to be the same as that of peroxysampsone A (**1**) by analysis of the ROESY spectra (*Fig. 2*), and this has not been reported previously.

In an antibacterial experiment, SA-1199B was used for drug-resistant inhibition bioassay. This strain is a fluoroquinolone-resistant *Staphylococcus aureus* which

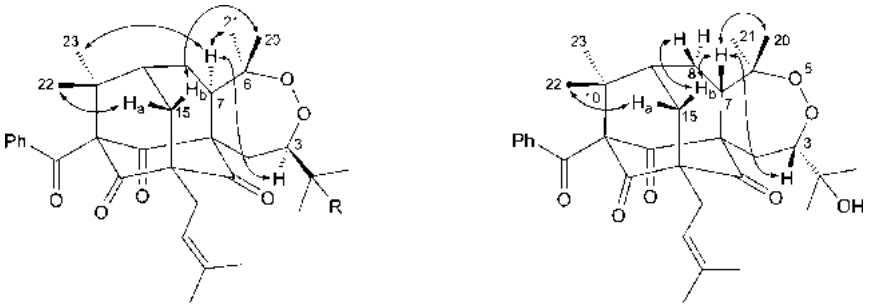

Fig. 2. *Selected ROESY cross-peaks* (H↔H) *of compounds* **1**, **2**, *and* **3**

possesses fluoroquinolone efflux mediated by NorA [7][8]. In the screening, only compound **1** exhibited comparable activity against SA-1199B with a *MIC* value of 110 μM, while the *MIC* value of norfloxacin, the positive control, was 100 μM. It is possible that the activity is largely due to the presence of the OOH group in peroxysampsone A.

Experimental Part

General. TLC: silica gel (SiO_2; *HGF254*, 10–40 μm, Yantai, Huanghai, P. R. China). Column chromatography (CC): SiO_2 (10–40 μm, *Merck*) and *ODS* (*C-18*, 15–35 μm, *Merck*). Optical rotations: *Jasco P-1020* polarimeter. UV Spectra: *Shimadzu UV-1600PC* spectrophotometer; λ_{max} (log ε) in nm. IR Spectra: *Avatar*™ *360 E.S.P.*™ FT-IR spectrophotometer; $\tilde{\nu}$ in cm^{-1}. ^{1}H- and ^{13}C-NMR Spectra: *Varian Mercury Plus* 400 MHz; δ in ppm rel. to Me_4Si as internal standard, *J* in Hz. ESI-, HR-MALDI-, EI-, and FAB-MS: *Agilent 1100* Series LC/MSD, *IonSpec 4.7 T* FT-MS; *Agilent 5973N* MSD (70 eV), and *VG AutoSpec 3000* spectrometer, resp.; in *m*/*z* (rel. %).

Plant Material. Hypericum sampsonii was collected from Cha Lin County in Hunan Province, P. R. China. A voucher specimen (No. HS-003) was deposited with the Natural Medicine Chemistry laboratory of the School of Pharmacy, Fudan University. The plant was identified by Dr. *Wen-Ju Zhang*, associate Professor in the Center of Biodiversity of the Biology School, Fudan University, P. R. China.

Extraction and Isolation. Powdered roots of the plant (1.1 kg) were extracted with 95% EtOH (3 l × 4) at 45° during 4 d, affording 90 g of extract after removal of the EtOH *in vacuo* at 45°. Petroleum ether (PE; 100 ml × 4), MeOH (100 ml × 4), and H_2O (90 ml), resp., were employed to dissolve the residue, then the resulting solns. were evapored to dryness. The EtOH extract (90 g) was thus fractionated into a PE part (40 g), a MeOH part (13 g), and H_2O-soluble fractions (400 ml). The PE-soluble fraction was subjected to CC over SiO_2, eluting with a gradient from PE to AcOEt, and final washing with MeOH afforded 15 fractions, *Frs. 1–15*. *Fr. 3* was subjected to repeated chromatography on SiO_2 columns with PE/AcOEt 3:7 to yield a brown gum-like fraction (260 mg), which contained a main yellowish spot on TLC at R_f (PE/AcOEt 3:7) 0.45. The fraction was separated as two constituents by SiO_2 CC, and compounds **1** (100 mg) and **3** (29 mg) were finally obtained, by further purification on SiO_2 CC alternatively with PE/AcOEt from 7:3 to 8:2 and $CHCl_3$/AcOEt 95:5, and on reversed-phase SiO_2 CC with MeOH/H_2O 82:18. *Fr. 8* was subjected to SiO_2 CC with PE/$CHCl_3$/acetone 5:4:1 to yield **2** (3.1 mg).

Peroxysampsone A (= rel-*(1*R*,3*S*,7*S*,9*S*,11*R*,13*S*)-11-Benzoyl-3-(1-hydroperoxy-1-methylethyl)-6,6,10,10-tetramethyl-13-(3-methylbut-2-en-1-yl)-4,5-dioxatetracyclo[9.3.1.1^{9,13}.0^{1,7}]hexadecane-12,14,15-trione*; **1**). $[\alpha]_D^{18} = +17.0$ (*c* = 0.128, $CHCl_3$). UV ($CHCl_3$): 247 (3.88), 210 (3.13). IR (film): 3424, 3060, 2981, 2931, 2848, 1734, 1698, 1666, 1596, 1581, 1447. ^{1}H- and ^{13}C-NMR, and HMBC: see *Table 1*. EI-MS:

Table 2. *NMR Data for Peroxysampsone B* (**2**[1]). δ in ppm, J in Hz.

	δ(H)	δ(C)	HMBC (H→C)	ROESY (H↔H)
C(1)		66.5		
CH_2(2)	3.10 (*dd*, J=11.0, 14.5, H_α)	31.1	1, 3, 13, 17	H_β–C(2), H_β–C(3), Me(19), Me(21)
	1.66 (*dd*, J=3.9, 14.5, H_β)		1, 7	H_α–C(2), H_β–C(3), Me(19), Me(18)
CH(3)	4.88 (*dd*, J=3.9, 11.0)	88.3	2	H_α–C(2), H_β–C(2), Me(19), Me(18)
C(6)		88.4		
CH(7)	2.56 (overlapped)	40.9	12, 1, 6, 11, 13	H_β–C(8), H_b–C(15), Me(20)
CH_2(8)	2.08 (*m*, H_α)	28.7	1, 6, 7, 9, 10	H_β–C(8), Me(21), Me(20), Me(23)
	1.90 (*m*, H_β)		1, 7, 9, 10	H_β–C(7), H_b–C(15)
CH(9)	2.06 (*m*)	42.8	11, 7, 8, 15, 14, 10	H_a–C(15), H_b–C(15), Me(23), Me(22)
C(10)		48.5		
C(11)		81.9		
C(12)		203.6		
C(13)		207.5		
C(14)		68.9		
CH_2(15)	2.56 (overlapped, H_a)	36.1	8, 9, 14, 16, 13	CH(9), H_b–C(15), Me(22)
	2.12 (*d*, J=14.8, H_b)		8, 9, 14, 16, 10, 13	H_β–C(7), H_β–C(8), CH(9), H_a–C(15)
C(16)		204.3		
C(17)		73.6		
Me(18)	1.16 (*s*)	25.5	3, 17, 19	Me(19), H_β–C(2), CH(3)
Me(19)	1.28 (*s*)	27.1	3, 17, 18	Me(18), CH_2(2), CH(3)
Me(20)	1.32 (*s*)	29.5	6, 7, 21	H_β–C(7), Me(21)
Me(21)	1.19 (*s*)	19.4	6, 7, 20	H_α–C(8), Me(20), Me(23)
Me(22)	1.43 (*s*)	25.0	11, 9, 10, 23	CH(9), H_a–C(15), Me(23)
Me(23)	1.36 (*s*)	22.4	11, 9, 10, 22	H_α–C(8), CH(9), Me(21), Me(22)
C(24)		193.0		
C(25)		135.4		
CH(26)	7.13 (*d*, J=7.4)	128.4	24, 28, 30	CH(27)
CH(27)	7.28 (*t*, J=8.2)	128.2	25, 29	CH(26), CH(28)
CH(28)	7.42 (*t*, J=7.4)	132.5	26, 30	CH(27), CH(29)
CH(29)	7.28 (*t*, J=8.2)	128.2	25, 27	CH(28), CH(30)
CH(30)	7.13 (*d*, J=7.4)	128.4	24, 26, 28	CH(29)
CH_2(31)	2.60 (*d*, J=7.4)	29.1	2, 14, 32, 33	CH(32), Me(35)
CH(32)	5.25 (*t*, J=7.4)	118.7	35, 34	CH_2(31), Me(34)
C(33)		135.7		
Me(34)	1.74 (*s*)	26.1	32, 33, 35	CH(32), Me(35)
Me(35)	1.68 (*s*)	18.1	32, 33, 34	CH_2(31), Me(34)

492 (1, $[M-(CH_3)_2COO]^+$), 459 (2, $[M-(CH_3)_2COO-O_2]^+$), 105 (100, $[PhCO]^+$). FAB-MS: 659 (1, $[M+H+glycerol]^+$), 567 (5, $[M+H]^+$), 493 (4, $[M+H-(CH_3)_2COO]^+$), 475 (5, $[M-(CH_3)_2COO-H_2O]^+$). HR-MALDI-MS: 589.2772 ($[M+Na]^+$, $C_{33}H_{42}NaO_8^+$; calc. 589.2777).

Peroxysampsone B (= rel-*(1*R,*3*R,*7*R,*9*S,*11*R,*13*S*)-11-Benzoyl-3-(1-hydroxy-1-methylethyl)-6,6,10,10-tetramethyl-13-(3-methylbut-2-en-1-yl)-4,5-dioxatetracyclo[9.3.1.1^{9,13}.0^{1,7}]hexadecane-12,14,15-trione*; **2**). $[\alpha]_D^{20}=-41.2$ (c=0.042, $CHCl_3$). UV ($CHCl_3$): 247 (3.91), 212 (3.08), 210 (3.08). IR (film): 3567, 3436, 2977, 2925, 2848, 1736, 1701, 1700, 1597, 1581, 1447. ^{1}H- and ^{13}C-NMR, HMBC, and ROESY correlations: see *Table 2*. EI-MS: 518 ($[M-O_2]^+$). HR-MALDI-MS: 573.2823 ($[M+Na]^+$, $C_{33}H_{42}NaO_7^+$; calc. 573.2828).

Plukenetione C (= rel-*(1*R,*3*S,*7*S,*9*S,*11*R,*13*S*)-11-Benzoyl-3-(1-hydroxy-1-methylethyl)-6,6,10,10-tetramethyl-13-(3-methylbut-2-en-1-yl)-4,5-dioxatetracyclo[9.3.1.1^{9,13}.0^{1,7}]hexadecane-12,14,15-trione*; **3**).

$[\alpha]_D^{18} = +27.5$ ($c = 0.272$, $CHCl_3$). UV ($CHCl_3$): 248 (3.98), 222 (3.33), 209 (3.20). IR (film): 3418, 3044, 2979, 2932, 1734, 1698, 1683, 1596, 1581, 1447. ^{1}H- and ^{13}C-NMR: see *Table 1*. EI-MS: 550 (1, M^+), 532 (1, $[M-H_2O]^+$), 517 (1, $[M-H-O_2]^+$); 105 (100, $[PhCO]^+$). FAB-MS: 501 ($[M-H_2O-O_2]^+$), 475 ($[M-(CH_3)_2COO]^+$). HR-MALDI-MS: 573.2823 ($[M+Na]^+$, $C_{33}H_{42}NaO_7^+$; calc. 573.2828).

Bioassay. Bacteria SA-1199B is a strain of *Staphylococcus aureus* overproducing the NorA MDR efflux protein, the major drug pump in *S. aureus*, and was resistant to norfloxacin (*MIC* 79 μg/ml) [7]. This strain was a gift of Prof. *G. K. Kaatz* [9].

Minimum Inhibitory Concentration (*MIC*) *Assay.* Bacteria were cultured on nutrient agar (*Oxoid*) and incubated for at 37° 24 h prior to *MIC* determination. The control antibiotic norfloxacin was obtained from *Sigma Chemical Co. Mueller–Hinton* broth (MHB; *Oxoid*) was adjusted to contain 20 and 10 mg/l of Ca^{2+} and Mg^{2+}, resp. An inoculum density of 5×10^5 cfu of *S. aureus* was prepared in normal saline (9 g/l) by comparison with a 0.5 *MacFarland* turbidity standard. The inoculum (125 μl) was added to all wells, and the microtitre plate was incubated at 37° for 18 h. For *MIC* determination, 20 μl of a 5 mg/ml MeOH soln. of 3-[4,5-dimethylthiazol-2-yl]-2,5-diphenyl1-2*H*-tetrazolium bromide (MTT; *Sigma*) was added to each of the wells and incubated for 20 min. Bacterial growth was indicated by a color change from yellow to dark blue. The *MIC* was recorded as the lowest concentration at which no growth was observed [9].

We thank for the financial supports from the *National Science Foundation of China* (30772630) and the *Initiating Financial for Returnee of Education Department of China* (2006).

REFERENCES

[1] Jiangsu New Medical College, 'Dictionary of Chinese Crude Drugs', Shanghai Scientific Technological Publishers, Shanghai, 1977, p. 345.
[2] L.-H. Hu, K.-Y. Sim, *Tetrahedron Lett.* **1998**, *39*, 7999; L.-H. Hu, K.-Y. Sim, *Tetrahedron Lett.* **1999**, *40*, 759; L. H. Hu, K. Y. Sim, *Org. Lett*. **1999**, *1*, 879; L.-H. Hu, K.-Y. Sim, *Tetrahedron* **2000**, *56*, 1379; Y.-L. Lin, Y.-S. Wu, *Helv. Chim. Acta* **2003**, *86*, 2156; M.-J. Don, Y.-J. Huang, R.-L. Huang, Y.-L. Lin, *Chem. Pharm. Bull.* **2004**, *52*, 866; D. Hong, F. Yin, L.-H. Hu, P. Lu, *Phytochemistry* **2004**, *65*, 2595.
[3] a) Z. Y. Xiao, W. P. S. Shiu, Y. H. Zeng, Q. Mu, S. Gibbons, *J. Nat. Prod.* **2007**, *70*, 1259; b) Z. Y. Xiao, W. K. P. Shiu, Y. H. Zeng, Q. Mu, S. Gibbons, *Pharm. Biol.* **2008**, *46*, 250.
[4] O. E. Christian, G. E. Henry, H. Jacobs, S. McLean, W. F. Reynolds, *J. Nat. Prod.* **2001**, *64*, 23.
[5] G. E. Henry, H. Jacobs, C. M. S. Carrington, S. McLean, W. F. Reynolds, *Tetrahedron* **1999**, *55*, 1581.
[6] G.-F. Chen, Z.-L. Li, K. Chen, C.-M. Tang, X. He, D.-J. Pan, D. R. McPhail, A. T. McPhail, K.-H. Lee, *Tetrahedron Lett*. **1990**, *31*, 3413.
[7] G. W. Kaatz, S. M. Seo, C. A. Ruble, *Antimicrob. Agents Chemother.* **1993**, *37*, 1086.
[8] H. Yoshida, M. Bogaki, S. Nakamura, K. Ubukata, M. Konno, *J. Bacteriol*. **1990**, *172*, 6942.
[9] S. Gibbons, E. E. Udo, *Phytother. Res.* **2000**, *14*, 139.

Received June 8, 2009

Fitoterapia 81 (2010) 656–658

Contents lists available at ScienceDirect

Fitoterapia

journal homepage: www.elsevier.com/locate/fitote

A new 7-oxygenated coumarin from *Clausena suffruticosa*

Rokeya Begum [a], Mohammad S. Rahman [b], Sarwaruddin Chowdhury [a], M. Mukhlesur Rahman [c,*], Simon Gibbons [c], Mohammad A. Rashid [b]

[a] Department of Applied Chemistry and Chemical Technology, University of Dhaka, Dhaka-1000, Bangladesh
[b] Department of Pharmaceutical Chemistry, Faculty of Pharmacy, University of Dhaka, Dhaka-1000, Bangladesh
[c] Department of Pharmaceutical and Biological Chemistry, The School of Pharmacy, University of London, 29–39 Brunswick Square, London WC1N 1AX, UK

ARTICLE INFO

Article history:
Received 16 December 2009
Received in revised form 5 March 2010
Accepted 9 March 2010
Available online 17 March 2010

Keywords:
Clausena suffruticosa
Rutaceae
Coumarin
7-[(2′*E*,6′*E*)-7′-carboxy-5′(ζ)-hydroxy-3′-methylocta-2′,6′-dienyloxy]-coumarin

ABSTRACT

A new coumarin, 7-[(2′*E*,6′*E*)-7′-carboxy-5′(ζ)-hydroxy-3′-methylocta-2′,6′-dienyloxy]-coumarin, was isolated from the leaf of *Clausena suffruticosa*. Its structure was established by means of spectroscopic data analyses, including mass spectrometry and both 1D and 2D NMR spectroscopy.

1. Introduction

Clausena suffruticosa, locally known as Kalomoricha (Rutaceae), is an understory shrub that is widely distributed in the hilly areas of the Chittagong and Sylhet districts of Bangladesh [1]. Although ethnopharmacological information on *C. suffruticosa* is not available, other members of this genus are known to have traditional medicinal uses. For example, *C. excavata* is used traditionally in Bangladesh as a diuretic [2]. In southeast Asian countries, this plant is also useful in paralysis, colic, stomach trouble, fever and headache, muscular pain and malarial fever [2,3] and additionally several of these species are known to be effective as diuretics, astringents, insecticides, tonics and as vermifuges [4]. In some countries, *C. excavata* has been used for cough, rhinitis, sore, wounds, yaws and detoxification [5]. In Taiwan and China, *Clausena lansium* has been used as a folk medicine for the treatment of coughs, asthma and gastro-intestinal diseases. The seeds are used for gastro-intestinal diseases such as acute and chronic gastro-intestinal inflammation, ulcers, and they are also used ethnomedically as a vermifuge and for digestive disorders [6]. Previous phytochemical studies with *Clausena* have led to the isolation of carbazole alkaloids [2], coumarins [7] and limonoids [8]. As a part of our continuing investigation for bioactive compounds from Bangladeshi rutaceous plants, we here report the isolation of a new coumarin (**1**) from the leaves of *C. suffruticosa*.

2. Experimental

2.1. General

Optical rotations: Perkin Elmer Polarimeter 341. IR: Perkin Elmer Spectrum 1000 FT-IR Spectrometer. UV: Thermo Electron Corporation UV/vis Spectrophotometer. HRTOFMS (positive-ion mode): Micromass Q-TOF Global Tandem Mass Spectrometer. NMR: Bruker AVANCE 500 Spectrometer (500 MHz for ^{1}H and 125 MHz for ^{13}C).

2.2. Plant material

The leaves of *C. suffruticosa* were collected from Ramakalanga, Sylhet, Bangladesh in October 2005. The plant was identified by Dr. Mahbuba Khanam, Bangladesh National Herbarium, Mirpur, Ministry of Environment and Forest

* Corresponding author. Tel.: +44 207 7535800/4853; fax: +44 207 7535964.
E-mail address: mukhlesur.rahman@pharmacy.ac.uk (M.M. Rahman).

0367-326X/$ – see front matter.
doi:10.1016/j.fitote.2010.03.013

Dhaka, Bangladesh, where a voucher specimen (DACB-31233) of this collection has been maintained.

2.3. Extraction and isolation

The air dried powdered leaves (124.5 g) were sequentially extracted with a Soxhlet apparatus using *n*-hexane, ethyl acetate and methanol to yield 6.1, 6.15 and 8.0 g of extracts, respectively. A portion of the *n*-hexane extract (3.5 g) was fractionated by VLC over Si gel 60H using hexane-EtOAc and EtOAc-MeOH mixtures of increasing polarity. Concentration of the VLC fraction eluted with 60% EtOAc in hexane yielded a white semisolid mass, which upon repeated washings with hexane led to the isolation of compound **1** (9.5 mg).

2.4. 7-[(2′E,6′E)-7′-carboxy-5′(ζ)-hydroxy-3′-methylocta-2′,6′-dienyloxy] coumarin (**1**)

White semisolid mass; $[\alpha]_D^{20}$ −27.2 (*c* 0.001, $CHCl_3$); UV λ_{max} (logε): 203 (3.56), 323 (2.88) nm; IR ν_{max} (solution in $CHCl_3$): 3367, 3022, 1753, 1615, 1508, 1217, 1129, 1003, 838 and 756 cm^{-1}; ^1H NMR (500 MHz, $CHCl_3$) and ^{13}C NMR (125 MHz, $CHCl_3$) see Table 1; positive-ion HRTOFMS *m/z*: 345.1353 $[M+H]^+$ (calcd for $C_{19}H_{21}O_6$, 345.1338).

3. Results and discussion

Extensive chromatographic separation and purification of the VLC fraction obtained from the *n*-hexane soluble materials of the leaf of *C. suffruticosa* yielded compound **1** as a white semisolid mass. It was visualized as a blue fluorescing as well as quenching spot on a TLC plate under UV light at 254 and 366 nm, respectively. Spraying the developed plate with vanillin–sulfuric acid followed by heating at 110 °C for 5 min gave a red color. The UV spectrum of **1** in MeOH displayed absorption maxima at 203 and 323 nm typical of a 7-oxygeneted coumarin [7]. The high resolution ESI-TOF MS of compound **1** exhibited the *pseudo*-molecular ion $[M+H]^+$, peak at *m/z* 345.1353, corresponding to the molecular formula $C_{19}H_{20}O_6$.

Table 1
^1H NMR, ^{13}C NMR and HMBC data of **1** in $CDCl_3$.

Position	^1H	^{13}C	HMBC	
			^2J	^3J
2	–	161.7	–	–
3	6.26, d, *J* = 9.5 Hz	113.4	–	–
4	7.65, d, *J* = 9.5 Hz	143.6	C-4a	C-8a, C-5
5	7.38, d, *J* = 8.5 Hz	129.0	C-4a	C-7, C-4
6	6.85, dd, *J* = 8.5, 2.0 Hz	113.3	C-7	–
7	–	162.1	–	–
8	6.81, d, *J* = 2.0 Hz	101.8	C-7	C-4a
8a	–	161.4	–	–
4a	–	156.1	–	–
1′	4.63, d, *J* = 6.0 Hz	65.3	C-2′	C-3′, C-7
2′	5.61, t, *J* = 6.0 Hz	123.2	C-1′	3′-Me, C-4′
3′	–	136.5	–	–
3′-Me	1.85, s	17.7	C-3′	C-4′, C-2′
4′	2.42, m	43.5	C-5′, C-3′	3′-Me, C-6′
5′	5.03, t, *J* = 6.0 Hz	79.6	C-4′	C-3′
6′	7.05, br s	148.3	C-5′	8′, 7′-COOH
7′	–	130.6	–	–
8′	1.92 br s	10.9	C-7′	C-6′, 7′-COOH
7′-COOH	–	174.1	–	–

The ^1H (500 MHz, Table 1) and ^{13}C NMR data (125 MHz, Table 1) of **1** revealed resonances which were typical of a 7-oxycoumarin [9]. The ^{13}C NMR spectrum displayed a total of 19 carbon resonances, while the DEPT135 and HMQC experiments indicated that 12 out of 19 carbons had attached protons. Analysis of the ^{13}C and DEPT135 spectra allowed discernment of the carbon resonances into two methyls, two methylenes, eight methines and seven quaternary carbons, including a carboxylic acid. A 7-substituted coumarin nucleus was evident from an AB doublet (*J* = 9.5 Hz) centered at δ 6.26 (H-3) and δ 7.65 (H-4) and further ABD resonances at 7.38 (d, *J* = 8.5 Hz, H-5), 6.85 (dd, *J* = 8.5, 2.0 Hz, H-6) and δ 6.81 (d, *J* = 2.0 Hz, H-8) from the ^1H NMR spectrum. The remaining signals in the ^1H NMR spectrum demonstrated the existence of a geranyl-derived (C_{10}) side chain. In the HMBC experiment, the methylene at δ 4.63 (H_2-1′; δ_C 65.3 from HMQC) showed ^3J connectivity to an oxygenated quaternary carbon at 162.1 ppm (C-7) which further supported the presence of the side chain at C-7. In the COSY spectrum, H_2-1′ showed a strong interaction with a methine proton at δ 5.61 (H-2′) which was further connected to methyl (δ_C 17.7) and methylene (δ_C 43.5; δ_H 2.42 from HMQC) carbons in the HMBC. Again, in the COSY experiment, an oxymethine proton at δ 5.03 (H-5′) showed a strong interaction with methylene protons at δ 2.42 (H-4′) and a methine hydrogen resonance at δ 7.05 (H-6′; δ_C 148.3 from HMQC). The downfield shift of this proton at δ 7.05 and its associated carbon at 148.3 suggested its position to be beta (β) to the carboxylic acid (174.1; ^3J HMBC connectivity to H-6′ and H_3-8′). In the NOESY experiment, the interaction between H-1′ and Me-3′ suggested this methyl to be *trans* to H-2′. Similarly, CH_3-8′ and H-6′ were in a *trans* orientation from the NOE interaction between CH_3-8′and H-5′. Accordingly, compound **1** was therefore identified as 7-[(2′*E*,6′*E*)-7′-carboxy-5′(ζ)-hydroxy-3′-methylocta-2′,6′-dienyloxy] coumarin which is reported here for the first time. The presence of this new 7-geranyloxycoumarin in the genus *Clausena* is of chemotaxonomic significance as the plant family Rutaceae is one of the richest sources of coumarins [10]. In particular, the genus *Clausena* is well known to produce coumarins [7]. 7-geranyloxycoumarins structurally similar to **1** are present in a number of rutaceous plants including those of *Aegle*, *Atalantia*, *Citrus*, *Geijera* and *Micromelum* [10,11].

This metabolite was evaluated for antibacterial activity against a panel of multidrug-resistant (MDR) and methicillin-resistant *Staphylococcus aureus* (MRSA), but exhibited no activity at 128 μg/ml.

1

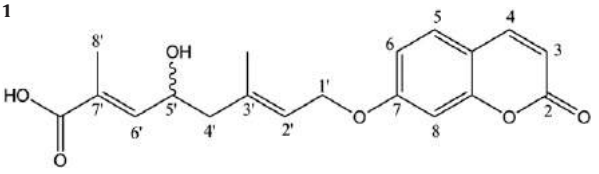

References

[1] Hooker JD. Flora of British India, vol. I. England: Reeve & Co. Ltd; 1875.
[2] Thuy TT, Ripperger H, Porzel A, Sung TV, Adam G. Counlarins, limonoids and an alkaloid from *Clausena excavate*. Phytochemistry 1999;52:511–6.

[3] Yusuf M, Chowdhury JU, Wahab MA, Begum J. Medicinal Plants of Bangldesh. Bangladesh Council of Scientific and Industrial Research (BCSIR), Dhakafirst ed. ; 1994.
[4] Perry LM. Medicinal plants of East and Southeast Asia: Attributed Properties and Uses. Cambridge: The MIT Press; 1980.
[5] Swarbrick JT. Environmental weeds and exotic plants on Christmas Island, Indian Ocean: A Report to Park Australia; 1997. p. 29–30.
[6] Lin JH. Cinnamamide derivatives from *Clausena lansium*. Phytochemistry 1989;28:621–2.
[7] Huang SC, Wu PL, Wu TS. Two coumarins from the root bark of the *Clausena excavata*. Phytochemistry 1997;44:179–81.
[8] Ngadjui BT, Ayafor JF, Sondengam BL. Limonoids from *Clausena anisata*. J Nat Prod 1989;52:832–6.
[9] Murray RDH, Mondez J, Brown SA. Chemistry and Biochemistry. Bristol: Wiley; 1982.
[10] Gray AI, Waterman PG. Coumarins in the Rutaceae. Phytochemistry 1978;17:845–64.
[11] Gray AI. In: Waterman PG, Grundon MF, editors. Chemistry and chemical taxonomy of the Rutales. London: Academic Press; 1983.

Phytochemistry 70 (2009) 403–406

Contents lists available at ScienceDirect

Phytochemistry

journal homepage: www.elsevier.com/locate/phytochem

Dibenzofuran and pyranone metabolites from *Hypericum revolutum* ssp. *revolutum* and *Hypericum choisianum*

Winnie Ka Po Shiu, Simon Gibbons *

Centre for Pharmacognosy and Phytotherapy, The School of Pharmacy, University of London, 29-39 Brunswick Square, London WC1N 1AX, UK

ARTICLE INFO

Article history:
Received 3 October 2008
Received in revised form 8 December 2008
Available online 4 February 2009

Keywords:
Hypericum revolutum
Hypericum choisianum
Guttiferae
Dibenzofuran
Pyranone
Pyran-2-one
Antibacterial
MRSA
Staphylococcus aureus
MDR

ABSTRACT

In a project to isolate and characterise anti-staphylococcal compounds from members of the genus *Hypericum*, a dibenzofuran and a pyranone were isolated from the dichloromethane and hexane extracts of *Hypericum revolutum* ssp. *revolutum* Vahl (Guttiferae) and *Hypericum choisianum* Wall. ex. N. Robson (Guttiferae), respectively. The structures of these compounds were elucidated by 1- and 2D-NMR spectroscopy and mass spectrometry as 3-hydroxy-1,4,7-trimethoxydibenzofuran (**1**) and 4-(3-*O*-3″)-3″-methylbutenyl-6-phenyl-pyran-2-one (**2**). The metabolites were evaluated against a panel of multi-drug-resistant strains of *Staphylococcus aureus*. Compound **1** exhibited a minimum inhibitory concentration (MIC) of 256 μg/ml, whereas compound **2** was inactive at a concentration of 512 μg/ml.

1. Introduction

Hypericum belongs to the Guttiferae family (alternative name Clusiaceae) and is a genus of approximately 450 species. The widespread interest in the use of *H. perforatum* (St. John's Wort) in mild to moderate depression has attracted much attention in investigating the bioactive metabolites from other species in this genus. Extracts from various *Hypericum* species have been shown to possess antibacterial (Rocha et al., 1995), anti-staphylococcal (Shiu and Gibbons, 2006), antiviral (Weber et al., 1994), anti-inflammatory (Trovato et al., 2001) and anti-oxidant (Conforti et al., 2002) activities. The most commonly isolated compounds from this genus include acylphloroglucinols (Gibbons et al., 2005; Shiu and Gibbons, 2006), xanthones (Bennett and Lee, 1989), flavonoids (Crockett et al., 2005), tannins (Ploss et al., 2001) and, less frequently, benzopyrans (Décosterd et al., 1986).

The anti-staphylococcal activity of 34 *Hypericum* species was studied previously by our group (Gibbons et al., 2002). In the preliminary study, 33 out of 34 chloroform extracts showed activity in a disk diffusion assay. The chloroform extract of *H. revolutum* ssp. *revolutum* Vahl exhibited a minimum inhibitory concentration (MIC) of 128 μg/ml against the methicillin-resistant *Staphylococcus aureus* (MRSA) strain, XU212. There is very little literature on this species although a paper by Kassu et al. (1999) refers to the use of *H. revolutum* as toothbrush sticks. This prompted us to carry out a large-scale plant collection and bioassay-guided isolation of antibacterial compounds from this plant. A new dibenzofuran (**1**) was isolated from *H. revolutum* ssp. *revolutum*. Previous phytochemistry of *H. choisianum* is limited to the characterisation of its essential oil content (Demirci et al., 2005), and we therefore investigated this species which afforded a new pyranone (**2**). The structural elucidation of these compounds is described in this paper. Extensive literature and internet searches indicate that the medicinal and traditional uses of these two species are unknown.

2. Results and discussion

Bioassay-guided fractionation of the dichloromethane (DCM) extract of the aerial parts of *H. revolutum* ssp. *revolutum* led to the isolation of (**1**) as a pale yellow oil. HRESI-MS suggested a molecular formula of $C_{15}H_{14}O_5$ $[M-H]^-$ (273.0763). In the ^{13}C NMR spectrum (Table 1), 12 signals in the aromatic region and three methoxyl signals were observed. The pattern of the aromatic carbon signals showed similarity to that of a xanthone nucleus, differing in the absence of a carbonyl signal in this compound. These data suggested that compound **1** was a dibenzofuran substituted with three methoxyl groups (Kokubun et al., 1995, 1995a). The

* Corresponding author. Tel.: +44 207 7535913; fax: +44 207 7535909.
E-mail address: simon.gibbons@pharmacy.ac.uk (S. Gibbons).

0031-9422/$ - see front matter © 2008 Elsevier Ltd. All rights reserved.
doi:10.1016/j.phytochem.2008.12.016

Table 1
^{1}H (500 MHz) and ^{13}C NMR (125 MHz) spectral data and ^{1}H–^{13}C long-range correlations of **1** recorded in $CDCl_3$.

Position	^{1}H (J, Hz)	^{13}C	^2J	^3J
1	–	143.9	–	–
2	6.25 s	94.2	C-1	C-4, C-9b
3	–	135.7	–	–
4	–	128.5	–	–
4a	–	144.0	–	–
5a	–	141.2	–	–
6	6.53 d (3)	102.6	C-5a, C-7	C-8, C-9a
7	–	155.9	–	–
8	6.47 dd (3, 8.5)	109.1	–	C-6, C-9a
9	6.89 d (8.5)	116.9	C-9a	C-5a, C-7
9a	–	135.9	–	–
9b	–	126.2	–	–
1-OCH_3	3.83 s	56.5	–	C-1
4-OCH_3	3.92 s	61.9	–	C-4
7-OCH_3	3.76 s	55.8	–	C-7
3-OH	5.42 bs	–	–	C-2, C-4

Table 2
^{1}H (500 MHz) and ^{13}C NMR (125 MHz) spectral data and ^{1}H–^{13}C long-range correlations of **2** recorded in $CDCl_3$.

Position	^{1}H (J, Hz)	^{13}C	^2J	^3J
1	–	–	–	–
2	–	161.7	–	–
3	–	163.9	–	–
4	–	99.3	–	–
5	6.42 s	97.8	C-4, C-6	C-3, C-1′
6	–	160.1	–	–
1′	–	131.3	–	–
2′/6′	7.78 m	125.6	–	C-6, C-4′, C-6′/2′
3′/5′	7.43 m	128.9	C-4′	C-1′, C-5′/3′
4′	7.42 m	130.9	–	C-2′/6′
1″	6.45 d (10)	116.4	–	C-3, C-3″
2″	5.42 d (10)	125.5	C-3″	C-4
3″	–	80.2	–	–
4″	1.48 s	28.6	C-3″	C-2″, C-5″
5″	1.48 s	28.6	C-3″	C-2″, C-4″

^{1}H NMR spectrum (Table 1) showed signals for three aromatic hydrogens in an ABD system with resonances at δ_H 6.89 (d, J = 8.5 Hz, H-9), δ_H 6.47 (dd, J = 3, 8.5 Hz, H-8) and δ_H 6.53 (d, J = 3 Hz, H-6), an aromatic hydrogen singlet (δ_H 6.25 s, H-2), a broad signal at δ_H 5.42 corresponding to an hydroxyl group and three methoxyl singlets (δ_H 3.92 s, 3.83 s, 3.76 s).

In the HMBC spectrum, correlations were seen between the methoxyl groups with resonances at δ_H 3.76 (C7–OCH_3), 3.83 (C1–OCH_3) and 3.92 (C4–OCH_3) and δ_C 155.9 (C-7), 143.9 (C-1) and 128.5 (C-4), respectively, confirming the chemical shifts of the carbons to which the methoxyl groups were attached. A cross-peak in the NOESY spectrum was observed between the methoxyl group at C-1 and the aromatic proton singlet (H-2), and the methoxyl group at C-4 and the hydroxyl group, thus placing them next to each other (Fig. 1). The hydrogen of the hydroxyl group showed a ^3J correlation with the carbon to which the aromatic hydrogen singlet was attached (δ_C 94.2, C-2) and to the carbon to which a methoxyl group was attached (δ_C 128.5, C-4). The hydroxyl group was placed between these groups in the same aromatic ring. The aromatic hydrogen (H-2) also displayed a ^3J HMBC correlation (Fig. 1) with C-9b (δ_C 126.2) but not to the oxygen-bearing carbon at δ_C 144.0 (C-4a), thus placing it at C-2 and not C-3.

For the other aromatic ring, a cross-peak could be seen between the methoxyl singlet at δ_H 3.76 (C7–OCH_3) and H-6 and H-8 in the NOESY spectrum (Fig. 1). This methoxyl group was therefore placed between the aromatic hydrogens in the ABD system. Since the *meta*- and *ortho*-coupled aromatic proton at δ_H 6.47 (H-8) showed a strong ^3J HMBC correlation with carbons at δ_C 135.9 (C-9a) but not δ_C 141.2 (C-10a), it could be implied that the methoxyl group was placed at C-7 and not C-8, which would also yield an ABD system. This completed the NMR assignment of compound **1**, which was characterised as the new natural product 3-hydroxy-1,4,7-trimethoxy-dibenzofuran. This compound was structurally related to a series of dibenzofurans, which are phytolexins isolated from *Mespilus* (Rosaceae) species (Kokubun et al., 1995, 1995a). To our knowledge, compound **1** is the first dibenzofuran to be isolated from the *Hypericum* genus to date.

Compound **2** was isolated as a yellow oil from the hexane extract of the aerial parts of *H. choisianum*. It showed an $[M + H]^+$ peak at m/z 255.1021 in the HRESI-MS, which corresponded to a molecular formula of $C_{16}H_{14}O_3$. The ^{1}H NMR spectrum (Table 2) revealed signals for five aromatic hydrogens in a mono-substituted benzene ring with resonances at δ_H 7.78 (m, 2H, H-2′, H-6′), δ_H 7.43 (m, 2H, H-3′, H-5′) and δ_H 7.42 (m, 1H, H-4′), an olefinic singlet (δ_H 6.42, H-5), two olefinic hydrogens with resonances at δ_H 6.45 (d, J = 10 Hz, H-1″) and δ_H 5.42 (d, J = 10 Hz, H-2″), and a methyl singlet integrating for six protons (δ_H 1.48 s, H_3-4″, H_3-5″). The ^{13}C NMR spectrum (Table 2) displayed signals for three highly deshielded aromatic carbons (δ_C 161.7, C-2; 163.9, C-3; 160.1, C-6), two quaternary aromatic carbons at δ_C 131.3 (C-1′) and 99.3 (C-4), three aromatic methines belonging to the mono-substituted benzene ring (δ_C 125.6, C-2′, C-6′; 128.9, C-3′, C-5′; 130.9, C-4′), two olefinic methines (δ_C 116.4, C-1″; 125.5, C-2″), a further olefinic methine at δ_C 97.8 (C-5), a deshielded quaternary aliphatic carbon at δ_C 80.2 (C-3″) and two methyl carbons at δ_C 28.6 (C-4″, C-5″). The molecular formula determined by mass spectrometry suggested that the deshielded carbons were oxygen-bearing.

In the HMBC spectrum, a cross-peak was seen between the methyl singlet (δ_H 1.48, 6H, H-4″, H-5″) and a methyl carbon at δ_C 28.6 (C-4″, C-5″), indicating the presence of a *gem*-dimethyl moiety (Fig. 2). The methyl groups also correlated to the oxygen-bearing quaternary carbon at δ_C 80.2 (C-3″) and an olefinic methine carbon at δ_C 125.5 (C-2″). A correlation between the olefinic hydrogen at C-2″ (δ_H 5.42) and the neighbouring olefinic proton (δ_H 6.45, H-1″) was seen in the COSY spectrum. The coupling constant between the olefinic hydrogens was 10 Hz, implying that they were in a *cis*-configuration. H-1″ exhibited an HMBC correlation to a highly deshielded oxygen-bearing carbon at δ_C 163.9 (C-3),

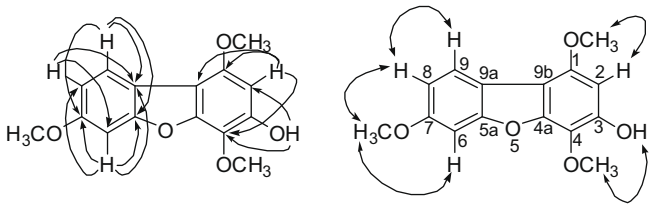

Fig. 1. Key HMBC (single headed arrows) and NOESY interactions (double headed arrows) correlations for **1**.

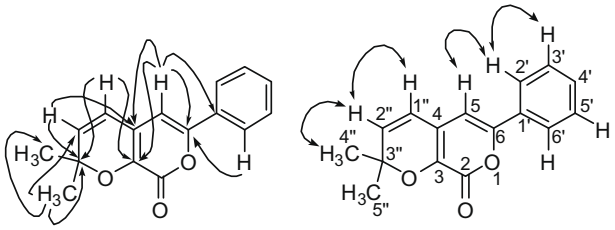

Fig. 2. Key HMBC (single headed arrows) and NOESY (double headed arrows) correlations for **2**.

whereas H-2″ showed an HMBC correlation to a quaternary aromatic carbon at δ_C 99.3 (C-4). These ^{1}H and ^{13}C NMR data were suggestive of the presence of a dimethylpyran ring (Seo et al., 1999).

Further inspection of the HMBC spectrum revealed correlations between the aromatic hydrogen singlet at δ_H 6.42 (H-5) and C-3, C-4, and two quaternary carbons at δ_C 160.1 (C-6) and 131.1 (C-1′), thus placing it at C-5 (Fig. 2). The presence of a mono-substituted phenyl group at C-6 was confirmed by investigating the HMBC spectrum. The hydrogen resonance at δ_H 7.42 (H-4′) was correlated to the equivalent carbons, C-2′ and C-6′, at δ_C 125.6 *via* three bonds. The two equivalent aromatic hydrogens at δ_H 7.43 (2H, H-3′, H-5′) showed a ^2J correlation to C-4′, and ^3J correlations to the corresponding equivalent carbon (C-5′, C-3′) and the substituent-bearing quaternary aromatic carbon (δ_C 131.3, C-1′). The remaining equivalent signals in the phenyl moiety (δ_H 7.78, 2H, H-2′, H-6′), showed ^3J correlations to the corresponding equivalent carbon (δ_C 125.6, C-6′, C-2′), C-4′, and to an oxygen-bearing carbon at δ_C 160.1 (C-6). Finally, the position of the phenyl substituent at C-6 was also confirmed by an NOE correlation between H-5 and H-2′/H-6′ (Fig. 2).

The remaining carbon (δ_C 160.1), which was not correlated to any hydrogen in the HMBC spectrum, was placed at C-2 to complete the structure of this compound, giving a pyran-2-one nucleus. The chemical shift of C-2 was typical of the carbonyl group in a pyran-2-one ring (Dharmaratne et al., 2002). Compound **2** was therefore identified as the new 4-(3-*O*-3″)-3″-methylbutenyl-6-phenyl-pyran-2-one, and is reported here for the first time.

Compounds **1** and **2** were assessed for antibacterial activity against a panel of *S. aureus* strains in an MIC assay (Table 3). Compound **1** was weakly active against the tested strains with an MIC value of 256 μg/ml against all strains. Unlike the control antibiotics, the antibacterial activity of compound **1** was constant against all the tested strains. This might imply that the mechanism of action of this compound was not affected by the multidrug-resistant mechanisms in these strains. A series of structurally similar dibenzofurans have been isolated from the sapwood of *Mespilus germanica* when challenged by *Nectria cinnabarina*, a coral spot fungus (Kokubun et al., 1995, 1995a). Those authors found that these dibenzofurans acted as the major phytoalexins and showed antifungal activity, with ED_{50}s in the range of 12–100 ppm. The antibacterial activity of these compounds has not been investigated, however. Compound **2** was inactive at a concentration of 512 μg/ml.

3. Experimental

3.1. General experimental procedures

NMR spectra were recorded on a Bruker AVANCE 500 MHz spectrometer. Chemical shifts values (δ) were reported in parts per million (ppm) relative to the appropriate internal solvent standard and coupling constants (J values) were given in Hz. IR spectra were recorded on a Nicolet 360 FT-IR spectrophotometer and UV spectra on a Thermo Electron Corporation Helios spectrophotometer. The specific rotation was measured on a Perkin–Elmer Polarimeter Model 343. Mass spectra were recorded on a Finnigan MAT 95 high resolution, double focusing, magnetic sector mass spectrometer. Accurate mass measurement was achieved using voltage scanning of the accelerating voltage. This was nominally 5 kV and an internal reference of heptacosa was used. Resolution was set between 5000 and 10,000.

Table 3
MICs of **1**, **2** and standard antibiotics in μg/ml.

Strain (MDR efflux protein)	**1**	**2**	Norfloxacin	Tetracycline	Erythromycin	Oxacillin
ATCC 25923	256	>512	1	–	–	–
SA-1199B (NorA)	256	>512	32	–	–	–
XU212 (TetK)	256	>512	–	128	–	–
RN4220 (MsrA)	256	>512	–	–	256	–
EMRSA-15	256	>512	–	–	–	32
EMRSA-16	256	>512	-	-	-	512

All MICs were determined in duplicate.

3.2. Plant material

The aerial parts of *H. revolutum* ssp. *revolutum* (Accession no. 1972–3163) and *H. choisianum* (Accession no. 1977–4670) were collected from the Royal Botanic Garden at Wakehurst Place in Surrey, England in August 2003 and August 2005, respectively. Voucher specimens were deposited in the herbarium at the Centre for Pharmacognosy and Phytotherapy at the University of London School of Pharmacy.

3.3. Extraction and isolation

Air-dried and powdered aerial parts of *Hypericum revolutum* ssp. *revolutum* (495 g) were extracted in a Soxhlet apparatus sequentially with hexane (3 l), dichloromethane (3 l) and methanol (3 l). The DCM extract (1.8 g) was subjected to LH-20 Sephadex chromatography, affording five fractions eluted with chloroform:methanol (1:1) and one fraction with a final methanol wash. Fractions five and six were combined and further separated on a LH-20 Sephadex column, giving eight fractions eluted with chloroform:methanol (1:1) and one fraction eluted with methanol. The fraction eluted with methanol was purified by preparative thin-layer chromatography (silica) using toluene-ethyl acetate-acetic acid (60:38:2), yielding compound **1** (4.5 mg; R_f = 0.58).

1.0 kg of air-dried, powered aerial parts of *H. choisianum* was extracted in a Soxhlet apparatus using sequential extraction as described above. The hexane extract (9.9 g) was subjected to vacuum liquid chromatography (VLC) on silica gel eluting with hexane containing 10% increments of ethyl acetate to yield 12 fractions. Fractions 5–7 showed similar TLC profiles and were combined (1.1 g) and this was further separated using LH-20 Sephadex chromatography. This resulted in seven fractions eluted with chloroform:methanol (1:1) and one fraction with a final methanol wash. Fractions 7 and 8 were combined (332.1 mg) and purified further by preparative reverse phase HPLC (Waters Prep C_{18} column, 19 × 300 mm, 10 μm) using a gradient of 5% acetonitrile in water to 100% acetonitrile over 30 min. The flow rate was 50 ml/min. Compound **2** (5.0 mg) had a retention time of 13.0 min.

VLC fraction 4 was subjected to reverse phase solid phase extraction (SPE; Phenomenex Strata, C_{18}, 10 g/60 ml Giga tubes), affording three fractions eluted with methanol and one fraction eluted with acetone. The first SPE fraction was further fractionated using reverse phase SPE, giving five fractions eluted with 80% acetonitrile in water and one fraction eluted with 100% acetone as a final wash. SPE fraction 1 was purified using preparative TLC (silica) with toluene-ethyl acetate-acetic acid (80:18:2), yielding compound **2** (7.2 mg, R_f = 0.59). A total of 12.2 mg of compound **2** was isolated using the two methods.

3.4. Bacterial strains

S. aureus standard strain ATCC 25923 and tetracycline-resistant strain XU212 which possesses the TetK tetracycline efflux protein were provided by (Gibbons and Udo (2000)). Strain SA-1199B

which overexpresses the norA gene encoding the NorA MDR efflux pump was provided by Kaatz et al. (1993). Strain RN4220 which possess the MsrA macrolide efflux protein was provided by (Ross et al. (1989). The epidemic strains EMRSA-15 and EMRSA-16 were provided by Richardson and Reith (1993) and Cox et al. (1995).

3.5. Minimum inhibitory concentration (MIC) assay

All strains were cultured on nutrient agar (Oxoid) and incubated for 24 h at 37 °C prior to MIC determination. Control antibiotics norflorxacin, tetracycline, erythromycin and oxacillin were obtained from Sigma Chemical Co. Mueller–Hinton broth (MHB; Oxoid) was adjusted to contain 20 and 10 mg/l of Ca^{2+} and Mg^{2+}, respectively. An inoculum density of 5×10^5 cfu of each *S. aureus* strain was prepared in normal saline (9 g/l) by comparison with a 0.5 MacFarland turbidity standard. The inoculum (125 μl) was added to all wells and the microtitre plate was incubated at 37 °C for 18 h. For MIC determination, 20 μl of a 5 mg/ml methanolic solution of 3-[4,5-dimethylthiazol-2-yl]-2,5-diphenyltetrazolium bromide (MTT; Sigma) was added to each of the wells and incubated for 20 min. Bacterial growth was indicated by a colour change from yellow to dark blue. The MIC was recorded as the lowest concentration at which no growth was observed (Gibbons and Udo, 2000).

3.6. 3-hydroxy-1,4,7-trimethoxydibenzofuran (**1**)

Pale yellow oil; $[a]_D^{22}$ 0° (*c* 0.19, $CHCl_3$); UV ($CHCl_3$) λ_{max} (log ε): 240 (3.87) nm; IR ν_{max} (thin film) cm^{-1}: 3412, 1504, 1472, 1264, 1208, 1155; ^1H NMR and ^{13}C NMR ($CDCl_3$): see Table 1; HR ESI-MS (*m*/*z*): 273.0763 $[M-H]^-$ (calc. for $C_{15}H_{14}O_5$, 273.0768).

3.7. 4-(3-O-3″)-3″-methylbutenyl-6-phenyl-pyran-2-one (**2**)

Yellow oil; $[a]_D^{22}$ 0° (*c* 0.24, $CHCl_3$); UV ($CHCl_3$) λ_{max} (log ε): 242 (4.03), 255 (3.98), 374 (3.82) nm; IR ν_{max} (thin film) cm^{-1}: 1717, 1700, 1696, 1653, 1616, 1558, 1506; ^1H NMR and ^{13}C NMR ($CDCl_3$): see Table 2; HR ESI-MS (*m*/*z*): 255.1021 $[M+H]^+$ (calc. for $C_{16}H_{14}O_3$, 255.1016).

Acknowledgements

We thank the Engineering and Physical Sciences Research Council for funding.

References

Bennett, G.J., Lee, H.H., 1989. Xanthones from Guttiferae. Phytochemistry 28, 967–998.

Conforti, F., Statti, G.A., Rundis, R., Menichini, F., Houghton, P., 2002. Antioxidant activity of methanolic extract of *Hypericum triquetrifolium* Turra aerial part. Fitoterapia 73, 479–483.

Cox, R.A., Conquest, C., Mallaghan, C., Marples, R.R., 1995. A major outbreak of methicillin-resistant *Staphylococcus aureus* caused by a new phage-type (EMRSA-16). J. Hosp. Infect. 29, 87–106.

Crockett, S.L., Schaneberg, B., Khan, I.A., 2005. Phytochemical profiling of new and old world *Hypericum* (St. John's Wort) species. Phytochem. Anal. 16, 479–485.

Décosterd, L., Stoeckli-Evans, H., Msonthi, J.D., Hostettmann, K., 1986. A new antifungal chromene and a related di-chromene from *Hypericum revolutum*. Planta Med. 52, 429.

Demirci, B., Baser, K.H.C., Crockett, S.L., Khan, I.A., 2005. Analysis of the volatile constituents of Asian *Hypericum* L. (Clusiaceae, Hyperidoideae) species. J. Essent. Oil Res. 17, 659–663.

Dharmaratne, H.R.W., Nanayakkara, N.P.D., Khan, I.A., 2002. Kavalactones from *Piper methysticum*, and their ^{13}C NMR spectroscopic analyses. Phytochemistry 59, 429–433.

Gibbons, S., Udo, E.E., 2000. The effect of reserpine, a modulator of multidrug efflux pumps, on the in vitro activity of tetracycline against clinical isolates of methicillin-resistant *Staphylococcus aureus* (MRSA) possessing the Tet(K) determinant. Phytother. Res. 14, 139–140.

Gibbons, S., Ohlendorf, B., Johnsen, I., 2002. The genus Hypericum – a valuable resource of anti-staphylococcal leads. Fitoterapia 73, 300–304.

Gibbons, S., Moser, E., Hausmann, S., Stavri, M., Smith, E., Clennett, C., 2005. An anti-staphylococcal acylphloroglucinol from *Hypericum foliosum*. Phytochemistry 66, 1472–1475.

Kaatz, G.W., Seo, S.M., Ruble, C.A., 1993. Efflux-mediated fluoroquinolone resistance in *Staphylococcus aureus*. Antimicrob. Agents Chemother. 37, 1086–1094.

Kassu, A., Dagne, E., Abate, D., Castro, A., Van Wyk, B.E., 1999. Ethnomedical aspects of the commonly used toothbrush sticks in Ethiopia. East Afr. Med. J. 76, 651–653.

Kokubun, T., Harborne, J.B., Eagles, J., Waterman, P.G., 1995. Dibenzofuran phytoalexins from the sapwood tissue of *Photinia*, *Pyracantha* and *Crataegus* species. Phytochemistry 39, 1033–1037.

Kokubun, T., Harborne, J.B., Eagles, J., Waterman, P.G., 1995a. Four dibenzofuran phytoalexins from the sapwood from *Mespilus germanica*. Phytochemistry 39, 1039–1042.

Ploss, O., Petereit, F., Nahrstedt, A., 2001. Procyanidins from the herb of *Hypericum perforatum*. Pharmazie 56, 509–511.

Richardson, J.F., Reith, S., 1993. Characterization of a strain of methicillin-resistant *Staphylococcus aureus* (EMRSA-15) by conventional and molecular methods. J. Hosp. Infect. 25, 45–52.

Rocha, L., Marston, A., Potterat, O., Kaplan, M.A., Stoeckli-Evans, H., Hostettmann, K., 1995. Antibacterial phloroglucinols and flavonoids from *Hypericum brasiliense*. Phytochemistry 40, 1447–1452.

Ross, J.I., Farrell, A.M., Eady, E.A., Cove, J.H., Cunliffe, W.J., 1989. Characterisation and molecular cloning of the novel macrolide-streptogramin B resistance determinant from *Staphylococcus epidermidis*. J. Antimicrob. Chemother. 24, 851–862.

Seo, E.K., Huang, L., Wall, M.E., Wani, M.C., Navarro, H., Mukherjee, R., Farnsworth, N.R., Kinghorn, A.D., 1999. New biphenyl compounds with DNA strand-scission activity from *Clusia paralicola*. J. Nat. Prod. 62, 1484–1487.

Shiu, W.K.P., Gibbons, S., 2006. Anti-staphylococcal acylphloroglucinols from *Hypericum beanii*. Phytochemistry 67, 2568–2572.

Trovato, A., Raneri, E., Kouladis, M., Tzakou, O., Taviano, M.F., Galati, E.M., 2001. Anti-inflammatory and analgesic activity of *Hypericum empetrifolium* (Guttiferae). Farmaco 56, 455–457.

Weber, N.D., Murray, B.K., North, J.A., Wood, S.G., 1994. The antiviral agent hypericin has *in vitro* activity against HSV-1 through non-specific association with viral and cellular membranes. Antiviral Chem. Chemother. 5, 83–90.

Fitoterapia 80 (2009) 226–229

Contents lists available at ScienceDirect

Fitoterapia

journal homepage: www.elsevier.com/locate/fitote

A new dihydrodibenzodioxinone from *Hypericum x 'Hidcote'*

Longru Sun [a,b], M. Mukhlesur Rahman [a], Brian W. Skelton [c], Simon Gibbons [a,*]

[a] Centre for Pharmacognosy and Phytotherapy, The School of Pharmacy, University of London, 29–39 Brunswick Square, London WC1N 1AX, UK
[b] Department of Natural Product Chemistry, School of Pharmacy, Shandong University, Jinan 250012, PR China
[c] Chemistry M313, School of Biomedical, Biomolecular & Chemical Sciences, University of Western Australia, Crawley, 6009, Western Australia, Australia

ARTICLE INFO

Article history:
Received 8 December 2008
Received in revised form 21 January 2009
Accepted 22 January 2009
Available online 2 February 2009

Keywords:
Hypericum x 'Hidcote'
Guttiferae

ABSTRACT

One new compound, 4-hydroxy-4a,7-dimethoxy-4,4a-dihydrodibenzo-p-dioxin-2(3H)-one (1), was isolated from the aerial parts of the hybrid *Hypericum x 'Hidcote'*, together with 8 known compounds: caryophyllene-4,5-epoxide, quercetin, quercitrin, quercetin-3-O-β-D-galactopyranoside, epicatechin, betulinic acid methyl ester, β-sitosterol and β-sitosterol glucoside. The structure of the new compound, as well as its absolute configuration, was established by means of spectroscopic data analyses, including 2D NMR spectroscopy and X-ray structural analysis.

1. Introduction

The genus *Hypericum* (Guttiferae) is known to produce antibacterial acylphloroglucinol metabolites, such as the drummondins from *Hypericum drummondii* [1], the hyperbrasilols from *Hypericum brasiliense* [2,3] and hyperforin from *Hypericum perforatum* [4]. These findings prompted us to investigate the antistaphylococcal activity of 34 *Hypericum* species collected from the National *Hypericum* collection at the Royal Botanic Gardens at Wakehurst Place, UK [5]. This work has led to the isolation of several new acylphloroglucinols displaying moderate levels of activity against methicillin-resistant and multidrug-resistant strains of *Staphylococcus aureus* [6,7]. As a part of our ongoing projects on the chemistry and biological activities of natural products from the genus *Hypericum*, we have recently investigated the chemical constituents of *Hypericum x 'Hidcote'*, which is a hybrid of *H. calycinum* and *H. cyathiflorum* widely grown in Europe for its attractive yellow flowers and foliage. To the best of our knowledge, the phytochemistry of this plant has not been investigated previously. Herein we report on the isolation of a new and unusual natural product based on a dibenzodioxinone skeleton given the trivial name hyperhidcotin, together with eight known compounds: caryophyllene-4,5-epoxide, quercetin, quercitrin, quercetin-3-O-β-D-galactopyranoside, β-sitosterol, β-sitosterol glucoside, epicatechin and betulinic acid methyl ester. The structure of the new compound was elucidated by extensive spectroscopic analyses of the 1D and 2D NMR, HRTOFMS spectra and single crystal X-ray structural analysis. The dibenzodioxinone skeleton has not been obtained from plants before, but similar derivatives have been reported from the synthesis literature [8]. The other known compounds were obtained for the first time from this plant.

The new metabolite was evaluated for antibacterial activity against a panel of multidrug-resistant (MDR) and methicillin-resistant *Staphylococcus aureus* (MRSA), but exhibited no activity at 128 μg/ml.

2. Experimental

2.1. General

Optical rotations: Perkin Elmer Polarimeter 341. IR: Perkin Elmer Spectrum 1000 FT-IR Spectrometer. UV: Thermo Electron Corporation UV/vis Spectrophotometer. HRTOFMS (positive-ion mode): Micromass Q-TOF Global Tandem Mass Spectrometer. NMR: Bruker AVANCE 500 Spectrometer (500 MHz for ^{1}H and 125 MHz for ^{13}C).

* Corresponding author. Tel.: +44 207 7535913; fax: +44 207 7535964.
E-mail address: simon.gibbons@pharmacy.ac.uk (S. Gibbons).

0367-326X/$ – see front matter © 2009 Elsevier B.V. All rights reserved.
doi:10.1016/j.fitote.2009.01.012

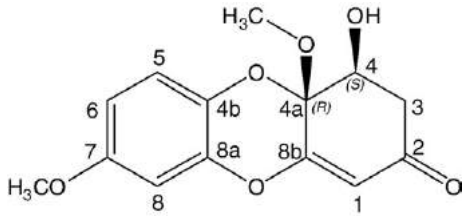

Fig. 1. The structure of compound **1**.

2.2. Plant material

The stem of *Hypericum x* '*Hidcote*' was collected from the National *Hypericum* Collection at the Royal Botanic Gardens Wakehurst Place in August 2005 with accession number 1969-31269. The authenticity of this species has been verified by Dr N.K.B. Robson. A voucher specimen of this collection is maintained at the Centre for Pharmacognosy and Phytotherapy (SG-2005-2/6).

2.3. Extraction and isolation

Dried stems of the plant (923.6 g) were powdered and sequentially extracted with hexane, chloroform and methanol in a Soxhlet apparatus.

VLC fractionation of the hexane extract (16.1 g) on silica gel was performed using the mobile phase hexane, EtOAc and methanol in order of increasing polarity. The fraction eluted with 5% EtOAc in hexane was further subjected to SPE (silica), eluting with hexane-EtOAc mixtures, and the fraction eluted with 6% EtOAc in hexane was separated by repeated preparative thin-layer chromatography (silica; 8% EtOAc in hexane; 5% EtOAc in toluene) to yield caryophyllene-4,5-epoxide (3.9 mg). The fraction eluted with 10% EtOAc in hexane yielded β-sitosterol (12.6 mg) by repeated preparative-TLC (silica; 25% EtOAc in hexane).

The chloroform extract (7.6 g) was fractionated by VLC over silica gel 60H, using hexane-EtOAc and EtOAc-MeOH mixtures of increasing polarity. The eluates were combined on the basis of TLC analysis. The VLC fraction eluted with 5% MeOH in ethyl acetate was separated by repeated preparative TLC (silica; 35% EtOAc in hexane; 30% EtOAc in toluene) to yield compound 1 (7.5 mg).

A portion of the methanol extract (15 g) was fractionated by VLC over silica gel 60H, eluted by $CHCl_3$-MeOH mixtures of increasing polarity and divided into several fractions. The fraction eluted with 5% MeOH in chloroform gave a semisolid residue, which was washed with methanol to afford β-sitosterol glucoside (9.2 mg) as a pale yellow powder. The fraction eluted with 20% MeOH in chloroform was separated by SPE (Strata S1-1 silica), eluting with $CHCl_3$-MeOH mixtures of increasing polarity. Its subfraction eluted with 6% MeOH in chloroform was subjected to preparative TLC (15% MeOH in chloroform) to yield quercetin (5.2 mg). The fraction eluted with 30% MeOH in chloroform, was separated again by VLC over silica gel 60H, eluting with $CHCl_3$-MeOH mixtures of increasing polarity. Its subfraction which was eluted with 15% MeOH in chloroform was later subjected to normal phase preparative TLC (developed with 25% MeOH in chloroform) and then to reversed-phase preparative TLC (developed with 50% MeOH in water) to yield epicatechin (18.9 mg), quercetin-3-O-β-D-galactopyranoside (11.5 mg) and quercitrin (4.3 mg). The known compounds were identified by comparison with data from the literature.

Compound 1, (Fig. 1) 4-hydroxy-4a,7-dimethoxy-4,4a-dihydrodibenzo-p-dioxin-2(3H)-one, colourless crystal; $[\alpha]_D^{20}$ −72.5 (c 0.001, MeOH); UV λ_{max} (logε): 202.5 (4.61), 247.5 (4.34), 295.0 (4.14) nm; IR ν_{max} (solution in $CHCl_3$): 3456, 1648, 1603, 1506, 1445, 1333, 1267, 1205, 1037, 919 cm^{-1}; ^1H NMR (500 MHz, $CHCl_3$) and ^{13}C NMR (125 MHz, $CHCl_3$) see Table 1; positive-ion HRTOFMS m/z: 279.0879 $[M+H]^+$ (calcd for $C_{14}H_{14}O_6$, 279.0863).

2.4. X-ray structure determination of compound **1**

$C_{14}H_{14}O_6$ (fw = 278.25), 100(2) K, monoclinic, $P2_1/n$, a = 13.0930(6), b = 5.1216(1), c = 17.8702(8) Å, β = 90.190 (4)°, V = 1198.32(8) $Å^3$, Z = 4, μ (Mo–K_α) = 0.122 mm^{-1}, ρ_{cal} = 1.542 g cm^{-3}; crystal dimensions: 0.44 × 0.29 × 0.18 mm; 22229 reflections measured (θ_{max} = 37.7°), 6124 were unique (R_{int} = 0.041) and of these 4172 had $I > 2\sigma(I)$ for which final $R1$, $wR2$ values were 0.047 and 0.140, respectively, for 185 parameters. Data were collected using an Oxford Diffraction Gemini diffractometer using Mo–K_α radiation. The structure was solved by direct methods followed by full-matrix refinement on $F2$ using Shelx-97 [9]. All hydrogen atoms were added at calculated positions and refined by use of a riding model with isotropic displacement parameters based on the isotropic displacement parameter of the parent atom. Anisotropic displacement parameters were employed throughout for the non-hydrogen atoms. The molecule is shown in Fig. 3 with non-H atoms drawn with 50% probability ellipsoids. CCDC 710303 contains the supplementary crystallographic data for this paper. These data can be obtained free

Table 1
NMR data of compound 1.

Position	δ_H	δ_C	COSY	NOESY	HMBC (H→C)	
					^2J	^3J
1	5.80 d (0.5)	109.0			C-8b	C-3, C-4a
2		194.6				
3	2.84 m	42.9	H-4	4α-H, 4β-OH	C-4, C-2	C-4a, C-1
4	4.44 m	72.7	H-3, 4-OH	3α-H, 3β-H		
4a		93.8				
4b		134.0				
5	7.04 d (8.5)	118.1	H-6	6-H	C-4b	C-8a, C-7
6	6.66 dd (8.5,2.5)	110.7	H-5,H-8	5-H, 7-OCH_3		C-4b, C-8
7		156.0				
8	6.68 d (2.5)	102.5	H-6	7-OCH_3	C-7	C-4b, C-6
8a		141.2				
8b		162.0				
4-OH	2.64 d (4.5)		H-4	4-H		
4a-OCH_3	3.54 s	54.0				C-4a
7-OCH_3	3.80 s	56.1		6-H, 8-H		C-7

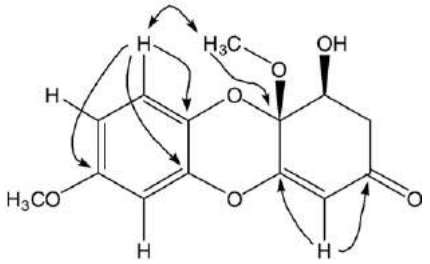

Fig. 2. HMBC correlations (single headed arrows) and NOESY correlations (double headed arrows) of **1**.

of charge from The Cambridge Crystallographic Data Centre via www.ccdc.cam.ac.uk/data_request/cif.

3. Results and discussion

The powdered stem and aerial parts of *Hypericum x* '*Hidcote*' was extracted sequentially with hexane, chloroform and methanol. Vacuum-liquid chromatography (VLC) fractionation of the chloroform extract was subjected to solid phase extraction (SPE) (Strata S1-1 silica, 55 µm, 70A) and preparative thin-layer chromatography (TLC) to yield compound **1** and betulinic acid methyl ester. Compound **1**, recrystallised from toluene and acetone, and its molecular formula was established as $C_{14}H_{14}O_6$ from the $[M+H]^+$ ion peak at m/z 279.0879 (calculated: 279.0863 for $C_{14}H_{14}O_6$) in positive ion HRTOFMS. The mass spectrum showed a further ion peak at m/z 247.0623 corresponding to the $[M-OCH_3]^+$ ion, indicating the presence of a methoxyl group in the molecule. The IR spectrum showed absorption bands for hydroxyl (3456 cm^{-1}), carbonyl (1648 cm^{-1}) and benzene ring (1603, 1506 cm^{-1}), which were confirmed by the ^{13}C NMR data (Table 1). The ^{13}C NMR spectrum exhibited 14 signals, which by ^1H NMR and ^{13}C DEPT-135 spectra corresponded to six quaternary carbons, five methines, one methylene and two methoxyl groups. The aromatic hydrogens at δ 6.66 (dd, $J=8.5$, 2.5 Hz), δ 7.04 (d, $J=8.5$ Hz) and δ 6.68 (d, $J=2.5$ Hz) in the ^1H NMR spectrum of 1 (Table 1) indicated the presence of a 1,2,4-trisubstituted benzene ring. ^1H and ^{13}C signals of this ring were assigned by the correlations of δ 7.04 (H-5) with δ 118.1 (C-5), δ 6.66 (H-6) with δ 110.7 (C-6) and δ 6.68 (H-8) with δ 102.5 (C-8) in the HMQC spectrum. Correlations in the HMBC experiment (Fig. 2) from H-5 to C-4b, C-7 and C-8a (134.0, 156.0 and 141.2), from H-6 to C-4b and C-8 and from H-8 to C-6, C-8a and C-4b (110.7, 141.2 and 134.0) enabled full unambiguous assignment of all of the resonances in this ring. Additionally a correlation of one of the methoxyl hydrogen resonances (δ3.80) with C-7 (156.0) in the HMBC spectrum revealed that this methoxyl was attached to the benzene ring at C-7. This was further supported by NOE correlations between the hydrogens of this methoxyl group and H-6 and H-8 in the NOESY spectrum. The hydrogen resonance at δ 2.64 (d, $J=4.5$ Hz) which had no correlation with any carbon in HMQC spectrum was associated with an hydroxyl group. In the ^1H–^1H COSY experiment, this hydroxyl hydrogen exhibited a correlation with H-4 (δ 4.44, m) which was attached to an oxygen-bearing carbon and H-4 further correlated to a methylene (δ 2.84, m) establishing the partial structure –CH_2–CHOH–. An olefinic hydrogen (H-1, δ5.80) was attached to a double-bond and its HMBC correlations with C-8b and the carbon of a carbonyl group (δ194.6) indicated the partial structure of an α,β-unsaturated ketone. The remaining methoxyl group was positioned on a quaternary carbon (C-4a), as was deduced by the correlation of its hydrogens with C-4a in the HMBC spectrum. In the HMBC spectrum, the correlations of H-1 and H-3 with C-4a, H-1 with C-3 and H-3 with C-1 confirmed that the partial structures –CH_2–CHOH–, α,β-unsaturated ketone and C_{4a}–OCH_3 completed an α,β-unsaturated six-ring ketone moiety (Fig. 2). This moiety was connected to the other benzene ring by two oxygen ether bonds from C-4a and C-8b to C-4b and C-8a, respectively. This was supported by a NOE correlation of the methoxyl group at position 4a with H-5 in the NOESY spectrum. An attempt at assignment of the relative configuration at positions 4 and C-4a however was made by analysis of its NOESY data (Fig. 2). However, no NOE correlation between the hydrogens of the methoxyl at 4a and H-4 could be observed which may indicate that the

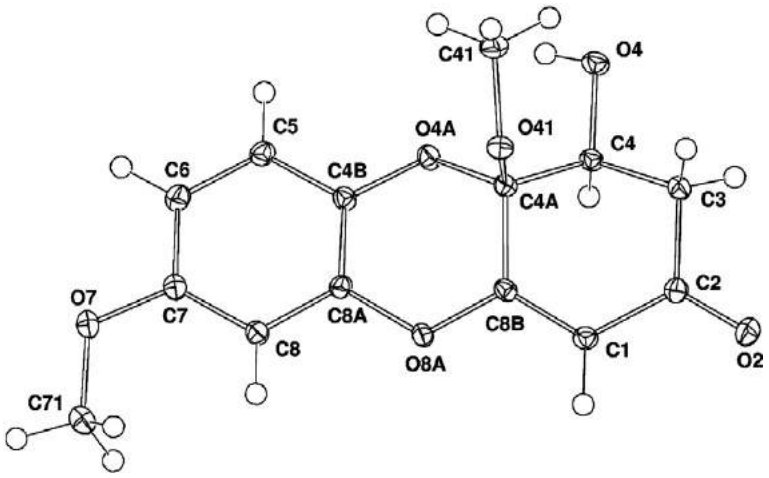

Fig. 3. X-ray crystal structure of compound **1**.

methoxyl at 4a and the hydrogen were *trans* to each other. To prove that this was the case and assign the absolute stereochemistry at these positions, compound **1** was recrystallised from a mixture of toluene and acetone and submitted to single crystal X-ray structural analysis (Fig. 3). This confirmed our NMR assignments and established the absolute stereochemistry at positions 4 and 4a as *S* and *R* respectively. In view of the above data, compound **1** was identified as 4-hydroxy-4a,7-dimethoxy-4,4a-dihydrodibenzo-p-dioxin-2(3H)-one, is given the trivial name hyperhidcotin (Fig. 1) and is reported here for the first time. Dihydrodibenzodioxinones are rare in nature and are presumably biosynthesised by simple phenolic coupling between two phenols. The oxygenation pattern in ring-C of **1** is typical for a phloroglucinol (1,3,5-trihydroxybenzene) natural product common to *Hypericum* and to the Guttiferae as a whole.

Acknowledgement

One of the authors (LS) is grateful to the China Scholarship Council and Shandong University for providing a scholarship to conduct this research at the School of Pharmacy, University of London.

References

[1] Jayasyriya H, Clark AM, McChesney JD. J Nat Prod 1991;54:1314.
[2] Rocha L, Marston A, Potterat O, Kaplan MAC, Stoeckli-Evans H, Hostettmann K. Phytochemistry 1995;40:1447.
[3] Rocha L, Marston A, Potterat O, Kaplan MAC, Hostettmann K. Phytochemistry 1996;42:185.
[4] Schempp CM, Pelz K, Wittmer A, Schopf E, Simon JC. Lancet 1999;353:2129.
[5] Gibbons S, Ohlendorf B, Johnsen I. Fitoterapia 2002;73:300.
[6] Gibbons S, Moser E, Hausmann S, Stavri M, Smith E, Clennett C. Phytochemistry 2005;66:1472.
[7] Shiu WKP, Gibbons S. Phytochemistry 2006;67:2568.
[8] Howe R, Rao BS. J Chem Soc C 1968;19:2436.
[9] Sheldrick GM. Acta Crystallogr 2008;A64:112.

Phytochemistry 69 (2008) 1915–1918

Contents lists available at ScienceDirect

Phytochemistry

journal homepage: www.elsevier.com/locate/phytochem

Guaianolide sesquiterpenes from *Pulicaria crispa* (Forssk.) Oliv.

Michael Stavri [a], K.T. Mathew [b], Andrew Gordon [c], Steven D. Shnyder [c], Robert A. Falconer [c], Simon Gibbons [a,*]

[a] *Centre for Pharmacognosy and Phytotherapy, The School of Pharmacy, University of London, 29-39 Brunswick Square, London WC1N 1AX, UK*
[b] *The Herbarium, Department of Biological Sciences, Kuwait University, P.O. Box 5969, Safat 13060, Kuwait*
[c] *Institute of Cancer Therapeutics, School of Life Sciences, University of Bradford, Bradford BD7 1DP, UK*

ARTICLE INFO

Article history:
Received 13 January 2008
Received in revised form 17 March 2008
Available online 28 April 2008

Keywords:
Pulicaria crispa
Sesquiterpene
Guaianolide
Pseudoguaianolide
Mycobacterium

ABSTRACT

A phytochemical study of the asteraceous herb *Pulicaria crispa* (Forssk.) Oliv. resulted in the characterisation of three guaianolide sesquiterpenes, 2α,4α-dihydroxy-7αH,8αH,10αH-guaia-1(5),11(13)-dien-8β,12-olide (**1**), 1α,2α-epoxy-4β-hydroxy-5αH,7αH,8αH,10αH-guaia-11(13)-en-8β,12-olide (**2**) and 5,10-*epi*-2,3-dihydroaromatin (**3**). The structures were assigned on the basis of extensive 1 and 2D NMR experiments. Compound **3** exhibited weak antimycobacterial activity against *Mycobacterium phlei* with a minimum inhibitory concentration of 0.52 mM and cytotoxicity (IC_{50} of 5.8 ± 0.2 μM) in a human bladder carcinoma cell line, EJ-138.

1. Introduction

Pulicaria crispa (Forssk.) Oliv. [syn. *Pulicaria undulata* (L.) C.A.Mey., *Francoeuria crispa* (Forssk.) Cass.] is an annual herb or sometimes a perennial sub shrub, belonging to the family Asteraceae, producing small bright yellow flowers. This species is distributed in Saudi Arabia, Kuwait, Iran, Iraq, Egypt, Afghanistan, Pakistan, India and parts of north and west tropical Africa (Boulos, 2002; Al-Rawi, 1987). *P. crispa* is a medicinal plant used by people of southern Egypt and Saudi Arabia to treat inflammation and also as an insect repellent (Ross et al., 1997) and is also used as an herbal tea. Phytochemical studies of this herb have identified it to be a rich source of sesquiterpene lactones of the guaianolide (Dendougui et al., 2000), eudesmanolide (San Feliciano et al., 1989) and xanthanolide classes as well as kaurane diterpenes (Abdel-Mogib et al., 1990).

2. Results and discussion

Compound **1** (Fig. 1) was isolated as a colourless oil and a molecular formula of $C_{15}H_{20}O_4$ $[M]^+$ (264.1355) was assigned by HR-EIMS. The ^1H and ^{13}C NMR signals (Table 1) were characteristic of a guaianolide sesquiterpene, which is distinctive of the genus *Pulicaria* (Dendougui et al., 2000). Assuming a guaianolide skeleton for compound **1**, a methyl singlet attributed to C-15 exhibited a ^2J correlation to C-4 and ^3J correlations to a methylene carbon (C-3) and an olefinic quaternary carbon (C-5). By inspection of the COSY spectrum, the methylene hydrogens at C-3 coupled to a deshielded oxymethine hydrogen (H-2, δ_H 4.86), which in turn gave a ^2J correlation to a second olefinic quaternary carbon (δ_C 140.8, C-1) as well as a ^3J correlation to C-5. H_2-3 confirmed the assignment of a cyclopentene ring system with two ^3J correlations to C-1 and C-5. The downfield appearance of C-2 and C-4 in the ^{13}C NMR spectrum as well as H-2, in the ^1H NMR spectrum indicated that hydroxyl groups should be placed at these positions therefore completing ring A. The oxymethine group at position 2 was allylic causing the appearance of both the carbon and hydrogen signals to be shifted further downfield. A second methyl (C-14) appearing as a doublet in the ^1H spectrum gave a COSY coupling to a methine proton (H-10) and in the HMBC spectrum exhibited two ^3J correlations to C-1 and C-9, placing the methyl adjacent to ring A. H_2-9 gave a strong COSY coupling towards a downfield methine hydrogen (H-8, δ_H 4.76) which in turn coupled to H-7. The 7-membered ring of ring B was completed by a COSY coupling between H-7 and methylene H_2-6 and by ^2J and ^3J HMBC correlations from H_2-6 and H-7 to C-5, respectively. A ^3J correlation between H-7 and an *exo*-cyclic olefinic methylene carbon (C-13) placed this *exo*-cyclic methylene on ring C of the molecule. ^2J and ^3J HMBC signals between the hydrogens of this *exo*-methylene and its olefinic quaternary partner (C-11) and an ester carbonyl carbon (C-12) confirmed the position of these groups as part of the guaianolide ring-C lactone. The deshielded nature of H-8, indicated that it was attached to a carbon bearing an oxygen, completing ring C by forming a 5-membered lactone ring system between C-8 and C-12.

* Corresponding author. Tel.: +44 207 7535913; fax: +44 207 7535909.
E-mail address: simon.gibbons@pharmacy.ac.uk (S. Gibbons).

0031-9422/$ - see front matter © 2008 Elsevier Ltd. All rights reserved.
doi:10.1016/j.phytochem.2008.03.012

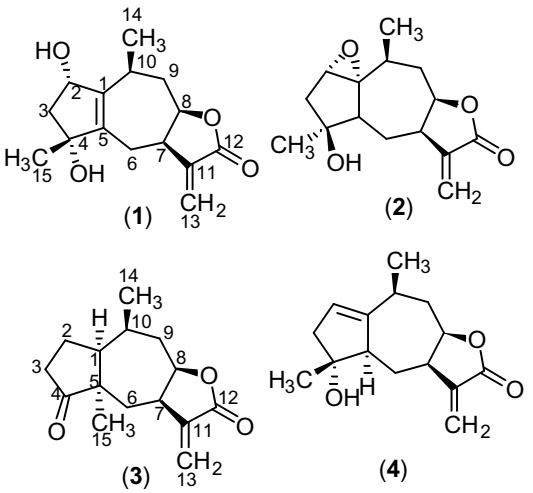

Fig. 1. Structures of **1–4**.

The relative stereochemistry of **1** was determined by inspection of the ^{1}H and NOESY spectra. An NOE correlation between H-7 and H-8 indicated that these two hydrogens are on the same face of the molecule. As only the coupling constants could be measured for H-8 and not for H-7, a model of this molecule indicated that these hydrogens were *cis* (α-oriented). This correlated well with one of the coupling constants measured for H-8 of 8.5 Hz and helped to confirm the *cis* orientation. A similar coupling constant measured for the known compound **4** also corroborated this assignment. A 1,3 NOE interaction between H-8 and H-10 allowed the assignment of H-10 as being α, therefore methyl-14 must be positioned in a β-orientation. A third NOE between methyl-14 and H-2 placed H-2 in a β-orientation and so the hydroxyl attached to C-2 must be α. An NOE between H-2 and the downfield hydrogen of the methylene at position 3 (δ_H 2.35) meant that this proton must be on the same face of the molecule (β). Thus a 1,3 interaction between $H_β$-3 and methyl-15 showed that this group should also be assigned as β. This was further confirmed by an NOE correlation between methyl-15 and both hydrogens of H_2-6. Compound **1** is therefore assigned as 2α,4α-dihydroxy-7αH,8αH,10αH-guaia-1(5),11(13)-dien-8β,12-olide and is reported here for the first time.

Compound **2** was isolated as a pale yellow oil and the HR-EIMS revealed a molecular formula of $C_{15}H_{20}O_4$ $[M]^+$ (264.1363). The NMR data were similar to those of **1**. The ^{13}C NMR spectrum indicated the presence of 15 carbons, including a carbonyl, two olefinic and two oxygenated quaternary carbons. The ^{1}H NMR spectrum provided signals for an *exo*-methylene group, two methyls and two deshielded methine hydrogens. The ^{1}H spectrum provided evidence to suggest that **2** was a guaianolide due to the similarity in the spectral data when compared with compound **1**. The structure of **2** (Fig. 1) was closely related to that of **1**, except for the absence of a double bond between C-1 and C-5 and the absence of an hydroxyl group attached at C-2. Instead ring A of **2** was saturated with the formation of an epoxide between C-1 and C-2. The remainder of the guaianolide structure was identical to that of **1** with similar HMBC and COSY correlations. The ^{13}C resonances at δ_C 72.4, (C-1) and δ_C 59.6, (C-2) were characteristic for epoxide carbons (Trifunovic et al., 2006) especially for methine C-2. The hydroxyl hydrogen was also detected in the ^{1}H spectrum as a sharp singlet and provided information on point of attachment, with a ^2J correlation to C-4 and a ^3J correlation to C-15. This further corroborated the structure of ring-A as a cyclopentane ring. The ^{1}H NMR data for **2** were in close agreement with that of the literature (Zdero et al., 1988). However, the NOESY spectrum provided evidence to indicate that **2** was in fact the epimer of the guaianolide isolated by Zdero et al., at the C-4 position and stereochemistry at C-2, 7, 8 and 10 were identical to that in **1**.

H-7 showed an NOE to H-5, which in turn gave a 1,3 interaction with the methyl hydrogens of C-15. This indicated that both H-5 and H_3-15 must also be on the same face of the molecule as H-7 in an α-orientation. The methylene hydrogens at C-6 each gave an NOE to H_3-15 and a molecular model of this molecule showed that these hydrogens were equidistant from the methyl group further confirming the relative stereochemical assignment at C-4. The hydroxyl group must therefore be in a β-orientation. This is the point of difference between the relative stereochemistry of **2** and that assigned by Zdero et al. The guaianolide detailed in the literature was described with the methyl group in a β-orientation and the hydroxyl group in an α-orientation. The C-14 methyl hydrogens gave a 1,3 interaction to the epoxide methine (H-2) placing this

Table 1
^{1}H (500 MHz) and ^{13}C (125 MHz) spectral data of **1–4**. **1** and **4** were recorded in CD_3OD, **2** was recorded in $CDCl_3$ and **3** was recorded in C_6D_6

Position	1		2		3		4	
	^{1}H	^{13}C	^{1}H	^{13}C	^{1}H	^{13}C	^{1}H	^{13}C
1	–	140.8	–	72.4	1.16 *m*	48.6	–	151.1
2	4.86 *m*	87.4	3.59 *s*	59.6	0.97 *ddd* (9.0, 3.0) 1.42 *dddd* (12.5, 9.5, 6.5, 1.0)	24.6	5.37 t (1.5)	120.3
3	2.09 *dd* (13.5, 4.5) 2.35 *dd* (13.5, 7.0)	46.0	1.77 *d* (14.5) 2.06 *d* (15.0)	40.6	1.72 *ddd* 2.01 *m*	35.6	2.37 *dd* (16.0)	47.5
4	–	81.6	–	78.2	–	222.4	–	82.1
5	–	144.9	2.02 *dd* (13.0, 2.0)	54.9	–	50.2	2.48 *d* (12.5)	59.7
6	2.41 *dd* (15.0, 5.0) 2.46 *ddt* (15.0, 5.0, 2.5)	25.5	1.38 *bdd* (12.5) 1.79 *m*	30.6	1.11 *dd* (13.0, 2.5) 2.19 *m*	35.4	1.46 *dd* (12.5) 1.99 *m*	32.7
7	3.44 *m*	44.1	3.21 *m*	41.9	2.21 *m*	45.1	3.37 *ddd* (12.0, 9.5, 4.0)	43.3
8	4.76 *ddd* (12.5, 8.5, 4.5)	81.5	4.72 *ddd* (12.0, 7.5, 4.5)	79.1	3.69 *ddd* (12.0, 9.0, 3.0)	81.0	4.82 *m*	82.6
9	1.99 *m*	37.2	1.73 *d* (14.0) 2.07 *dd* (13.5, 0.5)	35.3	0.95 *d* (12.5) 2.02 *d* (17.5)	44.8	1.56 *dd* (12.0) 1.93 *m*	39.1
10	2.65 *dq* (12.0, 7.0, 2.0)	31.0	2.14 *m*	30.0	1.24 *m*	30.0	2.24 *bs*	32.4
11	–	141.6	–	140.1	–	142.1	–	142.4
12	–	172.0	–	169.5	–	169.9	–	172.1
13	5.75 *d* (2.5) 6.21 *d* (3.0)	123.1	5.65 *d* (2.0) 6.29 *d* (2.5)	123.3	4.99 *d* (3.0) 6.04 *d* (3.5)	119.3	5.73 *d* (2.5) 6.20 *d* (3.0)	122.9
14	1.18 *d* (7.0)	20.6	0.90 *d* (7.0)	17.2	0.64 *d* (6.5)	20.4	1.22 *d* (6.5)	20.6
15	1.21 *s*	27.0	1.17 *s*	23.5	0.56 *s*	22.4	1.25 *s*	24.7
4-OH			3.70 *s*					

proton on the same face of the molecule as H_3-14 (β). Therefore the epoxide must be α-oriented and this follows the representation of the epimeric form of the molecule described by Zdero et al. (1988). Compound **2** is assigned as 1α,2α-epoxy-4β-hydroxy-5αH,7αH,8αϖ H,10αH-guaia-11(13)-en-8β,12-olide and is reported here for the first time.

Compound **3** was isolated as a white amorphous powder and the accurate EI-MS in the positive mode provided the molecular ion of *m/z* 248.1412 to establish a molecular formula of $C_{15}H_{20}O_3$. The ^{1}H NMR and ^{13}C NMR spectra provided signals for a sesquiterpene, but this time for a pseudoguaianolide sesquiterpene. The HMBC spectrum provided similar signals as for the previous guaianolide sesquiterpenes discussed above, again with notable differences occurring in ring A. The position of methyl-15 strongly indicated that a Wagner–Meerwein rearrangement had taken place, moving this group from C-4 to C-5 of the molecule to give a pseudoguaianolide. The normal biosynthetic pathway from the C_{15} precursor farnesyl pyrophosphate would place this methyl group at C-4. However, in the case of **3**, C-4 had been oxidised to a ketonic carbonyl. Methyl-15 appeared as a singlet and gave a ^2J correlation to a quaternary carbon C-5 (δ_C 50.2) as well as ^3J correlations to C-1 (δ_C 48.6), C-6 (δ_C 35.4) and the carbonyl of C-4 (δ_C 222.4). This ketonic carbonyl was highly deshielded and this was due to the highly strained nature of the cyclopentane ring (ring A). The methylene hydrogens of C-3 gave a COSY correlation with H_2-2, which in turn gave a further COSY correlation to H-1. The methine proton, H-1, also gave a COSY correlation to H-10, which in turn gave a COSY signal to H_2-9 and to a methyl doublet (H_3-14) placing these groups here. The methylene protons attached at C-9 then gave a COSY correlation to the oxymethine proton, H-8. A COSY correlation between H-8 and H-7 indicated that they should be placed at the ring junction of ring B and C as seen in compounds **1** and **2**. This was confirmed by an allylic coupling detected between H-7 and the *exo*-methylene hydrogens H_2-13. The COSY correlations detected for **3** were similar to those of the previously discussed guaianolides.

The relative stereochemistry of **3** (Fig. 1) was achieved by NOE's detected in the NOESY spectrum along with analysis of measured coupling constants. An NOE between H-8 and H-7 placed these protons on the same face of the molecule in an α-orientation. The large coupling constant (9.0 Hz) again indicated that these hydrogens were *cis*. A second NOE between H-8 and H-10 also placed these hydrogens on the same face of the molecule (α), therefore methyl-14 must be β-oriented. This was further confirmed by NOE's between both H_2-2α and H_2-2β to methyl-14. A molecular model showed that the methylene hydrogens were equidistant with respect to methyl-14, whereas if the methyl group were α-orientated this would not be possible. An NOE between H-8 and H-1 also placed this hydrogen in an α-orientation, thus confirming the relative stereochemistry at this position. Finally, methyl-15 exhibited NOE's with H-10 and H_2-3α placing this group on the same face of the molecule as H-1, H-7, H-8 and H-10 (α).

Compound **3** has been isolated previously (Abdel-Mogib et al., 1990; Bohlmann and Mahanta, 1979; Rustaiyan et al., 1987), however the relative stereochemistry of this compound differs from all of these compounds referred to in at least one position. All published literature has quoted the ^{1}H NMR data in deuterated chloroform, which suffers from signal overlap. However, for the purpose of comparing the ^{1}H NMR data with that of the literature, **3** was also analysed in deuterated chloroform. The ^{1}H NMR data for **3** was in agreement with that of the literature for 2,3-dihydroaromatin (Merfort and Wendisch, 1993) with the exception of H-7 and H-8 which were reported to be further downfield. The downfield values reported for these hydrogens are consistent with previous literature articles for guaianolides that have these protons in a *cis* (α) arrangement (Zdero et al., 1988), whereas they appear more upfield when H-7 (~2.75 ppm) and H-8 (~4.30 ppm) are *trans* (Abdel-Mogib et al., 1990; Rustaiyan et al., 1987). To confirm this relative assignment the NOESY experiment for **3** acquired in deuterated benzene again indicated that H-7 and H-8 should be *cis* (α-oriented). Compound **3** differs from 2,3-dihydroaromatin at positions 5 and 10. The methyl groups attached to these carbons in compound **3** are β- and α-oriented, respectively. However in 2,3-dihydroaromatin the methyl groups at positions 5 and 10 are α- and β-oriented, respectively. The pseudoguaianolide **3** is reported here for the first time as 5,10-*epi*-2,3-dihydroaromatin. 5,10-*epi*-2,3-Dihydroaromatin also exhibited weak antimycobacterial activity against *Mycobacterium phlei* with a minimum inhibitory concentration (MIC) of 0.52 mM. Whilst the activity recorded is weak it can provide a starting point for analogues with greater activity, particularly as the known guaianolide aromaticin, similar to **3**, has been reported to exert an antimycobacterial effect with an MIC of 0.064 mM (Cantrell et al., 2001; Copp, 2003).

Compound **3** was evaluated in vitro for anti-cancer activity in an established human bladder carcinoma cell line, EJ-138 and demonstrated promising activity in this cell line, with an IC_{50} of 5.8 ± 0.2 μM.

Compound **4** was isolated as a colourless oil and solved for a molecular formula of $C_{15}H_{20}O_3$ by ESI-MS. The ^{1}H NMR spectral data were identical to those of 1,2-dehydro-1,10α-dihydropseudoivalin (Zdero et al., 1988) which has previously been isolated from *Pulicaria sicula* and this is the first report of the ^{13}C NMR data for this compound and the first report of the full NMR data in deuterated methanol (Table 1).

3. Experimental

3.1. General experimental techniques

NMR spectra were recorded on a Bruker AVANCE 500 MHz spectrometer. Chemical shift values (δ) were reported in parts per million (ppm) relative to appropriate internal solvent standard and coupling constants (J values) are given in Hertz. Mass spectra were recorded on a Finnigan MAT 95 high resolution, double focusing, magnetic sector mass spectrometer. Accurate mass measurement was achieved using voltage scanning of the accelerating voltage. This was nominally 5 kV and an internal reference of heptacosa was used. Resolution was set between 5000 and 10,000.

IR spectra were recorded on a Nicolet 360 FT-IR spectrophotometer and UV spectra on a Thermo Electron Corporation Helios spectrophotometer.

The cancer cell growth inhibition assay details are provided in the supporting information.

3.2. Plant material

The plant material used for this study was collected from KSIR field station, in the Kebd area of Kuwait on the 27th of April 1999. The material was identified by K.T. Mathew and a voucher specimen (KTM 4612, collected by Simon Gibbons and K.T. Mathew) is deposited at the Kuwait University Herbarium (KTUH).

3.3. Extraction and isolation

The air dried aerial parts of *P. crispa* (185 g) were coarsely powdered and sequentially extracted in a Soxhlet apparatus with hexane (3.5 L), chloroform (3.5 L) and finally methanol (3.5 L). The hexane extract (6.7 g) was subjected to vacuum liquid chromatography (VLC) on silica gel (10 g) eluting with hexane containing 10% increments of ethyl acetate to yield 12 fractions. The fraction eluted with 80% ethyl acetate underwent further fractionation by Sephadex LH-20 chromatography eluting with dichloromethane (DCM) followed

by methanol. Final purification of the methanol fraction by multiple preparative thin layer chromatography (TLC) in reverse phase mode (C_{18}; H_2O:methanol, 1:1) (two times) afforded **1** (7.6 mg). Compound **4** was purified from the same VLC fraction as **1**. DCM fraction 3 of Sephadex LH-20 chromatography was subjected to solid phase extraction using a 6:4 methanol:H_2O system to purify **4** (12 mg). VLC fraction 7 (6:4 ethyl acetate:hexane) was subjected to Sephadex LH-20 chromatography eluting with DCM followed by multiple preparative TLC of fraction 2 in normal phase mode (65:35 hexane:ethyl acetate; two times). This afforded compound **2** (9.5 mg). VLC fraction 6 (1:1 hexane:ethyl acetate) was also subjected to Sephadex LH-20 chromatography, eluting with DCM. On addition of hexane to fraction 2 a white precipitate was observed. Three washes of the precipitate with hexane followed by decanting the supernatant enabled the purification of compound **3** (100 mg).

3.4. 2α,4α-Dihydroxy-7αH,8αH,10αH-guaia-1(5),11(13)-dien-8β,12-olide (**1**)

Colourless oil; $[\alpha]_D^{23} + 37.0^\circ$ (*c* 0.378, $CHCl_3$); UV (CH_3OH): λ_{max}: ($\log \varepsilon$) 218 (8.56) nm; IR ν_{max} (thin film) cm^{-1}: 3352, 2963, 1748, 1653, 1276, 986; ^1H NMR (500 MHz, CD_3OD) and ^{13}C NMR (125 MHz, CD_3OD) see Table 1. HREIMS *m/z* 264.1355 (calc. for $C_{15}H_{20}O_4$, 264.1362).

3.5. 1α,2α-Epoxy-4β-hydroxy-5αH,7αH,8αH,10αH-guaia-11(13)-en-8β,12-olide (**2**)

Pale yellow oil; $[\alpha]_D^{23} + 33.7^\circ$ (*c* 0.475, $CHCl_3$); UV (CH_3OH): λ_{max}: ($\log \varepsilon$) 214 (8.52) nm; IR ν_{max} (thin film) cm^{-1}: 3566, 2933, 1761, 1653, 1271, 1128; ^1H NMR (500 MHz, $CDCl_3$) and ^{13}C NMR (125 MHz, $CDCl_3$) see Table 1. HREIMS *m/z* 264.1363 (calc. for $C_{15}H_{20}O_4$, 264.1362).

3.6. 5,10-epi-2,3-Dihydroaromatin (**3**)

White amorphous powder; $[\alpha]_D^{25} + 104.8^\circ$ (*c* 4.75, $CHCl_3$); UV (ACN): λ_{max}: ($\log \varepsilon$) 222 (7.20) nm; IR ν_{max} (thin film) cm^{-1}: 2968, 2931, 1763, 1736, 1125, 996; ^1H NMR (500 MHz, C_6D_6) and ^{13}C NMR (125 MHz, C_6D_6) see Table 1. HREIMS *m/z* 248.1412 (calc. for $C_{15}H_{20}O_3$, 248.1413).

3.7. 1,2-Dehydro-1,10α-dihydropseudoivalin (**4**)

Colourless oil; $[\alpha]_D^{24} + 23.9^\circ$ (*c* 0.418, $CHCl_3$); UV (CH_3OH): λ_{max}: 218 nm; IR ν_{max} (thin film) cm^{-1}: 3420, 2963, 1759, 1270, 1128, 969; ^1H NMR (500 MHz, CD_3OD) and ^{13}C NMR (125 MHz, CD_3OD) see Table 1. Negative ESI-MS: *m/z* = 293.1 $[M-H+2Na]^-$.

3.8. Bacterial strain and antibacterial assay

M. phlei ATCC 11758 was obtained from NTCC. *M. phlei* was cultured on Columbia blood agar (Oxoid) supplemented with 7% defibrinated horse blood (Oxoid) and incubated for 72 h prior to MIC determination. A bacterial inoculum equivalent to 5×10^5 cfu/mL was prepared in normal saline using the 0.5 McFarland turbidity standard followed by dilution. The MIC was recorded as the lowest concentration at which no bacterial growth was observed (Gibbons and Udo, 2000). Ethambutol was used as a positive control, whilst growth and sterile controls were also performed.

3.9. Cancer cell line

The EJ-138 human bladder carcinoma cell line (ECACC, Salisbury, UK) was cultured in RPMI 1640 cell culture medium supplemented with 1 mM sodium pyruvate, 2 mM L-glutamine and 10% fetal bovine serum (all from Sigma, Poole, UK).

Acknowledgments

We thank the Engineering and Physical Sciences Research Council (Grant No. GR/R47646/01) for a multi-project equipment grant. The School of Pharmacy is thanked for a doctoral Scholarship to MS.

Appendix A. Supplementary data

Supplementary data associated with this article can be found, in the online version, at doi:10.1016/j.phytochem.2008.03.012.

References

Abdel-Mogib, M., Jakupovic, J., Dawidar, A.M., Metwally, M.A., Abou-Elzahab, M., 1990. Sesquiterpene lactones and kaurane glycosides from *Francoeuria crispa*. Phytochemistry 29, 2581–2584.

Al-Rawi, A., 1987. The Flora of Kuwait, vol. 2. Alden Press, Oxford.

Bohlmann, F., Mahanta, P.K., 1979. Zwei neue pseudoguajanolide aus *Telekia speciosa*. Phytochemistry 18, 887–888.

Boulos, L., 2002. Flora of Egypt, vol. 3. Al-Hadara Publishing, Cairo, Egypt.

Cantrell, C.L., Franzblau, S.G., Fischer, N.H., 2001. Antimycobacterial plant terpenoids. Planta Medica 67, 685–694.

Copp, B.R., 2003. Antimycobacterial natural products. Natural Product Reports 20, 535–557.

Dendougui, H., Benayache, S., Benayache, F., Connoly, J.D., 2000. Sesquiterpene lactones from *Pulicaria crispa*. Fitoterapia 71, 373–378.

Gibbons, S., Udo, E.E., 2000. The effect of reserpine, a modulator of multidrug efflux pumps, on the in vitro activity of tetracycline against clinical isolates of methicillin resistant *Staphylococcus aureus* (MRSA) possessing the tet(K) determinant. Phytotherapy Research 14, 139–140.

Merfort, I., Wendisch, D., 1993. Sesquiterpene lactones of *Arnica cordifolia*, subgenus *Austromontana*. Phytochemistry 34, 1436–1437.

Ross, S.A., El-Sayed, K.A., El-Sohly, M.A., Hamann, M.T., Abdel-Halim, O.B., Ahmed, A.F., Ahmed, M.M., 1997. Phytochemical Analysis of *Geigeria alata* and *Francoeuria crispa* essential oils. Planta Medica 63, 479–482.

Rustaiyan, A., Jakupovic, J., Chau-Thi, T.V., Bohlmann, F., Sadjadi, A., 1987. Further sesquiterpene lactones from the genus *Dittrichia*. Phytochemistry 26, 2603–2606.

San Feliciano, A., Medarde, M., Gordaliza, M., Del Olmo, E., Miguel del Corral, J.M., 1989. Sesquiterpenoids and phenolics of *Pulicaria paludosa*. Phytochemistry 28, 2717–2721.

Trifunovic, S., Vajs, V., Juranic, Z., Zizak, Z., Tesevic, V., Macura, S., Milosavljevic, S., 2006. Cytotoxic constituents of *Achillea clavennae* from Montenegro. Phytochemistry 67, 887–893.

Zdero, C., Bohlmann, F., Rizk, A.M., 1988. Sesquiterpene lactones from *Pulicaria sicula*. Phytochemistry 27, 1206–1208.

NPC Natural Product Communications

2008
Vol. 3
No. 1
1 - 3

A Novel Sesquiterpene from *Pulicaria crispa* (Forssk.) Oliv.

Michael Stavri[a], Koyippally T. Mathew[b] and Simon Gibbons[a]

[a]*Centre for Pharmacognosy and Phytochemistry*, *The School of Pharmacy*, *University of London*, *29-39 Brunswick Square*, *London WC1N 1AX*, *U.K.*

[b]*The Herbarium*, *Department of Biological Sciences*, *Kuwait University*, *P.O. Box 5969*, *Safat 13060*, *Kuwait*

simon.gibbons@pharmacy.ac.uk

Received: September 18th, 2007; Accepted: October 3rd, 2007

Dedicated to Professor Peter G Waterman, one of the pioneers of phytochemical research.

Using 1- and 2-dimensional NMR experiments and high-resolution mass spectrometry, a novel sesquiterpene, possessing a new skeleton, has been characterized from the *n*-hexane extract of the aerial parts of *Pulicaria crispa* (Asteraceae) as *rel*-2α,6α-dimethyltetracyclo-decal-3-en-2,12-diol-8α,13-olide and given the trivial name pulicrispiolide.

Keywords: *Pulicaria crispa,* Asteraceae, sesquiterpene lactone.

The genus *Pulicaria* Gaertner (syn. *Francoeuria* Cass.) comprises approximately 80 species widely distributed throughout Europe and Asia [1]. *Pulicaria crispa* (Forssk.) Oliv. [syn. *P. undulata* (L.) C.A. Mey., *Francoeuria crispa* (Forssk.) Cass.] is an annual herb producing small bright yellow flowers and is prevalent in Saudi Arabia, Kuwait, Iran, Iraq, Afghanistan, Pakistan, India, parts of north and west tropical Africa and Egypt [2, 3].

The species is used medicinally in southern Egypt and Saudi Arabia to treat inflammation and as an insect repellant [4]. Previous studies have centered on the isolation of many sesquiterpene lactones belonging to the guaianolide [5], eudesmanolide [6] and xantholide classes, and kaurane diterpenes [7].

Compound **1** was isolated as a pale yellow oil from the *n*-hexane extract of *P. crispa*. Accurate mass measurement yielded an ion at *m/z* 246.1264 [M-H_2O]+, which gave the expected formula, less a water molecule, of $C_{15}H_{18}O_3$. The ^1H and ^{13}C NMR spectra (Table 1) showed signals for two olefinic hydrogens, three methylene groups, two oxymethine groups, two methyl moieties, and an ester carbonyl carbon. From the HMBC data

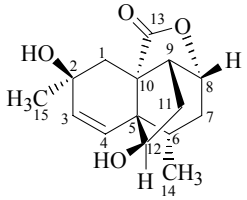

(**1**)

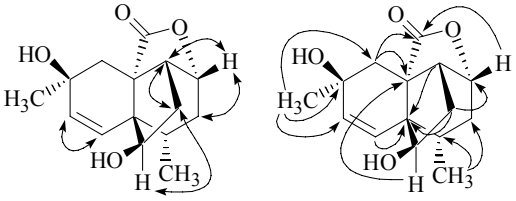

Figure 1: COSY (double headed arrows) and HMBC (single headed arrows) correlations for compound **1**.

(Figure 1), methyl-15 (δ_H 1.25) appeared as a singlet and gave a ^2J correlation with a quaternary carbon, C-2 (δ_C 69.8), and ^3J correlations to a methylene carbon (C-1, δ_C 44.7) and an olefinic carbon (δ_C 142.2, C-3). Due to the downfield resonance of C-2, an hydroxyl group was placed there.

The olefinic proton, H-3, exhibited a COSY correlation with its olefinic partner, H-4 (δ_H 5.98 d, J = 8.5 Hz, δ_C 129.2, C-4) and both showed

Table 1: ^{1}H (500 MHz) and ^{13}C (125 MHz) NMR spectroscopic data for **1**.

Position	^{1}H	^{13}C	^{2}J	^{3}J
1	1.31 d (13.0)	44.7	C-2, C-10	C-3, C-5, C-9, C-13, C-15
	2.15 d (13.5)			
2	-	69.8		
3	6.34 d (8.5)	142.2	C-2	C-5, C-15
4	5.98 d (8.5)	129.2	C-5	C-2, C-6
5	-	53.5		
6	1.45 t (8.0)	30.4	C-5, C-7, C-14	C-8, C-10, C-12
7	1.26 m	31.8	C-6, C-8	C-5, C-9, C-14
	1.36 bd (2.5)			
8	4.03 dt (7.0, 2.5)	80.5		C-6, C-13
9	2.21 bt (7.5)	50.9	C-8	C-1, C-5, C-7, C-12
10	-	49.6		
11	1.39 d (4.0)	35.2	C-9, C-12	C-5, C-8
	1.60 dd (15.0, 8.5)			
12	3.24 d (4.0)	83.7		C-9, C-10
13	-	177.7		
14	1.16 d (7.5)	21.7	C-6	C-5, C-7
15	1.25 s	24.3	C-2	C-1, C-3

an HMBC correlation with a quaternary carbon placed at C-5 (δ_C 53.5). The ^{13}C resonance for C-5 was characteristic of a quaternary carbon at a ring junction [8]. The olefinic hydrogen, H-4, also showed a ^{3}J correlation with a methine carbon (δ_C 30.4, C-6), which in turn exhibited a ^{2}J HMBC correlation and COSY correlation with a second methyl group (δ_H 1.16 d, J = 7.5 Hz, δ_C 21.7, C-14). Methyl-14 showed a ^{3}J correlation with C-5 and a methylene group at C-7. COSY correlations between H_2-7 and a deshielded proton H-8 (δ_H 4.03 dt, J = 7.5, 2.5 Hz), and H-8 and H-9 (δ_H 2.21 bt, J = 7.5 Hz) placed these groups there. ^{2}J and ^{3}J correlations between H_2-1 and H-6 respectively, with a quaternary carbon C-10 (δ_C 49.6) completed rings A and B of this sesquiterpene. The methine proton H-9 showed a COSY correlation with the methylene protons of H_2-11, which in turn gave a COSY correlation with a deshielded methine proton, H-12 (δ_H 3.24 d, J = 4.0 Hz, δ_C 83.7). Again, due to the downfield appearance of C-12, an hydroxyl group was placed here. ^{3}J HMBC correlations between H-9 and C-5, between H-9 and C-12 and also between H_2-11 and C-5 confirmed that C-12 should be connected to C-5 forming a cyclopentane ring (ring C). This was further confirmed by a ^{3}J signal between H-12 and C-10.

Ring D was identified as being a 5-membered lactone ring system. The position of the carbonyl (δ_C 177.7, C-13) was determined by two ^{3}J correlations between H_2-1 and C-13 and also between H-8 and C-13, therefore placing the carbonyl group of the lactone at C-10. This left the oxygen atom of the lactone group to be attached at C-8, which would explain why this group is deshielded. The HMBC data established the presence of a sesquiterpene with a novel skeleton and a molecular formula of $C_{15}H_{20}O_4$, which was confirmed by mass spectrometry, where an ion at *m/z* 246.1264 $[M\text{-}H_2O]^+$ (calculated for $C_{15}H_{18}O_3$: 246.1256) was detected.

The relative stereochemistry of **1** was established by signals obtained in the NOESY spectrum. The cyclopentane ring (ring C) was positioned β with respect to the plane of rings A and B, whilst the 5-membered lactone ring was α-orientated. H-6 showed a 1,3 interaction with H-12, suggesting that H-6 must be β-oriented. Therefore, H-12 must be orientated towards ring B, with the hydroxyl group attached to this carbon being orientated towards ring A. This was supported by a strong NOE between H-4 and H_3-14, placing this methyl group in an α-orientation. An NOE between H-3 and H_3-15 placed this methyl group in an α-orientation. Finally, NOE's between H_2-1β and H-9 and between H-9 and H-8 placed these protons in a β-orientation, thus completing the relative stereochemistry of this novel sesquiterpene skeleton. Compound **1** is, therefore, assigned as 2α,6α-dimethyltetracyclo-decal-3-en-2,12-diol-8α,13-olide (pulicrispiolide) and this is the first report of this sesquiterpene skeleton.

Experimental

General experimental techniques: NMR spectra were recorded on a Bruker AVANCE 500 MHz spectrometer. Chemical shift values (δ) were reported in parts per million (ppm) relative to an appropriate internal solvent standard, and coupling constants (*J* values) are given in Hertz. Mass spectra were recorded on a Finnigan MAT 95 high resolution, double focusing, magnetic sector mass spectrometer. Accurate mass measurement was achieved using voltage scanning of the accelerating voltage. This was nominally 5kV and an internal reference of heptacosa was used. Resolution was set between 5000 and 10,000.

IR spectra were recorded on a Nicolet 360 FT-IR spectrophotometer and UV spectra on a Thermo Electron Corporation Helios spectrophotometer.

Plant material: The plant material used for this study was collected from KSIR field station, in the Kebd area of Kuwait on the 27th April, 1999. The material was identified by K.T. Mathew and a voucher specimen (KTM 4612, collected by Simon Gibbons and K.T. Mathew) is deposited at the Kuwait University Herbarium (KTUH).

Extraction and isolation: The air dried aerial parts of *Pulicaria crispa* (185 g) were coarsely powdered and sequentially extracted in a Soxhlet apparatus with *n*-hexane (3.5 L), chloroform (3.5 L) and finally methanol (3.5 L). The *n*-hexane extract was concentrated under vacuum to yield 6.7 g of a green gum, which was subjected to vacuum liquid chromatography (VLC) on silica gel (12 g), eluting with *n*-hexane containing 10% increments of ethyl acetate to yield 12 fractions. The fraction eluted in 50% *n*-hexane underwent further separation by open column chromatography on Sephadex, eluting with dichloromethane, followed by normal-phase SPE (Phenomenex Strata Silica gel, 10 g / 60 mL giga tubes) eluting with 30% ethyl acetate in *n*-hexane. Fractions eluted from SPE were combined and subjected to multiple preparative TLC (two times) with toluene-ethyl acetate-acetic acid (80:18:2) as the mobile phase, to yield **1** (7.5 mg)

rel-2α,6α-Dimethyltetracyclo-decal-3-en-2,12-diol-8α,13-olide (**1**)

Pale yellow oil.
$[\alpha]_D$: 22.9º (*c* 0.35, $CHCl_3$).
Rf: 0.5 (toluene-EtOAc-AcOH).
IR (film):3649, 2968, 2931, 1770, 1507, 1015 cm^{-1}.
^1H NMR (500 MHz, C_6D_6): Table 1
^{13}C NMR (125 MHz, C_6D_6): Table 1
COSY and HMBC: Table 1 and Figure 1.
HREIMS: *m/z* $[M\text{-}H_2O]^+$ calcd for $C_{15}H_{18}O_3$: 246.1256; found 246.1264.

Acknowledgments - We thank the Engineering and Physical Sciences Research Council (Grant No. GR/R47646/01) for a multi-project equipment grant. The School of Pharmacy is thanked for a doctoral Scholarship to MS.

References

[1] Mabberley DJ. (**2002**) *The Plant Book*. 2nd Edition Cambridge University Press.

[2] Boulos, L. (**2002**) *Flora of Egypt.* Volume ***3***, Al-Hadara Publishing, Cairo, Egypt.

[3] Al-Rawi, A. (**1987**) *The Flora of Kuwait*. Volume 2, Alden Press, Oxford.

[4] Ross SA, El-Sayed, KA, El-Sohly MA, Hamann MT, Abdel-Halim OB, Ahmed AF, Ahmed MM. (**1997**) Phytochemical analysis of *Geigeria alata* and *Francoeuria crispa* essential oils. *Planta Medica*, ***63***, 479-482.

[5] Dendougui H, Benayache S, Benayache F, Connoly JD. (**2000**) Sesquiterpene lactones from *Pulicaria crispa*. *Fitoterapia*, ***71***, 373-378.

[6] San Feliciano A, Medarde M, Gordaliza M, Del Olmo E, Miguel del Corral JM. (**1989**) Sesquiterpenoids and phenolics *of Pulicaria paludosa*. *Phytochemistry*, ***28***, 2717-2721.

[7] Abdel-Mogib M, Jakupovic J, Dawidar AM, Metwally MA, Abou-Elzahab M. (**1990**) Sesquiterpene lactones and kaurane glycosides from *Francoeuria crispa*. *Phytochemistry*, ***29***, 2581-2584.

[8] Zdero C, Bohlmann F, King RM, Robinson H. (**1989**) Sesquiterpene lactones and other constituents from Australian *Helipterum* species. *Phytochemistry*, ***28***, 517-526.

Polyisoprenylated Benzoylphloroglucinol Derivatives from *Hypericum sampsonii*

Zhi Yong Xiao,[†] Qing Mu,*[,†] Winnie Ka Po Shiu,[‡] Yi Han Zeng,[†] and Simon Gibbons[‡]

School of Pharmacy, Fudan University, Shanghai 200032, People's Republic of China, and Centre for Pharmacognosy and Phytotherapy, The School of Pharmacy, University of London, London, United Kingdom

Received August 9, 2007

Bioassay-directed fractionation using multidrug-resistant (MDR) *Staphylococcus aureus* resulted in the isolation of four new polyprenylated benzophloroglucinol derivatives, sampsoniones N–Q (**1–4**), and four known compounds, 7-epiclusianone (**5**) and sampsoniones B, L, and R, from the roots of *Hypericum sampsonii*. The structures of these compounds were established by analysis of spectroscopic data, and the structures of **4** and **5** were determined by single-crystal X-ray diffraction crystallography. In the bioassay, 7-epiclusianone (**5**) showed promising activity with a minimum inhibitory concentration (MIC) of 7.3 μM against the NorA overexpressing MDR *S. aureus* strain SA-1199B; the positive control antibiotic norfloxacin showed activity at MIC 100 μM.

Multidrug-resistant *Staphylococcus aureus* infections, particularly those caused by methicillin-resistant *S. aureus* (MRSA), have been a major threat to public health in hospitals and the community in the past decade. Despite new advances in antibiotic development, MRSA infections remain a considerable concern due to the ability of this organism to rapidly acquire resistance to new agents. In 2002, MRSA strains fully resistant to vancomycin were isolated in the United States.[1] Resistance to linezolid, a member of the oxazolidinone class has also been reported in some patients followed by prolonged antibiotic treatment in the United States.[2] There is therefore a continuing need to discover and characterize new classes of antibiotics to reduce the pressures of bacterial resistance. In the search for antibacterial compounds with activity against MDR *S. aureus* from plants, a number of species of the genus *Hypericum* have been investigated due to their ability to produce extracts with antibacterial activity toward multidrug-resistant (MDR) strains.[3]

Hypericum sampsonii Hance (Guttiferae) is a Chinese herbal medicine used in the treatment of numerous disorders such as backache, burns, diarrhea, snakebites, and swellings.[4] Because of its various bioactivities, this species has been investigated and polyprenylated benzophloroglucinol derivatives and xanthones have been isolated from this plant.[5–8] Guided by antibacterial screening using SA-1199B, an MDR strain of *S. aureus* that overexpresses the NorA efflux protein, the major characterized drug pump in *S. aureus,* the petroleum fraction of the roots from *H. sampsonii* was found to possess activity at a minimum inhibitory concentration (MIC) of 64 μg/mL. Herein, we report the phytochemical investigation on the nonpolar fraction of the root extract of *H. sampsonii*.

Results and Discussion

The powdered roots of *Hypericum sampsonii* were extracted with 95% EtOH, and the extract was fractionated into petroleum ether-, methanol-, and water-soluble fractions. The active petroleum ether-soluble fraction was rechromatographed on silica gel and RP-18 to afford four new polyisoprenylated benzophenone derivatives, denoted sampsoniones N (**1**), O (**2**), P (**3**), and Q (**4**), and four known compounds, sampsonione L, 7-epiclusianone (**5**), and sampsoniones B and R. Of these, **5** showed promising activity with an MIC of 7.3 μM (4 μg/mL) against SA-1199B, while the positive control drug norfloxacin showed activity at MIC 100 μM (32 μg/mL).

Sampsonione N (**1**) was obtained as an optically active colorless oil, $[\alpha]_D^{20}$ +22.0 (*c* 0.090, $CHCl_3$); HR-MALDI-MS of **1** indicated

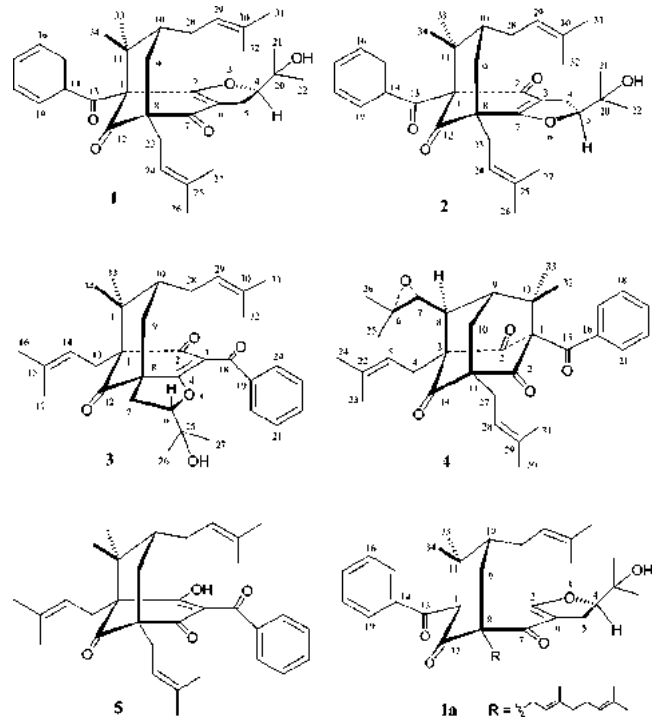

a molecular formula of $C_{33}H_{42}O_5$ ([M + Na]$^+$ 541.2924, calcd for $C_{33}H_{42}O_5Na^+$, 541.2915). The ^{13}C NMR spectrum of **1** (Table 1) showed signals for three carbonyls (δ_C 207.7, 193.0, 190.7), a benzoyl group (δ_C 173.2, 137.0, 128.2 × 2, 128.5 × 2, 132.7), eight methyls, four methylenes, four methines, and eight aliphatic quaternary carbons. These data, in combination with biogenetic considerations, suggested that the compound possessed a benzoylphloroglucinol structural feature.[5] The remaining 20 carbon signals were assigned to four isoprenyl moieties, and the NMR data for **1** were very similar to those of sampsonione M (**1a**), which was previously isolated from the same plant.[5] The difference between **1**and **1a** emerged at C-8, in which the substituent group was 3-methyl-2-butenyl in **1**, instead of a geranyl group in **1a**. Compound **1** was a new benzoylphloroglucinol and was named sampsonione N.

Sampsonione O (**2**), $C_{33}H_{42}O_5$, had the same molecular formula as **1**, and the ^{13}C NMR data (Table 1) of **2** were similar to those of **1** except for C-1, C-2, C-7, and C-8 (**1**: δ_C 69.0, 173.2, 190.7, and 63.5; **2**: δ_C 78.3, 188.7, 177.0, and 54.1). However, the dihydrofuran ring was formed through an oxygen atom at C-7 in **2** instead of at C-2 in **1** and was established by the presence in the HMBC

* To whom correspondence should be addressed. E-mail: muqing2000@yahoo.com.
† Fudan University, Shanghai.
‡ University of London.

10.1021/np0704147 CCC: $37.00
Published on Web 11/26/2007

Table 1. NMR Data for Sampsoniones N (**1**) and O (**2**)

1					**2**				
no.	δH (*J* in Hz)	δC	HMBC[a]	ROESY	no.	δH (*J* in Hz)	δC[b]	HMBC[a]	ROESY
1		69.0			1		78.3		
2		173.2			2		188.7		
3					3		119.3		
4α	4.66, dd (9.0, 10.6)	93.4		5α, 5*β*, 21, 22	4α	2.81, dd (10.6, 15.3)	28.2	3, 5, 7, 20	5α
					4*β*	2.96, dd (6.7,15.3)		3, 5, 7, 20	22
5α	2.81, dd (10.6, 14.9)	26.9	2, 6, 20	4α	5α	4.79, dd (6.7, 10.6)	93.5	4, 7, 21, 22	4α, 21, 22
5*β*	2.96, dd (8.6, 14.5)		2, 4, 6, 20	4α, 21, 22					
6		118.5			6				
7		190.7			7		177.0		
8		63.5			8		54.1		
9a	2.16, dd (7.4,14.1)	40.6	7, 8, 10, 12, 23	10, 34	9a	2.18, dd (6.6, 14.1)	39.4	7, 8, 10, 11, 23	10, 23, 34
9b	2.12, dd (0.8,14.1)			10	9b	2.22, dd (1.2, 14.1)		7, 8, 10, 23	10, 23
10	1.50, m	48.5	1, 8, 9, 11, 28	9a, 9b, 28	10	1.53, m	48.8	1, 8, 9, 11, 28, 33, 34	9, 34
11		48.9			11		49.9		
12		207.7			12		207.7		
13		193.0			13		193.8		
14		137.0			14		137.2		
15	7.57, m	128.2	13, 17, 19	16	15	7.56, dd (1.1, 8.2)	128.8	13, 17, 19	16
16	7.35, t (8.2)	128.5	14, 18	15, 17	16	7.26, dt (1.6,2.0,9.0)	128.6	14, 18	15, 17
17	7.49, t (7.4)	132.7	15, 19	16, 18	17	7.39, m	132.8	15, 19	16, 18
18	7.35, t (8.2)	128.5	14, 16	17, 19	18	7.26, dt (1.6,2.0,9.0)	128.6	14, 16	17, 19
19	7.57, m	128.2	13, 15, 17	18	19	7.56, dd (1.1, 8.2)	128.8	13, 15, 17	18
20		70.7			20		72.5		
21	0.89, s	26.3	4, 20, 22	5*β*, 22, 31	21	1.31, s	26.5	5, 20, 22	5α, 22, 31
22	0.88, s	23.7	4, 20, 21	5*β*, 21	22	1.22, s	23.8	5, 20, 21	4*β*, 5α, 21, 31
23a	2.60, dd (6.7, 14.1)	29.8	7, 8, 9, 12, 24, 25	27	23	2.53, d (6.6)	30.1	7, 8, 9, 12, 24, 25	23, 27
23b	2.49, dd (7.8, 14.4)								
24	5.08, t (7.4)	119.2	23, 26, 27		24	5.03, t (6.6)	120.8	23, 26, 27	
25		134.8			25		135.6		
26	1.68, s	26.1	24, 25, 27		26	1.70, s	26.6	24, 25, 27	
27	1.71, s	18.2	24, 25, 26	23	27	1.70, s	18.8	24, 25, 26	
28a	2.24, br, d	29.0	10, 30	10, 33	28a	2.25, br, d	30.5	9, 10, 29, 30	33
28b	2.0, m			10	28b	1.95, m		10, 29, 30	
29	4.89, t (7.04)	124.6	28, 31, 32		29	4.95, t (7.0)	125.4	28, 31, 32	31
30		132.8			30		133.0		
31	1.67, s	25.8	30, 32	21	31	1.70, s	26.4	29, 30, 32	21, 22, 32
32	1.55, s	17.9	30, 31		32	1.58, s	18.5	29, 30, 31	31
33	1.48, s	23.5	1, 10, 11, 34	10, 28	33	1.49, s	23.2	1, 10, 11, 34	28a, 34
34	1.43, s	26.7	1, 10, 11, 33	9a, 10	34	1.33, s	27.3	1, 10, 11, 33	9a, 33

[a] Carbons that correlate with the proton resonance.

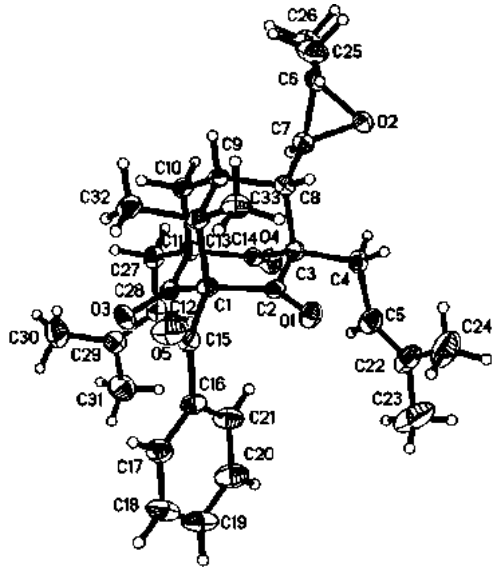

Figure 1. X-ray crystallography of sampsonione Q (**4**).

spectrum of a correlation between the methine proton of C-5 and the quaternary carbon at C-7 (177.0) of **2**. This assignment was supported by the presence of the corresponding correlation between H-23 and C-7. The structure for **2** is shown in Figure 1 and was confirmed by the ^{1}H–^{1}H COSY, HMQC, HMBC, and ROESY spectra, and compound **2** was named sampsonione O.

Sampsonione P (**3**) had a molecular formula of $C_{33}H_{42}O_5$ on the basis of HR-MALDI-MS ([M + Na]$^+$ 541.2924). The ^{13}C NMR and ^{1}H NMR data of **3** (Table 2) were compared with those of the known compound sampsonione L.[5] 2D NMR data also suggested that **3** and sampsonione L had the same skeleton and differed only with regard to the side chains attached to C-1 and C-3. Compound **3** possessed a 3-methyl-2-butenyl group and a benzoyl moiety. In the HMBC spectrum, the proton signals at δ_H 2.68 (H-13a) and 2.48 (H-13b) were correlated with the carbon signals at δ_C 68.5 (C-1), 194.0 (C-2), and 206.1 (C-12). In the ROESY spectrum, the proton signals at δ_H 2.68 (H-13a) and 2.48 (H-13b) were correlated with those at δ_H 1.20 (H-33) and 1.05 (H-34). These correlations suggested that the 3-methyl-2-butenyl group was connected to C-1 and the benzoyl group to C-3 in **3**, rather than the former connected to C-3 and the latter to C-1 as seen in sampsonione L.[5] Therefore, the structure of **3** was assigned as shown in Figure 1 and given the trivial name sampsonione P.

Sampsonione Q (**4**) was obtained as fine, colorless crystals, $[\alpha]_D^{20}$ −9.65 (*c* 0.401, $CHCl_3$); HR-MALDI-MS indicated a molecular formula of $C_{33}H_{40}O_5$ ([M + Na]$^+$ 539.2768, calcd for $C_{33}H_{40}O_5Na^+$, 539.2769). The analysis of 1D and 2D NMR spectra revealed that **4** was closely related to the adamantyl derivative sampsonione J, previously isolated from *H. sampsonii*.[5] The difference was in the side chain at C-11, with a geranyl group in sampsonione J being replaced by the 3-methyl-2-butenyl group in **4**. The α-configuration of H-8 in **4** was confirmed by the *W*-coupling between δ_H 2.51 (dt, *J* = 2.7, 5.5, 8.2, H-8) and 2.63 (dt, *J* = 2.7, 5.9, 14.1, H-10a), as well as an NOE interaction of H-8 with the C-32 methyl protons. Therefore, the structure of **4** was assigned as shown and named sampsonione Q, and the structure was confirmed by X-ray crystallography (Figure 1).

Compound **5** was isolated as colorless crystals, mp 98 °C, $[\alpha]_D^{20}$ −9.65 (*c* 0.401, $CHCl_3$) and existed as a mixture of 1,3-ene-one

Table 2. NMR Data for Sampsoniones P (**3**) and Q (**4**)

	3					**4**			
no.	δH (*J* in Hz)	δC	HMBC[a]	ROESY	no.	δH (*J* in Hz)	δC[b]	HMBC[a]	ROESY
1		68.5			1		81.8		
2		194.0			2		200.5		
3		116.6			3		72.5		
4		176.2			4a	2.82, dd (6.3, 15.3)	26.8	2, 3, 5, 22	24
					4b	2.44, dd (7.4, 15.3)		2, 3, 5, 8, 14, 22	24
5					5	4.96, br, t (7.1)	118.6	23, 24	23
6β	4.54, dd (5.4, 10.9)	91.5		9b, 26, 27	6		56.9		
7α	2.74, dd (10.9, 12.9)	30.6	6, 8, 9, 12, 25	7β, 26, 27					25
7β	1.78, dd (5.4, 12.9)		4, 8	7α, 9a	7β	2.69, d (8.6)	61.4	3, 8, 25	25
8		58.7			8α	2.51, dt (2.7, 5.5, 8.2)	55.8	7, 9	9, 26, 32
9a	2.12, dd (7.1, 14.5)	36.4	4, 8, 10, 28	7β, 10, 34	9	1.71, m	45.9	1, 3, 11	8, 10a, 10b
9b	2.34, d (14.5)		4, 8, 10, 11, 12, 28	6β, 10					26, 32, 33
10	1.51, m	46.2		9a, 9b, 28b, 29, 33, 34	10a	2.63, dt (2.7, 5.9, 14.1)	40.9	8, 13, 14	9, 33
					10b	2.28, dd (2.7, 14.1)		9, 11, 12, 13	9
11		47.5			11		68.7		
12		206.1			12		202.2		
13a	2.68, overlap	25.4	1, 12, 14, 15	13b, 14, 33	13		55.1		
13b	2.48, overlap		1, 2, 14, 15	13a, 14, 33, 34					
14	4.90, m	119.4		13a, 13b, 16	14		202.8		
15		135.0			15		192.8		
16	1.63, s	26.2	14, 15, 17	14	16		134.4		
17	1.60, s	18.1	14, 15, 16		17	7.16, m	129.3	15, 19, 21	18
18		191.7			18	7.27, m	127.9	16, 20	17, 19
19		137.5			19	7.42, m	132.5	17, 21	18, 20
20	7.68, dd (1.2, 8.2)	128.8	18, 22, 24	21	20	7.27, m	127.9	16, 18	19, 21
21	7.39, t (7.8)	128.5	19, 23	20, 22	21	7.16, m	129.3	15, 17, 19	20
22	7.52, t (6.3)	133.3	20, 24	21, 23	22		134.8		
23	7.39, t (7.8)	128.5	19, 21	22, 24	23	1.62, s	26.0	5, 22, 24	5, 24
24	7.68, dd (1.2, 8.2)	128.8	18, 20, 22	23	24	1.68, s	18.2	5, 22, 23	4, 23
25		70.4			25	1.33, s	24.7	7, 6, 26	7β
26	1.09, s	23.8	6, 25, 27	6β, 7α	26	1.29, s	19.1	7, 6, 25	8
27	1.10, s	26.7	6, 25, 26	6β, 7α	27	2.56, d (7.04)	27.4	10, 11, 12, 14, 28, 29	31
28a	2.21, m	29.0	29, 30	28b, 29, 33	28	5.18, br, t (7.1)	118.2	30, 31	30
28b	2.52, m			10, 28a, 29				30, 31	30
29	4.90, m	124.3		10, 28a, 28b, 31	29		135.4		
30		133.4			30	1.68, s	26.0	28, 29, 31	28, 31
31	1.69, s	25.9	29, 30, 32	29	31	1.66, s	18.1	28, 29, 30	27, 30
32	1.65, s	17.8	29, 30, 31		32	1.41, s	22.5	1, 9, 13, 33	8, 9
33	1.20, s	22.4	1, 10, 11, 34	10, 23a, 23b, 28a, 34	33	1.48, s	23.1	1, 9, 13, 32	9, 10a
34	1.05, s	26.9	1, 10, 11, 33	9a, 10, 23b, 33	34				

[a] Carbons that correlate with the proton resonance.

tautomers in the ratio of 3:2 in $CDCl_3$ solution. Its structure was confirmed as 7-epiclusianone by X-ray crystollagraphy (Figure 2).[9–12] In this experiment, **5** was isolated as the main constituent (2.8%) from 40 g of the petroleum ether residue. *S. aureus* strain SA-1199B, which is resistant to norfloxacin, overproduces the NorA MDR efflux protein, the major drug pump in *S. aureus*.[13] 7-Epiclusianone (**5**) showed promising activity against SA-1199B at an MIC of 7.3 μM (4 μg/mL), while norfloxacin showed activity at an MIC of 100 μM (32 μg/mL). Therefore, **5** was assumed to be the predominant active constituent of *H. sampsonii* root extract (256 μg/mL for the EtOH extract and 32 μg/mL for the petroleum fraction).

Other polyisoprenylated benzoylphloroglucinol derivatives were isolated and determined to be sampsonione B[5d] and sampsonione L,[5d] respectively. Also isolated was the known polyisoprenylated benzoylphloroglucinol derivative 1-benzoyl-7α-(1-hydroxy-1-methylethyl)-13,13-methyl-3,11-di(methyl-2-butenyl)tricycle[4.3.1.1^{3,11}]-undecane-2,12,14-trione,[14] which was given the trivial name sampsonione R. Absolute configurations of these compounds remain to be determined, and except for 7-epiclusianone (**5**), none of these metabolites exhibited activity against MDR *S. aureus* strain SA-1199B.

Experimental Section

General Experimental Procedures. Optical rotations were measured using a JASCO P-1020 polarimeter. IR spectra were recorded using an Avatar 360 ESP FTIR spectrophotometer and UV spectra on a Shimadzu UV-1600PC spectropolarimeter. ^{1}H and ^{13}C NMR spectra were obtained on a Varian Mercury Plus 400 MHz. Column chromatography was carried out with silica gel (10–40 μm, Merck) and ODS (C-18, 15–35 μm, Merck). Fractions obtained from column chromatography were monitored by TLC (silica gel HGF254, 10–40 μm, Yantai, Huanghai, China). ESI mass spectra were obtained on an Agilent 1100 Series LC/MSD spectrometer and HR-MALDI-MS spectra on an IonSpec 4.7 T FTMS. X-ray crystallographic analysis was carried out on a Bruker Smart Apex CCD diffractometer with graphite-monochromated Mo Kα radiation ($\lambda = 0.71073$ Å).

Plant Material. *Hypericum sampsonii* was collected from Cha Lin County in Hunan Province, China. A voucher specimen (No. HS-003) was deposited at the Natural Medicine Chemistry Laboratory of the School of Pharmacy, Fudan University. The plant was identified by Dr. Zhang Wen-Ju, Associate Professor in the Center of Biodiversity of the Biology School, Fudan University, China.

Extraction and Isolation. Powdered roots of the plant (1.1 kg) were extracted with 95% EtOH and afforded 90 g of extract after evaporation under vacuum at 45 °C. The extract was partitioned into petroleum ether- (40 g), methanol- (13 g), and water-soluble fractions.

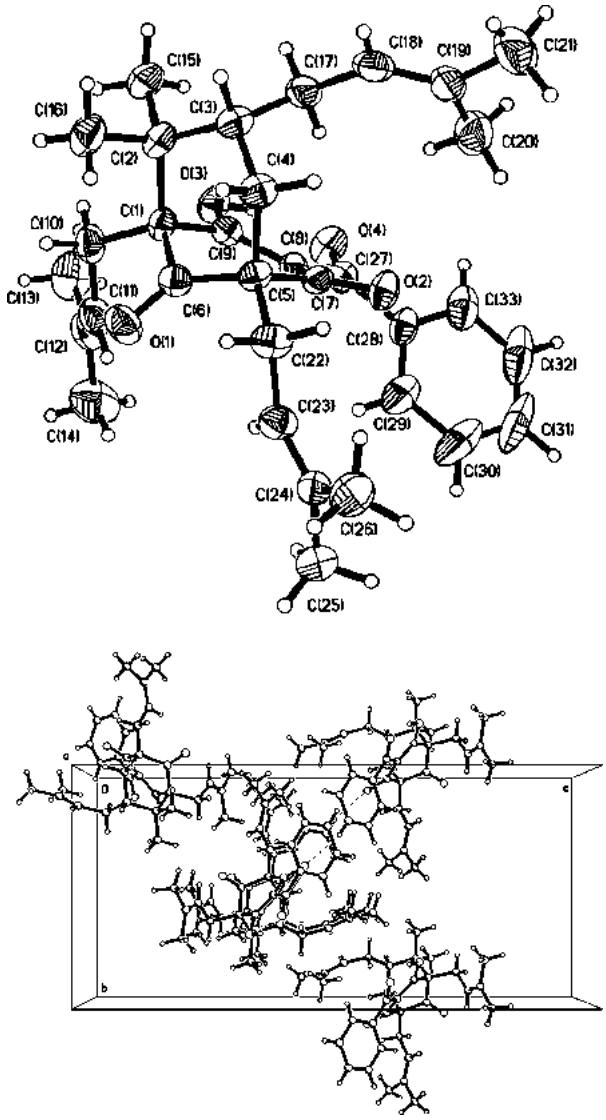

Figure 2. X-ray crystallography of 7-epiclusianone (**5**).

The petroleum ether-soluble fraction was subjected to column chromatography over silica gel, eluting with a gradient from petroleum ether to ethyl acetate and finally washed with methanol to afford 15 fractions (1–15). Fraction 1 (8.9g) was recrystallized from acetone to give **5** (1.1 g). Fraction 3 was chromatographed on silica gel columns eluted with petroleum ether–ethyl acetate to yield **4** (39.3 mg) and sampsonione B (19.4 mg). Fraction 8 was chromatographed on silica gel (petroleum ether–chloroform–acetone) and ODS (MeOH–H_2O) to yield **1** (9.7 mg), **2** (12.9 mg), **3** (2.4 mg), sampsonione L (3.9 mg), and sampsonione R (15.3 mg).

Sampsonione N (1): colorless oil; $[\alpha]_D^{20}$ +22.0 (*c* 0.090, $CHCl_3$); UV ($CHCl_3$) λ_{max} (log ε) 278 (3.88), 246 (3.99) nm; IR (film) ν 3434, 3064, 2965, 2925, 1724, 1699, 1655, 1632, 1600, 1580, 1446 cm^{-1}; ^1H NMR (400 MHz) and ^{13}C NMR ($CDCl_3$, 100 MHz) data, see Table 1; HR-MALDI-MS $[M + Na]^+$ 541.29245 (calcd for $C_{33}H_{42}O_5Na^+$, 541.2915).

Sampsonione O (2): colorless oil; $[\alpha]_D^{20}$ +87.9 (*c* 0.073, $CHCl_3$); UV ($CHCl_3$) λ_{max} (log ε) 284 (4.02), 248 (4.08), 216 (3.67) nm; IR (film) ν_{max} 3468, 3052, 2970, 2926, 2848, 1725, 1698, 1626, 1613, 1446 cm^{-1}; ^1H NMR (400 MHz) and ^{13}C NMR ($CDCl_3$, 100 MHz) data, see Table 1; HR-MALDI-MS $[M + Na]^+$ 541.29245 (calcd for $C_{33}H_{42}O_5Na^+$, 541.2930).

Sampsonione P (3): colorless oil; $[\alpha]_D^{20}$ +18.6 (*c* 0.022, $CHCl_3$); UV ($CHCl_3$) λ_{max} (log ε) 249 (4.08) nm; IR (film) ν_{max} 3479, 3056, 2969, 2924, 2851, 1732, 1682, 1631, 1448 cm^{-1}; ^1H NMR (400 MHz) and ^{13}C NMR ($CDCl_3$, 100 MHz) data, see Table 2; HR-MALDI-MS $[M + Na]^+$ 541.29245 (calcd for $C_{33}H_{42}O_5Na^+$, 541.2915).

Sampsonione Q (4): yellow oil; $[\alpha]_D^{20}$ –9.65 (*c* 0.401, $CHCl_3$); UV ($CHCl_3$) λ_{max} (log ε) 248 (3.98), 206 (3.27) nm; IR (film) ν_{max} 3055, 2962, 2923, 2851, 1745, 1704, 1597, 1582, 1447 cm^{-1}; ^1H NMR (400 MHz) and ^{13}C NMR ($CDCl_3$, 100 MHz) data, see Table 2; HR-MALDI-MS $[M + Na]^+$ 539.27680 (calcd for $C_{33}H_{40}O_5Na^+$, 539.2769).

X-ray Crystal Data for 4. Crystal data were as follows: colorless, fine crystal, C_{33} H_{40} O_5, fw 516.65, monoclinic, crystal size 0.15 × 0.12 × 0.05 mm, space group *P*2(1), a = 11.183(5) Å, b = 10.895(5) Å, c = 11.768(5) Å, V = 1427.1(11) $Å^3$, Z = 2, D_{calcd} = 1.202 g/cm^3, $F(000)$ = 556, reflections collected 7107, reflections unique 3266 (R_{int} = 0.0268), final R indices for $I > 2\sigma(I)$ R_1 = 0.0443, wR_2 = 0.1045, R indices for all data R_1 = 0.0561, wR_2 = 0.1104, completeness to 2θ (26.99) 99.8%, maximum transmission 0.9960, minimum transmission 0.9882. The structure was solved by direct methods using the program SHELXS. Refinement method was full-matrix least-squares on F^2, and goodness-of-fit on F^2 is 1.069. The X-ray diffraction material has also been deposited in the Cambridge Crystallographic Data Center (CCDC) as deposit no. CCDC 656236.

Bacteria. SA-1199B is a strain of *S. aureus* overproducing the NorA MDR efflux protein, the major drug pump in *S. aureus*, and was resistant to norfloxacin (MIC = 32 μg/mL). Additionally, some of this resistance is a result of a GrlA subunit substitution known to correlate with diminished fluoroquinolone susceptibility.[13]

Minimum Inhibitory Concentration (MIC) Assay. Bacteria were cultured on nutrient agar (Oxoid) and incubated for 24 h at 37 °C prior to MIC determination. The control antibiotic norflorxacin was obtained from Sigma Chemical Co. Mueller-Hinton broth (MHB; Oxoid) was adjusted to contain 20 and 10 mg/L of Ca^{2+} and Mg^{2+}, respectively. An inoculum density of 5 × 10^5 CFU of *S. aureus* was prepared in normal saline (9 g/L) by comparison with a 0.5 MacFarland turbidity standard. The inoculum (125 μL) was added to all wells, and the microtiter plate was incubated at 37 °C for 18 h. For MIC determination, 20 μL of a 5 mg/mL methanolic solution of 3-[4,5-dimethylthiazol-2-yl]-2,5-diphenyltetrazolium bromide (MTT; Sigma) was added to each of the wells and incubated for 20 min. Bacterial growth was indicated by a color change from yellow to dark blue. The MIC was recorded as the lowest concentration at which no growth was observed.[15]

Acknowledgment. We thank the National Science Foundation of China (30472068) and the Initiating Finance for Returnee of Education Ministry of China (2006) for financial support.

Supporting Information Available: NMR spectra of sampsoniones N–Q (**1**–**4**) and X-ray diffraction parameters of compound **5**. This material is available free of charge via the Internet at http://pubs.acs.org.

References and Notes

(1) Public Health Dispatch. *Morbidity Mortality Weekly Rep.* **2002**, *51*, 902.
(2) Peeters, M. J.; Sarria, J. C. *Am. J. Med. Sci.* **2005**, *330*, 102–104.
(3) Gibbons, S.; Ohlendorf, B.; Johnsen, I. *Fitoterapia* **2002**, *73*, 300–304.
(4) Jiang Su New Medical College. *Dictionary of Chinese Crude Drugs*; Shanghai Scientific Technological Publishers: Shanghai, 1977; pp 345–346.
(5) (a) Hu, L. H.; Sim, K. Y. *Tetrahedron Lett.* **1998**, *39*, 7999–8002. (b) Hu, L. H.; Sim, K. Y. *Tetrahedron Lett.* **1999**, *40*, 759–762. (c) Hu, L. H.; Sim, K. Y. *Org. Lett.* **1999**, *1*, 879–882. (d) Hu, L. H.; Sim, K. Y. *Tetrahedron* **2000**, *56*, 1379–1386.
(6) Lin, Y. L.; Wu, Y. S. *Helv. Chim. Acta* **2003**, *86*, 2156–2163.
(7) Don, M. J.; Huang, Y. J.; Huang, R. L.; Lin, Y. L. *Chem. Pharm. Bull.* **2004**, *52*, 866–869.
(8) Hong, D.; Yin, F.; Hu, L. H.; Lu, P. *Phytochemistry* **2004**, *65*, 2595–2598.
(9) McCandlish, L. E.; Hanson, J. C.; Stout, G. H. *Acta Crystallogr., Sect. B* **1976**, *32*, 1793.
(10) Alves, T. M. A.; Alves, R. O.; Romanha, A. J.; dos Santos, M. H.; Nagem, T. J.; Zani, C. L. *J. Nat. Prod.* **1999**, *62*, 369–371.
(11) Piccinelli, A. L.; Cuesta-Rubio, O.; Chica, M. B.; Mahmood, N.; Pagano, B.; Pavone, M.; Barone, V.; Rastrelli, L. *Tetrahedron* **2005**, *61*, 8206–8211.
(12) CCDC (Deposit No: 634436). Fax: +44-1223-336033. E-mail: deposit@ccdc.cam.ac.uk.
(13) Kaatz, G. W.; Seo, S. M. *Antimicrob. Agents Chemother.* **1997**, *41*, 2733–2737.
(14) Cruz, F. G.; Teixeira, J. S. R. *J. Brazil. Chem. Soc.* **2004**, *15*, 504–508.
(15) Gibbons, S.; Udo, E. E. *Phytother. Res.* **2000**, *14*, 139–140.

NP0704147

Amanicadol, a Pimarane-type Diterpene from *Phlomis amanica* Vierch.

Funda N. Yalçın[a], Tayfun Ersöz[a], Erdal Bedir[b], Ali A. Dönmez[c], Michael Stavri[d], Mire Zloh[e], Simon Gibbons[d], and İhsan Çalış[a]

[a] Hacettepe University, Faculty of Pharmacy, Department of Pharmacognosy, 06100, Sıhhiye, Ankara, Turkey
[b] Ege University, Faculty of Engineering, Department of Bioengineering, 35100, Bornova, İzmir, Turkey
[c] Hacettepe University, Faculty of Science, Department of Biology, 06532, Beytepe, Ankara, Turkey
[d] Centre for Pharmacognosy and Phytotherapy, The School of Pharmacy, University of London, 29 – 39 Brunswick Square, London WC1N 1AX, United Kingdom.
[e] Department of Pharmaceutical and Biological Chemistry, The School of Pharmacy, University of London, 29 – 39 Brunswick Square, London WC1N 1AX, United Kingdom

Reprint requests to Dr. Funda N. Yalçın. Fax: +90 312 311 4777. E-mail: funyal@hacettepe.edu.tr

Z. Naturforsch. **61b,** 1433 – 1436 (2006); received March 16, 2006

Fractionation of the methanol extract of *Phlomis amanica* resulted in the isolation of a new pimarane type diterpene, amanicadol (**1**), together with the known glycosides lamiide, verbascoside (= acteoside), syringaresinol-4-*O*-β-glucoside, liriodendrin, syringin, and a caffeic acid ester, chlorogenic acid. The structure of the new compound was established on the basis of extensive 1D and 2D NMR spectroscopic data interpretation. Molecular modeling studies on **1** were conducted and showed that it exhibited low conformational flexibility. Additionally, NMR chemical shifts were calculated for **1** *in vacuo*, and calculated values were in very close agreement with those found experimentally.

Key words: Phlomis amanica, Lamiaceae, Amanicadol, Diterpene, Pimarane

Introduction

The genus *Phlomis* (Lamiaceae) is represented by 34 species in the flora of Turkey [1]. Some *Phlomis* species are used as tonics and stimulants in Anatolian folk medicine [2]. A few members of the genus are used for their antiinflammatory, wound healing, and pain relief properties in Chinese medicine [3, 4].

Our previous phytochemical studies on Turkish *Phlomis* species were focused on glycosidic compounds. However, in a continuation of our phytochemical investigations on the same species, we have now isolated a new pimarane type diterpene, amanicadol (**1**) from the *n*-hexane extract of *Phlomis amanica*, an endemic species. Chromatographic separations on the *n*-BuOH extract of the title plant afforded the known glycosides lamiide, verbascoside (= acteoside), syringaresinol-4-*O*-β-glucoside, liriodendrin, syringin as well as a caffeic acid ester, chlorogenic acid.

Results and Discussion

Compound **1** was obtained as an amorphous powder. The molecular formula was established as $C_{20}H_{32}O$ on the basis of a HRESIMS molecular ion peak at $m/z = 299$ $[M+H]^+$, and the analysis of its ^{1}H and ^{13}C NMR spectroscopic data (Table 1). The IR spectrum of **1** displayed absorption bands typical for hydroxyl groups and double bonds. The combined analysis of the ^{13}C NMR and DEPT spectra revealed the presence of 20 carbon signals assigned to four methyls, seven methylenes, five methines (one tertiary alcohol and two olefinic carbon atoms), and four quaternary carbon atoms. These data, together with the molecular composition, suggested that **1** possessed 5 degrees of unsaturation. The presence of two π-bonds further indicated that the compound was a tricyclic diterpene. The ^{1}H NMR spectrum showed signals due to four tertiary methyl groups at $\delta = 1.01$, 0.91, 0.87 and 0.85, three vinylic protons from a monosubstituted double bond at $\delta = 5.90$, 4.93, and 5.02 [ABX pattern, $J_{AB} = 1.3$ Hz, $J_{AX} = 10.5$ Hz (*cis*-coupling), and $J_{BX} = 17.5$ Hz (*trans*-coupling)], a geminal proton of a secondary hydroxyl group at $\delta = 4.05$ (dt, $J = 4.8$ and 6.6 Hz), and a singlet resonance at $\delta = 5.30$ in addition to the proton signals assigned to the rings A, B and C. A detailed analysis of DQF COSY data

0932–0776 / 06 / 1100–1433 $ 06.00

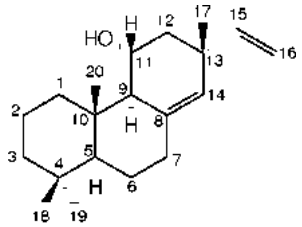

1

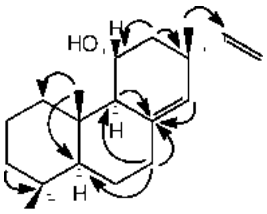

Fig. 1. Selected HMBC correlations of **1** (H → C).

revealed the identification of three spin systems arising from the rings A, B and C, H_2-1/H_2-2/H_2-3, H-5/H_2-6/H_2-7, and H-9/H-11/H_2-12, respectively. In the ^{13}C NMR spectrum the carbon resonances appearing at $\delta = 149.1$ (C-15) and 110.6 (C-16) supported the presence of an exocyclic vinyl group. This proposal was also confirmed by the long range ^{1}H-^{13}C NMR (Fig. 1) correlation between the methyl signal at $\delta = 1.01$ (H-17) and the carbon resonance at $\delta = 149.1$ (C-15) as well as HMBC correlations between the vinylic protons ($\delta = 4.93$ and 5.02) and the quaternary signal at $\delta = 37.5$ (C-13). An olefinic methine carbon signal was observed at $\delta = 127.4$ (C-14), which showed an HMQC correlation with the proton resonance at $\delta = 5.30$. In the HMBC spectrum this olefinic hydrogen coupled to C-8 ($\delta = 136.5$) indicating the presence of a trisubstituted double bond in the ring C. All of these findings indicated that compound **1** possessed a pimara-8(14),15-diene skeleton [5–7]. The signal at $\delta = 4.05$ (dt, $J = 4.8$ and 6.6 Hz), observed in the spin system of ring C, was attributed to a geminal proton signal of a secondary hydroxyl group. The location of the secondary hydroxyl group was determined as C-11 by analysing the DQF-COSY and HMBC spectra. The relative stereochemistry of **1** was established by NOE DIFF and NOESY experiments with mixing times of 400, 800 and 1200 msec. In all NOESY experiments NOE correlations were observed between Me-18 and Me-20, Me-20 and H-11, and also between H-11 and Me-17 which was suggestive of a relative β-axial orientation of H-11, revealing OH-11 to be α and equatorial [8]. Additionally, an NOE correlation observed between H-9 and H-5 indicated that both hydrogen atoms were in a relative α-axial orientation. This confirmed the *trans* A:B ring junction stereochemistry of **1**. Compound **1** was assigned as *rel*-(5*S*, 9*R*, 10*S*, 11*R*, 13*R*)-11-α-hydroxypimara-8(14), 15 diene.

Table 1. ^{13}C ($CDCl_3$, 100.0 MHz) and ^{1}H ($CDCl_3$, 400.0 Hz) NMR data for **1**. Values in parenthesis are calculated chemical shifts.

C	DEPT	δ_C (ppm)	δ_H (ppm)	J (Hz)
1	CH_2	40.2 (41.67)	1.33 (1.54) d	4.0
			1.89 (1.56) dd	12.7/1.4
2	CH_2	19.1 (21.81)	1.57 (1.59) t	3.1
3	CH_2	42.1 (41.89)	1.24 (1.31) d	4.4
			1.41 (1.41) m	–
4	C	33.4 (37.18)		
5	CH	54.9 (55.82)	1.13 (1.21) dd	12.5/2.6
6	CH_2	23.1 (25.60)	1.65 (1.57)*	–
			1.30 (1.52) dd	12.9/4.4
7	CH_2	36.3 (37.64)	2.34 (2.16)m	–
			2.10 (2.12) m	–
8	C	136.5 (134.55)		
9	CH	60.0 (62.1)	1.77 (1.89) d	4.8
10	C	39.1 (44.4)		
11	CH	66.2 (66.4)	4.05 (4.27) dt	4.8/6.6
12	CH_2	43.5 (43.16)	1.65 (1.59)*	–
13	C	37.5 (42.45)		
14	CH	127.4 (126.92)	5.30 (5.45) s	–
15	CH	149.1 (143.92)	5.90 (6.05) dd	17.5/10.5
16	CH_2	110.6 (106.02)	4.93 (5.09) dd	10.5/1.3
			5.02 (5.15) dd	17.5/1.3
17	CH_3	27.0 (23.23)	1.01 (1.14) s	–
18	CH_3	22.1 (22.66)	0.87 (0.86) s	–
19	CH_3	33.8 (33.87)	0.91 (0.92) s	–
20	CH_3	15.9 (16.96)	0.85 (1.00) s	–

* Unclear due to signal overlapping.

The 3D structure of **1** was built using the Maestro modelling software package and the conformational search was performed using Macromodel [9, 10]. It was found that **1** exibited low conformational flexibility. Furthermore, the geometry was optimized using DFT calculations utilizing the B3LYP/6-31** basis set [11]. The distances between different groups of hydrogen atoms were consistent with observed NOE signals (Fig. 2). The NMR chemical shifts were calculated for **1** *in vacuo*, which gave some remarkable agreements with experimentally found values (Table 1). Structures and chemical shifts for other possible stereoisomers were also calculated, but those could not explain the presence of the NOE signals, and the calculated values of chemical shifts did not agree so well with experimentally determined chemical shifts. This has suggested that our stereospecific assignments a correct. A literature survey revealed that **1** was a

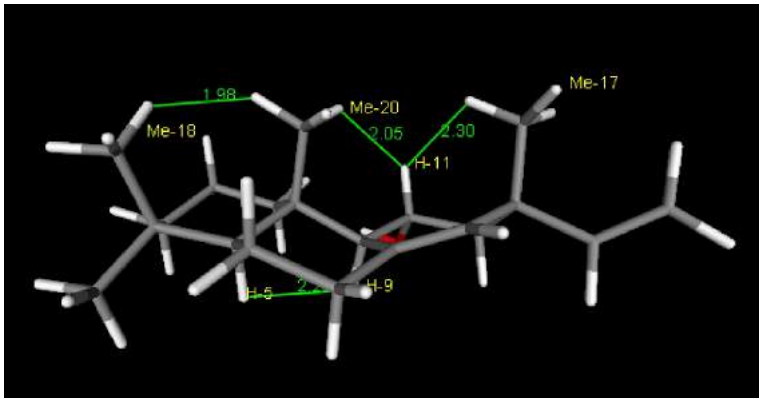

Fig. 2. 3D structure of **1**. Labels depict hydrogen atoms that exibit NOE correlations used for the assignment of the stereochemistry. (Distances in Å).

new compound from nature and the trivial name amanicadol is proposed.

The structures of the known compounds lamiide (**2**) [12], verbascoside (**3**) [13], syringaresinol-4-*O*-β-glucoside (**4**) [14], liriodendrin (**5**) [15], syringin (**6**) [16, 17], and chlorogenic acid (**7**) [18] were identified by their physical and spectroscopic (^{1}H NMR, ^{13}C NMR, DEPT, 2D NMR and MS) data and by comparing the data obtained with those published in the literature.

Conclusion

Phlomis species are generally known to contain glycosidic secondary metabolites such as iridoids, phenylethanoids, flavonoids, and lignans. Up to date only some labdane-type diterpenes have been reported from the genus [19, 20]. This is the first report of the isolation and characterization of a pimarane-type diterpene from a member of the genus *Phlomis*.

Experimental Section

General experimental procedures

Optical rotations were recorded on a Rudolph Autopol IV polarimeter. UV (CH_2Cl_2) spectra were recorded on a Shimadzu UV-160A spectrophotometer. FTIR (KBr) spectra were determined on a Perkin-Elmer 2000 FTIR spectrophotometer. NMR measurements in $CDCl_3$ were performed on a JEOL JNM-A400 FT-NMR (^{1}H: 400 and ^{13}C: 100 MHz) and a Bruker AVANCE 500 spectrometer (^{1}H: 500 and ^{13}C: 125 MHz). Chemical shifts were given in ppm with tetramethylsilane as an internal standard.

Accurate mass measurements were determined on a Micromass Q-TOF Ultima Global Tandem Mass Spectrometer. The sample was run under electrospray ionization mode using 50% acetonitrile in water and 0.1% formic acid as a solvent. The instrument was calibrated before analysis using the ions produced from [Glu]-fibrinopeptide B as an internal standard, $[M+2H]^{2+} = 785.8426$.

For open column chromatography (CC) Kieselgel 60 (0.063 – 0.200 mm, Merck) and Sephadex LH-20 (Fluka) were used. MPLC was performed on a Büchi (2.5×46 cm) glass column packed with LiChroprep RP-18 (Merck) (40 – 63 μm) using a Büchi B-684 pump. VLC separation was realized on a small glass column (5.2×10 cm) packed with LiChroprep RP-18 (Merck) (40 – 63 μm). TLC was carried out on pre-coated Kieselgel 60 F_{254} aluminium sheets (Merck). Compounds were detected by UV fluorescence and by spraying with 1% vanillin/H_2SO_4, followed by heating at 100 °C for 1 – 2 min.

Plant material

Phlomis amanica Vierch. was collected from Arsuz (Hatay), in the vicinity of Kale village, 151 m, Southwest Anatolia, Turkey. Voucher specimens have been deposited in the Herbarium of the Department of Biology, Faculty of Science, Hacettepe University (AAD 10654).

Extraction and isolation

Air-dried and powdered aerial parts of *P. amanica* (450 g), were extracted with MeOH (3×2 L) at 40 °C. The concentrated methanolic extract was suspended in H_2O (100 mL) and partitioned between *n*-hexane (4×100 mL), $CHCl_3$ (4×100 mL), and *n*-BuOH (4×100 mL). 8.8 g of the *n*-hexane extract was separated on a silica gel column (40×100 cm) with a solvent gradient of CH_2Cl_2-MeOH ($100:0 \rightarrow 50:50$), to afford six main fractions (Frs. I – VI, 200 mL, each). Fr. II (305 mg) was further rechromatographed by Sephadex LH-20, eluting with cyclohexane-acetone-dichloromethane-methanol (1 : 1 : 1 : 2). The elution volume of each fraction was (Frs II_{1-10}) 200 mL each. Fr. II_{5-6} (180 mg) was applied to a silica gel column eluting with a gradient of

n-hexane-EtOAc (99 : 1 → 95 : 5, 25 mL each) to give **1** (30 mg).

The *n*-BuOH extract (30 g) of *P. amanica* was first chromatographed on a polyamide column with MeOH-H_2O (0 : 100 → 100 : 0) mixtures to give Frs. A (1.49 g), B (8.5 g), C (1.2 g), D (3.3 g), and E (3.76 g). Fr. B was applied to VLC using a RP-18 column with MeOH-H_2O (0 : 100 → 45 : 55) mixtures to afford **2** (5 mg). Fr. B_{13-16} (134 mg), obtained from VLC, were subjected to repeated column chromatographic separations on Sephadex LH-20, RP-18 and silica gel to yield **5** (4 mg) and **6** (6 mg). Fr. C (1.2 g) was first subjected to MPLC and eluted with MeOH-H_2O (0 : 100 → 100 : 0) to give 120 fractions (Frs. C_{1-120}). Fr. C_{98-108} (200 mg) was rechromatographed by silica gel column chromatography, followed by VLC to afford **4** (4 mg) and **7** (12 mg). Fr. E (3.76 g) was applied to VLC using MeOH-H_2O (0 : 100 → 45 : 55) mixtures to yield **3** (15 mg).

*Amanicadol (**1**)*

Amorphous powder; $[\alpha]_D^{20} - 0.029°$ ($CHCl_3$, *c* 1) UV/vis (CH_2Cl_2): $\lambda_{max}(\lg \varepsilon_{max}) = 244$ nm (3.99). IR [KBr]: ν_{max} = 3400, 3080, 1634, 1595. ^{1}H and ^{13}C NMR data are given in Table 1, HRESIMS, *m/z* = 289.2522 $[M+H]^+$ (calcd. for $C_{20}H_{32}O$ 289.2526).

Molecular modelling

The 3D structure of **1** was generated using the Maestro 7.5 package [9]. The conformational searching was performed using the Monte Carlo method [21] and OPLS-AA force [22] included in Macromodel 9.1 [10]. The most stable conformers were further optimized using Jaguar 6.5 [23] at the B3LYP/6-31** level of theory. ^{1}H and ^{13}C shielding constants were computed by *pseudo* spectral methods [24]. The theoretical chemical shifts were calculated taking into account TMS as the reference compound whose shielding constants were calculated under the same conditions.

Acknowledgements

We gratefully thank Prof. Dr. Hasan Seçen and Asist. Prof. Dr. Cavit Kazaz (Atatürk University, Faculty of Science and Literature, Department of Chemistry, Erzurum, Turkey) for their help in NOE experiments. This work was supported by the Scientific and Technical Research Council of Turkey (TUBITAK Project No. SBAG-2304).

[1] A. Huber-Morath, Phlomis, in P. H. Davis (ed.): Flora of Turkey and the East Aegean Islands, Vol. 7. p. 102, University Press, Edinburgh (1982).
[2] T. Baytop, Therapy with Medicinal Plants in Turkey (Past and Present), 2nd ed., p. 193, Nobel Tıp Kitabevleri, İstanbul (1999).
[3] T. Tanaka, O. Tanaka, Z.-W. Lin, J. Zhou, H. Ageta, Chem. Pharm. Bull. **31**, 780 (1983).
[4] C.-Z. Zhang, C. Li, S.-I. Feng, J.-G. Shi, Phytochemistry **30**, 4156 (1991).
[5] L. C. Chang, L. L. Song, E. J. Park, L. Luyengi, K. J. Lee, N. R. Farnsworth, J. M. Pezzuto, A. D. Kinghorn, J. Nat. Prod. **63**, 1235 (2000).
[6] E. Wenkert, B. L. Buckwalter, J. Am. Chem. Soc. **94**, 4367 (1972).
[7] G. M. Woldemichael, M.-T. Gutierrez-Logo, S. G. Franzblau, Y. Wang, E. Suarez, B. N. Timmermann, J. Nat. Prod. **67**, 598 (2004).
[8] S. Thongnest, C. Mahidol, S. Sutthivaiyakit, S. Ruchirawat, J. Nat. Prod. **68**, 1632 (2005).
[9] Maestro 7.5, Schrodinger, LLC Portland, OR (2005).
[10] MacroModel 9.1, Schrodinger, LLC Portland, OR (2005).
[11] Chem3D Ultra version 7.0 2002, CambridgeSoft Corporation (1986 – 2002).
[12] H. Rimpler, Phytochemistry **11**, 3094 (1972).
[13] O. Sticher, M. F. Lahloub, Planta Med. **46**, 145 (1982).
[14] T. Deyama, T. Ikawa, S. Nishibe, Chem. Pharm. Bull. **33**, 3651 (1985).
[15] R. K. Chaudary, O. Sticher, Helv. Chim. Acta **64**, 3 (1981).
[16] K. Sano, S. Sanada, Y. Ida, J. Shoji, Chem. Pharm. Bull. **39**, 865 (1991).
[17] M. Sugiyama, E. Nagayama, M. Kikuchi, Phytochemistry, **33**, 1215 (1993).
[18] G. F. Pauli, U. Kuczkowiak, A. Nahrstedt, Magnetic Resonance in Chemistry **37**, 827 (1999).
[19] Ü. Ş. Harput, İ. Saracoğlu, İ. Çalış, K. Kojima, Y. Ogihara, Diterpenoids from *Phlomis bourgaei*, in İ. Çalış, T. Ersöz, A. Başaran (eds): New Trends and Methods in Natural Products' Research (Proceedings Book of XIIth International Symposium on Plant Originated Crude Drugs, Ankara, May 20 – 22, 1998), pp. 127 – 131, Rekmay Press, Ankara (2000).
[20] M. Katagiri, K. Ohtani, R. Kasai, K. Yamasaki, C.-R. Yang, O. Tanaka, Phytochemistry **35**, 439 (1994).
[21] I. Kolossváry, W. C. Guida, J. Am. Chem. Soc. **118**, 5011 (1996).
[22] W. L. Jorgensen, D. S. Maxwell, J. Tirado-Rives, J. Am. Chem. Soc. **118**, 11225 (1996).
[23] Jaguar 6.5, Schrodinger, LLC Portland, OR (2005).
[24] Y. Cao, M. D. Beachy, D. A. Braden, L. A. Morrill, M. N. Ringnalda, R. A. Friesner, J. Chem. Phys. **122**, 224116 (2005).

Available online at www.sciencedirect.com
ScienceDirect
Phytochemistry 67 (2006) 2110–2114
PHYTOCHEMISTRY
www.elsevier.com/locate/phytochem

An antibacterial hydroxy fusidic acid analogue from *Acremonium crotocinigenum*

Liam Evans [a], John N. Hedger [b], David Brayford [b], Michael Stavri [c], Eileen Smith [c], Gemma O'Donnell [c], Alexander I. Gray [d], Gareth W. Griffith [e], Simon Gibbons [c,*]

[a] *Hypha Discovery Ltd., School of Biosciences, University of Westminster, 115 New Cavendish Street, London W1W 6UW, UK*
[b] *School of Biosciences, University of Westminster, 115 New Cavendish Street, London W1W 6UW, UK*
[c] *Centre for Pharmacognosy and Phytotherapy, The School of Pharmacy, University of London, 29-39 Brunswick Square, London WC1N 1AX, UK*
[d] *Department of Pharmaceutical Sciences, University of Strathclyde, 27 Taylor Street, Glasgow G4 0NR, UK*
[e] *Institute of Biological Sciences, University of Wales, Aberystwyth, Penglais, Aberystwyth SY23 3DD, UK*

Received 3 May 2006; received in revised form 19 June 2006
Available online 22 August 2006

Abstract

A fusidane triterpene, 16-deacetoxy-7-β-hydroxy-fusidic acid (**1**), was isolated from a fermentation of the mitosporic fungus *Acremonium crotocinigenum*. Full unambiguous assignment of all ^{1}H and ^{13}C data of **1** was carried out by extensive one- and two-dimensional NMR studies employing HMQC and HMBC spectra.

Compound **1** was tested against a panel of multidrug-resistant (MDR) and methicillin-resistant *Staphylococcus aureus* (MRSA) strains and showed minimum inhibitory concentration values of 16 μg/ml.

Keywords: *Acremonium crotocinigenum*; Fusidane triterpene; Fusidic acid; Antibacterial; MRSA; MDR; *Staphylococcus aureus*

1. Introduction

Our studies on the production of metabolites by taxa of tropical rainforest fungi in fermentation, have led to the isolation and characterisation of a new metabolite, designated 16-deacetoxy-7β-hydroxy-fusidic acid (**1**), which is structurally related to the commercial antibiotic, fusidic acid, a widely used therapeutic for methicillin-resistant *Staphylococcus aureus* (MRSA) infections which is still of interest as a template for antibiotic activity improvement (Søtofte and Duvold, 2001). The metabolite is a prominent component of fermentation liquors from shake cultures of an isolate of the mitosporic fungus *Acremonium crotocinigenum*, cultured from rotting wood in Rio Palenque Forest Reserve, Pichincha Province, Ecuador in 1986, and currently held in the University of Westminster culture collection. *Acremonium* is a polyphyletic genus, often confused with *Cephalosporium* and is related to a number of ascomycete teleomorphs (Gams, 1971). It contains some 105 species, including a number which have been shown to produce biologically active metabolites (Kirk et al., 2001). Previous studies on *A. crotocinigenum* found sesquiterpenoid compounds of the isocrotonic acid type (Gyimesi and Melera, 1967).

The detection of **1** was part of a programme for screening tropical fungi for new antibiotics with activity against MRSA. There is currently an acute need for new effective antibiotics for MRSA treatment, especially since the appearance of vancomycin resistant (VRSA) strains (Centers for Disease Control and Prevention, 2003; Chang et al., 2003). Liquid fermentation was used in conjunction

* Corresponding author. Tel.: +44 207 7535913; fax: +44 207 7535909.
E-mail address: simon.gibbons@pharmacy.ac.uk (S. Gibbons).

0031-9422/$ - see front matter © 2006 Elsevier Ltd. All rights reserved.
doi:10.1016/j.phytochem.2006.06.033

with bioautography, to qualitatively indicate the presence of antibacterial compounds, facilitating the isolation of compound **1** by vacuum liquid chromatography.

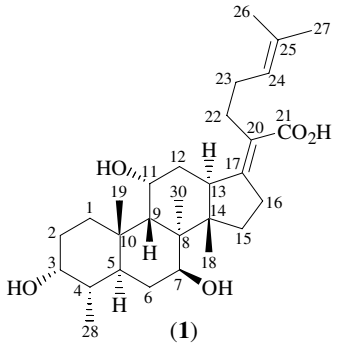

(**1**)

2. Results and discussion

Bioautography of the Diaion HP20 resin extract of the fermentation filtrate led to the isolation of compound **1** as a white solid. High-resolution ESI-TOFMS in the positive mode suggested a molecular formula of $C_{29}H_{46}O_5$. Signals in the ^1H and ^{13}C NMR spectra (Table 1) for five methyl singlets, one methyl doublet, four olefinic carbons and a carbonyl of a carboxylic acid (δ_C 173.8), were indicative of a fusidane class triterpene of the fusidic acid type (Rastup-Andersen and Duvold, 2002).

Table 1
^1H (400 MHz) and ^{13}C NMR (100 MHz) spectral data and ^1H–^{13}C long-range correlations of **1** recorded in $CDCl_3$

Position	^1H	^{13}C	^2J	^3J
1	1.50 *m*, 2.23 *m*	30.0		
2	1.75 *m*, 1.81 *m*	29.9		
3	3.73 *bq*	71.4	C-2	C-5
4	1.54 *m*	37.3		
5	2.31 *m*	36.2		
6	1.45 *m*, 1.67 *m*	34.1		
7	3.99 *t* (8.0)	70.9	C-6	C-14, C-30
8	–	45.6	–	–
9	1.52 *m*	50.8	–	–
10	–	36.7	–	–
11	4.37 *bs*	68.7	–	C-8
12	1.75 *m*, 2.39 *m*	36.4		
13	3.05 *bd* (12.1)	46.0	C-14, C-17	C-15, C-20
14	–	49.6	–	–
15	1.54 *m*, 1.77 *m*	33.4	–	–
16	2.68 *m*, 2.86*m*	33.0	C-15, C-17	C-20
17	–	160.4	–	–
18	0.89 *s*	15.9	C-14	C-8, C-13, C-15
19	0.95 *s*	24.4	C-10	C-5, C-1, C-9
20	–	125.0	–	–
21	–	173.8	–	–
22	2.44 *m*	28.5	C-20, C-23	C-17, C-21
23	2.02 *m*, 2.17 *m*	29.4	C-22, C-24	C-25
24	5.12 *t*, (7.2)	124.0	C-23	C-26, C-27
25	–	132.2	–	–
26	1.61 *s*	18.0	C-25	C-24, C-27
27	1.67 *s*	25.9	C-25	C-24, C-26
28	0.93 *d* (6.8)	16.0	C-4	C-3, C-5
30	1.36 *s*	14.6	C-8	C-7, C-9, C-14

By careful analysis of the HMBC, HMQC and COSY spectra it was possible to show that **1** was a new fusidic acid analogue. Assuming that the methyl doublet was C-28 of the fusidane skeleton, the protons of this group coupled to a methine proton (δ_H 1.54, H-4) in the COSY spectrum. H-4 formed part of a spin system with a deshielded methine (δ_H 3.73, H-3) and two methylene groups (at C-2 and C-1). In the HMBC spectrum, C-1 was coupled to by the protons of methyl-C19 (δ_H 0.95) which showed further couplings to C-10 (^2J), C-9 (^3J) and C-5 (^3J). In the COSY spectrum, H-5 (δ_H 2.31 *m*) coupled to both protons of a methylene moiety (C-6, δ_H 1.45, 1.67), which further coupled to a deshielded oxymethine proton (C-7, δ_H 3.00, *t*). Inspection of the HMBC spectrum showed that the carbon associated with this deshielded proton was coupled to by the protons of a further angular methyl singlet (C-30), which showed additional couplings to a methine carbon (C-9) and two quaternary carbons (C-8, δ_C 45.6 and C-14, δ_C 49.6). This completed the resonances for the A and B rings of compound **1**. Inspection of the COSY spectrum showed that the proton associated with C-9 (H-9) formed part of a CH–CH–CH_2–CH spin system which allowed identification of positions C-9, C-11, C-12 and C-13, respectively. C-11 was deshielded (δ_C 68.7, δ_H 4.37) indicating that an oxygen should be placed here. Furthermore, H-13 (delineated by inspection of the HMQC spectrum) was also deshielded (δ_H 3.05) suggesting that it was allylic and that an olefinic carbon (C-17) should be placed at the neighbouring carbon, which is typical for fusidic acid metabolites (Rastup-Andersen and Duvold, 2002). The protons of a methyl group (C-18) coupled to C-13 (^3J), C-14 (^2J) and to a methylene carbon (C-15, ^3J). CH_2-15 coupled to a deshielded allylic methylene group (δ_H 2.68, 2.86 (CH_2-16)) which again was supportive of being alpha to an olefinic carbon (C-17, δ_C 160.4). This completed rings C and D of **1**. H-13 and H_2-16 both gave a ^2J coupling to C-17 and a ^3J coupling to C-20, suggesting a C-17,20 double bond. In the HMBC spectrum C-17 was also coupled to by the protons of an allylic methylene (C-22, δ_H 2.44) which also coupled to a carbonyl carbon of a carboxylic acid group (C-21) and an olefinic methine carbon (C-24, δ_C 124.0). A further methylene (C-23) could be placed between C-22 and C-24 by couplings observed in the COSY spectrum. Finally, two deshielded geminal methyl groups could be placed on an olefinic carbon (C-25) *via* their HMBC correlations to this carbon and to the olefinic partner C-24 finalising the C-24–C-25 double bond. These resonances completed the eight carbon chain of the fusidane triterpene skeleton. HRESI-MS of **1** suggested a molecular formula of $C_{29}H_{46}O_5$ $[M]^+$ (475.3422). From the chemical shift values of H-3, H-7 and H-11, hydroxyl groups must be placed at these positions. From the molecular formula and chemical shift of the C-21 carbon, a car-

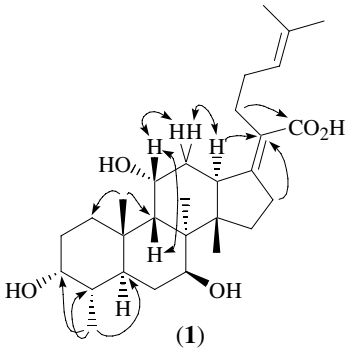

Fig. 1. Key COSY (double headed arrow) and HMBC (single headed arrow) correlations for compound **1**.

boxylic acid must be placed at C-21 and this is identical to that seen in fusidic acid (see Fig. 1).

The final consideration was to assign stereochemistry of hydroxyl groups at C-3, C-7 and C-11. The hydrogens at C-3 and C-11 were assigned as equatorial (rel β) on the basis of no large discernable couplings for these signals, which would make the hydroxyl groups at these positions both α and axial. The coupling constant for H-7 (δ 3.99, *t*) was 8.0 Hz indicating an axial-axial interaction with the axial partner of CH_2-6. This would make H-7 axial (α) and the OH at this position therefore equatorial (β). This was further supported by an NOE between H-7 and CH_3-30 indicating that they are both on the alpha face of the fusidane skeleton.

Fusidic acid and all known analogues to date have no substitution on carbon 7. Compound **1** possesses an hydroxyl at this position. *A. crotocinigenum* has also been found to produce analogues with an hydroxyl on carbon 16 and **1** is the first member of this class to be completely unsubstituted at the C-16 position.

Compound **1** was tested against a battery of drug-resistant bacteria and where active, possessed a minimum inhibitory concentration of 16 μg/ml, which although occasionally more active than erythromycin and norfloxacin, was significantly less potent than the fusidic acid comparator.

3. Experimental

3.1. General experimental procedures

NMR spectra were recorded on a Bruker AVANCE 500 MHz spectrometer. Chemical shift values (δ) were reported in parts per million (ppm) relative to appropriate internal solvent standard and coupling constants (*J* values) are given in Hertz. Accurate mass measurements were determined on a Micromass Q-TOF Ultima Global Tandem Mass Spectrometer. The sample was run under electrospray ionisation mode using 50% acetonitrile in water and 0.1% formic acid as solvent. [Glu]-fibrinopeptide B peptide was used as an internal standard, $[M+2H]^{2+} = 785.8426$.

IR spectra were recorded on a Nicolet 360 FT-IR spectrophotometer and UV spectra on a Thermo Electron Corporation Helios spectrophotometer.

3.2. Fungal strain

Cultures were maintained on malt extract agar (Oxoid) and for long term storage on malt extract agar plugs submerged in sterile distilled water at room temperature, as part of the University of Westminster culture collection (Culture No. cc56). The isolate was identified as *A. crotocinigenum* by David Brayford, initially through DNA sequencing of a PCR product amplified from the variable ITS (internal transcribed spacer) region of the ribosomal RNA locus using the conserved primers ITS1F and ITS4 (White et al., 1990; Gardes and Bruns, 1993). A search of DNA sequence databases with 508 bp of DNA sequence from this PCR product using the FASTA algorithm (Pearson and Lipman, 1988; http://www.ebi.ac.uk/fasta/) revealed the most closely related sequence accession to be AJ621773 (*Acremonium crotocinigenum*), which showed 98.2% identity over a 513 bp overlap. This *A. crotocinigenum* strain was isolated from the basidiome of *Trametes versicolor* in a Hungarian coal mine (Schol-Schwarz, 1965) and was named by Gams (1971). Comparisons of the conidia, chlamydospores and colony appearance with those described in Schol-Schwarz (1965) and Gams (1971) were used to confirm that cc56 was indeed morphologically the same as *A. crotocinigenum*. Further confirmation was obtained by direct comparison of cc56 with strain CABI 112775 (syn. CBS 129.64) kindly supplied by the International Mycological Institute, Egham, UK. The ITS sequence for isolate cc56 has been deposited in the GenBank database (accession number DQ882846).

3.3. Fermentation and extraction

Inoculum for the fermentation was prepared by vigorously shaking twenty 8 mm diameter plugs, excised from an actively growing culture of *A. crotocinigenum* on 2% malt extract agar (Oxoid), in 10 ml of sterile distilled water containing 2–3 ml of glass beads (VWR). The resulting mycelial suspension (2 ml) was added to each of twenty 1000 ml conical flasks, containing 200 ml of sterilised 2% potato dextrose broth (Difco). The flasks were incubated on a rotary shaker (200 rpm) for two weeks at 26 °C.

Biomass was removed from the culture broth by filtering through muslin prior to filtration through a Whatman No. 1 filter paper. The filtrate was then extracted with Diaion HP20 resin (400 ml; Mitsubishi) which had previously been washed with HPLC grade methanol (Merck) and thoroughly conditioned with distilled water. The resin was removed, washed with distilled water (2×1000 ml) and eluted with HPLC grade methanol (2×1000 ml). The methanolic eluent was evaporated to dryness.

3.4. Isolation

The crude HP20 resin extract of the culture filtrate was dissolved in methanol (5 ml) and combined with an equivalent mass of silica gel (flash chromatography grade; BDH; 1.6 g) and evaporated. The slurry was packed in a pre-column cartridge assembled in a Biotage™ chromatography apparatus along with a 40 mm diameter silica gel column.

The column was eluted with the following mobile phase fractions: 100% dichloromethane (100 ml), 2% methanol/dichloromethane (200 ml), 4% methanol/dichloromethane (200 ml), 6% methanol/dichloromethane (200 ml), 8% methanol/dichloromethane (200 ml) and finally 10% methanol/dichloromethane (200 ml). None of the fractions were observed to contain the desired metabolite which had correlated to a zone of inhibition in the bioautographical analysis. The column was therefore further eluted with 20% methanol/dichloromethane and a series of 30 ml volume fractions were collected. TLC analysis showed the target compound to be present in fractions 7–18. These fractions were combined, evaporated to dryness and re-dissolved in 9:1 ethyl acetate/*n*-hexane (2 ml) for further fractionation on a 10 mm diameter Biotage column, using isocratic 9:1 ethyl acetate/*n*-hexane as the mobile phase, fractionated into 7 ml fractions. The target compound was contained in fractions 5–15, these were combined, dried and reconstituted in 8% methanol/dichloromethane for further isocratic fractionation using the same solvent and a 10 mm Biotage column. Fractions of 3 ml volume were collected, TLC analysis showed the compound to be solely present in fractions 12–32. These fractions were combined and the dry weight of pure compound determined to be 17.1 mg.

3.5. Thin layer chromatography and bioautography analysis

Thin layer chromatography (TLC) separation was achieved using silica gel plates and three solvent systems (9:1 dichloromethane/methanol; 6:4 ethyl acetate/*n*-hexane and 9:1 ethyl acetate/*n*-hexane). All solvents used were HPLC grade.

Metabolites were visualised on the TLC plates by spraying with a 4% vanillin/concentrated sulphuric acid solution and heating with a hot air gun.

Bioautographic analysis was performed using *Staphylococcus aureus* (NCTC 6571) as the test organism.

S. aureus inoculum was prepared by seeding a 100 ml conical flask containing sterile nutrient broth (10 ml), the flask was shaken overnight at 200 rpm at 37 °C.

The inoculum was applied to the run TLC plates by gently dabbing with sterilised foam. The seeded plates were subsequently incubated overnight at 37 °C in a humidified chamber. The incubated plates were then sprayed with nitro-blue tetrazolium (Sigma Ltd.) in order to stain the live *S. aureus* and then re-incubated for 1 h to develop, the undeveloped areas of the plates indicating the presence of growth-inhibiting compounds.

3.6. Antibacterial assay

S. aureus strain ATCC 25923 was the generous gift of E. Udo (Kuwait University, Kuwait). *S. aureus* RN4220 containing plasmid pUL5054, which carries the gene encoding the MsrA macrolide efflux protein, was provided by J. Cove (Ross et al., 1989). Strain XU-212, which possesses the TetK tetracycline efflux protein, was provided by E. Udo (Gibbons and Udo, 2000). SA-1199B, which overexpresses the *norA* gene encoding the NorA MDR efflux protein was provided by G. Kaatz (Kaatz et al., 1993). All *Staphylococcus aureus* strains were cultured on nutrient agar and incubated for 24 h at 37 °C prior to MIC determination. Bacterial inocula equivalent to the 0.5 McFarland turbidity standard were prepared in normal saline and diluted to give a final inoculum density of 5×10^5 cfu/ml. The inoculum (125 μl) was added to all wells and the microtitre plate was incubated at 37 °C for 18 h. The MIC was recorded as the lowest concentration at which no bacterial growth was observed as previously described (Gibbons and Udo, 2000) (see Table 2).

3.7. 16-Deacetoxy-7β-hydroxyfusidic acid (*1*)

White powder; $[\alpha]_D^{21} - 113.64°$ (*c* 0.08, $CHCl_3$); UV (ACN) λ_{max} (log ε): 233 (3.96) nm; IR ν_{max} (thin film) cm^{-1}: 3369.62, 2924.39, 1715.97, 1696.02, 1558.27, 1436.56, 1375.42, 1255.07 1053.01, 934.01, 653.86; ^1H NMR and ^{13}C NMR ($CDCl_3$): see Table 1; HRES-MS (*m*/*z*): 475.3422 $[M+H]^+$ (calc. for $C_{29}H_{47}O_5$, 475.3418).

Table 2
MICs of **1** and standard antibiotics in μg/ml

Strain (resistance mechanism)	1	Fusidic acid	Norfloxacin	Erythromycin	Tetracycline
ATCC 25923	16	0.125	2	0.25	0.25
SA-1199B (NorA)	16	0.125	32	0.25	0.25
RN4220 (MsrA)	16	0.25	2	128	0.25
XU212 (TetK, mecA)	>64	>64	16	>256	128
EMRSA-15	16	0.125	0.5	2048	0.125
EMRSA-16 (mecA)	>64	4	128	4096	0.125

All MICs were determined in duplicate.

Acknowledgements

We acknowledge the contribution of the late David Brayford, who sadly passed away before the publication of this paper. We thank the Engineering and Physical Sciences Research Council (Grant No. GR/R47646/01). We also thank Ing. Raul Camacho and staff of the Facultad de Ciencias, Escuela Superior Politecnica de Chimborazo, Riobamba, Ecuador for assistance with field work in Ecuador, and Cal & Piedad Dodson for permission to collect in Rio Palenque Reserve.

References

Centers for Disease Control (CDC), 2002. Public health dispatch: vancomycin-resistant *Staphylococcus aureus* – Pennsylvania. Morbid. Mortal. Week. Rep. 51, 902.

Chang, S., Sievert, D.M., Hageman, J.C., Boulton, M.L., Tenover, F.C., Downes, F.P., Shah, S., Rudrik, J.T., Pupp, G.R., Brown, W.J., Cardo, D., Fridkin, S.K.and the Vancomycin-Resistant *Staphylococcus aureus* Investigative Team, 2003. Infection with vancomycin-resistant *Staphylococcus aureus* containing the *vanA* resistance gene. New Eng. J. Med. 348, 1342–1347.

Gams, W., 1971. Cephalosporium-*artige Schimmelpilze* (*Hyphomycetes*). Gustav Fischer Verlag, Jena, 262 pp.

Gardes, M., Bruns, T.D., 1993. ITS primers with enhanced specificity for basidiomycetes – application to the identification of mycorrhizae and rusts. Mol. Ecol. 2, 113–118.

Gibbons, S., Udo, E.E., 2000. The effect of reserpine, a modulator of multidrug efflux pumps, on the in vitro activity of tetracycline against clinical isolates of methicillin resistant *Staphylococcus aureus* (MRSA) possessing the Tet(K) determinant. Phytother. Res. 14, 139–140.

Gyimesi, J., Melera, A., 1967. Structure of crotocin, an antifungal antibiotic. Tetahedron Lett. 17, 1665–1673.

Kaatz, G.W., Seo, S.M., Ruble, C.A., 1993. Efflux-mediated fluoroquinolone resistance in *Staphylococcus aureus*. Antimicrob. Agents Chemother. 37, 1086–1094.

Kirk, P.M., Cannon, P.F., David, J.C., Stalpers, J.A., 2001. Ainsworth and Bisby's Dictionary of the Fungi, ninth ed. CAB International, Wallingford, UK, 624 pp.

Pearson, W.R., Lipman, D.J., 1988. Improved tools for biological sequence comparison. PNAS 85, 2444–2448.

Rastup-Andersen, N., Duvold, T., 2002. Reassignment of the ^{1}H NMR spectrum of fusidic acid and total assignment of ^{1}H and ^{13}C NMR spectra of some selected fusidane derivatives. Mag. Res. Chem. 40, 471–473.

Ross, J.I., Farrell, A.M., Eady, E.A., Cove, J.H., Cunliffe, W.J., 1989. Characterisation and molecular cloning of the novel macrolide-streptogramin B resistance determinant from *Staphylococcus epidermidis*. J. Antimicrob. Chemother. 24, 851–862.

Schol-Schwarz, M.B., 1965. *Cephalosporium crotocinigenum* sp. nov. Trans. Brit. Mycol. Soc. 48, 51–53.

Søtofte, I., Duvold, T., 2001. A new potent fusidic acid analogue. Acta Crystallogr. E57, o829–o831.

White, T.J., Bruns, T., Lee, S., Taylor, J.W., 1990. Amplification and direct sequencing of fungal ribosomal RNA genes for phylogenetics. In: Innis, M.A., Gelfand, D.H., Sninsky, J.J., White, T.J. (Eds.), PCR Protocols: A Guide to Methods and Applications. Academic Press, Inc., New York, pp. 315–322.

New Constituents of *Artemisia monosperma*

Michael Stavri,[†] K. Thomas Mathew,[‡] Trevor Gibson,[§] R. Thomas Williamson,[⊥] and Simon Gibbons*[,†]

Centre for Pharmacognosy and Phytotherapy, The School of Pharmacy, University of London, London, WC1N 1AX, U.K., The Herbarium, Department of Biological Science, Kuwait University, P.O. Box 5969, Safat 13060, Kuwait, Cubist Pharmaceuticals, Slough, U.K., and Wyeth Research, Global Chemical Sciences, 401 N. Middletown Road, Pearl River, New York 10965

Received December 31, 2003

A new eudesmane sesquiterpene (**1**) and a C_{10} diyne (**2**) were isolated from the aerial parts of *Artemisia monosperma*. The structures of these compounds were determined as *rel*-1*β*,3α,6*β*-trihydroxyeudesm-4-ene (**1**) and 1,3*R*,8*R*-trihydroxydec-9-en-4,6-yne (**2**) on the basis of spectral data interpretation. The absolute stereochemistry of **2** was determined using Mosher ester methodology in which the terminal primary hydroxyl group was first protected to simplify the stereochemical analysis.

In an ongoing phytochemical study of selected species of the Kuwaiti flora,[1] the aerial parts of *Artemisia monosperma* Del. (Asteraceae) have been investigated. This species grows along the northwestern border with Iraq, and its distribution in Kuwait is restricted to the sandy gullies of Wadi Al-Batin. Previous investigation of this plant has led to the isolation of a series of acetylenes and acetophenones,[2] an insecticidal aromatic acetylene,[3] and flavones and flavanol glycosides.[4]

The aerial parts of *A. monosperma* were dried and extracted in a Soxhlet apparatus. Compound **1** was isolated as an oil from the hexane extract. Signals in the ^{1}H and ^{13}C NMR spectra (Table 1) were characteristic of a eudesmane sesquiterpene,[5,6] this class being commonly found in the genus *Artemisia*.[7] By inspection of the HMBC and COSY spectra it could be shown that compound **1** had the connectivities typical of a eudesmane skeleton. From HMBC and DEPT-135 data, a methyl singlet (C-14) exhibited a ^2J correlation to C-10 and ^3J correlations to C-9 (CH_2), C-5 (quaternary), and an oxymethine carbon (C-1). From the HMQC spectrum, the proton directly attached to this carbon was a broad doublet (J = 12.9 Hz) and therefore axial. This proton coupled to two protons of a methylene group (C-2) that further coupled to another oxymethine proton (H-3, δ_H = 4.38, δ_C = 85.1), which was a broad singlet and equatorial in orientation. In the HMBC spectrum, the carbon to which this proton was attached was correlated with the protons of a downfield methyl group (C-15), which was deshielded (δ_H = 1.88) being directly attached to a double bond. This was confirmed by a ^2J correlation between these methyl protons to a quaternary olefinic carbon (C-4) and a ^3J correlation to a further quaternary carbon (C-5, δ_C = 144.7), which was also coupled to H-3 and the methyl protons of C-14, placing this carbon at C-5 and not C-4.

Further signals in the ^{1}H NMR spectrum included the most deshielded oxymethine proton (δ_H = 4.84), which gave HMBC correlations to carbons C-4 and C-5 and must therefore be placed at C-6. This resonance was a sharp singlet (equatorial) and coupled to a further methine proton (H-7) in the COSY spectrum. H-7 exhibited further couplings to a methine proton (H-11), which formed part of the typical eudesmane sesquiterpene isopropyl moiety commonly found at C-7 of this natural product class.[7] This was supported by the presence in the ^{1}H NMR spectrum of two methyl doublets, which in the COSY spectrum coupled to H-11. Additionally, H-7 coupled to a methylene group (C-8) that also correlated to the C-9 methylene group, therefore completing the B-ring and the 4-eudesmene skeleton.

From the coupling constant of 12.9 Hz for H-1 this proton must be axial, and lack of any discernible couplings for H-3 and H-6 (both singlets) implies that these protons are equatorial. Accurate mass determination indicated a molecular formula of $C_{15}H_{26}O_3$, which suggests that hydroxyl groups must be placed at C-1, C-3, and C-6. Compound **1** was therefore assigned as *rel*-1*β*,3α,6*β*-trihydroxyeudesm-4-ene and is reported here for the first time. A paucity of material prohibited determination of absolute stereochemistry.

Table 1. ^{1}H and ^{13}C NMR Data (δ) for Compounds **1** and **2**[a]

	1			**2**	
position	^{1}H	^{13}C	position	^{1}H	^{13}C
1	3.65 bd (12.9)	73.3	1	3.70 m	59.1
2	1.83 m, 2.31 bd (14.0)	30.8	2	1.89 m	41.3
3	4.38 bs	85.1	3	4.56 t (6.9)	60.2
4		125.5	4		82.0
5		144.7	5		68.9
6	4.84 s	67.4	6		70.1
7	0.91 m	48.9	7		79.5
8	1.62 m	19.2	8	4.88 d (5.4)	63.8
9	1.11 m, 1.99 (12.6)	37.7	9	5.91 ddd (17.0, 10.1, 5.4)	138.1
10		39.2	10	5.19 d (10.1), 5.40 bd (17.0)	116.1
11	1.70 m	28.9			
12	1.00 d (6.3)	20.7			
13	0.97 d (6.3)	21.2			
14	1.16 s	18.0			
15	1.88 s	17.2			

[a] Measured in $CDCl_3$. Coupling constants (Hz) in parentheses.

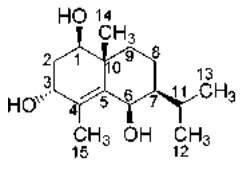

1

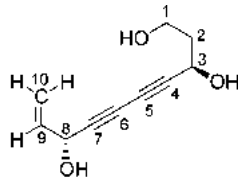

2

* To whom correspondence should be addressed. Tel: ++44 207 753 5913. Fax: ++44 207 753 5909. E-mail: simon.gibbons@ulsop.ac.uk.
[†] University of London.
[‡] Kuwait University.
[§] Cubist Pharmaceuticals.
[⊥] Wyeth Research.

10.1021/np030558v CCC: $27.50
Published on Web 04/01/2004

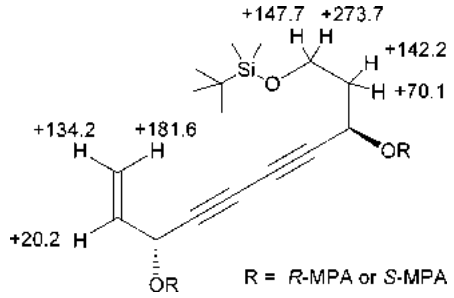

Figure 1. $\Delta\delta$ values [$\Delta\delta$ (in ppb) = $\delta_R - \delta_S$] obtained for the (*R*)- and (*S*)-MPA esters (**2a** and **2b**, respectively) of the TBDMS-protected **2**.

Compound **2** was isolated from the $CHCl_3$ extract by preparative TLC. Signals in the ^1H NMR and ^{13}C NMR spectra (Table 1) included two signals of an exomethylene, a highly coupled olefinic proton, two oxymethine protons, one oxymethylene group, and one methylene group. In addition to these resonances, the carbon spectrum showed the presence of four quaternary carbons, which were very similar to those seen in diacetylenic natural products such as falcarindiol;[8] in fact, the olefinic and oxymethine resonances were in close agreement with those reported for this diyne natural product.[8] The presence of triple bonds in compound **2** was confirmed by a weak absorption (2357 cm^{-1}) in the IR spectrum.

The COSY spectrum of **2** indicated that the exocyclic methylene protons coupled to the olefin, which in turn also coupled to an oxymethine proton (δ 4.88), and this exhibited ^2J and ^3J correlations in the HMBC spectrum to two acetylenic carbons (C-7 and C-6). Further couplings in the COSY spectrum included those between the oxymethylene, methylene, and remaining oxymethine proton, which resulted in a $CH(O)-CH_2CH_2OH$ spin system. In the HMBC spectrum the oxymethine resonance of this spin system also coupled to two acetylenic quaternary carbons (C-4 and C-5). The shielded nature of the two triple bonds suggested that they must be conjugated and connected, and this feature is commonly seen with other acetylenes such as falcarindiol.[8−10] HREIMS suggested a molecular formula of $C_{10}H_{12}O_3$, and therefore three hydroxyl groups must be placed at the oxymethine (C-3 and C-8) and oxymethylene carbons (C-1). Compound **2** was therefore assigned as 1,3,8-trihydroxydec-9-en-4,6-yne. The final problem that remained was the assignment of absolute stereochemistry at carbons 3 and 8, and this was resolved using a modified Mosher method.[11]

The *tert*-butyl dimethylsilyl (TBDMS)-protected **2** was treated with (*R*)-(−)- and (*S*)-(+) methoxyphenylacetic acid (MPA) in two separate reactions to give the bis-(*R*)- and bis-(*S*)-MPA esters (**2a** and **2b**, respectively). $\delta\Delta^{R,S}$ values ($\delta_R - \delta_S$) are shown in Figure 1. The $\delta\Delta^{R,S}$ values for H_2-1 and H_2-2 were positive, indicating *R* stereochemistry at C-3. By analogy, the $\delta\Delta^{R,S}$ values for H-9 and H_2-10 were positive, indicating *R* stereochemistry at C-8.

Both compounds were tested against methicillin- and multidrug-resistant strains of *Staphylococcus aureus* but were inactive (MIC > 128 μg/mL). This was surprising in the case of **2**, which shares some similarity with the anti-staphylococcal acetylene, falcarindiol.[12]

Experimental Section

General Experimental Procedures. Optical rotations were measured on a Bellingham and Stanley ADP 200 polarimeter. IR spectra were recorded on a Nicolet 360 FT-IR spectrophotometer. ^1H NMR (500 MHz) and ^{13}C NMR (125 MHz) spectra were recorded in $CDCl_3$ on a Bruker Avance 500 spectrometer. Chemical shift values (δ) are reported in parts per million (ppm) relative to NMR solvent $CDCl_3$ (δ_H = 7.27, δ_C = 77.0). Coupling constants (*J* values) are given in Hz. $^1H-^1H$ COSY, HMBC, and HMQC experiments were recorded with gradient enhancements using sine-shaped gradient pulses. Accurate mass measurement was performed on a Finnigan MAT 95 high-resolution magnetic sector mass spectrometer using electron ionization and voltage scanning at 10 000 resolution. Vacuum-liquid chromatography on Merck silica gel 60 $PF_{254+366}$ was used for fractionation and isolation. TLC was performed using Kieselgel 60 F_{254} (Merck) precoated plates, and spots were visualized by spraying with vanillin−sulfuric acid spray followed by heating.

Plant Material. *Artemisia monosperma* was collected from the sandy gullies in northwestern Kuwait bordering Iraq, interspersed with sandstone ridges and opening westwards into the extensive plains of the Wadi Al-Batin. The material was identified by K.T.M. A voucher specimen (KTM 4225, collected by K.T.M. and S.G. in February 1999) is deposited at the Kuwait University Herbarium (KTUH).

Extraction and Isolation. The aerial parts were air-dried for 3 days and ground to a fine powder. The powdered plant material (285 g) was extracted sequentially in a Soxhlet apparatus (3 L each) with hexane, chloroform, and methanol. Vacuum-liquid chromatography (VLC) of the hexane extract (10 g) was performed using a step gradient of 10% EtOAc in hexane followed by a final methanol wash to yield 12 fractions. Flash chromatography of VLC fraction 5 (1.4 g, 6:4 hexane−EtOAc) employing an 8:2 hexane−EtOAc isocratic system, followed by multiple preparative TLC (96 mg, 7:3 hexane−EtOAc, 3 developments), afforded 3 mg of compound **1**.

The chloroform extract (10 g) was subjected to VLC as described above. LH-20 Sephadex chromatography of VLC fraction 10 (231 mg; eluted using 90% EtOAc in hexane) using dichloromethane yielded nine fractions. Fractions 6 and 7 were combined (29 mg) and subjected to preparative TLC (toluene−EtOAc−AcOH, 30:68:2) to afford compound **2** (10 mg).

Compound 1 (*rel*-1β,3α,6β-trihydroxyeudesm-4-ene): colorless oil, $[\alpha]_D^{25}$ +314° (*c* 0.05, $CHCl_3$); IR ν_{max} (thin film) 3362, 2939, 2868, 1738, 1217, 781 cm^{-1}; ^1H and ^{13}C NMR data ($CDCl_3$), see Table 1; HREIMS *m/z* 254.1864 (calcd for $C_{15}H_{26}O_3$, 254.1882).

Compound 2 (1,3*R*,8*R*-trihydroxydec-9-en-4,6-yne): colorless oil, $[\alpha]_D^{25}$ +127° (*c* 0.24, MeOH); UV (MeOH) λ_{max} (log ϵ) 234 (3.18), 255 (3.05), 282 (3.05) nm; IR ν_{max} (thin film) 3259, 2357, 1635, 1507, 792 cm^{-1}; ^1H and ^{13}C NMR data ($CDCl_3$), see Table 1; HREIMS *m/z* 180.0788 (calcd for $C_{10}H_{12}O_3$, 180.0786).

Determination of Absolute Stereochemistry of Compound 2. TBDMS Protection of 2. Compound **2** (500 μg, 2.8 μmol) was dissolved in 750 μL of $CDCl_3$. To this mixture were added 20 μL aliquots of a 2.5:1 mixture of imidazole and TBDMS-Cl (1 μmol/mL). The reaction was monitored by NMR, and when complete protection of the primary alcohol was observed, the mixture was applied directly to a preconditioned 3 mL silica gel solid-phase extraction cartridge (Bakerbond). The TBDMS-protected **2** was eluted with 50% EtOAc−hexane and evaporated to dryness.

MPA Esterification of TBDMS-Protected 2. To a vial containing the TBDMS-protected **2** were added 1.5 mg of *R*- or *S*-MPA, 15 mg of polystyrene-carbodiimide (Argonaut Inc., Foster City, CA), and 200 μg of DMAP. The reaction mixture was dissolved in 750 μL of $CDCl_3$ and placed on a rotary shaker overnight. The reaction mixture was applied directly to a preconditioned 3 mL silica gel solid-phase extraction cartridge (Bakerbond). The desired product was eluted with $CDCl_3$ and evaporated to dryness.

Acknowledgment. We are grateful to the School of Pharmacy, University of London, for the award of a Ph.D. scholarship to M.S.

References and Notes

(1) Gibbons, S.; Ali-Amine, S.; Mathew, K. T.; Skelton, B. W.; White, A. H.; Gray A. I. *J. Nat. Prod.* **2000**, *63*, 839−840.

(2) Bohlmann, F.; Ehlers, D. *Phytochemistry* **1977**, *16*, 1450−1451.
(3) Saleh, M. A. *Phytochemistry* **1984**, *23*, 2497−2498.
(4) Saleh, N. A. M.; El-Negoumy, S. I.; Abd-Alla, M. F.; Abou-Zaid, M. M.; Dellamonica, G.; Chopin, J. *Phytochemistry* **1985**, *24*, 201−203.
(5) García-Granados, A.; Molina, A.; Sáenz de Buruaga A.; Sáenz de Buruaga, J. M. *Phytochemistry* **1985**, *24*, 97−101.
(6) Zhao, Y.; Yue, J.; Lin, Z.; Ding, J.; Sun, H. *Phytochemistry* **1997**, *44*, 459−464.
(7) Fraga, B. M. *Nat. Prod. Rep.* **2002**, *19*, 650−672.
(8) Furumi, K.; Fujioka, T.; Fujii, H.; Okabe, H.; Mihashi, K.; Nakano, Y.; Matsunaga, H.; Katano, M.; Mori M. *Bioorg. Med. Chem. Lett.* **1998**, *8*, 93−96.
(9) Bernart, M. W.; Cardellina, J. H., II; Balaschak, M. S.; Alexander, M. R.; Shoemaker, R. H.; Boyd, M. R. *J. Nat. Prod.* **1996**, *59*, 748−753.
(10) Kobaisy, M.; Abramowski, Z.; Lermer, L.; Saxena, G.; Hancock, R. E.; Towers, G. H. N.; Doxsee, D.; Stokes, R. W. *J. Nat. Prod.* **1997**, *60*, 1210−1213.
(11) Seco, J. M.; Quinoa, E.; Riguera, R. *Chem. Rev.* **2004**, *104*, 17−117.
(12) Lechner, D.; Stavri, M.; Oluwatuyi M.; Pereda-Miranda, R.; Gibbons, S. *Phytochemistry* **2004**, *64*, 331−335.

NP030558V

NMR Spectroscopy, X-ray Crystallographic, and Molecular Modeling Studies on a New Pyranone from *Haloxylon salicornicum*

Simon Gibbons,*[,†] Brian J. Denny,[‡] Sana'a Ali-Amine,[‡] K. T. Mathew,[§] Brian W. Skelton,[⊥] Allan H. White,[⊥] and Alexander I. Gray[∥]

Centre for Pharmacognosy and Phytotherapy, The School of Pharmacy, University of London, 29-39 Brunswick Square, London WC1N 1AX, U.K., Department of Pharmaceutical Chemistry, Faculty of Pharmacy, Kuwait University, P.O. Box 24923, Safat 13110, Kuwait, The Herbarium, Department of Biological Science, Kuwait University, P.O. Box 5969, Safat 13060, Kuwait, Department of Chemistry, University of Western Australia, Nedlands, WA 6907 Australia, and Department of Pharmaceutical Sciences, University of Strathclyde, 27 Taylor Street, Glasgow G4 0NR, Scotland, U.K.

Received October 22, 1999

A new pyranone, 5-hydroxy-3-methoxy-4*H*-pyran-4-one (**1**), was isolated from the aerial parts of the desert shrub *Haloxylon salicornicum*. The structure was elucidated by X-ray structural analysis, NMR spectroscopy, and mass spectrometry. The monoacetate was also prepared, and molecular modeling studies and full NMR data were recorded.

As part of a continuing study into the chemistry and chemotaxonomy of the desert flora of Kuwait,[1] we have studied the chemistry of *Haloxylon salicornicum* (Moq.) Bunge ex Boiss. (Chenopodiaceae) and isolated a new simple pyranone (**1**) from a chloroform extract of the aerial parts of the plant. Previous phytochemical studies on this species has led to the isolation of simple quinolines[2] and tyramine derivatives.[3] The family Chenopodiaceae is well represented in Kuwait,[4] and some of the most hardy perennial desert plants belong to this taxon. The family is known for its propensity for tolerance of salty and xeric conditions.

By Biotage flash chromatography and recrystallization, compound **1** was isolated as fine needles. The EIMS of compound **1** indicated a molecular ion at *m*/*z* 142. By recrystallization from methanol−ethyl acetate (1:1), a crystal of sufficient quality of **1** was obtained for X-ray structural analysis, which on completion led to the solution of the structure of compound **1** (Table 1, Figure 1). Natural product **1** is assigned as the new pyranone, 5-hydroxy-3-methoxy-4*H*-pyran-4-one monohydrate.

NMR studies on this natural product confirmed the X-ray analysis of **1**. Signals in the ^{1}H and ^{13}C NMR spectra indicated the presence of a methoxyl (δ_H 3.77, δ_C 57.8), two superimposed olefinic protons (δ_H 8.01 2H, δ_C 139.5, 142.0), and a broad hydroxyl moiety (δ_H 7.62). Compound **1** was acetylated to yield its acetate (**2**), which was subjected to 1D and 2D NMR studies. Both olefinic protons were now separate, but each of their corresponding carbon signals appeared as two signals. Analysis of the HMBC spectrum of **2** revealed correlations between an olefinic proton (H-6) and C-5 (^2J), the C-4 carbonyl and C-2 (both ^3J). The remaining olefinic proton, H-2, exhibited correlations with C-3 (^2J), C-4, and C-6 (^3J), which completed the pyran-4-one nucleus. The remaining cross-peaks could be attributed to the methoxyl protons to C-5 (^3J) and the acetyl methyl group to its carbonyl (^2J). To account for the doubling of the carbon resonances at positions C-2 and C-6 in compound **2**, molecular modeling was carried out to determine whether the acetylate adopted two low-energy conformations. Using semiempirical quantum mechanical energy calculations (MOPAC), conformational analysis about the C(4)−C(3)−O(3)−acetyl torsion angle revealed two different low-energy conformers that cannot interconvert (Figure 2). This would explain the doubling of NMR signals for the carbons at positions C-2 and C-6.

The demethyl parent compound, rubiginol (**3**), has been reported to be an insect sex pheromone from the male

Table 1. Atomic Positional and Isotropic Displacement Parameters

atom	*x*	*y*	*z*	U_{eq} (Å^2)
O(1)	0.1981(2)	0.3086(1)	0.0090(1)	0.0753(9)
C(2)	0.2678(2)	0.3768(2)	0.1033(2)	0.063(1)
C(3)	0.3205(2)	0.5379(2)	0.1100(1)	0.0466(8)
O(3)	0.3934(2)	0.6112(1)	0.20263(8)	0.0554(7)
C(31)	0.4276(3)	0.5034(2)	0.2961(2)	0.062(1)
C(4)	0.3036(2)	0.6489(2)	0.0145(1)	0.0445(8)
O(4)	0.3515(2)	0.7995(1)	0.01601(9)	0.0605(7)
C(5)	0.2284(2)	0.5708(2)	−0.0837(1)	0.0475(8)
O(5)	0.2117(2)	0.6711(2)	−0.17438(9)	0.0616(7)
C(6)	0.1807(3)	0.4072(2)	−0.0827(2)	0.062(1)
O(0)	0.5526(2)	0.9921(2)	0.1643(1)	0.0683(8)
H(2)	0.278(3)	0.303(3)	0.162(2)	0.086(6)
H(31a)	0.500(3)	0.566(3)	0.353(2)	0.084(6)
H(31c)	0.499(3)	0.405(3)	0.274(2)	0.079(6)
H(31b)	0.319(2)	0.467(2)	0.326(2)	0.072(5)
H(5)	0.154(3)	0.612(3)	−0.233(2)	0.083(6)
H(6)	0.133(3)	0.345(3)	−0.144(2)	0.080(6)
H(0a)	0.491(4)	0.926(3)	0.118(2)	0.103(8)
H(0b)	0.607(3)	1.058(3)	0.121(2)	0.093(7)

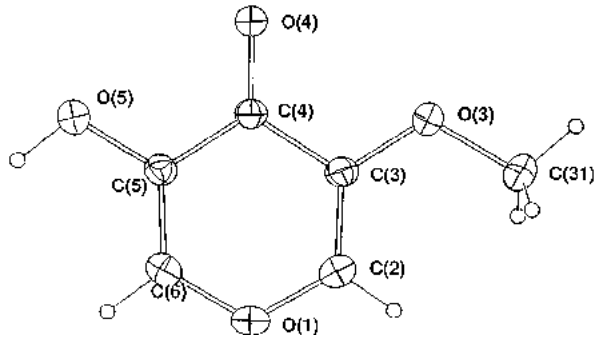

Figure 1. Molecular projection, normal to the plane of the molecule, showing 20% thermal ellipsoids for the non-hydrogen atoms, hydrogen atoms having arbitrary radii of 0.1 Å.

* To whom correspondence should be addressed. Tel: 0207 753 5913. Fax: 0207 753 5909. E-mail: sgibbons@cua.ulsop.ac.uk.
† University of London.
‡ Department of Pharmaceutical Chemistry, Kuwait University.
§ Herbarium, Kuwait University.
⊥ University of Western Australia.
∥ University of Strathclyde.

10.1021/np990535+ CCC: $19.00
Published on Web 04/26/2000

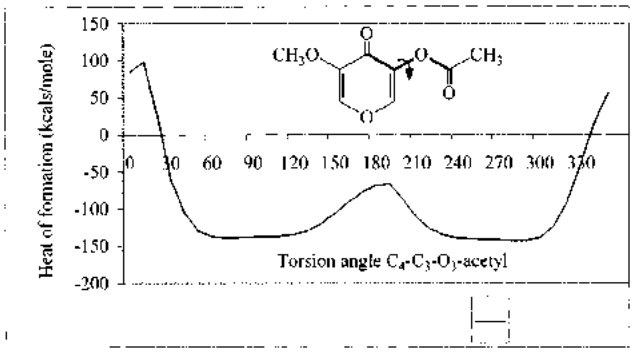

Figure 2. The change in the energy of the compound as the torsion angle shown was varied. The angle was changed in 10° increments, and the energy of the compound was measured with the semiempirical quantum mechanics program MOPAC using the AM1 Hamiltonian.

cotton harlequin bug *Tectoris diopthalmus*.[5] It is possible that *H. salicornicum* stores rubiginol as its monomethyl ether (**1**), which may then be demethylated to the sex pheromone, which could possibly act as a pollination aid.

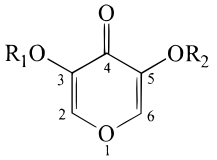

1 R_1 = Me, R_2 = H
2 R_1 = Ac, R_2 = Me
3 R_1 = R_2= H

Experimental Section

General Experimental Procedures. The NMR spectra of **1** and **2** (acetone-d_6, 400 MHz for ^{1}H, 100 MHz for ^{13}C) were run using a Bruker AMX-400 spectrometer with acetone as internal standard. EIMS were recorded on a Fisons AutospecQ instrument.

A sphere of X-ray data (8129 reflections) was measured using a Bruker AXS CCD detector instrument at ca. 300 K [specimen-detector 5 cm, $2\theta_{max} = 58°$; 5 s frames, ω scan (0.3° increments); monochromatic Mo $K\alpha$ radiation, $\lambda = 0.7107_3$ Å), and processed using proprietary software (SAINT/SADABS/XPREP) to yield 1382 independent reflections ($R_{int} = 0.031$), all being used in the full-matrix least-squares refinement, refining anisotropic thermal parameter forms for C, O as well as (x, y, x, U_{iso})$_H$. Some deterioration (dehydration?) of the crystal occurred during data collection and was compensated for by appropriate scaling. Conventional residuals R, R_w (statistical weights) on $|F|$ were 0.044, 0.059. Pertinent results are given in Figure 1 and Table 1. Crystallographic data for **1** has been deposited with the Cambridge Crystallographic Data Centre. Copies of data can be obtained, free of charge, on application to the Director, CCDC, 12 Union Road, Cambridge CB2 1EZ, U.K. (fax: +44-(0)1223-336033 or e-mail: deposit@ccdc.cam.ac.uk). Neutral atom complex scattering factors were employed, computation using the Xtal 3.5 program system.[6]

A search of the Cambridge Structural Database[7] revealed no structurally similar 3,5 disubstituted 4H-pyranone derivatives that have been crystallized. The structure was built using the molecular modeling package CHEMX[8] and was optimized by the ab initio quantum mechanics program GAMESS[9] with the 3-21G basis set. The conformational flexibility about the C(4)−C(3)−O(3)−acetyl torsion angle was examined by adjusting the angle in 10° increments with CHEMX and optimizing the structure using the semiempirical quantum mechanics package MOPAC (version 6) with the AM1 Hamiltonian.[10]

The torsion angle was fixed in each case. The keywords PRECISE, GEO-OK, GNORM=0.1 were specified with the BFGS optimizer.

Plant Material. Plant material was collected from the Jal-Az-Zoor in March 1998. A voucher specimen has been deposited at the Kuwait University Herbarium (KTUH), Khaldiyah, Kuwait.

Extraction and Isolation. The dried aerial parts of *H. salicornicum* (500 g) were extracted at room temperature in chloroform (3 × 2.5 L) and methanol (2 × 2.5 L). The chloroform extract was reduced under vacuum to give a residue of 20 g. This was then subjected to Biotage flash chromatography (Flash 75 S Si gel cartridge) eluting with hexane with increasing 10% amounts of ethyl acetate and finally 10% methanol in ethyl acetate. The residue from the fraction eluted with 70% ethyl acetate in hexane was then recrystallized from ethyl acetate to yield compound **1** (200 mg).

5-Hydroxy-3-methoxy-4*H*-pyran-4-one (1): colorless needles (acetone); mp 107−108 °C; UV (methanol) λ_{max} (log ϵ) 299 (1.3) nm; IR ν_{max} (film) 3200, 3070, 1580, 1470, 1312, 1216, 1079, 952 cm^{-1}; ^{1}H NMR (acetone-d_6, 400 MHz) δ 8.01 (2H, s, H-2, H-6), 7.62 (1H, s, OH), 3.77 (3H, s, MeO); ^{13}C NMR (acetone-d_6, 100 MHz) δ 169.8 (s, C-4), 148.2 (s, C-5), 147.1 (s, C-3), 142.0 (d, C-2), 139.5 (d, C-6), 57.8 (q, OMe); EIMS m/z 142 [M]$^+$ (100), 124 (35), 112 (55), 96 (30), 83 (35), 71 (20), 58 (60); FABMS m/z 165 [M+Na]$^+$ (40), 143 (100), 139 (25); HRFABMS m/z 143.0341 (calcd for $C_6H_7O_4$, 143.03443).

Crystal data: $C_6H_8O_5$, $M_r = 160.1$; monoclinic, space group $P2_1/c$ (C^5_{2h}, no. 14), $a = 7.615(2)$ Å, $b = 7.892(2)$ Å, $c = 12.013(3)$ Å, $\beta = 91.682(5)°$, $V = 721._6$ Å^3. D_c ($Z = 4$) = 1.47_4 g cm^{-3}; $F(000) = 336$. μ_{Mo} (no correction) = 1.3 cm^{-1}; specimen: 0.48 × 0.28 × 0.15 mm. $n_\nu = 133$; $|\Delta\rho_{max}| = 0.23$ e Å^{-3}.

Acetylation of Compound 1: Compound **1** (10 mg) was dissolved in pyridine (2 mL), and then acetic anhydride (1 mL) was added. The mixture was left overnight and then evaporated under nitrogen. The resulting solid was then recrystallized from acetone to afford compound **2** (8 mg).

3-Acetoxy-5-methoxy-4*H*-pyran-4-one (2): cubes (acetone); mp 87−88 °C; UV (acetone) λ_{max} (log ϵ) 324 (0.18) nm; IR ν_{max} (KBr) 2917, 2849, 1759, 1625, 1369, 1283, 1180, 1067 cm^{-1}; ^{1}H NMR (acetone-d_6, 400 MHz) δ 8.21 (1H, s, H-2), 8.00 (1H, s, H-6), 3.76 (3H, s, MeO), 2.24 (3H, s, Me); ^{13}C NMR (acetone-d_6, 100 MHz) δ 168.3 (s, C-4), 168.3 (s, acetyl carbonyl), 150.5 (s, C-5), 149.3 and 149.2 (d, C-2), 141.5 (s, C-3), 141.0 and 140.9 (d, C-6), 57.5 (q, OMe), 20.2 (q, Me); EIMS m/z 368 [2M]$^+$ (10), 340 (5), 312 (10), 181 (20), 137 (30); FABMS m/z 207 [M + Na]$^+$ (100), 185 [M + H]$^+$ (35), 176 (30), 143 (60); HRFABMS m/z 207.0270 (calcd for $C_8H_8O_5Na$, 207.0269).

Acknowledgment. This research was funded by Kuwait University Research Administration under grant no. FDC-111. NMR studies were undertaken in the Strathclyde University NMR laboratory. Professors C. W. T. Pilcher and C. H. J. Ford of the Faculty of Medicine, Kuwait University, are thanked for the use of laboratory space. Mr. John Alexander George, Department of Biological Sciences, Kuwait University, is thanked for running mass spectra.

References and Notes

(1) Gibbons, S.; Mathew, K. T.; Gray, A. I. *Phytochemistry* **1999**, *51* (3), 465−467.
(2) Michel, K. H.; Sandberg, F.; Haglid, F.; Norin, T. *Acta Pharm. Suec.* **1967**, *4*, 97−116.
(3) Michel, K. H.; Sandberg, F. *Acta Pharm. Suec.* **1968**, *5*, 67−70.
(4) Daoud, H. S.; Al-Rawi, A. *Flora of Kuwait;* KPI Publishers: London, 1985; Vol. 1.
(5) Knight, D. W.; Staddon, B. W.; Thorne, M. J. *Z. Naturforsch., C: Biosci.* **1985**, *40C* (11−12), 851−853.
(6) Hall, S. R., King, G. S. D., Stewart, J. M., Eds. *Xtal 3.4 User's Manual*; University of Western Australia, Lamb: Perth, 1995; Developmental Version 3.5.
(7) Allen, F. H.; Kennard, O. *Chem. Des. Automation News* **1993**, *8*, 131−137.
(8) CHEMX 1997. Marketed and distributed by Oxford Molecular, Ltd., Oxfordshire, U.K.
(9) Schmidt, M. W.; Baldridge, K. K.; Boatz, J. A.; Jensen, J. H.; Koseki, S.; Gordan, M. S.; Nguyen, K. A.; Windus, T. L.; Elbert, S. T. *QCPE Bull.* **1990**, *10*, 52−54.
(10) Stewart, J. J. P. *J. Comput. Aided Mol. Des.* **1990**, *4*, 1−145.

NP990535+

PERGAMON

Phytochemistry 51 (1999) 465–467

PHYTOCHEMISTRY

A caffeic acid ester from *Halocnemum strobilaceum*

Simon Gibbons[a,*], K.T. Mathew[b], Alexander I. Gray[c]

[a]*Department of Pharmaceutical Chemistry, Faculty of Pharmacy, Kuwait University, P.O. Box 24923, Safat 13110, Kuwait*
[b]*The Herbarium, Department of Biological Science, Kuwait University, P.O. Box 5969, Safat 13060, Kuwait*
[c]*Department of Pharmaceutical Sciences, University of Strathclyde, 27 Taylor street, Glasgow G4 0NR, Scotland, UK*

Received 3 November 1998

Abstract

A new *n*-alkyl ester of 3,4-dihydroxycinnamic acid (caffeic acid) has been isolated from the halophytic plant, *Halocnemum strobilaceum*. Its structure was elucidated by NMR and mass spectroscopy. © 1999 Published by Elsevier Science Ltd. All rights reserved.

Keywords: Halocnemum strobilaceum; Chenopodiaceae; Caffeic acid ester; Docosyl-3,4-dihydroxycinnamate; Docosyl caffeate

1. Introduction

The flora of Kuwait consists of ca. 400 species of native and naturalized vascular plants (Daoud & Al-Rawi, 1985; Al-Rawi, 1987). The largest plant families in the descending order of species representation are Gramineae, Asteraceae, Cruciferae, Leguminosae, Chenopodiaceae and Caryophyllaceae, accounting for (Boulos & Drosari, 1994) ca. 60% of the flora. Annuals that sprout after the November rains and complete their life cycle before summer (June onwards) account for the bulk of the taxa (ca. 70%). The rest of the flora is represented by perennials that tolerate a variety of stress conditions, such as salinity and extreme heat during the summer months.

The Chenopodiaceae has a cosmopolitan distribution with its centres of diversity in xeric and halophytic regions, such as the coastal areas of the Arabian Gulf. In Kuwait, the family is represented by 18 perennial taxa that are exceptionally hardy and tolerate very high temperatures, which at ground level may reach 84°C (ROPME, 1998). Some members of this family are known for their ability to produce alkaloids (Hegnauer, 1989), in particular pyridines from *Anabasis* (Sadykov, Mukhamedzhanov, & Aslanov, 1967) and quinolines from *Haloxylon* (Michel, Sandberg, Haglid, & Norin, 1967). In a start to a study of the natural products chemistry of the desert flora of Kuwait, we have investigated the halophyte, *Halocnemum strobilaceum* (Pall.) M. Bieb., from which we have isolated the new caffeic acid ester (**1**).

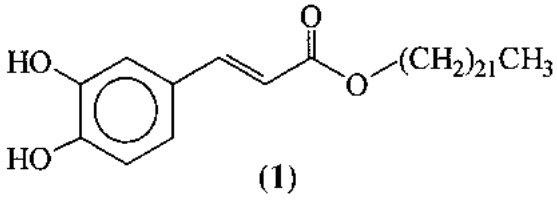

(1)

2. Results and discussion

By Biotage™ flash chromatography, compound (**1**) was isolated as a white waxy solid. The EI mass spectrum indicated the presence of an $[M]^+$ at m/z 488, with fragments that indicated the presence of a long-chain alkyl group with multiple losses of 14 mu (CH_2). The ^1H NMR spectrum (Table 1) exhibited signals for three aromatic protons in a 2,5,6 substitution pattern, two broad hydroxyl singlets (δ 5.65 and δ 6.05), which together with two protons of a *trans*-double bond ($J = 15.9$ Hz), indicated the presence of a 3,4-dihy-

* Corresponding author.

0031-9422/99/$ - see front matter
PII: S0031-9422(99)00007-2

droxy-*trans*-cinnamate (caffeate) moiety. Further signals for a deshielded methylene (δ 4.19), a methylene envelope and a methyl triplet, indicated the presence of a long alkyl chain. The carbon spectrum (Table 1) confirmed the presence of a dihydroxy cinnamate derivative with resonances attributable to a carbonyl group (δ 168.0), two deshielded oxygen bearing quaternary carbons, five methine carbons and a shielded aromatic quaternary carbon. Subtraction of the elements of 3,4-dihydroxy-cinnamate ($C_9H_7O_4$) from the M_r (488), left an alkyl chain of M_r 309, which was equivalent to the C_{22} *n*-alkyl docosyl chain from the parent alkane, docosane.

Compound (**1**) is therefore assigned as the new ester docosyl-3,4-dihydroxy-*trans*-cinnamate (docosyl caffeate). Such long-chain esters of caffeic acid are uncommon in nature, although hexacosanyl and triacontanyl caffeates have been isolated from *Pongamia glabra* (Saha, Mallik, & Mallik, 1991). Similar compounds with long-chain alcohols but with *p*-coumarate as the esterifying acid, have been encountered in Asteraceae growing in arid conditions, for example, in *Artemisia assoana* Willk. (Anthemidae) (Martinez, Barbera, Sanchez-Parareda, & Marco, 1987) and *A. campestris* (Vajs, Jeremic, Stefanovic, & Miloslavljevic, 1975).

It is possible that natural product (**1**) and related compounds may have a role in the stress management of halophytic plants. For example, they may be associated with water retention within the plant cells with the hydrophobic long alkyl chain being 'anchored' within the cell membrane and the hydrophilic hydroxycinnamate portion remaining within the cell, thus retaining a hydration shell.

3. Experimental

NMR were recorded in $CDCl_3$ using a Bruker AMX-400 spectrometer.

3.1. Plant material

This was collected from the Shuaikh campus of Kuwait University in March 1998. A voucher specimen (SG 983 102) has been deposited at the Kuwait University Herbarium (KTUH), Khaldiyah, Kuwait.

3.2. Extraction and isolation of compound (*1*)

Whole herb (800 g) was extracted at room temp. with $CHCl_3$ (3×2.5 l) and MeOH (2×2.5 l). The $CHCl_3$ extract was evapd under vacuum to give a residue of 19.1 g. This was then subjected to Biotage flash chromatography (Flash 75 S silica gel cartridge) eluting with hexane with increasing 10% amounts of EtOAc and finally 10% MeOH in EtOAc. The residue from the fr. eluted with 30% EtOAc in hexane was washed ($\times 5$) with hexane (10 ml) to yield compound (**1**) (30 mg).

Table 1
^1H and ^{13}C NMR data for compound (**1**). .Coupling constants Hz in parenthesis. Resonances denoted * may be interchangeable

Carbon	δ_H	δ_C
1	-	127.8
2	7.09 d (1.7)	114.6
3	-	144.0
4	-	146.5
5	6.87 d (8.2)	115.7
6	7.01 dd (1.7, 8.2)	122.6
7	7.57 d (15.9)	144.9
8	6.27 d (15.9)	116.0
9	-	168.0
OH-3*	6.05 br s	-
OH-4*	5.65 br s	-
CH_2-1′	4.19 t (6.7)	65.1
CH_2-2′	1.68 m	32.1
CH_2-3′- CH_2-21′	1.10-1.40 m	22-32
CH_3-22′	0.88 t (6.4)	14.3

3.3. Docosyl-3,4-dihydroxy-trans-cinnamate (*1*)

White waxy solid. Found: 488 $[M]^+$, $C_{31}H_{52}O_4$ requires 488. IR υ_{max} (film): 3446, 3286 (br, OH), 2954, 2915, 2848, 1686, 1600, 1527, 1471, 1271, 1178, 979, 719 cm^{-1}. EIMS *m/z*: 488 $[M]^+$, 460, 180, 163, 111, 97, 82, 69, 56.

Acknowledgements

This research was funded by Kuwait University Research Administration under grant No. FDC-111. NMR studies were undertaken in the Strathclyde University NMR laboratory. Professor C.W.T. Pilcher and Professor C.H.J. Ford of the Faculty of Medicine are thanked for the use of laboratory space. Mr John Alexander George, Department of Biological Sciences, is thanked for running MS.

References

Al-Rawi, A. (1987). In *Flora of Kuwait*, *2*. Oxford: The Alden Press Publishers.

Boulos, L., & Drosari, M. (1994). *J. Univ. Kuwait (Sci.)*, *21*, 203.

Daoud, H. S., & Al-Rawi, A. (1985). In *Flora of Kuwait*, *1*. London: KPI Publishers.

Hegnauer, R. (1989). In *Chemotaxonomie der Pflanzen*, *8*. Berlin: Birkhäuser Verlag.

Martinez, V., Barbera, O., Sanchez-Parareda, J., & Marco, J. A. (1987). *Phytochemistry*, *26*, 2619.

Michel, K. H., Sandberg, F., Haglid, F., & Norin, T. (1967). *Acta Pharm. Suec*, *4*, 97.

Regional Organisation for the Protection of the Marine Environment (ROPME) (1998), unpublished results.
Sadykov, K. S., Mukhamedzhanov, S. Z., & Aslanov, K. A. (1967). *Dokl. Akad. Nauk. Uzb. SSR*, *24* (4), 34.
Saha, M. M., Mallik, U. K., & Mallik, A. K. (1991). *Phytochemistry*, *30*, 3834.
Vajs, V., Jeremic, D., Stefanovic, M., & Miloslavljevic, S. (1975). *Phytochemistry*, *14*, 1659.